

**STELLAR  
STRUCTURE**

# **STELLAR STRUCTURE**

**ALLER and  
McLAUGHLIN**

**Edited by LAWRENCE H. ALLER  
and DEAN B. McLAUGHLIN**

**STARS  
AND  
STELLAR  
SYSTEMS  
VOLUME  
VIII**

## **CONTRIBUTORS**

**Stanley Bashkin, Robert R. Brownlee, T. G. Cowling, Arthur N. Cox,  
P. Ledoux, L. Mestel, Hubert Reeves, E. Schatzman, R. L. Sears,  
Bengt Strömberg, F. Zwicky**

**Volume VIII of STARS AND STELLAR SYSTEMS**

**...a nine-volume compendium of astronomy  
and astrophysics**



**CHICAGO**

**GERARD P. KUIPER, General Editor  
BARBARA M. MIDDLEHURST, Associate General Editor**



# STELLAR STRUCTURE

EDITED BY LAWRENCE H. ALLER *and* DEAN B. McLAUGHLIN

STARS  
AND  
STELLAR  
SYSTEMS

VOLUME  
VIII



CHICAGO



2nd printing

## STARS AND STELLAR SYSTEMS

### Volume VIII: STELLAR STRUCTURE

Edited by LAWRENCE H. ALLER  
and DEAN B. McLAUGHLIN

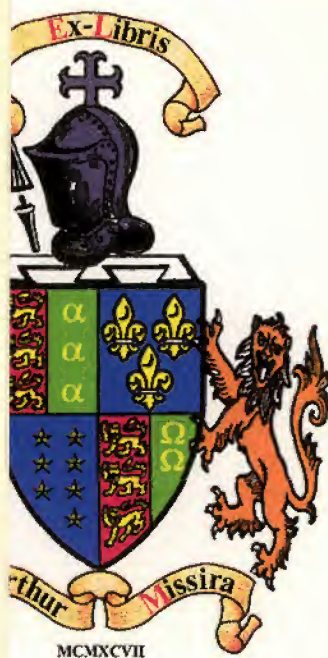
The theory of stellar structure is one of the classical topics in astrophysics. Starting with the investigations of Lane and Ritter a century ago, a steady succession of capable investigators have made fundamental contributions to the mathematical and physical theory, while others have supplied an understanding of essential data concerning opacity, degenerate matter, thermonuclear processes, and element-building in stars.

In this volume eleven experts discuss problems of the internal structure of stars, the sources of stellar energy, and the evolution of stars from several points of view. Among subjects treated here are the origin of the chemical elements, nuclear processes in stars, the theory of white dwarf stars, the observational and theoretical aspects of supernovae, and the nature of magnetic stars.

#### *About the editors . . .*

LAWRENCE H. ALLER is professor of astronomy and chairman of the Department of Astronomy at the University of California, Los Angeles.

DEAN B. McLAUGHLIN is professor of astronomy, University of Michigan.





# STARS AND STELLAR SYSTEMS

*Compendium of Astronomy and Astrophysics*

---

(IN NINE VOLUMES)

GERARD P. KUIPER, *General Editor*

BARBARA M. MIDDLEHURST, *Associate General Editor*

I

TELESCOPES

II

ASTRONOMICAL TECHNIQUES

III

BASIC ASTRONOMICAL DATA

IV

CLUSTERS AND BINARIES

V

GALACTIC STRUCTURE

VI

STELLAR ATMOSPHERES

VII

NEBULAE AND INTERSTELLAR MATTER

VIII

STELLAR STRUCTURE

IX

GALAXIES AND THE UNIVERSE



## CONTRIBUTORS

STANLEY BASHKIN	L. MESTEL
ROBERT R. BROWNLEE	HUBERT REEVES
T. G. COWLING	E. SCHATZMAN
ARTHUR N. COX	R. L. SEARS
P. LEDOUX	BENGT STRÖMGREN
	F. ZWICKY



# STELLAR STRUCTURE

*Edited by*

LAWRENCE H. ALLER

*and*

DEAN B. McLAUGHLIN



THE UNIVERSITY OF CHICAGO PRESS

CHICAGO & LONDON



*This publication has been supported in part by the*  
NATIONAL SCIENCE FOUNDATION

*Library of Congress Catalog Card Number: 63-16723*

THE UNIVERSITY OF CHICAGO PRESS, CHICAGO 60637  
The University of Chicago Press, Ltd., London W.C. 1  
© 1965 by The University of Chicago. All rights reserved

*Published 1965. Second Impression 1968*  
*Printed in the United States of America*

## *Preface to the Series*

THE SERIES "Stars and Stellar Systems, Compendium of Astronomy," comprising nine volumes, was organized in consultation with senior astronomers in the United States and abroad early in 1955. It was intended as an extension of the four-volume "Solar System" series to cover astrophysics and stellar astronomy. In contrast to the "Solar System" series, separate editors have been appointed for each volume. The volume editors, together with the general editors, form the editorial board that is responsible for the over-all planning of the series.

The aim of the series is to present stellar astronomy and astrophysics as basically empirical sciences, co-ordinated and illuminated by the application of theory. To this end the series opens with a description of representative telescopes, both optical and radio (Vol. 1), and of accessories, techniques, and methods of reduction (Vol. 2). The chief classes of observational data are described in Volume 3, with additional material being referred to in succeeding volumes, as the topics may require. The systematic treatment of astronomical problems starts with Volume 4, as is apparent from the volume titles. Theoretical chapters are added where needed, on dynamical problems in Volumes 4, 5, and 9, and on astrophysical problems in Volumes 6, 7, and 8. In order that the chapters may retain a greater degree of permanence, the more speculative parts of astronomy have been de-emphasized. The level of the chapters will make them suitable for graduate students as well as for professional astronomers and also for the increasing number of scientists in other fields requiring astronomical information.

The undersigned wish to thank both the authors and the volume editors for their readiness to collaborate on this series, which it is hoped will stimulate the further growth of astronomy.

The editors wish to acknowledge the support by the National Science Foundation both in defraying part of the costs of the editorial offices and in providing a publication subsidy.

GERARD P. KUIPER  
BARBARA M. MIDDLEHURST





# Preface and Introduction to Volume 8

THE theory of stellar structure is one of the classical topics in astrophysics. Starting with the investigations of Lane and Ritter a century ago, a steady succession of capable investigators—including Eddington, Rosseland, Chandrasekhar, Öpik, Cowling, Strömberg, Schwarzschild, and Henyey—have made fundamental contributions to the mathematical and physical theory, while others including Kramers, R. H. Fowler, Bethe, Salpeter, Critchfield, Von Weizsäcker, the Burbidges, W. A. Fowler, Hoyle, and Cameron have supplied an understanding of essential data concerning opacity, degenerate matter, thermonuclear processes, and element building in stars. It is worth noting that degenerate matter was recognized to exist in the stars before a degenerate electron gas (in metals) was recognized to exist on the earth.

Most of the earlier work on stellar structure was confined to chemically homogeneous models in hydrostatic equilibrium, i.e., to models appropriate to main-sequence stars. The basic equations and boundary conditions are so simple that we may quote them here, using well-known symbols.\*

$$\text{continuity of mass} \quad M_r = 4\pi \int_0^r r^2 \rho dr, \quad (1)$$

$$\text{hydrostatic equilibrium} \quad \frac{dP}{dr} = -\frac{GM_r}{r^2} \rho, \quad (2)$$

$$\text{energy production} \quad L_r = 4\pi \int_0^r r^2 \epsilon \rho dr. \quad (3)$$

In the zones where energy is transported by radiation, the net flux in ergs  $\text{cm}^{-2} \text{sec}^{-1}$  is

$$\mathfrak{F} = -\frac{4c a T^3}{3 \kappa \rho} \frac{dT}{dr}, \quad (4)$$

while in zones where the energy is transported mainly by convection and radiation pressure plays a negligible role, the pressure  $P$  and density  $\rho$  are connected approximately by the adiabatic gas law:

$$P = K \rho^\gamma. \quad (5)$$

\* Their derivation may be found in many places (e.g., L. H. Aller, *Nuclear Transformations, Stellar Interiors, and Nebulae* [New York: Ronald Press Co., 1954]).

Here  $\gamma$  is the ratio of specific heats,  $K$  is a constant, and the pressure obeys the equation of state

$$P = P_g + P_r = \rho \frac{\Re T}{\mu} + \frac{1}{3} a T^4, \quad (6)$$

where  $a$  is the radiative constant,  $\Re$  is the gas constant, and the molecular weight is

$$\mu = \mu(\rho, T, \text{chemical composition}).$$

The opacity  $\kappa = \kappa(\rho, T, \text{chemical composition})$  and the energy generation  $\epsilon = \epsilon(\rho, T, \text{chemical composition})$  must be evaluated from the data of atomic and nuclear physics.

As we approach the center of the star,  $r \rightarrow 0$ ,  $M_r$  (the mass inclosed within a sphere of radius  $r$ ), and  $L_r$  (the energy produced within a sphere of radius  $r$ ) must both approach zero.

Likewise as one approaches the surface of the star  $r \rightarrow R$ ,  $M_r \rightarrow M$ , and  $L_r \rightarrow L$ , whereas  $P$  and  $T$  must approach the values appropriate for these quantities in the visible layers of the stellar atmosphere.

When defined in this way, the problem admits of a solution when the mode of energy transport can be specified and the functional forms of  $\mu$ ,  $\kappa$ , and  $\epsilon$  are known. A literal solution of the equations is not possible; one must proceed by numerical integrations. Some very general conclusions may be drawn, at least for stars of *uniform* chemical composition. One of these is the mass-luminosity relation which can be expressed in the form

$$L = \text{const} \frac{M^a}{R^b} \mu^d, \quad (7)$$

where  $a \sim 4$ ,  $b \sim 0.5$ , and  $d \sim 7.5$  for plausible functional forms of  $\mu$ ,  $\kappa$ , etc. The important fact is that a mass-luminosity relation exists as a consequence of the temperature gradient in the star. The greater the mass, the steeper will be the pressure gradient. Hence the higher the temperature in the center, the greater the rate of energy generation, and therefore the greater the luminosity of the star. Even if the exact law of energy generation is not known, a mass-luminosity relation can be found. Eddington, who was the first to find this relation theoretically, thought that it substantiated his particular stellar model. Actually it is true quite generally for chemically homogeneous stars. The exact values of the exponents,  $a$ ,  $b$ , and  $d$  depend on the assumed opacity law, etc. A second relation involving the energy generation laws may also be desired. Clearly:

$$L = 4\pi \int_0^R \epsilon \rho r^2 dr. \quad (8)$$

The theories of the opacity and of nuclear energy generation are carefully reviewed here by Cox and by Reeves. (See chaps. 2 and 3.)



Chemically homogeneous models apply only to early stages of a star's life as a thermonuclear source. Although a brisk convection insures good mixing, stars are in convective equilibrium only in portions of their interiors and we can be reasonably sure that all portions of a star do not become evenly mixed—at least during those stages of its life now amenable to quantitative treatment. (See chap. 9 by Mestel on meridian circulation.) Hence chemical inhomogeneities are produced in the sense that hydrogen becomes replaced by helium in the core. Although Öpik was the first to realize the importance of chemically inhomogeneous models and important contributions were made by Chandrasekhar and Schoenberg, detailed applications to stellar evolution problems by Schwarzschild, Sandage, and Hoyle initiated great activity in this field. Chapter 4 by Strömgren and chapter 11 by Sears and Brownlee give detailed, clear, comprehensive accounts of stellar structure and evolution and the problems of age determination.

Intimately connected with advanced stages of evolution of massive stars is the problem of element building by thermonuclear reactions. We refer to Bashkin's thorough account of the origin of the chemical elements in chapter 1. What can be said of the late stages of stellar evolution? Some stars may evolve into white dwarfs in a relatively orderly way. Others may explode as supernovae. Nevertheless, the explosion (as a supernova) of a star previously recognized as a highly evolved object has never been observed. Zwicky authoritatively summarizes the observational data, which remain scanty in spite of intensive efforts by him and others to supply badly needed information. Novae and the nuclei of planetary nebulae certainly are stars in advanced stages of their evolution. In chapter 6, Schatzman carefully reviews current theories of novae and supernovae.

That the white dwarfs represent the last stage of stellar evolution was recognized nearly forty years ago. In fact, the first stellar models to stand the test of time were those worked out for these degenerate gas stars. Mestel treats the intriguing problem of these white dwarf stars in chapter 5.

Magnetic stars, treated by Cowling in chapter 8, present some of the most puzzling problems in modern astrophysics. The correlation of strong magnetic fields with chemical composition abnormalities and the apparent concentration of different elements in different places on the surface of a star suggest magneto-hydrodynamical interactions of a type not yet clearly envisaged.

Finally we come to the vital question of stellar stability. It is not sufficient that a stellar model be in equilibrium. It must also be stable. In chapter 10, Ledoux has given a very thorough summary of stability problems. Closely related to the problem of stellar stability is the theory of pulsations. In recent years, John Cox, Christie, and others have made important contributions to this subject. The importance of the role of the extensive convection zones in classical Cepheids and possibly also in long-period variables is now realized, and we can look forward to further significant advances in this field soon.

The relation of stellar structure and evolution to other problems in astronomy merits some attention which perhaps can be summarized best at this point. Quantitative checks on the theory at various stages of stellar evolution require accurate data on stellar masses, radii, and luminosities (particularly for highly evolved stars) and accurate color-magnitude diagrams for star clusters. In addition, reliable models for stellar atmospheres are required in order to derive the total luminosity or bolometric magnitude of a star from observations made in the usual spectral ranges. The chemical composition of a star provides revealing clues. Some effects, e.g., an abnormally small metal to hydrogen ratio, probably reflects a metal deficiency in the original medium from which the stars were made. Other phenomena, e.g., the presence of technetium, reflect effects of processes occurring within the interior of the star itself.

The interdependence of different branches of astronomy is no better illustrated than by the relationship between stellar structure and evolution on the one hand and cosmology on the other, in connection with the distance-scale problem. The classic methods of trigonometric parallaxes, dynamical parallaxes, and moving clusters are available only for the nearest stars. Use of the tau and epsilon components of proper motions often yield only rough to fair statistical results and are never available for more distant systems. Indeed, to establish the distances of the remote components of our stellar system and the nearest of external galaxies, we are dependent on a process of what might be called *photometric continuation*.

In a galactic cluster we may recognize not only stars like the sun but also main-sequence stars that are much more luminous, which could be identified if they appeared in much more remote systems. The absolute magnitudes and colors of these brighter stars, some examples of which may occur even in external galaxies, depend on their stage of evolution, i.e., on the age of the system. The stars observed in M31, M33, or even in the Magellanic clouds are massive objects that are undergoing rapid evolution. Their intrinsic luminosities are sometimes difficult to establish. Other methods involving Strömgren spheres, bright variable stars, etc., involve implicitly the same basic limitations. Only a better quantitative understanding of the evolutionary tracks of massive stars can improve the method of photometric continuation.

The rapidly increasing availability of electronic computers, the steadily mounting volumes of basic physical data on opacity, cross-sections for nuclear reaction, improved understanding of complex hydrodynamical phenomena provide a powerful stimulus for progress in stellar structure theory. Unfortunately, observational data essential to progress in this field are not being accumulated at a sufficient rate. Although certain useful material can be obtained with small telescopes, critical data on stellar luminosities, temperatures, masses, and chemical compositions depend increasingly on observations that can be secured only with instruments of large light-gathering power and these are grievously in short supply.

From the standpoint of stellar evolution studies, two of the most valuable objects known are the Magellanic clouds. In either of these, one may observe large stellar populations—all at essentially the same distance from us. The most luminous and easily observed stars are those that are evolving the most rapidly. Whereas one may compare only a handful of bright, rapidly evolving stars in any single cluster in our own Galaxy, in the Magellanic clouds one may compare multitudes of stars at almost any given epoch in their evolution. Unfortunately, there does not yet exist a single fully modern adequate telescope in the southern hemisphere! It is fervently to be hoped that these deficiencies in astronomical instrumentation will be remedied soon.

In an undertaking such as this, where ten different authors are involved, the dates of manuscript completion and submission cover a range of several years. Although opportunities have been provided for each author to update his manuscript, one cannot expect to keep up adequately with a rapidly moving field by this process. We are grateful to our authors for the patience and forbearance they have shown through the many delays that have beset the production of this book. Not the least of these delays has been caused by unwelcome administrative chores imposed on one of us (LHA).

It would have been impossible to produce this volume without the unflagging help of our associate general editor, Miss Barbara Middlehurst, who rendered services far beyond the responsibility of her assignment. We are also grateful to the many astronomers and physicists who critically read many of the chapters both in proof and manuscript form and offered helpful suggestions. Special mention must be made of the aid supplied by Alan Petty and Igor Jurkevich, who made a very detailed review of one of the chapters.

LAWRENCE H. ALLER

DEAN B. McLAUGHLIN





# *Table of Contents*

<b>1. THE ORIGIN OF THE CHEMICAL ELEMENTS . . . . .</b>	<b>1</b>
<i>Stanley Bashkin</i>	
1. Introduction . . . . .	1
2. Nuclear Abundances. . . . .	4
2.1. Stellar Nuclear Reactions Affecting Nuclear Abundances . . . . .	24
2.1.1. The Alpha Process . . . . .	24
2.1.2. The Equilibrium Process . . . . .	25
2.1.3. The Three-Alpha Process . . . . .	27
2.1.4. The <i>s</i> -Process . . . . .	28
2.1.5. The <i>r</i> -Process . . . . .	38
2.1.6. The <i>p</i> -Process . . . . .	49
2.2. Concluding Remarks on Solar Abundances . . . . .	49
2.3. Introduction to Anomalous Abundances in Stars . . . . .	50
2.4. Abundances in Globular and Galactic Clusters . . . . .	51
2.5. Anomalous Stars . . . . .	55
2.5.1. R Coronae Borealis . . . . .	56
2.5.2. Some G-Type Subdwarfs . . . . .	56
2.5.3. Magnetic Stars . . . . .	57
2.5.4. Manganese Stars and 53 Tauri . . . . .	58
2.5.5. 3 Centauri A . . . . .	58
2.5.6. Other Stars . . . . .	60
3. The Problem of the Nuclei of D, He <sup>3</sup> , Li, Be, and B . . . . .	60
4. The Age of Astronomical Objects . . . . .	87
4.1. Meteorites and the Earth . . . . .	87
4.2. The Solar System . . . . .	90
4.3. Stars and the Galaxy . . . . .	93
References . . . . .	98
 <b>2. STELLAR ENERGY SOURCES . . . . .</b>	 <b>113</b>
<i>Hubert Reeves</i>	
1. History of a Star . . . . .	113
2. Formalism . . . . .	114
2.1. Thermonuclear Reaction Rates . . . . .	119
2.2. Electron Screening Factors . . . . .	124

3. Hydrogen-burning Stage . . . . .	126
3.1. Electron Screening for Hydrogen-burning Cases . . . . .	127
3.2. Hydrogen Thermonuclear Reactions (Proton-Proton) . . . . .	130
3.3. Hydrogen Thermonuclear Reactions (CNO) . . . . .	135
3.4. Nucleosynthesis from the CNO Cycle . . . . .	142
3.5. Neutrinos from the Hydrogen-burning Stage . . . . .	145
3.6. Energy Generation from the Hydrogen-burning Stage . . . . .	152
4. Helium-burning Reactions . . . . .	158
4.1. Helium Thermonuclear Reactions . . . . .	159
4.2. Nucleosynthesis from Helium-burning Stage . . . . .	166
4.3. Energy Generation from the Helium-burning Stage . . . . .	169
5. Subsequent Burning Stages . . . . .	170
5.1.1. $C^{12} + C^{12} \rightarrow Mg^{24*}$ . . . . .	170
5.1.2. $C^{12} + O^{16}$ . . . . .	173
5.1.3. $O^{16} + O^{16} \rightarrow S^{32*}$ . . . . .	173
5.1.4. $Ne^{20} + \gamma \rightarrow O^{16} + He^4$ . . . . .	175
6. Neutrinos in the Late Stages of Stellar Evolution . . . . .	176
6.1. Neutrinos from the Urca Process . . . . .	176
6.2. Neutrinos from Weak Interaction Processes . . . . .	178
6.3. Neutrinos and Stellar Evolution . . . . .	183
7. More Thermonuclear Reaction Rates . . . . .	185
References . . . . .	190
 3. STELLAR ABSORPTION COEFFICIENTS AND OPACITIES . . . . .	195
<i>Arthur N. Cox</i>	
1. Introduction . . . . .	195
1.1. Conditions in Stellar Interiors and Atmospheres . . . . .	195
1.2. Derivation of the Radiation Diffusion Flux Formula . . . . .	198
1.3. Use of Opacities for Stellar Interiors . . . . .	202
1.4. Radiation Transfer in Stellar Atmospheres . . . . .	204
2. Summary of Absorption Coefficient and Opacity Data . . . . .	205
2.1. Eddington Approximations for the Stellar Interior Opacity . . . . .	205
2.2. Monochromatic Absorption Data for Stellar Atmospheres . . . . .	206
2.3. Strömgen Opacity Results . . . . .	206
2.4. Morse Opacities . . . . .	207
2.5. Monochromatic Absorption Coefficients . . . . .	207
2.6. Opacities with Free-free Absorption Improvements . . . . .	209
2.7. Keller and Meyerott Opacities . . . . .	209
3. Absorption and Scattering Processes and Electron Conduction . . . . .	211
3.1. Bound-free Absorption . . . . .	211
3.2. Free-free Absorption . . . . .	213
3.3. Compton Scattering . . . . .	215

## TABLE OF CONTENTS

xv

3.4. Bound-bound Absorption . . . . .	217
3.5. Negative Ion Absorption . . . . .	219
3.6. Coherent, Raman, and Rayleigh Scattering . . . . .	219
3.7. Molecular Absorption . . . . .	220
3.8. Pair Production . . . . .	221
3.9. Nuclear Absorption . . . . .	221
3.10. Photon-Photon Scattering . . . . .	221
3.11. Electron Conduction . . . . .	221
4. Methods of Opacity Calculations . . . . .	224
4.1. Strömgren Methods . . . . .	224
4.2. Morse Calculations . . . . .	227
4.3. Mayer Methods . . . . .	228
4.4. Vitense Monochromatic Absorption Coefficients and Opacities . . . . .	237
4.5. Present Equation of State Methods . . . . .	239
4.6. Present Methods for Absorption Calculations . . . . .	245
4.7. Current Limitations in Opacity Calculations . . . . .	247
5. New Results . . . . .	253
5.1. Comparisons with Previous Opacities . . . . .	253
5.2. Opacities for Mixture $X = 0.596$ , $Y = 0.384$ , $Z = 0.020$ . . . . .	256
6. Use of Opacities . . . . .	262
6.1. Analytic Fits to Opacity Tables . . . . .	262
6.2. Conclusions . . . . .	262
References . . . . .	263
<b>4. STELLAR MODELS FOR MAIN-SEQUENCE STARS AND SUBDWARFS . . . . .</b>	<b>269</b>
<i>Bengt Strömgren</i>	
1. General Considerations . . . . .	269
2. Main-Sequence Stars with Masses Larger than $1.7 M_{\odot}$ . . . . .	270
3. Main-Sequence Stars with Masses in the Range $0.8\text{--}1.7 M_{\odot}$ . . . . .	282
4. Subdwarfs . . . . .	288
5. Main-Sequence Stars with Masses Smaller than $0.8 M_{\odot}$ . . . . .	291
References . . . . .	292
<b>5. THE THEORY OF WHITE DWARFS . . . . .</b>	<b>297</b>
<i>L. Mestel</i>	
1. Zero-Temperature Stars . . . . .	297
1.1. The Pressure of the Degenerate, Perfect Electron Gas . . . . .	297
1.2. Corrections to the Perfect Gas Models . . . . .	300
1.3. Restrictions on Composition Imposed by Nuclear Physics . . . . .	303

1.4. Comparison with Observation . . . . .	305
1.5. Non-spherical Stars . . . . .	307
2. White Dwarfs of Finite Temperature . . . . .	309
2.1. The Internal Temperature . . . . .	309
2.2. A White Dwarf as a Cooling Body . . . . .	312
2.3. Nuclear Energy Generation and Stability . . . . .	315
3. The Origin and Evolution of White Dwarfs . . . . .	319
3.1. The Origin of White Dwarfs . . . . .	319
3.2. The Evolution of a White Dwarf . . . . .	322
References . . . . .	323
<b>6. THEORY OF NOVAE AND SUPERNOVAE</b> . . . . .	<b>327</b>
<i>E. Schatzman</i>	
1. Introduction . . . . .	327
2. Novae . . . . .	327
2.1. Historical Summary . . . . .	327
2.2. Basic Facts To Be Explained . . . . .	329
2.3. Recent Theories . . . . .	331
2.4. The Resonance Theory of Novae . . . . .	337
2.4.1. The Model . . . . .	338
2.4.2. Instability . . . . .	339
2.4.3. Energy and Recurrence . . . . .	341
2.4.4. Non-radial Oscillations . . . . .	343
2.4.5. The Explosive Process . . . . .	346
2.4.6. Changes in the Star during the Nova Stage . . . . .	347
2.5. The U Geminorum Stars . . . . .	348
3. Supernovae . . . . .	350
3.1. Introduction . . . . .	350
3.2. Short History . . . . .	351
3.3. Nuclear History of a Contracting Star . . . . .	354
3.4. Neutrino Astronomy . . . . .	356
3.5. Supernovae of Type II . . . . .	360
3.6. Supernovae of Type I . . . . .	361
3.7. Supernovae as Due to Chain Reactions . . . . .	362
3.8. Supernovae and Radio Galaxies . . . . .	363
References . . . . .	363
<b>7. SUPERNOVAE</b> . . . . .	<b>367</b>
<i>F. Zwicky</i>	
1. Historical . . . . .	367
1.1. The Search for Supernovae with the 18-inch Schmidt Telescope between September 5, 1936, and January 1, 1941. . . . .	371



1.2. Subsequent Search Programs, 1941-1956 . . . . .	372
1.3. Supernovae Discovered since 1956 . . . . .	372
2. Frequencies of Supernovae (Dimensionless Morphology) . . . . .	378
2.1. The Total Frequency of Supernovae . . . . .	378
2.2. The Frequency of Supernovae in Various Types of Galaxies . . . . .	379
2.3. The Frequency of Supernovae in Clusters of Galaxies . . . . .	381
3. Statistics as Related to Phenomenological Characteristics of Supernovae and of Galaxies in Which They Appear (Phenomenological Morphology) . . . . .	384
3.1. The Relative Luminosities of Galaxies and of Supernovae . . . . .	384
3.2. The Spatial Distribution of Supernovae within Their Parent Galaxies . . . . .	385
3.3. The Distribution of Supernovae in Apparent Magnitudes . . . . .	388
3.4. The Magnitude-Redshift Relation . . . . .	391
3.5. The Various Types of Supernovae . . . . .	392
3.5.1. Supernovae of Type I . . . . .	393
3.5.2. Supernovae of Type II . . . . .	401
3.5.3. Supernovae of Type III . . . . .	402
3.5.4. Supernovae of Type IV . . . . .	407
3.5.5. Supernovae of Type V . . . . .	410
3.6. Remarks on Recent Supernovae Spectra . . . . .	412
3.7. The Remnants of Supernovae . . . . .	415
4. The Intrinsic Properties of Supernovae (Absolute Morphology) . . . . .	416
4.1. Theory of Supernovae . . . . .	417
4.1.1. Possible Material Constellations Which May Become the Origins of Supernovae . . . . .	417
4.1.2. Possible Transformations of the Radiations from Supernovae by the Surrounding Interstellar Medium or by Neighboring Stars . . . . .	418
4.1.3. Reasons for the Collapse of Stars . . . . .	418
4.1.4. Reasons for the Collapse of Large Gas Clouds . . . . .	419
4.1.5. The Various Radiations from Supernovae . . . . .	420
5. Conclusion and Recommendations . . . . .	420
References . . . . .	422
<b>8. MAGNETIC STARS . . . . .</b>	<b>425</b>
<i>T. G. Cowling</i>	
1. Observational Data . . . . .	425
2. Basic Equations . . . . .	426
3. The Virial Theorem . . . . .	427
3.1. The Virial Theorem and Stability . . . . .	429

4. Surface Distortions Due to a Magnetic Field . . . . .	430
4.1. Ferraro's Equilibrium Solution . . . . .	430
4.2. Barocline Stars . . . . .	433
5. Force-free Magnetic Fields . . . . .	435
5.1. General Properties of Force-free Fields . . . . .	435
5.2. Magnetic Braking . . . . .	437
5.3. Theories of Flares . . . . .	440
6. Convection and Turbulence . . . . .	444
7. Origin of Stellar Magnetic Fields . . . . .	448
7.1. Fossil Magnetism . . . . .	449
7.2. Dynamo Theories . . . . .	451
8. Magnetic Variable Stars . . . . .	454
8.1. The Oblique-Rotator Theory . . . . .	455
8.2. The Magnetic-Oscillator Theory . . . . .	457
8.3. The Hydromagnetic-Cycle Theory . . . . .	458
9. Conclusion . . . . .	460
References . . . . .	461
 9. MERIDIAN CIRCULATION IN STARS. . . . .	465
<i>L. Mestel</i>	
1. Hydrostatic Equilibrium of Gaseous Stars . . . . .	465
2. Thermal Equilibrium: Conservative Perturbing Forces . . . . .	468
3. Thermal Equilibrium: General Perturbing Forces . . . . .	472
4. Conditions for Steady Circulation . . . . .	477
5. Meridian Circulation and Stellar Evolution . . . . .	482
6. Conditions for Steady Mixing . . . . .	485
7. Other Theoretical Consequences of Meridian Circulation . . . . .	490
8. Meridian Circulation in Convective Envelopes . . . . .	492
References . . . . .	496
 10. STELLAR STABILITY . . . . .	499
<i>P. Ledoux</i>	
1. Introduction . . . . .	499
2. General Equations and Local Stability . . . . .	503
2.1. Effects of Radiation . . . . .	504
2.2. Local Instability, Convection, and Turbulence, and Their Effects . . . . .	506

# TABLE OF CONTENTS

xix

2.2.1. Local Thermal Instability . . . . .	506
2.2.2. Turbulent Convection . . . . .	508
2.3. Effects of Ionization . . . . .	510
2.4. Effects of Nuclear Processes . . . . .	512
2.5. General Equations . . . . .	514
2.5.1. Conservation of Mass . . . . .	514
2.5.2. Conservation of Momentum . . . . .	514
2.5.3. Conservation of Mechanical Energy . . . . .	515
2.5.4. Conservation of Thermal Energy . . . . .	515
2.6. Small Motions and Linearized Equations . . . . .	516
2.7. Boundary Conditions . . . . .	518
3. The General Problem and Its Illustration for Purely Radial Motion . . . . .	521
4. Dynamical Stability . . . . .	524
4.1. Radial Perturbations . . . . .	525
4.2. Non-radial Perturbations . . . . .	528
5. Vibrational Stability . . . . .	534
5.1. Radial Perturbations . . . . .	534
5.1.1. The Main Stellar Interior . . . . .	535
5.1.2. Influence of the External Layers . . . . .	540
5.1.3. Phase Delays in Energy Generation . . . . .	542
5.1.4. Effects of Friction and Progressive Waves . . . . .	544
5.1.5. Vibrational Stability toward the Higher Modes of Pulsation . . . . .	545
5.2. Non-radial Oscillations . . . . .	546
6. Secular Stability . . . . .	547
6.1. General Considerations . . . . .	547
6.2. The Detailed Problem . . . . .	551
7. Some Comments on the Effects of Rotation, Magnetic Fields, or External Gravitational Fields . . . . .	554
7.1. Dynamical and Secular Stability . . . . .	555
7.1.1. Effects of a Rotation . . . . .	555
7.1.2. Effects of a Magnetic Field . . . . .	559
7.1.3. Effects of an External Gravitational Field . . . . .	562
7.1.4. Effects on the Small Perturbations of an Equilibrium State . . . . .	565
7.2. Local Stability . . . . .	566
7.2.1. Effects of a Rotation . . . . .	566
7.2.2. Effects of an External Gravitational Field . . . . .	569
7.2.3. Effects of a Magnetic Field . . . . .	569
References . . . . .	570
<b>11. STELLAR EVOLUTION AND AGE DETERMINATIONS . . . . .</b>	<b>575</b>
<i>R. L. Sears and Robert R. Brownlee</i>	
1. Introduction . . . . .	575

2. Physical Description of Stellar Evolution . . . . .	576
2.1. Pre-Main-Sequence Stages . . . . .	577
2.2. Main-Sequence Stages . . . . .	581
2.3. Post-Main-Sequence Stages . . . . .	585
3. Construction of Evolutionary Sequences . . . . .	593
3.1. Introduction . . . . .	593
3.2. Fitting Method . . . . .	594
3.3. Difference Methods . . . . .	603
4. Age Determinations . . . . .	613
4.1. Introduction . . . . .	613
4.2. Method of Age Determination . . . . .	614
4.3. Accuracy of Age Determinations . . . . .	621
References . . . . .	633
INDEX . . . . .	643



## CHAPTER 1

# *The Origin of the Chemical Elements*

STANLEY BASHKIN<sup>1</sup>

*State University of Iowa*

### § 1. INTRODUCTION

NUCLEAR astrophysics is conveniently divided into two parts, namely, the generation of stellar energy and all other topics. This division comes about because the problem of energy production has been fairly well solved in quantitative fashion, although some questions of detail remain. The remainder of nuclear astrophysics is notable for the absence of quantitative work. This does not mean that the extensive literature is devoid of calculations. Indeed, numerous papers are filled with equations and numbers. Unfortunately, the data and other premises on which such work is based, the methods of extracting results, and the conclusions are more often than not vigorously disputed by different authors. One can even find cases in which a given author has drastically altered his own arguments and numbers in the course of a brief lapse of time.

The present writer believes it important to emphasize the various viewpoints to make clear what is speculative and what is reasonably well understood. Consequently the present paper represents an attempt to summarize and compare the papers which have appeared prior to November, 1962.<sup>2</sup>

An immediate consequence of the fact that stellar energy derives from nuclear transmutations is that the nuclear composition—and, therefore, the chemical composition—of a star is a function of time. Since stars lose mass and new stars condense out of interstellar gas and dust, young stars will not have the same chemical constitution as older ones, nor will they experience identical nuclear

<sup>1</sup> Now at the Department of Physics, University of Arizona, Tucson, Arizona.

<sup>2</sup> A major development since this chapter was written has been the discovery of non-solar, astronomical, X-ray sources and the attempt to identify them as neutron stars, see, e.g., Giacconi *et al.* (1962), Gursky *et al.* (1963), Bowyer *et al.* (1964), Chiu (1964*a, b*), Chiu and Salpeter (1964), Morton (1964). Friedman and his associates observed an occultation of the Crab Nebula by the moon and found that the X-ray source there is not a point source. The angular size of the yet stronger Scorpio source is less than 10'. It is probably not a neutron star.

reactions. It is now generally recognized that many stars show marked differences in chemical abundances due to age, variations in the matter out of which the stars were formed, different mechanisms for mass loss, effects due to surface phenomena, mixing of the surface with interior regions, and so forth. Consequently, it no longer seems physically correct to discuss the Galaxy as though it were chemically homogeneous. It is still an interesting problem to know the present relative abundances for the elements for the entire Galaxy, but the literature on the subject is sometimes unclear as to whether the Galaxy or some portion thereof, such as the solar system, is under consideration. The more common approach in recent papers is to treat each star or group of related stars on an individual basis, which accounts for the composition within a framework which is qualitatively identical for all stars, but which takes advantage of the differences mentioned above to explain particular features.

Although stars differ in composition, it is possible to classify large numbers of them as being similar. Within any one population class, and especially within any one cluster, stars of similar mass and age are alike in most of their chemical characteristics, while the several population classes are distinguished from each other partly on the grounds of chemical disparities, the principal factor being the proportion of the metals relative to hydrogen. The sun is representative of the great majority of Population I stars, and we will first consider the various attempts that have been made to explain the chemical constitution of the sun and the solar system. Actually, certain peculiarities of other stellar bodies, like the presence of technetium in a few red giants and the linear time dependence of the magnitude of certain supernovae, provide important evidence for the operation of various nuclear reactions, and thereby assist in establishing the framework within which the abundance analysis is to be carried out. Basic to this approach is the assumption that the evolution of stars from birth to death is due primarily to the energy-producing requirements which only the core can satisfy. On the other hand, if the evolution of stars involves to an appreciable extent the continuous loss of mass (Fessenkov 1949; Masevich 1949, 1954), it may be necessary to modify many of the details of element formation as given in the present paper.

That framework was carefully constructed in the monumental paper by Burbidge, Burbidge, Fowler, and Hoyle (1957), hereafter denoted<sup>3</sup> by BBFH, in which knowledge of nuclear astrophysics was summarized and greatly extended. A brief account has been given by Cameron (1957) and by Burbidge and Burbidge (1958). A fuller treatment has been given by Frank-Kamenetskii (1959) and by Burbidge (1963). In BBFH, hydrogen was taken to be the original matter of the universe. The generation of stellar energy was ascribed to operation of the proton-proton sequence or carbon cycle for stars on the main sequence, while the three-alpha reaction was taken to be dominant in the red giants. In the course of these reactions, light nuclei up to perhaps  $\text{Mg}^{24}$ , but

<sup>3</sup> Abbreviations are used similarly in this chapter to denote other groups of workers.

excluding Li, Be, and B, were created. It is notable that the carbon cycle could not have taken place *ab initio* because it demands the prior generation of carbon and the intimate mixing of carbon with hydrogen. In any case, charged-particle reactions were not thought likely to lead directly to formation of the heavy elements because of the rapidly decreasing reaction rate which accompanies the growth of nuclear charge. Consequently, BBFH suggested that several processes were needed to create the chemical elements. The nuclei up to mass 44 or 48 were said to be synthesized by reactions initiated by alpha particles, the alpha particles themselves being liberated from  $\text{Ne}^{20}$  by photodisintegration. This is the alpha process. The mass group from  $A = 50$  to 60, where  $A$  is the atomic weight, contributes a large peak to the curve of abundance versus  $A$ , and was attributed to the *equilibrium*, or *e*-process under conditions of high temperature (about  $10^9$  °K) and density (about  $10^5$  gm/cm<sup>3</sup>). According to BBFH, these nuclei, especially  $\text{Fe}^{56}$ , then served as seeds for growing the more massive nuclei by neutron capture or, in rare cases, by proton capture or the photo-ejection of neutrons. These rare reactions were collectively termed the *p*-process.

Two neutron-capture schemes were postulated. In one, the time interval between successive captures was taken to be long compared to the half life of most of the radioactive nuclei which were produced. Here, beta decay generally preceded further neutron capture, the stable nuclei which resulted were close to the valley of nuclear stability, and nuclear species up to  $\text{Bi}^{209}$  could be formed. Capture of neutrons by  $\text{Bi}^{209}$  leads to alpha and beta activity which, on the slow time scale being discussed, causes cycling between  $\text{Pb}^{206}$  and  $\text{Bi}^{209}$ . This *s*-process was said to take place in the red giant phase of stellar evolution.

The second neutron-capture process was introduced to account for the existence of trans-bismuth elements and of others which, because of intervening radioactive nuclei of short half life, could not be made on a slow time scale. In the rapid, or *r*-process, a flood of neutrons is released so rapidly that all radioactive nuclei are capable of capturing further neutrons before decaying. The addition of neutrons ceases only when the neutron-binding energy falls to such an extent that photo-neutron processes compete with the radiative capture of the neutrons. When this condition is reached, beta decay takes place and neutron capture is once again possible. Sufficient neutrons for the *r*-process to be effective are set free during a supernova explosion. The stellar matter is dispersed after a brief, if intense, irradiation, and any beta-active nuclei later decay to their first stable or long-lived isobars, perhaps with some modification in abundance due to the emission and capture of delayed neutrons, fission, photo processes, and similar events. The *p*-process was also said to occur during a supernova explosion.

In accounting for the nuclear species of the solar system, it is fairly clear that the foregoing processes could not have taken place in a simple sequence of events in stars which may have been predecessors to the sun. For example, the *s*-process

depends on the prior creation of  $e$ - and  $\alpha$ -products, but these occur subsequent in time to the  $s$ -process. In addition, it is to be expected that the  $r$ -process, acting upon  $s$ -products, will markedly alter the abundance distribution which the latter alone would produce. Similarly, any  $r$ -products subjected to the  $s$ -process will undergo a drastic change of character. An identical remark applies to  $e$ -matter which later passes through an intense neutron flux. As a result, it seems necessary to accept the idea that the  $\alpha$ -,  $e$ -,  $s$ -, and  $r$ -products in the solar system came from different stars and happened to mix before the creation of the sun and planets. Details of this argument will be given below.

It is also important to recognize that the processes employed by BBFH are not the only ones that have been examined in efforts to explain the abundance of the nuclear species. As we will see, other investigators approach the problem from different points of view.

## § 2. NUCLEAR ABUNDANCES

A major purpose of the calculations based on the foregoing processes is to reproduce the observed abundance distribution of the nuclear species. Suess and Urey (1956, 1958) have provided a valuable summary of the data, as has Aller (1961). The emphasis in the SU papers was on solar system matter, but reference was made also to stars and planetary nebulae. Aller emphasized the astrophysical data. Some data from the sun's atmosphere were included by SU, but the bulk of the information was taken from studies of chondritic meteorites. In certain cases the meteoritic and solar values were quite different. Presumably the elements in the sun's atmosphere are representative of those out of which the solar system condensed, since, except for minor modifications due to surface reactions and surface-interior mixing, whatever changes have taken place in the sun's elements have been restricted to the core. It is, therefore, a matter of concern that meteoritic abundances seem not to be always the same as those in the sun. For example, the solar abundance of iron, relative to silicon, (Goldberg, Müller, and Aller 1960) is only 20 per cent of that for meteorites (SU 1958). Aller (1962) remarks that diffusion may influence surface abundances in very old stars, although possibly not as much as indicated by Aller and Chapman (1960).

So far as volatile substances go, and these include various chemical compounds, it is easy to understand why the earth and meteorites should be deficient as compared with the sun (Urey 1954). Moreover, the crust of the earth cannot be regarded as a reliable source of information about original matter because the crust is not even typical of the earth as a whole, and both physical and chemical processes have altered the crustal composition from its primordial nature (Vinoogradov 1958). What is more puzzling is that *isotopic* abundance ratios may not be the same on the earth and in the sun, the important case of carbon offering a good example of this. For terrestrial and meteoritic matter, the ratio of  $C^{12}/C^{13}$  is 89 (SU 1958); the atmosphere of Venus shows the same ratio (Kuiper 1962).

In the sun,  $C^{13}$  has not been seen, and limits on the ratio  $C^{12}/C^{13}$  have been given as 15 (McKellar 1948), 35 (Greenstein, Richardson, and Schwarzschild 1950), and  $10^4$  (Righini 1956). If one takes Righini's data at face value, the discrepancy in  $C^{12}/C^{13}$  between the sun and the earth is large. Fowler, Greenstein, and Hoyle (1962), using theoretical arguments to be reviewed below, find that the sun should be devoid of  $C^{13}$ , consistent with Righini's work. However, on the observational side, Righini's result has been questioned by Climenhaga (1960) and Aller (1961). Hopefully this situation will be re-examined in the near future with improved facilities. For stars in which the carbon cycle has reached equilibrium, the  $C^{12}/C^{13}$  ratio should be 4.6 (BBFH) when the hydrogen abundance exceeds the carbon abundance.

Of the meteorites which have been examined for abundances, SU selected the chondrites as being the most reliable sources of data. Chondrites appear to be fairly complete mixtures of the several phases in which matter has condensed in meteorites, although it is now well known that chondrites do differ in composition. Suess and Urey occasionally revised the measured abundances because of chemical properties, assumptions about evaporative losses, comparison with astronomical results, and the supposition that the abundances of even- $A$  and odd- $A$  nuclei should vary smoothly with  $A$  but along separate curves. Data which have been acquired since 1958 indicate that a number of element abundances vary from meteorite to meteorite. For example, DuFresne (1960) studied sulfur, selenium, and tellurium in 22 chondrites. The extreme variations were a factor of 40 in sulfur content, a factor of 3 in selenium, and a factor of 13 for tellurium. Now SU (1956) noted that sulfur is apt to be lost as  $H_2S$  and other gases more readily than Se, but DuFresne, commenting that the above variations were not correlated with each other, concluded that the chondrites are not reliable indicators of the primitive abundances of these chemically similar elements. DuFresne suggests further that the chondrites may not be reliable for other elements either. (See also Middlehurst and Kuiper 1963, chaps. 12–14.) Merz (1962) found the Zr/Hf ratio to vary by a factor of two for chondrites. Tin varies from less than 0.07 to 1.09 ppm in chondrites (Shima 1964).

In addition to such variations, the application of new experimental methods has led to changes in certain of the abundances given by SU (1958). One instance is that of indium for which Schindewolf and Wahlgren (1960) found a value not greater than one per cent of the SU listing, reminiscent of the earlier work by Shaw (1952). Column 1 of Table 1 lists the observed abundances as compiled by SU and modified by recent data. The abundances are relative to silicon =  $10^6$ . The data are plotted in Figures 1 and 2. Column 2 of Table 1 lists the solar abundances (GMA). It should be emphasized that the abundances are subject to further revision.

Of course, nuclear, rather than chemical, abundances are of primary concern, but non-terrestrial data on isotopic ratios are virtually non-existent. McKellar (1960) summarized the information on isotopes in stars. Only for the case of

TABLE 1  
RELATIVE ABUNDANCE OF STABLE NUCLEAR SPECIES

ELEMENT	A	SU 1958	CAMERON 1959 <sup>c</sup>	CFHZ 1961 CF 1961	GMA 1960	OTHERS		CF 1961	
						Abundance	Refer- ences*	s	r
1. H.....	1	3.2 × 10 <sup>10</sup>	2.50 × 10 <sup>10</sup>	.....	3.16 × 10 <sup>0</sup>	.....	.....	.....	.....
	2	3.2 × 10 <sup>10</sup>	2.50 × 10 <sup>10</sup>	.....	.....	.....	.....	.....	.....
2. He.....	3	4.5 × 10 <sup>6</sup>	3.56 × 10 <sup>6</sup>	.....	.....	D/H < 1/13,000	18	.....	.....
	4	.....	3.80 × 10 <sup>9</sup>	.....	.....	.....	.....	.....	.....
		.....	10 <sup>6</sup>	.....	.....	.....	.....	.....	.....
3. Li.....	6	4.1 × 10 <sup>6</sup>	3.80 × 10 <sup>9</sup>	.....	.....	.....	.....	.....	.....
	7	100	100	.....	0.29	.....	.....	.....	.....
		7.4	7.4	.....	.....	.....	.....	.....	.....
4. Be.....	9	92.6	92.6	.....	.....	3	14	.....	.....
5. B.....	10	20	20	.....	6.30	33	14	.....	.....
		24	24	.....	.....	1	17	.....	.....
	10	4.5	4.5	.....	.....	.....	.....	.....	.....
	11	19.5	19.5	.....	1.7 × 10 <sup>7</sup>	1.6	14	.....	.....
6. C.....	12	1.1 × 10 <sup>7</sup>	9.3 × 10 <sup>6</sup>	.....	.....	6.1	14	.....	.....
	13	1.09 × 10 <sup>7</sup>	.....	.....	.....	.....	.....	.....	.....
		1.22 × 10 <sup>6</sup>	.....	.....	.....	.....	.....	.....	.....
7. N.....	14	3.0 × 10 <sup>6</sup>	2.4 × 10 <sup>6</sup>	.....	3.0 × 10 <sup>6</sup>	.....	.....	.....	.....
	15	2.99 × 10 <sup>6</sup>	2.39 × 10 <sup>6</sup>	.....	.....	.....	.....	.....	.....
		1.1 × 10 <sup>4</sup>	8750	.....	.....	.....	.....	.....	.....

\* The references are as follows:

1. Vinogradov *et al.* (1960).
2. Stauffer (1961).
3. DuFresne (1960).
4. Reed *et al.* (1960).
5. Bate *et al.* (1960).
6. Fleisch *et al.* (1960).
7. Schindewolf and Wahlgren (1960).
8. Hara and Sandell (1960).
9. Schmitt *et al.* (1960).
10. Helliwell (1961).
11. Fowler's revised ratio of  $r$  to  $s$  contributions (see Macklin *et al.* 1962).
12. Rushbrook and Elmann (1962).
13. Bate, quoted in reference 12.
14. Shima (1962).
15. Stauffer and Honda 1962 (terrestrial samples).
16. White, Collins, and Rourke (1956).
17. Sill and Willis (1962).
18. Weinreb 1962 (interstellar ratio).
19. Schindewolf (1960).



TABLE 1—Continued

ELEMENT	A	SU 1958	CAMERON 1959c	CFHZ 1961 CF 1961	GMA 1960	OTHERS		CF 1961	
						Abundance	Refer- ences*	s	r
8. O.....	16	$3.1 \times 10^7$	$2.5 \times 10^7$	.....	$2.9 \times 10^7$	$O^{16}/O^{18}=490$	1	.....	.....
	17	$3.08 \times 10^7$	$2.49 \times 10^7$	.....	.....	.....	.....	.....	.....
	18	$1.16 \times 10^4$	9340	.....	.....	.....	.....	.....	.....
	19	$6.32 \times 10^4$	$5.10 \times 10^4$	.....	.....	.....	.....	.....	.....
9. F.....	19	1600	1600	.....	.....	.....	.....	.....	.....
10. Ne.....	20	$8.6 \times 10^6$	$8.0 \times 10^6$	.....	.....	.....	.....	.....	.....
	21	$7.74 \times 10^6$	$7.20 \times 10^6$	.....	.....	.....	.....	.....	.....
	22	$2.58 \times 10^4$	2400	.....	.....	.....	.....	.....	.....
	23	$8.36 \times 10^6$	$7.78 \times 10^4$	.....	.....	.....	.....	.....	.....
11. Na.....	22	$4.38 \times 10^4$	$4.38 \times 10^4$	.....	$6.3 \times 10^4$	$Ne^{20}/Ne^{22}=1 \text{ to } 12$	2	.....	.....
	23	$9.12 \times 10^6$	$9.12 \times 10^6$	.....	$7.9 \times 10^6$	$Ne^{21}/Ne^{22}=0.2 \text{ to } .9$	2	.....	.....
	24	$7.21 \times 10^6$	$7.21 \times 10^6$	.....	.....	.....	.....	.....	.....
	25	$9.17 \times 10^4$	$9.17 \times 10^4$	.....	.....	.....	.....	.....	.....
13. Al.....	26	$1.00 \times 10^6$	$1.00 \times 10^6$	.....	.....	.....	.....	.....	.....
	27	$9.48 \times 10^4$	$9.48 \times 10^4$	.....	$5.0 \times 10^4$	.....	.....	.....	.....
	28	$1.00 \times 10^6$	$1.00 \times 10^6$	.....	$1.00 \times 10^6$	.....	.....	.....	.....
	29	$9.22 \times 10^6$	$9.22 \times 10^6$	.....	.....	.....	.....	.....	.....
15. P.....	30	$4.70 \times 10^4$	$4.70 \times 10^4$	.....	.....	.....	.....	.....	.....
	31	$3.12 \times 10^4$	$3.12 \times 10^4$	.....	.....	.....	.....	.....	.....
	31	$1.00 \times 10^4$	$1.00 \times 10^4$	.....	$6.9 \times 10^3$	$3.39 \times 10^3 \text{ to } 1.36 \times 10^5$	3	.....	.....
	31	$3.75 \times 10^6$	$3.75 \times 10^6$	.....	$6.3 \times 10^6$	.....	.....	.....	.....
16. S.....	32	$3.56 \times 10^6$	$3.56 \times 10^6$	.....	.....	.....	.....	.....	.....
	33	$2.77 \times 10^3$	$2.77 \times 10^3$	.....	.....	.....	.....	.....	.....
	34	$1.57 \times 10^4$	$1.57 \times 10^4$	.....	.....	.....	.....	.....	.....
	36	51	51	.....	.....	.....	.....	.....	.....
17. Cl.....	36	8850	2610	.....	.....	.....	.....	.....	.....
	35	6670	1970	.....	.....	.....	.....	.....	.....
	37	2180	640	.....	.....	.....	.....	.....	.....
	37	.....	.....	.....	.....	.....	.....	.....	.....

TABLE 1—Continued

ELEMENT	A	SU 1958	CAMERON 1959c	CFHZ 1961 CF 1961	GMA 1960	OTHERS		CF 1961	
						Abundance	Refer- ences*	s	r
18. Ar.....									
	36	$1.50 \times 10^5$	$1.5 \times 10^5$						
	38	$1.26 \times 10^5$	$1.26 \times 10^5$						
	40	$2.4 \times 10^4$	$2.4 \times 10^4$						
19. K.....									
	39	3160	3160		$1.6 \times 10^3$	3280	4		
	40	2940	2940						
	41	0.38	0.38						
20. Ca.....									
	40	219	219		$4.5 \times 10^4$	$6.9 \times 10^4$	4		
	42	$4.90 \times 10^4$	$4.90 \times 10^4$			$40/44 = 46.8$	15		
	43	$4.75 \times 10^4$	$4.75 \times 10^4$			$42/44 = 0.314$	15		
	44	314	314			$43/44 = 0.641$	15		
	46	64	64						
	44	1040	1040						
	46	1.6	1.6			$46/44 = 0.00152$	15		
	48	87.7	87.7			$48/44 = 0.0893$	15		
21. Sc.....	45	28	28		21	32	5		
22. Ti.....					1500				
	46	2440	1680						
	47	194	134						
	47	189	130						
	48	1790	1230						
	49	134	92.2						
	50	130	89.5						
23. V.....									
	50	220	220		160				
	51	0.55	0.55						
24. Cr.....									
	50	220	220			$51/50 = 398$ and	16		
	52	7800	7800		7200	404	15		
	53	344	344			6400	5		
	54	6510	6510			$4.352\%$	6		
		744	744			83.764	6		
		204	204			9.509	6		
						2.375	6		

TABLE 1—Continued

ELEMENT	A	SU 1958	CAMERON 1959c	CFHZ 1961 CF 1961	GMA 1960	OTHERS		CF 1961	
						Abundance	Refer- ences*	s	r
25. Mn.....	55	6850	6850	.....	2300	.....	.....	.....	.....
26. Fe.....	54	6.00×10 <sup>5</sup>	8.50×10 <sup>4</sup>	.....	1.2 ×10 <sup>5</sup>	.....	.....	.....	.....
	56	3.54×10 <sup>4</sup>	5010	.....	.....	.....	.....	.....	.....
	57	5.49×10 <sup>5</sup>	7.76×10 <sup>4</sup>	.....	.....	.....	.....	.....	.....
	58	1.35×10 <sup>4</sup>	1910	.....	.....	.....	.....	.....	.....
	59	1.98×10 <sup>3</sup>	280	.....	.....	.....	.....	.....	.....
27. Co.....	59	1800	1800	.....	1380	.....	.....	.....	.....
28. Ni.....	58	2.74×10 <sup>4</sup>	2.74×10 <sup>4</sup>	.....	2.57×10 <sup>4</sup>	.....	.....	.....	.....
	60	1.86×10 <sup>4</sup>	1.86×10 <sup>4</sup>	.....	.....	.....	.....	.....	.....
	61	7170	7170	.....	.....	.....	.....	.....	.....
	62	342	342	.....	.....	.....	.....	.....	.....
	64	1000	1000	.....	.....	.....	.....	.....	.....
	64	318	318	.....	.....	.....	.....	.....	.....
	63	212	212	.....	.....	.....	.....	.....	.....
29. Cu.....	63	146	146	.....	3470	.....	.....	296	20
	65	66	66	.....	.....	.....	.....	146	10
	64	486	202	.....	.....	.....	.....	150	10
30. Zn.....	64	238	119	.....	790	.....	.....	320	40
	66	134	67	.....	.....	.....	.....	80	10
	67	20.0	10	.....	.....	.....	.....	125	10
	68	90.9	45.6	.....	.....	.....	.....	24	10
	70	3.35	1.68	.....	.....	.....	.....	91	10
31. Ga.....	69	11.4	9.05	.....	7.2	.....	.....	.....	.....
	71	6.86	5.45	.....	.....	.....	.....	21.5	11
	71	4.54	3.60	.....	.....	.....	.....	11	10
	70	50.5	25.3	.....	61.7	.....	.....	10.5	0.88
32. Ge.....	70	10.4	5.20	.....	.....	.....	.....	45.6	3.52
	72	13.8	6.90	.....	.....	.....	.....	10	.....
	73	3.84	1.92	.....	.....	.....	.....	13.2	0.88
	74	18.65	9.32	.....	.....	.....	.....	39	0.88
	76	3.87	1.94	.....	.....	.....	.....	18.5	0.88
				.....	.....	.....	.....	.....	0.88

† Shima (1963) has found the Ge isotopic abundances to be the same in meteorites and terrestrial matter.

TABLE 1—Continued

ELEMENT	A	SU 1958	CAMERON 1959c	CFHZ 1961 CF 1961	GMA 1960	OTHERS		CF 1961	
						Abundance	Refer- ences*	s	r
33. As.....	75	4.0	1.70	18.8		18.8	19	1.30	0.88
34. Se.....	74	67.6	0.181	0.18		10.2 to 29.1	3	7.4	23.5
	76	0.649	1.71	1.7				2.7	
	77	6.16	1.41	1.4				1.2	0.88
	78	5.07	4.45	4.4				2.0	1.44
	80	16.0	9.40	9.44				1.5	17.0
	82	33.8	1.66	1.7				4.2	4.2
		5.98	3.95					1.5	5.45
35. Br.....	79	13.4	2.00					0.8	1.25
	81	6.78	1.95					0.73	4.2
		6.62	42.0					2.6	15.3
	78	51.3	0.142						
36. Kr.....	80	0.175	0.14						
	82	1.14	0.928					1.1	
	83	5.90	4.80					0.55	4.2
	84	5.89	4.80					1.0	9.7
	86	29.3	23.90						
		8.94	7.28						
37. Rb.....		6.5	6.50	4.4		4.96	4	1.54	1.35
	85	4.73	4.73	3.2	9.6			1.54	2.70
	87	1.77	1.77	1.2				1.54	1.35
		18.9	61.0	18.9	12.6			16.2	1.35
38. Sr.....	84	0.106	0.342	0.11				1.86	
	86	1.86	6.00	1.85				1.26	
	87	1.33	4.30	1.32				13.1	1.35
	88	15.6	50.4	15.6				10.0	1.35
39. Y.....	89	8.9	8.9	8.9	5.6			35.3	4.5
40. Zr.....		54.5	14.2	21.8	5.4			20.0	0.9
	90	28.0	7.32	11.2				4.1	0.9
	91	6.12	1.60	2.4				5.8	0.9
	92	9.32	2.44	3.7				5.4	0.9
	94	9.48	2.48	3.8					0.9
	96	1.53	0.400	0.61					0.9
41. Nb.....	93	1.00	0.81		2.8			2.6	0.9

TABLE 1—Continued

ELEMENT	A	SU 1958	CAMERON 1959c	CFHZ 1961 CF 1961	GMA 1960	OTHERS		CF 1961	
						Abundance	Refer- ences*	s	r
42. Mo.....	92	2.42	2.42	.....	2.5	.....	.....	1.68	1.09
	94	0.364	0.364	.....	.....	.....	.....	.....	.....
	96	0.226	0.226	.....	.....	.....	.....	0.54	0.9
	95	0.382	0.382	.....	.....	.....	.....	0.53	.....
	96	0.401	0.401	.....	.....	.....	.....	0.28	0.063
	97	0.232	0.232	.....	.....	.....	.....	0.33	0.063
	98	0.581	0.581	.....	.....	.....	.....	.....	0.063
44. Ru.....	100	0.234	0.234	.....	0.85	.....	.....	0.57	0.26
	96	1.49	0.87	.....	.....	1.5	8	.....	.....
	98	0.0846	0.0452	.....	.....	.....	.....	.....	.....
	99	0.0321	0.0177	.....	.....	.....	.....	0.14	0.063
	100	0.191	0.112	.....	.....	.....	.....	0.17	.....
	101	0.189	0.111	.....	.....	.....	.....	0.077	0.063
	102	0.253	0.149	.....	.....	.....	.....	0.18	0.067
45. Rh.....	103	0.467	0.275	.....	.....	.....	.....	.....	0.067
	104	0.272	0.160	.....	.....	0.27	9	0.065	0.067
	105	0.214	0.15	0.27	0.19	.....	.....	0.415	0.186
	106	0.675	0.675	0.675	0.512	.....	.....	.....	.....
	107	0.0054	0.0054	.....	.....	.....	.....	0.135	.....
	108	0.0628	0.0628	.....	.....	.....	.....	0.065	0.067
	109	0.136	0.136	.....	.....	.....	.....	0.115	0.029
47. Ag.....	110	0.1839	0.1839	.....	.....	.....	.....	0.10	0.029
	111	0.180	0.180	.....	.....	.....	.....	0.108	0.023
	112	0.0911	0.0911	.....	0.044	0.131	9	0.055	0.058
	113	0.26	0.26	0.13	.....	.....	.....	0.053	0.029
	114	0.134	0.134	0.067	.....	.....	.....	0.659	0.115
	115	0.126	0.126	0.063	.....	.....	.....	.....	.....
	116	0.89	0.89	.....	0.91	.....	.....	.....	.....
48. Cd.....	117	0.0109	0.0109	.....	.....	.....	.....	.....	.....
	118	0.0079	0.0079	.....	.....	.....	.....	0.151	.....
	119	0.111	0.111	.....	.....	.....	.....	0.074	0.023
	120	0.114	0.114	.....	.....	.....	.....	0.145	0.023
	121	0.212	0.212	.....	.....	.....	.....	0.067	0.023
	122	0.110	0.110	.....	.....	.....	.....	0.152	0.023
	123	0.256	0.256	.....	.....	.....	.....	.....	0.023

TABLE 1—Continued

ELEMENT	A	SU 1958	CAMERON 1959c	CFHZ 1961 CF 1961	GMA 1960	OTHERS		CF 1961	
						Abundance	Refer- ences*	s	r
49. In.....	113	0.11	0.11	.....	0.46	0.0013	9	0.048	0.023
	115	0.0046	0.0046	.....	.....	0.000046	9	.....	.....
50. Sn.....	112	0.105	0.105	.....	1.10	0.00105	9	0.048	0.023
	114	1.33	.....	.....	.....	.....	.....	1.72	0.16
	116	0.0134	.....	.....	.....	.....	.....	.....	.....
	117	0.0090	.....	.....	.....	.....	.....	.....	.....
	118	0.00465	.....	.....	.....	.....	.....	.....	.....
	119	0.189	.....	.....	.....	.....	.....	.....	.....
	120	0.102	.....	.....	.....	.....	.....	.....	.....
	121	0.316	.....	.....	.....	.....	.....	.....	.....
	122	0.115	.....	.....	.....	.....	.....	.....	.....
	123	0.433	.....	.....	.....	.....	.....	.....	.....
	124	0.063	.....	.....	.....	.....	.....	.....	.....
51. Sb.....	121	0.079	.....	.....	.....	.....	.....	.....	.....
	122	0.246	0.227	.....	2.75	.....	.....	.....	.....
	123	0.141	0.130	.....	.....	.....	.....	0.304	0.012
	124	0.105	0.090	.....	.....	.....	.....	0.158	0.012
	125	4.67	2.91	1.83	.....	.....	.....	0.482	0.012
52. Te.....	120	0.00420	0.00262	0.0018	.....	0.28 to 3.8	3	0.608	0.018
	121	0.115	0.0712	0.045	.....	0.73	19	.....	0.084
	122	0.0416	0.0260	0.016	.....	.....	.....	0.040	0.051
	123	0.221	0.138	0.085	.....	.....	.....	0.040	0.018
	124	0.328	0.205	0.13	.....	.....	.....	.....	.....
	125	0.874	0.544	0.34	.....	.....	.....	.....	.....
	126	1.48	0.925	0.58	.....	.....	.....	0.091	0.070
	127	1.60	1.000	0.63	.....	.....	.....	0.018	0.20
	128	0.80	0.60	0.23	.....	.....	.....	0.130	0.59
53. I.....	130	.....	.....	.....	.....	.....	.....	.....	0.69
	131	.....	.....	.....	.....	.....	.....	0.038	0.17

TABLE 1—Continued

ELEMENT	A	SU 1958	CAMERON 1959c	CFHZ 1961 CF 1961	GMA 1960	OTHERS		CF 1961	
						Abundance	Refer- ences*	s	r
54. Xe.....	124	4.0	3.35	1.6	.....	.....	.....	0.477	2.13
	126	0.00380	0.00320	0.0016	.....	.....	.....	.....	.....
	128	0.00352	0.00296	0.0016	.....	.....	.....	0.066	.....
	129	0.0764	0.0640	0.030	.....	.....	.....	0.029	0.47
	130	1.050	0.880	0.42	.....	.....	.....	0.132	.....
	131	0.162	0.136	0.064	.....	.....	.....	0.060	0.69
	132	0.850	0.712	0.34	.....	.....	.....	0.190	0.69
	133	0.850	0.904	0.43	.....	.....	.....	.....	0.10
	134	1.078	0.420	0.17	.....	.....	.....	.....	0.18
	136	0.420	0.352	0.14	.....	.....	.....	0.032	0.10
	137	0.358	0.300	0.069	.....	.....	.....	3.22	0.46
	138	0.456	0.456	.....	3.98	3.75	4†	.....	.....
55. Cs.....	130	3.66	3.66	.....	.....	.....	.....	.....	.....
	132	0.00370	0.00370	.....	.....	.....	.....	0.083	.....
	134	0.00356	0.00356	.....	.....	.....	.....	0.226	0.10
	135	0.0886	0.0886	.....	.....	.....	.....	0.257	.....
	136	0.241	0.241	.....	.....	.....	.....	0.371	0.18
	137	0.286	0.286	.....	.....	.....	.....	2.28	0.18
	138	0.414	0.414	.....	.....	.....	.....	0.52	0.18
57. La.....	138	2.622	2.622	0.40 (exp)	.....	0.40	9	.....	.....
	139	2.000	0.50	0.0004	.....	.....	.....	0.52	0.18
	139	0.0018	0.00045	0.40	.....	.....	.....	0.81	0.36
58. Ce.....	136	2.00	0.575	0.62	.....	.....	.....	.....	.....
	138	2.26	0.0044	0.0012	.....	.....	.....	.....	.....
	140	0.00506	0.00144	0.0016	.....	.....	.....	0.81	0.18
	142	2.00	0.509	0.55	.....	.....	.....	.....	.....
	141	0.250	0.063	0.069	.....	0.068	9	0.154	0.022
59. Pr.....	141	0.40	0.23	0.15	.....	0.14	9	.....	.....

† Ba values for meteorites given by Moore and Brown (1963) vary widely from sample to sample and from other authors.



TABLE 1—Continued

ELEMENT	A	SU 1958	CAMERON 1959 <sup>c</sup>	CFHZ 1961 CF 1961	GMA 1960	OTHERS		CF 1961	
						Abundance	Refer- ences*	s	r
60. Nd.....	142	1.44	0.874	0.74	.....	.....	.....	0.531	0.246
	143	0.39	.238	.20	.....	.....	.....	.167	.....
	144	0.175	.106	.090	.....	.....	.....	.072	.022
	145	0.344	.209	.18	.....	.....	.....	.141	.022
	146	0.119	.0725	.061	.....	.....	.....	.049	.022
	147	0.248	.150	.13	.....	.....	.....	.102	.069
	148	0.0824	.0498	.042	.....	0.12	9	.....	.069
	149	0.0806	.0490	.041	.....	.....	.....	.....	.042
	150	0.664	.238	.25	.....	.....	.....	0.346	.249
	151	0.0108	.00386	.004	.....	.....	.....	.....	.....
62. Sm.....	144	0.100	.0480	.038	.....	.....	.....	.075	.069
	147	0.0748	.0358	.028	.....	.....	.....	.113	.....
	148	0.0920	.0442	.035	.....	.....	.....	.049	.042
	149	0.0492	.0248	.018	.....	.....	.....	.071	.....
	150	0.176	.0857	.066	.....	0.065	9	.038	.069
	152	0.150	.0726	.056	.....	.....	.....	.....	.069
	154	0.187	.115	.096	.....	0.078(5), 0.045	9	.038	.111
	151	0.0892	.0550	.046	.....	.....	.....	.029	.042
	153	0.0976	.0600	.050	.....	.....	.....	.009	.069
	154	0.684	.516	.36	.....	.....	.....	.126	.284
63. Eu.....	152	0.00137	.00103	.0007	.....	.....	.....	.....	.....
	154	0.0147	.0111	.008	.....	.....	.....	.032	.....
	155	0.101	.0755	.053	.....	.....	.....	.015	.046
	156	0.141	.1055	.074	.....	.....	.....	.032	.046
64. Gd.....	157	0.107	.0810	.056	.....	.....	.....	.015	.046
	158	0.169	.128	.089	.....	0.083	9	.032	.073
	160	0.149	.113	.079	.....	0.086	9	.....	.073
	159	0.0956	.090	.055	.....	0.055	9	0.010	0.073
	159	.....	.....	.....	.....	.....	.....	.....	.....
	159	.....	.....	.....	.....	.....	.....	.....	.....
	159	.....	.....	.....	.....	.....	.....	.....	.....

TABLE 1—Continued

ELEMENT	A	SU 1958	CAMERON 1959c	CFHZ 1961 CF 1961	GMA 1960	OTHERS		CF 1961	
						Abundance	Refer- ences*	s	r
66. Dy.....	156	0.556	0.665	0.39				0.224	0.449
	158	.00029	.00035	.0002					
	160	.000502	.00060	.0004					
	161	.0127	.0152	.0089				.051	.050
	162	.105	.107	.074				.058	.050
	163	.142	.170	.100				.026	.050
	164	.139	.166	.100				.067	.074
	165	.157	.188	.11				.010	.074
	166	.118	.180	.078			9	.127	.232
	167	.316	.583	.21			9		
67. Ho.....	162	.000316	.000583	.0002					
	164	.00474	.00875	.0031				.044	.074
	166	.104	.192	.069				.022	.046
	167	.0991	.132	.051				.061	.046
	168	.0850	.156	.057			9		
	170	.0228	.0855	.029			9		
	169	.0318	.090	.039			9	.014	.066
	168	.220	.393	.19	1.07			.174	.213
	170	.00030	.000535	.0003			9		
	171	.00666	.0119	.0058				.009	
69. Tm.....	171	.0316	.0560	.027				.022	.066
	172	.0480	.0750	.042				.045	.066
	173	.0356	.0635	.031				.034	.027
	174	.0678	.125	.059			9	.064	.027
	176	.0278	.050	.024					.027
	175	.050	.0358	.037				.0076	.027
	176	.0488	.0350	.036			9	0.0076	0.027
	176	0.0013	0.00093	0.001			9		
	175					.034			
	176					0.00095			
71. Lu.....	175						9		
	176						9		

TABLE 1—Continued

ELEMENT	A	SU 1958	CAMERON 1959c	CFHZ 1961 CF 1961	GMA 1960	OTHERS		CF 1961	
						Abundance	Refer- ences*	s	r
72. Hf.....	174	0.438	0.113	0.175	.....	.....	.....	0.167	0.069
	176	0.00078	.00020	.0003	.....	.....	.....	.....	.....
	177	0.0226	.00581	.0090	.....	.....	.....	.009	.....
	178	0.0806	.0211	.032	.....	.....	.....	.022	.027
	179	0.119	.0312	.048	.....	.....	.....	.048	.014
73. Ta.....	180	0.0604	.0158	.024	.....	.....	.....	.025	.014
	181	0.155	.0405	.062	.....	.....	.....	.063	.014
	182	0.065	.015	.026	.....	.....	.....	.016	.014
	183	0.49	.105	.20	.....	.....	.....	.128	.056
	184	0.0006	.00015	.0002	.....	.....	.....	.....	.....
74. W.....	185	0.13	.0278	.053	.....	.....	.....	.050	.014
	186	0.070	.0150	.029	.....	.....	.....	.018	.014
	187	0.15	.0322	.061	.....	.....	.....	.060	.014
	188	0.14	.0300	.057	.....	.....	.....	.....	.014
	189	0.135	.054	.054	.....	.....	.....	.008	.044
75. Re.....	190	0.0500	.0200	.020	.....	.....	.....	.008	.014
	191	0.0850	.0340	.034	.....	.....	.....	.008	.030
	192	1.00	.64	.40	.....	0.6	13	.063	.448
	193	0.00018	.000115	.00008	.....	.....	.....	.....	.....
	194	0.0159	.0102	.0064	.....	.....	.....	.007	.....
76. Os.....	195	0.0164	.0104	.0056	.....	.....	.....	.007	.....
	196	0.133	.0851	.053	.....	.....	.....	.014	.061
	197	0.161	.103	.064	.....	.1	13	.011	.056
	198	0.264	.169	.106	.....	.....	.....	.024	.103
	199	0.410	.262	.164	.....	.....	.....	.....	.228
77. Ir.....	200	0.821	.494	.328	.....	0.38	12	.063	.33
	201	0.316	.190	.126	.....	.....	.....	.021	.113
	202	0.505	.304	.202	.....	.....	.....	0.042	0.22
	203	.....	.....	.....	.....	.....	.....	.....	.....
	204	.....	.....	.....	.....	.....	.....	.....	.....

TABLE 1—Continued

ELEMENT	A	SU 1958	CAMERON 1959c	CPHZ 1961 CF 1961	GMA 1960	OTHERS		CF 1961	
						Abundance	Refer- ences*	s	r
78. Pt.....	190	1.625	1.28	0.650				0.209	0.59
	192	0.0001	0.00015	0.00007					
	194	0.0127	0.0100	0.0051				0.021	
	195	0.533	0.420	0.21				0.050	.35
	196	0.548	0.432	0.22				0.033	.11
	197	0.413	0.326	0.17				0.100	.11
	198	0.117	0.0923	0.047					.022
79. Au.....	197	0.145	0.145	0.058				0.019	.11
80. Hg.....	196	0.017	0.408	0.284				0.509	.11
	198	0.000027	0.00061	0.0005					
	199	0.0017	0.0408	0.0285				0.036	
	200	0.0029	0.0690	0.048				0.026	.022
	201	0.0040	0.0943	0.066				0.059	.022
	202	0.0022	0.0539	0.038				0.036	.022
	204	0.0051	0.122	0.084				0.352	.022
81. Tl.....	203	0.0012	0.0278	0.019		0.000297	4		.022
	205	0.0062	0.31	0.74				0.70	.044
	206	0.00183	0.095	0.22				0.20	.022
	207	0.00437	0.225	0.52				0.50	.022
	208	0.12	21.7	6.5	0.68	5.0 $^{+5.4}_{-1.7}$	10	5.6	.90
82. Pb.....	204	0.0023	0.321	0.13				0.13	
	206	0.022	5.10	1.2				0.95	.30
	207	0.024	4.89	1.3				0.93	.41
	208	0.068	11.35	3.7				3.59	.19
	209	0.078	0.300	0.92		0.0022	4	0.54	0.38
83. Bi.....	232	0.033	0.027						
90. Th.....	235	0.0178	0.0078			0.00071	4		
	238	0.0041	0.000056						
	238	0.0137	0.0078						

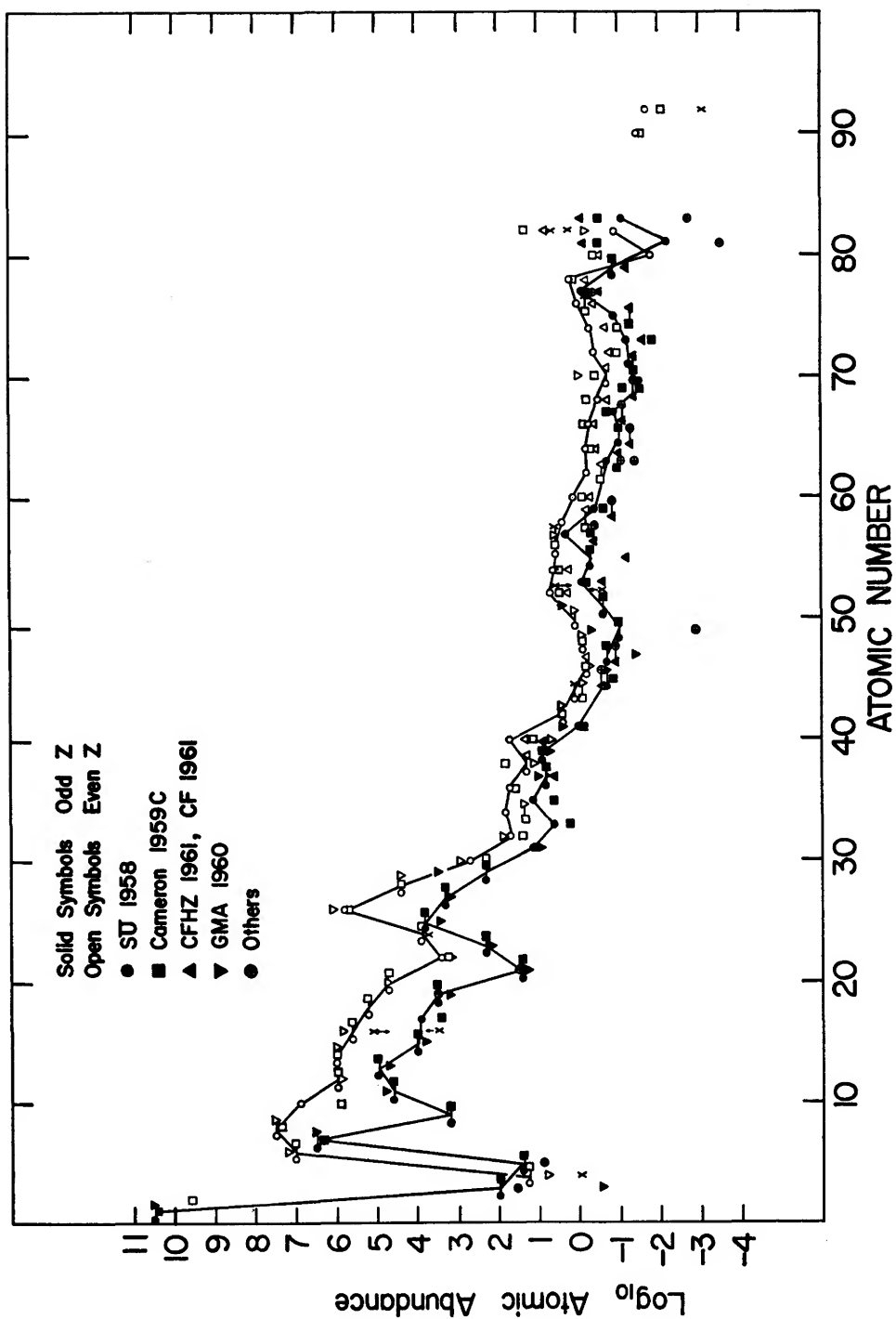


Fig. 1.—Log<sub>10</sub> of abundance *vs.* atomic number, relative to Si = 10<sup>6</sup>



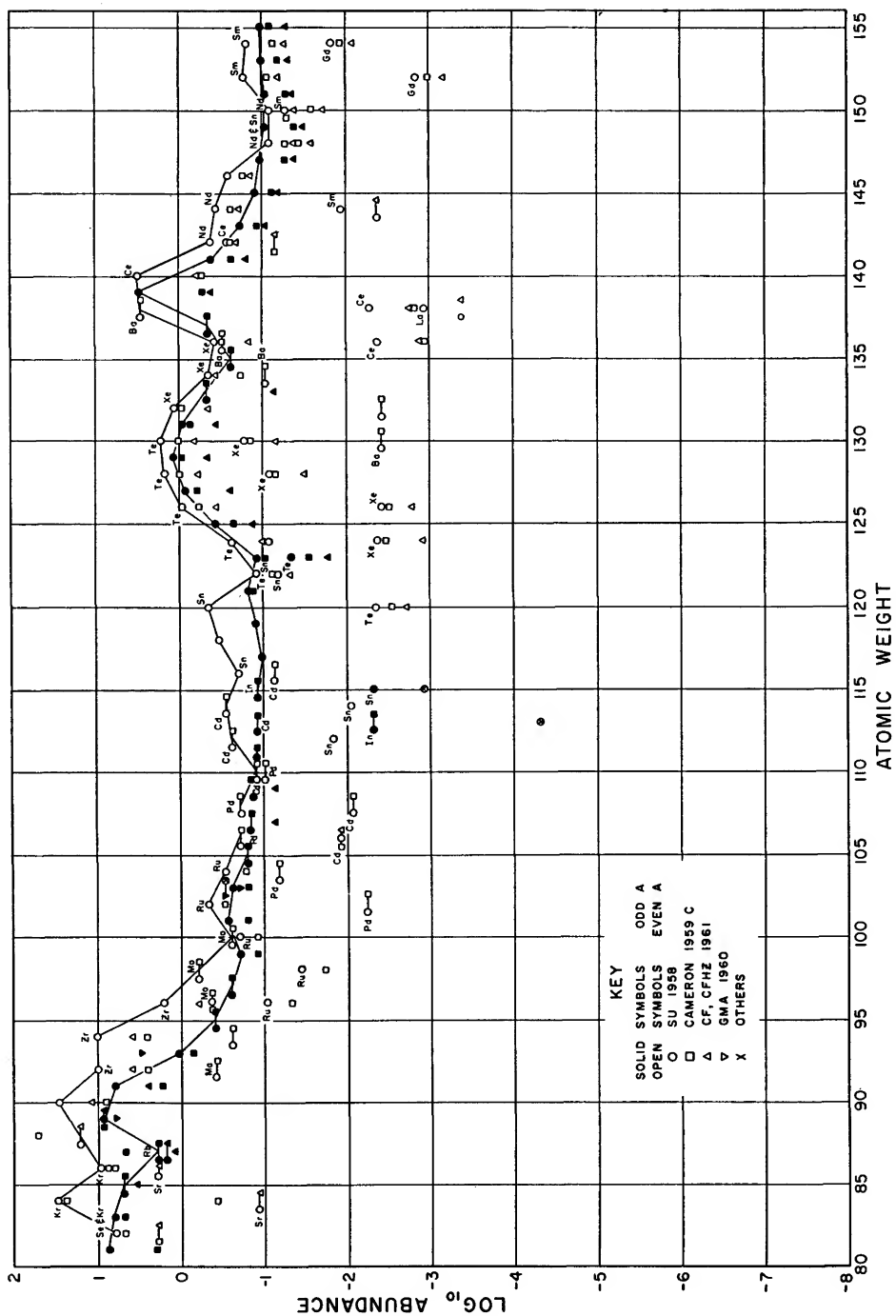


FIG. 2.—Continued

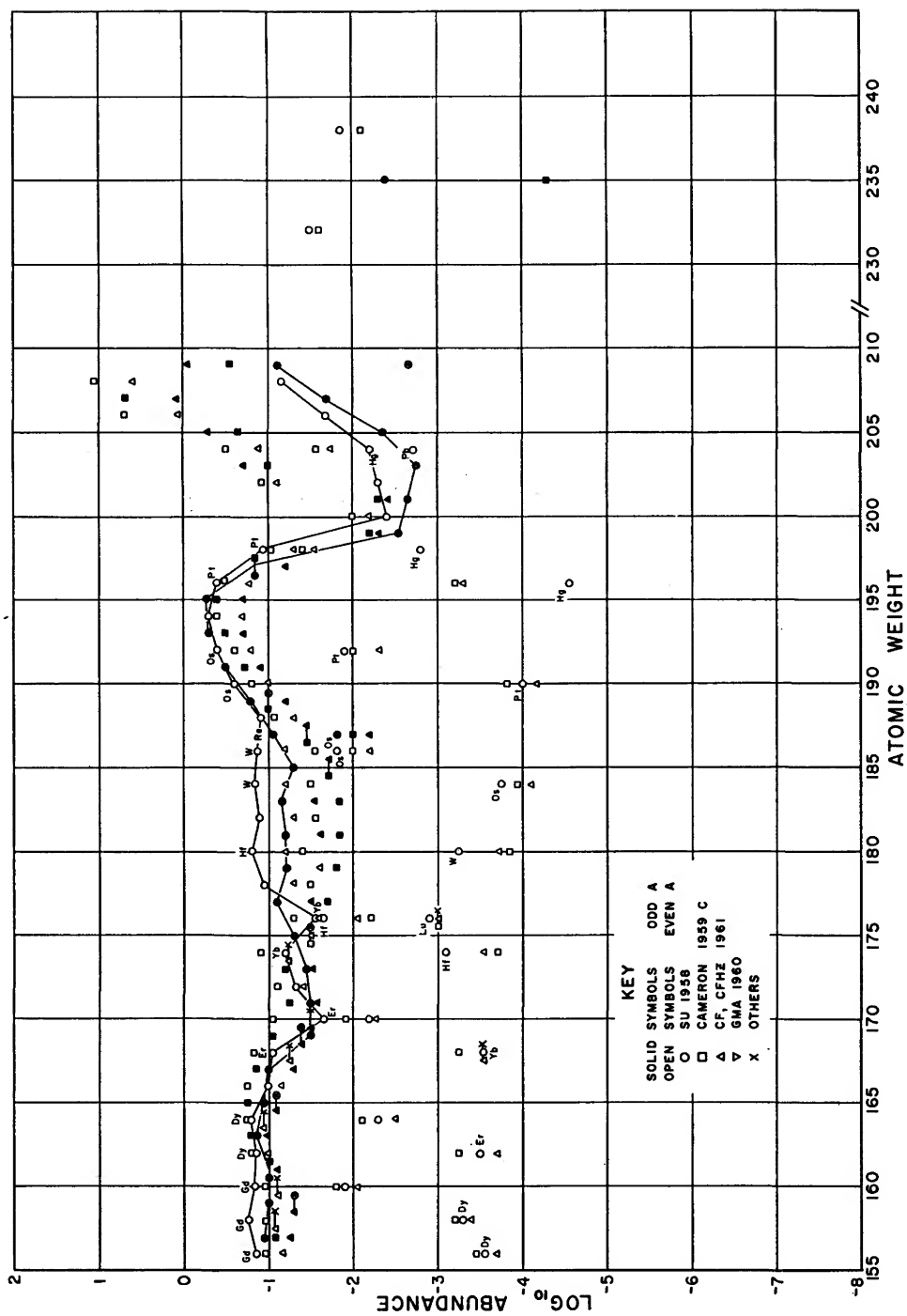


FIG. 2.—Continued



carbon is there any general, positive information on isotope abundances, the ratio  $C^{12}/C^{13}$  being anomalous, relative to the terrestrial ratio, for a number of R and N stars. The ratios in those stars seem to be variable from about 2 to 100. For example, Climenhaga (1960) found ratios from 4.7 to  $>100$  in various R and N stars. McKellar called attention to the uncertainties associated with the measurements, the major problems being that different observers do not always agree on the ratio and that bands in the blue-green and red spectral regions give different results. The  $C^{12}/C^{13}$  abundance ratio is presumably related to such nuclear developments as the carbon cycle. However, Bidelman (1961) has found that variations in the relative abundance of the carbon isotopes in some carbon stars deficient in hydrogen are unaccompanied by variations in the abundance of nitrogen, indicating that the carbon cycle has not been the only source of the carbon isotopes. Possibly Bidelman's result is connected with the fact that the  $C^{12}/C^{13}$  and C/N ratios depend on the number of available protons per  $C^{12}$  nucleus. It is interesting that R Coronae Borealis, a star deficient in hydrogen, is also lacking in  $C^{13}$  (Shajn and Hase 1954). Fowler (1962) states that if  $N_p \lesssim N_{C^{12}}$ , the CNO cycle can lead to  $C^{13}$  enhancement with little effect on the nitrogen abundance. Here  $N_p$  and  $N_{C^{12}}$  are hydrogen and  $C^{12}$  abundances, respectively.<sup>4</sup>

Herbig (1948) made a study of the titanium isotopes in nine giant and supergiant stars ranging in spectral class from K0 to M6. The bands of the TiO molecule were used. The relative abundances of the stellar titanium isotopes were not inconsistent with the terrestrial abundances, but the uncertainties in the data were large enough for quite serious deviations to have been undetectable.

Recently, Sargent and Jugaku (1961) established that  $He^3$  is highly overabundant in 3 Centauri A. Two He-rich stars were studied by Hill (1962) for possible  $He^3$  content, the conclusion being that  $He^3$  must be very rare.

Although the chondrites are generally regarded as the best sample of the non-volatile material of the solar system, these meteorites do differ in chemical composition among themselves. Carbonaceous chondrites are usually regarded as the most authentic samples and, of these, the Type II may be the best (Schmitt and Goles [in press]). The chondrules, which are the oldest constituents of the meteorite, differ in composition from the rest of it. They show Si/Fe ratios and abundances of sodium and other elements that agree more closely with the solar values.

Urey (1964) has reviewed the problem of abundance differences in chondrites. For a comparison of solar, terrestrial, and meteoritic abundances, see Runcorn (in press). Revisions of solar abundances based on new photospheric models and  $f$ -values have been given by Müller and Mutschlecner (1964) and by Aller (in

<sup>4</sup> Climenhaga (in press) has found  $C^{13}$  in five cool carbon stars (19 Psc, DS Peg, Y CVn, WZ Cas, and HD 52432) and reports that the ratio  $N(C^{12})/N(C^{13})$  lies between 4 and 20. Wyller (in press) reports that this ratio lies between 2 and 3 for Y CVn.

press). Further discussions of the solar iron abundance based on new atmospheric models and  $f$ -values by Goldberg, Dupree, and Kopp (1964) and by Aller, O'Mara, and Little (1964) reproduce the GMA values. Pottasch (1964) found a higher Fe/H ratio, more nearly in accord with the average chondritic value, from coronal lines, but the method differs from that employed in analyses of the dark-line spectrum of the sun and resembles closely those used for gaseous nebulae (Aller, 1957). D/H and  $\text{Li}^6/\text{Li}^7$  have been studied in the sun and elsewhere with D/H apparently very small and  $\text{Li}^6/\text{Li}^7$  apparently normal. See, however, the recent work of Herbig (in press). Virtually all data on isotopic abundances are derived from terrestrial and meteoritic samples. We have already called attention to the alleged discrepancy between the solar and terrestrial ratios of the carbon isotopes, and one is inclined to be cautious in assuming that other local isotopic ratios apply to the sun and distant stars.

We may note, also, that data on the helium content of the sun and stars are far from satisfactory, for reasons discussed by Underhill (1958). Briefly, Underhill points out that models of stellar atmospheres are essential to interpreting the equivalent widths, but such models rarely match all the observed features and reliance on the match between theory and data for just one feature leads to untrustworthy extrapolations. Similar comments have been made by Aller, Elste, and Jugaku (1957), Aller (1960), and by Underhill and deGroot (in press).

Cameron (1959c), taking general guidance from the SU compilations, has prepared an extensively revised table of nuclear abundances on the basis of theoretical calculations for stars in which particular nuclear reactions occurred. He assumed that most of the nuclei beyond neon originated in the  $s$ - and  $r$ -processes, neglecting the  $\alpha$ - and  $e$ -processes put forward by BBFH (see §§ 2.1.1 and 2.1.2). As discussed at length in BBFH, the  $s$ -process produces such abundances that the product  $\sigma(A, Z) N(A, Z)$  is a smooth function of  $A$ , where  $\sigma(A, Z)$  is the neutron-capture cross-section of the nucleus of mass  $A$  and charge  $Z$ , and  $N(A, Z)$  is the nuclear abundance. It is generally the case that odd- $A$  nuclei have higher neutron-capture cross-sections than neighboring even- $A$  nuclei because of an attractive pairing effect. Hence, the even- and odd- $A$  isotopes of an element should exhibit a characteristic oscillation in abundance provided they were created in an equilibrium  $s$ -process. This feature has been employed by Cameron to adjust some of the observed  $s$ -product abundances. Cameron's adjustments of the  $s$ -products depend on calculations (Cameron 1958) as to which nuclei will be created and preserved in supernova explosions. Equally important are his estimates of the neutron-capture cross-sections for many nuclei. These cross-sections and certain other features of Cameron's abundances will be discussed below.

Cameron states that, for a given mass region,  $r$ -products should have a smooth dependence on  $A$  because they all come from the final beta decay of neutron-rich nuclei produced under the same conditions. Consider the  $r$ -product  $\text{Zr}^{96}$ , the SU (1958) abundance of which, relative to  $\text{Si} = 10^6$ , is 1.53. The

*r*-products  $\text{Mo}^{100}$  and  $\text{Pd}^{110}$  have the SU abundances of 0.234 and 0.0911 respectively. Hence, Cameron asserts that the observed  $\text{Zr}^{96}$  abundance is too high to be truly indicative of its primitive value, and he extrapolates from  $\text{Pd}^{110}$  and  $\text{Mo}^{100}$  to give a "corrected"  $\text{Zr}^{96}$  abundance of 0.400. The abundances of the other Zr isotopes are fixed using the SU isotope ratios. Cameron's abundances are listed in column 3 of Table 1, and are plotted in Figure 2 when they differ from the SU values.

Cameron's abundance table has been criticized by Burbidge (1960, 1963) because of the many uncertainties which enter into the calculations. Not only are reaction rates often obtained from lengthly theoretical developments rather than from experiment, but the reactions themselves are not completely settled. Also, many astrophysical features of Cameron's work, such as theories of the nature of supernovae, are not always acceptable to other workers in the field. Hence Burbidge asserts that a more reliable procedure is to fit the theoretical analysis to the data rather than to use analytical methods to correct the measurements. A similar viewpoint has been advanced by Clayton, Fowler, Hull, and Zimmerman (1961). Further objections to Cameron's abundances have been given by Aller (1961) on empirical grounds. Cameron (1960*a*), however, has called attention to the ambiguities which attend both the choice of samples for obtaining abundance data and the history of the sample from its origin to the present. Since nuclear factors are of undoubted significance in the generation of the elements, Cameron observes that the application of nuclear theory can suggest whether the data are reliable or should be re-examined. While Cameron has taken an extreme stand in favor of a theoretical approach to the abundance problem, SU, BBFH, and CFHZ have also employed some theoretical arguments to revise the measurements. Thus, for reasons to be reviewed below, CFHZ have altered some abundances as noted in column 4 of Table 1.

## 2.1. STELLAR NUCLEAR REACTIONS AFFECTING NUCLEAR ABUNDANCES

2.1.1. *The alpha process.*—BBFH assumed that the alpha-particle nuclei beyond  $\text{Mg}^{24}$  were created by alpha-particle capture. The source of the alphas was the photodisintegration of  $\text{Ne}^{20}$ , and successive alpha captures were presumed to make the nuclear species up to mass 48. A possible objection to this process has arisen in connection with the abundance of  $\text{Ne}^{20}$ . According to Cameron's abundance table,  $\text{Ne}^{20}$  is rare. In addition, all the calculations of the  $\text{Ne}^{20}$  abundance have been made on the supposition that the capture of alpha particles by  $\text{O}^{16}$  is resonant through the 4.969 Mev state of  $\text{Ne}^{20}$  (see Fig. 3). However, that state is now known to have the wrong spin and parity (Gove, Litherland, and Clark 1961) to participate in that reaction. Consequently, the process must proceed through the higher levels in  $\text{Ne}^{20}$  and the abundance of  $\text{Ne}^{20}$  is predicted to be much smaller than assumed by BBFH, or *observed* in stars and gaseous nebulae. In B stars, for example, neon appears to be comparable in abundance with oxygen (Aller 1961), although it may be less so in plane-

tary nebulae (Aller 1957).<sup>5</sup> Reeves (1962) notes that new experimental data imply that  $\text{Ne}^{20}$  cannot be produced by helium burning in sufficient amounts to play an important role in formation of the heavier elements. Wallerstein (1962a) has reached the same conclusion. Reeves (1962), Cameron (1959d, e), Reeves and Salpeter (1959), and Hayashi, Nishida, Ohyama, and Tsuda (1958) have considered alternative reactions involving  $\text{C}^{12} + \text{C}^{12}$ ,  $\text{O}^{16} + \text{O}^{16}$ ,  $\text{C}^{12} + \text{O}^{16}$ , and so forth. HNOT conclude that the alpha-particle nuclei with  $A > 20$  might be

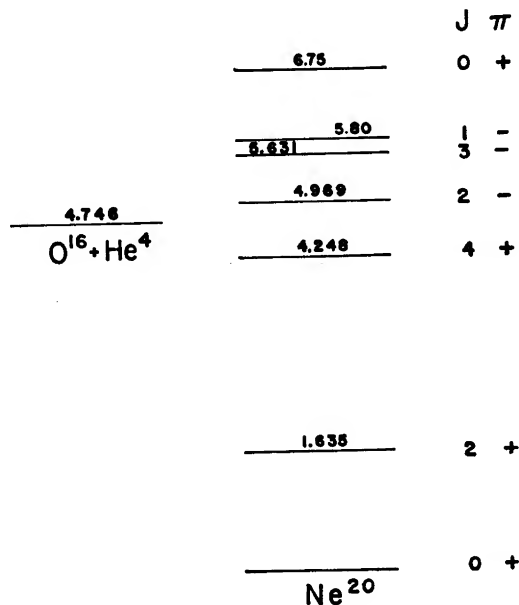


FIG. 3.—Energy-level diagram for  $\text{Ne}^{20}$  in the region of astrophysical interest. Energies (in mev) are given on each level. Spins and parities are listed under  $J\pi$ . Only even  $J$  even  $\pi$  or odd  $J$  odd  $\pi$  levels can be formed from  $\text{O}^{16} + \text{He}^4$ .

produced in supernova explosions. The other papers are discussed below. In connection with the problem of  $\text{Ne}^{20}$ , it is instructive to point out the desirability of having accurate information on isotopic abundances. Thus, Ne is actually abundant in stars (Aller 1953, 1954, 1961; Traving 1955); however, Cameron (1960b) has suggested that the source of the Ne lines is  $\text{Ne}^{22}$ , produced in the sequence  $\text{N}^{14}(\alpha, \gamma)\text{F}^{18}(\beta^+ \nu)\text{O}^{18}(\alpha, \gamma)\text{Ne}^{22}$ . This question cannot be resolved at the present time, but it is obviously of great importance to know which isotope of neon is responsible for the neon in stellar spectra. Aller (1962) proposes that stellar neon may have the same isotopic abundance as the earth. In solar cosmic rays, neon is much less abundant than oxygen.

2.1.2. *The equilibrium process.*—As shown in BBFH, the  $e$ -process occurs

<sup>5</sup> Aller (in press) finds neon more abundant in planetary nebulae than previously supposed, but it may show large variations from one object to another.

when the temperature reaches  $\sim 4 \times 10^9$  ° K and the density is in excess of  $10^5$  gm/cm<sup>3</sup>. In this circumstance there is a rapid exchange of neutrons and protons from one nuclear combination to another, the exchange being promoted by the large flux of energetic photons. The nuclear species near iron have the best chance of surviving because they have the highest binding energies per nucleon, and BBFH attributed the abundance peak in the iron-group elements (see Fig. 2) to the equilibrium event. Hoyle and Fowler (1960), make the matter more explicit as regards the site of the  $e$ -process.

It is well known that stars of large mass have short lives—a star of 30 solar masses may exist for only a few million years, and an evolutionary time scale of  $10^6$  years has been suggested for  $\zeta^1$  Scorpii (Code and Houck 1958). Were such stars produced in the early days of the life of the galaxy, they might possibly have quickly contaminated galactic matter with heavy elements. If, as assumed by HF, Type II supernovae are the source of the iron-group elements, with each supernova converting ten per cent of its mass into this portion of the abundance table, one such explosion per 400 years for  $\sim 10^{10}$  years would give rise to a relative  $e$ -product abundance comparable with what is now seen in the sun. *This assumes, to be sure, that these elements have never been subjected to any destructive reactions once they came into existence.*

Shklovskii (1960) also associates Type II supernovae with massive stars but suggests that the supernova mechanism is related to a *large* heavy-element content of these stars. Moreover, he gives the frequency of such outbursts as one every 50 years, which, in the absence of a means of destruction, would yield a 10-fold excess of the heavy elements.

Anders (1959) has noted from work on the energy released in supernovae that it is difficult to explain the ratio of  $r/e$  product abundances if they both come from the same star. HF offer a solution to this problem with their suggestion that Type II supernovae produce mainly iron-group elements while Type I supernovae yield the  $r$ -products.

HF examine the problem of the origin and structure of supernova explosions (see also chaps. 6 and 7). They conclude that the equilibrium process develops in both Type I and Type II supernovae, the distinction between the two types being one of the mass of the star—Type I is associated with stars having 1.5 or so solar masses, while Type II is attributed to very massive stars (30 solar masses). Stars of intermediate mass are presumed to lose matter in non-catastrophic ways. In the Type II case, the explosion is preceded by an implosion of the stellar core. The  $e$ -process operates, with nuclei clustering about  $\text{Fe}^{56}$ , and the  $e$ -nuclei are preserved on being expelled from the star. The Type I case is treated below (§ 2.1.5). For the Type II supernovae, HF find that the equilibrium mixture is frozen at  $3.8 \times 10^9$  ° K and  $10^5$  gm/cm<sup>3</sup>, conditions similar to those previously discussed.

There are grounds for regarding the HF calculations with care. For one thing,  $\text{Co}^{57}$ , with a 270-day half life, should be made in the  $e$ -process (Anders 1959) but

the Type II supernovae light curves do not exhibit a decay which can be ascribed to this isotope. Also, Colgate and Johnson (1960) find that the collapse of the core releases more than enough energy to convert the iron-group elements into alpha particles and neutrons. Thus, it is far from clear that the  $e$ -products can actually survive the explosion. Indeed, as emphasized by Frank-Kamenetskii (1959, 1961), the mechanism of freezing the abundances is poorly understood. Thirdly, the ultimate fate of a massive star is now believed to be seriously affected by photo-neutrino processes (Cameron 1960*b*; Chiu and Morrison 1960; Chiu 1961*a, b, c*; Chiu and Stabler 1961), but these were neglected by HF. Fourthly, the assumption mentioned above that the  $e$ -products have escaped further processing in nuclear reactions seems to be a weak point since other features of the stellar origin of nuclear abundances require that the  $e$ -matter be transmuted by the  $s$ -process (see below, sec. 2.1.4). Fifthly, Nemirovsky (1958) has offered an entirely different approach to understanding the iron-group abundance maximum. According to him, there is a closed nuclear shell with  $Z = 16$ ,  $N = 40$ , i.e.,  $S^{56}$ . Formation of this nucleus in a neutron burst such as characterizes the  $r$ -process would ultimately lead to  $Fe^{56}$  via beta decay. Si, Ar and Ca are taken by Nemirovsky to be suitable seeds for making the iron-group elements. As we will see in § 2.1.5, all  $r$ -process calculations are speculative because of our ignorance of the masses and lifetimes of ultra-neutron-rich nuclei, and one must consider Nemirovsky's idea as poorly founded. Nonetheless, this emphasizes the wide divergence of viewpoint among authors dealing with the origin of the elements.

2.1.3. *The three-alpha process.*—The three-alpha process is basic to the formation of all the elements beyond helium (Öpik 1951; Salpeter 1952*a*; Hoyle 1954). The reaction proceeds at a significant rate because of the unusually long life ( $\sim 10^{-16}$  sec) for the particle-unstable ground state of  $Be^8$  and because of the existence of a level in  $C^{12}$  at the proper energy for the radiative capture of alphas by  $Be^8$  to be resonant. A series of experiments, referred to in BBFH, demonstrated that the level in  $C^{12}$  has the correct character to participate in the capture reaction. The reaction rate contains the factor  $(\Gamma_\gamma + \Gamma_{e\pm}) \Gamma_\alpha / \Gamma$  where  $\Gamma_\gamma$  = radiative width,  $\Gamma_{e\pm}$  = the width for pair emission,  $\Gamma_\alpha$  = the alpha particle width and  $\Gamma$  = the total width, all referring to the resonant state in  $C^{12}$ . The rate also depends exponentially on the mass, or energy, difference between the excited state of  $C^{12}$  and three-alpha particles, and this difference was well known by BBFH along with the fact that  $\Gamma_\alpha \approx \Gamma$ . Later experiments by Alburger (1960, 1961), Ajzenburg-Selove and Stelson (1960) and by Seeger and Kavanagh (1963) resulted in

$$\frac{\Gamma_{e\pm}}{\Gamma} = 6.6 \pm 2.1 \times 10^{-6} \quad (\Gamma_\alpha = 8 \pm 5 \text{ ev}),$$

and

$$\frac{\Gamma_\gamma}{\Gamma} = 3.3 \pm 0.9 \times 10^{-4}.$$

The latest result, that of Seeger and Kavanagh, is  $(\Gamma - \Gamma_a)/\Gamma = 2.8 \pm 0.5 \times 10^{-4}$ . With the above numbers, one finds  $\Gamma_\gamma = 2.6 \times 10^{-3}$  ev, according to Alburger (1961), or  $2.5 \times 10^{-3}$  ev according to Seeger and Kavanagh (1963). With the larger number, which is 2.6 times the value used by BBFH, Table 2 gives the corrected rate of destruction of  $\text{He}^4$  per alpha particle per second as a function of temperature. A helium density of  $10^5$  gm/cm<sup>3</sup> is assumed. The correction for electron screening as given by BBFH is included. See also chapter 2.

2.1.4. *The s-process.*—Evidence for the operation of the *s*-process rests largely on three points. One is that the curve of nuclear abundance versus mass number exhibits relative maxima at the closed-shell nuclei with  $A = 90$ ,  $N = 50$ ;  $A = 120$ ,  $Z = 50$ ;  $A = 140$ ,  $N = 82$ ; and  $A = 208$ ,  $N = 126$ ,  $Z = 82$ . As shown in BBFH, these are nicely explained in terms of an *s*-type development. Secondly, there are a number of abundant shielded isotopes which, again, can originate only in the *s*-process. Thirdly, there is the observation (Merrill 1952,

TABLE 2  
RATE OF THREE-ALPHA REACTION PER ALPHA  
PER SECOND AT VARIOUS TEMPERATURES

$T(\times 10^8 \text{ }^\circ\text{K})$ . . . . .	0.5	0.75	1.0	1.4	2.0	3.0
Rate (sec <sup>-1</sup> ) . . . . .	$1.6 \times 10^{-32}$	$5.8 \times 10^{-21}$	$2.6 \times 10^{-16}$	$1.4 \times 10^{-10}$	$4.1 \times 10^{-7}$	$1.5 \times 10^{-4}$
$\tau$ (years) . . . . .	$2 \times 10^{14}$	$5.5 \times 10^{12}$	$1.2 \times 10^7$	$2.3 \times 10^3$	$7.7 \times 10^{-2}$	$2.1 \times 10^{-4}$

1956) that technetium, an element without any stable isotopes, occurs in some S, R, and N stars. Since the half life of the longest-lived isotope,  $\text{Tc}^{97}$ , is  $2.6 \times 10^6$  yr, it is clear that this element must be generated continuously. The isotope  $\text{Tc}^{99}$ , with a half life of  $2.1 \times 10^6$  yr, lies on the *s*-process path (BBFH), and has generally been considered to be the form of Tc seen in the red giants (for example, see Anders 1958). Cameron (1959a) has proposed that  $\text{Tc}^{97}$  is in fact the correct isotope, the production mechanism being such that, under very special conditions, the synthesis of Tc does not guarantee its continuous synthesis via neutron capture. This point is further treated below. Despite this possible reservation, it seems likely that the *s*-process is in current operation in red giant stars. Burbidge and Burbidge (1957) have analyzed the abundances in the Ba II star HD 46407 in terms of operation of the *s*-process. If one assumes that the star initially contained normal (i.e., solar) abundances, the *s*-process appears to explain satisfactorily how the present elements were created. Information on the isotopic composition of the elements would be valuable in refining this discussion, but such data are virtually impossible to obtain. We turn to particular problems.

a) *Neutron sources.*—The question of how the neutrons are generated on a slow time scale has yet to be answered definitively. BBFH surveyed the argu-

ments concerning the  $C^{13}(\alpha, n) O^{16}$  reaction, which has been favored by Cameron, and the  $Ne^{21}(\alpha, n) O^{16}$  reaction, which they preferred. The objections to the former may be stated as follows (BBFH):

1. If the  $C^{13}$  comes from operation of the carbon cycle, there is never enough  $C^{13}$  to generate a sufficient number of neutrons to make the heavy elements. Even in equilibrium in the carbon cycle,  $C^{12}/C^{13} = 4.6$ , and the observed ratio is often much larger than this. For hydrogen-poor stars, the  $C^{13}$  abundance may be quite small (Shajn and Hase 1954).

2. Should any hydrogen be present, the reaction  $C^{13}(p, \gamma)N^{14}$  takes place about four times as fast as  $C^{12}(p, \gamma)N^{13}$  (Caughlan and Fowler 1962), and the large cross-section for the reaction  $N^{14}(n, p)C^{14}$  consumes the neutrons. Indeed, this will happen even if the  $N^{14}$  is not continuously generated but simply is left over from the carbon-cycle reactions. Hydrogen is itself an efficient neutron poison, the deuterium which is made from  $n + p \rightarrow D + \gamma$  being converted eventually to  $He^3$ .  $He^3$  again rapidly changes neutrons into protons.

Cameron has attempted to overcome these drawbacks by suggesting (see BBFH) that  $C^{12}$ , synthesized in the 3- $\alpha$  reaction in a red giant core, mixes with hydrogen from the envelope at such a rate that  $C^{13}$  is made, but not  $N^{14}$ . The  $C^{13}$ , drawn into the core, can there interact with alphas to make the neutrons. Any protons liberated in the  $N^{14}(n, p)$  reaction are free to create more  $C^{13}$  by the carbon cycle process:  $C^{12}(p, \gamma)N^{13}(\beta^+ \nu)C^{13}$ . In more recent work Cameron (1959*d, e*) has proposed that the  $C^{13}(\alpha, n)O^{16}$  neutron source operates at high temperatures ( $T = 6$  to  $7.5 \times 10^8$  °K) in a carbon-burning core of a Type II pre-supernova.

Reeves (1962) has investigated high-temperature conditions, with a view toward neutron production, using recent data (Almqvist, Bromley, and Kuehner 1960; Bromley, Kuehner, and Almqvist 1960) on the rate of C + C reactions. The sequence of reactions is:

1.  $C^{12} + C^{12} \rightarrow Na^{23} + p + 2.230 \text{ Mev}$   
 $\rightarrow Ne^{20} + He^4 + 4.619 \text{ Mev}$
2.  $C^{12} + p \rightarrow N^{13} + \gamma + 1.941 \text{ Mev}$   
 $N^{13} \rightarrow C^{13} + \beta^+ + \nu + 1.200 \text{ Mev}$
3.  $C^{13} + He^4 \rightarrow O^{16} + n + 2.203 \text{ Mev}.$

There are certain problems associated with this possibility:

1. It is still necessary to avoid the formation of  $N^{14}$ .
2. If the temperature becomes too high,  $N^{13}$  is photodisintegrated before it can beta decay (Reeves and Salpeter 1959). At  $T = 7.5 \times 10^8$  °K, the neutron yield is reduced by 100 times as compared with  $T = 6 \times 10^8$  °K (Cameron 1959*a*).
3. At temperatures of  $\sim 7 \times 10^8$  °K or greater, neutrino losses (Cameron 1960*b*; Chiu 1961*b*; Strothers and Chiu 1962) may lead to a rapid collapse of the

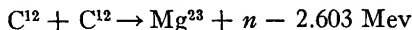


star and preclude satisfactory operation of the  $C + C$  reactions. If this does *not* happen, Reeves (1962) finds that enough neutrons are released to synthesize all the  $s$ -products. Contrariwise, Fowler (1962) observes that nuclei near  $Mg^{24}$  show many neutron-capture resonances at such temperatures. The effect of the resonances is to reduce the neutron concentration to too small a value to make the heavy elements, the deficiency being about a factor of ten. According to Fowler (1962) the  $s$ -process may be significant for a small-mass region above  $Fe^{56}$  when the temperature exceeds  $7 \times 10^8$  ° K.

Cameron (1960*b*), altering his earlier work (Cameron 1959*d*; see below, part *b*), finds that the neutrino loss will be too large for the carbon burning to occur at temperatures in excess of  $6 \times 10^8$  ° K, and proposes another neutron source which can operate at much lower temperatures. As noted above, Cameron (1960*b*) has suggested that  $Ne^{22}$  is the most important isotope of neon in stars. Neutrons can be generated from  $Ne^{22}$  by the endothermic reaction  $Ne^{22} + He^4 \rightarrow Mg^{26} + n - 481$  kev. Since the  $Ne^{22}$  is itself a product of reactions beginning with  $N^{14}$ , it is still necessary to scour out the  $N^{14}$  before the neutrons are liberated. Otherwise the neutrons will be converted into protons and will not be available for making the heavy elements.

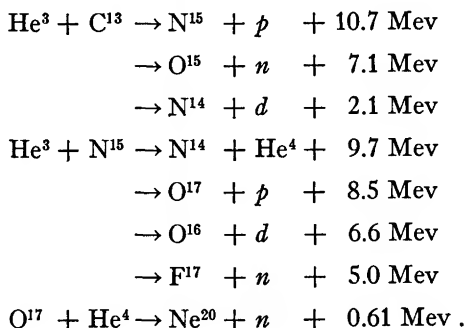
The arguments against the  $Ne^{21}(a, n) Mg^{24}$  reaction are also used in BBFH. It will be recalled from that paper that the  $Ne^{20}$  must be generated in a predecessor star so that it can react with protons in a hydrogen-burning shell surrounding the helium core of a red giant. The reaction gives  $Na^{21}$  which positron decays to  $Ne^{21}$ , this product then being in a favorable location to participate in the neutron-generating process. Of course, the  $(a, n)$  reaction must compete favorably with  $Ne^{21}(p, \gamma) Na^{22}$ , and Cameron, in various publications (for example, 1959*d*), argues that the radiative-capture process is resonant. Marion and Fowler (1957) show that  $Ne^{20}(p, \gamma) Na^{21}(\beta^+ \nu) Ne^{21}$  cannot give enough  $Ne^{21}$  if C and N are present because the latter convert the protons into helium too fast. Only if carbon is absent, and  $O^{16}$  and  $Ne^{20}$  present from a previous synthesis, can this reaction give enough neutrons in a red giant star. Data on this point are lacking. We have seen that the abundance of  $Ne^{20}$  *may* be too small to account for a satisfactory number of neutrons, which would weaken the case for  $Ne^{21}(a, n) Mg^{24}$  (but see § 2.1.1). As is the case with all other neutron sources, it is necessary that  $N^{14}$ , H, and  $He^3$  be absent.

Another possible neutron source is the endothermic reaction.



(RS), although Reeves (1962) states that this cannot be significant under astrophysical conditions. Cameron (1959*e*) studied neutrons from reactions involving  $O^{16}$  and  $Ne^{20}$  at a temperature of  $1.3 \times 10^9$  ° K, and concluded that at this temperature too few neutrons could be released to be a significant factor in the  $s$ -process. This conclusion is strongly reinforced if the later papers (Cameron 1960*b*; Chiu 1961*a, b, c*) on neutrino-induced collapse of hot stars are cor-

rect. The origin of the neutrons in the *s*-process is still a matter of conjecture. One can hypothesize that other neutron sources might be significant. Examples of exothermic reactions which produce neutrons are:



It is interesting to note that the first two sets of reactions, and especially the first one, largely bypass the neutron poison,  $\text{N}^{14}$ , since it appears only as a reaction product with small abundance. However,  $\text{He}^3$  is needed and it, too, destroys neutrons.

*b) Initial conditions of abundance and temperature and the time scale.*—Cameron (1959*d*) starts with a pure hydrogen star, and allows it to evolve to a core of 80 per cent  $\text{C}^{12}$  and 20 per cent  $\text{O}^{16}$ , after which the carbon-carbon reactions commence. Theoretical estimates are given for the production of elements up to  $\text{Ca}^{42}$  by virtue of proton- and alpha-particle capture. The principal means of reaching the heavy nuclei is, of course, neutron capture. With the neutron-capture cross-sections discussed below, nuclei up to bismuth result, although the heavy elements have a much smaller abundance than observed. Cameron then considers the results of adding solar-type abundances to the carbon-burning star, and of varying the temperature from  $T = 6 \times 10^8$  ° K to  $7.5 \times 10^8$  ° K. The chief effect of the former is to introduce some iron, which eases considerably the formation of the heavy nuclei on a slow time scale. Cameron concludes that the carbon reactions release the neutrons which, captured by the other nuclear species in the carbon-exhausted shell of a massive Population II pre-supernova, give rise to the *s*-products. These products must also survive the supernova explosion which follows quickly after completion of the *s*-process. In addition to the step-by-step buildup of heavy nuclei through neutron capture and beta decay, Cameron (1959*a*) introduces a "photo-beta" process which modifies the *s*-process. Consider a radioactive nucleus which decays with a long half life. The reasons for the slow decay are:

1. The energy release is small, since transition rates in (allowed) beta decay vary as the fifth power of the energy.
2. The change in nuclear spin and parity does not conform to the selection rules for allowed transitions.

Suppose, however, that the parent nucleus has an excited state with such spin and parity that the beta decay therefrom would be allowed. The half life would be shortened were the nucleus in this state. Cameron points out that a nucleus can be photoexcited provided the temperature is high enough. The photo-excitation produces a materially reduced beta-decay half life. A specific example is illustrated in Figure 4.

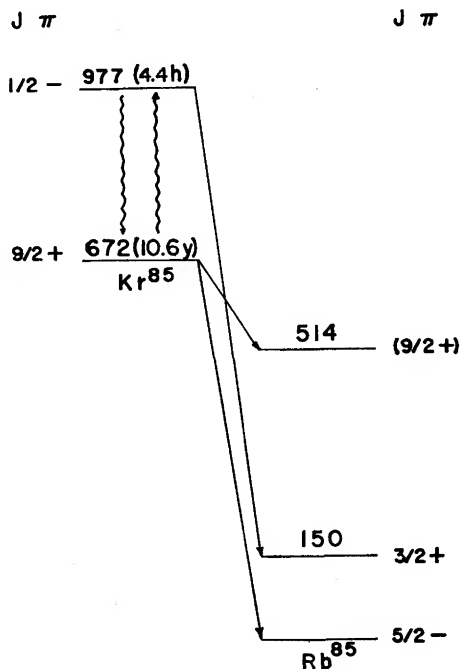


FIG. 4.—Beta decay of  $\text{Kr}^{85}$  from its ground and first-excited states. Uncertain spin-parity assignments are parenthetic. Energy levels are in kev with respect to the ground state of  $\text{Rb}^{85}$ . Half lives are in parentheses on the appropriate levels. The wavy lines indicate electromagnetic transitions in  $\text{Kr}^{85}$ .

As seen in Figure 4, the half life of the excited state of  $\text{Kr}^{85}$  is only 4.4 hours, in contrast with the 10.6 year half life of the ground state. At temperature,  $T$ , the fraction,  $N(E^*)$  of nuclei in an excited state is given

$$N(E^*) = \frac{2J+1}{2I+1} \exp\left(\frac{-E^*}{kT}\right),$$

where  $J$  is the spin of the excited state of energy  $E^*$ ,  $I$  is the ground-state spin, and  $k$  is Boltzmann's constant. At a temperature  $T = 7.5 \times 10^8$  °K, this amounts to 0.18 per cent of all  $\text{Kr}^{85}$  nuclei. The total transition rate,  $p$ , is

$$p = N^0 p^0 + N^* p^*,$$

where  $N^0$  is the fraction of nuclei in the ground state with a decay rate  $p^0$  and the other terms refer to the excited state. For  $\text{Kr}^{85}$  Cameron obtains an effective half life of 0.28 year. A more striking example is that of  $\text{Lu}^{176}$ , the half life of which is reduced from  $2.1 \times 10^{10}$  years to 0.03 year at  $7.5 \times 10^8$  ° K.

The importance of the photo-beta process is that it greatly reduces the probability of neutron capture by the radioactive nucleus. Were the mean time for neutron capture long compared with 0.25 year,  $\text{Kr}^{86}$  would be bypassed and its abundance anomalously low. Cameron analyzes the  $\text{Kr}^{86}$  abundance to give a mean neutron-capture time of 3 years. His results are summarized in Table 3. It is conjectural as to how much of a role the photo-beta process really has in the  $s$ -process, since Cameron (1960*b*) discards the carbon-carbon reactions at high temperature and, as has been mentioned earlier, gives the  $\text{Ne}^{22}(a, n) \text{Mg}^{25}$

TABLE 3  
COMPARISON OF NATURAL AND PHOTO-BETA HALF LIVES  
OF VARIOUS NUCLEI (CAMERON 1959*d*)

Nucleus	Natural Half Life (years)	Calculated Half Life at $7.5 \times 10^8$ ° K (years)
$\text{Se}^{79}$ .....	$6.5 \times 10^4$	$\sim 0.55$
$\text{Kr}^{86}$ .....	10.6	0.28
$\text{Pd}^{107}$ .....	$7 \times 10^6$	$\sim 3$
$\text{Cd}^{113}$ .....	$7.3 \times 10^{15}$	51
$\text{In}^{115}$ .....	$6 \times 10^{14}$	0.83
$\text{Dy}^{163}$ .....	stable	$\sim 0.5$
$\text{Lu}^{176}$ .....	$2.1 \times 10^{10}$	0.03

reaction as the neutron source. For this, the temperature is only  $2 \times 10^8$  ° K, and the photo-beta reactions are insignificant. We note that if the photo-beta process does take place at high temperature, it bears on the question of technetium production in the  $s$ -process. Cameron (1959*a*) has pointed out that  $\text{Mo}^{97}$ , which is stable in its ground state, can be photoexcited to a low-lying level from which beta decay to  $\text{Tc}^{97}$  can take place. Hence, Tc in red giants might be an indicator not of the  $s$ -process but of an internal temperature above  $6 \times 10^8$  ° K. Of course, mixing of the Tc to the surface must also occur.

The initial abundances, temperature, and time scale are all different in the  $s$ -process work of BBFH, CFHZ, and Clayton and Fowler (1961). Their stellar models are similar to those calculated, for example, by Schwarzschild and Selberg (1962) for the evolution of red giants. In Fowler's papers, it is assumed that elements up to iron have been synthesized in predecessor stars, the equilibrium process being of major importance. The  $s$ -process then takes place in a red giant which contains an appreciable amount of neon, from which the neutrons are eventually generated, and iron, which serves as the initial absorber of the neutrons. In this manner, the heavy elements are created up to  $\text{Bi}^{209}$ . A

temperature of  $\sim 3 \times 10^8$  ° K is postulated. The free-neutron density is low and the time interval between successive neutron captures by a given seed nucleus is  $10^4$ – $10^5$  years. A total time of  $\sim 10^7$  years is assumed. At the low temperature, the photo-beta process is generally unimportant, with a long time interval between successive neutron captures, all nuclei with half lives less than  $\sim 100$  years are assumed to decay, while a half life greater than  $10^5$  years means effective stability. Consequently, Fowler's *s*-chain is rather different here from Cameron's. Such a difference is illustrated in Figure 5, which shows two

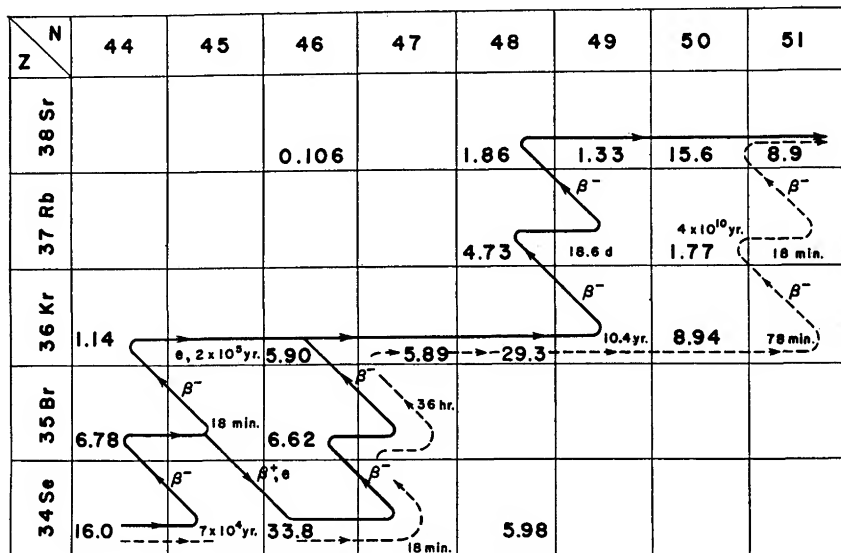


FIG. 5.—A portion of the *s*-chain. The solid arrow follows the work of Fowler and associates, the dotted arrow that of Cameron. Relative abundances ( $\text{Si} = 10^6$ ) are shown for the stable nuclei.

*s*-process chains through the radioactive nuclei  $\text{Se}^{79}$  and  $\text{Kr}^{85}$ . Cameron considers  $\text{Se}^{79}$  to be stable in the *s*-process, so  $\text{Br}^{79}$  and  $\text{Kr}^{80}$  are both bypassed. BBFH suggest that an appreciable fraction of the  $\text{Se}^{79}$  nuclei in fact decay to  $\text{Br}^{79}$ , so  $\text{Br}^{79}$  and  $\text{Kr}^{80}$  are both *s*-products. This point of view is maintained in CFHZ. Similarly, Cameron believes that  $\text{Kr}^{85}$  is largely stable on the *s*-time scale and asserts (Cameron 1959*a*, *d*) that  $\text{Kr}^{86}$  is an *s*-product, while BBFH and CFHZ reserve  $\text{Kr}^{86}$  for the *r*-process. Actually, operation of the photo-beta process somewhat modifies Cameron's sequence in the foregoing.

As seen from the remarks on photo-beta processes, the beta decay of a radioactive nucleus in a star is not identical with the decay of the same nucleus in a terrestrial sample of matter. Bahcall (1961, 1962) has shown that additional effects must be included. For example, the beta decay of an ion is slower than that of an atom, since the latter has an available energy greater than the former

because of the binding energy of atomic electrons. A contrary effect is that the ionization of a radioactive nuclide increases the decay rate because of an enhanced probability of decay into bound electronic states. Also, in dense matter the exclusion principle reduces the rate of beta decay. A proper treatment of stellar beta decay, including all these factors, may reveal lifetimes for unstable  $s$ -products which are substantially different from the normally observed lifetimes. Naturally this could alter considerably the abundances of certain  $s$ -products.

Again, at high temperatures ( $T > 6 \times 10^8$  ° K), Strothers and Chiu (1962) observe that the neutrino loss shortens the remaining life of a star by  $10^3$  times relative to what is calculated without neutrino losses. This, too, alters the  $s$ -process because some short-lived nuclei will no longer have the time to decay and the neutron-capture sequence is altered. Strothers and Chiu find that, for  $23 < A < 46$ ,  $\text{Cl}^{36}$  becomes effectively stable and can capture neutrons. The result is that, for  $36 < A < 46$ , the  $s$ -product abundances are about three times those calculated neglecting the neutrino loss.

Another suggestion concerning the temperature for the  $s$ -process comes from Frank-Kamenetskii (1959). He calls attention to the low abundance of scandium, an  $s$ -product. The rarity of  $\text{Sc}^{45}$  is attributed partly to the small neutron-capture cross-section of its precursor,  $\text{Ca}^{40}$ , and partly to a large neutron-capture cross-section for  $\text{Sc}^{45}$  itself.  $\text{Sc}^{45}$  has a large neutron-scattering resonance ( $\sigma_{\text{max}} = 100$  barn) at  $E_n = 4.1$  kev, and the (large) neutron-capture cross-section of 56 millibarn at 25 kev. Hence it is argued that the 4.1 kev resonance involves radiative capture with a large cross-section and this serves to deplete the scandium. From this, it appears that the relevant neutron energy is about 4 kev, corresponding to a temperature of about  $5 \times 10^7$  ° K, considerably lower than the other estimates.

CFHZ remark that the elements presently in the solar system probably represent a mixture of substances created in a number of stars. The nuclear reactions were likely not identical in all of those stars, and, even in one star, some part may experience a history different from that of another part. The growth of a given seed to some final form is affected only by the total number of neutrons captured, and not by interruptions in time or space in the neutron flux. Hence, it is reasonable to take advantage of a diversity of situations in accounting for the solar elements. Specifically, CFHZ find it possible to account for the  $s$ -products by assuming that iron-group elements, having the same abundance distribution that we now see, were subjected to neutron irradiation as summarized in Table 4. The listing in Table 4 is not to be thought of as unique. It is just one way of producing fairly good agreement with the observed abundance distribution. As discussed in detail in BBFH, the product of neutron-capture cross-section and abundance is expected to vary smoothly with  $A$ . In fact, if equilibrium is attained, the product should be constant. The entries in Table 4 show that most of the seeds were irradiated by a quite small number of neutrons, so that the product  $\sigma N$  must decline steeply for values of  $A$  just above

iron. Smaller and smaller fractions of the seeds were bombarded by increasing numbers of neutrons, the effect being to flatten the  $\sigma N$  product for the heavier  $A$ -values. One calculated curve obtained by CFHZ and the corresponding data are reproduced in Figure 6. It appears that the agreement is good, but one must note that the fit is not unique.

An interesting feature of the CFHZ work is that only 0.15 per cent of the original iron-group nuclei are presumed to have been converted into nuclei with  $A > 63$ . According to Fowler and his associates *this means that (prior to formation of the sun) the great majority of the solar iron-group elements were never*

TABLE 4  
IRRADIATION OF NUCLEI IN THE  
 $s$ -PROCESS (CFHZ 1961)

No. of Iron-Group Seeds	Average Number of Neutrons Captured per Initial Seed
2160	2.8
990	6.9
45	34.0
45	100.0

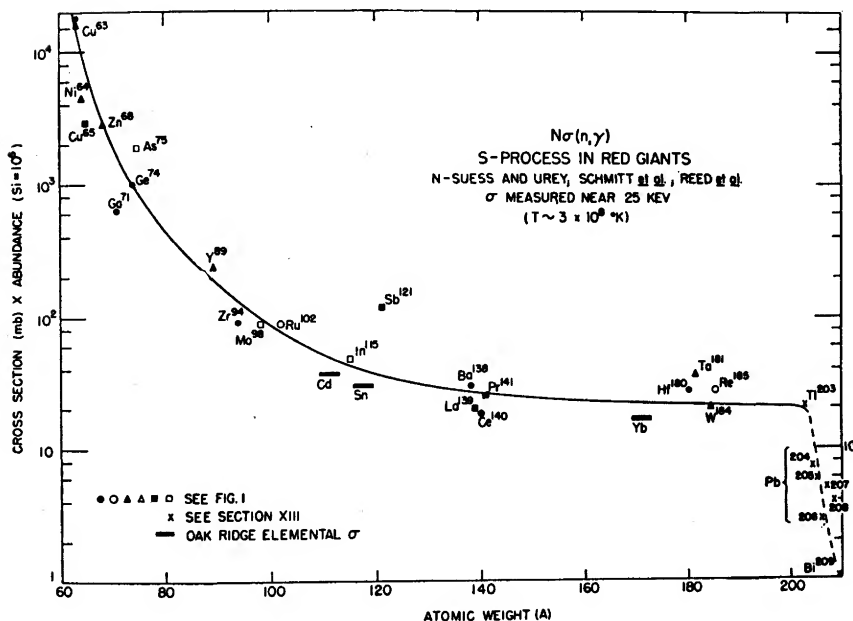


FIG. 6.—Calculated and experimental values of  $(\sigma_{n, \gamma} \times \text{abundance})$  vs. atomic weight. From Clayton, Fowler, Hull, and Zimmerman (1961).

recondensed into a stellar interior subsequent to the  $e$ -process in which they were generated. Furthermore, the  $s$ -products we now see in the solar system cannot have experienced presolar condensation either, for, as noted by HF, they would have been completely consumed in an ultimate  $r$ -process or  $e$ -process, depending on the mass of the star into which they had been incorporated. Of course, this neglects the possibility of non-catastrophic loss of mass from a star.

The suggestion that the  $e$ -,  $r$ -, and  $s$ -products in the solar system were separately the terminal elements in various stars is important for the calculation of the relative abundances of the solar  $s$ -nuclei. Consider that the general scheme for stellar evolution (BBFH) requires the  $s$ -process to be succeeded in time by the  $r$ -process, at least for small mass stars (HF). Now the  $r$ -process gives rise to such nuclei as  $\text{Te}^{130}$  (Fig. 7). In a recondensation, therefore, some  $\text{Te}^{130}$  would be

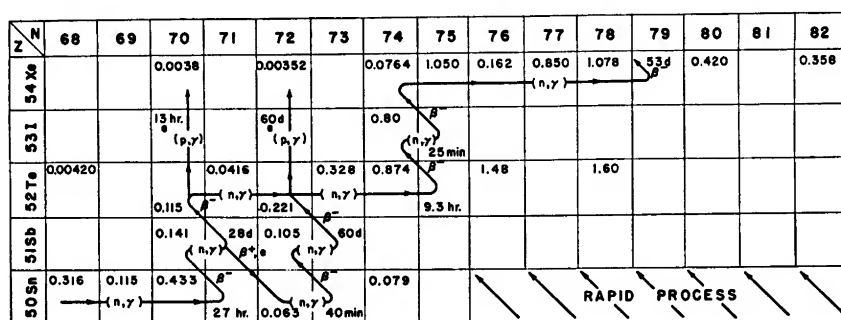


FIG. 7.—Element synthesis near  $A = 120$ . Relative abundances ( $\text{Si} = 10^6$ ) are shown for the stable nuclei.

present, and it could serve to create an overabundance of  $\text{Xe}^{131}$  in the next  $s$ -process. The assumption that such recondensations have *not* taken place, coupled with the reasonable expectation that  $\sigma N$  will be constant for the  $s$ -process *isotopes* of a particular element, enables CFHZ and CF to determine what fraction of the nuclei which can arise from both the  $s$ - and  $r$ -processes should be assigned to each. In the curve of Figure 6, the  $r$ -product contributions have been subtracted out. However, Fowler has recently revised the estimates of the fractions of the tin isotopes due to the  $s$ - and  $r$ -processes (quoted by Macklin, Inada, and Gibbons, 1962). The new ratios of  $r$ - to  $s$ -contributions differ by factors of five to fifteen from those given by CF. See insert in "others" column of Table 1 for the new estimates of abundance of the tin isotopes.<sup>6</sup>

Adjustment of the irradiation of various fractions of the iron-group elements is not sufficient to bring the calculated values of abundance into agreement with the empirical data over the entire range of  $A$ . CFHZ have used their computed curve to revise the abundance of certain nuclei (*all* isotopes of Zr, Hf, Ta, W, Re, Os, Ir, Pt, and Au) to 40 per cent of the SU values; this results in an im-

<sup>6</sup> See Shima (1964) for discussions of uncertainties in the abundance of tin.



proved fit. These adjusted values appear in Figure 6. Note that these abundance adjustments differ in one regard from Cameron's, namely that the CF changes are for elements whereas Cameron's are often for individual isotopes.

CFHZ study at length the termination of the slow process. The nuclei just beyond  $\text{Bi}^{209}$  have short half lives for beta and/or alpha activity, so that neutron capture by  $\text{Bi}^{209}$  leads to cycling between  $\text{Pb}^{206}$  and  $\text{Bi}^{209}$ , the principal result being the conversion of neutrons into alpha particles.<sup>7</sup>

*c) Neutron-capture cross-sections.*—Fundamental to the *s*-process calculations are the neutron-capture cross-sections which are functions of  $A$ ,  $Z$ , and the relative energy of the neutron and nucleus. For Cameron's work (Cameron 1959*d*, *e*) the average neutron energy is 60 to 75 kev, while CFHZ and CF assume the relevant energy to be 25 kev. As mentioned above, Frank-Kamenetskii uses 4.1 kev for the proper neutron energy. Only a few measured values have been obtained at the foregoing energies, most of these after Cameron's papers appeared. Consequently Cameron had to estimate practically all of his cross-sections. The other authors have had more data on which to base their conclusions, but still found it necessary to estimate some 130 cross-sections. The reader can gauge the difficulty these estimates pose by examining Table 5. The columns list in succession, with all cross-sections in millibarns: (1) The nucleus whose capture cross-section must be known; (2) Cameron's values at 60 kev; (3) CFHZ values at 25 kev; (4) measured values at 25 kev (where only the element symbol is shown, and not the mass, the measured value is for  $E_n = 30$  kev and the natural terrestrial element); (5) CFHZ values extrapolated to 60 kev assuming a  $1/\sqrt{E}$  dependence.

In general, the CFHZ estimates are close to the values subsequently measured, there being an occasional 50 per cent discrepancy. Cameron's cross-sections diverge more widely from the laboratory values. The purpose of column 6 is to compare the CFHZ and Cameron estimates for cases where measurements have not been made. Column 1 contains an asterisk where a discrepancy of a factor of 2 or greater occurs. Note well the comparison of the measured cross-sections for the tin isotopes (MIG) and the estimates.

*2.1.5. The  $r$ -process.*—As demonstrated in BBFH, the capture of neutrons on a very rapid time scale is an essential nuclear mechanism for synthesis of many of the nuclear species. The main feature of this *r*-process is the release of an enormous flood of neutrons in a total time of 100 seconds or less, the site being a supernova explosion of Type 1. Later work by Hoyle and Fowler (1960) substantiates this choice of site, as is described in chapter 6, which deals with supernovae. It is clear that with the locale in a supernova the temperature will

<sup>7</sup> The ground state of  $\text{Bi}^{210}$  is now known to have a half life of only 5 days (Erskine, Buechner, and Enge 1962). This information changes the CFHZ recycling equations (Clayton 1963). Specifically, products of neutron capture cross-sections and *s*-process abundances should be the same for  $\text{Pb}^{206}$ ,  $\text{Pb}^{207}$ ,  $\text{Pb}^{208}$ , and  $\text{Bi}^{209}$  if the *s*-process reaches equilibrium. The sensitivity of the calculations of nuclear astrophysics to even minor changes in laboratory data is high.

TABLE 5

NEUTRON-CAPTURE CROSS-SECTIONS FOR *s*-PROCESS NUCLEI

(All entries are in millibarns. Except where otherwise noted, the experimental data have been taken from the summary in CFHZ 1961.)

NUCLEUS	$\sigma_{n\gamma}$ (60 KEV) CAMERON 1959b	$\sigma$ (25 KEV) CFHZ 1961	$\sigma$ (25 KEV)		$\sigma$ (60 KEV) EXTRAPO- LATED FROM DATA OF CFHZ
			Experiment	Refer- ences†	
Ne <sup>20</sup> .....	0.014				
Ne <sup>21</sup> .....	1.17				
Ne <sup>22</sup> .....	0.014				
Na <sup>23</sup> .....	0.83				
Mg <sup>24</sup> .....	0.44				
Mg <sup>25</sup> .....	2.6				
Mg <sup>26</sup> .....	0.59				
Al <sup>27</sup> .....	5.0				
Si <sup>28</sup> .....	0.53				
Si <sup>29</sup> .....	3.7				
Si <sup>30</sup> .....	0.97				
P <sup>31</sup> .....	8.9				
S <sup>32</sup> .....	0.19				
S <sup>33</sup> .....	12.6				
S <sup>34</sup> .....	2.6				
Cl <sup>35</sup> .....	19.3				
Cl <sup>36</sup> .....	19.9				
Cl <sup>37</sup> .....	5.1				
Ar <sup>36</sup> .....	10.1				
Ar <sup>38</sup> .....	3.2				
K <sup>39</sup> .....	17.6				
K <sup>40</sup> .....	23				
K <sup>41</sup> .....	26				
Ca <sup>40</sup> .....	9.8				
Ca <sup>41</sup> .....	25				
Ca <sup>42</sup> .....	13.1				
Ca <sup>43</sup> .....	30.5				
Ca <sup>44</sup> .....	9.8				
Sc <sup>45</sup> .....	38				
Ti <sup>46</sup> .....	34				
Ti <sup>47</sup> .....	49				
Ti <sup>48</sup> .....	16.1				
Ti <sup>49</sup> .....	16.7				
Ti <sup>50</sup> .....	1.56				
V <sup>51</sup> .....	18				
Cr <sup>50</sup> .....	49				
Cr <sup>52</sup> .....	13.2				
Cr <sup>53</sup> .....	12.0				
Cr <sup>54</sup> .....	6.3				
Mn <sup>55</sup> .....	25				
Fe.....			12( $E_n=30$ kev)		
Fe <sup>54</sup> .....	31				
*Fe <sup>56</sup> .....	19.8	15			9.7
Fe <sup>57</sup> .....	36	40			26
Fe <sup>58</sup> .....	10.4	25			16
Co <sup>59</sup> .....	41				

\* Radioactive.

† The references are as follows:

1. Weston, Seth, Bilpuch, and Newson (1960).
2. Bilpuch, Weston, and Newson (1960).
3. Macklin, Inada, and Gibbons (1962).
4. Macklin, Inada, and Gibbons (1963).

TABLE 5—Continued

NUCLEUS	$\sigma_n\gamma$ (60 KEV) CAMERON 1959b	$\sigma$ (25 KEV) CFHZ 1961	$\sigma$ (25 KEV)		$\sigma$ (60 KEV) EXTRAPO- LATED FROM DATA OF CFHZ
			Experiment	Refer- ences†	
Ni.			16( $E_n=30$ kev)		
Ni <sup>58</sup>	40				
Ni <sup>59</sup>	66				
Ni <sup>60</sup>	26	30			19
Ni <sup>61</sup>	52	70			45
Ni <sup>62</sup>	17.1	30			19
Ni <sup>64</sup>	11.7	8.7			5.6
Cu.			39( $E_n=30$ kev)		
Cu <sup>63</sup>	65	115	116, 114		74
Cu <sup>65</sup>	30	47	46, 48		30
Zn.			31( $E_n=30$ kev)		
Zn <sup>64</sup>		87			
Zn <sup>66</sup>	43	66			43
Zn <sup>67</sup>	132	144			93
Zn <sup>68</sup>	34	32	32		21
*Ga <sup>69</sup>	178		93		32
Ga <sup>71</sup>	130		142		92
Ge <sup>70</sup>	107		97		63
Ge <sup>72</sup>	67		75		48
Ge <sup>73</sup>	184		262		169
Ge <sup>74</sup>	46		54		35
As <sup>75</sup>	310	695	740, 650, 600	1	449
Se <sup>76</sup>	143	300			194
Se <sup>77</sup>	430	600			387
*Se <sup>78</sup>	98	300			194
Se <sup>79</sup>	300	600			387
*Se <sup>80</sup>	51	300			194
Br.			650( $E_n=30$ kev)		
Br <sup>81</sup>	330	550			355
Kr <sup>82</sup>	139	330			213
Kr <sup>83</sup>	310	660			426
*Kr <sup>84</sup>	55	300			194
*Rb <sup>85</sup>	340	181	181		117
Sr.	340		155( $E_n=30$ kev)		
Sr <sup>86</sup>	139	140			90
*Sr <sup>87</sup>	290	190			123
*Sr <sup>88</sup>	23	16			10
*Y.	94	18	13.5( $E_n=30$ kev), 13, 28		12
Zr.			14( $E_n=30$ kev)		
*Zr <sup>90</sup>	62	8	11 ± 3( $E_n=30$ kev)	4	5.2
*Zr <sup>91</sup>	174	37	59 ± 10( $E_n=30$ kev)	4	24
*Zr <sup>92</sup>	57	24	34 ± 6( $E_n=30$ kev)	4	15
*Zr <sup>93</sup>	104	53			34
*Zr <sup>94</sup>	30	24	24; 19 ± 4( $E_n=30$ kev)	4	15
Nb <sup>93</sup>	30	264	264( $E_n=30$ kev)		
Mo.			140( $E_n=30$ kev)		
Mo <sup>95</sup>	220	224			145
*Mo <sup>96</sup>	63	217			140
Mo <sup>97</sup>	220	374			241
*Mo <sup>98</sup>	43	300	209, 390		194
Tc <sup>99</sup>	290	660			426
*Ru <sup>100</sup>	99	477			308
Ru <sup>101</sup>	400	880			568
*Ru <sup>102</sup>	70	386	386		249

TABLE 5—Continued

NUCLEUS	$\sigma_{n\gamma}$ (60 KEV) CAMERON 1959b	$\sigma$ (25 KEV) CFHZ 1961	$\sigma$ (25 KEV)		$\sigma$ (60 KEV) EXTRAPO- LATED FROM DATA OF CFHZ
			Experiment	Refer- ences†	
Rh <sup>103</sup> . . .	390	1000	1000	1	646
Pd . . .			454 ( $E_n = 30$ kev)		
*Pd <sup>104</sup> . . .	155	480			310
Pd <sup>106</sup> . . .	560	960			620
*Pd <sup>106</sup> . . .	88	520			536
Pd <sup>107</sup> . . .	410	1040			671
*Pd <sup>108</sup> . . .	61	560	540, 580, 560	1	361
Ag . . .			951 ( $E_n = 30$ kev)		
Ag <sup>109</sup> . . .	380	1000	1200	1	646
Cd . . .			330 ( $E_n = 30$ kev)		
Cd <sup>110</sup> . . .	138	337			218
Cd <sup>111</sup> . . .	480	660			426
Cd <sup>112</sup> . . .	129	324			209
Cd <sup>113</sup> . . .	370	672			434
*Cd <sup>114</sup> . . .	84	290			187
In . . .			763 ( $E_n = 30$ kev)		
In <sup>113</sup> . . .			8500		
In <sup>115</sup> . . .	530	900	805, 980, 600	1	581
Sn . . .			88 ( $E_n = 30$ kev)		
Sn <sup>116</sup> . . .	147	138	92 ± 19 ( $E_n = 30$ kev)	3	89
*Sn <sup>117</sup> . . .	400	258	390 ± 82 ( $E_n = 30$ kev)	3	167
*Sn <sup>118</sup> . . .	118	83	59 ± 12 ( $E_n = 30$ kev)	3	54
Sn <sup>119</sup> . . .	280	230	243 ± 51 ( $E_n = 30$ kev)	3	148
Sn <sup>120</sup> . . .	66	61	35 ± 7 ( $E_n = 30$ kev)	3	39
Sb . . .			436 ( $E_n = 30$ kev)		
*Sb <sup>121</sup> . . .	410	880	950, 810		568
Te <sup>122</sup> . . .	196	700			452
*Te <sup>123</sup> . . .	440	1930			1246
Te <sup>124</sup> . . .	149	363			234
*Te <sup>126</sup> . . .	360	1720			1110
Te <sup>126</sup> . . .	102	245			158
I <sup>127</sup> . . .	480	820	733 ( $E_n = 30$ kev), 820, 800	1	529
Xe <sup>128</sup> . . .	220	470			303
Xe <sup>129</sup> . . .	410	1030			665
Xe <sup>130</sup> . . .	179	227			147
Xe <sup>131</sup> . . .	360	500			323
Xe <sup>132</sup> . . .	103	153			99
Cs <sup>133</sup> . . .	440	900	900		581
Ba <sup>134</sup> . . .	210	337			218
*Ba <sup>136</sup> . . .	310	124			80
Ba <sup>136</sup> . . .	87	105			68
*Ba <sup>137</sup> . . .	92	73			47
Ba <sup>138</sup> . . .	12.3	11.4	11.4		7.4
La . . .			55 ( $E_n = 30$ kev)		
*La <sup>139</sup> . . .	86	50	50, 49		32
Ce <sup>136</sup> . . .			35 ( $E_n = 30$ kev)		
Ce <sup>140</sup> . . .	33	31	31		20
Pr <sup>141</sup> . . .	191	162	115 ( $E_n = 30$ kev), 155, 170		105
Nd <sup>142</sup> . . .	69	150			97
*Nd <sup>143</sup> . . .	107	335			216
*Nd <sup>144</sup> . . .	52	170			110
Nd <sup>146</sup> . . .	175	490			316
Nd <sup>146</sup> . . .	93	236			152

TABLE 5—Continued

NUCLEUS	$\sigma_n\gamma$ (60 KEV) CAMERON 1959b	$\sigma$ (25 KEV) CFHZ 1961	$\sigma$ (25 KEV)		$\sigma$ (60 KEV) EXTRAPO- LATED FROM DATA OF CFHZ
			Experiment	Refer- ences†	
Sm <sup>144</sup>			875 ( $E_n = 30$ kev)		
*Sm <sup>147</sup>	390	320	1173 ± 192 ( $E_n = 30$ kev)	4	207
Sm <sup>148</sup>	230	213	258 ± 48 ( $E_n = 30$ kev)	4	137
*Sm <sup>149</sup>	780	470	1622 ± 279 ( $E_n = 30$ kev)	4	303
*Sm <sup>150</sup>	420	324	370 ± 72 ( $E_n = 30$ kev)	4	209
*Sm <sup>151</sup>	1180	800			516
Sm <sup>152</sup>	440	600	668; 411 ± 72 ( $E_n = 30$ kev)	4	387
Eu <sup>153</sup>	1780	2560			1652
Gd			1175 ( $E_n = 30$ kev)		
Gd <sup>154</sup>	780	710			458
Gd <sup>155</sup>	1630	1560			1007
Gd <sup>156</sup>	530	710			458
Gd <sup>157</sup>	1220	1560			1007
Gd <sup>158</sup>	320	710	710		458
Tb <sup>159</sup>	1240	2280	1850 ( $E_n = 30$ kev)		1472
Dy			775 ( $E_n = 30$ kev)		
*Dy <sup>160</sup>	570	430			278
*Dy <sup>161</sup>	1470	940			607
Dy <sup>162</sup>	320	380			245
Dy <sup>163</sup>	970	840			542
Dy <sup>164</sup>	188	330	330		213
Ho <sup>165</sup>	920	2210	1720 ( $E_n = 30$ kev)		1427
Er			960 ( $E_n = 30$ kev)		
Er <sup>166</sup>	310	500			323
Er <sup>167</sup>	1030	1000			646
Er <sup>168</sup>	200	360			232
Tm <sup>169</sup>	650	1530	1310 ( $E_n = 30$ kev)		988
Yb			575 ( $E_n = 30$ kev)		
*Yb <sup>170</sup>	330	2340			1510
Yb <sup>171</sup>	740	1000			646
Yb <sup>172</sup>	230	486			314
Yb <sup>173</sup>	760	658			425
Yb <sup>174</sup>	161	344			222
Lu			2520 ( $E_n = 30$ kev)		
*Yb <sup>175</sup>	830	2900			1872
Yb <sup>176</sup>	1440				
Hf <sup>176</sup>		2400			
Hf <sup>177</sup>	870	1000			646
Hf <sup>178</sup>	190	456			294
Hf <sup>179</sup>	650	900			581
Hf <sup>180</sup>	133	350	441, 260		226
Ta <sup>181</sup>	800	1300	735 ( $E_n = 30$ kev), 1400, 1200		839
W			270 ( $E_n = 30$ kev)		
W <sup>182</sup>	250	420			271
W <sup>183</sup>	540	1155			746
W <sup>184</sup>	180	350			226
Re <sup>185</sup>	970	2650	2650		1711
*Os <sup>186</sup>	460	3000			1937
*Os <sup>187</sup>	800	3000			1937
*Os <sup>188</sup>	340	1500			968
*Os <sup>189</sup>	670	2000			1291
*Os <sup>190</sup>	240	886	886		572
Ir <sup>191</sup>	760	1000			646
Ir <sup>193</sup>		500			

TABLE 5—Continued

NUCLEUS	$\sigma_{n\gamma}(60 \text{ KEV})$ CAMERON 1959b	$\sigma(25 \text{ KEV})$ CFHZ 1961	$\sigma(25 \text{ KEV})$		$\sigma(60 \text{ KEV})$ EXTRAPO- LATED FROM DATA OF CFHZ
			Experiment	Refer- ences†	
Pt.....			330( $E_n = 30 \text{ kev}$ )		646
Pt <sup>192</sup> .....	330	1000			
Pt <sup>193</sup> .....	530				258
Pt <sup>194</sup> .....	230	400			452
Pt <sup>195</sup> .....	360	700			136
Pt <sup>196</sup> .....	180	210	210		710
Au <sup>197</sup> .....	540	1100	500( $E_n = 60 \text{ kev}$ ) 515( $E_n = 30 \text{ kev}$ ), 1120, 890, 1200, 850 295( $E_n = 30 \text{ kev}$ )	2	
Hg.....					361
Hg <sup>198</sup> .....	220	560			503
Hg <sup>199</sup> .....	430	780			219
Hg <sup>200</sup> .....	270	340			361
Hg <sup>201</sup> .....	370	560			37
*Hg <sup>202</sup> .....	97	57			58
Tl.....			71( $E_n = 30 \text{ kev}$ )		
*Tl <sup>203</sup> .....	143	90			36
Tl <sup>205</sup> .....		60			7.1
Pb.....			3( $E_n = 30 \text{ kev}$ )		1.8
*Pb <sup>204</sup> .....	77	55			3.6
*Pb <sup>205</sup> .....	109	11			0.7
*Pb <sup>206</sup> .....	37	2.8	5.3	‡	1.2
*Pb <sup>207</sup> .....	29	5.5			
*Pb <sup>208</sup> .....	1.88	1.1	0.53	§	
*Bi <sup>209</sup> .....	103	1.8	1( $E_n = 30 \text{ kev}$ ), 1.8±0.7		

† R. L. Macklin, quoted by Clayton (1963).  
§ Estimated by Clayton (1963).

be high ( $\sim 10^9 \text{ }^\circ \text{K}$ ), so that the stellar matter will be bathed in an intense flux of energetic photons as well as neutrons. The neutrons will be thermalized because, at the high densities involved ( $\sim 10^5 \text{ gm/cm}^3$ ), the time interval between successive collisions is short compared to 100 seconds. As a consequence of these conditions a given nucleus will absorb neutrons to an extent which is virtually independent of its neutron-capture cross-section, and neutron capture ceases only when the neutron-binding energy is low enough for equilibrium to be reached between ( $n, \gamma$ ) and ( $\gamma, n$ ) reactions.

The mass value for which this equilibrium condition holds can be found only if the neutron-binding energies are known with precision; BBFH noting that a 10 per cent error in the binding energy causes a 10-fold change in the relative abundance of  $N(A, Z)$  and  $N(A + 1, Z)$ . A 10 per cent change in temperature also introduces a 10-fold abundance change. The abundances are less sensitive to the neutron density.

When the probability of ( $n, \gamma$ ) equals that for ( $\gamma, n$ ), beta decay must occur. If the half life is short compared to a few seconds, the daughter nucleus will

again be capable of absorbing one or more neutrons. This sequence of events continues until the stellar explosion so reduces the temperature and density that the principal ultimate activity is beta decay by the neutron-rich nuclei until stable or long-lived isobars are reached. Since the various reactions are subject to statistical fluctuations, a small spread in  $A$  develops at each mass for which  $(n, \gamma)$  and  $(\gamma, n)$  have equal probability.

Suppose a particular nucleus with a small binding energy for the next neutron is beta active. If its half life is long, its chance of decaying while the neutrons are still present is small. Since it cannot absorb any more neutrons, it may survive until the neutron flux dies out, when it will decay to a stable or long-lived isobar. If the half life is short, decay will take place while neutrons are still present, so the mass number will rise. Therefore, the ultimate abundances of  $r$ -products are proportional to the half lives of their precursors, and it is necessary to know the half lives of nuclei which are rich in neutrons and far removed from the stability region. In the absence of experimental evidence on these half lives, recourse is had to beta-decay theory, which shows that the half life for allowed beta transitions is inversely proportional to  $W^5$ , where  $W$  is the total energy released in the decay. Like the neutron-binding energy,  $W$  must be obtained from theoretical estimates of the masses of the neutron-rich nuclei and of the level structures of the daughter nuclei. To find the masses, BBFH employed a modified form of the Weizsäcker semi-empirical mass formula, the modifications taking into account shell structure, pairing effects, and quadrupole deformation. Becker and Fowler (1959) carried out similar calculations, but were able to improve on the mass formula by virtue of further measurements of nuclear masses in the region between the neutron magic numbers of 80 and 126. This filled the  $A = 150$  to 185 gap in the BBFH calculations with results illustrated in Figure 8. Further improvements in the mass law have been made by Mozer (1959) and by Seeger (1961); these were presumably used by HF and CF. BF, HF, and CF also include the contributions from cycling due to fission. The beta-decay calculations, however, neglected the effects discussed by Bahcall (1961, 1962), and these could have major significance.

The starting nucleus for the  $r$ -process was assumed by BBFH and the other authors to be  $\text{Fe}^{56}$ . The terminal nucleus was calculated by BBFH to be  ${}_{91}\text{Pa}^{265}$ . Fission, both neutron-induced and spontaneous, brings a halt to the growth of heavy nuclei, and leads to cycling for the mass region between  $A = 110$  and the maximum. An especially important result of the  $r$ -process is its contribution to the abundances of the lead isotopes, both directly and via the alpha decay of the long-lived trans-bismuth alpha emitters. The significance stems from the application of these abundances to the problem of the age of the solar system and the Galaxy; a discussion of the Pb abundances will be found in § 4. Here we call attention to the fact that Cameron (1959c) finds a different heavy termination point for the  $r$ -process, and he suggests that the BBFH  $r$ -contributions to Pb, Bi, Th, and U might need extensive revision.

In BBFH and BF, it was assumed that a star proceeds steadily through the *s*-process to a supernova condition in which the  $\alpha$ -,  $e$ -,  $p$ -, and *r*-processes operate on the nuclear species previously synthesized. The neutron source for the *r*-process was taken to be ( $\alpha, n$ ) reactions on  $\text{Ne}^{21}$  and possibly other nuclei. However, Hoyle and Fowler (1960) state that the model of BBFH leads to a 100-fold overabundance of *r*-products. They (1960) offer a new model which proposes a very different source of neutrons and seed nuclei. Briefly, the

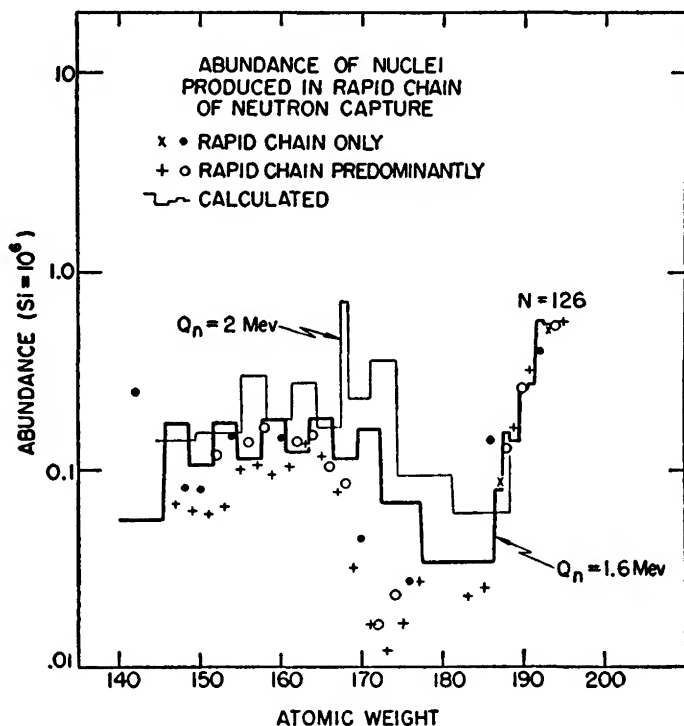


FIG. 8.—Observed and calculated abundance of *r*-product nuclei near  $A = 170$ . From Becker and Fowler (1959).

*r*-process is restricted to small-mass stars ( $\leq 1.5 M_{\odot}$ ).<sup>8</sup> In their final moments such stars are said to reach temperatures ( $T_{\text{core}} = 5.0 \times 10^9 \text{ }^{\circ}\text{K}$ ) and densities ( $\rho_{\text{core}} = 2 \times 10^9 \text{ gm/cm}^3$ ) which lead to the equilibrium process in which the most abundant nuclear type is  $\text{Fe}^{58}$  (not  $\text{Fe}^{56}$ ). The explosion, which follows shortly after this condition is reached, disrupts the entire star, the *e*-products in the core being transformed into alpha particles and neutrons (for example,  $\text{Fe}^{58} \rightarrow 13 \text{ He}^4 + 6n$ ). As the explosion proceeds, the central density falls to  $10^6$ – $10^8 \text{ gm/cm}^3$ , but the temperature stays at the high value of

<sup>8</sup> According to Colgate and White (in press), all stars with masses greater than 1.5 that of the sun explode, the matter ejected from the core being very neutron rich.



$5 \times 10^9$  ° K. Under this condition, a small fraction of the alphas unite to form  $C^{12}$  via the 9.63 Mev level (Fig. 9). The spin of that state, assumed by HF to be  $1-$ , has since been measured to be  $3-$  (Carlson 1961). The principal effect is to reduce the gamma-ray branching ratio. However, HF assumed a radiative width (0.01 ev) which is already much smaller than the experimental upper limit (2.5 ev, Carlson 1961) so their calculated rate of production of  $C^{12}$  is not affected. It would be helpful to have a direct measurement of the radiative width since the element-building process advanced by HF depends on its value.

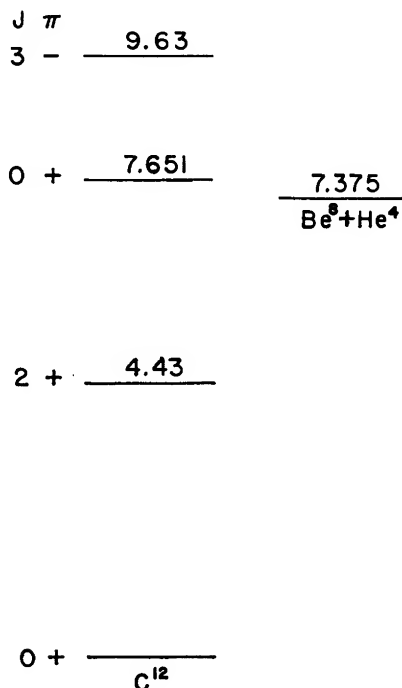


FIG. 9.—Energy-level diagram for  $C^{12}$  in the region of astrophysical interest. Energies are given for each level in Mev. Spins and parities are listed under  $J$  and  $\pi$ .

Assuming that only a small fraction of the helium is converted into carbon, there can then be radiative capture of the remaining helium to build elements up to mass values of 60 or 70. These nuclei serve to absorb the neutrons that were released in the disintegration of the  $Fe^{58}$ . Too large a value of the radiation width of the 9.63 Mev level in  $C^{12}$  would permit conversion of so much of the helium into carbon that the medium-weight seed nuclei needed for neutron capture would not be generated. HF do not consider the possible effects of carbon-carbon reactions or of neutrino-related developments.

The alpha building to  $A = 60$  or  $70$  takes place at high temperature ( $5 \times 10^9$  ° K) and low density ( $10^8$ – $10^6$  gm/cm<sup>3</sup>), and neutron addition commences.

Table 6 lists the nuclei at which  $(n, \gamma)$  competes with  $(\gamma, n)$  so that beta decay occurs; the lifetimes are also given. Beyond  $A = 90$ , the lifetimes become very short, and HF find that some 50 seconds are needed to reach the massive end of the  $r$ -process nuclei ( $A = 270$ ). With a characteristic expansion time of 10 seconds, the radius has increased by a factor of five, the density has fallen by  $5^3$ , and the temperature by a factor of five. It is at this temperature-density combination that the  $r$ -products with  $A > 110$ , namely those which cycle through the fission of the very massive nuclei, are created. In particular, the  $r$ -abundance peaks at  $A = 130$ ,  $N = 82$  and  $A = 196$ ,  $N = 126$  (see Fig. 2) are created. However, HF specifically observe that the lower  $r$ -peak ( $A = 80$ ,  $N = 50$ ) must arise in a supernova explosion in which the neutron flux is much smaller than in the case under discussion. It appears, therefore, that the solar system abundances are due to contributions from a variety of stars in which the nuclear processes were nominally the same but rather different in detail.

TABLE 6  
CHARACTERISTICS OF LONG WAITING POINTS IN THE  $r$ -PROCESS  
(HF 1960)

$A, Z, \dots\dots\dots$	78, 28	79, 29	80, 30	81, 31	84, 32	85, 33	90, 34
Mean Life (sec).	1.04	0.90	12.3	8.96	6.96	4.91	4.50

The foregoing ideas are difficult to make quantitatively satisfactory because of the lack of experimental data on the nuclear events and the uncertainties regarding the theory of supernova explosions. For example, Dicke (1962) and Cameron (1962) assigned the production of  $r$ -products to massive stars, contrary to the view of HF. While Shklovskii (1960) agrees that Type I presupernovae are small-mass stars, the energy he attributes to their explosion is three to four orders of magnitude less than assumed by HF. The available energy naturally strongly affects the nature and extent of element building.

It is interesting to examine the astrophysical observations that bear on the nature of Type I supernovae. A most important point is that the light curves of such supernovae exhibit an exponential decline with time (Baade, Burbidge, Hoyle, Christy, and Fowler 1956; Burbidge, Hoyle, Burbidge, Christy, and Fowler 1956; BBFH; Zwicky 1958). That phenomenon has been attributed to the transformation of the energy of radioactive decay into the visual wavelength region. From the half life, and considerations of energy release, BBFH and HF among others suggested that the substance primarily responsible for the observed decay is  $\text{Cf}^{254}$ , an  $r$ -product with a half life corresponding to the time scale of the supernova decline. This point of view does not have universal acceptance. Gordon (1960), for example, cites the inconsistency between the  $\text{Cf}^{254}$  hypothesis and the wide range of half lives of the luminosity decline of Type I supernovae. He gives the range as from 18.8 days (S Andromedae) to  $> 300$  days

(supernova in NGC 1003). He emphasizes that the optical spectra may be closely similar despite large differences in half life, the explosions in IC 4182 ( $t_4 = 55$  days) and NGC 1003 being given as particular illustrations. Moreover, while some Type I supernovae light curves exhibit an exponential decline after the initial outburst, this is sometimes followed by a relatively constant light output after which an exponential decline recurs (Kulikovskii 1944). This feature cannot be explained in terms of the  $\text{Cf}^{254}$  decay.

Gordon (1960) and Zwicky (1958) question whether the radioactive energy can be responsible for various observations. Thus Zwicky emphasizes the problem, described by BBFH, of efficiently converting the energy of radioactive decay into visible light. He suggests that the blue light, which alone demonstrates the exponential decay, represents but a tiny fraction of the total optical output, the bulk of which does not decline exponentially. Much energy must be present in the form of magnetic fields and thermal motion which do not follow an exponential decay. Anders (1959), however, finds that supernova energy can be efficiently transformed into blue light. Gordon argues that a radioactive origin of the light curves requires the radiation to be thermal. In fact, Type I supernovae are known to be strong sources of synchrotron radiation, presumably arising from relativistic electrons ( $10^{11}$ – $10^{12}$  eV per electron). If such radiation is thermal in nature, Gordon finds that impossibly large masses (e.g.,  $160 M_{\odot}$  for the envelope of Z Centauri) are needed.

Considering the synchrotron radiation, Gordon notes that the electron energies are far too great for them to result from radioactive decay, contrary to Woltjer's (1958) suggestion, and that synchrotron losses preclude the electrons from having been energized in changing magnetic fields. His conclusion is that the energetic electrons must result from a secondary process following upon the magnetic acceleration of protons to appropriate energies. If the electrons arise from the collisions of protons with protons, in the same way in which  $\pi$ -mesons are created, the exponential decline in light output follows directly from the exponential decline in the number of  $p$ - $p$  collisions as the supernova envelope expands. By varying the rate of expansion, any half life to the dying light can be reproduced.

It seems unlikely that Gordon's approach is correct. The production of electrons in  $p$ - $p$  interactions has an extremely small cross-section relative to that for creating  $\pi$ -mesons, since the former process takes place only through the (weak) electromagnetic field while the latter depends on a (strong) nuclear field. Hence, the analogy is not satisfactory. Also it is not clear why the energetic electrons cannot be accelerated in magnetic fields. If the field is weak, but extensive, the radiation losses need not be serious.

Another problem is that HF propose that the residue of a Type I supernova should be highly deficient in hydrogen, the hydrogen in the envelope of the dying star being consumed in the explosion. However, Woltjer (1958) found that the H/He ratio in the Crab is possibly half normal, and this indicates an

excess of hydrogen on the HF model. That the  $r$ -process *can* produce trans-bismuth elements has been demonstrated in the explosion of H-bombs (Hui-zenga and Diamond 1957; Cameron 1959e).

2.1.6. *The  $p$ -process.*—The  $p$ -process was suggested by BBFH as a means of explaining the existence of those stable nuclei which are bypassed in the neutron-capture reactions. For example, Figure 7 shows that  $\text{Te}^{120}$  cannot be generated by neutron capture by the lighter nuclei. According to BBFH,  $\text{Te}^{120}$  probably originated in the double sequence  $\text{Sn}^{118}(p, \gamma) \text{Sb}^{119}(p, \gamma) \text{Te}^{120}$ , or  $\text{Te}^{122}(\gamma, n) \text{Te}^{121}(\gamma, n) \text{Te}^{120}$ . Since many of the proton-rich nuclei in the same category as  $\text{Te}^{120}$  have rather large  $Z$ -values, the proton-capture sequences are expected to be infrequent, and, in actual fact, the relative abundances of such nuclei are generally much smaller than those of the neutron-richer isotopes. In addition, the intermediate nuclei invariably have short half lives,  $\text{Sb}^{119}$ , for example, decaying to  $\text{Sn}^{119}$  with a half life of 38 hours and  $\text{Te}^{121}$  decaying to  $\text{Sb}^{121}$  with a 17-day half life. Consequently, the captures must occur on a rapid time scale, probably in a supernova explosion.

Frank-Kamenetskii (1958, 1959, 1961) calls this the weakest point in the theory of element synthesis. At the temperatures involved ( $T \sim 10^9$  °K), he asserts that the reactions are reversible so that thermodynamic equilibrium among the bypassed nuclei and their near neighbors is rapidly reached. Therefore the abundances should show a smooth variation with neutron-binding energy for all nuclei containing the same number of neutrons, and Frank-Kamenetskii asserts that this condition has decidedly not been established.

As an alternative he has proposed that virtually all the bypassed nuclei can be created by single  $(p, 2n)$  reactions, with proton energies in excess of 10 Mev. These energetic protons are said to be due to electromagnetic acceleration processes in stellar atmospheres. Thus, his suggestion is similar to that employed in another connection (see below) by FGH, FBB, and BP, but has the additional interesting feature of providing a source of neutrons which might give rise to the iron-abundance peak, avoiding the  $e$ -process. One might expect on this basis that the  $p$ -process isotopes would be extremely rare since their source would be in a thin layer in stellar atmospheres rather than in the massive interiors.

## 2.2. CONCLUDING REMARKS ON SOLAR ABUNDANCES

Simply stated, there is not now any clear understanding of the specific events which led to the formation of the nuclear species in the solar system. The various and conflicting calculations by various authors suffer badly from our ignorance of the following factors: (1) the actual abundance distribution of the nuclear species; (2) nuclear reaction rates for numerous possible processes; (3) neutron absorption cross-sections; (4) a host of astrophysical matters which may conveniently be grouped as stellar formation, evolution, and decline on the one hand and the life history of the Galaxy on the other.

Further efforts to understand element formation will be aided by a useful

compilation prepared by CF in the spirit of BBFH. That compilation gives the amount of each nucleus which, according to Fowler and his associates, originated in the  $s$  or  $r$  process. These have been included as the last two columns of Table 1. Although there is no guarantee that any of those assignments are correct, they can still serve as a guide to new research. We have mentioned earlier that Fowler has revised the conclusions of Clayton and Fowler as regards the tin isotopes. Fundamentally, however, it is imperative to have more measured numbers before any quantitative reliance can be placed on the theories of element formation.

### 2.3. INTRODUCTION TO ANOMALOUS ABUNDANCES IN STARS

Much experimental evidence exists to show that element abundances are not the same from star to star. Thus Wilson (1960*a*) asserts that main-sequence K stars have a range of metal/hydrogen content of a factor of 100, and Preston (1961) has found RR Lyrae stars to vary in metal/hydrogen ratio from normal to 0.2 per cent of normal. In the magnetic A stars, certain metals are anomalously enhanced (Babcock 1958) and a careful study of oxygen in those stars (Sargent and Searle 1962*a*) gives an underabundance of up to 100 times. A general distinction can be drawn between halo stars on the one hand and stars of the disk and spiral-arm population on the other (Baade 1958*a*), in that the former appear to have substantially smaller metal/hydrogen ratios than the latter (see below). Beyond this finding there are stars which contain anomalous, i.e., non-solar abundances in particular elements, and the anomaly is often used to denote the star. Thus, there are helium stars, carbon stars, heavy-metal stars, silicon stars, and so forth. Numerous attempts have been made to explain these anomalies in terms of nuclear events. However, no completely satisfactory discussions have yet been presented. Part of the reason for this is that the data themselves are not always conclusive. The transition from observations on an optical spectrum to element abundances is made on the basis of educated guesses on the properties (temperature, electron pressure, turbulence, etc.) of the stellar atmosphere; oscillator strengths, partition functions, and atomic energy-levels for atoms and ions not yet thoroughly examined under laboratory conditions; and the conditions under which light is emitted and absorbed. As has been clearly pointed out by Aller (1962), the stellar spectrum can, at best, give information on the elements present in a star's atmosphere and this need not be indicative of the bulk of the stellar mass. Indeed, we can be sure that the stellar core will have been altered from the atmospheric (presumably original) composition by the reactions which generate energy and neutrons, so that a rather detailed calculation, involving the star's initial composition, age, and mass, is needed to determine the actual abundance distribution at any instant of time.

So far as the atmosphere of a star is concerned, it is often thought that abundance anomalies are evidence of special nuclear phenomena which occur only at the stellar surface. However, this viewpoint is not universal and the

subject of element anomalies is no better understood than is that of normal element abundances. It is unlikely that a clear understanding of stellar abundances will develop before those in the sun itself have been properly elucidated. Because of the countless uncertainties, the present review will consider only a few illustrative examples of the work in the field. Good reviews of the characteristics of anomalous stars have been written by BBFH, Burbidge and Burbidge (1958), Aller (1961), and Burbidge (1963). Aller (1961), in particular, has critically examined the data on which the abundance determinations are predicted. It should be kept in mind that anomalous stars taken together constitute but a tiny fraction of the stars in the Galaxy.

#### 2.4. ABUNDANCES IN GLOBULAR AND GALACTIC CLUSTERS

One curious feature of the Galaxy is the absence of stars with atmospheres of pure hydrogen or of hydrogen plus only the immediate products of the  $p$ - $p$  chain. Assuming the Galaxy has a finite age and that it actually began as hydrogen gas, such stars ought to exist. The closest approximation to this condition can be found in globular clusters and in high-velocity stars (Eggen, Lynden-Bell, and Sandage, 1962).

These objects, located in the galactic halo, generally show deficiencies in the metals, the range of metal content being from near normal to an underabundance of some hundreds or even a thousand times. Evidence for the high-metal end of this range comes from Morgan (1956), Sandage and Wallerstein (1960), Feast and Thackeray (1960), and Aller and Faulkner (1964). The cited work shows that 47 Tucanae and NGC 6356 have normal metal abundances. Morgan (1959*a*) observes that NGC 6528 and NGC 6553 have considerably stronger absorption in the blue-green spectral region than NGC 6356, implying excessive metal content for the two former clusters. Going down in metals, there is M13, a globular cluster with an age of  $10^{10}$  years (Baum, Hiltner, Johnson, and Sandage 1959) with a twenty-fold deficiency of the heavy elements (Helfer, Wallerstein, and Greenstein 1959).

The high velocity stars are undeniably metal poor, as shown, for example, by the work of Chamberlain and Aller (1951), Schwarzschild, Schwarzschild, Searle, and Meltzer (1957), Wallerstein and Helfer (1959*b*, 1961). Wilson (1959), Heiser (1960), Kron and Gordon (1961), and Thackeray (1962). The strong correlation between increasing distance from the galactic center of high space velocity and decreasing metal abundance has been demonstrated by numerous workers since Mayall (1946) noted that clusters of late spectral type are concentrated near the galactic center. Subsequent studies by Morgan (1956), Baade (1958*b*), Kinman (1959), Eggen and Sandage (1959), Merrill, Deutsch, and Keenan (1962), and ELS confirm the above-mentioned connection between metal abundance and galactic position and/or velocity. Occasional high-velocity stars are seen with normal metals (Greenstein, Hack, and Struve 1957), but these are sometimes discussed as runaway Population I stars (Feige 1958).

Complications such as a normal H-metal ratio but excessive He and C (Wallerstein, Stone, and Williams 1962) or greater deficiencies in C and N than in the metals (Greenstein and Keenan 1958) are also to be found.

Additional information on globular clusters is provided by observations on the Magellanic clouds. Johnson (1959) found He/H to be normal in LMC, and Hodge (1960*a, b*) obtained color-magnitude plots for globular clusters in LMC which were similar to those for the metal-normal cluster NGC 6356, suggesting that the metals are normal in LMC. Aller and Faulkner (1961) ascribe chemical normality to both clouds. There may be some uncertainty concerning the small cloud since Arp (1960) reports that the SMC cepheids are metal poor. This is disputed by Feast (1960), Feast, Thackeray, and Wesselink (1958, 1960), and Feast (1962). Arp and Kraft (1961) suggest the SMC cepheids are intermediate between Population I and Population II. This problem is further discussed in IAU Symposium No. 20 (Kerr and Rodgers 1964). The Andromeda Spiral also contains metal-poor Population II and metal-normal Population I stars (Baade 1958*a*).

There does not appear to be any intrinsic physical feature of globular clusters or of high-velocity stars that requires them to exclude the metals when they form. The most frequent explanation of the metal poverty of the Population II stars is that they are so old that they condensed before the Galaxy had had time to create many of the heavy metals (Baade 1958*a*). Indeed, the absence of metals from the Population II stars is cited as evidence for the chemical evolution of the Galaxy. Assume for the moment that this is true. It would then be instructive to know whether those few metals which are present in Pop II stars are *r*-products, as implied by Cameron (1962) and Dicke (1962), or *e*-products, as implied by Hoyle and Fowler (1960). It would be interesting to know whether the globular clusters contain uranium or thorium, since all isotopes of these elements are *r*-products and should be absent from the Pop II stars according to HF. Of course, data on isotopic compositions would also be decisive, but these are virtually impossible to obtain. The connection between stellar age and chemical composition is discussed below.

Another special feature of the globular clusters is that they are largely devoid of gas and dust. Even though some cluster stars have undoubtedly disintegrated over the aeons, there is little sign of debris from which new, perhaps massive, stars could be born. Osterbrock (1960) has seen some gas in a globular cluster, and Morton has suggested that the dust can be important. In addition, some B stars have been observed (Traving 1962).

The B stars in globular clusters also seem to have normal helium content (Traving 1962). Wallerstein (1959) has presented a shock-wave theory to interpret the spectra of Pop II cepheids. According to his theory, helium could well be normal in globular clusters. Since the helium allegedly derives from hydrogen burning, it is not easy to see how old stars born of essentially pure hydrogen could have a large helium abundance in their atmospheres unless the stars have

gone through a complete evolutionary sequence. This sequence must include the expulsion of helium from the cores of the original stars so that, on recondensation into new stars, the helium may become prominent in the atmospheres. Now the burning of hydrogen in the  $p$ - $p$  chain is very slow. Times of the order of  $10^9$  years characterize the mean life of a proton in the  $p$ - $p$  chain, so a long time must have passed before the hydrogen-pure stars could have generated a normal helium abundance. This we believe to be inconsistent with the evolutionary picture often given (Fowler 1961). Moreover, if hydrogen burning has occurred to the extent that normal helium abundances have resulted in the Pop II stars, the heavy elements should also be essentially normal, and this contradicts the observations. Thus it may be that the abundance distributions in the Pop II stars are *not* due to a chemical evolution of the Galaxy. There is the further problem that the planetary nebulae, which appear to be Population II objects, also seem to have normal helium abundance (Wyse 1942; Aller 1957; Mathis 1957 *a, b*, 1961; Osterbrock and Rogerson 1961). Aller (in press) has found a mean (He/H) ratio of  $0.165 \pm 0.005$  for some 40 planetary nebulae in good agreement with results of O'Dell. O'Dell, Kinman, and Peimbert (1964) find that in the planetary nebula in the globular cluster M15, oxygen is depleted with respect to hydrogen, although the He/H ratio is normal. We reiterate that a large (He/H) ratio for such old structures is puzzling if all helium has been produced from hydrogen in stellar interiors.

The galactic clusters, of which a few hundred are known in the Galaxy, are very different from the globular clusters. They are often closely associated with nebulosity, contain numerous young stars which are both bright and over-luminous, have normal metal compositions, are concentrated in the galactic disk, and have a spread in age from very old to rather young. Since the young metal-rich O and B stars are always formed in clusters (or associations) (Roberts 1957), it is tempting to attribute their metal content to a gradual galactic enrichment in the metals. Nonetheless, it is disturbing that a very old galactic cluster, like NGC 188, with an age of  $16 \times 10^9$  years (Sandage 1961) has a metal content (Wallerstein 1962*a*) essentially identical with that of the young Scorpio-Centaurus association (age =  $2 \times 10^7$  years, and abundances normal, Bertiau 1958; Traving 1955; Aller, Elste, and Jugaku 1957). Again, M67 (age =  $9 \times 10^9$  years, Hoyle 1959), Hyades (age =  $10^9$  years, Sandage 1957), and, of course, the sun (age =  $5 \times 10^9$  years, see sec. 4.2) have normal abundances (for Hyades, see Parker, Greenstein, Helfer, and Wallerstein 1961). Mathis (1957*a, b*), Aller (1957), Aller and Liller (1959), and Seaton (1960) have also demonstrated that the planetary nebulae have about the same helium abundance as the young Orion Nebula. Numerous writers, among the latest being Sandage (1962) and Wallerstein (1962*a*), have concluded that *the chemical abundances of stars in the galactic disk are independent of stellar age*. Eggen (1959) has made a similar point concerning stars in the Large Magellanic Cloud. Stars



in the galactic halo are certainly deficient in the metals, but this may *not* be connected with their age or with chemical evolution of the Galaxy.

On the last point, Heiser (1960) has suggested that the high-velocity star HD 25329, which he has found to be metal poor, might have this property solely because uncondensed matter far from the galactic plane lacks metals and that the star formed in that region. Abt (1960) made the same suggestion after a study of supergiants which are deficient in *s*-products. Wallerstein (1962*a*), analyzing the abundances, velocities of G dwarfs, and Arp (1962), considering the constitution of NGC 752, NGC 2158, and NGC 7789, offer the same idea. Implicit in these remarks is the suggestion that the metals are somehow concentrated near the galactic plane, rather than that the galactic metal/hydrogen ratio is growing with time. Van den Bergh (1961) and Dicke (1962) also propose that the heavy metal content of the Galaxy has not changed appreciably with time.

We may ask what physical features could produce a chemical fractionation of the observed nature. At least two effects could be important. Firstly, it is obvious that gravitational attraction is more effective in restricting the heavy elements to the plane than in confining hydrogen and helium thereto. If one thinks in terms of matter escaping from the disk to high latitudes, the light nuclei in the energetic tail of the Maxwell distribution are more easily lost than are the heavy elements. However, it is difficult on this picture to understand how the escaping gas could reach the densities which are essential for gravitational instability to occur. Moreover, it would appear that an enormous fraction of the original galactic mass would have escaped into intergalactic space. Since the Milky Way Galaxy is, in fact, one of the most massive to be seen, it seems rather unlikely that it could have lost any appreciable amount of mass. Münch and Zirin (1961) have given reasons for thinking that the evaporation of an ionized gas cloud could occur, aided by magnetic fields. We argue below that this has not happened.

Eggen, Lynden-Bell, and Sandage (1962) deduce that the Galaxy condensed in a time of the order of  $10^8$  years from a much larger volume than it now occupies. The gravitational effect mentioned above was operative and tended to leave the light elements behind. This effect, we suggest (Bashkin 1963), has been strongly enhanced by another, as follows. It is suggestive that the ionization potentials of the metals, and heavy elements generally, range from 5 to 7 or 8 electron volts, while the light elements have ionization potentials from 12 to 25 ev. Let us suppose that a low level of ionization existed in the nascent Galaxy, and that a weak magnetic field was present. The metals would be ionized to a far greater extent than hydrogen and helium. As a consequence, the metals were trapped around the magnetic field lines, whereas the neutral atoms were not, and the metals spiraled inward as the Galaxy collapsed under gravity. As the collapse proceeded, and the rate of star formation rose, the level of ionization increased because of the increased radiation, and the easily ionized atoms became more

and more restricted in their motions. Thus, the matter in the galactic disk became enriched in the metals relative to the halo. Since the halo stars are deficient in the metals, we suggest that the Münch and Zirin evaporation mechanism for ionized matter has not been operative.

We may conclude further that there are not now any unambiguous data to support the view that the over-all chemical content of the Galaxy is any different today from what it was at the birth of the Galaxy. Certainly elements are transmuted inside stars, and probably certain long-lived radioactive species ( $K^{40}$ ,  $Rb^{87}$ ,  $La^{138}$ ,  $Sm^{147}$ ,  $Lu^{176}$ ,  $Re^{187}$ ,  $Pt^{190}$ , Th, U) have been regenerated from time to time, but it seems that the evolution of stars can destroy, as well as create, the heavy elements. On this basis, it is reasonable to assume that old galactic clusters have the same heavy-element content as young ones and that the Population II stars are richer in helium than expected on the evolutionary argument. The chemical composition with which a star is formed may well be essentially independent of the time of formation of the star.

To achieve an over-all chemical equilibrium in the Galaxy, the reactions taking place in supernova explosions must be capable of converting some heavy elements into light ones. This is not at all impossible. The theories of Hoyle and Fowler, discussed earlier, show how helium can be liberated from heavy elements in the  $e$ -process, and there must also be a subsequent production of free neutrons, some of which will decay to protons. It is possible, therefore, that a better analysis of the course of supernova reactions will show in detail how the chemical equilibrium can be maintained. Our conclusion is that the initial substance of the Galaxy was quite possibly identical with what is now present. This makes reasonable, also, Morgan's finding (Morgan 1959*b*) that most external galaxies are metal normal. Indeed, it is tempting to revive the big-bang theory, with modifications involving the  $r$ - and  $p$ -processes on hydrogen to make  $He^4$  quickly, and the three-alpha process to make  $C^{12}$ . Thereafter the various reactions previously discussed could operate to synthesize the elements.

## 2.5. ANOMALOUS STARS

Turning to particular unusual stars, only a few have been selected for discussion. These stars show extreme deviations from normality and offer a good testing ground for the theories of nuclear effects in stars. One must, however, be constantly aware of the perplexing problem that stars which are similar in many respects may show quite different abundances for certain elements. Thus, Sargent and Searle (1962*c*) have shown that some A stars of like colors and absolute magnitudes differ considerably in their O/Mg ratios, and they remark that the abundance anomalies in Am and A pec stars cannot have the same origin. Also, the classification of stars is not always certain. For example, Bless (1960) interprets the Am stars as F stars deficient in calcium, rather than as metallic-line A stars. Underhill (1959) disputes the finding by Swings and Struve (1940) that 9 Sagittae is a carbon star. Unfortunately, there are a number of

classification discrepancies, and these obviously impede analysis which must take the observations at face value.

2.5.1. *R Coronae Borealis*.—This star is a supergiant variable with a carbon/metal ratio 25 times normal and a carbon/hydrogen ratio  $10^4$  times normal (Berman 1935; Searle 1961). The O/metal and N/metal ratios are normal (Searle 1962). Searle hypothesizes that this star is the core of a once-massive Population II star which lost its envelope, thereby exposing a region heavily contaminated by carbon from the three-alpha process. Presumably, neutrons were also set free at some time in the past, and these were absorbed by light nuclei to generate the heavy metals. One might expect such a star to be rich in He, O, and Ne; data on the inert gases are lacking. Aller (1961, 1962) suggests that the R Cr B stars may be fundamentally similar to other hydrogen-poor stars which show large He/H ratios and considerable variability in the C, N, and O abundances. They are also lacking in  $C^{13}$  (Shajn and Hase 1954). Aller (1961) treats this subject extensively.

2.5.2. *Some G-type sub-dwarfs*.—An extensive study of abundances in G dwarfs has been carried out in a series of papers (Wallerstein and Helfer 1959*a*, *b*; Helfer, Wallerstein, and Greenstein 1960; Parker, Greenstein, Helfer, and Wallerstein 1961; Wallerstein and Helfer 1961; Wallerstein 1962*a*). Several sub-dwarfs of type G and A have been studied by Baschek (1959) and by Aller and Greenstein (1960), on which we now comment briefly. Some of Wallerstein's conclusions have been mentioned above.

The data prove that the metals are not present to the same relative degree in the various stars. Thus, manganese, which BBFH attribute to the  $e$ -process, is often deficient, the Mn/Fe ratio decreasing as the iron content falls. A tentative explanation given by Wallerstein (1962*a*) is that the  $e$ -process temperature was slightly lower than that at which the solar  $e$ -elements were prepared. Wallerstein notes that the absence of abundance data on vanadium and cobalt, which are also  $e$ -products, makes this explanation uncertain. The neutron-capture cross-section given by BBFH for Mn is as much as two orders of magnitude higher than for V, but half that for Co. Consequently the Co and V abundances should be instructive as regards neutron fractionation effects.

Mg, Si, Ca, and Ti, all of which have some alpha-particle isotopes, are overabundant in seven iron-poor stars, and reasons are given for believing that these four elements represent a special anomaly. Using the treatment of BBFH, Wallerstein (1962*a*) finds that the alpha process is responsible and that the alpha-process time scale is about 1000 years, as first suggested by BBFH. It is unfortunate that data on sulfur and argon are not available, since the alpha-capture hypothesis requires them also to be overabundant. Again one can see the utility of knowing isotopic ratios, since each of the four elements concerned has several stable isotopes, only one of which can have an alpha-particle character. Finally, the alpha process depends on having enough  $Ne^{20}$  so that the reaction  $Ne^{20}(\gamma, \alpha) O^{16}$  can provide the alphas. Wallerstein (1962*b*) raises the

possibility that the non-resonant character of the reaction  $O^{16}(\alpha, \gamma) Ne^{20}$  might mean that the alpha process cannot take place, and a different source of alpha particles must be provided.

**2.5.3. Magnetic stars.**—Babcock (1960*a*) summarized the data on magnetic stars and included a discussion of the anomalous chemical abundances which are a common feature of such stars. Sargent and Searle (1962*a*) have published a careful study of the oxygen abundance in A pec stars. The essential features of these stars are an overabundance of such elements as Si, Mn, Cr, Sr, and Eu in various combinations and a dearth of oxygen. The oxygen deficiency is pronounced in stars having excessive amounts of Cr, Sr, or Eu. Since these stars have magnetic fields, various attempts have been made to explain the anomalies in terms of surface nuclear reactions initiated by protons accelerated magnetically to high energies (e.g., Fowler, Burbidge, and Burbidge 1955). FBB require spotty magnetic fields of the order of  $10^6$  gauss, whereas the highest general field so far seen in any star is  $3.4 \times 10^4$  gauss (Babcock 1960*b*). Curiously, the star with this magnetic field has a normal spectrum, and Babcock states that the evidence for a nuclear *cum* magnetic origin for the anomalies is hardly conclusive. A similar attitude is adopted by Bidelman (1962*a, b*). Sargent and Searle looked into the possibility that the oxygen is deficient because it was destroyed in surface nuclear reactions and that the fragments were combined to produce the observed overabundances. However, the processes invoked did not appear to the authors to be satisfactory. Bidelman (1962*a, b*) proposes that the overabundances were actually present in the matter out of which the A pec stars themselves formed and that surface interactions have at most modified a more fundamental peculiarity. He further postulates that the A pec stars are in a *late* stage of development, passing from the Population I red giant phase to the white dwarf phase.

Objections to the idea of peculiar abundances in prestellar matter are based on the fact that A pec stars may belong to clusters or associations the other members of which are normal. How element separations, and particularly of the kind observed, could arise has not been explained. We propose the following solution to the problem of the A pec stars.

In the A stars many of the elements (metals) observed to be overabundant are ionized. Assume that the A stars lose an appreciable portion of their atmospheric matter in a stellar wind. Because of the magnetic field, the ionized elements will be prevented from escaping from the star. On the other hand, elements like hydrogen, nitrogen, oxygen, and the inert gases are largely neutral in the A stars, and are therefore not constrained by the magnetic field. It is possibly for this reason that oxygen is deficient in stars showing excess Si, Cr, Sr, or Eu, since these elements have ionization potentials of 8.15, 6.77, 5.69, and 5.67 ev, respectively, and are ionized at relatively low temperatures. On this basis, one can predict that these stars will also be found lacking in nitrogen. On the other hand, stars with excess Mn (I.P. = 7.4 ev) may have normal oxygen

according to Sargent and Searle (1962*a*). These stars also seem to be hotter and have weaker magnetic fields than those with excess Cr, Sr, or Eu. Thus, the normality of oxygen may be due to a more uniform loss of matter of all kinds in the stellar wind. For HD 215441, the star with a field of 34,000 gauss, the spectral class is A0p. It may be so hot that all elements are ionized and have been retained magnetically. The mean surface temperature is about 1 ev.

On this picture it is not so hard to see how stars of a given association can have rather different compositions. If magnetic fields occur, they may either retain in, or exclude from, a given volume of space elements which are ionized. Hence, even small fluctuations in magnetic field and in ionization level may combine to produce marked chemical disparities from star to star.

2.5.4. *Manganese stars and 53 Tauri*.—53 Tauri is a well-studied example (Aller and Bidelman 1964) of a manganese-rich star. It is sharp-lined and shows excess amounts of Ga (100 times normal), C (2–3 times), Mn (16 times), Sr (13 times), Y (12 times), and Zr (15 times). Underabundances exist for Mg (5

TABLE 7  
Log<sub>10</sub> ELEMENT ABUNDANCES BY NUMBER OF ATOMS IN 3 CENTAURI A  
(JSG 1961) AND THE SUN (GMA 1960)

Element ...	H	He*	Be	C	N	O	Ne*	Mg	Si	P	S	Ar*	Ca	Fe	Ni	Ga	Kr*
3 Cen A...	12.0	10.4	≤ 6.3†	8.5	8.8	7.9	8.6	7.3	7.5	7.4	< 6.30	7.0	5.8	7.2	5.4	6.3	6.3
Sun.....	12.0	11.2	6.3	8.72	7.98	8.96	8.7	7.40	7.50	5.34	7.30	6.9	6.15	6.57	5.91	2.36	3.2

\* Quoted in JSG 1961.

† Jugaku and Sargent 1962.

times), Ca (13 times), Cr (8 times), and Fe (twofold). Oxygen is normal and silicon may be so (Sargent and Searle 1962*b*). No interpretation of these peculiarities has been offered. Since both the overabundant and deficient elements include species with low ionization potentials, the analysis proffered in § 2.5.3 appears inapplicable. More detailed quantitative studies of this star are currently in progress.

2.5.5. *3 Centauri A*.—One member of the young (age  $\approx 2 \times 10^7$  years) Scorpio-Centaurus association, 3 Cen A, is rich in He<sup>3</sup> (Sargent and Jugaku 1961) and has been identified as a phosphorus star (Bidelman 1960*a*). The star is sharp-lined, class B5 IV, and has a magnetic field not exceeding 200 gauss and probably zero (Babcock 1962). An abundance analysis by Jugaku, Sargent, and Greenstein (1961) gives the results summarized in Table 7. In addition, Be is not overabundant (Jugaku and Sargent 1962).

These data must be interpreted so as to be consistent with the fact that one other member of the association ( $\tau$  Scorpii) has normal abundances (Traving 1955; Aller, Elste, and Jugaku 1957).

The complications that attend accounting for the abundances in 3 Cen A are evident on comparison with  $\alpha$  Sculptoris (Jugaku and Sargent 1961). This is a B4 V star, also sharp-lined, but its chemical anomalies (excess Cr, Ti, Sr,

deficient He, O, weak C II and N II lines, no P) are quite different from those of 3 Cen A despite the similar spectral class of the two stars. Again, the sharp-lined B 8 star,  $\kappa$  Cancrī, differs from 3 Cen A, and Bidelman (1960*b*) calls attention to the unsatisfactory nature of an explanation of the  $\kappa$  Cancrī anomalies based on surface nuclear reactions. Possible sources of the abundance anomalies in 3 Cen A are:

1. 3 Cen A may be the remnant of a once-massive star so that evolution proceeded very rapidly (Greenstein 1962). However, there is no direct evidence for such a development nor is it clear that rapid evolution would produce the observed anomalies. Also, the same idea has been advanced to account for R Coronae Borealis (see above), the abundance anomalies of which are decidedly different from those of 3 Cen A.

2. Surface reactions involving the acceleration of protons to high energies destroyed the original normal constitution (JSG; Wallerstein 1962*c*). An objection to this is that the accelerations presumably depend on strong magnetic fields, whereas 3 Cen A has no observable field. Also, to convert most of the He<sup>4</sup> (10 per cent of the original atoms) to He<sup>3</sup> implies that the C, N, and O would be decimated, as, indeed, would be the He<sup>3</sup> itself (Bashkin and Middlehurst 1962), so that the net result would be only hydrogen and perhaps He<sup>4</sup>. Burbidge and Burbidge (1958) use data from H-bomb explosions to argue that surface stellar reactions would create overabundances of Cr and Mn at the expense of iron. While data on Cr and Mn in 3 Cen A are not available, Fe is actually overabundant by a factor of 4.

3. Heavy ion collisions in the surface are responsible. JSG show this to be highly unlikely.

4. Reactions induced by fast neutrons (JSG). In the first place, it is not easy to generate these neutrons; secondly, the neutrons would rapidly decelerate to thermal energies because of collisions with hydrogen. JSG remark that other anomalies might be expected from fast neutrons, but are not present.

5. An abbreviated rapid process (JSG quoting W. A. Fowler). This, like the other suggestions, has not yet been put in quantitative form, nor has the question been answered as to how this process started and stopped in such striking contrast to the usual  $r$ -process developments. It would be interesting to know if 3 Cen A has an overabundance of U and Th. We note that there is an abundance of H, He<sup>3</sup>, and N, all of which are effective neutron poisons, presenting difficulties for both (4) and (5).

6. The  $p$ - $p$  and CNO cycles operated, but never came close to equilibrium. This would account for the anomalous abundances of He<sup>3</sup>, He<sup>4</sup>, N, and O. However, SJ and Greenstein (1962) reject this because rapid mixing from the interior to the surface is needed and because the star is luminous enough to imply that these reactions would actually approach equilibrium very quickly. Also, they offer no way of accounting for the other anomalies, as with Ga and Kr.

7. Local fluctuations in the matter out of which Scorpio-Centaurus formed (Bashkin and Middlehurst 1962; Burbidge 1963). Since 3 Cen A and  $\tau$  Sco are now, at least, at almost opposite edges of the association, the apparent chemical normality of the latter need not imply normality for the former. It is difficult to make this interpretation quantitative.

We conclude that there is not now any quantitatively—or even qualitatively—satisfactory explanation of the anomalies in 3 Cen A.

2.5.6. *Other stars.*—There are many other stars that exhibit abundance peculiarities. Thus Przybylski (1963) has identified one star, HD 101065, as iron poor and holmium rich! Aller and Bidelman (Aller 1963) have found a large overabundance of iron and chlorine in HD 168733. Aller (1963) emphasizes the wide variation in relative abundances from star to star. It seems likely that highly individual factors enter into star formation, and general principles alone are not adequate to explain the observations. The situation is complicated by observational uncertainties. For example, Deutsch (1963) has pointed out that the inclusion of Rayleigh scattering in the opacity calculations for Mira stars reduces the presumed metal deficiency from a factor of *one hundred* to one of *three!*

These sources of opacity are taken into account in more recent calculations of atmospheric models (see, e.g., the illustrative graphs [Aller, 1963, pp. 255–260] and the discussion by Gingerich and Vardya [in press]). In cooler stars there appear to be additional sources of opacity and until these are identified, we cannot be confident of abundance determinations in such objects.

### § 3. THE PROBLEM OF THE NUCLEI OF D, He<sup>3</sup>, Li, Be, AND B

The idea that the present relative nuclear abundances have arisen from nuclear reactions in stellar interiors fails in connection with deuterons, He<sup>3</sup>, and the nuclei of the isotopes of Li, Be, and B. The reasons for this failure were recognized early (Fowler, Burbidge, and Burbidge 1955). Firstly, only D, He<sup>3</sup>, and Li<sup>7</sup>, out of the lot, are ever generated in the reactions common to stellar cores. In such cores, D is created in the  $p$ - $p$  chain, but the equilibrium ratio of D/H is  $\sim 10^{-17}$ , independent of the temperature (Salpeter 1952*a*), whereas the value in terrestrial-meteoritic matter is  $1.5 \times 10^{-4}$  (Suess and Urey 1958). The small equilibrium ratio of D/H is a consequence of the slow rate of deuteron formation in

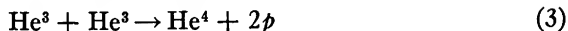


and the rapid destruction in



From this, it seems quite impossible to explain the observed D/H ratio on the basis of events within the stellar core.

A rather different situation obtains for  $\text{He}^3$ , which comes into existence in reaction (2) and is consumed in the slow processes



and



An alternative possibility, namely the reaction



which has most recently been discussed by Reeves (1959) and Fowler (1958, 1959), has been shown experimentally not to occur (Bashkin, Kavanagh, and Parker 1959).

Reactions (3) and (4) proceed slowly at low temperatures. For (3), the equilibrium ratio of  $\text{He}^3/\text{H}$  for stars operating on the  $p$ - $p$  sequence is given as a function of temperature in Table 8. In the table,  $x_3$  and  $x_1$  refer to the mass fractions of  $\text{He}^3$  and hydrogen, respectively.

TABLE 8  
TEMPERATURE DEPENDENCE OF  $x_3/x_1$

$T(\times 10^6 \text{ }^\circ \text{K}) \dots$	4	8	12	16
$x_3/x_1 \dots \dots \dots$	1.34	$4.18 \times 10^{-3}$	$2.56 \times 10^{-4}$	$4.44 \times 10^{-5}$

Fowler (1958, 1959) has given a recent treatment of reaction (4) using the cross-section as measured by Holmgren and Johnston (1959) and has shown that the rate is very low for  $T_6 < 13$ . The latest value of the cross-section (Parker 1961; Parker and Kavanagh 1963) is a factor of two lower than that found by Holmgren and Johnston (1959), and the rate of (4) is correspondingly half that in Fowler's papers (Fowler 1958, 1959). Thus it develops that  $\text{He}^3$  can survive well in stellar cores. Diffusion, convection, or explosive expulsion from the core could then lead to an appreciable  $\text{He}^3/\text{H}$  ratio in stellar atmospheres and extra-stellar matter.

The foregoing implies that  $\text{Li}^7$ , which has its birth in stellar cores in electron capture by  $\text{Be}^7$ , is generated only in hot stars at a rate which depends on  $x_3/x_4$  as well as on the temperature and density. Moreover, if any hydrogen is present,  $\text{Li}^7$  is rapidly consumed by

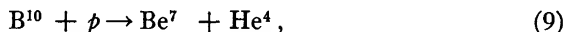
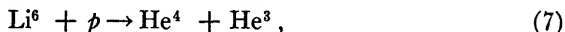


In the absence of hydrogen, a set of processes, starting with  $\text{Li}^7$ ,  $\text{He}^3$ , and  $\text{He}^4$  can, in principle, produce  $\text{Li}^6$ ,  $\text{B}^{10}$ ,  $\text{B}^{11}$ , and other light nuclei. In reality, there will always be protons, either from the initial condition, or from the operation



of (3). If a star had a core of  $\text{Li}^7$  and  $\text{He}^4$ , it could create  $\text{B}^{11}$  and  $\text{N}^{15}$ , but the condition is so artificial as not to warrant further comment.

As mentioned earlier,  $\text{Li}^6$ ,  $\text{Be}^9$ ,  $\text{B}^{10}$ , and  $\text{B}^{11}$  do not originate in stellar interiors. Moreover, were they somehow introduced into such a region, they would be destroyed promptly by the reactions



Should deuterium be present to an appreciable degree, other processes come into play to burn the light elements. These are of the form  $(\text{D}, p)$ ,  $(\text{D}, n)$ , and  $(\text{D}, \text{He}^4)$  and proceed at high rates. The fragility of the light nuclei can be appreciated by reference to Table 9, which is taken from Fowler, Greenstein, and Hoyle (1962) and is based on the calculations by Salpeter (1955) and Fowler (1959). This table gives  $\log_{10} (\bar{l}\rho x)$  for various events. Here  $\bar{l}$  is the mean life in years of the nucleus in the top row,  $\rho$  is the density in  $\text{gm/cm}^3$ ,  $x$  is the mass fraction of the nucleus listed in row 3, and the temperature is in units of  $10^6$  degrees. For the reaction  $\text{He}^3 (\text{He}^4, \gamma) \text{Be}^7$ , the table makes use of Parker's cross-section factor (Parker 1961).

The conclusion contained in Table 9 is that the stellar core is an inhospitable environment for maintaining the light nuclei, even were they present in the original matter. Only H and the helium isotopes are sufficiently refractory to live very long, and, in stars with internal temperatures exceeding  $15 \times 10^6$  °K, protons alone have a chance to leave the core unscathed. It is clear that the D,  $\text{He}^3$ , Li, Be, and B, which are directly observed, could not have originated in stellar cores.

Defer, for a moment, the question of the productive mechanism, and consider whether these substances could have been present in the matter out of which the stars themselves condensed or could have been accreted subsequent to formation of the stars. The first possibility is considered unlikely for the following reasons:

1. One study (Bonsack and Greenstein 1960) of lithium in T-Tauri stars showed that the surrounding nebulosity out of which the stars are presumably condensing contains not more than 10 per cent as much lithium as the stellar atmospheres. Consequently, it is unlikely that the T-Tauri lithium was a prime substance. By the kind of extrapolation common to the present subject, we argue that none of the light nuclei other than H and  $\text{He}^4$  occurs in any prestellar matter. The data on which this conclusion is based are still difficult to interpret. Bonsack (1961a) calls attention to the highly approximate nature of the Li

TABLE 9  
DEPENDENCE OF  $\text{LOG}_{10}(\dot{\rho}x)$  ON TEMPERATURE (FGH 1961)

NUCLEUS BURNED	$\dot{\rho}$	D	D	D	He <sup>3</sup>	He <sup>3</sup>	He <sup>3</sup>	Li <sup>6</sup>	Li <sup>7</sup>	Be <sup>9</sup>	B <sup>10</sup>	B <sup>11</sup>
Reaction	$\dot{\rho}(p, \beta^+\gamma)D$	$D(p, \gamma)He^3$	$D(D, \pi)He^4 + D(D, p)H^3$	$He^4(He^3, 2p)\alpha$	$He^3(\alpha, \gamma)Be^7$	$Li^6(p, \alpha)He^3$	$Li^7(p, \alpha)\alpha$	$Be^9(p, D)2He^4 + Be^9(p, \alpha)Li^6$	$B^{10}(p, \alpha)Be^7$	$B^{11}(p, \alpha)2He^4$		
$x$ for $T(\times 10^6 \text{ } ^\circ \text{K})$	$\dot{\rho}$	$\dot{\rho}$	D	He <sup>3</sup>	He <sup>4</sup>	$\dot{\rho}$	$\dot{\rho}$	$\dot{\rho}$	$\dot{\rho}$	$\dot{\rho}$		
1.....	19.61	3.77	0.35	34.05	39.91	16.18	18.13	23.80	31.36	30.81		
2.....	16.78	0.64	- 3.25	23.25	28.61	8.84	10.74	14.72	20.75	20.17		
3.....	15.42	-0.86	- 4.99	18.02	23.14	5.29	7.17	10.32	15.61	15.02		
4.....	14.58	-1.80	- 6.08	14.72	19.69	3.06	4.92	7.55	12.37	11.77		
5.....	13.98	-2.47	- 6.85	12.38	17.24	1.47	3.32	5.59	10.07	9.47		
8.....	12.87	-3.70	- 8.29	7.99	12.66	- 1.48	0.34	1.91	5.77	5.15		
10.....	12.40	-4.22	- 8.88	6.14	10.72	- 2.72	- 0.91	0.36	3.95	3.33		
15.....	11.66	-5.05	- 9.85	3.13	7.57	- 4.75	- 2.95	- 2.15	1.00	0.36		
20.....	11.20	-5.57	-10.46	1.24	5.59	- 6.02	- 4.23	- 3.74	- 0.85	- 1.49		

abundance in nebulae. In addition, Herbig (1962*a*) states that too little is known about the composition of the dust-rich HI regions, in which the T-Tauri stars are formed, to rule out the possibility that the T-Tauri lithium has a prestellar origin. Herbig suggests that interstellar lithium might be detected if a suitable star could be found imbedded in the dust. So far all results are negative, but not necessarily decisive.

2. Various authors have shown that the red dwarfs (Osterbrock 1953; Limber 1958*a*, *b*; Weymann 1957) and giant stars (Hoyle and Schwarzschild 1955) have convective outer zones, the depths of which increase as the effective temperature decreases. Limber (1958*a*) concludes that the cool dwarfs have completely convective interiors. Kaminisi (1960) has calculated that the convective envelope for middle M dwarfs (Kruger 60 A, O<sup>2</sup> Eri, Kruger 60 B) extends inward for 40 per cent of the stellar radius.

It seems inescapable, therefore, that any combustible substances initially present in the atmosphere of a cool star must be transported into the deep

TABLE 10  
MEAN LIFE OF Li<sup>7</sup> AT THE BASE OF THE CONVECTIVE ZONE  
(Bonsack 1959)

Star Type	$T(\times 10^6 \text{ }^\circ \text{K})$	$\rho(\text{gm/cm}^3)$	$\bar{t}$ (years)
G2V.....	1.04	0.020	$3.1 \times 10^{19}$
K1V.....	2.5	0.545	$1.3 \times 10^9$
M0V.....	2.6	1.93	$1.5 \times 10^8$

interior where they will burn. Since all stars with 1.5 solar masses or less are presumably cool at some time, original light nuclei must disappear during the star's evolution. Massive stars will consume light nuclei in supernovae. Bonsack (1959) has computed the mean life of Li<sup>7</sup> at the base of the convective zone for three main-sequence stars, assuming hydrogen to compose 70 per cent of the stellar mass. His results are displayed in Table 10. Deuterons and Li<sup>6</sup> are consumed far faster than Li<sup>7</sup>, and FGH have pointed out that the combustion of appreciable amounts of deuterons at the base of the convective zone would liberate enough energy to strengthen the convective currents, likely driving them deeper into the star where the other light substances would be transmuted. Neglecting this possibility, we see from Table 10 that lithium would not suffer convective depletion in the present sun, but would so in cooler stars. Weymann and Moore (1964) find that the deuterium would be consumed slowly without significantly increasing the luminosity of a star of one solar mass, and that, despite deep convection, the lithium survives because the internal temperature does not get high enough for effective burning. However, this conclusion is extremely sensitive to the model. Be and B are more refractory than Li, so their survival in cool stars is a possibility.

3. The accretion of matter by stars has been examined by many authors, among them Eddington (1926), Hoyle and Lyttleton (1939, 1940, 1941), Bondi and Hoyle (1944), Bondi (1952), Dodd and McCrae (1952), McCrea (1953, 1955), Schatzman (1955), Mestel (1954), Takebe and Matsunami (1957), Huang (1957), Stephenson (1957), Lambrecht (1959), and Traving (1962). The earlier papers were devoted largely to establishing the necessary kinematic relationship between the star and the surrounding nebulosity for accretion to take place, and it appeared that the relative velocity of star and cloud must be very small. Schatzman (1955) showed, however, that even were that relationship satisfied the radiation pressure from a hot star precludes the acquisition of matter by accretion, a point agreed to by Hoyle (1955). For a cool star, Schatzman emphasizes that the release of gravitational energy by the incoming particles quickly raises the surface temperature, and, again, radiation pressure brings an early halt to accretion. One gram of matter falling on the sun from infinity brings  $2 \times 10^{15}$  erg with it, and Schatzman argues that this energy is not easily dissipated by the star. It has further been noted (Menzel 1955) that the presence of a stellar magnetic field would virtually preclude the accretion of ions. Mestel (1959) also shows that a magnetic field inhibits accretion. Traving (1962), however, has proposed that the roughly normal He/H ratio in Barnard 29 (a star of small mass in the globular cluster M13) might be due to accretion. The accreted matter would have to come from red giants in the same cluster. Why this matter should have normal He/H is not clear if the globular clusters represent original stars. Perhaps mixing brings helium from the core to the surface.

A second objection to explaining the atmospheric abundances of the light nuclei by an accretion process comes from the fact that many observations on stars have shown that stars lose matter to interstellar space, but there is no evidence for their accepting any. This is true even for T-Tauri stars (Herbig 1958), and for giants and supergiants later than M0 (Deutsch 1959, Rubbra and Cowling 1959, De Jager 1959, Schatzman 1959). Red giants of spectral class earlier than M0 seem not to lose mass (Wilson 1960*b*). The problem has been reviewed by Deutsch (1960) in Volume 6 of this series. Biermann and Lüst (1960) have treated some aspects of the problem in the same volume.

We are forced to the conclusion that Li, Be, B cannot originate in stellar cores, while D cannot escape from the core even though it is formed in that region. Also, the light elements are probably not part of prestellar matter, at least in the observed amounts, nor can the abundances we find in stars be a result of accretion. Finally, if D and Li were somehow present in the atmosphere of a star, they could not survive the epochs in the star's evolution when the star is cool and possesses deep convective zones. He<sup>3</sup>, Be, and B might survive the convective periods.

Having determined where the light nuclei cannot occur, we may now inquire where they are actually found. Then it will be important to find mechanisms

for creation and stability consistent with the abundances. As will be seen, the data are very unsatisfactory. A recent review has been given by McKellar (1960) in Volume 6 of this series. For example, D has never been detected with certainty outside of terrestrial-meteoritic matter. This is especially discomfiting because the assumption that the local D/H ratio is universal means that D is the sixth most abundant of all the nuclear species. Attempts have been made, of course, to see D in the quiescent sun (Kinman 1956, Severny 1957), solar flares (Severny 1956; Goldberg, Mohler, and Müller 1958), interstellar space (Adgie and Hey 1957), and a flare star (Wilson 1961). In no case has better than an upper limit to D/H been determined; the latest value of that limit for interstellar space is 1/13,000 (Weinreb 1962) or about one-half the terrestrial ratio. As a consequence, any hypothesis dealing with the abundance of D must be based on a fundamental assumption—that the local D/H value is universal. Both assumptions have been followed by various authors. Most recently, Cameron (1962) has taken the local value to be universal, but this has been disputed by Burbidge (1963) on the basis of new empirical evidence. Weinreb's conclusion that the local value of D/H is an isolated anomaly is suggestive, but not conclusive.

$\text{He}^3$  is seen in terrestrial-meteoritic matter, but its origin is ascribed to cosmic ray-induced spallation rather than to original events. Greenstein (1951) placed an upper limit of 2 per cent on  $\text{He}^3/\text{He}^4$  for the sun, based on He I lines shorter than 10,830 Å, and 10 per cent based on the triplet at 10,831.69 Å. An observation by Burbidge and Burbidge (1956) on the He I lines in the magnetic star 21 Aquilae was interpreted by them as suggesting the ratio  $\text{He}^3/\text{He}^4 \sim 1$ . However, the conclusion is uncertain because the Stark effect introduces a wavelength shift comparable to that observed.

Sargent and Jugaku (1961) have provided convincing evidence that the helium in the phosphorous star 3 Centauri A is about 80 per cent  $\text{He}^3$ , the total helium content being smaller than normal by a factor of 6 relative to silicon (Jugaku, Sargent, and Greenstein 1961). In that same star Sargent and Jugaku put an upper limit on D/H of 1 per cent. These, disappointingly enough, represent the only data on the abundance of a nucleus whose creation is believed essential to the present structure of the universe.

Lithium has been seen relatively widely. In terrestrial-meteoritic matter (SU 1958), the abundance is some 350 times the current value for the sun (GMA 1960). It has already been mentioned that lithium has been detected in T-Tauri stars, where its abundance approximates the local value (Bonsack and Greenstein 1960; Bonsack 1959, 1961*b*; Herbig 1962*b*). Bonsack (1959) has also measured the lithium/vanadium ratio in 46 normal stars ranging in spectral type from G8 through M0. A wide range of luminosity within each spectral class was studied. Bonsack gives good evidence for believing that the vanadium abundance is essentially constant among these stars, and concludes that the lithium content may differ by a factor of 100 from star to star of the same spec-

tral class (Fig. 10). Most suggestive is the fact that the lithium content shows a decided decrease as the surface temperature declines. We have already pointed out the strong correlation between low surface temperatures and deep convective zone and Bonsack has interpreted his data in terms of destruction of the lithium at the inner edge of the convective region.

Other work in which stellar lithium has been seen includes Merrill and Greenstein's identification (1956) of Li in the S-type star R Andromedae 001838. McKellar and Stilwell (1944) saw Li weakly in some 40 red carbon stars and strongly in one (WZ Cas), where it had previously been noted by McKellar

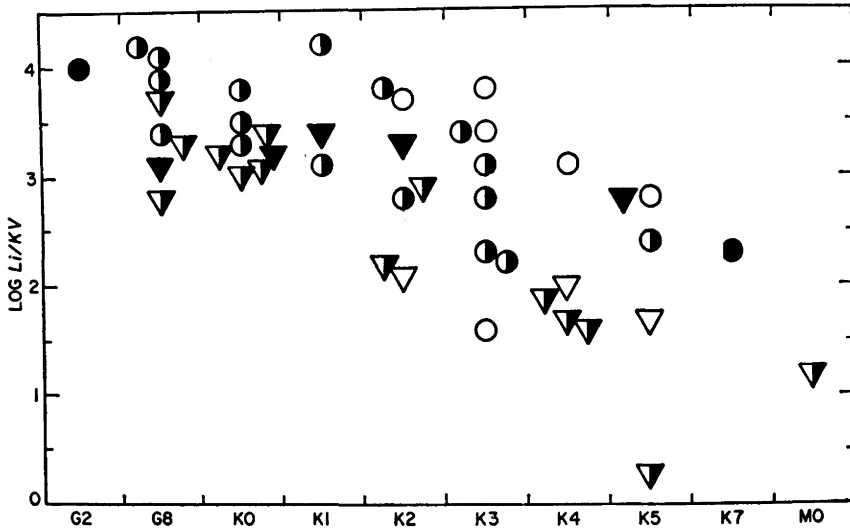


FIG. 10.— $\text{Log}_{10} (\text{Li abundance}/K \times \text{vanadium abundance})$  vs. spectral type, where  $K$  is a constant. Circles are values from measured lines; triangles are upper limits. Open figures are for stars of luminosity classes Ib and II; filled figures are classes IV and V; and half-filled figures are intermediate luminosities. From Bonsack (1959).

(1940, 1941). Sanford (1950) has also remarked on the range of the Li equivalent widths in stars of classes R and N. He pointed out that the Li equivalent width was unrelated to that for Na, so the observed variations could not have been due to variations in excitation conditions. Neither can they be attributed to the failure of local thermodynamic equilibrium. Earlier Sanford (1944) had found one type-N star (WX Cygni) with a large lithium abundance. Keenan and Teske (1956) and Teske (1956) have shown that Li is enhanced in S-stars but not as much as in carbon stars. Bonsack (1961*b*) has observed Li in a number of additional T-Tauri stars.

The isotopic composition of stellar lithium is as important to our subject as the relative abundance of the element. The lighter isotope is the more readily consumed, as may be seen from Table 9. In terrestrial-meteoritic samples, the

isotopic ratio is (SU 1958)  $\text{Li}^6/\text{Li}^7 = 0.08$ ; Shima (1962) gives 0.091 for chondrites with lithium one third as abundant as used by SU (1958).<sup>9</sup> Recently Boyarchuk and Herbig (1961) have studied lithium spectra in K and M stars, and have found  $\text{Li}^7/\text{Li}^6$  to be large, possibly comparable with the terrestrial value. A positive determination of the isotopic abundance has not yet been made in the sun or in non-solar system matter. Greenstein and Richardson (1951) made a careful study of the lithium doublet in the solar penumbra and disk. They obtained moderately good agreement (Figs. 11 and 12) between the

<sup>9</sup> Shima and Honda (1963) confirm the lower abundance of Li and also that the  $\text{Li}^6/\text{Li}^7$  ratio is 20 per cent higher in stony meteorites than in terrestrial matter.

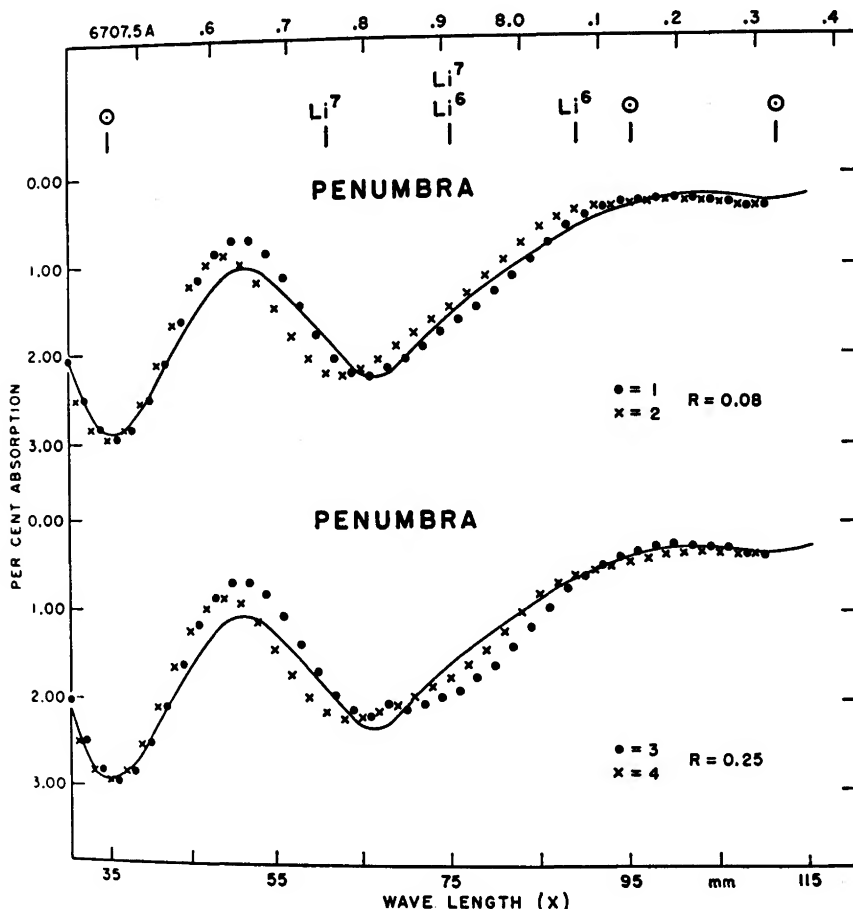


FIG. 11.—Absorption spectrum near Li I lines in the penumbra of the sun. The solid curve represents smoothed data. The dots and crosses are calculated according to choices of the  $\text{Li}^6/\text{Li}^7$  isotope ratio,  $R$ , and other parameters. Numbers 1–4 refer to sets of parameters used in the solution of the equation for the absorption spectrum. From Greenstein and Richardson (1951).

observed and computed line profiles, the presence of  $\text{Li}^6$  showing up as a long-wavelength asymmetry. The adjustable parameters of the theoretical line shapes included a displacement of the lithium line from the wavelength measured in laboratory experiments, and they recall reports by King (1916) that the appearance of the Li lines is a function of excitation conditions. The equivalent width and central absorption were other free parameters. Despite the uncertainties, Greenstein and Richardson concluded that the solar ratio of  $\text{Li}^6/\text{Li}^7$  is possibly zero, probably not as high as 0.25, and most likely 0.08. No other measurements on  $\text{Li}^6/\text{Li}^7$  have come to our attention, and we face another major deficiency in fundamental data. This inevitably weakens any argument that can be offered on the means of production and loss of the light elements.

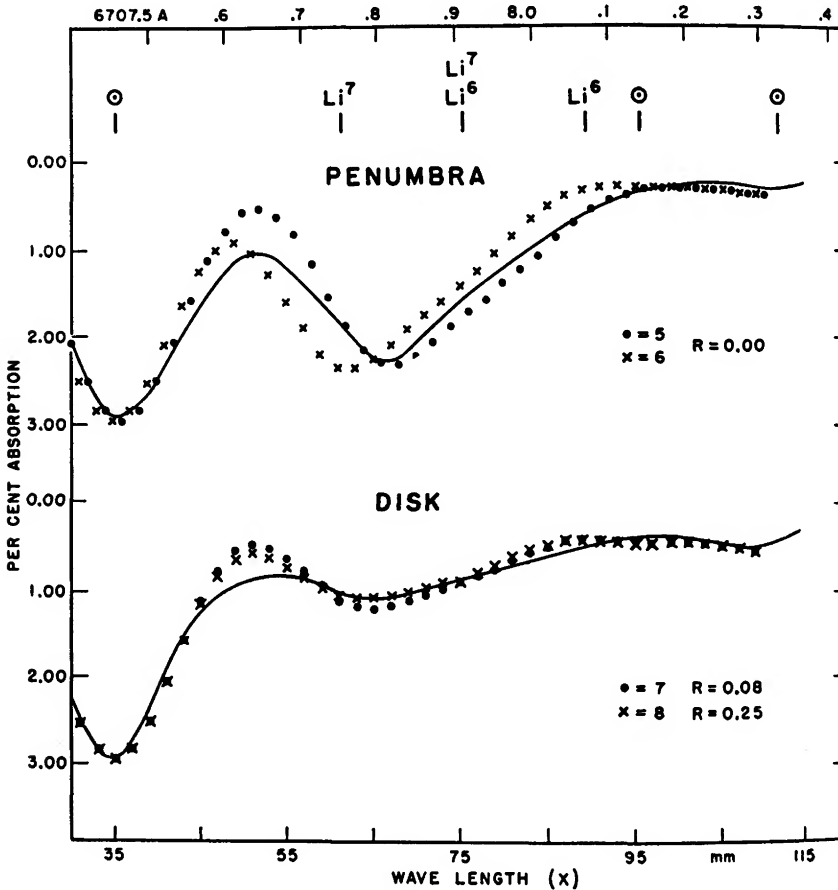


FIG. 12.—Absorption spectrum near Li I lines in the penumbra and disk of the sun. The solid curve represents smoothed data. The dots and crosses are calculated according to choices of the  $\text{Li}^6/\text{Li}^7$  isotope ratio,  $R$ , and other parameters. Numbers 5–8 refer to sets of parameters used in the solution of the equation for the absorption spectrum. From Greenstein and Richardson (1951).



At this point, we have the results that lithium has a large abundance (i.e., the terrestrial-meteoritic value) only in T-Tauri stars, is rather thoroughly decomposed in cool main-sequence stars, and is weakly present in stars as hot as the sun. The isotopic abundance is unknown outside the solar system and uncertain for the sun.

In the case of beryllium, the SU meteoritic value of 20, relative to  $\text{Si} = 10^6$ , is to be compared with the GMA determination of 7. This difference may not be significant. Sill and Willis (1962) have found an abundance of 1 in chondrites, so the sun now appears overabundant in Be relative to chondrites. With Shima's lithium abundance, it appears that the solar  $\text{Li}/\text{Be}$  ratio is 1/700 that of meteoritic matter; previously this ratio was thought to be 1/20 that of meteorites (see Table 1). In the interstellar medium, Be is at least 10 times less abundant than the SU (1958) value (Spitzer and Field 1955). Be can be observed in the spectra of distant stars only if the stars are bright. Bonsack (1961*c*) has examined four of the A dwarfs and found the abundance to be extremely variable, reminiscent of the situation for lithium. Of the four stars studied, two showed Be abundances essentially identical with that in the sun, the observed difference of a factor of four being probably of no significance. In one star ( $\alpha$  CMa), which is a member of a visual binary, the abundance is low by approximately 160 times. Bonsack suggests this might be due to dilution by a large amount of matter which was transferred some time ago from the other member of the pair. This star is also overabundant in Fe and Ti (Wallerstein, Stone, and Williams 1962). The fourth star shows a sixteen-fold overabundance of Be relative to the sun. This star,  $\alpha^2$  CVn, is also noted for its strong magnetic field, and it is speculated by Bonsack, as it had been earlier by FBB, that the overabundance is directly related to that field. This will be discussed more fully below.

Boron is spectroscopically invisible in all stars. Russell (1934) reported boron to be present as BO in a sun spot, but not in the disk. BH was absent. Russell estimated  $\text{B}/\text{H} \sim 3 \times 10^{-6}$ , which seems exceptionally high. Goldschmidt (1954) has accepted this abundance, Babcock (1945) saw solar bands attributed to BH, but none due to BO. Moore (1951), presumably on the basis of Babcock's and Russell's work, listed BH and BO as solar constituents. Rankama and Sahama (1949) questioned the existence of solar boron, and atomic boron was not found in the solar spectra obtained on a rocket flight (Malitson, Pursell, Tousey, and Moore 1960). The solar data are ambiguous but tend to the negative side. Underhill (1960) has suggested that two lines of the B IV spectrum might be present in O-type stars. We consider only the local data. SU give B an abundance of 24, relative to  $\text{Si} = 10^6$ , with  $\text{B}^{10}/\text{B}^{11} = 0.25$ . Shima (1962) finds meteoritic boron to be 10 per cent as abundant as terrestrial boron, with  $\text{B}^{10}/\text{B}^{11}$  about 10 per cent higher in meteorites than in rocks. Boron, in these data, has an abundance, relative to silicon, about one third the value given by Suess and Urey.

One final introductory comment regarding  $\text{DHe}^3\text{LiBeB}$  is that the last three

are exceptionally rare compared to nuclei of nearby atomic weights, whereas D is strongly overabundant and  $\text{He}^3$  is essentially unknown. We turn our attention to theories of the origin of D,  $\text{He}^3$ , Li, Be, and B.

Consider the case of the deuteron under the assumption that the local abundance is universal. With this condition in mind, Heller (1957) has examined the formation of deuterium according to the theories that the elements were synthesized in an equilibrium process (Beskow and Treffenberg 1947), in the early moments of an exploding universe (Alpher and Herman 1950), or, following his own suggestion, in supernovae. He makes the important points that, for  $x_D/x_H = 1.5 \times 10^{-4}$ , the reactions



are faster than (2), and that in hot regions photodisintegration of D is significant independent of the density. His calculations predict that the observed  $x_D/x_H$  ratio could not derive from an equilibrium situation followed by expansion and a freezing-in of the equilibrium abundances. Reactions (11) and  $\text{D}(\gamma, n)p$  are too fast. A contrary difficulty arises from the exploding universe theory, for there the production of D by the radiative coalescence of a neutron and a proton leads to a large overabundance of D. This necessitates destruction of D in subsequent reprocessing in stars. Moreover, the exploding universe theory is beset by so many problems (Alpher and Herman 1953) that it is unlikely to account for D.

The supernova origin of D is based on the supposition that D is made in reaction



the capture taking place with low-energy neutrons and protons. Using the then current model of supernovae (BHBCF 1956) neutrons were assumed liberated in  $(\alpha, n)$  reactions on  $\text{C}^{13}$ ,  $\text{O}^{17}$ , and  $\text{Ne}^{21}$ , thermalized by collision with protons, and eventually captured by the latter. The fact that new models of supernovae have been published since 1956 (Hoyle and Fowler 1960; Colgate and Johnson 1960) alters Heller's argument in two respects. Firstly, HF find that small-mass stars consume all their hydrogen prior to exploding, so that the supernovae which develop from such stars cannot yield deuterium by reaction (12). This excludes Type I supernovae from consideration. Secondly, for the large-mass stars which account for the Type II supernovae, the source of neutrons is no longer taken to be  $(\alpha, n)$  reactions but to be in the disruption of  $e$ -process nuclei like  $\text{Fe}^{56} \rightarrow 13\text{He}^4 + 4n$ . Now Heller ascertains that appreciable amounts of D can be made in supernovae only if:

a)  $\text{He}^3$  and  $\text{N}^{14}$  are absent, since they have extremely large cross-sections for consuming neutrons in  $(n, p)$  reactions.

b) The density is low ( $\sim 10^{-5}$  gm/cm<sup>3</sup>) to avoid destruction of D in particle reactions.

c) The temperature is  $< 10^8$  °K to reduce the rate of photodisintegration.

Even meeting these severe restrictions, estimates of the yield of D per supernova and the fraction of the galactic mass ( $10^{-4}$ ) which has suffered through a supernova explosion lead to a galactic D/H of  $\sim 10^{-8}$ , some  $10^4$  times smaller than the local value. This number must be further reduced because only Type II supernovae can contribute. Only on the further supposition that the substance of the solar system coagulated without any dilution in the general interstellar gas could the local D/H ratio be achieved. It thus appears that supernovae cannot be the source of supply of D.

An entirely different approach to the problem of D was adopted by Hayakawa (1960), according to whom the local D/H value is not to be thought of as universal. Following a solar model proposed by Urey (1954), it is asserted that in an early period the solar planetary matter consisted of massive objects, which collided, fragmented with heating, and later recondensed over a time of the order of  $10^8$  years. Among other things, this model is offered as an explanation of the terrestrial reduction of hydrogen relative to that in the sun. On the assumption that the fragments had a size comparable with one mean free path for a cosmic-ray proton (roughly 25 cm), Hayakawa suggests that D is made in spallation collisions of the form



Taking the average cross-section,  $\sigma$ , to be 0.1 barn, the cosmic-ray flux,  $I$ , to be one/cm<sup>2</sup> sec, and an irradiation time,  $T$ , of  $10^8$  years, the number of deuterons made per target nucleus is

$$N_D = I\sigma T \sim 3 \times 10^{-10}. \quad (14)$$

Since the fractional number of H atoms in meteorites is  $10^{-2}$ , this yields D/H  $\sim 3 \times 10^{-8}$ , too small by  $\sim 10^4$  times. The discrepancy is removed by the assumption that the sun, during this early period, generated  $10^4$  times as many energetic protons as are now seen in cosmic rays. It is stated, without numerical argument, that Li, Be, and B can be generated to the correct amount in this way. Hayakawa's paper is interesting in that it specifically avoids the use of neutrons to produce D. This is in direct contrast to the conclusion by Frank-Kamenetskii (1961) that the existence of deuterium must be due to neutron capture in hydrogen. As will be seen below, Hayakawa's idea has been treated with greater numerical attention by Bashkin and Peaslee (1961) who, however, find an effective spallation cross-section some 4 or 5 times smaller than that used by Hayakawa. Hayakawa justifies the assumption of an increased solar activity early in the history of the planetary system by comparison with the T-Tauri stars. Those stars are believed to exhibit frequent and intense flare activity of the

kind now known to accelerate protons on the sun, and it is assumed that the sun passed through a T-Tauri phase while the planets were coagulating. This idea is common to the other theories we will summarize.

In 1955, Fowler, Burbidge, and Burbidge (1955) attempted to explain the anomalous abundances of heavy elements in Apm stars. A revised discussion was given by Burbidge, Burbidge, and Fowler (1958). Two alternatives were offered. In one, protons and alpha particles were flare-accelerated, thanks to the magnetic fields, to energies up to 100 Mev. Bombardment of the atmospheric nuclei was to produce neutrons which, thermalized by hydrogen, were captured by the Mg to Fe nuclei so as to create the anomalous abundances. At the same time, a considerable amount of D was said to result. The second method assumed that all the matter in a flare was energized to  $\sim 1$  Mev ( $10^{10}$  ° K), at which energy neutrons were released in  $(p, n)$  reactions and their subsequent capture again led to deuterium and the heavy elements. The estimated D/H ratio approached 1 or 2 per cent.

The first suggestion may be questioned because of the important restriction that the particle energy be less than 100 Mev. This restriction arises because higher energy protons and alpha particles are apt to destroy, rather than create, the heavy elements in spallation reactions. It is known that the sun, whose magnetic fields are modest compared with the  $5 \times 10^6$ – $10^7$  gauss postulated by FBB, generates substantial numbers of protons out to 20 Bev (Parker 1957) so the cut-off at 100 Mev in the Apm stars is hard to justify. Moreover, the desired enhancement in the heavy nuclei is achieved only at the expense of C, N, O, and Ne with which the fast protons and alphas will also interact. Thus, if the elements of the Mg to Fe group are to serve, as suggested by FBB, as the targets for  $(\alpha, n)$  reactions, about 50 reactions per Mg nucleus are needed to create the observed abundances. At this rate, all the C, N, O, and Ne would be destroyed 25 times over.

The second method suffers because it seems likely that the hot spots will very rapidly reach thermodynamic equilibrium and photodisintegration will reduce all nuclei to neutrons and protons. In subsequent cooling down, or in diffusion of the neutrons out of the hot spots, the principal end effect will be production of D, but not of the heavy elements. Bonsack (1961*c*) offers the comment that, if the strong magnetic fields in Apm stars result in nuclear reactions, one should also expect to find associated optical effects. In fact, Bonsack points out, no such effects are known (Provin 1953). However, this may argue only that the Be in  $\alpha^2\text{CVn}$  is not the result of current production, but has survived since an early epoch when flares, absorbing energy from the magnetic fields, were effective in stimulating spallation reactions.

Despite these drawbacks, the FBB paper calls attention to the possibility that the light elements might be created in stellar atmospheres where the

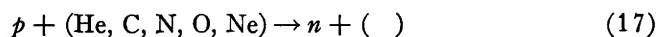
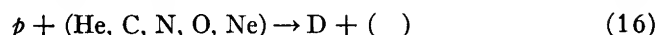
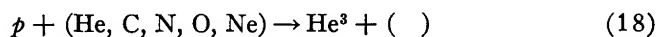
quiescent density and temperature are sufficiently low to allow preservation of D, Li, Be, and B.

We might take note at this point of the suggestion, to be met with over and over in these theories, that stellar-surface magnetic fields are an essential ingredient in accelerating charged particles to high energy. It is patent that, to be effective in this manner, the magnetic fields must vary rapidly with time, and such variations should be correlated with flares. In this connection, recent solar observations are of interest. Howard and Babcock (1960) took periodic magnetograms during the large solar flare of July 16, 1959, the intensity being 3+. The magnetograph was sensitive to the longitudinal Zeeman effect for H $\alpha$  and H and K emission lines. Data were obtained from 12 minutes after the flare began until two hours after the maximum flare intensity was reached. The spectrograph was adjusted to give information on field strengths of 5, 10, 20, and 40 gauss. Subsequent to the large flare, four smaller ones were studied with the same apparatus. Quoting the authors: "The most striking result disclosed by the magnetograms is the essential constancy of the magnetic pattern." Those small differences which occurred are attributed to changes in seeing and to scanning imperfections. It is also remarked that this negative result could not be due to having had too low an upper limit to the observed magnetic intensity. This experimental conclusion contrasts with quoted work by Severny, so the general situation may still be doubtful. Thus, Gopasyuk (1961) and Severny (1961) have found that the region near flares shows marked variations in magnetic field near the time of formation of the flare. Babcock (1960a) has surveyed the data on stellar magnetic fields.

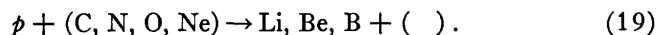
In a general attack on the problem of the light nuclei, Bashkin and Peaslee (1961) have assumed that the local abundances of the light nuclei are to be treated as characteristic only of the solar system. Briefly, the experimental fact that the sun does accelerate protons to high energies when flares occur is the basis for their calculations. The flare is considered to be a rather stable region of hot gas which floats at a height of some  $10^4$  km above the photosphere and emits energetic protons, assumed to be distributed isotropically. The method of creating the flare or accelerating the protons is not specified, reliance being placed simply on the observation that such flares and such particles exist. A certain fraction of the high-speed protons enter the photosphere of the sun and give rise to spallation reactions in the normal matter, chiefly, p, He<sup>4</sup>, C, N, O, and Ne, of which the sun's atmosphere is composed. Where known, cross-sections for the spallation reactions are used, with a proper weighting over the abundances of the target substances. Cosmic ray and other data are taken into account in order to estimate the frequency of flare production, the proton energy distribution, and the efficiency of each flare in generating the fast protons. An additional assumption is that the planetary system has been contaminated by matter expelled from the surface of the sun.

The reactions taken to be important in producing the light nuclei are:

## A) Deuterons

B) He<sup>3</sup>

## C) Li Be B



Quite generally, one may write

$$Y(x) = 2 R N_p N_t \sigma(x) \text{ where} \quad (20)$$

$Y(x)$  is the rate of production of nucleus  $x$ ,

$R$  is the rate of occurrence of flares,

$N_p$  is the number of effective protons per flare,

$N_t$  is the number of target nuclei per cm<sup>2</sup>,

$\sigma(x)$  is the cross-section for producing nucleus  $(x)$ .

The factor 2 arises because, as first shown by FBB, the heavy nuclei which are accelerated in the flare are as effective in causing spallation when they strike protons as the fast protons are on hitting targets of heavy nuclei. Now  $R$  is not a constant, nor is  $N_p$  always the same for different flares. Moreover, the protons have an energy distribution which is a function of the flare. The cross-section, of course, is energy dependent. In principle, these variations must be taken into account in calculating  $Y(x)$ . In fact, so little information is available that BP were able to make only crude approximations. It is especially disappointing to note that  $\sigma(x)$ , which can be measured in standard experiments in nuclear laboratories housing large proton accelerators, is virtually unknown for the reactions of interest in this work. The only available information on  $\sigma(x)$  is based on experiments in which radioactive products result. For example, the production of H<sup>3</sup>, He<sup>6</sup>, Be<sup>7</sup>, C<sup>10</sup>, and C<sup>11</sup> from various bombardments has been measured. These nuclei decay respectively to He<sup>3</sup>, Li<sup>6</sup>, Li<sup>7</sup>, B<sup>10</sup>, and B<sup>11</sup>. Hence BP assumed that the total production of the stable nuclei was just twice the measured value for making the radioactive isobars. (In the case of B<sup>10</sup>, a third source, Be<sup>10</sup>, is also a contributor). On weighting over an assumed energy dependence for the flare protons and the relative number of He, C, N, O, and Ne atoms in the sun's photosphere, they obtained

$$Y(D) = 7 \times 10^{27} \text{ sec}^{-1} \text{ for direct production of deuterons,} \quad (21a)$$

$$Y'(D) = 2 \times 10^{29} \text{ sec}^{-1} \text{ for indirect production of deuterons} \quad (21b)$$

through the generation and capture of  
neutrons,

$$Y(\text{He}^3) = 2 \times 10^{27} \text{ sec}^{-1}, \quad (21c)$$

$$Y(\text{Li}) \approx Y(\text{Be}) \approx (B) \approx 3 \times 10^{25} \text{ sec}^{-1}. \quad (21d)$$

Whether or not the rates of (21) are sufficient to explain the observed abundances depends on subsequent developments in the sun. An unknown fraction will be mixed inward and consumed, while some may be expelled from the sun in the corona. An estimate of the coronal loss was made, neglecting any inward loss, by equating the magnetic energy density at the earth's orbit to the kinetic energy density due to the outward flow of protons. The argument is that a gross imbalance of these quantities would lead to fluctuations in, if not destruction of, the magnetic field. The equations are

$$U = \frac{1}{2} n m v^2 = B^2 / 8\pi \quad (22)$$

and

$$\psi = 4\pi R^2 n v = 8\pi R^2 U / m v = 2.5 \times 10^{34} T_6^{-1/2} \text{ sec}^{-1}, \quad (23)$$

where  $U$  is the energy density,  $n$  is the number of protons per  $\text{cm}^3$ ,  $m$  is the mass of the proton,  $v$  is the proton velocity,  $B$  is the quiescent magnetic field at the earth's orbit,  $\psi$  is the net proton flux from the sun,  $R$  is the radius of the earth's orbit,  $T_6$  is the coronal temperature in units of  $10^6$  °K. With  $T_6$  in the range 1 to 4 and  $U$  uncertain by  $10^2$ , the result is

$$\psi = 10^{35 \pm 1} \text{ per sec}, \quad (24)$$

and the solar fractional abundances are found by dividing the yields of (21) by  $\psi$ . This gives abundances,  $f$ , relative to hydrogen of

$$f(\text{Li}, \text{Be}, \text{B}) = 10^{-9} \quad (25a)$$

$$f(\text{He}^3) = 2 \times 10^{-8} \quad (25b)$$

$$f(\text{D}) = 4 \times 10^{-7} \quad (25c)$$

with an over-all uncertainty of at least a factor of ten.

With the exception of D, therefore, it appears that the proposed mechanism is capable of explaining the terrestrial-meteoritic *presence* of the light elements, although the *abundances* are still subject to question. To offset any loss due to inward mixing, BP fall back on the assumption that the sun, when in its T-Tauri phase, was probably far more efficient than the present sun in creating the light substances and in dispersing them throughout the volume of the solar system, so that, qualitatively, the spallation process on the common solar constituents can account for all the light nuclei with the possible exception of deuterium.

To explain the large value of D/H, BP are forced to introduce a model of formation of the planets. In this model (Urey 1952, Ringwood 1957) much of the local matter external to the sun was in the form of dust grains incapable of retaining much gas but holding a small amount of hydrogen and the light nuclei ejected from the active sun. It is postulated that successive condensa-

tions and evaporations of H and D produced a 100-fold increase in D/H, which brings the result (25c) to the correct value.

There is no question but that the foregoing is quantitatively unsatisfactory because of the nature of the approximations and assumptions, especially as regards D. The major uncertainties are in the model of formation of the planets, the nature of the sun's surface activity, mixing characteristics, and coronal mass loss from its earliest days to the present and the spallation cross-sections. Various balloon and satellite studies have been made on the fast protons emitted from the sun. The general conclusion is that even the quiescent sun loses numerous protons with energies up to a few hundred Mev, while a large flare may be orders of magnitude more productive of energetic protons than BP assumed. These factors tend, of course, to ease the problem of generating enough of the light nuclei, but only in a qualitative sense: calculations based on the still scanty data about the number and energy distribution of solar protons must be treated with reserve. There is, however, one suggestive feature in the limited

TABLE 11  
SPALLATION CROSS-SECTION RATIO FOR  
He<sup>6</sup>/Be<sup>7</sup> IN VARIOUS TARGETS

Target	C	Al	Cu	Ag	Au, Pb
He <sup>6</sup> /Be <sup>7</sup> . . . . .	0.05	0.13	0.5	1	4

cross-section data on the spallation origin of the lithium and boron isotopes. For protons with energies between 400 Mev and 1 Bev on targets of carbon and oxygen, the ratio of C<sup>10</sup>/C<sup>11</sup> varies from 0.1 to 0.2 (Symonds, Warren, and Young 1957). For  $E_p$  between 1 Bev and 3 Bev, the results for He<sup>6</sup>/Be<sup>7</sup> are as shown in Table 11 (Rowland and Wolfgang 1958; Baker, Friedlander, and Hudis 1958). It thus appears that the spallation yields of the radioactive contributors to the lithium and boron isotopes are almost the same as the relative isotopic abundances thereof. This was the justification for BP's assumption that the direct spallation yield was the same as the indirect yield, and that spallation in the solar atmosphere gave us these light nuclei. As we shall see shortly, this point of view is subject to severe criticism.

By far the most detailed study of the light nuclei has been carried out by Fowler, Greenstein, and Hoyle (1962), who also consider the observed abundance of the light nuclei to be a local phenomenon.<sup>10</sup> Spallation induced by energetic protons is the mechanism for creating the light nuclei. As in the papers by Hayakawa and BP, quantitative agreement with the observed abundances can be attained only with the help of numerous assumptions. Three features distinguish the FGH calculations from the others. These are:

1. A model of the early solar system is adopted which spells out in consider-

<sup>10</sup> Mitler (1963) has used the FGH model to calculate the abundance of He<sup>3</sup> in planetesimals.



able detail the chemical and physical form of the preplanetary matter, the nature of the link between that matter and the active sun, and the process whereby the planets eventually coalesced. The time scale and chronological order for many of the necessary events are largely specified.

2. The spallation reactions are taken to occur in the preplanetary matter, the principal target nuclei being O, Si, and Fe. That choice of nuclei derives from the solar model.

3. An appreciable neutron flux, generated in the spallation reactions, irradiates the preplanetary matter, thereby introducing a preferential destruction of the light isotopes of lithium and boron, and giving rise to deuterons by virtue of the reaction  $p(n, \gamma)D$ . That neutrons are generated prolifically in such reactions is substantiated by the work of Gusakow, Albouy, and Poffe (1961), Waddell, Henderson, and Lewis (1961), and Albouy, Gusakow, and Poffe (1961). Table 12 gives the results of GAP.

TABLE 12  
NEUTRON YIELDS FROM SPALLATION ON  
VARIOUS TARGETS (GAP 1961)

Target	$\sigma_{\max}$ (mb)	$E_p$ (Mev) for $\sigma_{\max}$	$\sigma$ (mb) at $E_p = 150$ Mev
F <sup>19</sup> .....	220 ± 35	30 ± 5	30 ± 8
Na <sup>23</sup> .....	140 ± 25	24 ± 3	45 ± 8
Mn <sup>55</sup> .....	460 ± 50	25 ± 3	90 ± 12
Y <sup>89</sup> .....	170 ± 30	30 ± 5	90 ± 15
Cs <sup>133</sup> .....	250 ± 40	60 ± 10	130 ± 20
Au <sup>197</sup> .....	190 ± 30	80 ± 5	75 ± 15

The solar model is most fully explained by Hoyle (1960). In some respects, it is similar to, but more explicit than the solar system models employed by Hayakawa and by BP. Gold (1960) has briefly described a similar source of planetary matter. The starting point is the marked difference in angular momentum per unit mass in planetary matter and the sun, the ratio of the former to the latter being  $5 \times 10^4$ . Hoyle assumes that the matter, and angular momentum, of the solar system originally resided in the spinning sun. As the sun contracted, a discoidal volume was filled with matter expelled from the sun, and, because of the decreased temperature with increasing distance from the sun, condensation of the less volatile materials (Mg, Si, Fe, and common metals) occurred. The low-density gas (hydrogen at  $10^{-13}$  gm/cm<sup>3</sup>) which remained between the solid particles and the sun was ionized to roughly one part in  $10^7$ . This level of ionization was sufficient to maintain a magnetic linkage between the sun and the grains. This linkage enabled the sun to transfer angular momentum to the planetary system. FGH extend the model from this point,

but the final formation of the planets themselves is not treated except for the assumption that the terrestrial planets coagulated in a gas-free region.

FGH assert that the sun passed through a T-Tauri phase at the end of its gravitational contraction. The outermost portions of the solar atmosphere were cool, and possibly contained grains of silicon, magnesium, and the common metals, which have low volatility. These grains did not follow the contracting gas but remained in circular orbits around the sun. The condensing sun ejected large quantities of mass which cooled on moving outward, and further condensation of grains of the less volatile substances occurred. Among these substances was water ice which developed on the metallic grains until "planetesimals" with radii near 50 cm were formed, the size being limited by the mechanical strength of the ice. At this size, any viscous drag from the out-flowing gas was inadequate to carry the planetesimals along, so they stayed in orbits near those of the present terrestrial planets.

In addition to a general loss of matter, the sun ejected some  $10^{45}$  erg of energy in the form of fast protons. The protons were accelerated in the frequent and powerful flares which are presumably characteristic of T-Tauri stars. The protons, spiraling about the magnetic lines of force, were focused on to the planetesimals where they fragmented the common metals, taken to have the solar atmospheric relative abundances. These spallation reactions produced the light nuclei. Such reactions also took place in the atmosphere of the sun where the presently observed abundances of the light nuclei were made, but the solar light nuclei did not mix with those in the planetary material.

The details of the situation are as follows. In the first place, the targets in the planetesimals are primarily silicon and the common metals, along with some oxygen because of the probable presence of oxides and water. Indeed, the model of the planetesimals gives  $\rho = 1.8 \text{ gm/cm}^3$ ,  $r \approx 50 \text{ cm}$ ,  $H = 8 \times 10^6$ ,  $O = 7.5 \times 10^8$ , Si-group  $= 2.5 \pm 10^8$ , and Fe-group  $= 1.6 \times 10^8$ , all relative to Si  $= 10^6$ . However, carbon and nitrogen are absent because they occur mostly in the form of gases with low boiling points. With the medium-weight targets, FGH state that the even-A isotopes of lithium and boron ought to be produced at least as often as the odd-A isotopes. Since the present abundances show that the even-A isotopes are rare relative to those with odd A, some process must be introduced to reduce the relative abundances of the light isotopes. For the lithium isotopes, a differential reduction could be effected with either protons or neutrons, as  $\text{Li}^6$  interacts far more readily with such particles than does  $\text{Li}^7$ . Table 9 shows, for example, that  $\text{Li}^6$  is consumed approximately 70 times faster than  $\text{Li}^7$  in proton reactions at all temperatures. Also, the thermal-neutron cross-section for  $\text{Li}^6(n, \alpha)\text{H}^3$  is 945 barn, while the capture of neutrons by  $\text{Li}^7$  has a cross-section of 33 millibarn.

The case of boron is different. Reference to Table 9 shows that it is the heavier isotope which reacts preferentially with protons. However, neutrons

are far more effective in destroying the lighter isotope than the heavy one, the relevant cross-sections being 3800 barn and 50 millibarn, respectively. Hence the simplest way to reduce the abundance of the light isotopes of both Li and B is to postulate irradiation by neutrons.

The neutrons are generated in the planetesimals along with the other spallation products. This is the best location for their appearance, for, were they expelled from the sun, they would be subject to radioactive decay and, not following the magnetic lines of force, the flux would have to be enormous in order to have an adequate number collide with the planetesimals. On the other hand, with their origin in the planetesimals proper, the hydrogen in the water ice serves to thermalize the neutrons before they can diffuse out of the solids. Once thermalized, they are subject to capture by hydrogen, to make deuterons, and by  $\text{Li}^6$  and  $\text{B}^{10}$ , depleting these nuclei. Only a modest neutron flux is needed and it does not impose any serious strain on the model.

There are certain requirements which must be satisfied.

1. There cannot be an overabundance of hydrogen, for then the neutrons would all go into deuterons and not be available to consume  $\text{Li}^6$  and  $\text{B}^{10}$ . It is for this reason that FGH propose that the planetesimals existed in a volume essentially devoid of gas except for the tenuous stream which maintained the magnetic link with the sun.

2. Another restriction of the gas density is that the energetic protons may not interact until they reach the planetesimals which are at a distance of some  $10^{12}$  cm from the sun. Taking into account the fact that spiraling about the magnetic field lines makes for an effective path length much greater than  $10^{12}$  cm, FGH find a density of  $10^{-12}$  or  $10^{-13}$  gm/cm<sup>3</sup>.

3.  $\text{He}^3$  must be absent from the original planetesimal matter, and virtually all of the  $\text{He}^3$  that is generated in spallation of  $\text{Li}^6(n, \alpha)\text{H}^3(\beta^- \bar{\nu})\text{He}^3$  reactions must evaporate. The reason is that the sequence of events  $\text{He}^3(n, p)\text{H}^3(\beta^- \bar{\nu})\text{He}^3$  is initiated with a thermal cross-section of 5500 barn, and  $\text{He}^3$  would convert so many neutrons into protons that the other required uses for the neutrons would not be met.

4. The neutron flux cannot be too large. To illustrate this, FGH describe the case of certain isotopes of gadolinium.  ${}_{64}\text{Gd}^{157}$  has a thermal neutron-capture cross-section of  $2.4 \times 10^5$  barn, while the corresponding value for  ${}_{64}\text{Gd}^{158}$  is only 4 barn. Making the reasonable assumption that the original production ratio of these isotopes was largely dependent on their respective even Z-odd N *versus* even Z-even N constitutions, calculations of the type elaborated by BBFH suggest that the abundance ratio  $\text{Gd}^{157}/\text{Gd}^{158}$  should be a bit less than 1. The ratio given by SU 1958 is  $\text{Gd}^{157}/\text{Gd}^{158} = 0.63$ . This is clear evidence that the odd isotope has not been preferentially destroyed, and it follows that there cannot have been too many neutrons flooding through the planetesimals. FGH assert that only some 10 per cent of the planetesimal matter was subjected to neutron bombardment. The remainder of the matter avoided contact with neutrons

simply because it was condensed in objects too large to have been thoroughly permeated by the primary protons or because the original protons missed.<sup>11</sup>

Taking an average proton energy near 400 Mev, the average depth of penetration into the planetesimals is 40 cm; those protons which travel farther than this are taken to cause spallation, while shorter range protons are neglected. This division is adopted for simplicity. Clearly, the spallation cross-sections are fundamental, for, given the nature of the targets from the planetary model, the cross-sections fix the number of protons and the total energy in the form of fast protons that the early sun had to produce. Once those numbers are known, one can see whether they are consistent with the other demands on the sun, such as the need for transfer of angular momentum to the planetary system. However, as is the case for the light targets employed by BP, the cross-sections are either poorly known or entirely unknown, and, again, various assumptions are called for.

For example, it is pointed out that the nuclei  $\text{Li}^6$  and  $\text{B}^{10}$  have even mass numbers, while the other stable isotopes of those elements have odd mass numbers. Since it is generally true that even-A nuclei are more stable than odd-A nuclei, it is concluded that the even-A isotopes should be generated in spallation *at least* as often as the others. It is further argued that there seems to be no reason why  $\text{Li}^7$  should be made more readily than  $\text{B}^{11}$ , but the abundance ratio of  $\text{Li}^7/\text{B}^{11}$  is roughly five to one. This is interpreted in terms of an equal original abundance of the lithium and boron isotopes, and the subsequent irradiation by neutrons to augment  $\text{Li}^7$  relative to  $\text{B}^{11}$  as well as to reduce  $\text{Li}^6$  and  $\text{B}^{10}$ . The augmentation of  $\text{Li}^7$  comes from the reaction  $\text{B}^{10}(n, \alpha)\text{Li}^7$ .

FGH chose spallation cross-sections from experimental work, which has been summarized by Miller and Hudis (1959), and from theoretical papers by Dostrovsky and his associates (Dostrovsky, Fraenkel, and Friedlander 1959; Dostrovsky, Fraenkel, and Rabinowitz 1960; Dostrovsky, Fraenkel, and Winsburg 1960). The calculations are based on the idea that the incident proton produces a nucleus which is highly excited and which, after statistical equilibrium is reached, haphazardly concentrates enough energy in one or another combination of nucleons to permit their evaporation from the nucleus. Since the stable light nuclei can be produced directly or through the decay of radioactive isobars which themselves appear as spallation products, FGH find it necessary to estimate the relative spallation yields of the stable and unstable isobars. This is done by noting that where the isobars have even A, the mass difference between the stable and radioactive forms is generally greater than when the isobars have

<sup>11</sup> Murthy and Schmitt (1963) have found that the isotopic abundances for Sm, Eu, and Gd are the same in meteorites and terrestrial matter. From this they offer three alternatives: (1) the planetesimals could not have contained enough water to thermalize the neutrons, for large isotope anomalies would have resulted. They further state that the physical structure of the FGH planetesimals must be modified in a major way; (2) the planetesimals and terrestrial matter received exactly the same neutron irradiation; and (3) the planetesimals were never irradiated.

odd A. Thus, the  $\text{He}^6\text{-Li}^6$  mass difference is 3.54 Mev, while the  $\text{Be}^7\text{-Li}^7$  difference is only 860 kev. In the evaporation of light isobars from the nucleus which has absorbed an energetic proton, the cross-section falls exponentially with increasing mass of the emitted particle, and the radioactive isobars are assumed to occur less frequently than the stable ones, with  $\text{He}^6$  expected to be rare relative to the others.

The number of fast protons ejected from the sun is obtained by consideration of the angular momentum and energy which the sun must lose to the planetary matter. Then the calculations of the various yields follow directly. The neutrons that are liberated and thermalized are shared, according to capture cross-sections and relative abundance, by all the nuclear constituents of the planetesimals.

The time scale for the irradiation is significant, as may be appreciated from the case of  $\text{B}^{10}$ , to the abundance of which the radioactive nucleus  $\text{Be}^{10}$  is a contributor. The mean life of  $\text{Be}^{10}$  is  $3.9 \times 10^6$  yr. If the neutron flux lasts for a time short compared with that value,  $\text{Be}^{10}$  will be preserved and will eventually add to the  $\text{B}^{10}$  abundance. However, if the  $\text{Be}^{10}$  decays before termination of the neutron irradiation, the ultimate amount of  $\text{B}^{10}$  will be reduced. FGH give the Kelvin contraction time for the sun as  $\sim 3 \times 10^7$  years, and suggest that the irradiation period is  $\sim 10^7$  years, so that much of the  $\text{Be}^{10}$  spallation yield is converted into surviving  $\text{B}^{10}$ .

Putting the above factors together in numerical fashion, FGH conclude that the local abundances of D, Li, Be, and B can be explained provided  $7.6 \times 10^{46}$  protons carrying  $6.5 \times 10^{48}$  erg of energy irradiated 10 per cent of planetary matter. A total of  $7.6 \times 10^{46}$  neutrons, or a neutron flux of  $10^7$  n/sec  $\text{cm}^2$ , permeated the planetesimals over a time interval of  $10^7$  years. Approximately 100 times as much energy was lost by the sun to produce the rotational braking. Thus, if the chance of a collision between a fast proton and a planetesimal was about 10 per cent, some 10 per cent of the total solar energy loss had to be expended in fast particles. Comparison with flares on the present sun suggests that the sun was  $10^7$  times more active in its T-Tauri phase than now. This is to be compared with Hayakawa's estimate of  $10^4$ .

Finally, FGH consider spallation reactions in the solar atmosphere proper to explain the abundance of the light nuclei there. Although it is recognized that the target substances are  $\text{He}^4$ , C, N, O, and Ne rather than the common metals, it is assumed that the spallation cross-sections for creating the nuclei of interest will not be very different. Mixing of the surface matter to a depth at which  $\rho x_{\text{H}} = 10^2$  gm/ $\text{cm}^3$  and  $T_6 = 1$  presumably occurred just as the sun settled onto the main sequence. Under those conditions, the mean life of a deuteron is  $\sim 10^6$  years, and the energy released in its destruction suffices to drive the convection currents to  $\rho x_{\text{H}} = 2$  gm/ $\text{cm}^3$ ,  $T_6 = 3.4$ , where the lithium isotopes can burn but not Be or B. This, then accounts for a Li/Be ratio in the sun roughly 100 times less than in meteoritic matter and serves, also, to deplete  $\text{Li}^6$  relative to  $\text{Li}^7$ .

We have pointed out earlier that new data by Shima (1962) and Sill and Willis (1962) make the factor 750 instead of 100 (see Table 1).

Our discussion of this paper will deal largely with the spallation cross-sections, although the model of the formation of the solar system is also subject to question. For example, Lyttleton (1961) has proposed that the planets were accreted by the sun, in which case planetary matter need not bear any relation whatever to solar developments.

One basic assumption advanced by FGH is that the cross-sections for creating isotopes of Li, Be, and B are closely the same. Virtually no measurements have yet been made on the direct production of the stable nuclei, and only fragmentary data on the radioactive isobars are available. A summary of the experimental and theoretical information on the spallation yield of various light substances is given in Table 13 (DFR 1960).

TABLE 13  
EXPERIMENTAL AND CALCULATED SPALLATION CROSS-SECTIONS  
(MILLIBARN)(DFR 1960)

TARGET	$E_p(\text{MEV})$	He <sup>6</sup>		Be <sup>7</sup>		Li <sup>8</sup>		Li <sup>6</sup>	Li <sup>7</sup>
		Exp.	Calc.	Exp.	Calc.	Exp.	Calc.	Calc.	Calc.
Cu.....	460	2±1	2±.5	0.6	1.4	.....	.....	.....	.....
	940	4±2	6±1	4±1	5±1	.....	2±.4	14±1	10±1
	1840	.....	.....	12±3	11±1	3	3±.6	26±2	18±1
Ag.....	460	.....	.....	0.1	1.1	.....	.....	.....	.....
	940	4±2	6±1	2.5	6.8	.....	3±1	24±2	16±2
	1840	7±4	11±2	11±3	14±2	4	9±2	44±4	40±3
Au.....	460	0.01	0.40	.....	.....	.....	.....	.....	.....
	940	.....	.....	1±3	4±1	.....	6±1	21±2	32±3
	1840	.....	.....	6±2	15±2	9	19±2	63±4	82±5
Pb.....	940	10±5	13±2	.....	.....	.....	.....	.....	.....
	1840	21±11	40±5	.....	.....	.....	.....	.....	.....
	.....	.....	.....	.....	.....	.....	.....	.....	.....

The table indeed shows that  $\sigma(\text{Li}^6) \approx \sigma(\text{Li}^7)$ ,  $\sigma(\text{He}^6) \ll \sigma(\text{Li}^6)$ , and  $\sigma(\text{Be}^7) < \sigma(\text{Li}^7)$ . The agreement, to within a factor of 2, between the calculated and experimental cross-sections is taken as justification for using the theoretical values even in cases where corresponding experiments have not been performed. The agreement depends, however, on choices of parameters, which vary markedly not only as the target nucleus changes but also with the bombarding energy. The parameters are in no sense determined from fundamental nuclear theory, but are essentially *ad hoc*. In this circumstance, the application of the calculations to reactions for which data do not exist must be regarded as speculative. Attention is also called to the fact that not even calculations are available for Be<sup>9</sup>, B<sup>10</sup>, and B<sup>11</sup>. Moreover, for reactions of the form  $(p, p\ n)$ , experiment and theory are not in agreement (Markowitz, Rowland, and Friedlander 1958; Porile 1962) for proton energies above 300 Mev and a variety of targets.

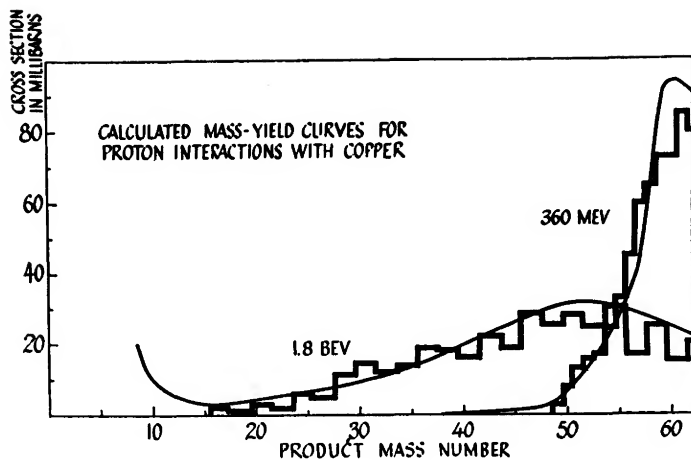


FIG. 13.—Cross-section (millibarns) for production of various mass products from proton bombardment of copper for two bombarding energies. From Miller and Hudis (1959).

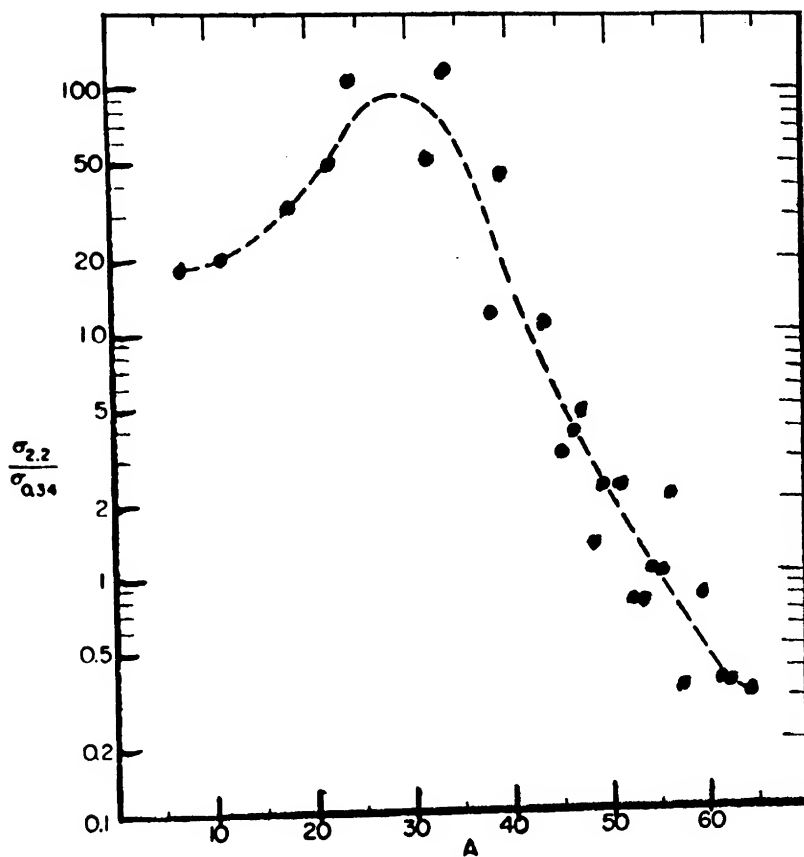


FIG. 14.—Ratio of formation cross-sections at 2.2 BeV proton energy to those at 340 Mev as a function of the atomic weight of the product particle from the bombardment of copper. From FMWHB (1954).

We note, from Tables 11 and 13, that the spallation cross-sections for making  $\text{He}^6$  and  $\text{Be}^7$  vary rapidly with the mass of the target and with bombarding energy. The energy dependence is of great importance, as seen in Figure 13 from MH (1959) and Figure 14 from Friedlander, Miller, Wolfgang, Hudis, and Baker (1954). Clearly the number of small-mass fragments is very small for  $E_p \sim 400$  Mev. However, one can suggest that the bulk of the energy transported from the sun by fast protons could very well be in large numbers of protons with energies below 400 Mev, and the spallation yields of Li, Be, and B would then be extremely small. While Li, Be, and B *might* be associated with the observed mass fragments between  $A = 50$  and  $A = 60$ , the assertion that  $\sigma(\text{Li}) \approx \sigma(\text{Be}) \approx \sigma(\text{B})$  is not yet substantiated by experiment. Some data on this point have been offered by Nakagawa, Tamai, and Nomoto (1958), who bombarded the Ag and Br of photographic emulsions with 6.2 Bev protons and distinguished the light nuclei on the basis of the density of tracks in the nuclear stars which occurred. Their results appear in Table 14. From a survey of all such data, Miller and Hudis (1959) conclude that  $\sigma(\text{He}) > \sigma(\text{Li}) > \sigma(\text{Be}) > \sigma(\text{B})$ .

TABLE 14  
FREQUENCY OF PRODUCTION OF NUCLEAR FRAGMENTS  
(NTN 1958) WITH CHARGE Z

Charge Z.....	3	4	5	6	7	8
Frequency.....	$145 \pm 21$	$46 \pm 10$	$18 \pm 7$	$5 \pm 3$	$2 \pm 3$	$5 \pm 4$

The FGH cross-sections for spallation of the light nuclei (He, C, N, O, and Ne) in the sun are based on the assumption that variations in target are unimportant. Evidence to the contrary appears in Table 13, where the calculated  $\sigma(\text{Li}^7)$  for  $E_p = 1840$  Mev is 18 mb for a copper target and 82 for a gold target. The table suggests that small targets should be completely ineffective in making He, Li, Be, and B. However, it must be kept in mind that light nuclei are not simply pieces of heavy ones but have a structure all their own. In particular, experimental evidence is now accumulating that nuclei with masses from 2 to 8 or 10 may maintain a quasi-independent existence within larger nuclei. Thus, the ejection of D, He, Li, Be, and B may result from a direct interaction between a fast proton and a substructure of the necessary character. For example, consider  $\text{C}^{12}$ ,  $\text{O}^{16}$ , and  $\text{Ne}^{20}$  to consist of alpha particles (Peaslee 1962). Bombardment by fast protons causes the ejection of nuclei of the type  $(na + \text{D})$  or  $(na + t)$ , where  $n = 1$  or 2 for Li and B. Considering only knock-out,  $\text{D}/t$  should be very small for  $n = 0$  because of the small binding energy of the deuteron. If alpha particles accompany the emergent D or t, the deuteron is somewhat stabilized by the presence of the other particles, so  $(na + \text{D})/(na + t)$  should increase with  $n$ . This is in qualitative accord with the observed isotope ratios  $\text{Li}^6/\text{Li}^7 = 0.08$ ,  $\text{B}^{10}/\text{B}^{11} = 0.23$ , for  $n = 1, 2$ . The production



ratio for  $(na + 2)/(na + 3)$  may also increase with nuclear size because of the increasing applicability of the statistical model, in agreement with Table 13. Production of B relative to Li should also be inhibited by the Coulomb barrier in medium-weight targets.

Another feature of spallation is that, as seen in Figure 13, the nuclei produced with the greatest frequency are those with mass numbers only a few removed from that of the target. This is generally true for medium and heavy targets (MH 1959). From studies of stable isotopes produced in iron meteorites by cosmic rays, Stauffer and Honda (1962) conclude that the spallation contribution to a nuclear species is given approximately by  $C \sim (dA)^{-2.4}$  where  $dA$  is the mass loss. Were copper the principal target substance, Figure 13 shows a relatively large yield of nuclei with  $A \approx 50$  to 60, the production cross-sections being

TABLE 15  
ABUNDANCES OF SELECTED NUCLEI ( $Si = 10^6$ )

Nucleus	Abundance	Nucleus	Abundance
${}^3\text{Li}^6$ .....	7.4 <i>sp</i>	${}^{22}\text{Ti}^{47}$ .....	189 <i>s, e, r</i>
${}^3\text{Li}^7$ .....	92.6 <i>sp</i>	${}^{22}\text{Ti}^{49}$ .....	134 <i>s</i>
${}^4\text{Be}^9$ .....	20 <i>sp</i>	${}^{22}\text{Ti}^{50}$ .....	130 <i>s</i>
${}^6\text{B}^{10}$ .....	4.5 <i>sp</i>	${}^{23}\text{V}^{51}$ .....	220 <i>e</i>
${}^6\text{B}^{11}$ .....	19.5 <i>sp</i>	${}^{24}\text{Cr}^{54}$ .....	204 <i>e</i>
${}^{19}\text{K}^{41}$ .....	219 <i>s</i>	${}^{28}\text{Ni}^{61}$ .....	342 <i>e</i>
${}^{20}\text{Ca}^{42}$ .....	314 <i>s</i>	${}^{28}\text{Ni}^{64}$ .....	318 <i>s</i>
${}^{20}\text{Ca}^{48}$ .....	64 <i>s</i>	${}^{29}\text{Cu}^{63}$ .....	146 <i>s</i>
${}^{21}\text{Sc}^{45}$ .....	28 <i>s</i>	${}^{29}\text{Cu}^{65}$ .....	66 <i>s</i>
${}^{22}\text{Ti}^{46}$ .....	194 <i>s</i>		

of the same order as those taken by FGH for Li, Be, and B. A closely similar result has been obtained in the bombardment of  $\text{As}^{75}$  by 2.9 Bev protons (Kaufman 1962). Consequently, with light metal targets, one should find abundances of nuclei with  $A = 40$  to 65 to be comparable with those of Li, Be, and B. Indeed, SU (1958) lists values, relative to  $Si = 10^6$ , as in Table 15. The abundances of Li, Be, and B are included for comparison. Below the abundance figure is a letter indicative of the presumed mode of formation according to the code: *sp* = spallation product, *s* = slow neutron absorption, *r* = rapid neutron absorption, *e* = equilibrium process. The information on *s*- and *e*-yields is from BBFH.

The point is that spallation of the light metals will itself produce relative abundances at least comparable with those given in the table, whereas many of the listed nuclei are attributed to the *s*-process. Moreover, the FGH argument concerning even- $A$  versus odd- $A$  spallation cross-sections suggests that  ${}^{22}\text{Ti}^{46}$ ,  ${}^{22}\text{Ti}^{50}$ , and  ${}^{28}\text{Ni}^{64}$  ought to be considerably more abundant than their odd- $A$  isotopes, which, in fact, they are not. Similarly, Stauffer and Honda (1962) find that the cosmogenic production of calcium isotopes varies as  $\text{Ca}^{42}:\text{Ca}^{43}:\text{Ca}^{44}:\text{Ca}^{46} = 90:100:140:2.5$ . The relative rarity of  $\text{Ca}^{46}$  is readily explained in terms of its large neutron excess, but the production ratio of the other isotopes is at

variance with the FGH assumption. Stauffer and Honda also estimated the  $V^{51}/V^{50}$  production ratio as between 3 and 5, the  $V^{50}$  enrichment varying from a factor of 3 to a factor of 100. The enrichment of  $K^{40}$  exceeded 100 times. From this information we argue that the spallation contribution to the medium-weight nuclei would exceed the  $s$ -contributions taken by Fowler and his associates to account for nearly all of their abundance.

We see from this discussion that the interesting work by FGH and the narrower efforts of Hayakawa and BP have certain features in common. Di, Li, Be, and B are found to arise from spallation reactions; these reactions accompanied heavy flare activity in the sun's T-Tauri stage; the targets were in the outer regions, either the sun's nebula proper (Hayakawa and FGH) or the photosphere from which matter was evaporated. Hayakawa explains the large D/H ratio as due to differential losses from small dust grains as they combined to make the planets, whereas BP rely on cycling, and FGH introduce slow neutron irradiation of strategically organized planetesimals. These efforts all suffer from grave uncertainties in spallation cross-sections. While it may never be possible to eliminate all ambiguities from the astrophysical aspects of the creation of D,  $He^4$ , Li, Be, and B, it is well within present capabilities to determine the spallation cross-sections with good precision. It is deeply to be regretted that these measurements, which call only for relatively standard techniques of nuclear physics and a large proton accelerator, have not yet been done. Hopefully some laboratories will soon devote a portion of their machine time to problems of this fundamental nature; the best approach seems to the present author to be to construct a 1-3 bev accelerator solely for astrophysical purposes.

## § 4. THE AGE OF ASTRONOMICAL OBJECTS

### 4.1. METEORITES AND THE EARTH

The existence of naturally radioactive nuclei like  $Th^{232}$  and the isotopes of uranium gives positive proof that the age of the earth is not infinite. Moreover, measurement of the relative abundance of the long-lived parent and stable daughter nuclei in the thorium and uranium decay chains can be used to determine the age of the sample of matter under study (Nier 1939). Let the chemical symbol stand for the relative number of nuclei of that type, the subscript zero referring to the time at which the sample was formed and the subscript  $t$  referring to the present time. Radioactive decay constants are denoted by  $\lambda$  and a subscript giving the mass number. From the law of radioactive decay,

$$N_t = N_0 \exp(-\lambda t),$$

where  $N_0$  is the original number of radioactive nuclei with decay constant  $\lambda$ , and  $N_t$  is the number remaining at time  $t$ , we readily find

$$\begin{aligned} Pb_t^{206} &= Pb_0^{206} + U_t^{238} [\exp(\lambda_{238}t) - 1], \\ Pb_t^{207} &= Pb_0^{207} + U_t^{235} [\exp(\lambda_{235}t) - 1], \\ Pb_t^{208} &= Pb_0^{208} + Th_t^{232} [\exp(\lambda_{232}t) - 1]. \end{aligned}$$

Two procedures can be followed. If an estimate can be made of the original relative abundances of the Pb isotopes, those abundances can be subtracted, and Pb-U, Pb-Th, or Pb-Pb ages can be deduced from the foregoing equations. Knowledge of the initial relative abundances is based on the fact that  $\text{Pb}^{204}$  is non-radiogenic. Hence, samples which have the largest relative concentration of  $\text{Pb}^{204}$  may be assumed to have the primordial isotopic distribution. This is particularly justified if the sample is free of uranium and thorium. However, caution must still be exercised because of the possible loss of uranium and thorium relative to lead sometime during the life of the sample (Patterson 1953).

An alternative is to use two samples: say, two meteorites believed to have the same age. If the samples have different Pb/U or Pb/Th ratios, the original amounts of the Pb isotopes may be eliminated. To see this, let primed and unprimed symbols stand for the contents of the two samples, respectively. Then, for example,

$$\frac{\text{Pb}_t^{206}}{\text{Pb}_0^{204}} - \frac{\text{Pb}_t'^{206}}{\text{Pb}_0'^{204}} = \frac{\text{Pb}_0^{206}}{\text{Pb}_0^{204}} - \frac{\text{Pb}_0'^{206}}{\text{Pb}_0'^{204}} + \left( \frac{\text{U}_t^{238}}{\text{Pb}_0^{204}} - \frac{\text{U}_t'^{238}}{\text{Pb}_0'^{204}} \right) [\exp(\lambda_{238}t) - 1].$$

Since the initial ratio  $\text{Pb}_0^{206}/\text{Pb}_0^{204}$  is independent of the sample, the first two terms on the right cancel and a Pb-U age can be found.

The assumptions which underlie the foregoing as applied to meteorites have been clearly stated by Patterson (1956) as: (1) The samples were formed at the same time; (2) they have existed as isolated and closed systems since their formation; (3) their original relative abundance of the Pb isotopes was the same.

On this basis, Patterson (1956) concluded that meteorites have an age of  $4.55 \pm 0.07 \times 10^9$  years. Moreover, comparison of the non-radiogenic Pb abundances in meteorites and on the earth (ocean sediment) shows them to be the same. Hence, the further assumption that the composition of terrestrial uranium is the same as that of meteoritic uranium enables one to equate the age of the earth with the age of the meteorites. Masuda (1958) obtained a Pb-Pb age of  $4.55 \times 10^9$  years, and Marshall (1962a) finds  $4.6$  to  $4.7 \times 10^9$  years with a possible (but unlikely) age of  $5.1 \times 10^9$  years for the Indarch carbonaceous chondrite. Fowler and Hoyle (1960) take Patterson's result as the most reliable age of the earth, although more recent measurements (Hess and Marshall 1960) indicate a spread in meteoritic age from 4.27 to 4.69, with the most radiogenic lead sample giving 4.6, the units being billions of years. Fowler (1961), assessing the various uncertainties in the age determination, remarks that a condensation time for the earth  $10^8$  years after that for the meteorite would be consistent with the data.

It is worthwhile to examine some of the basic assumptions, especially since careful selection of samples is needed if concordant  $\text{Pb}^{207}$ - $\text{U}^{235}$  and  $\text{Pb}^{206}$ - $\text{U}^{238}$  ages are to be obtained. Stieff and Stern (1961) note that the calculated ages of uranium ores are discordant, with  $\text{Pb}^{206}$ - $\text{U}^{238}$  ages  $<$   $\text{Pb}^{207}$ - $\text{U}^{235}$  ages  $\ll$   $\text{Pb}^{207}$ - $\text{Pb}^{206}$  ages as a general rule. Occasionally the sequence is reversed. Discussions of dis-

cordance have often centered on the possible loss of matter intermediate between the parent and ultimate daughter substances. Of the intermediate elements, only one (radon) is a gas. However, the half lives of the radon isotopes of interest in this connection are quite short (4 sec, 52 sec, and 3.8 days), and it is difficult to explain the observed deviations in terms of the loss of this element. We call attention to the fact that among the long-lived intermediate species are three from  $U^{238}$  ( $Th^{230}$ ,  $8 \times 10^4$  yr;  $Ra^{226}$ , 1620 yr;  $Bi^{210}$ ,  $2.6 \times 10^6$  yr), one from  $U^{235}$  ( $Pa^{231}$ ,  $3.4 \times 10^4$  yr), and none from  $Th^{232}$ . Ehmann and Huizenga (1959) have measured the relative abundances of Bi, Ti, and Hg in chondrites, and have concluded that there is strong evidence that Bi has been fractionated relative to U and Th. Should this be the case, the existence of  $Bi^{210}$  in the  $U^{238}$  chain could have the effect of depleting the sample in  $Pb^{206}$  and give too small an age. This is in the correct direction to explain the tabulation by Stieff and Stern.<sup>12</sup>

In addition to chemical fractionation, other possibilities can be mentioned. For example, were the meteorites containing U, Th, and radiogenic Pb irradiated with slow neutrons, fission of  $U^{235}$  would lead to too great an age as calculated from  $Pb^{207}$ , the error depending on how long after the original condensation the irradiation took place. As mentioned in § 3 on D, Li, Be, and B, Fowler, Greenstein, and Hoyle (1961) have studied the problem of neutron irradiation and have argued that only 10 per cent of solar system matter outside the sun underwent such an effect.

In the work on age, the abundance of lead is of major importance. Unfortunately, it is not clear that this number is well known. For ordinary chondrites, Reed, Kigoshi, and Turkevich (1960) estimate an uncertainty of a factor of 3. Since lead has a low melting point ( $327^\circ C$ ), it has been proposed by RKT that lead has been lost by evaporation from the ordinary chondrites, which have presumably been heated during their history. Using the concentration of Hg as an indication, RKT find that the carbonaceous meteorites have probably not been hot. For such meteorites, the Pb concentration is some 80 times that in ordinary chondrites. It is this latter result which is used by CFHZ in their study of the termination of the *s*-process and by Fowler and Hoyle (1960) in their calculations on age (see below).

The decay of  $K^{40}$  (to  $Ar^{40}$ ) and of  $Rb^{87}$  (to  $Sr^{87}$ ) can also be used to fix the age of very old samples of matter. Aldrich and Wetherill (1958) have reviewed those determinations. For  $K^{40}$ , which decays to  $Ca^{40}$  as well as to  $Ar^{40}$ , there is still some uncertainty in the decay constants. The expression for the age is

$$t = \frac{1}{\lambda_e + \lambda_\beta} \ln \left( 1 + \frac{\lambda_e + \lambda_\beta}{\lambda_e} \frac{Ar^{40}}{K^{40}} \right),$$

<sup>12</sup> Erskine, Buechner, and Enge (1962) find that the ground state of  $Bi^{210}$  actually has a half life of 5 days, the figure  $2.6 \times 10^6$  years belonging to an isomeric state. Hence, the foregoing analysis is incorrect if  $Bi^{210}$  is formed in its ground state.

where the subscripts  $e$  and  $\beta$  refer to electron capture and  $\beta$ -emission respectively. At an age near  $5 \times 10^9$  years, a 10 per cent error in either decay constant introduces a 5 per cent error in  $t$ . A measurement of the K-Ar age in the Richardton meteorite as carried out by Reynolds (1960a) gave  $4.47 \pm 0.2 \times 10^9$  years, while an earlier study (Geiss and Hess 1958) gave  $4.15 \pm 0.01 \times 10^9$  years. Two points are worth noting about such age measurements. For one, where a noble gas is involved, the time that is measured is merely the time for which the sample has been cool enough to retain the gas, and this time is a function of the size of the original object of which the sample was a part (Fish, Goles, and Anders 1960). Secondly, it might be worth recognizing that  $K^{40}$  is an  $s$ -product, while all of the other nuclei used in dating are  $r$ -products. It will shortly be shown that age calculations have been made on the basis of the relative production rates for certain  $r$ -products, but similar work based on  $s$ -products has not been carried out.

#### 4.2. THE SOLAR SYSTEM

A question which has received much recent study is: how long did it take the solar system to condense? (Reynolds 1960a, b, c; Wasserburg, Fowler, and Hoyle 1960; Fowler and Hoyle 1960; Goles and Anders 1960; Anders and Stevens 1960; Kohman 1961; Fowler 1961). An answer to this question can be found, as always, provided certain assumptions are introduced. To begin with, let us assume that the matter of the solar system was synthesized in a single supernova explosion. The  $r$ -process took place, and among the  $r$ -products were  $I^{127}$  (stable) and  $I^{129}$  ( $t_{1/2} = 1.7 \times 10^7$  yr). According to CF (1960), 80 per cent of  $I^{127}$  is due to the  $r$ -process and 20 per cent to the  $s$ -process.  $I^{129}$  decays to  $Xe^{129}$ , so the latter is shielded from direct formation in the  $r$ -process. CF find that 6 per cent of  $Xe^{129}$  comes from the  $s$ -process, the remainder arising from the decay of  $I^{129}$ .

Subsequent to the supernova explosion, the expanding gas and dust coalesced into solid objects. The exact size of these objects is a matter of importance but also of conjecture. We have seen that FGH describe planetesimals with radii of the order of a meter. FGA discuss the formation of meteorites as taking place within planetesimals with radii of the order of 25 km. Urey (1959) has suggested a different model according to which the meteorites came from the fragmentation of lunar-sized objects. FGA argue that this could not be the case, and we will adopt the point of view that the planetesimals were rather small in size.

It follows that the planetesimals captured very little of the noble gases present in the original residue of the supernova, and, in particular, little xenon was retained. On the other hand, iodine combined chemically with other elements to form solids which were readily incorporated into the planetesimals. Since the  $I^{129}$  eventually decayed to  $Xe^{129}$ , any  $Xe^{129}$  found in a meteorite could be attributed to the decay of  $I^{129}$  after solidification. Were the original amount of  $I^{129}$  known, the xenon content would give the interval of time required for solidification. For

$$Xe_i^{129} = I_c^{129} = I_0^{129} \exp(-\lambda_{129} t_c),$$

where the subscript “*t*” refers to the present time, “*c*” to the time when condensation occurred, and “0” to the instant after the supernova explosion. Then,

$$\exp(\lambda_{129} t_c) = \frac{I_0^{129}}{I_t^{127}} \frac{I_t^{127}}{Xe_t^{129}} = \frac{I_0^{129}}{I_0^{127}} \frac{I_t^{127}}{Xe_t^{129}},$$

whence

$$t_c = \frac{1}{\lambda_{129}} \left( \ln \frac{I_t^{127}}{Xe_t^{129}} + \ln \frac{I_0^{129}}{I_0^{127}} \right).$$

Reynolds (1960*b*) found that the Richardton meteorite contained an excess amount of  $Xe^{129}$ , relative to the terrestrial composition, of  $1.3 \times 10^{-3}$  cm<sup>3</sup> per gram of meteorite.<sup>13</sup> He assumed that the initial ratio of the iodine isotopes was unity. Correcting his assumption that the iodine content was a microgram per gram of meteorite to the later measured value (Goles and Anders 1960) of  $4.7 \times 10^{-8}$  gram per gram of meteorite, it follows that  $t_c = 2.7 \times 10^8$  yr. Jeffrey and Reynolds (1961) showed that Xe and I are correlated in one enstatite chondrite.

It is clear from the discussion of the origin of the elements that the solar system did not result from a single supernova explosion. Rather, there were many contributors distributed in time from the “origin” of the Galaxy to approximately  $5 \times 10^9$  years ago. Support for this conclusion has been given earlier, but a further argument can be offered. Were a single event responsible for the solar elements, the calculated relative production rates for  $U^{235}$  and  $U^{238}$  (BBFH, HF 1960, Kohman 1961, Fowler 1961), coupled with their present relative abundance, shows that that event must have taken place at least  $6.9 \times 10^9$  yr ago. Indeed, the  $U^{238}$ -Th<sup>232</sup> data give an age of  $8 \times 10^9$  yr (Fowler 1961). Such long times are consistent with the Pb-Pb and Pb-U ages obtained for meteorites and the earth only if the solar system condensed about  $2 \times 10^9$  yr after the supernova.

Now FGA (1960) have found that the meteorites were heated internally to temperatures of 2000–3000° K, the source of the heat being short-lived radioactivities. Detailed calculations on such heating have been carried out by Kohman (1961). The point is that the required radionuclei, principally  $Al^{26}$  ( $t_{1/2} = 7.4 \times 10^5$  yr), were generated in the supernova and lasted for only a few million years at most. Thus, a single *r*-event would create these nuclei some two billion years before they were needed to heat the meteorites. Kohman (1961) shows that continuous element formation, capped by a modest supernova explosion, gives a reasonable time sequence with a condensation time for the meteorites of  $6 \times 10^7$  yr. Marshall (1962*b*) finds there were three periods of supernova activity—one some  $13 \times 10^9$  years ago, a second  $7.5 \times 10^9$  years

<sup>13</sup> Merrihue (1963) has found a very large excess of  $Xe^{129}$  in the chondrules of the Bruderheim meteorite, but the excess varies with the sample selected. He states that the Xe is the result of  $I^{129}$  decay in the final element synthesis prior to the condensation of the meteorite.

ago, and the third about  $4.5 \times 10^9$  years ago, the last two contributing perhaps 15 per cent of the  $r$ -elements in the solar system.

The more-or-less continuous synthesis of the heavy elements has among its consequences that the time,  $t_c$ , found from the xenon work described above, is an upper limit to the condensation period. To get a more accurate value of  $t_c$  requires knowing how the supernovae occurred in time. Work by Salpeter (1959) and by Schmidt (1959) suggests that the rate of formation and evolution of stars has decreased exponentially with time. For such a situation, FH (1960) show that one must take account of the time constant of stellar evolution and the time interval over which production of the elements occurred. The details of this are given below (§ 4.3). For our immediate purpose we simply note that gross uncertainties in the two latter times have but a small effect on the calculation of  $t_c$ . In recent papers (Reynolds 1960c; Goles and Anders 1960), it is concluded that the condensation time of the solar system could have been as short as  $86 \times 10^6$  years. On this basis, one may, therefore, put the age of the solar system at  $4.55 \pm 0.09 = 4.64$ , in units of  $10^9$  years.

It happens that the foregoing interpretation of Reynolds' discovery is not free from criticism. For one thing CFHZ find  $I_0^{129}/I_0^{127}$  to be two instead of unity, and this slightly increases  $t_c$ .

More seriously, FGH and Fowler (1961) argue that the  $I^{129}$ , which led to the excess of  $Xe^{129}$  in meteorites, was *not* the result of the  $r$ -process in a supernova explosion. Rather, they put forward the idea that the same spallation of the planetesimals which, in their view, created D, Li, Be, and B, also generated the  $Al^{26}$  needed to heat the meteorites and the  $I^{129}$  which then gave rise to the anomalous  $Xe^{129}$ . Hence, it is claimed that the  $Xe^{129}$  cannot be used to fix the time interval between the termination of synthesis of solar matter and the condensation thereof. Having broken that link, there is greater freedom in choosing that interval, and Fowler (1961) suggests that the solar matter mixed in the Galaxy for at least  $10^8$  years before its withdrawal into the solar system. FGH take the mixing time to exceed  $2 \times 10^8$  years. Fowler (1961) gives a condensation time, subsequent to withdrawal, of  $\sim 7 \times 10^7$  years, so that the solar system has an age of  $4.55 \pm 0.07 = 4.62$  in units of  $10^9$  years. The last contribution to solar matter was produced  $\sim 4.8 \times 10^9$  years ago. However, Panasyuk (1961) questions the approximations which enter into the derivation of the equations used by Reynolds and Fowler, and concludes that there is no single way of using the  $I/Xe$  ratio to fix the times of interest.<sup>14</sup>

Another suggestion has been made by Cameron (1962). According to him, a brief burst of supernovae immediately preceded formation of the sun, and all the short-lived radioactivities were produced in those explosions. These explosions occurred over a time interval of  $3 \times 10^8$  years, after which the meteorite parents condensed in  $3 \times 10^6$  years, the time interval between cessation of the

<sup>14</sup> Butler, Jeffrey, Reynolds, and Wasserburg (1963) have found excess  $Xe^{129}$  in granite and attributed it to the decay of  $I^{129}$  soon after the formation of the earth.

supernovae explosions and condensation of the meteorites being  $1.47 \times 10^8$  years.

#### 4.3. STARS AND THE GALAXY

Not many years ago, it was thought that the Galaxy and the solar system had about the same age (Tolman 1949). Since then, revisions of the distance scale (Baade 1952; Humason, Mayall, and Sandage 1956) have led to the view that the Galaxy is considerably more ancient than the sun. At the present time, the age of the Galaxy is less certain than it was believed to be a few years ago, and it is no longer so certain that the sun and Galaxy have widely disparate ages (Dicke 1962). The principal methods of determining the ages of stars and the Galaxy are: (1) locating the point at which the stars in a cluster deviate to the right of the main sequence in a Hertzsprung-Russell diagram; (2) calculating the time it takes a star of given mass and chemical composition to attain its observed luminosity and radius; (3) calculating the time it takes to contaminate the Galaxy with the observed concentration of heavy elements; (4) by means of cosmological theory.

The first method has received a general discussion by Sandage (1958*a, b*) and Oort (1958*a, b*). By its use, very great ages have been reported for various objects, among them the following: Sandage (1961, 1962) has found an age of  $2.6 \times 10^{10}$  years for the globular clusters M3 and M5,  $2.2 \times 10^{10}$  years for M13, and  $1.6 \times 10^{10}$  years for the galactic cluster NGC 188. Hoyle (1959) and Sandage (1962) have reported M67 to have an age of  $9.2 \times 10^9$  years, while Oke (1959) and Wilson (1959) have found ages in excess of  $1.4 \times 10^{10}$  years for some stars. In this work, much depends on the choice of chemical composition, and it is important to recall that Hoyle (1959) gave reasons for believing that the helium content of very old objects is small. However, this has been questioned by Sandage (1962). Earlier we mentioned that the helium content of globular clusters appears to be normal (Traving 1962; O'Dell *et al.* 1964). It would clearly be helpful to have additional data on the helium concentration at various points in the Galaxy. Sandage (1962) notes that the globular-cluster ages could be smaller by a factor of 1.6 if the helium content is normal.

The stellar models employed to yield the great ages of the globular clusters have been questioned by Woolf (1962). He has considered the maximum age the cluster M3 can have based on the initial mass of the horizontal branch stars in M3, i.e., the initial amount of available fuel of those stars. According to him, the maximum age M3 can have is  $6.8 \times 10^9$  years for an initial mass of  $1.25 M_{\odot}$  for the horizontal branch stars and  $20.6 \times 10^9$  years for an initial mass of  $0.95 M_{\odot}$ . Thus, there is considerable uncertainty regarding the age as found from the turn-off points on the color-magnitude plots.

One would expect that the second method would be most precisely applied to the sun. However, it is noted by Dicke (1962) that the uncertainty in the contribution which helium makes to the mean molecular weight of the sun



introduces a possible spread of ages from 4 to  $15 \times 10^9$  years. It seems unlikely that similar calculations for other stars can give narrower limits.

The third method has been explored in considerable detail by BBFH, Fowler and Hoyle (1960), Kohman (1961), and Fowler (1961). The basis for this approach consists of the assumptions that stellar formation has declined exponentially with time during the life of the Galaxy and that the synthesis of the heavy elements, taking place in stellar interiors, follows that same time variation. One must further assume that particular heavy elements are the result of particular stellar developments. Thus, the authors quoted above consider that the  $r$ -products are created in Type I supernovae, which terminate the lives of stars with small masses. Dicke (1962) and Cameron (1962) adopt the contrary point of view that the  $r$ -nuclei come from the explosion of massive stars. That this divergence affects the estimates of the age of the Galaxy is readily seen. If massive stars are the source of the  $r$ -products, the rapid evolution of such stars means that the  $r$ -products contaminated the Galaxy well within the first  $10^9$  years of the Galaxy's life. If small mass stars are responsible, there is a time delay of 3 to  $8 \times 10^9$  years before such stars can have reached the supernova condition. Consequently, Dicke and Fowler, for example, find galactic ages which differ by this time interval even though they use the same data and technique for determining the time which has elapsed since the  $r$ -products appeared in the Galaxy.

Consider a model in which the Galaxy had a definite time of birth and has existed as a closed system. Then the age of the Galaxy is the sum of the age of the solar system, the time during which the elements were generated prior to formation of the solar system and the mean age of stars which give rise to the heavy elements. This method of finding the galactic age depends heavily on the relative abundance of the nuclear species and the theory of element formation.

BBFH used the present abundance ratio of the  $r$ -products  $U^{235}$  and  $U^{238}$  and the calculated relative production rates for these isotopes to find the interval of time over which the  $r$ -process took place prior to condensation of the solar system. FH (1960), Kohman (1961), and Fowler (1961) have revised the work of BBFH.<sup>15</sup> Suppose the Galaxy were born at a time  $t_0$  (Fig. 15). Thereafter, star formation declined exponentially with a characteristic time  $T$ , and decay constant,  $\Lambda = T^{-1}$ . When  $t_1$  was reached, those supernovae which generate the  $r$ -products started to contaminate the Galaxy with uranium and thorium. This supernova activity also decreased with the decay constant  $\Lambda$ . At time  $t_2$  the synthesis of the matter destined to become the solar system ceased, and at time  $t_3$  the solar system came into being. From  $t_2$  to the present time,  $t_4$ , the solar uranium and thorium decayed according to the radioactive law. Some neutron fractionation may also have occurred (FGH 1960; Fowler 1961). Schmidt (1960) has discussed the possibility that the rate of formation of those

<sup>15</sup> Clayton (1963) has revised some of the FH (1960) calculations.

stars which eventually yield  $r$ -products might differ from the rate for the Galaxy as a whole. Neglecting that,

$$\frac{dn}{dt} = K \exp[-\lambda(t-t_1)] - \lambda n \quad (t_1 \leq t \leq t_2),$$

whence

$$N(t_2) = \frac{K}{\lambda - \Lambda} [\exp(-\Lambda D) - \exp(-\lambda D)] \quad (D = t_2 - t_1),$$

and

$$N(t_4) = N(t_2) \exp(-\lambda \theta) \quad (\theta = t_4 - t_2);$$

$K$  is the production rate for the species with disintegration constant  $\lambda$ .

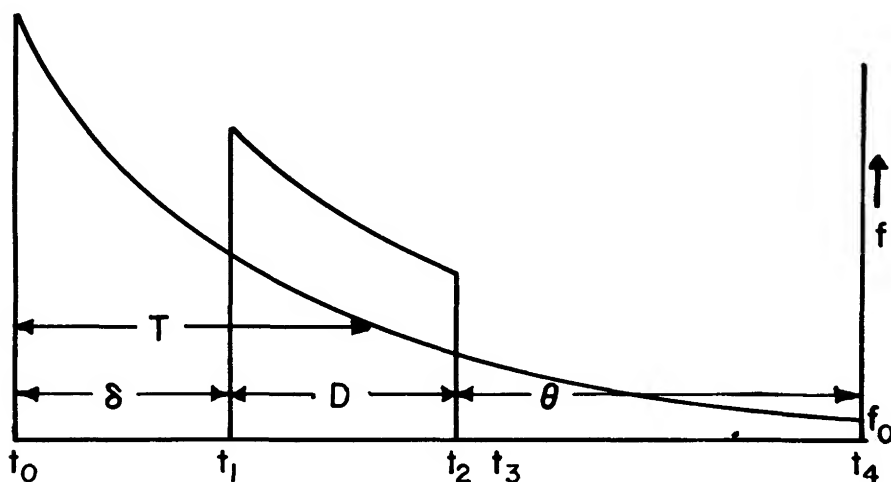


FIG. 15.—An evolutionary scheme for the galaxy. From Fowler and Hoyle (1960)

Determination of the significant time intervals is simplified by taking ratios of  $r$ -products. Experimental data on  $U^{235}/U^{238}$ ,  $U^{238}/Th^{232}$ , and the decay constants of these nuclei are available (Stromiger, Hollander, and Seaborg 1958; Marshall 1957; Bate, Huizenga, and Potratz 1959; König and Wänke 1959). BBFH showed how the relative production rates of the above  $r$ -products might be calculated in terms of the number of predecessor isobars created in the  $r$ -process. FH (1960) and Fowler (1961) used the same method to find

$$\frac{K_{235}}{K_{238}} = 1.65 \quad \text{and} \quad \frac{K_{238}}{K_{232}} = 1.65.$$

From these production ratios, FH and Fowler (1961) show that the assumption of a single event for preparation of solar matter gives discordant U-Th ages, the discrepancy amounting to  $\sim 1.5 \times 10^9$  yr (Fowler 1961). Concordance demands continuous synthesis of  $r$ -elements over a long period of time.

FH (1960) obtained an expression for  $\Lambda$  in terms of  $D$ ,  $\theta$ ,  $\delta = t_1 - t_0$ , and the

fraction,  $f$ , of the galactic mass, which is still in the form of gas and dust, the basis for the derivation being the exponential model of the Galaxy. The result was

$$\Lambda = -\frac{\ln f}{\delta + D + \theta},$$

and values of  $f$  ranging from zero to 100 per cent were considered. For  $0.02 < f < 0.37$ , concordant U-Th ages could be obtained, the best agreement being reached for  $f = 0.26$ . The experimental value is 0.02 (Oort 1958*b*). Fowler (1961) then finds  $D = 7.7 \times 10^9$  years.

Finally,  $\delta$  must be evaluated. This measures the average time it took the original stars to begin making  $r$ -elements. HF (1960) associated the  $r$ -process with stars of small mass. With this in mind, the mass chosen in that paper was 1.5 solar masses for which  $\delta = 3 \times 10^9$  years. Fowler (1961) takes 1.33 solar

TABLE 16  
THE EFFECT OF CHANGING U-TH PARAMETERS ON GALACTIC AGE  
(Kohman 1961)

$k_{235}/k_{238}$	$k_{232}/k_{238}$	$N_{235}/N_{238}$	$N_{232}/N_{238}$	$\theta \times 10^9$ yr	$\lambda (\times 10^{-9} \text{ yr}^{-1})$	$D (\times 10^9 \text{ yr})$
1.65	1.65	0.00726	3.80	4.70	0.015	7.2
1.65	1.65	0.00726	3.68	4.70	0.085	6.0
1.80	1.65	0.00726	3.80	4.70	0.095	6.6
1.80	1.65	0.00726	3.68	4.70	0.19	5.4

masses for which  $\delta = 7.6 \times 10^9$  years, while Dicke (1962) assumes  $\delta < 0.5 \times 10^9$  years. Fowler (1961) gives the age of the Galaxy as  $7.6 + 7.7 + 4.6 \sim 20 \pm 4$  in units of  $10^9$  years. Of these three numbers, the first depends critically on the mass distribution of the stars at the birth of the Galaxy.

The sensitivity of the second number to uncertainties in the basic data is well illustrated by Table 16, from Kohman (1961). The top row corresponds closely to the values used by FH (1960) and Fowler (1961). In the second row, the change in the  $\text{Th}^{232}/\text{U}^{238}$  value is based on König and Wänke (1959), while rows three and four use a ratio of production rates for the two uranium isotopes different by one standard deviation from the number in the upper two rows. A 3 per cent change in  $\text{Th}^{232}/\text{U}^{238}$  produces a 20 per cent change in  $D$ . From these considerations, Kohman (1961) concludes only that the solar system abundances derive from synthesizing events which took place over a time interval probably greater than  $5 \times 10^9$  years.

The third of the above numbers is the best known, although it is still necessary to have this reservation—the value of  $4.6 \times 10^9$  years is for the earth and meteorites and not for the sun. This age is assigned to the sun on the grounds that planetary matter came from the sun, but, as mentioned earlier, this need not be correct (Lyttleton 1960, 1961).

The discussion so far has rested on the assumption that the Galaxy has neither lost nor gained matter since its creation. FG (1960) investigated the consequences of a strategic injection of matter into the Galaxy. This idea is introduced because the calculated absolute solar abundances of  $r$ -elements appear to be about 100 times too large if Type I supernovae have contributed over the time  $D$ . Hence it is suggested that the Galaxy evolved as described until the original Type I presupernovae were all consumed, but the next generation of stars had not yet reached the supernova stage. The rate of formation of  $r$ -elements was then very small. FH set the time of this quiescent period about  $5 \times 10^9$  years ago and allow an absorption of extra-galactic  $r$ -matter at that time. Kahn and Woltjer (1959) have shown that the local group of galaxies contains about three times as much mass in the form of gas as in stellar systems and give a mean density for the local group of  $1.6 \times 10^{-28}$  gm/cm<sup>3</sup>. However, the density of galaxies in the local group is greater than the average in the universe, and FH take the mean density to be  $10^{-29}$  gm/cm<sup>3</sup>, of which they say only one per cent is condensed matter. In this case the galactic abundance of  $r$ -elements is diluted by a factor of 100 relative to what is seen in the stars, and matter absorbed from intergalactic space would be reduced by this factor in its  $r$ -component. (Van Albada [1960] assumes the mass ratio of invisible matter to galactic matter as 10.) FH suggest that the solar system was created just after the Galaxy acquired some extra-galactic substance.

For a steady state model of the universe, the appropriate equation for the rate of change of a given nuclear species with time is

$$\frac{dN}{dt} = K - \lambda N - 3NH = 0,$$

whence

$$N = \frac{K}{\lambda + 3H}.$$

In the foregoing  $H$  is the Hubble constant.

Suppose the gas collected by the galaxy were isolated from new sources of  $r$ -matter  $T$  years ago. Then the radioactive  $r$ -nuclei have undergone free decay for time  $T$ , and we have the expressions

$$\begin{aligned} \frac{U^{235}(T)}{U^{238}(T)} &= \frac{K_{235} \lambda_{238} + 3H}{K_{238} \lambda_{235} + 3H} \\ \frac{U^{235}}{U^{238}} &= \frac{U^{235}(T) \exp(-\lambda_{235}T)}{U^{238}(t) \exp(-\lambda_{238}T)}, \end{aligned}$$

where the last relation gives the present-day ratio. From that equation, and a similar one for  $U^{238}$  and  $Th^{232}$ , both  $T$  and  $H$  can be found; they are given by FH as

$$T \approx 5.3 \pm 0.3 \times 10^9 \text{ years},$$

$$H^{-1} \approx 11 \pm 6 \times 10^9 \text{ years}.$$

The above value of  $T$ , coupled with the age of the solar system, implies that the extragalactic gas took  $6 \times 10^8$  years to condense. Were this the case, the  $\text{I}^{29}$  discussed above, and, indeed, all of the  $r$ -products with short half lives, would have decayed before formation of the planetary system, and one would have to turn to the spallation argument to account for the abundance anomalies in xenon and similar elements.

It is interesting to note that the value of the Hubble constant obtained by FH is close to the value of  $13 \pm 6 \times 10^9$  years found by Sandage (1958*b*). However, Sandage (1961) has called attention to the possibility of error in the value of that constant, and Dicke (1962) cautions that  $H^{-1}$  was thought to be  $2 \times 10^9$  years only a decade ago. In any event, a consequence of the model just described is that the age of the Galaxy is indeterminate.

Dicke (1962) has summarized the results that cosmological theory give for galactic age and has emphasized the discrepancy in the age that the various methods yield. Thus, he observes that the average age of all the galaxies should be only one-third the Hubble age for the steady state model and about two-thirds the Hubble age for other cosmologies. The Hubble age is about three times the age of the earth but far less than that of the clusters and stars mentioned above. Dicke points out that there does not seem to be any feature of our Galaxy that would make one believe it to be significantly older than any of the other galaxies, but the existence of the old stars implies that our Galaxy is in fact older than the others. If we assume that our Galaxy is a rare object, the age of which is greater than the Hubble age, one expects to see other features that would distinguish our Galaxy from the bulk of the others. No such features can be specified, however. It may further be pointed out that if the surrounding galaxies are only 4 or so billion years old, stellar evolution therein could not have enriched the extra-galactic matter with heavy elements. Indeed, if stars of small mass with a lifetime of  $3$  to  $8 \times 10^9$  years are essential for production of the  $r$ -products, one would expect that the neighboring galaxies would be very deficient in heavy elements. Such is not the case, at least for the Magellanic Clouds.

At the present time, it would seem that only the age of the earth and meteorites can be considered as well established. In order to improve on age calculations for stars, including the sun and the Galaxy, one must have a better grasp of the conditions needed to synthesize the  $r$ -products and a more certain understanding of the connection between the sun and the planetary system. These are minimum requirements.

#### REFERENCES

- |   |      |                                       |
|---|------|---------------------------------------|
| ABT, H. A.                                  | 1960 | <i>Ap. J.</i> , <b>130</b> , 99.      |
| ADGIE, R. L., and<br>HEY, T. S.             | 1957 | <i>Nature</i> , <b>179</b> , 370.     |
| AJZENBURG-SELOVE, F.,<br>and STELSON, P. H. | 1960 | <i>Phys. Rev.</i> , <b>120</b> , 500. |

- ALBOUY, G., GUSAKOW,  
M., and POFFE, N. 1961 Proceedings of Rutherford Jubilee International  
Conference, Manchester, England, ed. J. B.  
BIRNS.
- ALBURGER, D. E. 1960 *Phys. Rev.*, **118**, 235.  
1961 *Ibid.*, **124**, 193.
- ALDRICH, L. T., and  
WETHERILL, G. W. 1958 *Ann. Rev. Nuclear Sci.*, **8**, 257.
- ALLER, L. H. 1953 *Atmospheres of the Sun and Stars* (New York:  
Ronald Press).  
1954 *Ap. J.*, **120**, 411.  
1957 *Ibid.*, **125**, 84.  
1960 *Stellar Atmospheres*, ed. J. L. GREENSTEIN  
(Chicago: University of Chicago Press).  
1961 *Abundance of the Elements* (New York, London:  
Interscience Publishers), p. 164.  
1962 Private communication.  
1963 *Astrophysics: Atmospheres of the Sun and Stars*  
(New York: Ronald Press Co.).  
1964 *Publ. Astron. Society Pacific*, Vol. **76**, in press.  
1965 *Advances in Astron. and Astrophysics*, ed. Z. KOPAL  
(New York: Academic Press).
- ALLER, L. H., and  
BIDELMAN, W. P. 1964 *Ap. J.*, **139**, 171.
- ALLER, L. H., and  
CHAPMAN, S. 1960 *Ap. J.*, **132**, 461.
- ALLER, L. H., ELSTE, G.,  
and JUGAKU, J. 1957 *Ap. J., Suppl.*, **3**, 1.
- ALLER, L. H., and  
FAULKNER, D. J. 1961 *A.J.*, **66**, 37.  
1962 *Pub. A.S.P.*, **74**, 219.  
1964 *International Astronomical Union Symposium*, No.  
20, "The Southern Milky Way and the Magel-  
lanic Clouds," ed. F. KERR and A. RODGERS,  
Canberra.
- ALLER, L. H., and  
GREENSTEIN, J. L. 1960 *Ap. J., Suppl.*, **5**, 139.
- ALLER, L. H., and  
LILLER, W. 1959 *Ap. J.*, **130**, 45.
- ALLER, L. H., O'MARA,  
B. J., and LITTLE, S. 1964 *S. Proc. Nat'l Acad. Sci.* (Washington), **51**, 1238.
- ALMQVIST, E.,  
BROMLEY, D. A., and  
KUEHNER, J. A. 1960 *Phys. Rev., Letters*, **4**, 515.
- ALPHER, R. A., and  
HERMAN, R. C. 1950 *Rev. Mod. Phys.*, **22**, 153.  
1953 *Ann. Rev. Nuclear Sci.*, **2**, 1.

- ANDERS, E. 1958 *Ap. J.*, **127**, 355.  
 1959 *Ibid.*, **129**, 327.
- ANDERS, E., and  
 STEVENS, C. M. 1960 *J. Geophys. Res.*, **65**, 3043.
- ARP, H. 1960 *A.J.*, **65**, 404.  
 1962 *Ap. J.*, **136**, 66.
- ARP, H., and  
 KRAFT, R. P. 1961 *Ap. J.*, **133**, 420.
- BAADE, W. 1952 *Trans. I.A.U.*, **8**, 397.  
 1958a *Stellar Populations*, ed. D. J. K. O'CONNELL (New York, London: Interscience Publishers), p. 1.  
 1958b *Ibid.*, p. 303.
- BAADE, W., BURBIDGE,  
 G. R., HOYLE, F.,  
 CHRISTY, R. F., and  
 FOWLER, W. A. 1956 *Pub. A.S.P.*, **68**, 296.
- BABCOCK, H. D. 1945 *Ap. J.*, **102**, 154.
- BABCOCK, H. W. 1958 *Ap. J., Suppl.*, **3**, 141.  
 1960a *Stellar Atmospheres*, ed. J. L. GREENSTEIN (Chicago: University of Chicago Press), p. 282.  
 1960b *Ap. J.*, **132**, 521.  
 1962 Private communication to B. M. Middlehurst.
- BAHCALL, J. N. 1961 *Phys. Rev.*, **124**, 495.  
 1962 *Ibid.*, **126**, 1143.
- BAKER, E., FRIEDLANDER,  
 G., and HUDIS, J. 1958 *Phys. Rev.*, **112**, 1319.
- BASCHEK, B. 1959 *Zs. f. Ap.*, **48**, 95.
- BASHKIN, S. 1963 *Nature*, **197**, 1091.
- BASHKIN, S.,  
 KAVANAGH, R. W., and  
 PARKER, P. D. 1959 *Phys. Rev., Letters*, **3**, 518.
- BASHKIN, S., and  
 MIDDLEHURST, B. M. 1962 *Communications Lunar and Planetary Lab.*, **1**, No. 20, 155.
- BASHKIN, S., and  
 PEASLEE, D. C. 1961 *Ap. J.*, **134**, 981.
- BATE, G. L. 1962 Quoted by Rushbrook and Ehmann (1962).
- BATE, G. L.,  
 HUIZENGA, J. R., and  
 PORTRATZ, H. A. 1959 *Geochim. et Cosmochim. Acta*, **16**, 88.
- BATE, G. L.,  
 PORTRATZ, H. A., and  
 HUIZENGA, J. R. 1960 *Geochim. et Cosmochim. Acta*, **18**, 101.
- BAUM, W. A., HILTNER,  
 W. A., JOHNSON, H. L.,  
 and SANDAGE, A. R. 1959 *Ap. J.*, **130**, 749.
- BECKER, R. A., and  
 FOWLER, W. A. 1959 *Phys. Rev.*, **115**, 1410.

- BERMAN, L. 1935 *Ap. J.*, **81**, 369.
- BERTIAU, F. C. 1958 *Ap. J.*, **128**, 533.
- BESKOW, G., and  
TREFFENBERG, L. 1947 *Arkiv. f. Mat. Astr. o. Fysik, A*, **34**, No. 17.
- BIDELMAN, W. P. 1960a *Pub. A.S.P.*, **72**, 24.  
1960b *Ibid.*, p. 471.  
1961 *A.J.*, **66**, 453.  
1962a *Ibid.*, **67**, 111.  
1962b Private communication.
- BIERMANN, L., and  
LUST, R. 1960 *Stellar Atmospheres*, ed. J. L. GREENSTEIN (Chicago: University of Chicago Press), p. 260.
- BILPUCH, E. G.,  
WESTON, L. W., and  
NEWSON, H. W. 1960 *Ann. Phys.*, **10**, 455.
- BLESS, R. C. 1960 *Ap. J.*, **132**, 532.
- BONDI, H. 1952 *M.N.* **112**, 195.
- BONDI, H., and HOYLE, F. 1944 *M.N.*, **104**, 273.
- BONSACK, W. K. 1959 *Ap. J.*, **130**, 843.  
1961a Private communication.  
1961b *Ap. J.*, **133**, 340.  
1961c *Ibid.*, p. 551.
- BONSACK, W. K., and  
GREENSTEIN, J. L. 1960 *Ap. J.*, **131**, 83.
- BOWYER, S., BYRON,  
E. T., CHUBB, T. A.,  
and FRIEDMAN, H. 1964 *Nature*, **201**, 1307.
- BOYARCHUK, A. A., and  
HERBIG, G. H. 1961 *A.J.*, **66**, 453.
- BROMLEY, D. A.,  
KUEHNER, J. A., and  
ALMQVIST, E. 1960 *Phys. Rev., Letters*, **4**, 365.
- BURBIDGE, E. M., and  
BURBIDGE, G. R. 1957 *Ap. J.*, **126**, 357.  
1958 *Hdb. d. Phys.*, **51**, 134.
- BURBIDGE, E. M.,  
BURBIDGE, G. R., and  
FOWLER, W. A. 1958 *I.A.U. Symp.*, No. 6, 222.
- BURBIDGE, E. M., BUR-  
BIDGE, G. R., FOWLER,  
W. A., and HOYLE, F. 1957 *Rev. Mod. Phys.*, **29**, 547.
- BURBIDGE, G. R. 1960 *Ap. J.*, **131**, 519.  
1963 *Ann. Rev. Nuclear Sci.*, **12**, 507.
- BURBIDGE, G. R., and  
BURBIDGE, E. M. 1956 *Ap. J.*, **124**, 655.  
1958 *Ibid.*, **127**, 557.



- BURBIDGE, G. R., HOYLE,  
F., BURBIDGE, E. M.,  
CHRISTY, R. F., and  
FOWLER, W. A. 1956 *Phys. Rev.*, **103**, 1145.
- BUTLER, W. A.,  
JEFFERY, P. M.,  
REYNOLDS, J. H., and  
WASSERBURG, G. J. 1963 *J. Geophys. Res.*, **68**, 3283.
- CAMERON, A. G. W. 1957 *Pub. A.S.P.*, **69**, 201.  
1958 Joint Discussion on Nucleogenesis in Stars, Tenth  
General Assembly of the I.A.U., Moscow  
(Chalk River Reprint PD-304).  
1959a *Ap. J.*, **130**, 452.  
1959b *Canadian J. Phys.*, **37**, 322.  
1959c *Ap. J.*, **129**, 676.  
1959d *Ibid.*, **130**, 429.  
1959e *Ibid.*, p. 895.  
1960a *Ibid.*, **131**, 521.  
1960b *A.J.*, **65**, 485.  
1962 *Icarus*, **1**, 13.
- CARLSON, R. R. 1961 *Nuclear Phys.*, **28**, 443.
- CAUGHLAN, G. R., and  
FOWLER, W. A. 1962 *Ap. J.*, **136**, 453.
- CHAMBERLAIN, J. W.,  
and ALLER, L. H. 1951 *Ap. J.*, **114**, 52.
- CHIU, H. Y. 1961a *Ann. Phys.*, **15**, 1.  
1961b *Phys. Rev.*, **123**, 1040.  
1961c *Ann. Phys.*, **16**, 321.  
1964a *Ibid.*, **26**, 364.  
1964b *A.J.* (in press).
- CHIU, H. Y., and  
MORRISON, P. 1960 *Phys. Rev., Letters*, **5**, 573.
- CHIU, H. Y., and  
SALPETER, E. E. 1964 *Phys. Rev., Letters*, **12**, 413.
- CHIU, H. Y., and  
STABLER, R. C. 1961 *Phys. Rev.*, **122**, 1317.
- CLAYTON, D. D. 1963 *J. Geophys. Res.*, **68**, 3715.
- CLAYTON, D. D., and  
FOWLER, W. A. 1961 *Ann. Phys.*, **16**, 651.
- CLAYTON, D. D., FOWLER,  
W. A., HULL, T. E., and  
ZIMMERMAN, B. A. 1961 *Ann. Phys.*, **12**, 331.
- CLIMENHAGA, J. L. 1960 *Pub. Dom. Ap. Obs. Victoria*, **11**, 307.  
1964 *A.J.* (in press).
- CODE, A. D., and  
HOUCK, T. E. 1958 *Pub. A.S.P.*, **70**, 261.

- COLGATE, S. A., and  
JOHNSON, M. H. 1960 *Phys. Rev., Letters*, **5**, 235.
- COLGATE, S. A., and  
WHITE, R. H. 1964 *A. J.* (in press).
- DE JAGER, C. 1959 *Ninth International Astrophys. Symp. Liège*, p. 280.
- DEUTSCH, A. J. 1959 *Ninth International Astrophys. Symp. Liège*, p. 54.  
1960 *Stellar Atmospheres*, ed. J. L. GREENSTEIN (Chicago: University of Chicago Press), p. 543.  
1963 *Observatory*, **83**, 28.  
1962 *Rev. Mod. Phys.*, **34**, 110.
- DICKE, R. H. 1962 *Rev. Mod. Phys.*, **34**, 110.
- DODD, K. N., and  
McCRAE, W. H. 1952 *M.N.*, **112**, 205.
- DOSTROVSKY, I.,  
FRAENKEL, Z., and  
FRIEDLANDER, G. 1959 *Phys. Rev.*, **116**, 683.
- DOSTROVSKY, I.,  
FRAENKEL, Z., and  
RABINOWITZ, P. 1960 *Phys. Rev.*, **118**, 791.
- DOSTROVSKY, I.,  
FRAENKEL, Z., and  
WINSBURG, L. 1960 *Phys. Rev.*, **118**, 781.
- DUFRESNE, A. 1960 *Geochim. et Cosmochim. Acta*, **20**, 141.
- EDDINGTON, A. E. S. 1926 *Internal Constitution of the Stars* (Cambridge: Cambridge University Press), p. 39.
- EGGEN, O. J. 1959 *Observatory*, **79**, 165.
- EGGEN, O. J.,  
LYNDEN-BELL, D., and  
SANDAGE, A. R. 1962 *Ap. J.*, **136**, 748.
- EGGEN, O. J., and  
SANDAGE, A. R. 1959 *M.N.*, **119**, 255.
- EHMANN, W. D., and  
HUIZENGA, J. R. 1959 *Geochim. et Cosmochim. Acta*, **17**, 125.
- ERSKINE, J. R.,  
BUECHNER, W. W.,  
and ENGE, H. A. 1962 *Phys. Rev.*, **128**, 720.
- FEAST, M. W. 1960 *Observatory*, **80**, 104.  
1962 *Ibid.*, **81**, 73.
- FEAST, M. W., and  
THACKERAY, A. D. 1960 *M.N.*, **120**, 463.
- FEAST, M. W.,  
THACKERAY, A. D.,  
and WESSELINK, A. J. 1958 *Observatory*, **78**, 156.  
1960 *M.N.*, **121**, 337.
- FEIGE, J. 1958 *Ap. J.*, **128**, 267.
- FESSENKOV, V. G. 1949 *A.J., U.S.S.R.*, **26**, 67.

- FISH, R. A., GOLES, G. G.,  
and ANDERS, E. 1960 *Ap. J.*, **132**, 243.
- FLESCH, G. D., SVEC,  
H. J., and STALEY, H. G. 1960 *Geochim. et Cosmochim. Acta*, **20**, 300.
- FOWLER, W. A. 1958 *Ap. J.*, **127**, 551.  
1959 *Ninth International Astrophys. Symp. Liège*, p.  
207.  
1961 Proceedings of Rutherford Jubilee International  
Conference, Manchester, England, ed. J. B.  
BIRNS.  
1962 Private communication.
- FOWLER, W. A.,  
BURBIDGE, G. R., and  
BURBIDGE, E. M. 1955 *Ap. J., Suppl.*, **2**, 167.
- FOWLER, W. A.,  
GREENSTEIN, J. L.,  
and HOYLE, F. 1962 *Geophys. J.*, **6**, 148.
- FOWLER, W. A., and  
HOYLE, F. 1960 *Ann. of Phys.*, **10**, 280.
- FRANK-KAMENETSKII,  
D. A. 1958 Joint Discussion on Nucleogenesis in Stars, Tenth  
General Assembly of the I.A.U., Moscow.  
1959 *Soviet Physics Uspekhi*, **2**(68), 600.  
1961 *Soviet Astr.*, **5**, 66.
- FRIEDLANDER, G.,  
MILLER, J. M., WOLF-  
GANG, R., HUDIS, J.,  
and BAKER, E. 1954 *Phys. Rev.*, **94**, 727.
- GAMOW, G. 1953 *Math. Fys. Medd.*, **27**, No. 10.
- GEISS, J., and  
HESS, D. C. 1958 *Ap. J.*, **127**, 224.
- GIACONI, R., GURSKY, H.,  
PAOLINI, F. R., and  
ROSSI, B. B. 1962 *Phys. Rev., Letters*, **9**, 439.
- GOLD, T. 1960 *Ap. J.*, **132**, 274.
- GOLDBERG, L., DUPREE,  
A. K., and KOPP, R. 1964 *A.J.*, **69**, 140.
- GOLDBERG, L.,  
MOHLER, O. C., and  
MÜLLER, E. A. 1958 *Ap. J.*, **127**, 302.
- GOLDBERG, L.,  
MÜLLER, E. A., and  
ALLER, L. H. 1960 *Ap. J., Suppl.*, **5**, 1.
- GOLDSCHMIDT, V. N. 1954 *Geochemistry* (Oxford: Clarendon Press).
- GOLES, G. G., and  
ANDERS, E. 1960 *J. Geophys. Res.*, **65**, 4181.
- GOPASYUK, S. I. 1961 *Soviet Astr.*, **5**, 158.

- GORDON, I. M. 1960 *Soviet Astr.*, 4, 234.
- GOVE, H. E.,  
LITHERLAND, A. E.,  
and CLARK, M. A. 1961 *Nature*, 191, 1381.
- GREENSTEIN, J. L. 1951 *Ap. J.*, 113, 531.
- 1962 Private communication.
- GREENSTEIN, J. L., HACK,  
M., and STRUVE, O. 1957 *Ap. J.*, 126, 281.
- GREENSTEIN, J. L., and  
KEENAN, P. C. 1958 *Ap. J.*, 127, 172.
- GREENSTEIN, J. L., and  
RICHARDSON, R. S. 1951 *Ap. J.*, 113, 536.
- GREENSTEIN, J. L.,  
RICHARDSON, R. S., and  
SCHWARZSCHILD, M. 1950 *Pub. A.S.P.*, 62, 15.
- GURSKY, H., GIACONI, R.,  
PAOLINI, F. R., and  
ROSSI, B. B. 1963 *Ann. Phys.*, 11, 530.
- GUSAKOW, M., ALBOUY,  
G., and POFPE, N. 1961 Proceedings of Rutherford Jubilee International  
Conference, Manchester, England.
- HARA, T., and  
SANDELL, E. B. 1960 *Geochim. et Cosmochim. Acta*, 21, 145.
- HAYAKAWA, S. 1960 *Pub. Astr. Soc. Japan*, 12, 115.
- HAYASHI, C., NISHIDA,  
M., OHYAMA, N., and  
TSUDA, H. 1958 *Progress of Theoretical Phys.*, 20, 110.
- HEISER, A. M. 1960 *Ap. J.*, 131, 506.
- HELPER, H. L.,  
WALLERSTEIN, G., and  
GREENSTEIN, J. L. 1959 *Ap. J.*, 129, 700.
- 1960 *Ap. J.*, 132, 553.
- HELLER, L. 1957 *Ap. J.*, 126, 341.
- HELLIWELL, T. M. 1961 *Ap. J.*, 133, 566.
- HERBIG, G. H. 1948 *Pub. A.S.P.*, 60, 378.
- 1958 *Stellar Populations*, ed. D. J. K. O'CONNELL (Am-  
sterdam: North-Holland Publishing Co.), p.  
127.
- 1962a Private communication.
- 1962b *Advances in Astronomy and Astrophysics*, ed. Z.  
Kopal (New York: Academic Press), p. 47.
- 1964 *Ap. J.* (in press).
- HESS, D. C., and  
MARSHALL, R. R. 1960 *Geochim. et Cosmochim. Acta*, 20, 284.
- HILL, P. W. 1962 *Observatory*, 82, 60.
- HODGE, P. W. 1960a *Ap. J.*, 132, 341.
- 1960b *Ibid.*, p. 346.

- HOLMGREN, H. D., and  
JOHNSTON, R. L. 1959 *Phys. Rev.*, **113**, 1556.
- HOWARD, R., and  
BABCOCK, H. W. 1960 *Ap. J.*, **132**, 218.
- HOYLE, F. 1954 *Ap. J., Suppl.*, **1**, 121.  
1955 *Gas Dynamics of Cosmic Clouds* (New York, London: Interscience Publishers), p. 208.  
1959 *M.N.*, **119**, 124.  
1960 *Quart. J.R.A.S.*, **1**, 28.
- HOYLE, F., and  
FOWLER, W. A. 1960 *Ap. J.*, **132**, 565.
- HOYLE, F., and  
LYTTLETON, R. A. 1939 *Proc. Cambridge Phil. Soc.*, **35**, 405 and 592.  
1940 *Ibid.*, **36**, 325 and 424.  
1941 *M.N.*, **101**, 227.  
1957 *Pub. A.S.P.*, **69**, 427.
- HUANG, S.  
HUIZENGA, J. R., and  
DIAMOND, H. 1957 *Phys. Rev.*, **107**, 1087.
- HUMASON, M. L.,  
MAYALL, N. U., and  
SANDAGE, A. R. 1956 *A.J.*, **61**, 97.
- JEFFERY, P. M., and  
REYNOLDS, J. H. 1961 *Zs. f. Naturforsch.*, **16a**, 431.
- JOHNSON, H. M. 1959 *Pub. A.S.P.*, **71**, 425.
- JUGAKU, J.,  
SARGENT, W. L. W.,  
and GREENSTEIN, J. L. 1961 *Ap. J.*, **134**, 782.
- JUGAKU, S., and  
SARGENT, W. L. W. 1961 *Pub. A.S.P.*, **73**, 249.  
1962 Private communication from L. SEARLE and J. JUGAKU.
- KAHN, F., and  
WOLTJER, J. 1959 *Ap. J.*, **130**, 705.
- KAMINSI, K. 1960 *Pub. Astr. Soc. Japan*, **12**, 398.
- KAUFMAN, S. B. 1962 *Phys. Rev.*, **126**, 1189.
- KEENAN, P. S., and  
TESKE, R. G. 1956 *Ap. J.*, **124**, 499.
- KING, A. S. 1916 *Mt. Wilson Contr.*, No. 122; *Ap. J.*, **44**, 169.
- KINMAN, T. D. 1956 *M.N.*, **116**, 77.  
1959 *M.N.*, **119**, 538.  
1961 *J. Chem. Educ.*, **38**, 73.
- KOHMAN, T. P.  
KÖNIG, H., and  
WÄNKE, H. 1959 *Zs. f. Naturforsch.*, **14a**, 866.
- KRON, G. E., and  
GORDON, K. C. 1961 *Pub. A.S.P.*, **73**, 267.
- KUIPER, G. P. 1962 *Communications Lunar and Planetary Lab.*, **1**, No. 15, 83.

- KULIVKOSKII, P. G. 1944 *A.J., U.S.S.R.*, **21**, 211.
- LAMBRECHT, H. 1959 *Ninth International Astrophys. Symp. Liège*, 318.
- LIMBER, D. N. 1958a *Ap. J.*, **127**, 362.  
1958b *Ibid.*, p. 387.
- LYTTLETON, R. A. 1960 *Observatory*, **80**, 41.  
1961 *M.N.*, **122**, 399.
- MCCRAE, W. H. 1953 *M.N.*, **113**, 162.  
1955 *Gas Dynamics of Cosmic Clouds* (New York, London: Interscience Publishers), p. 186.
- McKELLAR, A. 1940 *Pub. A.S.P.*, **52**, 407.  
1941 *Observatory*, **64**, 4.  
1948 *Pub. Dom. Ap. Obs. Victoria*, **7**, 395.  
1960 *Stellar Atmospheres*, ed. J. L. GREENSTEIN (Chicago: University of Chicago Press), p. 569.
- McKELLAR, A., and  
STILWELL, W. H. 1944 *J. R. Astr. Soc. Canada*, **38**, 237.
- MACKLIN, R. L., INADA,  
T., and GIBBONS, J. H. 1962 *Nature*, **194**, 1272.  
1963 *Ibid.*, **197**, 369.
- MALITSON, A. H. H.,  
PURSELL, J. D.,  
TOUSEY, R., and  
MOORE, C. E. 1960 *Ap. J.*, **132**, 746.
- MARION, J. B., and  
FOWLER, W. A. 1957 *Ap. J.*, **125**, 221.
- MARKOWITZ, S. S.,  
ROWLAND, F. S., and  
FRIEDLANDER, G. 1958 *Phys. Rev.*, **112**, 1295.
- MARSHALL, R. R. 1957 *Geochim. et Cosmochim. Acta*, **12**, 225.  
1962a *J. Geophys. Res.*, **67**, 2005.  
1962b *Icarus*, **1**, 95.
- MASEVICH, A. G. 1949 *A.J., U.S.S.R.*, **26**, 207.  
1954 *Fifth International Astrophys. Symp. Liège*, p. 170.
- MASUDA, A. 1958 *Geochim. et Cosmochim. Acta*, **13**, 143.
- MATHIS, J. S. 1957a *Ap. J.*, **125**, 328.  
1957b *Ibid.*, **126**, 493.  
1961 *A.J.*, **67**, 276.  
1962 *Ap. J.*, **136**, 374.
- MAYALL, N. U. 1946 *Ap. J.*, **104**, 290.
- MENZEL, H. 1955 *Gas Dynamics of Cosmic Clouds* (New York, London: Interscience Publishers), p. 209.
- MERRIHUE, C. M. 1963 *J. Geophys. Res.*, **68**, 325.
- MERRILL, P. W. 1952 *Ap. J.*, **116**, 21.  
1956 *Pub. A.S.P.*, **68**, 70.
- MERRILL, P. W.,  
DEUTSCH, A. J., and  
KEENAN, P. C. 1962 *Ap. J.*, **136**, 21.

- MERRILL, P. W., and  
GREENSTEIN, J. L. 1956 *Ap. J., Suppl.*, 2, 225.
- MERZ, E. 1962 *Geochim. et Cosmochim. Acta*, 26, 327.
- MESTEL, L. 1954 *M.N.*, 114, 437.
- 1959 *Observatory*, 79, 35.
- MIDDLEHURST, B. M.,  
and KUIPER, G. P. 1963 *Moon, Meteorites, and Comets* (Chicago: University of Chicago Press).
- MILLER, J. M., and  
HUDIS, J. 1959 *Ann. Rev. Nuclear Sci.*, 9, 159.
- MITLER, H. E. 1963 *J. Geophys. Res.*, 68, 4587.
- MOORE, C. B., and  
BROWN, H. 1963 *J. Geophys. Res.*, 68, 4293.
- MOORE, C. E. 1951 *Science*, 113, 669.
- MORGAN, W. W. 1956 *Pub. A.S.P.*, 68, 509.
- 1959a *A.J.*, 64, 432.
- 1959b *Pub. A.S.P.*, 71, 92.
- MORTON, D. C. 1964 *Nature*, 201, 1308.
- MOZER, F. S. 1959 *Phys. Rev.*, 116, 970.
- MÜLLER, E. A., and  
MUTSCHLECNER, J. P. 1964 *Ap. J., Suppl.*, 9, 1.
- MÜNCH, G., and  
ZIRIN, H. 1961 *Ap. J.*, 133, 11.
- MURTHY, V. R., and  
SCHMITT, R. A. 1963 *J. Geophys. Res.*, 68, 911.
- NAKAGAWA, S., TAMAI,  
E., and NOMOTO, S. 1958 *Nuovo Cimento*, 9, 780.
- NEMIROVSKY, P. E. 1958 Joint Discussion on Nucleogenesis in Stars, Tenth  
General Assembly of the I.A.U., Moscow.
- NIER, A. O. C. 1939 *Phys. Rev.*, 55, 153.
- O'DELL, C. R., KINMAN,  
T. D., and PEIMBERT, M. 1964 *Ap. J.*, 140, 119.
- ÖPIK, E. J. 1951 *Proc. Roy. Irish Acad.*, A54, 49.
- OKE, J. B. 1959 *Ap. J.*, 130, 487.
- OORT, J. H. 1958a *Stellar Populations*, ed. D. J. K. O'CONNELL (New  
York, London: Interscience Publishers), p.  
63 ff.
- 1958b *Ibid.*, p. 415.
- OSTERBROCK, D. E. 1953 *Ap. J.*, 118, 529.
- 1960 *Ibid.*, 132, 325.
- OSTERBROCK, D. E., and  
ROGERSON, J. B. 1961 *Pub. A.S.P.*, 73, 129.
- PANASYUK, I. S. 1961 *Soviet Astr.*, 5, 141.
- PARKER, E. N. 1957 *Phys. Rev.*, 107, 830.
- PARKER, P. D. 1961 Private communication.
- PARKER, P. D., and  
KAVANAGH, R. W. 1963 *Phys. Rev.*, 121, 2578.

- PARKER, R., GREENSTEIN,  
J. L., HELFER, H. L.,  
and WALLERSTEIN, G. 1961 *Ap. J.*, **133**, 101.
- PATTERSON, C. 1953 Rept. on Conference on Nuclear Processes in Geologic Settings, p. 36.
- 1956 *Geochim. et Cosmochim. Acta*, **10**, 230.
- PEASLEE, D. C. 1962 Private communication.
- PORILE, N. J. 1962 *Phys. Rev.*, **125**, 1379.
- POTTASCH, S. R. 1964 *M.N.*, **128**, 73.
- PRESTON, G. W. 1961 *Ap. J.*, **134**, 633.
- PROVIN, S. S. 1953 *Ap. J.*, **118**, 489.
- PRZYBYLSKI, A. 1963 Private communication from B. Bok.
- RANKAMA, K., and  
SAHAMA, T. G. 1949 *Geochemistry* (Chicago: University of Chicago Press), p. 485.
- REED, G., KIGOSHI, K.,  
and TURKEVICH, A. 1960 *Geochim. et Cosmochim. Acta*, **20**, 122.
- REEVES, H. 1959 *Phys. Rev., Letters*, **2**, 423.
- 1962 *Ap. J.*, **135**, 779.
- REEVES, H., and  
SALPETER, E. E. 1959 *Phys. Rev.*, **116**, 1505.
- REYNOLDS, J. H. 1960a *Phys. Rev., Letters*, **4**, 351.
- 1960b *Ibid.*, p. 8.
- 1960c *J. Geophys. Res.*, **65**, 3843.
- RIGHINI, G. 1956 *Mem. Soc. R. Sci. Liège*, 4th ser., **18**, 265.
- RINGWOOD, A. E. 1957 *Geochim. et Cosmochim. Acta*, **15**, 257.
- ROBERTS, M. S. 1957 *Pub. A.S.P.*, **69**, 59.
- ROWLAND, P. S., and  
WOLFGANG, R. L. 1958 *Phys. Rev.*, **110**, 175.
- RUBBRA, F. T., and  
COWLING, T. G. 1959 *Ninth International Astrophys. Symp. Liège*, 274.
- RUNCORN, S. K. 1965 *Encyclopedia of Geophysics* (London: Pergamon Press [in press]).
- RUSHBROOK, P. R., and  
EHMANN, W. D. 1962 *Geochim. et Cosmochim. Acta*, **26**, 649.
- RUSSELL, H. N. 1934 *Ap. J.*, **70**, 11.
- SALPETER, E. E. 1952a *Phys. Rev.*, **88**, 547.
- 1952b *Ap. J.*, **115**, 326.
- 1955 *Phys. Rev.*, **97**, 1237.
- 1957 *Ibid.*, **107**, 516.
- 1959 *Ap. J.*, **129**, 608.
- SANDAGE, A., and  
WALLERSTEIN, G. 1960 *Ap. J.*, **131**, 598.
- SANDAGE, A. R. 1957 *Ap. J.*, **125**, 435.
- 1958a *Stellar Populations*, ed. D. J. K. O'CONNELL (New York, London: Interscience Publishers), pp. 41 ff.



- 1958b *Ap. J.*, **127**, 513.  
 1961 *A.J.*, **66**, 53.  
 1962 *Ap. J.*, **135**, 349.  
 SANFORD, R. F. 1944 *Ap. J.*, **99**, 145.  
 1950 *Ibid.*, **111**, 262.
- SARGENT, W. L. W., and  
 JUGAKU, J. 1961 *Ap. J.*, **134**, 777.
- SARGENT, W. L. W., and  
 SEARLE, L. 1962a *Ap. J.*, **136**, 408.  
 1962b Quoted by Aller and Bidelman (1964)  
 1962c *Ap. J.*, **136**, 673.
- SCHATZMAN, E. 1955 *Gas Dynamics of Cosmic Clouds* (New York, London: Interscience Publishers), p. 193.  
 1959 *Ninth International Astrophys. Symp. Liège*, 295.  
 1960 *Geochim. et Cosmochim. Acta*, **19**, 134.
- SCHINDEWOLF, U.  
 SCHINDEWOLF, U., and  
 WAHLGREN, M. 1960 *Geochim. et Cosmochim. Acta*, **18**, 36.  
 SCHMIDT, M. 1959 *Ap. J.*, **129**, 243.  
 1960 *Symposium on Stellar Evolution* (La Plata: National University of La Plata), p. 67.
- SCHMIDT, R. A., and  
 GOLES, G. G., In press.  
 SCHMITT, R. A., MOSEN,  
 A. W., SUFFREDINI,  
 C. S., LASCH, J. E.,  
 SHARP, R. E., and  
 OLEHY, D. A. 1960 *Nature*, **186**, 863.
- SCHWARZSCHILD, M.,  
 SCHWARZSCHILD, B.,  
 SEARLE, L., and  
 MELTZER, A. 1957 *Ap. J.*, **125**, 123.  
 SEARLE, L. 1961 *Ap. J.*, **133**, 531.  
 1962 Private communication.
- SEATON, M. J. 1960 *M.N.*, **120**, 326.  
 SEEGER, P. A. 1961 *Nuclear Phys.*, **25**, 1.
- SEEGER, P. A., and  
 KAVANAGH, R. W. 1963 *Ap. J.*, **137**, 704.  
 SEVERNY, A. B. 1956 *Pub. Crimean Ap. Obs.*, **16**, 12.  
 1957 *Russian Astr. J.*, **34**, 328.  
 1961 *Soviet Astr.*, **5**, 299.
- SHAJN, G. A., and  
 HASE, V. 1954 *Fifth International Astrophys. Symp. Liège*, p. 397.  
 SHAW, D. M. 1952 *Geochim. et Cosmochim. Acta*, **2**, 118.  
 SHIMA, M. 1962 *J. Geophys. Res.*, **67**, 4521.  
 1963 *Ibid.*, **68**, 4289.  
 1964 *Geochim. et Cosmochim. Acta*, **28**, 517.

- SHIMA, M., and  
HONDA, M. 1963 *J. Geophys. Res.*, **68**, 2849.
- SHKLOVSKII, L. S. 1960 *Soviet Astr.*, **4**, 355.
- SILL, C. W., and  
WILLIS, C. P. 1962 *Geochim. et Cosmochim. Acta*, **26**, 1209.
- SMAK, J. 1960 *Acta Astronomica*, **10**, 153.
- SPITZER, L., and  
FIELD, G. B. 1955 *Ap. J.*, **121**, 300.
- STAUFFER, H. 1961 *Geochim. et Cosmochim. Acta*, **24**, 70.
- STAUFFER, H., and  
HONDA, M. 1962 *Geochim. et Cosmochim. Acta*, **67**, 3503.
- STEPHENSON, C. B. 1957 *Ap. J.*, **126**, 195.
- STIEFF, L. R., and  
STERN, T. W. 1961 *Geochim. et Cosmochim. Acta*, **22**, 176.
- STROMINGER, D.,  
HOLLANDER, J. M.,  
and SEABORG, G. T. 1958 *Rev. Mod. Phys.*, **30**, 585.
- STROTHERS, R., and  
CHIU, H. Y. 1962 *Ap. J.*, **135**, 963.
- SUESS, H. E., and  
UREY, H. C. 1956 *Rev. Mod. Phys.*, **28**, 53.  
1958 *Hdb. d. Phys.*, **51**, 296.
- SWINGS, P., and  
STRUVE, O. 1940 *Ap. J.*, **91**, 564.
- SYMONDS, J. L., WARREN,  
J., and YOUNG, J. D. 1957 *Proc. Phys. Soc., ser. A*, **70**, 824.
- TAKEBE, H., and  
MATSUNAMI, N. 1957 *Pub. Astr. Soc. Japan*, **9**, 136.
- TESKE, R. G. 1956 *Pub. A.S.P.*, **68**, 520.
- THACKERAY, A. D. 1962 *Observatory*, **82**, 72.
- TOLMAN, R. C. 1949 *Rev. Mod. Phys.*, **21**, 374.
- TRAVING, G. 1955 *Zs. f. Ap.*, **36**, 1.  
1962 *Ap. J.*, **135**, 439.
- UNDERHILL, A. B. 1958 *Observatory*, **78**, 127.  
1959 *Ap. J.*, **130**, 1027.  
1960 *Ibid.*, **131**, 395.
- UNDERHILL, A. B., and  
DEGROOT, M. 1964 *A. J.* (in press).
- UREY, H. C. 1952 *The Planets* (New Haven: Yale University Press).  
1954 *Ap. J., Suppl.*, **1**, 147.  
1959 *J. Geophys. Res.*, **64**, 1721.  
1964 *Reviews in Geophys.*, **2**, 1.
- VAN ALBADA, G. B. 1960 *B.A.N.*, **15**, 165.
- VAN DEN BERGH, S. 1961 *Pub. A.S.P.*, **73**, 135.
- VINOGRADOV, A. P. 1958 *Geochim. et Cosmochim. Acta*, **15**, 80.

- VINOGRADOV, A. P.,  
DONTSOVA, E. I., and  
CHUPAKHIN, M. S. 1960 *Geochim. et Cosmochim. Acta*, **18**, 278.
- WADDELL, C. N.,  
HENDERSON, T. M.  
and LEWIS, P. S. 1961 Proceedings of Rutherford Jubilee International  
Conference, Manchester, England.
- WALLERSTEIN, G. 1959 *Ap. J.*, **130**, 560.  
1962a *Ap. J., Suppl.*, **6**, 407.  
1962b Private communication.  
1962c *Phys. Rev., Letters*, **9**, 143.
- WALLERSTEIN, G., and  
HELPER, H. L. 1959a *Ap. J.*, **129**, 347.  
1959b *Ibid.*, p. 720.  
1961 *Ibid.*, **133**, 562.
- WALLERSTEIN, G.,  
STONE, Y. H., and  
WILLIAMS, J. A. 1962 *Ap. J.*, **135**, 459.
- WASSERBURG, G. J.,  
FOWLER, W. A., and  
HOYLE, F. 1960 *Phys. Rev., Letters*, **4**, 112.  
1962 *Nature*, **195**, 367.
- WEINREB, S.
- WESTON, L. W., SETH,  
K. K., BILPUCH, E. G.,  
and NEWSON, H. W. 1960 *Ann. Phys.*, **10**, 477.
- WEYMANN, R., and  
MOORE, E. 1964 *Ap. J.*, **137**, 552.
- WEYMANN, R. J. 1957 *Ap. J.*, **126**, 208.
- WHITE, F. A.,  
COLLINS, T. L., and  
ROURKE, F. M. 1956 *Phys. Rev.*, **101**, 1786.  
1959 *Ap. J.*, **130**, 496.  
1960a *Ibid.*, **133**, 457.  
1960b *Ibid.*, **132**, 136.  
1961 *Pub. A.S.P.*, **73**, 15.
- WILSON, O. C. 1958 *B.A.N.*, **14**, 39.  
1962 *Ap. J.*, **135**, 644.  
1964 *A.J.* (in press).  
1942 *Ap. J.*, **95**, 356.
- WOLTJER, L.
- WOOLF, N. J.
- WYLLER, A. A.
- WYSE, A. B.
- ZAHRINGER, J., and  
GENTNER, W. 1961 *Zs. f. Naturforsch.*, **16a**, 239.  
1958 *Hdb. d. Phys.*, **51**, 766.
- ZWICKY, F.

## CHAPTER 2

# *Stellar Energy Sources*<sup>1</sup>

HUBERT REEVES

*University of Montreal and Institute for Space Studies*

### § 1. HISTORY OF A STAR

THROUGHOUT its life a star transforms nuclear and gravitational energy into photons and neutrinos. The star lives on its nuclear resources during the so-called nuclear burning stages. During such stages the rate of energy release from some particular nuclear reaction is just sufficient to compensate for the radiation loss. The star stops its gravitational contraction for the time being, to resume it only after exhaustion of the particular fuel involved.

By now, two neatly defined burning stages can be identified with fair confidence: the hydrogen- and helium-burning stages. During the hydrogen-burning stage, four hydrogen nuclei are transformed into one helium nucleus with an energy release of 26.730 Mev (6.682 Mev per nucleon). Four main mechanisms are responsible for this conversion. They are described in § 3 (cf. Tables 3 and 5). According to the mass of the star, the hydrogen-burning stage will take place at temperatures ranging from ten to thirty million degrees. Some of these reactions are accompanied by neutrino emission. About five per cent of the energy will escape under the form of neutrinos.

Stars in the hydrogen-burning stage are identified with those in the main sequence of the Hertzsprung-Russell diagram. The upper half of the main sequence represents stars living mostly on the C-N cycles (PP IV), while the lower half represents stars living on some combination of the first three cycles. After the exhaustion of the hydrogen in the core, a star resumes its contraction again but still obtains some of its energy from hydrogen burning in a thin shell surrounding the helium core. The red giant branch in the HR diagram can be considered with good confidence as representing stars in this stage of evolution.

The helium-burning stage starts when the core becomes hot enough to initiate thermonuclear reactions between the helium nuclei themselves (§ 4 and

<sup>1</sup> This work was done while the author was the guest of the Institute for Space Studies, under an appointment by NASA as a NASA Research Associate.

Table 10). This occurs at temperatures ranging from  $10^8$ ° K to  $3 \times 10^8$ ° K, ( $T_8 = 1$  to 3). The isotopic outcome of the burning consists mainly of  $C^{12}$  and  $O^{16}$ . Only in very massive stars does it appear possible to obtain heavier elements from the helium-burning stage. The energy released during this stage depends on the final isotopic abundance. It is 7.275 Mev for each  $C^{12}$  made (0.6062 Mev per nucleon); 14.436 Mev for each  $O^{16}$  (0.9022 Mev per nucleon); 19.167 Mev for  $Ne^{20}$  (0.9583 Mev per nucleon) and 28.481 Mev for  $Mg^{24}$  (1.187 Mev per nucleon). These reactions do not create neutrinos.

Stars in the helium-burning stage are usually identified with those in the tip of the red giant branch. The presence of any further burning stages is still quite hypothetical. The next candidate as fuel nuclei is  $C^{12}$  (through its fusion with another  $C^{12}$ ). Rough estimates show that it would become active at temperatures varying from 0.6 to 1.0 billion degrees. After that, the photodisintegration of  $Ne^{20}$  could trigger another burning stage, and still later the fusion of two  $O^{16}$  nuclei (both in the range from  $T_9 = 1.3$  to 2.0). We have good reason to believe that at this stage the core becomes the seat of intense neutrino-producing reactions. As the temperature rises, these neutrinos carry away an increasingly large fraction of the stellar energy. At temperatures neighboring the billion degree mark, these neutrinos appear to have become the main source of energy dissipation.

The following nuclear reactions (further photodisintegration and re-combination) would be spread over a range of temperature (from two to about four billion degrees). They would most likely not succeed in halting the gravitational contraction; they would merely slow it down to some extent. These reactions could build up elements all the way to the iron peak. If still higher temperatures are attained, the iron peak nuclei would find themselves disintegrating all the way down to  $He^4$  and neutrons. These reactions would, of course, absorb some energy from the core and could lead to some instability. This instability is sometimes considered to be a trigger for supernovae explosions.

In the following three graphs we have *roughly* sketched the development of a star. The first graph (Fig. 1) pictures the energy generation history; the second one (Fig. 2), the nuclear history. In the third graph (Fig. 3) we give an illustration of the neutrino intensities reached in a typical stellar core as a function of the temperature.

## § 2. FORMALISM

This chapter attempts to review somewhat critically the whole problem of nuclear energy generation rates during stellar evolution. The computation of these rates depends, among other things, upon the cross-sections for the various nuclear events responsible for energy production. Except for one case (the  $H^1 + H^1$  reaction) these cross-sections cannot be calculated; they must be measured by laboratory experiments. Furthermore, in most cases the measurements were made at energies somewhat higher than the energies of stellar in-

terest (a few times  $kT$ ). In these cases some methods of extrapolation are used to find the cross-section in the proper range of energies.

We intend to consider each reaction of interest in detail. The diagrams exhibiting the energy levels of the nuclei involved will be given for most reactions. In these diagrams we shall include the break-up energies for some constituents of interest, together with the stellar energy ranges at various temperatures. Through this one can judge whether the reaction should be resonant or not, and if so, which resonance levels are expected to play a dominant role. Further, if any new levels are discovered in the future or if the existence of some of the levels already shown become dubious, the diagram will allow a quick estimate of the importance of the resulting modifications in the computed rate.

Most of the parameters relevant to the various reactions are given in the tables. We shall give for each reaction the range of energy which has been ex-

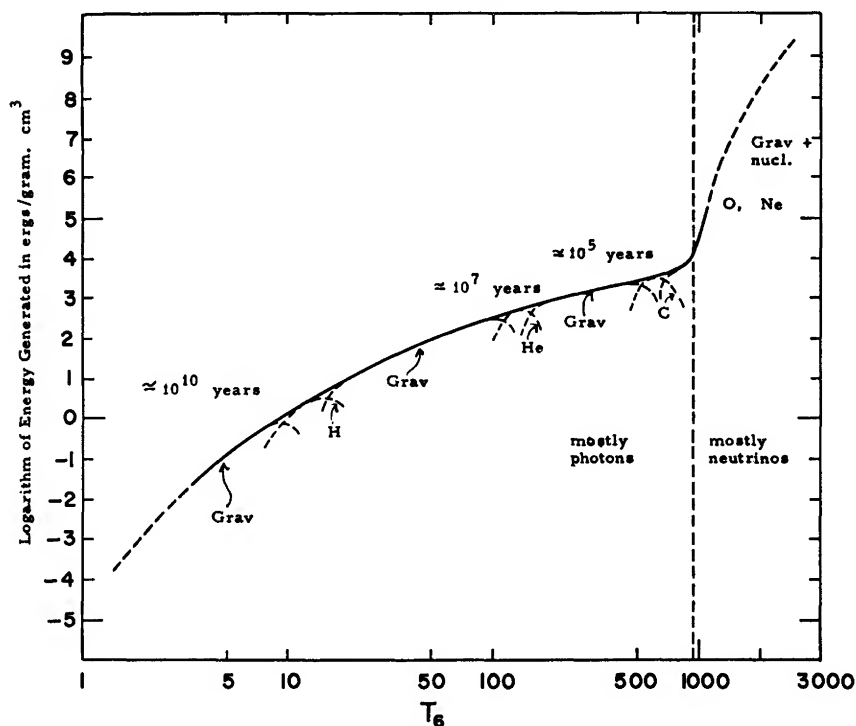


FIG. 1.—Over-all energy generation rate. A very rough sketch of the energy generated by a star of about one solar mass which (we assume) would reach up to a few billion degrees. The origin of the energy is identified by "Grav" for gravitational contraction, and by the name of the nuclear fuel for nuclear burning stages. The dashed lines represent the individual contributions of these two modes. The solid (envelope) line is the sum of both: the total luminosity of the star in erg/gm/sec. We identify roughly the region where the luminosity switches from photons to neutrinos.

plotted experimentally. We shall then describe the method of extrapolation and give the accuracy of the results. In a number of cases the experimenters have been contacted to obtain a re-evaluation of the uncertainty in their results. Using these new estimates, values will be recommended here that may differ somewhat from those used by previous authors. The margin of errors quoted will tend to be pessimistic, although not unduly so.

From the computed reaction rates, energy generation rates will be calculated. These last rates depend on the slowest reaction of a given set of reactions, but also, in some cases, on the rate of some other reactions. These effects will be discussed. Calculations will be made, however, which will not prejudice the chemical composition of the gas considered.

For uniformity, the masses and  $Q$  values (with the  $O^{16}$  scale) were all taken

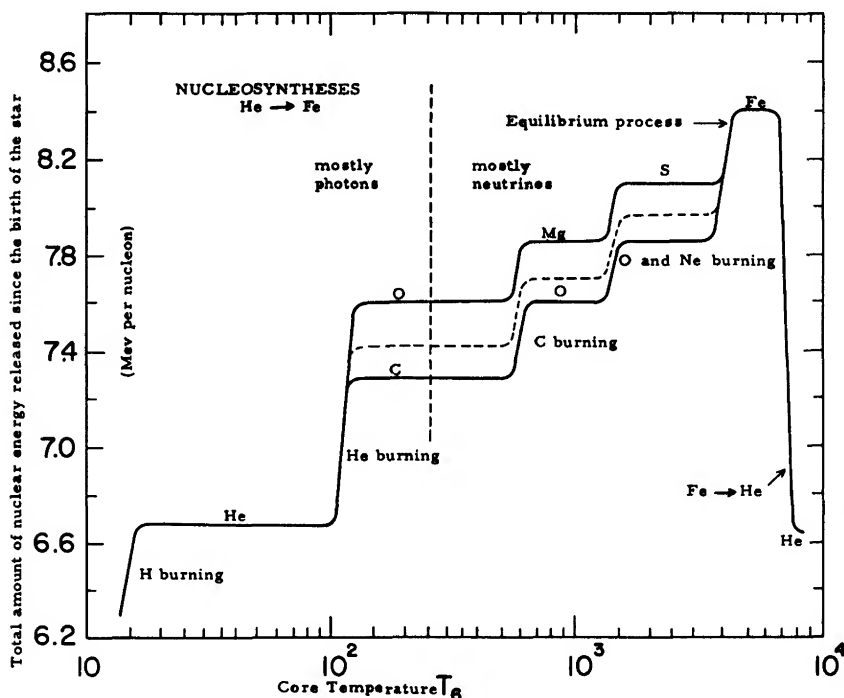


FIG. 2.—Nuclear history of a star. The curve represents the total amount of nuclear energy (per nucleon) released since the birth of the star, as a function of the core temperature. During the nuclear burning stages the curve rises sharply (almost isothermal processes). During the periods of gravitational contraction the isotopic composition does not change (flat regions). After the He-burning stage the core contains  $C^{12}$  and  $O^{16}$  in fractional abundances depending upon the initial mass. The C and O curves are then lower and upper limits respectively, as they represent cases in which the core is pure C or pure O. To the left of the vertical dashed line most of the energy escapes as photons; to the right, most of it escapes as neutrinos. The dashed line is a typical case. The same kind of statement applies to the rest of the graph.

from the latest (1960) nuclear data tables of the U.S.A.E.C. (Everling, Koenig, Mattauch, and Wapstra 1960). In Table 1 these masses are given in a.m.u. (scale of  $O^{16}$ ) together with the mass excesses in kev. The energy diagrams were taken from the Landolt-Börnstein handbook (1961) but again with the  $Q$  values from the U.S.A.E.C. Corrections to the diagram were made whenever newer data were available.

Unless otherwise noted, the kinetic energies quoted are always energies in the center of momentum system. We shall use three units of temperature;  $T_6$  (units of  $10^6$  °K) for the hydrogen burning,  $T_8$  (units of  $10^8$  °K) for helium burning, and  $T_9$  (units of  $10^9$  °K) for the rest of the stages. In analytical formulae the temperature units will always be identified. The stable chemical

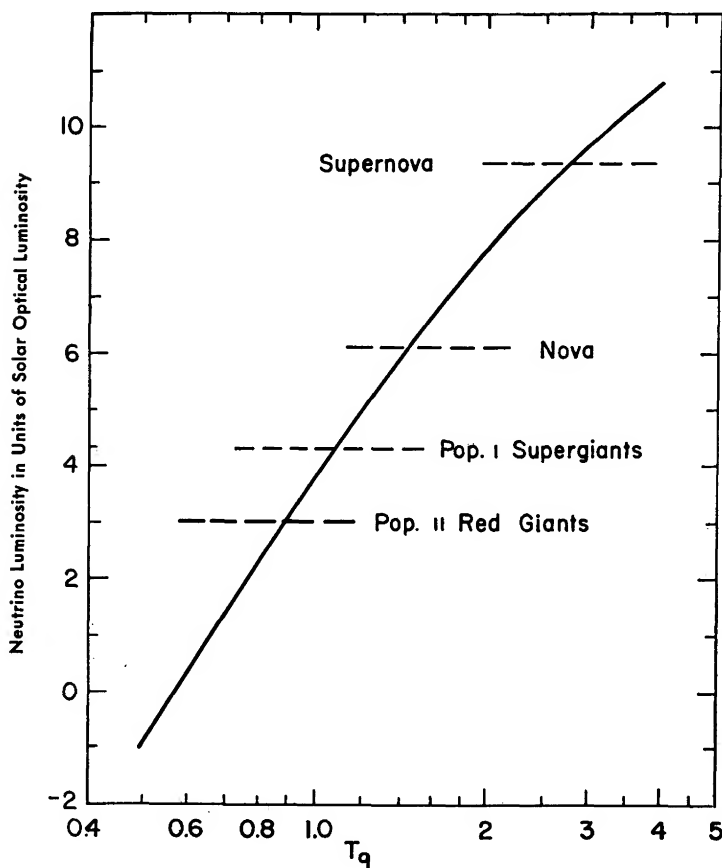


FIG. 3.—Average neutrino luminosity of a typical star. This graph was obtained by dividing the central neutrino luminosity per gm/cm/sec by about one hundred, in order to obtain an average value over the whole star. For comparison, average optical luminosities are given for various steady states of stars (giants) and also transient states (novae and supernovae). The ordinate is the logarithm of the luminosity.



TABLE 1

ATOMIC MASSES OF STABLE ISOTOPES FROM  $A = 1$  TO 58

Symbol	Name	Z	Mass (a.m.u.: $O^{16} = 16.00$ ) (Error in milli-a.m.u.)	Mass Excess (kev: $O^{16} = 0.00$ )
H <sup>1</sup>	Hydrogen	1	1.00814563 ± 0.00007	7584.76 ± 0.06
D <sup>2</sup>	Deuterium	1	2.01474251 ± 0.00009	13727.42 ± 0.08
He <sup>3</sup>	Helium	2	3.0169888 ± 0.0002	15819.0 ± 0.2
He <sup>4</sup>	Helium	2	4.0038761 ± 0.0004	3609.2 ± 0.3
Li <sup>6</sup>	Lithium	3	6.017039 ± 0.001	15865 ± 1
Li <sup>7</sup>	Lithium	3	7.018236 ± 0.001	16980 ± 1
Be <sup>9</sup>	Beryllium	4	9.0150509 ± 0.0009	14014.6 ± 0.8
B <sup>10</sup>	Boron	5	10.0161222 ± 0.0007	15012.1 ± 0.7
B <sup>11</sup>	Boron	5	11.0128051 ± 0.0005	11923.4 ± 0.4
C <sup>12</sup>	Carbon	6	12.0038150 ± 0.0002	3552.3 ± 0.2
C <sup>13</sup>	Carbon	6	13.0074883 ± 0.0008	6972.7 ± 0.7
N <sup>14</sup>	Nitrogen	7	14.0075262 ± 0.0002	7008.0 ± 0.2
N <sup>15</sup>	Nitrogen	7	15.0048769 ± 0.0009	4541.1 ± 0.8
O <sup>16</sup>	Oxygen	8	16.000000	0
O <sup>17</sup>	Oxygen	8	17.0045377 ± 0.0009	4225.3 ± 0.8
O <sup>18</sup>	Oxygen	8	18.0048821 ± 0.0003	4545.9 ± 0.2
F <sup>19</sup>	Fluorine	9	19.0044445 ± 0.0007	4138.5 ± 0.6
Ne <sup>20</sup>	Neon	10	19.9987964 ± 0.0004	— 1120.8 ± 0.4
Ne <sup>21</sup>	Neon	10	21.000524 ± 0.002	488 ± 2
Ne <sup>22</sup>	Neon	10	21.9983759 ± 0.0004	— 1512.3 ± 0.4
Na <sup>23</sup>	Sodium	11	22.997081 ± 0.002	— 2718 ± 2
Mg <sup>24</sup>	Magnesium	12	23.992670 ± 0.002	— 6825 ± 2
Mg <sup>25</sup>	Magnesium	12	24.993738 ± 0.002	— 5788.8 ± 2
Mg <sup>26</sup>	Magnesium	12	25.990851 ± 0.002	— 8519 ± 2
Al <sup>27</sup>	Aluminium	13	26.990113 ± 0.002	— 9206 ± 2
Si <sup>28</sup>	Silicon	14	27.985822 ± 0.003	— 13202 ± 3
Si <sup>29</sup>	Silicon	14	28.985703 ± 0.004	— 13313 ± 3
Si <sup>30</sup>	Silicon	14	29.983290 ± 0.004	— 15560 ± 4
P <sup>31</sup>	Phosphorus	15	30.983611 ± 0.002	— 15261 ± 1
S <sup>32</sup>	Sulfur	16	31.982238 ± 0.001	— 16538.8 ± 0.9
S <sup>33</sup>	Sulfur	16	32.981943 ± 0.003	— 16814 ± 3
S <sup>34</sup>	Sulfur	16	33.978663 ± 0.003	— 19867 ± 3
Cl <sup>35</sup>	Chlorine	17	34.979972 ± 0.003	— 18649 ± 3
S <sup>36</sup>	Sulfur	16	35.978524 ± 0.004	— 19996 ± 3
Ar <sup>36</sup>	Argon	18	35.978983 ± 0.003	— 19570 ± 3
Cl <sup>37</sup>	Chlorine	17	36.977648 ± 0.002	— 20813 ± 2
Ar <sup>38</sup>	Argon	18	37.974794 ± 0.003	— 23471 ± 2
K <sup>39</sup>	Potassium	19	38.976101 ± 0.003	— 22253 ± 3
Ar <sup>40</sup>	Argon	18	39.9750886 ± 0.006	— 23196.2 ± 0.6
K <sup>40</sup>	Potassium	19	39.976713 ± 0.004	— 21683 ± 3
Ca <sup>40</sup>	Calcium	20	39.975294 ± 0.004	— 23005 ± 4
K <sup>41</sup>	Potassium	19	40.974858 ± 0.005	— 23411 ± 4
Ca <sup>42</sup>	Calcium	20	41.971967 ± 0.004	— 26103 ± 4
Ca <sup>43</sup>	Calcium	20	42.972437 ± 0.005	— 25665 ± 5
Ca <sup>44</sup>	Calcium	20	43.969464 ± 0.005	— 28434 ± 5
Sc <sup>45</sup>	Scandium	21	44.970211 ± 0.004	— 27738 ± 4
Ca <sup>46</sup>	Calcium	20	45.968298 ± 0.004	— 29519 ± 4
Ti <sup>46</sup>	Titanium	22	45.967242 ± 0.004	— 30502 ± 3
Ti <sup>47</sup>	Titanium	22	46.966685 ± 0.008	— 31021 ± 8
Ca <sup>48</sup>	Calcium	20	47.96776 ± 0.02	— 30017 ± 14
Ti <sup>48</sup>	Titanium	22	47.963191 ± 0.005	— 34274 ± 4
Ti <sup>49</sup>	Titanium	22	48.963428 ± 0.005	— 34054 ± 4
Ti <sup>50</sup>	Titanium	22	49.960667 ± 0.006	— 36624 ± 5
V <sup>50</sup>	Vanadium	23	49.963044 ± 0.005	— 34412 ± 5
Cr <sup>50</sup>	Chromium	24	49.961929 ± 0.005	— 35449 ± 5
V <sup>51</sup>	Vanadium	23	50.960174 ± 0.005	— 37084 ± 5
Cr <sup>52</sup>	Chromium	24	51.957027 ± 0.005	— 40015 ± 4
Cr <sup>53</sup>	Chromium	24	52.957482 ± 0.005	— 39591 ± 4
Cr <sup>54</sup>	Chromium	24	53.956027 ± 0.007	— 40945 ± 5
Fe <sup>54</sup>	Iron	26	53.956769 ± 0.007	— 40254 ± 6
Mn <sup>55</sup>	Manganese	25	54.955519 ± 0.005	— 41418 ± 5
Fe <sup>56</sup>	Iron	26	55.952714 ± 0.007	— 44030 ± 6
Fe <sup>57</sup>	Iron	26	56.953494 ± 0.007	— 43304 ± 6
Fe <sup>58</sup>	Iron	26	57.951690 ± 0.008	— 44984 ± 7

elements will be identified by their mass numbers (although we shall sometimes write  $\alpha$  for the  $\text{He}^4$  particle).  $N_i$  will represent the number densities and  $X_i$  the fractional mass (in a given gas) of an element of mass number  $i$ .

In the diagrams the energy levels are in Mev, the notation "2-; 0" under a level indicates that the spin is 2, the parity is (-), and the isotopic spin is 0. Bracketed numbers are doubtful. Whenever we have taken away a part of the diagram, the number of levels in that range is given. Finally, a vertical bar outside the diagram with the label  $T_8 = 20$  means that at this temperature the most likely candidate for a given nuclear reaction is to be found in the corresponding energy range (the Gamow peak). The center of the range is also indicated.

In the tables of the reaction rates, we have often identified the level which gives the dominant contribution at a given temperature. For instance, the notation (6.87-n.r.-10) attached to a certain portion of a column means that in the corresponding range of temperatures the 6.87 Mev level in the compound nucleus is dominant, the contribution is non-resonant (n.r.), and the rate may be inaccurate by a factor of 10.

### 2.1. THERMONUCLEAR REACTION RATES

We consider a gas composed of two types of particles, 1 and 2, reacting to give two new particles, 3 and 4. The number of reactions per second per unit volume can be written as

$$I_{1,2} = \int_{v_t}^{\infty} N(v) [v \sigma(v)] dv. \quad (2.1)$$

Here  $v$  is the relative velocity between two reacting particles;  $\sigma(v)$  is the nuclear cross-section for the reaction under consideration, at the velocity  $v$ ;  $N(v)$  is the number of pairs of particles with velocity  $v$ ;  $v_t$  is the threshold velocity for the reaction (usually  $v_t = 0$ ).

In most cases of astrophysical interest, the atomic gas is not degenerate and may be represented adequately by a Maxwellian distribution. The distribution of the *relative* velocities between pairs of particles (the only one that matters for us) is easily seen to be Maxwellian as well, and is given by

$$N(v) = \frac{2 N_1 N_2}{(2\pi)^{1/2}} \frac{M^{3/2} v^2}{(kT)^{3/2}} \exp(-Mv^2/2kT). \quad (2.2)$$

$M$  is the reduced mass,  $M = A_1 A_2 / A_1 + A_2$  in a.m.u.;  $N_1, N_2$  are the numbers of atoms 1 and 2 per unit volume. We shall frequently use the following quantity,  $\langle \sigma v \rangle$ ;

$$\langle \sigma v \rangle_{2,1} = \int N(v) [\sigma(v) v] dv / \int N(v) dv = I_{1,2} / N_1 N_2. \quad (2.3)$$

In words,  $\langle \sigma v \rangle$  is the reaction probability per unit pair of particles 1 and 2 in a unit volume per unit time.

In terms of  $\langle \sigma v \rangle$  one can obtain a collection of useful quantities;

$$P_{2,1} = N_1 \langle \sigma v \rangle_{2,1} \quad (2.4)$$

is the probability of a reaction between an atom of species 2 with  $N_1$  atoms of species 1 per unit volume. We recall that  $N_1 = \mathfrak{N} \rho X_{A_1} / A_1$ , where  $\mathfrak{N}$  is Avogadro's number ( $6.02 \times 10^{23}$  in c.g.s.),  $\rho$  is the total density of the gas,  $A_1$  is the mass number of species 1, and  $X_{A_1}$  is the fractional density of that species.  $1/P_{2,1}$  is the mean life of the atom of species 2 in these conditions.

$$r_{2,1} = \frac{N_2 N_1 \langle \sigma v \rangle_{2,1}}{\rho} = N_2 \frac{P_{2,1}}{\rho} \quad (2.5)$$

is the number of reactions per gram per second, if the species 1 and 2 are different. If we are considering reactions of a certain species with itself (e.g.,  $H^1 + H^1$ ), then

$$r_{1,1} = \frac{N_1^2 \langle \sigma v \rangle_{1,1}}{2\rho} = \frac{N_1 P_{1,1}}{2\rho}. \quad (2.6)$$

If  $Q_{2,1}$  is the energy released in any one reaction, then  $\epsilon$ , the rate of energy generation per gram per second, is

$$\epsilon_{2,1} = r_{2,1} Q_{2,1} = \frac{N_1 N_2 \langle \sigma v \rangle_{2,1} Q_{2,1}}{\rho} = \frac{N_2 P_{2,1} Q_{2,1}}{\rho} \text{ erg/gm-sec} \quad (2.7)$$

for different reacting species, or

$$\epsilon_{1,1} = \frac{N_1^2 \langle \sigma v \rangle_{1,1}}{2\rho} Q_{1,1} = \frac{N_1 P_{1,1} Q_{1,1}}{2\rho} \quad (\text{same species}). \quad (2.8)$$

The heart of the problem is the estimation of  $\sigma(E)$ . In some cases  $\sigma(E)$  has been measured experimentally in the region of astrophysical interest. In other cases,  $\sigma(E)$  must either be extrapolated from higher energy measurements or estimated from various nuclear models.

When the rest-mass energy of the two particles 1 and 2 corresponds to a region of the energy diagram of the compound system (compound nucleus) where the resonances are well separated (which happens mostly for light nuclei), the contribution from any one of these resonances at energy  $E_r$  to the process involved ( $1 + 2 \rightarrow 3 + 4$ ) is well represented by a Breit-Wigner one-level formula (see, however, the discussion following eq. [2.24b]):

$$\sigma_{B.W.}(E_r) = \pi \lambda^2 \omega \Gamma_{2,1} \Gamma_{3,4} / [(\Gamma^2/4) + (E - E_r)^2]. \quad (2.9)$$

Here  $\lambda$  is the DeBroglie wavelength ( $\lambda = \hbar/P$ ); (numerically,  $\pi \lambda^2 = [0.647/E] \times [1/M]$  barns; 1 barn =  $10^{-24}$  cm<sup>2</sup>, if  $E$  is in Mev and  $M$  in a.m.u.);  $\Gamma_{2,1}$  is the partial width for the reaction ( $2 + 1$ );  $\Gamma_{3,4}$  is the partial width for the  $3 + 4$  breakup. Finally, the term  $\omega$  is a statistical factor

$$\omega = (2j_{C.N.} + 1) / (2j_1 + 1)(2j_2 + 1), \quad (2.10)$$

$j_1$  is the spin of particle 1,  $j_2$  the spin of particle 2, and  $j_{C.N.}$  is the spin of the resonant level in the compound nucleus.

The partial widths can be further factored into the product of a transmission factor and a so-called reduced width  $\gamma^*$ . Then we write

$$\gamma^* = \theta_{1,2}^2 \gamma_w^*,$$

where  $\gamma_w^*$  is the Wigner-Teichmann upper limit to the reduced width ( $\gamma_w^* = 1.5\hbar^2/MR^2$ ) and  $\theta_{1,2}^2$  is a constant, smaller than unity, which depends upon the internal structure of the resonance level.  $R$  is the nuclear radius of interaction, as usually defined.

If we consider a collision of particles with relative angular momentum  $l$  and relative energy  $E = \hbar^2 k^2/2M$ , the transmission factor is often written as  $T_l(E) \frac{1}{2}(kR)$ . This factor expresses the probability that the two constituents will overcome their various barriers (Coulomb, centrifugal, and also the sudden change in the potential as the nuclear surface is crossed), and will penetrate each other. When written down explicitly,  $T_l(E)$  (for charged particles) presents itself as a complicated mixture of the regular ( $F_l$ ) and irregular ( $G_l$ ) solution to the wave equation outside of the nuclear boundary (Feshbach, Shapiro, and Weisskopf 1953). However, at low energy (low compared to the height of the barriers) the factor  $T_l(E)$  can be approximated by simpler expressions.

The highest barrier is usually the Coulomb barrier [ $B_c = (Z_1 Z_2 e^2/R) \simeq (1.44 Z_1 Z_2/R)$  in Mev, if  $R$  is in fermis ( $1f = 10^{-13}$  cm)]. In cases where  $E \ll B$  we are justified in writing

$$\Gamma_{1,2} = \gamma^* \xi_l^2 e^{-2\pi\eta}, \quad (2.11)$$

where

$$\xi_l^2 = (G_0^2/G_l^2) (2y^{1/2} e^{4y^{1/2}})$$

with

$$4y^{1/2} = 4[(2Z_1 Z_2 e^2 MR)/\hbar^2]^{1/2} = 1.054[Z_1 Z_2 M(\text{a.m.u.})R(f)]^{1/2}.$$

Here  $\xi_l^2$  is almost independent of energy. The penetration factor  $\exp(-2\pi\eta) = \exp(-2\pi Z_1 Z_2 e^2/\hbar v)$  (the so-called Gamow factor) represents the strong energy dependence brought in by the Coulomb repulsion. Numerically, if  $E$  is in kev,

$$\exp(-2\pi\eta) = \exp(-31.285 Z_1 Z_2 M^{1/2}/E^{1/2}). \quad (2.12)$$

Away from the resonances the Breit-Wigner formula is no longer accurate. However, again if  $E \ll B$  the experimental cross-sections still exhibit the Gamow factor energy dependence. Then it is customary to use the so-called astrophysical  $S$  factor defined as

$$\sigma = (S/E) e^{-2\pi\eta}. \quad (2.13)$$

Then the  $S$  factor is almost energy-independent. If we introduce (2.13) into (2.3) we see that the integrand has a peak (the Gamow peak) which represents the best candidates for nuclear reactions. The center,  $E_0$ , and the width,  $\Delta E_0$ , of

the peak are both increasing functions of the temperature. Numerical values for different frequently used temperature units are given in Table 2.

The expression  $\langle \sigma v \rangle$  can be approximately integrated by a technique described in Salpeter (1952). The result, usually called the non-resonant (n.r.) approximation, is

$$\log_{10} \langle \sigma v \rangle_{\text{n.r.}} = -15.14 - \log(MZ_1Z_2) + \log S + 2 \log \tau - 0.434 \tau \quad (2.14)$$

where  $S$  is in Mev-barn,  $M$  is in a.m.u., and  $\tau$ , a dimensionless parameter, is given by  $\tau = 3E_0/kT$  (see Table 2). In many cases the factor  $S$  was found ex-

TABLE 2

USEFUL PARAMETERS FOR COMPUTATION OF THERMONUCLEAR REACTION RATES

	kev	Mev
$2\pi\eta E^{1/2}/(Z_1^2 Z_2^2 M)^{1/2} \dots\dots\dots$	$3.1285 \times 10^4$	$9.8935 \times 10^{-1}$
$y^{3/2}/6\eta^2 [MR^3/(Z_1 Z_2)]^{-1/2} E^{-1} \dots\dots\dots$	$1.2150 \times 10^{-4}$	$1.2150 \times 10^{-1}$

	$T_6$	$T_8$	$T_9$
$E_0/T^{2/3}(Z_1^2 Z_2^2 M)^{+1/3} \text{ (kev)} \dots\dots\dots$	1.22	26.3	122
$\Delta E_0/T^{5/6}(Z_1^2 Z_2^2 M)^{+1/6} \text{ (kev)}^* \dots\dots\dots$	.75	35	237
$\tau(Z_1^2 Z_2^2 M)^{-1/3} T^{1/3} \dots\dots\dots$	$4.2483 \times 10^1$	9.1528	4.2483
$\epsilon/(MR^3/Z_1 Z_2)^{1/2} T \dots\dots\dots$	$1.05 \times 10^{-5}$	$1.05 \times 10^{-3}$	$1.05 \times 10^{-2}$
$kT \text{ (kev)} \dots\dots\dots$	$8.6164 \times 10^{-2} T_6$	$8.6164 T_8$	$8.6164 \times 10^1 T_9$

\* Note:  $\Delta E_0$  is the full width at half-maximum.

perimentally to be slightly energy-dependent. In such cases, we use the first two terms of a series expansion

$$S(E) = S(0) + E(dS/dE). \quad (2.15)$$

Various workers have analyzed their data to obtain by extrapolation the value of  $S(0)$  at zero energy, and an average value  $\langle dS/dE \rangle$  at low energies. In these cases we use in (14) the value of  $S$  at the Gamow peak ( $S_{\text{eff}}$ ):

$$S_{\text{eff}}(T) = S(0) g(T) = S(0) \left[ 1 + \frac{5}{12\tau} + \frac{\langle dS/dE \rangle}{S(0)} (E_0(T) + \frac{35}{36} kT) \right] \quad (2.16)$$

(the term  $5/12\tau$  is actually a correction term to the integral itself). For convenience in tabulation we also define

$$g(T) = [1 + UT^{1/3} + VT^{2/3} + WT]. \quad (2.17)$$

The values of  $U$ ,  $V$ ,  $W$ , and  $g$  can be calculated with the help of Table 2 if the proper experimental information is available.

In most instances we shall characterize a non-resonant reaction by giving it  $(P_{2,1}/\rho X_1)$  (see eq. [2.4]). We shall write it as

$$\frac{P_{2,1}}{\rho X_1} = A f_{2,1} g_{2,1} e^{-B/T^{1/3}} / T^{2/3}, \quad (2.18)$$

where  $A$  is a numerical constant (obtained from [2.14]),  $f_{2,1}$  is the electron screening factor (discussed later);  $g_{2,1}$  is defined in (2.16) and  $B = \tau T^{1/3}$ . From equations (2.7) or (2.8) we can obtain  $(\epsilon)$ , the energy generation rate for a given reaction. We shall also introduce  $n$ , the logarithmic derivative of  $\epsilon$  with respect to  $T$ :

$$n \equiv \frac{T}{\epsilon} \frac{d\epsilon}{dT}. \quad (2.19)$$

In certain cases the “non-resonant” contribution from a given resonance can be approximated by evaluating its Breit-Wigner cross-section at the Gamow peak  $(E_0)$ . Comparing (2.9), (2.11), and (2.13), we get an effective  $S$  factor given by

$$S_{B.W.} = (\pi \lambda^2 E) (\omega \xi_i^2 \gamma^* \Gamma_{3,4}) / \left[ \frac{\Gamma^2(E_0)}{4} + (E_0 - E_r)^2 \right]. \quad (2.20)$$

Experimental determination of  $\Gamma_{1,2}$  at the resonances yields immediately the value of  $[\gamma^* \xi_i^2]$ . If no experimental results are available one must guess the value of  $R$ , the nuclear radius of interaction, to be used in computation of  $\xi_i^2$  and of  $\theta_{1,2}^2$ . The uncertainty in  $\theta_{1,2}^2$  usually brings the greatest uncertainty in the rate.

For the later stages of stellar evolution one has to deal with particles having energies approaching the Coulomb barrier energies. In such cases one has to include an extra term in the expansion of the Coulomb wave function. To take into account this modification we shall redefine and prime some of the expressions used previously. First we want to extract from some of the “constants” the energy dependence inflicted on them by the increased bombarding energies. We define

$$\xi_i'^2 = \xi_i^2 \exp(y^{3/2}/6\eta^2) = (G_0/G_i)^2 2y^{1/2} \exp(4y^{1/2}); \quad (2.21)$$

$$S' = S \exp(y^{3/2}/6\eta^2) = \sigma E \exp(2\pi\eta + y^{3/2}/6\eta^2). \quad (2.22)$$

For numerical values of  $y^{3/2}/6\eta^2$  see Table 2. Then  $\xi_i'^2$  and  $S'$  are almost energy-independent and we have

$$\Gamma_{1,2} = \gamma^* \exp(-2\pi\eta - y^{3/2}/6\eta^2) \xi_i'^2. \quad (2.23)$$

The effect of this term will be to “reduce” the value of the Gamow energy to  $E_0' = E_0 [1 - (2\epsilon/3)]$ ;  $\epsilon \simeq (y^{3/2}/6\eta^2) kT$ , the Gamow width to  $\Delta E_0' = \Delta E_0 [1 - (5\epsilon/6)]$ . Finally, we replace  $\tau$ , such as in (2.14), by  $\tau' = (1 + \epsilon/3)\tau$  to obtain the correct rate. Numerical values of  $\epsilon$  are given in Table 2.

Lastly, when some resonance falls in (or close to) the Gamow peak, the term

$\langle \sigma v \rangle$  comes dominantly from this resonance, and we have (the so-called resonant contribution)

$$\frac{P_{1,2}}{\rho X_1} = \frac{\omega \mathfrak{N}}{A_1} e^{-E_r/kT} \left( \frac{2\pi\hbar^2}{MkT} \right)^{3/2} \frac{\Gamma_{1,2}\Gamma_{3,4}}{\Gamma\hbar} \quad (\text{in c.g.s. units}). \quad (2.24)$$

This yields (in units of  $T_8$ )

$$\begin{aligned} \log_{10} \langle \sigma v \rangle_r = & -11.09 + \log \omega \left( \frac{\Gamma_{1,2}\Gamma_{3,4}}{\Gamma} \right) \\ & - \frac{3}{2} \log M - \frac{3}{2} \log T_8 - 50.4 E_r / T_8 \end{aligned} \quad (2.24a)$$

with  $\Gamma$ 's and  $E_r$  in Mev, or:

$$\begin{aligned} \log \left( \frac{P_{2,1}}{\rho X_1} \right) = & \left[ 12.69 - \log A_1 - \log \frac{\omega \Gamma_{1,2}\Gamma_{3,4}}{\Gamma} \right. \\ & \left. - \frac{3}{2} \log T_8 - \frac{3}{2} \log M - \frac{50.4 E_r}{T_8} \right]. \end{aligned} \quad (2.24b)$$

If we are dealing with identical particles, the cross-section for allowed partial waves has twice the value it would have for non-identical particles leading to the same compound state (with given widths). Indeed for identical particles the R.H.S. of equations (2.9), (2.20), and (2.24) should be multiplied by two, while the R.H.S. of equations (2.24a) and (2.24b) should be increased by +0.3. On the other hand, since the factor  $S$  in (2.13) is usually obtained experimentally for the reaction under consideration (e.g.,  $\text{He}^3 + \text{He}^3$ ), it needs no further correction.

## 2.2. ELECTRON SCREENING FACTORS

Electron screening factors were first calculated by Schatzman (1948). The limiting cases were considered by Salpeter (1954). He has shown that the effective increase in the nuclear reaction rate due to electron screening can be described in terms of a potential energy term  $U_0$ . He gives recipes to evaluate this term and shows that the correct rate is obtained by multiplying the unscreened rate by  $\exp(-U_0/kT)$  ( $U_0$  is always a negative quantity).

To evaluate  $U_0$  one must first determine whether the screening is weak or strong, i.e., if the electrostatic interaction energy between neighboring nuclei is small or large compared to the thermal energy. Intermediate cases require special attention. If the weak screening condition applies one obtains

$$-U_0/kT = 0.188 Z_1 Z_2 \zeta \rho^{1/2} / T_6^{3/2}, \quad (2.25)$$

where  $Z_1, Z_2$  are the charges of the two particles involved ( $Z_1 \geq Z_2$ ),  $\rho$  is the density in grams, and  $\zeta$  is defined by

$$\zeta = \left\{ \sum_i \frac{X_i (z_i + z_i^2)}{A_i} \right\}^{1/2}, \quad (2.26)$$

where  $z_i$  are the charges of the various nuclei in the stellar core. The sum over  $i$  refers to a sum over all the constituents of the gas.

The criterion for the validity of the weak screening approximation can be written as  $(-U_0/kT)(z/Z_2) < 1$ , where  $z$  is the average charge of the gas. If the electron gas is partly degenerate one has to redefine  $\zeta$ :

$$\zeta_{\text{deg.}} = \left\{ \sum X_i \frac{z_i}{A_i} + (f'/f) \sum X_i \frac{z_i}{A_i} \right\}^{1/2}. \quad (2.27)$$

In Figure 4 the function  $f'(z)/f(z)$  is plotted as a function of  $D$ , the degeneracy parameter (the ratio of the Fermi energy to the mean thermal energy). The

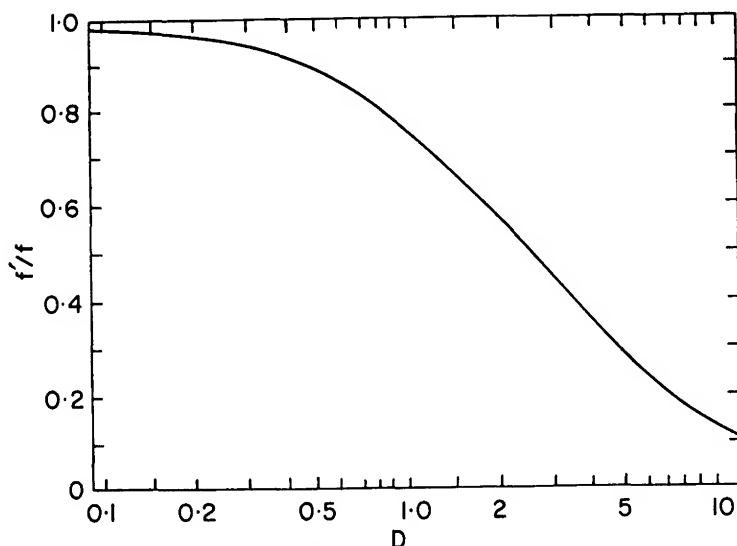


FIG. 4.—Plot of the electron screening parameter as a function of  $D$ , the degeneracy parameter.

value of  $D$  is given by (a)  $D = 0.3 (\rho/\mu)^{2/3} (1/T_6)$  for non-relativistic cases  $(\rho/\mu) \ll 10^6$ , and (b)  $D = (60/T_6)(\rho/\mu)^{1/3}$  for relativistic cases  $(\rho/\mu) \gg 10^6$ .  $\mu$  is the number of nucleons per electron in the gas;

$$\mu = \left( \sum X_i \frac{Z_i}{A_i} \right)^{-1}.$$

If the condition for weak screening is violated, one computes the strong screening potential by the formula

$$-\frac{U_0}{kT} = 0.20 [(Z_1 + Z_2)^{5/3} - Z_1^{5/3} - Z_2^{5/3}] \left( \frac{\rho}{\mu} \right)^{1/3} \frac{1}{T_6}. \quad (2.28)$$

This formula is valid if (1)  $Z_1 \ll \rho^{1/3}$ , and (2)  $(0.23 Z_1^{2/3}/T_6) z (\rho/\mu)^{1/3} \gg 1$ . If these two conditions do not apply (intermediate screening) one has to consider



more involved techniques. However, a graphical interpolation between weak screening and strong screening may yield a first approximation to the correct value.

The results of Salpeter are based on the assumption that all atoms in the gas are completely ionized. To test this assumption, we define an ionization parameter ( $I_*$ ) for a given atom of charge  $Z$  as the ratio of the ionization potential of a  $K$ -shell electron in a hydrogen-like atom to the mean thermal energy. The assumption is valid if

$$I_* = \left( \frac{Z e^2}{2 a_{0z}} \right) \frac{1}{(kT)} = \frac{0.16 Z^2}{T_6} \ll 1, \quad (2.29)$$

where  $a_{0z}$  is the Bohr radius for an atom of charge  $Z$ . This parameter is usually much smaller than one. One notable exception is the CNO cycle at low temperatures. There one would have to use a more accurate formalism such as that given by Schatzman (1958) or Keller (1953). However, it usually turns out that in such cases the CNO cycle is not the dominant mode of energy production. The formalism of Salpeter, while somewhat inaccurate, still remains then perfectly adequate.

### § 3. HYDROGEN-BURNING STAGE

In the stars the fusion of four protons into one helium nucleus is accomplished through two important mechanisms: the proton-proton chain and the carbon-nitrogen cycle. In the proton-proton chain one starts by adding three protons together to form a helium-3 nucleus. This nucleus then reacts with another helium-3 or with an already present helium-4 nucleus to become eventually a helium-4 nucleus. The detailed possible mechanisms are given in Table 3.

The rate of energy generation is governed mostly by the rate of the proton-proton reaction. It is also governed by the number of subsequent reactions which can obtain equilibrium with this reaction. One should notice here that the PP I requires for its completion two helium-3 nuclei while PP II and PP III require only one (the helium-4 used in these modes acts only as a catalyst). Hence the *rate* of energy generation is twice as large for these modes. In that sense the energy generation rate depends also on the abundance of helium-4.

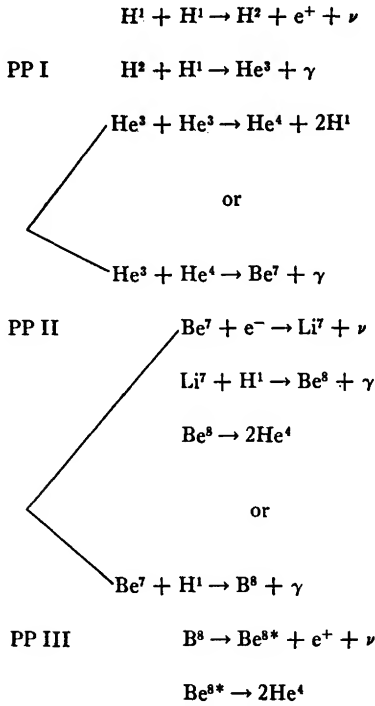
In the carbon-nitrogen cycle (also referred to as PP IV) four protons are successively added to a nucleus of  $C^{12}$ . With the addition of the last proton the nucleus breaks into  $C^{12}$  and  $He^4$ . Sometimes the break-up does not occur and  $O^{16}$  is formed. This nucleus then accepts two more protons and breaks into  $N^{14}$  and  $He^4$ . This is called the CNO bi-cycle.

We shall discuss in detail the set of nuclear reactions involved in hydrogen burning. Recent improvements in experimental techniques as well as in theoretical understanding allow one to compute the rates with fair confidence and even permit the addition of some refinements.

The set of reactions considered are listed in Tables 4 and 6, together with

some of the relevant nuclear parameters. It appears fairly certain that with the exception of the  $O^{17}$  ( $H^1$ ,  $He^4$ )  $N^{14}$ , the reactions involved in the proton-proton branches or the CNO cycle are all non-resonant, although the presence of resonances in the stellar energy range cannot yet be completely ruled out. To discuss these reaction rates it is convenient to use  $T_6$  as a unit of temperature. The results will all be given in terms of this unit. The results concerning the CNO bi-cycle came mostly from the work of Caughlan and Fowler (1962).

TABLE 3  
REACTIONS INVOLVED IN THE PROTON-PROTON CHAINS



In the diagram we have indicated the position and width of the Gamow peak at  $T_6 = 100$ , which is certainly an upper limit to the temperature of the hydrogen-burning stage.

### 3.1. ELECTRON SCREENING FOR HYDROGEN-BURNING CASES

For stars on the main sequence, the factor  $\rho^{1/2}/T_6^{3/2}$  varies from 0.02 for  $M = 10 M_\odot$  to 2.4 for  $M = 0.1 M_\odot$  (Kumar 1962). For  $M > 0.6 M_\odot$ ,  $D$  is less than 0.6, then from Figure 4,  $f'/f \simeq 1$ . In this case  $\zeta$  is  $\simeq 1.4(1 - 0.13X_4)$ . (Again  $X_4$  is the concentration by weight of the helium in the gas.)  $(-U_0/kT)$  becomes  $0.27(Z_1Z_2)(1 - 0.13X_4) \rho^{1/2}/T_6^{3/2}$ . The product  $Z_1Z_2$  is never larger

TABLE 4  
PARAMETERS FOR THE PROTON-PROTON CHAINS

Reaction	Reduced Mass $M = (A_1 A_2) / (A_1 + A_2)$ a.m.u.	$Z_1 Z_2 \sqrt{M}$	Gamow Peak $E_0/T_e^{1/2} =$ $1.220(Z_1^2 Z_2^2 M)^{1/2}$ (kev)	Full Width $\Delta E_0/T_e^{1/2} =$ $0.75 (Z_1^2 Z_2^2 M)^{1/2}$ (kev)
$H^1 + H^1 \rightarrow H^2 + e^+ + \nu$	$0.5041 \pm 0.0001$	$0.70998 \pm 0.00009$	$0.971$	$0.67$
$H^1 + H^2 \rightarrow He^3 + \gamma$	$0.6719 \pm 0.0001$	$0.81971 \pm 0.00006$	$1.07$	$0.70$
$He^3 + He^3 \rightarrow He^4 + 2H^1$	$1.5085 \pm 0.0001$	$4.9128 \pm 0.0002$	$3.53$	$1.3$
$He^3 + He^4 \rightarrow Be^7 + \gamma$	$1.7205 \pm 0.0001$	$5.2468 \pm 0.0002$	$3.68$	$1.3$
$Be^7 + e^- \rightarrow Li^7 + \nu$				
$Li^7 + H^1 \rightarrow He^4 + He^4$	$0.8815 \pm 0.0001$	$2.8167 \pm 0.0002$	$2.43$	$1.1$
$Be^7 + H^1 \rightarrow B^8 + \gamma$	$0.8815 \pm 0.0001$	$3.7556 \pm 0.0003$	$2.95$	$1.2$
$B^8 \rightarrow Be^8 + e^+ + \nu$				

TABLE 4—Continued

Reaction	$B_0 = 42.483(Z_1^2 Z_2^2 M)^{1/2}$ $B_0 = \tau T_e^{1/2}$	$2\pi\eta E^{1/2}$ (kev) = $31.285(Z_1^2 Z_2^2 M)^{1/2}$	Q value (kev) $(4H^1 \rightarrow He \rightleftharpoons$ $26.730 \text{ Mev})$	Neutrino $E_{\max}$ (kev) = $(\Delta m - 2m_e c^2)$
$H^1 + H^1 \rightarrow H^2 + e^+ + \nu$	$33.810 \pm 0.003$	$22.212 \pm 0.003$	$1442.10 \pm 0.20$	$420.16 \pm 0.20$
$H^1 + H^2 \rightarrow He^3 + \gamma$	$37.210 \pm 0.002$	$25.645 \pm 0.003$	$5493.15 \pm 0.16$	
$He^3 + He^3 \rightarrow He^4 + 2H^1$	$122.774 \pm 0.004$	$153.70 \pm 0.02$	$12859.31 \pm 0.48$	
$He^3 + He^4 \rightarrow Be^7 + \gamma$	$128.277 \pm 0.004$	$164.15 \pm 0.02$	$1587.4 \pm 1.2$	
$Be^7 + e^- \rightarrow Li^7 + \nu$			$860.7 \pm 2.2$	
$Li^7 + H^1 \rightarrow He^4 + He^4$	$84.731 \pm 0.004$	$88.121 \pm 0.010$	$17346.5 \pm 1.2$	
$Be^7 + H^1 \rightarrow B^8 + \gamma$	$102.645 \pm 0.005$	$117.50 \pm 0.01$	$133.1 \pm 1.8$	
$B^8 \rightarrow Be^8 + e^+ + \nu$			$17980.0 \pm 2.3$	$16958.1 \pm 2.3$

TABLE 4—Continued

Reaction	Average Neutrino Energy Loss (Mev)	$S(0)$ (keV-barns)	$\langle dS/dE \rangle$ barns	$A$ $[P/\rho X_1 = A f g \exp(-B_0/T_e^{1/3}) T_e^{-2/3}]$
$H^1 + H^1 \rightarrow H^2 + e^+ + \nu$	0.263	$(3.36 \pm 0.4) \times 10^{-22}$ $(2.5 \pm 0.4) \times 10^{-4}$ $1.2 \times 10^3$	$2.7 \times 10^{-24}$ $7.9 \times 10^{-6}$ .....	$(3.3 \pm 0.4) \times 10^{-13}$ $(2.2 \pm 0.4) \times 10^5$ $(P_{3,3}/\rho x_3)$ $(4.3) \times 10^{11}$
$H^1 + H^2 \rightarrow He^3 + \gamma$				
$He^3 + He^3 \rightarrow He^4 + 2H^1$				
$He^3 + He^4 \rightarrow Be^7 + \gamma$	0.80	$(0.47 \pm 0.07)$ ..... $(100 \pm 25)$ $(2 \pm 1) \times 10^{-2}$	$-2.8 \times 10^{-4}$ ..... ..... .....	$(P_{3,4}/\rho x_4)(1.2 \pm 0.2) \times 10^8$ ..... $(1.2 \pm 0.3) \times 10^{11}$ $(2.6 \pm 1.3) \times 10^7$
$Be^7 + e^- \rightarrow Li^7 + \nu$				
$Li^7 + H^1 \rightarrow He^4 + He^4$				
$Be^7 + H^1 \rightarrow B^8 + \gamma$	7.2	.....	.....	.....
$B^8 \rightarrow Be^8 + e^+ + \nu$				

TABLE 4—Continued

REACTION	$g = (1 + UT_e^{1/3} + VT_e^{2/3} + WT_e)$			$f$ ELECTRON SCREENING FACTOR (WEAK)
	$U$ $(U = 5/12B)$	$V$ $\{V = E_0/T_e^{2/3} [ \langle dS/dE \rangle / S(0) ]\}$	$W$ $\{W = 35/36 [ \langle dS/dE \rangle / S(0) ]^2\}$	
$H^1 + H^1 \rightarrow H^2 + e^+ + \nu$	$1.23 \times 10^{-2}$ $1.12 \times 10^{-2}$ $3.39 \times 10^{-3}$ $3.25 \times 10^{-3}$	$7.80 \times 10^{-3}$ $3.12 \times 10^{-2}$ ..... $-2.15 \times 10^{-3}$	$6.73 \times 10^{-4}$ $2.45 \times 10^{-3}$ ..... $-4.90 \times 10^{-5}$	$(1 + 0.25\rho^{1/2}/T_e^{3/2})$ $(1 + 0.25\rho^{1/2}/T_e^{3/2})$ $(1 + 1.0\rho^{1/2}/T_e^{3/2})$ $(1 + 1.0\rho^{1/2}/T_e^{3/2})$
$H^1 + H^2 \rightarrow He^3 + \gamma$				
$He^3 + He^3 \rightarrow He^4 + 2H^1$				
$He^3 + He^4 \rightarrow Be^7 + \gamma$				
$Be^7 + e^- \rightarrow Li^7 + \nu$	$4.92 \times 10^{-3}$ $4.06 \times 10^{-3}$	.....	.....	$(1 + 0.75\rho^{1/2}/T_e^{3/2})$ $(1 + 1.0\rho^{1/2}/T_e^{3/2})$ .....
$Li^7 + H^1 \rightarrow He^4 + He^4$				
$Be^7 + H^1 \rightarrow B^8 + \gamma$				
$B^8 \rightarrow Be^8 + e^+ + \nu$	.....	.....	.....	.....

than 8, hence all main-sequence stars with  $M > 0.6M_{\odot}$  are eligible for the weak screening formula.

The maximum value of  $0.27Z_1Z_2 \rho^{1/2}/T_6^{3/2}$  is about 0.40 when the proton-proton branch is dominant, and even less when the CNO cycle is dominant. Hence, in view of the approximation already used in deriving these formulae one may well put  $X_4 = 0.5$  everywhere and expand the exponential

$$\exp(-U_0/kT) = \left[1 + 0.25Z_1Z_2 \frac{\rho^{1/2}}{T_6^{3/2}}\right] \equiv f.$$

In Tables 4 and 6 we list the value of  $f$ , assuming that the weak screening approximation applies. As discussed before, it should apply inside all main-sequence stars with  $M > 0.6M_{\odot}$ . In hydrogen-burning shells the electron screening is usually negligible. For main-sequence stars with  $M < 0.6M_{\odot}$ , the strong screening approximation or some accurate estimates should be used.

The case of C-N burning stars of low temperature has been discussed previously.

### 3.2. HYDROGEN THERMONUCLEAR REACTIONS (PROTON-PROTON)

3.2.1.  $H^1 + H^1 \rightarrow H^2 + e^+ + \nu$ .—Since there is no bound system to be formed with two protons, this reaction can occur only if the protons are brought together by a nuclear collision. During the short time of the encounter, one of the protons has a chance to beta decay thereby becoming a neutron, a positive electron, and a neutrino. The neutron can then be captured by the other proton to form a deuteron. This reaction has never been observed in the laboratory. Its extremely small calculated cross-section ( $10^{-28}$  barns) explains this fact and suggests that it might never be detected directly. However, the present state of nuclear physics and of weak interaction theories makes its existence practically compelling.

The computation of the cross-section for this reaction requires knowledge of the Gamow-Teller beta-decay coupling constant. The decay rate is given by

$$\beta = 4 \left( \frac{G^2}{2\pi^3} \right) \left( \frac{m_e c^2}{\hbar} \right) f(w) |\phi_i \phi_f d\tau|^2,$$

where  $G$  is the interaction coupling constant which will be explained below,  $w$  is the maximum energy of the electron (or positron) in units of  $m_e c^2$ , and  $f(w)$  is computed in Fermi's theory.  $\phi_i$  is the initial wave function, and  $\phi_f$  is the final wave function. The uncertainties in  $\beta$  come from two sources; the uncertainty due to a lack of knowledge of the initial and the final state wave functions, and a lack of knowledge of the coupling constant  $G$ .

In most literature, instead of  $G$ ,  $g_{\beta}$  is quoted.  $g_{\beta}$  is defined as

$$g_{\beta} = 4 \left( \frac{G^2}{2\pi^3} \right) \left( \frac{m_e c^2}{\hbar} \right) \quad (3.1)$$

and

$$G = g m_P^2 \left( \frac{m_e}{m_P} \right)^2 \left( \frac{g_G T}{g_F} \right).$$

Experimentally  $g(m_p^2) = (1.01 \pm 0.01) \times 10^{-5}$ .  $g_{GT}$  and  $g_F$  are the Gamow-Teller part and the Fermi part of the weak coupling constants.

We write  $a = g_{GT}/g_F$ . Numerically,

$$g_B = 4.49 \times 10^{-4} a^2.$$

To determine  $a$ , one may use the experimentally determined half-life of the neutron and the decay of  $O^{14}$  nuclei. Wu (private communication) has determined

$$a^2 = 1.42 \pm 0.08.$$

Hence

$$g_B = (6.36 \pm 0.36) \times 10^{-4}.$$

Fowler has substantially revised the above data. The uncertainty in our knowledge of  $g_B$  is thus around 5 per cent. With this value of  $g_B$ , the  $S$  factor becomes  $S(0) = (3.36 \pm 0.4) \times 10^{-22}$  kev-barns while  $\langle dS/dE \rangle = 2.7 \times 10^{-24}$  barns (Chiu, private communication).

3.2.2.  $H^1 + H^2 \rightarrow He^3 + \gamma$ .—This reaction has recently been analyzed by Griffiths, Lal, and Scarfe (1961) down to energies of 16 kev (24 kev lab). The cross-section can be accounted for in terms of a direct capture process. Both the  $S$  and the  $P$  waves contribute significantly to the capture rate, even at the lowest energies. The reaction can be characterized by the following parameters.

$$S(0) = (2.5 \pm 0.4) \times 10^{-4} \text{ kev-barns},$$

$$\langle dS/dE \rangle = 0.079 \times 10^{-4} \text{ barns}.$$

It is worthwhile noting that this value of  $S$  is some three to four times larger than the values used previously. The ratio of  $H^2/H^1$  in stars should consequently be decreased by the same amount.

3.2.3.  $He^3 + He^3 \rightarrow He^4 + 2H^1$ .—The reaction has been studied in the laboratory (Good, Kunz, and Moak 1954) at energies from 50 to 400 kev (c.m.). The cross-section follows a simple Gamow-type curve up to  $E \simeq 175$  kev. These experimenters find that at  $E = 100$  kev, the cross-section is at least  $2.5 \mu\text{b}$ . From this one sees that the  $S(0)$  factor is larger than  $1.2 \times 10^3$  kev-barns. Dr. Good (private communication) believes that this number should be at the same time a good estimate and a lower limit. He sets the upper limit as  $2.4 \times 10^3$  kev-barns, although such a high value of  $S$  appears very unlikely. The experiments do not allow a determination of  $\langle dS/dE \rangle$ .

3.2.4.  $He^3 + He^4 \rightarrow Be^7 + \gamma$ .—The importance of this reaction for stellar energy sources was first pointed out by Fowler (1951) and Schatzman (1951). Measurements have been made by Holmgren and Johnston (1959) and by Parker and Kavanagh (1963). From the energy diagram (Fig. 5) the process is clearly non-resonant. In fact, it shows the characteristics of a direct capture process (Christy and Duck 1961, Tombrello and Parker 1963). The experimental curve can be fitted by a Gamow-type curve. We obtain  $S(0) = 0.47 \pm 0.07$  kev-barns and  $\langle dS/dE \rangle = -2.8 \times 10^{-4}$  barns.

3.2.5.  $\text{Li}^7 + \text{H}^1 \rightarrow \text{He}^4 + \text{He}^4; \rightarrow \text{Be}^8 + \gamma$ .—These two reactions have been studied in the range from 30 to 250 kev (c.m.) (Sawyer and Phillips 1953). The first one is more than one hundred times faster than the second everywhere in the range. Previous measurements had shown an isotropic yield at 100 kev. Assuming isotropy all through the range, the cross-sections were calculated from the  $90^\circ$  yield.

The product of the yield times the energy was plotted as a function of  $E^{-1/2}$  in order to detect any energy dependence of the factor  $S$  (Fig. 6). Within the experimental uncertainty no such dependence could be found. The value of  $S_0$  is 100 kev-barns with a probable error of 25 per cent.

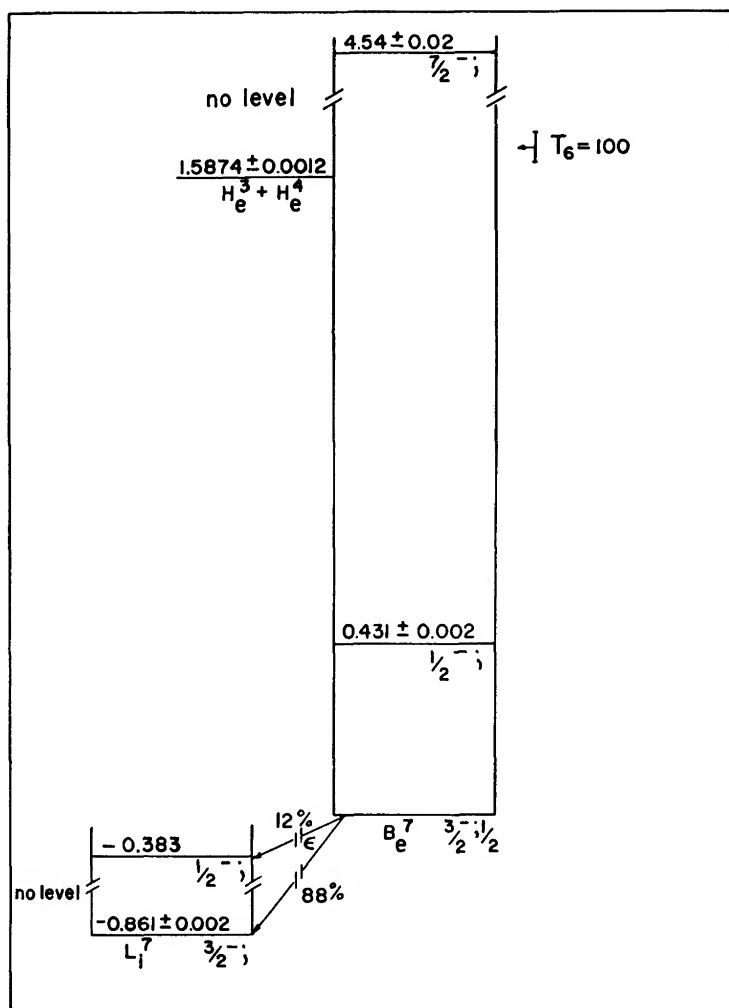


FIG. 5.—Energy diagram of  $\text{Be}^7$

3.2.6.  $\text{Be}^7 + \text{H}^1 \rightarrow \gamma + \text{B}^8$ .—The existence of an excited level at  $E_r = 600$  kev has been questioned. We have not included this level in the diagram (Fig. 7). This reaction has been described by Christy and Duck (1961) as a direct capture process. Its cross-section has been measured by Kavanagh (1960) at  $E_{\text{c.m.}} = 700$  kev, and 1225 kev. He finds  $\sigma(700) = (0.48 \pm 0.18 \mu\text{b})$  and  $\sigma(1225) = (0.50 \pm 0.20 \mu\text{b})$ . Although the first measurement could be expected to feel the influence of the resonance at 790 kev, Kavanagh estimates that the resonant contribution is probably negligible. He evaluates  $S_0 = 0.020 \pm 0.010$  kev-barn.

3.2.7.  $\text{Be}^7 + e^- \rightarrow \text{Li}^7 + \nu$ .—The free electron gas in a stellar core is ex-

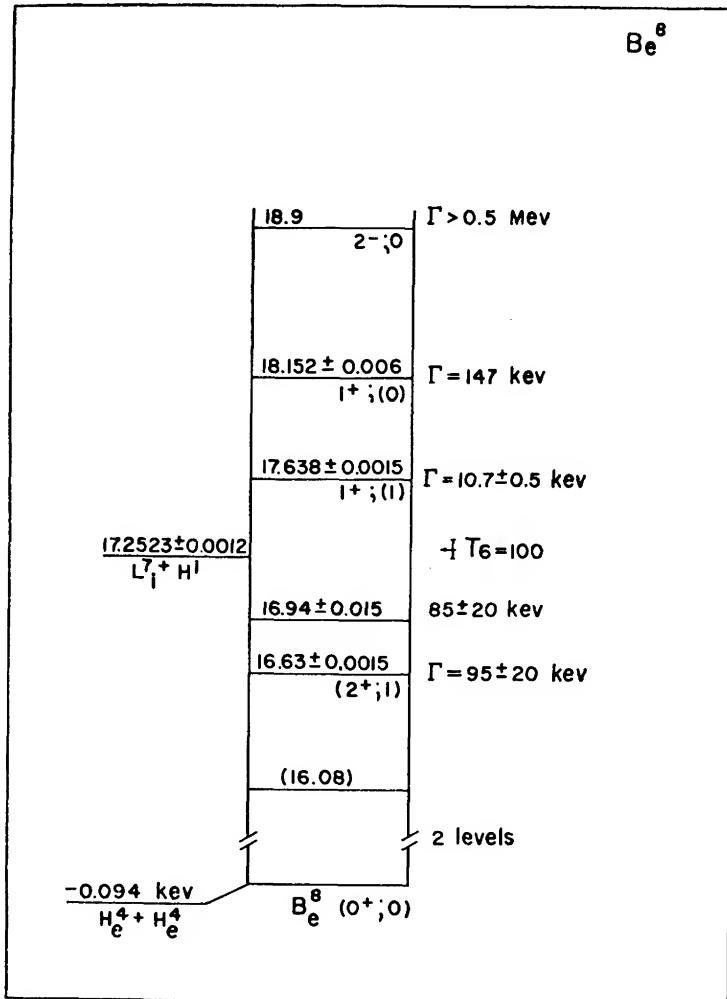


FIG. 6.—Energy diagram of  $\text{Be}^8$



pected to initiate this reaction. An accurate calculation has been made by Bahcall *et al.* (1963) taking into account the nucleus electron (Coulomb interaction, relativistic and nuclear size corrections, the imperfect overlap between initial and final atomic states, and electron screening in bound decay. The probability of electron capture is given as

$$P_{\text{Be}^7 + e^- \rightarrow \text{Li}^7 + \nu} = \frac{2.12 \times 10^{-9} \rho (1 + X_1)}{T_6^{1/2}} \text{ sec}^{-1} \quad (3.2)$$

within a few per cent ( $X_1$  is the fractional weight of hydrogen).

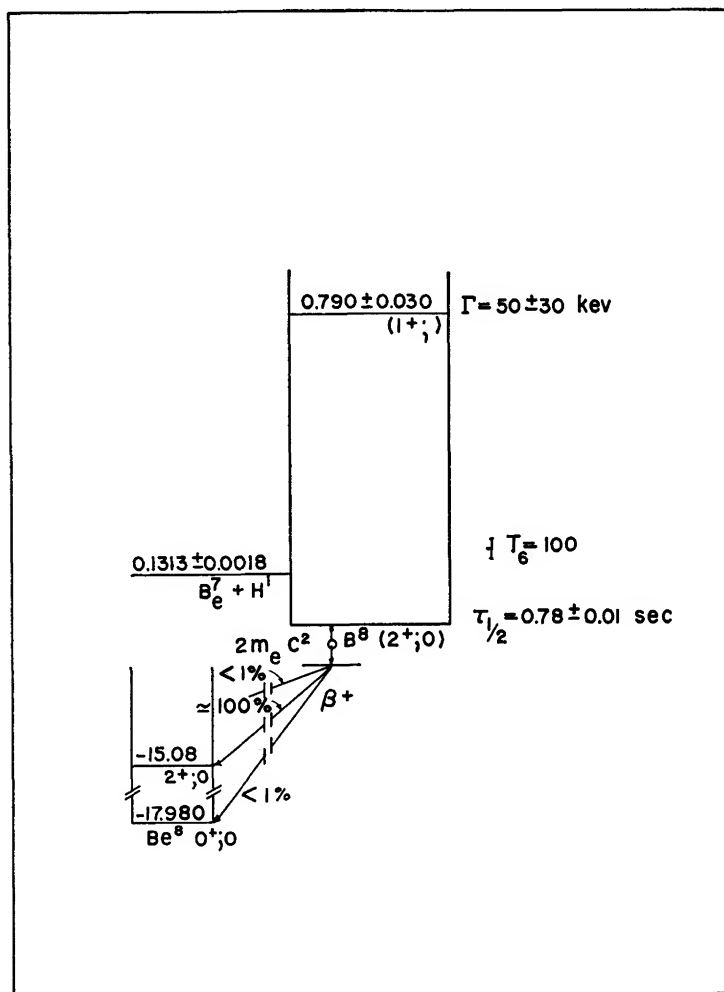
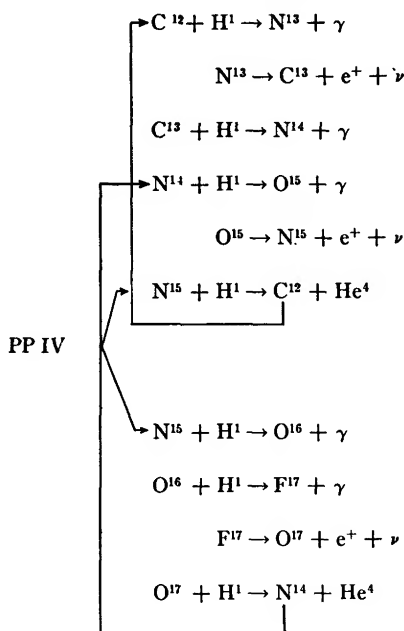


FIG. 7.—Energy diagram of  $B^8$

## 3.3. HYDROGEN THERMONUCLEAR REACTIONS (CNO)

3.3.1.  $C^{12} + H^1 \rightarrow N^{13} + \gamma$ .—Measurements have been made down to  $E_p = 80$  kev ( $E_{e.m.} = 74$  kev) by Lamb and Hester, (Lamb 1957*a*) and others. A resonance at  $E_{lab} = 462$  kev ( $E^* = 2.367$  Mev;  $\gamma_p^2 = 1695$  kev;  $\omega\Gamma_\gamma = 1.52$  ev) is the most important factor in the cross-section. In the low energy part of the range one has to consider the interference of the resonance tail with the non-resonant rate (Fig. 8).

TABLE 5  
REACTIONS INVOLVED IN THE CNO BI-CYCLE



The extrapolation to low energy has been made by Hebbard and Vogl (1960) in the following way. First they have calculated the contribution of the resonance tail of the 462 kev level from a single-level Breit-Wigner formula, including all energy dependences. Then, they have divided the experimental cross-section by this computed cross-section. In this way the non-resonant factor could be obtained and extrapolated to low energies. They find  $S = 1.33 \pm 0.15$  kev-barn at  $E_{e.m.} = 25$  kev.

The lifetime of  $N^{13}$  against photodisintegration is given by  $\log t = [119/T_8 - 15.3]$  sec. For  $T_8 > 7.5$  it becomes shorter than the lifetime against beta disintegration.

3.3.2.  $C^{13} + H^1 \rightarrow N^{14} + \gamma$ .—As seen from the diagram (Fig. 9) the  $Q$  value

for the ( $C^{13} + H^1$ ) break-up is situated in a rather well populated area of the energy spectrum of  $N^{14}$ . For this reason, the extrapolation of the capture cross-section to low energies has always been a difficult problem. The resonances are, in this area, separated by a few hundred kev. One of these resonances may well be located in the region just above the break-up point. Because of the Coulomb effect it would be very difficult to analyze the contribution of this reaction to the thermonuclear reaction rate. An experiment on  $N^{14}(H^1, H^1)N^{14*}$  (Burge and Prowse 1956) had suggested in particular the presence of a level at 7.60 Mev. However, a recent examination of the energy level scheme of  $N^{14}$  through

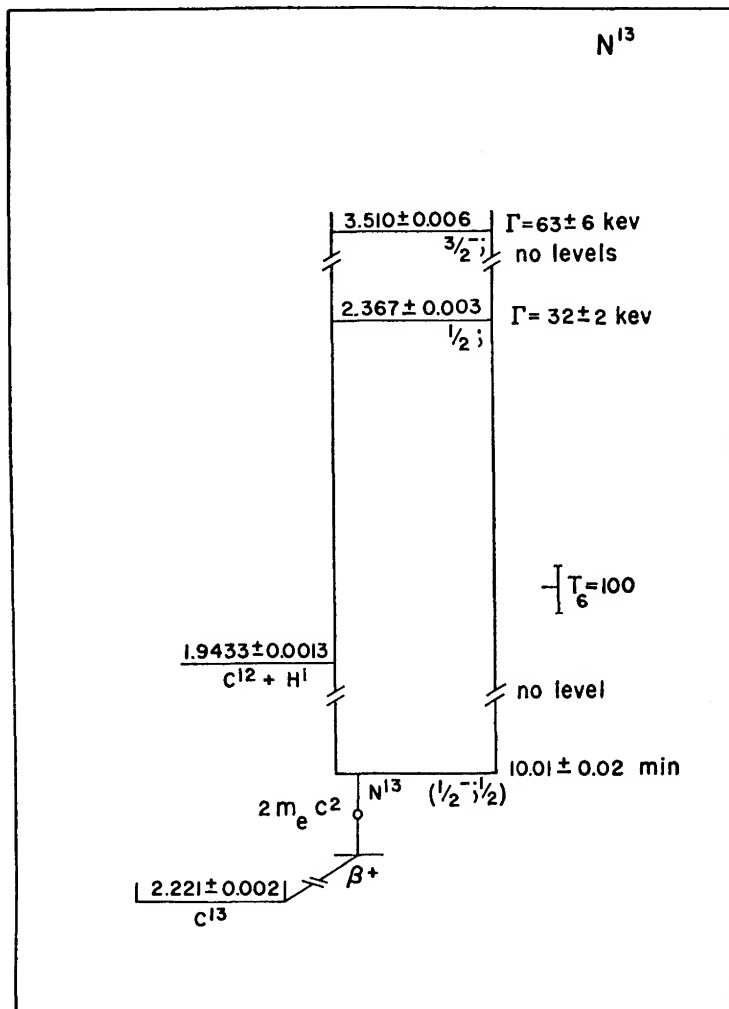


FIG. 8.—Energy diagram of  $N^{13}$





3.3.4.  $N^{15} + H^1 \rightarrow C^{12} + He^4; \rightarrow O^{16} + \gamma$ .—The cross-section for the  $N^{15} + H^1 \rightarrow C^{12} + He^4$  reaction has been measured down to  $E_{lab} = 100$  kev by Schardt, Fowler, and Lauritsen (1952) and other workers. Two groups of alpha particles are observed; one group ( $\alpha_0$ ) accompanies  $C^{12}$  nuclei in the ground state, another group ( $\alpha_1$ ) with  $C^{12}$  in the first excited state (4.43 Mev). The yield for the first group is by far the largest at low energies, as can be expected from arguments concerning the Coulomb barrier. It is the only one that we shall consider.

As  $C^{12}$  and  $He^4$  are both spinless particles, they can only come from the state of so-called “natural” parity in  $O^{16}$  ( $0^+, 1^-, 2^+, 3^-$ , etc.). Indeed the cross-section exhibits maxima at the 12.44, 13.10, and 13.25 Mev levels, which are respectively  $1^-, 1^-$ , and  $3^-$ . The  $N^{15} + H^1 \rightarrow O^{16} + \gamma$  reaction has been measured by Hebbard (1960) to  $E_{lab} \cong 200$  kev. The cross-section is resonant at  $E^* = 12.44$  and 13.10 (Fig. 11).

Hebbard has analyzed the integrated cross-sections with the multi-channel two-level Breit-Wigner expression. He included in his analysis the four channels of  $O^{16}$  breaking up into  $N^{15} + H^1$ ,  $C^{12} + \alpha_0$ ,  $C^{12} + \alpha_1$ , and  $O^{16} + \gamma$ . The experimental points are reasonably well fitted by his theoretical curve. Extrapolation of the theoretical curve allows a determination of the  $S$  factor. He obtains:  $S = 32$  kev-barns and  $7.2 \times 10^4$  kev-barns, respectively, for  $N^{15} + H^1 \rightarrow O^{16} + \gamma$  and  $N^{15} + H^1 \rightarrow C^{12} + He^4$ , at  $E = 25$  kev.

3.3.5.  $O^{16} + H^1 \rightarrow F^{17} + \gamma$ .—Measurements of the radiative proton capture by oxygen have been made by Tanner (1959) at 616 kev (lab) and by Hester, Pixley, and Lamb (1958) in the range from 140 to 170 kev (lab). Tanner finds  $S = 6 \pm 1.4$  kev-barns. Using the formalism of Christy and Duck, Fowler and Caughlan have extrapolated these results to low energies. They get  $S(0) = 10.6$  kev-barns and  $\langle dS/dE \rangle = -2.8 \times 10^{-2}$  (Fig. 12). (Note: A theoretical analysis of the same data plus newer points has been made by Lal [1961]. He finds  $S(0) = 12$  kev-barns.)

3.3.6.  $O^{17} + H^1 \rightarrow N^{14} + He^4; \rightarrow F^{18} + \gamma$ .—Because of the abundance of levels in the corresponding region of the compound nucleus the rate is most likely resonant. Close to the break-up point one finds two ( $1^-$ ) resonances at  $E_r = -3 \pm 7$  kev and at  $E_r = 65 \pm 7$  kev. Silverstein, Hardie, Oppliger, and Salisbury (1960) have made some measurements of the properties of these levels. In both cases the total width is  $\cong 200$  ev, and is most likely due to the alpha particle width. Hence, one can obtain a good estimate of  $\theta_\alpha^2$ , (the alpha reduced width of these levels): one gets  $\theta_\alpha^2 \cong 0.14$  (Fig. 13). (The  $[H^1, \gamma]$  reaction is neglected as its radiation width is undoubtedly much smaller than 200 ev.)

Brown (1962) has used these two levels to compute the reaction rate. One important quantity for computation of the resonant nuclear reaction is  $\theta_p^2$ , the proton reduced width. Unfortunately nothing is known about the  $\theta_p^2$  of these

two levels. To obtain an estimate Brown assumed that the  $\theta_p^2$  of these levels is similar to the  $\theta_p^2$  of some neighboring levels at higher excitation energy. He sets  $\theta_p^2 \simeq 7 \times 10^{-3}$ . This estimate is probably within a factor 10 of the correct value but may possibly be wrong by a factor of one hundred.

Since the two levels are both  $(1^-)$  and since they are so close to each other one should worry about interference effects. In particular, one does not know whether the interference will be destructive or constructive. Brown has carried out calculations for the two cases and has shown that the thermonuclear rates would be the same for  $T_6 > 22$  but could differ by factors of 10 to 100 at lower

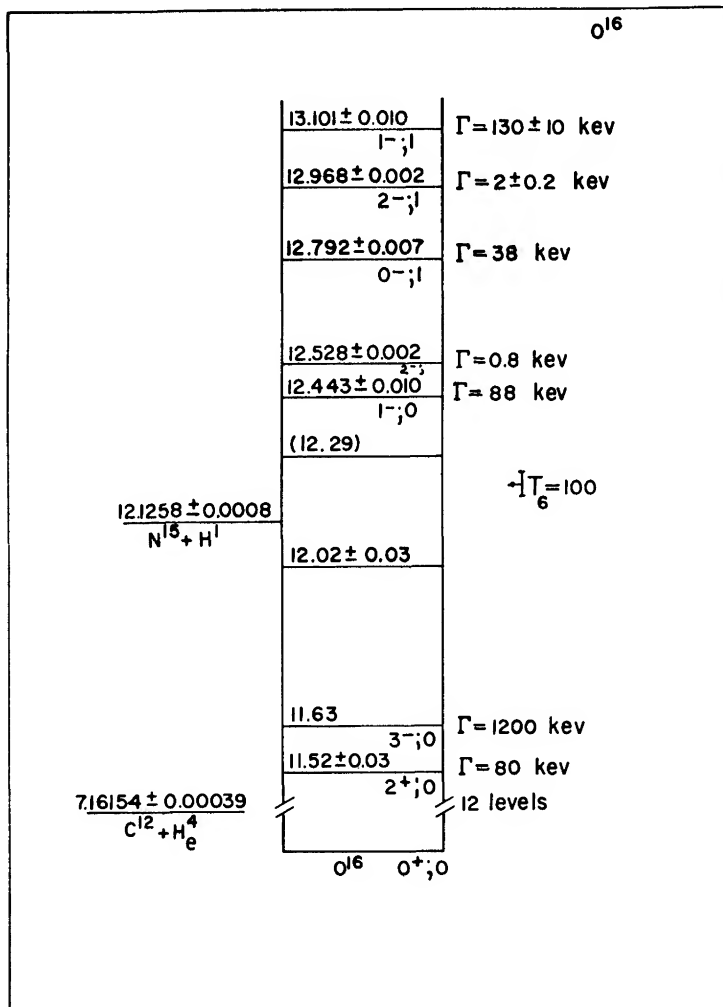


FIG. 11.—Energy diagram of  $O^{16}$

temperatures. He then shows that the observed terrestrial  $O^{17}/O^{16}$  ratio is better explained in terms of destructive interference. On this account Fowler and Caughlan accept the choice of destructive interference. In the absence of better argumentation we shall make the same choice but remember that it rests on unsafe grounds.

Above  $T_6 = 30$ , the rate can be written with the help of a resonant formula of the form

$$\frac{P}{\rho X_1 f_{17,1}} = 10^{2.4} e^{-755/T_6} / T_6^{3/2}, \quad T_6 > 30.$$

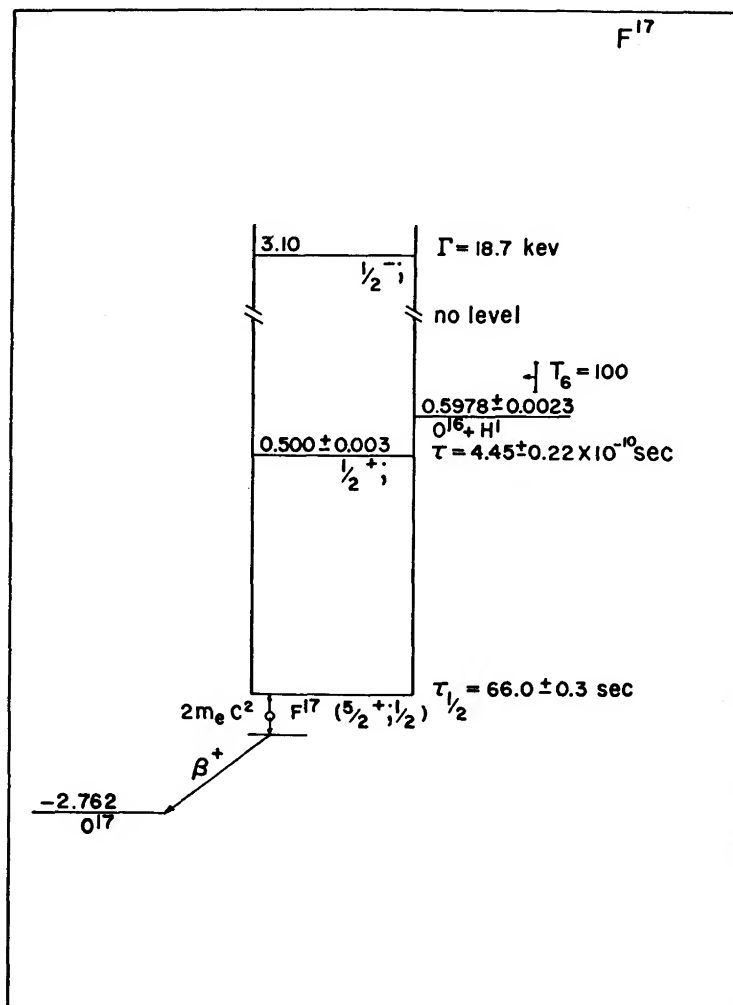


FIG. 12.—Energy diagram of  $F^{17}$



At lower temperatures the values of  $P/\rho X_{17,1}$  were computed numerically by Brown. The results are given in Table 7. This rate is the poorest known of all those discussed so far. The influence of the uncertainties attached to this particular reaction rate on our knowledge of the energy generation rate will be discussed in later paragraphs.

### 3.4. NUCLEOSYNTHESIS FROM THE CNO CYCLE

Caughlan and Fowler (1962) have considered the equilibrium production of CNO during the carbon cycle. The relative abundance of a given isotope is ob-

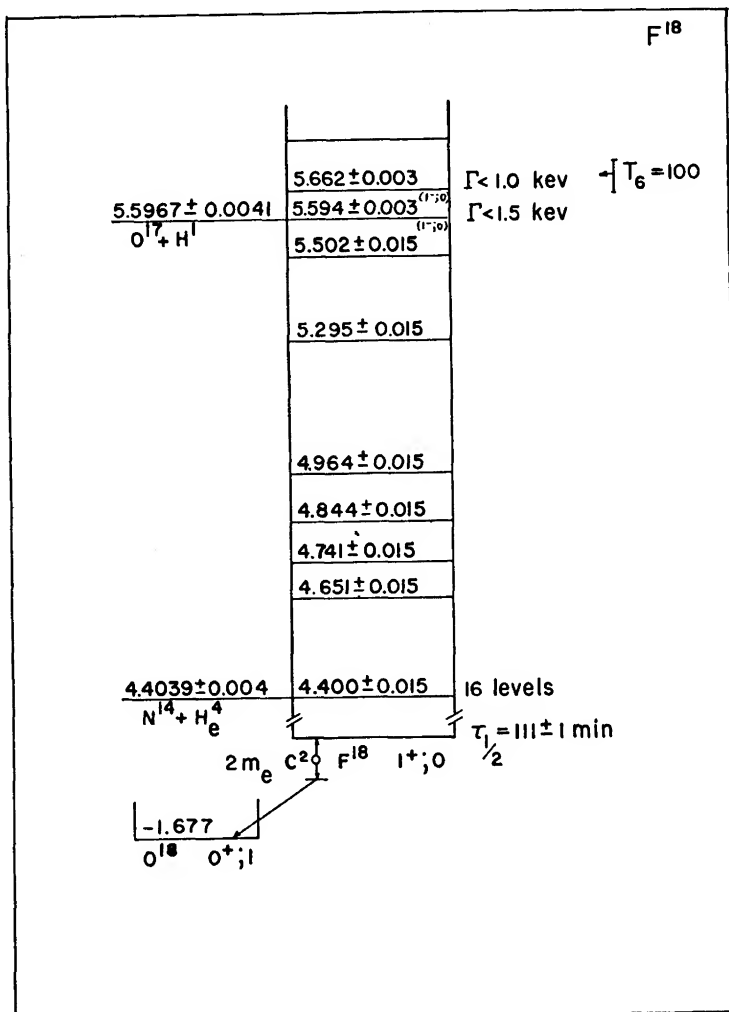


FIG. 13.—Energy diagram of  $F^{18}$

TABLE 6  
PARAMETERS FOR THE CNO BI-CYCLE

Reaction	Reduced Mass $M = (A_1 A_2) / (A_1 + A_2)$ a.m.u.	$Z_1 Z_2 \sqrt{M}$	Gamow Peak $E_0 / T_9^{3/4} =$ $1.220 (Z_1^2 Z_2^2 M)^{1/2}$ (kev)	Full Width $\Delta E_0 / T_9^{3/4} =$ $0.75 (Z_1^2 Z_2^2 M)^{1/2}$ (Mev)
$C^{12} + H^1 \rightarrow N^{13} + \gamma$	$0.93004 \pm 0.00004$	$5.7863 \pm 0.0003$	3.93	1.4
$N^{13} \rightarrow C^{13} + e^+ + \nu$				
$C^{13} + H^1 \rightarrow N^{14} + \gamma$	$.93563 \pm .00006$	$5.8037 \pm .0002$	3.94	1.4
$N^{14} + H^1 \rightarrow O^{15} + \gamma$	$.94046 \pm .00003$	$6.7884 \pm .0001$	4.38	1.4
$O^{15} \rightarrow N^{15} + e^+ + \nu$				
$N^{15} + H^1 \rightarrow C^{12} + He^4$	$.94467 \pm .00006$	$6.8036 \pm .0002$	4.38	1.4
$N^{15} + H^1 \rightarrow O^{16} + \gamma$	$.94467 \pm .00006$	$6.8036 \pm .0002$	4.38	1.4
$O^{16} + H^1 \rightarrow F^{17} + \gamma$	$.94839 \pm .00002$	$7.79082 \pm .00006$	4.80	1.5
$F^{17} \rightarrow O^{17} + e^+ + \nu$				
$O^{17} + H^1 \rightarrow N^{14} + He^4$	$0.95172 \pm 0.00005$	$7.8045 \pm 0.0002$	4.80	1.5

TABLE 6—Continued

Reaction	$B_0 = 42.4834 (Z_1^2 Z_2^2 M)^{1/2}$ $B_0 = \tau T_9^{1/2}$	$2\pi\eta E^{1/2}$ (kev) = $31.2853 (Z_1^2 Z_2^2 M)^{1/2}$	Q value (kev)	Neutrino $E_{max}$ (kev) = $(\Delta m - 2m_e c^2)$
$C^{12} + H^1 \rightarrow N^{13} + \gamma$	$136.926 \pm 0.002$	$181.03 \pm 0.02$	$1943.3 \pm 1.3$	
$N^{13} \rightarrow C^{13} + e^+ + \nu$			$2221.1 \pm 2.0$	$1199.0 \pm 2$
$C^{13} + H^1 \rightarrow N^{14} + \gamma$	$137.200 \pm .003$	$181.57 \pm .02$	$7549.4 \pm 0.7$	
$N^{14} + H^1 \rightarrow O^{15} + \gamma$	$152.311 \pm .002$	$212.38 \pm .03$	$7291.1 \pm 1.7$	
$O^{15} \rightarrow N^{15} + e^+ + \nu$			$2760.6 \pm 2.6$	$1739 \pm 3$
$N^{15} + H^1 \rightarrow C^{12} + He^4$	$152.538 \pm .003$	$212.85 \pm .03$	$4964.3 \pm 0.9$	
$N^{15} + H^1 \rightarrow O^{16} + \gamma$	$152.538 \pm .003$	$212.85 \pm .03$	$12125.8 \pm 0.8$	
$O^{16} + H^1 \rightarrow F^{17} + \gamma$	$166.958 \pm .001$	$243.74 \pm .03$	$597.8 \pm 2.3$	
$F^{17} \rightarrow O^{17} + e^+ + \nu$			$2761.7 \pm 3.1$	$1740 \pm 2$
$O^{17} + H^1 \rightarrow N^{14} + He^4$	$167.154 \pm 0.003$	$244.17 \pm 0.03$	$1192.9 \pm 0.9$	

TABLE 6—Continued

Reaction	Average Neutrino Energy Loss (Mev)	$S(0)$ (kev-barns)	$\langle dS/dE \rangle$ barns	$\begin{matrix} A \\ [P/\rho X_1 = \\ Afg \exp(-B_0/T_0^{1/3})T_0^{-2/3}] \end{matrix}$
$C^{12}+H^1 \rightarrow N^{13}+\gamma$			$5.81 \times 10^{-3}$	$(1.7 \pm 0.3) \times 10^9$
$N^{13} \rightarrow C^{13}+e^++\nu$	0.710	$(1.20 \pm 0.15)$		
$C^{13}+H^1 \rightarrow N^{14}+\gamma$		$(5.52 \pm 0.7)$	$1.94 \times 10^{-4}$	$(8.0 \pm 1.0) \times 10^9$
$N^{14}+H^1 \rightarrow O^{15}+\gamma$		$(3.12 \pm 0.25)$	$-2.67 \times 10^{-3}$	$(4.7 \pm 0.4) \times 10^9$
$O^{15} \rightarrow N^{15}+e^++\nu$	1.00			
$N^{15}+H^1 \rightarrow C^{12}+He^4$		$(5.34 \pm ) \times 10^4$	$8.22 \times 10^2$	$(8.0 \pm ) \times 10^{13}$
$N^{15}+H^1 \rightarrow O^{16}+\gamma$		$(2.74 \pm ) \times 10^4$	$1.86 \times 10^{-1}$	$(4.2 \pm ) \times 10^{10}$
$O^{16}+H^1 \rightarrow F^{17}+\gamma$		$(1.06 \pm 0.18) \times 10^4$	$-2.81 \times 10^{-2}$	$(1.7 \pm 0.3) \times 10^{10}$
$F^{17} \rightarrow O^{17}+e^++\nu$	0.94			
$O^{17}+H^1 \rightarrow N^{14}+He^4$				

TABLE 6—Continued

REACTION	$g = (1 + UT_0^{1/3} + VT_0^{2/3} + WT_0)$			$f$ ELECTRON SCREENING FACTOR (WEAK)
	$U$ $(U = 5/12B_0)$	$V$ $\{V = E_0/T_0^{1/3} \\ [ \langle dS/dE \rangle / S(0) ] \}$	$W$ $\{W = 35/36 \\ [ \langle dS/dE \rangle / S(0) ]^2 \}$	
$C^{12}+H^1 \rightarrow N^{13}+\gamma$	$3.04 \times 10^{-3}$	$1.90 \times 10^{-2}$	$4.05 \times 10^{-4}$	$(1 + 1.5\rho^{1/2}/T_0^{3/2})$
$N^{13} \rightarrow C^{13}+e^++\nu$				
$C^{13}+H^1 \rightarrow N^{14}+\gamma$	$3.04 \times 10^{-3}$	$1.38 \times 10^{-2}$	$2.94 \times 10^{-4}$	$(1 + 1.5\rho^{1/2}/T_0^{3/2})$
$N^{14}+H^1 \rightarrow O^{15}+\gamma$	$2.74 \times 10^{-3}$	$-3.74 \times 10^{-3}$	$-7.17 \times 10^{-6}$	$(1 + 1.75\rho^{1/2}/T_0^{3/2})$
$O^{15} \rightarrow N^{15}+e^++\nu$				
$N^{15}+H^1 \rightarrow C^{12}+He^4$	$2.73 \times 10^{-3}$	$6.74 \times 10^{-2}$	$1.29 \times 10^{-3}$	$(1 + 1.75\rho^{1/2}/T_0^{3/2})$
$N^{15}+H^1 \rightarrow O^{16}+\gamma$	$2.73 \times 10^{-3}$	$2.97 \times 10^{-2}$	$5.69 \times 10^{-4}$	$(1 + 1.75\rho^{1/2}/T_0^{3/2})$
$O^{16}+H^1 \rightarrow F^{17}+\gamma$	$2.50 \times 10^{-3}$	$-1.27 \times 10^{-2}$	$-2.22 \times 10^{-4}$	$(1 + 2.0\rho^{1/2}/T_0^{3/2})$
$F^{17} \rightarrow O^{17}+e^++\nu$				
$O^{17}+H^1 \rightarrow N^{14}+He^4$	$2.50 \times 10^{-3}$			

tained by comparing its lifetime against destruction with the lifetime of the cycle as a whole (remembering that for  $T_6 \gtrsim 17$  the full bi-cycle gets into operation). In Table 7, the lifetime of the cycle is given as a function of the temperature while in Figures 14 and 15, the relative isotopic abundances are plotted, normalized to the total abundance of carbon and nitrogen isotopes (C-N) or to the total abundance of carbon, nitrogen, and oxygen isotopes (CNO).

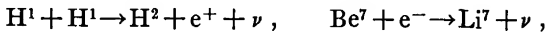
TABLE 7

RATE OF THE  $O^{17} + H^1 \rightarrow N^{14} + He^4$  AND TOTAL LIFETIME OF THE BI-CYCLE

$T_6$	$\frac{P_{17+1 \rightarrow 14+4}}{\rho X_{17,1}}$	$\tau \rho X_{17,1} \rho X_{14,1}$ bi-cycle sec	$T_6$	$\frac{P_{17+1 \rightarrow 14+4}}{\rho X_{17,1}}$	$\tau \rho X_{17,1} \rho X_{14,1}$ bi-cycle sec
5.....	-31.6	29.7	25.....	-12.8	13.9
6.....	-29.7	27.4	26.....	-12.3	13.6
7.....	-28.0	25.6	27.....	.....	.....
8.....	-26.2	24.1	28.....	-11.4	13.1
9.....	-24.8	22.9	29.....	.....	.....
10.....	-23.7	21.8	30.....	-10.7	12.6
11.....	-22.8	20.8	35.....	-9.3	11.6
12.....	-22.1	20.0	40.....	-8.2	10.8
13.....	-21.4	19.3	45.....	-7.4	10.1
14.....	-20.7	18.6	50.....	-6.7	9.5
15.....	-20.0	18.0	55.....	-6.2	8.9
16.....	-19.2	17.4	60.....	-5.7	8.5
17.....	-18.4	16.9	65.....	-5.4	8.1
18.....	-17.6	16.4	70.....	-5.1	7.7
19.....	-16.7	16.0	75.....	-4.8	7.3
20.....	-15.9	15.6	80.....	-4.6	7.0
21.....	.....	.....	85.....	-4.4	6.7
22.....	-14.5	14.9	90.....	-4.2	6.5
23.....	.....	.....	95.....	-4.0	6.2
24.....	-13.3	14.2	100.....	-3.9	6.0

### 3.5. NEUTRINOS FROM THE HYDROGEN-BURNING STAGE

From Tables 6 and 7 we see that there are six nuclear reactions which involve beta decay; namely



In principle each beta-decaying nucleus ( $A \rightarrow B + e^+ + \nu$ ) can also undergo an electron capture process ( $A + e^- \rightarrow B + \nu$ ). In certain cases (e.g.,  $Be^7$ ) where the first mode is energetically forbidden, only the second mode is actually possible.

The importance of the second mode will be briefly investigated for the case of free electron capture (completely ionized gas) since, if it turned out to be important it would reduce the mean life of the beta-decaying nucleus. This second

mode is also interesting in the sense that it will generate sharp lines in the neutrino spectrum of the sun. Indeed, whereas the first mode produces a hump spread from zero energy to  $(\Delta M - 2m_e c^2)$  where  $\Delta M$  is the energy difference between the mother and daughter atoms, the second mode (because it ends in a two-body break-up) will emit monoenergetic neutrinos (within  $kT$ ; the thermal energy spread of the electrons) with  $E_\nu = \Delta M$ .

The relative rate of the two modes can be obtained by simply comparing the volume of phase space available to these modes (the  $f$  factor of beta decay).

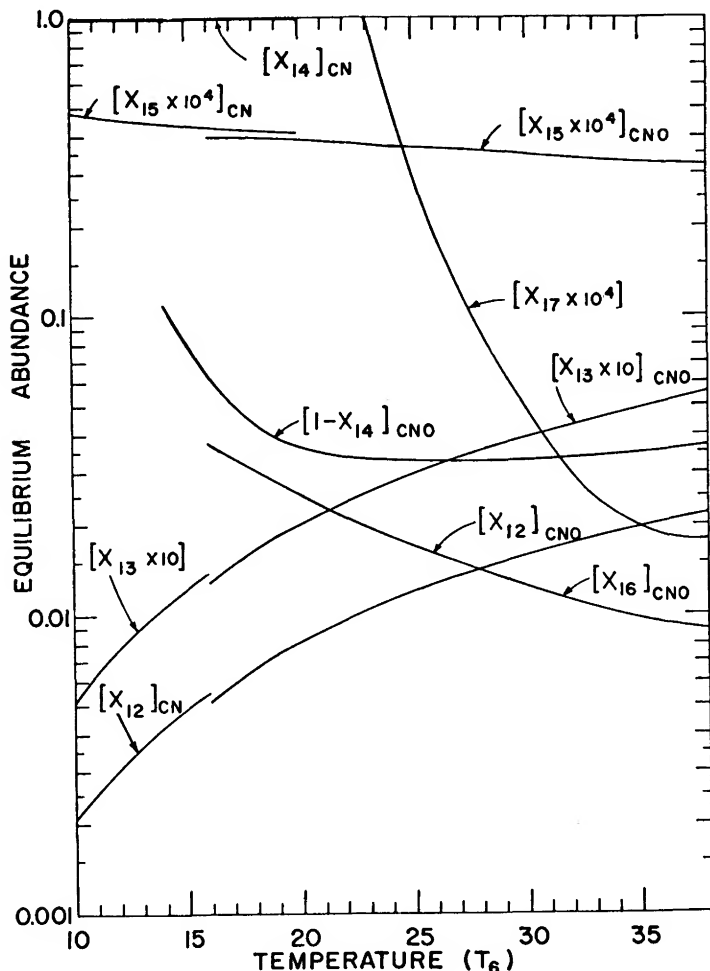


FIG. 14.—Isotopic abundances from the CNO bi-cycle, normalized to  $X_{CN} = 1$ , or to  $X_{CNO} = 1$ . In these graphs the quantities  $X_i$  are number (not mass) densities.

The volume of phase space available to the free electron capture can be obtained to a reasonable accuracy ( $\approx 25\%$ ) by the following formula

$$f_{f.e.} = 4.7 \times 10^{-7} (Z)(\Delta M)^2 \frac{\rho(1+X_1)}{T_6^{1/2}}, \quad (3.3)$$

where  $Z$  is the charge of the *mother* nucleus,  $\Delta M$  is the mass difference defined above, in  $m_e c^2$  ( $m_e c^2 = 0.51/\text{Mev}$ ).

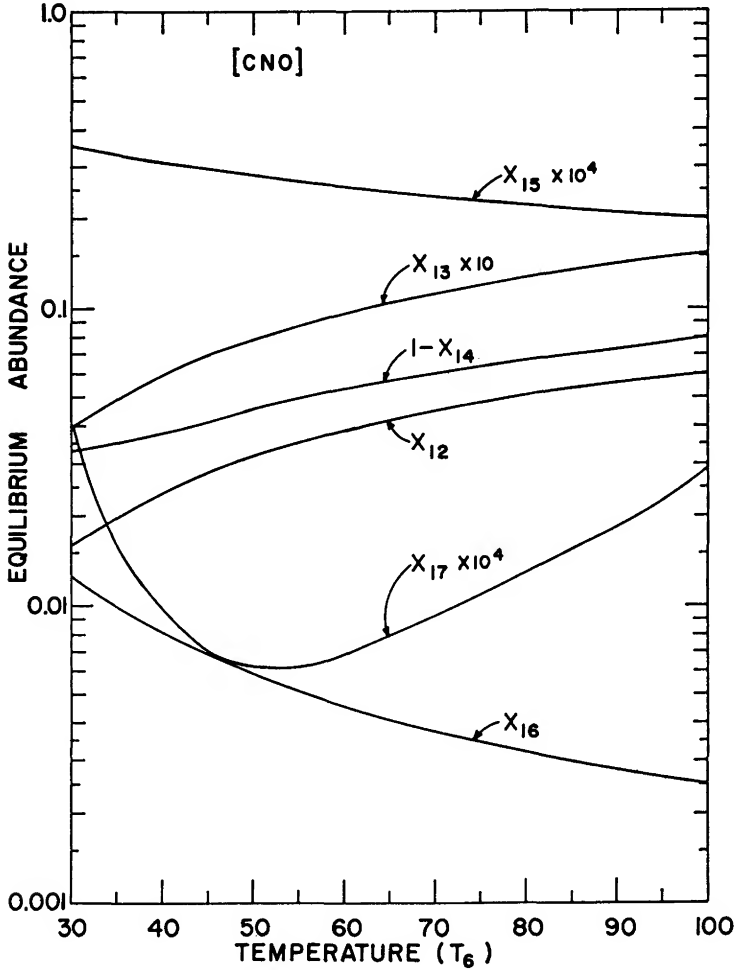


FIG. 15.—Isotopic abundances from the CNO bi-cycle normalized to  $X_{\text{CNO}} = 1$ . In these graphs the quantities  $X_i$  are number (not mass) densities.

Using the experimentally known value of  $\tau_{1/2}$  (the half life) and of the factor  $f$  for the reaction  $A \rightarrow B + e + \nu$  we have

$$P_{A+e \rightarrow B+\nu} = P_{A \rightarrow B+e+\nu} \left( \frac{f_{A+e \rightarrow B+\nu}}{f_{A \rightarrow B+e+\nu}} \right) = \frac{\ln 2}{(f \tau_{1/2})} (f_{A+e \rightarrow B+\nu}),$$

where  $P_{A+e \rightarrow B+\nu}$  is the inverse of the lifetime of  $A$  against electron capture.

Salpeter has calculated the  $f$  factor for the first reaction ( $H^1 + H^1$ ): he gets  $f_{H^1+H^1 \rightarrow H^2+e+\nu} = 0.145 [1 + 0.054(T_6/15)^{2/3}]$ . From our formula, the free capture rate is:

$$f_{H^1+H^1+e \rightarrow H^2+\nu} = 7.5 \times 10^{-6} \rho (1 + X_1) / T_6^{1/2}. \quad (3.4)$$

The ratio of the two processes is  $[5 \times 10^{-5}(X_1 + 1)\rho] / T_6^{1/2}$ . In the center of the sun this ratio is about 0.003, hence, the contribution is negligible. In smaller stars it could well be much more important. It should be noticed, however, that (3.3) is valid only for a non-degenerate gas. The case of a degenerate gas has been treated by Schatzman (1958). The neutrino spectrum from this reaction contains a hump from  $E_\nu = 0$  to 0.42 Mev and then a peak at 1.440 Mev. In the sun the peak is slightly higher than the hump.

As mentioned before, because of its low  $Q$  value the  $Be^7$  decays only by electron capture. The decaying nucleus goes eighty-eight per cent of the time to the ground state of  $Li^7$  (0.861 Mev neutrino) and twelve per cent of the time to the first excited state (0.383 Mev neutrino). In the previous section a detailed calculation of the electron capture probability by Bahcall *et al.* (1963) was mentioned. Our approximate formula would give here a numerical constant eighteen per cent smaller. The spectrum in this case consists of two narrow lines. The relative heights are 7.3:1.

The  $B^8$  isotope decays almost one hundred per cent of the time to the 2.9 Mev level in  $Be^8$  ( $\log ft = 5.72$ ) and less than one per cent of the time to the ground state ( $\log ft > 7.3$ ). The outcoming neutrinos have on the average 7.2 Mev. They are by far the most energetic neutrinos coming from ordinary stars. The peaks from the  $B^8$ ,  $N^{13}$ ,  $O^{15}$ ,  $F^{17}$  electron captures are all negligibly small in areas and in heights, as compared to the respective humps.

Looking at these neutrinos from the point of view of the cycles, we have the following situation: each PP I cycle is accompanied by two ( $H^1 + H^1$ ) neutrinos (total  $E_\nu = 0.53$  Mev). PP II has one ( $H^1 + H^1$ ) and one  $Be^7$  neutrino (total  $E_\nu = 1.06$ ). PP III has one ( $H^1 + H^1$ ) and one  $B^8$  neutrino (total  $E_\nu = 7.5$ ). PP IV has one  $N^{13}$  and one  $O^{15}$  neutrino (total  $E_\nu = 1.71$ ).  $F^{17}$  contributes negligibly to the spectrum.

In the next chapter we shall evaluate the relative contribution of each of these cycles in a star. If we call  $\epsilon_I$  the rate of energy generation from the PP I, etc., the intensity of the ( $H^1 + H^1$ ) neutrinos will be proportional to  $2\epsilon_I + \epsilon_{II} + \epsilon_{III}$ ; the intensity of the  $Be^7$  neutrinos to  $\epsilon_{II}$ , the intensity of the  $B^8$  neutrinos to  $\epsilon_{III}$  and the intensity of the  $N^{13}$  and  $O^{15}$  proportional to  $\epsilon_{IV}$ . Using

the results of the next chapter and a model of the sun by Pochoda and Reeves (1964), we have built a neutrino spectrum from the sun. We recognize over the general background, made by the various humps, the three main lines of the spectrum (Fig. 16).

Is there any hope of observing these solar neutrinos? To answer this question

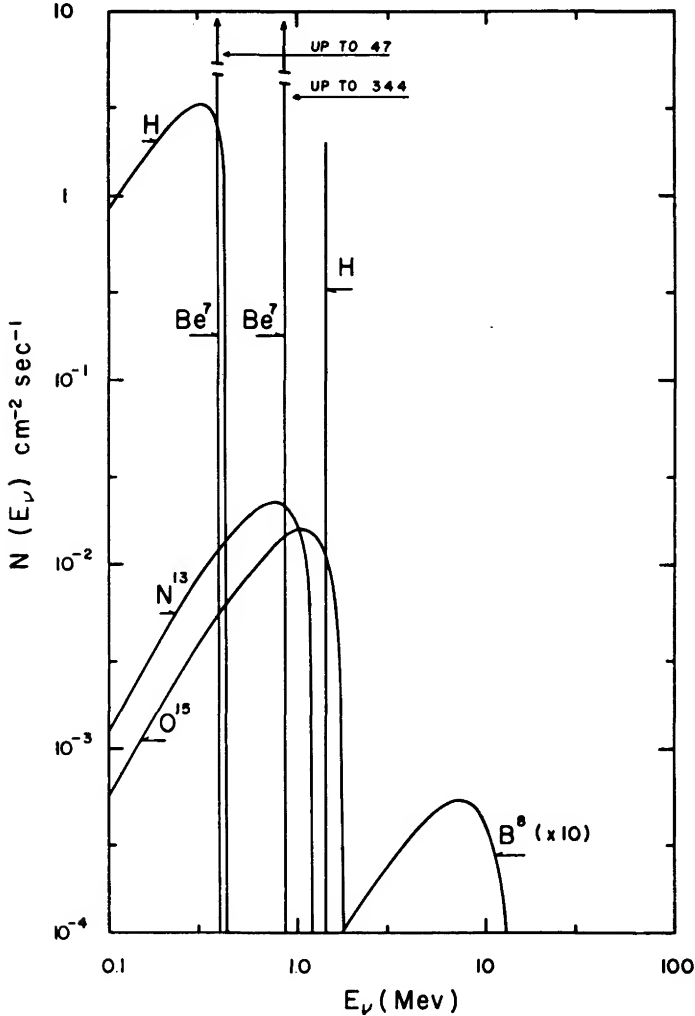
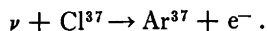


FIG. 16.—Using the energy generation rates quoted in this chapter, a revised solar model has been built, in order to calculate the solar neutrino spectrum. We notice the presence of high and thin lines associated with free electron capture. The width of these lines is about 1 kev ( $\approx kT$ , the thermal energy spread).

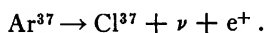
This flux could be detected with present day technology. Plans are already under way for the "Brookhaven Solar Neutrino Observatory."



we shall briefly review the state of affairs in neutrino astronomy. The anti-neutrino was detected some two or three years ago in a famous experiment by Reines and Cowan (1960). Let it be repeated for the sake of completeness that the decay of neutron or neutron-rich isotopes is accompanied by the emission of antineutrinos ( $\bar{\nu}$ ) while the decay of proton (or proton-rich isotopes) is accompanied by neutrinos ( $\nu$ ). In a reactor, the nuclear reactions are sources of abundant fluxes of  $\bar{\nu}$ . Setting a detecting apparatus in a flux of  $\simeq 10^{13} \bar{\nu} \text{ cm}^{-2} \text{ sec}^{-1}$ , the experimenters succeeded in detecting a few  $\bar{\nu}$  every hour. The neutrino ( $\nu$ ) has not yet been detected experimentally. The detection of  $\nu$  is far more difficult than the detection of  $\bar{\nu}$ . Indeed, the fundamental process is now  $n + \nu \rightarrow p + e^-$  instead of  $p + \bar{\nu} \rightarrow n + e^+$ . While the pair ( $n, e^+$ ) is easily identified by the gamma rays it produces, the pair, ( $p, e^-$ ) makes no effect of comparable ease in identification. One technique already used by Dr. Davis (Davis and Harmer, 1959) at Brookhaven is the following: a huge tank is filled with a material containing chlorine isotopes (1000 gallons of  $\text{CCl}_4$ ). A flux of neutrinos may induce the following reaction in the  $\text{Cl}^{37}$  isotope of the material:



The  $\text{Ar}^{37}$  is beta-unstable with a period of 35 days:



So, depending upon the flux, there is an equilibrium concentration of  $\text{Ar}^{37}$  in the tank (a few hundred atoms). To isolate these atoms one bubbles some helium gas through the tank. The argon atoms stick to the helium and the whole is brought to a detection counter. Isotopes of  $\text{Ar}^{37}$  are detected by their beta activity. The number of  $\text{Ar}^{37}$  atoms detected allows us to evaluate:

$$\begin{aligned} & \text{number of } \text{Ar}^{37} \text{ decaying per second} \\ &= \text{number of } \text{Ar}^{37} \text{ formed per second} \\ &= \int \sigma N(E_\nu) c dE_\nu, \end{aligned}$$

where  $\sigma$  is the cross-section for absorption of a neutrino by a  $\text{Cl}^{37}$  atom.

The strongest source of neutrinos which reach the earth is the sun. The sun emits neutrinos almost exclusively. Indeed, the nuclear reactions leading to beta-unstable nuclei are of the ( $p, \gamma$ ) form. They produce proton-rich isotopes which in turn decay to stable isotopes by emitting a neutrino ( $\nu$ ). According to the previous model of the sun, the flux of neutrinos at the earth would be:

$$\int N(E_\nu) c dE_\nu \simeq 6.5 \times 10^{10} \nu \text{ cm}^{-2} \text{ sec}^{-1}.$$

So far, the neutrino detection experiment of Dr. Davis has failed to yield positive results. However, he has obtained an upper experimental limit:  $\int \sigma N dE: < 5 \times 10^{-33}$  captures per second per atom. Such a rate is much more

than the solar model predicts. It is about equal to the rate that would obtain if the PP III process were the only one active. Indeed, the decay of  $B^8$  produces a high energy neutrino ( $E = 7$  Mev). As the capture cross-section varies with  $E^2$ , such a decay has a far better chance to produce a click in Dr. Davis' tank than any other. Dr. Davis plans to do another experiment with a tank of  $10^5$  gallons of  $CCl_4$ . He hopes to detect a flux if as little as 4 per cent of the solar energy comes from PP III. Due to the uncertainties in our knowledge of the solar structure, such a contribution is indeed still quite possible.

This problem was first considered by Marx and Menyhard (1960). Bahcall *et al.* (1963) and Pochoda and Reeves (1964) have made detailed analyses of this question from revised solar models. The detection power of the new apparatus is still too low, by a factor of about ten. However, an increase of  $\Delta T_6 \simeq 3$  in the solar central temperature would bring the flux above threshold. The possibility of such a variation cannot be ruled out at the present time.

Note: Experimental results on the  $Cl^{37}(p, n)Ar^{37}$  have shown that the neutrino capture cross-section is considerably larger than expected. Bahcall (to be published) has re-evaluated the integrated solar neutrino cross-section. The number of counts expected is now far above threshold. Plans are already under way for the "Brookhaven Solar Neutrino Observatory."

It is worth mentioning that if Dr. Davis obtains a positive result, that is, if he actually detects some neutrinos from the sun, he will have given us for the first time a direct proof of the occurrence of nuclear reactions in the stars. He will then have settled definitely an age-old problem: how do the sun and stars generate energy at such a rate during so long a time. Today everybody believes in the nuclear mode of energy generation. At first this particular answer to the problem was accepted because no other one was available. Later, as stellar structures were studied in more detail, it became more and more evident in the light of the physical laws that nuclear reactions must go on inside the stars. The coherence of the whole framework necessitates their occurring. However, all these proofs remain indirect in nature. The clicks in Dr. Davis' tank would put a magnificent end point to our speculations. By the same token the clicks could tell us more about the nature of stellar interiors. One could hope, for instance, that with improved techniques one would eventually, at least grossly, be able to analyze the spectrum. As we have discussed before, the respective shape of its various humps and lines would be a function of the physical conditions in the core.

It is amusing to realize that a star of anti-matter would produce the same spectrum but with antineutrinos ( $\bar{\nu}$ ). The lines identify the hydrogen-burning core, the  $\bar{\nu}$  identify the anti-matter nature of the whole star. Before we finish the subject of the hydrogen-burning stage, it might be worthwhile to consider one interesting corollary. All through the discussion we have neglected the reaction  $He^3 + H^1 \rightarrow Li^4 + \gamma$ ,  $Li^4 \rightarrow He^4 + e^+ + \nu$ . Indeed, there are good reasons for neglecting that reaction;  $Li^4$  is most likely a very unstable nucleus. It would

much sooner break apart than beta decay. All the experimental evidence (analyzed in the light of good theoretical models) points toward the particle-instability of  $\text{Li}^4$  (Bashkin, Kavanagh, and Parker 1959, Imhof *et al.* 1962).

In the chain of events leading to the formation of  $\text{He}^4$  particles the stability of  $\text{Li}^4$  would produce some drastic changes. Because of the difference in Coulomb repulsion, the reaction  $\text{He}^3 + \text{H}^1$  would be thousands of times faster than the  $\text{He}^3 + \text{He}^4$ . The solar energy would then be entirely obtained through that reaction. The crucial point now is that the decay of  $\text{Li}^4$ , leading to  $\text{He}^4$  would be accompanied by a high energy neutrino of maximum energy  $\sim 19$  Mev, mean energy  $\sim 10$  Mev. Since the capture cross-section varies as  $E_\nu^2$ , on the average these neutrinos have twice as large a capture probability as the  $\text{B}^8$  neutrinos. Further, since the average neutrino emission per fusion of four protons into one helium would be larger than in the hypothetical case of pure PP III burning, we should have to assume a higher rate of hydrogen burning to understand the present solar light output. This in turn implies a larger number (flux) of neutrinos.

Such a flux would produce an easily detectable effect in the  $\text{Cl}^{37}$  tank (far above the experimental limit quoted earlier). The absence of such an effect is an astronomical proof of the nuclear instability of  $\text{Li}^4$ .

### 3.6. ENERGY GENERATION FROM THE HYDROGEN-BURNING STAGE

The first three PP cycles are governed by the rate for the proton-proton reaction. The number of reactions per sec per gram of matter is

$$r = (1.0 \pm 0.1) \times 10^{11} f_{1,1} g_{1,1} \rho X_1^2 e^{-33.810 T_6^{-1/3}} / T_6^{2/3}. \quad (3.5)$$

At temperatures below  $T_6 \simeq 8$ , only the two first reactions can come into equilibrium ( $\text{H}^1 + \text{H}^1$  and  $\text{H}^2 + \text{H}^1$ ). Excluding the energy carried by the neutrinos, these two reactions yield together  $Q = 6.675$  Mev ( $1.069 \times 10^{-5}$  ergs). We obtain then for  $T_6 \simeq 8$ :

$$\epsilon = (1.1 \pm 0.1) \times 10^6 f_{1,1} g_{1,1} \rho X_1^2 e^{-33.810 T_6^{-1/3}} / T_6^{2/3}. \quad (3.6)$$

At higher temperatures the  $\text{He}^3$  nuclei can react with themselves (leading to PP I) or with  $\text{He}^4$  (leading to PP II or PP III). PP II will be favored in the region of lower temperatures or of smaller  $\text{He}^4/\text{H}^1$  ratio. Both factors will be found during the early periods of hydrogen burning.

In the case of PP II one needs two  $\text{H}^1 + \text{H}^1$  reactions to form a  $\text{He}^4$  nucleus, hence, the energy production *per proton-proton reaction* is only half of the nuclear energy released by the formation of  $\text{He}^4$ . In other words, although  $Q_I = 26.20$  Mev, we have to use here

$$\epsilon'_I = \frac{1}{2} Q_I r_{1,1} = 2.06 \pm 0.2 \times 10^6 f_{1,1} g_{1,1} \rho X_1^2 e^{-33.810 T^{-1/3}} / T_6^{2/3} \quad (3.7)$$

( $\epsilon'_I$ , we define to be the energy generation rate when  $X_4 = 0$ .) As the temperature increases (and/or the  $\text{He}^4/\text{H}^1$  ratio increases), the PP II and PP III

branches may take over. The competition between these two cycles is tantamount to the competition between  $\text{Be}^7(e^-, \nu)\text{Li}^7$  and  $\text{Be}^7(\text{H}^1, \gamma)\text{B}^8$ . Comparing the reaction rates (see [3.13]) it appears that PP III could predominate only at temperatures above  $T_6 = 20$ . For both processes each  $\text{H}^1 + \text{H}^1$  reaction brings in the whole  $4\text{H}^1 \rightarrow \text{He}^4$  process. Excluding neutrino losses again, we have  $Q_{\text{II}} = 25.67$  Mev and  $Q_{\text{III}} = 19.2$  Mev.

Thanks to the fact that for equilibrium conditions the relative abundances of the various elements involved can be expressed in terms of  $\text{H}^1$  and  $\text{He}^4$ , the contribution from the three first branches can be grouped together in a formula which contains only the fractional densities of  $\text{H}^1$  and  $\text{He}^4$ . Indeed, the rate of energy generation from these proton-proton branches can be written as

$$\rho \epsilon_{\text{PP}} = Q_{\text{I}} N_3^2 \frac{\langle \sigma v \rangle_{3,3}}{2} + Q_{\text{II}} N_7 p_{7+e} + Q_{\text{III}} N_7 N_1 \langle \sigma v \rangle_{7,1} \quad (3.8)$$

while the equilibrium abundance equations give the relation

$$\frac{1}{2} \langle \sigma v \rangle_{1,1} N_1^2 = \langle \sigma v \rangle_{3,3} N_3^2 + \langle \sigma v \rangle_{3,4} N_3 N_4 \quad (3.9)$$

for the equilibrium abundance of  $\text{He}^3$ , and  $\langle \sigma v \rangle_{3,4} N_3 N_4 = \langle \sigma v \rangle_{7,1} N_1 N_7 + N_7 p_{7+e}$  for  $\text{Be}^7$ . We write our result in the form, after Iben (1962),

$$\epsilon_{\text{PP}} = \epsilon'_{\text{I}} \psi_{\text{PP}}(\alpha, W), \quad (3.10)$$

where  $\rho \epsilon'_{\text{I}} = \frac{1}{4} Q_{\text{I}} N_1^2 \langle \sigma v \rangle_{1,1}$  as in (3.7). Then

$$\psi_{\text{PP}}(\alpha, W) = \left[ 1 + \gamma \left( 0.959 - \frac{0.492W}{1+W} \right) \right] \quad (3.11)$$

with the following definitions:

$$\gamma = \left[ \left( 1 + \frac{2}{\alpha} \right)^{1/2} - 1 \right] \alpha; \quad \frac{S_{3,4}^2}{S_{1,1} S_{3,3}} = 5.48 \times 10^{17}; \quad (3.12)$$

$$\alpha = \frac{\langle \sigma v \rangle_{3,4}^2}{\langle \sigma v \rangle_{1,1} \langle \sigma v \rangle_{3,3}} \left( \frac{N_4}{N_1} \right)^2 = \frac{S_{3,4}^2}{S_{1,1} S_{3,3}} e^{-100/T_6^{1/2}} \left( \frac{X_4}{4X_1} \right)^2.$$

The factor  $\alpha/(X_4/4X_1)^2$  has been plotted in Figure 18 and tabulated in Table 8 as a function of temperature. The factor  $\gamma$  varies from zero to one as the temperature increases.

In the last bracket

$$W = \frac{\langle \sigma v \rangle_{7,1} N_1}{p_{7+e}} = 1.22 \times 10^{16} f_{7,1} g_{7,1} e^{-102.6/T_6^{1/2}} (T_6^{-1/6}) (1 + 1/X_1)^{-1} \quad (3.13)$$

represents the influence of PP III (through its high neutrino loss). Again, the contribution from this cycle is always negligible for  $T_6 < 20$  and is usually negligible even for  $T_6 > 20$ , as the C-N cycle becomes dominant. It could become important if the CNO abundance is abnormally low. In Figure 17 we have plotted  $\psi_{\text{PP}}(\alpha, W)$  for two values of the ratio  $X_4/X_1$ .

The contribution from the three branches can be individually calculated from the following expression:

$$\epsilon_{\text{PP}} = \epsilon_{\text{I}} + \epsilon_{\text{II}} + \epsilon_{\text{III}} = \epsilon_{\text{I}}' \left[ (1 - \gamma) + \frac{1.96\gamma}{1+W} + \frac{1.47\gamma W}{1+W} \right]. \quad (3.14)$$

Using now a scheme described in the second section, we write

$$\epsilon_{\text{PP}} = \rho X_1^2 f_{1,1} g_{1,1} \psi_{\text{PP}}(a, W) \epsilon_0 \left( \frac{T}{T_0} \right)^n, \quad (3.15)$$

where  $[f_{1,1} = 1. + 0.25\rho^{1/2}/T_0^{3/2}]$  (the electron screening factor) and  $[g_{1,1} = 1 + 0.012T_0^{1/3} + 0.0078T_0^{2/3} + 0.0006T_0]$  (a correction term) (see Tables 4 and 8).  $\psi(a)$  is defined above with  $a$  plotted in Figure 18.

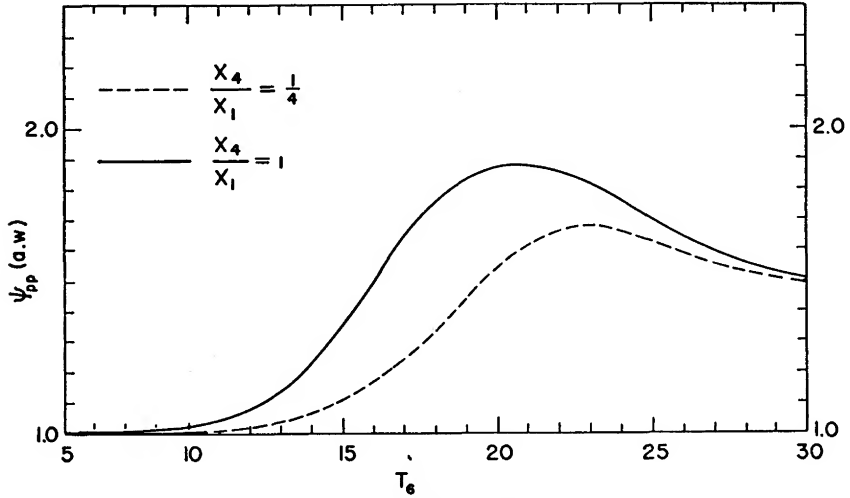


FIG. 17.—Plot of  $\psi_{\text{PP}}(a, W)$  for  $X_4/X_1 = 1$  and  $\frac{1}{4}$

$\psi(a)$  is plotted in Figure 17 for two values of  $(X_4/X_1)$ . In other words,  $\epsilon_0$  becomes the unscreened rate of energy generation at temperature  $T_0$  per unit gram of hydrogen when helium-4 is absent from the core. Then  $n$  is the temperature exponent of the energy generation rate for the three PP branches of hydrogen burning. Although  $f_{1,1}$  and  $g_{1,1}$  and  $\psi_{\text{PP}}(a)$  are functions of the temperature, their effect on the value of  $n$  is negligible.

The fourth PP cycle is governed by the rate of the  $\text{N}^{14} + \text{H}^1$  reaction (the slowest one in the CNO cycle). The number of such reactions per unit gram is

$$r = 1.98 \times 10^{32} f_{14,1} g_{14,1} \rho X_{14} X_1 e^{-152.313/T_0^{1/3}} / T_0^{2/3}. \quad (3.16)$$

The non-neutrino energy release is 25.02 Mev per cycle, hence,

$$\epsilon_{\text{CN}} = (7.94 \pm 0.8) \times 10^{27} f_{14,1} g_{14,1} \rho X_{14} X_1 e^{-152.313/T_0^{1/3}} / T_0^{2/3} \text{ erg/gm/sec.} \quad (3.17)$$

At temperatures below  $T_6 \simeq 16$ , the period of the CNO bi-cycle is too long to let the  $O^{16}$  atoms reach an equilibrium abundance concentration with the rest of the elements of the C-N cycle. In this case, one only needs to consider the abundance of the carbon and nitrogen isotopes in the original stellar gas. Within the rate given here, for temperatures below  $T_6 = 17$ , the equilibrium abundance of  $N^{14}$  will always exceed 99 per cent of  $(X_{CN})$  the original abundance of C and N. Hence, we replace  $X_{14}$  by  $X_{CN}$  in the formula. We write again

$$\epsilon_{CN} = \rho X_1 X_{C-N} f_{1,14} g_{1,14} \epsilon_0 (T/T_0)^n, \quad (3.18)$$

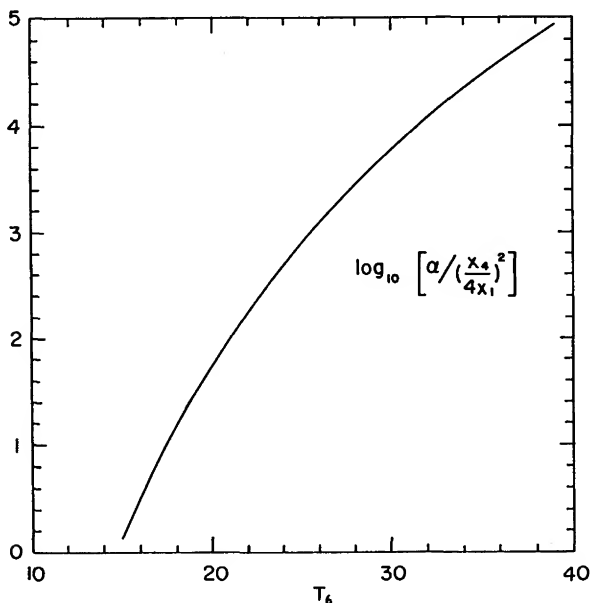


FIG. 18.—Plot of the parameter  $\alpha/(X_4/4X_1)^2$  as a function of  $T_6$

where  $X_{CN}$  is the original abundance of carbon and nitrogen, ( $X_{CN} = X_{14}$ ),  $f_{14,1} = [1. + 1.75\rho^{1/2}/T_6^{3/2}]$ , and  $g_{14,1} = [1. + 0.0027T_6^{1/3} - 0.0037T_6^{2/3} - 0.00007T_6]$ . In Tables 6 and 9 one finds  $g_{14,1}$ ,  $\epsilon_0$ , and  $n$  at various temperatures.

At higher temperatures the bi-cycle is fully active and the  $O^{16}$  isotopes of the original stellar gas participate in the energy generation process. We can express the energy generation rate in terms of the  $(N^{14} + H^1)$  rate and the fractional abundance of carbon, nitrogen, and oxygen together. In this case

$$\epsilon = \epsilon_0 X_{CNO} \rho X_1 (X_{14}/X_{CNO}) f_{14,1} g_{14,1} (T/T_0)^n. \quad (3.19)$$

In Table 9 the values of  $X_{14}/X_{CNO}$  are tabulated. The effect of this quantity on  $n$ , the temperature exponent, is negligible.

The large uncertainty in the rate of  $O^{17} + H^1 \rightarrow N^{14} + He^4$  introduces an uncertainty in the quantity  $X_{14}/X_{CNO}$  and also in the temperature at which

TABLE 8  
ENERGY GENERATION FROM THE PROTON-PROTON BRANCHES

$T_6$	$g_{1,1}$	$\epsilon_0$	$n$	$a/(X_4/4X_1)^2$
1.....	1.02	4.27(-9)	10.61	2.03(-26)
2.....	1.03	2.88(-6)	8.29	1.85(-17)
3.....	1.04	6.53(-5)	7.17	4.22(-13)
4.....	1.04	4.60(-4)	6.46	2.39(-10)
5.....	1.05	1.82(-3)	5.95	2.19(-8)
6.....	1.05	5.18(-3)	5.56	6.88(-7)
7.....	1.06	1.19(-2)	5.26	1.08(-5)
8.....	1.06	2.34(-2)	5.00	1.06(-4)
9.....	1.07	4.16(-2)	4.79	7.23(-4)
10.....	1.07	6.79(-2)	4.60	3.80(-3)
11.....	1.07	1.04(-1)	4.44	1.62(-2)
12.....	1.08	1.52(-1)	4.30	5.87(-2)
13.....	1.08	2.12(-1)	4.17	1.85(-1)
14.....	1.08	2.87(-1)	4.06	5.23(-1)
15.....	1.09	3.77(-1)	3.95	1.34
16.....	1.09	4.83(-1)	3.86	3.18
17.....	1.09	6.07(-1)	3.77	7.04
18.....	1.10	7.49(-1)	3.69	1.47(1)
19.....	1.10	9.09(-1)	3.61	2.90(1)
20.....	1.10	1.09	3.54	5.48(1)
21.....	1.11	1.29	3.48	9.92(1)
22.....	1.11	1.51	3.42	1.73(2)
23.....	1.11	1.75	3.36	2.93(2)
24.....	1.12	2.01	3.30	4.81(2)
25.....	1.12	2.29	3.25	7.68(2)
26.....	1.12	2.59	3.21	1.20(3)
27.....	1.13	2.92	3.16	1.83(3)
28.....	1.13	3.26	3.12	2.73(3)
29.....	1.13	3.63	3.07	4.00(3)
30.....	1.13	4.01	3.03	5.77(3)
31.....	1.14	4.42	3.00	8.19(3)
32.....	1.14	4.85	2.96	1.14(4)
33.....	1.14	5.29	2.93	1.58(4)
34.....	1.14	5.76	2.89	2.15(4)
35.....	1.15	6.25	2.86	2.89(4)
36.....	1.15	6.75	2.83	3.85(4)
37.....	1.15	7.28	2.80	5.07(4)
38.....	1.16	7.82	2.77	6.61(4)
39.....	1.16	8.38	2.74	8.54(4)
40.....	1.16	8.96	2.72	1.09(5)
41.....	1.16	9.56	2.69	1.39(5)
42.....	1.17	1.02(1)	2.67	1.75(5)
43.....	1.17	1.08(1)	2.64	2.20(5)
44.....	1.17	1.15(1)	2.62	2.73(5)
45.....	1.17	1.21(1)	2.60	3.37(5)
46.....	1.18	1.28(1)	2.57	4.14(5)
47.....	1.18	1.35(1)	2.55	5.06(5)
48.....	1.18	1.42(1)	2.53	6.14(5)
49.....	1.18	1.49(1)	2.51	7.41(5)
50.....	1.19	1.57(1)	2.50	8.90(5)
55.....	1.20	1.96(1)	2.40	2.08(6)
60.....	1.21	2.38(1)	2.33	4.41(6)
65.....	1.22	2.84(1)	2.26	8.64(6)
70.....	1.23	3.32(1)	2.19	1.59(7)
75.....	1.24	3.82(1)	2.14	2.75(7)
80.....	1.25	4.34(1)	2.08	4.56(7)
85.....	1.26	4.88(1)	2.04	7.25(7)
90.....	1.27	5.43(1)	1.99	1.11(8)
95.....	1.28	5.99(1)	1.95	1.66(8)
100.....	1.29	6.56(1)	1.92	2.41(8)

TABLE 9  
ENERGY GENERATION FROM THE CNO BI-CYCLE (PP IV)

$T_6$	$g_{14, 1}$	$\epsilon_0$	$n$	$X_{14}/X_{\text{CNO}}$
6.....	0.99	9.45(-10)	27.3	.....
7.....	.99	5.67(-8)	25.9	.....
8.....	.99	1.66(-6)	24.7	.....
9.....	.99	2.87(-5)	23.7	.....
10.....	.99	3.35(-4)	22.9	.....
11.....	.99	2.86(-3)	22.2	.....
12.....	.99	1.91(-2)	21.5	.....
13.....	.98	1.04(-1)	20.9	.....
14.....	.98	4.82(-1)	20.4	0.89
15.....	.98	1.94	19.9	.91
16.....	.98	6.90	19.5	.93
17.....	.98	2.22(+1)	19.1	.95
18.....	.98	6.52(+1)	18.7	.95
19.....	.98	1.77(+2)	18.3	.96
20.....	.98	4.51(+2)	18.0	.96
21.....	.98	1.08(+3)	17.7	.....
22.....	.98	2.44(+3)	17.4	.97
23.....	.98	5.27(+3)	17.2	.....
24.....	.98	1.09(+4)	16.9	.97
25.....	.97	2.16(+4)	16.7	.....
26.....	.97	4.14(+4)	16.4	.97
27.....	.97	7.66(+4)	16.2	.....
28.....	.97	1.38(+5)	16.0	.97
29.....	.97	2.41(+5)	15.8	.....
30.....	.97	4.11(+5)	15.6	.97
31.....	.97	6.85(+5)	15.5	.....
32.....	.97	1.12(+6)	15.3	.....
33.....	.97	1.78(+6)	15.1	.....
34.....	.97	2.79(+6)	15.0	.....
35.....	.97	4.30(+6)	14.8	.....
36.....	.97	6.52(+6)	14.7	.....
37.....	.97	9.73(+6)	14.5	.....
38.....	.96	1.43(+7)	14.4	.....
39.....	.96	2.08(+7)	14.3	.....
40.....	.96	2.98(+7)	14.1	.96
41.....	.96	4.22(+7)	14.0	.....
42.....	.96	5.90(+7)	13.9	.....
43.....	.96	8.18(+7)	13.8	.....
44.....	.96	1.12(+8)	13.7	.....
45.....	.96	1.52(+8)	13.6	.....
46.....	.96	2.05(+8)	13.5	.....
47.....	.96	2.74(+8)	13.4	.....
48.....	.96	3.62(+8)	13.3	.....
49.....	.96	4.76(+8)	13.2	.....
50.....	.96	6.20(+8)	13.1	.95
55.....	.95	2.11(+9)	12.6	.....
60.....	.95	6.24(+9)	12.3	.95
65.....	.95	1.64(+10)	11.9	.....
70.....	.94	3.93(+10)	11.6	.94
75.....	.94	8.66(+10)	11.3	.....
80.....	.94	1.78(+11)	11.1	.93
85.....	.93	3.46(+11)	11.0	.....
90.....	.93	6.39(+11)	10.6	.93
95.....	.93	1.13(+12)	10.4	.....
100.....	0.93	1.91(+12)	10.2	0.92

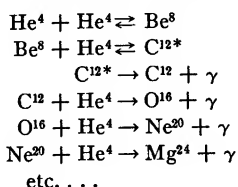


the bi-cycle gets in motion. With the values given in the table the contribution of the bi-cycle is governed by the  $O^{16} + H^1$  rate at all temperatures where the bi-cycle plays any role ( $T_8 > 14$ ). Hence, any increase in the rate of  $O^{17} + H^1$  would be unnoticed as far as energy generation is concerned. On the other hand, a reduction of the rate by a factor of 30 would raise the effective operation of the bi-cycle to  $T_8 = 17$  or 18, and would reduce by a non-negligible amount the fraction  $X_{14}/X_{CNO}$ .

#### § 4. HELIUM-BURNING REACTIONS

The fusion of two helium-4 produces the highly unstable  $Be^8$  nucleus (lifetime  $\simeq 10^{-16}$  sec). In thermal equilibrium a certain concentration of  $Be^8$  is established. A small number of these  $Be^8$  will capture an extra  $He^4$  to form  $C^{12}$  in its second excited state. The  $C^{12}$  may decay to its ground state liberating a gamma ray. After a certain concentration of  $C^{12}$  has been built one may have  $C^{12} + He^4 \rightarrow O^{16} + \gamma$ ,  $O^{16} + He^4 \rightarrow Ne^{20} + \gamma$ , etc. (Table 10). These

TABLE 10  
REACTIONS INVOLVED IN  
HELIUM BURNING



exothermic reactions (mostly the first one, as we shall see later on) are expected to become the source of energy generation when the stellar core reaches temperatures of  $T_8 = 1$  to 3 ( $kT \simeq 10$  to 30 kev).

In this section we shall study in detail the three reactions mentioned above. The parameters for these reactions are given in Table 11. Every resonance level in the range of stellar energies has been represented by a Breit-Wigner one-level cross-section formula (with  $\Gamma_a$ 's and  $\Gamma_\gamma$ 's). The value of  $\langle \sigma v \rangle$  has then been integrated numerically. The rate is well approximated by the resonant and non-resonant rate formulae when the Gamow peak is close or far from the resonance. In the intermediate region, the agreement is not so good. However, since the rates are poorly known anyway, and since analytic approximations are useful for interpolation formulae, we have given such formulae whenever convenient. We have given the rates for temperature up to  $T_8 = 5$ . More complete discussion together with more extensive calculations have appeared in Cartledge, Thibaudau, and Reeves (1963).

At high densities we expect the rate to be accelerated by the effect of electron screening. For the first reaction ( $3a \rightarrow C^{12}$ ) the electron screening acts twice; once for the  $He^4 + He^4$  reaction and then for the  $He^4 + Be^8$  reaction. We

shall consider a gas consisting mostly of  $\text{He}^4$  atoms. According to the degree of degeneracy the value of  $\zeta$  would vary from 1.22 to 1.0. We choose  $\zeta = 1.1$  everywhere. Then

$$\begin{aligned}
 -U_0/kT &\simeq 0.2 Z_1 Z_2 \rho^{1/2} / T_8^{3/2}, & \text{for weak screening;} \\
 &= 2.4 \rho^{1/2} / T_8^{3/2}, & \text{for } 3\alpha \rightarrow \text{C}^{12}; \\
 &= 2.4 \rho^{1/2} / T_8^{3/2}, & \text{for } \text{C}^{12} + \text{He}^4 \rightarrow \text{O}^{16} + \gamma; \\
 &= 3.2 \rho^{1/2} / T_8^{3/2}, & \text{for } \text{O}^{16} + \text{He}^4 \rightarrow \text{Ne}^{20} + \gamma.
 \end{aligned} \quad (4.1)$$

TABLE 11  
PARAMETERS FOR THE HELIUM THERMONUCLEAR REACTIONS

Reaction	$\text{He}^4 + \text{Be}^9 \rightarrow \text{C}^{12} + \gamma$	$\text{He}^4 + \text{C}^{12} \rightarrow \text{O}^{16} + \gamma$	$\text{He}^4 + \text{O}^{16} \rightarrow \text{Ne}^{20} + \gamma$
Reduced Mass $M = (A_1 A_2) / (A_1 + A_2)$ a.m.u. ....	$2.66926 \pm 0.00015$	$3.00242 \pm 0.00008$	$3.20248 \pm 0.00005$
$Z_1 Z_2 \sqrt{M}$ .....	$13.0703 \pm 0.0004$	$20.7930 \pm 0.0003$	$28.6328 \pm 0.0002$
$E_0 / T_8^{2/3} =$ $26.3 (Z_1^2 Z_2^2 M)^{1/3}$ (kev) .	146	199	246
$\Delta E_0 / T_8^{3/8} = 35 (Z_1^2 Z_2^2 M)^{1/6}$ (kev) .....	82	96	107
$B_8 = 9.1527 (Z_1^2 Z_2^2 M)^{1/3}$ ( $B_8 = \tau T_8^{1/3}$ ) .....	$50.786 \pm 0.001$	$69.209 \pm 0.001$	$85.663 \pm 0.001$
$2\pi\eta E^{1/2}$ (kev) = $31.1285 (Z_1^2 Z_2^2 M)^{1/2}$ .	$408.908 \pm 0.048$	$650.52 \pm 0.08$	$895.78 \pm 0.10$
$Q$ value (kev) .....	$7369.5 \pm 1.0$	$7161.54 \pm 0.39$	$4729.98 \pm 0.47$

In massive stars ( $M \gtrsim 2M_\odot$ ) the weak electron screening should apply. In smaller stars, and especially before the helium flash, one may have to consider the strong screening or even the extremely strong screening (pynconuclear reactions) (Cameron 1962).

#### 4.1. HELIUM THERMONUCLEAR REACTIONS

4.1.1.  $3\text{He}^4 \rightarrow \text{C}^{12} + \gamma$ .—As seen from the diagram (Fig. 19) the reaction is expected to be resonant through the  $7.656 \pm 0.0007$  Mev level in  $\text{C}^{12}$ . The energy difference between this level and the masses of three  $\text{He}^4$  has been determined by Cook, Fowler, Lauritsen, and Lauritsen (1957); they find  $372 \pm 4$  kev. Using the tables of USAEC (based on an ensemble of experimental data) one gets  $381 \pm 0.008$  kev. We choose here 375 kev.

As a result of a series of experiments (Alburger 1960, Alburger and Pixley 1960, Alburger 1961, and Ajzenberg-Selove and Stelson 1960), we have the following sets of ratios:  $(\Gamma_e \pm \Gamma) = (6.6 \pm 2.2) \times 10^{-6}$ ,  $(\Gamma_\gamma / \Gamma) = (3.3 \pm 0.9)$

$\times 10^{-4}$ , which yields  $\Gamma_\gamma/\Gamma_{e^\pm} = 50^{+50}_{-25}$ , where  $\Gamma_\gamma$ ,  $\Gamma_{e^\pm}$  and  $\Gamma$  are, respectively, the radiation width to the 4.43 Mev state, the width for pair emission to the ground state and the total width of the 7.656 Mev level. The matrix element (M.E.) for the decay of this level through electron-positron pair emission has been estimated by Fregeau (1956) from an analysis of the inelastic electron scattering. He gets (M.E.) =  $(5.0 \pm 1.2) \times 10^{-26}$  cm<sup>2</sup>. To obtain from this matrix element the pair emission width, one must use a specific model. Using an incompressible liquid drop model of C<sup>12</sup> (Walecka 1962), we obtain (with Fregeau's M.E.)  $\Gamma_{e^\pm} = 4.5 \times 10^{-5}$  ev (this model also predicts M.E., one gets

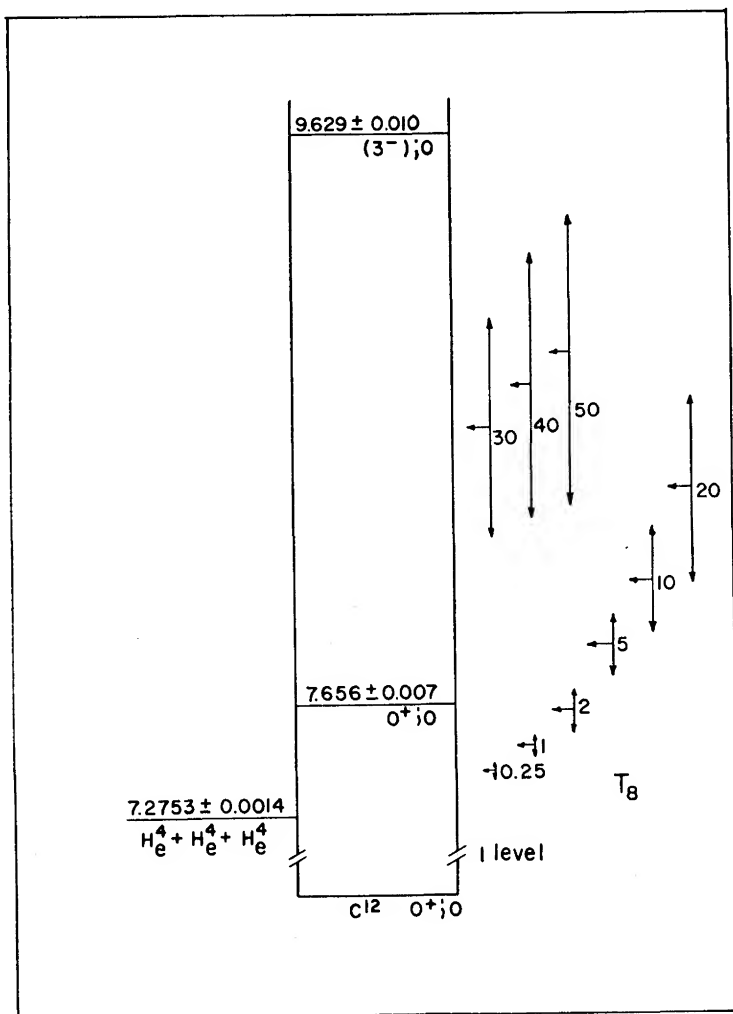


FIG. 19.—Energy diagram of C<sup>12</sup>

M.E. =  $4.2 \times 10^{-26}$  cm<sup>2</sup>). Since this value is model-dependent it cannot be considered very accurate. Dr. L. I. Schiff (private communication) has estimated for it an uncertainty of a factor two.

Using the experimental ratios quoted above, one gets  $\Gamma_\gamma = 2.5 \times 10^{-3}$  ev (within a factor four) and  $\Gamma = 7$  ev (within a factor three). Clearly  $\Gamma \simeq \Gamma_\alpha$  (the alpha particle width). The Wigner-Teichmann limit of  $\Gamma_\alpha$  is 7 ev (using a radius of 5.2 f. for the Be<sup>8</sup> + He<sup>4</sup> system). Hence, the level is almost a pure alpha level. Consequently, the upper limit of 21 ev for  $\Gamma_\alpha$  is rather unlikely as well as the upper limit on  $\Gamma_\gamma$ . The theoretical model of Walecka predicts  $\Gamma_\gamma = 1.0 \times 10^{-2}$  ev. In the view of the present discussion this appears somewhat high. It does seem that his model gives a better estimate of  $\Gamma_{e^\pm}$  than of  $\Gamma_\gamma$ . P. A. Seeger and R. W. Kavanagh (1963) have recently obtained  $(\Gamma_\gamma/\Gamma) = (2.8 \pm 0.3) \times 10^{-4}$ . Their analysis yields  $\Gamma_\gamma = (2.4 \pm 1.5) \times 10^{-3}$  ev.

There is now strong evidence for an assignment of  $J\pi = 3^-$  for the 9.63 Mev level (Bradford and Robson 1961, Carlson 1961). We know also that the alpha width has the value  $\Gamma_\alpha = 30 \pm 8$  kev (Douglas, Broer, Chiba, Herring, and Silverstein 1956); however, the radiation width is unknown. The most likely mode of radiative decay would be by a cascade through the 2<sup>+</sup> first excited state. If the width had an average value for uninhibited electric dipole transitions, then  $\Gamma_\gamma = 2.5$  ev (Carlson 1961); however, this transition would be of the form  $0 \rightarrow 0$  in isotopic spin, so that selection rules will probably reduce the width by an order of magnitude. A calculation of  $\Gamma_\gamma$  has been quoted (Hoyle and Fowler 1960) which shows that an admixture of 4 per cent of the  $T = 1$  level at 17.63 Mev will reduce  $\Gamma_\gamma$  to 0.01 ev. We choose  $\Gamma_\gamma = 0.03$  ev with an uncertainty of about a factor ten either way.

Salpeter (1957) has shown that the resonant contribution from these two levels can be written as

$$P_\alpha = \omega (3)^{5/2} N_4^2 \left( \frac{2\pi\hbar^2}{M_\alpha k T} \right)^3 \left( \frac{\Gamma_\gamma + \Gamma_{e^\pm}}{\hbar} \right) e^{-E_r/kT}, \quad (4.2)$$

where  $M_\alpha$  is the mass of the helium-4 nucleus, and  $\omega$  a statistical factor defined earlier, involving this time the He<sup>4</sup> and the Be<sup>8</sup> nuclei.  $P_\alpha$  is then the rate of destruction of He<sup>4</sup> per alpha particle per second.

With the data given earlier we find

$$\frac{P_\alpha}{(\rho X_4)^2 f_{3\alpha \rightarrow C^{12}}} = \frac{5.92 \times 10^{-7}}{T_8^3} \times 10^{-18.9/T_8} \quad (7.65 \text{ level}) \quad (4.3)$$

within about 60 per cent. The resonant rate from the second level (9.63) is given by

$$\frac{P_\alpha}{(\rho X_4)^2 f_{3\alpha \rightarrow C^{12}}} = \frac{5.0 \times 10^{-5}}{T_8^3} \times 10^{-119.0/T_8}. \quad (4.4)$$

In our range of temperatures ( $T_8 < 6$ ), the first level dominates everywhere. The resonant rate given in (48) is valid for  $T_8 > 0.85$ . At lower temperatures

the rate has been integrated numerically, and the result is given in Table 12. We recall here that  $P_\alpha$  is the rate of destruction of  $\text{He}^4$  per alpha particle per second. The mean rate of formation of  $\text{C}^{12}$  per alpha particle  $P_{3\alpha \rightarrow \text{C}^{12}}$  is three times smaller.

4.1.2.  $\text{C}^{12} + \alpha \rightarrow \text{O}^{16} + \gamma$ .—The level at 7.12 Mev lies 40 kev below the sum of the masses of  $\text{C}^{12} + \text{He}^4$ . Its radiation width is  $6.6 \times 10^{-2}$  ev within 30 per cent (Swann and Metzger 1957, Reibel and Mann 1960).

The value of the alpha width is still unknown. More specifically, we know nothing of the value of  $\theta_\alpha^2$  which measures the overlap of this state with the system of  $\text{C}^{12} + \text{He}^4$ . Statistically, the spectrum of values of  $\theta_\alpha^2$  is distributed between 0.001 and 1 (Roth and Wildermuth 1960). There is some theoretical reason (quoted in Cameron 1958) to believe that this state should have a rather large alpha particle width. We shall choose  $\theta_\alpha^2 = 0.1$  with a possible error of a factor ten each way. The rate has been integrated numerically. The non-resonant approximation comes to within 30 per cent of the computed value everywhere except at the highest temperature,

$$\frac{P_{12,4}(7.12)_{\text{n.r.}}}{(\rho X_4 f_{12,4})} = \frac{4.6 \times 10^3 \times 10^{-(30.05/T_8^{1/4} - \delta)}}{T_8^2 [1 - 4 \times 10^{-3} T_8 + 0.2 T_8^{-2/3}]^2}, \quad (4.5)$$

where  $\delta = 0.06 T_8^{2/3} (1 + 0.07 T_8^{1/3})$ . This rate is uncertain by a factor of about twenty.

The level at 8.88 Mev is a  $2^-$ , hence it cannot contribute to the capture process. The next level at 9.58 Mev has  $\Gamma_\alpha = (0.65 \pm 0.03)$  Mev (Segel, Olness, and Sprenkel 1961). Its radiation width is  $\Gamma_\gamma = 6 \times 10^{-3}$  ev within a factor of about two (Bloom, Toppel, and Wilkinson 1957). The computed rate should be correct within a factor of five:

$$\frac{P_{12,4}(9.58)_r}{(\rho X_4) f_{12,4}} = \frac{4.3 \times 10^3 \times 10^{-122/T_8}}{T_8^{3/2}}. \quad (4.6)$$

The next level ( $2^+$  at 9.84 Mev) has  $\Gamma_\gamma = (2 \pm 1) \times 10^{-2}$  ev (Meads and McIlldowie 1960) and  $\Gamma_\alpha = (7.5 \pm 4) \times 10^2$  ev (Hill 1953). This makes the rate uncertain by less than a factor of two:

$$\frac{P_{12,4}(9.84)_r}{(\rho X_4) f_{12,4}} = \frac{2.35 \times 10^4 \times 10^{-135/T_8}}{T_8^{3/2}}. \quad (4.7)$$

The 7.12 level contribution dominates the rate for  $T_8 < 5$ . The 9.58 level enters the picture at  $T_8 > 5$ , while the 9.85 level comes in only above  $T_8 = 20$  to 30. The total reaction rate (the sum of these contributions) is given in Table 12.

4.1.3.  $\text{O}^{16} + \alpha \rightarrow \text{Ne}^{20} + \gamma$ .—The situation is described in Figure 21. Here we have incorporated the new data from the Chalk River group (Kuehner, Gove, Litherland, Clark, and Almqvist 1961). The  $Q$  value and the various resonance energies are known within about 10 kev. The 4.97 level is a  $(2^-)$ ;

hence not active for  $O^{16}(\alpha, \gamma) Ne^{20}$ . For the 5.64 Mev ( $3^-$ ) level, we have two independent measurements:  $(2l+1)(\Gamma_\alpha \Gamma_\gamma / \Gamma) = 0.003 \pm 0.002$  ev, and  $\Gamma_\gamma / \Gamma = 0.07 \pm 0.01$ . From these we get  $\Gamma_\alpha = 6 \pm 4 \times 10^{-3}$  ev, and  $\Gamma_\gamma = 4 \pm 3 \times 10^{-4}$  ev. For the 5.80 Mev ( $1^-$ ) level we have only one piece of information:  $\Gamma_\gamma / \Gamma < 0.006$ . The single particle limit for  $\Gamma_\alpha$  is 16 ev; the actual  $\Gamma_\alpha$  has been estimated to be about 10 per cent of this value, or  $\Gamma_\alpha \approx 2$  ev. We adopt this value and from the experimental information,  $\Gamma_\gamma / \Gamma_\alpha < 0.006$ , we choose,  $\Gamma_\gamma = 0.01$  ev. Both choices should be valid within factors of 10 either way. The product  $(2l+1) \times (\Gamma_\alpha \Gamma_\gamma / \Gamma)$  should be about 0.03 ev, again within a factor of

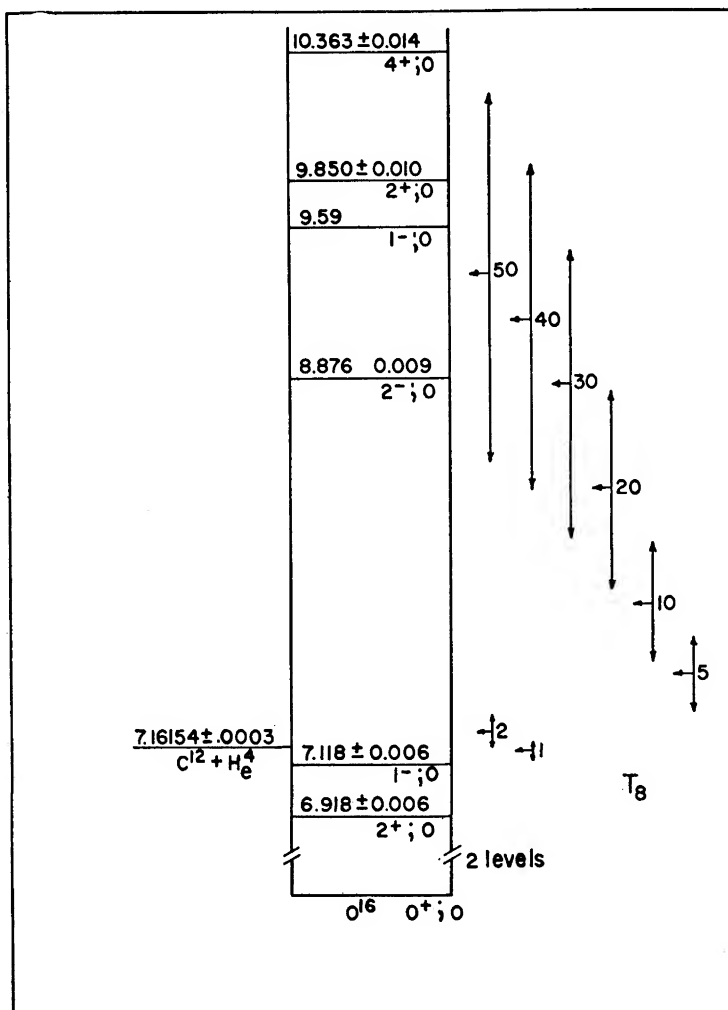


FIG. 20.—Energy diagram of  $O^{16}$

ten. For the 6.75 Mev level the radiation width is not known. On the basis of single particle estimates, we take  $\Gamma_\gamma = 0.1$  ev. The alpha width is 19 kev (J. R. Cameron 1953).

In the range  $1 < T_8 < 2.1$  the total rate comes mostly from the non-resonant contribution of the 5.80 Mev and 6.72 Mev levels;

$$\frac{P_{16,4}(5.8+6.7)_{n.r.}}{(\rho X_4)f_{16,4}} = \frac{4.5 \times 10^9 \times 10^{-37.2/T_8^{1/2}}}{T_8^{2/3}} \quad (\text{within a factor of } 10). \quad (4.8)$$

TABLE 12  
HELIUM-BURNING RATES AND ENERGY GENERATION

$T_8$	$P_{\alpha}/(\rho X_4)^2 f_{3\alpha \rightarrow C^{12}}$	$P_{12,4}/(\rho X_4)f_{12,4}$	$P_{16,4}/(\rho X_4)f_{16,4}$	$\epsilon_0$	$n$
0.7....	7.2(-33)			4.2(-15)	42
0.8....	3.1(-30)			1.8(-12)	49
0.9....	8.1(-28)			4.7(-10)	45
1.0....	7.5(-26)	3.4(-22)		4.4(-8)	41
1.1....	2.9(-24)	3.3(-21)	3.0(-28)	1.7(-6)	37
1.2....	6.1(-23)	2.4(-20)	4.1(-27)	3.6(-5)	33
1.3....	7.8(-22)	1.4(-19)	4.1(-26)	4.6(-4)	31
1.4....	6.8(-21)	6.5(-19)	3.3(-25)	4.0(-3)	29
1.5....	4.4(-20)	2.6(-18)	2.1(-24)	2.6(-2)	26
1.6....	2.2(-19)	9.5(-18)	1.2(-23)	1.3(-1)	24
1.7....	9.2(-19)	3.0(-17)	5.4(-23)	5.4(-1)	23
1.8....	3.2(-18)	8.7(-17)	2.2(-22)	1.9	21
1.9....	9.7(-18)	2.3(-16)	8.4(-22)	5.7	20
2.0....	2.6(-17)	5.8(-16)	2.8(-21)	1.5(1)	19
2.1....	6.4(-17)	1.3(-15)	8.8(-21)	3.7(1)	18
2.2....	1.4(-16)	3.0(-15)	3.0(-20)	8.3(1)	17
2.3....	2.9(-16)	6.2(-15)	2.7(-19)	1.7(2)	16
2.4....	5.7(-16)	1.2(-14)	2.1(-18)	3.3(2)	15
2.5....	1.0(-15)	2.4(-14)	1.3(-17)	6.1(2)	14
2.6....	1.8(-15)	4.4(-14)	7.2(-17)	1.1(3)	14
2.7....	3.0(-15)	7.9(-14)	3.4(-16)	1.8(3)	13
2.8....	4.8(-15)	1.4(-13)	1.5(-15)	2.8(3)	13
2.9....	7.4(-15)	2.3(-13)	5.6(-15)	4.3(3)	12
3.0....	1.1(-14)	3.8(-13)	2.0(-14)	6.4(3)	12
3.1....	1.6(-14)	6.1(-13)	6.3(-14)	9.3(3)	11
3.2....	2.2(-14)	9.6(-13)	1.9(-13)	1.3(4)	11
3.3....	3.1(-14)	1.5(-12)	5.1(-13)	1.8(4)	10
3.4....	4.2(-14)	2.2(-12)	1.3(-12)	2.4(4)	9.8
3.5....	5.5(-14)	3.3(-12)	3.3(-12)	3.2(4)	9.4
3.6....	7.1(-14)	4.9(-12)	7.6(-12)	4.2(4)	9.1
3.7....	9.1(-14)	7.0(-12)	1.7(-11)	5.3(4)	8.8
3.8....	1.1(-13)	1.0(-11)	3.6(-11)	6.7(4)	8.5
3.9....	1.4(-13)	1.4(-11)	7.3(-11)	8.3(4)	8.2
4.0....	1.7(-13)	2.0(-11)	1.4(-10)	1.0(5)	7.9
4.1....	2.1(-13)	2.7(-11)	2.7(-10)	1.2(5)	7.6
4.2....	2.5(-13)	3.6(-11)	4.9(-10)	1.5(5)	7.4
4.3....	3.0(-13)	4.9(-11)	8.8(-10)	1.8(5)	7.1
4.4....	3.5(-13)	6.5(-11)	1.5(-9)	2.1(5)	6.9
4.5....	4.1(-13)	8.5(-11)	2.6(-9)	2.4(5)	6.7
4.6....	4.7(-13)	1.1(-10)	4.2(-9)	2.7(5)	6.5
4.7....	5.4(-13)	1.4(-10)	6.8(-9)	3.2(5)	6.3
4.8....	6.2(-13)	1.9(-10)	1.1(-8)	3.6(5)	6.1
4.9....	7.0(-13)	2.4(-10)	1.7(-8)	4.1(5)	5.9
5.0....	7.9(-13)	3.0(-10)	2.5(-8)	4.6(5)	5.7
		3.8(-10)	3.8(-8)		

For  $2.5 < T_8 < 8$ , the resonant contribution from the 5.64 Mev level dominates;

$$\frac{P_{16,4}(5.64)_r}{\rho X_4} = \frac{6.3 \times 10^2 \times 10^{-45.9/T_8}}{T_8^{3/2}} \quad (\text{within a factor of } 2). \quad (4.9)$$

Above  $T_8 = 8$ , the resonant rate from the 5.80 Mev level takes over;

$$\frac{P_{16,4}(5.80)}{\rho X_4} = \frac{6.3 \times 10^3 \times 10^{-54.4/T_8}}{T_8^{3/2}} \quad (\text{within a factor of } 10). \quad (4.10)$$

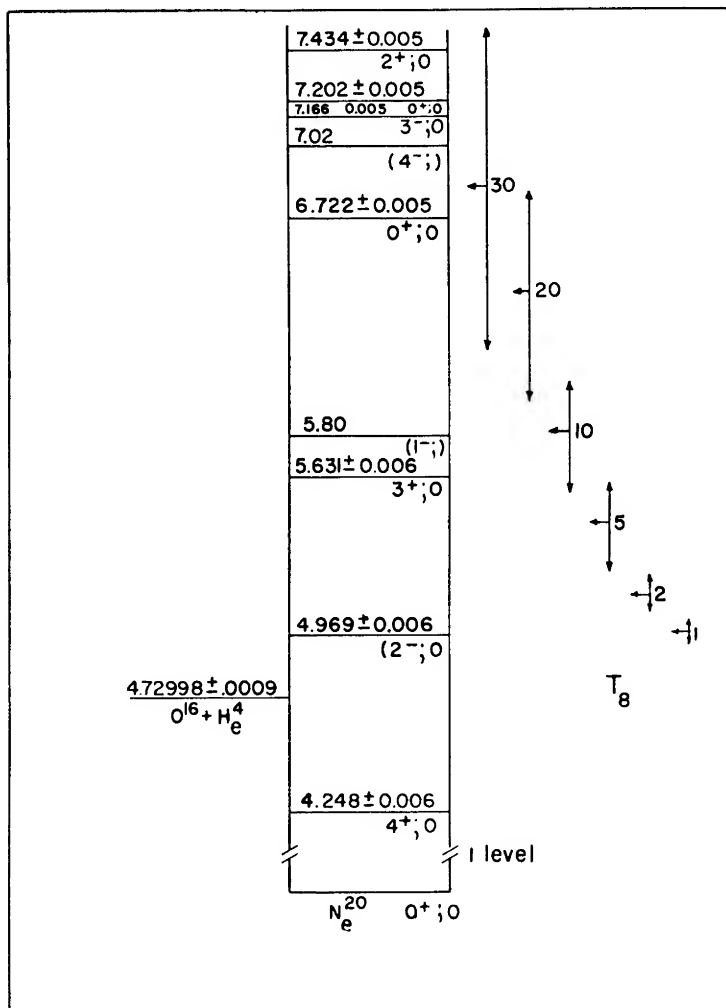


FIG. 21.—Energy diagram of  $\text{Ne}^{20}$



Note: Almqvist and Kuehner (to be published 1965) have obtained new results on this reaction. They give:  $[(2l+1)\Gamma_a\Gamma_\gamma/\Gamma] = (1.0 \pm 0.1) \times 10^{-3}$  ev for the 5.64 Mev level and  $(\Gamma_\gamma/\Gamma) < (3 \times 10^{-4})$  for the 5.80 Mev levels. Consequently, equation (4.8) (unchanged) remains valid in about the same range of temperature while equation (4.9) (with a numerical coefficient of  $(2.1 \pm 0.2) \times 10^3$ ) becomes dominant for  $2 < T_8 < 30$ . The 5.80 level becomes unimportant. The corresponding numbers in Table 12 should be reduced by a factor of three. The curve " $q_{20\rho}$ " in Figure 24 should be brought down by 0.5 units for  $T_8 \geq 2.5$ .

#### 4.2. NUCLEOSYNTHESIS FROM HELIUM-BURNING STAGE

The rate of isotope formation in the helium thermonuclear reactions can be obtained by solving the following equations:

$$\begin{aligned}\frac{dN_{12}}{dt} &= N_4N_8\langle\sigma v\rangle_{4,8} - N_4N_{12}\langle\sigma v\rangle_{4,12}, \\ \frac{dN_{16}}{dt} &= N_4N_{12}\langle\sigma v\rangle_{4,12} - N_4N_{16}\langle\sigma v\rangle_{4,16}, \text{ etc.}, \\ \frac{dN_4}{dt} &= -3N_4N_8\langle\sigma v\rangle_{4,8} - N_4N_{12}\langle\sigma v\rangle_{4,12} - N_4N_{16}\langle\sigma v\rangle_{4,16}, \text{ etc.}\end{aligned}\tag{4.11}$$

From our previous definitions we have

$$\begin{aligned}N_4N_8\langle\sigma v\rangle_{4,8} &= P_{3a \rightarrow C^{12}}N_4 = P_aN_4/3, \\ N_4N_{12}\langle\sigma v\rangle_{4,12} &= P_{12,4}N_{12},\end{aligned}\tag{4.12}$$

together with  $N_{12} = \mathfrak{N}\rho X_{12}/12$ , etc., where  $\mathfrak{N}$  is Avogadro's number. We rewrite these equations in a more convenient form:

$$\begin{aligned}\frac{dX_4}{d\tau} &= -3X_4^3 - \frac{q_{16}X_4X_{12}}{3} - \frac{q_{20}X_4X_{16}}{4} \text{ etc.}, \\ \frac{dX_{12}}{d\tau} &= 3X_4^3 - q_{16}X_4X_{12}, \\ \frac{dX_{16}}{d\tau} &= \frac{4}{3}q_{16}X_4X_{12} - q_{20}X_4X_{16}, \text{ etc.},\end{aligned}\tag{4.13}$$

where

$$\log(q_{16}\rho) = \log \frac{P_{12,4}}{\rho X_4} - \log \frac{P_{3a \rightarrow C^{12}}}{(\rho X_4)^2}.\tag{4.14}$$

Note that  $q_{16}$  is unaffected by electron screening (4.1).

$$\log(q_{20}\rho) = \log \frac{P_{16,4}}{\rho X_4} - \log \frac{P_{3a \rightarrow C^{12}}}{(\rho X_4)^2}.\tag{4.15}$$

The variable  $\tau \equiv [(P_{3\alpha \rightarrow C^{12}})/(X_4)^2]t$  is a convenient time scale. The equations are solved with the assumption that

$$X_4(0) = 1, \quad X_i(0) = 0, \quad \text{all other } i,$$

in other words, a pure helium core.

The behavior of the variables  $X_i$  as a function of  $q$  is depicted in Figure 22. The fractional weight of  $C^{12}$  at the end of the process depends only upon the value of  $q_{16}$ . In the graph we give the final value of  $X_{12}$  as a function of  $q_{16}$ . It

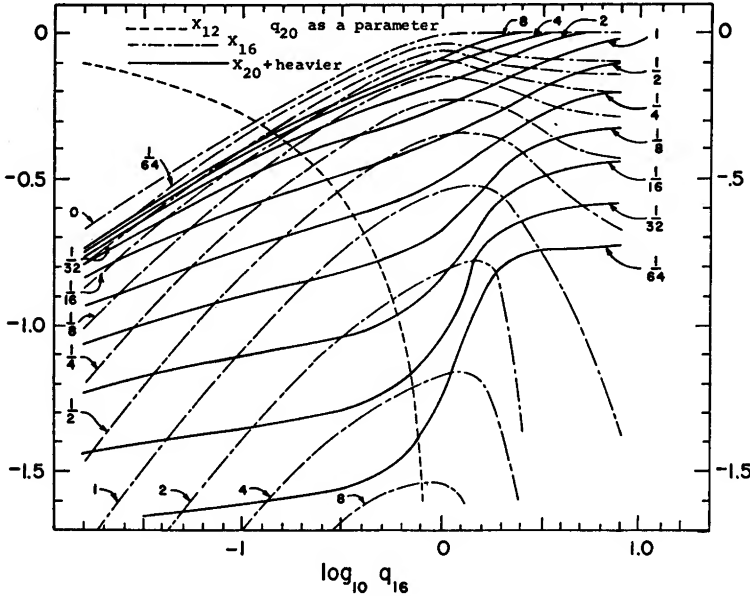


FIG. 22.—Plot of the isotopic abundances at the end of the helium burning

appears that if  $q_{16} > 0.1$ ,  $X_{12} < 0.5$ , and if  $q_{16} > 1.0$ ,  $X_{12}$  is completely negligible. On the same graph we have used  $q_{20}$  as a parameter and studied the effect of a variation in  $q_{16}$ . The combination of  $q_{16}$  and  $q_{20}$  fixes the weight of all the material heavier than  $O^{16}$  ( $Ne^{20}$ ,  $Mg^{24}$ , etc.).

Except for very heavy stars the production of  $Ne^{20}$  and heavier elements ( $Mg^{24}$ ,  $Si^{28}$ , etc.) is negligible. In the foregoing calculations we set  $q_{20} = 0$ . In Figure 23 we have plotted the ratio  $X_{16}/X_{12}$  as a function of  $X_4$ , with  $q_{16}$  as a parameter. Using the fact that  $X_4 + X_{12} + X_{16} = 1$ , one may obtain at any time the abundance of  $X_{12}$  and  $X_{16}$ . This will be useful later when we shall consider over-all energy generation rates.

Using the rate computed previously we have plotted  $\log_{10} (q_{16}\rho)$  and  $\log_{10} (q_{20}\rho)$  as a function of  $T_8$  (Fig. 24). Then from a given set of  $\rho_c$  and  $T_c$  (cen-

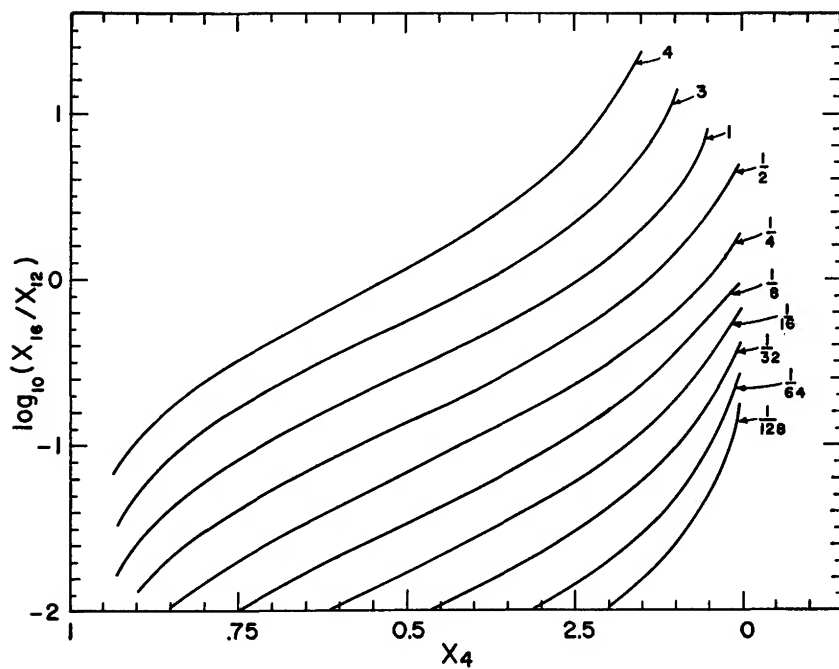


FIG. 23.—Plot of  $X_{16}/X_{12}$  as a function of  $X_4$  for various values of  $q_{16}$

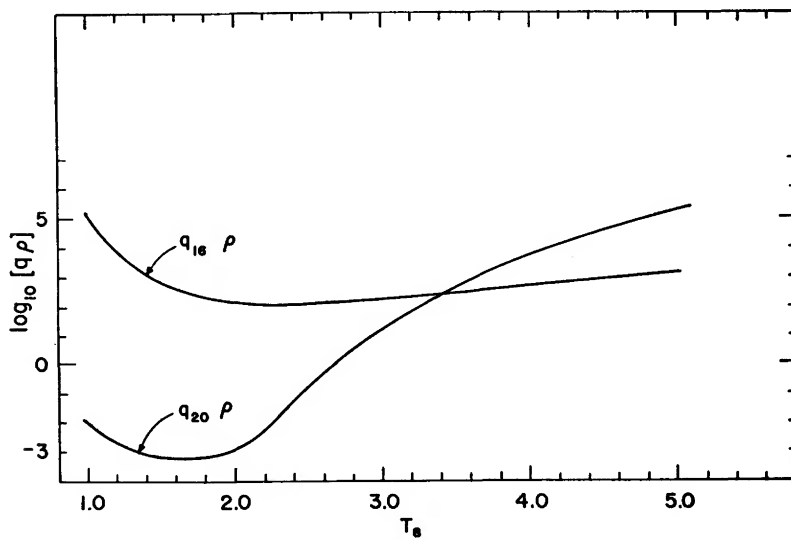


FIG. 24.—Plot of  $q_{16}\rho$  and  $q_{20}\rho$  as a function of  $T_s$

tral density and temperature), one can obtain first  $q_{16}$  and  $q_{20}$  (Fig. 24) and then  $X_{12}$ ,  $X_{16}$ ,  $X_{20}$  (Fig. 22) at the end of the helium-burning process. Although we have made the underlying assumption that  $\rho_c$  and  $T_c$  were remaining constant all through the helium-burning stage, the isotopic abundances obtained should not be badly approximated.

#### 4.3. ENERGY GENERATION FROM THE HELIUM-BURNING STAGE

The rate of energy generation from the helium-burning reactions depends primarily on the rate of the  $3\text{He}^4 \rightarrow \text{C}^{12}$  ( $Q = 7.275$  Mev per reaction). We write the rate of energy production in ergs/gm/sec of the  $3\text{He}^4 \rightarrow \text{C}^{12}$  reaction as

$$\epsilon_{3\alpha \rightarrow \text{C}^{12}} = 1.75 \times 10^{18} P_{3\alpha \rightarrow \text{C}^{12}} X_4 f_{3\alpha \rightarrow \text{C}^{12}}. \quad (4.16)$$

In the resonant range ( $0.85 < T_8 < 50$ ) we have

$$\begin{aligned} \epsilon_{3\alpha \rightarrow \text{C}^{12}} &= 3.46 \times 10^{11} \rho^2 X_4^3 T_8^{-3} (10^{-18.9/T_8}) f_{3\alpha \rightarrow \text{C}^{12}} \\ &= \rho^2 X_4^3 f_{3\alpha \rightarrow \text{C}^{12}} \epsilon_0 (T/T_0)^n. \end{aligned} \quad (4.17)$$

The values of  $\epsilon_0$  and  $n$  are tabulated in Table 12. For  $T_8 > 0.85$ ;  $n = (43.5/T_8) - 3$ . Below that value of  $T$ , the  $n$  were computed by numerical interpolation.

There has recently been some dispute on the correct way of calculating the

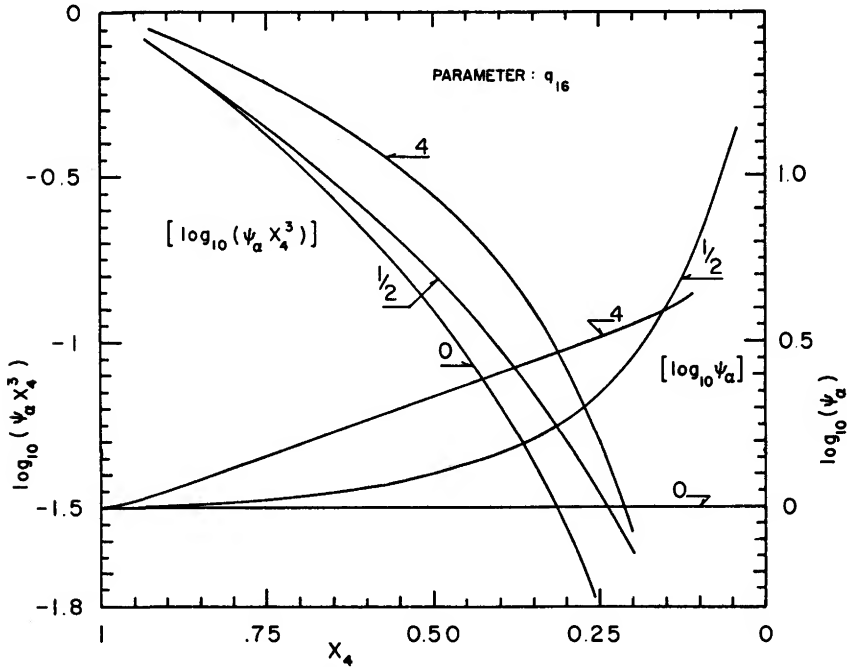


FIG. 25.—Plot of  $\psi_\alpha$  as a function of  $X_4$  and  $q_{16}$

$3\text{He}^4 \rightarrow \text{C}^{12}$  rate. Indeed, the rate as calculated from reaction rate theory seems to be only one-half of the rate obtained from the proper statistical-mechanics arguments. However, as we are dealing with identical particles (bosons here), the cross-section for  $2\text{He}^4 \rightarrow \text{Be}^8$  through even 1 states is twice as large as it would be if the particles were not identical, e.g., the R.H.S. of equation (2.24) should be multiplied by two.

To take into account the contributions of the subsequent reactions we write

$$\epsilon = \epsilon_{3\alpha \rightarrow \text{C}^{12}} \psi_a \quad (4.18)$$

with

$$\psi_a = (1 + 0.33 q_{16} X_4^{-2} X_{12} + 0.15 q_{20} X_4^{-2} X_{16} + \dots). \quad (4.19)$$

In Figure 25 we have plotted the values of  $\psi_a(X_4)$  and  $\psi_a X_4^2$  for various  $q_{16}$ , neglecting again the formation of  $\text{Ne}^{20}$ .

### § 5. SUBSEQUENT BURNING STAGES

After the exhaustion of  $\text{He}^4$ , the least charged nucleus to be found in a stellar core is  $\text{C}^{12}$ . If the temperature keeps on rising, the rate of nuclear reaction between  $\text{C}^{12}$  will become large enough to meet the energy requirements of the star. Approximate models have shown that the consequent carbon-burning stage would take place around  $T_9 = 0.6$  to 1.0. The set of reactions following the initial fusion are described in Table 13.

The next source of energy generation will be either the  $\text{O}^{16} + \text{O}^{16}$  reaction or the photodisintegration of  $\text{Ne}^{20}$  ( $\text{Ne}^{20} + \gamma \rightarrow \text{O}^{16} + \text{He}^4$ ) (followed by the capture of the  $\text{He}^4$ ), depending upon the physical conditions in the stars. The  $\text{Ne}^{20}$  mode will precede the  $\text{O}^{16}$  mode when the densities are low and/or the temperature is high. The same models mentioned before show that stars with less than one solar mass will go through the  $\text{O}^{16}$  stage before the  $\text{Ne}^{20}$  stage. In the range  $1 \lesssim M_\odot \lesssim 4$  the two stages should be about simultaneous (at  $T_9 \simeq 1.2$ ) while more massive stars should see the order reversed. Again it should be repeated that these estimates are approximate.

5.1.1.  $\text{C}^{12} + \text{C}^{12} \rightarrow \text{Mg}^{24*}$ .—The low energy yield of the  $\text{C}^{12} + \text{C}^{12}$  reaction has been studied experimentally by the Chalk River group (Almqvist, Bromley, and Kuehner 1960; Bromley, Kuehner, and Almqvist 1960). The results have been studied by Reeves (1962a) and by Fowler (private communication), with the help of rather different extrapolation methods. The rates obtained are numerically in very good agreement, although the analytic formulation is slightly different. Agreement was reached that Reeves's formula is accurate over a wider range of temperature.

$$\log_{10} \frac{P_{12,12}}{\rho X_{12}} \frac{1}{f_{12,12}} = 27.0 - \frac{36.55}{T_9^{1/3}} (1 + 0.1 T_9)^{1/3} - \frac{2}{3} \log_{10} T_9. \quad (5.1)$$

It is difficult to estimate the accuracy of these rates; although the experimental points were valid within 50 per cent, they were still quite remote from

the energies of astrophysical interests. The extrapolations were not easy since the  $C^{12} + C^{12}$  reaction is a rather complicated process (e.g., exhibiting resonances in the excitation curve). At the lowest temperature ( $T_9 \simeq 0.5$ ) the uncertainty in the rate may reach a factor of ten each way. At higher temperatures ( $T_9 \simeq 1$ ) it is probably less than five. For large densities we must again consider the effect of electron screening ( $f_{12,12} = e^{-U_0/kT}$ ). For weak screening cases we use  $\xi \simeq 1.7$ ; then  $-U_0/kT \simeq 12\rho^{1/2}/T_9^{3/2}$ . When this last quantity is larger than one, we use  $-U_0/kT = 3.5\rho^{1/3}/T_9$  (strong screening).

The  $Q$  value of the  $C^{12} + C^{12}$  reactions brings these particles into a region of the energy diagram of the compound nucleus ( $Mg^{24}$ ) where the levels overlap each other. The experimental branching ratio between the  $Na^{23} + H^1$  mode and the  $Ne^{20} + He^4$  mode is about one-to-one at all measured energies. Comparing the  $Q$  values with the respective Coulomb barrier energies, it seems

TABLE 13  
REACTION INVOLVED IN  $C^{12} + C^{12}$ ,  $O^{16} + O^{16}$   
AND RELEVANT NUCLEAR PARAMETERS

PARAMETERS	REACTIONS	
	$C^{12} + C^{12}$	$O^{16} + O^{16}$
Reduced Mass $M = A_1 A_2 / (A_1 + A_2)$ a.m.u. ....	$6.00191 \pm 0.00007$	$8.00000 \pm 0.00000$
$Z_1 Z_2 \sqrt{M}$ .....	$88.1956 \pm 0.0005$	$181.019 \pm 0.000$
$E_0/T_9^{2/3} = 122 (Z_1^2 Z_2^2 M)^{1/3}$ (kev) .....	2418	3905
$\Delta E_0/T_9^{5/6} = 237 (Z_1^2 Z_2^2 M)^{1/6}$ (kev) .....	1056	1342
$B_9 = 4.248 (Z_1^2 Z_2^2 M)^{1/3}$ .....	$84.175 \pm 0.001$	$135.947 \pm 0.000$
$2\pi\eta E^{1/2}$ (kev) $= 31.285 (Z_1^2 Z_2^2 M)^{1/2}$ .....	$2759.22 \pm 0.01$	$5663.24 \pm 0.00$

TABLE 13—Continued

Reaction	$Q$ Value (kev)
$C^{12} + C^{12} \rightarrow Mg^{24} + \gamma$ .....	$13930.1 \pm 2.2$
$C^{12} + C^{12} \rightarrow Na^{23} + H^1$ .....	$2237.5 \pm 2.0$
$C^{12} + C^{12} \rightarrow Mg^{23} + n$ .....	$-2605 \pm 11$
$C^{12} + C^{12} \rightarrow Ne^{20} + He^4$ .....	$4616.2 \pm 1.1$
$C^{12} + C^{12} \rightarrow O^{16} + He^4 + He^4$ .....	$-113.8 \pm 1.1$
$O^{16} + O^{16} \rightarrow S^{32} + \gamma$ .....	$16538.8 \pm 0.9$
$O^{16} + O^{16} \rightarrow P^{31} + H^1$ .....	$7676.2 \pm 1.5$
$O^{16} + O^{16} \rightarrow S^{31} + n$ .....	$1459 \pm 17$
$O^{16} + O^{16} \rightarrow Si^{28} + He^4$ .....	$9593.1 \pm 3.3$
$O^{16} + O^{16} \rightarrow Mg^{24} + He^4 + He^4$ .....	$-393.0 \pm 2.5$

safe to assume that this ratio is the same in the stellar energy region. In view of its negative  $Q$  value, the branching ratio to  $\text{Mg}^{23} + n$  is negligible. The protons and the alphas released by this reaction will in turn be captured by some of the nuclei in the gas, thereby building some of the isotopes, mainly in the range  $20 < A < 28$ . On the average, the net amount of energy released in each  $\text{C}^{12} + \text{C}^{12}$  collision is about 13 Mev. Hence, we write as before

$$\epsilon_c = 10^{17.7} X_{12} p_{12, 12} = \rho (X_{12})^2 f_{12, 12} \epsilon_0 (T/T_0)^n \text{ erg/gm/sec.} \quad (5.2)$$

In Table 14 values of  $\epsilon_0$  are given, together with  $n$ , the logarithmic derivative.

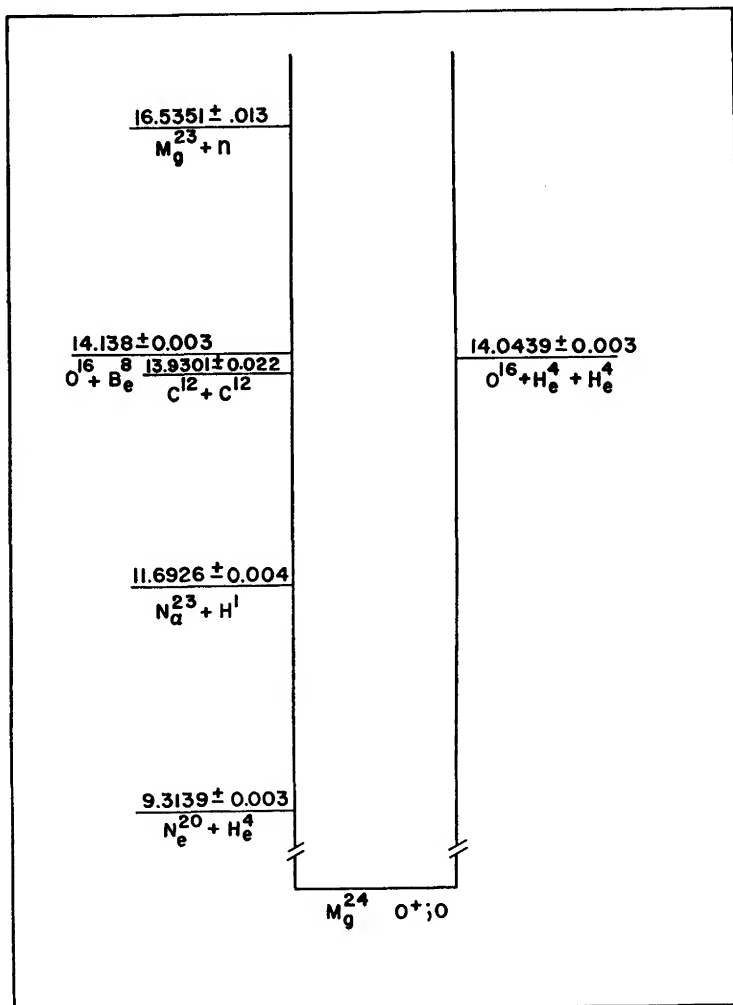


FIG. 26.—Energy diagram of  $\text{Mg}^{24}$

5.1.2.  $C^{12} + O^{16}$ .—Experimental results show that, as expected from Coulomb barrier comparison, this reaction is much slower than  $C^{12} + C^{12}$ . Hence,  $C^{12}$  will be almost completely exhausted before it has a chance to start. It most likely never plays an important astrophysical role so far as energy generation is concerned.

5.1.3.  $O^{16} + O^{16} \rightarrow S^{32*}$ .—Again we have experimental information from the Chalk River group but of much poorer value this time. The yield has been obtained at only one angle, and only the alpha break-up has been studied (Fig. 27). The data have been studied by Reeves (1962*a*) and Fowler (private communication). The rate obtained by Fowler is about ten to twenty times smaller than that obtained by Reeves. Such a difference is within the expected uncertainties since the extrapolation has to be brought quite a long way down. In a

TABLE 14  
ENERGY GENERATION FROM  $C^{12} + C^{12}$ ,  $O^{16} + O^{16}$  AND  $Ne^{20}$

$T_9$	$C^{12} + C^{12}$		$O^{16} + O^{16}$		$Ne^{20} + \gamma$	
	$\epsilon_0$	$\eta$	$\epsilon_0$	$\eta$	$\epsilon_0$	$\eta$
0.4.....	5(−6)	38	.....	.....	.....	.....
0.45.....	3(−4)	36	.....	.....	.....	.....
0.50.....	1(−2)	35	.....	.....	.....	.....
0.55.....	3(−1)	34	.....	.....	.....	.....
0.60.....	5	32	.....	.....	.....	.....
0.65.....	5(1)	32	.....	.....	.....	.....
0.70.....	5(2)	31	.....	.....	.....	.....
0.75.....	4(3)	30	.....	.....	.....	.....
0.80.....	2(4)	29	3(−8)	47	3(−6)	81
0.85.....	1(5)	29	.....	.....	.....	.....
0.90.....	6(5)	28	5(−6)	45	.....	73
0.95.....	3(6)	27	.....	.....	.....	.....
1.0.....	9(6)	27	4(−4)	43	5(1)	65
1.05.....	3(7)	26	.....	.....	.....	.....
1.1.....	1(8)	26	(2−2)	42	2(4)	59
1.15.....	3(8)	25	.....	.....	.....	.....
1.2.....	.....	.....	6(−1)	40	4(6)	54
1.3.....	6(9)	24	1(1)	39	2(8)	50
1.4.....	3(10)	24	2(2)	38	9(9)	47
1.5.....	1(11)	23	2(3)	37	3(11)	44
1.6.....	5(11)	22	2(4)	36	4(12)	41
1.7.....	2(12)	22	1(5)	35	4(13)	38
1.8.....	6(12)	21	7(5)	34	3(14)	36
1.9.....	2(13)	21	4(6)	34	2(15)	34
2.0.....	5(13)	20	2(7)	33	2(16)	33
2.1.....	1(14)	20	7(7)	32	.....	.....
2.2.....	3(14)	20	3(8)	31	.....	.....
2.3.....	6(14)	19	1(9)	31	.....	.....
2.4.....	1(15)	19	3(9)	30	.....	.....
2.5.....	3(15)	19	9(9)	30	.....	.....
2.6.....	5(15)	18	3(10)	29	.....	.....
2.7.....	1(16)	18	7(10)	29	.....	.....
2.8.....	2(16)	18	2(11)	28	.....	.....
2.9.....	3(16)	17	4(11)	28	.....	.....
3.0.....	5(16)	17	1(12)	27	2(21)	22



private discussion it was agreed that Reeves's analysis gave a better fit to the data.

$$\log_{10} \frac{P_{16,16}}{\rho X_{16} f_{16,16}} = 40.5 - \frac{59.02}{T_9^{1/3}} [1 + 0.14 T_9]^{1/3} - \frac{2}{3} \log T_9. \quad (5.3)$$

The weak electron screening factor is  $\exp 25 (\rho^{1/2}/T_6^{3/2})$  and the strong screening factor,  $\exp (6.2 \rho^{1/3}/T_6)$ .

Again the compound nucleus ( $S^{32}$ ) will be formed in a region of excitation energy where the levels are heavily crowded. The proton decay mode has not been studied but it is probably safe to assume a one-to-one ratio between alpha

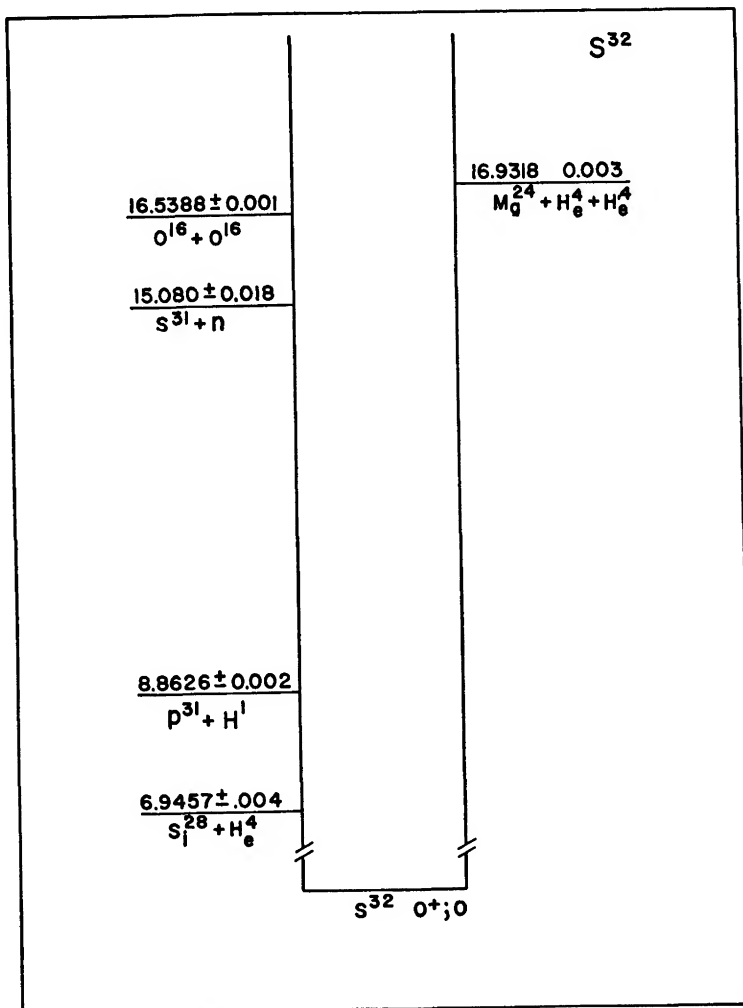


FIG. 27.—Energy diagram of  $S^{32}$

and proton branching ratio. Although the neutrons have a positive  $Q$  value their branching ratio should still be negligible. The mean energy release per  $O^{16} + O^{16}$  reaction is 19 Mev. Hence

$$\epsilon_0 = 10^{17.8} X_{16} P_{16,16} = \rho X_{16}^2 f_{16,16} \epsilon_0 (T/T_0)^n \text{ erg/gm, sec.} \quad (5.4)$$

Values of  $\epsilon_0$ , together with the logarithmic derivative are to be found in Table 14.

5.1.4.  $Ne^{20} + \gamma \rightarrow O^{16} + He^4$ .—The experimental situation has been analyzed in the section on helium thermonuclear reactions. The rate of photodisintegration from the level at 5.64 Mev is

$$\log_{10} P_{20 \rightarrow 16+4}(5.64) = 12.7 \left( \begin{smallmatrix} +0.2 \\ -0.5 \end{smallmatrix} \right) - \frac{28.4}{T_9} \quad (5.5)$$

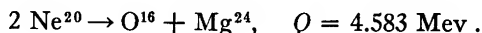
while the level at 5.80 gives

$$\log_{10} P_{20 \rightarrow 16+4}(5.81) \simeq 13.40 - \frac{29.3}{T_9} \quad (\text{within a factor of } 10). \quad (5.6)$$

Below  $T_9 = 1.3$ , the 5.64 Mev level dominates the rate while in the region from 1.3 to 2.0, they become very similar. The total rate is given in Table 14. The uncertainty is about a factor three in the low temperature range and (due to the uncertainty in the second level) grows to about a factor of five in the higher temperature range. The effect of electron screening is negligible.

Note: With the new measurements reported in § 4.1.3, the R.H.S. of equation (5.5) becomes  $(12.15 \pm 0.05) - 28.4/T_9$ . This contribution to the total photodisintegration rate becomes dominant up to  $T_9 = 3$  or 4. The contribution of the next level (eq. [5.6]) should be reduced by a factor of twenty and hence becomes unimportant. All the numbers in the next to last column in Table 14 should be decreased by three.

The alpha coming out could be captured by some of the constituents of the gas ( $O^{16}$ ,  $Ne^{20}$ ,  $Mg^{25}$  are probably the best represented isotopes at this point in the game). Of these  $Ne^{20}$  has by far the largest cross-section (by a factor of about ten). Hence, the most frequent set of reactions will be represented by



The two reactions involved will almost always be in equilibrium, hence, the energy generation rate will be given by the photodisintegration rate

$$\epsilon_{Ne} = 10^{17.13} (P_{20 \rightarrow 16+4}) X_{20} = X_{20} \epsilon_0 (T/T_0)^n. \quad (5.7)$$

The values of  $\epsilon_0$  and  $n$  are given in Table 14.

The carbon-burning stage generates elements in the range  $A = 20$  to 27. Detailed calculations indicate that  $Ne^{20}$  would retain its preponderance over its neighbors, but it is doubtful whether  $Mg^{24}$  would be much more abundant than  $Mg^{25}$  or  $Mg^{26}$ . Neon burning, on the other hand, would be an important source of  $Mg^{24}$ , most likely the dominant one. Oxygen burning is responsible

for the isotopes in the range  $A = 25-32$ , with a strong peak at  $\text{Si}^{28}$ , most likely strong enough to make it preponderant over the background of the isotope-curve. It does seem, then, that the alpha process of Burbidge, Burbidge, Fowler, and Hoyle (1957) could be responsible for isotopes 36-46 but may not be the main source of the isotopes 24, 28, and 32.

Carbon burning gives rise to a neutron flux which is strong enough to produce large amounts of metals in over-abundance. Such a process could be an important mechanism for heavy-nuclei building (Cameron 1959*a*, Reeves and Salpeter 1959, Reeves 1960, Tsuda 1963).

## § 6. NEUTRINOS IN THE LATE STAGES OF STELLAR EVOLUTION

### 6.1. NEUTRINOS FROM THE URCA PROCESS

One factor which will play an ever more important role in the energy balance of stars is the emission of neutrinos. As we saw before, in the hydrogen-burning

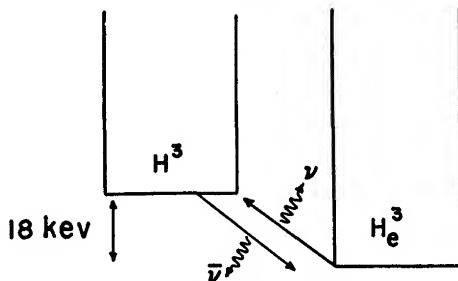


FIG. 28.—Ordinary Urca process

phase, at most ten per cent of the energy was carried away by neutrinos. In the helium-burning reactions no neutrinos were emitted accompanying the formation of carbon, oxygen, or neon. However, another mechanism was becoming increasingly operant, the so-called Urca process of Gamow and Schoenberg (1941). One isotope of the gas can capture an electron and decay into a new isotope with the emission of an antineutrino. The new isotope is unstable and would soon beta decay to the original nucleus with the emission of a neutrino, and the process could start again. At every round of the game the star loses a pair of neutrino-antineutrinos. Such a process represents a leak through which the star could in principle lose energy at a very high rate. In reality the energy loss depends on the electron capture rate, hence, on the temperature and also on the actual isotopic abundances of the gas. More exactly it depends to a very high degree on the presence of some special nuclei which differ very little in mass from another (unstable) nucleus into which they can be transformed by a weak interaction. In that case an electron of very small energy could generate the transformation. Since low energy electrons are well represented in a Maxwell-Boltzmann or Fermi distribution, the rate would be correspondingly higher. In Figure 28 we have described the best Urca nucleus ( $\text{He}^3$ ). The mass differ-

ence between a tritium nucleus plus an electron and a helium nucleus is only 18 kev. At a temperature of  $T_8 = 1$  the value of  $kT$  is  $\sim 9$  kev, hence, the mean kinetic energy is about 14 kev. Other privileged nuclei are  $N^{14}$  (150 kev),  $S^{33}$  (249 kev) and  $Cl^{35}$  (167 kev). Unfortunately, at the temperatures where the process could become important  $He^3$  has completely disappeared and the  $C^{14}$  formed by electron capture on  $N^{14}$  decays too slowly back to the original state (lifetime of 5600 years). The stellar abundance of  $Cl^{35}$  and  $S^{33}$  is not known, but these isotopes could well catalyze a large production of neutrinos shortly after the end of the helium-burning stage.

These neutrino producing processes can be further enhanced by the stellar heat. Consider a beta-unstable nucleus, newly formed, e.g., by the Urca process, waiting for its lifetime to run out. By a thermal collision it can be excited in a

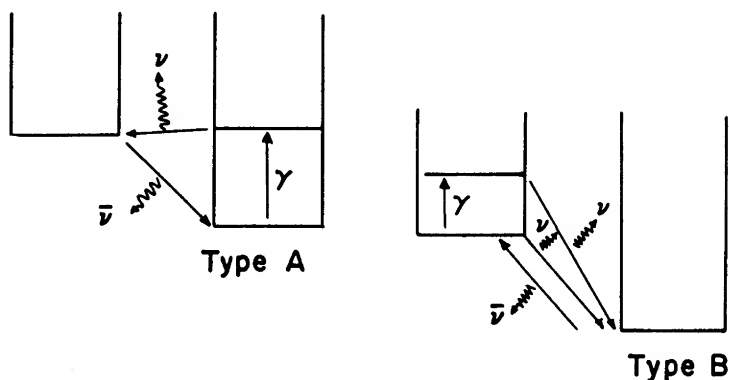


FIG. 29.—Enhanced Urca process

higher state, out of which it can beta decay back directly to the original nucleus possibly with a much reduced lifetime, thereby decreasing the period of the cycle and increasing its energy output (see Fig. 29). Consider next a nucleus which has a beta-stable ground state but a low energy beta-unstable excited state. From Figure 29 it is easy to see how such a nucleus could itself participate in the process under investigation.

Chiu (1961*a*) gives a table illustrating the Urca energy loss for various elements. The rate of energy loss in ergs per gram per sec, in a gas entirely made of a given element  $i$  (i.e.,  $X_i = 1$ ), is given at various temperatures. In this work, Chiu had not considered the possible enhancement of the Urca process. Hence, the rate of energy loss becomes "saturated" when the time for electron capture becomes much smaller than the time for beta decay. The enhancement of the Urca process (the photo-beta reaction) is treated by Cameron (1959*a*). He shows that the lifetime of certain beta-decaying nuclei can be shortened by several orders of magnitude, thereby postponing the onset of saturation.

In the next section we shall describe other modes of neutrino emission. The modes turn out to be much more important than the Urca process for just about

any realistic conditions of temperature, density, and chemical composition. However, as it turns out that there is still a slight aura of doubt surrounding the existence of the newly discovered neutrino processes, the Urca process should be kept in the background.

## 6.2. NEUTRINOS FROM WEAK INTERACTION PROCESSES

Experiments in recent years have called for a revision of the classical beta-decay theory. A new formalism has been put forward by a number of theorists, in particular by Feynman and Gell-Mann (1958). The form of the theory suggests the possibility of a direct interaction between electrons and neutrinos even in the absence of nucleons (Pontecorvo 1959). Indeed, in this theory (called the universal Fermi interaction), the transition amplitude is written down as

$$J = (e, \nu_e) + (p, \bar{n}) + (\mu, \nu_\mu). \quad (6.1)$$

In the language of quantum mechanics, this means that the transition probability formula,  $P = J^*J$ , should describe all the processes made possible by the weak interaction. In other words, we should observe in nature the processes  $(\nu_e, \bar{e})$   $(e, \bar{\nu}_e)$ ,  $(\mu, \bar{\mu})$   $(e, \bar{\nu}_e)$ ,  $(\nu_\mu, \bar{\mu})$   $(p, \bar{n})$ , etc. And with due regard to kinetic variables, the probability of each such process should be the same.

So far in laboratories, only the cross term  $(n, \bar{p})$   $(e, \bar{\nu}_e)$  (for instance,  $n \rightarrow p + e^- + \bar{\nu}$ , the decay of the neutron),  $(\bar{\nu}_\mu, \mu)$   $(e, \bar{\nu}_e)$  (i.e.,  $\mu \rightarrow e + \nu_e + \nu_\mu$ , the decay of the muon), and  $(n, \bar{p})$   $(\mu, \bar{\nu}_\mu)$  (i.e.,  $p + \bar{\mu} \rightarrow n + \nu_\mu$ , the muon capture) have been observed. Their transition probabilities are as predicted by the theory. None of the square terms has been observed, which, indeed, is not a drawback for the theory; their cross-sections are too small for present technologies.

We shall assume that these square terms represent real physical processes. Such an assumption is most probably correct, although it is not easy to evaluate its degree of validity. Later we shall discuss how a confirmation of its validity may actually come from astrophysical observations.

In particular, we concentrate our attention on the first square terms, i.e., we assume the existence of a direct weak interaction between electrons and neutrinos. We consider two different groups of processes; group A involves the fundamental process

$$e^- \rightarrow e^- + \nu + \bar{\nu}. \quad (A)$$

From energy momentum considerations this process will always require another particle. We shall have

$$\gamma + e^- \rightarrow e^- + \nu + \bar{\nu}, \quad (\text{photoneutrinos}), \quad (A1)$$

$$e^- + e^- \rightarrow e^- + e^- + \nu + \bar{\nu}, \quad (A2)$$

$$e^- + (Z, A) \rightarrow e^- + (Z; A) + \nu + \bar{\nu}, \quad (\text{bremsstrahlung}). \quad (A3)$$

The second group (B) involves the reaction

$$e^- + e^+ \rightarrow \nu + \bar{\nu} \quad (\text{actually or virtually}), \quad (\text{B})$$

$$e^- + e^+ \rightarrow \nu + \bar{\nu} \quad (\text{pair annihilation, neutrinos}), \quad (\text{B1})$$

$$\gamma + \gamma \rightarrow (e^+ + e^-) \rightarrow \nu + \bar{\nu}, \quad (\text{B2})$$

$$\gamma + \gamma \rightarrow (e^+ + e^-) \rightarrow \gamma + \nu + \bar{\nu}, \quad (\text{B3})$$

$$\gamma + (Z, A) \rightarrow (Z, A) + \nu + \bar{\nu}, \quad (\text{B4})$$

$$\text{plasmon} \rightarrow \nu + \bar{\nu}. \quad (\text{B5})$$

The process (B2) is absent if the weak interaction is a local interaction and if there is no intermediate boson (Gell-Mann 1961). Even if the intermediate boson exists the cross-section is expected to be vanishingly small. We shall not consider it.

The rates for the processes (A1), (A3), (B1), (B4), and (B5) have been computed (Chiu and Stabler 1961, Ritus 1962, Gandel'man and Pinaev 1960, Chiu 1960*b*, Matinyan and Tsilosani 1962, Adams, Ruderman, and Woo 1962, Levine 1963). (A2) is presently being computed; preliminary results show that it is of less importance than the other processes. (B3) has been evaluated approximately (Chiu and Morrison 1960). It also seems to be of less importance. Of course, these rates are functions of the density and the temperature. For astrophysical discussion we shall consider the region of the  $\rho$ - $T$  plane defined by the following inequalities:

$$10^2 < \rho < 10^8 \text{ gr/cm}^3, \\ 1 < T_8 < 50.$$

At such temperatures all the stellar constituents have atomic numbers equal to or larger than four. Hence, we have  $A/Z \simeq 2$ . So the mean number of nucleons per electron is  $\mu_e \simeq 2$ . However, if the temperature is high enough, electron-positron pairs will be created, which should be taken into account. Then  $\mu_e$  should be computed by proper statistical consideration. (See, e.g., Levine 1963; Landau and Lifschitz 1958.)

In this range, three main processes are dominant: (A1), (B1), and (B5). In Figure 30 their respective domains are roughly delineated. (B5) (plasma neutrinos) takes over the low  $T$ -high  $\rho$  part of the range; it is far less affected by the onset of degeneracy than any of the other processes. This process can be described as resulting from the interaction of electromagnetic waves with an ionized gas. The coupled system then has a normal mode (plasmon) whose frequency  $\omega_p$  is greater than  $(2\pi/\lambda)c$  where  $\lambda$  is the wavelength, i.e., it acts like a particle with non-zero mass. In particular it can decay into a  $\nu$ - $\bar{\nu}$  pair with energy-momentum conservation. Although neutrinos are generated by the action of both transverse and longitudinal electromagnetic waves, the first type is more effective in our range of physical conditions.

The computation of the rate is too involved to be repeated here. We shall merely quote the results together with some useful approximations. One important parameter is  $\omega_p$ , the natural frequency of the plasma. For a completely degenerate gas

$$\left(\frac{\hbar\omega_p}{m_e c^2}\right)^2 \simeq \frac{4a x_f^3}{3\pi(1+X^2)^{1/2}} \quad (6.2)$$

where  $x_f$  is the Fermi momentum in units of  $m_e c[x_f^3 \simeq 1.02 \times 10^{-6}(\rho/\mu_e)]$ , and  $a$  is the fine structure constant. Numerically

$$\frac{\hbar\omega_p}{m_e c^2} = 5.62 \times 10^{-5} \left(\frac{\rho}{\mu_e}\right)^{1/2} \left[1 + 1.01 \times 10^{-4} \left(\frac{\rho}{\mu_e}\right)^{2/3}\right]^{-1/4}. \quad (6.3)$$

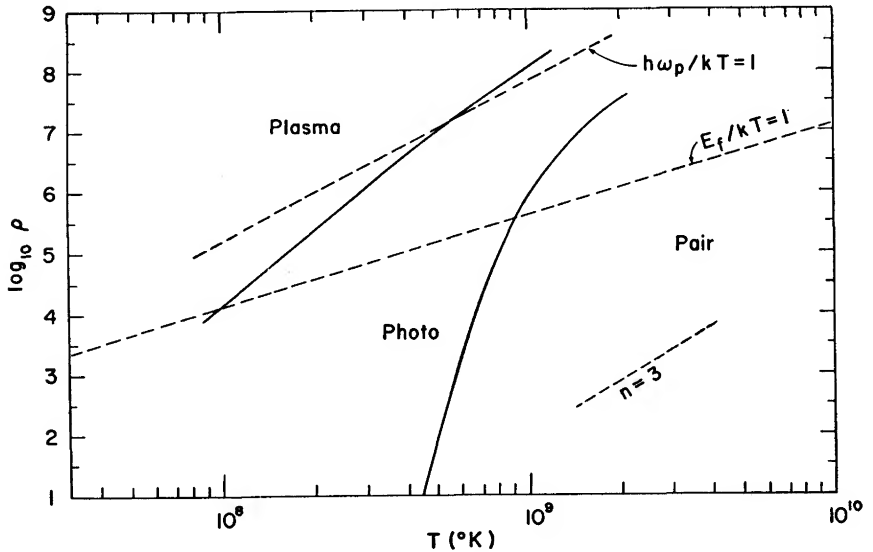


FIG. 30.—Respective domains of the various neutrino processes. On the same graph are shown the lines  $\hbar\omega_p/kT = 1$ ,  $E_f/kT = 1$  (bordering the region of degeneracy) and the slope of the  $\rho \propto T^3$  function applicable to the interior of an  $n = 3$  polytropic model.

We shall also use

$$\frac{\hbar\omega_p}{kT} = \frac{3.34 \times 10^{-4}}{T_9} \left(\frac{\rho}{\mu_e}\right)^{1/2} \left[1 + 1.01 \times 10^{-4} \left(\frac{\rho}{\mu_e}\right)^{2/3}\right]^{-1/4} \quad (6.4)$$

and  $(kT/m_e c^2) = 0.169 T_9$ .

For  $T_9 < 5$  the plasma frequency is quite insensitive to the temperature; accordingly these formulas remain approximately valid even in partially degenerate gases. The rate is given by

$$\epsilon_{B5}^{\nu} = \frac{2.96 \times 10^{22}}{\rho} \left(\frac{\hbar\omega_p}{m_e c^2}\right)^6 \left(\frac{kT}{m_e c^2}\right)^3 \text{ ergs/gm/sec for } \frac{\hbar\omega_p}{kT} \ll 1, \quad (6.5)$$

and

$$\epsilon_{B5}^{\nu} = \frac{1.54 \times 10^{22}}{\rho} \left( \frac{\hbar \omega_p}{m_e c^2} \right)^{7.5} \left( \frac{kT}{m_e c^2} \right)^{1.5} \exp \left( -\frac{\hbar \omega_p}{kT} \right) \text{ ergs/gm/sec, (6.6)}$$

for  $\hbar \omega_p/kT \gg 1$  (see Fig. 30). The intermediate region has not been investigated adequately. However a first approximation can be obtained by a smooth joining of the curves. Numerically we get

$$\epsilon_{B5}^{\nu} = \frac{5.55 \times 10^{-7} \rho^{2/3} T_9^3}{[1 + 0.63 \times 10^{-4} \rho^{2/3}]^{3/2}} \quad \text{for } \frac{\hbar \omega_p}{kT} \ll 1; \quad (6.7)$$

$$\epsilon_{B5}^{\nu} = \frac{10^{-12} \rho^{2.75} T_9^{1.5} e^{-\hbar \omega_p/kT}}{[1 + 0.63 \times 10^{-4} \rho^{2/3}]^{15/8}} \quad \text{for } \frac{\hbar \omega_p}{kT} \gg 1. \quad (6.8)$$

The temperature exponent  $n$  is always small. It has the value  $n = 3$  in the region  $\hbar \omega_p/kT < 1$ , while in the region  $\hbar \omega_p/kT > 1$  it gets slightly larger. Only for extreme conditions such as  $T_9 < 0.2$ ,  $\rho > 10^8$  does it ever reach values larger than five or six.

Next we have to investigate the photoneutrino mechanism. The probability of the photoneutrino process depends linearly on the density of the electron gas (provided the electrons are non-degenerate). It depends very strongly on the temperature, since both the density of the photon gas and the phase space available to the outgoing neutrinos are rapidly increasing with the temperature.

The detailed calculation is too complicated to be reproduced here. We shall only quote a result valid in the non-degenerate non-relativistic range. We define  $\epsilon_{A1}^{\nu}$  as the rate of neutrino energy generation per gram per sec from photoneutrino processes. Then

$$\epsilon_{A1}^{\nu} = \frac{10^8 T_9^8}{\mu_e} \text{ erg/gm/sec.} \quad (6.9)$$

Because of the definition of  $\epsilon_{A1}^{\nu}$  we expect this quantity to be independent of the density. In Table 15 values of  $\epsilon_{A1}^{\nu}$  are given for several temperatures at which the photoneutrino rate may dominate over the pair annihilation process (if the density is high enough). The effect of degeneracy would be to reduce the rate. Indeed, in the process (A1) the electron is expected to change its momentum and hence its cell of momentum space. Degeneracy, however, implies that very few cells are still available, except at higher energies. This reduces considerably the total probability of a reaction. Indeed, computations show this effect. However, some discrepancies have recently appeared between different computations, so that the results cannot be used at the present time. A recalculation is being made and should soon be available.

The third process of importance is the pair annihilation neutrino process (B1). It owes its presence to the existence of electron-positron pairs in the gas. These pairs are themselves created by the gamma rays populating the high energy tail of the black body radiation. As the temperature is increased, the



number of these photons increases enormously ( $\sim T^3$ ) and so does the equilibrium concentration of the positron-electron gas. A small fraction of the ensuing recombination results in the neutrino-antineutrino pairs

$$\gamma + \gamma \rightarrow (e^+ + e^-) \rightarrow \nu + \bar{\nu}.$$

In a vacuum, the neutrino energy output *per unit volume* would be a function of the temperature *only* (since the population of photons is a function of  $T$  only) and, again, a very steep function for reasons similar to those given in the discussion of the (A1) process.

We shall derive approximately (Chiu and Morrison 1960) the expression for  $\epsilon_{B1}$  as this derivation illustrates the nature of the processes involved. For electrons of energies less than  $m_e c^2$  (0.5 Mev) the probability of the reaction

TABLE 15  
NON-DEGENERATE NEUTRINO RATES

$T_e$	PHOTO $\log_{10}(\epsilon_{A1})$ (with $\mu_e = 2$ )	PAIR		RANGE [ $\log \rho <$ ]	$T_e$	PHOTO $\log_{10}(\epsilon_{A1})$ (with $\mu_e = 2$ )	PAIR		RANGE [ $\log \rho <$ ]
		$\log_{10}(\rho \epsilon_{B1})$	$n$				$\log_{10}(\rho \epsilon_{B1})$	$n$	
0.2.....	2.1	.....	.....	4.6	1.4.....	8.9	16.1	13	6.0
0.3.....	3.5	.....	.....	4.8	1.6.....	9.3	16.8	12	6.4
0.4.....	4.5	4.70	32	5.0	1.8.....	.....	17.4	11	.....
0.5.....	5.3	7.7	27	5.2	2.0.....	.....	17.9	.....	6.8
0.6.....	5.9	9.7	23	5.4	2.5.....	.....	19.0	.....	7.0
0.7.....	6.5	11.2	20	5.4	3.0.....	.....	19.7	.....	7.5
0.8.....	6.9	12.3	18	5.6	3.5.....	.....	20.4	.....	.....
0.9.....	7.3	13.2	16	5.6	4.0.....	.....	21.0	.....	.....
1.0.....	7.7	14.0	15	5.6	5.0.....	.....	21.9	.....	.....
1.2.....	8.3	15.2	14	5.8	6.0.....	.....	22.6	.....	.....

$e^+ + e^- \rightarrow \nu + \bar{\nu}$  per unit pair of electron and positron per  $\text{cm}^3$  is almost independent of energy:

$$P_{B1} \simeq 1.35 \times 10^{-34} / \text{sec/cm}^3. \quad (6.10)$$

Each reaction releases about  $2m_e c^2$  in the form of neutrinos. Hence, the total rate of energy generation should be given by

$$E \simeq \int P_{B1}(2m_e c^2) \times N e^-(p_-) \times N e^+(p_+) d^3 p_+ d^3 p_-. \quad (6.11)$$

The population of electrons or positrons in a vacuum can be found from statistical thermodynamics. Since these are fermions we have

$$N(p) d^3 p = \frac{2 d^3 p}{h^3 [e^{+(a+E/kT)} + 1]}. \quad (6.12)$$

Now we need not impose the restriction that  $N$  (their total number) be constant (it is a function of  $T$ ). Hence, we set  $a = 0$ . Further, since these par-

icles can be annihilated, we must use for  $E$  the total  $E^2 = (p^2c^2 + m_e^2c^4)$ . Defining  $x = p/m_e c$  and  $\beta = m_e c^2/kT$ , we have

$$\int N e - (p_-) d^3 p_- = \frac{1}{\pi^2} \left( \frac{\hbar}{m_e c} \right)^{-3} f(\beta), \quad (6.13)$$

with

$$f(\beta) = \int_0^\infty \exp[-\beta(1+x^2)^{1/2}] x^2 dx. \quad (6.14)$$

If  $\beta$  is large (as will be the case for  $T_9 \gtrsim 3$ ), the integrand decreases very rapidly with increasing  $x$ . Indeed, most of its value comes from  $x < 1$ . So we can expand

$$(1+x^2)^{1/2} \simeq 1 + \frac{x^2}{2} - \frac{x^4}{8} + \dots \quad (6.15)$$

and keep only the first terms

$$f(\beta) = \frac{\pi^{1/2}}{4} \left( \frac{2}{\beta} \right)^{3/2} e^{-\beta}, \quad \beta > 1. \quad (6.16)$$

$\epsilon_{B1}^p$  becomes

$$\epsilon_{B1}^p = \frac{P_{B1}(2m_e c^2) f^2(\beta)}{\rho \pi^4 (\hbar/m_e c)^6} = \frac{10^{18.7} e^{-2m_e c^2/kT}}{\rho} T_9^3 \quad (\text{vacuum}). \quad (6.17)$$

We note that  $\epsilon$  is actually a decreasing function of the density. This explains why it becomes dominated by the photoneutrinos in the high density range.

The previous discussion was restricted to a vacuum. What happens if we introduce a gas of matter into the box? The answer depends upon the state of degeneracy of the gas. A non-degenerate gas will not modify the rate of neutrino energy production; true enough the electron gas will reduce the equilibrium concentration of positrons but it will not affect the rate of creation of positrons and, also, the rate of annihilation since both are (by definition of equilibrium) equal. Hence, the neutrino energy output per unit volume is independent of the density of the gas, provided again that the density corresponds to a state of non-degeneracy. The presence of degenerate electrons will hinder the formation of electron-positron pairs, and consequently decrease the output of neutrinos. Extensive calculations have been made all through the relevant range of density and temperature. Table 16 reproduces some of the results (Chiu 1961b).

### 6.3. NEUTRINOS AND STELLAR EVOLUTION

The intensity of neutrino emission in the temperature range above a few hundreds of millions of degrees is quite remarkable (see Fig. 3). If we realize that the sun pours out 2 ergs/gm/sec and that the most brilliant steady stars yield only a few thousand times more optical photons, we see that neutrino emission may be of paramount importance during the late stages of the life of a star. Supernovae do reach luminosities of  $10^{10}$  erg/gm/sec and novae  $10^6$  erg/gm/sec, but only for very short periods of time (hours to days) denoting highly unstable situations.

The effects on stellar evolution of neutrino-emitting mechanisms are far from being well understood. Through the virial theorem (which applies to photons and neutrino emission as well) we learn that to every quantum of energy emitted there must correspond a quantum of energy to be used in increasing the internal (kinetic) energy of the star. In a non-degenerate core (for a stellar mass exceeding the solar mass) this growth in the thermal energy raises the temperature. The specific effect of these neutrino processes is then to accelerate the contraction rate and hence to shorten the life of the star (that is, compared to what would be the case if these mechanisms were inactive).

On the nuclear burning of the remaining isotopes the neutrino emission has the following effect: as discussed before, contraction of a star can be halted only

TABLE 16  
PAIR ANNIHILATION NEUTRINO RATES, INCLUDING  
DEGENERACY (FROM CHIU 1961*b*)  
 $\log (\epsilon_{\text{B1}})$  in erg/gm/sec

$T_e$	$\log_{10} \rho$ (gr/cm <sup>3</sup> )							
	2	3	4	5	6	7	8	9
0.5.....	5.7	4.7	3.7	2.6	1.2	.....	.....	.....
0.6.....	7.7	6.7	5.7	4.6	3.3	0.3	.....	.....
0.7.....	9.2	8.2	7.2	6.1	4.9	2.3	.....	.....
0.8.....	10.3	9.3	8.3	7.3	6.1	3.8	.....	.....
0.9.....	11.2	10.2	9.2	8.2	7.0	5.0	0	.....
1.0.....	12.0	11.0	10.0	9.0	7.8	5.9	1.5	.....
1.2.....	13.2	12.2	11.2	10.2	9.1	7.4	3.7	.....
1.4.....	14.1	13.1	12.1	11.1	10.0	8.5	5.4	.....
1.6.....	14.8	13.8	12.8	11.8	10.8	9.4	6.6	0.4
1.8.....	15.4	14.4	13.4	12.4	11.4	10.1	7.6	2.1
2.0.....	15.9	14.9	13.9	12.9	11.9	10.7	8.4	3.5
2.5.....	17.0	16.0	15.0	14.0	13.0	11.8	10	6.1
3.0.....	17.7	16.7	15.7	14.7	13.7	12.7	11.1	7.9

if the nuclear energy generation is high enough to provide the energy requirement of the star, and will be halted at the temperature where such a condition is met. For a specific nuclear fuel this temperature range can be obtained by comparing the rate of nuclear energy generation from this fuel with the rate of neutrino and photon emission. The temperature range will be much higher than it would have been in a case of pure photonic emission. The equivalent burning stage would be postponed until this higher temperature is reached. Experimental evidence for or against the existence of neutrino emission from a direct coupling between electrons and neutrinos (such as discussed in the beginning of this chapter) may actually come from astrophysics.

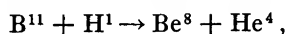
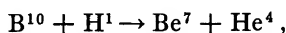
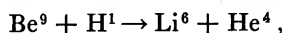
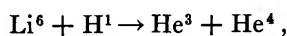
The plasma neutrinos appear to be intense enough to influence even the helium-burning stage. Hayashi and Cameron (1962) have recently discussed models of carbon-burning red supergiants with and without neutrino emission. Reeves (1963) has investigated crudely the effect of neutrino emission on car-

bon, oxygen, and neon stages. Finally we expect the supernova explosion and cooling to be highly influenced by neutrino losses.

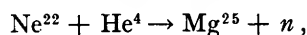
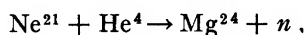
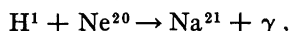
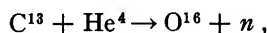
Although the present neutrino emission hypothesis seems to rest on fairly safe ground, we would have to reject it, should improved models persistently find better agreement with experimental results when the neutrinos from such processes are ignored. In the meantime experimental physicists are busy preparing a crucial experiment; the scattering of antineutrinos from a reactor by electrons. Detection of scattered electrons would confirm the validity of our assumption.

### § 7. MORE THERMONUCLEAR REACTION RATES

In this section we shall consider a number of nuclear reactions which are of interest especially for studies of nucleosynthesis. For instance, the reactions



are most important for theories of the origin of the solar system (Cameron 1962; Fowler, Greenstein, and Hoyle 1962; Bashkin and Peaslee 1961), while the reactions



are expected to provide neutron fluxes for the formation of heavy elements (Clayton, Fowler, Hull, and Zimmerman 1961). The reaction  $\text{N}^{14} + \text{He}^4 \rightarrow \text{O}^{17} + \text{H}^1$  may act as a trigger for the helium-burning flash (Cameron 1959b). The parameters belonging to the proton reactions are given in Table 17. They come mostly from the work of Salpeter (1955), Fowler (1959) and Fowler, Greenstein, and Hoyle (1962). Most of them *have not been* revised during the course of the present work.

Three reactions involving  $\text{He}^4$  ( $\text{C}^{13} + \text{He}^4$ ,  $\text{N}^{14} + \text{He}^4$ ,  $\text{N}^{15} + \text{He}^4$ ) have been recomputed by Thibaudau (1962).<sup>2</sup> The most recent data on the energy levels of  $\text{F}^{18}$  do allow the  $\text{N}^{14} + \text{He}^4$  reaction to be resonant through the 4.651 Mev level. Consequently the rate given here is much larger than the rate given by Burbidge, Burbidge, Fowler, and Hoyle (Table 18 and Table 19). Other helium reactions have been listed in Tables 18 and 19; they come from Salpeter (1955) or Burbidge, Burbidge, Fowler, and Hoyle (1957).

<sup>2</sup> Some of these rates are taken from a recent analysis of Dr. G. R. Caughlan.

TABLE 17  
PARAMETERS FOR SOME SECONDARY PROTON REACTIONS

Reaction	Reduced Mass $M = [(A_1 A_2) / (A_1 + A_2)] \text{ a.m.u.}$	$Z_1 Z_2 \sqrt{M}$	Gamow Peak $E_0 / T_0^{1/2} =$ $1.220 (Z_1^2 Z_2^2 M)^{1/2} \text{ (kev)}$	Full width $\Delta E_0 / T_0^{1/2} =$ $0.75 (Z_1^2 Z_2^2 M)^{1/2} \text{ (kev)}$
$\text{H}^1 + \text{Li}^6 \begin{cases} \swarrow \text{He}^3 + \text{He}^4 \\ \searrow \text{Be}^7 + \gamma \end{cases}$	$0.8635 \pm 0.0001$	$2.7877 \pm 0.0002$	2.42	1.1
$\text{H}^1 + \text{Be}^9 \begin{cases} \swarrow \text{Li}^6 + \text{He}^4 \\ \searrow \text{B}^{10} + \gamma \end{cases}$	$0.90675 \pm 0.00009$	$3.8089 \pm 0.0002$	2.98	1.2
$\text{H}^1 + \text{B}^{10} \begin{cases} \swarrow \text{Be}^7 + \text{He}^4 \\ \searrow \text{C}^{11} + \gamma \end{cases}$	$0.91595 \pm 0.00008$	$4.7853 \pm 0.0002$	3.47	1.3
$\text{H}^1 + \text{B}^{11} \begin{cases} \swarrow \text{Be}^8 + \text{He}^4 \\ \searrow \text{C}^{12} + \gamma \end{cases}$	$0.92360 \pm 0.00006$	$4.8052 \pm 0.0002$	3.48	1.3
$\text{H}^1 + \text{O}^{18} \begin{cases} \swarrow \text{N}^{15} + \text{He}^4 \\ \searrow \text{F}^{19} + \gamma \end{cases}$	$0.95469 \pm 0.00002$	$7.8167 \pm 0.0001$	4.81	1.5
$\text{H}^1 + \text{F}^{19} \begin{cases} \swarrow \text{O}^{16} + \text{He}^4 \\ \searrow \text{Ne}^{20} + \gamma \end{cases}$	$0.95736 \pm 0.00004$	$8.8060 \pm 0.0002$	5.20	1.6
$\text{H}^1 + \text{Ne}^{20} \rightarrow \text{Na}^{21} + \gamma$	$0.95976 \pm 0.00003$	$9.7968 \pm 0.0002$	5.59	1.6
$\text{H}^1 + \text{Ne}^{21} \rightarrow \text{Na}^{22} + \gamma$	$0.96197 \pm 0.00006$	$9.8080 \pm 0.0003$	5.59	1.6
$\text{H}^1 + \text{Ne}^{22} \rightarrow \text{Na}^{23} + \gamma$	$0.96397 \pm 0.00003$	$9.8182 \pm 0.0002$	5.60	1.6
$\text{H}^1 + \text{Na}^{23} \begin{cases} \swarrow \text{Ne}^{20} + \text{He}^4 \\ \searrow \text{Mg}^{24} + \gamma \end{cases}$	$0.96581 \pm 0.00005$	$10.8103 \pm 0.0003$	5.97	1.7

TABLE 17—Continued

Reaction	$B_0 = T_0$ $B_0 = 42.483 (Z^2 Z_0^2 M)^{1/2}$	$2\pi\eta E^{1/2}$ (kev) = $31.285 (Z^2 Z_0^2 M)^{1/2}$	Q value (kev)
$H^1 + Li^6 \begin{cases} \swarrow He^3 + He^4 \\ \searrow Be^7 + \gamma \end{cases}$	84.149 $\pm$ 0.005.....	87.21 $\pm$ 0.01	4021.9 $\pm$ 1.0
$H^1 + Be^9 \begin{cases} \swarrow Li^6 + He^4 \\ \searrow B^{10} + \gamma \end{cases}$	103.615 $\pm$ 0.004.....	119.16 $\pm$ 0.01	5609.3 $\pm$ 1.4
$H^1 + B^{10} \begin{cases} \swarrow Be^7 + He^4 \\ \searrow C^{11} + \gamma \end{cases}$	120.640 $\pm$ 0.003.....	149.71 $\pm$ 0.02	2124.7 $\pm$ 0.9
$H^1 + B^{11} \begin{cases} \swarrow Be^8 + He^4 \\ \searrow C^{12} + \gamma \end{cases}$	120.974 $\pm$ 0.003.....	150.33 $\pm$ 0.02	6587.2 $\pm$ 1.0
$H^1 + O^{18} \begin{cases} \swarrow N^{15} + He^4 \\ \searrow F^{19} + \gamma \end{cases}$	167.327 $\pm$ 0.002.....	244.55 $\pm$ 0.03	1146.8 $\pm$ 1.0
$H^1 + F^{19} \begin{cases} \swarrow O^{16} + He^4 \\ \searrow Ne^{20} + \gamma \end{cases}$	181.164 $\pm$ 0.003.....	275.50 $\pm$ 0.03	8691.1 $\pm$ 3.1
$H^1 + Ne^{20} \rightarrow Na^{21} + \gamma$	194.510 $\pm$ 0.002.....	306.49 $\pm$ 0.04	8586.4 $\pm$ 1.1
$H^1 + Ne^{21} \rightarrow Na^{22} + \gamma$	194.658 $\pm$ 0.004.....	306.85 $\pm$ 0.04	15955.87 $\pm$ 0.44
$H^1 + Ne^{22} \rightarrow Na^{23} + \gamma$	194.793 $\pm$ 0.002.....	307.17 $\pm$ 0.04	3980.4 $\pm$ 0.9
$H^1 + Na^{23} \begin{cases} \swarrow Ne^{22} + He^4 \\ \searrow Mg^{24} + \gamma \end{cases}$	207.704 $\pm$ 0.004.....	338.20 $\pm$ 0.04	7992.2 $\pm$ 0.7
			8114.0 $\pm$ 0.7
			12843.93 $\pm$ 0.7
			2454 $\pm$ 3.0
			6743.0 $\pm$ 4.9
			8790.1 $\pm$ 1.5
			2378.7 $\pm$ 1.5
			11692.6 $\pm$ 2.2

TABLE 17—Continued

REACTION	$S^{(0)}$ (kev - barns)	$A$ $P/\rho X_1 =$ $Afg \exp (-B/T_e^{1/3})T_e^{-1/2}$	$g = (1 + UT_e^{1/3})$		ELECTRON SCREENING FACTOR $f$
			$U$ ( $U = 5/12B$ )		
$H^1 + Li^6 \begin{array}{c} \diagup \\ He^3 + He^4 \\ \diagdown \end{array} \begin{array}{c} \\ Be^7 + \gamma \end{array}$	$5.06 \times 10^3$	$5.96 \times 10^{12}$	$4.95 \times 10^{-3}$		$(1 + 0.75\rho^{1/2}/T^{3/2})$
$H^1 + Be^9 \begin{array}{c} \diagup \\ Li^6 + He^4 \\ \diagdown \end{array} \begin{array}{c} \\ B^{10} + \gamma \end{array}$	$3.01 \times 10^4$	$3.84 \times 10^{13}$	$4.02 \times 10^{-3}$		$(1 + 1.00\rho^{1/2}/T^{3/2})$
$H^1 + B^{10} \begin{array}{c} \diagup \\ Be^7 + He^4 \\ \diagdown \end{array} \begin{array}{c} \\ C^{11} + \gamma \end{array}$	$1.79 \times 10^4$	$2.45 \times 10^{13}$	$3.45 \times 10^{-3}$		$(1 + 1.25\rho^{1/2}/T^{3/2})$
$H^1 + B^{11} \begin{array}{c} \diagup \\ Be^9 + He^4 \\ \diagdown \end{array} \begin{array}{c} \\ C^{12} + \gamma \end{array}$	$8.99 \times 10^4$	$1.23 \times 10^{14}$	$3.44 \times 10^{-3}$		$(1 + 1.25\rho^{1/2}/T^{3/2})$
$H^1 + O^{18} \begin{array}{c} \diagup \\ N^{15} + He^4 \\ \diagdown \end{array} \begin{array}{c} \\ F^{19} + \gamma \end{array}$	$10^5$	$1.5 \times 10^{14}$	$2.49 \times 10^{-3}$		$(1 + 2.00\rho^{1/2}/T^{3/2})$
$H^1 + F^{19} \begin{array}{c} \diagup \\ O^{16} + He^4 \\ \diagdown \end{array} \begin{array}{c} \\ Ne^{20} + \gamma \end{array}$	$10^6$	$1.5 \times 10^{15}$	$2.30 \times 10^{-3}$		$(1 + 2.25\rho^{1/2}/T^{3/2})$
$H^1 + Ne^{20} \longrightarrow Na^{21} + \gamma$	$55 \pm 20$	$9.33 \times 10^{10}$	$2.14 \times 10^{-3}$		$(1 + 2.50\rho^{1/2}/T^{3/2})$
$H^1 + Ne^{21} \longrightarrow Na^{22} + \gamma$	$> 5.6$	$> 10^{10}$	$2.14 \times 10^{-3}$		$(1 + 2.50\rho^{1/2}/T^{3/2})$
$H^1 + Ne^{22} \longrightarrow Na^{23} + \gamma$	$> 550$	$> 10^{12}$	$2.14 \times 10^{-3}$		$(1 + 2.50\rho^{1/2}/T^{3/2})$
$H^1 + Na^{23} \begin{array}{c} \diagup \\ Ne^{20} + He^4 \\ \diagdown \end{array} \begin{array}{c} \\ Mg^{24} + \gamma \end{array}$			$2.01 \times 10^{-3}$		$(1 + 2.75\rho^{1/2}/T^{3/2})$

TABLE 18  
PARAMETERS FOR SOME SECONDARY He<sup>4</sup> REACTIONS

Reaction	He <sup>4</sup> +C <sup>12</sup> $\begin{cases} \nearrow \text{O}^{17}+\gamma \\ \searrow \text{O}^{16}+n \end{cases}$	He <sup>4</sup> +N <sup>14</sup> →F <sup>18</sup> +γ	He <sup>4</sup> +N <sup>16</sup> →F <sup>19</sup> +γ
Reduced Mass $M=(A_1A_2)/(A_1+A_2)$ a.m.u.	3.06150±0.00011	3.11383±0.00007	3.16053±0.00011
$Z_1Z_2\sqrt{M}$ .....	20.9966±0.0004	24.7045±0.0003	24.8890±0.0004
$E_0/T_8^{2/3}=26.3 (Z_1^2Z_2^2M)^{1/3}$ (kev).....	200	223	224
$\Delta E_0/T_8^{5/6}=35 (Z_1^2Z_2^2M)^{1/6}$ (kev).....	96	101	101
$B_8=9.1527 (Z_1^2Z_2^2M)^{1/3}$ $B_8=\tau T_8^{1/3}$ .....	69.660±0.001	77.637±0.001	78.023±0.001
$2\pi\eta E^{1/2}$ (kev) = 31.1285 $(Z_1^2Z_2^2M)^{1/2}$ .....	652.97±0.08	768.86±0.09	774.77±0.09
Q value (kev).....	6356.6±1.1(O <sup>17</sup> +γ) 2214.5±0.9(O <sup>16</sup> +n)	4403.9±4.0	4011.8±1.1

TABLE 19  
RATES FOR SOME SECONDARY He<sup>4</sup> REACTIONS

$\log_{10} \left( \frac{P_{13,4}}{\rho X_4 f_{13,4}} \right) = 17.1 - \frac{2}{3} \log T_8 - 30.24 T_8^{-1/3}$
$\log_{10} \left( \frac{P_{14,4}}{\rho X_4 f_{14,4}} \right) = -3.8 - 12.4 T_8^{-1} - \frac{3}{2} \log T_8$
$\log_{10} \left( \frac{P_{20,4}}{\rho X_4 f_{20,4}} \right) = 19.8 - \frac{2}{3} \log T_8 - 43.73 T_8^{-1/3} - 0.09 T_8^{2/3}$
$\log_{10} \left( \frac{P_{24,4}}{\rho X_4 f_{24,4}} \right) = 20.7 - \frac{2}{3} \log T_8 - 49.8 T_8^{-1/3} - 0.1 T_8^{2/3}$
$\log_{10} \left( \frac{P_{28,4}}{\rho X_4 f_{28,4}} \right) = 22.0 - \frac{2}{3} \log T_8 - 55.6 T_8^{-1/3} - 0.12 T_8^{2/3}$

I wish to thank Dr. R. Jastrow and the Institute for Space Studies for their hospitality; Drs. A. G. W. Cameron, H. Y. Chiu, E. E. Salpeter and B. Ström-gren for their comments; Messrs. J. Hauben, W. Hatt, Miss B. Forman, Mr. A. Weisswasser, and M. Golub for their help in the numerical calculations. Finally I acknowledge gratefully the patience of Mrs. Judith Sprott, Mr. Ted Psaropulos, and Mr. W. Cartledge in preparing and revising the manuscript.



## REFERENCES

- ADAMS, J. B., RUDERMAN,  
M. A., and WOO, C. H. 1963 *Phys. Rev.*, **129**, 1383.
- AJZENBERG-SELOVE, F.,  
and STELSON, P. H. 1960 *Phys. Rev.*, **120**, 500.
- ALBURGER, D. E. 1960 *Phys. Rev.*, **118**, 235.  
1961 *Ibid.*, **124**, 193.
- ALBURGER, D. E., and  
PIXLEY, R. W. 1960 *Phys. Rev.*, **119**, 1970.
- ALMQVIST, E.,  
BROMLEY, D. A., and  
KUEHNER, J. A. 1960 *Phys. Rev., Letters*, **4**, 515.
- BAHCALL, J. N., FOWLER,  
W. A., IBEN, I., and  
SEARS, R. L. 1963 *Ap. J.*, **137**, 344.
- BASHKIN, S.,  
KAVANAGH, R. W., and  
PARKER, P. D. 1959 *Phys. Rev., Letters*, **3**, 518.
- BASHKIN, S., and  
PEASLEE, D. C. 1961 *Ap. J.*, **134**, 981.
- BLOOM, S. D.,  
TOPPEL, B. J., and  
WILKINSON, D. H. 1957 *Phil. Mag.*, **2**, 57.
- BRADFORD, E., and  
ROBSON, B. A. 1961 *Nuclear Phys.*, **29**, 442.
- BROMLEY, D. A.,  
KUEHNER, J. A., and  
ALMQVIST, E. 1960 *Phys. Rev., Letters*, **4**, 365.
- BROWN, R. E. 1962 *Phys. Rev.*, **125**, 347.
- BURBIDGE, E. M., Bur-  
BIDGE, G. R., FOWLER,  
W. A., and HOYLE, F. 1957 *Rev. Mod. Phys.*, **29**, 547.
- BURGE, E. J., and  
PROWSE, D. J. 1956 *Phil. Mag.*, **1**, 912.
- CAMERON, A. G. W. 1958 *Chalk River Rept.*, CRL-41.  
1959a *Ap. J.*, **130**, 452.  
1959b *Ibid.*, p. 916.  
1962 *Icarus*, **1**, 13.
- CAMERON, J. R. 1953 *Phys. Rev.* **90**, 839.
- CARLSON, R. R. 1961 *Nuclear Phys.*, **28**, 443.
- CARTLEDGE, W.,  
THIBAudeau, M., and  
REEVES, H. 1963 *Helium Thermonuclear Reactions* (New York:  
Institute for Space Studies).
- CAUGHLAN, G. R., and  
FOWLER, W. A. 1962 *Ap. J.*, **136**, 453.

- CHIU, H. Y. 1961a *Ann. Phys.*, **15**, 1.  
 1961b *Phys. Rev.*, **123**, 1040.
- CHIU, H. Y., and MORRISON, P. 1960 *Phys. Rev., Letters*, **5**, 573.
- CHIU, H. Y., and STABLER, R. C. 1961 *Phys. Rev.*, **122**, 1317.
- CHRISTY, R. F., and DUCK, I. 1961 *Nuclear Phys.*, **24**, 89.
- CLAYTON, D. D. 1962 *Phys. Rev.*, **128**, 2254.
- CLAYTON, D. D., FOWLER, W. A., HULL, T. E., and ZIMMERMAN, B. A. 1961 *Ann. Phys.*, **12**, 331.
- COOK, C. W., FOWLER, W. A., LAURITSEN, C. C., and LAURITSEN, T. 1957 *Phys. Rev.* **107**, 508.
- DAVIS, R., and HARMER, D. S. 1959 *Bull. Amer. Phys. Soc.* **4**, 217.
- DOUGLAS, R. A., BROER, J. W., CHIBA, REN, HERRING, D. F., and SILVERSTEIN, E. A. 1956 *Phys. Rev.*, **104**, 1059.
- EVERLING, F., KOENIG, L. A., MATTAUCH, J. H. E., and WAPSTRA, A. H. 1960 *Nuclear Data Tables, Part I, U.S.A.E.C. Rept.*
- FESHBACH, H., SHAPIRO, M. M., and WEISSKOPF, V. F. 1953 *Tables of Penetrabilities of Charged Particle Reactions* (N.Y.O.-3077).
- FEYNMAN, R. P., and GELL-MANN, M. 1958 *Phys. Rev.*, **109**, 193.
- FOWLER, W. A. 1951 *Phys. Rev.*, **81**, 655.  
 1959 *Ninth Internat. Astr. Symp.*, Liège, p. 203.
- FOWLER, W. A., GREENSTEIN, J. L., and HOYLE, F. 1962 *Geophys. J. of the R.A.S.*, **6**, 148.
- FREGEAU, J. H. 1956 *Phys. Rev.*, **104**, 225.
- GAMOW, G., and SCHOENBERG, M. 1941 *Phys. Rev.*, **59**, 539.
- GANDEL'MAN, G. M., and PINAEV, V. S. 1960 *Soviet Physics—J.E.T.P.*, **10**, 764.
- GOOD, W. M., KUNZ, W. E., and MOAK, C. D. 1954 *Phys. Rev.*, **94**, 87.
- GRIFFITHS, G., LAL, M., and SCARFE, C. 1961 *Bull. Amer. Phys. Soc.*, **6**, 506.

- HAYASHI, C., and  
CAMERON, R. C. 1962 *Ap. J.*, **136**, 166.
- HEBBARD, D. F. 1960 *Nuclear Phys.*, **15**, 289.
- HEBBARD, D. F., and  
VOGL, J. L. 1960 *Nuclear Phys.*, **21**, 652.
- HESTER, R. E.,  
PIXLEY, R. E., and  
LAMB, W. A. B. 1958 *Phys. Rev.*, **111**, 1604.
- HILL, R. W. 1953 *Phys. Rev.*, **90**, 845.
- HOLMGREN, H. D., and  
JOHNSTON, R. L. 1959 *Phys. Rev., Letters*, **2**, 275, 381.
- HOYLE, R., and  
FOWLER, W. A. 1960 *Ap. J.*, **132**, 565.
- IBEN, I., and  
EHRMAN, J. R. 1962 *Ap. J.*, **135**, 770.
- IMHOF, W. L., *et al.* 1962 *Lockheed Rept.*, AF 29(601)-1765.
- KAVANAGH, R. W. 1960 *Nuclear Phys.*, **15**, 411.
- KELLER, G. 1953 *Ap. J.*, **118**, 142.
- KUEHNER, J. A., GOVE,  
H. E., LITHERLAND,  
A. E., CLARK, M. A.,  
and ALMQVIST, E. 1961 Chalk River Rept., PD-317.
- KUMAR, S. S. 1963 *Ap. J.*, **137**, 1121.
- LAL, M. 1961 Thesis, University of British Columbia.
- LAMB, W. A. S., and  
HESTER, R. E. 1957a *Phys. Rev.*, **107**, 550.  
1957b *Ibid.*, **108**, 1304.
- LANDAU, L. D., and  
LIFSCHITZ, E. M. 1958 *Statistical Physics*, trans. E. and R. F. PEIERLS  
(London: Pergamon Press, Ltd.).
- LANDOLT-BÖRNSTEIN, R. 1961 *New Series Group I* (Berlin: Springer-Verlag),  
Vol. 1.
- LEVINE, M. J. 1963 Thesis, California Institute of Technology.
- MARX, C., and  
MENYHARD, N. 1960 *Mitteilungen der Sternwarte der Ungarischen*  
(Budapest: Akademie der Wissenschaften).
- MATINYAN, G., and  
TSILOSANI 1962 *J.E.T.P.*, **14**, 1195.
- MEADS, R. E., and  
MCILDOWIE, J. E. C. 1960 *Proc. Phys. Soc.*, **A75**, 257.
- PARKER, P. D., and  
KAVANAGH, R. W. 1963 *Phys. Rev.*, **131**, 2578.
- POCHODA, P., and  
REEVES, H. 1964 *Planetary and Space Science*, **12**, 119.
- PONTECORVO, N. M. 1959 *Soviet Physics—J.E.T.P.*, **9**, 1148.

- REEVES, H. 1960 Thesis, Cornell University.  
 1962 *Ap. J.*, **135**, 779.  
 1963 *Ibid.*, **138**, 79.
- REEVES, H., and  
 SALPETER, E. E. 1959 *Phys. Rev.*, **116**, 1505.
- REIBEL, K., and  
 MANN, A. K. 1960 *Phys. Rev.*, **118**, 701.
- REINES, R., and  
 COWAN, C. L., JR. 1960 *Phys. Rev.*, **117**, 159.
- RITUS, V. I. 1962 *Soviet Physics—J.E.T.P.*, **14**, 915.
- ROTH, B.; and  
 WILDERMUTH, K. 1960 *Nuclear Phys.*, **20**, 10.
- SALPETER, E. E. 1952 *Phys. Rev.*, **88**, 547.  
 1954 *Australian J. Phys.*, **7**, 373.  
 1955 *Phys. Rev.*, **97**, 1237.  
 1957 *Ibid.*, **107**, 516.
- SAWYER, G. A., and  
 PHILLIPS, J. A. 1953 *Los Alamos Rept.*, 1578.
- SCHARDT, A.,  
 FOWLER, W. A., and  
 LAURITSEN, C. C. 1952 *Phys. Rev.*, **86**, 527.
- SCHATZMAN, E. 1948 *J. de Phys. et Radium*, **9**, 46.  
 1951 *Compt. Rend.*, **232**, 1740.  
 1954 *Ap. J.*, **119**, 464.  
 1958 *White Dwarfs* (Amsterdam: North-Holland Pub. Co.)
- SEARS, R. L. 1959 *Ap. J.*, **192**, 489.
- SEEGER, P. A., and  
 KAVANAGH, R. W. 1963 *Ap. J.*, **137**, 704.
- SEGEL, R. E.,  
 OLNES, J. W., and  
 SPRENKEL, E. L. 1961 *Phys. Rev.*, **123**, 1382.
- SILVERSTEIN, E. A.,  
 HARDIE, G., OPPLIGER,  
 L., and SALISBURY, S. 1960 *Bull. Amer. Phys. Soc.*, **5**, 405.
- SWANN, C. P., and  
 METZGER, F. R. 1957 *Phys. Rev.*, **108**, 982.
- TANNER, N. 1959 *Phys. Rev.*, **114**, 1060.
- THIBAudeau, M. 1962 Thesis, University of Montreal.
- TOMBRELLO, T. A., and  
 PARKER, P. D. 1963 *Phys. Rev.*, **131**, 2582.
- TSUDA, H. 1963 *Progress of Theor. Phys.*, **29**, 29.
- WALECKA, J. D. 1962 *Phys. Rev.*, **126**, 663.



## CHAPTER 3

# *Stellar Absorption Coefficients and Opacities*

ARTHUR N. COX

*Los Alamos Scientific Laboratory, University of California*

### § 1. INTRODUCTION

#### 1.1. CONDITIONS IN STELLAR INTERIORS AND ATMOSPHERES

TO PREPARE for the calculation of photon absorption in stars it is convenient to review the conditions with which we must deal. The ranges of temperature and density are very large; nevertheless the absorption calculations can be made and for extreme temperatures and densities we shall even find that theoretical simplifications are possible.

The coolest visible star has a surface temperature just over  $2000^{\circ}$  K, but for special problems material properties are required at  $1000^{\circ}$  K. Much lower temperatures exist in the universe, but those cases of solid bodies or interstellar matter will not be considered here. The highest temperatures, perhaps  $10^{10}$  ° K in the interiors of highly evolved stars, are high enough to convert all matter to the most stable element, iron. It is possible that at such temperatures or even lower ones, nuclear reactions occur which cause stellar explosions. Our temperature range is then  $10^3$  ° K to  $10^{10}$  ° K.

The densities at which we need absorption data also cover a large range. In the solar atmosphere the density is about  $10^{-7}$  gm/cm<sup>3</sup>, and considerably lower densities occur in the high-temperature solar corona. At these low densities an equilibrium assumption about the state of the matter may not be valid. Non-equilibrium problems are not treated here, for we assume that the state of the matter can be uniquely described by a temperature. Special methods of treating radiation flow are necessary when the gas-kinetic temperature at a point in space is not the same as the temperature which describes the radiation. Even more complicated situations (called departures from local thermodynamic equilibrium) are possible when neither the matter nor the radiation at a given point can be

described by a temperature. When the matter does have a definite temperature, its average properties are known and absorption coefficients can be readily determined.

Except for possible neutron stars, the highest densities, perhaps  $10^9$  gm/cm<sup>3</sup>, seem to occur in white dwarfs, but at this extreme we need not worry about absorption processes in energy transfer problems, because all the energy is carried by electronic heat conduction. (There are, of course, intermediate densities that give some computation difficulties when electronic conduction has not yet become dominant.) The high densities go with the high temperatures in astrophysical situations, and when, at the high densities, electron conduction becomes important, almost all the elements are completely ionized. This fact makes our calculations easier and enables absorption and electron conduction calculations to be made at the high densities met in stellar interiors.

The gas and radiation pressures that exist in these temperature and density ranges display a larger range of values than either the temperature or density, but only at high pressures and densities are there effects such as electron-electron interactions that influence the state of the matter and complicate absorption calculations.

The temperature and density ranges indicate that we must deal with molecules and atoms in all possible stages of ionization, though not all need to be considered simultaneously at a point in a star. Atmospheres have temperatures that permit association of molecules and even negative atomic ions, i.e., atoms with an extra electron loosely attached. The complicated absorption coefficients in these very low temperature regions, due to continuous absorption as well as molecular bands and atomic lines, have not been fully worked out as yet. As the temperature increases, the molecules dissociate and atoms ionize. It is necessary to know accurately the degree of ionization for each element in our stellar mixtures in order to compute the absorption of photons by the matter. Complete ionization for stellar mixtures depends on the density but occurs at about  $5 \times 10^7$  °K, and at these and higher temperatures absorption processes are simplified.

By the Pauli exclusion principle free electrons are required to avoid a state already occupied by another free electron. At densities of  $10^2$  gm/cm<sup>3</sup> and higher, assuming an astrophysical temperature condition of  $10^7$  °K as at the solar center, the available free states are beginning to be filled by electrons ionized from the atoms in the mixture. Complete electron degeneracy, where all lower free states are filled by electrons moving at relativistic velocities, occurs roughly at  $10^6$  gm/cm<sup>3</sup>. Only in the partially degenerate range do we need to consider the state of the matter for absorption calculations. At higher densities where there is simultaneously high degeneracy and complete ionization all the transport of energy is by electron conduction. Fortunately, the degeneracy of atomic nuclei with or without bound electrons does not have to be considered in astrophysics.

Our discussion here should also include the conditions of stellar matter which enable thermonuclear reactions to occur. It is the energy generated by these processes which must be transported by radiation, conduction, convection, or by mechanical means, such as expansion or pulsation, to the stellar surface where it is radiated away. Also, as the thermonuclear processes change the composition, the equation of state and opacity change.

During the early stages in the life of a star the low temperature reactions burning deuterium, lithium, beryllium, and boron occur at the stellar center. When temperatures near  $5 \times 10^6$  ° K are reached in the contracting stellar center, hydrogen can be transmuted to  $\text{He}^3$ . Above  $8 \times 10^6$  ° K the hydrogen reaction can be completed to produce  $\text{He}^4$  in astronomical time scales. As the hydrogen is depleted in the life of a star the core contracts to release more potential energy. This energy allows the temperature to increase to about  $10^8$  ° K when all the hydrogen is either burned or can be burned very rapidly.

At  $10^8$  ° K the helium can transmute to  $\text{Be}^8$  which has a small equilibrium concentration. This  $\text{Be}^8$  can react with the  $\text{He}^4$  to produce the stable nucleus  $\text{C}^{12}$ . The resulting alpha-particle fusion, forming carbon, yields, per unit mass of transmuted matter, about 10 per cent as much thermonuclear energy as has already been generated by hydrogen burning. Again, depletion of helium can occur by its being converted to  $\text{O}^{16}$  and  $\text{Ne}^{20}$ . The exact processes which occur between  $10^8$  ° K and  $10^{10}$  ° K are not completely known, but between  $10^9$  and  $10^{10}$  ° K the matter exists mostly as  $\text{Fe}^{56}$ , the most stable nucleus.

These thermonuclear changes after the complete hydrogen consumption need not concern us very much in opacity calculations for stellar mixtures, because above  $5 \times 10^7$  ° K all elements that ever can attain appreciable abundance (i.e., those lighter than about iron) are completely ionized. The calculations needed for the photon absorption and scattering are simplified when there are no bound electrons as in most of the mass of highly evolved stars.

Considering now in more detail the most important energy transfer process in stars, namely radiation, we can notice how closely conditions in stars approach those of an ideal blackbody. The mean free path of the average photon in the hot stellar interior is usually of the order of a few centimeters or less, and particle mean free paths are also very small. With collisions keeping the matter in a steady state of ionization and excitation at a point in the interior, the matter is said to be in local thermodynamic equilibrium. Temperature gradients in stars can be approximated by considering the drop of about  $10^7$  ° K over a radius of  $10^{11}$  cm in a typical star. This gradient of the order of  $10^{-4}$  ° K/cm means that a photon, before absorption, moves to a region whose temperature is only a very small fraction of degree different from that at its point of origin. The photons then can be said to diffuse through the star, and a photon is absorbed in material that is at the same temperature as the emitting material. This is the condition of local thermodynamic equilibrium with the matter and radiation temperatures almost equal. We shall use this condition later when we



derive the absorption coefficient for a mean photon. This mean absorption coefficient is called the opacity, and as used in astrophysics it has the units of  $\text{cm}^2/\text{gm}$ .

A temperature gradient, however, must exist in stellar interiors. This temperature gradient is produced primarily by the condition of hydrostatic equilibrium. Due to this gradient, energy flows outward. If there were perfect thermodynamic equilibrium we could use Planck's law which gives the emitted specific intensity at frequency  $\nu$  from a blackbody (completely absorbing) in thermodynamic equilibrium at temperature  $T$ ,

$$B_\nu(T) d\nu = \frac{2h\nu^3}{c^2} \frac{d\nu}{\exp\left(\frac{h\nu}{kT}\right) - 1} \frac{\text{ergs}}{\text{cm}^2 \text{ sec ster}}, \quad (1)$$

where cgs units are given to indicate the dimensions of this specific intensity,  $h$  is the Planck constant,  $c$  is the velocity of light, and  $k$  is the Boltzmann constant. Quite small deviations from this intensity cause the flow of energy in stellar interiors.

In some stellar atmospheres the mean free paths of photons are long enough so that photons from a point at one temperature can, before absorption, reach material which is at another temperature. Also, it is possible to have the situation where only wavelength independent (Thomson) scattering hinders the radiation flow without changing its spectrum. True absorption and re-emission at the local temperature changes the spectrum of the radiation as it passes through a stellar atmosphere. But if scattering dominates absorption, or if photon mean free paths are very long, it may happen, at some point in the atmosphere, that the character of the incident radiation (i.e., its spectral distribution) may not be coincident with the blackbody energy distribution at the local matter temperature. These situations which do occur in the very outer layers of stars must be dealt with monochromatically at all space points as opposed to the treatment which we discuss immediately where the flow of radiation can be calculated accurately considering only the mean photon. We shall return to this point in section 1.4, after a discussion of the radiation transfer equation.

## 1.2. DERIVATION OF THE RADIATION DIFFUSION FLUX FORMULA

When the conditions of local thermodynamic equilibrium obtain, and matter and radiation have almost equal temperatures, a simple formula which is a function of the local temperature, its gradient, the local density, and the opacity gives the flux of energy due to radiation transfer.

The transfer of energy by radiative processes is described by an equation of transfer. At a given frequency,  $\nu$ , we write for the steady (time independent) state

$$\frac{\partial I_\nu(s)}{\rho \partial s} = -(\kappa'_\nu + \sigma_\nu) I_\nu(s) + \sigma_\nu \int I_\nu(s') p(\cos \Theta) \frac{d\omega}{4\pi} + \kappa'_\nu B_\nu(T), \quad (2)$$

where  $\kappa'_\nu$  is the absorption coefficient normally calculated by atomic physics and corrected by a reduction factor so that finally:

$$\kappa'_\nu = \kappa_\nu \left[ 1 - \exp \left( -\frac{h\nu}{kT} \right) \right]. \quad (3)$$

This factor, discussed below, allows for induced emission or negative absorption in the absorption term. In the equation of transfer,  $I_\nu(s)$  is the monochromatic specific intensity which is varying in the direction  $s$ ,  $\rho$  is the density of matter,  $\sigma_\nu$  is the monochromatic scattering coefficient in the same units as  $\kappa'_\nu$  but uncorrected for induced emission,  $p(\cos \Theta)$  is a scattering phase function, normalized to unity, which indicates how the energy is distributed in angle  $\Theta$  in the solid angle  $d\omega$  about direction  $s'$ , and  $B_\nu(T)$  is the previously given Planck function.

The sources of radiation are spontaneous emission, induced emission, and scattered photons. The flux of scattered photons is  $\sigma_\nu \int I_\nu(s') p(\cos \Theta) (d\omega/4\pi)$ , and the attenuation due to scattering is  $\sigma_\nu I_\nu$ . The induced emission (i.e., negative absorption), which is proportional to and in the same direction as the radiation intensity, equals  $\kappa_\nu I_\nu e^{-h\nu/kT}$ , and is considered by reducing the true absorption term  $\kappa_\nu I_\nu$  to  $\kappa'_\nu I_\nu$ . In local thermodynamic equilibrium, the equation of transfer should have only the spontaneous emission  $\kappa'_\nu B_\nu(T)$  instead of  $\kappa_\nu B_\nu(T)$ , the total blackbody emission in thermodynamic equilibrium because the induced emission is taken into account in the absorption term. Another term representing other sources of radiation, for example thermonuclear energy, could also be added to the right-hand side of equation (2) to make a more exact expression. A detailed derivation of the equation of transfer not considering electron degeneracy is given by Chandrasekhar (1939). His induced emission correction and the equation of transfer, however, are valid even when the free electrons are degenerate.

The equation of transfer allows photons to be absorbed and scattered. Even if there were no absorption ( $\kappa'_\nu = 0$ ), in stellar interiors the photons diffuse to a different temperature region only after many scatterings. The radiation always changes to the blackbody character at the local matter temperature because a Compton scattering photon has an energy different from that of the original photon. This energy shift by Compton scattering is not as efficient as a true absorption process where the emission has a spectrum determined by the matter in local thermodynamic equilibrium, but even slight energy shifts can keep the matter and radiation temperatures almost equal.

Quantitatively, our postulates of local thermodynamic equilibrium and almost equal matter and radiation temperature can be expressed by assuming an intensity given by the blackbody function reduced slightly or,

$$I_\nu(s) = B_\nu(T) - \frac{1}{\rho(\kappa'_\nu + \sigma_\nu)} \frac{\partial B_\nu(T)}{\partial s}, \quad (4)$$

higher-order derivatives being negligible. If we try this expansion for  $I_\nu(s)$  as a solution of the equation of transfer (2) we find that only the term

$$\frac{\sigma_\nu}{\rho(\kappa'_\nu + \sigma_\nu)} \int \frac{\partial B_\nu(T)}{\partial s'} p(\cos \Theta) \frac{d\omega}{4\pi} \quad (5)$$

does not cancel. This integral is then

$$\frac{1}{2} \frac{\sigma_\nu}{\rho(\kappa'_\nu + \sigma_\nu)} \frac{\partial B_\nu(T)}{\partial s} \int_0^\pi \cos \Theta p(\cos \Theta) \sin \Theta d\Theta, \quad (6)$$

where  $\Theta$  is the angle between  $s'$  and  $s$ . This integral is zero if the phase function is isotropic

$$p(\cos \Theta) = 1 \quad (7)$$

or if it is the Rayleigh function,

$$p(\cos \Theta) = \frac{3}{4} (1 + \cos^2 \Theta), \quad (8)$$

which holds for Rayleigh and Thomson scattering. Thus equation (4) is an approximate solution of the equation of transfer.

We can see also that the expansion for  $I(s)$  is rather accurate for the average point in stellar interiors. Using the definition of  $B_\nu(T)$ , we obtain

$$\begin{aligned} \frac{\partial B_\nu(T)}{\partial s} &= \frac{\partial B_\nu(T)}{\partial T} \frac{\partial T}{\partial s} \\ &= \frac{B_\nu(T) \left( \frac{h\nu}{kT^2} \right) \exp \left( \frac{h\nu}{kT} \right) \frac{\partial T}{\partial s}}{\exp \left( \frac{h\nu}{kT} \right) - 1}. \end{aligned} \quad (9)$$

The ratio,  $R$ , of the second-order term in the intensity expansion to  $B_\nu(T)$  is, therefore,

$$R = \frac{\left( \frac{h\nu}{kT^2} \right) \exp \left( \frac{h\nu}{kT} \right)}{\rho(\kappa'_\nu + \sigma_\nu) \left[ \exp \left( \frac{h\nu}{kT} \right) - 1 \right]} \frac{\partial T}{\partial s}. \quad (10)$$

The value of  $\partial T/\partial s$  can be taken as less than  $10^{-3}$ , the bulk of the energy in the blackbody spectrum is at  $h\nu/kT = 1-10$ ,  $(\kappa'_\nu + \sigma_\nu)^{-1}$  is almost always less than about 5, and  $T$  is always greater than  $10^3$  °K. The ratio,  $R$ , then is less than about  $5 \times 10^{-5}/\rho$ , and for densities greater than about  $10^{-3}$ – $10^{-4}$  gm/cm<sup>3</sup>, the expansion is quite accurate. Only in stellar atmospheres and the envelopes of giant stars is the expansion for  $I_\nu(s)$  to be questioned. One must usually investigate the intensity approximation to see if it is valid in low density cases where, however, temperature gradients are also low.

The definition of the monochromatic radiative flux in direction  $x$  is given by

$$F_{\nu,x} = \int I_\nu(s) \cos \Theta d\omega, \quad (11)$$

where  $\cos \Theta$  is now the projection factor for the intensity on to the direction  $x$  at angle  $\Theta$  from direction  $s$ . Insertion of the expansion of  $I_\nu$  yields the expression

$$F_{\nu, x} = - \int_0^\pi \int_0^{2\pi} \frac{1}{\rho (\kappa'_\nu + \sigma_\nu)} \frac{\partial B_\nu(T)}{\partial x} \cos^2 \Theta \sin \Theta d\Theta d\phi, \quad (12)$$

where the first isotropic term in the intensity vanished due to the symmetry of the integral. The integral is thus

$$F_{\nu, x} = - \frac{4\pi}{3\rho (\kappa'_\nu + \sigma_\nu)} \frac{\partial B_\nu(T)}{\partial x}. \quad (13)$$

Now the total flux at all frequencies in direction  $x$  is

$$\begin{aligned} F_x &= \int_0^\infty F_{\nu, x} d\nu \\ &= - \frac{4\pi \partial T}{3\rho \partial x} \int_0^\infty \frac{1}{(\kappa'_\nu + \sigma_\nu)} \frac{\partial B_\nu(T)}{\partial T} d\nu \\ &= - \frac{4\pi \partial T}{3\rho \kappa \partial x} \int_0^\infty \frac{\partial B_\nu(T)}{\partial T} d\nu, \end{aligned} \quad (14)$$

defining  $\kappa$  as a harmonic mean of  $(\kappa'_\nu + \sigma_\nu)$  (see eq. [62]). Thus,

$$\begin{aligned} F_x &= - \frac{4\pi}{3\rho \kappa} \frac{\partial}{\partial x} \int_0^\infty B_\nu(T) d\nu \\ &= - \frac{4\pi}{3\rho \kappa} \frac{\partial}{\partial x} \frac{\sigma}{\pi} T^4 \\ &= - \frac{ac}{3\rho \kappa} \frac{\partial T^4}{\partial x}, \end{aligned} \quad (15)$$

which is our desired result. Here  $\sigma = ac/4$ , where  $\sigma$  and  $a$  are radiation constants and  $c$  is the velocity of light. The derivation is originally due to Roseland (1924). Another early derivation was given by Eddington (1926, chap. V).

Note the physical interpretation of the flux equation when written in the form

$$F_x \frac{\kappa \rho}{c} = - \frac{\partial P_r}{\partial x}, \quad (16)$$

where

$$P_r = \frac{aT^4}{3} \quad (17)$$

is the radiation pressure. The rate of decrease of the radiation pressure with distance  $x$  is given by the change in momentum of the radiation per unit area at  $x$ . This change in momentum per unit area at  $x$  per  $dx$  is the flux passing through, multiplied by  $\kappa \rho$  to give the fraction of energy per unit area per unit time absorbed per  $dx$ , divided by  $c$ , the velocity of light.

### 1.3. USE OF OPACITIES FOR STELLAR INTERIORS

The construction of models to represent the interior of stars dates back to Kelvin (1862, 1887), Lane (1869), and Ritter (1878–99)<sup>1</sup> in the last half of the nineteenth century. Schuster (1903, 1905), as others before, suggested that radiation is an important energy transfer process, and later Schwarzschild (1906) studied atmospheric problems of pure radiation transport. In those times, however, the favorite model for stellar interiors was one with all the energy transported by convection.

The discovery of the correlation of luminosity (absolute magnitude) and effective temperature (spectral type or color) discussed in papers by Hertzsprung (1905) and Russell (1913) provided data for theories of stellar models and stellar evolution. Recourse was made to a suggestion by Helmholtz (1854) that the potential energy release by slow contraction of a gravitating mass could produce the observed luminosity of the stars. Kelvin (1861) also developed the idea, but he stated that for long periods of time this energy source would not suffice. Nevertheless, until the early 1920's the theory of stellar evolution envisioned a contraction of the M giants to the earliest type giants of smaller radius and then further contraction down the main sequence from the A stars to the M dwarfs.

These ideas were finally rejected when the age of terrestrial rocks, and presumably also the solar age, was shown to be several billion years. The solar contraction age was certain to be only about  $10^7$  years. Better mass determinations of giant and dwarf stars also show that the requirement, for this older theory, of equal mass along the main sequence of dwarfs in the Hertzsprung-Russell diagram is not met. Nuclear energy sources eventually were discovered which could keep the sun shining for periods like  $10^{10}$  years.

The radiation theory introduced by K. Schwarzschild (1906) for stellar atmospheres was exploited by Eddington (1926) from 1916 to 1926, and for the first time it was demonstrated that radiation transport can be more important in stellar interiors than convection.

In 1924 Rosseland showed that the definition given above for the average absorption coefficient is the correct one to use in Eddington's radiative stellar-model work. At about the same time Kramers (1923) developed absorption formulas using semiclassical methods. Considerations of quantum-mechanical models of atoms show that corrections to the Kramers formulas are small. Using the Kramers absorption formulae and the Rosseland mean, the theoretical average absorption coefficient called the opacity was only about one-tenth the value needed in Eddington's purely radiative stellar models. The discrepancy, to be discussed in detail later, could only be removed by allowing stars to have low mean molecular weights, that is, large hydrogen abundances.

Further theoretical work on opacities by Strömgren (1932, 1933) allowed

<sup>1</sup> See Chandrasekhar (1939, p. 178) for a complete list of Ritter's papers.

more detailed interpretation of the magnitude-spectral type or Hertzsprung-Russell diagram. Using opacity data computed by Strömberg, Cowling (1930, 1935) was able to construct a point source model. Further work on Cowling-type models has shown that the model has a convective core containing about 15 per cent of the stellar mass, but outside of this core radiation carries all the energy.

With the discovery of nuclear sources of stellar energy by von Weizsäcker (1938) and Bethe (1939), it became possible to construct models which could be used to obtain the stellar composition. M. Schwarzschild (1946), using Kramers' absorption formulas, and also a formula integrated over frequencies for the opacity, was able to obtain a homogeneous solar composition which seemed reasonable when compared with the composition inferred spectroscopically from the outer solar layers. This composition is

$$X = .47, \quad Y = .41, \quad Z = .12, \quad (18)$$

respectively, the mass fractions of hydrogen, helium, and heavy elements.

Modern Cowling models using the Bethe carbon-nitrogen cycle for converting hydrogen to helium to produce energy seem to represent actual stars more massive than the sun on the main sequence of the Hertzsprung-Russell diagram. Details of the convective core structure are easily determined using polytrope models computed by Emden (1907) and others early in this century.

In 1950 papers by Epstein, Oke, and Aller showed that main-sequence models of solar mass and less should have an appreciable energy source in the proton-proton chain. These reactions proceed at lower temperatures than the catalytic carbon-nitrogen cycle, and because of the lower temperature sensitivity of the  $p$ - $p$  chain, only about 30 per cent of the total energy is generated in the convective core. The composition for the sun determined by Epstein is

$$X = .82, \quad Y = .17, \quad (19)$$

where the composition is the same throughout the sun.

Only within the last few years have stellar models been calculated that are not homogeneous. The inevitable evolution of dwarf stars (except possibly those of very low mass) to the giant stage was discovered by Sandage and Schwarzschild (1952). The consumption of hydrogen in the central parts of stars slowly changes the central composition to mostly helium and affects the structure.

The transmutation of helium to carbon was suggested by Salpeter (1952); and this reaction changes the central composition even further. The temperature dependence of this energy source is so large that most of the energy is produced at the stellar center. The flow of energy cannot be handled by radiation alone, and a convective core results. This helium-burning core, like the Cowling-model core, is then well mixed and is homogeneous in composition.

The various stages, through which it is now known that a stellar interior

passes, are hydrogen burning with or without a convective core, core contraction to release potential energy and heat the core, and then the appearance of a convective core as helium burning commences. The detailed course of evolution beyond the red giant stage to the final white dwarf configuration is still not known. Mass loss from these stars is observed and may be an important influence on their evolution (see Deutsch [1956]).

For our opacity calculations we need to consider a range of compositions from almost pure hydrogen with perhaps only a few per cent by mass of the heavier elements like carbon, nitrogen, oxygen, neon, sodium, magnesium, aluminum, silicon, argon, and iron to a mixture of almost pure helium with the same heavy-element mixture. Fortunately, energy generation processes operate effectively only above temperatures of several million degrees, and therefore only the high-temperature material changes composition. Opacities for the wide range of mixtures in the normal evolution then do not have to be calculated for all temperatures unless, as in red dwarfs (see Osterbrock [1953] and Limber [1958*a*, 1958*b*]), convection mixes the hot transmuted material to the outer cooler regions. Only in very late evolutionary stages of stars when hydrogen burning occurs in the outer layers or in red dwarfs do we need to worry about a wide range of hydrogen and helium composition throughout the entire star.

#### 1.4. RADIATION TRANSFER IN STELLAR ATMOSPHERES

The development of models to explain the details of the emergent intensity from the solar surface and the emergent flux from the stars dates back to about the beginning of this century. Important papers were written by Schuster (1905) and Schwarzschild (1906). These papers considered that the entire gaseous atmosphere absorbed and emitted radiation at all frequencies as contrasted with the idea that there was a bright surface (photosphere) due to condensation clouds and an overlying absorbing gaseous atmosphere. A very complete discussion of stellar atmospheres by Schwarzschild produced results which could be compared with solar observations assuming that the absorption coefficient  $\kappa$  was independent of frequency.

Today the approximate analytic and numerical solutions of equation (2) give the structure of purely radiative stellar atmospheres. An atmosphere transfer problem must be solved using absorption and scattering at a number of definite frequencies or energy groups and angles from the radial direction, especially when the intensity source is largely scattered photons from incident radiation.

The absorption coefficient is not only important for determining the structure of an atmosphere, but its value can also affect the convective stability of the atmosphere. If the atmospheric absorption is low, the emergent photons will come from deep, high-pressure layers. When the absorption finally begins to increase with depth, because of the H and H<sup>-</sup> absorption, the energy transport in an extensive zone below may take place more efficiently by convection.

If the atmospheric absorption is high, as in stars of Type A or hotter, the photosphere is at a much lower pressure, and only a very thin convection zone occurs. In many cases the convection influences the observable emergent radiation intensity and spectrum.

## § 2. SUMMARY OF ABSORPTION COEFFICIENT AND OPACITY DATA

### 2.1. EDDINGTON APPROXIMATIONS FOR THE STELLAR INTERIOR OPACITY

With certain assumptions, which will be discussed later, it is possible to make the proper Rosseland integral over frequencies and obtain an approximate opacity expression

$$\kappa = \kappa_0 \rho \frac{T^{-3.5}}{t}, \quad (20)$$

where  $\kappa_0$  is a constant,  $\rho$  is the density,  $T$  the temperature, and  $t$  is Eddington's so-called guillotine factor to express the temperature and density dependent degree of ionization. With this opacity law Eddington derived a theoretical mass-radius-luminosity law

$$L = \text{constant} \frac{M^{5.5}}{\frac{\kappa_0}{t} R^{0.5}} (\mu \beta_c)^{7.5}, \quad (21)$$

where  $L$  is the luminosity of a stellar model,  $M$  the total mass,  $R$  the radius,  $\mu$  the mean molecular weight, and  $\beta_c$  the central ratio of gas pressure to the sum of the gas and radiation pressures. From this law one finds  $\kappa_0$  for the bright component of the double star Capella to be  $9 \times 10^{26}$  with  $\mu = 2.11$  and  $\beta_c = 1$ . The guillotine factor has been set to unity at the temperatures expected to be important in most of the mass of Capella, and the assumption of  $\mu = 2.11$  means that hydrogen is absent.

According to Strömberg (1932, 1933), for the Russell mixture  $\kappa_0$  is  $3.9 \times 10^{25}$ , less than one-twentieth the astronomical value. The Russell mixture, which is O, Na + Mg, Si, K + Ca, Fe in the ratios by weight 8:4:1:1:2, was expected to exist throughout a star like Capella or the sun since it was derived from the spectrum of the solar surface. Eddington had no measure of the hydrogen or helium abundances and assumed that they were very low, even though hydrogen and helium lines appeared in the sun and other stars.

One way out of the opacity discrepancy is to assume a high abundance of hydrogen and helium so that the mean molecular weight,  $\mu$  in equation (21), is reduced. This smaller  $\mu$  then lowers the astronomical opacity determination, and addition of hydrogen and helium to the Russell mixture increases the theoretical opacity somewhat. The crude models of Eddington are not able to tell us more about the opacity, especially since stars like Capella and the sun are not homogeneous in composition. Further progress in understanding stellar structure has come from improved opacity values obtained from physical principles.



## 2.2. MONOCHROMATIC ABSORPTION DATA FOR STELLAR ATMOSPHERES

The first attempt to calculate absorption coefficients for material in stellar atmospheres was made by Milne (1925*a, b*) using the Kramers formulae. The absorption was assumed to be constant with depth in the atmosphere. Stellar-atmosphere absorption coefficients were incorrect at first because of imperfect knowledge of the composition. McCrea (1929) considered the absorption due to the dominant hydrogen instead of pure calcium which was assumed by Milne, but his opacity was inaccurate and the derived gas pressure in the solar photosphere still was not enough to support the atmosphere as observed.

The new quantum mechanics now was able to correct the Kramers formulae, and Gaunt (1930) and Stobbe (1930) introduced a factor to be applied to the semiclassical formulae to make them more nearly correct. These Gaunt factors were used by Pannekoek (1935), Unsöld (1938), etc., for atmosphere problems, but no one was able to predict the emergent intensity versus wavelength for the solar surface.

Wildt (1939) discovered that the negative ion of hydrogen has a large enough abundance in the solar surface to cause considerable absorption. Theoretical  $H^-$  absorption coefficients were soon accurately calculated by Chandrasekhar and Breen (1946), and immediately the predictions of the emergent spectrum of the sun showed great improvement. The recent inclusion of absorption by pseudo-molecular hydrogen according to Zwaan (1962) makes the predicted solar spectrum agree very well with observations. The best available monochromatic absorption coefficients including absorption by the negative hydrogen ion and the heavier elements have been given by Vitense (1951), and are discussed in section 2.5.

## 2.3. STRÖMGREN OPACITY RESULTS

Strömgren (1932, 1933) presented opacity results for various proportions of hydrogen and the Russell mixture of heavy elements. Mixtures were made by assuming the hydrogen was transparent and only changed the average molecular weight. More modern calculations show that hydrogen is capable of producing a sizable fraction of the opacity at stellar centers by free-free absorption, and in stellar envelopes by bound-free absorption.

In the second Strömgren paper the contribution to the opacity due to electron scattering is considered. The large number of electrons from hydrogen can produce Thomson or Compton scattering at very high temperatures where pure absorption processes are not very important. A rule for combining the effects of absorption,  $\alpha$ , and scattering,  $\sigma$ , at a given temperature and electron density has been given: "The resulting opacity is equal to the greater of the quantities  $\alpha$  and  $\sigma$  plus 1.5 times the smaller." Accurate computations over a wide range of temperature and density show that this simple rule is not of very high accuracy.

The Strömgren papers present a method for opacity calculations which is described in § 4. This method can consider all the absorption and scatter-

ing processes mentioned briefly in this section and discussed in detail in § 3. Using the original Strömgren method, opacities have been calculated by Harrison (1948, 1950) and by Epstein and Motz (1954).

#### 2.4. MORSE OPACITIES

Morse (1940), using improved ideas about the occupation of various energy levels by electrons, presented new opacities for the Russell mixture and three other new mixtures. The improved occupation numbers affect the absorption due to the photoelectric or bound-free process. Also better values for the number of bound electrons in atoms affect the number of free electrons that can absorb photons by the free-free process.

All the Rosseland mean opacities were computed without including electron (Thomson and Compton) scattering. An approximate procedure is therefore given to combine the true absorption opacity with the scattering effect. Results are given in a tabular form where the ratio of  $\bar{\kappa}_s/\bar{\kappa}_a$  is given versus  $\bar{\kappa}/\bar{\kappa}_a$ .  $\bar{\kappa}_s$  is the scattering opacity evaluated at the energy of the photon distribution peak, i.e., at four times the  $kT$  values in energy units.  $\bar{\kappa}_a$  is the Rosseland mean for only the true absorption processes.  $\bar{\kappa}$  is the total opacity including both absorption and scattering, and this opacity can be obtained, if  $\bar{\kappa}_a$  and  $\bar{\kappa}_s$  are known, from tables and formulae given by Morse.

The four Morse mixtures include the elements iron, potassium, calcium, silicon, sodium, magnesium, and oxygen. In order to obtain the opacity of an intermediate mixture, an elaborate interpolation formula is given which allows one to change the abundances of Fe, K + Ca, Si, Na + Mg, and O over small ranges. The opacities, while much more accurate than those of Strömgren, are not as accurate as 10 per cent except at the Compton limit.

The opacities are given by the Kramers opacity formula form, such as in equation (20). The guillotine factor tabulated by Morse has its own dependence on temperature and density. It is noted that for the Russell mixture the guillotine factors give an opacity variation from the zero to the negative 9/2 power of the temperature. The reason for these departures from the Kramers opacity formula is due to particular electron shells in the atoms becoming suddenly depleted as the temperature rises, reducing the photoelectric absorption.

Morse did not use his results to discuss stellar models. Other opacities, however, obtained later by Biermann (1943) were used in the study of stellar interiors at about that time. Until the results of Keller and Meyerott (1955), the Morse data were the only extensive high temperature opacity results.

#### 2.5. MONOCHROMATIC ABSORPTION COEFFICIENTS

The Morse results could not be improved until better Gaunt factors and more efficient computing methods were available, but there are other early tabulations that are worth mentioning here because of their use even today.

A tabulation by Strömgren (1944) for pure hydrogen and the negative hydro-

gen ion has been extensively used for work on stellar atmospheres. Metals are present in the mixtures, but they only contribute to the electron pressure. These tables give  $\log \kappa$  versus  $\log P$  and  $5040/T = 0.3\text{--}1.1$  for most cases. Methods described by Unsöld (1938) and similar to ones described in section 4.4 are used to obtain the absorption from the highly excited states of hydrogen. Only bound-free absorption with unit Gaunt factors is considered along with the constant bound-free  $H^-$  cross-section of  $26 \times 10^{-18} \text{ cm}^2$  per  $H^-$  ion. These monochromatic absorption coefficients have been recalculated by Strömgren with improved absorption data. The newer tables have been extensively used, but no publication of these improved data has been made.

Other useful data are the Vitense (1951) continuous monochromatic absorption coefficients and opacities at the temperatures and densities of stellar atmospheres. The Vitense mixture has the composition

$$X = .561, \quad Y = .407, \quad Z = .032, \quad (22)$$

with the number fractions and weight fractions given by Unsöld (1955). Data for the mean molecular weight and gas pressure (pressure equation of state) are available from Rosa (1948). Unsöld (1948), and Rosa and Unsöld (1948) give the entropy, adiabats, specific heats, and the enthalpy (caloric equation of state). The temperature range in this absorption tabulation goes from  $3877^\circ \text{ K}$  to  $100,800^\circ \text{ K}$ , with the electron pressure ranging from about  $10^{-1}$  to  $10^7$  dynes/cm<sup>2</sup> in such a manner that only low electron pressures are considered at the low temperatures and only the high electron pressures are considered at the highest temperatures.

Monochromatic absorptions are allowed due to atomic hydrogen, the negative hydrogen ion, neutral and once ionized helium, the ions C, Ne,  $\text{Ne}^+$ , Fe, Si, Mg, Ca. Also included are Thomson and Rayleigh scattering. No molecular absorptions are allowed because their effect is small. The heavy ions are considered using a simplified Kramers bound-free absorption formula for hydrogen with an effective nuclear charge determined from observed energy levels. This effective nuclear charge is about 4 or 5 for deep levels. The abundances of these ions and their excited states are determined by a combination of the Boltzmann excitation and Saha ionization formulas to be discussed in section 4.4. The highly ionized ions of oxygen, neon, nitrogen, and carbon are considered only approximately because their absorption lies in the far ultraviolet. There is no allowance for line absorptions (blanketing).

These Vitense data are plotted as  $\kappa_\lambda/P_e$  versus  $\lambda$ , the wavelength. Values can be obtained easily and accurately, but unfortunately if one desires absorption for another mixture, this tabulation cannot be used.

Monochromatic absorption coefficients for neutral hydrogen including free-free absorption, neutral helium, and once ionized helium have been tabulated by Ueno, Saito, and Jugaku (1954). These data have been used by Ueno (1954)

who tabulates equations of state and opacities for a mixture similar in composition to that used by Vitense. In the mixture, absorption is allowed by hydrogen, the negative hydrogen ion, and helium. Consideration is given also to electron scattering, but no absorption due to elements heavier than helium is included.

## 2.6. OPACITIES WITH FREE-FREE ABSORPTION IMPROVEMENTS

As knowledge of stellar structure advanced, it was realized that at the centers of many stars absorption is due largely to free-free transitions in the field of the hydrogen ions. The central opacity influences the structure of a star and determines whether a convective core exists. To improve models and predict accurate stellar evolution, one needs free-free Gaunt factors at these temperatures. The free-free Gaunt factor expansion of Menzel and Pekeris (1935), used so widely, is really valid only at very low temperatures or at high frequencies.

Tsao (1954), Zirin (1954), and Kulsrud (1954) attempted calculations for free-free Gaunt factors. Tsao and Zirin have not tabulated averages of the Gaunt factors over either a Maxwell-Boltzmann or Fermi-Dirac electron distribution. However, Kulsrud did average his Gaunt factors over a Maxwell-Boltzmann electron velocity distribution, and they agree well with the more detailed recent results at very high temperatures. The early limited results have been surpassed by more extensive calculations of Rudkjøbing (1955, 1959), Berger (1956), Karzas and Latter (1958*a*, 1961), and Greene (1959). Gaunt factors for a wide range of electron velocities, their average over a Maxwell distribution, and the effects of screening of the nucleus by surrounding bound electrons are discussed by Grant (1958). Green (1958, 1960) has calculated corrections to the hydrogen-like free-free Gaunt factors due to both electron degeneracy and screening of the nuclear fields by other free charged particles.

Only opacities for pure hydrogen at four densities have been calculated by Tsao. Kulsrud confines his discussion to Gaunt factors and does not present any new opacities.

Using his own Gaunt factors Zirin gives opacity tables for three new mixtures. These tables contain errors which have been corrected in a second paper by Zirin (1958). This second paper also has typographical errors such that in Table 5 the opacities are given in the wrong order except the opacities at  $3.14 \times 10^6$  °K and density 1 gm/cm<sup>3</sup>. In this second paper, however, Zirin has given opacities which for the first time consider ionic splitting of absorption edges. We shall discuss this improvement in opacity calculations in more detail later.

## 2.7. KELLER AND MEYEROTT OPACITIES

In 1955 a tabulation of opacities for thirteen mixtures was published by Keller and Meyerott (1955). Principles previously established by Strömgren (1932), Morse (1940), and Mayer (1947) were used.

Opacities for each mixture are given at 63 pairs of temperature and density.

The compositions of the mixtures cover the range of interest in modern astrophysics, but leave gaps a little too large for accurate interpolation. For example, the solar composition is thought to be about  $X = 0.60$ ,  $Y = 0.38$ ,  $Z = 0.02$  (Aller 1961), which is not near any of the listed compositions. One heavy element mixture is given to show the effects of very low hydrogen and helium abundances.

The opacities have been calculated using the usual Kramers absorption formulas together with Gaunt factors. For hydrogen and helium the bound-free Gaunt factors are those tabulated by Mayer. For elements heavier than hydrogen and helium, special methods of obtaining cross-sections were developed, and these methods involving Hartree-type wave functions are described by Meyerott (1954) and Moszkowski and Meyerott (1956). These heavy-element cross-sections were also used by Zirin (1954, 1958).

The free-free Gaunt factor for hydrogen and helium is again the Menzel-Pekeris expansion, which is not accurate at high temperatures. Unity is used as the free-free Gaunt factor for the heavier elements. The free-free effects considered by Tsao, Zirin, and Kulsrud are not used, because none of these latter authors gives Gaunt factors that are general enough or in a form that can be used easily.

Unlike the Strömgren and Morse data, the Keller and Meyerott opacities include electron scattering according to Mayer (see § 4.3).

Keller and Meyerott were the first to calculate extensively on an electronic computing machine, though Zirin did do some work previously. Computations of the positions and amplitudes of absorption edges were done by hand with a degeneracy parameter  $\eta$  and the temperature as independent variables. Use of  $\eta$  and  $T$  yield occupation numbers directly without the iteration needed when input data are temperature and density. The occupation number data are in a form such that mixtures other than the original thirteen are easily calculated. The computing program which now exists at Indiana University can calculate opacities for any mixture of certain elements but only for a certain set of temperatures and degeneracy parameters.

The Keller and Meyerott results for astrophysical mixtures were preceded by opacities for pure elements and mixtures reported by Moszkowski and Meyerott (1951) and Meyerott and Moszkowski (1951) in Argonne National Laboratory reports. Some of these opacities have been calculated considering the approximate effect of line absorptions. Olson (1958) has extended the Keller and Meyerott continuous opacity methods to other compositions.

Almost all the recent work on stellar interior models has been based on Keller and Meyerott opacities. However, some workers in stellar structure are now using high speed computers to calculate their own opacities for the exact mixture being used, making the uncertain interpolation in the Keller-Meyerott data unnecessary.

### § 3. ABSORPTION AND SCATTERING PROCESSES AND ELECTRON CONDUCTION

#### 3.1. BOUND-FREE ABSORPTION

The absorption and scattering processes in this section are discussed in order of their importance in studies of stellar structure.

The photoelectric ejection of an orbital electron from either the ground state or from an excited state is usually the primary mechanism of photon absorption in stars. For *bound-free absorption*, the photon to be absorbed must have at least enough energy to ionize the electron, however. Photon energy in excess of the binding energy can go into kinetic energy of the free electron. Kramers was the first to give a reasonably accurate expression for the bound-free absorption.

Both the bound-free and the free-free absorption, which is discussed next, were considered by Kramers on the basis of classical radiation from electrons being accelerated in the field of the nuclear charge. The resulting radiation in the frequency range corresponding to the bound edge is arbitrarily assigned to free-bound radiation. With the free-bound emission known, equilibrium arguments give the bound-free absorption. Quantum-mechanical corrections to Kramers formula are usually small, and they are accounted for by multiplication by a Gaunt factor  $g$ .

The bound-free cross-section for an atom with an electron in level  $n$  is written<sup>2</sup>

$$\begin{aligned}\sigma_{bf} &= \frac{2^6 \pi^4}{3 \sqrt{3}} \frac{Z^{*4} m e^{10}}{c h^6 n^5 \nu^3} g_{bf} \\ &= 2.82 \times 10^{29} \frac{Z^{*4}}{n^5 \nu^3} g_{bf} \text{ cm}^2,\end{aligned}\tag{23}$$

where  $Z^*$  is an effective nuclear charge,  $n$  is the principal quantum number of the initial state,  $\nu$  is the frequency in  $\text{sec}^{-1}$ , and the other atomic constants have their usual meaning.

The Gaunt factor depends on the quantum numbers of the initial states and the photon energy in excess of the ionization energy. All extensive opacity calculations have assumed that the bound-free transitions occur in hydrogen-like atoms where the electric fields are Coulomb. In this case the free-electron energy parameter, on which  $g$  depends, can be scaled by the effective nuclear charge for ease in tabulation.

The most accurate and recent hydrogen-like Gaunt factors, due to Karzas and Latter (1958b, 1961) show that for all the principal and orbital quantum numbers ( $n$  and  $l$ ) of the initial states which they list, the Gaunt factor is always within about 50 per cent of unity at the absorption edge where the free electron has just zero kinetic energy. Most initial states have Gaunt factors only 20 per

<sup>2</sup> Note  $\sigma_\nu$  and later  $\sigma_e$  and  $\sigma_{ei}$  are the scattering opacity in  $\text{cm}^2/\text{gm}$  whereas other  $\sigma$ 's which have subscripts like  $\sigma_i$  or  $\sigma_{bf}$  are cross-sections in cgs units of  $\text{cm}^2$ .

cent from unity at the edge. For high photon energies (high frequencies) the Gaunt factors sometimes grow to over 30 (for the  $6s$  initial state), while for others, like the  $6h$  initial state, the Gaunt factor decreases exponentially to less than 0.1 at a free-electron energy equal to the ionization energy. In spite of these extremes at free-electron energies somewhat greater than zero, the average value of this correction factor to the Kramers formula is close to unity, because at photon energies near the edges the absorption is largest.

In a mixture of elements whose absorption is desired, one must add at each photon energy (frequency) the absorptions due to all processes. This means that photons can be absorbed by liberating bound electrons from all those shells where the binding energy is less than or equal to the incoming photon energy. While the Kramers formula says that absorptions are most important right at the edge, one must sum over all possible absorptions by bound electrons even far from the edge. The abundance of electrons in certain shells may outweigh the approximate  $1/\nu^3$  decrease at increasing frequency, and one absorption far from an edge may still dominate other absorption processes. At very low frequencies there is no bound-free absorption, but as the frequency increases one must sum over an ever increasing number of initial bound states.

The bound-free absorption depends on the equilibrium number of electrons which are bound in the various atomic states. These *occupation numbers* for each state are obtained by applying ionization and excitation formulas as will be seen later. When ionization of an element is complete, no more bound-free absorption due to that element can occur. The ultimate guillotine has then fallen on that element, according to Eddington. In astrophysical mixtures, the abundance of iron is enough so that its bound-free absorption by the  $K$  shell electrons keeps the opacity moderately large even up to several million degrees.

A correction factor to the cross-section is needed to allow for the availability of a final state for the ejected electron in the continuum. This probability of finding an unoccupied free state is

$$q_{bf} = 1 - \frac{1}{\exp\left(\frac{E_f}{kT} - \eta\right) + 1} \quad (24)$$

$$= \frac{1}{\exp\left(\eta - u - \frac{E_{ijk}}{kT}\right) + 1} \leq 1,$$

where  $E_f$  is the final free-electron energy and  $E_{ijk}$  is the (negative) energy of the bound state  $k$  corrected for the depression of the continuum level. Here  $u = h\nu/kT$  with  $h$  the Planck constant,  $\nu$  the incoming photon frequency,  $k$  the Boltzmann constant,  $T$  the temperature, and  $\eta$  is a degeneracy parameter to be discussed in the next section.

## 3.2. FREE-FREE ABSORPTION

After most elements in an astrophysical mixture have been ionized and absorption of photons by the photoelectric process is no longer important, it is still possible for a free electron to absorb a photon and change its free orbit to another free orbit in the field of a nuclear charge. Again, Kramers, on the basis of semiclassical arguments, gives a formula for the cross-section per ion of charge  $Z^*$ :

$$\begin{aligned}\sigma_{ff} &= \frac{2^4 \pi^2 Z^{*2} e^6}{3 \sqrt{3} h c (2 \pi m)^{3/2}} \frac{N_e}{(kT)^{1/2} \nu^3} g_{ff} \\ &= 3.69 \times 10^8 \frac{Z^{*2} N_e g_{ff}}{T^{1/2} \nu^3} \text{ cm}^2,\end{aligned}\quad (25)$$

where  $Z^*$  is an effective nuclear charge,  $N_e$  is the number of electrons per cubic centimeter, and  $T$  and  $\nu$  are in cgs units. This *free-free cross-section* has to be multiplied by the number density of ions of effective charge  $Z^*$  which exist in the mixture, and a sum over all ions must be made to get the total free-free absorption.

A Gaunt factor for free-free transitions exists for each free-electron energy and each photon energy being absorbed. The  $g_{ff}$  in the above formula has been averaged over the Maxwell velocity distribution for the electrons to make it depend only on the temperature and photon frequency. These data for hydrogen-like fields have been given in great detail by Karzas and Latter (1958a, 1961).

In case the density is high and the temperature is low, i.e., the electron distribution is degenerate, we must look at the averaging more closely. The Kramers cross-section for an electron at velocity  $v$  relative to the nucleus of charge  $Z^*$  is

$$d\sigma_{ff}(v) = \frac{4\pi Z^{*2} e^6 N_e(p) dp}{3 \sqrt{3} h c m v^3} g_{ff}(v), \quad (26)$$

with  $N_e(p)dp$  the electron density in the velocity range  $dv = dp/m$ . Now neglecting relativistic effects

$$N_e(p) dp = \frac{8\pi p^2}{h^3} \frac{dp}{\exp\left(\frac{p^2}{2mkT} - \eta\right) + 1}, \quad (27)$$

where  $p$  is the electron momentum,  $m$  the electron mass, and  $\eta$  is the degeneracy parameter. To evaluate the quantity

$$\frac{N_e(p) dp}{m v} g_{ff}(v), \quad (28)$$



we need to obtain the integral

$$\frac{8\pi}{h^3} \int_0^\infty \frac{p dp g_{ff} q_{ff}}{\exp\left(\frac{p^2}{2mkT} - \eta\right) + 1}, \quad (29)$$

where

$$q_{ff} = \frac{1}{\exp(\eta - u - x) + 1} \leq 1 \quad (30)$$

is a factor for the availability of a final state which we introduce here just as in the bound-free absorption. Here, as also below,

$$\frac{p^2}{2mkT} = x. \quad (31)$$

Note that in the Fermi-Dirac statistics we ignore the potential energy of the electrons due to their interactions with other electrons. Later, we shall be able to adjust the energy zero point by a quantity  $E_0$  so that the potential energy of the free electrons does not need to be considered in the Fermi-Dirac statistics.

The cross-section integral becomes

$$\begin{aligned} \frac{8\pi mkT}{h^3} \int_0^\infty \frac{g_{ff} q_{ff} dx}{\exp(x - \eta) + 1} &= \frac{8\pi mkT}{h^3} \bar{g}_{ff} \int_0^\infty \frac{dx}{\exp(x - \eta) + 1} \\ &= \frac{8\pi mkT \bar{g}_{ff}}{h^3} \ln(1 + e^\eta), \end{aligned} \quad (32)$$

where here the averaged Gaunt factor includes the  $q_{ff}$  factor. Therefore

$$\sigma_{ff} = \frac{2^5 \pi^2 Z^{*2} e^6 kT}{3 \sqrt{3} h^4 c \nu^3} \ln(1 + e^\eta) \bar{g}_{ff}, \quad (33)$$

where  $\bar{g}_{ff}$  depends on the frequency, temperature, and, if degenerate, on  $\eta$ . The  $\bar{g}_{ff}$  for degenerate cases have been tabulated by Green (1960).

The quantity  $\eta$  depends on the electron density and temperature by the non-relativistic expression

$$\begin{aligned} N_e &= \frac{8\pi}{h^3} \int_0^\infty \frac{p^2 dp}{\exp\left(\frac{p^2}{2mkT} - \eta\right) + 1} \\ &= \frac{4\pi}{h^3} (2mkT)^{3/2} \int_0^\infty \frac{x^{1/2} dx}{\exp(x - \eta) + 1} \\ &= \frac{4\pi}{h^3} (2mkT)^{3/2} F_{1/2}(\eta), \end{aligned} \quad (34)$$

where  $F_{1/2}(\eta)$  is the Fermi-Dirac integral of order one-half. This  $F_{1/2}(\eta)$  is the same quantity as  $(\sqrt{\pi}/2)N_e/G(T)$  used by Chandrasekhar (1939). Other Fermi-

Dirac integrals of half-integral or integral orders are defined by the power of  $x$  in the integrand numerator. For use of  $F_{3/2}(\eta)$  for electron pressure see equation (135). The Fermi-Dirac integrals are compiled by McDougall and Stoner (1939).

For small degeneracy (large negative  $\eta$ ),

$$F_{1/2}(\eta) \cong \frac{\sqrt{\pi}}{2} e^{\eta} \quad (35)$$

$$\ln(1 + e^{\eta}) \cong e^{\eta} \quad (36)$$

and

$$\begin{aligned} \sigma_{ff} &= \frac{2^6 \pi^{3/2} Z^{*2} e^6 k T}{3 \sqrt{3} h^4 c \nu^3} F_{1/2}(\eta) \bar{g}_{ff} \\ &= \frac{2^6 \pi^{3/2} Z^{*2} e^6 k T N_e h^3}{3 \sqrt{3} h^4 c \nu^3 4\pi (2 m k T)^{3/2}} \bar{g}_{ff}, \end{aligned} \quad (37)$$

which can be simplified to what was obtained before. Note that a possible normalizing factor for  $\bar{g}_{ff}$  is  $\ln(1 + \eta^3)$  in equation (32) though other normalizations, such as  $F_{1/2}(\eta)$ , or none at all, are possible (Marshak 1941).

At temperatures approaching  $10^7$  ° K in astrophysical mixtures, free-free absorption in the field of hydrogen ions is very important. Thus, accurate Gaunt factors are necessary, and in many cases the average should be over the correct Fermi-Dirac distribution.

Another effect in free-free transitions is the shielding of the nuclear charge by free electrons and ions. Sagdeev (1956) has investigated the effects of screening and the simultaneous interaction of an electron with many ions. A first-order screening theory by Green (1958) assuming a Debye-Hückel shape of the electrostatic potential function has been found to be adequate for most applications in astrophysics. Both degeneracy and screening reduce the free-free absorption, but these effects are found to have a maximum effect of only 10 per cent or less at moderate densities and  $10^6$  ° K.

### 3.3. COMPTON SCATTERING

The derivation of the formula for the average absorption or opacity showed that to the true absorption-process cross-sections one should also add the cross-section for *electron scattering*. It can be shown that a classical oscillator will absorb energy from a radiation field according to the formula

$$\sigma_R = \frac{\pi e^2}{m c} \frac{2\nu^2 \left(\frac{\nu}{\nu_0}\right)^2 \frac{\gamma}{2\pi^2}}{(\nu^2 - \nu_0^2)^2 + \nu^2 \left(\frac{\gamma}{2\pi}\right)^2}, \quad (38)$$

where  $\gamma$  indicates the width of the resonance which occurs at  $\nu_0$ .

From the classical expression for the radiation of this accelerating oscillator

with electron mass and charge, one gets a classical width or damping constant (Heitler 1954; Unsöld 1955; Aller 1963)

$$\gamma = \frac{8\pi^2\nu_0^2e^2}{3mc^3}. \quad (39)$$

The quantum-mechanical damping constant has almost the same value even though it is a function of the bound level. This variation of the absorption of radiation around the resonance of a classical oscillator is called natural broadening. Unfortunately, other effects of broadening are important for the "line" absorption near resonance, but here we concern ourselves only with frequencies far removed from  $\nu_0$ . Coherent scattering which uses equation (38) will be discussed in § 3.6.

When the photon frequency is large compared to  $\nu_0$ ,

$$\sigma_T = \frac{\pi e^2}{mc} \frac{\gamma}{\nu_0^2 \pi^2} = \frac{8\pi e^4}{3m^2 c^4} = .665 \times 10^{-24} \text{ cm}^2. \quad (40)$$

This is the Thomson cross-section. Our present situation has an electron being excited by a frequency so high that it essentially does not get a chance to move with any amplitude around its equilibrium position. Thus, we have an electron cross-section which will be applied only to free electrons.

At higher photon frequencies or energies, energy is actually given to an electron by photon recoil, and the cross-section at a given frequency is less than the above Thomson value. The Thomson cross-section for unpolarized photons depends on the relative angle  $\Theta$  between the incident and scattered photon in the form

$$\frac{3}{4} (1 + \cos^2 \Theta). \quad (41)$$

For photon energies small compared to the electron rest-mass energy  $mc^2$ , the Compton cross-section has the approximate form

$$(1 + \cos^2 \Theta) \left[ 1 + \frac{h\nu}{mc^2} (1 - \cos \Theta) \right]^{-2}. \quad (42)$$

More accurate formulas due to Klein and Nishina are given by Heitler (1954), and they must be considered for opacities at very high stellar temperatures.

Recently Sampson (1959) has shown that for Compton scattering, where the energy of the photon is significantly changed by the scattering process, the scattering of photons into and out of a beam of radiation does not cancel as previously assumed. The equation of transfer as given in equation (2) is not correct when the scattered photon energy differs from the incident photon energy. Sampson's results are opacities even lower than one expects from the Klein-Nishina formula, unless densities are so low that extensive pair production occurs. The production of positrons at temperatures approaching the threshold energy of  $2mc^2$  can increase the number of scatterers and therefore the opacity if

the density is not high enough to suppress positron formation. For example, at  $10^9$  ° K one must have densities above about  $5 \times 10^8$  gm/cm<sup>3</sup> to prevent appreciable increase in electron and positron numbers.

One should note that nuclei can also scatter photons, but, due to their much larger mass, the Thomson and Compton cross-sections are smaller by a factor of about  $(1840)^2$  times the square of the atomic mass.

Some corrections may be needed for the free-electron Compton scattering due to collective effects of neighboring electrons. These possible corrections are discussed in § 4.7.

Improvements to the Strömberg and Morse methods of treating free-electron scattering in opacity calculations, given by Mayer and used by Keller and Meyerott, are discussed in § 4.3.

### 3.4. BOUND-BOUND ABSORPTION

The effects of many lines close together (blanketing) have been important in studies of stellar atmospheres for many years. Accurate quantitative calculations of *bound-bound absorption* have not yet been made very extensively either for the high temperature stellar-interior case where one uses the opacity or for the atmospheric case where monochromatic absorption coefficients are needed. Mayer (1947) treats the problem in some detail, but he obtains moderately accurate numerical results only for pure iron at  $1.16 \times 10^7$  ° K and 7.85 gm/cm<sup>3</sup>. See also Moszkowski and Meyerott (1951) and Carpenter (1957).

From our discussion of the classical oscillator (eq. [38]), the naturally broadened cross-section for resonant absorption near the line center can be approximately written as

$$\sigma_R d\nu = \frac{\pi e^2}{m c} f \left( \frac{\frac{\gamma}{4\pi^2}}{(\nu - \nu_0)^2 + \left(\frac{\gamma}{4\pi}\right)^2} \right) d\nu, \quad (43)$$

where  $f$  is the oscillator strength which corrects this expression for quantum-mechanical effects. Collisions of the absorbing atom with neighbors during the time of absorption also broadens the line according to the same formula with a different  $\gamma$ .

We must add to natural and collisional broadening the effects of Doppler and Stark broadening. The cross-section for the Doppler case is

$$\sigma_D d\nu = \frac{\pi e^2}{m c} f \left( \frac{M c^2}{2\pi kT} \right)^{1/2} \frac{d\nu}{\nu_0} \exp \left[ -\frac{M c^2}{2kT} \left( \frac{\nu - \nu_0}{\nu_0} \right)^2 \right], \quad (44)$$

where now  $M$  is the mass of the atom in which the bound-bound transition occurs. For all temperatures at which there are bound electrons so that line absorption can occur, Doppler cores are too narrow to affect significantly either the monochromatic absorption or the opacity. For hydrogen lines in a stellar

atmosphere, Stark broadening is dominant (Griem, Kolb, and Shen 1959; Griem 1960), but for opacity calculations in the deep interior it appears that collisional broadening alone is important. A combination of natural, collisional, and Doppler broadening is discussed by Hjerting (1938) and Harris (1948). Recent reviews of the theories for line shapes have been given by Margenau and Lewis (1959), by Traving (1960), and by Aller (1963).

The Moszkowski-Meyerott (1951) formula, due to Sternheimer in an unpublished report "Line Widths for Opacities" and used extensively in this chapter, is

$$\frac{\delta_u}{4\pi} = \frac{1}{4\pi} \frac{h\gamma}{kT} = 0.0134\rho \frac{y}{\sum_i x_i \mu_i} \frac{n_{ik}^4 + n_{ik'}^4}{T^{3/2} Z_{ik}^{*2}}, \quad (45)$$

where  $n_{ik}$  and  $n_{ik'}$  are the initial and final principal quantum numbers,  $Z_{ik}^*$  an effective nuclear charge of the initial level, and  $T$  the temperature in kilovolts (one kilovolt =  $11.6052 \times 10^6$  °K). The number  $y$  is the number of free electrons per average atom at density  $\rho$  as is discussed later, and the sum over the individual molecular weights gives the total molecular weight of the mixture unit atom which has  $\sum_i x_i$  particles in it. The principal quantum numbers here are raised to the fourth power, but if detailed line splitting is not taken into account, another power of  $n$  can allow for the splitting in the line-width formula. This formula for the collisional width is very similar to the collisional width used by Griem (1960). An uncertainty in  $\delta$  means the same uncertainty in the cross-section because at moderate distances from  $\nu_0$  the cross-section is proportional to  $\delta$ .

The influence of line absorption on the opacity, of course, depends on the position of the line in the emission spectrum of the matter. The shape of an individual line seems to be less important in most absorption calculations than an accounting of the positions of all the components of the lines. For a given line the wing can be allowed to extend only to the centers of the neighboring lines, which have the same initial level.

At temperatures that occur in the atmospheres of stars, hydrogen and helium lines are very strong, and a more accurate shape may be required for these lines. An approximate theory of Stark line shapes due to Griem (1960) is therefore used for H and He II lines, while equation (45) is still used for the neutral He lines. Later discussion shows that the opacity, at least, is not very sensitive to the line widths, but the use of the Stark shape for H and He II is not absolutely necessary for accurate values.

Line absorption is important for the determination of stellar structure at and below temperatures of  $5 \times 10^6$  °K. At lower temperatures lines can increase the opacity by a factor of two or more. At temperatures such as at the center of the sun, however, line absorption contributes less than 10 per cent of the total opacity.

### 3.5. NEGATIVE ION ABSORPTION

At low temperatures such as are met in the very outer layers of a star, it is possible that neutral atoms and molecules attach another electron to become a negative ion. The *photoionization* of these ions is a source of continuous photon absorption. As in atomic bound-free absorption, the photon to be absorbed has to have enough energy to liberate the bound electron. Free-free absorption in the field of the neutral atom or molecule is also possible.

Numbers of negative ions are known, but apparently the only negative ion of importance in astrophysics is that of hydrogen. Its importance has been shown by Wildt (1939), and many have contributed to the intricate quantum-mechanical calculations to obtain the bound-free and free-free absorption coefficient. The absorption edge is at 0.75 electron volt, the binding energy of the extra electron, and this corresponds to a wavelength of about 16,500 Å. In typical cases like the solar atmosphere, the  $H^-$  free-free absorption, which depends on the number of free electrons, is not important except at wavelengths near or longer than the  $H^-$  bound-free edge. Tables of the  $H^-$  bound-free absorption cross-sections are available from John (1960*a*, *b*) and from Geltman (1962), and Ohmura and Ohmura (1960, 1961) have made available free-free cross-sections per unit electron pressure and per neutral hydrogen atom.

Most negative ions have ionization potentials of only one volt or so. Thus, their importance in astrophysics is limited to stellar atmospheres where the Rosseland mean absorption or opacity is not used very often. However, the continuous absorption coefficients needed in computing radiation transport are determined partly or even completely by negative hydrogen ion absorption.

### 3.6. COHERENT, RAMAN, AND RAYLEIGH SCATTERING

*Coherent scattering* by atoms leaves them in the same energy state after the scattered photon departs in a direction different from the incident photon. *Raman scattering*, neglected in all opacity calculations to date, leaves the atom in a state different from the original one. Consideration of both coherent and Raman scattering by Heitler (1954) shows that the cross-sections are similar to the Compton cross-section. Equations (38) and (39) give the coherent scattering cross-section. Mayer (1947) recommends that to include these effects one should treat all electrons, bound or free, as contributing to the Compton scattering. When there are many bound electrons, the photoelectric absorption will dominate. In the case where all or almost all electrons are free, there is essentially no coherent or Raman scattering by bound electrons anyway. A more correct treatment, however, uses the Compton formula for only the free electrons and the coherent scattering formula for the bound electrons.

An interesting case of coherent scattering is that considered by Rayleigh (1899). When one is at some distance from a resonance as given by the classical theory, one can have either *Thomson* or *Rayleigh scattering*. The first case was

the extreme when the incident photon had a frequency so high that one could neglect  $\nu_0$  compared to  $\nu$ . In the other extreme  $\nu_0 \gg \nu$ , the Rayleigh total cross-section becomes

$$\sigma_{\text{Ray}} = \frac{\pi e^2}{m c} \frac{\nu^4 \gamma}{\nu_0^2 \pi^2} f \quad (46)$$

at a distance from the resonance center large compared to  $\gamma$ . Here the  $f$  value corrects the expression for quantum-mechanical effects. Using the previously described classical damping constant, at large distances from the true line

$$\sigma_{\text{Ray}} = \frac{8\pi e^4 \nu^4 f}{3 m^2 c^4 \nu_0^4} = \sigma_T \frac{\nu^4}{\nu_0^4} f. \quad (47)$$

Rayleigh scattering can be the only source of photon attenuation at very low temperatures in atmospheres with low metal abundance. This is because at the low temperatures bound-free edges and their associated lines are far in the ultraviolet, and free-free absorption, free-electron scattering, and negative hydrogen ion absorption are small because there are very few free electrons. Indeed, in the terrestrial atmosphere molecular Rayleigh scattering dominates the small amount of molecular-band and atomic-line absorption in the visible region of the spectrum. This scattering is large enough to make the sky appear blue, but small enough so that the atmosphere is very transparent to visible light.

In the earth's atmosphere and in many astrophysical cases, the spacing between atomic and molecular oscillators is small compared to the wavelength of the incident light. This would lead one to suspect that the total scattered light would not be the sum of the contributions from the individual atoms or molecules but would depend on the particle correlations. Actually in a gas there is no permanent ordering of the oscillators, as in a crystal, and therefore there is no permanent interference between the scattered waves from different oscillators. Thus, in computing Rayleigh scattering for a gas, one can assume the oscillators are all independent.

Anisotropic molecules, which cannot oscillate in perfect resonance with the incoming wave, scatter according to the Rayleigh formula with a small correction factor. A discussion of this point and some applications of molecular Rayleigh scattering are given by Chandrasekhar (1950) and Van de Hulst (1957).

### 3.7. MOLECULAR ABSORPTION

The absorption due to *molecules* that form in stellar atmospheres is poorly known and is only partially accounted for in the results given in this chapter. While molecular bands do appear in spectra of many stars, only for the coolest stars with surface temperatures of less than 4000° K are absorption data necessary. Monochromatic absorption coefficients for  $\text{H}_2^+$  ions (Bates 1952), quasi- $\text{H}_2$  molecules (Erkovich 1960; Zwaan 1962), water vapor, or other molecules

may be necessary to construct models of cool atmospheres for studies of stellar abundances. The blanketing effect due to overlapping molecular bands is probably a very important source of absorption in low temperature atmospheres.

### 3.8. PAIR PRODUCTION

High energy photons called gamma rays have enough energy to create an electron-positron pair. The threshold is at about 1.02 Mev energy for this process, and photon energies can get that high even below the maximum temperatures supposed to exist in stars, i.e.,  $10^{10}^{\circ}$  K.

The cross-section for *pair production* depends on quantum-mechanical considerations. We only note that the cross-section (Heitler 1954) is of the order of magnitude of

$$\sigma_P \sim Z^2 \frac{e^4}{m^2 c^4} \frac{1}{137}, \quad (48)$$

where the production takes place in the field of a nucleus with charge  $Z$ . Pair production can also occur in the field of an electron or positron with a cross-section given approximately by (48) with  $Z = 1$ . Thus, the Compton absorption must decrease rather greatly with a photon energy increase before pair production can become important. Even for elements with large  $Z$ , such as lead, the Compton absorption is not surpassed for photon energies below 2 Mev. This absorption seems unimportant for astrophysical situations and is neglected in the calculations reported later.

### 3.9. NUCLEAR ABSORPTION

In the range of a few Mev, photons can be absorbed and excite *atomic nuclei* to states above the ground state. These are similar to bound-bound electronic transitions of atomic theory. *Nuclear photodisintegrations* similar to the electronic photoelectric absorptions can also occur in the range of 2 Mev and larger. Both these cross-sections are smaller than that for pair production. These mechanisms are not of importance in calculations of absorptions for astrophysical problems.

### 3.10. PHOTON-PHOTON SCATTERING

A recent discussion by Milford (1957) has indicated that at high temperatures like  $2 \times 10^9^{\circ}$  K the scattering of one photon by another may contribute to radiative transfer. Sampson (1959), however, discussing *photon-photon* scattering has shown that the abundance of extra electron and positron pairs produced at these temperatures may keep Compton scattering dominant at all temperatures.

### 3.11. ELECTRON CONDUCTION

A process which is not one of absorption or scattering is to be considered here because it can dominate effects of radiation transport. This process is that of *electron conduction*. In highly ionized stellar interiors, the density can get high enough so that the bulk of the energy is transported by hot electrons migrating in one direction and cooler electrons moving in the opposite direction. There is



no charge separation in this process. Theories have been worked out by Marshak (1941) and by Mestel (1950) (see also Schatzman 1958), but more work in this field needs to be done.

According to Mestel the flux of energy in the  $x$  direction can be written as

$$F_x = -\nu_c \frac{\partial T}{\partial x}, \quad (49)$$

where the conductivity  $\nu_c$  is a function of six integrals of the form

$$K_p(\eta) = \int_{-\eta}^{\infty} \frac{x^p e^x dx}{(e^x + 1)^2}. \quad (50)$$

In the non-degenerate case ( $\eta \leq -4$ ) the integrals can be evaluated analytically, and the resulting formula for  $\nu_c$  is

$$\nu_c = \frac{128 m k^5 T^4 e^\eta}{h^3 e^4 \rho N_0 \sum_i \frac{y_i^2 X_i \Theta_i}{\mu_{ci}}} = \frac{64 m k^{7/2} N_e T^{5/2}}{(2\pi m)^{3/2} e^4 \rho N_0 \sum_i \frac{y_i^2 X_i \Theta_i}{\mu_{ci}}}, \quad (51)$$

where

$$\theta_0 = \frac{1}{2} \ln \frac{2}{1 - \cos \theta_0}; \quad (52)$$

and

$$\begin{aligned} \theta_{0i} &= \frac{2^{2/3} F_{1/2}^{5/6}(\eta)}{(3\pi y_i)^{1/3} F_{3/2}^{1/2}(\eta)} \\ &= .8475 y_i^{-1/3} \quad (\eta \rightarrow \infty) \\ &= .5894 \left( \frac{e^\eta}{y_i} \right)^{1/3} \quad (\eta \rightarrow -\infty). \end{aligned} \quad (53)$$

For high degeneracies ( $\eta \geq 8$ ),

$$\nu_c = \frac{16\pi^2 m k^5 T^4 \left( \eta^{3/2} + \frac{\pi^2}{8} \eta^{-1/2} \right)^2}{9 h^3 e^4 \rho N_0 \sum_i \frac{y_i^2 X_i}{\mu_{ci}} \Theta_i (1 + x^2)} \left[ 1 + 9.376 \left( \eta^{3/2} + \frac{\pi^2}{8} \eta^{-1/2} \right)^{-4/3} \right]. \quad (54)$$

In these formulae  $m$  is the electron mass,  $k$  is the Boltzmann constant,  $T$  the temperature,  $h$  Planck's constant,  $e$  the electronic charge,  $\rho$  the matter density,  $N_0$  Avogadro's number,  $y_i$  the number of free electrons per atom of element  $i$ ,  $X_i$  the weight fraction of element  $i$  in the mixture,  $\mu_{ci}$  the cold (neutral) molecular weight of element  $i$ ,  $F_{1/2}(\eta)$  and  $F_{3/2}(\eta)$  the Fermi-Dirac integrals which are functions of the degeneracy parameter  $\eta$ , and  $x$  the relativistic degeneracy parameter given by Chandrasekhar (1939):

$$x = \left( \frac{3 N_e h^3}{8 \pi m^3 c^3} \right)^{1/3}, \quad (55)$$

with  $N_e$  the electron density.

For partially degenerate situations one can tabulate the quantities

$$\frac{\nu_c \rho \sum_i \frac{y_i^2}{\mu_{ci}} X_i \theta_i}{T^4 e^\eta} \quad (56)$$

and

$$\theta_{0i} y_i^{1/3} \quad (57)$$

as functions of  $\eta$  alone. For a mixture with known temperature, density  $\eta$ , and the number of free electrons per atom (approximately  $Z_i$  in most degenerate

TABLE 1  
CONDUCTIVITY INTEGRALS

$\eta$	$\theta_{0i} y_i^{1/3}$	$10^{13} \nu_c \rho \frac{\sum_i \frac{y_i^2}{\mu_{ci}} X_i \theta_i}{T^4 e^\eta} \times \frac{\text{erg mole}}{\text{sec cm}^4 \text{ deg}^5}$
-4.0.....	0.1548	6.252
-3.0.....	.2146	6.218
-2.0.....	.2947	6.142
-1.0.....	.3952	5.948
-0.2.....	.4842	5.634
0.4.....	.5494	5.268
1.0.....	.6084	4.779
1.6.....	.6582	4.188
2.2.....	.6982	3.543
2.8.....	.7292	2.895
3.4.....	.7531	2.290
4.0.....	.7712	1.759
5.0.....	.7926	1.070
6.0.....	.8066	0.6133
7.0.....	.8161	0.3346
8.0.....	0.8228	0.1752

cases), one can interpolate for  $\theta_{0i}$ , obtain  $\theta_{0i}$ , and thus get the conductivity  $\nu_c$ . The values of these two functions at appropriate  $\eta$ 's are given in Table 1.

It is possible to express the conductive flux in the same form as the radiation diffusion flux (eq. [15]) or

$$F_c = -\frac{a c}{3 \kappa_C \rho} \frac{\partial T^4}{\partial x} = -\frac{4 a c T^3}{3 \kappa_C \rho} \frac{\partial T}{\partial x}, \quad (58)$$

where

$$\frac{4 a c T^3}{3 \kappa_C \rho} = \nu_c \quad (59)$$

is the coefficient of electronic conduction, and  $\kappa_C$  is the conductive opacity. In general, the total flux due to radiation and conduction is given by

$$F = -\frac{a c}{3 \kappa_T \rho} \frac{\partial T^4}{\partial x}, \quad (60)$$

where

$$\frac{1}{\kappa_T} = \frac{1}{\kappa_C} + \frac{1}{\kappa_R} \quad (61)$$

with  $\kappa_R$  the radiative opacity and  $\kappa_T$  the total opacity.

## § 4. METHODS OF OPACITY CALCULATIONS

### 4.1. STRÖMGREN METHODS

We have seen (eq. [14]) that the average absorption, according to Rosseland, is given by

$$\frac{1}{\kappa} = \frac{\int_0^\infty \frac{1}{(\kappa'_\nu + \sigma_\nu)} \frac{\partial B_\nu(T)}{\partial T} d\nu}{\int_0^\infty \frac{\partial B_\nu(T)}{\partial T} d\nu}, \quad (62)$$

as discussed in section 1.2. Strömgren (1932), whose method is also described by Chandrasekhar (1939), has written this integral in the form

$$\mathfrak{J} = \int_0^\infty \frac{W(u) du}{\sum_i X_i^s D_i(u)}, \quad (63)$$

where

$$X_i^s D_i(u) = \frac{\rho_i}{\rho} \kappa_i(u) u^3 = \frac{N_i \sigma_i(u) u^3}{\rho} \quad (64)$$

and

$$u = \frac{h\nu}{kT}. \quad (65)$$

Here  $\sigma_i(u)$  is the cross-section for  $N_i$  particles of matter density  $\rho_i$  and mass fraction  $X_i$  involved in process  $i$  (not the scattering coefficient), and the sum is over all absorption and scattering processes. A more recent definition of  $D$ , due to Mayer (1947), which will be used later, is

$$D_i(u) = \frac{\kappa_i(u) \rho_i u^3}{A} = \frac{N_i \sigma_i(u) u^3}{A} \quad (66)$$

with the definition, in inverse length units,

$$A = \frac{2^4}{3\sqrt{3}} \frac{h e^2}{m c} \frac{N}{kT}, \quad (67)$$

and  $N$  the number of unit atoms per unit volume. There are  $\sum_i x_i$  atoms per unit atom in the mixture. Here

$$W(u) = \frac{15}{4\pi^4} u^7 e^{2u} (e^u - 1)^{-3}, \quad (68)$$

and the induced emission factor is included in this definition of  $W(u)$ . This  $W(u)$  is tabulated by Mayer. The Strömgren  $^*D$  has cgs units of  $\text{cm}^2/\text{gm}$ . According to the newer definition  $D$  is dimensionless.

In the case of only non-degenerate free-free absorption in the field of an ion of charge  $Z^*$ , the integral is equal to

$$\mathfrak{J} = \frac{\mu_e}{N_0} \frac{3\sqrt{3}c}{16\pi^2 Z^{*2}} \frac{(2\pi m)^{3/2} (kT)^{3.5}}{e^6 h^2 N_e g_{ff}} \int_0^\infty W(u) du, \quad (69)$$

using the Strömgren  $^*D$  and equation (25). The integral has the value 196.51947 and the opacity, which is the reciprocal of  $\mathfrak{J}$ , is

$$\kappa = \text{constant} \frac{N_e g_{ff}}{T^{3.5}}. \quad (70)$$

The constant depends on the mixture. For the Russell mixture it is 130  $(1 - X - Y)$  in which  $(1 - X - Y)$  is the weight fraction of the Russell mixture. This expression is that of a Kramers opacity, which shows that the opacity goes linearly as the density and inversely as temperature to the 3.5 power. This form of the opacity has had wide use since Eddington's work (see eq. [20]), even though it only applies rigorously to free-free absorption.

Absorption due to the bound-free processes changes the opacity law because the integral is discontinuous at absorption edges. When bound-free absorption dominates there is no direct dependence of the opacity on density. The indirect density dependence comes from the relation of the number of bound electrons in the atomic levels to the electron pressure. A brief discussion of this density dependence is given later in § 4.3.

From § 3.1 the Strömgren  $^*D_{bf}$  can be written as

$$\begin{aligned} ^*D_{bf} &= ^*D_{ff} \frac{2\pi^2 Z^{*2} m e^4}{h^5 n^5} \frac{2(2\pi m)^{3/2} (kT)^{1/2}}{N_e} \frac{g_{bf}}{g_{ff}} x_n \\ &= ^*D_{ff} \frac{I_n}{n^3 kT} e^{-\eta} \frac{g_{bf}}{g_{ff}} x_n, \end{aligned} \quad (71)$$

where

$$I_n = \frac{2\pi^2 Z^{*2} m e^4}{n^2 h^2} \quad (72)$$

is the ionization energy from the  $n$  shell,  $\eta$  is the previously mentioned degeneracy parameter (see eqs. [34] and [35]), and  $x_n$  is the number of atoms in the mixture that are in state  $n$  of the particular element which gives the bound-free  $^*D$ .

The evaluation of  $x_n$  is the next step, and the accuracy must be reasonably high because bound-free absorption usually is the main contributor to the opacity. We can see that

$$x_n = x_i x_{ik}, \quad (73)$$

where in the mixture  $x_i$  is the number fraction of element  $i$  which is giving absorption from level  $n$ , and  $x_{ik}$  is the number of atoms of element  $i$  in state  $k$ . Here state  $k$  in this case means that the electron to be absorbed is in a level with principal quantum number  $n$ . The quantity  $x_i$  is given by the composition, but for the present discussion, both  $x_i$  and  $x_{ij}$ , to be used later as the fraction of atoms of type  $i$  in ionization stage  $j$ , are taken as unity. Now, according to statistical mechanics,

$$x_{ik} = \frac{2n^2}{1 + \exp\left(-\frac{I_n}{kT} - \eta\right)}. \quad (74)$$

In the case of high free-electron degeneracy, that is high electron pressure, the occupation is a maximum of  $2n^2$ , and in the case of low electron pressure, where  $\eta$  is large and negative, the occupation goes to zero.

The expression for the occupation of level  $n$  can be thought of as applying Fermi-Dirac statistics to electrons which are allowed certain energy levels  $E_n = -I_n$ . For these energies Strömberg assumed the Bohr theory of hydrogen-like atoms. It is possible to use Slater (1930) screening constants to calculate an effective nuclear charge, which is assumed to have a Coulomb field, and then use of the Bohr theory gives  $E_n$  values. However, screening of the nuclear charge by bound electrons was not used by Strömberg to calculate energy levels.

The integral over frequency is seen to consist of a sum of integrals which are easily evaluated between bound-free edges. Up to the lowest energy edge, only free-free absorption occurs. This gives

$$\mathfrak{J}_1 = \frac{1}{\kappa_{ff}} \int_0^{u_1} W(u) du = \frac{1}{\kappa_{ff}} S(u_1), \quad (75)$$

where  $S(u)$  is the Strömberg function, tabulated by Strömberg (1932), Morse (1940), and Mayer (1947). Between the first edge and the second edge, the integral is

$$\begin{aligned} \mathfrak{J}_2 &= \int_{u_1}^{u_2} \frac{W(u) du}{\kappa_{ff} + \kappa_{bf}^{(1)}} \\ &= \frac{1}{\kappa_{ff} + \kappa_{bf}^{(1)}} [S(u_2) - S(u_1)]. \end{aligned} \quad (76)$$

These integrals never have to be evaluated beyond  $u = 30$  because the weighting function there is very small, and usually the sum of the bound-free  $D$ 's from all levels with ionization energy less than  $ukT$  is very large. The opacity is then evaluated by taking the reciprocal of the sum of these  $\mathfrak{J}$ 's. Later when the newer definition of  $D$  will be used, the opacity is the reciprocal of the integral multiplied by  $A/\rho$ .

While it is true that the procedure is relatively simple once the composition, the temperature, and the electron pressure (or degeneracy parameter) are given,

there are several complications which are necessary if one wishes to obtain opacities accurate to within 10 per cent. For example, occupation numbers  $x_{ik}$  are often influenced by density effects, which perturb the energy levels,  $E_n$ , of bound electrons. These effects simultaneously change the positions of absorption edges needed when computing the opacity.

If one wishes to specify a temperature and density for a mixture instead of a temperature and an electron density or electron pressure, an iteration is necessary in the calculations to divide the electrons properly into the free and all the bound states. This iteration procedure is given in § 4.3.

When the absorption is being calculated, Gaunt factors must be considered and the integrands are not constant between bound-free edges. Electron scattering, which was not considered by Strömgren when evaluating the integral, also makes the total  $D$  vary between bound-free edges. Strömgren has considered the Gaunt factors only approximately by using for the bound-free Gaunt factor its value at the absorption edge, which then is set equal to 0.9. In the calculations of the Russell mixture by Strömgren, the free-free absorption is small, and the free-free Gaunt factor uncertainty is unimportant.

#### 4.2. MORSE CALCULATIONS

Morse considers three processes: bound-free absorption, free-free absorption, and electron scattering. For these calculations Gaunt factors had become available from Menzel and Pekeris (1935) for both bound-free and free-free absorption, and these corrections were applied to the Kramers formulae. The Klein-Nishina formula for the electron-scattering cross-section as a function of photon energy is used. The integral over frequency to obtain the average absorption or opacity is done just as specified by Strömgren. Scattering is not included in the opacity integral, but Morse gives instructions for considering Compton scattering which have been outlined in § 2.4.

These opacity calculations are an improvement over the Strömgren work because more accurate occupation numbers are derived. Fermi-Dirac statistics (i.e., eq. [74]) are applied to electrons which are confined to energies given by the Bohr theory scaled to the proper effective nuclear charge. This effective nuclear charge is given by the actual nuclear charge less screening due to the other bound electrons, calculated by using screening constants derived by Slater (1930).

The ionization energy from some state  $k$  is reduced in this treatment by an energy representing the depression of the continuum. In the continuum-depression calculations, use is made of the zero-temperature Thomas-Fermi (Thomas 1927; Fermi 1928) statistical theory of the atom. For example, this depression is about one electron volt at electron densities of about one-tenth of an electron per cubic Bohr radius ( $1.48 \times 10^{-25} \text{ cm}^3$ ). This continuum depression, which changes the position of the absorption edge, varies appreciably with nuclear charge in this theory.

Morse has included for the first time another effect which appears at high density when the free electrons are partially or highly degenerate. Sometimes there is a lack of space in the continuum for the absorbing electron to fit into. The effect reduces both bound-free and free-free absorption as discussed in § 3.1 and 3.2.

Morse calculates opacities for densities up to  $10^4$  gm/cm<sup>3</sup>. Beyond that point there is pressure ionization of everything except the *K* shell of iron, and the free electrons are degenerate even at stellar temperatures. In this degenerate situation, it is clear that electron conduction dominates radiation transport of energy, but Morse does not give any quantitative conduction data.

The Morse results are given by a formula

$$\kappa = 7.23 \times 10^{24} \Gamma \rho (1 + X)(1 - X - Y) T^{-3.5} \frac{\bar{g}}{l} \frac{\text{cm}^2}{\text{gm}}, \quad (77)$$

where

$$\Gamma = \sum_i \frac{X_i Z_i^2}{\mu_i} = 5.4 \quad (\text{for the Russell mixture}) \quad (78)$$

and the  $X_i$  are the weight fractions of the elements in the mixture with nuclear charge  $Z_i$  and molecular weight  $\mu_i$ . As usual

$$\begin{aligned} X_{\text{H}} &= X & (\text{for hydrogen}), \\ X_{\text{He}} &= Y & (\text{for helium}). \end{aligned} \quad (79)$$

The guillotine factor is  $\bar{g}/l$ , and this quantity is tabulated as a function of density and temperature.

#### 4.3. MAYER METHODS

In a report, unfortunately not available in the normal literature, Harris Mayer (1947) has given very detailed methods of opacity calculations. All the necessary steps in the opacity calculation are improved somewhat, and, in addition, methods are given for adding the absorption due to bound-bound transitions. This report should be read by all serious workers in the field of opacity calculations. The only opacity obtained in this work is for pure iron at the density of 7.85 gm/cm<sup>3</sup> and the temperature of 11,600,000° K. However, the results are interesting because the effects of line absorption increase the opacity by a factor of more than three over the continuous opacity.

The usual Kramers formulas are used by Mayer for the bound-free and free-free absorption. A Gaunt factor expression due to Menzel and Pekeris (1935) is used to correct the free-free absorption formula, and bound-free Gaunt factors are given as functions of the free-electron energy for absorption from various shells. The bound-bound transitions have *f*-values which are the counterpart of Gaunt factors, and these have also been tabulated by Mayer and by many others since Menzel and Pekeris.

Scattering processes are discussed, and the conclusion is that for frequencies

not too close to a bound-electron resonance, one can approximately use the Klein-Nishina cross-section for photons, which have energies either above or below the resonance energy. In the Mayer opacity calculations, therefore, all electrons, whether bound or free, are counted as being able to scatter according to the electron-scattering (Thomson or Compton) formula. The error due to this rule is usually very small because, except at high temperatures where all the electrons are free anyway, other absorption processes dominate. However, this rule will not be correct at low temperatures and densities that exist in stellar atmospheres. There Rayleigh scattering due to bound electrons may be important, and use of the Thomson cross-section for this electron scattering will not give the correct absorption.

An error in the weighting function for the pure-electron scattering opacity has been pointed out by Mayer and independently by Rudkjøbing (1947). Emission induced by a photon beam produces more photons, which act to make the absorption appear less. The scattering process does not obey this simple rule for induced emission, and it requires a weighting function when the opacity integral is being made, which does not include the normal correction factor  $(1 - e^{-u})$  for induced emission. The older integral over frequency for the pure scattering opacity is

$$\mathfrak{S} = \frac{15}{4\pi^4} \int_0^\infty \frac{1}{\sigma_e} \frac{u^4 e^{2u}}{(e^u - 1)^3} du = \frac{1.055}{\sigma_e}, \quad (80)$$

as given by Chandrasekhar (1939). A more nearly correct integral is

$$\mathfrak{S} = \frac{15}{4\pi^4} \int_0^\infty \frac{1}{\sigma_e} \frac{u^4 e^u}{(e^u - 1)^2} du = \frac{1}{\sigma_e}. \quad (81)$$

Sampson (1959) has discussed induced scatterings and the Compton effect, which we consider later.

For a mixture of elements we now investigate the total effect of electron scattering on the opacity. We have for element  $i$ ,

$$\sigma_{ei} = \left( \frac{8\pi e^4}{3m^2 c^4} \right) \frac{Z_i N_0}{\mu_{ci}}, \quad (82)$$

where the Thomson cross-section is multiplied by Avogadro's number,  $N_0$ , and the number of  $Z_i$  electrons, which are scattering from the atom of (cold) molecular weight  $\mu_{ci}$ . This formula gives for all the elements in the mixture

$$\sigma_e = .401 \sum_i \frac{Z_i \rho_i}{\mu_{ci} \rho} \text{ cm}^2/\text{gm} \quad (83)$$

or, in another form,

$$\sigma_e = .401 \frac{\sum_i x_i Z_i}{\sum_i x_i \mu_{ci}} \text{ cm}^2/\text{gm}, \quad (84)$$



where the  $x_i$  are the number fractions of the elements in the mixture. If mass fractions  $X_i = \rho_i/\rho$  for a mixture are available, it is most convenient to use equation (83), but when number fractions only are known, equation (84) is easier to use.

The equivalence of formulas (83) and (84) is seen by the fundamental sum rule for adding absorption and scattering coefficients

$$\sum_i \rho_i \sigma_{ei} = \rho \sigma_e, \quad (85)$$

where  $\rho_i$  are the densities of the elements having electron scattering  $\sigma_{ei}$ ,  $\rho$  is the total density, and  $\sigma_e$  is the total scattering opacity. We have then, by the previous formula (83),

$$\rho \sigma_e = .401 \sum_i \frac{Z_i \rho_i}{\mu_{ci}} \text{ cm}^{-1}. \quad (86)$$

Since  $x_i$  are the number fractions of species  $i$ ,

$$\sum_i x_i Z_i \frac{\rho}{\sum_i x_i \mu_{ci}} = \sum_i \frac{Z_i \rho_i}{\mu_{ci}}, \quad (87)$$

because the units of the right-hand side are moles of electrons per unit volume summed over all elements  $i$ , and those of the left side are total moles of atoms, with molecular weight  $\sum_i x_i \mu_{ci}$ , per unit volume multiplied by the number of electrons per atom. Thus, either formula for  $\sigma_e$  can be used.

Now, for a mixture of hydrogen, helium, and heavy elements, we have, from equation (83),

$$\sigma_e = .401 \left[ \frac{X}{1.008} + \frac{2Y}{4.003} + \frac{1}{2}(1 - X - Y) \right] \frac{\text{cm}^2}{\text{gm}}, \quad (88)$$

where the heavy elements are assumed to have weight fraction of  $(1 - X - Y)$  and their  $Z_i/A_i = \frac{1}{2}$ . Approximately, then, the scattering opacity is

$$\sigma_e = .200(1 + X) \frac{\text{cm}^2}{\text{gm}}. \quad (89)$$

Chandrasekhar (1939) gives the average  $\sigma_e$  as  $\sigma_e/1.055$  and therefore obtains

$$\sigma_e = .19(1 + X) \frac{\text{cm}^2}{\text{gm}} \quad (90)$$

as the scattering opacity. This error, still seen in the current literature, is small for almost all work, however, and usually there are simultaneously other sources of opacity which reduce the effect of this error.

Bound-free and free-free absorptions depend on the number of electrons in the various bound and free states. The opacity calculation then requires first a calculation of the equation of state. While the equation of state discussed here

does not include the pressure and energy at the temperature and density under consideration for the selected composition, it is an easy step from the occupation numbers and electron densities to these ordinary equation of state quantities.

Mayer describes a method for obtaining occupation numbers which he calls the independent electron approximation. This is the same method used by Strömberg, and it is very similar to the procedure followed by Morse. Given a composition, temperature, and density, one assumes first that all electrons are ionized from the atoms. The number of free electrons per average atom is then

$$y = \sum_i x_i Z_i, \quad (91)$$

where  $\sum_i x_i$ , the sum of the abundances by number, does not necessarily have to be equal to unity. The electron density is

$$N_e = \frac{\rho N_0}{\sum_i x_i \mu_{ei}} y, \quad (92)$$

and this number, together with the temperature, can be used to calculate  $\eta$  using the Fermi-Dirac integral  $F_4(\eta)$  given in equation (34). This  $\eta$  assumes the free electrons have only kinetic energy and no interaction energy. Corrections to this  $\eta$  are discussed below. The independent electron approximation then uses Fermi-Dirac statistics to calculate the number of electrons in bound state  $k$  of element  $i$  (see also eq. [74]):

$$x_{ik} = \frac{g_{ik}}{\exp\left(\frac{E_{ik}}{kT} - \eta\right) + 1}, \quad (93)$$

where  $g_{ik}$  is the degeneracy of state  $k$ , and the energy of state  $k$  is the interaction energy of the electron with the nucleus. The occupation of each level is then computed in this first approximation.

A sum can be made over all the bound states of each element, and then these sums can be summed over all elements to give the total number of bound electrons per average atom in the system. Therefore,

$$n_b = \sum_i x_i \sum_k x_{ik}, \quad (94)$$

and also the number of free electrons

$$y = \sum_i x_i \left( Z_i - \sum_k x_{ik} \right) \quad (95)$$

can be compared with the original assumption that *all* electrons are free. If the successive  $y$  values differ from each other, one can iterate until  $y$  is accurately determined.

If one wants to start with  $T$  and  $\eta$  for a given composition as Strömgren did, then iteration is not necessary at all, provided the positions of energy levels do not depend on the density. At low temperatures where the iteration is difficult and may not converge,  $T$  and  $\eta$  (or even  $N_e$  or  $P_e$ ) are often the starting data, and a density is derived. Keller and Meyerott, for example, have tabulated opacities and densities as a function of  $T$  and  $\eta$ , or really  $T$  and  $a_e = -\eta$ .

We now look at this energy-level calculation on the basis of a modified independent (or dependent) electron model as Morse did to a limited extent. Morse considers perturbations of the bound electron energies by other bound electrons and by a continuum depression due to the free electrons. The Mayer modified independent electron method also attempts to consider as perturbations the interactions of bound electrons both with other bound electrons and with those that are free. Use of statistical mechanics and quantum mechanics shows that the occupation number formula (93) retains its form in this modified approximation, but the electron energy  $E_{ik}$  is calculated by a new prescription.

Energies are given by the usual Bohr hydrogen-like theory with the nuclear charge shielded by the bound electrons according to screening constants. A complete table of these screening constants is given by Mayer. Interaction energies between the free and bound electrons and a depression of the continuum are also included. The composite energy level, assuming each atom is surrounded by a uniformly charged sphere with enough free electrons to neutralize the net nuclear charge is

$$E_{ik} = -\frac{Z_{ik}^{*2}}{n_{ik}^2} + \frac{y_i}{r_i} \left[ 3 - \left( \frac{\langle r_k^2 \rangle}{r_i^2} \right) \right] + \frac{3}{5} \sum_i \frac{x_i y_i^2}{y r_i} \text{ Rydbergs,} \quad (96)$$

where

$$Z_{ik}^* = Z_i - \sum_{k' \neq k} x_{ik'} \sigma_{kk'} - x_{ik} \left( 1 - \frac{1}{g_{ik}} \right) \sigma_{kk}, \quad (97)$$

$n_{ik}$  is the principal quantum number of the state  $ik$ ,  $y_i$  is the number of free electrons from element  $i$ , (taken as an approximation to the effective nuclear charge seen in state  $k$ ),  $\langle r_k^2 \rangle$  is the average radius-squared of this state in Bohr radii units as given by a quantum-mechanical average, and the quantity  $r_i$  is the average radius of a sphere which contains enough electronic charge to neutralize the ionic charge of atom  $i$ :

$$r_i = \frac{\left( \frac{y_i}{y} \frac{3}{4\pi} V \right)^{1/3}}{a_0} \text{ Bohr radii.} \quad (98)$$

Here

$$V = \frac{\mu_c}{\rho N_0} = \frac{\sum_i x_i \mu_{ci}}{\rho N_0} \quad (99)$$

is the volume per average atom and  $a_0$  is the Bohr radius. A Rydberg is the hydrogen-atom ionization energy, 13.60 electron volts.

The last term in (96), the negative of the potential energy of the free electrons averaged over all ion spheres, is usually called  $E_0$ . This shift in the energy zero point enables one to ignore the interaction energy of the free electrons with themselves and with the ions which are assumed to have bound electrons in orbits small compared with  $r_i$ . One can then retain equation (34) for calculating  $\eta$ . The correct  $\eta$  to be used in equation (93) is the  $\eta$  calculated with the free electrons having both kinetic and potential energy ( $-E_0$ ), but in practice one calculates  $\eta$  and  $E_0$  separately and uses them always in the form  $\eta - E_0/kT$ .

Note that the interactions depress the continuum by a constant energy plus another which varies from state to state. When the electron energy is greater than the depressed continuum, the electron is counted as being free. Use of equation (93) does not give incorrect occupation numbers when  $E_0$  is included in the electron energy, but the absorption edge for the bound-free process is shifted by  $E_0$ . Since merging lines tend to depress the edge anyway, moving the edge by  $E_0$  and calling bound-bound absorptions bound-free gives a very small error.

The screening constants  $\sigma_{kk}$  consider shielding of the nucleus by electrons in the same shell  $k$  and in different shells  $k'$ . The appropriate screening constants and

$$\delta = \langle r_k^2 \rangle Z^{*2} (\text{Bohr radii})^2 \quad (100)$$

are tabulated by Mayer. In the application,  $\delta/(Z^{*2} r_i^2)$  should be limited at less than or equal to unity for geometrical reasons.

This modified independent electron method converges rapidly except when atoms are nearly neutral. For astrophysical mixtures which contain mostly hydrogen and/or helium, convergence can be assumed down to  $10^6$  °K or a little lower. This method will not work for the temperatures and densities in stellar atmospheres, because the energies needed in the expression for occupation number are very sensitive to the presence of other bound electrons in the same atom. This sensitivity does not exist if the electrons are truly independent or if the temperature is so high that  $E_{ik}/kT$  is small. Actually, at the higher temperatures there are fewer bound electrons, and the electrons are indeed more independent.

Mayer also discusses slightly more accurate formulas which do not assume that the free electrons are uniformly distributed over the atom. The criterion for the above approximations is

$$\frac{y_i e^2}{r_i k T} < 1 \quad (101)$$

or

$$\frac{2 y_i}{r_i k T} < 1, \quad (102)$$

where  $kT$  now is in Rydbergs and  $r_i$  in Bohr radii. Using the definition of  $r_i$  in equations (98) and (99), with  $\rho$  in  $\text{gm/cm}^3$ , the expression is

$$1.4 \left( \frac{y}{y_i \sum_i x_i \mu_{ei}} \right)^{1/3} y_i \left( \frac{\rho^{1/3}}{kT} \right) < 1. \quad (103)$$

In the sun, for example,  $\rho^{1/3}/kT$  is less than .1 throughout, so the criterion is satisfied except for the heaviest elements at the higher temperatures when complete ionization takes place. The low abundance of these heavier elements in astrophysically interesting mixtures fortunately allows the opacity to be calculated with good accuracy over the entire temperature and density range. Discussions of a more accurate interaction energy between the free and bound charges are given by Stewart and Pyatt (1961) and Armstrong *et al.* (1961) who use, in addition to the above ion sphere model, the Debye-Hückel model.

Shortly after the Mayer work, Marshak, Morse, and York (1950) published an extension of the occupation number work of Morse. The Thomas-Fermi theory of the atom extended to non-zero temperatures was used to calculate the depression of the continuum. Only data for the equation of state were calculated in this work, but the method could be used in opacity calculations. Further improvements have been discussed by Keller and Meyerott (1952) who derived another method for obtaining  $E_0$ .

Instead of using the Bohr theory for the unperturbed binding energy of electrons in atoms, in some applications Mayer uses relativistic energy levels which depend on the element and the effective nuclear charge. Energy levels become relativistic when orbital velocities become comparable with the velocity of light. In Mayer's table one can see that for uranium, energy levels are changed by 15 per cent due to these relativistic effects. The energy levels are always displaced deeper below the continuum. By ignoring this energy shift for the worst case (1s level in uranium), an absorption edge that should appear at  $u = 10$  will appear at  $u = 8.5$ , a rather bad error for opacity calculations.

For 1s electrons of iron, Bohr scaling gives an energy which is only one per cent different from the relativistic energy. As an example, this gives an error of 7 Rydbergs out of  $Z^2 = 676$  Rydbergs at temperatures like 30 Rydbergs where the 1s bound-free absorption is not completely dominated by other iron edges. The 1s edge is then displaced  $\Delta u = 7/30 \approx 0.2$  from where it should be placed according to the relativistic energy levels. This is not a large error because the edge appears at  $u = 676/30 \approx 20$ , where the weighting function for the opacity is well down in value from its peak at  $u = 7$ . Relativistic energy levels need not be considered in most absorption problems of astrophysics.

Mayer gives an interesting discussion on how to use the average occupation numbers of an atom of each element to determine the approximate probabilities for the existence of the various ionic configurations. The value of this ionic calculation is that it splits bound-free absorption edges correctly, and, more im-

portant, it allows the proper line splitting in bound-bound absorption. Other ionic methods which are capable of even more detail have been worked out more recently and are described later in § 4.5.

It is assumed that the Boltzmann factor,  $\exp(-E/kT)$ , which influences the occupation of the levels at energy  $E$  has been correctly considered in obtaining the average occupation numbers, and that this factor no longer needs to be considered when computing occupations in the various specific ionic configurations. The assumption is valid if energies of specific configurations do not differ much from the energy of the average configuration. In this case, the average occupation in a shell of an atom can be used to give the probability  $p_{ik}$  of finding an electron in shell  $k$  in any of the various ions of element  $i$ . Thus

$$p_{ik} = \frac{x_{ik}}{g_{ik}} \quad (104)$$

and

$$q_{ik} = 1 - p_{ik}, \quad (105)$$

where  $q_{ik}$  is the probability of there being no electron in level  $k$ . The probability of finding  $\nu_k$  electrons and  $g_{ik} - \nu_k$  vacancies in level  $k$  is

$$p_{i\nu k} = \left( \frac{g_{ik}}{\nu_k} \right) p_{ik} q_{ik}^{g_{ik} - \nu_k}, \quad (106)$$

where the binomial coefficient normalizes the probability.

One can list ions with a priori configurations close to the configuration given by the average occupations. It is of no value to list possible ionic configurations which look considerably different from the average atom, because these ions are very improbable. Full shells have unit probability of being full and zero probability of having any holes. Almost empty shells have the greatest probability of zero electrons in them and very low probability of one electron in them. For those few shells where various integral numbers of electrons are likely, one can form the products of the probabilities that each shell has a given number of electrons in it, and therefore compute the probability of these configurations occurring.

In each configuration one can recompute the energy levels by using screening constants. These new, more accurate energy levels are used by Mayer for computing the bound-free absorption edges and the bound-bound line transitions. In heavy elements and at high temperatures, a very complex spectrum of lines can occur from all the ionic configurations, and this spectrum may have a tremendous influence on the opacity.

Mayer has also given an approximate scaling law for continuous opacities of pure elements. If one is given the continuous opacity (no bound-bound absorption) of element 1 at  $T_1$ , and  $\rho_1$ , then at

$$T_2 = T_1 \left( \frac{Z_2}{Z_1} \right)^2 \quad (107)$$

and

$$\rho_2 = \rho_1 \left( \frac{Z_2}{Z_1} \right)^3 \quad (108)$$

the opacity of element 2 is

$$\kappa_2 \approx \kappa_1 \left( \frac{Z_1}{Z_2} \right)^3. \quad (109)$$

Unfortunately, this scaling law is not of much value for the complicated mixtures of interest in astrophysics. In these mixtures it is necessary to calculate each case separately for reliable opacities. Table 2 shows how this scaling compares to actually calculated opacities for oxygen, neon, and aluminum.

Of more interest in astrophysics are some limiting values of the opacity or limiting forms of the opacity function discussed by Mayer. If there are no

TABLE 2  
COMPARISON OF SCALED AND ACTUAL CONTINUOUS OPACITIES

Element	$kT$ (kilovolts)	$\rho$ (gm/cm <sup>3</sup> )	$\kappa/\kappa_0$ Predicted	$\kappa/\kappa_0$ Actual	$\kappa$ (cm <sup>2</sup> /gm)
O. ....	0.1	1	1	1	157
Ne. ....	.156	1.95	0.512	0.650	102
Al. ....	0.264	4.29	0.233	0.369	58

bound electrons, only free-free absorption and electron scattering can contribute to the opacity. At high density and high temperatures free-free absorption given by equations (70) and (20) is more important, and the opacity varies linearly with density and as the  $-3.5$  power of the temperature. Thus

$$\kappa \approx \rho T^{-3.5}. \quad (110)$$

At low densities one gets the Compton limit. The Compton limit is really not a fixed constant for a given mixture, but decreases slowly with increasing temperature due to the behavior of the Compton scattering process.

At lower temperatures, electrons can be bound to atoms. The bound-free absorption is less dependent on the density because the occupation of nearly full shells is independent of density. Only when the occupation of shells is very small is the occupation approximately proportional to density, as equation (93) indicates. When there is no electron degeneracy,  $\eta \leq -4$ , and  $x_{ik}$  is small,

$$x_{ik} = g_{ik} \exp \left( -\frac{E_{ik}}{kT} + \eta \right) \quad (111)$$

and, using (34), (35), and (92),

$$x_{ik} \propto \rho y. \quad (112)$$

If the number of free electrons per average atom of the mixture,  $y$ , is moderately large and due mostly to hydrogen and helium, it will not vary greatly with small changes of  $x_{ik}$ , and the occupation is proportional to density.

Bound-free absorption drops rapidly when the positions of absorption edges move to large  $u$  at low temperatures. However, in a hydrogen-metal mixture, the opacity does not decrease very much because of the formation of  $H^-$  ions by combination of H atoms with electrons from the metals. Other elements which do not have the negative ion complication show a very rapid drop in opacity when the temperature gets much below

$$kT \approx \frac{1}{10} \frac{Z^{*2}}{n_0^2} \text{ Rydbergs,} \quad (113)$$

where  $Z^{*2}/n_0^2$  is the ionization energy of the outermost ground state electron in the level with principal quantum number  $n_0$ . When bound-bound absorption is dominant, the opacity can vary more rapidly with density than the linear relation which is the limit for the continuous opacity.

Mayer devotes much of his effort to the calculation of opacities including line absorption. This work is not described here though its statistical features should not be overlooked in the blanketing problem of stellar atmospheres. In the case of complex splitting of bound-bound transitions from state  $k$  to state  $k'$ , the statistical method is able to group all these lines together and treat the absorption as continuous. Several methods for adding line absorption are outlined for specific circumstances. Unfortunately, one can have problems where just a few lines are important, and in that case the only available method is to calculate the detailed absorption at many frequencies at all important positions in the line.

#### 4.4. VITENSE MONOCHROMATIC ABSORPTION COEFFICIENTS AND OPACITIES

The only available modern absorption data for low temperature have been given by Vitense (1951). A description of the mixture, the absorption processes considered, and the results have been given in § 2.5.

One of the unusual features of this work is the method used to calculate the bound-free absorption by the metals. The levels in each metal element are not considered in detail as necessary in precise work; instead, only average level properties are considered. In order to obtain occupation numbers the Boltzmann excitation formula

$$x_{ijk} = \frac{\nu_k g_{ijk}}{B_{ij}} \exp \left( -\frac{E_{ijk} + \chi_{ij}}{kT} \right) \quad (114)$$

is used, where  $x_{ijk}$  is the occupation of level  $k$  in ion  $j$  of element  $i$ ,  $g_{ijk}$  is the number of ways state  $ijk$  can exist with energy  $E_{ijk} < 0$ ,  $\nu_k$ , an integer, is the number of electrons in level  $k$  in the excitation state  $ijk$ ,  $B_{ij}$  is the partition function or sum over all states  $k$ , that is, the number of ways ion  $j$  can exist, and  $\chi_{ij}$  is the ionization energy of ion  $j$ .

The Kramers bound-free absorption due to  $x_i x_{ij} x_{ijk}$  electrons in the level



with principal quantum number  $n$  can be written from equation (23):

$$\kappa_\nu = \frac{N_0}{\sum_i x_i \mu_{ci}} \frac{2^6 \pi^4}{3 \sqrt{3}} \frac{Z^{*2} m e^{10}}{c h^6 \nu^3} x_i x_{ij} \frac{Z^{*2}}{n^5} \frac{g_{ijk} \nu_k}{B_{ij}} \exp\left(-\frac{E_{ijk} + \chi_{ij}}{kT}\right), \quad (115)$$

where  $x_i$  and  $x_{ij}$  are the number fractions, respectively, of element  $i$  in the mixture and of ion  $j$  in element  $i$ ,  $N_0$  is Avogadro's number, and the unit molecular weight is  $\sum_i x_i \mu_{ci}$ . The bound-free Gaunt factor and the correction for the availability of a final state have been set to unity here. Now,

$$g_{ijk} = 2n^2 \quad (116)$$

and

$$E_{ijk} = -\frac{Z^{*2}}{n^2} \text{ Rydbergs} \quad (117)$$

if we allow hydrogen-like levels with only one excited electron ( $\nu = 1$ ). The absorption from levels in  $dn$  becomes

$$\frac{d\kappa_\nu}{dn} = \frac{N_0 x_i}{\sum_i x_i \mu_{ci}} \frac{2^5 \pi^2}{3 \sqrt{3}} \frac{Z^{*2} e^6}{c h^4 \nu^3} \frac{x_{ij}}{B_{ij}} \frac{dE_{ijk}}{dn} \exp\left(-\frac{E_{ijk} + \chi_{ij}}{kT}\right). \quad (118)$$

This *bound-free* formula can also be derived from the *free-free* cross-section (with  $g_{ff} = 1$ ) given in equation (26) and the free-electron concentration in equation (27), noting that the free-electron occupation number per available state  $N_e(p)/(8\pi p^2/h^3)$  has a bound state equivalent of  $x_{ijk}/g_{ijk}$ .

One can assume the levels are close together and integrate over all photon energies that can be absorbed, hence

$$\exp\left(-\frac{\chi_{ij}}{kT}\right) \int_{-h\nu}^{\infty} \exp\left(-\frac{E_{ijk}}{kT}\right) dE_{ijk} = kT \exp\left(-\frac{\chi_{ij}}{kT}\right) \exp\left(\frac{h\nu}{kT}\right). \quad (119)$$

where the integral has been extended to include the free-free transitions. The formula now is

$$\kappa_\nu = \frac{N_0 x_i}{\sum_i x_i \mu_{ci}} \frac{2^5 \pi^2}{3 \sqrt{3}} \frac{Z^{*2} e^6}{h c u^3} \frac{x_{ij}}{B_{ij} (kT)^2} \exp\left(-\frac{\chi_{ij}}{kT} + u\right). \quad (120)$$

The Vitense formulas are somewhat different from those given here because of her definition of

$$g_{ijk} = 2n^2 B_{ij}, \quad (121)$$

but the degree of ionization,  $x_{ij}$ , is always required. A similar treatment is also given by Unsöld (1955) and Raizer (1960). Formula (120) allows one to calculate the absorption at any  $u$ ,  $\eta$ , and  $kT$  with the composition, its degree of ionization, effective nuclear charges, ionization potentials, and partition functions known.

Vitense has considered in her method the absorption due to the negative

hydrogen ion. Allowance for this absorption is straightforward using tables of Chandrasekhar and Breen (1946). Use of the Saha ionization equation at the temperature and density of interest with the known ionization energy of .75 ev for the  $H^-$  ion yields the  $H^-$  ion abundance per neutral hydrogen atom. This ratio

$$\frac{x_{H^-}}{x_{H,0}} = 4.158 \times 10^{-10} P_e \theta^{5/2} e^{1.726\theta}, \quad (122)$$

where  $\theta = 5040/T$  and other units are cgs, is multiplied by the bound-free cross-section and the abundance of neutral H atoms to give the bound-free cross-section for each hydrogen atom in the mixture. Only the electron pressure and temperature are required to enter the Chandrasekhar and Breen tables, which give the free-free cross-section per neutral H atom. The absorption due to the  $H^-$  ion is very important at low temperatures and its consideration is necessary in the construction of most stellar atmospheres.

Another feature of the Vitense method is the addition of Rayleigh scattering to the absorption. The cross-section for Rayleigh scattering used is

$$\sigma_{\text{Ray}} = \sigma_T \frac{\lambda_r^4}{\lambda^4}, \quad (123)$$

where  $\sigma_T$  is the Thomson cross-section of  $.665 \times 10^{-24} \text{ cm}^2$ , and  $\lambda_r$  is the resonant wavelength. The Vitense work assumes Rayleigh scattering only from hydrogen and takes the resonant wavelength equal to 1000 Å or approximately the wavelength corresponding to the ionization of the hydrogen atom from its highly occupied ground state (911 Å). From the Vitense results it appears that Rayleigh scattering is not usually important. Only when the metal content and the temperature get very low can this scattering effectively influence radiation transfer.

#### 4.5. PRESENT EQUATION OF STATE METHODS

Efforts have been devoted at the Los Alamos Scientific Laboratory to the accurate calculation of monochromatic absorption coefficients and opacities over the entire range of density and temperature met in problems of stellar structure. The first region to be described here is the temperature range from  $5 \times 10^3$  °K where molecular formation may be of some importance, to  $10^6$  °K above which the more conventional methods are accurate.

We start this *ionic method* by calculating the equation of state of a mixture when the temperature  $T$  and the degeneracy parameter  $\eta$  are given. According to statistical mechanics one must use the Saha ionization equation. The form we use, applicable to any degree of electron degeneracy, is

$$\frac{x_{i,j+1}}{x_{i,j}} = \frac{B_{i,j+1}}{B_{i,j}} \exp \left[ -\frac{x_{ij} - \frac{(j+1)e^2}{R_D}}{kT} - \eta + \frac{E_0}{kT} \right], \quad (124)$$

where, for element  $i$ ,  $x_{i,j}$  is the number fraction of ion  $j$  with  $j$  electrons missing;  $B_{i,j}$  is the partition function for that ion;  $\chi_{ij}$ , the energy needed to ionize the ion  $j$  to ion  $j+1$ , is corrected for interactions between charged particles;  $\eta$ , corrected by  $E_0/kT$ , is the degeneracy parameter, which may have any value; and  $R_D$  is the Debye radius. The corrections for the interactions between the charged particles are discussed by Armstrong *et al.* (1961) and Stewart and Pyatt (1961). The Debye radius considering all charged particles depends on the density and is

$$R_D = \left[ \frac{kT}{4\pi N_i e^2 \left( y + \sum_i x_i \sum_j x_{ij} j^2 \right)} \right]^{1/2}. \quad (125)$$

The electrostatic corrections to  $\chi_{ij}$  are accurate only when  $e^2/R_D kT$  is small compared to unity. This form of the ionization equation reduces to the familiar non-degenerate form by use of equations (34) and (35). Equation (124) can be written for every adjacent pair of ions of each element in the mixture. For studies of molecular abundances, a formula similar to (124) is used, but for this discussion molecules are not allowed to exist.

The partition function sums for equation (124) are given by

$$B_{ij} = \sum_k g_{ijk} \exp \left[ - \frac{\epsilon_{ijk} + \frac{y_i}{r_i^3} (\langle r_k^2 \rangle - \langle r_0^2 \rangle) R h c}{kT} \right], \quad (126)$$

where  $g_{ijk}$  is the statistical weight of the excited level  $k$ ,  $\epsilon_{ijk}$  is the excitation energy above the ground state, and  $R h c = 13.60$  electron volts. These data, which sometimes include states where more than one electron is excited above the ground level, are obtained from Moore (1949, 1952). The energy-level corrections in equation (126) are those derived from Mayer's ion sphere model, with  $\langle r_k^2 \rangle$  and  $\langle r_0^2 \rangle$  the orbital radii squared in state  $k$  and in the ground state. The cutoff of the partition function sum is at that perturbed energy level which is at the continuum depressed by  $(j+1)/(e^2/R_D)$ .

If observed energy-level data are not available, screening constants, given by Mayer and corrected by Karzas (private communication), are used with the Bohr theory to obtain the energy levels of the one excited electron. Also,  $g_{ijk} = 2n^2$  or  $2(2l+1)$  is used. For a definite configuration, the screening by electrons in the same shell as the electron being considered is not given by the average in (97) but merely by the screening of the other electrons in the shell.

In cases at low temperatures where most atoms are neutral, the perturbation of the energy levels is due principally to neutral atoms. Therefore, a partition function is cut off when the orbit of the excited level has a radius greater than the mean separation between nuclei.

The procedure for the solution of the resulting set of equations uses two polynomials:

$$P_i = \frac{\text{no. nuclei of element } i}{x_{i0}} = 1 + \frac{x_{i1}}{x_{i0}} + \frac{x_{i2}}{x_{i1}} \frac{x_{i1}}{x_{i0}} + \dots + \frac{x_{iZ}}{x_{iZ-1}} \dots \frac{x_{i1}}{x_{i0}} \quad (127)$$

and

$$Q_i = \frac{\text{no. electrons from element } i}{x_{i0}} = \frac{x_{i1}}{x_{i0}} + 2 \frac{x_{i2}}{x_{i1}} \frac{x_{i1}}{x_{i0}} + \dots + Z \frac{x_{iZ}}{x_{iZ-1}} \dots \frac{x_{i1}}{x_{i0}}, \quad (128)$$

so that

$$\frac{Q_i}{P_i} = y_i \frac{\text{free electrons from element } i}{\text{element } i \text{ nuclei}}. \quad (129)$$

Now

$$\sum_i x_i y_i = y \frac{\text{free electrons}}{\text{average atom}}, \quad (130)$$

and since the electron density from equation (34),

$$N_e = 4\pi \frac{(2mkT)^{3/2}}{h^3} F_{1/2}(\eta), \quad (131)$$

is known from the known temperature and  $\eta$  for the case in question, the average atom density is

$$N_t = \frac{N_e}{y} = \rho \frac{N_0}{\sum_i x_i \mu_{ei}}. \quad (132)$$

The matter density of the mixture can now be computed using (132). The fraction of neutral atoms in the mixture,  $x_{i0}$ , is  $1/P_i$  for each element, and the  $x_{i,j+1}/x_{i,j}$  can be used to calculate all  $x_{i,j}$  once  $x_{i,0}$  is known.

It is possible to define  $P_i$  and  $Q_i$  with respect to the most abundant ion instead of the neutral ion. In that case, equations (127) and (128) are changed appropriately. The redefinition, which can vary from one element to another, prevents excessively large values of  $P_i$  and  $Q_i$  and makes numerical solution easier.

Actually, the density affects the value of the partition functions, through energy-level corrections, and the ionization potential reduction in the ionization equation, due to electrostatic effects. Therefore, it is often convenient to obtain an approximate  $\eta$  from a given starting density by estimating the number of electrons from each element,  $y_i$ , and the average number of free electrons per average atom,  $y$  in (130), using the method of the dominant potential (Chandrasekhar 1951). Solution of the ionization equation is then made, assuming  $\rho$ ,  $T$ , and  $\eta$  are all given and that  $\eta$  and  $\rho$  are self-consistent.

After an approximately correct density corresponding to the starting  $T$  and

$\rho$  and the approximate  $\eta$  has been derived, one can select a new  $\eta$  which will give a resulting density closer to the starting value. A few iterations with improved density corrections can give a consistent set of  $T$ ,  $\rho$ , and  $\eta$  with the first two values specified in advance.

When the density has converged in the iterations to about 0.01 per cent the results can be tabulated. The material (gas) pressure is

$$P_g = b' \rho T, \quad (133)$$

where

$$b' = \frac{R \sum_i x_i}{\sum_i x_i \mu_{ci}} + \frac{P_e(\eta, T)}{\rho T} \quad (134)$$

with  $R$  the gas constant. In general (see eq. [34] and following), in the non-relativistic case

$$P_e = N_e k T \frac{\frac{2}{3} F_{3/2}(\eta)}{F_{1/2}(\eta)}. \quad (135)$$

If the case is non-degenerate,

$$P_e = \frac{\rho N_0 y}{\sum_i x_i \mu_{ci}} k T, \quad (136)$$

then

$$b' = b = \frac{R}{\sum_i x_i \mu_{ci}} \left( \sum_i x_i + y \right). \quad (137)$$

The occupation of state  $k$  is given by equation (114), or

$$x_{ijk} = \frac{\nu_k g_{ijk} \exp\left(-\frac{\epsilon'_{ijk}}{kT}\right)}{B_{ij}}, \quad (138)$$

where the  $\epsilon'_{ijk}$  is the excitation energy corrected for the free-charge perturbations as written in equation (126). The state  $k$  may have more than one excited electron, and in that case each electron level with its occupation in that configuration is listed. A table including the ionic abundance  $x_i x_{ij}$ , the level abundance  $x_{ijk}$ , the corrected energy  $E_{ijk}$  below the depressed continuum, the  $n$  and  $l$  quantum numbers of the state  $k$ , and the effective nuclear charge of the electron in the level is made for all reasonably abundant excited electron levels.

The average energy levels of the electrons in the cores of each ionization stage are computed using screening constants and the average occupation of the excited levels. They are also listed as above. Note that  $x_{ijk}$  can be greater than unity for core levels or excited levels which contain  $\nu_k > 1$  excited electrons. Energy-level data for the core and excited states,  $1s$ ,  $2s$ ,  $2p$ ,  $3s$ ,  $3p$ ,  $3d$ ,  $4$ ,  $5$ ,  $6$ ,

7, 8, 9, 10 along with other data such as the temperature,  $\eta$ , density of free electrons, etc., are required for the absorption calculations.

The matter-energy equation of state can now be computed by adding the energy of ionization and excitation to the kinetic energy of the free electrons. If densities are high, electrostatic corrections for interactions between all the free charged particles must be made to both the pressure and energy values.

An ionization equation for the  $H^-$  ion is also written. Equation (122), with a more modern value of the ionization energy and consideration of the neutral hydrogen partition function, and  $P$  and  $Q$  values for hydrogen take into account the fact that  $H^-$  can exist. It may happen that most of the electrons for the negative hydrogen ion come not from hydrogen in astrophysical mixtures, but from the more easily ionized metals.

More detailed ionic calculations have been given by Plass *et al.* (1957), Bernstein and Dyson (1959), Armstrong *et al.* (1958), and Rouse (1963). The Plass *et al.* report is a very useful extension to the somewhat sketchy Mayer (1947) report. Armstrong uses fractional parentage coefficients which make the consideration of multiply-excited levels even more detailed in calculating the splitting of the bound-free absorption edges. The Rouse equation of state data have been checked at  $T = 20,000^\circ \text{K}$  and  $\rho = 10^{-4} \text{ gm/cm}^3$  and at  $T = 7750^\circ \text{K}$  and  $\rho = 4.68 \times 10^{-7} \text{ gm/cm}^3$ . The greatest differences are only a few per cent for all quantities when allowance is made for his approximate partition functions and neglect of excitations in his total energy.

If the temperature is above  $10^6^\circ \text{K}$  for astrophysical mixtures, it is faster to use the Mayer modified independent-electron method described in section 4.3 for getting occupation numbers. Actual checks show that the "ionic" and "atomic" methods give essentially the same occupation numbers and opacities. The value of the "ionic" method just described is in its sole applicability at low temperatures and densities and its greater detail in splitting of absorption edges. The ionic method often takes into account actual observed configurations, and, except for the core electrons, which are considered to exist only in the average ion, energy-level data are of high accuracy.

The occupation of the various bound levels determines the absorption line spectrum which, together with the oscillator strengths  $f_{kk'}$  and the line shapes, gives the line absorption. One difficult problem in line absorption is the tabulation of all the possible lines that exist. When the ionic method is being used, the assumption is made that all important ionic configurations have been observed and are therefore represented in the energy-level data. The positions, strengths, and widths of all important lines from each ion are then tabulated. For the "atomic" cases, where detailed energy-level data are not available, one can use the Mayer ionic method (see § 4.3) in which one lists various probable configurations, proceeds to evaluate their exact abundances from the occupations in the average atoms, and then tabulates data for the strongest lines which occur in these ionic configurations. However in this chapter, for "atomic"

cases, the line absorption spectrum is computed by another method described below. The equivalence of the Mayer "ionic" method and the method given below is shown by Plass *et al.* (1957).

We calculate from essentially all the possible configurations, a partition function for the entire atom

$$B_i = \sum_{j'} g_{ij'} \exp \left[ -\frac{E_{ij'}}{kT} + \eta \sum_k (\nu_k - x_{ik}) \right], \quad (139)$$

where the sum is over the entire set of configurations  $j'$ , which contains the levels  $k$  with  $\nu_k$  electrons in them. The  $\nu_k$  here is adjusted by the average occupation  $x_{ik}$  to keep the exponential from reaching extreme values. The  $g_{ij'}$  is the appropriate product of binomial coefficients which expresses the number of ways configuration  $j'$  can exist with no appreciable change in energy of the configuration  $E_{ij'}$ .

The energy  $E_{ij'}$  is calculated by using screening constants and is corrected for free-electron perturbations and the continuum depression according to Mayer (1947). Thus, using the ion sphere model,

$$E_{ij'} = -\frac{9}{5} \frac{y_i^2}{r_i} + \sum_k \nu_k \left( -\frac{Z_{ik}^{**2}}{n_k^2} - \frac{y_i \langle r_k^2 \rangle}{r_i^3} + E_0 \right) \text{ Rydbergs} \quad (140)$$

with

$$Z_{ik}^{**} = Z_i - \sum_{k' < k} \sigma_{kk'} \nu_{k'} - \frac{1}{2} (\nu_k - 1) \sigma_{kk}. \quad (141)$$

Note that  $E_0$  is added  $\sum_k \nu_k$  times to compensate for  $\sum_k \nu_k \eta$  values, as discussed in § 4.3. The factor of one half in the screening of electrons in the  $k$  level by other electrons in the same level is due to the definition of screening constants and how they are used in calculating the interaction of electrons in the same shell. This energy of the whole ion differs from that given in equation (96), because the interaction energy between the free electrons and the nucleus as well as the potential energy of the free electron cloud have been included.

The probability of configuration  $ij'$  then is

$$p_{ij'} = \frac{g_{ij'} \exp \left[ -\frac{E_{ij'}}{kT} + \eta \sum_k (\nu_k - x_{ik}) \right]}{B_i}, \quad (142)$$

and occupations can be obtained by multiplying this probability by the number of electrons which exist in each shell of the configuration.

For each important configuration the entire ion energies before and after the line transition, again obtained by using screening constants, can now be used to compute the energies of possible transitions. The thermal fluctuation in occupation numbers results in a complex spectrum which does become simpler at lower temperatures. Further line splitting, which appears as fine structure in

spectra, probably needs to be considered at low temperatures where accurate monochromatic absorption coefficients are required. The spreading of line absorption over a band of frequencies can have a large effect on absorption coefficients and opacities.

#### 4.6. PRESENT METHODS FOR ABSORPTION CALCULATIONS

Processes discussed in § 3 and considered for the opacities to be tabulated later are: bound-free absorption, free-free absorption, Compton electron scattering, bound-bound absorption,  $H^-$  bound-free and free-free absorption, coherent scattering by bound electrons, calculated together with bound-bound absorption, and  $H_2^+$  and  $N+H$  molecular absorption. One follows the Ström-gren and Mayer methods closely by calculating:<sup>3</sup>

$$D_{bf} = \frac{\kappa_{bf} \rho u^3}{A} = \sum_{i,j,k} x_i x_{ij} \frac{x_{ijk} 4\pi^4 m^2 e^8 Z_k^{*/4}}{h^4 n_k^5 (kT)^2} q_{bf} g_{bf} \left[ n_k, \frac{kT(u - u_e)}{Z_k^{*/2}} \right], \quad (143)$$

$$D_{ff} = \frac{\kappa_{ff} \rho u^3}{A} = \sum_i x_i \frac{2\pi^2 m e^4 y_i^2}{h^2 kT} \ln(1 + e^\eta) g_{ff}(\eta, y_i^2/kT, u), \quad (144)$$

$$D_s = \frac{\sigma_e \rho u^3}{A} = \sum_i x_i y_i \frac{u^3}{1 - e^{-u}} \frac{kT \sqrt{3}}{8} \left( \frac{2\pi e^2}{hc} \right)^3 \frac{h^2}{2\pi^2 m e^4} G(u), \quad (145)$$

$$D_l = \frac{\kappa_l \rho u^3}{A} = \sum_{i,j,k} x_i x_{ij} x_{ijk} f_{kk'} P(k') \pi b(u) \frac{3\sqrt{3}}{2^4} u^3, \quad (146)$$

$$D_{H_{bf}^-} = \frac{\kappa_{H_{bf}^-} \rho u^3}{A} = \sigma_{H_{bf}^-} \frac{x_{H^-}}{x_{H0}} \frac{x_H x_{H0} u^3 3\sqrt{3} m c kT}{2^4 h e^2}, \quad (147)$$

$$D_{H_{ff}^-} = \frac{\kappa_{H_{ff}^-} \rho u^3}{A} = \left( \frac{\sigma_{H_{ff}^-}}{P_e x_{H0}} \right) \frac{P_e x_H x_{H0} u^3 3\sqrt{3} m c kT}{2^4 h e^2}, \quad (148)$$

$$D_m = \frac{\kappa_m \rho u^3}{A} \quad (149)$$

$$= [A_{H_2^+} N_i^2 x_H^2 x_{H0} x_{H^+} + A_{H+H} (P_o - P_e)^2 x_H^2 x_{H0}^2] \frac{u^3 3\sqrt{3} m c kT}{2^4 h e^2 N_i},$$

with  $A$  defined in equation (67).

Bound-free and free-free Gaunt factors are from Karzas and Latter (1958a, b, 1961). The bound-free Gaunt factor depends on the difference of  $u$  from its value at the absorption edge,  $u_e$ . Bound-free absorption is corrected for the availability of the final state by  $q_{bf}$  discussed in section 3.1. The  $Z^{*}$  is the effec-

<sup>3</sup> See footnote in § 3.1 concerning the double use of  $\sigma$  for the scattering opacity and cross-sections following conventions of previous authors.



tive nuclear charge considering screening due to both bound and free electrons, though perhaps only the bound electrons should be considered.

The free-free Gaunt factors used have been averaged over the Fermi-Dirac distribution and are also corrected for screening of the nuclear charge and the availability of a final state. These improvements are due to Green (1958, 1960). For free-free absorption the nuclear charge seen by the free electron is taken as  $y_i$ , and even if data for individual ions are known, the sum here has only one term per element. This simplified treatment is possible because free-free absorption is never important when there is only partial ionization.

$G(u)$ , the ratio of the effective electron-scattering cross-section to the Thomson cross-section, is given by Sampson (1959). The induced emission correction  $(1 - e^{-u})$  for pure absorption processes is not to be applied to free-electron scattering and is therefore put in  $D_*$  to cancel out this factor in  $W(u)$  in equation (68). The appropriate induced effects are included in  $G(u)$ .

The  $f_{kk'}$  is the  $f$ -value listed by Karzas and Latter (1961) for the bound-bound transition  $k$  to  $k'$ . These  $f$ -values are preferred over those given by Green *et al.* (1957) because they have more detail for low quantum numbers. The Green *et al.*  $f$ -values are used for transitions from levels with principal quantum number  $n = 4$  and above. Bound-bound transitions between levels with the same principal quantum number are not considered when using the hydrogen-like  $f$ -values. Nevertheless, these same shell transitions are likely to be important.

We take

$$P(k') = \frac{2(2l_{k'} + 1) - x_{ijk'}}{2(2l_{k'} + 1)}, \quad (150)$$

or

$$P(k') = \frac{2n_{k'}^2 - x_{ijk'}}{2n_{k'}^2}, \quad (151)$$

if detailed data about a level are not known.

The line shape for all lines except those of H, He II, and resonance lines, is given by

$$\pi b(u) = \frac{\frac{\delta_u}{4\pi}}{(u - u_c)^2 + \left(\frac{\delta_u}{4\pi}\right)^2}, \quad (152)$$

with  $\delta_u/4\pi$  the distance from  $u_c$  where the collisionally broadened line has one-half its central value, and this half width is given in equation (45). For all H and He II lines the approximate Stark theory of Griem (1960) is used.

Coherent scattering by bound electrons is included, considering both the emission before absorption and emission after absorption. This is given by

$$\pi b_{cs}(u) = \frac{8\pi e^2 kT}{3m c^3 h} \frac{u^4 \left[ 1 + \frac{x_{ijk'} P(k)}{x_{ijk'} P(k')} \right]}{(u^2 - u_c^2)^2 + u^2 \left( \frac{4\pi e^2 kT}{3m c^3 h} u_c^2 \right)^2}, \quad (153)$$

and, as seen before in §§ 3.3 and 3.6, Thomson and Rayleigh scattering result at the extremes of  $u \gg u_c$  and  $u \ll u_c$ . Equation (153) is used instead of (152) only for scattering by ground-state electrons (resonance lines only), and then only in the wings beyond  $\delta_u$  when  $\Pi b_{os}(u)$  is larger.

The bound-free  $H^-$  cross-sections which are used have been published by John (1960*a*, *b*). Ohmura and Ohmura (1960, 1961) have tabulated the required free-free  $H^-$  cross-sections. Above  $T = 23,210^\circ \text{ K}$  (2 v.)  $H^-$  is not allowed to exist in this method.

The  $H_2^+$  and  $H+H$  molecular effects, described respectively by Bates (1952) and Zwaan (1962), are applied only in the temperature ranges ( $2500\text{--}12,000^\circ \text{ K}$  for  $H_2^+$  and  $3000\text{--}8000^\circ \text{ K}$  for  $H+H$ ) where  $A_{H_2^+}$  and  $A_{H+H}$  are tabulated.

The opacity integral, using Mayer's  $D$  definition, is

$$\mathfrak{I}_M = \int_0^\infty \frac{W(u) du}{D} = \frac{A}{\kappa \rho}, \quad (154)$$

where

$$D = \Sigma D_{bf} + D_{ff} + D_s + D_l + D_{H^-} + D_M. \quad (155)$$

The bound-free sum is over all the edges which have an ionization energy less than  $ukT$  and  $D_l$  is summed over all lines which exist at the  $u$  value. For opacities given in § 5, a line wing is considered to extend only to the line center of the neighboring line with the same initial state.  $D_{ff}$  and  $D_s$  are summed over all elements in the mixture. The integral is calculated by partial sums between absorption edges using Simpson's rule.

At any edge beyond the maximum of the weighting function at  $u \approx 7$ , one can estimate the remaining integral by assuming the  $D$  will be no smaller at larger  $u$  values than it is at the edge where  $u = u_e$  and  $D = D_e$ . Then,

$$\Delta \mathfrak{I}_M \leq \frac{1}{D_e} \int_{u_e}^\infty W(u) du = \frac{1}{D_e} [S(\infty) - S(u_e)] \text{ (remaining)}. \quad (156)$$

If this remainder is sufficiently small compared to  $\mathfrak{I}_M$ , it is neglected.

Recent work has been done on maximum values for the continuous- and line-absorption opacities. Some data are given by Armstrong *et al.* (1961) and Liberman (1962), and the early work is due to Bernstein and Dyson (1959). For astrophysical work, however, opacities cannot be obtained for mixtures to any moderate degree of accuracy unless all details are included.

At densities so high that electron degeneracy becomes important, one needs to consider electron conduction in competition with radiation flow for the transport of energy. The conduction due to molecules, atoms, and ions is important only in the high atmosphere of stars and is not considered here. A discussion of how to calculate the electron-conductive opacity and how to combine it with the radiative opacity has already been given in § 3.11.

#### 4.7. CURRENT LIMITATIONS IN OPACITY CALCULATIONS

Some of the limitations on the method now being used at the Los Alamos Scientific Laboratory, apart from neglect of some molecular effects, can be

TABLE 3  
HIGH TEMPERATURE OPACITIES

T(deg K)	$\rho$ (gm/cm <sup>3</sup> )						
	10 <sup>-3</sup>	10 <sup>-2</sup>	10 <sup>-1</sup>	1.00	10 <sup>+1</sup>	10 <sup>+2</sup>	10 <sup>+3</sup>
2.0×10 <sup>7</sup> :							
$\eta$ .....	-13.72	-11.41	-9.11	-6.81	-4.50	-2.16	.49
$\gamma$ .....	1.15+00	1.15+00	1.15+00	1.15+00	1.15+00	1.15+00	1.15+00
$\kappa_C$ .....	3.04-01	3.05-01	3.06-01	3.18-01	3.80-01	6.04-01	1.51+00
$\kappa_L$ .....	3.04-01	3.05-01	3.07-01	3.24-01	3.90-01	6.11-01	1.51+00
$\kappa_{TL}$ .....	3.04-01	3.05-01	3.07-01	3.24-01	3.90-01	6.10-01	1.43+00
Lines.....	189	243	345	443	384	34	1
1.0×10 <sup>7</sup> :							
$\eta$ .....	-12.68	-10.37	-8.07	-5.77	-3.45	-1.05	2.20
$\gamma$ .....	1.15+00	1.15+00	1.15+00	1.15+00	1.15+00	1.15+00	1.15+00
$\kappa_C$ .....	3.12-01	3.15-01	3.35-01	4.54-01	8.95-01	2.16+00	8.58+00
$\kappa_L$ .....	3.12-01	3.16-01	3.44-01	4.87-01	9.80-01	2.20+00	8.58+00
$\kappa_{TL}$ .....	3.12-01	3.16-01	3.44-01	4.87-01	9.79-01	2.18+00	5.00+00
Lines.....	309	582	936	951	532	25	0
7.0×10 <sup>6</sup> :							
$\eta$ .....	-12.14	-9.84	-7.54	-5.23	-2.91	-.44	3.44
$\gamma$ .....	1.15+00	1.15+00	1.15+00	1.15+00	1.15+00	1.15+00	1.15+00
$\kappa_C$ .....	3.15-01	3.27-01	4.04-01	7.86-01	1.96+00	5.54+00	2.39+01
$\kappa_L$ .....	3.15-01	3.31-01	4.32-01	8.93-01	2.16+00	5.62+00	2.39+01
$\kappa_{TL}$ .....	3.15-01	3.31-01	4.32-01	8.93-01	2.16+00	5.47+00	5.58+00
Lines.....	437	923	1693	1620	740	27	0
5.0×10 <sup>6</sup> :							
$\eta$ .....	-11.64	-9.33	-7.03	-4.73	-2.40	.19	5.00
$\gamma$ .....	1.15+00	1.15+00	1.15+00	1.15+00	1.15+00	1.15+00	1.15+00
$\kappa_C$ .....	3.21-01	3.61-01	6.29-01	1.89+00	4.94+00	1.50+01	6.22+01
$\kappa_L$ .....	3.23-01	3.71-01	7.25-01	2.24+00	5.37+00	1.54+01	6.22+01
$\kappa_{TL}$ .....	3.23-01	3.71-01	7.25-01	2.24+00	5.36+00	1.39+01	4.05+00
Lines.....	613	1594	3023	5047	866	10	0
3.5×10 <sup>6</sup> :							
$\eta$ .....	-11.10	-8.80	-6.50	-4.19	-1.84	.93	7.27
$\gamma$ .....	1.15+00	1.15+00	1.15+00	1.15+00	1.15+00	1.15+00	1.15+00
$\kappa_C$ .....	3.40-01	5.08-01	1.68+00	6.51+00	1.51+01	4.51+01	1.70+02:
$\kappa_L$ .....	3.47-01	5.77-01	2.33+00	8.09+00	1.62+01	4.53+01	1.70+02:
$\kappa_{TL}$ .....	3.47-01	5.77-01	2.33+00	8.09+00	1.60+01	3.08+01	2.25+00
Lines.....	1063	3103	6414	6929	734	7	0
2.0×10 <sup>6</sup> :							
$\eta$ .....	-10.26	-7.96	-5.66	-3.35	-.93	2.43	12.85
$\gamma$ .....	1.15+00	1.15+00	1.15+00	1.14+00	1.15+00	1.15+00	1.15+00
$\kappa_C$ .....	4.92-01	1.41+00	8.22+00	3.48+01	7.95+01	2.56+02	9.68+02:
$\kappa_L$ .....	5.41-01	2.25+00	1.66+01	5.01+01	8.55+01	2.56+02	9.68+02:
$\kappa_{TL}$ .....	5.41-01	2.25+00	1.66+01	5.00+01	7.96+01	4.08+01	8.43-01
Lines.....	2968	8852	8046	2832	150	3	0
1.0×10 <sup>6</sup> :							
$\eta$ .....	-9.22	-6.92	-4.62	-2.31	.33	5.40	25.81
$\gamma$ .....	1.15+00	1.15+00	1.14+00	1.12+00	1.15+00	1.15+00	1.15+00
$\kappa_C$ .....	1.28+00	7.23+00	4.05+01	1.30+02	5.26+02	1.86+03:	3.19+04:
$\kappa_L$ .....	2.07+00	2.03+01	8.54+01	1.89+02	5.31+02	1.86+03:	3.19+04:
$\kappa_{TL}$ .....	2.07+00	2.03+01	8.54+01	1.86+02	2.80+02	1.65+01	2.18-01
Lines.....	8482	16270	7104	950	43	1	0

listed. A bibliography of current opacity work has been given by Huebner and Stuart (1964).

At normal temperatures and densities there is some uncertainty in the bound-free and free-free Gaunt factors. The uncertainty arises because the electric fields seen by electrons may not be accurately Coulomb. Very few quantum-mechanical calculations of non-Coulomb absorption are available, but some recent results are available, for example, see Burgess and Seaton (1960). Huang (1948) has given quantum-mechanical absorptions for the helium atom, without the Coulomb field assumption.

The methods developed for opacity calculations do not give accurate occupation numbers and energy levels for elements with many bound electrons. Such

TABLE 4  
INTERMEDIATE TEMPERATURE OPACITIES

T(deg K)	$\rho(\text{gm/cm}^3)$						
	$10^{-7}$	$10^{-6}$	$10^{-5}$	$10^{-4}$	$10^{-3}$	$10^{-2}$	$10^{-1}$
$1.0 \times 10^3$ :							
$\eta$ .....	-18.43	-16.13	-13.83	-11.53	-9.23	-6.95	-4.65
$\gamma$ .....	1.15+00	1.15+00	1.15+00	1.15+00	1.14+00	1.12+00	1.12+00
$\kappa_C$ .....	3.18-01	3.22-01	3.45-01	4.89-01	1.46+00	8.43+00	4.35+01
$\kappa_L$ .....	3.19-01	3.24-01	3.50-01	5.36-01	2.16+00	1.92+01	9.05+01
$\kappa_{TL}$ .....	3.19-01	3.24-01	3.50-01	5.36-01	2.16+00	1.92+01	9.04+01
Lines.....	396	590	932	1401	1163	933	556
$5.0 \times 10^3$ :							
$\eta$ .....	-17.39	-15.09	-12.79	-10.49	-8.20	-5.95	-3.73
$\gamma$ .....	1.15+00	1.15+00	1.15+00	1.14+00	1.13+00	1.07+00	1.09+00
$\kappa_C$ .....	3.22-01	3.53-01	5.74-01	2.29+00	1.52+01	7.29+01	1.98+02
$\kappa_L$ .....	3.24-01	3.60-01	6.45-01	3.47+00	3.35+01	1.38+02	2.89+02
$\kappa_{TL}$ .....	3.24-01	3.60-01	6.45-01	3.47+00	3.35+01	1.38+02	2.88+02
Lines.....	623	1049	1331	1139	1169	800	742
$2.0 \times 10^4$ :							
$\eta$ .....	-16.02	-13.72	-11.42	-9.14	-6.88	-4.59	-2.32
$\gamma$ .....	1.15+00	1.15+00	1.14+00	1.12+00	1.07+00	1.06+00	1.08+00
$\kappa_C$ .....	4.89-01	1.70+00	1.30+01	1.15+02	7.67+02	2.88+03	3.01+03
$\kappa_L$ .....	5.23-01	2.11+00	1.96+01	2.46+02	1.50+03	3.48+03	3.17+03
$\kappa_{TL}$ .....	5.23-01	2.11+00	1.96+01	2.46+02	1.50+03	3.46+03	2.95+03
Lines.....	1768	1615	1383	1208	1330	704	479
$1.0 \times 10^5$ :							
$\eta$ .....	-14.98	-12.69	-10.40	-8.16	-5.94	-3.77	-1.25
$\gamma$ .....	1.14+00	1.14+00	1.12+00	1.06+00	9.70-01	9.32-01	1.02+00
$\kappa_C$ .....	1.61+00	1.16+01	1.31+02	1.42+03	9.09+03	2.46+04	1.86+04
$\kappa_L$ .....	2.19+00	2.08+01	2.79+02	4.05+03	2.60+04	4.58+04	1.86+04
$\kappa_{TL}$ .....	2.19+00	2.08+01	2.79+02	4.05+03	2.59+04	3.99+04	1.01+04
Lines.....	1979	1513	1114	1176	1283	952	218
$5.0 \times 10^4$ :							
$\eta$ .....	-13.99	-11.76	-9.52	-7.28	-5.09	-2.96	.....
$\gamma$ .....	1.09+00	1.01+00	9.59-01	8.99-01	8.01-01	6.76-01	.....
$\kappa_C$ .....	2.17+01	1.70+02	1.33+03	9.47+03	5.65+04	1.46+05	.....
$\kappa_L$ .....	3.42+01	3.07+02	3.05+03	2.75+04	1.56+05	1.91+05	.....
$\kappa_{TL}$ .....	3.42+01	3.07+02	3.05+03	2.75+04	1.45+05	7.63+04	.....
Lines.....	1707	1253	1143	1478	1211	700	.....

large occupation numbers are not usually encountered in astrophysical situations. Special methods of obtaining bound energy levels in the Thomas-Fermi potential have been worked out, but they are not discussed here.

Improvements in non-relativistic screening constants have recently been made by Layzer (1959). The nuclear charge of ions should not be so high that the non-relativistic screening constants which are used to get energy levels are inaccurate. These relativistic effects are small for elements with  $Z$  no larger than 26.

For high temperatures like  $10^{10}$  °K one gets absorption by pair production

TABLE 5  
LOW TEMPERATURE OPACITIES

5040/T (1/deg K)	$P_e$ (erg/cm <sup>2</sup> )						
	10 <sup>-1</sup>	1.00	10 <sup>1</sup>	10 <sup>2</sup>	10 <sup>3</sup>	10 <sup>4</sup>	10 <sup>5</sup>
0.2:							
$\eta$ .....	-27.23	-24.93	-22.63	-20.33	-18.02	-15.72	-13.42
$\gamma$ .....	1.12+00	1.04+00	1.01+00	1.00+00	1.00+00	9.97-01	9.83-01
$\rho$ .....	6.21-14	6.63-13	6.88-12	6.92-11	6.93-10	6.95-09	7.05-08
$P_\theta$ .....	1.90-01	1.96+00	1.99+01	2.00+02	2.00+03	2.00+04	2.01+05
$\kappa_C$ .....	3.09-01	2.95-01	3.18-01	4.19-01	8.73-01	4.41+00	3.71+01
$\kappa_L$ .....	3.10-01	2.96-01	3.19-01	4.26-01	1.00+00	6.85+00	8.36+01
Lines.....	566	593	712	1022	1545	1914	1629
0.4:							
$\eta$ .....	-25.50	-23.20	-20.90	-18.59	-16.29	-13.99	-11.69
$\gamma$ .....	9.96-01	9.69-01	8.96-01	8.61-01	8.21-01	5.90-01	1.61-01
$\rho$ .....	1.39-13	1.43-12	1.55-11	1.61-10	1.69-09	2.35-08	8.61-07
$P_\theta$ .....	2.00-01	2.03+00	2.12+01	2.16+02	2.22+03	2.69+04	7.19+05
$\kappa_C$ .....	2.79-01	2.98-01	4.62-01	1.81+00	1.40+01	9.65+01	2.82+02
$\kappa_L$ .....	2.87-01	3.04-01	4.81-01	2.02+00	1.84+01	1.63+02	7.29+02
Lines.....	459	541	647	809	1071	1559	1947
0.6:							
$\eta$ .....	-24.49	-22.18	-19.88	-17.58	-15.28	-12.97	-10.67
$\gamma$ .....	8.55-01	8.06-01	5.16-01	1.13-01	1.30-02	1.40-03	1.45-04
$\rho$ .....	2.43-13	2.58-12	4.03-11	1.85-09	1.60-07	1.49-05	1.43-03
$P_\theta$ .....	2.17-01	2.24+00	2.94+01	9.87+02	7.79+04	7.16+06	6.88+08
$\kappa_C$ .....	2.63-01	4.10-01	9.89-01	2.07+00	6.05+00	3.23+01	2.59+02
$\kappa_L$ .....	2.66-01	4.17-01	1.10+00	2.61+00	9.58+00	6.57+01	5.34+02
Lines.....	382	444	479	554	724	962	812
0.8:							
$\eta$ .....	-23.77	-21.47	-19.16	-16.86	-14.56	.....	.....
$\gamma$ .....	1.05-01	1.20-02	1.29-03	1.73-04	3.40-05	.....	.....
$\rho$ .....	2.63-12	2.30-10	2.15-08	1.61-06	8.15-05	.....	.....
$P_\theta$ .....	1.05+00	8.40+01	7.76+03	5.79+05	2.94+07	.....	.....
$\kappa_C$ .....	4.12-02	2.36-02	1.23-01	1.30+00	1.56+01	.....	.....
$\kappa_L$ .....	4.24-02	2.57-02	1.40-01	1.62+00	2.03+01	.....	.....
Lines.....	302	314	324	447	557	.....	.....
1.0:							
$\eta$ .....	-23.21	-20.91	-18.60	-16.30	-14.00	.....	.....
$\gamma$ .....	2.00-04	6.48-05	2.88-05	7.07-06	7.40-07	.....	.....
$\rho$ .....	1.73-09	5.35-08	1.20-06	4.90-05	4.69-03	.....	.....
$P_\theta$ .....	5.00+02	1.54+04	3.47+05	1.41+07	1.35+09	.....	.....
$\kappa_C$ .....	2.39-03	2.33-02	2.38-01	2.53+00	3.21+01	.....	.....
$\kappa_L$ .....	2.90-03	2.57-02	2.77-01	2.94+00	3.37+01	.....	.....
Lines.....	227	251	326	338	243	.....	.....

and production of an abundance of electron-positron pairs, all of which can give rise to Compton scattering. If the density is very high, as is likely to be the case, one possibly does not have to worry about the excess electron and positron density. Attempts by Milford (1957) and Sampson (1959) have already been made to calculate opacities at temperatures up to  $10^9$  °K.

In the present calculations it is assumed that the free electrons scatter independently. Actually, however, collective interactions in the plasma introduce a partial ordering of the charged particles which tends to reduce the scattering cross-section per electron. Kahn (1959) has studied this effect. He shows that in the limit of low temperatures and high densities the Compton cross-section is reduced by a factor  $Z/(Z + 1)$  for a completely ionized gas of a pure element with atomic number  $Z$ . Using Kahn's work and a correction to it pointed out by Salpeter (1960), one can estimate this effect on the total opacity of a typical stellar mixture. Indeed, in many cases the Compton scattering should be reduced

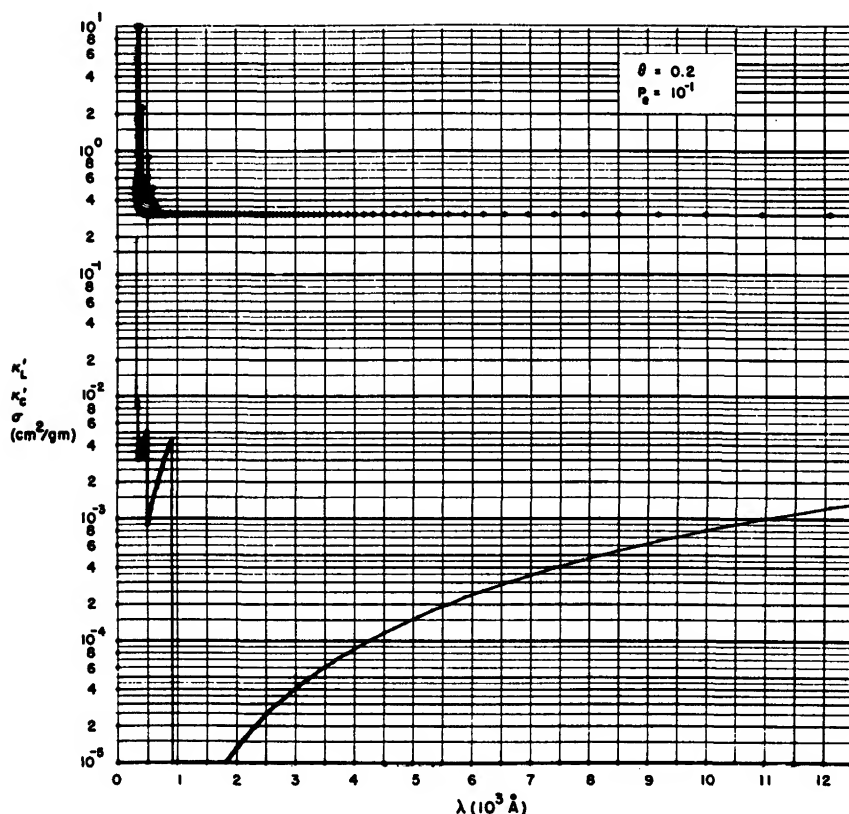


FIG. 1.—Monochromatic line absorption, continuous absorption, and scattering coefficients versus wavelength for  $\theta = 5040/T = 0.2$  and  $P_e = 10^{-1}$ . The Rosseland mean of these data is given in Table 5.

to perhaps one-half its value. These corrections have not been applied because of other simultaneous effects. For astrophysical mixtures when the photon wavelengths become large compared to the Debye length, a condition necessary for the photons to notice the plasma ordering, the number of ions in the Debye sphere gets very small. With numbers of ions as small as a few per Debye sphere, relaxation times are short, and the ordering theory is not accurate. It is perhaps better to ignore the ordering effects until the theory has been worked out in some detail.

The cutoff of photon transmission at the plasma frequency may affect radiation flow at high densities. The cutoff does not appreciably affect any of the data presented here because at high densities electron conduction is dominant.

The most important defect of the present opacity results is in the line absorption. There are two problems: the number of possible lines must be tabulated with proper strengths, and the line width and shape must be known. There

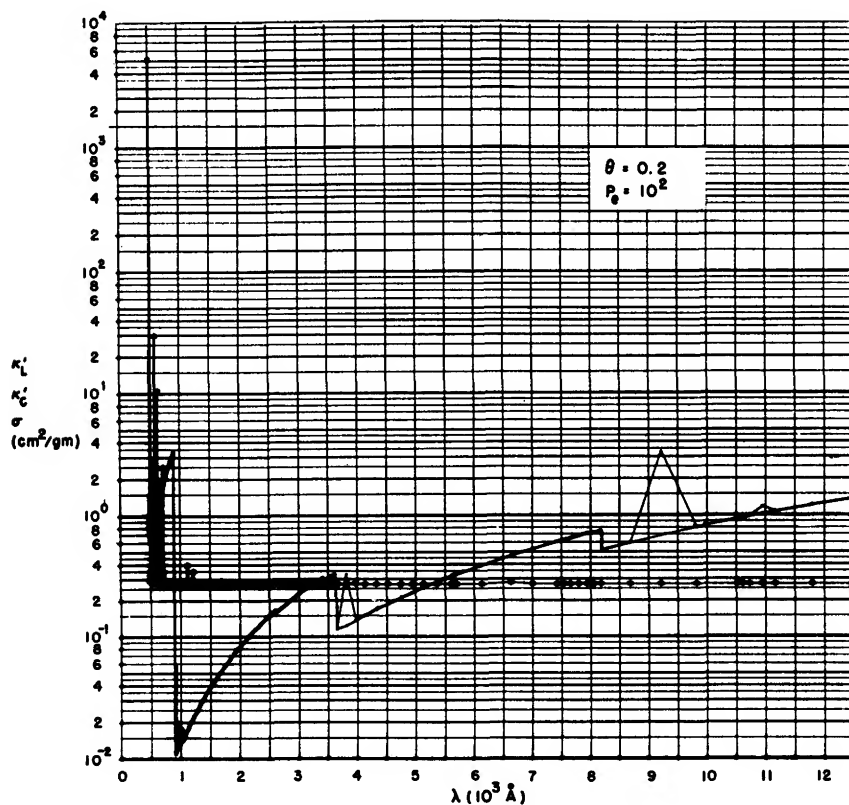


FIG. 2.—Monochromatic line absorption, continuous absorption, and scattering coefficients versus wavelength for  $\theta = 5040/T = 0.2$  and  $P_e = 10^2$ . The Rosseland mean of these data is given in Table 5.

is still uncertainty in the line widths, but usually the exact shape of lines does not seem very important because so many lines merge to give a band of absorption. However, at low temperatures exact line shapes may be important.

The absorption by exotic compounds such as  $\text{HeH}^+$ ,  $\text{He}^3$ ,  $\text{He}^-$ ,  $\text{He}_2$ , etc., has been neglected in all absorption calculations to date. Conceivably one or more could contribute noticeably to the total absorption in special cases.

## § 5. NEW RESULTS

### 5.1. COMPARISONS WITH PREVIOUS OPACITIES

A recalculation, by this author, of the Zirin continuous opacities shows that, at the highest densities, electron conduction should dominate all radiative energy transport. Morse also gave opacities which he admitted were probably not relevant because of electron heat conduction. A closer comparison of the Zirin opacities, given in his second paper, with the more modern results shows

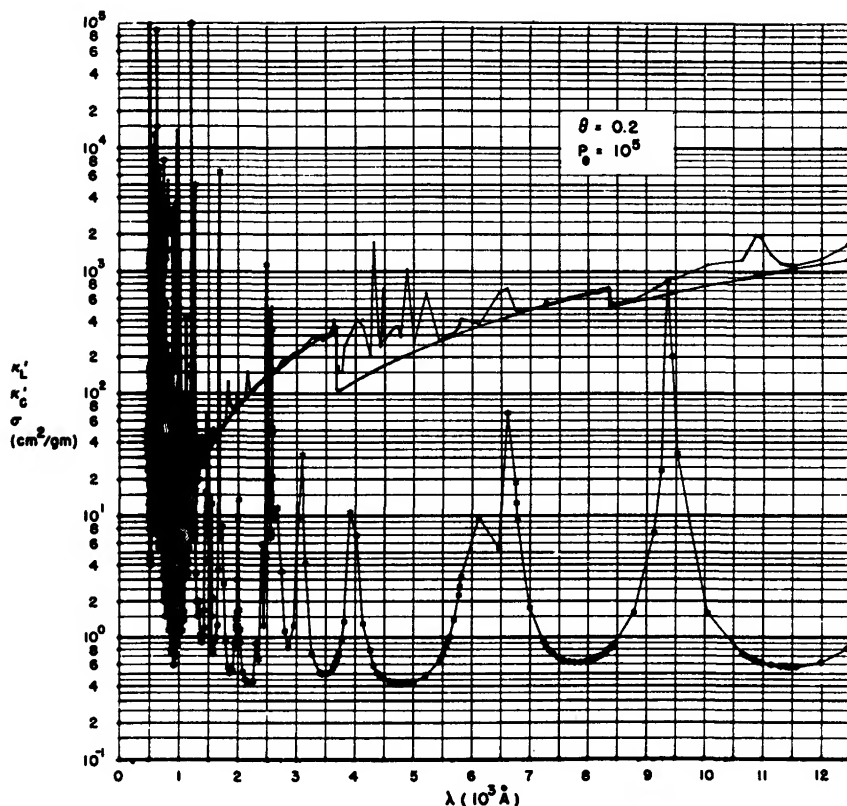


FIG. 3.—Monochromatic line absorption, continuous absorption, and scattering coefficients versus wavelength for  $\theta = 5040/T = 0.2$  and  $P_e = 10^5$ . The Rosseland mean of these data is given in Table 5.



that his rapid method may introduce appreciable errors at some points. Errors are usually less than 30 per cent when there is no electron degeneracy, but the Zirin values are almost always too small. The Zirin opacities are sometimes almost a factor of 2 too small at moderate degeneracies. At the temperature and density of the solar center, the error is less than 50 per cent.

All the Keller-Meyerott mixtures have been redone by this author. Except at the lowest temperatures where occupation numbers are uncertain in both series of computations, agreement between continuous opacities is better than 20 per cent. The hoped for accuracy of 10 per cent in the Keller-Meyerott opacities seems to be almost always achieved. The reason for the quality of the results is probably due to partial application of high-speed computing machines. All previous work had to be limited to some extent, and certain sources of opacity were neglected or wrongly estimated. Even with the use of the IBM card program calculator, there is suspicion that a few bound-free absorption edges have

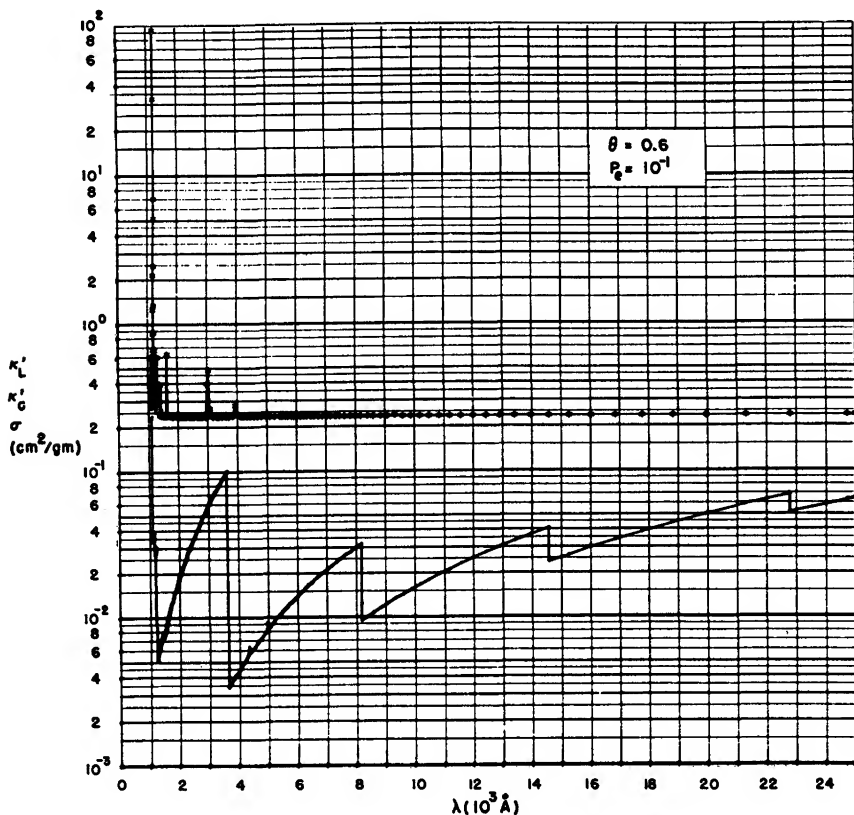


FIG. 4.—Monochromatic line absorption, continuous absorption, and scattering coefficients versus wavelength for  $\theta = 5040/T = 0.6$  and  $P_e = 10^{-1}$ . The Rosseland mean of these data is given in Table 5.

been neglected, because the Keller-Meyerott opacities are systematically low compared with even more elaborate recent calculations using the IBM 704 and IBM 7090.

Some of the monochromatic absorption cross-sections for hydrogen and helium given by Ueno, Saito, and Jugaku (1954) have also been recalculated at  $\theta = 5040/T = 0.2$  and  $\log P_e = 5$ . At the highest temperatures in their tabulation, one must be sure to consider these cross-sections as relative to the number of atoms in the ground state and not relative to the total number of atoms in the appropriate ionization stage. With this understanding the cross-sections seem to be accurate to better than 10 per cent. The Ueno (1954) opacities, based on these monochromatic absorption data, seem to be of good quality.

Monochromatic absorption coefficients calculated by Vitense (1951) and Lyast (1954) have also been checked at  $\theta = 0.2$  and  $\log P_e = 5$  for Vitense and  $\log P_e = 3$  for Lyast. The Vitense results are apparently accurate to only a few

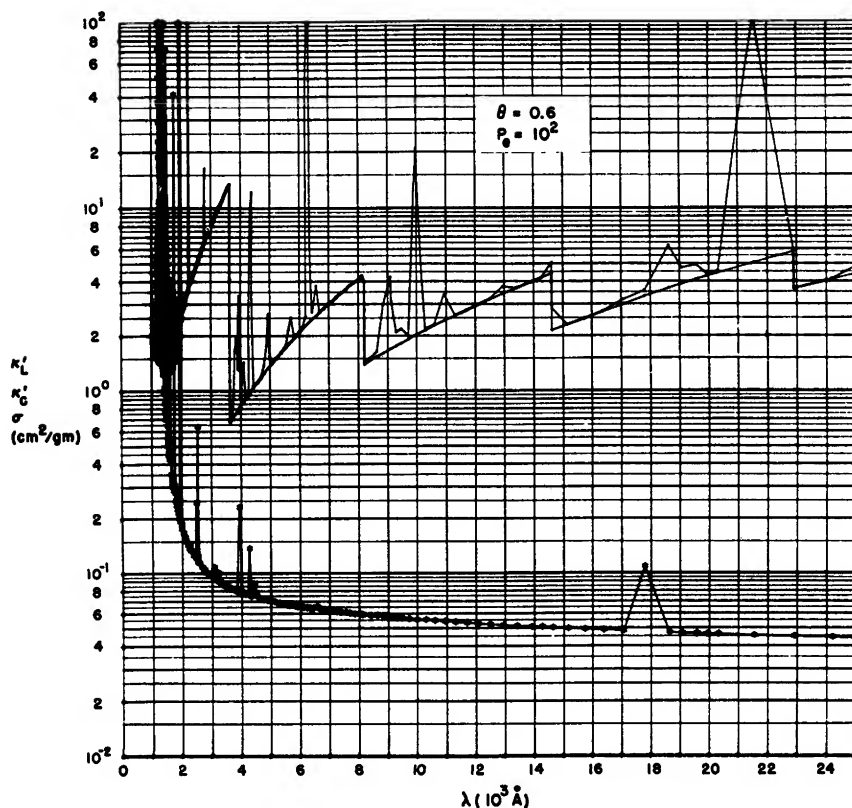


FIG. 5.—Monochromatic line absorption, continuous absorption, and scattering coefficients versus wavelength for  $\theta = 5040/T = 0.6$  and  $P_e = 10^2$ . The Rosseland mean of these data is given in Table 5.

per cent where they have been checked. However, the Lyast data seem to be based on only approximate partition functions, and differences of more than a factor of two are possible at absorption edges where occupation numbers are uncertain. However, the plotted opacities at  $\theta = 0.2$  seem to be accurate to better than 10 per cent.

The new widely used Strömngren tables for pure H, including  $H_2^+$ , which unfortunately have never been published, are accurate to about 10 per cent at all frequencies at  $\theta = 0.3$  and  $\log P_e = 4$ .

## 5.2. OPACITIES FOR MIXTURE $X = 0.596$ , $Y = 0.384$ , $Z = 0.020$

A mixture which is supposed to be close to the primordial composition of the sun (Aller 1961) has been calculated in detail. The number fractions, respectively, for H, He, C, N, O, Ne, Na, Mg, Al, Si, A, and Fe are 0.858971, 0.139309, 0.000342, 0.000096, 0.000766, 0.000431, 0.000002, 0.000022, 0.000001, 0.000027,

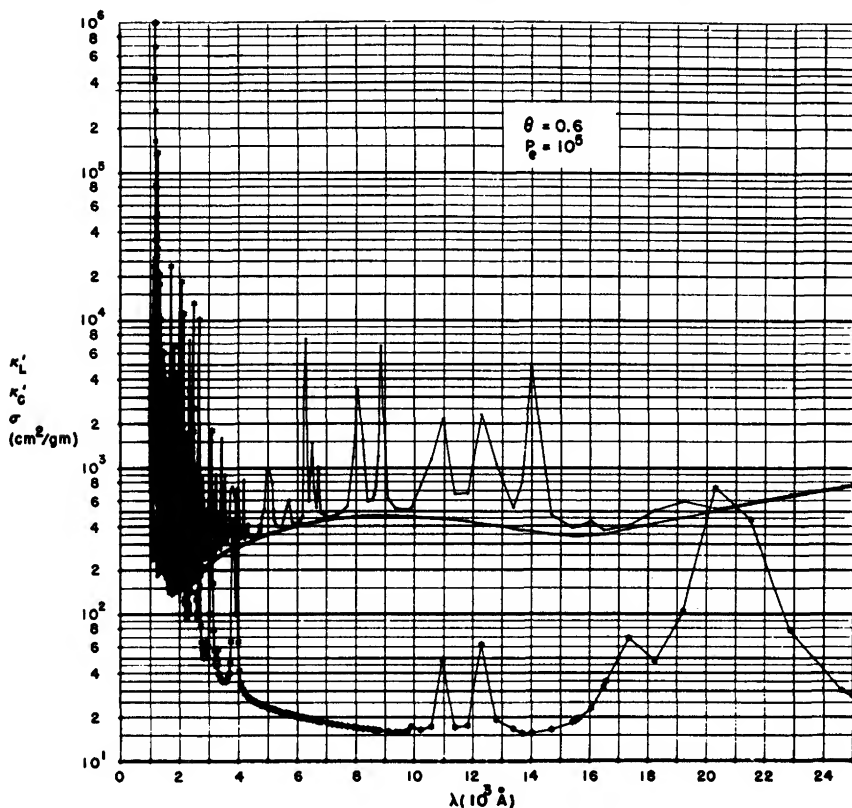


FIG. 6.—Monochromatic line absorption, continuous absorption, and scattering coefficients versus wavelength for  $\theta = 5040/T = 0.6$  and  $P_e = 10^5$ . The Rosseland mean of these data is given in Table 5.

0.000029, and 0.000004. The respective weight fractions are 0.59603, 0.38388, 0.00283, 0.00093, 0.00843, 0.00599, 0.00003, 0.00036, 0.00003, 0.00053, 0.00079, and 0.00017.

Table 3 gives, versus temperature and density, the degeneracy parameter  $\eta$ , the number of free electrons per average atom  $y$ , the continuous opacity  $\kappa_c$ , an estimate of the radiative opacity including line absorption as described in section 4.6,  $\kappa_L$ , the total-line and continuous opacity with conduction  $\kappa_{TL}$ , and the number of lines strong enough to be considered. Lines from no more than 390 levels have been tabulated for the bound-bound absorption. Opacities in all tables are in units of  $\text{cm}^2/\text{gm}$ , and the power of ten which applies to some of the values is given immediately after the number. These opacities have been calculated using occupation numbers for the average atom only (Mayer method), and the method discussed in § 4.5 for obtaining abundances of specific ionic configurations has been used to determine the line spectrum.

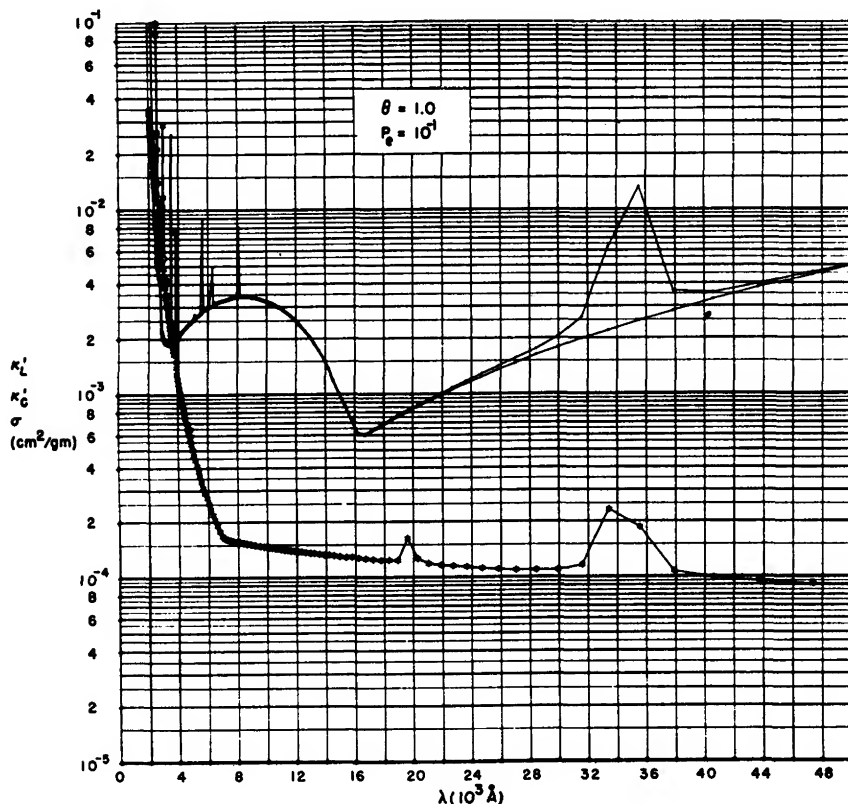


FIG. 7.—Monochromatic line absorption, continuous absorption, and scattering coefficients versus wavelength of  $\theta = 5040/T = 1.0$  and  $P_e = 10^{-1}$ . The Rosseland mean of these data is given in Table 5.

Table 4 continues these opacities at lower temperatures and densities using the ionic method in § 4.5. The occupation numbers for these lower temperatures are those in the important configurations in the mixture except that occupations for core electrons are the average for each stage of ionization. At  $10^6$  °K there is overlap with Table 3 which shows the differences between the "ionic" and "atomic" methods. Ionic opacities are preferred over the atomic opacities.

Table 5 gives opacities from the "ionic" method at even lower temperatures as a function of temperature and electron pressure. The spectrum is dominated by the hydrogen and helium lines at these low temperatures, and the shapes of H and He II lines at all temperatures have been calculated using an approximate Stark theory due to Griem (1960). At each point is given the degeneracy parameter  $\eta$ , the number of free electrons per average atom  $y$ , the density  $\rho$  in gm/cm<sup>3</sup>, the gas pressure  $P_g$  in dynes/cm<sup>2</sup> or erg/cm<sup>3</sup>, the continuous opacity

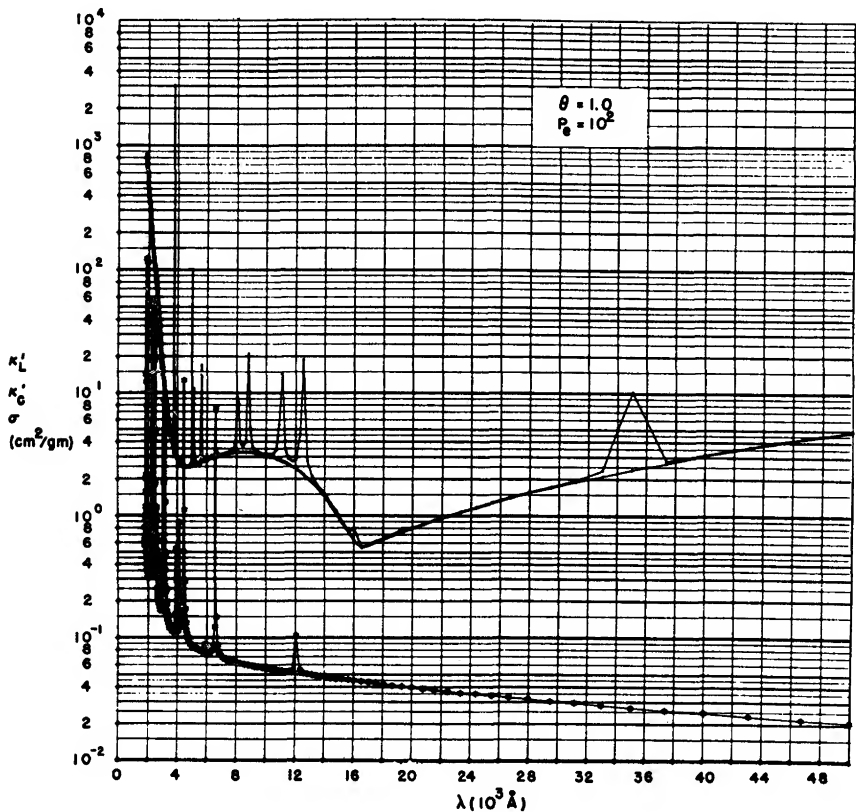


FIG. 8.—Monochromatic line absorption, continuous absorption, and scattering coefficients versus wavelength for  $\theta = 5040/T = 1.0$  and  $P_e = 10^2$ . The Rosseland mean of these data is given in Table 5.

$\kappa_C$ , the line opacity  $\kappa_L$ , and the number of lines strong enough to be considered. Electron conduction does not contribute to energy flow at these low temperatures and densities.

At high densities in Table 3 some of the radiative opacities listed are not strictly correct due to the impossibility of photon propagation at frequencies below the plasma frequency. These opacities have been calculated assuming infinite absorption at frequencies less than the plasma frequency, and they are marked with a colon in the tables. For example, at  $T = 10^6$  °K and  $\rho = 10^3$  gm/cm<sup>3</sup>, the plasma frequency corresponds to  $u = 9.4$ . The total opacity in-

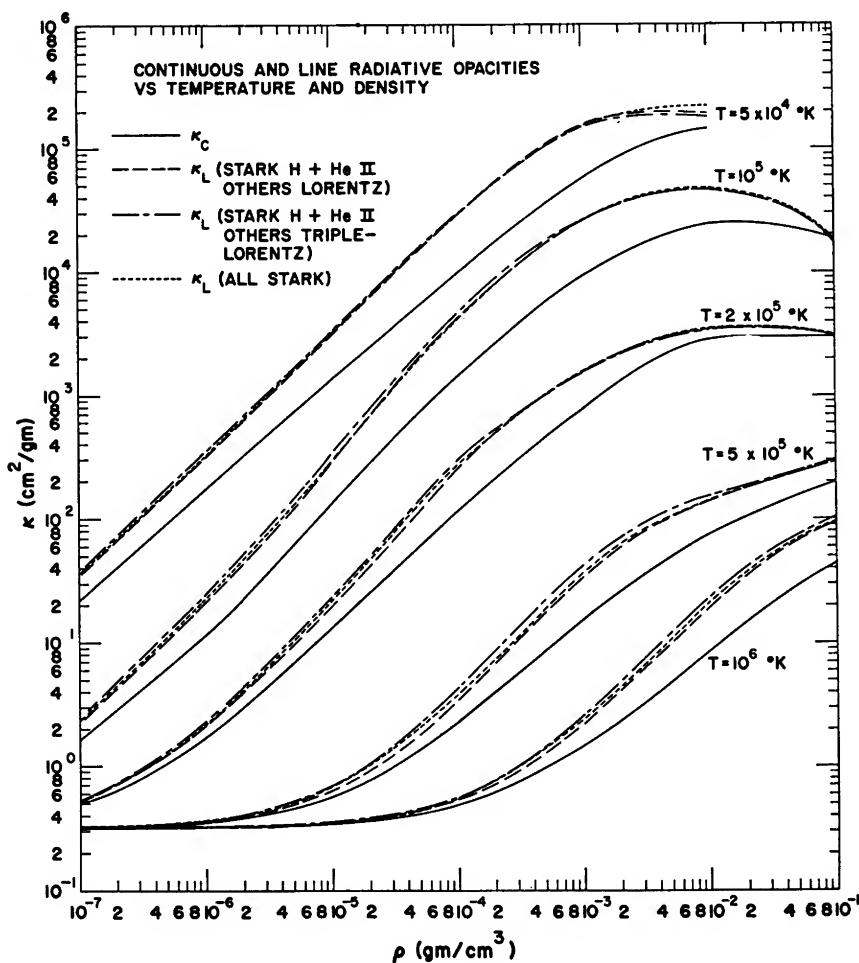


FIG. 9.—Continuous and line opacities using various line shapes versus density with temperature as a parameter.

cluding electron conduction is not affected, however, because when these plasma effects are important, electron conduction is also important.

For illustration, Figures 1 through 8 give the monochromatic  $\kappa'_\lambda$  and  $\sigma_\lambda$ , with the  $\kappa'_\lambda$  corrected for induced emission, as functions of the wavelength,  $\lambda$ , for several stellar atmosphere electron pressures and temperatures. Each figure shows the continuous, the continuous plus line absorption coefficients and the scattering coefficients in units of  $\text{cm}^2/\text{gm}$ . Very fine detail in the absorption is not calculated by the methods discussed in this chapter, but the general behavior of the absorption is accurately displayed.

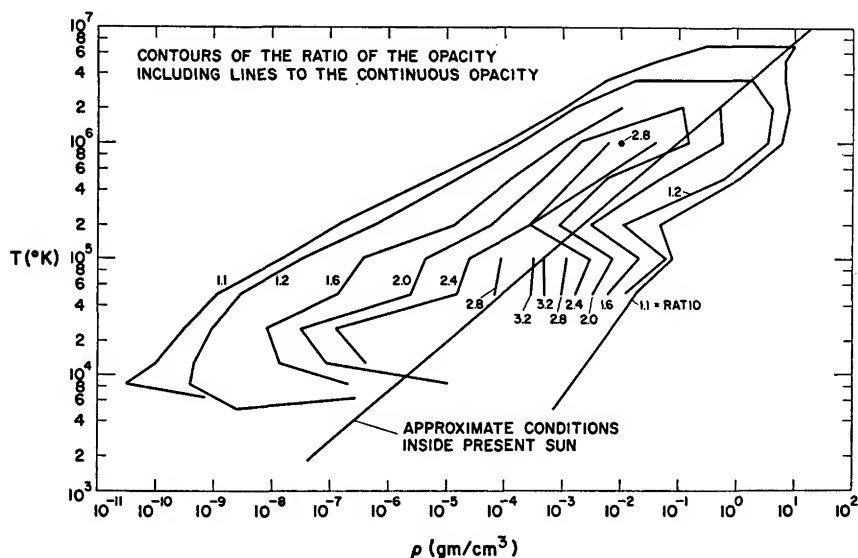


FIG. 10.—Contours of the ratio of the line opacity to the continuous opacity on the temperature-density plane.

Figure 9 gives plots of the continuous and continuous plus line opacities in Table 4. Figure 9 also shows opacities calculated with line widths three times greater than those given by equation (45) (except that the Stark H and He II lines are unchanged), and opacities calculated using the Griem (1960) approximate Stark shape for *all* lines. For high density, the Lorentz formula with the triple width gives a lower opacity than the usual formula because the lines spread outside the region of the  $W(u)$  maximum. The opacity is not strongly dependent on the line shape at any temperature and density point for this mixture, and most of the data in Table 4 are accurate to better than 30 per cent.

The effects of the line absorption on the opacity are given in Figure 10, where ratios of the line to continuous radiative (not radiative and conductive) opacity are plotted as contours on the temperature-density plane. The data come from the preceding tables and a few other opacity values not given here. Also plotted

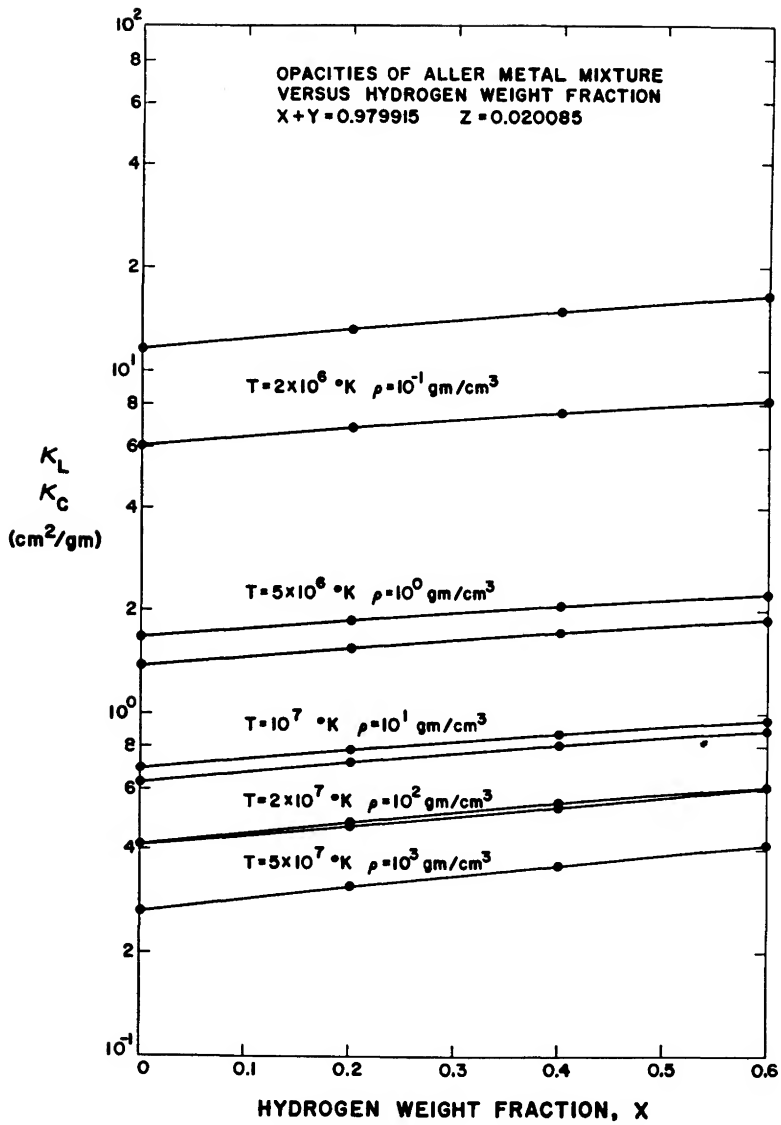


FIG. 11.—The variation of the Aller mixture opacity with hydrogen content for selected temperature-density pairs. Line opacity is the upper and continuous opacity is the lower of each pair of curves.



are approximate conditions within the present sun. It is apparent that large effects due to line absorption do occur in the outer convection zones of stars.

Figure 11 shows how the line and continuous opacities decrease with hydrogen content. Data from Table 3 and others are indicated to show how linear interpolation in the hydrogen weight fraction,  $X$ , can give opacities to better than about 5 per cent accuracy with tables spaced as far apart as 0.6 in  $X$ .

## § 6. USE OF OPACITIES

### 6.1. ANALYTIC FITS TO OPACITY TABLES

Two recent attempts have been made to fit opacities by an analytic formula which can be used over a wide range of temperature, density, and composition. The Henyey, LeLevier, and Levee (1959) formula has been evaluated by this author at all the temperatures and densities given by Keller and Meyerott. Since the fit is supposed to reproduce the Keller and Meyerott data, the differences between the formula and the actual opacities are disappointingly large at many points. The fits are a convenient method of computing opacities in a program for stellar model construction, but it does not seem possible to fit entire tables to within 30 per cent. At a point like the center of the sun and for compositions given by Keller and Meyerott, the Henyey *et al.* formula gives opacities too low by about 30 per cent. Similar differences also appear when using the Hoyle-Hazelgrove (1959) opacity formula which has also been evaluated by this author.

Experience with stellar-evolution calculations at Los Alamos has shown that the most reliable method of obtaining opacities is to put into the computing machine complete opacity tables for the primordial mixture and one or two other hydrogen depleted mixtures. Linear interpolations in  $\log \kappa$  versus  $\log T$  and  $\log \rho$  can give 15 per cent accuracy in the opacity with a table containing between 50 and 100 points.

Presumably material that is entirely depleted of hydrogen is at such a high temperature that the Compton limit opacity is rather accurately independent of composition. If this is not true, probably two opacity tables with the maximum and zero helium contents are the only data required for accurate interpolation. There is also the case of hydrogen-depleted material at moderate temperatures in envelopes of highly evolved stars, but for those stars the composition may not be changing with time, and perhaps a single opacity table can be used.

### 6.2. CONCLUSIONS

While many features of absorption calculations still require attention (e.g., energy-level calculations, bound-bound absorption, and plasma effects), one now has available reasonably accurate opacities over the entire range of temperature and density needed in studies of stellar structure. Additional opacity data can readily be calculated using up to three programs at the Los Alamos Scientific Laboratory for the IBM 7094. These programs are: an ionization code

for the low temperature equation of state, the continuous opacity code, and the code to add line absorption and coherent scattering to the opacity.

The recent work by the author has been made possible by considerable help from Donald L. Bowers. Much theoretical advice has been generously supplied by Douglas H. Sampson and Walter F. Huebner. The extensive tabulations of opacities reported here have been calculated by machine codes developed by Herrick S. Lauson, Donald D. Eilers, and John N. Stewart, Jr. Thomas L. Swihart and Robert R. Brownlee have kindly read the manuscript and have offered useful suggestions. Thanks are also due to Mrs. Margaret Lang, Mrs. Zoe Ciscon, and Mrs. Helen LaMonica for the typing of the manuscript.

#### REFERENCES

- |   |      |   |
|---|------|---|
| ALLER, L. H.  | 1950 | <i>Ap. J.</i> , <b>111</b> , 173.   |
|   | 1961 | <i>The Abundance of the Elements</i> (New York: Interscience Publishers).   |
|   | 1963 | <i>Atmospheres of the Sun and Stars</i> (2d ed.; New York: Ronald Press Co.).   |
| ARMSTRONG, B., BUTTREY, D. E., SARTORI, L., SIEGERT, A. J. F., and WEISNER, J. D. | 1961 | Air Force Special Weapons Center, Kirtland Air Force Base, New Mexico, rept. AFSWC-TR-61-72.  |
| ARMSTRONG, B., HOLLAND, D. H., and MEYEROTT, R. E.                                | 1958 | Air Force Special Weapons Center, Kirtland Air Force Base, New Mexico, rept. AFSWC-58-36.   |
| BATES, D. R.  | 1952 | <i>M.N.</i> , <b>112</b> , 40.  |
| BERGER, J. M.   | 1956 | <i>Ap. J.</i> , <b>124</b> , 550.   |
| BERNSTEIN, J., and DYSON, F. J.   | 1959 | General Atomics, rept. G.A. 848.  |
| BETHE, H. A.  | 1939 | <i>Phys. Rev.</i> , <b>55</b> , 434.  |
| BIERMANN, L.  | 1943 | <i>Zs. f. Ap.</i> , <b>22</b> , 244.  |
| BURGESS, A., and SEATON, M. J.  | 1960 | <i>M.N.</i> , <b>120</b> , 121.   |
| CARPENTER, J. W.  | 1957 | Thesis, Massachusetts Institute of Technology.  |
| CHANDRASEKHAR, S.   | 1939 | <i>An Introduction to the Study of Stellar Structure</i> (Chicago: University of Chicago Press). (Reprinted by Dover Publications, New York, 1957.) |
|   | 1950 | <i>Radiative Transfer</i> (Oxford: Clarendon Press). (Reprinted by Dover Publications, New York, 1960.)   |
|   | 1951 | <i>Astrophysics</i> , ed. J. A. HYNEK (New York: McGraw-Hill Book Co., Inc.), p. 606.   |

- CHANDRASEKHAR, S., and  
BREEN, F. 1946 *A p. J.*, **104**, 430.
- COWLING, T. G. 1930 *M.N.*, **91**, 92.  
1935 *Ibid.*, **96**, 42.
- DEUTSCH, A. J. 1956 *A p. J.*, **123**, 210.
- EDDINGTON, A. S. 1926 *The Internal Constitution of the Stars* (Cambridge: Cambridge University Press). (Reprinted by Dover Publications, New York, 1959.)
- EMDEN, V. R. 1907 *Gaskugeln* (Leipzig: Teubner).
- EPSTEIN, I. 1950 *A p. J.*, **112**, 207.
- EPSTEIN, I., and MOTZ, L. 1954 *A p. J.*, **120**, 156.
- ERKOVICH, S. P. 1960 *Optics and Spectroscopy*, **8**, 162.
- FERMI, E. 1928 *Zs. f. Phys.*, **48**, 73.
- GAUNT, J. A. 1930 *Phil. Trans. R. Soc. London, ser. A*, **229**, 163.
- GELTMAN, S. 1962 *A p. J.*, **136**, 935.
- GRANT, I. P. 1958 *M.N.*, **118**, 241.
- GREEN, J. M. 1958 The Rand Corp., rept. AECU-4133.  
1960 *Ibid.*, RM-2580-AEC.
- GREEN, L. C., RUSH, P. P.,  
and CHANDLER, C. D. 1957 *A p. J., Suppl.*, **3**, 37.
- GREENE, J. 1959 *A p. J.*, **130**, 693.
- GRIEM, H. R. 1960 *A p. J.*, **132**, 883.
- GRIEM, H. R., KOLB, A. C.,  
and SHEN, K. Y. 1959 *Phys. Rev.*, **116**, 4.
- HARRIS, D. L. 1948 *A p. J.*, **108**, 114.
- HARRISON, M. H. 1948 *A p. J.*, **108**, 310.  
1950 *Ibid.*, **111**, 446.
- HEITLER, W. 1954 *The Quantum Theory of Radiation* (Oxford: Clarendon Press).
- HELMHOLTZ, H. 1854 *Popular Lecture for the Kant Commemoration in Königsberg*.
- HENYEY, L. G.,  
LELEVIER, R., and  
LEVÉE, R. D. 1959 *A p. J.*, **129**, 2.
- HERTZSPRUNG, E. 1905 *Zs. f. Wissensch. Photographie*, **3**, Abt 2.
- HJERTING, F. 1938 *A p. J.*, **88**, 508.
- HOYLE, F., and  
HAZELGROVE, C. B. 1959 *M.N.*, **119**, 112.
- HUANG, S. S. 1948 *A p. J.*, **108**, 354.
- HUEBNER, W. F., and  
STUART, R. S. 1964 Los Alamos Scientific Laboratory Report, LAMS 3002.
- HULST, H. C. VAN DE 1957 *Light Scattering by Small Particles* (New York: John Wiley & Sons).
- JOHN, T. L. 1960a *A p. J.*, **131**, 743.  
1960b *M.N.*, **121**, 41.

- KAHN, F. D. 1959 *Ap. J.*, **129**, 205.
- KARZAS, W. J., and  
LATTER, R. 1958a The Rand Corp., rept. AECU-3703, revised.  
1958b *Ibid.*, RM-2091-AEC.  
1961 *Ap. J., Suppl.*, **6**, 167.
- KELLER, G., and  
MEYEROTT, R. E. 1952 Argonne National Laboratory, rept. ANL-4771.  
1955 *Ap. J.*, **122**, 32.
- KELVIN, LORD 1861 Brit. Assoc. Repts., Pt. II, 27-28, reprinted as  
*Mathematical and Physical Papers* (Cambridge:  
The University Press), **5**, 141-44.  
1862 *Ibid.*, **3**, 255-60.  
1887 *Phil. Mag.*, **22**, 287.
- KRAMERS, H. A. 1923 *Phil. Mag.*, **46**, 836.
- KULSRUD, R. M. 1954 *Ap. J.*, **119**, 386.
- LANE, J. H. 1869 *Amer. J. Sci.*, 2d ser., **50**, 57-74.
- LAYZER, D. 1959 *Ann. of Phys.*, **8**, 271.
- LIBERMAN, D. 1962 Los Alamos Scientific Laboratory, rept. LA 2700.
- LIMBER, D. N. 1958a *Ap. J.*, **127**, 263.  
1958b *Ibid.*, p. 387.
- LYAST, E. T. 1954 *Uchenye Zapiski*, Gorky University, **27**, 46.
- MCCREA, W. H. 1929 *M.N.*, **89**, 483.
- MCDUGALL, J., and  
STONER, E. C. 1939 *Phil. Trans. R. Soc. London, ser. A*, **237**, 67.
- MARGENAU, H., and  
LEWIS, M. 1959 *Rev. Mod. Phys.*, **31**, 569.
- MARSHAK, R. E. 1941 Ann. New York Acad. Sci., **41**, 49.
- MARSHAK, R. E.,  
MORSE, P. M., and  
YORK, H. 1950 *Ap. J.*, **111**, 214.
- MAYER, H. 1947 Los Alamos Scientific Laboratory, rept. LA-647.  
Also known as AECD-1870 available at  
USAEC depository libraries.
- MENZEL, D. H., and  
PEKERIS, C. H. 1935 *M.N.*, **96**, 77.
- MESTEL, L. 1950 *Proc. Cambridge Phil. Soc.*, **46**, 331.
- MEYEROTT, R. E. 1954 *Phys. Rev.*, **95**, 72.
- MEYEROTT, R. E., and  
MOSZKOWSKI, S. A. 1951 Argonne National Laboratory, rept. ANL-4594.
- MILFORD, S. N. 1957 *Ap. J.*, **125**, 213.
- MILNE, E. A. 1925a *M.N.*, **85**, 750.  
1925b *Ibid.*, p. 768.
- MOORE, C. E. 1949 National Bureau of Standards, Circ. 467, **1**.  
1952 *Ibid.*, **2**.
- MORSE, P. M. 1940 *Ap. J.*, **92**, 27.

- MOSZKOWSKI, S. A., and  
MEYEROTT, R. E. 1951 Argonne National Laboratory, rept. ANL-4743.  
1956 *Ap. J.*, **124**, 537.
- OHMURA, T., and  
OHMURA, H. 1960 *Ap. J.*, **131**, 8.  
1961 *Phys. Rev.*, **121**, 513.
- OKE, J. B. 1950 *J. R. Astr. Soc. Canada*, **44**, 135.
- OLSON, E. C. 1958 *Ap. J.*, **128**, 146.
- OSTERBROCK, D. E. 1953 *Ap. J.*, **118**, 529.
- PANNEKOEK, A. 1935 *Pub. Astr. Inst. Amsterdam*, No. 4.
- PLASS, G. N., MAYER,  
H. L., WRIGHT, R. S.,  
ROSENGREN, J. W.,  
SCHLESINGER, S. I.,  
SASHKIN, L., and  
BROWNE, E. J. 1957 Air Force Special Weapons Center, Kirtland Air  
Force Base, New Mexico, rept. SWC-TR-  
57-34.
- RAIZER, Y. P. 1960 *Soviet Physics—JETP*, **10**, 769.
- RAYLEIGH, LORD 1899 *Scientific Papers* (Cambridge: Cambridge Uni-  
versity Press), **1**, 87, 104, 518.
- RITTER, A. 1878 *Widemann Ann.*, **5**, 573 (1878); **6**, 135 (1878); **8**,  
-83 157 (1880); **11**, 332, 978 (1880); **16**, 166 (1882);  
20, 137, 897 (1883).
- ROSA, A. 1948 *Zs. f. Ap.*, **25**, 1.
- ROSA, A., and UNSÖLD, A. 1948 *Zs. f. Ap.*, **25**, 20.
- ROSSELAND, S. 1924 *M.N.*, **84**, 525.
- ROUSE, C. A. 1963 *Ap. J.*, **137**, 1286.
- RUDKJØBING, M. 1947 *Pub. Copenhagen Obs.*, No. 145.  
1955 *Ann. d'ap.*, **18**, 11.  
1959 *Mem. Soc. R. Sci. Liège*, 5th ser., **3**, 224.
- RUSSELL, H. N. 1913 *Nature*, **91**, 645.
- SAGDEEV, R. Z. 1956 *Ap. J. USSR*, **33**, 840.
- SALPETER, E. E. 1952 *Ap. J.*, **115**, 326.  
1960 *Phys. Rev.*, **120**, 1528.
- SAMPSON, D. H. 1959 *Ap. J.*, **129**, 734.
- SANDAGE, A. R., and  
SCHWARZSCHILD, M. 1952 *Ap. J.*, **116**, 463.
- SCHATZMAN, E. 1958 *Hdb. d. Phys.*, **51**, 729.
- SCHUSTER, A. 1903 *Ap. J.*, **17**, 165.  
1905 *Ap. J.*, **21**, 1.
- SCHWARZSCHILD, K. 1906 *Göttingen Nach.*, **1**, 41.
- SCHWARZSCHILD, M. 1946 *Ap. J.*, **104**, 203.
- SLATER, J. C. 1930 *Phys. Rev.*, **36**, 57.
- STEWART, J. C., and  
PYATT, K. D., JR. 1961 Air Force Special Weapons Center, Kirtland Air  
Force Base, New Mexico, rept. AFSWC-TR-  
61-71.

- |  |      |  |
|--|------|--|
| STOBBE, M.                             | 1930 | <i>Ann. d. Phys.</i> , <b>7</b> , 661.   |
| STRÖMGREN, B.                          | 1932 | <i>Zs. f. Ap.</i> , <b>4</b> , 118.  |
|  | 1933 | <i>Ibid.</i> , <b>7</b> , 222.   |
|  | 1944 | <i>Pub. Copenhagen Obs.</i> , No. 138.   |
| THOMAS, L. H.                          | 1927 | <i>Proc. Cambridge Phil. Soc.</i> , <b>23</b> , 542.                                     |
| TRAVING, G.                            | 1960 | <i>Über die Theorie der Druckverbreiterung von Spectrallinien</i> (Karlsruhe: G. Braun). |
| TSAO, H. T. H.                         | 1954 | <i>Ap. J.</i> , <b>119</b> , 70.   |
| UENO, S.                               | 1954 | Contr. Inst. Ap. Univ. of Kyoto, No. 42.   |
| UENO, S., SAITO, S., and<br>JUGAKU, J. | 1954 | Contr. Inst. Ap. Univ. of Kyoto, No. 43.   |
| UNSÖLD, A.                             | 1938 | <i>Physik der Sternatmosphären</i> (Berlin: Springer-Verlag).                            |
|  | 1948 | <i>Zs. f. Ap.</i> , <b>25</b> , 11.  |
|  | 1955 | <i>Physik der Sternatmosphären</i> (2d ed.; Berlin: Springer-Verlag).                    |
| VITENSE, E.                            | 1951 | <i>Zs. f. Ap.</i> , <b>28</b> , 81.  |
| WEIZSÄCKER, C. F. VON                  | 1938 | <i>Phys. Z.</i> , <b>39</b> , 633.   |
| WILDT, R.                              | 1939 | <i>Ap. J.</i> , <b>89</b> , 295.   |
| ZIRIN, H.                              | 1954 | <i>Ap. J.</i> , <b>119</b> , 371.  |
|  | 1958 | <i>Ibid.</i> , <b>128</b> , 342.   |
| ZWAAN, C.                              | 1962 | <i>B.A.N.</i> , <b>16</b> , 225.   |



## CHAPTER 4

# *Stellar Models for Main-Sequence Stars and Subdwarfs*

BENGT STRÖMGREN

*Institute for Advanced Study, Princeton, New Jersey*

### § 1. GENERAL CONSIDERATIONS

WITH the development by Bethe and von Weizsäcker of the theory of stellar-energy generation through transmutation of hydrogen into helium, quantitative study of the structure and evolution of main-sequence stars became possible. When it was realized that thorough mixing of material in the interior of main-sequence stars is limited to regions in convective equilibrium (Sweet 1950, Mestel 1953), significant progress was made in the analysis of changes of stellar structure with age during the hydrogen-burning phase.

The early work on chemically inhomogeneous models by Öpik (1938), by Hoyle and Lyttleton (1942), and by Schönberg and Chandrasekhar (1942) was followed by investigations of sequences of stellar models representing the evolutionary changes of main-sequence stars caused by the transmutation of hydrogen into helium (Tayler 1954, Kushwaha 1957, and Blackler 1958).

Extensive calculations of evolutionary model sequences for main-sequence stars were carried out by Henyey, LeLevier, and LeVée (1959), Haselgrove and Hoyle (1959), and Hoyle (1960), and for the sun by Schwarzschild, Howard, and Härm (1957).

The principles and the basic equations according to which the calculations in question are carried out are developed and discussed by Schwarzschild (1958) in the monograph *Structure and Evolution of the Stars* (referred to as *SES*). Chapter 11 of the present volume, by Sears and Brownlee, contains a detailed description and discussion of the numerical techniques employed in high-speed computer calculations of evolutionary model sequences and, in particular, for main-sequence stars.

In order to compute the models, it is necessary to have analytical expressions



or numerical tables giving the total pressure  $P$ , the opacity  $\kappa$ , and the energy generation  $\epsilon$  as functions of the temperature  $T$  and the density  $\rho$  for the ranges of these variables encountered in the stellar interiors under consideration. The problems of ionization, equation of state, and opacity of stellar interior matter are dealt with by Cox in chapter 3 of this volume, those pertaining to the thermonuclear energy generation by Reeves in chapter 2.

In the present chapter, we present and discuss results of numerical calculations of evolutionary model sequences for main-sequence stars. In many respects the stellar-model work in question is based on assumptions more realistic than those made in previous efforts. However, it should be emphasized that throughout this chapter we consider non-rotating, spherically symmetrical stars; that we assume the effects of magnetic fields to be negligible; and that we regard mass losses, and mass gains, through interaction with the surroundings as vanishingly small.

In discussing stellar models we refer in each case to the specific assumptions, in particular with regard to opacity and energy generation, upon which the calculations were based.

In § 2 we discuss main-sequence stars with masses larger than  $1.7 M_{\odot}$ . For this mass range the outer convection zone has a negligibly small influence upon the internal constitution, and the discussion is correspondingly simplified.

For the mass range  $0.8$ – $1.7 M_{\odot}$ , considered in § 3, the presence of a deep outer convection zone complicates the discussion. For this mass range the available material of evolutionary model sequences is less complete than for the range regarded in § 2. In § 2 and § 3 the discussion is limited to models representing stars of initial chemical compositions that do not differ strongly from the initial solar composition (Population I and old disk population).

§ 4 deals with models representing stars of relatively low heavy-element content, i.e., extreme Population II.

For the stars of masses under  $0.8 M_{\odot}$ , which are the subject of § 5, the evolutionary effects that develop during time intervals shorter than the age of our Galaxy are quite small. The contraction phase of evolution lasts relatively longer here; however, discussion of this phase is outside the scope of the present chapter. Consequently, we limit the discussion for masses smaller than  $0.8 M_{\odot}$  to homogeneous hydrogen-burning models.

## § 2. MAIN-SEQUENCE STARS WITH MASSES LARGER THAN $1.7 M_{\odot}$

The work of Biermann (1935, 1945) on convective energy transport in stars led to the conclusion that the sun has an outer convective zone extending from the lower layers of the photosphere inward through an appreciable fraction of the solar radius. In a recent investigation Baker (1963), using the mixing-length theory of convective transport as developed by Böhm-Vitense (1958), has shown that main-sequence stars in the mass range of from  $1 M_{\odot}$  to  $1.4$  or  $1.5 M_{\odot}$  have extensive outer convective zones. The relative thickness of the outer convective zone decreases with increasing mass, and Baker confirmed the result

found in previous investigations that the outer convective zone has a negligible influence upon the internal constitution for main-sequence stars of masses close to  $2 M_{\odot}$  or larger. According to Baker, the transition occurs near  $M = 1.6 M_{\odot}$ , and for masses larger than  $1.7 M_{\odot}$  the influence of the outer convective zone is small or negligible through the hydrogen-burning phase. In the construction of models for these stars the outer part of the star can be assumed to be in radiative equilibrium.

In the interior of the sun the proton-proton process of energy generation dominates over the carbon-cycle process (see Reeves, chap. 2). For main-sequence stars of masses about  $2 M_{\odot}$  and larger, most of the energy generation is due to the C-N or CNO cycle, and the energy production  $\epsilon$  then varies with a high power of  $T$ . When this is the case the star will have a convective core, as was first demonstrated by Cowling (1935).

The calculations discussed in this section show that the stars with  $M > 1.7 M_{\odot}$  have convective cores throughout the hydrogen-burning phase. At the beginning of this evolutionary phase when the star is chemically homogeneous, the fraction of the mass contained in the convective core increases with the mass of the star; for  $M = 30 M_{\odot}$  the fraction is over one-half.

For a given mass the convective-core mass fraction  $q$  (core) decreases with age  $t$ . Consider now the role of mixing for different values of  $q = M_r/M$ , where  $M_r$  is the mass inside a sphere of radius  $r$  concentric with the surface of the star. In the part of the star where  $q$  is larger than the largest value of  $q$  (core), i.e.,  $q$  (core) at the beginning of the hydrogen-burning phase ( $t = 0$ ), there is no mixing of matter, and the rate of change of the relative hydrogen content  $X$  with time at a given  $q$  is then determined by the local rate of transmutation of hydrogen into helium. On the other hand, for any  $q$  smaller than  $q$  (core) for the age considered, there is thorough mixing with all other matter in the convective core, so that  $X = X$  (core); in other words,  $X$  has the same value for all layers with  $q < q$  (core). The rate of change of  $X$  (core) with time is given by a weighted mean of the rate of transmutation of hydrogen into helium taken throughout the convective core.

Between the convective core with  $X = X$  (core) and the part of the star with  $q$  larger than the value of  $q$  (core) at the beginning of the hydrogen-burning phase, there is an intermediate zone in which mixing has played a role in determining  $X(q)$ . This is true, however, only for part of the time from the beginning of the hydrogen-burning phase (age zero) to the epoch in question (age  $t$ ). Consider a layer  $q'$  in the intermediate zone, where  $q$  is larger than  $q$  (core) corresponding to  $t$  and smaller than  $q$  (core) for age zero. At a certain epoch,  $0 < t' < t$ , the surface of the convective core was located at  $q'$ ; until this epoch  $X(q')$  was equal to  $X$  (core), and at the age  $t'$  the value of  $X(q')$  was  $X$  (core,  $t'$ ). After this epoch the layer  $q'$  was unaffected by mixing, and the rate of change of  $X(q')$  with time was given by the local rate of transmutation of hydrogen into helium.

In the evolutionary model sequences considered in this section the hydrogen

content is constant and equal to the initial hydrogen content in the outer parts of the models where the hydrogen transmutation rates are negligibly small; it decreases continuously toward the center and reaches the value  $X$  (core) at the surface of the convective core.

The question of the criterion for convective instability in models with continuously varying chemical composition has been discussed by Härm and Schwarzschild (1955) who concluded that the stability condition

$$\left| \frac{1}{T} \frac{dT}{dr} \right| < \frac{\gamma - 1}{\gamma} \left| \frac{1}{P} \frac{dP}{dr} \right|,$$

which is valid in a chemically homogeneous medium, also holds for zones in stellar interiors of the type just considered, characterized by continuously varying chemical composition.

In chapter 11 of this volume the problem of determining the structure of a chemically homogeneous star is considered in detail. The methods described are applicable to stars that are in the initial stage of the hydrogen-burning phase, i.e., to zero-age stars. For a zero-age star of specified chemical composition—the same throughout the star—the pressure  $P$ , the opacity  $\kappa$ , and the energy generation  $\epsilon$  are known functions of the temperature  $T$  and the density  $\rho$ . The boundary-value problem, defined by the fundamental differential equations and the boundary conditions at the center and at the surface of the star, then has a well-defined solution. The numerical techniques through which the solution is found are discussed in chapter 11.

When the structure of a star of given mass and specified initial chemical composition has been ascertained for age zero, the changes of chemical composition through a time interval  $\Delta t$  caused by nuclear processes can be determined for each separate layer in the interior, characterized by, say,  $q = M_r/M$ . Thus the transmutation rates can be computed, and the influence of mixing can be taken into account following the procedures just referred to. At the epoch considered the chemical composition is no longer constant through the stellar interior, but since it is known as a function of  $q$  the quantities  $P$ ,  $\kappa$ , and  $\epsilon$  can be evaluated as before, in terms of  $T$  and  $\rho$ , allowing for the chemical-composition changes in question. Again, the boundary-value problem has a well-defined solution. The techniques by which the solution is obtained numerically are described in detail in chapter 11.

The choice of initial chemical composition for stellar models with masses larger than  $1.7 M_\odot$  is generally made in such a way that the models will correspond to Population I stars. The initial hydrogen content  $X$ , the helium content  $Y$ , and the heavy-element content  $Z$  are chosen so that the theoretically computed zero-age line coincides as well as possible with the observed zero-age line of Population I stars through the mass range under consideration, and so that there is agreement with the empirical mass-luminosity relation. With regard to the relative abundances of the elements within the heavy-element group, the

choice is guided by the results of cosmic abundance determinations (e.g., Aller 1961), in particular those for atmospheres of Population I stars. The question is discussed in the investigations by Henyey, LeLevier, and Levée (1959), and Haselgrove and Hoyle (1959) already referred to; see also Morton (1959), Iben and Ehrman (1962), and Iben (1963).

In an investigation of the empirical mass-luminosity relation based on data for visual binaries in the Hyades group, the Sirius group, the Pleiades group, and among nearby field stars, Eggen (1963) has found considerable variations from group to group and has interpreted these in terms of variations in the relative hydrogen content  $X$ . On general grounds, and in particular in view of this result, it appears desirable to construct evolutionary model sequences for suitable sets of  $(X, Y, Z)$  values rather than for a single composition, even when the study is limited to Population I stars.

Although the various calculations of evolutionary model sequences that we have referred to differ considerably with regard to basic assumptions, particularly regarding the energy generation  $\epsilon$  and the chemical composition, they yield rather similar pictures of the evolution through the hydrogen-burning phase; the changes of structure with age and the tracks of evolution through the Hertzsprung-Russell diagram are not very different.

The evolutionary model sequences presented in this section were computed by Kelsall (1965).<sup>1</sup> The energy generation function  $\epsilon(\rho, T)$  was taken in accordance with Reeves (chap. 2 this vol.). The opacity function  $\kappa(\rho, T)$  was computed according to the procedure described by Cox in chapter 3 of this volume, with one exception, namely that the absorption-line contribution to the opacity was taken from an investigation by Arking and Herring (1964). Tables of the opacity due to continuous absorption and scattering as functions of  $\rho$  and  $T$  were computed with the Los Alamos high-speed computer code (see chap. 3), and corrections were applied to allow for the line effect according to Arking and Herring.

The computational technique used by Kelsall is similar to that described by Sears and Brownlee in chapter 11, § 3.2, of this volume. Numerical solutions running inward from the surface and outward from the center were fitted at a point ( $q = 0.4$ ) sufficiently far from the center for the chemical composition at this point to be very nearly equal to the initial chemical composition throughout the hydrogen-burning phase.

The energy production function  $\epsilon(\rho, T)$  was taken as the sum of the  $\epsilon$  values for the proton-proton process and the CNO cycle, respectively. The latter value is by far the largest for the larger masses. Following Reeves (chap. 2), Kelsall adopted for the processes of the CNO cycle the rates of transmutation given by Caughlan and Fowler (1962). It was assumed that the abundances of the C, N, and O isotopes were those reached in equilibrium at the relevant temperature.

<sup>1</sup> The author is very grateful to Mr. Kelsall for having put the results of this investigation at his disposal prior to publication.

The relative abundance of  $N^{14}$  is then nearly equal to the sum of the relative abundances for  $C^{12}$ ,  $N^{14}$ , and  $O^{16}$  of the initial composition, and, accordingly, the relative mass of  $N^{14}$  was set equal to  $0.6 Z$ , where  $Z$ , as before, denotes the relative mass of the heavy-element group (all elements except hydrogen and helium, i.e.,  $X + Y + Z = 1$ ). For the mass range in question the central temperatures are larger than  $19 \times 10^6$  throughout the hydrogen-burning phase, and, according to Caughlan and Fowler, the equilibrium composition is then reached in about  $10^8$  years or less, so that the assumption just referred to should give  $\epsilon$  values of adequate accuracy.

TABLE 1  
PARAMETERS OF STARS AS A FUNCTION OF MASS, AT AGE ZERO  
FOR DIFFERENT CHEMICAL COMPOSITIONS\*

LOG ( $M/M_{\odot}$ )	LOG ( $R/R_{\odot}$ )		$M_{bol}$		LOG $T_e$		$Z$
	$X=0.60$	$X=0.70$	$X=0.60$	$X=0.70$	$X=0.60$	$X=0.70$	
0.25.....	{ 0.16	0.16	+1 <sup>m</sup> 4	+1 <sup>m</sup> 9	4.01	3.96	0.02
	.19	.19	+1.6	+2.1	3.98	3.93	.03
	.21	.20	+1.7	+2.3	3.96	3.91	.04
.45.....	{ .27	.27	-0.5	0.0	4.15	4.10	.02
	.30	.29	-0.4	+0.2	4.12	4.07	.03
	.32	.31	-0.2	+0.3	4.10	4.05	.04
.65.....	{ .39	.38	-2.3	-1.8	4.27	4.23	.02
	.41	.41	-2.2	-1.7	4.25	4.20	.03
	.43	.42	-2.1	-1.6	4.23	4.19	.04
0.85.....	{ .51	.50	-4.0	-3.5	4.38	4.34	.02
	.53	.52	-3.9	-3.5	4.36	4.32	.03
	0.54	0.55	-3.9	-3.4	4.35	4.31	0.04

\* Source: Kelsall (1965).

Table 1 gives the radius  $R$ , the bolometric magnitude  $M_{bol}$ , and the effective temperature  $T_e$  at age zero, for  $\log M/M_{\odot}$  equal to 0.25, 0.45, 0.65, and 0.85, respectively, and for six different sets of  $(X, Y, Z)$  values. For each chemical composition the  $M_{bol}-T_e$  relation defines the zero-age line for the mass range in question. Similarly the  $M/M_{\odot}-M_{bol}$  relation defines the mass-luminosity law on the zero-age line.

The question of the zero-age relation between color index  $B - V$  and visual absolute magnitude  $M_v$  is discussed by Blaauw (1963) in Volume 3 of this Compendium (chap. 20, § 3.1). In chapter 14 Harris (1963) considered the relation between effective temperature  $T_e$  and color index, and that between  $T_e$  and the bolometric correction  $BC = M_{bol} - M_v$ . In chapter 15 Harris, Strand, and Worley (1963) treated the empirical data on stellar masses, luminosities, and radii. In the present context we refer to these three chapters, and to the references given there.

Comparison of the theoretical  $M_{\text{bol}}-T_e$  and  $M/M_\odot-M_{\text{bol}}$  relations given in Table 1 with the observational material just referred to suggests that the choice of  $X$  values 0.60 and 0.70 and  $Z$  values 0.02, 0.03, and 0.04 provides composition ranges that are adequate for Population I stars. In fact, the choice  $X = 0.65$  and  $Z = 0.035$  yields agreement with the observational data practically within their uncertainty range. The investigation by Eggen (1963) on the Hyades visual binaries leads to  $X$  values lower than 0.6, but still within the range of reasonably accurate extrapolation.

In this connection it should be noted that the theoretical  $M/M_\odot-M_{\text{bol}}$  relations given by Table 1 are valid for age zero only. However, with the help of evolutionary tracks such as are discussed further on in this section, corrections can be applied to the observed  $M_{\text{bol}}$  values in individual cases to allow for the change in  $M_{\text{bol}}$  from  $t = 0$  to the actual age of the star in question.

Since the comparison of observation and theory for the mass range considered does not yield a very accurate simultaneous determination of  $X$  and  $Z$ , it is of interest to note that the range of  $Z$  values for Population I stars is indicated by other considerations. The  $Z$  value for the sun is close to 0.02 (see § 3), and comparison of atmospheric metal contents of F and G Population I stars of the age range in question with that of the sun suggests  $Z$  values for the latter between 0.02 and 0.04 (e.g., Strömgren [1963], § 3). Once  $Z$  is thus limited,  $X$  cannot be chosen very far outside the range 0.6–0.7 without serious conflict with the empirical mass-luminosity relation as defined by the most reliable visual-binary and spectroscopic-binary material.

Tables 2 and 3 give stellar models, for age zero, for two masses and three chemical compositions. It is seen that the internal structure is not strongly affected by changes in chemical composition within the ranges considered.

Principal characteristics of evolutionary model sequences are given in Table 4 for  $\log M/M_\odot$  equal to 0.25, 0.45, 0.65, and 0.85. The relative hydrogen content  $X_c$  at the center of the star is the argument, and the corresponding age is given in the following column. The next four columns describe the evolutionary track in the Hertzsprung-Russell diagram;  $\Delta M_{\text{bol}}$  indicates the increase in luminosity over that of a zero-age star of the same effective temperature. The last six columns pertain to properties of the convective core and conditions at the center. The quantity  $\beta_c$  is the value of Eddington's  $\beta = \text{gas pressure}/(\text{gas pressure} + \text{radiation pressure})$  at the center of the star.

Table 5 corresponds to Tables 2 and 3, but gives the stellar structure at  $X_c = 0.10$ , i.e., near the end of the hydrogen-burning phase.

Evolutionary model sequences for  $\log M/M_\odot$  equal to 0.45 and initial chemical composition  $X = 0.70$ ,  $Y = 0.27$ ,  $Z = 0.03$  are given in Table 6. Only the central parts of the stars, where the hydrogen content changes with age, are represented. The space argument is  $q = M_r/M$ , while the time argument is  $X_c$ . The relation between  $X_c$  and age is given in Table 4. Comparison of rows with equal  $X_c$  and different  $q$  indicate the stellar structure at the age in question,

TABLE 2  
STELLAR MODELS FOR AGE ZERO, FOR THREE INITIAL  
COMPOSITIONS AS INDICATED\*

$\tau/R$	$\log (M/M_{\odot})=0.45$							
	$M_{\tau}/M$	$L_{\tau}/L$	$\log T$	$\log \rho$	$\kappa$	$X$	$Y$	$Z$
0.95.....	{ 1.000	1.00	5.42	-4.81	7.6	0.60	0.36	0.04
	{ 1.000	1.00	5.44	-4.74	7.0	.60	.37	.03
	{ 1.000	1.00	5.41	-4.73	8.9	.70	.27	.03
.85.....	{ 1.000	1.00	5.92	-3.04	4.1	.60	.36	.04
	{ 1.000	1.00	5.94	-2.97	3.5	.60	.37	.03
	{ 1.000	1.00	5.91	-2.97	4.4	.70	.27	.03
.75.....	{ 0.998	1.00	6.20	-2.09	3.8	.60	.36	.04
	{ 0.998	1.00	6.22	-2.02	3.3	.60	.37	.03
	{ 0.998	1.00	6.19	-2.02	4.0	.70	.27	.03
.65.....	{ 0.992	1.00	6.43	-1.43	3.8	.60	.36	.04
	{ 0.992	1.00	6.44	-1.36	3.2	.60	.37	.03
	{ 0.992	1.00	6.42	-1.36	4.0	.70	.27	.03
.55.....	{ 0.975	1.00	6.60	-0.85	2.78	.60	.36	.04
	{ 0.973	1.00	6.61	-0.77	2.31	.60	.37	.03
	{ 0.974	1.00	6.59	-0.77	2.90	.70	.27	.03
.45.....	{ 0.926	1.00	6.75	-0.26	1.78	.60	.36	.04
	{ 0.922	1.00	6.76	-0.18	1.45	.60	.37	.03
	{ 0.925	1.00	6.74	-0.19	1.86	.70	.27	.03
.35.....	{ 0.806	1.00	6.90	+0.34	1.20	.60	.36	.04
	{ 0.795	1.00	6.92	+0.41	1.01	.60	.37	.03
	{ 0.804	1.00	6.89	+0.41	1.25	.70	.27	.03
.25.....	{ 0.546	1.00	7.06	+0.91	0.80	.60	.36	.04
	{ 0.527	1.00	7.08	+0.96	0.72	.60	.37	.03
	{ 0.544	1.00	7.05	+0.98	0.84	.70	.27	.03
.20.....	{ 0.365	1.00	7.15	+1.14	0.66	.60	.36	.04
	{ 0.347	1.00	7.17	+1.18	0.60	.60	.37	.03
	{ 0.362	0.99	7.14	+1.21	0.71	.70	.27	.03
.15.....	{ 0.190	0.98	7.24	+1.32	0.56	.60	.36	.04
	{ 0.179	0.98	7.25	+1.35	conv.	.60	.37	.03
	{ 0.188	0.97	7.22	+1.38	0.59	.70	.27	.03
.10.....	{ 0.065	0.82	7.31	+1.43	conv.	.60	.36	.04
	{ 0.062	0.80	7.32	+1.45	conv.	.60	.37	.03
	{ 0.065	0.79	7.30	+1.49	conv.	.70	.27	.03
.05.....	{ 0.010	0.26	7.35	+1.49	conv.	.60	.36	.04
	{ 0.008	0.24	7.36	+1.51	conv.	.60	.37	.03
	{ 0.009	0.25	7.34	+1.56	conv.	.70	.27	.03
.00.....	{ 0.000	0.00	7.36	+1.51	conv.	.60	.36	.04
	{ 0.000	0.00	7.37	+1.53	conv.	.60	.37	.03
	{ 0.000	0.00	7.35	+1.58	conv.	.70	.27	.03
.148†.....	0.183	0.98	7.24	+1.32	0.55	.60	.36	.04
.155†.....	0.194	0.98	7.24	+1.33	0.53	.60	.37	.03
0.147†.....	0.179	0.97	7.23	+1.39	0.59	0.70	0.27	0.03

\* Source: Kelsall (1965).

† Boundary of convective core.

TABLE 3  
STELLAR MODELS FOR AGE ZERO, FOR THREE INITIAL  
COMPOSITIONS AS INDICATED\*

$r/R$	$\log (M/M_{\odot})=0.85$							
	$M_r/M$	$L_r/L$	$\log T$	$\log \rho$	$\kappa$	$X$	$Y$	$Z$
0.95.....	{ 1.000	1.00	5.59	-4.77	1.88	0.60	0.36	0.04
	{ 1.000	1.00	5.61	-4.70	1.72	.60	.37	.03
	{ 1.000	1.00	5.58	-4.72	2.09	.70	.27	.03
.85.....	{ 1.000	1.00	6.09	-3.06	1.34	.60	.36	.04
	{ 1.000	1.00	6.10	-2.99	1.22	.60	.37	.03
	{ 1.000	1.00	6.08	-2.99	1.42	.70	.27	.03
.75.....	{ 0.997	1.00	6.38	-2.18	1.33	.60	.36	.04
	{ 0.997	1.00	6.39	-2.10	1.19	.60	.37	.03
	{ 0.997	1.00	6.37	-2.10	1.43	.70	.27	.03
.65.....	{ 0.987	1.00	6.59	-1.52	1.10	.60	.36	.04
	{ 0.987	1.00	6.60	-1.44	0.95	.60	.37	.03
	{ 0.987	1.00	6.58	-1.44	1.16	.70	.27	.03
.55.....	{ 0.958	1.00	6.75	-0.92	0.81	.60	.36	.04
	{ 0.955	1.00	6.77	-0.85	0.70	.60	.37	.03
	{ 0.957	1.00	6.74	-0.85	0.87	.70	.27	.03
.45.....	{ 0.880	1.00	6.91	-0.35	0.64	.60	.36	.04
	{ 0.872	1.00	6.93	-0.28	0.58	.60	.37	.03
	{ 0.878	1.00	6.90	-0.28	0.68	.70	.27	.03
.35.....	{ 0.705	1.00	7.07	+0.18	0.50	.60	.36	.04
	{ 0.689	1.00	7.08	+0.24	0.47	.60	.37	.03
	{ 0.702	1.00	7.06	+0.25	0.53	.70	.27	.03
.25.....	{ 0.410	1.00	7.23	+0.61	0.41	.60	.36	.04
	{ 0.393	1.00	7.24	+0.65	0.39	.60	.37	.03
	{ 0.407	1.00	7.22	+0.67	0.44	.70	.27	.03
.20.....	{ 0.252	1.00	7.31	+0.75	conv.	.60	.36	.04
	{ 0.239	0.99	7.32	+0.78	conv.	.60	.37	.03
	{ 0.249	1.00	7.30	+0.82	conv.	.70	.27	.03
.15.....	{ 0.123	0.94	7.37	+0.86	conv.	.60	.36	.04
	{ 0.116	0.93	7.38	+0.89	conv.	.60	.37	.03
	{ 0.125	0.94	7.36	+0.93	conv.	.70	.27	.03
.10.....	{ 0.041	0.66	7.42	+0.94	conv.	.60	.36	.04
	{ 0.038	0.64	7.43	+0.96	conv.	.60	.37	.03
	{ 0.040	0.67	7.41	+1.00	conv.	.70	.27	.03
.05.....	{ 0.006	0.16	7.45	+0.99	conv.	.60	.36	.04
	{ 0.005	0.11	7.45	+1.01	conv.	.60	.37	.03
	{ 0.005	0.16	7.44	+1.05	conv.	.70	.27	.03
.00.....	{ 0.000	0.00	7.45	+1.00	conv.	.60	.36	.04
	{ 0.000	0.00	7.46	+1.02	conv.	.60	.37	.03
	{ 0.000	0.00	7.45	+1.06	conv.	.70	.27	.03
.211†...	{ 0.282	1.00	7.29	+0.73	0.39	.60	.36	.04
.218†...	{ 0.290	1.00	7.30	+0.74	0.38	.60	.37	.03
0.207†...	{ 0.270	1.00	7.29	+0.80	0.42	0.70	0.27	0.03

\* Source: Kelsall (1965).

† Boundary of convective core.



TABLE 4

PRINCIPAL CHARACTERISTICS OF EVOLUTIONARY MODEL SEQUENCES FOR FOUR MASSES AS INDICATED<sup>\*</sup>  
INITIAL CHEMICAL COMPOSITION:  $X = 0.70$ ,  $Y = 0.27$ ,  $Z = 0.03$ \*

$\log (M/M_{\odot})$	$X_c$	Age (million years)	$R/R_{\odot}$	$M_{\text{bol}}$	$\log T_e$	$\Delta M_{\text{bol}}$	Conv. Core Rel. Mass $q$ (core)	Conv. Core Rel. Radius	Conv. Core Rel. Energy Production	Control Tempera- ture $T_c$	Control Density $\rho_c$	$\beta_c$
0.25.....	0.70	0	1.54	+2 <sup>m</sup> 1	3.93	0 <sup>m</sup> 0	0.12	0.11	0.81	$20 \times 10^6$	68	1.00
	.60	210	1.64	+2.0	3.92	0.1	.11	.10	0.83	20	72	1.00
	.50	390	1.74	+2.0	3.92	0.3	.10	.09	0.84	21	76	1.00
	.40	540	1.86	+2.0	3.90	0.5	.09	.08	0.86	21	82	1.00
	.30	670	1.99	+1.9	3.89	0.7	.08	.07	0.87	22	89	1.00
	.20	770	2.14	+1.9	3.88	0.9	.07	.06	0.89	22	99	1.00
	.10	860	2.28	+1.9	3.86	1.0	.06	.05	0.90	24	117	1.00
	.70	0	1.96	+0.2	4.07	0.0	.18	.15	0.96	$23 \times 10^6$	38	0.99
	.60	70	2.11	+0.1	4.07	0.2	.16	.13	0.96	23	39	0.99
	.50	120	2.28	-0.0	4.06	0.4	.14	.11	0.97	24	41	0.99
.45.....	.40	170	2.46	-0.1	4.05	0.6	.12	.10	0.97	24	43	0.99
	.30	210	2.67	-0.1	4.03	0.8	.10	.08	0.97	25	46	0.99
	.20	240	2.91	-0.1	4.02	1.1	.08	.07	0.97	25	50	0.99
	.10	260	3.15	-0.1	4.00	1.3	.07	.06	0.97	27	59	0.99
	.70	0	2.54	-1.7	4.20	0.0	.22	.18	0.99	$25 \times 10^6$	21	0.99
	.60	23	2.75	-1.8	4.20	0.2	.20	.15	0.99	26	21	0.98
	.50	42	2.99	-1.9	4.19	0.4	.17	.13	0.99	26	22	0.98
	.40	56	3.26	-2.0	4.18	0.7	.15	.12	0.99	27	22	0.98
	.30	68	3.57	-2.0	4.16	0.9	.12	.10	0.99	28	24	0.98
	.20	78	3.91	-2.1	4.15	1.2	.10	.08	0.99	28	26	0.97
0.85.....	.10	86	4.27	-2.1	4.13	1.5	.08	.07	0.98	30	30	0.97
	.70	0	3.3	-3.5	4.32	0.0	.27	.21	1.00	$28 \times 10^6$	12	0.97
	.60	9	3.6	-3.6	4.32	0.2	.24	.18	1.00	29	12	0.96
	.50	16	3.9	-3.7	4.31	0.4	.21	.16	1.00	29	12	0.96
	.40	21	4.3	-3.8	4.30	0.7	.18	.14	0.99	30	12	0.95
	.30	26	4.7	-3.9	4.29	1.0	.16	.12	0.99	31	13	0.94
	.20	29	5.2	-3.9	4.27	1.3	.13	.10	0.99	32	14	0.94
	.10	32	5.8	-4.0	4.26	1.5	.11	.08	0.99	33	16	0.93
	.70	0	3.3	-3.5	4.32	0.0	.27	.21	1.00	$28 \times 10^6$	12	0.97
	.60	9	3.6	-3.6	4.32	0.2	.24	.18	1.00	29	12	0.96

\* Source: Kelsall (1965).

and, in particular, the run of  $X$  with  $\bar{q}$  through the central regions, while comparison of rows with equal  $q$  and different  $X_c$  shows the time changes of a given mass element.

Sakashita, Ono, and Hayashi (1959) computed evolutionary model sequences for a star with  $M = 15.6 M_\odot$  through the hydrogen-burning phase. The evolution through the hydrogen-exhaustion phase for  $M = 15.6 M_\odot$  was studied by Hayashi and Cameron (1962) who followed the further development through the helium-burning and carbon-burning phases for this particular mass. An evolutionary model sequence covering the hydrogen-exhaustion phase was computed by Polak (1962) for a star of five solar masses.

Schwarzschild and Härm (1958) investigated the hydrogen-burning phase for masses in the range  $30 M_\odot$ – $300 M_\odot$ . They found that for these massive stars

TABLE 5  
STELLAR MODELS FOR  $X_c = 0.10^*$   
(Near End Hydrogen Burning)

$r/R$	$M_r/M$	$L_r/L$	$\log T$	$\log \rho$	$\kappa$	$X$
$\log (M/M_\odot) = 0.45$ $X = 0.70, Y = 0.27, Z = 0.03$						
0.85.....	1.000	1.00	5.70	-3.74	5.0	0.70
.75.....	0.999	1.00	5.98	-2.79	3.4	.70
.65.....	0.994	1.00	6.19	-2.09	3.5	.70
.55.....	0.980	1.00	6.39	-1.51	3.6	.70
.45.....	0.945	1.00	6.56	-0.96	2.8	.70
.35.....	0.864	1.00	6.71	-0.39	1.85	.70
.25.....	0.685	1.00	6.88	+0.24	1.16	.70
.20.....	0.538	1.00	6.97	+0.55	0.88	.70
.15.....	0.360	1.00	7.07	+0.84	0.73	.70
.10.....	0.190	0.99	7.18	+1.09	0.57	.69
.05.....	0.048	0.93	7.34	+1.63	conv.	.10
.00.....	0.000	0.00	7.43	+1.77	conv.	0.10
$\log (M/M_\odot) = 0.85$ $X = 0.70, Y = 0.27, Z = 0.03$						
.85.....	1.000	1.00	5.84	-3.92	1.40	0.70
.75.....	0.998	1.00	6.12	-3.01	1.18	.70
.65.....	0.992	1.00	6.33	-2.35	1.18	.70
.55.....	0.973	1.00	6.52	-1.78	1.06	.70
.45.....	0.927	1.00	6.68	-1.24	0.86	.70
.35.....	0.824	1.00	6.84	-0.68	0.62	.70
.25.....	0.617	1.00	7.01	-0.13	0.48	.70
.20.....	0.472	1.00	7.10	+0.12	0.45	.70
.15.....	0.320	1.00	7.20	+0.35	0.39	.70
.10.....	0.179	1.00	7.32	+0.70	0.32	.39
.05.....	0.036	0.81	7.47	+1.12	conv.	.10
0.00.....	0.000	0.00	7.52	+1.22	conv.	0.10

\* Source: Kelsall (1965).

TABLE 6  
EVOLUTIONARY MODEL SEQUENCE, CENTRAL PART OF STAR\*  
CHEMICAL COMPOSITION:  $X = 0.70$ ,  $Y = 0.27$ ,  $Z = 0.03$ ;  $\log M/M_{\odot} = 0.45$

$q = M_r/M$	$X_c$	$\tau/R$	$L/L_r$	$\log T$	$\log \rho$	$\kappa$	$X$
0.26.....	0.70	0.172	0.98	7.19	1.32	0.63	0.70
	.60	.162	0.99	7.18	1.28	.62	.70
	.50	.152	0.99	7.18	1.28	.62	.70
	.40	.143	0.99	7.17	1.17	.62	.70
	.30	.136	1.00	7.16	1.11	.63	.69
	.20	.128	1.00	7.14	1.05	.64	.69
	.10	.122	1.00	7.13	0.99	.64	.69
.24.....	.70	.166	0.98	7.20	1.34	.61	.70
	.60	.156	0.98	7.20	1.30	.60	.70
	.50	.146	0.99	7.19	1.25	.60	.70
	.40	.137	0.99	7.18	1.19	.60	.69
	.30	.130	0.99	7.17	1.14	.61	.69
	.20	.122	1.00	7.16	1.07	.62	.69
	.10	.116	1.00	7.14	1.02	.62	.69
.22.....	.70	.160	0.97	7.21	1.36	.60	.70
	.60	.150	0.98	7.21	1.32	.59	.70
	.50	.140	0.99	7.20	1.27	.58	.69
	.40	.131	0.99	7.19	1.22	.58	.69
	.30	.124	0.99	7.18	1.16	.59	.69
	.20	.116	1.00	7.17	1.10	.59	.69
	.10	.110	1.00	7.16	1.05	.60	.69
.20.....	.70	.154	0.97	7.22	1.38	.60	.70
	.60	.143	0.98	7.22	1.34	.59	.70
	.50	.134	0.98	7.21	1.29	.58	.69
	.40	.125	0.99	7.21	1.24	.57	.69
	.30	.117	0.99	7.20	1.19	.56	.69
	.20	.110	0.99	7.18	1.13	.57	.69
	.10	.103	1.00	7.17	1.08	.58	.69
.18.....	.70	.148	0.96	7.23	1.39	.59	.70
	.60	.137	0.97	7.23	1.36	.58	.69
	.50	.127	0.98	7.22	1.31	.57	.69
	.40	.118	0.98	7.22	1.27	.56	.69
	.30	.110	0.99	7.21	1.22	.55	.68
	.20	.103	0.99	7.20	1.16	.55	.68
	.10	.096	0.99	7.19	1.11	.56	.68
.16.....	.70	.141	0.95	7.24	1.41	conv.	.70
	.60	.130	0.96	7.24	1.40	.55	.61
	.50	.121	0.97	7.24	1.36	.54	.61
	.40	.112	0.98	7.23	1.32	.53	.60
	.30	.104	0.99	7.23	1.27	.53	.60
	.20	.096	0.99	7.22	1.22	.52	.60
	.10	.089	0.99	7.21	1.17	.52	.60
.14.....	.70	.134	0.94	7.25	1.43	conv.	.70
	.60	.124	0.95	7.25	1.43	conv.	.60
	.50	.114	0.97	7.25	1.42	.51	.51
	.40	.105	0.97	7.25	1.38	.50	.50
	.30	.097	0.98	7.24	1.34	.49	.50
	.20	.089	0.99	7.23	1.29	.49	.50
	.10	.082	0.99	7.23	1.25	.49	.50
0.12.....	.70	.126	0.92	7.26	1.45	conv.	.70
	.60	.116	0.94	7.27	1.45	conv.	.60
	.50	.107	0.96	7.27	1.45	conv.	.50
	.40	.098	0.97	7.26	1.45	.46	.40
	.30	.090	0.98	7.26	1.41	.46	.40
	.20	.082	0.98	7.25	1.37	.46	.40
	0.10	0.075	0.99	7.25	1.33	0.45	0.40

\*Source: Kelsall (1965).

TABLE 6—*Continued*

$q = M_r/M$	$X_c$	$r/R$	$L/L_r$	$\log T$	$\log \rho$	$\kappa$	$X$
0.10.....	0.70	0.118	0.89	7.28	1.46	conv.	0.70
	.60	.109	.92	7.28	1.47	conv.	.60
	.50	.100	.94	7.28	1.47	conv.	.50
	.40	.092	.95	7.28	1.47	conv.	.40
	.30	.083	.97	7.28	1.48	conv.	.30
	.20	.075	.98	7.27	1.45	0.42	.29
	.10	.068	.98	7.27	1.42	.41	.29
.08.....	.70	.108	.85	7.29	1.48	conv.	.70
	.60	.100	.88	7.29	1.49	conv.	.60
	.50	.092	.91	7.29	1.49	conv.	.50
	.40	.084	.93	7.30	1.50	conv.	.40
	.30	.076	.95	7.30	1.51	conv.	.30
	.20	.069	.97	7.30	1.53	conv.	.20
	.10	.061	.97	7.29	1.52	0.37	.17
.06.....	.70	.098	.78	7.30	1.50	conv.	.70
	.60	.090	.81	7.31	1.51	conv.	.60
	.50	.083	.85	7.31	1.51	conv.	.50
	.40	.075	.88	7.31	1.53	conv.	.40
	.30	.068	.91	7.32	1.54	conv.	.30
	.20	.061	.94	7.32	1.57	conv.	.20
	.10	.054	.96	7.32	1.61	conv.	.10
.04.....	.70	.084	.66	7.31	1.52	conv.	.70
	.60	.078	.70	7.32	1.53	conv.	.60
	.50	.071	.74	7.33	1.54	conv.	.50
	.40	.065	.79	7.33	1.55	conv.	.40
	.30	.059	.83	7.34	1.57	conv.	.30
	.20	.053	.87	7.34	1.60	conv.	.20
	.10	.047	.91	7.35	1.65	conv.	.10
.02.....	.70	.066	.45	7.33	1.55	conv.	.70
	.60	.061	.48	7.34	1.55	conv.	.60
	.50	.056	.53	7.34	1.57	conv.	.50
	.40	.051	.57	7.35	1.58	conv.	.40
	.30	.046	.63	7.36	1.61	conv.	.30
	.20	.041	.69	7.37	1.64	conv.	.20
	.10	.036	.75	7.38	1.70	conv.	.10
0.00.....	.70	.000	.00	7.35	1.58	conv.	.70
	.60	.000	.00	7.36	1.59	conv.	.60
	.50	.000	.00	7.37	1.61	conv.	.50
	.40	.000	.00	7.38	1.63	conv.	.40
	.30	.000	.00	7.39	1.66	conv.	.30
	.20	.000	.00	7.41	1.70	conv.	.20
	0.10	0.000	0.00	7.43	1.77	conv.	0.10

the relative mass of the convective core increases with stellar age through the hydrogen-burning phase, in contrast to the pattern of shrinking convective cores that holds for the evolution of masses smaller than  $10 M_{\odot}$ . The change in pattern is connected with the important role played by radiation pressure in very massive stars. The analysis of Schwarzschild and Härm shows that for the very massive stars considered the convective core is surrounded by a semi-

convective intermediate zone in which the composition at every point is adjusted by convective mixing to maintain convective neutrality (Ledoux 1947). Outside the intermediate zone there is a homogeneous radiative envelope of unchanging composition, as is the case in the mass range considered before.

The question of pulsational stability of very massive stars was studied by Schwarzschild and Härm (1959) who concluded that main-sequence stars with masses larger than  $65 M_{\odot}$  are pulsationally unstable.

Stothers (1963) has computed an evolutionary model sequence through the hydrogen-burning phase for a star of mass  $M = 30 M_{\odot}$  and with initial chemical composition  $X = 0.70$ ,  $Y = 0.27$ ,  $Z = 0.03$ . In these calculations the energy generation  $\epsilon$  was taken according to Caughlan and Fowler (1962); see also Reeves (chap. 2). It was found that for the temperature range in question  $\epsilon$  could be represented with sufficient accuracy by a power law  $\epsilon \sim \rho T^{15}$ . Since

TABLE 7

STELLAR PARAMETERS AND PHYSICAL CONDITIONS AT THE CENTER\*  
INITIAL CHEMICAL COMPOSITION:  $X = 0.70$ ,  $Y = 0.27$ ,  $Z = 0.03$ ;  $M = 30 M_{\odot}$

$X_c$ †	Age	Average Relative Hydrogen Content through Entire Star, $\bar{X}$	$\log R/R_{\odot}$	$M_{\text{bol}}$	$\log T_e$	$\log T_c$	$\log \rho_c$	$\beta_c$
0.70 . . .	0	0.70	0.82	$-8^m1$	4.64	7.56	0.48	0.77
0.07 . . .	$4.7 \times 10^6$ years	0.40	1.12	$-8.8$	4.56	7.65	0.65	0.58

\* Source: Stothers (1963).

† The two rows pertain to age zero and a stage near the end of the hydrogen-burning phase.

scattering by free electrons is the principal contributor to the opacity for the models in question,  $\kappa$  was taken to be  $0.19 (1 + X)$ . Following Sakashita, Ono, and Hayashi (1959), Stothers took into account the development during the hydrogen-burning phase of an inner radiative zone between the convective core and the semiconvective zone. Table 7 gives a comparison of the initial homogeneous model ( $X_c = 0.70$ ) for  $M = 30 M_{\odot}$  with the model for which  $X_c$  has decreased to 0.07. The lifetime of the star considered in the hydrogen-burning phase is found to be close to 5 million years.

### § 3. MAIN-SEQUENCE STARS WITH MASSES IN THE RANGE $0.8$ – $1.7 M_{\odot}$

As mentioned in § 1, the main-sequence stars in this mass range have a deep outer convective zone. With the exception of a relatively thin outer fringe, the relation between pressure gradient and temperature gradient is given in this zone, to a high degree of approximation, by the adiabatic relation (see *SES*, p. 50). Since the adiabatic constant  $\gamma$  is close to  $\frac{5}{3}$  throughout most of the zone, the relation between pressure  $P$  and temperature  $T$  is, to a good approximation,

$P = KT^{5/2}$ . Here, however, the value of the constant  $K$  depends in a sensitive way upon conditions in the thin outer fringe of the convectively unstable zone where the transition between radiative equilibrium and nearly adiabatic equilibrium occurs. The present form of the mixing-length theory (see *SES*, § 11, references), although it gives a good general picture of the physical conditions in the outer convective zone, does not yield the value of  $K$  with sufficient accuracy for the purpose of stellar interior model computations. Therefore,  $K$  is here introduced as a parameter, along with the relative hydrogen content  $X$  and the relative heavy-element content  $Z$  (Osterbrock 1953; Schwarzschild, Howard, and Härm 1957).

The mass range  $0.8\text{--}1.7 M_{\odot}$  of the main sequence is not quite as well covered by evolutionary model sequences as the range  $M > 1.7 M_{\odot}$  discussed in § 2. However, the case of  $M = M_{\odot}$  has been thoroughly investigated, and we turn to this case first.

The work of Epstein (1950) and Oke (1950), based on Salpeter's calculations of the energy production  $\epsilon$  by the proton-proton reaction (Salpeter 1952), showed that in the solar interior the main contribution to  $\epsilon$  comes from the proton-proton process. It was realized that this leads to solar models characterized by radiative equilibrium in the region from the center to the lower limit of the outer convective zone. With regard to the evolutionary changes of chemical composition, this means that the rate of change of  $X$  and  $Y$  in each layer is given by the local rate of transmutation of hydrogen into helium and is not influenced by mixing.

Schwarzschild, Howard, and Härm (1957) computed evolutionary model sequences for  $M = M_{\odot}$ , choosing the parameters  $X$ ,  $Z$ , and  $K$  in such a way that the luminosity and radius of the sun at its present age (about  $4.5 \times 10^9$  years) are reproduced, while the ratio  $Z/X$  agrees with results of quantitative spectroscopic analysis of the solar atmosphere. The resulting  $K$  value is compatible with the (rather uncertain) value obtained from the application of the mixing-length theory. We refer to *SES*, § 16 and § 23, where the procedure is described in detail.

Osterbrock and Rogerson (1961) used the value of the oxygen-hydrogen ratio obtained from spectroscopic analysis of the solar atmosphere in combination with available information on cosmic abundances within the heavy-element group (where oxygen predominates) for a derivation of  $Z/X$  and a redetermination of the initial values of  $X$ ,  $Y$ , and  $Z$  for the solar interior. Gaustad (1964) revised the calculation, taking into account the results of measurements of relative abundances of nuclei (He, C, N, O, and Ne) in solar cosmic rays (Biswas, Fichtel, and Guss 1962; Ney and Stein 1962; and Biswas, Fichtel, Guss, and Waddington 1963). Gaustad concluded that the initial composition of the solar interior is closely approximated by the values  $X = 0.72$ ,  $Y = 0.26$ , and  $Z = 0.02$ .

In connection with the use of results of spectroscopic analysis of the solar atmosphere in the present context, it should be emphasized that in the case of the sun the atmosphere is well mixed with a fraction of the solar matter (the outer convective zone) which is not very small. Furthermore, investigations of the pre-main-sequence contraction phase of evolution of the sun by Hayashi and others (see chap. 11 of this volume) have led to the conclusion that the sun during that phase was fully convective and therefore well mixed throughout the interior.

TABLE 8

MODEL FOR AGE ZERO\*

INITIAL CHEMICAL COMPOSITION:  $X = 0.708$ ,  $Y = 0.272$ , AND  $Z = 0.020$ ;  $M = M_{\odot}$ 

$M_r/M_{\dagger}$	$r_{\dagger}$ unit $10^{11}$ cm	$T$ unit $10^6$	$\rho$ unit $\text{g cm}^{-3}$	$L_r_{\dagger}$ unit $10^{33}$ erg sec $^{-1}$	$\epsilon$ ( $p$ - $p$ ) proton- proton process	$\epsilon$ (CN) CN cycle	$\kappa$
0.0 . . . . .	0.00	13.7	90	0.00	13.8	0.11	1.38
.05 . . . . .	.07	12.3	74	0.95	7.2	.011	1.64
.1 . . . . .	.09	11.6	65	1.54	4.8	.002	1.82
.2 . . . . .	.11	10.4	51	2.20	2.3	.000	2.16
.3 . . . . .	.14	9.4	40	2.53	1.1	.000	2.50
.4 . . . . .	.16	8.5	30.5	2.68	0.5	.000	2.87
.5 . . . . .	.18	7.6	22.4	2.75	0.2	.000	3.3
.6 . . . . .	.20	6.8	15.7	2.77	0.04	.000	3.8
.7 . . . . .	.23	5.9	10.0	2.78	0.01	.000	4.4
.8 . . . . .	.26	5.0	5.5	2.78	0.00	.000	5.2
.9 . . . . .	.32	3.8	2.09	2.78	0.00	.000	7.0
.95 . . . . .	.37	3.0	0.87	2.78	0.00	.000	8.6
.99 . . . . .	.46	1.73	0.142	2.78	0.00	.000	11.1
0.99968 . . .	0.60	0.62	0.0057	2.78	0.00	0.000	$\dagger$

\* Source: Sears (1964).

 $\dagger$  The radius of the model is  $0.659 \times 10^{11}$  cm, the luminosity  $2.78 \times 10^{33}$  erg sec $^{-1}$ . $\ddagger$  Bottom of outer convective zone.

However, the effect of diffusive drainage of the heavier elements from the outer convective zone into the interior may not be negligible. Aller and Chapman (1960) estimate that the reduction of the atmospheric abundance of silicon in the sun through this effect is at least 10 per cent, while the corresponding estimate for iron is 12 per cent, and the reduction would be smaller for oxygen. So far, the effect in question has been neglected in the applications of stellar atmosphere abundances to the problem of deducing stellar-interior compositions.

Following Gaustad, Sears (1964)<sup>2</sup> adopted  $Z/X = 0.028$  for the initial solar-interior composition, and computed an evolutionary model sequence for

<sup>2</sup> The author is very grateful to Dr. Sears for having put the results of this investigation at his disposal prior to publication.

$M = M_{\odot}$  covering the age range  $0-4.5 \times 10^9$  years. The conditions that  $L = L_{\odot}$  and  $R = R_{\odot}$  for the present age were satisfied through proper choice of  $X$  and  $K$ . Tables 8 and 9 show the properties of the resulting models for age zero and age  $4.5 \times 10^9$  years.

Similar calculations for  $M = M_{\odot}$  have been carried out by Demarque and Percy (1964). The opacities used are those of Keller and Meyerott (1955), while the energy generation is taken according to Reeves (see chap. 2). Evolutionary tracks were determined for the following  $Z$  values: 0.020, 0.025, 0.030, 0.035, 0.040. For each  $Z$  value sequences corresponding to a number of  $X$  values were computed, and  $X$  was then chosen so that  $L = L_{\odot}$  for age  $4.5 \times 10^9$ . The

TABLE 9  
MODEL FOR AGE  $4.5 \times 10^9$  YEARS\*  
INITIAL CHEMICAL COMPOSITION:  $X = 0.708$ ,  $Y = 0.272$ ,  $Z = 0.020$ ;  $M = M_{\odot}$

$M_r/M_{\dagger}$	$r_{\dagger}$ unit $10^{11}$ cm	$T$ unit $10^6$	$\rho$ unit $\text{g cm}^{-3}$	$L_r_{\dagger}$ unit $10^{33}$ erg sec $^{-1}$	$\epsilon(p-p)$ proton- proton process	$\epsilon(\text{CN})$ CN cycle	$\kappa$	$X$
0.0.....	0.00	15.7	158	0.00	15.9	1.6	1.09	0.36
.05.....	.06	13.8	103	1.30	10.0	0.13	1.32	.52
.1.....	.08	12.8	83	2.13	6.8	0.023	1.48	.58
.2.....	.10	11.3	59	3.09	3.3	0.001	1.78	.65
.3.....	.13	10.1	43	3.55	1.6	0.000	2.09	.68
.4.....	.15	9.0	31.5	3.77	0.7	0.000	2.42	.69
.5.....	.17	8.1	22.4	3.86	0.3	0.000	2.79	.70
.6.....	.20	7.1	15.2	3.90	0.06	0.000	3.2	.70
.7.....	.23	6.2	9.4	3.90	0.02	0.000	3.8	.71
.8.....	.26	5.1	5.0	3.90	0.00	0.000	4.5	.71
.9.....	.32	3.9	1.84	3.90	0.00	0.000	6.0	.71
.95.....	.38	3.0	0.74	3.90	0.00	0.000	7.4	.71
.99.....	.48	1.73	0.117	3.90	0.00	0.000	9.6	.71
0.99955.....	0.62	0.66	0.0063	3.90	0.00	0.000	‡	0.71

\* Source: Sears (1964).

† The radius of the model is  $0.694 \times 10^{11}$  cm, the luminosity  $3.90 \times 10^{33}$  erg sec $^{-1}$ .

‡ Bottom of outer convective zone.

TABLE 10  
VALUE OF THE HYDROGEN CONTENT  $X$   
WITH CORRECT SOLAR LUMINOSITY  
FOR  $Z$  VALUES\*

$Z$	$X$	$Z/X$
0.02.....	0.703	0.028
.03.....	.666	.045
0.04.....	0.637	0.062

\* Source: Demarque and Percy (1964).



value of  $K$  was determined by the condition that  $R$  for this age should be equal to  $R_{\odot}$ . Table 10 shows the relation between  $Z$  and the proper  $X$ , as well as  $Z/X$ . With  $Z/X$  equal to 0.028, the resulting initial composition is  $X = 0.70$ ,  $Y = 0.28$ , and  $Z = 0.020$ .

Demarque and Larson (1964)<sup>3</sup> have computed evolutionary model sequences for masses equal to  $0.8 M_{\odot}$ ,  $0.9 M_{\odot}$ ,  $0.95 M_{\odot}$ ,  $1.0 M_{\odot}$ , and  $1.03 M_{\odot}$ . The initial chemical composition was chosen to be  $X = 0.67$ ,  $Y = 0.30$ , and  $Z = 0.03$ . The assumptions regarding the opacity  $\kappa$  and the energy generation  $\epsilon$  were the same as in the investigation just referred to. The structure of the outer convection zone was computed according to a procedure developed by Demarque and Geisler (1963), which corresponds to the Vitense (1953) mixing-length theory,

TABLE 11  
RADIUS, BOLOMETRIC MAGNITUDE, AND EFFECTIVE TEMPERATURE  
AS A FUNCTION OF MASS FOR AGE ZERO\*  
CHEMICAL COMPOSITION:  $X = 0.67$ ,  $Y = 0.30$ ,  $Z = 0.03$

$M/M_{\odot}$	LOG ( $R/R_{\odot}$ )		$M_{\text{bol}}$		LOG $T_{\text{e}}$	
	$l/H = 1.6$	$l/H = 2.0$	$l/H = 1.6$	$l/H = 2.0$	$l/H = 1.6$	$l/H = 2.0$
0.8.....	-0.11	.....	+6 <sup>m</sup> 4	.....	3.65	.....
0.9.....	- .08	-0.09	+5.7	+5 <sup>m</sup> 7	3.70	3.71
1.0.....	- .05	- .06	+5.1	+5.1	3.75	3.75
1.1.....	+ .01	- .02	+4.6	+4.6	3.78	3.79
1.2.....	+ .03	+ .01	+4.2	+4.2	3.81	3.82
1.3.....	+0.06	+0.05	+3.8	+3.8	3.83	3.84

\* Source: Demarque and Larson (1964).

except that the radiative interaction between the turbulent rising and sinking elements and the surroundings is neglected. The ratio of mixing-length  $l$  and pressure scale height  $H$  was taken to be 1.6; with this ratio and the chosen chemical composition, the radius and luminosity of the sun are very closely reproduced for  $M = M_{\odot}$  and age  $4.5 \times 10^9$  years. Table 11 gives the properties of the zero-age line corresponding to the choice  $X = 0.67$ ,  $Y = 0.30$ ,  $Z = 0.03$ , and  $l/H = 1.6$ . Also shown are the zero-age line results for the same chemical composition, but with  $l/H = 2.0$ .

Evolutionary model sequences for  $M = 0.8 M_{\odot}$  and  $M = 1.0 M_{\odot}$  are given in Table 12 ( $X = 0.67$ ,  $Y = 0.30$ ,  $Z = 0.03$ ;  $l/H = 1.6$ ). It is seen that the evolutionary track for  $M = 0.8 M_{\odot}$  practically coincides with the zero-age line through 15 billion years. For  $M = M_{\odot}$  evolution is very nearly along the zero-age line through 4 billion years, but after 10 billion years location of the star in the Hertzsprung-Russell diagram is 1<sup>m</sup>0 above the zero-age line.

<sup>3</sup> The author is very grateful to Dr. Demarque for having put the manuscript of this paper, as well as the paper with Mr. Percy, at his disposal prior to publication.

Comparing the models for stars in the mass range  $0.8\text{--}1.7 M_{\odot}$  to those for  $M > 1.7 M_{\odot}$  considered in § 2, we note that the densities in the stellar interior, at points with the same temperature, are considerably higher in the former case. This has the consequence that the theoretically calculated opacities are generally less accurate for the models with  $M$  between  $0.8$  and  $1.7 M_{\odot}$ . More accurate opacity tables and an improved theory of energy transport in the upper part of the outer convection zone are desiderata in the field considered in this section. With regard to the latter point, the insensitivity of computed radii and luminosities of stellar models to the value of the parameter  $l/H$  in the mixing-length theory (cf. table 11, table 14) is encouraging. Nevertheless, the development of a better procedure for the theoretical calculation of the structure of the outer convection zone remains an important problem.

TABLE 12  
EVOLUTIONARY MODEL SEQUENCES\*  
INITIAL CHEMICAL COMPOSITION:  $X = 0.67$ ,  
 $Y = 0.30$ ,  $Z = 0.03$ ;  $l/H = 1.6$

Age (billion years)	$R/R_{\odot}$	$M_{\text{bol}}$	$\log T_{\text{e}}$	$\Delta M_{\text{bol}}$ (from zero- age line, equal $T_{\text{e}}$ )
$M = 0.8 M_{\odot}$				
0.....	0.78	+6 <sup>m</sup> 4	3.65	0 <sup>m</sup> 0
2.5.....	.79	6.3	3.66	.0
5.0.....	.80	6.2	3.66	.0
7.5.....	.81	6.1	3.67	.0
10.0.....	.82	6.0	3.68	.0
12.5.....	.84	5.9	3.68	.1
15.0.....	0.87	+5.8	3.69	0.1
$M = 1.0 M_{\odot}$				
0.....	0.90	+5 <sup>m</sup> 1	3.75	0 <sup>m</sup> 0
2.0.....	0.93	5.0	3.75	0.0
4.0.....	0.97	4.8	3.76	0.1
5.2.....	1.01	4.7	3.76	0.2
6.4.....	1.06	4.6	3.76	0.3
7.09.....	1.10	4.5	3.76	0.3
7.87.....	1.15	4.4	3.77	0.4
8.39.....	1.19	4.3	3.77	0.5
8.85.....	1.24	4.2	3.77	0.6
9.32.....	1.31	4.2	3.77	0.7
9.66.....	1.37	4.1	3.76	0.8
9.94.....	1.45	4.0	3.76	1.0
10.15.....	1.53	3.9	3.75	1.1
10.35.....	1.63	+3.9	3.74	1.3

\* Source: Demarque and Larson (1964).

## § 4. SUBDWARFS

The category of stars at present referred to as extreme Population II subdwarfs was recognized spectroscopically by Adams *et al.* (1935). On the basis of the metallic-line strengths Adams and Joy classified the stars in question as A stars, and the trigonometric parallaxes indicated that the stars were considerably fainter than main-sequence A stars. Further work on this category of stars was done by Kuiper (1940), by Morgan, Keenan, and Kellman (1943), and by Parenago (1946). See also Greenstein, Volume 5 of this series.

Chamberlain and Aller (1951) carried out a quantitative analysis of the spectra of two typical stars of the category in question and, on the basis of the observed strengths of the Balmer lines, concluded that the effective temperature is only slightly higher than that of the sun. The metallic lines are very weak for this effective temperature, and Chamberlain and Aller showed that this is due to very low abundance of the metals relative to hydrogen. On the basis of this finding, confirmed by many other investigations, this category of stars is referred to as extreme Population II. Comparison of the effective temperature derived from the Balmer line strengths with the absolute magnitudes (not very accurately known) shows that the location of the stars in the Hertzsprung-Russell diagram is not far removed from the main sequence of Population I stars.

Roman (1954) carried out photoelectric *UBV* photometry of a number of extreme Population II stars of spectral type F and showed that they have an ultraviolet excess of about 0<sup>m</sup>2. It became clear that the ultraviolet excess is mainly due to the fact that the reduction of broad-band intensities, such as the *B* intensity, and particularly the *U* intensity, through absorption lines is much smaller for extreme Population II stars than for Population I stars of the same effective temperature (e.g., Reiz 1954).

The effect of the absorption lines in *UBV* photometry, and the dependence of this effect upon the metal-hydrogen ratio, was investigated by Schwarzschild, Searle, and Howard (1955), by Sandage and Eggen (1959), and by Wildey, E. M. Burbidge, Sandage, and G. R. Burbidge (1962), also Burbidge, Burbidge, Sandage, and Wildey (1959). After correction according to the amount of ultraviolet excess, the color index  $B - V$  can give the effective temperature practically without bias, due to the effect of chemical composition. Similarly, the color index  $b - \gamma$  of photoelectric *uvby* photometry (Strömgren 1963) yields unbiased effective temperatures after a small correction has been applied, according to the value of the metal index,  $m_1$ . Code (1959) has shown that the  $G - I$  color index of the six-color photometric system gives effective temperatures of F and G stars, practically unaffected by the absorption line effects. Swihart (1956) showed, through a theoretical investigation of model atmospheres, that the relation between color indices and effective temperature is little affected by the metal-hydrogen ratio, once a correction for the absorption-line effect has been applied.

Thus, the determination of effective temperatures for extreme Population II stars presents no great problems. However, the problem of observational determination of absolute magnitudes remains a difficult one (Greenstein 1956, Code 1959), because the trigonometric parallaxes of even the brighter representatives are small. Eggen (1964) derived the result that the location of the extreme Population II stars in the  $M_{\text{bol}}-T_{\text{eff}}$  diagram is close to the zero-age line of the Hyades cluster, the separation being less than  $0^{\text{m}}5$ . Code (1959) utilized trigonometric parallaxes for seven extreme Population II stars at relatively small distances from the sun and found that they are located about  $1^{\text{m}}$  below the Population I main sequence.

Models of stars with very low heavy-element content have been computed in a number of investigations. With a view to applications to observable extreme Population II stars, the masses considered are generally in a fairly narrow range around  $M = M_{\odot}$ . However, Ezer (1961) calculated models of pure-hydrogen stars of large masses for the purpose of discussion of element formation during the first phase of star formation in the Galaxy.

Reiz (1954) computed models for stars with negligible content of heavy elements applicable to masses in the range  $0.7-1.3 M_{\odot}$ . For a star consisting of a mixture of hydrogen and helium, the energy production is by the proton-proton process. The main contributors to the opacity are continuous absorption corresponding to free-free transitions of electrons in the fields of the hydrogen and helium nuclei and electron scattering. Reiz found that, for the interiors of stars in the mass range considered, the opacity can be rather well represented by a power law of the form  $\kappa \sim \rho^{0.5} T^{-1.75}$ .

The models of pure hydrogen-helium stars computed by Reiz for the mass range  $0.7-1.3 M_{\odot}$  are similar to those considered in the previous section in that they have no convective cores. Assuming radiative equilibrium throughout the models, Reiz computed the location of the zero-age line in the  $M_{\text{bol}}-T_e$  diagram. For the composition  $X = 0.70$ ,  $Y = 0.30$  the line is located about  $1^{\text{m}}$  below that of the Population I zero-age line in the spectral range of late F and early G stars. The zero-age line for a pure-hydrogen star ( $X = 1.00$ ,  $Y = 0.00$ ), however, was found to coincide very nearly with the Population I line. The distribution of temperature, density, mass, and energy flux for the models considered is shown in Table 13.

A comparison of the location of the zero-age lines for extreme Population II and Population I stars was made by Haselgrove and Hoyle (1959) who took into account the effect of the outer convective zone. Again, the lines for pure-hydrogen stars and Population I stars were found to have only a small separation. If equal helium content,  $Y$ , is assumed, then the zero-age line for the stars with low heavy-element content is located below that of the Population I stars, but Haselgrove and Hoyle found that the separation is considerably smaller than  $1^{\text{m}}$ .

Using a similar technique, Hoyle (1959) computed evolutionary model se-

quences for extreme Population II stars with masses and compositions as follows:  $M = 1.35 M_{\odot}$ ,  $X = 0.99$ ,  $Y = 0.01$ ,  $Z = 0.0001$ , and  $M = 1.17 M_{\odot}$ ,  $X = 0.75$ ,  $Y = 0.25$ ,  $Z = 0.0001$ . In discussing the results of these calculations, Hoyle emphasized that in a star with low heavy-element content, in which the proton-proton process dominates even in regions where most of the hydrogen has been converted to helium, a considerably larger fraction of the hydrogen

TABLE 13  
TEMPERATURE, DENSITY, RELATIVE MASS, AND RELATIVE FLUX  
AS A FUNCTION OF RELATIVE RADIUS\*

$r/R$	$T/T_c$	$\rho/\rho_c$	$M_r/M$	$L_r/L$
0.0.....	1.00	1.00	0.00	0.00
.2.....	0.75	0.62	0.20	0.75
.4.....	0.40	0.14	0.72	1.00
.6.....	0.19	0.014	0.96	1.00
0.8.....	0.07	0.0005	1.00	1.00

\* For a stellar model with negligible heavy-element content, assumed to be in radiative equilibrium. Source: Reiz (1954).

TABLE 14  
PRINCIPAL CHARACTERISTICS OF ZERO-AGE MODELS OF STARS WITH  
LOW HEAVY-ELEMENT CONTENT\*

$M/M_{\odot}$	LOG ( $R/R_{\odot}$ )		$M_{\text{bol}}$		LOG $T_e$		$X$	$Z$
	$l/H=1$	$l/H=2$	$l/H=1$	$l/H=2$	$l/H=1$	$l/H=2$		
0.8.....	-0.14	-0.16	+6.6	+6.6	3.63	3.64	0.999	0.001
	- .14	- .15	+7.4	+7.4	3.56	3.56	.990	.010
	- .13	- .14	+4.9	+4.9	3.80	3.80	.75	.001
	- .13	- .13	+5.8	+5.8	3.71	3.71	.75	.010
1.0.....	- .04	- .06	+5.1	+5.1	3.74	3.75	.999	.001
	- .04	- .06	+6.0	+6.0	3.65	3.66	.990	.010
	- .09	- .09	+3.6	+3.6	3.91	3.91	.75	.001
	-0.07	-0.08	+4.5	+4.5	3.81	3.82	0.75	0.010

\* Source: Demarque (1960, 1961).

content of the star is burned before the star moves away from the main sequence into the subgiant region of the Hertzsprung-Russell diagram. Consequently the main-sequence lifetimes of extreme Population II stars are longer than those of Population I stars, comparison being made for the same main-sequence luminosity.

Reiz and Torgård (1961) computed an evolutionary model sequence for an extreme Population II star with initial luminosity about equal to that of the sun. In  $16 \times 10^9$  years the absolute magnitude of the star increased by about  $0^m.3$ , and the star remained very close to the zero-age line.

For a discussion of the problems of age determinations for Population II stars we refer to Sears and Brownlee, chapter 11 of the present volume.

Demarque (1960) investigated the structure of stars of low heavy-element content for zero age in the mass range  $0.6\text{--}1.0 M_{\odot}$ , taking into account the effect of the outer convection zone. The opacities were taken according to Keller and Meyerott (1955), and the energy generation was represented by  $\epsilon = 10^{-29} X^2 \rho T^4$ . The ratio of mixing-length  $l$  to pressure scale height was assumed to be 1. In a following investigation Demarque (1961) computed corresponding models with  $l/H = 2$ .

For equal helium content Demarque found the zero-age line corresponding to  $Z = 0.001$  to lie about one-third of a magnitude lower than that for  $Z = 0.01$  in the spectral range of late F and early G stars. The principal characteristics of the models for two masses, and four chemical compositions are given in Table 14.

Naur (1956) has computed models for chemically homogeneous stars in radiative equilibrium, for which the energy generation is given by the expression  $\epsilon = \epsilon_0 \rho T^4$ . Tables of the structure are given for 11 different power-law representations of the opacity. Results valid for the opacities adopted by Reiz (1954) and Demarque (1960, 1961) can be interpolated with fair accuracy from the data given in these tables.

#### § 5. MAIN-SEQUENCE STARS WITH MASSES SMALLER THAN $0.8 M_{\odot}$

In § 1 we referred to the fact that the evolutionary changes during the lifetime of the Galaxy are small for stars with masses under  $0.8 M_{\odot}$ . The discussion in this section is limited to the structure of chemically homogeneous stars.

The application by Aller *et al.* (1952) of the results of the investigations of the proton-proton reaction to the structure of main-sequence M stars resulted in computed luminosities for these stars that were much higher than the observed luminosities. In the calculations of the models, radiative equilibrium was assumed throughout the interior. It was concluded that either the models or the adopted  $p$ - $p$  cross-sections had to be discarded. Osterbrock (1953) showed that the discrepancy is removed when the role of the outer convective zone is properly taken into account.

Schwarzschild (*SES*, § 16) has discussed the problem of the structure of the practically identical components of the spectroscopic binary YY Gem. The techniques are similar to those utilized for the sun except that evolutionary effects are negligible here. The spectral type is M1 V, the mass  $0.64 M_{\odot}$ , the radius  $0.62 R_{\odot}$ , the bolometric magnitude  $+7^m.7$ , while  $\log T_e = 3.56$  (Harris, Strand, and Worley 1963). A homogeneous model with  $X = 0.70$ ,  $Y = 0.27$ , and  $Z = 0.03$  gives a radius and luminosity agreeing well with the observed values. The central temperature is  $9 \times 10^6$ , the central density  $76 \text{ gm cm}^{-3}$ . The electron gas is not approaching degeneracy anywhere in the interior. The thickness of the outer convective zone amounts to one-third of the radius, and the zone contains 11 per cent of the mass of the star.

Limber (1958*a, b*) investigated the structure of middle and late M main-sequence stars, with masses ranging from  $0.27 M_{\odot}$  (Krüger 60A) to  $0.08 M_{\odot}$  (Ross 614B). For these masses the outer convective zone extends all the way to the center. The stellar model is thus completely convective except for a thin atmospheric fringe in radiative equilibrium. Limber finds that the models satisfactorily reproduce the values of radii and luminosities obtained from a rediscussion of the observational material. For the composition  $X = 0.75$ ,  $Y = 0.23$ , and  $Z = 0.02$ , the central temperature  $T_c$  and central density  $\rho_c$  are computed as functions of stellar mass  $M$  and stellar radius  $R$  and represented in an M-R diagram. The role of electron-gas degeneracy is discussed in terms of this diagram. For Krüger 60B ( $M = 0.16 M_{\odot}$ ),  $T_c$  is close to  $5 \times 10^6$  and  $\rho_c$  about  $150 \text{ gm cm}^{-3}$ . The degeneracy effect is noticeable but not pronounced.

Completely convective models of the type investigated by Limber have been applied by Kumar (1963) to the study of the contraction phase of stars in the mass range  $0.05\text{--}0.09 M_{\odot}$ . For stars with a chemical composition typical of Population I it is found that when the mass is smaller than  $0.07 M_{\odot}$  the main-sequence stage is never reached because temperature and density at the center remain too low for energy generation through hydrogen burning to become appreciable. Instead, the contracting mass becomes a degenerate black-dwarf star.

#### REFERENCES

- ADAMS, W. S., JOY, A. H.,  
HUMASON, M. L., and  
BRAYTON, A. M. 1935 *A p. J.*, **81**, 187.
- ALLER, L. H. 1961 *The Abundance of the Elements* (New York: Interscience Publishers).
- ALLER, L. H., and CHAPMAN, S. 1960 *A p. J.*, **132**, 461.
- ALLER, L. H., *et al.* 1952 *A p. J.*, **115**, 328.
- ARKING, A., and  
HERRING, J. 1964 Unpublished. For a summary, see *Pub. A.S.P.*, **75**, 226.
- BAKER, N. 1963 "The depth of the outer convection zone in main-sequence stars," *Pub. Inst. for Space Studies, New York*.
- BIERMANN, L. 1935 *A.N.*, **257**, 269.  
1945 *Ergebnisse d. exakten Naturwiss.*, **21**, 1.
- BISWAS, S., FICHTEL,  
C. E., and GUSS, D. E. 1962 *Phys. Rev.*, **128**, 2756.
- BISWAS, S., FICHTEL,  
C. E., GUSS, D. E., and  
WADDINGTON, C. J. 1963 *J. Geophys. Res.*, **68**, 3109.
- BLAAUW, A. 1963 *Stars and Stellar Systems*, Vol. 3, ed. K. AA. STRAND (Chicago: University of Chicago Press), chap. 20.

- BLACKLER, J. M. 1958 *M.N.*, **118**, 37.
- BÖHM-VITENSE, E. 1958 *Zs. f. Ap.*, **46**, 108.
- BURBIDGE, E. M.,  
BURBIDGE, G. R.,  
SANDAGE, A. R., and  
WILDEY, R. L. 1959 *Coll. Internat. d'Astrophys., Liège*, No. 9, p. 427.
- CAUGHLAN, G. R., and  
FOWLER, W. A. 1962 *Ap. J.*, **136**, 453.
- CHAMBERLAIN, J. W.,  
and ALLER, L. H. 1951 *Ap. J.*, **114**, 52.
- CODE, A. D. 1959 *Ap. J.*, **130**, 473.
- COWLING, T. G. 1935 *M.N.*, **96**, 42.
- DEMARQUE, P. R. 1960 *Ap. J.*, **132**, 366.  
1961 *Ibid.*, **134**, 9.
- DEMARQUE, P. R., and  
GEISLER, J. E. 1963 *Ap. J.*, **137**, 1102.
- DEMARQUE, P. R., and  
LARSON, R. B. 1964 *Ap. J.*, **140**, 544.
- DEMARQUE, P. R., and  
PERCY, J. R. 1964 *Ap. J.*, **140**, 541.
- EGGEN, O. J. 1963 *Ap. J. Suppl.*, **8**, 125.  
1964 *Roy. Obs. Bull.*, No. 82, p. 4.
- EPSTEIN, I. 1950 *Ap. J.*, **112**, 207.
- EZER, D. 1961 *Ap. J.*, **133**, 159.
- GAUSTAD, J. E. 1964 *Ap. J.*, **139**, 406.
- GREENSTEIN, J. L. 1956 *Proc. Third Berkeley Symp. Math. Stat. Prob.*, ed.  
J. NEYMAN (Berkeley: University of California  
Press), **3**, 11.
- HÄRM, R., and  
SCHWARZSCHILD, M. 1955 *Ap. J.*, **121**, 445.
- HARRIS, D. L. 1963 *Stars and Stellar Systems*, Vol. **3**, ed. K. AA.  
STRAND (Chicago: University of Chicago  
Press), chap. 14.
- HARRIS, D. L.,  
STRAND, K. AA., and  
WORLEY, C. E. 1963 *Stars and Stellar Systems*, Vol. **3**, ed. K. AA.  
STRAND (Chicago: University of Chicago Press),  
chap. 15.
- HASELGRÖVE, C. B., and  
HOYLE, F. 1959 *M.N.*, **119**, 112.
- HAYASHI, C., and  
CAMERON, R. C. 1962 *Ap. J.*, **136**, 166.
- HENYEX, L. G.,  
LELEVIER, R., and  
LEVÉE, R. D. 1959 *Ap. J.*, **129**, 2.
- HOYLE, F. 1959 *M.N.*, **119**, 124.  
1960 *Ibid.*, **120**, 22.



- HOYLE, F., and  
 LYTTLETON, R. A. 1942 *M.N.*, **102**, 218.
- IBEN, I. 1963 *Ap. J.*, **138**, 452.
- IBEN, I., and  
 EHRLMAN, J. 1962 *Ap. J.*, **135**, 770.
- KELLER, G., and  
 MEYEROTT, R. E. 1955 *Ap. J.*, **122**, 32.
- KELSALL, T. 1965 Unpublished.
- KUIPER, G. P. 1940 *Ap. J.*, **91**, 269.
- KUMAR, S. S. 1963 *Ap. J.*, **137**, 1121.
- KUSHWAHA, R. S. 1957 *Ap. J.*, **125**, 242.
- LEDoux, P. 1947 *Ap. J.*, **105**, 305.
- LIMBER, D. N. 1958a *Ap. J.*, **127**, 363.  
 1958b *Ibid.*, p. 387.
- MESTEL, L. 1953 *M.N.*, **113**, 716.
- MORGAN, W. W.,  
 KEENAN, P. C., and  
 KELLMAN, E. 1943 *An Atlas of Stellar Spectra* (Chicago: University  
 of Chicago Press).
- MORTON, D. C. 1959 *Ap. J.*, **129**, 20.
- NAUR, P. 1956 *Pub. Copenhagen Obs.*, No. 168.
- NEY, E. P., and  
 STEIN, W. A. 1962 *J. Geophys. Res.*, **67**, 2087.
- OKE, J. B. 1950 *J. R. Astr. Soc. Canada*, **44**, 135.
- ÕPIK, E. 1938 *Pub. Obs. Tartu*, Vol. **30**, No. 3.
- OSTERBROCK, D. E. 1953 *Ap. J.*, **118**, 529.
- OSTERBROCK, D. E., and  
 ROGERSON, J. B. 1961 *Pub. A.S.P.*, **73**, 129.
- PARENAGO, P. P. 1946 *A.J.*, *U.S.S.R.*, **23**, 31.
- POLAK, E. J. 1962 *Ap. J.*, **136**, 465.
- REIZ, A. 1954 *Ap. J.*, **120**, 342.
- REIZ, A., and TORGÅRD, I. 1961 *Ann. Acad. Sci. Fennicae, ser. A*, Vol. **3**, p. 217.
- ROMAN, N. G. 1954 *A.J.*, **59**, 307.
- SAKASHITA, S., ONO, Y.,  
 and HAYASHI, C. 1959 *Progress of Theoret. Phys.* **21**, 315.
- SALPETER, E. E. 1952 *Phys. Rev.*, **88**, 547.
- SANDAGE, A. R., and  
 EGGEN, O. J. 1959 *M.N.*, **119**, 278.
- SCHÖNBERG, M., and  
 CHANDRASEKHAR, S. 1942 *Ap. J.*, **96**, 161.
- SCHWARZSCHILD, M. 1958 *Structure and Evolution of the Stars* (Princeton,  
 N.J.: Princeton University Press).
- SCHWARZSCHILD, M., and  
 HÄRM, R. 1958 *Ap. J.*, **128**, 348.  
 1959 *Ibid.*, **129**, 637.

- SCHWARZSCHILD, M.,  
HOWARD, R. F., and  
HÄRM, R. 1957 *Ap. J.*, **125**, 233.
- SCHWARZSCHILD, M.,  
SEARLE, L., and  
HOWARD, R. 1955 *Ap. J.*, **122**, 353.
- SEARS, R. L. 1964 *Ap. J.*, **140**, 477.
- STOTHERS, R. 1963 *Ap. J.*, **138**, 1074.
- STRÖMGREN, B. 1963 *Stars and Stellar Systems*, Vol. 3, ed. K. AA.  
STRAND (Chicago: University of Chicago Press),  
chap. 9.
- SWEET, P. A. 1950 *M.N.*, **110**, 548.
- SWIHART, T. L. 1956 *Ap. J.*, **123**, 151.
- TAYLER, R. J. 1954 *Ap. J.*, **120**, 332.
- VITENSE, E. 1953 *Zs. f. Ap.*, **32**, 135; see also BÖHM-VITENSE (1958).
- WILDEY, R. L.,  
BURBIDGE, E. M.,  
SANDAGE, A. R., and  
BURBIDGE, G. R. 1962 *Ap. J.*, **135**, 94.



## CHAPTER 5

# *The Theory of White Dwarfs*

L. MESTEL

*University of Cambridge, England*

A WHITE dwarf is a body of stellar mass, but of planetary dimensions. It is self-luminous, with a surface temperature that can be as high as  $20,000^\circ\text{K}$  in the hottest or as low as  $4000^\circ\text{K}$  in the coolest white dwarfs observed. Because of its small surface area, the star is far fainter than a main-sequence star of the same color; equally, the light it emits is much whiter than that from main-sequence stars of similar luminosity. The basic theoretical problem is to reconcile hydrostatic equilibrium under the enormous gravitational field with the observed low luminosity: for if the normal gaseous equation of state is assumed valid, the theory of stellar structure predicts a luminosity rather greater than the main-sequence value. The resolution of the problem by Fowler (1926) was a triumph for the recently formulated Fermi-Dirac statistics—the application of the Pauli exclusion principle to the electron gas. In addition to thermal energy—the microscopic kinetic energy associated thermodynamically with a temperature  $T$ , identical, for example, with the temperature of Planck radiation present—a dense electron gas at low enough temperatures has a much larger “exclusion” energy, due to the requirement that only two electrons (with oppositely directed spins) may occupy the same energy state. It is this zero-point kinetic energy that supplies most of the pressure balancing the gravitational field; accordingly, it is both physically realistic and convenient to study first zero-temperature stars—black dwarfs—in which the electron gas is fully “degenerate,” i.e., stars with as low an energy as is allowed by the exclusion principle. A white dwarf of observable luminosity is found to have a fairly high internal temperature, but most of its mass is still almost completely degenerate, so that the zero-temperature model remains an excellent approximation.

### § 1. ZERO-TEMPERATURE STARS

#### 1.1. THE PRESSURE OF THE DEGENERATE, PERFECT ELECTRON GAS

We consider first the non-relativistic approximation, and suppose all the energy states are occupied up to a maximum momentum  $p_0$ . The number density

$n_e$  and the energy density  $U$  are then given by

$$n_e = 2 \int_0^{p_0} \frac{4\pi p^2 dp}{h^3} = \frac{8\pi}{3} \frac{p_0^3}{h^3}, \quad (1.1)$$

and

$$U = 2 \int_0^{p_0} \left( \frac{p^2}{2m_e} \right) \frac{4\pi p^2 dp}{h^3} = \frac{4\pi}{5} \frac{p_0^5}{m_e h^3}, \quad (1.2)$$

where use is made of the equivalence of one quantum energy state to a volume  $h^3$  of phase space. By its definition as the mean rate of momentum transfer across unit area, the pressure  $P_e$  is

$$P_e = \frac{1}{3} \int_0^{p_0} (p v_p) \frac{8\pi p^2 dp}{h^3}, \quad (1.3)$$

where  $v_p$  is the velocity associated with momentum  $p$ ; in the non-relativistic limit,  $v_p = p/m_e$ , and  $P_e = \frac{2}{3}U$ . Thus we arrive at the expression for the pressure of a non-relativistically degenerate electron gas at zero temperature:

$$P_e = \frac{h^2}{5m_e} \left( \frac{3}{8\pi} \right)^{2/3} n_e^{5/3} = K \left( \frac{\rho}{\mu_e} \right)^{5/3}, \quad (1.4)$$

where  $\rho$  is the mass density,  $\mu_e$  is the number of proton masses per free electron, and

$$K = \frac{h^2}{5m_e m_H^{5/3}} \left( \frac{3}{8\pi} \right)^{2/3}. \quad (1.5)$$

Anticipating that the gas in a white dwarf is almost completely "pressure-ionized" (cf. § 1.2), we have

$$\mu_e = \frac{\rho}{m_H n_e} = \frac{A}{Z}, \quad (1.6)$$

where  $A$  is the mean atomic weight and  $Z$  the mean ionic charge of the nuclear species present. With the equation of state (1.4), a cold body of any mass may exist in gravitational equilibrium, its mass  $M$  and radius  $R$  given by (Chandrasekhar 1939, chap. 4)

$$M = 4\pi \left( \frac{5K}{8\pi G \mu_e^{5/3}} \right)^{3/2} \rho_c^{1/2} \left( -\xi^2 \frac{d\theta_{3/2}}{d\xi} \right)_1, \quad (1.7)$$

$$R = \left( \frac{5K}{8\pi G \mu_e^{5/3}} \right)^{1/2} \rho_c^{-1/6} \xi_1 \propto M^{-1/3}, \quad (1.8)$$

where  $\rho_c$  is the central density,  $\theta_{3/2}(\xi)$  the Emden function of index  $3/2$ ,  $\xi$  the non-dimensional Emden radial coordinates, as in equation (1.8), and the suffix unity refers to the first zero of  $\theta_{3/2}$ .

The first and most serious modification to the theory arises at densities high enough for the energy  $p_0^2/2m_e$  at the Fermi surface to be comparable with the

electronic rest energy  $m_e c^2$ : by (1.1), when  $n_e^{1/3} \simeq m_e c/h$ , requiring  $\rho \simeq 10^6$ —less than the central densities of most white dwarfs. When the relativistic relations

$$\begin{aligned} T &= \text{kinetic energy per electron} \\ &= c (m_e^2 c^2 + p^2)^{1/2} - m_e c^2, \\ v &= \frac{c p}{(m_e^2 c^2 + p^2)^{1/2}} \end{aligned} \quad (1.9)$$

are used in (1.2) and (1.3), we arrive at (Anderson 1929, Stoner 1930, Chandrasekhar 1939, chap. 10)

$$\begin{aligned} P_e &= \frac{\pi m_e^4 c^5}{3 h^3} f(x) \\ &= \frac{\pi m_e^4 c^5}{3 h^3} [x(2x^2 - 3)(x^2 + 1)^{1/2} + 3 \sinh^{-1} x], \end{aligned} \quad (1.10)$$

$$n_e = \frac{8 \pi m_e^3 c^3}{3 h^3} x^3, \quad (1.11)$$

$$\begin{aligned} U &= \frac{\pi m_e^4 c^5}{3 h^3} g(x) \\ &= \frac{\pi m_e^4 c^5}{3 h^3} \{ 8x^3 [(x^2 + 1)^{1/2} - 1] - f(x) \}, \end{aligned} \quad (1.12)$$

where

$$x = \frac{p_0}{m_e c} \quad (1.13)$$

is the maximum momentum in non-dimensional form. The mean energy per electron is

$$E_0 = \frac{U}{n_e} = \frac{m_e c^2}{8} \frac{g(x)}{x^3}. \quad (1.14)$$

The zero-temperature pressure (1.10)—written now as  $P_0$ —is given by the thermodynamic relation  $P_0 = -\partial E_0 / \partial (1/n_e)$ .

For substitution in the equation of hydrostatic support, (1.10) and (1.11) are written, with use of (1.6), as

$$P_0 = A f(x), \quad \rho = n_e \mu_e m_H = \frac{8 \mu_e m_H}{m_e c^2} A x^3 = B x^3. \quad (1.15)$$

It is readily verified that, for  $x \ll 1$ , the earlier, non-relativistic formulae are recovered. At the limit  $x \gg 1$ ,  $f(x) \simeq 2x^4$ ,  $g(x) \simeq 6x^4$ , and

$$P_0 = \frac{1}{3} U = \frac{1}{8} \left( \frac{3}{\pi} \right)^{1/3} h c n_e^{4/3} = \frac{1}{8} \left( \frac{3}{\pi} \right)^{1/3} \frac{h c}{m_H^{4/3}} \left( \frac{\rho}{\mu_e} \right)^{4/3} = \frac{2 A}{B^{4/3}} \rho^{4/3}. \quad (1.16)$$

Since the constant multiplying  $\rho^{4/3}$  is fixed (once  $\mu_e$  is given), the theory of polytropes (Chandrasekhar 1939) predicts just one mass for which equilibrium is possible under the extreme relativistically degenerate pressure (1.16):

$$M_e = 4\pi \left( \frac{2A}{\pi G} \right)^{3/2} \frac{1}{B^2} \left( -\xi^2 \frac{d\theta_3}{d\xi} \right)_1 = \frac{5.75 M_\odot}{\mu_e^2}. \quad (1.17)$$

This is the well-known Chandrasekhar limiting mass. Stars of mass less than  $M_e$  achieve equilibrium, with radii systematically less than those of the corresponding  $3/2$  polytrope (1.8), the deviation being already marked at  $M \simeq 0.15 M_e$ . There is no homology relation between models with different central densities—each mass has its own density function; when normalized to the same central density and radius, the different density laws all lie, as expected, between the polytropes  $n = 3/2$  and  $n = 3$ . If a star with  $M < M_e(\mu_e)$  were to find itself so condensed that its electron pressure approximated to the  $\rho^{4/3}$  law, its self-gravitation would be insufficient to maintain it in equilibrium: it would expand until the drop in  $\rho$  modifies the pressure law so that it depends more strongly on  $\rho$ , and equilibrium can be reached (after some energy dissipation) with the Chandrasekhar density function appropriate to its mass. Equally, a (non-rotating) star with mass  $M > M_e(\mu_e)$  can never achieve equilibrium under the pressure (1.10), however far it contracts: there is no place in physics for a *cold* spherical body in hydrostatic equilibrium if its mass exceeds  $M_e(\mu_e)$ .

Savedoff (1963) has computed the total energy of a series of Chandrasekhar models, including the limiting case, which he shows has a finite negative energy.

## 1.2. CORRECTIONS TO THE PERFECT GAS MODELS

The implicit assumption of the Fowler-Chandrasekhar theory is that at zero temperature the electrons and ions together form an electrically neutral gas of free particles in its lowest quantum state, its energy being primarily that of the degenerate electron gas. In a cold body of sufficiently low density, each ion would recombine with electrons to form a neutral atom, and the resultant gas pressure would be due to the very much lower zero-point motions of the heavy particles. The “mean radius”  $d$  of such a neutral atom is given approximately by the Fermi-Thomas atomic model (e.g., Seitz 1940). With  $Z$  electrons confined to a sphere of radius  $d$ , the “uncertainty” energy per electron is  $\sim [\hbar/(d/Z^{1/3})]^2/2m_e$ ; equating this to the potential energy per electron,  $Ze^2/d$ , yields

$$d \simeq \frac{Z^{-1/3} \hbar^2}{m_e e^2} = \frac{Z^{-1/3} \hbar}{\alpha m_e c} = Z^{-1/3} a_0, \quad (1.18)$$

where  $\alpha$  is the fine-structure constant and  $a_0$  the Bohr radius. The Fermi-Thomas distance  $d$  is the quantum analogue of the Debye shielding length in normal plasma theory, the exclusion energy playing the role of the thermal energy. If  $Z^{-1/3} a_0$  is large compared with the mean ionic distance  $Z^{1/3} (4\pi n_e/3)^{-1/3}$ , then even at absolute zero the atoms are “pressure-ionized,” the electron gas is

nearly uniform, and the energy (1.14) is the dominant term; the biggest fractional correction is of order  $Z^{1/3}n_e^{-1/3}/Z^{-1/3}a_0 \simeq Z^{2/3}r_e$ , where  $r_e$  is the inter-ionic distance in units of  $a_0$ . Numerically, the above condition for pressure ionization is  $\rho \gg 2.5AZ$ , which is easily satisfied over the bulk of a white dwarf. The approximation would not be good in the extreme outer layers of low density, where, however, the finite temperature in any observable white dwarf implies that degeneracy has disappeared (§ 2.1).

Various attempts have been made to estimate deviations from the Chandrasekhar formulae. A recent systematic discussion is by Salpeter (1961). His most striking conclusion is that the ions in a white dwarf do not form a nearly uniform gas like the electrons, but a nearly rigid lattice of spacing  $\simeq Z^{1/3}r_e a_0$ . The demonstration proceeds by assuming the result, and computing corrections to the energy (1.14). The largest term is the classical Coulomb energy of a lattice cell, computed according to the Wigner-Seitz approximation (Seitz 1940): each ion  $Ze$  is supposed to be surrounded by a uniform, negatively charged sphere of radius  $Z^{1/3}r_e a_0$ , the total electronic charge being  $-Ze$ . This Coulomb energy per electron (discussed earlier by Auluck and Mathur [1959]), is

$$E_c = -\frac{9}{10} \frac{Z^{2/3}}{r_e} a^2 m_e c^2 \propto n_e^{1/3}. \quad (1.19)$$

This is less than  $E_0$  of (14) by the factor  $Z^{2/3}r_e$  for non-relativistic electrons ( $x \ll 1$ , or  $r_e \gg a$ ), and by  $Z^{2/3}a$  when  $x \gg 1$ . This must be compared with the positive contribution of the zero-point kinetic energy associated with the precise specification of ionic lattice sites: roughly,

$$E_{z.p.} \simeq \frac{3}{2} \left( \frac{m_e}{Zm_i} \right)^{1/2} r_e^{-3/2} a^2 m_e c^2 \quad (1.20)$$

(Salpeter 1961), which is less than  $|E_c|$  by the factor  $f \simeq (0.065x/ZA)^{1/2}$ . The amplitude of the zero-point oscillations is of order  $f^{1/2}$  times the lattice spacing. If this were of order unity or more, the lattice model would certainly break down: the ions would also form a nearly uniform gas and the Coulomb correction (1.19) would nearly disappear. (The kinetic energy of the ions would then depend on the quantum statistics obeyed by the nuclei; for Fermi-Dirac nuclei [odd  $A$ ] it would be approximately the exclusion energy of a gas of non-interacting nuclei, given by eqs. [1.11] and [1.12], with  $m_i$  replacing  $m_e$ ; for Bose-Einstein nuclei [even  $A$ ] it would be nearly zero.) But the breakdown in the lattice model demands a very high value of  $x$ , enhanced by the fact that at the correspondingly high densities only fairly heavy nuclei occur (cf. § 1.3). Salpeter concludes that the lattice model is the state of lowest energy which a zero-temperature star must adopt: the sizable negative correction (1.19) is reduced only slightly by the zero-point kinetic energy (1.20). The large Fermi-Thomas screening radius (compared with the lattice spacing) is responsible for the effect. If this radius were small, motion of an individual ion from its site would not be



inhibited by the neighboring ions, since the ion would be effectively screened by the  $Z$  electrons it would carry with it. As it is, the ionic lattice is permeated by a nearly uniform electron gas, and the ions are kept close to their lattice sites by their mutual repulsion. This striking difference from a thermal plasma is a characteristically quantum effect: the high Fermi-Thomas radius is due to the Pauli principle's forcing up the electron energy, while the zero-point energy of the ions in their lattice is much weaker. In a normal plasma, however, the same thermal energy that forces up the Debye length well above the interparticle distance also keeps the ionic thermal energy above the interaction energy: the ions cannot condense without the electrons falling simultaneously into Bohr orbits.

Salpeter estimates several other corrections to the Chandrasekhar energy (1.14). Because of the smallness of the parameter  $Z^{2/3}r_e$ , the correction to  $E_c$  due to the non-uniformities in the electron distribution (the Fermi-Thomas effect) is smaller still by the same factor. A larger effect is the exchange energy of the antisymmetrical electronic wave functions, which makes a negative contribution of about  $E_c/2Z^{2/3}$ .

In any self-gravitating star there is a radial electric field that transfers the electronic pressure to the ions, so enabling the electron gas to contribute to balance against the gravitational force that acts essentially on the ions. This macroscopic electrostatic energy is therefore comparable with the mean kinetic energy, which in a relativistically degenerate star is greater than the electronic rest mass. However, as emphasized by Salpeter, this does not affect the equation of state, because the spacing of the energy levels is unaltered. The effect of the electric potential gradient is negligible, the macroscopic scale of variation being far larger than the De Broglie wavelength of the electrons; contrary to an erroneous earlier derivation of a large correction to the equation of state.

Once the total energy per electron,  $E$ , is known, the pressure  $P$  (at zero temperature) is given by the thermodynamic relation  $P = -\partial E/\partial(1/n_e)$ . At the extreme relativistic limit, Salpeter's pressure reduces to Chandrasekhar's pressure (1.10) multiplied by a constant less than but close to unity, its precise value depending on  $Z$ . At lower densities, the deviations become more marked; the dominant correcting term, due to the Coulomb energy (1.19), decreases as  $\rho^{4/3}$ , compared with the  $\rho^{5/3}$  decrease of the non-relativistically degenerate electrons. When the lattice spacing becomes comparable with the Fermi-Thomas radius, i.e.,  $r_e Z^{2/3} \simeq 1$ , the scheme of approximation breaks down. For example with  $Z = 26$ , the new formula gives a negative pressure for densities less than about  $2.5 \times 10^2 \text{ gm/cm}^3$ . Thus the formulae cannot be applied to the extreme edges of cold white dwarfs (though this is not a real restriction on observable white dwarfs because of the finite temperature).

Hamada and Salpeter (1961) have used the modified equation of state to construct homogeneous models, analogous to Chandrasekhar's, for different values of  $\mu_e$  and  $Z$ . A value of  $\rho_e$  is assumed, and the outward integrations terminated

at the radius  $R$  for which the pressure vanishes (i.e., the thin outermost regions are neglected, a good approximation for masses above  $0.2 M_{\odot}$ ). As expected, the computed models have smaller radii and higher central densities than the Chandrasekhar models of the same mass. The deviations are quite small at high densities, but are marked for low masses: e.g., with  $\rho_c \simeq 10^5$ , a model consisting of  $\text{Fe}^{56}$  has a mass of  $\simeq M_{\odot}/10$ , about 25 per cent lower than the Chandrasekhar mass  $0.136 M_{\odot}$ . As  $\rho_c$  decreases still farther,  $M$  decreases, but  $R$  reaches a maximum, after which it decreases: for example, with  $\text{Fe}^{56}$  again assumed to be the dominant nuclear species, the maximum occurs near  $\rho_c = 10^4$ , with  $M \simeq 0.02 M_{\odot}$  and  $R \simeq 0.021 R_{\odot}$ . These values are only rough, because the derivation of the pressure by the perturbation method is doubtful at these densities. However, they provide a semi-quantitative illustration of the early remark of Russell (1935) that white dwarfs and planets of given composition must form a linear series depending on the mass, with the radius reaching a maximum and subsequently decreasing as the matter changes from the gaseous to the solid state (see also Ramsey 1950).

### 1.3. RESTRICTIONS ON COMPOSITION IMPOSED BY NUCLEAR PHYSICS

For masses of stellar rather than planetary order, the Salpeter pressure formula does not cause very striking changes in the Chandrasekhar models. Since at high densities  $P/P_0$  is approximately a constant (less than but close to unity), then by (1.16) the new homogeneous models with prescribed  $\mu_e$  and sufficiently large  $\rho_c$  are simply derived by using an effective  $\mu'_e = \mu_e(P/P_0)^{-0.75}$ . More serious are the consequences of nuclear reactions at high densities, which alter  $A$  and  $Z$  and hence also alter  $\mu_e = A/Z$ . For normal nuclei other than hydrogen,  $\mu_e \simeq 2$ ; for hydrogen  $\mu_e = 1$ , so that if one ignores nuclear reactions, the fraction of hydrogen in a homogeneous white dwarf is a parameter that can be varied to assist in fitting observed theoretical radii (e.g., Chandrasekhar 1939). However, we are interested in nuclear species that are stable on astronomical time scales against both beta-decay and also inverse beta-decay—the absorption of electrons from the Fermi sea. If the energy at the Fermi surface,  $E_F = mc^2[(1 + x^2)^{1/2} - 1]$ , exceeds the energy for beta emission by the nucleus,  $(Z - 1, A)$ , then the nucleus  $(Z, A)$  will spontaneously transform into  $(Z - 1, A)$ . Conversely, the  $(Z - 1, A)$  nucleus cannot undergo beta-decay into  $(Z, A)$ , because the energy level into which the emitted electron would have to fall is already occupied by an electron. If, then, we prescribe the dominant nuclear species in a homogeneous model, we arrive at a maximum *finite* central density, with an associated maximum mass, beyond which no homogeneous model can exist; for inverse beta-decay increases  $\mu_e$ , so lowering the number of degenerate electrons per massive particle. The first estimate for the maximum mass was made by Schatzman (1958); more accurate and extensive results were obtained by Hamada and Salpeter (1961) for different chemical compositions assumed present before the nuclear transformations. Thus, with  $\text{C}^{12}$ ,  $\text{Mg}^{24}$ ,  $\text{Si}^{28}$ , and  $\text{Fe}^{56}$

the respective initial nuclei, the maximum masses decrease steadily from  $1.396 M_{\odot}$  to  $1.11 M_{\odot}$ , as compared with the Chandrasekhar limit (1.17), which is  $1.44 M_{\odot}$  for  $\mu_e = 2$ . The corresponding values of  $\rho_c$  are  $\simeq 10^{9.778}$ ,  $10^{9.499}$ ,  $10^{9.290}$ ,  $10^{9.060}$ . Models with higher  $\rho_c$  are necessarily inhomogeneous, with  $\mu_e$  higher in the center, and of correspondingly lower mass: for example, a star which "initially" consists of  $\text{Mg}^{24}$ , and which is imagined to reach equilibrium with a prescribed central density of  $10^{10}$ , must have achieved a central core of  $\text{Ne}^{24}$  through inverse beta-decay, and must have a mass of  $1.205 M_{\odot}$ , as compared with the maximum mass of  $1.363 M_{\odot}$ , and associated central density of  $10^{9.499}$  for a pure  $\text{Mg}^{24}$  star. In fact, a magnesium star of this mass can achieve equilibrium near  $\rho_c = 10^{8.3}$ , below the density at which inverse beta-decay starts, and we may expect that a homogeneous star of mass below the maximum mass (for its composition) will achieve homogeneous equilibrium; but masses above the maximum cannot settle down into a cold equilibrium state.

Inverse beta-decay reduces  $Z$  but leaves  $A$  unaltered. But even at zero temperature, exoenergetic nuclear reactions take place (in astronomically short times) if the density is sufficiently high—"pynconuclear" as opposed to thermonuclear reactions—due to screening of the nuclear Coulomb field by the electrons (Schatzman 1948 and 1958, Zeldovich 1958, Cameron 1959*b*; cf. § 2.3). It is found that  $\text{H}^1$  transmutes into  $\text{He}^4$  at densities  $\simeq 5 \times 10^4$  or  $10^5$ ,  $\text{He}^4$  into  $\text{C}^{12}$  at  $\simeq 8 \times 10^8$ , and  $\text{C}^{12}$  into  $\text{Mg}^{24}$  (followed by beta-decay into  $\text{Ne}^{24}$ ) at  $\simeq 6 \times 10^9$ —all densities lower than those for inverse beta-decay. Since a Chandrasekhar white dwarf of pure hydrogen would have a central density of about  $10^5$  even if its mass is as low as  $0.16 M_{\odot}$ , it follows, quite apart from any restrictions imposed by thermonuclear transformations during the previous history, that no white dwarf of even moderate mass can have hydrogen deep in its interior.

Further integrations by Hamada and Salpeter (1961) impose similar restrictions on the amount of hydrogen that the star may have in an envelope surrounding a hydrogen-free core; for again the density at the interface must be less than the critical value for zero-temperature fusion. The smaller the mass, the larger the fraction that can be put into the model as a hydrogen envelope. A non-homogeneous model with a sharp decrease in  $\mu_e$  at the interface has a radius larger than the homogeneous model with the same fraction of hydrogen, an effect similar to (but weaker than) that of a hydrogen envelope in a red giant model. Thus an iron-core star of mass  $M_{\odot}/3$  can have a hydrogen envelope containing up to one-fifth of the mass, and with a radius up to  $2.28 (R_{\odot}/100)$ , as compared with  $2 (R_{\odot}/100)$  for a homogeneous model with the same fraction of hydrogen, and  $\simeq 1.65 (R_{\odot}/100)$  for the homogeneous model with  $\mu_e = 2$ . The allowed fraction decreases rapidly with mass; beyond  $M = 0.75 M_{\odot}$  the possible increase in the radius is very small. Slightly more favorable numbers are found for a helium-core star: a star with  $M = 0.4 M_{\odot}$  can have  $0.44 M$  as a hydrogen envelope. Models with a discontinuity from iron to helium are hardly

distinguishable in their parameters from homogeneous models, since the change in  $\mu_e$  is much smaller than to a hydrogen layer.

At higher densities electron capture and emission occur sufficiently fast for statistical equilibrium to be set up between nuclei with different  $A$  and  $Z$  values; given the density  $\rho$ ,  $Z$  and  $A$  are determined by optimizing the free energy (Schatzman 1958, Salpeter 1960, 1961). Beyond  $\rho \simeq 3.4 \times 10^{11}$  there begins a rapid production of free neutrons, and when  $\rho \simeq 10^{13}$  is reached it is the partial pressure of the imperfect, degenerate neutron gas that dominates (Cameron 1959*a*). Study of matter at such high densities, and in particular of neutron stars, belongs rather to the theory of supernovae and quasi-stellar radio sources than to white dwarf theory, especially since general relativistic effects lead to dynamical instability when  $\rho_e \simeq 2.3 \times 10^{10}$  (Chandrasekhar and Tooper 1964).

#### 1.4. COMPARISON WITH OBSERVATION

We may anticipate here (cf. § 2.3) that the final restrictions on the extent of a hydrogen outer zone in a radiating white dwarf are much more severe than those found at zero temperature, so that it is entirely reasonable to put  $\mu_e = 2$  in the mass-radius relation (bearing in mind the possibility of inhomogeneous structures, with  $\mu_e > 2$  in superdense central regions of stars close to the limit [§ 1.3]). It is unfortunate that there are available only three white dwarfs with masses well determined from their motions as components of binary systems: 40 Eridani B, of mass  $0.43 M_\odot$  (Popper 1954), and Sirius B and Procyon B, respectively  $0.98 M_\odot$  and  $0.65 M_\odot$  (van de Kamp 1954). Radii are normally estimated from observed parallaxes, magnitudes, and surface temperatures. The Einstein shift, due to the loss of energy of a photon in escaping from the enormous gravitational field, in principle yields a value for  $M/R$ ; expressed as a velocity, the shift is

$$c \frac{\Delta\nu}{\nu} = \frac{GM}{cR} = 0.635 \frac{M/M_\odot}{R/R_\odot} \text{ km/sec.} \quad (1.21)$$

For Sirius B, both methods were originally claimed to yield nearly the same value of  $1.36 \times 10^9 = 1.95 \times 10^{-2} R_\odot$  for the radius, and the closeness of the agreement was hailed as a triumph for general relativity. But this radius exceeds the theoretical value for a hydrogen-free star by a factor 2: a hydrogen content of about fifty per cent would be required for agreement. Attempts to iron out the discrepancy by building a model with a hydrogen envelope (Schatzman 1945, Lee 1950, Mestel 1952*a*) fail because of excess nuclear energy generation. Nor would the return of the Fowler pressure formula (1.4), as urged by Eddington (1947) (also in Shaler 1941), remove the difficulty, as the Fowler radius is still only about seven-tenths of the observed value.

A report has appeared (Gamow and Critchfield 1949) that the radius of Sirius B does in fact conform to the Chandrasekhar formula with  $\mu_e = 2$ . This must be treated with reserve until new red-shift measurements have been made

when Sirius A and B are at their greatest separation to minimize blending of the light of the bright component with that of the white dwarf. This is now being attempted by Oke and Greenstein. The possibility that Sirius B is in fact a close double white dwarf with a correspondingly smaller red-shift cannot be completely ruled out (Greenstein 1963).

Popper (1954) has found the Einstein shift in 40 Eridani B to be 21 km/sec, as compared with Greenstein's prediction (1958) of 16 km/sec from the known mass and the radius inferred from the effective temperature.<sup>1</sup> Both values satisfy the theoretical relation for a small (but not vanishing) hydrogen content. For the very faint white dwarf van Maanen 2, Kuiper derived an effective temperature of 8200°, yielding  $R/R_\odot = 10^{-2.05}$ . A high positive velocity of 238 km/sec has been measured; with all of it assumed to be Einstein shift, a mass of  $3.38 M_\odot$  was deduced, requiring about 66 per cent of hydrogen (Chandrasekhar 1939). However, these figures have been drastically revised. Greenstein (1958) and Weidemann (1960), respectively, estimate temperatures of 5140° and 5800°, corresponding to radii of  $10^{-1.77} R_\odot$  and  $10^{-1.88} R_\odot$ . The velocity found by Greenstein (1954) is only about 70 km/sec; but since the spatial velocity of the star is unknown, so is the Einstein shift, and no reliable mass estimate can be made.

Greenstein (1958) includes van Maanen 2 and 40 Eridani B in the twenty-seven stars he uses to compute an average of  $-1.88$  for  $\log R/R_\odot$ . Assuming  $\mu_e = 2$ , he derives from the theoretical  $M$ - $R$  relation an average mass of  $0.56 M_\odot$ , with averages for mean and central densities of  $3.5 \times 10^5$  and  $2.6 \times 10^6$  gm/cm<sup>3</sup>, respectively.<sup>2</sup>

An outstanding feature of the theory of relativistic degeneracy is the rapid decrease in radius as the mass approaches the limiting mass appropriate to its composition. Chandrasekhar (1939) has remarked that the discovery of stars that are exceptionally dense even by white dwarf standards, even if we have no independent knowledge of their masses, would be powerful support for the theory of relativistic degeneracy against the claim of Eddington (1947) that the Fowler pressure (1.4) is valid up to the highest densities. Chandrasekhar quoted as evidence the star AC 70°8247, which was originally estimated (Kuiper 1935) to have  $R = 10^{-2.38} R_\odot$ . With  $\mu_e = 2$ , the Fowler mass formula (1.7) would yield  $28 M_\odot$ , as compared with about  $0.95 M_\odot$  for the limiting mass on the Chandrasekhar theory. This is certainly remarkably large, if not quite the

<sup>1</sup> There is now a suggestion (Greenstein 1963) that A-type white dwarfs are hotter than was thought: the revised effective temperature may remove this discrepancy.

<sup>2</sup> Weidemann (1963) has attempted a new check on the  $M$ - $R$  relation. He shows that the varieties of  $H\gamma$  line profiles observed by Greenstein can be explained by variations in effective temperature and surface gravity  $g$ , from star to star. Thus, from the absolute magnitude, effective temperature, and the observed line profiles, without making any assumptions about internal structure,  $R$ ,  $g$ , and so also  $M$ , can be estimated. The scatter in the  $M$ - $R$  diagram is quite large, due primarily to uncertainties in the luminosities. However, the results do not contradict the assumption that  $\mu_e = 2$ .

*reductio ad absurdum* of Eddington's contention. However, it now appears that Kuiper's temperature of  $28,000^\circ \text{K}$  was too high: Greenstein's estimate (1958) is  $11,500^\circ \text{K}$ , with nearly the same absolute magnitude, and the revised radius is that of a "normal" white dwarf ( $10^{-1.93} R_\odot$ ). Two other stars that were originally reported to have exceptionally small radii (Shaler 1941) appear in Greenstein's table as rather larger: Ross 627, from  $10^{-2.62} R_\odot$  to values that lie between  $10^{-2.01} R_\odot$  and  $10^{-2.25} R_\odot$ ; and Wolf 219, from  $10^{-2.5} R_\odot$  to  $10^{-2.19} R_\odot$ . Wolf 219 is the smallest star in Greenstein's list, with a radius of about seven-tenths of the earth's; for this, the Fowler formula predicts about  $7.5 M_\odot$ .

The discovery by Luyten (1963*a*) of a white dwarf with  $R/R_\odot$  less than  $10^{-2.94}$ , if confirmed, could be claimed as a dramatic vindication of the theory, for the Fowler-Eddington mass would need to be about  $10^3 M_\odot$  as against a value near the appropriate limit on the relativistic theory. (The inevitable increase in  $\mu_e$  at such enormous densities [§ 1.3] would reduce this estimate somewhat, but it would still be very large.) However, with some theorists now speculating—admittedly with the relativistically degenerate formulae assumed valid—on the collapse of super-massive "stars" and the possible link with radio sources, the mere prediction of large masses by the Fowler-Eddington theory will not be universally accepted as a *reductio ad absurdum*. We still await discovery of a super-dense white dwarf for which at least two of the three measurements—of effective temperature, Einstein shift, or of the orbital motion of a binary member—are good enough to yield reliable  $M$  and  $R$  estimates. It is certain that many more white dwarfs are waiting to be discovered—Luyten (1963*a*) estimates that the Palomar survey will yield a few thousand—so that we may hope that such a case will arise. (For a review of the present observational position, see Luyten [1963*b*].)

### 1.5. NON-SPHERICAL STARS

Theorists will await with interest new estimates for the radii of Sirius B and Procyon B. One would like to know definitely whether or not radii estimated from color, line profiles, and Einstein shift agree within the limits of observational error, and how they compare with the theoretically predicted radii of spherical, hydrogen-free stars. We have already noted the apparently genuine (though slight) discrepancies between the theoretical radius of 40 Eridani B (assuming  $\mu_e = 2$ ) and both Popper's (1954) and Greenstein's (1958) observations. It is satisfactory that the discrepancies all seem to demand radii larger than the theoretical values. But in view of the serious energetic difficulties (§ 1.3 and § 2.3) consequent on assuming any but the slightest hydrogen content, it is far more plausible to retain  $\mu_e = 2$  (except for very dense stars) and to explain persisting discrepancies as due to forces other than pressure, such as centrifugal and magnetic force. Once such an essentially non-spherical model has been constructed, one must relate observations of its integrated color and Einstein shift to the variation of surface flux with effective gravity (cf. eq. 2.3), limb darken-

ing and variation of the gravitational potential over the surface, as well as the orientation of the axis of symmetry to the line of sight: it need not then be surprising if the "radius" given by  $[L/(\pi acT_e^4)]^{1/2}$  differs from the "radius" appearing in the Einstein shift formula (1.21).

Some work has been done on slowly rotating, nearly spherical white dwarfs, in which the centrifugal force is treated as a small perturbation (Chandrasekhar, in Shaler 1941, Bandyopadhyay 1952, Kaminski 1953, Kazuo Suda 1953, Krishan and Kushwaha 1963). For the other extreme of very rapid rotation, Hoyle (1947*a*) has discussed the state of disk-like equilibrium, in which gravity is balanced by centrifugal force in two dimensions and by the degenerate pressure in the third dimension. (Chandrasekhar's limit does not apply to such non-spherical structures: since a self-gravitating, rotating cloud of isothermal classical gas [ $P \propto \rho$ ] can reach equilibrium as a disk [Spitzer 1942, Ledoux 1951] whatever its mass, it is not surprising that this is also possible for a body of degenerate gas with its stronger  $P$ - $\rho$  law.) However, such a highly flattened model is certainly quite unrealistic as a description of a single body: gravitational instabilities, analogous to those occurring in the isothermal classical disk, would almost certainly cause it to break up into degenerate subcondensations, each of mass below the limit, in mutual orbital motion. Moreover, there is the strong probability that during the contraction into the flattened state the star would become rotationally unstable, shedding mass at its equator until it loses enough mass and angular momentum to achieve stable equilibrium as a rapidly rotating fairly oblate star of mass below Chandrasekhar's limit. It is this type of model that may be relevant to observed white dwarfs.

However, current ideas on formation of white dwarfs (§ 3.1) do not unambiguously support the suggestion that the star has a centrifugal field comparable with gravity. Main-sequence stars of mass below the Chandrasekhar limit have low rotations: e.g., a contraction of the sun by a factor of one hundred to white dwarf dimensions would yield a centrifugal force at the surface no higher than about two per cent of gravity. One would not, therefore, expect a white dwarf forming from a main-sequence star of similar mass to rotate very rapidly. More massive main-sequence stars do rotate rapidly, and it is possible that a white dwarf born as the burnt-out, degenerate core of such a star may possess a high centrifugal field. But if the parent star has just a moderate general magnetic field, the contracting core will systematically lose angular momentum to the expanding envelope (cf., e.g., chap. 9, this volume) so that the centrifugal force in the ultimate white dwarf will again be negligible.

An alternative possibility, not yet explored, is that a white dwarf may possess a large internal magnetic energy, which can have dilatory effects within the bulk of the star, without the likelihood of surface instabilities. No exceptional postulates need be made to achieve this. For example, suppose that the parent main-sequence star has a magnetic energy as low as one per cent of its gravita-

tional energy, so that the field exerts negligible forces over the bulk of the star. Now suppose that at the end of the star's evolution away from the main sequence the central fifth of the mass condenses into a white dwarf, retaining its magnetic flux; the resultant ratio of magnetic to gravitational energy in the white dwarf would be about one quarter, and so could yield a model observationally distinguishable from a spherically symmetric model. It is easy to confirm that in spite of the much reduced length-scale in a white dwarf, the Cowling decay-time,  $\tau$ , of a dipole-type component is longer than the galactic age. The electrical conductivity,  $\sigma$ , of degenerate matter is related to the thermal conductivity,  $\nu$  (cf. eq. 2.8) by the Wiedemann-Franz law (Seitz 1940):

$$\sigma \simeq \left(\frac{e}{k}\right)^2 \frac{\nu}{T} \simeq 10^{16} \rho \quad (1.22)$$

in the degenerate bulk of the star; thus,

$$\tau = 4\pi \frac{\sigma}{c^2} R^2 \simeq 10^{-4} \rho R^2 = 2 \times 10^{10} \frac{M/M_{\odot}}{R/R_{\odot}} \text{ yrs}, \quad (1.23)$$

which is longer than the  $10^{10}$  years found for main-sequence stars.

## § 2. WHITE DWARFS OF FINITE TEMPERATURE

### 2.1. THE INTERNAL TEMPERATURE

Any observable white dwarf must have a finite internal temperature  $T$ . An extreme upper limit is found from the condition that the degenerate electron pressure be a good zero-order approximation. In the non-relativistic limit, the mean electron energy (114) reduces to

$$3(m_e c x)^2 / 10 m_e = (3/10)(3/8\pi)^{2/3} \times (\rho / \mu_e m_H)^{2/3} h^2 / m_e$$

by (1.10) and (1.15). Degeneracy has set in when this exceeds  $\frac{3}{2} kT$ , the energy per electron of a classical gas, i.e., when

$$\frac{10^8 \rho}{T^{3/2}} \gg 10^8 \mu_e m_H \left(\frac{5k m_e}{h^2}\right)^{3/2} \left(\frac{8\pi}{3}\right) \simeq 1. \quad (2.1)$$

With a mean density of  $10^5 \text{ gm/cm}^3$ , degeneracy would be incipient at  $T = 4 \times 10^8 \text{ }^\circ \text{K}$ .

In fact, the temperature in a faint white dwarf must be much lower than this, otherwise the luminosity would be of main-sequence order or higher. Given the observed low luminosity, it can be shown that degeneracy sets in at densities much lower than the mean (Strömgren 1936). As an example, we adopt Kramers' opacity law  $\kappa = \kappa_0 \rho T^{-7/2}$ ; then the equations to a non-degenerate envelope of negligible self-gravitation yield (e.g., Chandrasekhar 1939)

$$T = \frac{4}{17} \frac{\mu}{\Re} \frac{GM}{R} \left(\frac{1}{\xi} - 1\right), \quad (2.2)$$

$$\rho = \left(\frac{64\pi}{51} \frac{a c \mu}{\kappa_0 \Re} \frac{GM}{L}\right)^{1/2} T^{13/4} = a T^{13/4}, \quad (2.3)$$



say, where  $M$ ,  $R$ , and  $L$  are the mass, radius, and luminosity,  $\xi$  the radial distance in units of  $R$ , and  $\mu$  the mean molecular weight. Insertion of numerical values shows that with  $M/L \simeq 300$  (as for Sirius B),  $10^3 \rho / T^{3/2}$  reaches unity at a depth equal to a few per cent of the radius, with  $\rho$  and  $T$  respectively about  $1700 \text{ gm/cm}^3$  and  $1.7 \times 10^7 \text{ }^\circ \text{K}$ , and with the non-degenerate envelope containing only about  $\frac{1}{4}$  per cent of the mass. The larger the ratio  $M/L$ , the closer is the star to the zero-temperature state.

To get a more precise estimate of the thermal state of the bulk of a white dwarf, we need to study more carefully both the equation of state in the range of incipient degeneracy, and the transport of energy through the star. At finite temperature, the equation of state for a non-relativistic Fermi gas of free electrons is given implicitly (e.g., Mestel 1950) by

$$\frac{P_e h^3}{8\pi kT (2m_e kT)^{3/2}} = F(\lambda) = \int_0^\infty x^2 \log(1 + \lambda e^{-x^2}) dx, \quad (2.4)$$

and

$$\frac{n_e h^3}{8\pi (2m_e kT)^{3/2}} = G(\lambda) = \int_0^\infty \frac{x^2 dx}{1 + e^{x^2}/\lambda}. \quad (2.5)$$

When  $\lambda \ll 1$ , both  $F(\lambda)$  and  $G(\lambda)$  reduce to  $(\sqrt{(\pi)/4})\lambda$ , and  $P_e = n_e kT$ ; as estimated earlier, the criterion for non-degeneracy is  $10^3 \rho / \mu_e T^{3/2} \ll 1$ . For  $\lambda \gg 1$ , the integrals can be evaluated, yielding  $K(\rho/\mu_e)^{5/3}$  for the dominant term in the  $P$ - $\rho$  relation as in (1.4). The energy density of a strongly degenerate, non-relativistic, electron gas has as the largest correcting temperature-dependent term

$$4\pi^2 \left(\frac{\pi}{3}\right)^{2/3} \frac{m_e (kT)^2 n_e}{h^2 n_e^{2/3}} \quad (2.6)$$

(yielding a specific heat proportional to  $T$ ). The ratio of (2.6) to the energy  $(3/2)n_e kT$  of the non-degenerate ions is

$$(n_e/n_i)(8\pi^2/3)(\pi/3)^{2/3}(m_e/h^2)(kT/n_e^{2/3}),$$

which is just  $2\pi^2 Z/15$  times the ratio of the thermal energy  $(3/2)n_e kT$  of a non-degenerate electron gas to the exclusion energy of a degenerate electron gas. Thus, even for large  $Z$ , over the bulk of the star the ions make the larger thermal correction to the zero-temperature equation of state.

Over the bulk of the star, effectively all the electrons are free through "pressure-ionization" (cf. § 1.2). In the extreme outer layers, the ordinary Saha equation is adequate for a computation of  $n_e$ , but as  $\rho/T^{3/2}$  increases inward there is initially some recombination of electrons and stripped heavy ions, but at higher densities pressure ionization forces all the bound states into the continuum. For pure Russell mixture, Lee (1950) estimates that  $\mu_e$  in the zone of incipient degeneracy can become as much as four times its value at high densities.

We have seen that the opacity of the non-degenerate envelope is high enough

for a temperature of about  $10^7$  ° K to be reached very quickly. It is important to know whether the temperature increase remains rapid, in order to verify that the zero-temperature star is a good approximation. It was early recognized (Chandrasekhar 1931, Majumdar 1931, 1932, Swirles 1931) that the opacity of degenerate matter would be less than the extrapolated non-degenerate opacity, for the rate of photo-electric absorption of a photon  $h\nu$  by an electron of energy  $\epsilon$  would need to be multiplied by the probability  $1/[1 + \lambda \exp - (h\nu + \epsilon)/kT]$  that the state  $\epsilon + h\nu$  is empty. Marshak (1940a) gives as a good approximation to the opacity over the whole range of  $\lambda$ ,

$$\kappa = \frac{6 \times 10^{17} X}{T^2} \log \left( \frac{1 + \lambda}{1 + \lambda e^{-t}} \right) \frac{1}{t}, \quad (2.7)$$

where  $t$  is the guillotine factor, and  $X$  is the proportion by mass of the absorbing matter (in this case, Russell mixture; for pure hydrogen there is a similar expression). When  $\lambda \ll 1$ , (2.7) reduces to the usual Kramers law; when  $\lambda \gg 1$ ,  $\kappa \propto 1/T^2 t$ . Accurate values of  $t$  are not required for large  $\lambda$ , because over the bulk of the star thermal conduction is by far the dominant mechanism of energy transport (Kothari 1932a, b, Marshak 1940a, Lee 1950, Mestel 1950, Schatzman 1958): the high mean velocity of the degenerate electrons cuts down the rate of Coulomb scattering by the ionic lattice. An adequate approximation for the thermal conductivity  $\nu$  under strong degeneracy is

$$\nu = \frac{1.88 \times 10^3 \rho T}{Z^2 A \Theta}, \quad (2.8)$$

where  $\Theta$  is an integral of order unity, involving the angle at which electron screening of the nucleus cuts off the small angle contributions to the Coulomb scattering.

Several authors have used the previously summarized physical properties to estimate the internal temperatures of white dwarfs; however, their assumptions about the composition of the outermost layers and the sources of the radiated energy have been different (Marshak 1940b, Lee 1950, Schatzman 1952, Mestel 1952a, Schwarzschild 1958). All agree that once the region of incipient degeneracy is reached the temperature gradient decreases sharply through the drop in opacity and increase in conductivity: the degenerate bulk of the star is nearly isothermal, at about  $10^7$  ° K for observable white dwarfs. It is this sharp decline in the temperature gradient that makes the zero-temperature star such a good approximation. Even the reduction (1.19) in the zero-temperature electronic energy, associated with the lattice structure of the ions, does not disappear over the bulk of a dense white dwarf; for the mean ionic thermal energy  $\frac{3}{2}kT$ , though greater than the zero-point energy (1.20), is lower than  $|E_c|$  by the factor  $0.7/Z^{2/3}x$ , which is less than unity over the bulk of a star with  $Z \gg 1$ .

A simple, standard relation between the internal temperature  $T_c$  and  $L$  is given by assuming radiative equilibrium up to the point of incipient degeneracy

and isothermality due to conduction farther in. Assuming, as in (2.2) and (2.3), a simple Kramers opacity due to heavy elements, we find (Mestel 1952*a*; Schwarzschild 1958)

$$T_c = 5 \times 10^7 \left( \frac{L}{M} \right)^{2/7}, \quad (2.9)$$

or

$$\frac{L}{M} = 3.6 \times 10^{-3} \left( \frac{T_c}{10^7} \right)^{7/2} = k T_c^{7/2}, \quad (2.10)$$

say. This procedure slightly exaggerates the internal temperature as found by accurate integrations through the transition layer.

Schatzman (1952) has studied in detail models with an outer layer of pure hydrogen. He finds somewhat lower temperatures, summarized approximately by the formulae

$$T_c = 2.9 \times 10^7 \left( \frac{L}{M} \right)^{0.349}, \quad (2.11)$$

$$\frac{L}{M} = 4.7 \times 10^{-2} \left( \frac{T_c}{10^7} \right)^{2.87}. \quad (2.12)$$

However, from stability considerations (cf. § 2.3) these models are unlikely to be realistic, and we shall use only relations (2.9) and (2.10).

Given the internal temperature, we may estimate as the next approximation the deviation of the star from the black dwarf density distribution and the associated increase in radius. Marshak (1940*b*) made such an estimate, but assumed the thermal part (2.6) of the electronic energy rather than the ionic energy to be the dominant perturbation. New integrations are required, not for any direct observational check, but for more accurate age estimates (§ 2.2).

To sum up, a radiating white dwarf has the bulk of its mass as a highly degenerate, nearly isothermal, hot core. It is surrounded by an opaque envelope which acts as a blanket, keeping down the luminosity. The black dwarf density distribution is an excellent zero-order approximation.

## 2.2. A WHITE DWARF AS A COOLING BODY

Relation (2.9) is derived for a white dwarf of prescribed mass and radius by integrating the envelope equations inward, assuming a definite luminosity. In estimating the temperature at the point of onset of degeneracy, required to drive out the observed flux against the envelope opacity, we simultaneously assert that the isothermal core must have a definite high thermal energy, mainly ionic kinetic energy. In a more physical sense, we can reverse the statement: given a core temperature  $T_c$ , and assuming that the sources of radiated energy lie in the core, we may determine the luminosity, as an eigen-parameter of the equations to the envelope, by the requirement that  $T$  and  $\rho$  vanish together (an adequate approximation to the physical boundary conditions, by which  $T \rightarrow T_c$  and  $\rho$  approaches the appropriate photospheric value). If the opacity of the surface

layers were lower, the flux from the hot core to the photosphere would be greater, and the surface would heat up until the enhanced surface loss balanced the flux from the core.

Since Eddington's work, it is a commonplace that a non-degenerate star radiates energy because it cannot help doing so: the internal temperature must be high in order to maintain hydrostatic equilibrium, and the consequent slow radiative energy leak to the surface determines at least lower limits to the luminosity and effective temperature at the given radius (any convective transport will augment the flux). Provided  $\gamma > \frac{4}{3}$  (necessary if the star is to be dynamically stable), contraction following energy loss releases more than enough gravitational energy to compensate for the loss and the star heats up to the new temperature required by the virial theorem. Alternatively, if we prescribe a star of known mass to have a definite amount of thermal energy, we can estimate its radius from the condition of hydrostatic equilibrium and its luminosity from the opacity of its material. But as long as the gas is non-degenerate, there is no way by which a spherical star with exhausted nuclear sources can cut off the continuous transformation of gravitational energy into radiated energy and internal heat.

The white dwarf case is similar in one respect: if we prescribe the core temperature, then, as discussed in § 2.1, we can estimate the luminosity and also the excess of the radius over that of a cold body. A hot white dwarf radiates because it is not in thermodynamic equilibrium with the rest of the universe (the presence or absence of nuclear energy sources [to be discussed below] is again not relevant to the issue). But it is clear, merely from the existence of zero-temperature equilibria for stars below the appropriate limiting mass, that for such stars there is a limit to the amount of gravitational energy convertible into radiation. High thermal energy is not now a necessary condition for hydrostatic equilibrium—it is in fact a small addition to the Fermi energy that balances most of the gravitational energy even at temperatures of  $10^7$ ° K or higher. A perturbation analysis will yield the change in the core density field due to the finite temperature. If the star has no nuclear sources, its thermal energy will decline as it radiates. The slight reduction in the total pressure will cause a slight over-all contraction, with some release of gravitational energy, partly to be transformed into extra exclusion energy, the rest to supply part of the energy radiated. But the amount of gravitational less exclusion energy available is strictly limited to the difference between that of the finite-temperature and zero-temperature models; its release merely slows up the rate of cooling. As a dynamically stable non-degenerate star loses energy it heats up; as a degenerate star of low enough mass loses energy, it cools down.

We now suppose that the star, in fact, has no nuclear energy sources, and estimate its age as a cooling body. When its internal temperature is  $T$ , the thermal energy is  $\frac{3}{2} \mathfrak{R}MT/A$ , where again  $A$  is the mean atomic weight of the heavy particles, the thermal contribution of the electrons being small. A lower

limit to the cooling time is given by ignoring the release of gravitational energy: by (2.9), the equation of cooling is then (Kaplan 1950, Mestel 1952a)

$$-\frac{d}{dt}\left(\frac{3}{2}\frac{\mathfrak{R}MT}{A}\right) = L = kMT^{7/2}. \quad (2.13)$$

The time for the star to reach present-day temperature  $T$  and luminosity  $L$ , from earlier values  $T'$  and  $L'$ , is then

$$0.6 \frac{\mathfrak{R}M}{A} \left(\frac{T}{L} - \frac{T'}{L'}\right) \approx 0.6 \frac{\mathfrak{R}M}{A} \frac{T}{L} \quad (2.14)$$

if  $T'/T$  differs even only slightly from unity. The picture of a white dwarf implied by (2.13) is valid only when the non-degenerate, radiative envelope is a small fraction of the total mass; but it is easy to verify that the time the star spends as a partially degenerate, very hot body is only a fraction of its lifetime as a cool body (Mestel 1952a).

For Sirius B and 40 Eridani B, the known masses and the  $T$ - $L$  relation (2.9) yield  $1.5 \times 10^9/A$  and  $10^9/A$  as lower limits to their ages (the improved opacity used by Schwarzschild [1958] reduces by a factor 2 the estimates in Mestel [1952a]). With theoretically estimated masses for other white dwarfs, one finds ages that range from  $5 \times 10^7/A$  for Wolf 1346 to  $5 \times 10^{10}/A$  for van Maanen 2, Wolf 457, and Wolf 489. Fortunately the theory predicts white dwarfs of all ages up to the galactic age, for the processes giving birth to white dwarfs (cf. § 3.1) should have been continuous since star formation began. It is reasonable that Population I stars of low velocity have few of the faintest white dwarfs among them—they are just not old enough (Greenstein 1958). It is also significant that for the oldest white dwarfs observed so far, it is barely sufficient to have  $A = 4$  (pure helium) in order that the ages should not exceed that of the oldest galactic clusters studied: discovery of even fainter stars may provide definite support for the view that synthesis of heavy elements necessarily occurs in the cores of stars that are evolving toward the pre-white dwarf state.

Since the zero-temperature, black dwarf state is one of equilibrium between gravitational force and degenerate pressure, the algebraic sum of the gravitational and exclusion energies in the slightly perturbed state with a finite temperature is greater than that for the black dwarf state by terms of only second order in the ratio of thermal to gravitational energy. Thus more accurate estimates of the ages are unlikely to increase 2.14 by more than a small fraction.

The radius of a cooling white dwarf changes so little that its path in the theorists' Hertzsprung-Russell diagram is given by

$$\text{Magnitude} = -10 \log T_e + C, \quad (2.15)$$

the constant  $C$  depending on mass and composition. There is clearly no question of arranging the stars in a regular sequence which would depend on mass and

composition, as with normal stars in thermal equilibrium: the position of a given star depends on its internal temperature and hence on its age, but is not correlated with significant changes of composition and structure. The greater the mass, the farther to the left in the diagram is the cooling path; hence, there is no reason for surprise at the irregular spread of the white dwarfs in their corner of the HR diagram.

### 2.3. NUCLEAR ENERGY GENERATION AND STABILITY

We have seen that a satisfactory picture of a white dwarf is that of a slowly cooling body, supplying its luminosity from its thermal energy and the associated difference between its gravitational and exclusion energies at finite temperature and absolute zero, respectively. However, actual white dwarfs probably result at the end of a line of stellar evolution that is not yet fully explored (see § 3.1), and we cannot be certain (from the discussion so far) that a white dwarf will not be born with some nuclear sources in its outer layers. There is also the possibility (§ 3.2) of a source-free star's acquiring surface hydrogen, in quantities greater than the slight amount required to account, e.g., for the presence of hydrogen lines in the spectrum of Sirius B. The simplest procedure is to suppose that nuclear sources are present and to discuss the possibility of thermal equilibrium and the associated stability questions.

Suppose, then, that a white dwarf does contain nuclear sources which liberate energy at a rate that depends on the density and temperature. If the total rate of energy liberation  $\epsilon$  is less than the luminosity (see eq. [2.10]) at the given temperature, then the star continues to cool in the long time scale (2.14). Further, if  $\epsilon$  decreases with temperature more rapidly than  $L$ , the disparity between  $\epsilon$  and  $L$  increase with time—the nuclear energy liberation is just a small perturbation on the cooling process. This is in striking contrast to the behavior of a non-degenerate (dynamically stable) star, for which loss of energy implies contraction and *heating*, so that energy sources more temperature-sensitive than the luminosity restore thermal equilibrium. On the other hand, if  $\epsilon$  decreases with  $T$  less rapidly than  $L$ , then there is available a state of thermal equilibrium that the star will reach after it has cooled sufficiently.

Now suppose that the energy generation  $\epsilon$  exceeds  $L$  so that the star heats up, the high conductivity insuring isothermality over the degenerate bulk. If  $\epsilon$  is less temperature-sensitive than  $L$ , there again exists a state of thermal equilibrium. Provided the strength of the nuclear sources is not too great, this state, though having a higher internal temperature and luminosity, will still be recognizably a white dwarf state, with the bulk of the star degenerate. Provided no other instabilities intervene (see below), the star would subsequently evolve slowly in thermal equilibrium, the temperature decreasing just at the rate to offset the consumption of nuclear sources. But if  $\epsilon$  increases more rapidly than  $L$ , then thermal equilibrium cannot be reached in the white dwarf state. Further, even if  $\epsilon$  and  $L$  happen to balance initially, the equilibrium will be secularly

unstable. A slight increase in temperature will start an *accelerating* energy gain, while a slight decrease will force the star into the cooling state: with  $\epsilon$  more temperature-sensitive than  $L$ , the star in thermal equilibrium is on a “razor’s edge” (Lee 1950, Mestel 1952a).

The argument as stated does depend on the simple model of a white dwarf, with an isothermal degenerate core surrounded by a thin radiative envelope and with the active nuclear sources within the core, so that the core temperature is also that of the energy source. Then the condition for secular instability is that  $\epsilon$  should depend on temperature more strongly than the index  $\frac{7}{2}$  of (2.10) or 2.87 of the hydrogen-layer models (2.12). However, if the star gains energy and heats up, the point of incipient degeneracy moves in, and ultimately all the surface hydrogen will be in the non-degenerate, radiative envelope. The  $\rho$ - $T$  relation for the envelope will still be approximately  $\rho = \alpha T^{13/4}$ , with  $\alpha \propto L^{-1/2}$ , as in (2.3), but  $\alpha$  can now be related to the temperature  $\bar{T}$  of the hottest hydrogen by use of the condition that the mass of the hydrogen is prescribed:

$$\int \rho r^2 dr \propto \int_0^{\bar{T}} \alpha T^{13/4} dT \propto \alpha \bar{T}^{17/4} = \text{constant}. \quad (2.16)$$

Thus,

$$L \propto \bar{T}^{17/2} \quad (2.17)$$

replaces (2.10); however,  $\bar{T}$  is now not the temperature of the isothermal core, but the temperature at a prescribed mass shell in the envelope. If the energy generation per unit mass is proportional to  $\rho^\mu T^\nu$ , the total energy generation is approximately proportional to

$$\int_0^{\bar{T}} \rho^{\mu+1} T^\nu dT \propto \alpha^{(\mu+1)} \bar{T}^{[13/4(\mu+1)+\nu+1]} \propto \bar{T}^{(\nu-\mu)} \quad (2.18)$$

by equation (2.16). Thus the condition for secular instability is now  $\nu > \mu + \frac{17}{2}$ , which is more stringent than that found earlier, but still valid for a highly sensitive reaction such as the Bethe cycle.

The Chandrasekhar white dwarf models (with a prescribed  $\mu_e$ ) are necessarily dynamically stable (Sauvenier-Goffin 1950): the period of small oscillations is always real and very short—of the order of a minute. (In fact, instability sets in for masses of high density just below the Chandrasekhar limit, because of the variation of  $\mu_e$  with  $\rho$  at high densities [Schatzman 1958], and through general relativistic departures from Newtonian gravitation [Chandrasekhar and Tooper 1964].) However, just as for non-degenerate stars, it is possible that the fluctuations in energy generation and energy transport over an oscillatory cycle will feed energy into the oscillations, so that the star becomes vibrationally unstable. Ledoux and Sauvenier-Goffin (1950) have shown that the amplitude of the fundamental mode stays nearly constant throughout the star, similar to the case of a convective non-degenerate star, and in contrast to, e.g., a Cowling-type star, for which the amplitude is much larger in the outer than in the inner regions (e.g., Ledoux and Walraven 1958). The restrictions imposed by the re-

quirement of vibrational stability on the density and temperature exponents in the energy-generation law are consequently found to be very severe, whether the nuclear sources are located in the radiative envelope or the degenerate core.

Before models in thermal equilibrium can be constructed and their stability studied, it is important to estimate carefully nuclear reaction rates under high-density conditions. We have already noted (§ 1.3) that even at zero temperature certain nuclear reactions occur fairly rapidly inside white dwarfs. This is a consequence (Schatzman 1948, 1958, Cameron 1959*b*) of using, for the mutual Coulomb energy of two interacting nuclei of charges  $Z_1e$  and  $Z_2e$ , the expression

$$U(r) = \frac{Z_1 Z_2 e^2}{r} \left( 1 - \frac{3}{2} \frac{r}{R} + \frac{1}{2} \frac{r^3}{R^3} \right), \quad (2.19)$$

where, if  $Z_2 > Z_1$ ,  $R$  is the radius of the spherical volume containing  $Z_2$  electrons. The first term in (2.19) is the ordinary unshielded Coulomb potential; the second represents the shielding effect of a uniform sea of electrons (see § 1.2); and the third represents the effect of the other nuclei which neutralize the total charge. It is this modified potential that must be used in estimating the probability  $P$  that a bombarding particle of kinetic energy  $E$  will penetrate the potential barrier:

$$P = \exp \left[ -2 \left( \frac{2\bar{m}}{\hbar^2} \right)^{1/2} \int_{R_n}^{R_c} [U(r) - E]^{1/2} dr \right], \quad (2.20)$$

where  $\bar{m}$  is the reduced mass of the bombarding particle,  $R_n$  is the nuclear radius, and  $R_c$  the radius at which the integrand in (2.20) vanishes (the classical turning point of the bombarding nucleus). The particle then behaves approximately as if it were incident on an ordinary Coulomb barrier with the elevated energy  $E^* = E + (3Z_1 Z_2 e^2 / 2R)$ . The zero-temperature reaction rate is given by putting  $E = 0$ : at high densities  $R$  is so small that the rate is not negligible ("pycnonuclear reactions"). At finite temperature most of the particles have an energy close to  $\frac{3}{2}kT$ ; if  $T$  is low enough this will be small compared with  $E^*$ , so that the integrated penetration rate will depend primarily on the density (through  $R$ ) and only weakly on  $T$ . At higher temperatures the small number of particles with energy much higher than the mean begin to make comparatively large contributions to the penetration rate. The total number of reactions per second is an integrated product of the penetration probability, which increases sharply with energy, and the number of nuclei of given energy, which in the Maxwellian tail decreases sharply with energy: there results a well-defined energy for which most of the reactions occur, and the familiar strong temperature-sensitivity.

For detailed application of these principles to the proton-proton reactions, the Bethe cycle, and the helium cycles under white dwarf conditions, the reader is referred to Schatzman (1958). The general conclusion is that it is very difficult, if not impossible, to construct a stable white dwarf model in thermal equi-



librium that is also plausible on evolutionary grounds. It is always possible to adjust the hydrogen or helium content in the *core* to the low values required for thermal balance. Thus, even if one ignores the increased rate at high densities, the fraction by mass of hydrogen in the core must be less than  $5 \times 10^{-4}$ , yet it has enough available energy to maintain the luminosity for  $10^9$  years or more. The fraction of helium deep in a dense white dwarf must similarly be very low. At these densities and temperatures the proton-proton reaction is of pycnonuclear rather than thermonuclear type, with a low temperature-dependence, so that the secular and vibrational stability conditions are not violated. It is also possible, though not certain, that a dense white dwarf can remain stable while generating its energy through the helium cycle.

However, a powerful objection to these models is the difficulty of fitting them into a plausible evolutionary path. All the sources within the bulk should have been consumed at much higher temperatures before the star became a white dwarf: the relic of both the hydrogen and helium would have decayed exponentially through reactions with  $C^{12}$ . More plausible are models with a superficial layer of hydrogen, either an unconsumed relic of earlier stages, or the result of subsequent accretion (cf. § 3.2). Such models have been studied in detail, with particular attention to the sorting of the elements under the enormous gravitational field (Schatzman 1945, 1958, Lee 1950): after a fairly long diffusion time, the elements would reach an asymptotic state with a layer of pure hydrogen floating on the bulk and an intermediate mixed layer. But these models are either secularly or vibrationally unstable and so are not relevant to most white dwarfs, though, as pointed out by Schatzman (1958), vibrational instability in some white dwarfs may lead to recurrent ejection of gaseous shells, for which some observational support has been claimed (Greenstein 1957).

To sum up, the assumption that a white dwarf radiates in thermal equilibrium at the expense of nuclear sources leads to serious difficulties. By contrast, the picture of a white dwarf as a cooling body leads to no physical difficulties, and so far does not appear to conflict with independent estimates of the ages of star clusters containing white dwarfs.<sup>3</sup> The considerable effort spent in studying nuclear reactions in white dwarfs should not be regarded as in vain, but rather as affording additional support for the cooling picture. Further, our understanding of secular instability caused by temperature-sensitive nuclear reactions in degenerate matter, studied first in the white dwarf context (Lee 1950, Mestel 1952*a*), has borne fruit in the much more important application to the evolution of red giants (Hoyle and Schwarzschild 1955, Schwarzschild and Härm 1962, Osaki 1963).

<sup>3</sup> There is evidence that the Hyades cluster, judged "young" from the point of turn-off of the giant branch from the main-sequence, contains also some white dwarfs that are very faint and so considerably older than the bright stars (Greenstein 1963). This discrepancy is clearly not an argument for nuclear energy supply, which would only slow up the rate of cooling. Rather it is a clue suggesting that star formation within the gas cloud that generated the Hyades has occurred at more than one epoch.

### § 3. THE ORIGIN AND EVOLUTION OF WHITE DWARFS

#### 3.1. THE ORIGIN OF WHITE DWARFS

The contraction of a proto-star is halted at the main-sequence radius, when the central temperature is high enough for nuclear energy liberation to offset the leak to the surface. If one were to imagine nuclear reactions to cease, the Kelvin-Helmholtz contraction would continue until degeneracy set in, at a radius about one-tenth of the main-sequence radius, and a central temperature correspondingly ten times higher. If the mass is below the appropriate limit, the contraction would slow up, the release of gravitational energy would only partially compensate for the energy radiated, and the star would enter the cooling white dwarf state, described in § 2.

Direct formation of white dwarfs from interstellar matter was put forward by Eddington (1939), shortly after Bethe's discovery of the carbon-nitrogen cycle leading to the synthesis of helium from hydrogen. As already noted, the then accepted radius of Sirius B demanded a high hydrogen content; but during the contraction of a star of solar mass it is certain that even a very slight admixture of carbon and nitrogen—one part in  $10^{16}$ —would insure thermal equilibrium at something like a main-sequence radius. Impressed by the difficulty in seeing how a star could reach a degenerate state without passing through regimes of very high temperature, and consequently enormous nuclear energy liberation, Eddington proposed that the catalytic ingredients—carbon and nitrogen—necessary for the Bethe cycle to proceed were, in fact, entirely absent, along with all the other heavy elements and helium: he proposed white dwarfs of pure hydrogen. The change in the Einstein shift required to yield the correct radius was from 20 to 15 km/sec, not outside possible observational errors.

Eddington did not take account of the proton-proton reaction, which will certainly prevent direct formation of a hydrogen white dwarf. At one time there was doubt as to whether the proton-proton reaction is quantum-mechanically "allowed" or not, i.e., whether Gamow-Teller or Fermi selection rules apply to this beta-reaction. Hoyle (1947*b*) pointed out that if the Fermi rules apply, Eddington white dwarfs could form in large numbers early in the galactic life, provided the primeval galactic material was pure hydrogen. Nucleosynthesis inside the collapsed massive stars (Hoyle 1946), followed by adulteration of the interstellar gas by slight amounts of carbon and nitrogen, would enable the Bethe cycle to operate in the next generation of stars, so that no more Eddington white dwarfs would be born.

Since it is now accepted that the proton-proton reaction is allowed—so that even at the absolute zero, hydrogen within the bulk of a white dwarf would be transmuted fairly rapidly into helium (see § 1.3)—Eddington's proposal is only of historical interest; but his argument did make clear that a white dwarf could form only from gas without strong nuclear energy sources in its bulk. The obvious alternative is that a white dwarf is the end-product of stellar evolution,

following exhaustion of nuclear sources. This is very plausible, but immediately raises a number of questions.

In the oldest star clusters studied so far (Sandage 1962), the stars that have just left the main sequence to evolve into the giant region are of mass near  $1.15 M_{\odot}$ . Stars slightly more massive will have passed through the giant region, with a progressive extension of the partially degenerate helium core. According to Hoyle and Schwarzschild (1955), helium burning in the degenerate core center brings the star down from the overluminous giant branch to the "horizontal branch" in the Hertzsprung-Russell diagram. When the helium in the core is all transmuted into carbon, the star again acquires an inert degenerate core which gradually extends through the bulk of the star as it evolves into a white dwarf. The results of Ledoux and Sauvenier-Goffin (1950) on vibrational instability, referred to in § 2.3, suggest that any remaining hydrogen envelope will be ejected before the star has reached a white dwarf luminosity. Thus, very old stars less massive than the Chandrasekhar limit  $1.44 M_{\odot}$  for a hydrogen-free star are able to evolve directly into white dwarfs within the galactic lifetime. But in younger clusters, the mass must be well above the limit if the star is to have had time to leave the main sequence. The argument is not circular, even though it depends on age estimates derived by considering just main-sequence and giant stars, and ignoring the white dwarfs. If we were to assert, for example, that the galaxy is old enough for 40 Eridani B, of mass  $0.43 M_{\odot}$ , to have evolved without substantial mass loss from a main-sequence star, we should have to explain why we do not observe clusters with giant branches that meet the main sequence at points corresponding to masses even less than  $0.43 M_{\odot}$ . We are forced to accept the short time scales for most clusters and look for processes by which a massive evolved star is able to lose a large fraction of its mass, so it can settle down into a cooling white dwarf; thus, we link the problem of the origin of white dwarfs with that of the ultimate fate of stars well above the Chandrasekhar limit.

Evolutionary studies of more massive stars are still in their early stages. At one time it was thought that a rapidly rotating, early-type main-sequence star would stay homogeneous in composition until all of its hydrogen has been transmuted into helium, after which it would contract more or less homologously; helium burning would temporarily halt the contraction, but ultimately a homogeneous carbon star would contract, with more and more gravitational energy becoming electronic exclusion energy, ionic energy, and centrifugal energy. Stars of initially high angular momentum would become rotationally unstable early in their contraction: they were identified with P Cygni and Wolf-Rayet stars. At the other extreme, stars of moderately low rotation could contract unimpeded to such high densities that rapid formation of free neutrons is the prelude to a supernova explosion (Hoyle 1946, 1947*a*).

It is now clear that the early stages of evolution are more complicated, because even a rapidly rotating star is unlikely to stay homogeneous (see chap. 9,

this volume). This is certainly no disadvantage for stellar theory, as now giant stars fit naturally into the evolutionary scheme, without implausible assumptions about accretion of interstellar hydrogen. Further, there is the possibility of substantial mass loss from the highly extended envelope of a giant, as observed by Deutsch (1959), though it is not clear whether this steady, non-catastrophic "corpuscular radiation" will ever be sufficient to reduce the mass below the Chandrasekhar limit. If not, then the star will have become a pre-white dwarf once the burnt-out core contains most of the stellar mass, but it must again find some means of getting rid of its excess mass.

Detailed study of these late stages of stellar evolution is beyond the scope of this chapter. An adequate theory must explain why the mean white dwarf mass—as estimated theoretically by Greenstein (1958) from observed surface temperatures and magnitudes and by Weidemann (1963) from line profiles—is only two-fifths of the Chandrasekhar limit. Rotational instability may again be an important cause of mass loss. Perhaps vibrational instability induced by nuclear reactions in the surface layers of a prewhite dwarf results in enough mass ejection. And finally there is the possibility that some white dwarfs are supernova remnants. We may quote here the remark of Hamada and Salpeter (1961) that their more accurate discussion of zero-temperature equilibrium models, taking account of inverse beta-decay, is relevant to the Hoyle-Fowler (1960) theory of one type of supernova, which requires a presupernova star of very high density but moderate temperature. On the Chandrasekhar theory, only stars that are very slightly larger than the limiting mass satisfy this condition. However, inverse beta-decay has the consequence (cf. § 1.3) of making less precise the concept of a "limiting mass": depending on the initial composition, there is a moderately wide range of mass, from about  $1.1 M_{\odot}$  to  $1.4 M_{\odot}$ , which may exceed the appropriate limit for zero-temperature equilibrium.

Observational support for mass loss as an essential feature in the evolution to the white dwarf state comes from O'Dell's studies of planetary nebulae (1963). The changing size of the nebular shell indicates that the central star is contracting from  $R \simeq R_{\odot}$  to  $R \simeq 10^{-2} R_{\odot}$ —i.e., from a non-degenerate to an almost fully degenerate state—in a time-scale of about 25,000 years. The estimated mass of the central star is  $\simeq 1.2 M_{\odot}$ , and that of the nebula  $\simeq 0.2 M_{\odot}$ , suggesting that the parent star had a mass close to the limit. However, the central star is twice as massive as the mean white dwarf mass estimated by Greenstein (1958) and Weidemann (1963), so unless there is subsequently even more efficient emission of mass, evolution to the white dwarf state via a planetary nebula would not appear to be typical.

The suggestion has been made (Schatzman 1958) that white dwarfs may form directly from a primeval nebula: the hope is that locally the temperature may be high enough for hydrogen and helium to be lost, while the heavier elements can agglomerate to form cooling, source-free stars. In the solar system, the heavier planets—all much less massive than a star—do in fact *retain* a fair

fraction of hydrogen, and only the minor planets are comparatively free of hydrogen. However, at least until we have more precise ideas on the formation of the solar system, the possibility suggested by Schatzman should be borne in mind.

### 3.2. THE EVOLUTION OF A WHITE DWARF

Left to itself, the evolution of a typical white dwarf is likely to be very unspectacular—just the slow cooling to the asymptotic “black dwarf” state, described in § 2.2. However, if the star were to receive a supply of energy in excess of its surface loss, a simple reversal of the argument shows that the star will *heat up*: the increased thermal energy will expand the star slightly, releasing a little exclusion energy and increasing the gravitational energy, while the fraction of the mass in the non-degenerate envelope increases. Once the bulk of the star is non-degenerate (at temperatures near  $10^8$  °K) further steady supplies of energy will expand the star sufficiently to cool it—the reverse of the Kelvin-Helmholtz contraction.

A white dwarf that begins to accrete interstellar hydrogen before it has been cooled much below  $10^8$  °K would evolve in this way: as the hydrogen settled on the surface it would be at once transmuted into helium. However, once the non-degenerate outer parts of the star have expanded and cooled, accreted hydrogen would tend to accumulate, and the star would settle into an equilibrium state with a burnt-out, partially degenerate core, and a shell energy source surrounding the core. Such a process was suggested (Mestel 1952*b*) for the origin of subgiants—stars of low mass that seemed to have evolved further from the main sequence than the then-accepted galactic age would warrant.

Steady accretion by a *cool* white dwarf differs in one crucial way: since at  $10^7$  °K the nuclear reactions are fairly slow, the time of heating of the star is  $10^7$  years or so, giving the star time, if circumstances are favorable, to acquire a stock of surface hydrogen. When  $10^8$  °K is reached, the hydrogen is all transmuted in a few seconds, liberating far more energy than the gravitational binding energy of the hydrogen, and so blowing off these layers to infinity. This phenomenon was tentatively identified as a type of supernova.

Substantial gravitational accretion from the interstellar medium is not likely to occur often. However a white dwarf that is a member of a binary system may acquire surface hydrogen from the expanding envelope of its companion as it evolves through the giant stage (Schatzman 1959). (As it heats up, the star becomes vibrationally unstable, but the *e*-folding time is of the same order as the time of heating up.) Deutsch (Schatzman 1959) has, in fact, noted that the giant star Mira has an abnormal companion which shows instabilities, and he has suggested that it is an unstable white dwarf. Kraft (1962) has concluded that U Geminorum cataclysmic variables (dwarf novae) are binary systems with one component a white dwarf; the nova eruption is again traced to the white dwarf's picking up mass from the expanding envelope of the companion giant.

The author wishes to thank Dr. W. J. Luyten, Dr. M. P. Savedoff, and Dr. J. L. Greenstein for private communication of unpublished results. He is especially indebted to Dr. Greenstein and to Dr. V. Weidemann for commenting on the manuscript.

## REFERENCES

- |   |       |  |
|---|-------|--|
| ANDERSON, W.                            | 1929  | <i>Zs. f. Phys.</i> , <b>54</b> , 433.   |
| AULUCK, F. C., and<br>MATHUR, V. S.     | 1959  | <i>Zs. f. Ap.</i> , <b>48</b> , 28.  |
| BANDYOPADHYAY, G.                       | 1952  | <i>Bull. Calcutta Math. Soc.</i> , <b>44</b> , 2 and 89.   |
| CAMERON, A. W. G.                       | 1959a | <i>Ap. J.</i> , <b>130</b> , 884.  |
|   | 1959b | <i>Ibid.</i> , p. 916.   |
| CHANDRASEKHAR, S.                       | 1931  | <i>Proc. R. Soc. London, ser. A</i> , <b>133</b> , 241.  |
|   | 1939  | <i>Introduction to the Study of Stellar Structure</i><br>(Chicago: University of Chicago Press). |
| CHANDRASEKHAR, S.,<br>and TOOPER, R. F. | 1964  | <i>Ap. J.</i> , <b>139</b> , 1936.   |
| DEUTSCH, A. J.                          | 1959  | <i>Liège Symp.</i> , <b>9</b> , 54.  |
| EDDINGTON, A. S.                        | 1939  | <i>M.N.</i> , <b>99</b> , 595.   |
|   | 1947  | <i>Fundamental Theory</i> (Cambridge University Press).  |
| FOWLER, R. H.                           | 1926  | <i>M.N.</i> , <b>87</b> , 114.   |
| GAMOW, G., and<br>CRITCHFIELD, C. L.    | 1949  | <i>Theory of Atomic Nucleus and Nuclear Energy Sources</i> (Oxford: Clarendon Press).            |
| GREENSTEIN, J. L.                       | 1954  | <i>A.J.</i> , <b>59</b> , 322.   |
|   | 1957  | <i>I.A.U. Symp.</i> , No. 3, p. 41.  |
|   | 1958  | <i>Hdb. d. Phys.</i> , ed. S. FLÜGGE (Berlin: Springer-Verlag), Vol. 50.                         |
|   | 1963  | Private communication.   |
| HAMADA, T., and<br>SALPETER, E. E.      | 1961  | <i>Ap. J.</i> , <b>134</b> , 683.  |
| HOYLE, F.                               | 1946  | <i>M.N.</i> , <b>106</b> , 343.  |
|   | 1947a | <i>Ibid.</i> , <b>107</b> , 231.   |
|   | 1947b | <i>Ibid.</i> , p. 253.   |
| HOYLE, F., and<br>FOWLER, W. A.         | 1960  | <i>Ap. J.</i> , <b>132</b> , 565.  |
| HOYLE, F., and<br>SCHWARZSCHILD, M.     | 1955  | <i>Ap. J., Suppl.</i> , <b>2</b> , 1.  |
| KAMINSKI, K.                            | 1953  | <i>Kumanuto J. of Sci., ser. A</i> , <b>1</b> , No. 2, 49.                                       |
| KAMP, P. VAN DE                         | 1954  | <i>A.J.</i> , <b>59</b> , 447.   |
| KAPLAN, S. A.                           | 1950  | <i>A.J. U.S.S.R.</i> , <b>27</b> , 31.   |
| KAZNO SUDA                              | 1953  | <i>Sendai Astr. Repts</i> , <b>2</b> , 20 and 32.  |
| KOTHARI, D. S.                          | 1932a | <i>Phil. Mag.</i> , <b>13</b> , 361.   |
|   | 1932b | <i>M.N.</i> , <b>93</b> , 61.  |

- KRAFT, R. P. 1962 *Ap. J.*, **135**, 408.
- KRISHAN, S., and  
KUSHWAHA, R. S. 1963 *Pub. Astr. Soc. Japan*, **15**, 253.
- KUIPER, G. P. 1935 *Pub. A.S.P.*, **47**, 307.
- LEDoux, P. J. 1951 *Ann. d'ap.*, **14**, 438.
- LEDoux, P. J., and  
SAUVENIER-GOFFIN, E. 1950 *Ap. J.*, **111**, 611.
- LEDoux, P. J., and  
WALRAVEN, TH. 1958 *Hdb. d. Phys.*, ed. S. FLÜGGE (Berlin: Springer Verlag), Vol. **51**, 353.
- LEE, T. D. 1950 *Ap. J.*, **111**, 625.
- LUYTEN, W. J. 1963a Private communication.  
1963b *Advances in Astronomy and Astrophysics*, Vol. **2**,  
ed. Z. KOPAL (New York: Academic Press).
- MAJUMDAR, R. C. 1931 *A.N.*, **243**, 5.  
1932 *Ibid.*, **247**, 217.
- MARSHAK, R. E. 1940a *Ann. New York Acad. Sci.*, **51**, 49.  
1940b *Ap. J.*, **92**, 321.
- MESTEL, L. 1950 *Proc. Cambridge Phil. Soc.*, **46**, 331.  
1952a *M.N.*, **112**, 583.  
1952b *Ibid.*, **1**, 598.  
1963 *Ibid.*, **126**, 553.
- O'DELL, C. R. 1963 *Ap. J.*, **138**, 67.
- OSAKI, Y. 1963 *Pub. Astr. Soc. Japan*, **15**, 336.
- POPPER, D. M. 1954 *Ap. J.*, **120**, 316.
- RAMSEY, W. H. 1950 *M.N.*, **110**, 444.
- RUSSELL, H. N. 1935 *Observatory*, **58**, 259.
- SALPETER, E. E. 1960 *Ann. of Phys.*, **11**, 393.  
1961 *Ap. J.*, **134**, 669.
- SANDAGE, A. R. 1962 *Ap. J.*, **135**, 349.
- SAUVENIER-GOFFIN, E. 1950 *Mem. Soc. R. Sci. Liège*, **10**, 1.
- SAVEDOFF, M. P. 1963 *Ap. J.*, **138**, 291.
- SCHATZMAN, E. 1945 *Ann. d'ap.*, **8**, 143.  
1948 *J. Phys. et Rad.*, **9**, 46.  
1952 *Ann. d'ap.*, **15**, 361.  
1958 *White Dwarfs* (New York: Interscience Publishers).  
1959 *Liège Symp.*, **9**, 320.
- SCHWARZSCHILD, M. 1958 *Structure and Evolution of the Stars* (Princeton, N.J.: Princeton University Press).
- SCHWARZSCHILD, M., and  
HÄRM, R. 1962 *Ap. J.*, **136**, 158.
- SEITZ, F. 1940 *Modern Theory of Solids* (New York: McGraw-Hill Book Co.).
- SHALER, A. J., ed. 1941 *Novae and White Dwarfs* (Paris: Hermann et Cie)

- |               |      |  |
|---------------|------|--|
| SPITZER, L.   | 1942 | <i>A p. J.</i> , <b>95</b> , 329.              |
| STONER, E. C. | 1930 | <i>Phil. Mag.</i> , <b>9</b> , 944.            |
| STRÖMGREN, B. | 1936 | <i>Hdb. d. Phys.</i> , <b>7</b> , 160.         |
| SWIRLES, B.   | 1931 | <i>M.N.</i> , <b>91</b> , 861.                 |
| WEIDEMANN, V. | 1960 | <i>A p. J.</i> , <b>131</b> , 638.             |
|               | 1963 | <i>Zs. f. A p.</i> , <b>57</b> , 87.           |
| ZELDOVICH, B. | 1958 | <i>Soviet Phys.—J.E.T.P.</i> , <b>6</b> , 760. |





## CHAPTER 6

# *Theory of Novae and Supernovae*

E. SCHATZMAN

*Institut d'Astrophysique, Paris, France*

### § 1. INTRODUCTION

BY "THEORY of novae and supernovae," we shall understand the theory of the origin of outbursts and of the observed changes in the structure of a star. Concerning novae, available information now makes possible the presentation of a fairly reliable model of these stars and of the mechanism of the explosion. Concerning supernovae, very interesting work has been done, but there is still little connection between observation and theory. As it is now quite certain that novae and supernovae have different origins, this chapter considers separately (i) the novae, including recurrent and dwarf novae, and (ii) supernovae. In each case, a short historical summary of the theories is given.

It should be borne in mind that, in any case, theories of novae and supernovae are still largely speculative. It is not possible yet to explain all observations, but the author will try to present his own point of view, which, on several points, is not necessarily shared by other astrophysicists.

### § 2. NOVAE

The theory of novae being a problem of stellar structure, a model to explain all the gross properties of a nova must be found.

#### 2.1. HISTORICAL SUMMARY

The main problem is to explain the total amount of energy liberated in the explosion. In a typical nova, this is of the order of  $10^{44}$ – $10^{45}$  ergs.

It has been suggested by Milne (1931) that the energy lost during a nova outburst is the accompaniment of the collapse of a star from a centrally condensed configuration of ordinary density to a white dwarf configuration of high density. For a polytrope with  $n = 3$ , the total energy is  $E = -(\frac{3}{4}) (GM^2/R)$ . For the solar values of  $M$  and  $R$ ,  $|E| = 2.8 \times 10^{48}$  ergs. A white dwarf configuration has a total energy of the order of  $10^{50}$  ergs, one million times the

energy needed. A minor change in the radius would be sufficient to provide  $10^{44}$ – $10^{46}$  ergs.

Considering only the energy balance, contraction could provide the necessary amount, even if the star had a smaller mass. Some objections raised against Milne's model do not seem convincing now; Biermann's considerations (1939) on stellar evolution, excluding the possibility of such a collapse, are, however, still valid. Nowadays, the main criticism against the theory of collapse would be that it does not rest on any theory of instability of the star.

Biermann (1939) considered not only the energy balance but also the fact, deduced from statistical considerations on the total number of novae per year per galaxy, that outbursts occur many times in the same star. Therefore, Biermann sought a recurrent phenomenon. He considered a star with mass  $M \simeq (\frac{1}{2})M_{\odot}$  and radius  $R \simeq \frac{1}{2}R_{\odot}$  exhausted of hydrogen and helium, the main constituents being oxygen, neon, and magnesium. In the region where the temperature,  $T$ , is of the order of a few million degrees, the matter is not fully ionized, and the adiabatic gradient is near to, but smaller than, the radiative gradient; the change from radiative equilibrium to convective equilibrium would be accompanied by a partial recombination of the ions and the electrons and would provide the necessary amount of energy. Strömgren (1941) suggested that the increase in instability could simply be associated with the contraction of the prenova. However, Ledoux has raised an important objection to Biermann's theory. The change from radiative to convective equilibrium can be prevented only by viscosity. As shown by Rayleigh's theory of the instability, the maximum thickness,  $h$ , of a stable layer is given by

$$h^4 = \frac{27\pi^4}{4} \frac{K\nu T}{C_p \rho g} \frac{1}{|(dT/dh) - (dT/dh)_{ad}|}, \quad (2.1)$$

where  $K$  is the effective conductivity,  $\nu$  is the coefficient of kinematic viscosity, and other symbols have their usual meanings. With

$$K = \frac{4a c T^3}{3 \kappa \rho},$$

we find easily that, for the conditions which prevail in the region considered by Biermann,  $h$  is of the order of 1 meter. Consequently, if in the course of stellar evolution a part of a radiative zone becomes radiatively unstable, convection develops almost immediately, and no large unstable radiative zone can exist. Therefore, it is not clear how the mechanism that Biermann imagined could lead to a sudden release of energy and provide a recurrent mechanism.

Hoyle (1946, 1947) linked the nova phenomenon to the contraction of a rotating star, after exhaustion of its hydrogen. In the first paper, Hoyle gave an analysis of the nuclear reactions which could develop in a collapsing star. This analysis was later extended by Burbidge, Burbidge, Fowler, and Hoyle (1957). Hoyle's idea was that when a rotating star contracts, it takes a lenticular shape,

filling the Roche equipotential surface, and then becomes unstable, the instability being accompanied by ejection of matter. At a certain critical density the endothermic transformation of iron and heavy elements into helium occurs, and the star collapses further. If the star becomes rotationally unstable before this point is reached, the instability produces an ejection of matter, which stabilizes the star until, further contraction leading to instability, another mass ejection takes place.

Hoyle's reasoning is based on the theory of stability exchange and on Cartan's theory on the stability of Jacobi ellipsoids. Cartan (1928) showed that ellipsoids with three unequal axes (Jacobi ellipsoids) are dynamically unstable for a deformation by the third ellipsoidal harmonic. But it is not clear how it is possible to deduce from these results that mass loss through the equator is due to violent ejection and dynamical instability. According to Poincaré (1911), the way in which matter is shed through the equator, continuously or by discrete steps, depends on the physical processes underlying contraction. If the contraction is continuous, the mass loss will not show any discrete steps. Furthermore, as mentioned by Ledoux (1958), following a discussion by Jeans, an actual gaseous star may become lenticular without going through the spheroidal and pear-shaped configurations.

## 2.2. BASIC FACTS TO BE EXPLAINED

If the main aspects of a typical nova outburst can be explained, the phenomena which appear in stars of related types, such as slow novae (RT Serpentis), dwarf novae (SS Cygni stars) also are likely to find an explanation.

We have already mentioned the following characteristics of novae: (1) energy of the outburst,  $10^{44}$ – $10^{45}$  ergs; (2) recurrence, the postnova being very similar to the prenova. To these, we must add the following: (3) the mass ejected is of the order of  $10^{-3}M_{\odot}$ ; (4) the prenova is below the main sequence, intermediate between white dwarfs and main-sequence stars; (5) the outburst takes place in a very short interval of time; the rise to 2 mag. below maximum takes 2–3 days, but the process itself takes certainly much less time, possibly as little as a few hours; (6) further changes take place in the star, as will be explained below (§ 2.4.6), but the star returns to a final stage very similar to the prenova stage.

The first consideration is the sudden ejection of matter, with a velocity of the order of several hundred kilometers per second. The first mention of the possible role of shock waves in astronomical phenomena is due to Muraour (1941, 1945). However, the first consistent idea of a link between the nova phenomenon and a shock wave was due almost simultaneously to Lebedinsky (1946), Schatzman (1946*a, b*) and Rosseland (1946). Schatzman draws attention to the fact that, in first-order discontinuities, matter ahead of the discontinuity can be at rest but that matter behind the discontinuity is moving. This postfrontal wind would, in the case of a nova, correspond to the outward velocity observed for the surface material.

As will be seen later, a considerable amount of work has been devoted to the

study of the propagation of spherical shocks in stellar models. It has been shown that the arrival of a shock front at the surface of a star is followed by an ejection of a shell of matter. Observations of some novae, e.g., Nova Aquilae 1918, raise some doubt as to whether the ejected shell is spherical or not; furthermore, it is quite certain that, after fast ejection of the first shell, ejection of matter continues for some time; consequently, the interpretation of the nova phenomenon cannot be reduced to the propagation of a shock which, after a time of the order of a few minutes, leaves behind a practically unaltered star. However, shock seems to be a characteristic phenomenon associated with the nova outburst, and it is necessary to look for a type of instability that finally leads to a kind of explosive process.

It is now well understood that in all cepheids a shock front propagates in the atmosphere of the star, the amplitude of the shock, as shown by Whitney (1956), being quite small. It could be concluded that the only difference between the shock in novae and in cepheids is its amplitude and that it would not be necessary to seek a violent kind of instability to explain the novae. However, the continuous ejection of matter that follows the blast wave cannot be explained by the wind of the wake of the shock, and another process should be sought.

Referring to the detailed discussion of the various kinds of instabilities by Ledoux (1958), it is possible to accept the idea that, for small velocities, there are only three kinds of instabilities. If we suppose that the expression for the velocity contains a term in  $\exp(\sigma t)$ , we have the following cases:

1.  $\sigma^2$  is real. The star is said to be dynamically unstable. This case will be considered in greater detail in the case of supernovae (§ 3.2).
2.  $\sigma$  is complex, with a small real part. If the real part is negative, the star is vibrationally stable, and the small oscillations die out; if the real part is positive, the star is vibrationally unstable. The rate of increase in the amplitude will always be small and the time scale long compared with the period of the oscillation.
3. If the star is dynamically and vibrationally stable, it can pass slowly through a set of states departing from equilibrium only by a very small amount. It remains to find whether this slow motion is stable or not. This is the problem of secular stability.

It can readily be seen that none of these instabilities can directly explain the novae outbursts; dynamical instability leads to major changes in the system and cannot be used to explain the minor changes observed in novae. Vibrational instability in itself is not sufficient to provide an explosive phenomenon, as the time scale of the amplitude increase is very long, of the order of magnitude of the Kelvin-Helmholtz scale of gravitational contraction, within one or two orders of magnitude.

This reasoning suggests that the instability may be initiated or stimulated in some way, so that it could lead to a sudden release of energy. This hypothesis will be considered in § 2.4.

## 2.3. RECENT THEORIES

Several other suggestions have been made concerning the origin of novae. They stress one aspect or another of the basic facts to be explained; Schatzman's theory is an attempt to reconcile all the facts.

(i) Struve (1955) and Huang (1956, 1957) suggested that novae and nova-like objects may all be components of close binary systems. The idea, developed by Huang (1957), is based on the theory of stellar evolution. A star, evolving as a close binary, can never become a giant. When the isothermal core develops and contracts, the star grows until it fills the critical equipotential surface of the dynamical system. The star then begins to lose mass through the Lagrange point,  $L_1$ , and evolves approximately with a constant radius. Huang assumes that there exists a region of instability through which all stars evolve. A star that has evolved with no mass loss (a single star) or with little mass loss (well-separated binary) would become an RR Lyrae star or an RR Lyrae-like star (e.g., UX Monocerotis). A star that has evolved with a large mass loss (close binary) would become a nova. The ejection of matter would restore stability, until further evolution brings instability again.

The binary nature of novae and nova-like stars is probably very important; however, as the instability is supposed to be vibrational instability, it is necessary to discuss the assumptions more closely. Huang assumes that the instability is due to the properties of the core. In RR Lyrae stars, damping due to the envelope is large, so that we observe pulsations. Since novae have very thin envelopes, the damping due to the envelopes is small, so that the oscillation is amplified until an explosion occurs. The loss of energy and mass restores stability until instability again develops inside the core.

In this theory, the binary nature simply provides a way of removing mass from the surface of the star; but the interpretation of the explosion is entirely based on the idea of vibrational instability. In this respect, the theory is not essentially different from Schatzman's theory (1953*b*). The principal criticism to be made of this theory is that the time scale of the amplitude increase is of the order of the Kelvin-Helmholtz contraction time scale. The interval between two outbursts would be essentially given by the Kelvin time scale, and this is far too large, for example, to explain the recurrence.

To be more specific, for a core of mass  $M$ , radius  $R$ , and luminosity of the star,  $L$ , the time scale is of the order of

$$t = 30 \times 10^6 \left( \frac{M}{M_\odot} \right)^2 \frac{L_\odot R_\odot}{L R}. \quad (2.2)$$

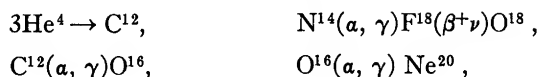
To take the most favorable case, considered by Walker (1958),  $(M/M_\odot) = 0.4$ ,  $(R/R_\odot) = 0.06$ ,  $L/L_\odot = 0.38$ , we nevertheless obtain  $t \simeq 2 \times 10^8$  years.

Even if the actual time scale of the amplitude increase were smaller than the Kelvin scale, we would still find a time much longer than that which can be de-

duced from the period-amplitude relation of Kopylov (1957). The discrepancy is even greater for the SS Cygni stars, where the period is of the order of 50 days and the Kelvin scale of the order of several hundred thousand years.

(ii) Schatzman's theory, developed below, assumes in its first version that the reaction  $\text{He}^3(\text{He}^3, 2p)\text{He}^4$  might trigger nova explosions. However, as mentioned by Cameron (1959), the rate of production of  $\text{He}^3$  is very slow, and this might limit the number of explosions in  $5 \times 10^9$  years. The amount of mass ejected in a nova explosion is small, and the total number of explosions would be too small to allow for the reduction of the stellar mass to a value appreciably less than the white dwarf limit. Though these objections can be met, it is worth considering, with Cameron, other reactions that might also trigger nova explosions.

Cameron considers the following reactions:



and takes into account the effect of the screening potential, following a method suggested by Schatzman (1948). He shows that the rate of energy production by these reactions increases considerably when the density becomes of the order of  $10^6 \text{ gm cm}^{-3}$  or larger. Figure 1 shows what Cameron calls the "ignition diagram" for the  $\text{C}^{12}(\alpha, \gamma)\text{O}^{16}$  reaction. Figure 2 shows the evolutionary tracks of stars in the ignition diagram. Cameron's idea is the following: The evolution can lead to the formation of a helium-burning core. Later an isothermal core, consisting mostly of  $\text{Ne}^{20}$  can appear, and the helium shell source, moving outward, leaves behind a large degenerate core composed mostly of  $\text{Ne}^{20}$ .

If the star has a mass not much larger than the white dwarf limit, it is unlikely that the core can contract fast enough to raise the temperature to about  $1.2 \times 10^8 \text{ }^\circ \text{K}$ , where  $\text{Ne}^{20}$  would start to react.

Cameron's suggestion is that the helium-burning shell source can cease operation, leaving incompletely burned helium with a fair admixture of  $\text{C}^{12}$ . By further contraction, the matter of this shell source can become degenerate, and its density may increase steadily with little increase in temperature. This is indicated by the dashed line, marked *prenova* in the ignition diagram, Figure 2. Cameron suggests that when the density of the matter becomes high enough, the energy production can start. Because the equation of state of the degenerate gas is very insensitive to temperature, the energy-generation rate can "run away," raising the temperature but not expanding the gas, until the point where the gas is no longer degenerate. This would produce the shock wave and the nova explosion.

Let us consider more closely the nature of the instability. The star contracts because it has no other source of energy than contraction. Physically, this has two meanings: (1) the energy flux outward can be compensated for only by the energy gained by contraction; (2) the weight of the outer layers on the inner

layers is the driving force of the contraction. When the energy generation starts in the degenerate region, it is true that the rise in temperature will be insufficient to stop contraction and to stabilize directly the energy production. However, this stabilization can be achieved indirectly, as a very small temperature gradient will be sufficient in a degenerate region to allow all the generated heat to leak away.

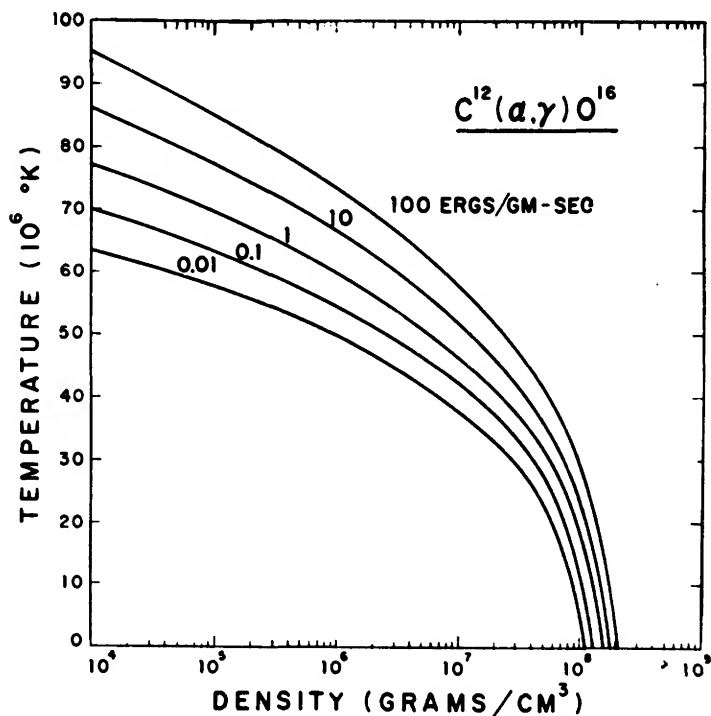


FIG. 1.—Ignition diagram for the reaction  $C^{12}(\alpha, \gamma)O^{16}$ , according to Cameron. The curves give the temperature as a function of the density for a constant rate of energy generation per gram.

As soon as the heat flux balances the luminosity of the star, the contraction will stop. An explosive process can take place only if the time needed by the star to adjust itself to the new situation is large compared with the rate of energy generation.

However, it can be seen, simply by considering orders of magnitude, that the star will always have time to adjust itself to the new situation before the start of an explosive generation of energy.

In the region of densities considered by Cameron, the energy-generation rate can be written

$$\epsilon = \epsilon_0 \rho^n, \quad (2.3)$$



where  $n$  is of the order of 12. The radius of the core decreases as  $(t + a)^{-1}$ , and the density increases as  $(t + a)^3$ , where  $a$  is a constant. The rate of energy production increases as  $(t + a)^{3n}$ . The rise of temperature in the central part of the degenerate core is of the order of

$$\Delta T = \frac{1}{C_v} \int \epsilon dt,$$

where  $C_v$  is the specific heat at constant volume. We can write

$$\Delta T = \frac{(t + a)\epsilon}{C_v(3n + 1)}, \quad (2.4)$$

$\epsilon$  being the rate of energy production at time  $t$ . We suppose that  $a^{3n+1} \ll (t + a)^{3n+1}$ , which seems a fairly reasonable assumption, since  $3n + 1 \simeq 37$ .

The temperature gradient is of the order of  $\Delta T/R$ , and the heat flux  $l$  is of the order of  $4\pi R^2\lambda(\Delta T/R)$ , that is to say,

$$l = 4\pi R \frac{\lambda}{C_v} \frac{(t + a)\epsilon}{(3n + 1)}, \quad (2.5)$$

where  $\lambda$  is the thermal conductivity.

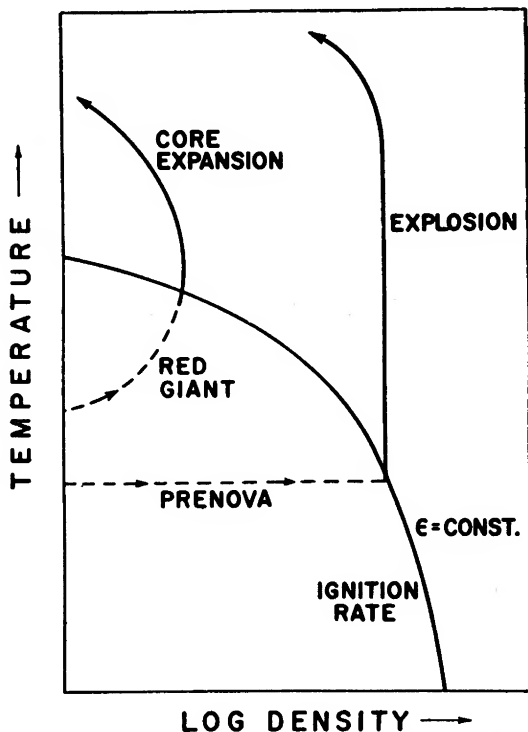


FIG. 2.—Evolutionary tracks of stars in the ignition diagram, as suggested by Cameron

Let us now consider the time  $\Delta t$  needed to establish this temperature gradient. From the equation of heat, we have the dimensional relation,

$$\Delta t \simeq \frac{C_v}{\lambda} R^2.$$

No explosive process will take place if, for  $l = L$ ,  $\Delta t < t$ . This condition can be written

$$\frac{C_v}{\lambda} R^2 + a < (3n + 1) \frac{C_v}{\lambda} \frac{L}{4\pi R\epsilon}. \quad (2.6)$$

The contraction time scale,  $a$ , should satisfy the condition

$$a < R^2 \frac{C_v}{\lambda} \left[ \frac{(3n + 1)L}{4\pi R^3\epsilon} - 1 \right]. \quad (2.7)$$

To the same approximation, it can be seen that the energy flux is of the order of

$$\frac{4\pi}{3} R^3 \epsilon \simeq L,$$

$a$  is of the order  $GM^2/RL$ , and we obtain the approximate condition

$$\frac{C_v}{\lambda} > \frac{GM^2}{nR^3L}. \quad (2.8)$$

Let us now consider the expressions for  $C_v$  and  $\lambda$  (Schatzman 1958a):

$$\begin{aligned} C_v &= \frac{8\pi^3 M^2 c k^2 T}{3 h^3} x (x^2 + 1)^{1/2}, \\ \lambda &= \frac{2\pi^2}{g} \frac{M^4 c^6 k^2 T}{h^3 e^4 I} \frac{x^6}{x^2 + 1}, \end{aligned} \quad (2.9)$$

with the following notation:  $x = P/m_e c$  is the Fermi limit. It is related to the number of free electrons by

$$N_e = \frac{8\pi m_e^3 c^3 x^3}{3 h^3}$$

and

$$I = \frac{\rho}{m_H} \sum_i \frac{X_i Z_i^{-2}}{A_i} \left( \frac{1}{3} \log 12\pi + \frac{1}{3} \log Z_i + \frac{5}{6} \log \frac{3}{2} - \frac{1}{2} \log \frac{5}{2} \right),$$

$$\rho = N_e \mu_e,$$

$$\mu_e = \sum_i \frac{A_i}{Z_i} X_i m_H,$$

where  $X_i$  is the concentration by weight of the element  $i$ . Other symbols have their usual meanings.

We then have, for  $C^{12}$ ,

$$\frac{C_v}{\lambda} = 64\pi^2 \frac{r_0^2}{c\lambda_0^3} \frac{(x^2 + 1)^{3/2}}{x^2} \log_e \left( \frac{9}{10} 72\pi \sqrt{\frac{3}{5}} \right). \quad (2.10)$$

Numerically,

$$\frac{C_v}{\lambda} = 319 \frac{r_0^2}{c\lambda_0^3} \frac{(x^2 + 1)^{3/2}}{x^2},$$

where  $r_0$  is the classical radius of the electron and  $\lambda_0$  is the Compton wave length.

With

$$r_0 = 2.817 \times 10^{-13} \text{ cm}, \quad \lambda_0 = 2.426 \times 10^{-10} \text{ cm},$$

we obtain the expression

$$\frac{M^{*2}}{R^{*3}L^*} < 3490 \frac{(x^2 + 1)^{3/2}}{x^2}, \quad (2.11)$$

where  $L^*$ ,  $M^*$ , and  $R^*$  are in solar units. In the range of densities considered by Cameron,  $\rho \simeq 10^6$ – $10^7$ ,  $x \simeq 0.8$ – $1.71$ , and the expression on the right-hand side is  $[(x^2 + 1)^{3/2}/x^2] \simeq 3.3$ – $2.66$ , the minimum value being 2.598. In order of magnitude, we can write

$$\frac{M^{*2}}{R^{*3}L^*} < 10^4.$$

If the mass is of the order of the solar mass, the luminosity a fraction of the solar luminosity, or higher, we obtain, for the radius of the degenerate core,  $R^* > 10^{-2}$ , which is of a reasonable order of magnitude for the densities we have considered.

From this discussion, we can conclude that the star has time to adjust itself to the energy generated by the thermonuclear reactions. It does not seem that the instability considered by Cameron can actually exist. Furthermore, it should be noticed that the time scale of the contraction  $a$  is of the order of  $3 \times 10^9$  years for  $R^* \simeq 10^{-2}$ . Even if it were much shorter, it would still be too long for an explanation of the recurrence phenomena.

(iii) Kraft (1962, 1963) considers also the consequence of duplicity in novae and U Geminorum stars. In his model, a U Geminorum star consists of a star filling the Lagrange surface and a white dwarf-like star. The large star is losing matter through the Lagrange point  $L_1$  and the dwarf is accreting matter. Kraft (1963) suggests that energy generation in the hydrogen-rich accreted matter produces an instability followed by an explosion. The period of recurrence would correspond to the time needed to collect enough matter to make the star unstable again.

Let us consider more closely the nature of the instability in Kraft's hypothesis. As the equation of state of the white dwarf does not depend on the temperature, the energy generation in the accreted hydrogen raises the temperature of the star without changing its structure. The rise of temperature is not stopped by a structural change and continues until an explosion occurs. We can say that Kraft assumes a secular instability. The change in temperature due to this instability is assumed to be so fast that it leads to an explosion.

Schatzman (1960) has considered the structure of a white dwarf after accretion of hydrogen-rich material. He has shown that the white dwarf becomes vibrationally unstable when the energy generation in the hydrogen envelope exceeds three times the gravitational energy generation. As shown by Mestel (1952, and chap. 5, § 2.3, this volume) a white dwarf is secularly unstable when the energy generation increases faster with the internal temperature than do the radiative losses. However, the time scale of the secular changes, or the time scale of the exponential increase of the oscillations, is of the order of magnitude of the Kelvin-Helmholtz time scale. Even if the actual time scale were much shorter than the contraction time scale, it would still be too long to account for the recurrence of the outbursts.

Let us assume now that the energy produced in hydrogen is partly radiated outside and partly transmitted by heat conduction inside. The time scale of the heating of the hydrogen is of the order of

$$t_0 = \frac{\pi \lambda C_v T^2}{4F^2}, \quad (2.12)$$

where  $\lambda$  is the thermal conductivity,  $C_v$  the specific heat,  $F$  the flux of thermonuclear energy. With the following values,  $T \simeq 10^7$  degrees,  $C_v \simeq 10^{12}$ ,  $F \simeq F_\odot \simeq 4 \cdot 10^{10}$  and assuming the conductivity  $\lambda = 10^{11.1}$  of a perfect gas at a temperature of  $10^7$  degrees, we find  $t_0 \simeq 10^{16}$  seconds  $\simeq 3 \cdot 10^8$  years. The actual conductivity is greater, and the time scale correspondingly longer.

It seems difficult to account for the explosion by an instability induced by the accretion of hydrogen. The reason is that heat is brought inside by thermal conductivity and that the total heat capacity of the star is very large. Furthermore, the continuous ejection which takes place after the production of the shock wave would remain to be explained.

The question naturally arises whether there is a difference between a nova like T Coronae Borealis, which is a double star with a period of revolution of 227<sup>d</sup>6, and DQ Herculis with a period of 4<sup>h</sup>39<sup>m</sup>. A non-radial oscillation with a period of 200 days would correspond to such a high mode that it would certainly be damped by viscous friction. T Coronae Borealis seems to be so exceptional among all the stars listed by Kraft (1963) that it is suggested here that T Cr B is a triple star, and that the nova belongs to a close binary of short period in the triple system.

#### 2.4. THE RESONANCE THEORY OF NOVAE (SCHATZMAN 1958b)

We shall consider, first, the principle of the resonance theory. Let us assume that one of the non-radial modes of oscillation has an eigen-period near the period of the orbital motion of the double star. Using canonical variables to describe the amplitude of the mode, we can formally write that the oscillation is described by the following equation:

$$\ddot{q} + \kappa \dot{q} + \sigma^2 q = a e^{i\lambda t}. \quad (2.13)$$

The amplitude of the forced oscillation then is

$$A = \frac{a}{[(\sigma^2 - \lambda^2)^2 + \lambda^2 \kappa^2]^{1/2}}. \quad (2.14)$$

Let us consider the physical meaning of this relation.

1. If  $\sigma = \lambda$ , the amplitude is finite but increases indefinitely when  $\kappa$  goes to zero. For  $\kappa = 0$ , the well-known solution of the differential equation is

$$q = \frac{a}{2i\sigma} t e^{i\sigma t}, \quad (2.15)$$

and the amplitude increases linearly with time.

We can see that in such a case, starting from forced oscillations of finite amplitude, the change of the damping constant  $\kappa$  from a positive to a negative value leads in a few oscillations to a large amplitude, able to produce a large energy generation and an explosive phenomenon.

2. If  $\sigma \neq \lambda$ , the amplitude remains finite when  $\kappa$  goes to zero, during stellar evolution, but has a maximum for  $\kappa = 0$ ; the higher the maximum, the smaller is the difference  $\sigma - \lambda$ .

As long as  $\kappa > |\sigma - \lambda|$ , the situation is not different from that described in paragraph 1. The amplitude increases roughly as  $\kappa^{-1}$  until the non-linear and explosive process can take place.

In this description of the generation of the explosive phenomenon, the time scale of the recurrence is associated only with the characteristic time of decrease of the damping constant,  $\kappa$ . No important lag can appear when the star becomes vibrationally unstable, and the explosion can occur as soon as the amplitude has become great enough. The resonance theory of the outburst is strongly suggested by the discovery of several double stars among novae and by the affirmation by Kraft that all SS Cygni stars are double stars.

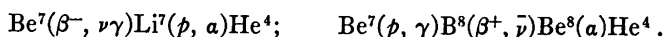
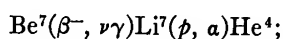
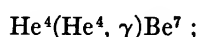
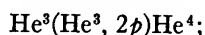
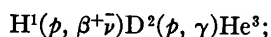
Assuming the correctness of the assumption of duplicity, the following problems have to be solved: (1) the theory of the energy of the outburst; (2) the theory of the recurrence; (3) the model of the prenova; (4) the theory of the outburst itself; and (5) the theory of the changes occurring in the star after outburst and of the continuous ejection of matter.

Points 1 and 2 can be considered as solved, at least in their main features; point 3 is still speculative; point 4 is well advanced, as far as the hydrodynamics of the ejection is concerned, but is still very uncertain for all questions concerning the nuclear processes associated with the large-amplitude oscillation; finally, a few new suggestions can be made concerning point 5, and will be given below (§ 2.4.6).

2.4.1. *The model.*—It is assumed that the star has an isothermal core and a hydrogen-burning shell providing the energy radiated by the star. As we shall see below (stability problems), the shell source of the energy has to be near the

surface of the star. This model is roughly in agreement with the ideas we have concerning stellar evolution. The isothermal core could be a neon or oxygen core that has never reached a temperature or a density high enough for further reactions to take place. The contraction was stopped or had been slowed down when the hydrogen-burning shell source became able to provide the energy radiated away by the star.

In the hydrogen-burning shell, according to Fowler (1958), the following reactions probably take place:



Can we get, at least, orders of magnitude of the temperature and density in the hydrogen-burning shell? To have enough  $\text{He}^3$  to allow a detonation wave to

TABLE 1  
FRACTION  $\xi$  OF THE MASS OF THE  
HYDROGEN-BURNING SHELL

$\rho$	$T$	
	$10 \times 10^6$	$15 \times 10^6$
$10^3$ .....	0.025	0.0056
$10^4$ .....	0.0017	0.00045

be produced eventually, the temperature must not be too high. Let us assume, for the moment, a temperature of the order of  $10^7$  degrees. To have an energy production of the order of  $L_\odot$ , the density must not be too small.

Assuming that the energy production occurs in the fraction  $\xi$  of the stellar mass, we obtain the luminosity, using the expression given by Fowler (1960) and the correction term due to screening given by Schatzman (1948),

$$L = 2.06 \times 10^6 \rho \xi M T_{\frac{1}{6}}^{-2/3} \exp(-33.804 T_{\frac{1}{6}}^{-1/3}) \times \exp\left(\frac{3.38 \times 10^5 \rho^{1/3}}{T \mu_e^{1/3}}\right).$$

For  $L/M \simeq 2$  ergs gm cm $^{-3}$ , we obtain the values of  $\xi$  for  $\rho = 10^3$  and  $10^4$  and  $T = 10^7$  and  $1.5 \times 10^7$  in Table 1.

2.4.2. *Instability.*—The theory of the sensitivity of energy-generation rate to temperature and density changes has been made by Rosseland (1949). Schatzman (1953*b*) has applied it to the proton-proton chain. It is necessary now to take into account the  $\text{He}^3(\alpha, \gamma) \text{Be}^7$  reaction. Let us call  $p_i$  the number of reactions per gram per second. The rate of these reactions, in the neighborhood of

$\rho$  and  $T$  varies as  $\rho T^\nu$ , and the exponents  $\nu$  are given in the following list, with the energy release in mev:

$$\begin{aligned}
 p(p, \beta\nu) D^2, \quad \nu_1 &= -\frac{2}{3} + \frac{11.27}{T_6^{1/3}}, \quad E_1 = 2.38; \\
 p(p, D^2) \text{He}^3, \quad \nu_2 &= -\frac{2}{3} + \frac{12.41}{T_6^{1/3}}, \quad E_2 = 10.98; \\
 \text{He}^3(\text{He}^3, 2p) \text{He}^4, \quad \nu_3 &= -\frac{2}{3} + \frac{41.00}{T_6^{1/3}}, \quad E_3 = 12.85; \\
 \text{He}^3(\text{He}^4, \gamma) \text{Be}^7, \quad \nu_4 &= -\frac{2}{3} + \frac{42.7}{T_6^{1/3}}, \quad E_4 = 1.58; \\
 \text{Be}^7(\beta^-, \nu\gamma) \text{Li}^7, \quad \nu_5 &= 0, \quad E_5 = 0.05; \\
 \text{Li}^7(p, \alpha), \alpha, \quad \nu_6 &= -\frac{2}{3} + \frac{28.2}{T_6^{1/3}}, \quad E_6 = 17.34.
 \end{aligned}$$

The second and last reactions are very fast, and the lifetimes of  $D^2$  and  $\text{Li}^7$  are very short compared with the pulsation time. The electron capture by  $\text{Be}^7$  is slow compared with the period of pulsation.

It can be shown that the effective exponent of the temperature will be

$$\nu_{\text{eff}} = \frac{(E_1 + E_2)p_1\nu_1 + E_3p_3\nu_3 + (E_4 + E_6)p_4\nu_4}{E_1p_1 + E_2p_2 + E_3p_3 + E_4p_4 + E_5p_5 + E_6p_6}. \quad (2.16)$$

For a given chemical composition (hydrogen, helium), the only variable is the content of  $\text{He}^3$ . It is readily seen that  $\nu_{\text{eff}}$  increases with the content of  $\text{He}^3$ . The maximum value of  $\nu_{\text{eff}}$  is reached for the stationary conditions. We always have  $p_1 = p_2$ ,  $p_5 = p_6$ . For stationary conditions, we also have  $2p_3 = p_1$ ,  $p_1 = 2p_4$ ,  $p_4 = p_5$ , and we find

$$(\nu_{\text{eff}})_{\text{max}} = \frac{(E_1 + E_2)\nu_1 + [E_3\nu_3 + (E_4 + E_6)\nu_4]/2}{E_1 + E_2 + (E_3 + E_4 + E_6)/2}. \quad (2.17)$$

Using the expressions for  $\nu$  given above, we obtain

$$(\nu_{\text{eff}})_{\text{max}} = -\frac{2}{3} + \frac{28.2}{T_6^{1/3}}. \quad (2.18)$$

The minimum value is obtained for a  $\text{He}^3$  concentration  $x_3 = 0$ ,  $p_3 = p_4 = 0$ ,

$$(\nu_{\text{eff}})_{\text{min}} = -\frac{2}{3} + \frac{11.27}{T_6^{1/3}}. \quad (2.19)$$

It is worth giving the values of  $(\nu_{\text{eff}})_{\text{max}}$  and  $(\nu_{\text{eff}})_{\text{min}}$  for several values of the temperature (Table 2).

The actual values are slightly smaller, because of the change in reaction

rates by electron screening of the nuclei. However, it is not necessary here to consider this effect, as the only important point for us is the increase in  $\nu_{\text{eff}}$  when the  $\text{He}^3$  content increases.

The mechanism would be the following: assuming that at some time the  $\text{He}^3$  content is low and is increasing,  $\nu_{\text{eff}}$  increases too until the star becomes unstable. After an explosion, the  $\text{He}^3$  content has decreased, the star is stable again, the amplitude of the oscillation is finite. The increase in the  $\text{He}^3$  content leads back to instability and to a new explosion.

TABLE 2  
MAXIMUM AND MINIMUM VALUES OF  $(\nu_{\text{eff}})$

$T_8$	$(\nu_{\text{eff}})_{\text{max}}$	$(\nu_{\text{eff}})_{\text{min}}$
8.....	13.53	4.97
10.....	12.53	4.56
12.....	11.65	4.25
14.....	11.05	4.01
16.....	10.55	3.80

2.4.3. *Energy and recurrence.*—We shall assume that the  $\text{He}^3$  content always remains small. If the concentration rises from  $x_{30}$  to  $x_{31}$ , the time needed for such a growth is

$$t = \frac{x_{31} - x_{30}}{p_1}. \quad (2.20)$$

The luminosity of the star is given by

$$L = p_1 m (E_1 + E_2), \quad (2.21)$$

where  $m$  is the mass of stellar matter in which the thermonuclear reactions occur; the contribution of  $E_3$  is small, if we suppose  $x_3$  small.

During the explosion, the energy liberated comes from the decrease in the  $\text{He}^3$  content from  $x_{31}$  to  $x_{30}$  and from further transformation of hydrogen into helium.

Designate by  $x_1, x_3, x_4$  the concentrations by weight of  $\text{H}^1, \text{He}^3, \text{He}^4$ ; then the energy produced during the explosion is an integral taken over the time of the explosion:

$$E_{\text{expl}} = \int_{\text{expl}} [(E_1 + E_2) K_1 \rho x_1^2 + E_3 K_3 \rho x_3^2 + (E_4 + E_5 + E_6) K_4 \rho x_3 x_4] m dt.$$

The duration  $\Delta t$  of the explosion is related to the change in  $\text{He}^3$  content by the relation

$$\Delta t = \frac{x_{31} - x_{30}}{2p'_3 + p'_4 - p'_1}, \quad (2.22)$$



where  $p'_i$  is the number of reactions per cubic centimeter per second during the explosive process. We then obtain

$$E_{\text{expl}} = \frac{m(x_{31} - x_{30})}{2p'_3 + p'_4 - p'_1} [p'_1(E_1 + E_2) + p'_3E_3 + p'_4(E_4 + E_5 + E_6)], \quad (2.23)$$

and we obtain the fundamental recurrence relation:

$$\frac{Lt}{E_{\text{expl}}} = \frac{(E_1 + E_2)(2p'_3 + p'_4 - p'_1)}{p'_1(E_1 + E_2) + p'_3E_3 + p'_4(E_4 + E_5 + E_6)}. \quad (2.24)$$

If we suppose that the destruction of  $\text{He}^3$  is essentially due to the reaction with  $\text{He}^4$ , we obtain

$$\frac{Lt}{E_{\text{expl}}} = \frac{p'_4 - p'_1}{p_1 + 1.42p'_4} = k, \quad (2.25)$$

and the constant  $k$  can take any value from 0 to 0.7. For typical novae,  $k$  is likely to be nearer the upper limit, as the contribution of the  $p(p, \beta\nu)\text{D}^2$  reaction is probably small; for U Geminorum stars and recurrent novae, the ratio is certainly smaller, as the contribution of the proton-proton reaction is larger. This is in agreement with the observations, as analyzed by Zuckermann (1954) and by Payne-Gaposchkin (1957).

We conclude this section by emphasizing the fact that the production and destruction of the nuclear fuel give simultaneously the explanation of the energy output and of the recurrence.

It should be noticed that the appearance of vibrational instability should be associated with the possibility of an explosive generation of energy. A simple change of structure during stellar evolution, leading to vibrational instability (as in RR Lyrae stars), would not be sufficient to explain the recurring explosions. It is necessary to assume that the explosion establishes stability again. This could be achieved either by a chemical change or by a change in mass.

Let us now consider different possibilities: (a) the energy generation is due to thermonuclear reactions; (b) the energy production is due to gravitational contraction or both; (A) the instability is due to a change in structure; (B) the instability is due to a chemical change. The combination (a, B) is the one which has just been described. Huang's theory belongs to the group (b, A). An improvement of this theory could be the following: Instead of assuming that in the HR diagram the star crosses the region of instability from right to left, we can suppose that, following the blue-white sequence of Vorontsov-Velyaminov, the star crosses the region of instability from left to right. Mass ejection would remove the surface of the star; the new surface layer would be slightly warmer, and the star would thus leave the unstable zone. Further cooling would bring the star back to the unstable zone.

If the energy of the outburst is of the order of the potential energy of the ejected mass, we have

$$E_{\text{expl}} = \alpha \frac{GM\Delta M}{R}, \quad (2.26)$$

with  $\alpha > 1$ . On the other hand, the time scale of the evolution, back to the unstable zone, is of the order of the contracting scale

$$\Delta t = \frac{GM^2}{R^2} \frac{\Delta R}{L}, \quad (2.27)$$

where  $\Delta R$  is the change of radius that brings the star back to the unstable zone;  $\Delta R$  is related to the change of mass by the expression

$$\frac{\Delta R}{R} = \beta \frac{\Delta M}{M}, \quad (2.28)$$

where  $\beta$  is a constant, which, in the case of an homology relation, is of the order of 7. We then find a relation of recurrence

$$\frac{L\Delta t}{E_{\text{expl}}} = \frac{\beta}{\alpha}, \quad (2.29)$$

and the star would slide down along the edge of the region of instability.

Though a recurrence relation can be proposed in this case, the energy source of the explosion is not found. It cannot be the contraction, as the contraction here is not an explosive phenomenon. It must be a nuclear phenomenon, though the above reasoning does not include any reference to nuclear processes.

**2.4.4. Non-radial oscillations.**—In the double-star hypothesis the oscillation is enhanced by the tidal action of the companion. We suppose that the star has an angular velocity of rotation  $\omega$  and that the plane of the orbit coincides with the equatorial plane of the star. If the star of mass  $M_2$  is at a distance  $R$  from the disturbed star, in a direction  $\alpha$ , the perturbing potential at a point with co-ordinates  $a, \phi, \theta$ , is given by

$$W = \frac{GM_2}{R} \sum_2^4 P_j [\sin \theta \cos(\phi - \alpha)] - \frac{1}{3} \omega a^2 P_2(\cos \theta). \quad (2.30)$$

We can develop this expression, taking into account the addition theorem for spherical harmonics and Lagrange's development in powers of the eccentricity for the root of the Euler equation.

To the first power of the eccentricity, the distance  $R$  and the anomaly  $w$  are given by

$$R = R_0(1 - e \cos \Omega t), \quad w = \Omega t + e \sin \Omega t.$$

In the rotating system of co-ordinates, the angle  $\alpha$  is

$$\alpha = (\Omega - \omega)t + e \sin \Omega t.$$

We can finally obtain the potential  $W$  as a sum of potentials, which are given, to the first power of the eccentricity by the following expressions:

$$\begin{aligned}
 \frac{R^3}{GM_2 a^2} W_2 &= \frac{1}{4} P_2^2 [\cos 2\phi \cos 2(\Omega - \omega)t + \sin 2\phi \sin 2(\Omega - \omega)t] \\
 &+ e \left\{ -\frac{3}{2} P_2 \cos \Omega t + \frac{1}{4} P_2^2 [\cos 2\phi \sin 2(\Omega - \omega)t \right. \\
 &\times 2 \sin \Omega t + 3 \cos 2\phi \cos 2(\Omega - \omega) \cos \Omega t \\
 &\left. + \sin 2\phi \cos 2(\Omega - \omega)t \times 2 \sin \Omega t + 3 \sin 2(\Omega - \omega) \cos \Omega t \right\}; \\
 \frac{R^4}{GM_2 a^3} W_3 &= \frac{1}{4} P_3^1 [\cos \phi \cos(\Omega - \omega)t] - \frac{P_3^3}{24} [\cos 3\phi \cos 3(\Omega - \omega)t + \sin(\Omega - \omega)t] \\
 &+ e \left\{ \frac{1}{4} P_3^1 \cos \phi [-\sin(\Omega - \omega)t \sin \Omega t + 4 \cos(\Omega - \omega)t \cos \Omega t] \right. \\
 &+ \frac{1}{4} P_3^1 \sin \phi [\cos(\Omega - \omega)t \sin \Omega t + 4 \sin(\Omega - \omega)t \cos \Omega t] \\
 &- \frac{P_3^3}{24} \cos 3\phi [-3 \sin 3(\Omega - \omega)t \sin \Omega t + 4 \cos 3(\Omega - \omega)t \cos \Omega t] \\
 &\left. - \frac{P_3^3}{24} \sin 3\phi [3 \cos 3(\Omega - \omega)t \sin \Omega t + 4 \sin 3(\Omega - \omega)t \cos \Omega t] \right\}; \\
 \frac{R^5}{GM_2 a^4} W_4 &= -\frac{P_4^2}{24} [\cos 2\phi \cos 2(\Omega - \omega)t + \sin 2\phi \sin 2(\Omega - \omega)t] \\
 &+ \frac{P_4^4}{192} [\cos 4\phi + \cos 4(\Omega - \omega)t + \sin 4\phi \sin 4(\Omega - \omega)t] + e \left\{ \frac{5}{8} P_4 \cos \Omega t \right. \\
 &- \frac{P_4^2}{24} \cos 2\phi [-2 \sin 2(\Omega - \omega)t \sin \Omega t + 5 \cos 2(\Omega - \omega)t \cos \Omega t] \\
 &- \frac{P_4^2}{24} \sin 2\phi [2 \cos 2(\Omega - \omega)t \sin \Omega t + 5 \sin 2(\Omega - \omega)t \cos \Omega t] \\
 &+ \frac{P_4^4}{192} \cos 4\phi [-4 \sin 4(\Omega - \omega)t \sin \Omega t + 5 \cos 4(\Omega - \omega)t \cos \Omega t] \\
 &\left. + \frac{P_4^4}{192} \sin 4\phi [4 \cos 4(\Omega - \omega)t \sin \Omega t + 5 \sin 4(\Omega - \omega)t \cos \Omega t] \right\}.
 \end{aligned} \tag{2.31}$$

The perturbing potentials can be written

$$W_i^s(a) P_i^s e^{i\lambda t}. \tag{2.32}$$

Each of these potentials produces a forced oscillation

$$\delta \mathbf{r} = \delta \mathbf{r}_{ij}^s b_{ij}^s e^{i\lambda t}, \tag{2.33}$$

where  $i$  and  $s$  are the indices of the spherical harmonics and  $j$  is the index of the mode of the non-radial oscillation.

If we describe the amplitude of the oscillation with the help of the functions  $a_j(r)$  and  $b_j(r)$  introduced by Ledoux (1951), we shall write

$$\begin{aligned}\delta r &= a_j(r) P_i^s e^{\pm i s \phi}, \\ r \delta \theta &= b_j(r) \frac{\partial P_i^s}{\partial \theta} e^{\pm i s \phi}, \\ r \delta \phi \sin \theta &= \pm i s b_j(r) \frac{P_i^s}{\sin \theta} e^{\pm i s \phi}, \\ \delta \rho &= -P_i^s e^{\pm i s \phi} \left[ \frac{1}{r^2} \frac{\partial}{\partial r} r^2 a_{j,\rho} - i(i+1) \frac{b_{j,\rho}}{r} \right],\end{aligned}$$

and we can finally calculate the amplitude  $b_{ij}^s$ :

$$b_{ij}^s = \frac{1}{\sigma_i^2 - \lambda^2} \frac{\int W_i^s(r) [(d/dr) r^2 a_{j,\rho} - i(i+1) b_{j,\rho}] dr}{\int [a_j^2 + i(i+1) b_j^2] \rho r^2 dr}. \quad (2.34)$$

The  $b_{ij}^s$ 's have been calculated by Schatzman (1958*b*) for the case  $\Omega = \omega$  and for three potentials  $W_2$ ,  $W_3$ , and  $W_4$ :

$$\begin{aligned}b_2 &\sim -\frac{3}{2} P_2 \cos \Omega t + \frac{3}{4} P_2^2 \cos 2\phi \cos \Omega t + \frac{1}{2} P_2^2 \sin 2\phi \sin \Omega t, \\ b_3 &\sim P_3^1 \cos \phi \cos \Omega t + \frac{1}{4} P_3^1 \sin \phi \sin \Omega t - \frac{1}{6} P_3^3 \cos 3\phi \cos \Omega t \\ &\quad - \frac{1}{8} P_3^3 \sin 3\phi \sin \Omega t, \quad (2.35) \\ b_4 &\sim \frac{5}{8} P_4 \cos \Omega t - \frac{5}{14} P_4^2 \cos 2\phi \cos \Omega t - \frac{1}{12} P_4^2 \sin 2\phi \sin \Omega t \\ &\quad + \frac{5}{192} P_4^4 \cos 4\phi \cos \Omega t + \frac{1}{48} P_4^4 \sin 4\phi \sin \Omega t.\end{aligned}$$

The lowest mode is of special interest. If we calculate the modulus of the amplitude, we find

$$|b_2|^2 \sim \frac{9}{4} \sin^4 \theta \sin^2 2\phi + \left( \frac{9}{2} \sin^2 \theta \cos^2 \phi - \frac{9}{2} \right)^2. \quad (2.36)$$

Figure 3 shows the position of the maxima and minima of  $(b_2)^2$  and of a few lines of equal amplitude.<sup>1</sup> The amplitude is a maximum at the equator and at the pole and vanishes on the meridian  $\phi = 0$ , for  $\sin^2 \theta = \frac{1}{3}$ ,  $\theta = 35^\circ 16'$ .

From this picture, we can derive some speculations concerning the nova outburst:

1. The maxima of the amplitude being at the equator and near the pole, we can expect the explosion to eject an equatorial belt and two polar caps. This result seems to agree with the interpretation by Weaver (1957) of the spectra of Nova Aql 1918.

2. There is a phase difference between the oscillation at the pole and at the

<sup>1</sup> Note added in proof: Mrs. Lortet (unpublished) has found that the lines of equal amplitude are not exactly as shown in Figure 3 and that the amplitudes are slightly different.

equator. Let us consider the points  $\theta = \pi/2$ ,  $\phi = 0$ , and  $\theta = 0$ . The amplitude is

$$b_{2 \text{ equator}} \sim -3 \cos \Omega t, \quad b_{2 \text{ pole}} \sim \frac{3}{2} \cos \Omega t,$$

which means that a maximum at the pole can correspond to a minimum at the equator.

3. The existence of two regions of large amplitude of the oscillation leads to the explanation of the alternation of two kinds of outbursts in U Geminorum stars.

The resonance cannot take place between the orbital motion and the fundamental mode of the non-radial oscillations. As stressed by Kraft (1963), the fundamental mode has a much shorter period than the orbital motion. However,

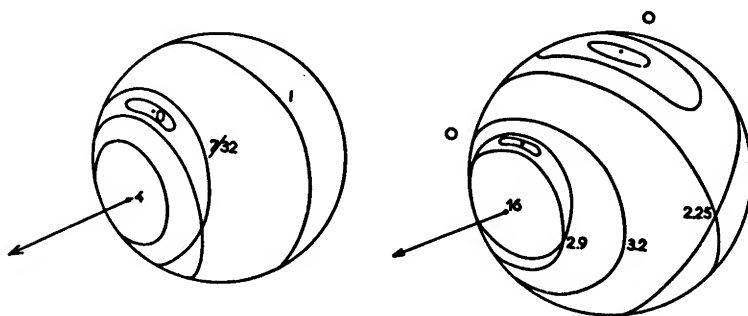


FIG. 3.—Amplitudes of forced oscillations for the first and second non-radial modes (Schatzman).

the non-radial oscillations are divided into compressive modes of shorter period and gravitational modes of longer period. The fundamental mode has a large amplitude near the center of the star. On the contrary, a high gravitational mode has a long period and a high amplitude near the surface.

2.4.5. *The explosive process.*—We have no very clear idea at the date of writing how the non-linear explosive process develops. Assuming that the explosive process has taken place, several papers have been published concerning the propagation of a spherical shock wave in a sphere of gas.

In its full generality, the problem is not tractable, but the method of similarity gives the possibility of finding a solution in a few peculiar cases. Classical works now are those of Sedov (1955, 1959) and Kopal and co-workers (1951*a*, *b*, 1954). A very important work is a paper of Hazlehurst (1962). In principle, the method of similarity consists in finding a solution of the *progressive type*, i.e., motions for which the velocity, pressure, and density of the disturbed field of flow can be made to depend on a single variable  $\xi = t^\psi/r$ , where  $r$  denotes the radial distance,  $t$  the time, and  $\psi$  a suitably chosen constant.

Assuming a density in the undisturbed fluid in front of the shock wave varying as  $r^{-a}$ , the hydrostatic pressure is found to vary as

$$p \sim \frac{r^{2(1-a)}}{(3-a)(a-1)} + C, \quad (2.37)$$

and it is found that a similarity condition exists if  $C = 0$ , and  $a\psi = 2$ . The positivity and finiteness of the equilibrium pressure imply

$$1 < a < 3.$$

It is found that the front moves, its co-ordinate being given by  $\xi = \xi_1$ , and that inside there exists an empty sphere of radius  $\xi_2$ . The Mach number is given by

$$M^2 = \frac{4(3-a)(a-1)}{a^2 \gamma \xi_1^a}. \quad (2.38)$$

Calculating the total energy between the spheres  $\xi_1$  and  $\xi_2$  in two different ways gives a relation between  $a$ ,  $\xi_1$ , and  $\xi_2$ , so that the solutions form only a one-parameter family.

We can consider the solution as showing that a shell of finite thickness can be ejected from a star. However, the existence of a sphere effectively devoid of matter can be understood only if there is inside such a volume of finite pressure that maintains it. These methods, as shown by Hazlehurst, give the possibility of explaining the sudden ejection of a very thin, transparent shell, as has often been observed in novae; but they do not explain the continuous ejection, which sometimes lasts several weeks after the beginning of the outburst.

*2.4.6. Changes in the star during the nova stage.*—We shall give here some speculations as to the origin of the changes present in the star during the nova stage. These speculations seem to give the possibility of explaining simultaneously the continuous ejection and the change in radius of the photosphere of the star.

The basic idea of the explanation is to assume that, through non-linear coupling between different oscillatory modes, the non-radial instability also excites oscillations of higher frequency. We shall assume that these radial waves change the structure of the star through the following effects: (1) transport of momentum and (2) dissipation of mechanical energy as heat.

Let us assume that the transport of momentum due to the oscillations provides the main part of the pressure. If the mechanical flux is roughly constant,

$$F_{\text{mec}} = 4\pi r^2 \rho v^3, \quad (2.39)$$

the mechanical pressure is

$$P = \rho v^2,$$

and the equation of equilibrium can be solved to give

$$\rho = \frac{F}{4\pi} (GM)^{-3/2} r^{-1/2}. \quad (2.40)$$

As we could have expected, the effect of the transfer of momentum is to build an extended envelope in which the density decreases very slowly. Assuming that the radius has tripled and has passed from 0.2 to 0.6 solar radius, and supposing a large mechanical flux,  $F = 4 \times 10^{37}$  ergs sec<sup>-1</sup>, we calculate the mass of the extended envelope:

$$m = 2 \times 10^{-9} M_{\odot}.$$

To have a confirmation of the size of the envelope, let us write that the flux  $F$  is dissipated into heat in the envelope. The dissipation per cubic centimeter per second is given (Schatzman 1949) by

$$\epsilon = \frac{2}{9} \frac{\rho v^3}{V t_0}, \quad (2.41)$$

where  $t_0$  is the characteristic period of the compression waves and  $V$  is the velocity of propagation. With  $V = 2v$ , we obtain the energy dissipated as heat:

$$F = \frac{2F}{27t_0} \frac{r^{3/2} - R^{3/2}}{(GM)^{1/2}}, \quad (2.42)$$

from which we calculate the value of  $r$ . For  $t_0 = 10^2$  seconds and  $M = M_{\odot}$ , we find  $r = 6.25 \times 10^{10}$  cm. This is obviously an overestimate, but it is surprisingly close to the radius of the photosphere of the central star of a nova at its maximum.

The very high equivalent temperature in the outer layers of the star will provide the powerful source for a *stellar wind* that will last as long as instability is present. As soon as the instability has disappeared, the flux of mechanical waves will die, and the extended envelope will collapse, the photosphere will shrink and return to its original size.

## 2.5. THE U GEMINORUM STARS

The distribution of the amplitude of the oscillation at the surface of the unstable star seems to provide an explanation for the remarkable alternation of strong and weak explosions in SS Cygni stars. To see the principle of the explanation, it is sufficient to reduce the oscillation to two zones of constant amplitude, one consisting of the equatorial belt (region I), the other one consisting of the two polar caps (region II).

The star becomes vibrationally unstable when the average concentration of the explosive fuel becomes larger than a certain value,  $a_0$ . The amplitude increases linearly with time until the non-linear explosive process occurs. The explosion process will start in the region where the amplitude first becomes critical (for example, in region II). When the explosive process starts, it burns in one region a fraction of the explosive fuel, until the star becomes stable again. The secular increase in explosive fuel leads to instability again, but this time the amplitude is likely to become critical first in the other region (for ex-

ample, region I). The explosive process then occurs alternately in one region and the other. This could explain the alternation of two types of explosions.

Physically, this implies that, for each concentration  $\alpha$  of the explosion fuel, there exists a critical amplitude for which a mild explosive process starts. The outer layers of the star experience a considerable change during the time of the extra generation of energy and then return to their initial structure.

If no other phenomena influence the outbursts, we should expect a strict alternation and close relation between two maxima of different types. Though the two types can alternate regularly for some time, for example, in U Geminorum, the alternation is not so regular in SS Cygni and is almost missing in Z Cam.

A detailed analysis of 440 maxima of SS Cygni by Martel (1961) shows that the nature of the maxima is determined by a simple Markov chain; the probability that a maximum will be of a certain type (strong or weak) depends only on the nature of the preceding maximum.

The transition matrix is

$$\|P^{(1)}\| = \begin{vmatrix} 0.285 & 0.836 \\ 0.715 & 0.164 \end{vmatrix},$$

and the numerical values show clearly that there is a preference for a strong maximum to be followed by a weak one and for a weak maximum to be followed by a strong one.

From this matrix, it is possible, for example, to predict the number of certain successions and to check the result by comparison with the observations. Martel obtains the results in the accompanying table. This agreement is remarkable and shows clearly the preference for the alternation of the two types.

Type of Successions	Observed Frequency	Predicted Frequency
SWS.....	113	119.6
SWWS.....	43	34.0
SWWWS.....	9	9.7
SWWWWS.....	2	2.7
WSW.....	141	140.4
WSSW.....	22	23.0
WSSSW.....	4	3.8
WSSSSW.....	1	0.6

However, the preference is only a statistical one, in contradiction to the strict relation predicted by the simple model. It can be suggested that the rotation period  $2\pi/\omega$  of the unstable star differs from the period  $(2\pi/\Omega)$  of the double star. Consequently, the zones of oscillation slide continuously at the surface of the star, sweeping regions of different chemical composition. The regularity of the alternation would be continuously altered, and it can be shown that a minor



change in chemical composition in one zone can considerably disturb the succession of the types of outbursts.

Let us, with Martel, use the term *accident* for the succession of two maxima having the same type (weak, weak, called "accident A"; strong, strong, called "accident B"). A diagram on which the place of accidents A and B in the succession of outbursts has been plotted shows obviously that they are not distributed

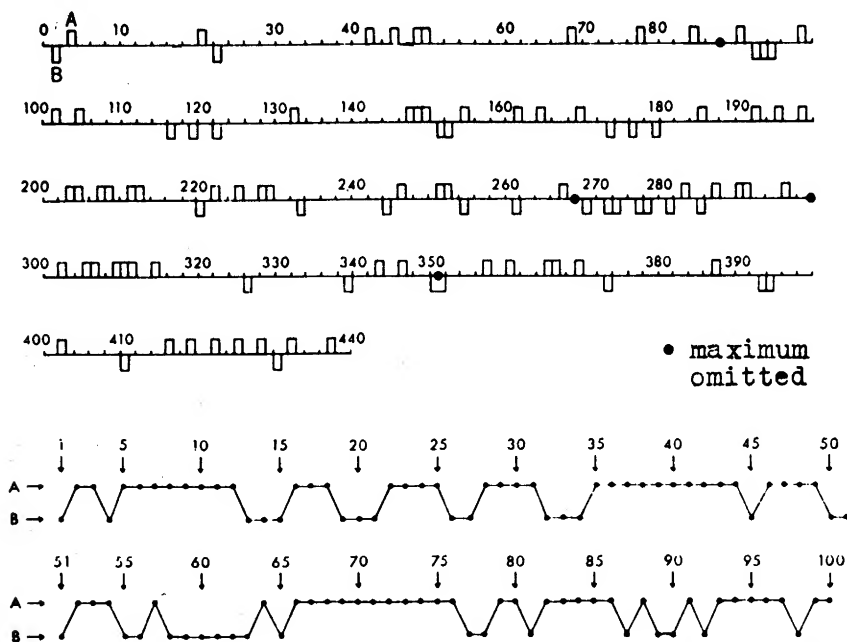


FIG. 4.—Analysis of the light variations of SS Cygni (after Martel, 1961). An *accident* is defined as a succession of two maxima having the same type (weak, weak, called "accident A"; strong, strong, called "accident B"). The succession of accidents A and B is plotted in the figure. *Above*: the place of accidents A and B in the series of maxima SS Cygni; *below*: the chronological series of the accidents. It is obvious that accidents A and B are not randomly distributed.

at random (Fig. 4). Applying a probability test, Martel can show that the configuration of the hundred observed accidents has a probability of only 0.005. The presence of a trend in the distribution of accidents A and B seems to indicate an evolution which at some time favors accidents A and at some other time favors accidents B.

### § 3. SUPERNOVAE

#### 3.1. INTRODUCTION

It is now proved that a supernova explosion is a completely different process from a nova outburst. The main characteristics are the following:

1. The total energy emitted by a supernova is three to four orders of magnitude larger than the energy radiated by a nova; it is of the order of  $10^{49}$  ergs, of the same order as the total energy of the sun.

2. The mass of the ejected matter is much larger than in the case of the novae. This can be deduced from the great duration of the visibility of the supernova: from several weeks to several months. The Crab Nebula, remnant of the supernova of 1054, has a mass of the order of 0.1 solar mass or larger. It has been suggested that some supernovae might have a mass of the order of several solar masses.<sup>2</sup>

3. Supernovae fall into two main classes: supernovae of type I, with an uninterpreted spectrum and a very slow decline of the light-curve; supernovae of type I can be found in galaxies of all types and are probably related to population II stars; supernovae of type II decline faster but are probably of a larger mass; their spectrum has been identified and is rich in iron and other metals; supernovae of type II have been found only in spirals and are probably related to population I stars. Three additional types of supernovae listed by Zwicky (chap. 7, this volume) cannot be discussed here, as our knowledge of them is still scanty.

4. The supernova phenomenon is relatively rare. Its frequency in the Galaxy is probably not greater than one supernova every 50 years. A statistical analysis by Baade (1939) gave one supernova per galaxy per 300 years; but naturally, in any given galaxy, the frequency depends on the total number of stars in the system, and this effect was not considered by Baade. As recently suggested by Burbidge (1961), radio sources can appear in a galaxy in consequence of the successive outburst of many supernovae in a short interval of time. The question of the possibility of a triggering mechanism for supernovae explosions has thus been raised.

Considering the large mass ejected by a supernova, it has long been suggested that, in the supernova process, most of the mass of the star is blown off. Nuclear phenomenon which possibly take place during the outburst have been considered in detail by Burbidge *et al.* (1957) and by Fowler and Hoyle (1960), and we shall only sketch this aspect of the phenomenon. We shall consider in more detail the instability problem, the shift from stability to instability, the types of supernovae, the possible triggering of supernovae explosions.

The theory of supernovae is still fairly speculative, as we have no observation of a presupernova. We can rely, for the time being, only on the internal consistency of the physical theory which is suggested.

### 3.2. SHORT HISTORY

The first suggestion concerning the theory of supernovae stems from energy considerations. The total internal energy of the sun is of the order of  $2 \times 10^{48}$  ergs. Only the collapse of the sun to a radius one hundred times smaller than the actual radius could provide  $2 \times 10^{50}$  ergs. Zwicky (1938) suggested, first, that the collapse of an ordinary star to a neutron star could provide the necessary amount of energy. Further work by Zwicky (1939) led to the determination of

<sup>2</sup> Note added in proof: Poveda (1964) has shown that the mass can be as small as  $0.01 \odot$  for Type II supernovae.

the structure of a neutron star of uniform density, taking into account relativistic effects. Zwicky finds the values for gravitational energy, released by contraction, as given in the last column of Table 3. The table also gives the density and the radius of the star. The maximum value of the mass corresponds to the velocity of light vanishing at the center of the star. In all these models, the proper density is constant and equal to  $10^{14}$  gm cm $^{-3}$ . We see from these numbers that the collapse to a neutron star provides a large amount of energy, of the order of what is observed or larger.

In a recent work, Ambartsumian and Saakian (1960) have considered the equation of state of a superdense gas of elementary particles; for increasing densities, they consider successively electron degenerate gas, neutron gas, meson gas, and several hyperon gases. Later (1961) they used their result to calculate the internal structure of stars of nuclear densities. The order of magnitude of the radii and masses are comparable with Zwicky's values. However, as they have

TABLE 3  
NEUTRON STARS: DIMENSIONS AND ENERGY  
RELEASED BY COLLAPSE

Mass	$\rho$	$R$ (Km)	$E_g$
$2.16 \times 10^{32}$ .....	$10^{14}$	8	$2.3 \times 10^{51}$
$2.0 \times 10^{33}$ .....	$1.18 \times 10^{12}$	74	$2.16 \times 10^{52}$
$3.0 \times 10^{34}$ .....	$5.2 \times 10^9$	1100	$3.24 \times 10^{53}$
$3.8 \times 10^{34}$ .....	.....	.....	$4.08 \times 10^{53}$

used an equation of state, they find a mass-radius relation very similar in form to that for white dwarfs (Fig. 5) with maximum mass.

For a given mass, a star with larger radius is more stable, as can be found from simple considerations of dynamical stability. It is not excluded that such hyperdense stars can appear as remnants of supernovae. Zwicky recognized that the collapse to a neutron star could only be the effect of nuclear reactions. However, he did not consider the possible mechanism nor the nuclear reactions in detail.

Gamow and Schönberg (1941) considered that the emission of a large number of neutrinos would produce the collapse of a star of already high central temperature and density. When the temperature and the density are sufficiently high, reactions of the type

$$X_Z^A + e^- \rightarrow X_{Z-1}^A + \nu,$$

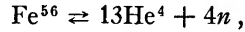
$$X_{Z-1}^A \rightarrow X_Z^A + e^- + \bar{\nu},$$

can proceed at a very fast rate.

We shall consider the neutrino problem later in greater detail. We shall deal here only with the conclusions drawn by Gamow and Schönberg. When neutrino

production begins, a large amount of energy that can be replaced only by gravitational contraction is carried away and the star collapses.

Burbidge, Burbidge, Fowler, and Hoyle (1957), following an idea of Hoyle (1946), consider the equilibrium



which is reached at a very late stage of stellar evolution, when the central temperature of a star is of the order of several times  $10^9$  degrees. They show that,

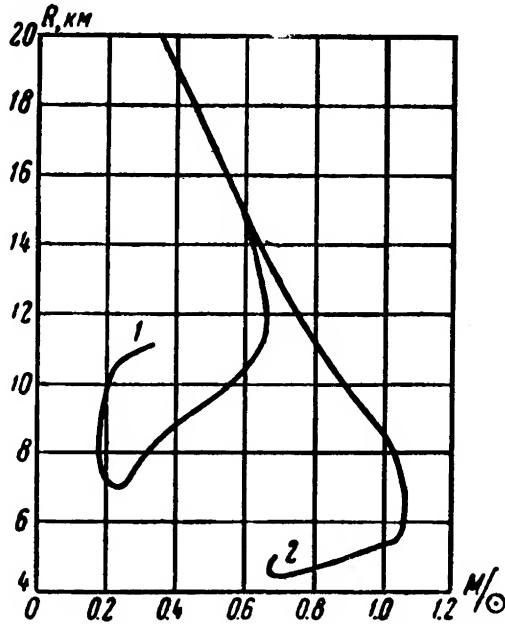


FIG. 5.—The mass-radius relation for neutron stars, according to Ambartsumian and Saakian. Curve 1 refers to configurations consisting of real baryon gas.

at a temperature of  $8 \times 10^9$  degrees, a small increase in the central temperature produces an almost complete dissociation of a core of iron, the energy of the dissociation being so large that it can be provided only by the gravitational collapse of the star.

However, Burbidge *et al.* (1957) have not considered what seems to be the main reason for instability—the decrease in the adiabatic compressibility in a dissociative equilibrium below  $\frac{4}{3}$ . At such temperatures, we have to consider the following equilibria:



and the calculation of the adiabatic compressibility  $\Gamma_1$  is better achieved by numerical methods. The first three reactions by themselves can decrease  $\Gamma_1$ , where

$$\Gamma_1 = \frac{d \log p}{d \log \rho},$$

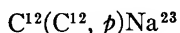
below  $\frac{4}{3}$  for a temperature slightly below  $8 \times 10^9$  degrees. It can therefore be concluded that a detailed analysis of the instability of pre-supernova stars must also include a determination of the adiabatic compressibility  $\Gamma_1$ .

### 3.3. NUCLEAR HISTORY OF A CONTRACTING STAR

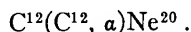
We shall consider here the thermal history of a contracting star of large mass (e.g.,  $30M_\odot$ ). As we shall see later (§ 3.5) when considering other types of instability, the explosive process following the implosion of such a star probably gives the model of type II supernovae.

When the temperature in the core of a star reaches about  $2 \times 10^8$  degrees, the  $3\alpha$  process, leading to  $C^{12}$ , proceeds with a time scale of the order of 1 year for a density  $\rho \simeq 10^5$ . The  $\alpha$ -capture is sufficiently rapid to lead to  $Mg^{24}$  in a time of the order of  $10^3$  years. For other  $\alpha$ -capture processes to proceed at a fast rate, further heating of the core is necessary. It is not until  $T \simeq 10^9$  degrees that formation of silicon, sulfur, . . . can proceed with a time scale smaller than 1,000 years. Considering that the most important term for the rate of thermonuclear reaction is the term coming from the potential barrier, we easily obtain an estimate of the time scale for different reactions.

Following Cameron (1960), we consider that, after  $He^4$  exhaustion, the first reaction to occur is the reaction of  $C^{12}$  on itself:



and



Twice as many alpha particles are produced as protons. The rate is

$$p \simeq 5.6 \times 10^{27} \frac{\rho x_c}{T_8^{2/3}} \exp\left(-\frac{181}{T_8^{1/3}}\right), \quad (3.1)$$

where  $x_c$  is the concentration in weight of carbon and  $T_8$  is the temperature in units of  $10^8$  ° K. The mean reaction rate is  $10^3$  years at a temperature of  $6.7 \times 10^8$  degrees. Following these reactions,  $O^{16}$ ,  $Ne^{20}$ ,  $Ne^{23}$ , and  $Mg^{24}$  are built. The same time scale for the  $O^{16}-O^{16}$  reaction is reached only at a temperature of  $1.5 \times 10^9$  degrees.

The oxygen reactions lead to  $P^{31}$ ,  $Si^{30}$ , and  $Si^{28}$ . When the temperature rises again to  $2.1 \times 10^9$  degrees, part of  $Si^{28}$  is partly dissociated by photodisintegration; the other part builds elements of the iron group in the vicinity of mass number 56.

We shall find in a pre-supernova a succession of shells of different chemical composition, He and light elements in the outer layers and Fe in the center (Fig. 6).

When a temperature of  $8 \times 10^9$  degrees is reached, Fe dissociates into He. Gravitational contraction then has to provide 2 mev per nucleon, that is to say,  $1.65 \times 10^{18}$  ergs per gram. At the same temperature, the total thermal energy of 1 gm of material is  $3 \times 10^{17}$  ergs. Evidently, the conversion of iron into helium demands a supply of energy much greater than the thermal content of the material.

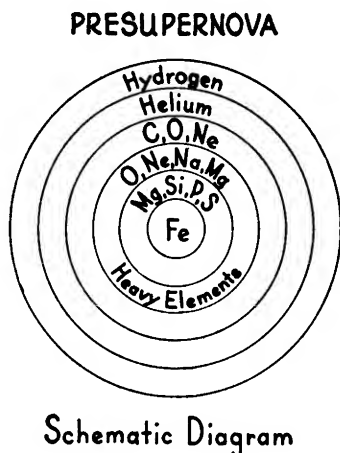


Fig. 6.—Distribution of the elements in a pre-supernova (type I) star, according to Cameron

It is interesting to draw in the  $\log T$ - $\log \rho$  plane the curve which separates the region of pure  $\text{He}^4$  from the region of pure  $\text{Fe}^{56}$  (Fig. 7). The relation between the two abundances is approximately

$$\log [\text{He}^4] - \frac{1}{14} \log [\text{Fe}^{56}] = 32.08 + 1.39 \log T_9 - \frac{34.62}{T_9}.$$

The material will be half  $\text{Fe}^{56}$  by mass and half alpha particles and neutrons when

$$\log \rho = 11.62 + 1.5 \log T_9 - \frac{39.17}{T_9}. \quad (3.2)$$

It is assumed that a star of  $30M_{\odot}$  will contract along a curve  $\rho \sim T^3$ , toward the  $(\text{Fe}^{56}\text{-He}^4)$  equilibrium. When the dissociation equilibrium is reached, the star will evolve along the equilibrium curve, as there is no energy available to achieve the dissociation. Moving along the dissociation-curve, the gravitational energy will increase much faster than the thermal energy. In equilibrium conditions, as shown by the virial theorem, the ratio of gravitational energy to thermal energy is roughly constant. This equilibrium condition is not

satisfied along the curve of dissociative equilibrium. Therefore, the equilibrium is disrupted, and a catastrophic implosion takes place.

### 3.4. NEUTRINO ASTRONOMY

The production of neutrinos by nuclear reactions has been called by Gamow and Schönberg the "URCA process" because of the evident similarity between the traceless disappearance of heat by means of these nuclear reactions and the

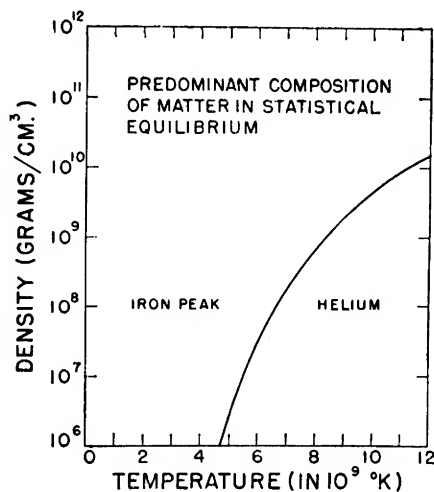
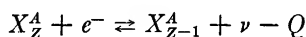


FIG. 7.—The temperature-density diagram, showing the curve separating the region of pure iron from the region of helium and neutrons.

fate of the gambler's money in the crowded playrooms of the famous Casino da Urca in Rio de Janeiro. The reaction

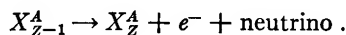


is possible only if the energy of the electron is above threshold. For a non-degenerate gas, there are always, in the tail of the Maxwell-Jüttner velocity-distribution function of the electrons, some electrons above threshold. However, it is only when  $kT$  is of the order of the energy  $W$  of the reaction, that electron capture can proceed sufficiently fast.

At equilibrium, if  $[X_Z^A]$  and  $[X_{Z-1}^A]$  are the concentrations of the two elements, we have

$$K[X_Z^A]N_e \rightleftharpoons \lambda[X_{Z-1}^A],$$

where  $\lambda$  is the decay constant of the  $\beta$ -process:



The ratio of the concentrations is

$$\frac{[X_{Z-1}^A]}{[X_Z^A]} = \frac{KN_e}{\lambda}.$$

When an electron of energy  $E$  is captured, a neutrino of energy  $E - Q$  is emitted. The transition probability per free electron of energy  $E$  is

$$P_i = 16\pi^3 g^2 \frac{m^2 c}{h^4} (E - Q)^2. \quad (3.3)$$

For a velocity-distribution function,

$$\mathfrak{N}(p) dp \sim \exp\left(-\frac{E}{kT}\right) p^2 dp, \quad (3.4)$$

with

$$p = mc \operatorname{sh} \theta, \quad z = \frac{m_e c^2}{kT} = \frac{5.93 \times 10^9}{T},$$

$$E = mc^2 \operatorname{ch} \theta,$$

$$Q = mc^2 \operatorname{ch} \theta_0$$

(where we write sh for sinh and ch for cosh), we obtain the number of transitions  $KN_e$  per atom:

$$KN_e = \frac{8\pi^3 g^2 m^2 c}{h^4} N_e \frac{\int_{\operatorname{ch} \theta_0}^{\infty} \exp(-z \operatorname{ch} \theta) (\operatorname{ch} \theta - \operatorname{ch} \theta_0)^2 \operatorname{sh} \theta \operatorname{ch} \theta d(\operatorname{ch} \theta)}{\int_1^{\infty} \exp(-z \operatorname{ch} \theta) \operatorname{sh} \theta \operatorname{ch} \theta d(\operatorname{ch} \theta)}. \quad (3.5)$$

Then the average energy of the neutrino per reaction is given by

$$\langle (\operatorname{ch} \theta - \operatorname{ch} \theta_0) \rangle = \frac{\int_{\operatorname{ch} \theta_0}^{\infty} \exp(-z \operatorname{ch} \theta) (\operatorname{ch} \theta - \operatorname{ch} \theta_0)^3 \operatorname{sh} \theta \operatorname{ch} \theta d(\operatorname{ch} \theta)}{\int_{\operatorname{ch} \theta_0}^{\infty} \exp(-z \operatorname{ch} \theta) (\operatorname{ch} \theta - \operatorname{ch} \theta_0)^2 \operatorname{sh} \theta \operatorname{ch} \theta d(\operatorname{ch} \theta)}. \quad (3.6)$$

The energy loss is

$$\frac{8\pi^3 g^2 m^2 c}{h^4} mc^2 N_e N_Z \frac{\int_{\operatorname{ch} \theta_0}^{\infty} \exp(-z \operatorname{ch} \theta) (\operatorname{ch} \theta - \operatorname{ch} \theta_0)^3 \operatorname{sh} \theta \operatorname{ch} \theta d(\operatorname{ch} \theta)}{\int_1^{\infty} \exp(-z \operatorname{ch} \theta) \operatorname{sh} \theta \operatorname{ch} \theta d(\operatorname{ch} \theta)}. \quad (3.7)$$

The energy loss through beta decay is

$$\frac{2}{3} m_e c^2 (\operatorname{ch} \theta_0 - 1) \lambda N_{Z-1}. \quad (3.8)$$

Assuming  $KN_e \gg \lambda$ , the total loss of energy is

$$mc^2 \left[ \frac{2}{3} (\operatorname{ch} \theta_0 - 1) + \langle (\operatorname{ch} \theta - \operatorname{ch} \theta_0) \rangle \right] \lambda N_A, \quad (3.9)$$



where  $N_A$  is the total number of nucleons ( $A, Z$ ). It is possible to find that an approximate expression is

$$\langle (\text{ch } \theta - \text{ch } \theta_0) \rangle = \frac{2.25}{z}. \quad (3.10)$$

We can write

$$\frac{2}{3}Q \left( 1 + \frac{3.36kT}{Q} \right) \lambda N_A. \quad (3.11)$$

We see that the energy loss does not depend strongly on the temperature, as soon as the probability of electron capture becomes very large.

Let us now consider some numerical values for  $\lambda$  and  $Q$  (Table 4).

TABLE 4  
LIFETIMES AND ENERGIES OF SOME NUCLEAR REACTIONS

Nuclear Reaction	(Lifetime) $^{-1} = \lambda$	Energy $Q$	Energy Loss per Gram: $\frac{2}{3}\lambda Q$ (1/AH)
$\text{H}^3 \rightarrow \text{He}^3 + e^-$ .....	$2 \times 10^{-9}$	18.6 kev	$7.92 \times 10^6$
$\text{C}^{14} \rightarrow \text{N}^{14} + e^-$ .....	$4 \times 10^{-12}$	155 kev	$2.84 \times 10^2$
$\text{Mn}^{56} \rightarrow \text{Fe}^{56} + e^-$ .....	$7.7 \times 10^{-5}$	1.7 mev	$1.48 \times 10^{12}$
$\text{N}^{16} \rightarrow \text{O}^{16} + e^-$ .....	$9.3 \times 10^{-2}$	6 mev	$2.24 \times 10^{16}$

Pontecorvo (1959) has considered the possibility that the process

$$e^- + A \rightarrow e^- + A + \nu + \bar{\nu},$$

due to the collision of an electron with a positive ion, could produce a large number of neutrinos and antineutrinos. Such a reaction is much less probable than the ordinary production of photons by bremsstrahlung:

$$e^- + A \rightarrow e^- + A + \gamma.$$

The ratio of the probabilities is estimated to be

$$\frac{W_{\nu\bar{\nu}}}{W_\gamma} = \frac{G^2 (E/m_e c^2)^4}{(e^2/\hbar c)}, \quad \text{with } G = \frac{gm_e^2 c}{\hbar^3} \quad \text{and} \quad g = 1.4 \times 10^{-49} \text{ erg cm}^3.$$

If we now consider an electron of energy  $E$  and velocity  $v$ , its energy loss by bremsstrahlung is, per second (Heitler 1954),

$$\frac{dE}{dt} = -N_A E v \phi_{\text{rad}}, \quad (3.12)$$

where  $\phi_{\text{rad}}$  is the cross-section for the energy loss; for low energies,

$$\phi_{\text{rad}} = \frac{1}{3} \bar{\phi},$$

and, for high energies,

$$\phi_{\text{rad}} = 4 \left( \log \frac{2E}{m_e c^2} - \frac{1}{3} \right) \bar{\phi},$$

with

$$\bar{\phi} = \frac{Z^2 e^4}{2\pi (e^2/\hbar c)} \frac{1}{(m_e c^2)^2}.$$

Multiplying the rate of energy loss by bremsstrahlung by the probability of the neutrino process and integrating over the energy of the electrons, we obtain the rate of energy loss per cubic centimeter,

$$\frac{dW}{dt} = - \frac{G^2}{(e^2/\hbar c)} N_A N_e c (m_e c^2) \phi_{\text{rad max}} \frac{\int_1^\infty t^3 (t^2 - 1) e^{-zt} dt}{\int_1^\infty t (t^2 - 1)^{1/2} e^{-zt} dt}, \quad (3.13)$$

with

$$\phi_{\text{rad max}} = \phi_{\text{rad}} \left( \text{ch } \theta = \frac{3.4}{z} \right); \quad z = \frac{m_e c^2}{kT}.$$

TABLE 5

ENERGY LOSSES IN THE REACTION  $e^+ + e^- \rightarrow \nu + \bar{\nu}$

log <i>N</i> (Ions+)	<i>T</i>		
	10 <sup>9</sup>	5 × 10 <sup>8</sup>	10 <sup>8</sup>
25.78.....	1.43 × 10 <sup>14</sup>	1.1 × 10 <sup>21</sup>	1.01 × 10 <sup>23</sup>
26.78.....	1.42	1.1	1.01
27.78.....	1.40	1.1	1.01
28.78.....	1.34	1.1	1.01
29.78.....	0.74	1.1	1.01
30.78.....	0.17	0.96	1.00
31.78.....	.....	0.31	0.835
32.78.....	.....	.....	0.136

As already mentioned by Gandel'man and Pinaev (1959), this process begins to be of some importance at a temperature of 10<sup>8</sup> degrees. If we consider the temperatures and densities that seem to be present in pre-supernovae stars, we find a rate of energy loss by the neutrino process that is extremely large.

This effect has to be compared with that considered by Chiu:

$$e^+ + e^- \rightarrow \nu + \bar{\nu}.$$

The cross-section of this reaction is about 10<sup>-44</sup> cm<sup>2</sup>. The number of pairs is a function of the temperature and the density. Table 5 gives the energy loss as a function of temperature, for various densities of positive charges carried by the nucleons. The number of pairs has been taken from a table given by Dumézil-Curien (1951). The figures are very close to those given by Chiu (1961*b*). It is readily seen that, even at a temperature of 10<sup>9</sup> degrees, the rate of energy loss by this process is much larger than by the URCA process. Even if only a small fraction of a star's mass was at such a temperature, the rate of energy loss would

be much greater than by radiative processes. This is even more true if the Pontecorvo process occurs and its cross-section has been correctly estimated.

Assuming a star of  $30M_{\odot}$ , the generation of neutrinos in a fraction  $10^{-1}$  of the stellar mass, we obtain the luminosities given in Table 6. The central densities have been supposed to be proportional to  $T_c^3$ . Using the relation of Fowler and Hoyle (1960),

$$\rho_c = 4.3 \times 10^4 T_c^3 \text{ gm cm}^{-3},$$

we obtain the results of Table 6. The time of free fall has been calculated from the relation  $t_{ff} = (R^3/2GM)^{1/2}$ ; the central density has been taken equal to 100 times the average density. For  $T_c = 10^9$ , the energy losses due to the Pontecorvo process are still dominant. At higher temperature, the process considered by Chiu is much more important. The results differ slightly from those of Chiu (1961*c*) because the conventions concerning the central densities are not exactly the same.

TABLE 6  
PARAMETERS OF NEUTRINO-EMITTING STARS WITH MASS  $30M_{\odot}$

$T_c$	$\rho_c$	$L_{\nu}/L_{\odot}$	$t_{\nu}$	$t_{ff}$
$10^9$ .....	$4.3 \times 10^4$	$3.33 \times 10^7$	$1.51 \times 10^8$	210
$5 \times 10^9$ .....	$5.4 \times 10^6$	$2.01 \times 10^{12}$	$1.24 \times 10^4$	20
$10^{10}$ .....	$4.3 \times 10^7$	$2.35 \times 10^{13}$	$2.15 \times 10^3$	0.7

### 3.5. SUPERNOVAE OF TYPE II

The results we have just given show that the picture of Fowler and Hoyle (1960) is not drastically changed, unless the Pontecorvo process is taken into account. Fowler and Hoyle suggest that implosion is followed by an explosion taking place in the outer part of the star, where an explosive fuel is still available (Fig. 8). Assuming a stellar mass of  $30M_{\odot}$ , Fowler and Hoyle give an estimate of  $2.6M_{\odot}$  for the mass of the explosive fuel, with an available energy of  $5 \times 10^{17}$  ergs  $\text{gm}^{-1}$ . The total potential explosive output is  $2.6 \times 10^{51}$  ergs.

However, Colgate and Johnson (1960) have found that the gravitational collapse supplies approximately twice the energy necessary to convert iron into helium and neutrons. Thus the surplus energy available is about  $10^{53}$  ergs in the collapse of a core with a mass equal to  $20M_{\odot}$ , much larger than the energy available in the explosive envelope.

Later, Colgate, Grasberger, and White (1961) studied the shock produced by the collapse of a star of  $10M_{\odot}$ . They have shown that a shell of 1 solar mass can be ejected, with a specific energy of  $2 \times 10^{18}$  ergs  $\text{gm}^{-1}$ . It is suggested that the elements of the iron group are synthesized in type II supernovae and ejected into the galaxy.

## 3.6. SUPERNOVAE OF TYPE I

The fact that the temperature can rise very quickly without much change in the equation of state of degenerate matter leads Fowler and Hoyle (1960) to the suggestion that degenerate stars may be unstable. This idea has to be compared with the hypothesis of pycno-nuclear reactions (Cameron 1959).

It is very likely that a star near to the critical mass (Fig. 9) could collapse. In this case, it is quite possible that the whole star could be blown off, the core of iron being dissociated into alpha particles and neutrons, providing the large number of neutrons necessary to produce the heavy elements, including Californium,  $\text{Cf}^{254}$ .

Hamada and Salpeter's (1961) recent result concerning the structure of white dwarfs confirms and improves the result of Schatzman (1958*a*). They showed that, as a function of radius, there exists a maximum mass for white dwarfs. The collapsing star considered by Fowler and Hoyle could be either a star having a

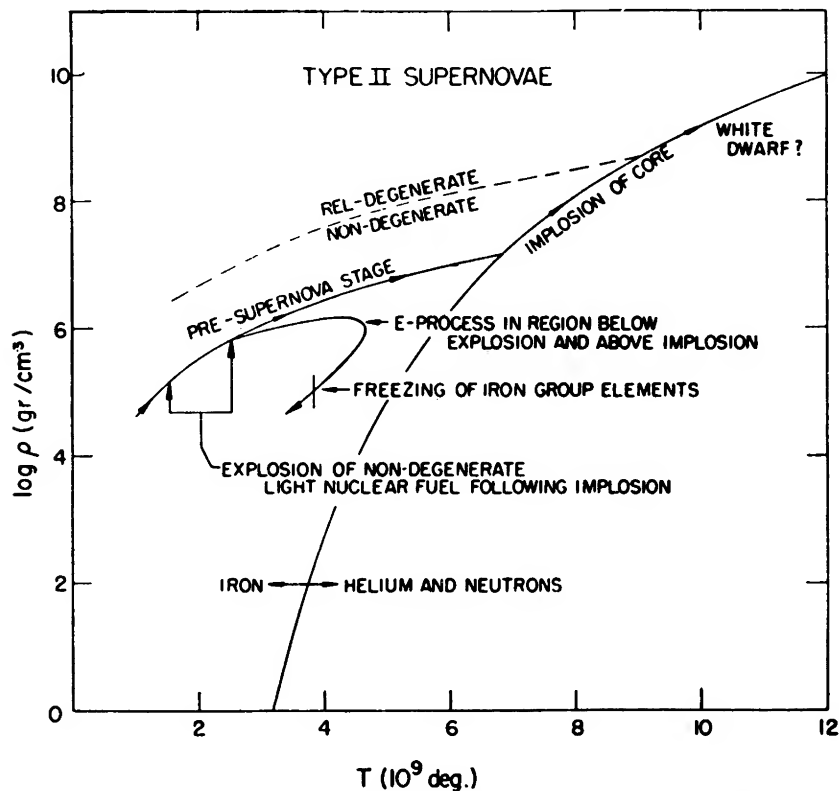


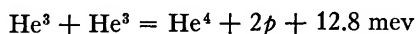
FIG. 8.—Evolutionary track of a pre-supernova in the temperature-density diagram (Fowler and Hoyle).

mass larger than the critical mass or a white dwarf near the critical mass and becoming dynamically unstable after collecting a small amount of interstellar material.

### 3.7. SUPERNOVAE AS DUE TO CHAIN REACTIONS

Gryźński (1958, 1959) has shown that the stopping power of matter decreases when the mean kinetic energy of the electrons increases. Therefore, a degenerate gas of electrons has a small stopping power.

The protons produced by the reaction



can accelerate  $\text{He}^3$  nuclei by elastic collisions and overpopulate the tail of the velocity-distribution function above the Maxwellian value. The number of  $\text{He}^3$  reactions can increase in such a way that a real chain reaction begins. For pure  $\text{He}^3$  the critical density is  $1.1 \times 10^{28}$  electrons  $\text{cm}^{-3}$ .

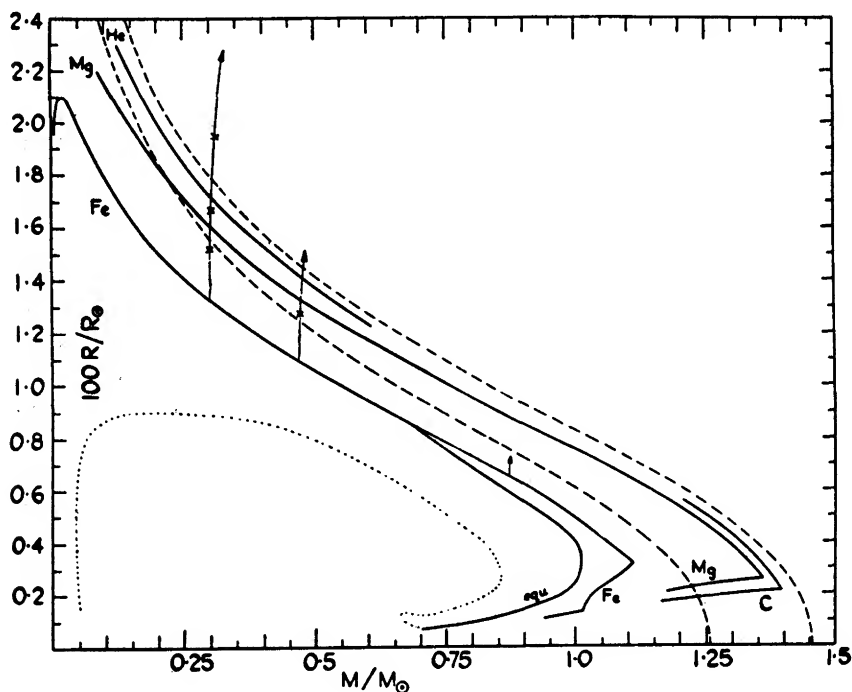


FIG. 9.—Mass-radius relation for white dwarfs, according to Hamada and Salpeter (1961). The curves take into account the change in  $(A/Z)$  due to inverse beta-process in a degenerate gas. The curve marked *equ* denotes equilibrium composition at each density. The dashed curves are for the Chandrasekhar models, the upper one for  $\mu = 2$  and the lower for  $\mu = 2.15$ . The dotted curves are for neutron stars. The vertical arrows are for stars with  $\text{H}^1$  in the outer layers.

Gryźński suggests that a pure  $\text{He}^3$  star could explode as a supernova. Though it is not clear how such a star could be produced, it is necessary to bear in mind the importance of the process suggested by Gryźński. The release of energy by *in statu nascendi* reactions could well be a very important process in astrophysics.

### 3.8. SUPERNOVAE AND RADIO GALAXIES

The instability of white dwarfs near the critical mass could eventually be the basic explanation of radio sources (cf. Vols. 5 and 9 of this series).

From energy considerations, Burbidge (1961) has shown that a large number of simultaneous supernovae outbursts could provide the sudden release of a large amount of energy in a galaxy, which is needed to explain the radio sources. A triggering mechanism is necessary to make the explosions almost simultaneous. White dwarfs near instability could collect a small amount of matter in a short interval of time—for example, after a first supernova outburst which would have pushed this matter toward the region of space occupied by these white dwarfs. Though this idea may seem highly speculative, it has the advantage of providing a simple and efficient triggering mechanism.

### REFERENCES

- |   |       |   |
|---|-------|---|
| AMBARTSUMIAN, V., and<br>SAAKIAN, G. S.                       | 1960  | <i>A.J.</i> , U.S.S.R., <b>37</b> , 193 ( <i>Soviet Astr.—A.J.</i> , <b>4</b> , 187). |
|   | 1961  | <i>A.J.</i> , U.S.S.R., <b>38</b> , 785.  |
| BAADE, W.   | 1939  | <i>Novae and White Dwarfs</i> (Paris: Hermann et Cie, 1941).                          |
| BIERMANN, L.  | 1939  | <i>Zs. f. Ap.</i> , <b>18</b> , 344.  |
| BURBIDGE, G.  | 1961  | <i>Nature</i> , <b>190</b> , 1053.  |
| BURBIDGE, G., BUR-<br>BIDGE, M., FOWLER,<br>W., and HOYLE, F. | 1957  | <i>Rev. Mod. Phys.</i> , <b>29</b> , 547.   |
| CAMERON, A. G. W.   | 1959  | <i>Ap. J.</i> , <b>130</b> , 916.   |
|   | 1960  | <i>Mém. Soc. R. Sci. Liège</i> , <b>3</b> , 163.                                      |
| CARTAN, E.  | 1928  | <i>Proc. Inst. Math. Cong. at Toronto</i> (1924), <b>2</b> , 9.                       |
| CHIU, H. Y.   | 1961a | <i>Phys. Rev.</i> , <b>123</b> , 1040.  |
|   | 1961b | <i>Ann. Phys.</i> , <b>15</b> , 1.  |
|   | 1961c | <i>Ibid.</i> , <b>16</b> , 321.   |
| COLGATE, S. A.,<br>GRASBERGER, W. H.,<br>and WHITE, R. H.     | 1961  | <i>A.J.</i> , <b>66</b> , 280.  |
| COLGATE, S. A., and<br>JOHNSON, M. H.                         | 1960  | <i>Phys. Rev. Letters</i> , <b>5</b> , 235.   |
| DUMÉZIL-CURIEN, P.  | 1951  | <i>Ann. d'ap.</i> , <b>14</b> , 40.   |
| FOWLER, W.  | 1958  | <i>Ap. J.</i> , <b>127</b> , 551.   |
|   | 1960  | <i>Mém. Soc. R. Sci. Liège</i> , <b>3</b> , 207.                                      |

- FOWLER, W., and  
HOYLE, F. 1960 *Ap. J.*, **132**, 565.
- GAMOW, G., and  
SCHÖNBERG, M. 1941 *Phys. Rev.*, **59**, 539.
- GANDEL'MAN, G. M., and  
PINAEV, V. S. 1959 *Soviet Physics—J.E.T.P.*, **37**, 1072, *Trans. J.E.T.P.*, **37** (10), 764, 1960.
- GRYZIŃSKI, M. 1958 *Phys. Rev.*, **111**, 900.  
1959 *Ibid.*, **115**, 1087.
- HAMADA, T., and  
SALPETER, E. E. 1961 *Ap. J.*, **134**, 683.
- HAZLEHURST, J. 1962 *Advances in Astronomy and Astrophysics*, ed. Z. KOPAL (New York: Academic Press), Vol. 1.
- HEITLER, W. 1954 *Quantum Theory of Radiation* (Oxford: Clarendon Press).
- HOYLE, F. 1946 *M.N.*, **106**, 343.  
1947 *Ibid.*, **107**, 231.
- HUANG, S.-S. 1956 *A.J.*, **61**, 49.
- HUANG, S.-S.,  
and STRUVE, O. 1957 *Occasional Notes Roy. Soc.*, **19**, 161.
- KOPAL, Z. 1954 *Ap. J.*, **120**, 159.
- KOPAL, Z., CARRUS,  
P. A., FOX, P. A., and  
HAAS, F. 1951a *Ap. J.*, **113**, 193.  
1951b *Ibid.*, p. 496.
- KOPYLOV, I. M. 1957 *I.A.U. Symp.*, No. 3: *Non-stable Stars*, p. 71.
- KRAFT, R. P. 1962 *Ap. J.*, **135**, 408.  
1963 *Advances in Astronomy and Astrophysics*, ed. Z. KOPAL (New York: Academic Press), Vol. 3.
- LEBEDINSKY, A. I. 1946 *A.J.*, *U.S.S.R.*, **23**, 15.
- LEDoux, P. 1951 *Ap. J.*, **114**, 373.  
1958 *Hdb. d. Phys.*, **51**, 605.
- MARTEL, L. 1961 *Ann. d'ap.*, **24**, 267.
- MESTEL, E. 1952 *M.N.*, **112**, 583.
- MILNE, E. A. 1931 *Observatory*, **54**, 144.
- MURAOUR, H. 1941 *J. d. Obs.*, **24**, 97.  
1945 *C.R.*, **221**, 200.
- PAYNE-GAPOSCHKIN, C. 1957 *The Galactic Novae* (Amsterdam: North Holland Publishing Co.)
- POINCARÉ, H. 1911 *Leçons sur les hypothèses cosmogoniques* (Paris: Hermann et Cie), chap. iii.
- PONTECORVO, B. 1959 *Soviet Physics—J.E.T.P.*, **36**, 1615; *Trans. J.E.T.P.*, **36**, (9), 1148.
- POVEDA, A. 1964 *Ann. d'ap.*, **27**, 522.
- ROSSELAND, S. 1946 *Ap. J.*, **104**, 329.  
1949 *The Pulsation Theory of Variable Stars* (Oxford: Clarendon Press).

- |                   |       |   |
|-------------------|-------|---|
| SCHATZMAN, E.     | 1946a | C.R., 222, 722.   |
|                   | 1946b | Ann. d'ap., 9, 199.   |
|                   | 1948  | J. Phys. Rad., 9, 46.   |
|                   | 1949  | Ann. d'ap., 12, 203.  |
|                   | 1953a | Mém. Soc. R. Sci. Liège, 14, 163.   |
|                   | 1953b | Ann d'ap., 16, 162.   |
|                   | 1958a | White Dwarfs (Amsterdam: North Holland Publishing Co.).                                   |
|                   | 1958b | Ann. d'ap., 21, 1.  |
|                   | 1960  | 9ème colloque de Liège, p. 320.   |
| SEDOV, L. I.      | 1955  | Questions of Cosmogony (in Russian) (Moscow: Academy of Sciences, U.S.S.R.), 4, 133.      |
|                   | 1959  | Similarity and Dimensional Methods in Mechanics (New York: Academic Press, 1959), p. 334. |
| STRÖMGREN, B.     | 1941  | Novae and White Dwarfs (Paris: Hermann et Cie), p. 157.                                   |
| STRUVE, O.        | 1955  | Sky and Telescope, 14, 275.   |
| WALKER, M. F.     | 1958  | Ap. J., 127, 319.   |
| WEAVER, H.        | 1957  | Private communication.  |
| WHITNEY, C.       | 1956  | Ann. d'ap., 19, 142.  |
| ZUCKERMANN, N. C. | 1954  | Ann. d'ap., 17, 243.  |
| ZWICKY, F.        | 1938  | Ap. J., 88, 522.  |
|                   | 1939  | Phys. Rev., 55, 726.  |





## CHAPTER 7

# *Supernovae*

F. ZWICKY

*Mount Wilson and Palomar Observatories  
Carnegie Institution of Washington, California Institute of Technology*

### § 1. HISTORICAL

THE existence of supernovae, as events distinct from common novae, has been clearly recognized only after many decades of painstaking investigation. Our knowledge of how many different types of supernovae there are is still meager, and the origin and the absolute physical characteristics of supernovae remain largely unknown. The reasons for this slow progress are many. Some of them are of interest for our understanding of the subject, and they will be touched upon in the course of this review.

Supernovae are characterized by absolute magnitudes far brighter than those of ordinary novae. Their spectra also are distinctive. While the brightest common novae have luminosities at maximum ranging only a little above  $10^6$  times that of the sun, nearly all supernovae for which adequate data exist were much brighter than  $10^8$  times the sun. The separation of the two classes is well illustrated by those known in the Andromeda spiral galaxy. Common novae there are seldom brighter than apparent magnitude 15, while the supernova S Andromedae was near sixth magnitude at maximum. It is only recently that a proposed variety of supernova (type V) has been recognized in the intermediate range of luminosities, about  $10^7$  times the sun (see § 3.55 below).

If our knowledge of supernovae were fairly advanced, a review of this knowledge in terms of concepts developed by the so-called morphological approach (Zwicky 1957, 1959) would be most illuminating. In the case at hand, this would mean the classification and analysis of all phenomena related to supernova outbursts in the light of the following three concepts: (a) *dimensionless morphology*, which involves essentially the *identification* of various objects and phenomena, as well as pure *number relations* among them; (b) *phenomenological morphology*, which treats of the observed and the deduced relations among the various phenomena exhibited by supernovae; for instance, the relations be-

tween the spectra and the light-curves; (c) *absolute morphology*, which is concerned with the absolute characteristics of supernovae in terms of standards of length, time, mass, luminosity, temperature, etc., as they have been determined by terrestrial experiments.

Even in the present rudimentary state of the art it will be useful to view our scanty knowledge of supernovae in the light of the concepts just mentioned, although a systematic presentation is as yet impossible.

Until fairly powerful telescopes became available and extragalactic stellar systems were surveyed regularly, various temporary phenomena could be observed only if they occurred within the confines of the Milky Way system. Among these temporary events, nova outbursts attracted particular attention. All that could be deduced by the most discerning observers, however, was that occasionally a star, or what was thought to be a star, flared up enormously within a day or so, that its brightness declined within a few months, and that the star then faded from sight again. In a number of cases which occurred during the last thousand years, alert observers also recorded color variations of novae in terms of the colors of permanent stars or colors of the planets.

While in the astronomical records of various peoples in the past many temporary flareups of an apparently stellar nature were recorded, most of the respective data still remain to be worked up and related to observations made with modern optical and radio telescopes, as well as to data obtained from the observations of cosmic rays and of other phenomena. Only a few of the novae observed in the more distant past have been given detailed attention by modern astronomers. Among these, four events which we believe to have been supernova outbursts are the best known. These events relate to (1) the "guest" star observed by the Chinese in 1054 A.D., whose remnant has been identified with the Crab Nebula; (2) Tycho's star of 1572; (3) Kepler's star of 1604; and (4) Nova Carinae ( $\eta$  Carinae), which reached maximum brightness in 1843.

Although these stars were, at maximum, brighter than all other novae, no distinction between supernovae and novae could be made on the basis of the statistics of the apparent brightness of all novae. Indeed, such statistics lead to a distribution of apparent brightness of the seemingly most luminous novae observed, shown in Figure 1.

The novae of 1054, 1572, and 1604 lie in the ranges of apparent magnitudes  $-5$  to  $-4$ ,  $-4$  to  $-3$ , and  $-3$  to  $-2$ , respectively. We now know that supernovae and common novae cannot be separated in a diagram of this kind because of the much greater frequency of occurrence of common novae. Because of this greater frequency, the less luminous common novae will so often be located closer to the earth that their apparent luminosities will inextricably intermingle with those of the supernovae. As we shall see, this confusion does not occur if we plot a diagram similar to that of Figure 1 for the novae in extragalactic stellar systems.

On closer inspection and with the aid of large reflectors, it became possible

to derive data which indicated that the afore-mentioned four stars must be regarded as objects quite different from ordinary novae. The considerations involved are as follows. Ordinary novae from their maximum brightness to their final stage have a range of at most 15 mag. This means that Tycho's star, whose apparent magnitude in 1572 was about  $-4$ , should now not be fainter than  $+11$ . No star of this brightness, however, can be found in the position given by Tycho which would at all fit the characteristics of the remnant of a nova. In fact, no peculiar star which might be the remnant of the star of 1572 can be found in the proper location, even when searched for with the 200-inch telescope. We must therefore conclude that Tycho's star could not have been a common nova but was a much more distant and much brighter outburst.

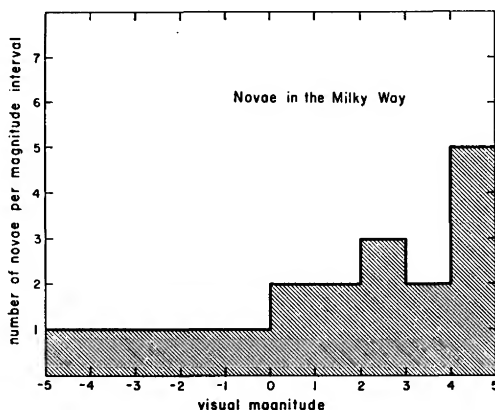


FIG. 1.—Distribution in apparent visual magnitudes  $m_v$  of the brightest known novae which appeared during the last 700 years and for which reliable data are available.

Second, if Tycho's star had been a common nova, whose absolute visual magnitudes we know to be in the range of about  $0 > M_v > -10$ , we could argue as follows. Even at  $M_v = -10$ , Tycho's star, which was at maximum of the apparent magnitude  $-4$ , could have been at most at a distance of 150 parsecs, and its remnant would therefore be subject to easy detection by present-day methods of observing proper motions.

From the above considerations it may be concluded that Tycho's star was located at a far greater distance than 100 parsecs and that, at maximum, its brightness was much greater than that of the brightest common novae. W. Baade and the writer (1934) therefore proposed in 1933 to designate stars of this kind as "supernovae."

Still more decisive were the deductions that could be made about some of the temporary stars which, between 1885 and 1930, had been observed in extragalactic stellar systems. In contradistinction to the novae in the Milky Way system, even the earliest observations with large telescopes should have forcibly

suggested that there exist two classes of novae. An important fact about novae in extragalactic systems is as follows. If the number of novae in different apparent brightness ranges within a group of a few dozen nearby galaxies such as Messier 31, 32, 33, and NGC 205, 145, 187, etc., is plotted, a diagram of the type shown in Figure 2 is arrived at. In these nearby systems we may expect, on the average, about 100 common novae per year, but perhaps only one supernova in 20 years. From a diagram of this sort it becomes evident that there are two types of novae, provided that one can make sure that the brighter type of object is not some kind of temporary star, such as SS Cygni or U Geminorum, which belongs to our own Galaxy and which might simply have happened to be in the line of sight to an extragalactic stellar system. It is not necessary to

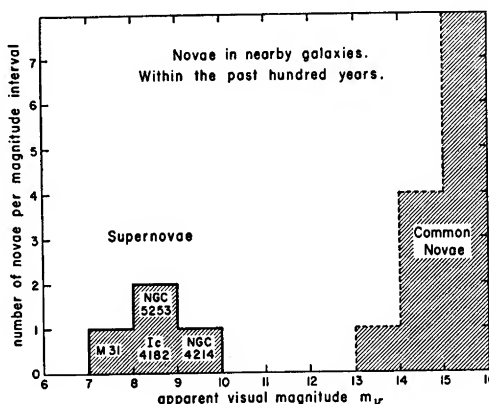


FIG. 2.—Distribution of the brightest novae and supernovae which have been observed during the last 100 years in galaxies of the local group.

reproduce here the facts and arguments which make it most unlikely that all the temporary stars that appeared superposed on the images of external galaxies such as Messier 31, Messier 87, NGC 4321, NGC 6946, and others in the period from 1885 to 1930 were common variable stars. In addition to the improbability of such a supposition, it is known that the light-curves of the objects in question are quite different from those of any of the variable or eruptive stars which make their appearance only once in many decades.

From the above-mentioned considerations and observations it thus appeared reasonable to suggest a grouping of novae as a preliminary measure into the following three major classifications: (a) supernovae whose visual brightness corresponds to absolute visual magnitudes in the range  $-11 > M_v > -20$ ; (b) common novae in the range  $-5 > M_v > -11$ ; and (c) dwarf novae in the range  $M_v > -5$ .

As time goes on, we shall have to go into ever greater details of a classification which has meaning in an astrophysical sense. We shall not get very far with supernovae at the present time, but we shall be able to present a variety of ob-

servations that will allow us to make some meaningful suggestions for future investigators.

From the outset we also wish to clarify the relation between supernovae and the stellar systems in which they appear. The latter can be classified according to their structures, their material content, and their absolute luminosity. As to the latter, we suggest, for purposes of easy terminology, the following classes of stellar systems or galaxies.  $L_{\odot}$  is the absolute visual luminosity of the sun:

A. *Giant galaxies* whose absolute visual brightness,  $L_v$ , is in the range

$$\frac{L}{L_{\odot}} > 10^8.$$

B. *Medium galaxies*, for which

$$10^6 < \frac{L}{L_{\odot}} < 10^8.$$

C. *Dwarf galaxies*, for which

$$10^4 < \frac{L}{L_{\odot}} < 10^6.$$

D. *Pygmy galaxies*, for which

$$10^2 < \frac{L}{L_{\odot}} < 10^4.$$

E. *Swarms or groups of intergalactic stars*, for which

$$\frac{L}{L_{\odot}} < 10^2.$$

Independent stellar systems of all the above classes are now known, examples of types D and E having been identified only very recently, in the immediate neighborhood of the Milky Way system (Bowen 1959, 1960, 1961).

Although Knut Lundmark and H. D. Curtis seriously considered the idea, the conviction that supernovae are a separate and unique class of stars never reached the stage of bringing about a systematic search for these elusive objects until the present author in 1932 initiated such a search, first, in a desperate and unsuccessful attempt between 1933 and 1936 with a 3-inch  $f/4.5$  camera on the roof of the astrophysics building of the California Institute of Technology in Pasadena and later, after its installation on Palomar Mountain on September 5, 1936, with the 18-inch Schmidt telescope.

All the data and discussions presented in the following must be considered as no more than prototype examples of a most complex subject. It is hoped that a detailed presentation of the available knowledge can be made in a special monograph in the near future.

#### 1.1. THE SEARCH FOR SUPERNOVAE WITH THE 18-INCH SCHMIDT TELESCOPE BETWEEN SEPTEMBER 5, 1936, AND JANUARY 1, 1941

The author and his assistant, Dr. J. J. Johnson, worked during this period on a search for supernovae. This search yielded a total number of 19 supernovae,

which at maximum were all brighter than the fifteenth magnitude. Their detailed observation by observers at the Mount Wilson and Palomar Observatories led to the conclusions which follow.

1. Supernovae at maximum have a brightness that is only about 2 mag. fainter than that of the brightest galaxies.

2. Supernovae in the brighter galaxies—those listed in the Shapley-Ames (1932) catalogue—appear with an average frequency of one per galaxy per 360 years. There seem to exist, however, galaxies with a far greater number of supernovae. For instance, 3 supernovae have appeared in NGC 3184, in April and December, 1921, and in December, 1937.

3. Supernovae appear in spiral, elliptical, and irregular galaxies with the same average frequencies per individual galaxy.

4. Supernovae seem to appear surprisingly often in the outlying regions of the galaxies.

5. At least two types of supernovae could be recognized both by their light-curves and by their spectra.

6. The spectra of type I supernovae consist of wide bands that have defied identification to the present day. The spectra of type II supernovae appeared to be analogous to those of common novae, with, however, the emission lines of H, He, and other elements widened because of expansion velocities of the order of 7000 km/sec of the supernova shells.

#### 1.2. SUBSEQUENT SEARCH PROGRAMS, 1941–1956

No systematic search was undertaken, but sporadic discoveries brought the number of supernovae to 54, which are reported in the *Handbuch der Physik*, 51, 766–785 (Berlin: Springer-Verlag, 1958).

#### 1.3. SUPERNOVAE DISCOVERED SINCE 1956

During the past few years, that is, 1956 to the present, an international co-operative search for supernovae has been organized by this author. At present the following observatories are participating: Palomar and Mount Wilson, Steward (at Tucson), Tonantzintla, Meudon, Asiago, Berne, Crimea, and Córdoba. The program is supported by the U.S. National Science Foundation, by the Swiss National Science Fund, and by the various governments of the countries mentioned. To date, 57 supernovae have been discovered in this program, which brings the total number to 111. Some of the preliminary results are as follows:

The conclusions derived from the original search of 1936–1941 have been confirmed and strengthened and important new insights have been gained.

a) The over-all average frequency of all types of supernovae in the nearby individual brighter galaxies and in the brighter galaxies of the Virgo Cluster is of the order of one per galaxy in about 350 years.

*b*) Supernovae appear in normal and barred spirals, as well as in elliptical galaxies, at a rate commensurate with their relative numbers. There was a poor representation, however, of supernovae among the irregular galaxies.

*c*) During the last 50 years, three supernovae have appeared in each of the four galaxies NGC 3184, 4321, 5236, and 6946, and two supernovae each have appeared in NGC 2841 and 4303.

*d*) Although the general character of the light-curves of type I supernovae is fairly uniform, the rate of decline per day over the semistraight-line, long portion of the light-curve may vary by as much as a factor of 2.

*e*) Judging from their absolute luminosities, light-curves, and spectra, we now find at least five types, I, II, III, IV, and V of supernovae, representatives of which are the objects in IC 4182 (1937), in NGC 4725 (1940), NGC 4303 (1961), NGC 3003 (1961), and NGC 1058 (1961). Type V is the faintest in absolute magnitude; types I and II reach about the same brightness at maximum; but little is known about types III and IV. Throughout the remainder of this chapter, types referred to are those discussed here.

*f*) Ten well-observed supernovae in the Virgo Cluster had a mean photographic apparent brightness at maximum of about +11.6. By comparison with the estimated absolute magnitudes of the Chinese supernova in 1054 A.D. and some of the supernovae in the nearby resolved galaxies like M31 and IC 4182, it appears unlikely that the distance modulus of the Virgo Cluster is greater than  $\mu = 29.0$  or that the constant for the universal redshift-distance relation is less than 175 km/sec per million parsecs.

*g*) Supernovae appear frequently on the far outskirts of galaxies where the surface brightness is too low for photographic recording. A striking example was the recent supernova in the E0 galaxy at  $\alpha = 12^{\text{h}}48^{\text{m}}30^{\text{s}}$ ,  $\delta = +28^{\circ}06'5$  (1950), a member of the Coma Cluster of galaxies (Zwicky 1961*a*).

*h*) In the renewed search for supernovae, much stress has been laid on the survey of clusters of galaxies that are considerably more distant than the Virgo Cluster, because within the Virgo Cluster the dispersion in distance is too great to allow for an accurate determination of the dispersion in absolute magnitudes of supernovae. The search in more distant clusters is therefore vital for the use of supernovae in establishing a reliable distance scale. Gratifying success has resulted from this effort, inasmuch as a dozen supernovae have been found in clusters of galaxies whose symbolic velocities of recession lie in the range from 3000 to 15000 km/sec.

*i*) The spectra of many supernovae, especially those of type I, still defy interpretation. There is considerable hope, however, that an identification of significant features will be possible on the following lines: within the expanding gas shells from a supernova, local explosive events (jets, shock waves, etc.) may be expected to produce sharp emission lines that are superposed on the luminous bands that defy interpretation because of their width (due to Doppler



effects of the integrated shell spectrum and overlaps with other wide bands). Through a succession of spectroscopic recordings made within a few hours, and even within 1 hour, it has been found that such sharp, temporary, but recurring features in the spectra actually exist. A particular attempt will be made to photograph short-term recurring patterns of sharp features in the expectation that such patterns can be correlated to and identified with patterns known from the study of other light-sources.

j) A study of *past supernovae* in neighboring galaxies has also been started, since they betray themselves by luminous, often circular, gas clouds whose expansion velocities may be determined through a spectroscopic analysis of their emission lines. Objects like the local galaxy IC 10 appear to be particularly suitable subjects for this study.

Before we proceed, it is advisable to list those objects found recently which, by various characteristics, have been identified with great probability as being supernovae. In doing this, we confine ourselves to the years following 1885, the year of the appearance of the supernova near the nucleus of the great galaxy in Andromeda. Also, we shall not repeat the data for the first 54 supernovae which were published by the author (Zwicky 1958), except to mention three corrections which concern the co-ordinates of the supernovae Nos. 9, 29, and 33. The correct positions for these objects for the epoch 1950.0 are as follows: No. 9,  $\alpha = 12^{\text{h}}20^{\text{m}}4$ ;  $\delta = +16^{\circ}6'$ ; No. 29,  $\alpha = 2^{\text{h}}34^{\text{m}}36^{\text{s}}$ ;  $\delta = +34^{\circ}16'$ ; No. 33,  $\alpha = 0^{\text{h}}55^{\text{m}}00^{\text{s}}$ ;  $\delta = -5^{\circ}16'$ .

Furthermore, we call the attention of the specialists and especially of the members of the committee for supernovae of Commission 28 of the International Astronomical Union to the fact that three of the supernovae which the present author had mentioned in his four Circular Letters to the members of the committee have been dropped from the final list as not having been sufficiently confirmed. These objects are those which were given the numbers 61, 62, and 89 in my four Circular Letters of October 30, 1960, and January 23, May 22, and December 20, 1961, respectively. It is proposed that inclusion in a contemplated appendix list of supernovae be postponed for all doubtful supernovae until multiple confirmation can be obtained from past records stored at various observatories. Continuation of the list of supernovae previously published is given in Table 1.

In the master list of Table 1 we have, for the time being, refrained from incorporating the most interesting star, which was discovered in November, 1961, by Professor L. Rosino in a location about  $7.5$  of arc from the nucleus of NGC 4501 (M88). Our dilemma, at present, consists in the fact that this star fits the characteristics neither of any known types of supernovae nor of any of the many types of stars in our own Galaxy. Unfortunately, because of continuous bad weather, none of the observers who collaborate with us at the three large observatories in California was able to obtain observations that would allow

TABLE 1  
LIST OF KNOWN SUPERNOVAE\*

No.	GALAXY	TYPE OF GALAXY	1950		$m_p$ GAL-AXY	$V_p$ (km/sec)	PROBABLE DATE OF MAXIMUM BRIGHTNESS	$\Delta_i$	$\Delta_s$	SN $m_{\max}$	TYPE OF SUPERNOVA	CLUSTER MEMBER	DISCOVERER	YEAR OF DISCOVERY	LITERATURE AND REMARKS
			R.A.	Decl.											
55.....	NGC 2841	Sb	9 <sup>h</sup> 18 <sup>m</sup> 36 <sup>s</sup>	+51°12'	10.5	+	Mar. 1957	106° W	73° N	<14.0	.....	.....	M. Schürer	1957	
56.....	NGC 4374	E	12 22 36	+13 10	10.9	+	May 1957	8 W	47 N	<13.0	.....	.....	G. Romano	1957	
57.....	NGC 1365 (M84)	Sb	3 31 48	-36 18	11.2	+	(Oct.) 1957	54 W	75 N	<16.5	.....	.....	H. S. Gates	1957	
58.....	NGC 5236	Sb	13 34 18	-29 37	8.0	+	(Dec.) 1957	41 W	145 N	<15.0	.....	.....	H. S. Gates	1957	
59.....	NGC 23	Sb	0 07 18	+25 39	12.7	+	Sept. 1955	10 E	10 N	<16.0	.....	.....	A. R. Sandage	1958	
60.....	NGC 1350	SbC	3 29 06	-33 48	11.8	+	Jan. 1959	22 E	70 N	<16.0	.....	.....	H. S. Gates	1959	
61.....	NGC 4921	SbC	12 59 12	+28 07	14.5	+	May 1959	16 E	48 S	<18.5	I	.....	M. L. Humason	1959	
62.....	Anon	SbC	13 08 51	+3 40	16.0	+	May 1959	7 E	3 S	14.1	II	.....	M. L. Humason	1959	
63.....	NGC 7331	Sb	22 34 48	+34 10	11.2	+	June 1959	32 W	13 N	13.0	.....	.....	M. L. Humason	1959	
64.....	Anon	SbC	2 47 12	-0 43	15.0	.....	Dec. 1959	28 E	20 N	18.5	.....	.....	C. E. Kearns	1960	
65.....	Anon	Sb	12 32 12	+9 10	15.5	+	Feb. 1960	5 E	6 S	16.0	.....	.....	M. L. Humason	1960	
66.....	Anon	Sb	12 04 36	+17 16	15.5	+	Feb. 1960	4 W	9 N	17.0	.....	.....	M. L. Humason	1960	
67.....	NGC 4321	Sc	12 20 24	+16 06	10.8	+	Sept. 1959	58 E	21 S	<<17.5	I	.....	M. L. Humason	1960	
68.....	Anon	SbC	8 17 21	+21 02	15.5	+	Mar. 1960	18 E	26 S	<16.0	.....	.....	M. L. Humason	1960	
69.....	NGC 4496	SbC	12 29 06	+4 12	12.0	.....	Apr. 1960	42 E	25 S	~11.0	.....	.....	M. L. Humason	1960	
70.....	Anon	Sc	11 28 30	+18 40	16.0	.....	Apr. 1960	14 E	16 S	<17.5	.....	.....	M. L. Humason	1960	
71.....	NGC 4096	Sc	12 03 30	+47 45	12.2	.....	June 1960	17 E	114 N	<14.5	.....	.....	P. Wild, M. L. Humason	1960	
72.....	Anon	SbB	12 24 24	+48 34	14.5	.....	June 1960	5 E	11 S	<18.5	.....	.....	M. L. Humason	1960	
73.....	NGC 4375	Sa	12 22 42	+28 58	14.0	+	June 1960	37 E	17 N	<18.5	.....	.....	M. L. Humason	1960	
74.....	Anon	SbC	22 42 42	+17 08	15.5	+	June 1960	10 W	6 S	<19.0	.....	.....	M. L. Humason	1960	
75.....	NGC 7177	Sb	21 58 28	+17 26	12.5	+	Aug. 1960	6 E	58 S	<16.0	.....	.....	M. L. Humason	1960	
76.....	Anon	Sb	8 32 55	+1 53	16.1	.....	Jan. 1960	5 E	5 S	<16.0	.....	.....	M. L. Humason	1960	
77.....	NGC 2565	SbB	8 32 54	+22 10	13.3	+	Aug. 1960	13 W	38 N	<17.5	I	.....	A. M. Gomes	1960	
78.....	Anon	Sc	8 33 12	+21 37	15.0	+	Sept. 1960	11 E	12 N	<16.5	.....	.....	A. M. Gomes	1960	
79.....	Anon	Sc	23 33 54	+27 39	17.0	.....	Nov. 1960	1 W	10 N	<18.5	.....	.....	M. L. Humason	1960	

\* Some supernovae which have only been announced in local observatory publications may have been intentionally omitted from our master list. This is, for instance, the case with the supernova of November 7, 1955, in an anonymous peculiar spiral galaxy ( $m_p \sim 15.1$ ), which is located at R.A. 08 40m45, decl. -16°41' (1950). The supernova, whose magnitude in November, 1955, was about  $m_p = 15.5$ , was discovered by G. Haro in the fall of 1957 ( $m_p > 18.5$  at that time) and announced in *Bulletin* No. 17, April, 1958, of the Tonantzintla and Tacubaya Observatories.

In order to have a more consistent listing of supernovae that will avoid the necessity of constant renumbering, we intend to adopt in the future a system similar to that of the numbering of the comets.

TABLE 1—Continued

No.	Galaxy	Type of Galaxy	1950		$m_V$ Gal-axy	$V_s$ (km/sec)	Probable Date of Maximum Brightness	$\Delta_1$	$\Delta_2$	SN $m_{\max}$	Type of Supernova	Cluster Member	Discoverer	Year of Discovery	Literature and Remarks
			R.A.	Decl.											
80.....	Anon	SO	2h34m30s	+1°07'	16.0	.....	Dec. 1958	1° W	7° N	<18.0	.....	.....	M. L. Humason	1960	Pub. A.S.P., 73, 175, 1961
81.....	Anon	Sc	1 03 30	+31 08	17.5	.....	Nov. 1960	4 E	2 N	<17.5	.....	.....	A. M. Gomes	1960	Pub. A.S.P., 73, 175, 1961
82.....	Anon	Sb	1 33 24	-5 45	18.5	.....	Dec. 1960	1 E	2 S	<17.5	.....	.....	M. L. Humason	1960	Pub. A.S.P., 73, 175, 1961
83.....	Anon	SBb	2 41 30	+0 34	16.1	.....	Jan. 1961	9 E	27 N	19.0	.....	.....	M. L. Humason	1961	Pub. A.S.P., 74, 215, 1962
84.....	IC 2363	SBc	8 22 52	+19 37	15.2	.....	Jan. 1961	9 E	18 N	18.5	.....	.....	M. L. Humason	1961	Pub. A.S.P., 74, 215, 1962
85.....	Anon	Sc	2 12 19	+40 53	16.4	.....	Jan. 1961	3 E	8 S	18.2	.....	.....	M. L. Humason	1961	Pub. A.S.P., 74, 215, 1962
86.....	NGC 4382 (M85)	SO	12 22 48	+18 28	10.5	+ 773	Dec. 1960	8 E	132 S	(12.0)	I	.....	H. S. Gates, L. Rosino	1961	Pub. A.S.P., 74, 215, 1962
87.....	Anon	EO	12 48 30	+28 06	14.7	+ 7638	Jan. 1961	32 E	12 S	16.5	I	Coma Cluster	C. E. Kearns	1961	Pub. A.S.P., 73, 185, 1961
88.....	Anon	SO	15 15 06	+5 14	15.7	+12899	Jan. 1961	10 W	2 S	<17.0	.....	Shane Cloud	A. M. Gomes	1961	Pub. A.S.P., 74, 215, 1962
89.....	NGC 3003	Sc irr	9 45 36	+33 39	12.5	+ 1476	Feb. 1961	34 E	17 N	<15.0	IV	.....	P. Wild	1961	Pub. A.S.P., 74, 215, 1962
90.....	Anon	Sa	12 15 08	+48 10	17.8	.....	Feb. 1960	1 E	8 S	~16.5	.....	.....	M. L. Humason	1961	Pub. A.S.P., 74, 215, 1962
91.....	Anon	Sb	10 19 36	+21 29	16.3	.....	May 1961	9 W	2 S	18.2	I	.....	M. L. Humason	1961	Pub. A.S.P., 74, 215, 1962
92.....	NGC 4564	E7	12 34 00	+11 43	12.1	.....	May 1961	0 EW	5 N	11.0	.....	.....	G. Romano	1961	Pub. A.S.P., 74, 215, 1962
93.....	NGC 4303 (M61)	SBc	12 19 18	+4 45	10.2	+ 1671	June 1961	82 E	12 S	13.0	III	Virgo Cluster	M. L. Humason	1961	Pub. A.S.P., 74, 215, 1962
94.....	Anon	Sc	16 09 47	+29 42	19.5	.....	June 1961	1°5 W	1°5 S	16.0	(III)	.....	C. E. Kearns	1961	Pub. A.S.P., 74, 215, 1962
95.....	Anon	Sc	12 00 48	+16 47	14.6	.....	June 1961	10 W	5 S	<16.3	.....	.....	M. L. Humason	1961	Pub. A.S.P., 74, 215, 1962
96.....	NGC 1058	Sc	2 40 12	+37 08	12.7	+ 440	July 1961	76 E	17 N	~14.0	V	.....	P. Wild	1961	Pub. A.S.P., 74, 215, 1962
97.....	Anon	Sb	1 07 11	+32 06	14.3	.....	Aug. 1961	16 E	37 N	17.0	.....	.....	C. E. Kearns	1961	Pub. A.S.P., 74, 215, 1962
98.....	IC 5342	EO	23 36 08	+26 44	15.3	.....	Sept. 1961	1 E	7 S	16.8	.....	Pisces (ZCs)	M. L. Humason	1961	Pub. A.S.P., 74, 215, 1962
99.....	Anon	Sc	2 32 32	+43 23	17.0	.....	Sept. 1961	2 W	10 N	17.0	.....	.....	M. L. Humason	1961	Pub. A.S.P., 74, 215, 1962
100.....	Anon	Sc	2 32 30	+37 25	14.2	.....	Sept. 1961	0 EW	36 S	15.0	.....	.....	P. Wild	1961	Pub. A.S.P., 74, 215, 1962
101.....	NGC 3221	Sc irr	10 19 37	+21 51	16.2	.....	(July 1961)	19 E	53 N	<17.5	.....	.....	P. Wild	1961	Pub. A.S.P., 74, 215, 1962
102.....	Anon	Sa	10 18 16	+21 58	15.8	.....	Nov. 1961	19 E	6 S	18.3	.....	.....	C. E. Kearns	1961	Pub. A.S.P., 74, 215, 1962
103.....	NGC 550	EO	1 07 15	+32 39	14.3	.....	Oct. 1961	11 W	5 N	17.0	.....	Pisces (ZCs)	M. L. Humason	1961	Pub. A.S.P., 74, 215, 1962
104.....	NGC 3938	Sb	11 50 06	+44 24	11.6	+ 874	Oct. 1961	20 W	13 N	17.2	.....	.....	M. L. Humason	1961	Pub. A.S.P., 74, 215, 1962
105.....	Anon	Sc	13 04 18	+28 08	15.6	.....	Dec. 1961	81 E	104 N	<14.0	II	.....	P. Wild	1961	Pub. A.S.P., 74, 215, 1962
106.....	Anon	E	10 30 48	-27 39	17.4	.....	Jan. 1962	11 W	7 N	16.5	I	Coma Cluster	F. Zwicky	1962	Pub. A.S.P., 75, 236, 1963
107.....	Anon	Irr	10 30 48	-27 39	17.4	.....	Jan. 1962	0 EW	2 S	<16.0	.....	Field of Hydra 1 Cluster	F. Zwicky	1962	Pub. A.S.P., 75, 236, 1963
108.....	Anon	Sa	15 20 42	+29 57	14.3	.....	Jan. 1962	5 E	1 S	<17.0	I	.....	F. Zwicky	1962	Pub. A.S.P., 75, 236, 1963
109.....	Anon	Sc	16 02 08	+17 43	18.5	.....	Jan. 1962	12 E	6 N	<18.0	.....	Field of Hercules Cluster	F. Zwicky	1962	Pub. A.S.P., 75, 236, 1963
110.....	Anon	Irr	9 36 00	+33 40	19.5	.....	Nov. 1961	3 W	5 N	<17.5	.....	.....	H. S. Gates	1962	Pub. A.S.P., 75, 236, 1963
111.....	Anon	EO	11 12 24	+26 10	17.5	.....	Feb. 1962	4 W	14 S	<19.0	.....	.....	K. Rudnicki	1962	Pub. A.S.P., 75, 236, 1963

us to draw any final conclusions. In a letter of March 16, 1962, Dr. F. Bertola of the Asiago Observatory reports as follows:

I give you the photographic magnitudes (in a provisional scale) of the star near M88, determined by Rosino.

17 Nov. 61	UT	3 <sup>b</sup> 47 <sup>m</sup>	13.0	Schmidt
19 "		3 55	13.0	"
30 "		4 8	13.0	"
4 Dec.		3 47	13.6	"
8 "		3 5	16.5	"
8 "		3 13	17.0	Telescope of 122 cm (GG 13)
9 "		3 00	14.0	Schmidt
10 "		4 55	14.0	"
12 "		3 37	14.2	"
15 "		2 3	14.0	"
16 "		2 39	14.3	"
18 "		3 40	14.0	"
20 "		4 45	14.5	"
6 Jan. 62		1 8	17.5	"
8 "		3 39	18.8	122 (GG 13)

From Jan. 10 to the last observations in March the star is seen near 18<sup>m</sup> or fainter (March 15 invisible,  $m > 18.0$ ).

In the Schmidt plates taken in 1959–60 and spring of 61 the object is not visible or faintly visible ( $\sim 18$ ).

I took two spectra in the nights of 21–22 Nov. and 1–2 Dec. 1961. In the opinion of Professor Rosino and myself the star may have been a supernova of type II for the following reasons:

- a) Continuum featureless spectrum with a far extension in the ultraviolet (through  $\lambda 3500$ ). The abnormal ultraviolet intensity is confirmed by some UBV photographic observations made near the maximum with the 122 cm.
- b) Rapid general fall of luminosity (5 magnitudes in 50 days).

Two things, however, are abnormal:

- 1) The presence in the same position of the supernova of a faint object, visible in the Palomar chart and perhaps in some of the Schmidt plates of 1959–60.
- 2) The very deep and sudden minimum between Dec. 4 and Dec. 8–9. Minima of this type might easily have escaped in other supernovae of type II for their short duration.

There are no variable stars which have spectral and light-curves of this type.

In February 1964 I observed that the brightness of the star rose again from  $m_p = 21.0$  (approximately) in 1962–63 to 19.0. This suggests that it is a galactic variable and not a supernova.

Unless the star brightens up again and allows some easy interpretation of its spectrum, it is intended to attempt the following tests: (a) Check on the position, proper motion, and magnitude of the star which existed in the position of the flareup on all the records obtained with large telescopes prior to November, 1961. (b) Obtain direct photographs with the 200-inch telescope under the very best conditions of seeing, in order to check whether or not the remnant of

Rosino's star is identical with the star that existed previously in the same position or near it. (c) Attempt, if possible, to obtain a readable spectrum of the remnant of the object which flared up twice in November and December, 1961. It is hoped that, along one of these avenues, results can be obtained which will allow us to recognize the true nature of Rosino's object.

## § 2. FREQUENCIES OF SUPERNOVAE (DIMENSIONLESS MORPHOLOGY)

### 2.1. THE TOTAL FREQUENCY OF SUPERNOVAE

We may inquire about the total number of supernovae that occur per year in a very large volume of space, or we may inquire about the frequency of occurrence in an average galaxy of a certain type. The first problem cannot be solved at the present time because we do not yet possess a reliable distance scale and because it has not so far proved feasible to survey constantly any given volume of space. The second question can be answered on the basis of the two systematic searches that have been made, namely, the searches from the Palomar Observatory in the respective periods from 1936 to 1941 and from 1956 to 1962. Calculations have actually been made only for the first period. Although voluminous, the reduction of the data for the first-mentioned period was much simpler than the reduction still to be made for the second period because only one telescope and two observers (F. Zwicky and J. J. Johnson) were involved. Very much work remains to be done to derive values for the frequency of occurrence from the more recent program, not only because at least six observatories are involved but also because even the reduction of the data obtained from the two Schmidt telescopes on Palomar Mountain will be laborious, since the not always equal efforts of at least five observers (Humason, Gates, Wild, Kearns, and Gomes) must be evaluated. It may be said, however, with some degree of assurance that the reduction of the data of the recent, much more extended search will not materially alter the original results obtained twenty years ago from the author's search for supernovae with the 18-inch Schmidt telescope (Zwicky 1942). These results are as follows:

a) In the period from September 6, 1936, to January 1, 1940, 837 galaxies listed in the Shapley-Ames catalogue were searched at exactly known intervals, and five supernovae were discovered in these galaxies. Taking into account the intervals between observations and the general behavior of the light-curves of supernovae, an average frequency of occurrence of

$$\nu_1 = \text{One supernova per 359 years per galaxy} \quad (1)$$

was derived. Additional estimates from a less well-controlled collection of about 3000 galaxies brighter than the apparent photographic magnitude  $m_p = 15$ , in which we found 12 supernovae in the period mentioned, resulted in a frequency of

$$\nu_2 = \text{One supernova per 430 years per galaxy.} \quad (1a)$$

The first value  $\nu_1$  is to be taken as the more reliable, since it refers to nearer and better-controlled galaxies and since these galaxies all lie in a definite range of apparent luminosities ( $m < 13$ ) and presumably also in a definite range of absolute photographic luminosities ( $M_p < -16$ ), belonging to the classes of giant and intermediate galaxies.

*b)* As to the occurrence of supernovae in various types of galaxies, it could be said from the original search only that supernovae occur in spirals and in ellipticals at a rate roughly proportional to the relative numbers of these types.

*c)* Some galaxies, like NGC 3184, 4321, 5236, 6946, etc., had two or three supernovae each within a few decades.

*d)* Finally, it was observed that, remarkably enough, supernovae were found in pronounced dwarf galaxies, indicating that either these galaxies must exist in rather unexpectedly large numbers or that, quite inexplicably, per star they are far more prolific producers of supernovae than are the bright galaxies.

TABLE 2  
FREQUENCIES OF SUPERNOVAE WITH RESPECT  
TO TYPE OF GALAXY

	Per Cent in Shapley- Ames Catalogue	Per Cent Supernovae
Elliptical galaxies.....	23.8	13.2
Irregular galaxies.....	3.4	5.7
Spiral galaxies.....	72.8	81.1

## 2.2. THE FREQUENCY OF SUPERNOVAE IN VARIOUS TYPES OF GALAXIES

As mentioned above, the few supernovae discovered during the first systematic search with the 18-inch Schmidt telescope were distributed over the various structural types of galaxies roughly in proportion to the numbers of the various galaxies included in the search. A more extensive statistics has just been published by Ch. Bertaud (1961), using all the supernovae discovered between 1885 and July, 1961, in 806 galaxies selected from the Shapley-Ames catalogue. These supernovae were distributed over the various types of galaxies as shown in Table 2. As to the distribution of the various normal spiral galaxies in the Shapley-Ames catalogue and the relative numbers of supernovae which appeared in them, Bertaud (1961) arrives at the data given in Table 3.

It appears from these data that the ellipticals do not have as many supernovae, per galaxy, as the spirals and, likewise that the Sa's do not produce as many supernovae (none was found, in fact) as the types Sb and Sc. It may, however, not be too safe to take these results at face value and therefore to conclude that the frequency of supernovae is really smaller in ellipticals and in Sa spirals, since it was found that selective effects may have vitiated the results.

Indeed, if supernovae had appeared in the dense and normally overexposed, very luminous central disks of the bright elliptical and spiral Sa galaxies, they would almost certainly have been missed by most searchers. For instance, the supernova No. 92 discovered by G. Romano (5'' north of the nucleus on a short-exposure plate), in NGC 4564 was missed for this reason by the Palomar observers, although they had scanned plates near the maximum brightness of that supernova. To check on the real frequency of supernovae in the types of galaxies that possess a large and very luminous central disk, a renewed and laborious search on underexposed plates will therefore be necessary.

TABLE 3  
FREQUENCIES OF SUPERNOVAE WITH RESPECT  
TO SUBTYPE OF SPIRAL GALAXY

	Type	Per Cent in Shapley- Ames Catalogue	Per Cent Supernovae
Spirals.....	Sa	16.4	0
Spirals.....	Sb	33.6	35.1
Spirals.....	Sc	50.0	64.9

TABLE 4  
FREQUENCIES OF TYPE I SUPERNOVAE WITH RESPECT  
TO TYPE OF GALAXY (AFTER BERTAUD)

	Type	No. of Supernovae of Type I	Percentages
Elliptical galaxies.....		5	26
Irrregular galaxies.....		2	11
Spiral galaxies.....	Sa	0	0
Spiral galaxies.....	Sb	1	5
Spiral galaxies.....	Sc	11	58

In a later section we shall discuss the various types of supernovae. The type I among these is the most frequent so far, and Bertaud (1961) finds 19 objects of this type distributed over the various types of galaxies in the proportions shown in Table 4. The percentages of Sc and ellipticals in the Shapley-Ames catalogue are, respectively, 50 and 23.8 per cent, so that they are about in the same proportion as the numbers of supernovae of type I that appeared in these two types of galaxies.

Since, so far, no supernovae of type II have been found in elliptical galaxies, the relative deficiency of supernovae of all types in elliptical galaxies might be blamed on the non-occurrence of supernovae of type II or, generally, on the

non-occurrence of types of supernovae other than type I in the elliptical galaxies. Also, as Bertaud and others have pointed out, supernovae, on the basis of the present slim data, seem to occur relatively too frequently in irregular galaxies. Considering, however, selectivities of the type that I have mentioned above, it would seem too early to draw any too definite conclusions as to the relative frequency of occurrence of supernovae in general and of various special types of supernovae in particular in various structural types of galaxies.

### 2.3. THE FREQUENCY OF SUPERNOVAE IN CLUSTERS OF GALAXIES

Until recently, far too few clusters of galaxies have been searched for supernovae. If we wish not only to obtain values for the frequency of supernovae in clusters but also to differentiate between the different types of clusters of

TABLE 5  
SUPERNOVAE FOUND IN WELL-KNOWN  
CLUSTERS OF GALAXIES

Cluster	$V_s$ (km/sec)	No. of Supernovae
Pisces Cloud.....	5340	3
Fornax I Cluster.....	1700	2
Perseus Cluster.....	5433	.....
Cancer Cluster.....	4865	5
Virgo Cluster.....	1136	14
Coma Cluster.....	6728	5
Hydra I Cluster.....	4000	1
A-cluster.....	.....	(1)
Corona Borealis Cluster.....	21651	0
Shane Cloud (1 redshift only).....	(13000)	(1)
Hercules Cluster.....	10400	(1)

galaxies, perhaps only the 48-inch Schmidt telescope on Palomar Mountain and similar instruments are suitable. If enough manpower were available, a survey for supernovae along the following lines would be most desirable: (*a*) search for supernovae in compact, medium-compact, and open clusters of galaxies which have the same redshifts; (*b*) search for supernovae in compact or medium-compact clusters of galaxies which have the same redshift but whose populations contain different relative numbers of elliptical, spiral, and irregular galaxies; and (*c*) search for supernovae in clusters at widely varying distances.

Because only one observer has, on a part-time basis, pursued these aims, our results are naturally most incomplete, and only very preliminary data have been obtained on the above program *b*. On program *c* the data are still more scanty and concern, so far, only clusters whose redshifts are in the range from 1000 to about 15000 km/sec. The numbers of supernovae found in various clusters are given in Table 5.

The distribution of the supernovae found so far in the clusters in Cancer,



Coma, and Virgo are shown in Figures 3, 4, and 5. The distribution of the supernovae in the spherically symmetrical and apparently stationary clusters of Coma, Cancer, and Hydra is of great interest for the following two reasons.

In the first place, if the galaxies in a stationary spherical cluster are distributed as the mass in an isothermal gravitational gas sphere, the number of supernovae in rings of equal width  $d$  around the center of the cluster should tend

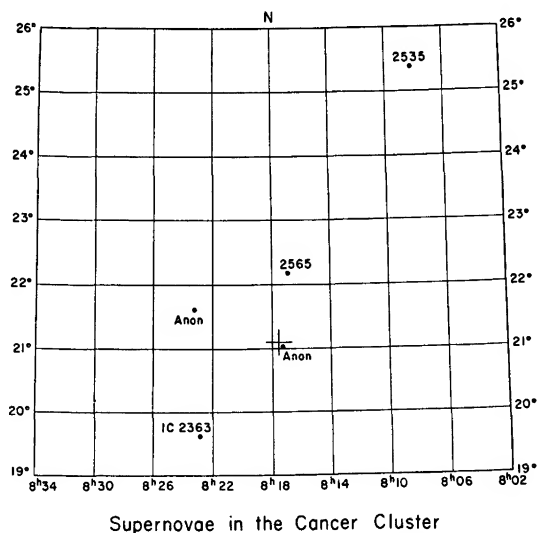


FIG. 3.—Distribution of supernovae which have appeared in the Cancer Cluster of galaxies, whose center at R.A.  $8^{\text{h}}17^{\text{m}}6$  and Decl.  $+21^{\circ}06'$  (epoch 1950.0) is marked by a cross.

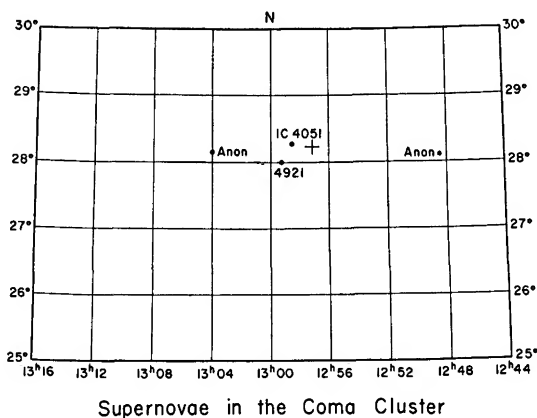


FIG. 4.—Distribution of supernovae found in the Coma Cluster of galaxies. The center of the cluster at R.A.  $12^{\text{h}}56^{\text{m}}5$ , Decl.  $+28^{\circ}13.5'$  (1950.0) is marked by a cross. As mentioned in the text, supernova No. 73 in NGC 4375 probably should also be assigned to the Coma Cluster. It is not included in Fig. 4.

toward a *constant value* as the radius  $r$  of the ring increases. Beyond the periphery of the cluster, the number  $n(r)$  of supernovae per ring of equal width should increase *proportional to the radius*. The scant data (see Figs. 3, 4, 5) so far available confirm the first conclusion. The field around the Coma Cluster or any other compact spherical cluster of galaxies has, however, not been searched far enough to determine the turning point in the frequency function

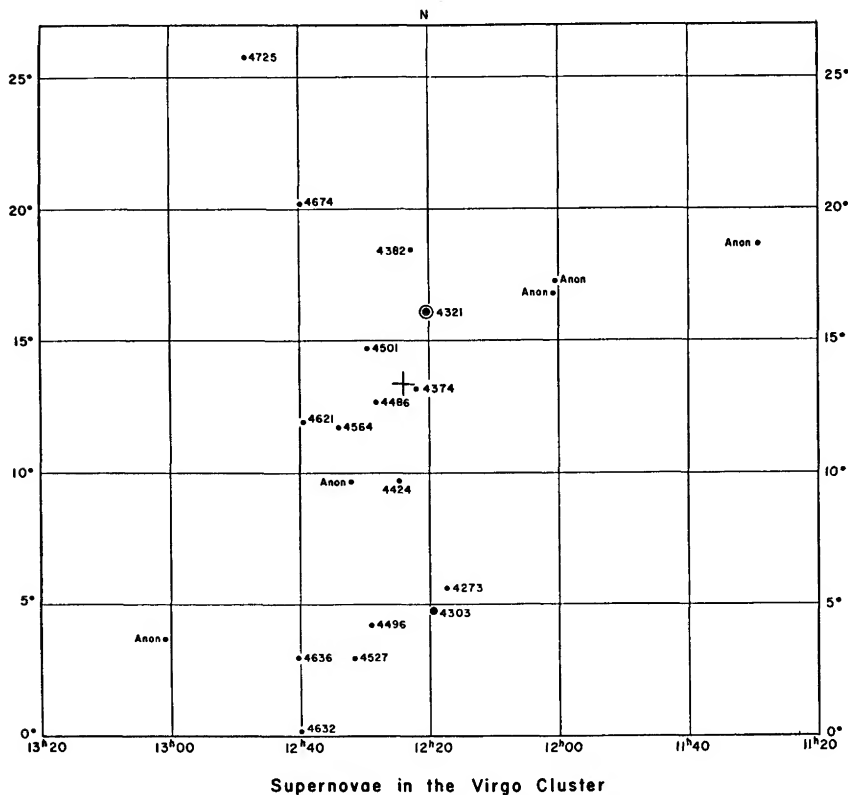


FIG. 5.—Distribution of supernovae in the Virgo Cluster of galaxies. The center of the cluster at R.A.  $12^{\text{h}}24^{\text{m}}00^{\text{s}}$  and Decl.  $+13^{\circ}20'$  (1950.0) is marked by a cross.

$n(r)$ . Nevertheless, from the data available on the supernovae in the clusters in Coma and Cancer, we see that the turning points appear to be at radii greater than about  $4^{\circ}$ . For this reason, the criticisms (Noonan 1961) voiced during the past decades of the determination by the author (Zwicky 1957, 1959) of a minimum diameter of  $12^{\circ}$  for the Coma Cluster find here an additional rejection.

The contention that the diameter of the Coma Cluster is much greater than the  $3^{\circ}$  advocated by recent critics of the author's value of at least  $12^{\circ}$  is also vastly strengthened by recent observations by the author of the dispersion in redshifts (or in symbolic velocities of recession  $V_s = c\Delta\lambda/\lambda$ ) at various distances

from the center of the clusters in Coma, Cancer, and Hydra I. These results will be presented and discussed elsewhere. I wish only to mention in passing that, as we explore the region around the Coma Cluster to ever greater distances from the center, the new results gained invariably tend to confirm the suspicion that the radius of the cluster may be even greater than the  $6^\circ$  derived from a study (Zwicky 1957, 1959) of the isopleths (equal population contours). For instance, in the course of finishing this manuscript, I had the good fortune to obtain a spectrum of NGC 4375, the parent galaxy of the supernova No. 73 of Table 1. With an apparent photographic magnitude of  $m_p = 14.0$  (equal to that of some of the brightest galaxies in the Coma Cluster) and a diameter of about  $50''$  of arc, the chance for this galaxy to have a symbolic velocity of recession in the range  $5000 \text{ km/sec} < V_s < 10000 \text{ km/sec}$  is less than one-tenth the chance for it to be in the range  $2500 \text{ km/sec} < V_s < 5000 \text{ km/sec}$ . My measures show that, actually,  $V_s = 9165 \text{ km/sec}$ , at the upper limit of our expectation for the values of  $V_s$  of members of the Coma Cluster. This is a remarkable result, since NGC 4375 is at a distance of almost  $8^\circ$  from the center of the Coma Cluster.

### § 3. STATISTICS AS RELATED TO PHENOMENOLOGICAL CHARACTERISTICS OF SUPERNOVAE AND OF GALAXIES IN WHICH THEY APPEAR (PHENOMENOLOGICAL MORPHOLOGY)

#### 3.1. THE RELATIVE LUMINOSITIES OF GALAXIES AND OF SUPERNOVAE

If the difference in apparent magnitudes  $m_s$  and  $m_g$  of a supernova and the galaxy in which it appears is

$$\Delta m = m_s - m_g, \quad (2)$$

the difference in their absolute magnitudes is

$$\begin{aligned} \Delta M &= (m_s - \delta) - m_g \\ &= \Delta m - \delta. \end{aligned} \quad (3)$$

Since we may, in general, assume that both the supernova and the galaxy have been dimmed in the same manner by interstellar and intergalactic dispersed matter, the quantity  $\delta$  has its origin entirely in the action of interstellar dispersed matter *within* the parent galaxy of the supernova.

From Table 1 it is seen that the values of  $\Delta m$  so far observed lie in the range  $+2$  to  $-5$ , the upper values applying to cases like the supernova of 1885 in Andromeda and  $\Delta m = -5$  for the supernova of 1937 in IC 4182, for instance. If, however, we assume that, for supernova No. 17 (probably type V) in NGC 5236 ( $m_p = +8.0$ ), the magnitude  $m_p(SN) = +14.0$  corresponds to the brightness near maximum, we would have values for  $\Delta m$  as high as  $+6$ , and the range for  $\Delta m$  would be from  $+6$  to  $-5$  at least.

A very important conclusion suggests itself when we consider the fact that a fair number of supernovae have appeared in dwarf galaxies, in which cases

$\Delta m < 0$ . For instance, the relative number of supernovae for which  $\Delta m$  lies, respectively, in the ranges  $2 > \Delta m > -1.5$  and  $-1.5 > \Delta m > -5$  appears to be only about 5 to 1. If, therefore, the frequency of supernovae is roughly proportional to the amount of luminous matter in a galaxy, the number of galaxies in the range of absolute magnitudes  $M_{\max} + 3.5$  to  $M_{\max} + 7.0$ , in a given large volume of space, must be about five times greater than the number of galaxies in the range  $M_{\max}$  to  $M_{\max} + 3.5$ , where  $M_{\max}$  is the absolute magnitude of the brightest galaxy that has been searched for supernovae. This result is in excellent agreement with the luminosity function  $n(M) \sim 10^{0.2(M-M_{\max})}$ , which was derived by the author from an investigation of clusters of galaxies (Zwicky 1957).

### 3.2. THE SPATIAL DISTRIBUTION OF SUPERNOVAE WITHIN THEIR PARENT GALAXIES

For large enough redshifts, that is, for values of the symbolic velocities of recession  $V_*$  greater than 500 km/sec, we shall assume the *indicative* distances  $D_i$  (see Zwicky and Humason 1960, 1961, 1964 for the definition of indicative distances) of the respective galaxies to be given by

$$D_i = V_*/100 \quad \text{million parsecs,} \quad (4)$$

where  $V_*$  is expressed in km/sec. This assumption corresponds to a Lundmark-Hubble<sup>1</sup> constant for the universal nebular redshift of 100 km/sec per million parsecs.

If a supernova appears at a distance of  $\Delta$  seconds of arc from the nucleus of a galaxy, the *indicative distance* of this supernova from the nucleus, in a plane normal to the line of sight from the observer, is

$$\Delta_{SN} = V_* \Delta \times 10^4 / 206250 \quad \text{parsecs.} \quad (5)$$

In Table 6 we give the values of  $\Delta_{SN}$  for some of the best-investigated supernovae listed in Table 1.

In Figure 6 we have plotted the results listed in Table 6. We expect that, as a first approximation, for all distances involved, the statistical distribution of the values of  $\Delta$  should be the same. The plot in Figure 6 tends to confirm this expectation, although, for a final proof, data on several hundred supernovae will be needed. Since the distribution of the values of  $\Delta$ , in contradistinction to most other tests for the properties of various cosmological models, is entirely independent of obscuration by interstellar and intergalactic dust and is not affected

<sup>1</sup> Knut Lundmark was the first to relate the universal redshift to the distance  $D$ , expressing the relative shift in wavelengths as  $\Delta\lambda/\lambda = aD + bD^2$ , or, as it is now commonly written, the "symbolic velocity of recession"  $V_* = HD + D^2$ . E. P. Hubble later derived for  $H = 550$  km/sec per million parsecs a value which is now thought to be too large by a factor of the order of 4 or 5. (For some of the history on the subject see my article "Knut Lundmark and Man's March into Space" in *Knut Lundmark: A Memorial Volume*, published by Värld och Velande, Göteborg, Sweden, in 1961.)

TABLE 6\*

INDICATIVE DISTANCES, NORMAL TO LINE OF SIGHT, OF A  
NUMBER OF RECENT SUPERNOVAE FROM CENTERS  
OF THEIR PARENT GALAXIES

No.†	NGC	$V_s$ (km/sec)	$\Delta_{SN}$ (In $10^3$ Parsecs)
54. ....	3992	+ 1059	3.51
55. ....	2841	584	3.74
56. ....	Messier 84	954	2.17
57. ....	1365	1672	7.49
58. ....	5236	491	3.59
59. ....	23	4568	3.14
60. ....	1350	1780	6.30
61. ....	4921	5459	13.4
62. ....	Anon	2994	1.1
63. ....	7331	+ 780	1.3
65. ....	Anon	12924	4.8
66. ....	Anon	6741	3.1
67. ....	4321	1617	4.8
68. ....	Anon	5008	7.8
77. ....	2565	3684	6.5
78. ....	Anon	4349	3.4
85. ....	4382 (M85)	773	4.8
87. ....	Anon	7638	12.6
88. ....	Anon	12899	6.8
89. ....	3003	1476	2.7
93. ....	4303 (M61)	1671	6.7
105. ....	3938	+ 874	5.6

\* After finishing this manuscript, the author obtained a spectrum of NGC 4375, the parent galaxy of the supernova No. 73 and derived, for its symbolic velocity of recession,  $V_s = 9165$  km/sec. This value, combined with  $\Delta = 40.7$  results in an indicative distance of the supernova from the nucleus of the galaxy equal to  $\Delta_{SN} = 18.8 \times 10^3$  parsecs, the greatest yet found.

† The numbers given in this column are those assigned to the supernovae in master list, Table I, and *Handbuch der Physik*, Vol. 51, 1958.

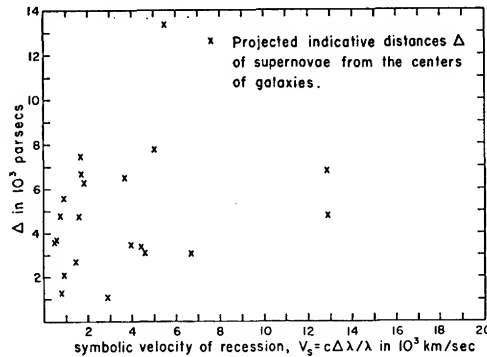


FIG. 6.—Indicative distances  $\Delta$  of supernovae from the centers of their parent galaxies, as projected on the planes normal to the lines of sight to these centers, are plotted in dependence on the symbolic velocities of recession  $V_s = c\Delta\lambda/\lambda$  of their parent galaxies. ( $\Delta\lambda$  = redshift.)

by the universal redshift, it will be most important to extend the plot of Figure 6 to as great values of  $V_s$  as possible. A more complete plot of the type shown in Figure 6 will also enable us to fix a physically significant diameter for galaxies.

In Figure 7 we plot the number of supernovae whose distances  $\Delta$  from the nuclei of their parent galaxies fall into the intervals 0-2, 2-4, and so on, in units of 1000 parsecs. It is seen that the greatest values of  $\Delta$  correspond roughly to half the diameter of the largest galaxies, such as the Milky Way system and Messier 31. As more data become available, the maximum values of  $\Delta$  will indicate what the most probable value of the Lundmark-Hubble constant might be. Furthermore, it will be interesting to see from a more complete diagram whether  $n(\Delta)$  for moderate and large values of  $\Delta$  is essentially independent of  $\Delta$ , as we might expect it to be for galaxies within which the distribution of matter, on the average, is roughly similar to that in an Emden isothermal gravitational gas sphere.

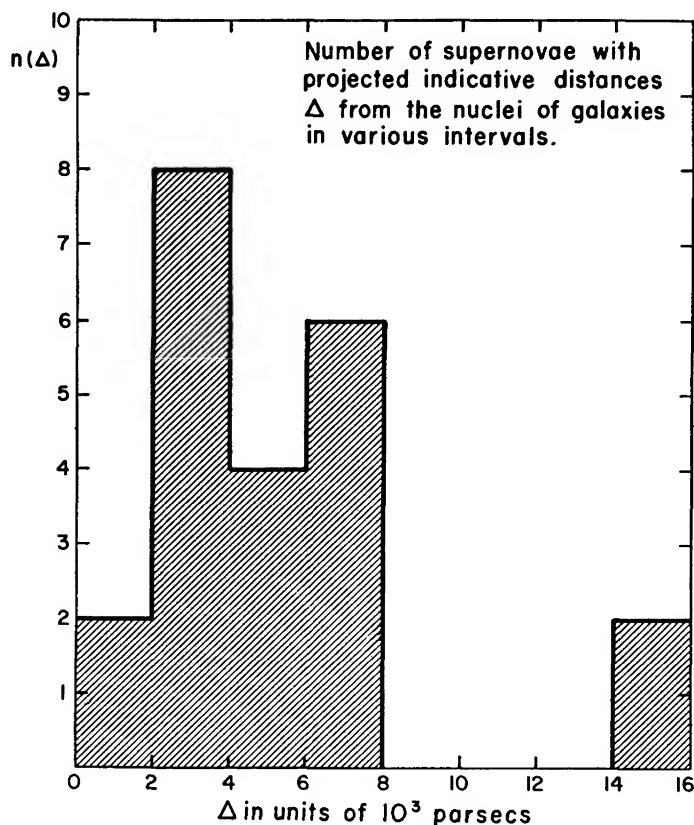


FIG. 7.—Number of supernovae  $n(\Delta)$  with projected indicative distances  $\Delta$  from the nuclei of their parent galaxies in various intervals of  $\Delta$ , which latter are expressed in units of 1000 parsecs.

Finally, it is of interest that very small values of  $\Delta$  seem to be rather infrequent. This, however, for the time being, we interpret as being due to the difficulty already mentioned, that supernovae are easily missed in a photographic search if they flare up in the central luminous disks of galaxies.

### 3.3. THE DISTRIBUTION OF SUPERNOVAE IN APPARENT MAGNITUDES

The distribution in apparent magnitudes  $m = m_{\max}$  at maximum luminosity of all supernovae in a given part of the sky would be given by the relation

$$\log_{10} N = 0.6 m - c, \quad (6)$$

where  $c$  is a constant, provided that (a) the distribution-curve of the absolute magnitudes  $M_{\max}$  is bell-shaped around some value  $M_{\max}^0$ ; (b) all supernovae in the said part of the sky were discovered; and (c) the distribution of the galaxies searched for supernovae is uniform in space.

As a first approximation we may assume (a) and (c) to be correct for the searches conducted at Palomar for supernovae whose apparent magnitudes at maximum were  $m_{\max} < 16.0$ . Assumption (b), however, is certainly far from the truth and must be replaced by a better one, which we shall now formulate.

We first rewrite equation (6) as

$$K \log_e N = 0.6 m - c, \quad (7)$$

where  $K = \log_{10} e = 0.4343$ . Differentiating equation (7), we obtain

$$\frac{dN}{N} = \frac{0.6}{K} dm. \quad (8)$$

The actually found number,  $dN^1$ , of supernovae per magnitude interval  $dm$  is, of course, the smaller, relative to  $dN$ , the fainter the supernovae are, since images of these supernovae appear above the limiting magnitude  $m_L$  of a given search for ever shorter intervals  $\tau$  of time. These intervals can be determined for known light-curves of supernovae. For purposes of calculation, we use the formalized light-curve shown in Figure 8.

The probability  $P(m)$  for a supernova of maximum magnitude  $m$  to be detected is

$$P(m) = a(m_L - m), \quad (9)$$

where  $a = \text{const.}$

The number  $dN^1$  of supernovae in the magnitude interval  $m$  to  $m + dm$  which we may expect to detect is, therefore,

$$dN^1 = P dN = a(m_L - m)dN. \quad (10)$$

As applied to the continuous search over many years with the 18-inch Schmidt telescope and similar instruments, we have  $m_L \sim 16.0$  and  $a \sim \frac{1}{8}$ , since a

supernova of  $m_{\max} = 8$  may be expected to be detectable as long as one year. We therefore find

$$\begin{aligned} \text{A. } dN^1 &= dN && \text{for } m_{\max} < m_0 (=8.0), \\ \text{B. } dN^1 &= a(m_L - m)dN && \text{for } m_0 < m_{\max} < 16.0, \\ \text{C. } dN^1 &= 0 && \text{for } 16.0 < m_{\max}. \end{aligned} \quad (11)$$

In order to derive the function  $N^1(m)$ , we must obviously integrate relation (10) for the region B. We obtain from equations (7), (8), and (10)

$$dN^1 = \frac{0.6a}{K} (m_L - m) N dm = \frac{0.6a}{K} e^{-c/K} (m_L - m) e^{0.6m/K} dm. \quad (12)$$

The number  $\Delta N^1$  of supernovae expected in the interval of apparent magnitudes at maximum  $m_{\max} = 8.0$  to  $m_{\max} = m$  is, therefore,

$$\begin{aligned} \Delta N^1 &= \frac{0.6a}{K} e^{-c/K} \left( m_L \int_{m_0}^m e^{0.6m/K} dm - \int_{m_0}^m e^{0.6m/K} m dm \right), \\ \Delta N^1 &= aN \left[ \left( m_L - m + \frac{K}{0.6} \right) - \left( m_L - m_0 + \frac{K}{0.6} \right) e^{(0.6/K)(m_0 - m)} \right]. \end{aligned} \quad (13)$$

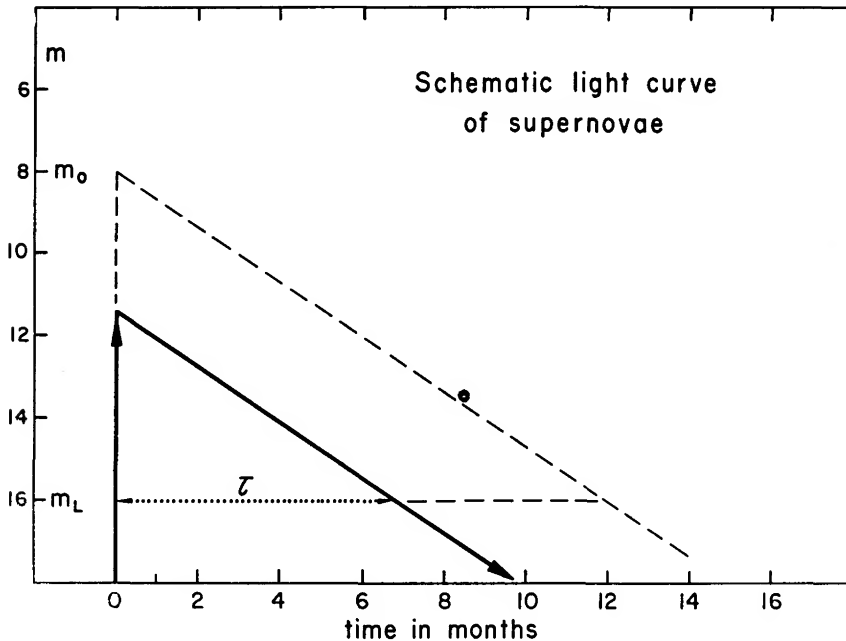


FIG. 8.—Schematic light-curve of supernovae.  $\tau$  = period of detectability;  $m_L$  = limiting apparent magnitude to be reached with the telescope used in the search for supernovae. The inclined dashed line is the light-curve of a supernova whose detection on a yearly search with the 18-inch Schmidt telescope at Palomar is certain.



In the limits, we have, for  $m = m_0$ ,

$$\Delta N^1 = 0, \quad (14)$$

$$\text{for } m = m_L, \quad \Delta N^1 = a N \left[ \frac{K}{0.6} - \left( m_L - m_0 + \frac{K}{0.6} \right) e^{(0.6/K)(m_0 - m_L)} \right],$$

or, numerically, for  $m_L = 16.0$ ,  $m_0 = 8$ ,  $a = \frac{1}{8}$ ,

$$\Delta N^1 = \frac{N(16)}{8} (1.38 - 9.38 e^{-11})$$

$$= 1.38 \frac{N(16)}{8} = 0.17 N(16). \quad (15)$$

The theoretically expected (relative) number of supernovae, as a function of  $m_{\max}$ , is plotted in Figure 9 as the solid curve. For  $m_{\max} < 8.0$ , we have  $\log N = 0.6 m_{\max} + \text{const.}$ ; for  $8 < m < 16$ , the values given by formula (13) are plotted, and for  $m > 16.0$ , the number  $N$  remains constant, since fainter supernovae cannot be detected with a telescope which reaches only objects brighter than those of the limiting magnitude  $m_L = 16.0$ .

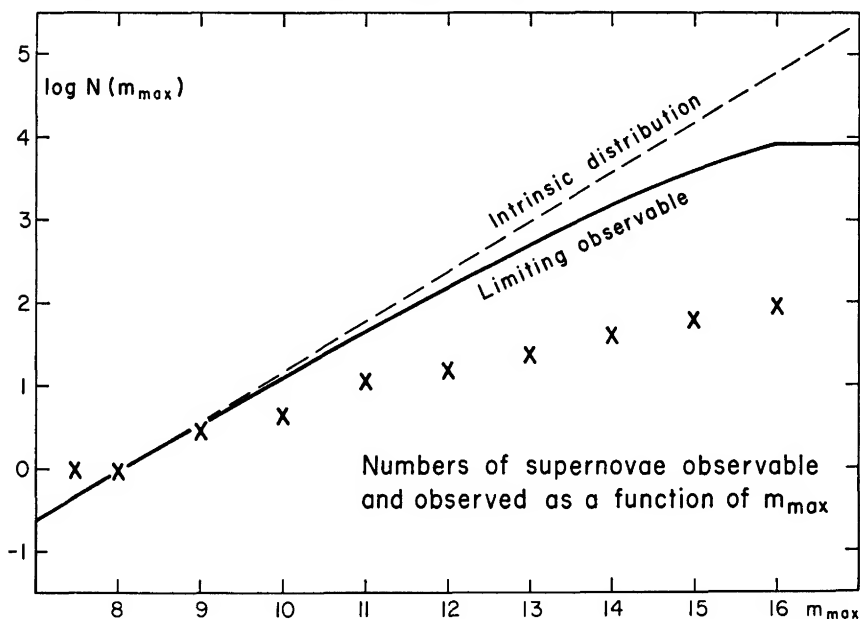


FIG. 9.—Numbers  $N(m_{\max})$  of supernovae which are ideally observable and which are actually observed (indicated by the crosses) in dependence upon their apparent visual magnitudes at maximum brightness. The dashed line characterizes their intrinsic distribution in the absence of clustering of galaxies according to relation (6). The solid line represents the expected number of supernovae according to relation (13) for the range  $8 < m < 16$ , relation (6) for  $m < 8$ , and  $n = \text{constant}$  for  $m > 16$ . The crosses represent the actual distribution for which fair upper limits of  $m_{\max}$  are known.

It is seen that, for all values  $m > 9$ , the number of supernovae discovered ( $\times$ ) falls far short of those expected by formula (13). Some of the reasons for this shortage are as follows:

a) For most of the fainter supernovae the magnitudes at maximum remain undetermined, and the very conservative values which I have used are certainly much too faint.

b) The galaxies in which the brighter supernovae appear are selectively searched much more often than the galaxies in which the fainter supernovae appear.

c) Because of the inclusion of the large clusters in Virgo, Fornax, and so on, the space density of the brighter supernovae in our collection is relatively much too great when compared with the space density of fainter supernovae.

Corrections for all these effects will become possible only when good data on several hundred supernovae are available. If the theory which led to relation (13) is then applied to the results of the recent systematic searches exclusively, good agreement between the predicted and the actually discovered numbers of supernovae to the limit  $m_L$  should be expected. Indeed, the very great discrepancy between the theoretical curve and the distribution of the 77 supernovae found certainly results mainly from having plotted the data for all supernovae found since 1885. From 1885 until the first Palomar search in 1936, only apparently bright supernovae were at all likely to be found. The same is true for all search programs and especially for most accidental discoveries for the whole period covered from 1885 to 1962. Fainter supernovae were thus heavily discriminated against. In a few years, however, using only data from the modern search programs, significant statistical data should become available.

### 3.4. THE MAGNITUDE-REDSHIFT RELATION.

If the universal redshift or the symbolic velocity of recession  $V_s$  were strictly proportional to the distance and if all supernovae, say those of type I, had the same absolute visual magnitude  $M_{\max}$  at maximum brightness, we should have

$$\log_{10} V_s = 0.2 m_{\max} + \text{constant}, \quad (16)$$

provided that no interstellar or intergalactic absorption affects the relation between the apparent and the absolute magnitudes. In Figure 10 we present a preliminary plot of the observed relation between  $V_s$  and  $m_{\max}$  for a few supernovae of type I. The point marked *Virgo* represents the average of seven supernovae of type I in the Virgo cluster. The numbers of the other three points correspond to the numbering in the master list established by F. Zwicky (1958) (see Table 1). The apparent magnitudes in Figure 10 need to be corrected eventually for interstellar absorption both in the Milky Way and in the parent galaxy, as well as for intergalactic obscuration. Although no reliable data are available at the present time to evaluate these corrections, the plot in Figure 10 suggests that the dispersion in absolute magnitudes of type I supernovae seems

surprisingly small and that, for the range plotted, relation (16) holds good. From recent discoveries, data are available on about ten additional supernovae of the type I, but these have not been analyzed sufficiently as yet to be incorporated in the plot of Figure 10.

### 3.5. THE VARIOUS TYPES OF SUPERNOVAE

In order to classify supernovae, all our knowledge on the character of the light-curves in various colors, the spectral characteristics as well as available

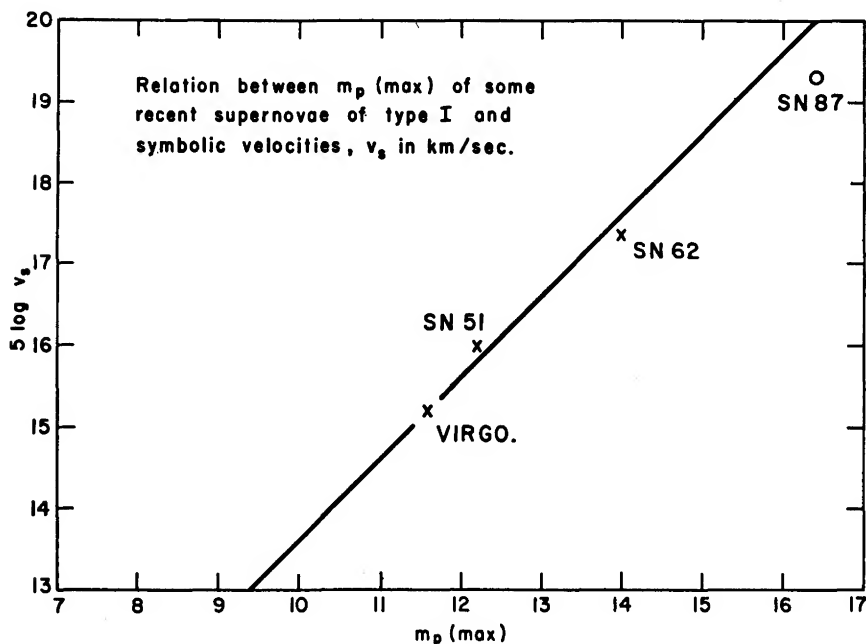


FIG. 10.—Relation between the photographic apparent magnitude  $m_p$  (max) at maximum brightness and the symbolic velocity of recession  $V_s = c\Delta\lambda/\lambda$  (expressed in km/sec) for some recent supernovae of type I.

information on absolute magnitudes, frequencies, and appearance in different types of galaxies and locations within them needs to be mobilized. It now appears, indeed, that some supernovae which have similar light-curves have quite different spectra. Vice versa, supernovae which have similar spectra over long periods of time may have different light-curves and in some cases (types II and V, for instance) quite different absolute magnitudes. We shall in the following discuss some of the available facts on these various characteristics. So far, the spectra have furnished the most useful pointers for a comprehensive classification, this in spite of the fact that most of them have not yet proved interpretable! On the other hand, the usefulness of  $U$ ,  $B$ ,  $V$  magnitudes for the physical

interpretation of the intrinsic properties of supernovae has been greatly overrated by many investigators for reasons which will be presented below.

3.5.1. *Supernovae of type I.*—The apparently brightest supernova discovered at Palomar was the one in IC 4182 of 1937 (No. 25 in the master list). Its photographic and photovisual magnitudes at maximum were about  $m = 8.2$ , and its light-curve, which could be followed for over 600 days, is shown in Figure 11, while on Plate I, *A*, four successive stages of the supernova, as photographed with the 18-inch Schmidt telescope, are reproduced. The light-curves of all supernovae of type I are quite similar to that of the supernova in IC 4182, but the spectra which are described below serve best to distinguish type I supernovae from all other types.

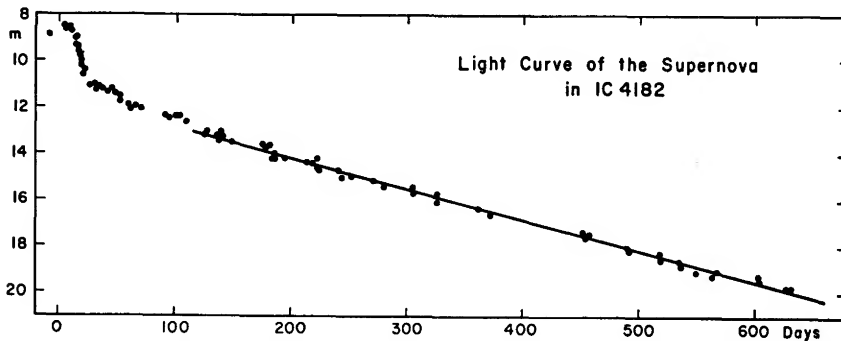


FIG. 11.—Photographic light-curve of the bright supernova No. 25 in IC 4182 as it was originally determined by W. Baade and F. Zwicky (1934). In view of subsequent developments in the photometry of stars and galaxies, some of the magnitude sequences established for the earlier supernovae found in our searches may need to be recalibrated.

*a) Some features of the light-curves of type I supernovae.*—In Figure 12 we show schematically some features of the light-curves of type I supernovae which are significant for the use of supernovae as distance indicators and for the ultimate analysis of their intrinsic characteristics. First, there is a sharp and immense rise in luminosity, which is followed by a broad maximum, lasting several days. A sharp decline leads to the point  $P_1$ . The width of the top of the light-curve at  $P_1$  always seems to be of the order  $\tau_1 \sim 50$  days. Curiously enough, the small protrusion between  $P_1$  and  $P_2$  always seems to be present. Between  $P_2$  and  $P_3$  the decline of the photographic and photovisual magnitudes  $m_p$  and  $m_v$  seem to be more or less linear in time  $t$ , with, however, considerable excursions in different colors. The linear declines,  $1 \text{ mag. loss per } \tau_2 \text{ days}$ , for several supernovae of the type I are listed in Table 7.

There are thus much wider variations in  $\tau_2$  than has been assumed by investigators who have attempted to associate the semilinear decline in  $m$  with the idea that the source of the light of a supernova of type I during its later stages is to be looked for in the disintegration of certain radioactive isotopes,

such as californium 254 (Baade, Burbidge, Hoyle, Burbidge, Christy, and Fowler 1956).

From the theoretical viewpoint it would seem that the parameters  $\tau_1$  and  $\Delta m$ , which refer to the initial stages of the outbursts, are more significant than the angle  $\alpha$ , which is subject to alteration of the light emitted by dispersed interstellar matter surrounding the supernova and by the non-uniformity of the clouds of gases ejected from it. The increment in magnitudes  $\Delta m$  is of the order of 2.5.

As to the point  $P_3$ , where the light-curve turns and the luminosity of all the matter involved in a supernova outburst converges toward some steady value  $m_L$ , the following may be said.

For the supernova of 1937 in IC 4182, the point  $P_3$  had not yet been reached at a time 600 days after maximum. The author feels that the apparent magni-

TABLE 7  
TIMES OF DECLINE THROUGH 1 MAG. FOR SUPERNOVAE OF TYPE I

Supernova in	$\tau_2$ (Days)	Supernova in	$\tau_2$ (Days)
IC 4182.....	73	NGC 5658.....	63
NGC 4214.....	56	Anon (SN 62).....	56
NGC 3992.....	67	NGC 4382 (M85).....	50

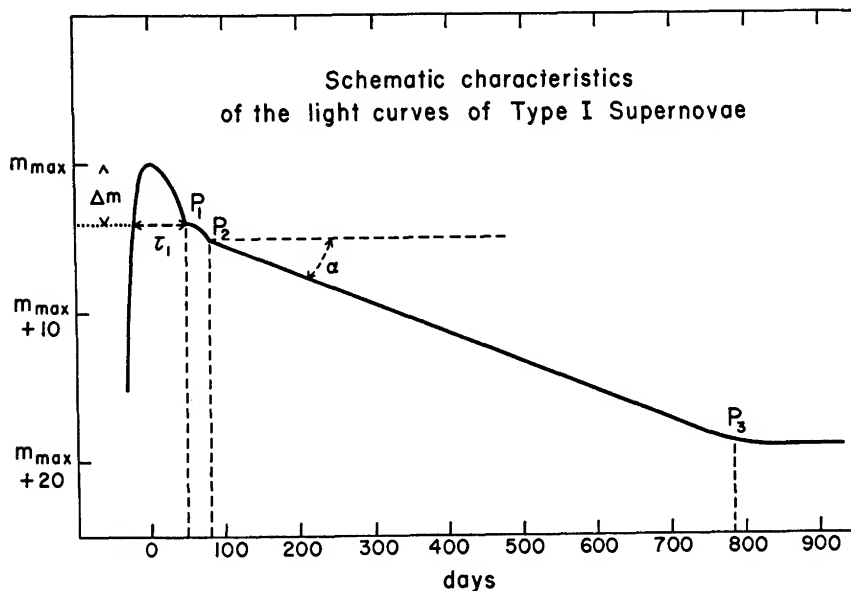


FIG. 12.—Schematic characteristics of the light-curves of type I supernovae

tude might be of the order of  $m_L = 23$  at the present time, and he is attempting to locate the remnant with the 200-inch telescope, using perhaps Dr. I. S. Bowen's lens attachment to the Cassegrain focus of the Hale telescope, which seems to reach a limiting magnitude 24.

An apparent range  $m_L - m_{\max} = 15$  suggests itself also from the fact that, for the supernova of 1054 A.D., it was  $m_{\max} = -4$ , while the remnant Crab Nebula has an apparent luminosity  $m_L \cong +11.0$ . On the other hand, for Tycho's star  $m_L - m_{\max}$  appears to be considerably greater than 15 mag.

*b) Some features of the spectra of type I supernovae.*—Plate I, *B*, shows direct photographs of Messier 85, with the supernova bright and faint. In Plate II, *A*,

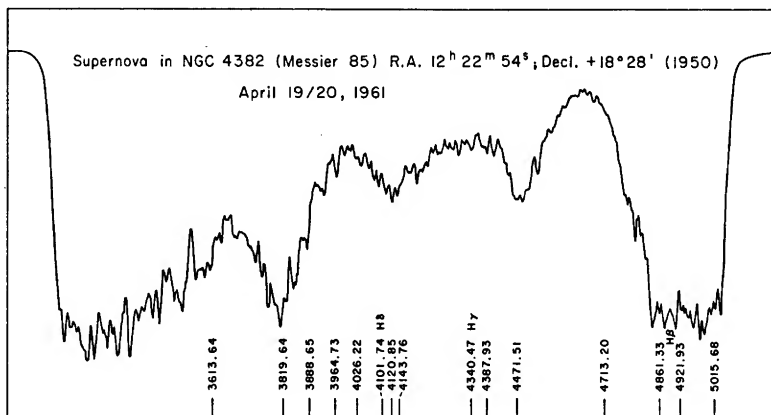


FIG. 13.—Linear microphotometer record of the spectrum of type I supernova No. 86 in NGC 4382 (Messier 85) which is shown on Pl. II, *A*. No attempt at correcting for the plate sensitivity or atmospheric transmission has been made either in this or in any of the direct tracings which are reproduced in subsequent figures.

we reproduce a spectrum of the type I supernova (No. 86) in NGC 4382 = Messier 85 about 4 months after maximum. Figure 13 shows a tracing of this spectrum.

The most persistent features in the visual spectrum of supernovae of type I appear in the region from 5000 to 3500 Å. These are the bands which, on Plate II, *A*, and in Figure 13, are seen around the wavelengths 4680, 4400, 4200, 4000, and 3700 Å. When corrected for the redshifts of the parent galaxies, these bands are always roughly centered around the same wavelengths. They do, however, show variations in position, shape, and particularly in intensity as a function of time elapsed after the date of maximum brightness, as well as when compared for different supernovae. While the band at 4680 Å is generally the brightest and the band at 3700 Å the weakest, recent observations on about three supernovae have shown that these conditions may be exactly reversed, as is shown for supernova No. 87 on Plate II, *B*, and the tracing in Figure 14.

There are not enough successive observations available to ascertain beyond doubt whether or not the discussed reversal of intensity between the bands at  $\lambda 4680$  and  $\lambda 3700$  occurs in the course of the evolution of the spectra of all supernovae of type I or whether it is to be ascribed to fairly basic variations in the evolution of different supernovae. In view of the absence of the said reversal in a long series of spectra which R. Minkowski and M. L. Humason obtained of the supernovae Nos. 25, 26, and 30 in IC 4182, NGC 1003, NGC 4636, and others, it is most likely to conclude that the evolution of supernova No. 87 shown in Plate II, *B*, and Figure 14 represents a wide deviation from the evolution of the spectra of the supernovae 25, 26, and 30. For the bands in the spectra

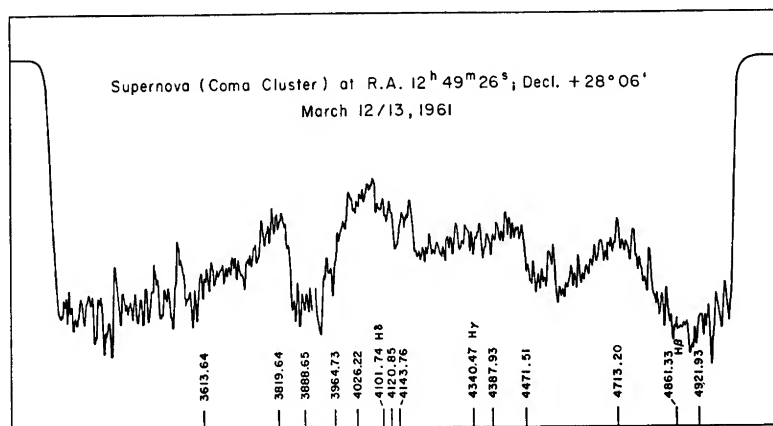


FIG. 14.—Linear microphotometer record of the spectrum of type I supernova No. 87 in the Coma Cluster which is shown in Pl. II, *B*. It is seen that, in contradistinction to all other supernovae of type I, the strongest bands in the blue region of the spectrum lie at 4090 and 3820 Å rather than at 4750 Å.

of the latter, Dr. R. Minkowski has worked out valuable sequences of average wavelengths and intensities, which are shown in Plate III. I am indebted to Dr. Minkowski for permission to incorporate his chart in the present treatise. As to the wanderings of the average positions of the bands and of their intensities, they have been variously interpreted as being due to changes in the configurations of the gas clouds ejected from supernovae, to accelerations and decelerations, as well as to local excitations of these clouds, to immense negative gravitational potentials on the remnant cores, and so forth.

The spectra of supernovae of type I, in contradistinction to the behavior of other types, show a featureless continuum for only a very few days around maximum brightness. Also, mysteriously enough, in the initial stages they seem to emit very little ultraviolet light in the range from 3200 to 3600 Å.

As to the spectra in the final stages of a supernova of type I, we have no knowledge whatever, except if we assume that the Crab Nebula, Messier 1, is

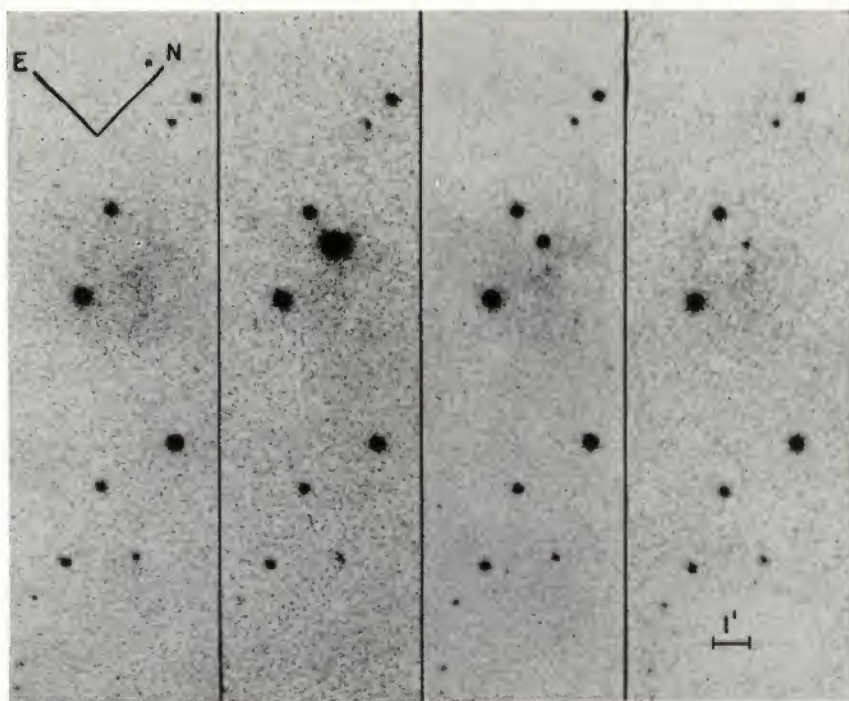


PLATE I.—A: Photographs of supernova No. 25, obtained with the 18-inch Schmidt telescope on Palomar Mountain on the following dates, *from left to right*: April 10, 1937; August 26, 1937; December 31, 1937; June 8, 1938. Scale as indicated.

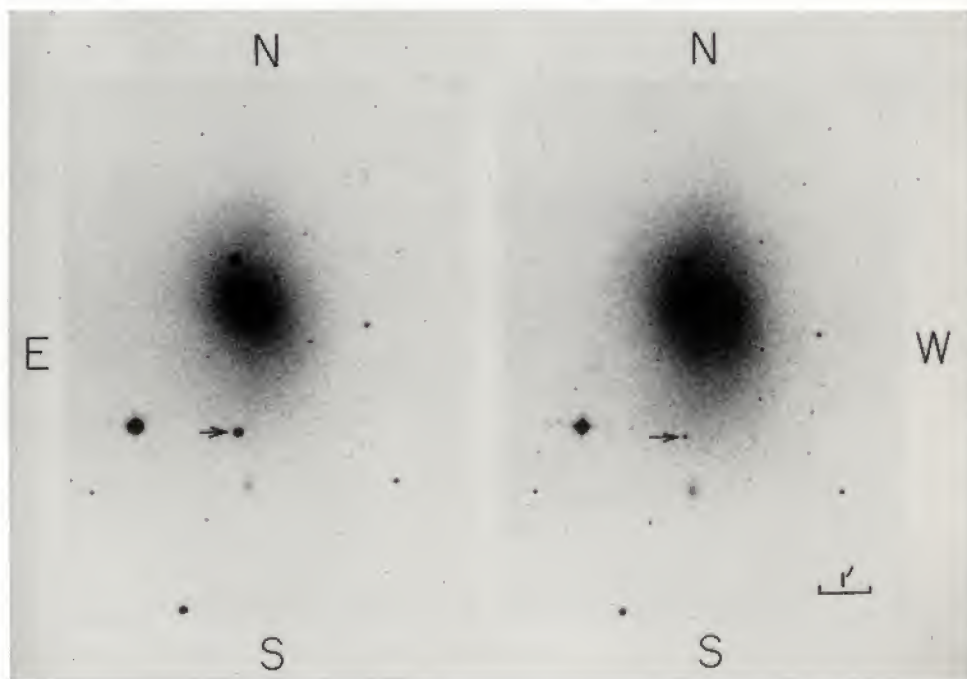


PLATE I.—B: NGC 4382 (Messier 85) with supernova No. 86 of type I bright and faint. Scale is as indicated. The two photographs were obtained with the 48-inch Schmidt telescope on Palomar Mountain on January 15, 1961, on emulsion 103a-O and June 6, 1961, on emulsion 103a-D.



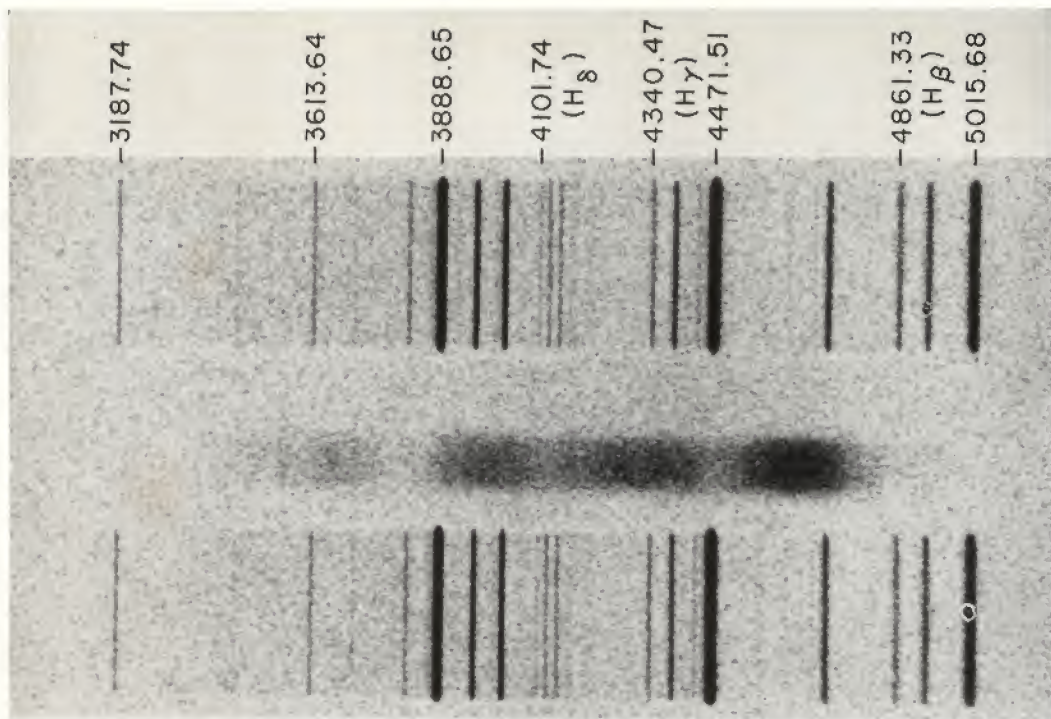


PLATE II.—A: Spectrum of type I supernova in Messier 85, obtained with the prime-focus spectrograph of the 200-inch telescope on April 19/20, 1961, four months after maximum. Emulsion 103a-O, with an exposure time of 91 minutes at seeing 1-2. Comparison spectrum He plus H. Dispersion on the original equal to 385 Å/mm.

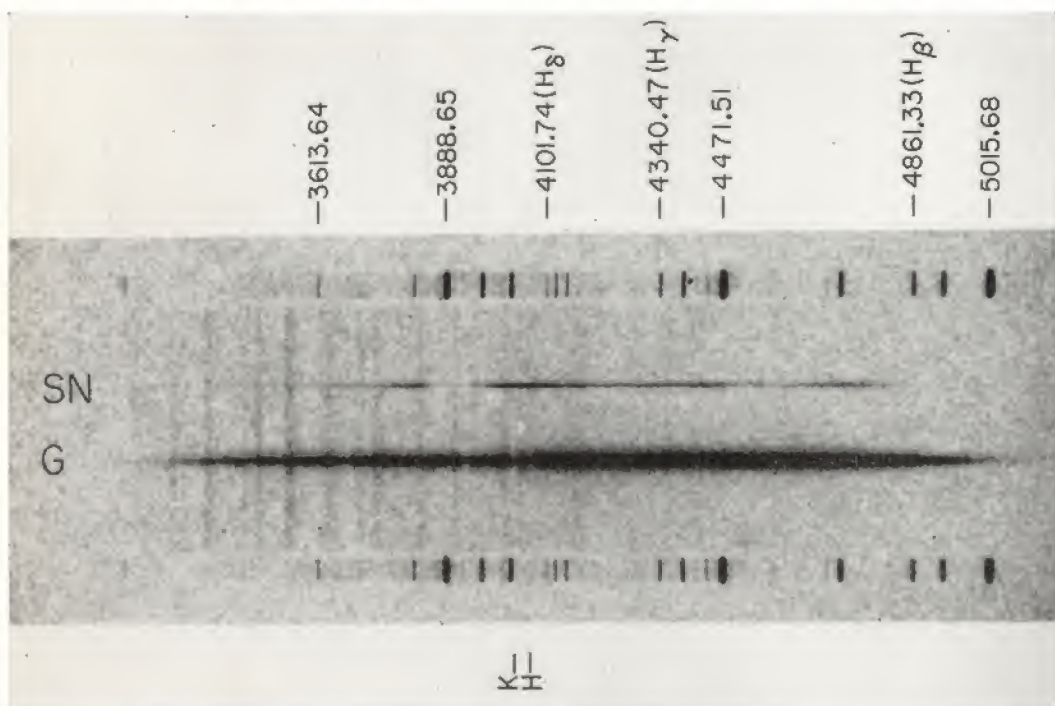


PLATE II.—B: Spectrum of type I supernova No. 87 in anonymous galaxy in the Coma Cluster, obtained with the prime-focus spectrograph of the 200-inch telescope on March 12/13, 1961, about 60 days after maximum. Emulsion 103a-O and exposure time of 227 minutes at seeing 4-5. Comparison spectrum He + H, dispersion 185 Å/mm. The spectra of the galaxy and of the supernova on its far outskirts appear side by side. Since the apparent photographic magnitude of the supernova was about 19.5, this is the faintest celestial source of continuous light for which a spectrum has been photographed so far.

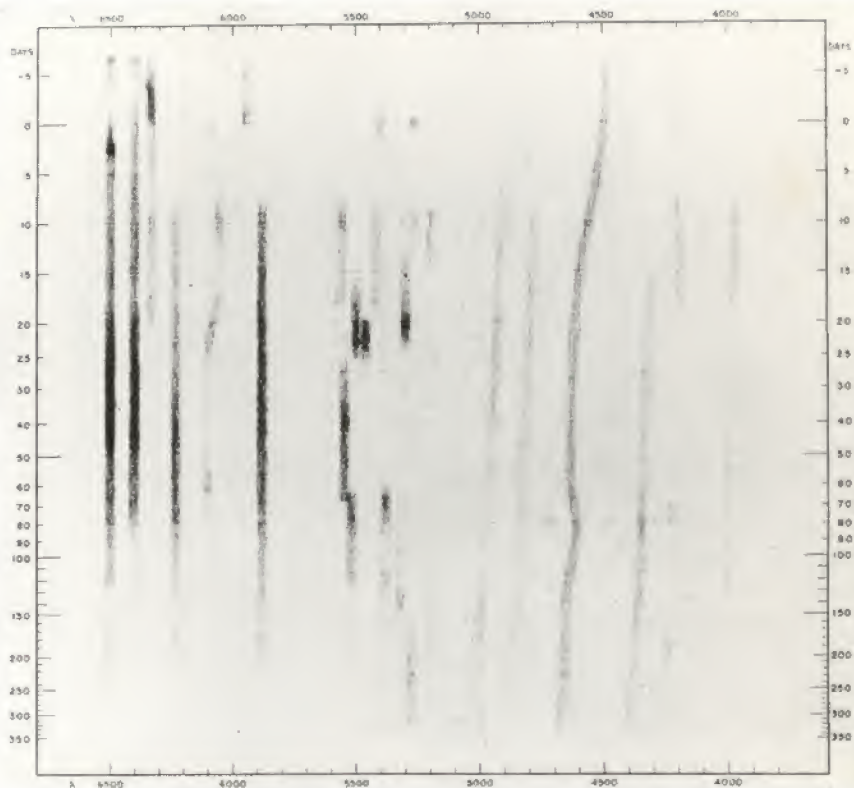


PLATE III.—On the ordinate the days to and elapsed from the date (0) of maximum brightness are plotted. The shaded bands indicate changes of intensity and of average wavelengths of the various characteristic bands of supernovae of type I. Diagram by R. Minkowski.

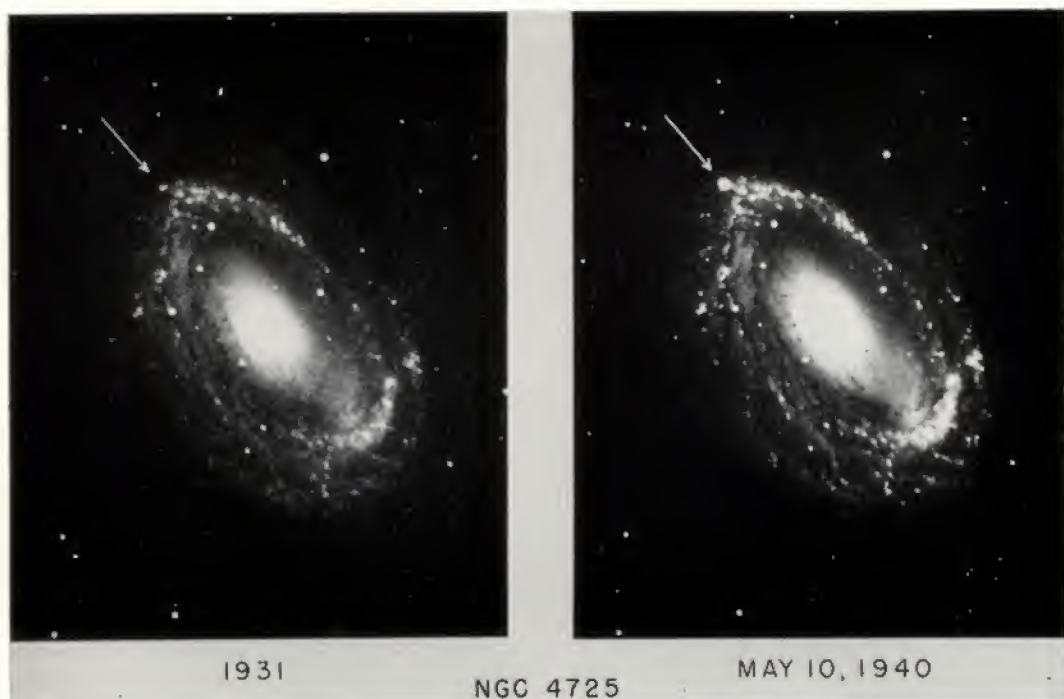


PLATE IV.—A: NGC 4725 without and with supernova No. 35

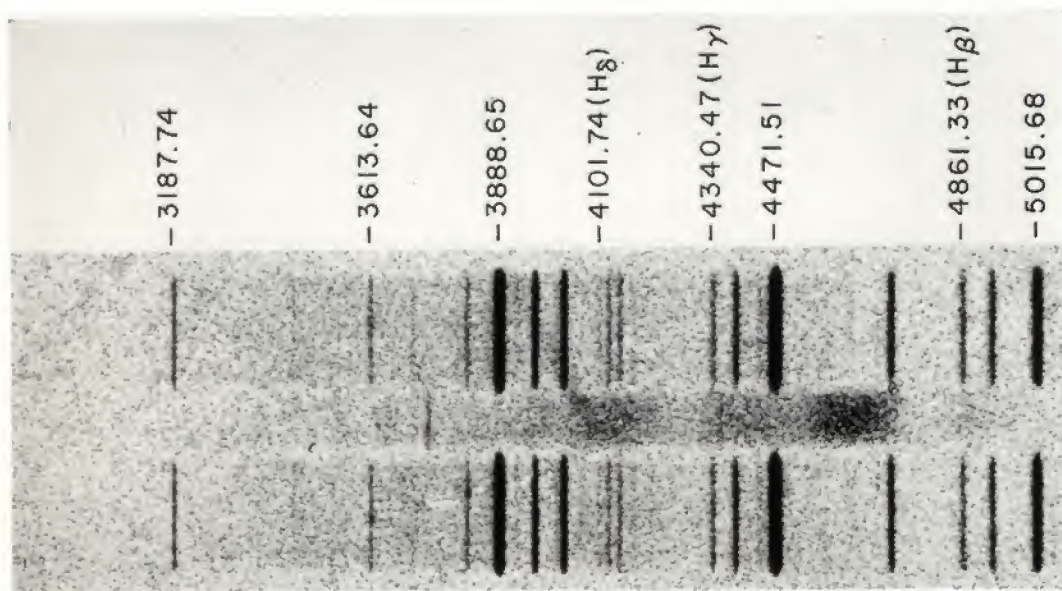


PLATE IV.—B: Spectrum of type II supernova No. 105 in NGC 3938 which was obtained with the prime-focus spectrograph of the 200-inch telescope on February 27/28, 1962, about 2 months after maximum brightness of the supernova. Emulsion 103a-O, exposure time 92 minutes, seeing  $1''$ , dispersion of the original 385 Å/mm.



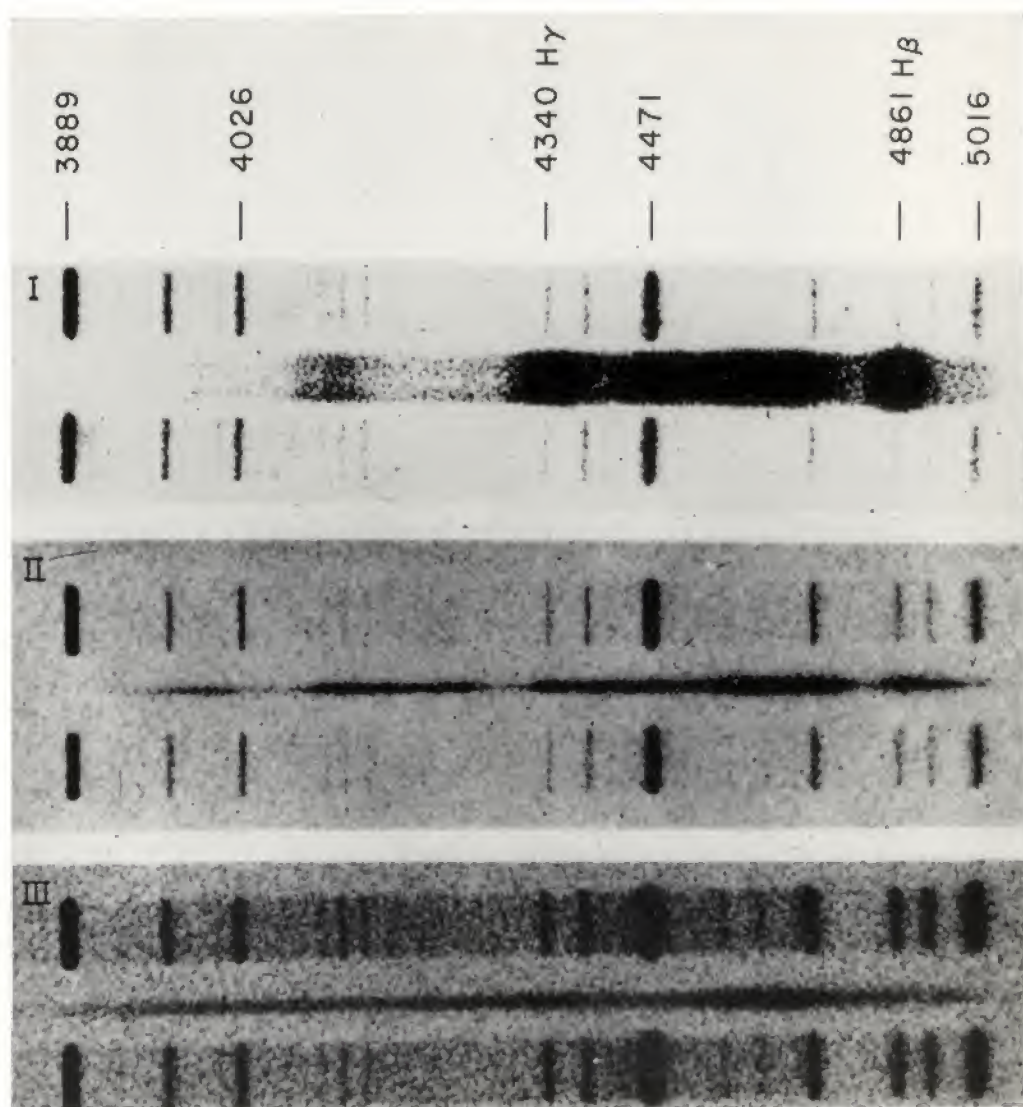


PLATE V.—Spectra of *I*: common Nova Sagittarii on October 13, 1936. *II*: type II supernova No. 34 in NGC 5907 on April 6, 1940. *III*: type I supernova No. 26 in NGC 1003 on November 3, 1937. The wavelengths of some of the lines of the comparison spectrum He + H are indicated.

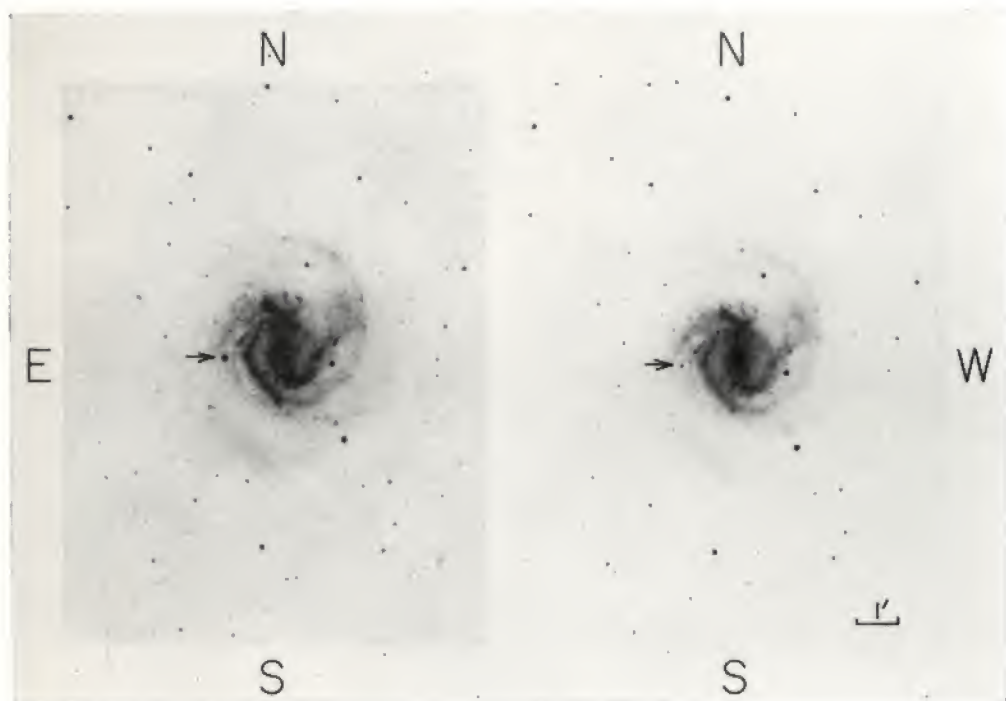


PLATE VI.—A: NGC 4303 with supernova No. 93 bright and faint. Photographs obtained with the 48-inch Schmidt telescope on June 3, 1961, and January 6, 1962. Emulsion 103a-D. Scale as indicated.

PLATE VI.—*B*: Spectrum of type III supernova No. 93 in NGC 4303 obtained on June 14/15, 1961, with the 200-inch telescope prime-focus spectrograph about 2 weeks after maximum brightness. The widened and the unwidened spectra correspond to exposures of 15 minutes and 1 minute, respectively, on emulsion 103a-O at seeing 3. Dispersion 185 Å/mm. Comparison He + H. The almost featureless continuum which extends far into the ultraviolet is typical of supernovae of type III, and it persists for several weeks, after which time bands begin to appear which seem to owe their origin to emission of H, He, and other light atoms.

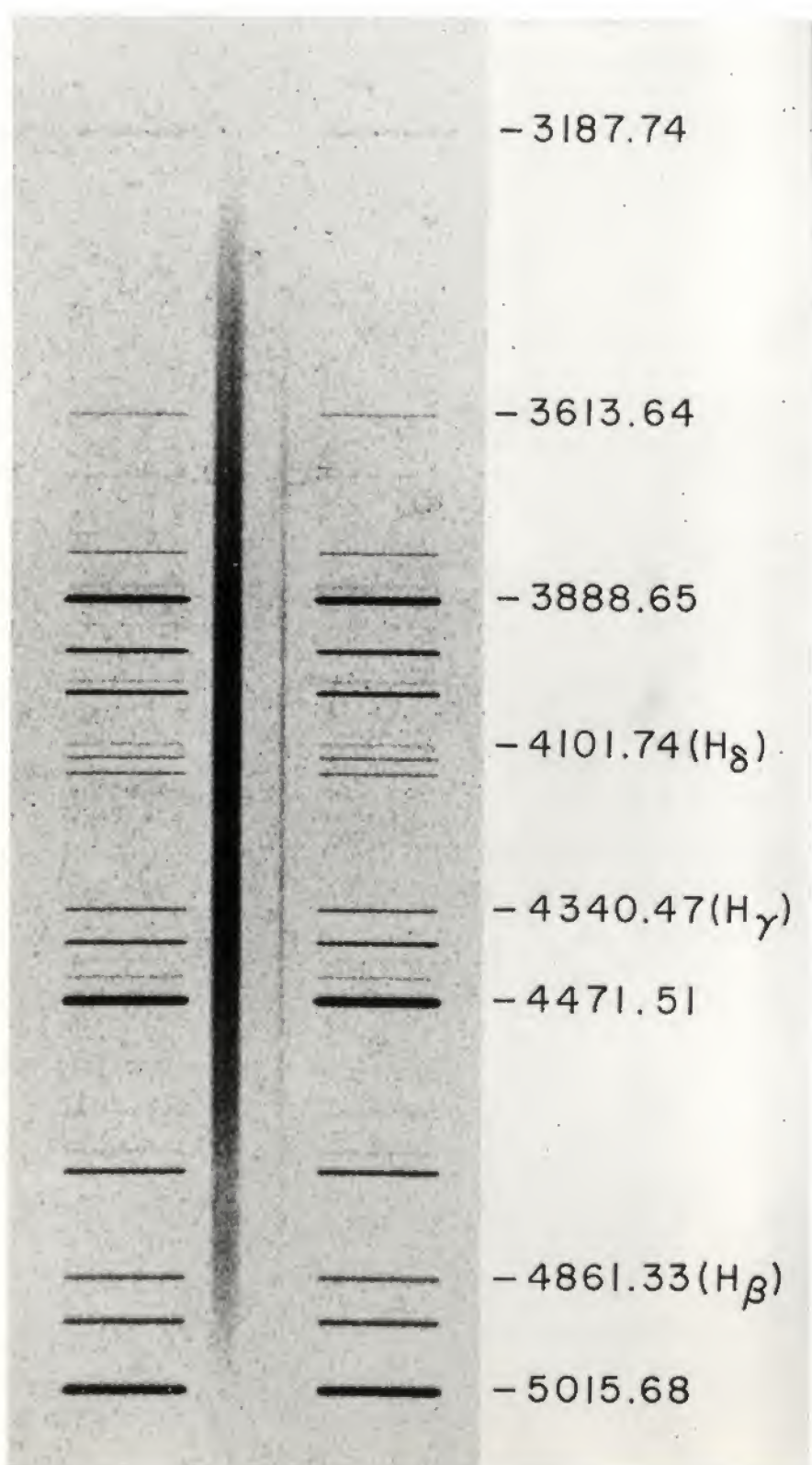
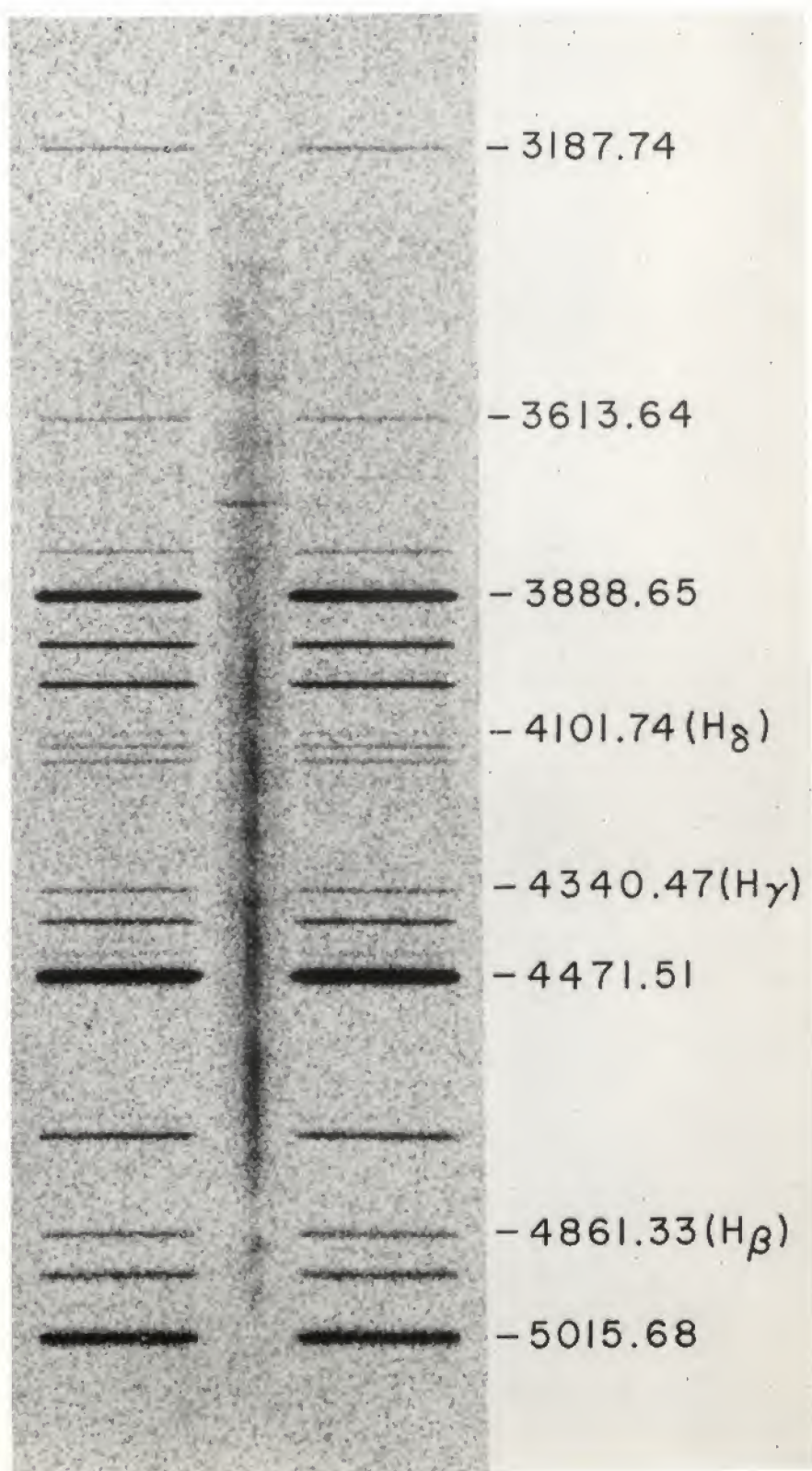




PLATE VI. C: Spectrum of type III supernova No. 93 in NGC 4303 obtained on February 1/2, 1962, with the 200-inch telescope prime-focus spectrograph at the approximate apparent photographic magnitude  $m_p = +19.5$  about 8 months after maximum brightness. Exposure 190 minutes on emulsion 103a-O at seeing 3-5. Dispersion 385 Å/mm. Comparison spectrum He + H. The spectrum of the supernova, in the center, is flanked by the washed-out spectrum of the adjacent parts of the galaxy in which the bright line  $\lambda 3727$  is very strong and the H and K absorption lines are barely discernible. H $\delta$  and H $\gamma$  in emission appear distinct in the spectrum of the supernova, their width corresponding to a velocity of expansion of about 6000 km/sec. On the violet side of both H $\delta$  and H $\gamma$  there appears to be the sharp absorption edge present that is a familiar feature in the spectra of common novae and is due to the absorption of the continuous light from the central parts or the stellar core of the supernova by the gases approaching exactly in the line of sight.



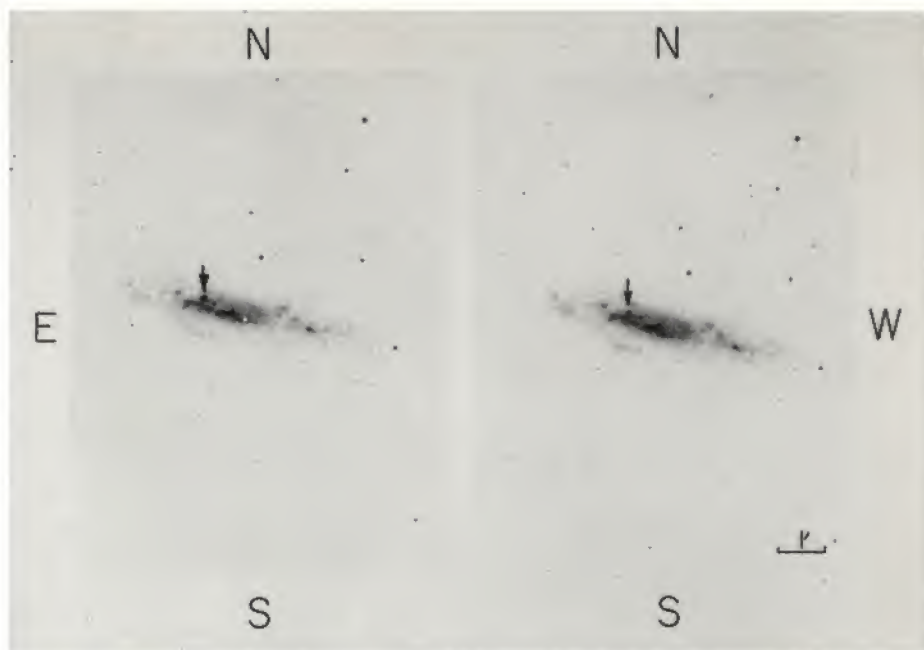


PLATE VII.—A: NGC 3003 with supernova No. 89 bright and faint. Photographs obtained with the 48-inch Schmidt telescope on February 22, 1961, and on November 9, 1961, both on emulsion 103a-O.

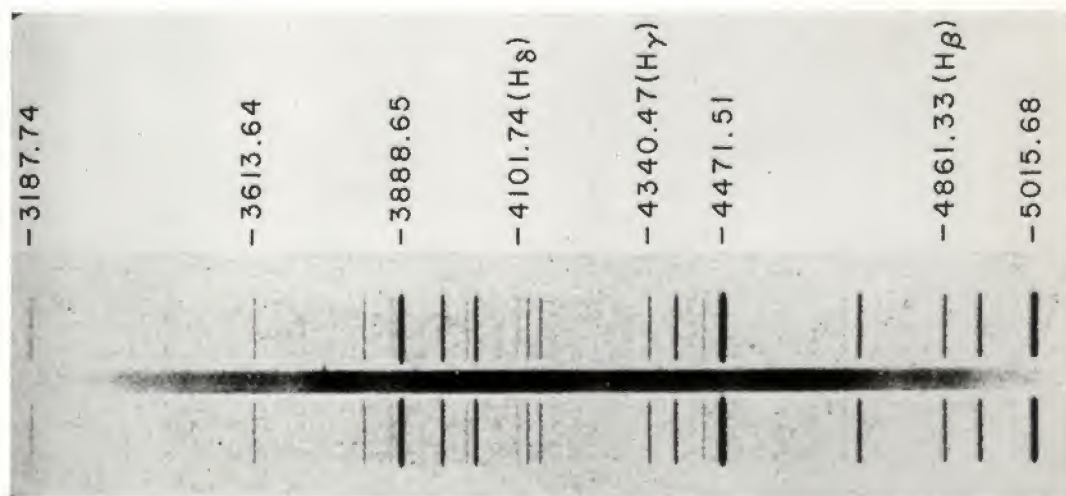


PLATE VII.—B: Spectrum of type IV supernova No. 89 in NGC 3003 obtained with the prime-focus spectrograph of the 200-inch telescope on March 12/13, 1960, about 3 weeks after maximum brightness. Exposure time for the widened spectrum 45 minutes on emulsion 103a-O at scieing 5. Dispersion of the original plate 185 Å/mm. Comparison spectrum He + H. The spectrum is continuous, with some flat, broad bands, and extends far into the ultra-violet. The bright line  $\lambda$  3727 is seen to protrude beyond the widened spectrum of the supernova and thus is due to an emission nebulosity of NGC 3003. The same is probably true for the sharp emissions at H $\beta$  and H $\gamma$ , the latter of which is also seen to protrude beyond the widened supernova spectrum. It is to be noted from the light-curve shown in Fig. 26 that, on March 12/13, the supernova was just reaching the first lower steady level after a rapid decline of 1 mag. from maximum brightness.



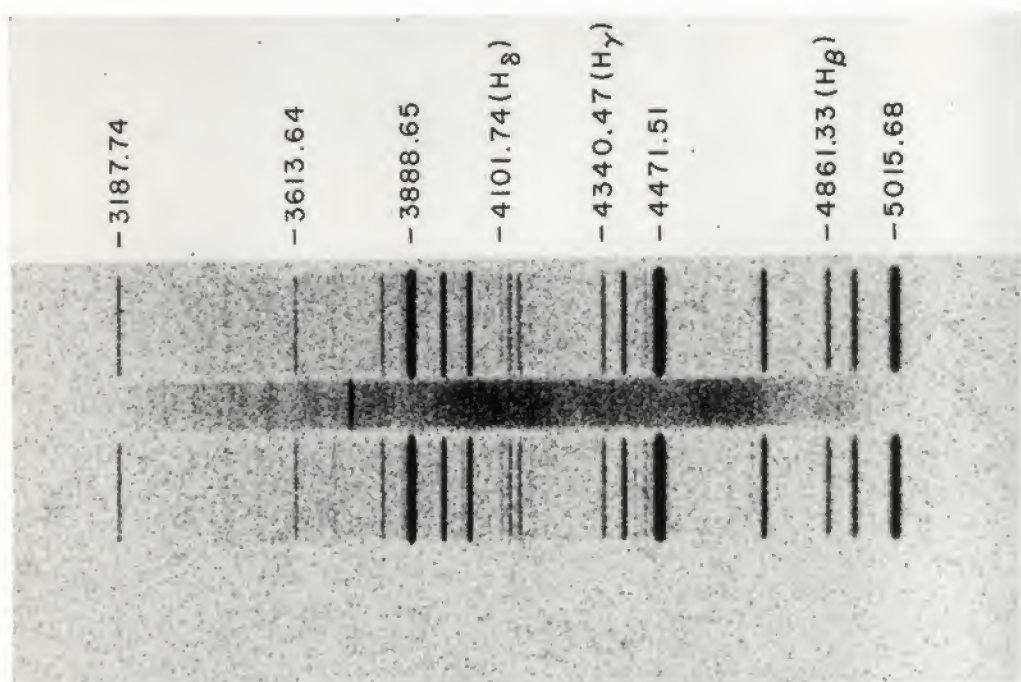


PLATE VIII.—A: Spectrum of type IV supernova No. 89 in NGC 3003 obtained with the prime-focus spectrograph of the 200-inch telescope on April 19/20, 1961, about 8 weeks after maximum brightness. Exposure time 96 minutes on emulsion 103a-O at seeing  $1''$  and some moonlight. Dispersion of the original plate 385 Å/mm. Comparison spectrum He + H. Sharp emission lines  $H\gamma$  and  $\lambda$  3727 from permanent emission nebulosities are superposed on the widened supernova spectrum, which shows five broad bands at about 4900, 4600, 4400, 4100, and 3800 Å. It is not certain to what degree the slight addition of moonlight intensified the longer-wave-length regions relative to the ultraviolet below 4000 Å. (Compare with the spectrum on Pl. VIII, B, which had no moonlight.) Note that the H and K absorption lines which are distinct on Pl. VIII, B, are not visible in the spectrum on Pl. VIII, A. This must be due to the fact that the slit of the spectrograph cut across some bright spot of late-type stars on the one exposure but not on the other, although it was oriented exactly in the same way.

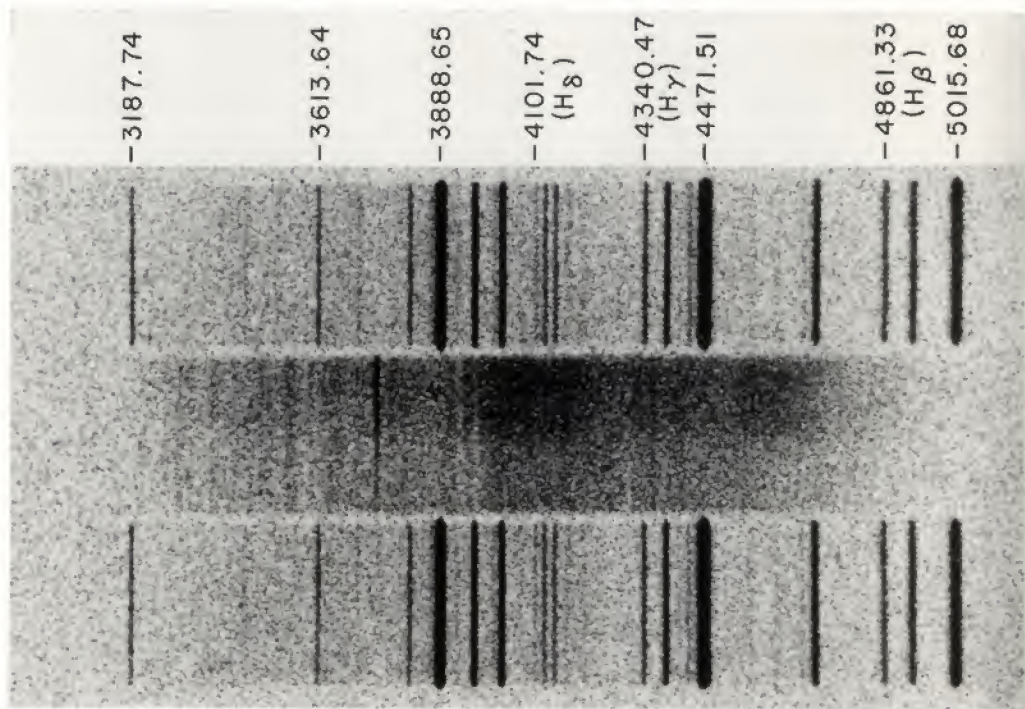


PLATE VIII.—*B*: Spectrum of type IV supernova No. 89 in NGC 3003 obtained with the prime-focus spectrograph of the 200-inch telescope on April 20/21, 1961, one day after the spectrum shown on Pl. VIII, *A*, and an estimated 8 weeks after maximum brightness. Exposure time 75 minutes on emulsion 103a-O at seeing 1-2. Dispersion 385 Å/mm on the original. Comparison spectrum He + H. The same remarks apply as to Pl. VIII, *A*. Note that the H and K absorption lines, as well as the G band, are present and no doubt due to a permanent knot of late-type stars in NGC 3003.



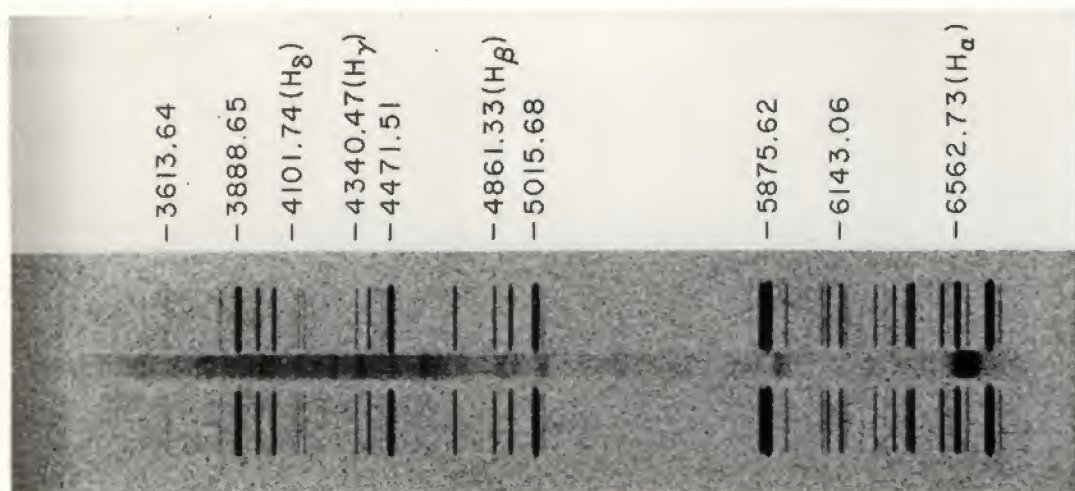


PLATE IX.—A: Widened spectrum of type V supernova No. 96 in NGC 1058 obtained with the prime-focus spectrograph of the 200-inch telescope on February 1/2, 1962, about 7 months after (the first) maximum brightness. Exposure time 65 minutes on emulsion 103a-F, at seeing 3. Dispersion 385 Å/mm on original. Comparison spectrum He + H + Ne. Distinct and not excessively broad emission bands H $\alpha$ , H $\beta$ , H $\gamma$  (with sharp absorption on the violet edge) are clearly visible. Other lines, structural features, and temporal variations are discussed by Dr. J. L. Greenstein in § 3.6 of this chapter.

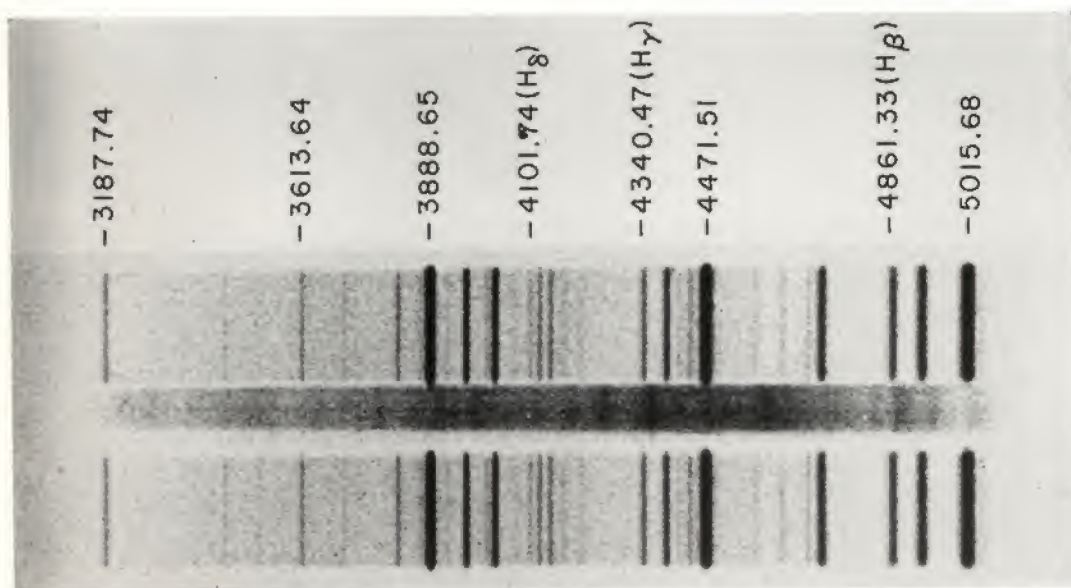


PLATE IX.—B: Spectrum of type V supernova No. 96 in NGC 1058 obtained with the prime-focus spectrograph of the 200-inch telescope on February 28/March 1, 1962, about 8 months after the first maximum outburst of the supernova. Exposure time 90 minutes on emulsion IIa-O baked, at seeing 3–4. Dispersion 385 Å/mm. Comparison spectrum He + H. As in the spectrum of February 1/2, many emission lines are visible the interpretation of which is discussed in § 3.6, written by Dr. J. L. Greenstein. The spectrum extends far into the ultraviolet.

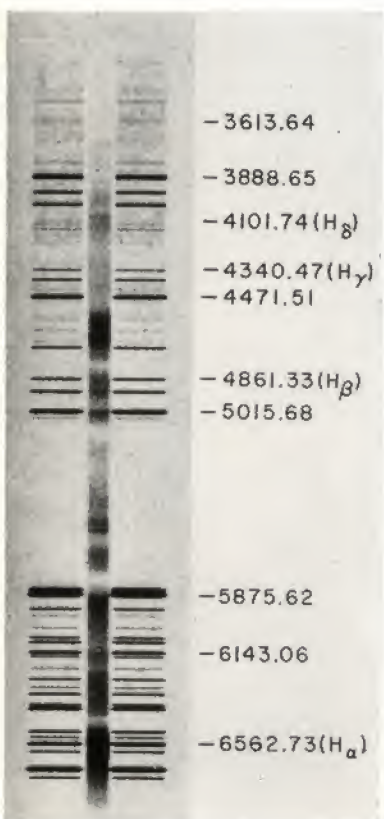
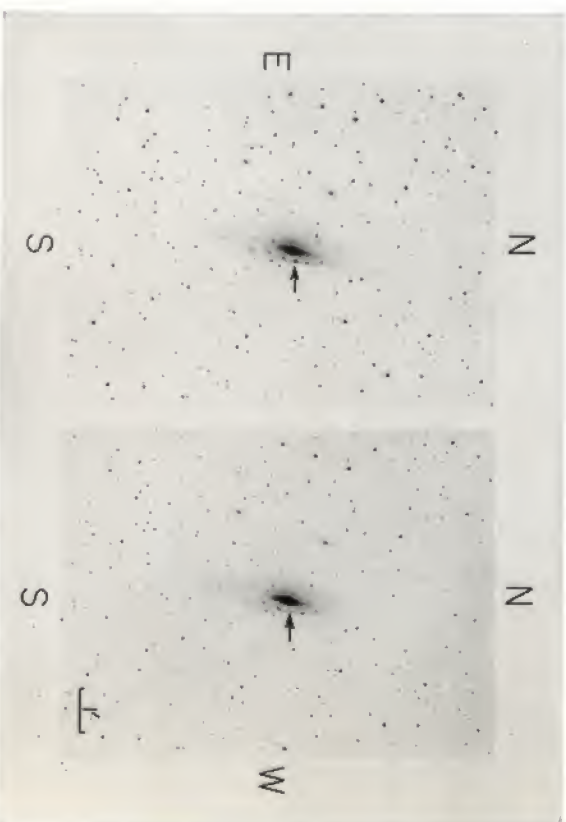
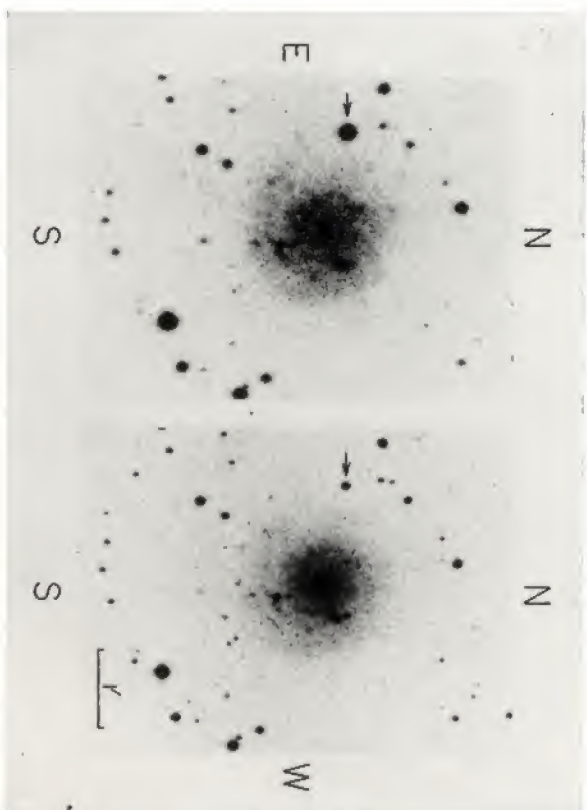


PLATE X.—A: NGC 1038, with supernova No. 96 of type V bright and faint. The two photographs were obtained with the 48-inch Schmidt telescope on December 4, 1961, and February 2, 1962, respectively, on emulsions 103a-O and 103a-D.

PLATE X.—B: NGC 7331, with supernova No. 63 of type II bright and faint. The two photographs were obtained with the 48-inch Schmidt telescope on June 29, 1959, and September 8, 1959, both on emulsion 103a-O.

PLATE X.—C: Spectrum of type II supernova No. 63 in NGC 7331 obtained with the prime-focus spectrograph of the 200-inch telescope by J. L. Greenstein on September 1, 1959. Emulsion 103a-F. Comparison spectrum He + H + Ne.



part of the remnant of the supernova of 1054 A.D. and that this supernova was of type I. Nevertheless, even with these assumptions, we do not know how much of the matter in the Crab Nebula is due to the original supernova body and how much interstellar matter became involved.

Curiously enough, in spite of extremely arduous work by observational, experimental, and theoretical experts, the origin and the meaning of the spectra of supernovae of type I have remained completely mysterious. Not a single feature in these spectra has as yet been definitely identified. Only recently has some faint hope arisen that decisive clues might be obtained through the analysis of a group of spectra taken in rapid sequence. Indeed, from our knowledge of the phenomena in common nova outbursts and in geometrically uncontrolled explosions of all kinds, it may be expected that very local sources of light flare up. These are due to local accumulations of "explosive" matter, to jets, shock waves, and so on. Such local flares may be expected to give rise to sharp patterns of lines and bands that are superposed on the broad bands in the supernova spectra, the width of which is probably due in great part to a tremendous dispersion in the velocities of the different luminous sources. Preliminary observations by the author on some bright supernovae indeed indicate that sharp patterns occur and that they persist for matters of minutes, hours, or perhaps even days.

In this connection it may be of interest to reprint some remarks about the interpretation of the spectra of supernovae which R. Minkowski made in his original paper (1939) and to suggest that we are not much more enlightened even today:

Any attempt to identify these lines is difficult and may easily lead to an overinterpretation. Owing to the very low dispersion and the faintness of the details, the measures may be in error by several angstroms; and true absorption-line details may be shifted by an unknown amount toward the violet because of outward flow of matter in the atmosphere of the star. Suggested identifications, which are far from satisfactory, are given in Table 8. Two lines which might be expected, He II  $\lambda$  4540 and Si IV  $\lambda$  4075, cannot be identified with observed details; and the displacements which follow from the identifications scatter more than would be expected from the errors of the measures. On the other hand, the amount of the displacement, about 45 Å, is in general agreement with the width of about 100 Å shown by the narrowest emission bands in the early spectra. This displacement would indicate a radial velocity of about 3000 km/sec. Altogether, the identifications are hardly convincing enough to be considered as evidence for the reality of the suspected absorption lines.

The question may be raised whether the abrupt end of the spectrum in the ultraviolet is an indication of continuous absorption. The absence of strong emission bands in this region would warrant the assumption of continuous absorption only if identifications in other regions should lead us to expect the appearance of strong emission bands in the ultraviolet. The absence even of a continuous spectrum, however, deserves some discussion. The very strongly overexposed spectrogram of supernova IC 4182 obtained with a quartz spectrograph on September 10, 1937, shows no trace of a record

below  $\lambda$  3300. With the same instrument and exposure time, an early-type star of apparent photographic magnitude 12 would give a faint record in this region. Thus, one may conclude that, if only the continuous spectrum of the supernova were observed, the absolute photographic magnitude on this date would have been only  $-13$  or fainter, instead of  $-16.2$ , as observed. The value  $-13$  is an upper limit for the intensity of the continuous spectrum; and, on the assumption of black-body radiation, an upper limit for the temperature can be obtained for any value of the radius of the star. For a radius equal to that of the sun, we obtain  $2.6 \times 10^9$  degrees as upper limit for the temperature, and, for smaller radii, values which increase with the inverse square of the radius. Temperatures of this order of magnitude would lead to the

TABLE 8\*  
TENTATIVE IDENTIFICATIONS FOR SPECTRUM OF SUPER-  
NOVA NGC-1003 ON SEPTEMBER 12.444, 1937

$\lambda$ Obs.	Identification	Displacement
4813.....	4861 H $\beta$ ; 4859 He II	-47
4747.....	4798-4783 O IV	-43
4646.....	4687 He II	-41
4580.....		
4530.....		
4450.....		
4380.....		
4294.....	4340 H $\gamma$ ; 4339 He II	-46
4252.....		
4218.....	4262 O IV	-44
4160.....	4199 He II	-39
4048.....	4102 H; 4100 He II; (4089 Si II)	-49
4011.....		
3988.....	4025 He II	-37
3950.....	3995 O IV	-45
3934.....	3975, 3977 O IV	-42

\* Transitions  $n = 5$  to  $n = 6$  of O IV are to be expected in this region (cf. B. Edlén, *Zs.f. Ap.*, 7, 383, 1933). All units are in angstroms.

emission of an amount of energy which, integrated over the duration of the outburst, exceeds the equivalent of ordinary stellar masses converted into radiation.

The actual temperature must have been lower; and if the radius of the star was not much larger than that of the sun, the absence of a continuous spectrum thus needs no explanation. For large values of the radii, on the other hand, the upper limit for the temperature decreases rapidly. Only if the star were greatly expanded would it be necessary, therefore, to explain the faintness of the continuous spectrum by continuous absorption in the ultraviolet.

From about two weeks on, after the star has reached its maximum brightness, the appearance of the spectrum leaves little doubt that the spectrum is composed essentially of wide and partially overlapping emission bands. These may be divided into three classes. The independence of the spectral regions below and above  $\lambda$  5000, which has already been discussed, can lead only to the conclusion that the permanent bands below  $\lambda$  5000 differ in origin from the others. The variations in the relative intensities

of the two parts of the spectrum indicate that the separation is complete in the sense that none of the strong original bands above  $\lambda$  5000 is connected with the permanent bands below  $\lambda$  5000. The two narrow bands which appeared in the red of supernova IC 4182 from February 21, 1938, on are of a different type from the other bands in the red; they increase in intensity while the others fade out.

The average wave lengths of the two narrow bands are  $\lambda$  6299 and  $\lambda$  6359. Within the errors of measurement they agree with the wave lengths of the [O I] lines  $\lambda$  6300 and  $\lambda$  6364. The relative intensities of the bands are also in good agreement with those of the [O I] lines. The fluctuations in the measured wave lengths of these only partially resolved bands are easily understood as due to variations in the intensity distribution, such as occur frequently in emission bands in ordinary novae. There can be hardly any doubt that these bands are to be identified as the nebular lines of [O I]. The absence of the auroral [O I] line  $\lambda$  5577 may be taken as an indication that the lines are excited at extremely low pressure. One difficulty presents itself, however. It is remarkable that only the two nebular lines of [O I] appear, unaccompanied by the lines of other origin which usually are seen with them. It is possible that this peculiarity may be explicable on the basis of the very small pressure, indicated by the absence of  $\lambda$  5577, and the very small transition probability. Nevertheless, it is hard to understand how the lines can be excited without the appearance of other lines, unless the mechanism of the excitation is entirely different from that usually assumed for forbidden lines. With all reserve, the possibility of an increased abundance of oxygen as a result of nuclear reactions should, however, be mentioned.

The difficulties met in any attempt to identify the permanent bands below  $\lambda$  5000 are obvious. The true wave lengths of these bands may be smaller than in the beginning or larger than in the latest spectra, depending on whether the explanation of the red shift is a real red shift or a decreasing violet shift. The discussion of the red shift shows that these bands are probably emitted under conditions which are so peculiar that an identification with lines of known origin can hardly be expected. The merely temporary coincidence of one of the bands with a line of known origin cannot be considered as evidence. For this reason former identifications of these bands with lines of N III and H cannot be maintained. Besides, they are contradicted by the absence of lines above  $\lambda$  5000, the presence of which should be expected; such lines should remain when the red part of the spectrum becomes faint. The invalidation of these identifications removes the only quantitative argument for the contention that the spectra of supernovae are similar to those of ordinary novae.

The red part of the spectrum is not subject to any considerable red shift. The main obstacle to identifications is thus missing. The fact that no lines below  $\lambda$  5000 remain strong when the blue part of the spectrum becomes relatively faint, about 40 days after maximum, allows for bands above  $\lambda$  5000 only such identifications as would not imply the presence of strong lines below  $\lambda$  5000. Almost all known lines which could provide identifications for the strong and more permanent bands above  $\lambda$  5000 are thus excluded. In particular, the hydrogen lines cannot be present; the assumption that H $\alpha$  forms part of the first intensive band around  $\lambda$  6500 is refuted by the absence of all other hydrogen lines. Similarly, the presence of He becomes at least extremely improbable; the band at about  $\lambda$  5900 could be identified with He  $\lambda$  5876, but all other He lines are certainly not present. The absence of H and He shows that the ionization in that part of the star's atmosphere in which the red lines appear is either very high



or very low. The assumption of low ionization, which would permit an identification of the band at about  $\lambda$  5900 with the Na D lines, is contradicted by the complete absence of other lines which would be expected to accompany the D lines, such as Ca I or Ca II, or numerous other lines in the observed range of the spectrum. We are thus led to the conception that the bands above  $\lambda$  5000 are emitted by highly ionized atoms. The close coincidence, on September 11, 1938, of the two bands at  $\lambda$  6085 and  $\lambda$  5300 in supernova IC 4182, which emerged and disappeared simultaneously, with the forbidden lines of Ca V at  $\lambda$  6086 and  $\lambda$  5309 deserves mention in this connection as possible identifications. If the assumption of very high ionization is justified, the failure to obtain identifications may be due merely to the incompleteness of our knowledge of the spectra of highly ionized atoms.

The conception that all bands in the spectra of supernovae are emitted under unique conditions of ionization and excitation possibly finds some support in the observations of the Crab nebula. It has become increasingly certain that the Crab nebula is the remnant of a former supernova. If such is really the case, the final stage of a supernova does not differ from that of an ordinary nova. The Crab nebula shows the usual nebular spectrum, developed by ordinary novae a few months after the outbreak; and the velocity of expansion of the nebula, about 1300 km/sec, is of the same order as that observed in ordinary novae. If the ejection of matter from a supernova coincides with the outbreak, as in ordinary novae, we might therefore expect the formation of a nebular spectrum only a few months after the maximum. The present observations show indisputably that this does not occur; at the most, the appearance of the [O I] lines may be the first step toward such a development. The absence of the nebular spectrum may be considered as a direct indication that, even a year after the supernova outbreak, the conditions of ionization and excitation are still widely different from those in ordinary novae.

As to the localization of supernovae of type I, it has already been pointed out that they appear indiscriminately in all types of galaxies, that is, in normal and barred spirals, ellipticals, and irregulars. They also have flared up in giant and in dwarf galaxies such as Messier 31 and IC 4182, respectively. So far, there has been no success in picking them up in intergalactic space.

Baade (1942, 1943) made the attempt to reconstruct the light-curves of the supernovae of 1054 A.D., Tycho's star of 1572, and Kepler's star of 1604 (SN Oph). These light-curves seem to be remarkably similar to those of supernovae of type I, especially to the one of 1937 in IC 4182. Nevertheless, the remnants of the three events are so entirely different in character that it would seem hazardous to conclude rashly that the outbursts of 1054, 1572, and 1604 were really all supernovae of type I. While the supernova of 1054 A.D. has left us with the massive and luminous Crab Nebula and, possibly, with a clearly distinguishable stellar remnant of the sixteenth apparent magnitude, the more recent supernovae of 1572 and 1604 have left no stellar remnants that can be found with the large telescopes, and the identification of any very faintly luminous gas-cloud remnants is of the most dubious value. The investigation of these remnants by optical and radio telescopic means is therefore most important and is now in full swing.

As to the behavior of the "debris" from supernovae, the following possibility may be kept in mind. While a supernova probably attains maximum luminosity in terms of ordinary light during the first few days of the outburst, it is conceivable that, much later, considerable relative increases in luminosity of the remnants may occur, which are due to a number of causes. In particular, the impingement of the very energetic electromagnetic and corpuscular radiations from supernovae on surrounding interstellar clouds, as well as other stars must be kept in mind (Zwicky 1962). In this connection a claim by Simon Marius (Zinner 1920) may be of interest. He reported that in 1614 he saw a reappearance (telescopic) of Tycho's star of 1572. This might mean, for instance, that a formation such as the Crab Nebula, perhaps at various times between now and its start in 1054 A.D., was much brighter than it is now. As a matter of fact, local changes in brightness have even been observed during the past few decades and are being followed by G. Münch and others.

As to delayed actions it must be further kept in mind that the emission of radio waves and of cosmic-ray particles may become most efficient long after the original supernova outburst. For the cosmic rays the slight difference in their speed relative to that of light would, of course, complicate matters still further, since, because of the great distance of most supernovae, cosmic rays would arrive on the earth many years after the light of the outburst, although both might have been emitted at the same time.

3.5.2. *Supernovae of type II.*—On Plate IV, *A*, we reproduce two photographs of the spiral galaxy NGC 4725 with and without the supernova No. 35 of May, 1940. The spectrum of this supernova was quite different from the spectra of supernovae of type I, and Minkowski therefore proposed to classify SN 35 as a supernova of type II. On closer inspection it appears that spectra of supernovae of type II are in many respects quite similar to the spectra of very luminous common novae and that the main difference between them lies in the fact that the gas clouds from supernovae of type II are ejected with velocities of the order of 7000 km/sec rather than with considerably smaller velocities (see Pls. IV, *B*, and V and Fig. 15).

H $\alpha$  in emission is always prominent, and H $\beta$  can likewise almost always be seen. It is not certain, however, whether the absorption on the violet side of the wide emission lines has ever been seen as in the spectrum of the type V supernova in NGC 1058, which is discussed below.

As to the time sequences of the spectra of supernovae of type II, far less material is available than for type I. No supernovae of type II have ever been discovered that were anywhere near as bright (apparent brightness) as the type I in IC 4182. Observations were therefore more difficult, and no great range in magnitude has as yet been covered.

Although the spectra of supernovae of type II, in contradistinction to those of type I, seem, luckily enough, to be interpretable, the structural features of

the light-curves are most disappointingly varied, as is seen from the light-curves plotted in Figures 16 and 17.

Type II supernovae, so far, have never been found in globular and elliptical galaxies. In addition to having appeared in spiral galaxies, some of the fainter galaxies in which they were found were almost certainly dwarf, irregular systems.

It should also be noted that, so far, supernovae of type II have never flared up in the peripheral, featureless regions of galaxies, and often they seem to be associated with emission patches in or between the spiral arms.

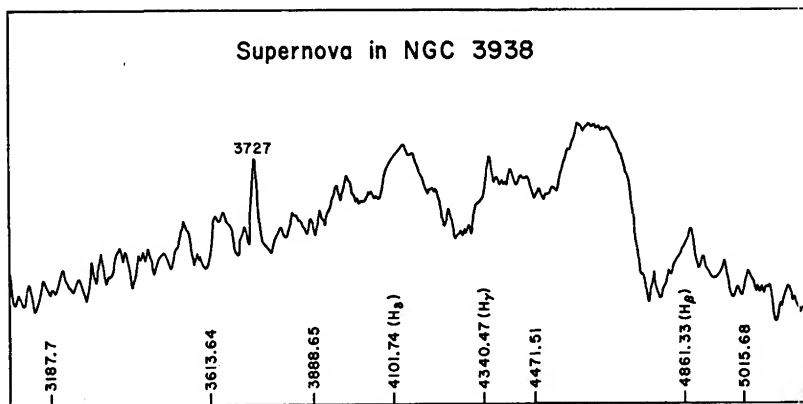


FIG. 15.—Linear microphotometer record of the spectrum, shown in Pl. IV, *B*, of type II supernova 105 in NGC 3938, about 70 days after maximum. The peaks of  $H\beta$ ,  $H\gamma$ , and  $\lambda$  3727 seem to be too sharp to have originated wholly in the supernova. A check for the emission of a permanent luminous nebulosity which is coincident with the supernova will have to be made at a later time when the supernova has faded away.

If no spectra are available, supernovae of types I and II can usually be told apart by their colors at and near maximum brightness, the supernovae of type II having stronger ultraviolet radiation, that is, lower values of  $B - V$ , than type I.

3.5.3. *Supernovae of type III.*—Although it may turn out that type III is only a variant of type II, this author prefers, for the time being, to class a supernova such as No. 93 of 1961 in NGC 4303 as being of type III. In Plate VI, *A*, we reproduce the barred spiral galaxy NGC 4303 in two stages, with the supernova, respectively, bright and faint.

In Plate VI, *B* and *C*, two spectra of the supernova and the emission nebulosity on which it is superposed are shown, while in Figures 18, 19, 20, and 21 some tracings of these spectra are given.

Unfortunately, the late discovery of the supernova in NGC 4303, shortly before it started disappearing in the west, as well as bad weather in the winter 1961–1962, left us with a gap of almost half a year, as to the observation of both the spectra and the light-curve. An appeal to the observatories in the Southern

Hemisphere, who could have helped materially in closing this gap through observations in August and September, 1961, unfortunately produced no visible results.

From partial light-curves and colors of some very faint supernovae (for instance, No. 94, which, by the way, may be the most distant supernova ever observed spectroscopically) we infer that these objects were also of type III.

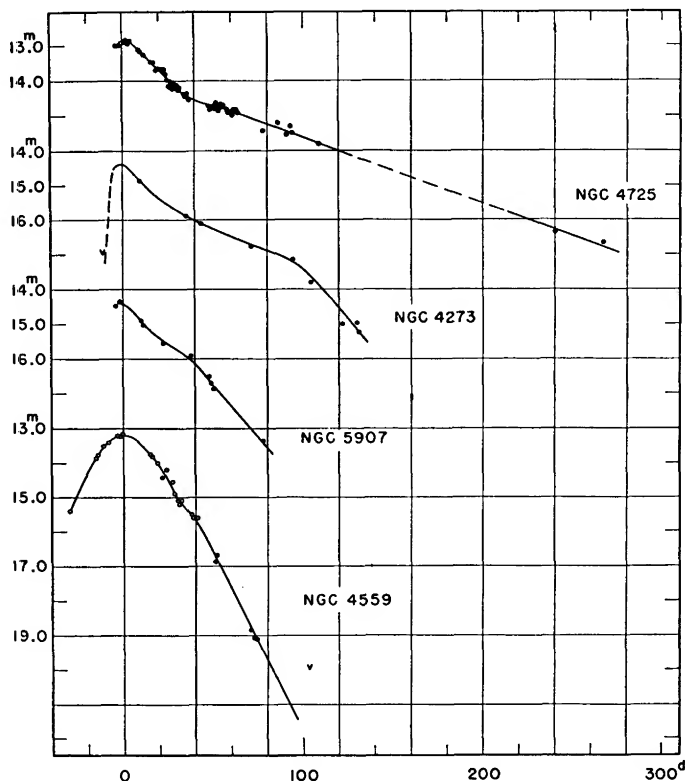


FIG. 16.—The light-curves of supernovae of type II show considerably greater variations in shape than those of supernovae of type I, which, except for the variability in the inclination  $\alpha$ , are well represented by the schematic light curve of Fig. 12.

As a very preliminary appraisal of the characteristics of this type we may state the following:

a) Supernovae of type III hover around maximum for many weeks, rather than only for a few days, as do types I and II. For instance, although the data have not yet been reduced, the light-curve of SN 93 seems to have the general character depicted in Figure 22.

b) During the many weeks near maximum brightness the spectrum is essentially a featureless continuum, with the blue and violet radiation strong.

c) At the next stage, weeks after maximum brightness, the continuum falls

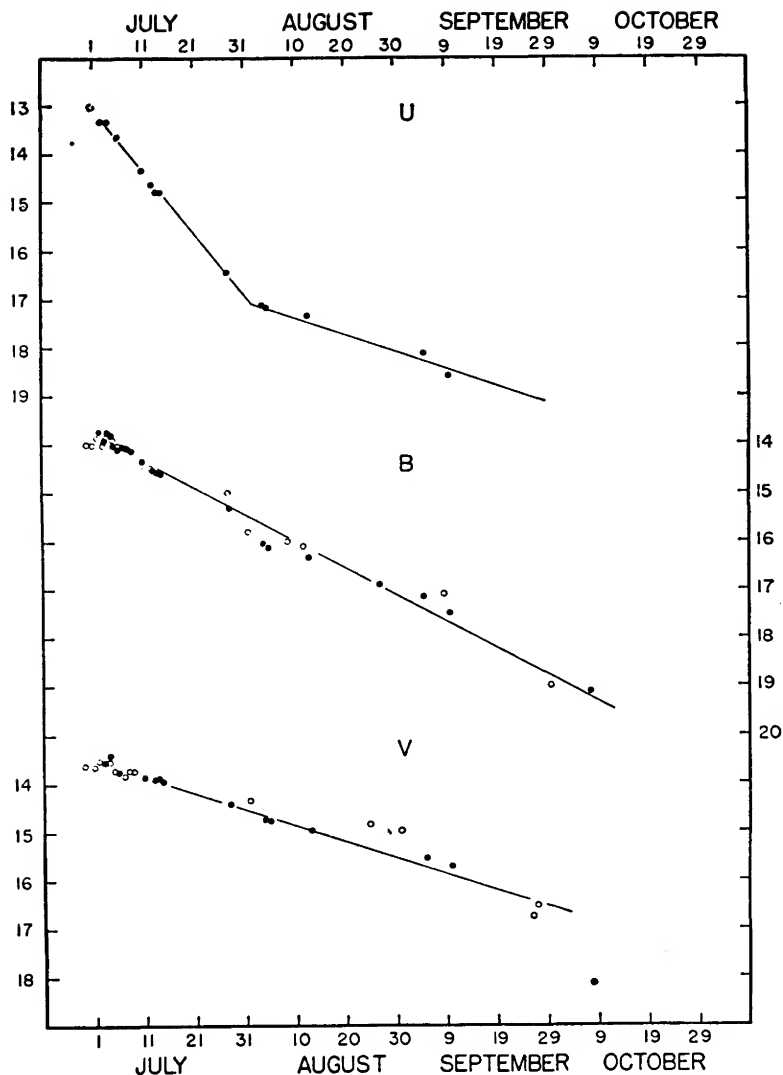


FIG. 17.—“Light-curves in three colors for the supernova No. 63 in NGC 7331.  $U$  points are from photoelectric observations only. The first point (*open symbol*) is from an extrapolation of the  $U - B$  color-curve, added to  $B$  magnitude at that time. In the  $B$ -curve the open symbols are magnitudes transformed to  $B$  from  $m_{pg}$  (Schmidt plates). The closed circles are measures directly on the  $B$  system (reflector plates and photoelectric observations). In the bottom,  $V$ -curve, the open and closed circles represent photographic and photoelectric observations, respectively.” Although the spectra of all supernovae of type II are surprisingly similar, it can be seen from Figs. 16 and 17 that the light-curves of these objects show few common features. (Curves and quote from H. C. Arp, *Astrophysical Journal*, 133, 883, 1961.)

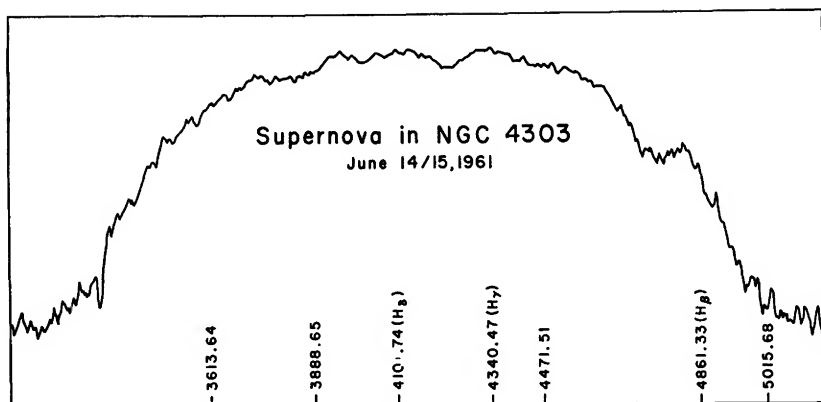


FIG. 18.—Linear microphotometer record of the spectrum of June 14/15, 1961, shown on Pl. VI, B, of type III supernova in NGC 4303. The spectrum is almost completely featureless and extends far into the ultraviolet, characteristics which for this type of supernova persist for many weeks about maximum brightness and which indicate that very large masses of gases are ejected from the supernova at very high temperatures.

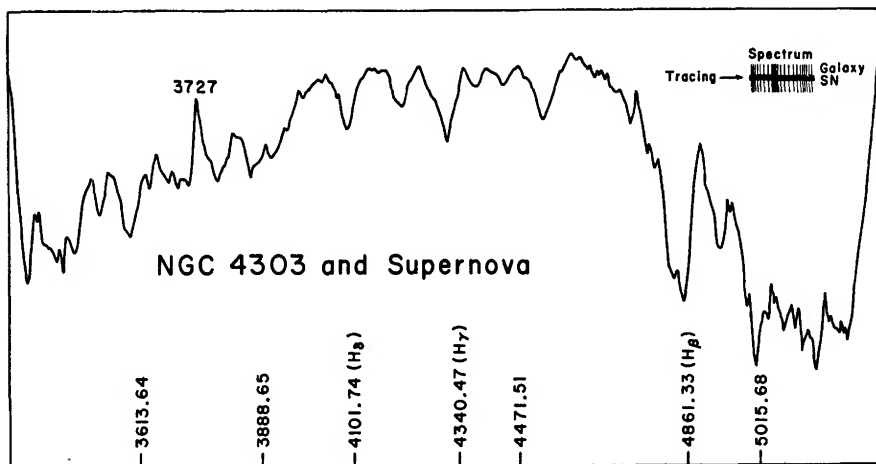


FIG. 19.—Linear microphotometer record of the spectrum of February 1/2, 1962, shown on Pl. VI, C, of type III supernova in NGC 4303. The tracing was made exactly through the central horizontal ribbon of the spectrum, as shown in the sketch at the upper right. The tracing therefore gives the main features of the supernova, at a late stage, partly distorted and washed out by the superposed light from parts of the galaxy which are in the line of sight with the supernova. Nevertheless, many of the emission bands, such as  $H\beta$  and the broad complex around  $\lambda$  4600 seem to be caused by the supernova, while the bright line  $\lambda$  3727 originates in a permanent and compact emission nebosity which can be seen on 48-inch Schmidt plates taken prior to the date of flareup of the supernova.

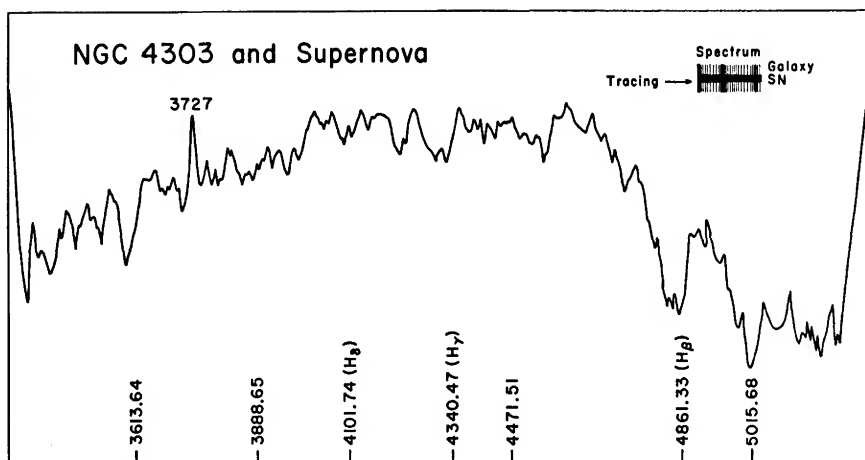


FIG. 20.—Linear microphotometer record of the spectrum shown on Pl. VI, C. In contradistinction to the curve reproduced in Fig. 19, this record was obtained by tracing along the edge of the spectrum of the supernova and the adjacent parts of the galaxy, as indicated by the arrow in the upper right of the figure. It is seen that certain features of the supernova spectrum, such as the  $H\beta$  emission, begin to be depressed relative to the superposed features of the spectrum of the galaxy.

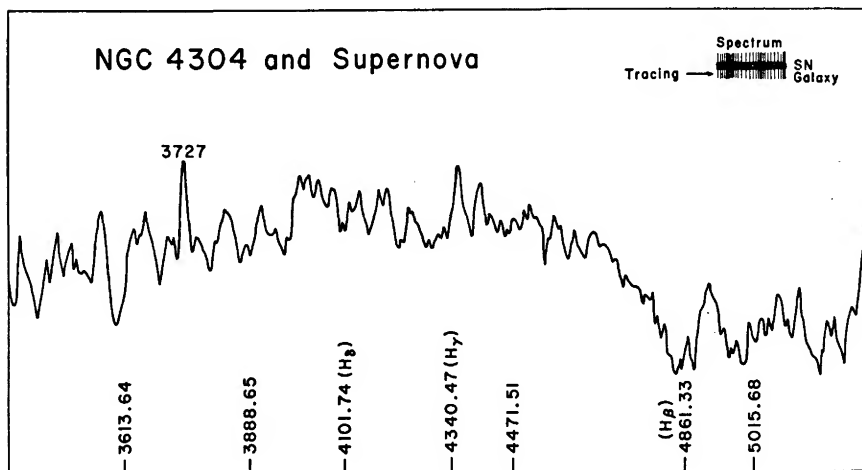


FIG. 21.—Linear microphotometer record of the spectrum shown on Pl. VI, C. In contradistinction to the curves reproduced in Figs. 19 and 20, this record was obtained by avoiding the spectrum of the supernova and tracing through the spectrum of the parts of the galaxy NGC 4303 which lie adjacent to the supernova. While the broad band around  $\lambda 4600$  has disappeared, emission at  $H\beta$  persists,  $H\gamma$  has become distinct and sharp, and  $\lambda 3727$ , of course, remains pronounced and sharp; also, the absorption at H and K has now become distinct.

apart into bands, the distribution of which is very similar to that in type II. As in the latter case the bands seem to be mostly due to emission of the lines of simple atoms, such as hydrogen, helium, and so on.

d) On February 1, 1962, I succeeded in photographing the spectrum of SN 93 at approximately magnitude  $m_p = 19.5$ . From the appearance of the bright line  $\lambda 3727$ , as well as from the direct photographs, it is obvious that the supernova is superposed on an emission nebulosity the total brightness of which rivals the brightness of the supernova on February 1, 1962. It is therefore difficult to make a clear-cut assignment of all emission lines to the supernova. Nevertheless, it seems that many among these lines are the same as those in fast common novae and in supernovae of type II and that they originate as allowed or as forbidden lines of hydrogen, helium, and other light atoms in the periodic system.

3.5.4. *Supernovae of type IV.*—Only one specimen of this type has so far been discovered. This is the object SN 89 in NGC 3003. Both its light-curve and its

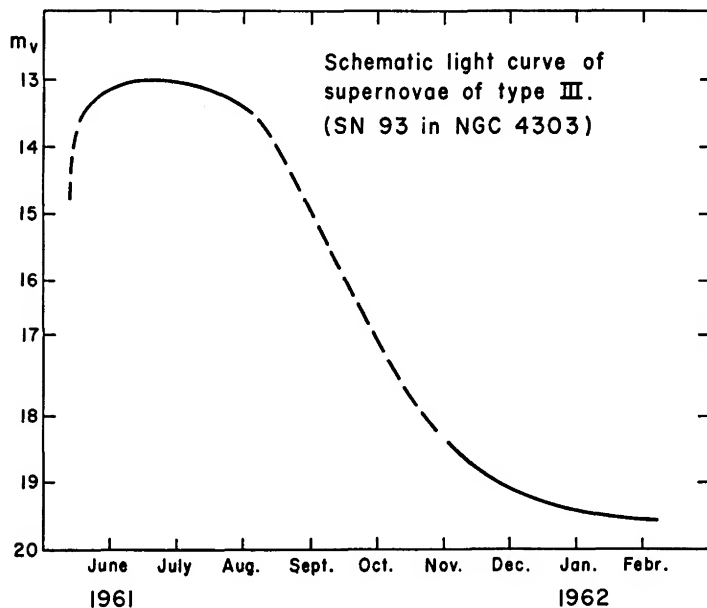


FIG. 22.—Schematic light-curve of a type III supernova. Although the magnitudes for supernova No. 93 in NGC 4303 have not yet been determined, we present here some very approximate estimates. It is seen that a very broad maximum which extends over several months is followed by a rapid decline which amounts to over 6 mag. We hope to follow the supernova with the 200-inch telescope in order to ascertain whether or not the final decline is as slow as depicted in the plot shown here. It is to be noted that supernovae Nos. 34 and 39 in NGC 5907 and NGC 4559 exhibited similarly rapid declines, as shown in Fig. 16. The maxima of their light-curves were, however, not particularly broad; while the spectrum of supernova No. 34 in NGC 5907 was definitely classified by R. Minkowski as being of type II, the character of the spectrum of supernova No. 39 in NGC 4559 at the time was thought to be peculiar.



spectrum seem to be different from all other types of supernovae. In Plate VII, *A*, photographs are shown of NGC 3003 with the supernova bright and faint. On Plates VII, *B*, VIII, *A* and *B*, and Figures 23, 24, and 25, spectra and their respective tracings are reproduced.

Since the supernova seems to have been at maximum on about February 20, 1961, the first spectrum (*a*) which was obtained on March 12 already appears well resolved into about a dozen very broad bands in the wavelength range from 3400 to 5000 Å. These bands are more numerous and somewhat better separated than those in spectra of supernovae of type I, but so far they are

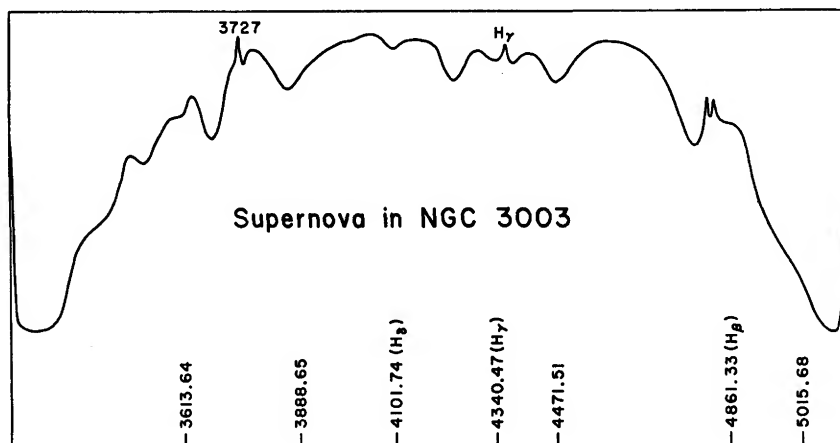


FIG. 23.—Linear microphotometer record of the spectrum of March 12/13, 1961, shown on Pl. VII, *B*, of type IV supernova No. 89 in NGC 3003. A number of broad bands are seen which, like those in type I supernovae, cannot as yet be identified. The discovery of more supernovae of type IV must be awaited before we can even tell to what extent the bands seen on the tracing are characteristic. Sharp lines such as  $H\gamma$  and  $\lambda$  3727 no doubt originate in permanent features of the parent galaxies.

equally uninterpretable. They appear to be about 100 Å in (half-)width, indicating that gas clouds were ejected from this supernova at velocities of about 6000 km/sec, similar to those characteristic of supernovae of type II.

Between March 12 and the date of the second spectrum on April 20, there occurred some rather drastic changes. Two broad bands remained on April 20, the relative intensity of which changed considerably from the spectrum (*b*) of April 20 to that (*c*) of April 21. The only sharp and identifiable features are  $H\gamma$  and  $\lambda$  3727, whose origin is presumably in some emission nebulosities of NGC 3003.

For a partial light-curve, reproduced in Figure 26, I am greatly indebted to Professor G. Haro, director of the Tonantzintla Observatory. As seen from Figure 26, the light-curve is quite unique and totally different in character from any of the other known supernovae.

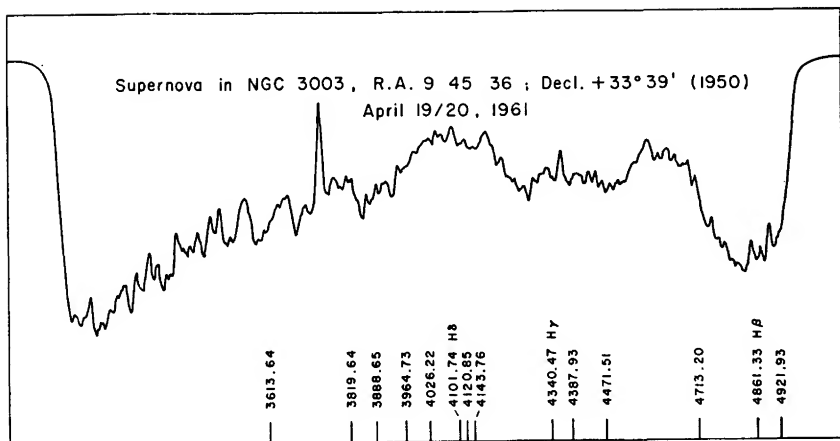


FIG. 24.—Linear microphotometer record of the spectrum obtained on April 19/20, 1961, and shown on Pl. VIII, A, of type IV supernova No. 89 in NGC 3003. The same broad bands which are indicated on the tracing of Fig. 23 are present and better pronounced, at about 4900, 4600, 4400, 4100, and 3800 Å. The ultraviolet continuum is relatively weak.

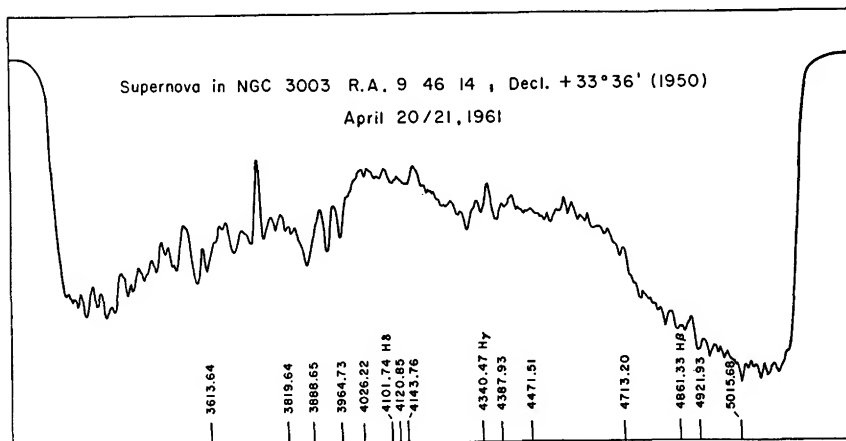


FIG. 25.—Linear microphotometer tracing of the spectrum obtained on April 20/21, 1961, and shown on Pl. VIII, B, of type IV supernova No. 89 in NGC 3003. All features seen on the tracing of Fig. 24 are present, but the band at 4600 Å has much declined in intensity relative to the band at 4100 Å, and the ultraviolet continuum is much weaker, although the spectra analyzed in Figs. 24 and 25 were photographed only 1 day apart.

The spectrum and light-curve of SN 89 seem therefore distinctive enough to suggest the classification of this supernova as one of a new type IV.

3.5.5. *Supernovae of type V.*—Several supernovae in the past appeared to be excessively faint at maximum, with  $\Delta m = m_s - m_G$  assuming values as high as 6. The four objects SN 7 in NGC 5457, SN 17, SN 49, SN 58, in NGC 5236 are particularly noteworthy. Unfortunately, SN 7 occurred so long ago and so few observations are available that one could not be certain whether or

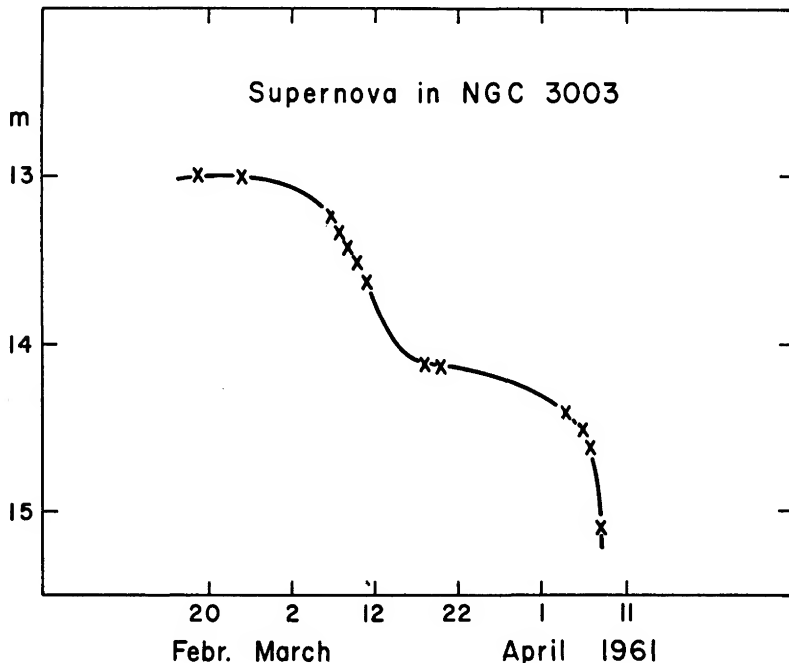


FIG. 26.—Partial light-curve of type IV supernova No. 89 in NGC 3003. The values plotted were kindly supplied by Professor G. Haro, director of the Tonantzintla Observatory.

not the maximum had been missed. To some extent the same uncertainty applies to the three objects which flared up in NGC 5236, because this galaxy is located so far south that the records obtained by the observers at Palomar and the Northern Hemisphere in general are very scanty. Also, no spectrum of any of these supernovae could ever be secured. On the other hand, the light-curves which show hovering of the luminosity around maximum for many months suggested that we here deal with some sort of subluminescent supernovae, similar perhaps to  $\eta$  Carinae of 1843, whose absolute magnitude may be of the order  $M \sim -13.0$  instead of  $-18.0$  for all other supernovae.

Fortunately, a flareup of the type described was recently discovered by P. Wild in NGC 1058. Many direct observations, as well as spectra, have been ob-

tained of this supernova, and I entertain high hopes that significant records can be secured for quite some time to come. These hopes are based on the expectation that SN 96 is a supernova of the type of  $\eta$  Carinae (Bok 1932). The general record, to date is as follows. For many years, in the present position of SN 96 a star of approximately the eighteenth magnitude was present, showing no perceptible variations. This statement, however, will be checked upon more thoroughly. In July, 1961, P. Wild reported a flareup to about the fourteenth magnitude in the exact position of this star. All supernova observers on the Palomar program were unfortunately absent during that time (attending the I.A.U. meeting in Berkeley and various associated symposia). Fortunately, however, Dr. F. Bertola, of the Asiago Observatory, secured spectra and announced in Berkeley that they were different from those of supernovae of type I.

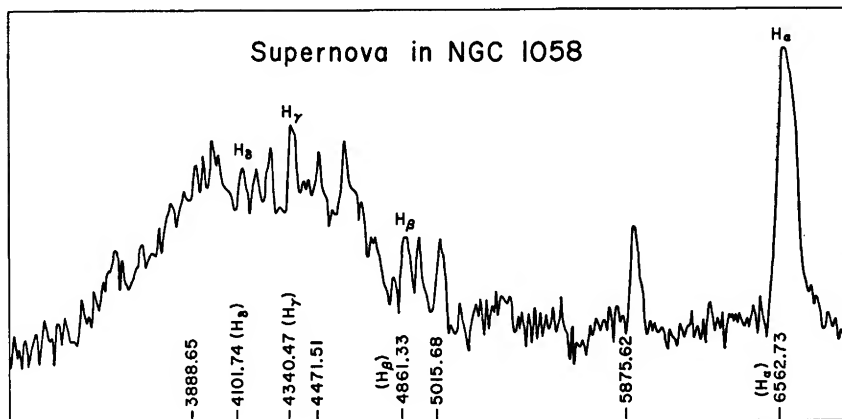


FIG. 27.—Linear microphotometer record of the spectrum of February 1/2, 1962, shown on Pl. IX, *A*, of type V supernova in NGC 1058. Emission bands such as H $\alpha$ , H $\beta$ , H $\gamma$ , H $\delta$ , etc., are clearly discernible. A detailed analysis of all the significant features remains as yet to be carried through.

Later on, the Palomar observers obtained a series of good spectra, some of which are reproduced on Plate IX, *A* and *B*, together with straight tracings in Figures 27 and 28.

These spectra show emission lines or bands of moderate widths, which are due to hydrogen, helium, and so on, as described in Dr. Greenstein's account, which follows. The supernova slowly declined in brightness through September and October, 1961, and then flared up in November to about the fourteenth magnitude again. On the assumption that good information could be obtained at that time, Greenstein secured a spectrum with a dispersion of 18 Å/mm, which, however, turned out to be an almost featureless continuum, characteristic of a very hot (O-type) star. Since December, 1961, the nova has steadily declined in brightness and in February, 1962, showed a spectrum as seen above in Plate IX, *A* and *B*.

Since NGC 1058 has a redshift of only 80 km/sec and an apparent magnitude of  $m_p = 12.7$ , it is probably a nearby dwarf spiral. Photographs of the galaxy with the supernova bright and faint are reproduced in Plate X, A. In view of the uniqueness of this star, it will, however, be important to attempt resolution of NGC 1058 with the Hale telescope and under the very best conditions of seeing, in order to obtain a good estimate of the absolute brightness of this star. In the meantime, I have succeeded in getting better spectra of NGC 1058 which show that its redshift is +439 km/sec. An extended light-curve of this supernova has been published (Zwicky 1964).

For the time being, I repeat that the account presented in the preceding of the various types of supernovae must be considered as a groping attempt at

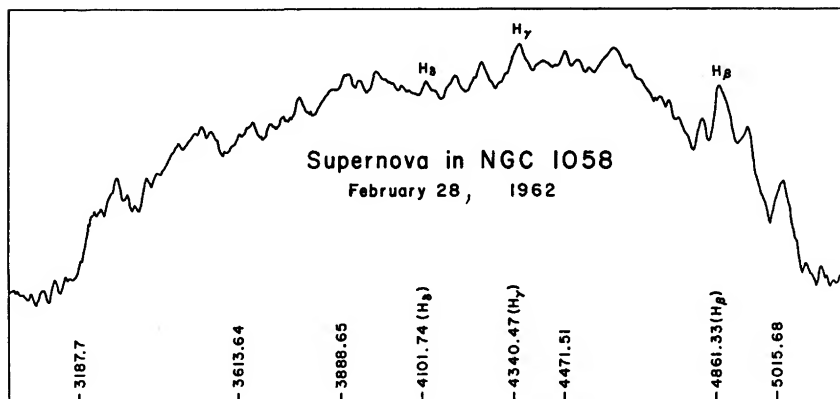


FIG. 28.—Linear microphotometer tracing of the spectrum of February 28, 1962, shown on Pl. IX, B, of type V supernova in NGC 1058. Note the far extension into the ultraviolet.

classification. Unfortunately, a great number of the really significant observations have been obtained only during the past year, and it has not yet been possible to analyze them and incorporate any final results in this report. Some more detailed considerations, however, were kindly put at my disposal by Professor J. L. Greenstein, and they are presented in the following section.

### 3.6. REMARKS ON RECENT SUPERNOVAE SPECTRA

While no very bright supernovae have appeared in recent years, improvement of spectrographic techniques has permitted observation of several objects for long periods of time, at higher resolution than had previously been obtained. In addition, a spectrophotometric program gave the relative intensities of individual bands, in widely different portions of the spectrum, as functions of time. These very detailed measurements are still being collected, but a few major results can be mentioned.

Without prejudging the number of different types of supernovae that exist, it is clear that a large number follow the spectral evolution sketched by Min-

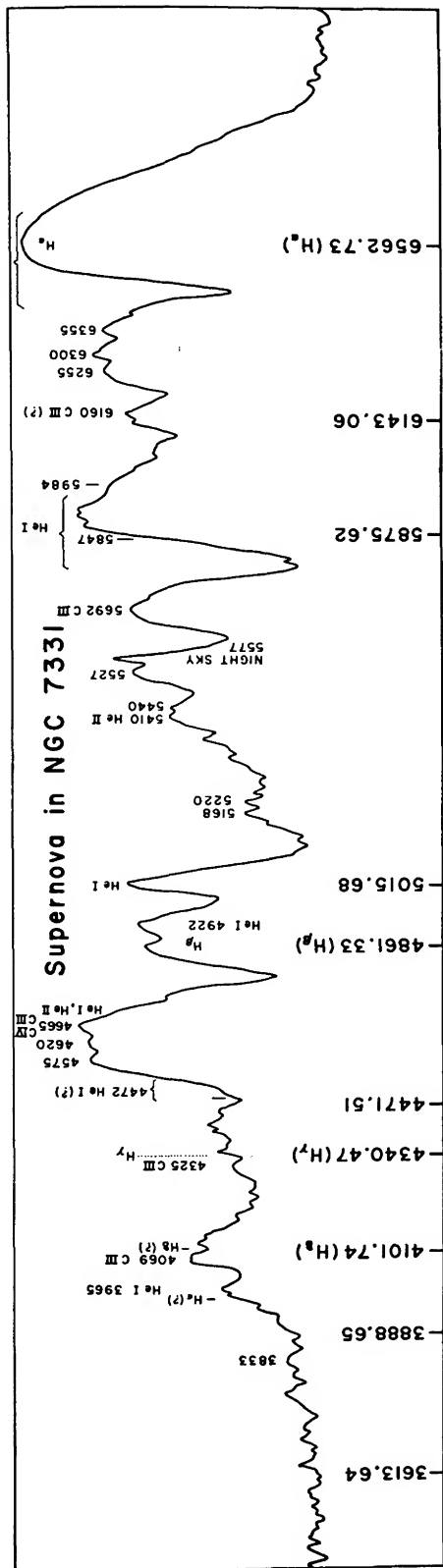


FIG. 29.—Linear microphotometer tracing of the spectrum of September 1, 1959, shown in Pl. X, C, of type II supernova in NGC 7331

kowski and are members of a fairly homogeneous class of type I. Both the spectral features and wavelength shifts follow a consistent general pattern. I will assume, without definite proof, that the features are emission on a background of continuum or weak emission. Near light-maximum, all features show a relatively low contrast, with maximum rising about 50 per cent above a base level. At later phases, many features rise to about 300 per cent of the base level. The strong emission bands have half-widths in the range 60–200 Å, or 4000–10000 km/sec. It is not yet possible to identify any spectral feature with certainty. Since it seems probable that the very broad bands are composite, the ejection velocities may be as low as 3000 km/sec. The sharper features appear for a limited period, the sharpest being near  $\lambda$  3700 and  $\lambda$  4920, with total widths near the background of 1000–1500 km/sec, i.e., a quite low expansion velocity. The shift to longer wavelengths discussed by Minkowski is confirmed, amounting to about 40 Å for bands in the supernova in NGC 4496, over a period of 60 days. Its possible interpretation will be discussed later.

Most effort has been expended in the study of the supernovae of type II in NGC 4303<sup>2</sup> and NGC 7331 (Plate X, *B* and *C*). These objects were remarkably similar from a spectroscopic point of view. Near maximum the spectra were essentially featureless, showing a blue continuous background on which were visible very wide, low-contrast emissions. These may have had very broad violet-shifted absorption components. The total width from one minimum to the next was 170 Å or 12000 km/sec, for about 3 days after discovery (magnitudes,  $V = 13.6$ ,  $B - V \approx +0.3$ ). The next spectra, 34 days later, showed a fully developed absorption and emission-band spectrum, which strengthened in contrast, and also showed velocity changes until the object became too faint 65 days after discovery (magnitude  $V = 15.3$ ,  $B - V = +1.6$ ). On the last spectrogram, the very strong band at  $\lambda$  4650 was 190 Å wide at half-intensity, although other features were only 70 Å in half-width. In type II supernovae, therefore, it is almost certain that some of the strong bands, like  $\lambda$  4650, are a composite of many atomic lines. It is very interesting to note that one of the strongest features in type I spectra is also centered near  $\lambda$  4600 soon after maximum and has a half-width of 200 Å. According to Minkowski, this feature drifts from  $\lambda$  4500 to  $\lambda$  4680 in about 350 days in type I supernovae. It is therefore plausible that at least some of the atomic contributors to the band are the same in type I and type II spectra, possibly He I, He II, C III, C IV, N III, N IV(?), O V(?). (See Fig. 29.)

The most interesting aspect of the spectra of type II supernovae, 30–60 days after maximum, is that a number of features can be identified as H, He I, C III, with H $\alpha$  and  $\lambda$  5876 of He I very clearly present and accompanied by a deep, displaced violet absorption component. H $\beta$ ,  $\lambda$  4922,  $\lambda$  5015 of He I are also present, but higher members of the series are not recognizable. After 60 days, H $\alpha$  is more than 200 Å wide in emission, and the absorption core is displaced

<sup>2</sup> Note that Zwicky classifies this supernova as type III.

110 Å, i.e.,  $-5000$  km/sec;  $\lambda$  5876 is displaced to  $-4000$  km/sec. The most striking phenomena, however, are connected with the wavelength shifts of the relatively sharp line  $\lambda$  4861 soon after maximum. The violet side of the absorption edge was displaced  $-11000$  km/sec, when first seen in NGC 4303, and was displaced to  $-8000$  km/sec, 33 days later. The center of the emission line was at  $-7500$  km/sec, shifted to  $-3000$  km/sec in the same period, and later to nearly zero. The plausible interpretation is that the star was opaque and that cool, high-velocity gas up to  $-11000$  km/sec existed. The displaced emission line can be ascribed to the forward side of the expanding shell, and its drift back to zero velocity was caused either by deceleration or by growing transparency, which revealed the far side of the shell or both. Thus an enormous gas mass is required, which became transparent only after more than 30 days, in spite of a speed exceeding  $10000$  km/sec, i.e., at a radius of more than 200 astronomical units.

The spectrum of the supernova in NGC 1058 presents very many interesting problems, although it has a close resemblance to the spectra of supernovae of type II. The emission lines are quite sharp, with half-widths of approximately  $2000$  km/sec. Lines of hydrogen and neutral helium, as well as many other features similar to those in type II supernovae, are visible. There is no doubt that a few shortward-displaced absorption lines appeared early, and there seems to be a persistent absorption at  $\lambda$  3888, presumably due to the metastable helium atoms in the  $2^3S$  level. Because of the combination of emission and absorption, there are quite conspicuous velocity shifts at an early phase which seem to be disappearing toward the end of the period of observation. Thus the lines became sharper, by approximately a factor of 2, and shifted by approximately half their width, to shorter wavelengths between November 12, 1961, and January 29, 1962. The complexity of the spectrum and the fact that some material is available at  $18$  Å/mm dispersion suggest that a very detailed study of this type of object will be valuable. In spite of the peculiarity of the light-curve, there is little doubt that this object is more closely related to supernovae of type II than it is to ordinary galactic novae even of high luminosity. Forbidden lines had not yet appeared at the end of January, 1962.

*End of Dr. Greenstein's remarks*

### 3.7. THE REMNANTS OF SUPERNOVAE

The investigation of the remnants of supernovae and their relation to historical records, both written and unwritten, will be one of the most fascinating tasks awaiting the next generation of astronomers. These records may also include various features of a geological and a biological nature, referring back to evolutionary phenomena of the earth's surface and the life on it. Already at the present time a book could be written about the subject of the remnants of supernovae and about the efforts which have been made to elucidate their characteristics. These efforts have mainly followed along two avenues, namely, (a) the



investigation by optical means of the remnants of supernovae in the Milky Way, as well as in neighboring galaxies, and (b) the investigation by radio astronomy (Harris 1961) of some of the remnants of past supernovae in the Milky Way and in extragalactic systems.

The radio investigation of supernovae remnants was, of course, initiated when Bolton and Stanley (1949) identified the Taurus A source with the remains of the galactic supernova of 1054 A.D., that is, with the Crab Nebula (Messier 1).

#### § 4. THE INTRINSIC PROPERTIES OF SUPERNOVAE (ABSOLUTE MORPHOLOGY)

The final aim of any specifically astronomically-oriented investigation must naturally be to understand qualitatively and quantitatively the intrinsic properties of the celestial objects and of the phenomena which govern their interactions. Applied to supernovae, this means that we wish to know their average frequency of occurrence per year and per cubic megaparsec of cosmic space at all distances, their distribution in absolute luminosities, the masses of the gases expelled, and the masses of the remnants. The temperatures generated during the outbursts and the generation of cosmic rays are also of the greatest interest. The answers of these questions depend obviously on a fairly accurate knowledge of the cosmic distance scale. Since this scale has not yet been reliably established, any absolute assertions which we make about supernovae are still in part speculative. On the other hand, studies of the apparent characteristics of supernovae, such as we have discussed in this review, can be of great help in our efforts to establish, first, a relative and, later on, an absolute cosmic distance scale. Without committing ourselves to any definite distance scale and to any definite value of the Lundmark-Hubble redshift constant, we present the following thoughts.

From the distance of the Crab Nebula it follows that the absolute visual luminosity of the supernova of 1054 A.D. at maximum brightness could hardly have been greater than that corresponding to an absolute visual magnitude of  $M_v = -18$ .

Assuming that the distance modulus of Messier 31 is  $\mu = 24.4$ , the supernova of 1885 would have had an absolute visual magnitude  $M_v = -17.2$  at maximum brightness, provided that its apparent brightness had not been greatly affected by interstellar and intergalactic obscuration.

Likewise, from a comparison of the brightest stars in IC 4182 and NGC 4214 with the two type I supernovae Nos. 25 and 50 which respectively flared up in the two systems, the absolute magnitudes of the two supernovae are probably near  $M_v = -18.0$ .

As to more decisive observational criteria for the determination of the absolute magnitudes of type I supernovae, I suggest the following:

a) An attempt to investigate the remnants of supernovae, both in the Milky

Way system and in nearby galaxies. Direct determinations of the angular sizes of the expanding disks of gases will give us a trigonometric means of distance determination, analogous to that used in the case of the Crab Nebula, as well as for some common novae.

b) The comparison of the distribution  $n(\Delta)$  (see Fig. 7) for a group of nearby galaxies, whose distances are known by independent means, and for galaxies at very much greater distances will provide us with an independent statistical method for the determination of the Lundmark-Hubble redshift constant,  $H$ . For instance, if maximum values of the indicative  $\Delta$ 's (see Fig. 6) should be found for very remote galaxies that are consistently greater than the maximum values of the  $\Delta$ 's for the giant nearby galaxies, we could conclude that the Lundmark-Hubble redshift constant must be correspondingly greater than 100 km/sec per million parsecs.

From the estimates of the absolute magnitudes ( $M_v \cong -18.0$ ) of type I supernovae mentioned above, as well as from the fact that some  $\Delta$  values for remote galaxies are excessively large, I am inclined to conclude in a preliminary way that  $H$  is perhaps of the order of 175 km/sec per million parsecs rather than 100 km/sec. In any event, if further discoveries of supernovae in remote clusters confirm the presently probable fact that supernovae of type I have a small dispersion ( $< 1.0$ ) in their absolute photovisual magnitudes, very low values of  $H$  of the order 75 km/sec per million parsecs, such as have been advocated by Sandage (1958) and others, would appear to be unrealistic.

As to the determination of both a relative and an absolute cosmic distance scale, it should be emphasized that, so far, supernovae and the study of the structural features of spherical clusters of galaxies provide the only rational means (Zwicky 1960).

#### 4.1. THEORY OF SUPERNOVAE

Since the theory of supernovae will be treated in another article of this volume,<sup>3</sup> I shall confine myself to a brief exposition of some of the ideas that I have suggested in the course of the last thirty years. A few of these ideas have gradually found increasing confirmation by subsequent observations, as well as growing support by other investigators, while others, as yet unproved, may be useful for future investigations on supernovae.

4.1.1. *Possible material constellations which may become the origins of supernovae.*—(1) The seats of supernovae may be individual stars; (2) the seats of supernovae may be multiple stars; (3) some supernovae may not be related to stars at all but may be the result of catastrophic collapses of gas and dust clouds; (4) supernovae may be the results of the collapse of gas and dust clouds on stars; (5) any of the above-mentioned types of events may, for the observer, assume appearances that are vastly different from the appearances of the intrinsic events. This will happen, for instance, if the radiations issuing from

<sup>3</sup> Chapter 6, by E. Schatzman.

supernovae impinge on matter such as gas clouds which surround them and are thereby fundamentally transformed in their composition and intensity.

4.1.2. *Possible transformations of the radiations from supernovae by the surrounding interstellar medium or by neighboring stars.*—(a) Transformations of the electromagnetic radiation from supernovae may be of the following types: reflection and scattering by dust clouds; excitation of fluorescence radiation in surrounding gas clouds, including ionization of the gases in these clouds; transmission of momentum to the interstellar gas and dust clouds because of the above effects. (b) Cosmic rays from supernovae not only will excite and ionize surrounding dust clouds but will also induce various nuclear reactions and thus vastly change the relative abundances of the elements in the interstellar clouds around a supernova outburst. In a case of this sort it would be quite impossible to deduce the composition of the material ejected from a supernova by the direct analysis of the integrated spectra. (c) The gas clouds ejected from a supernova are conjectured to possess mass<sup>4</sup> velocities of up to 30000 km/sec. In supernovae of type II they have, according to present interpretations of their spectra, velocities of at least 7000 km/sec. Such clouds, impinging on interstellar material, will cause a great variety of effects, while they themselves lose energy and momentum and thereby carry the interstellar material with them.

Impinging on very nearby stars, the cosmic rays and the gas clouds ejected from supernovae may actually induce nuclear fusion reactions and thus possibly give rise to *chains of supernovae* (Zwicky 1961a, 1962). Events of this sort are particularly likely in the most crowded parts of galaxies, such as the dense nuclei.

So far, only supernovae of type I, which have appeared in elliptical galaxies or in regions far removed from the crowded central regions of spirals, have exhibited uniform traits as to the time sequences of their spectra and the shapes of their light-curves. This leads to the suspicion that some of the other types of supernovae—that is types II, III, and IV—might not all be really different intrinsically from type I but might appear to be so partly or entirely because of secondary actions of the types mentioned above.

4.1.3. *Reasons for the collapse of stars.*—In addition to non-degenerate hot gaseous and almost completely ionized interiors of stars, electronically degenerate states of such gases under high gravitational pressure have been studied for many years, especially with a view to understanding the physical characteristics of white dwarfs. In this connection the idea has been advanced that the rapid transition from the ordinary state of matter into degenerate matter—that is, the transition from densities of a few grams per cm<sup>3</sup> to densities of the order of 100000 grams per cm<sup>3</sup>—might account for some of the outbursts of novae and of supernovae.

<sup>4</sup> Those which refer to the average directed motions of macroscopic or cosmic bodies of matter are called mass velocities. Particle velocities are those of individual elementary particles whose motions may be random or directed. There is no doubt that particle velocities nearly that of light exist in supernova outbursts.

In addition, the present author pointed out (Baade and Zwicky 1934; Zwicky 1938) that the ultimate states of collapsed matter are to be looked for in *nuclear matter*, in which the electrons have essentially been entirely absorbed by protons or nuclei, which are closely packed with internuclear distances of the order of  $10^{-13}$  cm and densities of the order of  $10^{13}$  gm/cm<sup>3</sup>. In transitions of stars from the ordinary or electronically degenerate states of matter into nuclear matter, energies would be liberated that are of the order of  $\text{Mc}^2$  of the stars themselves, and the tremendous radiation from supernovae would thus be easily understandable.

The idea of neutron stars, neutron cores, and nuclear goblins for many years did not seem to find any particular appeal until, in recent years, Cameron (1959) started new and detailed investigations of the nuclear evolution of stars which ultimately results in the collapse into neutron stars and the flareup of supernovae.

Cameron (1959) and Ambartsumian and Saakian (1960) also suggested that beyond the neutron stars we should visualize the possibility of hyperon stars of still greater densities ( $10^{19}$  gm/cm<sup>3</sup> instead of  $10^{13}$  gm/cm<sup>3</sup>). It should be noted that the general concept leading to the idea of neutron stars and hyperon stars is related to the fact that, under very high pressures, some of the unstable nucleons and strange particles become stable. Indeed, once the electron states or Fermi levels in the highly compressed matter are filled up to energies corresponding to the energies liberated on disintegration of the said particles—for instance, 780000 electron volts for the neutrons—the particles cannot decay any more.

In connection with the ideas mentioned above, much work remains to be done that will allow us to associate some of the modes of collapse of stars with specific events observed among the novae and supernovae. For the present it is not yet possible to identify any particular supernova with any particular model of a stellar collapse.

4.1.4. *Reasons for the collapse of large gas clouds.*—The gravitational collapse of gas clouds has been studied with the idea in mind that it might be one of the major processes leading to star formation. In particular, such clouds seem to become easily unstable if their masses are greater than some critical mass that is much greater than that of the sun. Also, it would seem that if the mass of the gas cloud is too great, complications will set in, and an orderly collapse toward one central condensation will become impossible. Uniform aspects and small dispersion in the absolute luminosities of supernovae of some of the types would thus find an explanation.

For some of the supernovae observed, we have felt for a long time that masses much greater than the sun's mass were involved and that the theory of collapsing gas clouds might therefore be of importance for our understanding of supernovae. The suspicion that greater-than-stellar masses are involved in some supernova outbursts arises, first, from the size of certain remnants such as the Crab Nebula and, second, from the fact that the bands of supernovae of types

II and III are first present with their violet half-width only and later on widen to their full width, as Dr. Greenstein has pointed out in his section of this review.

4.1.5. *The various radiations from supernovae.*—Without going into any details, mention may be made of some conclusions and suggestions made by the author more than twenty years ago and which now have been either confirmed or have become highly probable. These conclusions were as follows:

a) A very bright supernova reaches a visual luminosity of several billion times that of the sun (Zwicky 1940).

b) The total energy radiated away in the form of visual light is greater than  $10^{48}$  ergs (Zwicky 1940).

c) The total energy radiated away in the form of electromagnetic radiation may be as high as  $10^{51}$ – $10^{55}$  ergs, since I estimated that the surface temperature at some of the very initial stages could be of the order of up to 3 million degrees Kelvin. Integrated amounts of radiation of the mentioned orders would mean mass losses of from  $3 \times 10^{30}$  to  $10^{34}$  gm (or five solar masses).

As to the kinetic energy imparted to gas clouds and individual particles, the following conclusions have been reached:

d) Maximum mass velocities for the ejected gas clouds up to 30000 km/sec or more may be expected.

e) Cosmic rays are directly generated by two processes, namely, first, because electrical potential differences of about  $10^{11}$  volts exist between any two large parts of any hot star, cosmic rays of the energy of  $10^{11}$  electron volts will be generated by the collapse of the permanent (but fluctuating) electric field when the star violently flies apart because of some excessive liberation of internal energy (Zwicky 1939a). Second, during the ejection and expansion of the gas clouds, positive and negative particles are separated by persistently and differentially acting light-pressure (Zwicky 1939b). Fields of up to  $10^{19}$  volts are built up in the process, which, after the radiation has decreased materially in intensity, will collapse and generate cosmic-ray particles of up to  $10^{19}$  electron volts. This type of energy, which at the time of my prediction was unheard of, has, of course, been confirmed.

f) Likewise confirmed was the conclusion from the above consideration (Zwicky 1939b) that the cosmic rays must contain nuclei of all atomic weights.

g) Finally, from the frequency of supernovae known, it was calculated that the cosmic-ray intensity created by them on the surface of the earth's atmosphere should be of the order of  $10^{-3}$  ergs/cm<sup>2</sup> sec, which is in accordance with the observed intensities.

## § 5. CONCLUSION AND RECOMMENDATIONS

Astronomy and astrophysics, as compared with all the other sciences, are vastly handicapped because of the present impossibility of experimenting with the celestial objects outside the solar system. Fortunately, most of the celestial objects can be observed for indefinitely long periods of time. The investigation

of supernovae shares the difficulties mentioned with general astronomy. In addition, however, research on supernovae is seriously plagued because supernovae are difficult to discover at the proper time and can be observed for only short periods. Also, for detailed investigations of their spectra, fairly large telescopes are generally necessary. All these factors have enormously slowed down our progress. In order to achieve greater efficiency, a special committee for research on supernovae was organized within Commission 28 (extragalactic nebulae) of the International Astronomical Union at the meeting of August, 1961, at Berkeley. This committee comprises representatives of the following observatories: Asiago, Italy (L. Rosino); Berne, Switzerland (P. Wild); Córdoba, Argentina (J. L. Sérsic); Crimea (B. V. Kukarkin); Meudon, France (Ch. Bertaud); Tonantzintla, Mexico (G. Haro); Tucson, United States (E. F. Carpenter); Mount Wilson and Palomar (F. Zwicky, *Chairman*). The program on supernovae will be greatly aided if astronomers who possess pertinent data communicate either with one of the members of the committee or with the chairman, who will include them in his *Circular Letters on Supernovae*, which are being sent to actively participating observatories.

In conclusion, it is worthwhile to emphasize a few points which appear to be of prime importance:

a) It is of the greatest importance not to miss any apparently bright supernova in one of the perhaps thousand nearest galaxies. Of such a supernova, short exposure spectra could be obtained in fast succession and in various wavelength ranges, which would give us the possibility of observing the short-lived sharp patterns in supernovae whose spectra are not yet identifiable and thus lead to an identification, as described previously in § 2. Nearby supernovae can also be followed for a long time, their remnants might be observable, and the emission of cosmic rays and of radio waves might be detectable.

b) Sequences of good spectra will be of importance in finding out how many types of supernovae actually occur. Integral features of the light-curves will also be significant in this connection, while detailed features of light-curves are probably much less important for our understanding of the phenomena involved than detailed features of the spectra.

c) Both in order to establish the dispersion in absolute magnitudes of various types of supernovae and for the construction of a reliable relative and absolute cosmic distance scale, it is imperative that we obtain the following three data on as many supernovae as possible: (1) apparent brightness at maximum, preferably the photographic and photovisual magnitudes; (2) the type of the supernova as indicated by its spectrum; and (3) the symbolic velocity of recession of the parent galaxy.

d) For purposes of cosmological theory, it will be desirable to search for supernovae in exceedingly distant clusters of galaxies and compare their characteristics and especially the frequencies with those in nearby similar clusters of galaxies.

Finally, a few remarks as to the usefulness of very exact light-curves for the theory of supernovae. My own present opinion on this matter, as I have already stated, is as follows: Because of the banded structure of the supernova spectra and because of the displacements and intensity variations of these bands by intrinsic effects, as well as by the universal redshift, exact  $U$ ,  $B$ ,  $V$  light-curves are of relatively little use to the theory unless at the same time a sufficient number of spectra are available. The latter are likely to give us far more information about the intrinsic happenings in supernovae than light-curves alone. For instance, it would appear to be highly speculative to deduce temperatures from light-curves. This applies even to the  $U$ ,  $B$ ,  $V$  magnitudes during the first days of the outbursts. It can be expected that infrared and far ultraviolet magnitudes of supernovae, to be obtained from observations with balloons and rockets, will lead to new surprises.

The author has been asked by nuclear physicists if exact  $U$ ,  $B$ ,  $V$  light-curves would not allow us to check the theory that the monotone decline with time of the apparent magnitude of supernovae of type I is due to the decay of several isotopes of californium and other elements. Both in view of the observational characteristics of the spectra of supernovae of type I and the disturbing influences on the light-curves discussed in § 4.12, any analysis of the light-curves, no matter how exact they be, in terms of decay-curves of unstable nuclei would seem to be a futile undertaking.

On the other hand, integral characteristics of light-curves, in combination with pertinent features in the spectra, will no doubt be necessary and useful to arrive at a first classification of supernovae of different types such as we have attempted in a very preliminary way in this review.

For co-operation in organizing the supernova search on an international scale I am indebted to all the members of the Committee on Supernovae within Commission 28 of the I.A.U., as well as to astronomers too numerous to be mentioned individually. My thanks go to them anonymously and collectively. For the many new results which have been already achieved, my sincere thanks go to my close collaborators at the Palomar Observatory (M. L. Humason, H. S. Gates, A. M. Gomes, K. Rudnicki, and C. E. Kearns), as well as to all my colleagues of the Department of Astrophysics, California Institute of Technology, and to a number of guest investigators at Palomar, who have occasionally secured for us badly needed plates with the 48-inch Schmidt telescope.

#### REFERENCES<sup>5</sup>

- |  |      |  |
|--|------|--|
| AMBARTSUMIAN, V. A.,<br>and SAAKIAN, G. S. | 1960 | <i>A.J.</i> , U.S.S.R., <b>37</b> , 193 ( <i>Soviet Astron.</i> , <b>4</b> , 187). |
| BAADE, W.                                  | 1942 | <i>A.p. J.</i> , <b>96</b> , 188.  |
|  | 1943 | <i>Ibid.</i> , <b>97</b> , 119.  |

<sup>5</sup> Additional references for data on individual supernovae appear in Table 1 (p. 375).

- BAADE, W., BURBIDGE,  
 G. R., HOYLE, F.,  
 BURBIDGE, E. M.,  
 CHRISTY, R. F., and  
 FOWLER, W. A. 1956 *Pub. A.S.P.*, **68**, 296.
- BAADE, W., and  
 ZWICKY, F. 1934 *Proc. Nat. Acad. Sci. U.S.*, **20**, 254.
- BERTAUD, CH. 1961 *Ann. d'ap.*, **24**, 516.
- BOK, BART J. 1932 *Harvard Obs. Rept.*, No. 77.
- BOLTON, J. G., and  
 STANLEY, G. J. 1949 *Australian J. Sci. Res.*, **2**, 139.
- BOWEN, I. S. 1959 *Carnegie Inst. Washington Year Book*, **58**, 60.  
 1960 *Ibid.*, **59**, 26.  
 1961 *Ibid.*, **60**, 80.
- CAMERON, A. G. W. 1959 *Ap. J.*, **130**, 884.
- HARRIS, D. E. 1961 *Observations of the C.I.T. Radio Obs., Owens Valley, Calif.*, No. 6.
- MINKOWSKI, R. 1939 *Ap. J.*, **89**, 156.
- NOONAN, T. 1961 *Pub. A.S.P.*, **73**, 212.
- SANDAGE, A. R. 1958 *Ap. J.*, **127**, 513.
- SHAPLEY, H., and  
 AMES, A. 1932 *Ann. Astr. Obs. Harvard College*, Vol. **88**, No. 2.
- ZINNER, E. 1920 *Geschichte und Literatur der veränderlichen Sterne*,  
 ed. G. MÜLLER and E. HARTWIG (Leipzig: Verlag Poeschel and Trepte), **2**, 416.
- ZWICKY, F. 1938 *Ap. J.*, **88**, 522.  
 1939a *Phys. Rev.*, **55**, 986.  
 1939b *Proc. Nat. Acad. Sci. U.S.*, **25**, 338.  
 1940 *Rev. Mod. Phys.*, **12**, 66.  
 1942 *Ap. J.*, **96**, 28.  
 1957 *Morphological Astronomy* (Berlin: Springer-Verlag).  
 1958 *Handbuch der Physik*, ed. S. FLÜGGE (Berlin: Springer-Verlag), **51**, 766.  
 1959 *Morphologische Forschung* (Zurich: Buchdruckerei Winterthur, A. G.).  
 1960 *Pub. A.S.P.*, **72**, 465.  
 1961a *Ibid.*, **73**, 185.  
 1961b *Physikalische Blätter*, **17**, 393.  
 1962 *Pub. A.S.P.*, **74**, 70.  
 1964 *Ap. J.*, **139**, 519.
- ZWICKY, F., and  
 HUMASON, M. L. 1960 *Ap. J.*, **132**, 627.  
 1961 *Ap. J.*, **133**, 794.  
 1964 *Ap. J.*, **139**, 269.





## CHAPTER 8

# *Magnetic Stars*

T. G. COWLING  
*University of Leeds, England*

### § 1. OBSERVATIONAL DATA

AS NOTED in Volume 6, chapter 10, of this series, strong magnetic fields, of order 1000 gauss or more—in one case 30,000 gauss (Babcock 1960)—have been observed in a number of stars. These stars are distributed over a large number of spectral types; they include, for example, B stars, M giants, an S star, and the cluster-type variable RR Lyrae. However, they are most regularly found in the peculiar A stars. The main peculiarities of these Ap stars concern their spectra; as regards their bulk properties, the only known peculiarity is that they appear to lie a little (about half a magnitude) above the main sequence.

The magnetic fields are measured by observing Zeeman shifts; these are relatively small and so can be measured only for sharp-line stars. In particular, fields cannot be measured if the spectral lines show broadening due to rapid rotation; that is, the fields can be measured only for slowly rotating stars or for stars nearly pole-on to the observer. Thus many more stars than are actually observed to possess strong magnetic fields may, in fact, do so, and the actually observed fields may be underestimated. Again, a magnetic field like the sun's is far too weak to be observable in a distant star. It therefore seems possible that most stars may possess magnetic properties to some extent.

The Zeeman observations give the mean field directed toward the observer, averaged over the visible hemisphere. They do not show the distribution of the field over this hemisphere, save that they indicate that the field extends over a large fraction of the total area. It is natural, for simplicity, to assume in the first instance that the surface field approximates to a dipole field. However, indirect evidence suggests that the actual surface field may deviate very considerably from a dipole form; in particular, small spots with a highly enhanced field may be superimposed on a general field.

Virtually without exception, the observed magnetic fields show variations, which in certain cases are periodic or cyclic. In many stars the variations pro-

ceed as far as actual reversals of polarity. The actual moment of reversal is often accompanied by a peculiar crossover effect—a systematic difference in width between the right-handed and left-handed circularly polarized components into which a line is split by an analyzer. This effect is ascribed to a difference in motions of the parts of the star's surface on which the field is directed toward, or away from, the observer.

Finally, certain elements—notably Mn, Si, Sr, Cr, Eu, and many rare earths—are often far more abundant in magnetic A stars than in stars with no observable field; certain other elements—notably Fe and Ca—are less abundant. The anomalous abundances may be a surface phenomenon, and, indeed, the abundances appear to vary from point to point on a star's surface. In a periodic magnetic variable, the strengths of the spectral lines of many elements vary with the period of the magnetic variation. In particular, the lines of two groups of elements, typified by Cr and Eu, vary in antiphase with each other.

In comparing theory with experiment, we shall normally regard a typical magnetic star as being of type Ap. The radius  $R$  and mass  $M$  of the typical magnetic star will be taken as  $R = 2R_{\odot}$ ,  $M = 2.4M_{\odot}$ ; on the assumption that the surface magnetic field is a dipole field, the surface polar field,  $H_p$ , will be taken to be 1000–7000 gauss. In the case of periodic magnetic variables, a typical period will be taken to be 6–9 days.

## § 2. BASIC EQUATIONS

The basic equations for magnetic stars have already been discussed in *The Sun*, chapter 8 (Cowling 1953); here they will simply be stated with the minimum of discussion. Let  $\rho$  be the density,  $p$  the pressure, and  $\mathbf{v}$  the material velocity, with  $\mathbf{H}$  and  $\mathbf{j}$  the magnetic field and electric current density, both measured in electromagnetic units. Then

$$\text{curl } \mathbf{H} = 4\pi\mathbf{j}, \quad \text{div } \mathbf{H} = 0. \quad (2.1)$$

The equation of continuity is

$$\frac{d\rho}{dt} + \rho \text{ div } \mathbf{v} = 0, \quad (2.2)$$

where  $d/dt$  is the time derivative following the motion. Also, if  $\mathbf{g}$  is the (vector) acceleration of gravity, the equation of motion of the material is

$$\rho \frac{d\mathbf{v}}{dt} = \rho \mathbf{g} - \text{grad } p + \mathbf{j} \times \mathbf{H}. \quad (2.3)$$

In electrically conducting masses of the size of stars, the lines of magnetic force leak so slowly through the material that, for most purposes, they can be regarded as “frozen” into it (Cowling 1953, p. 543). This means that in the star each line of force can be regarded as possessing an individuality of its own; the material can be regarded as attached to the lines of force much like beads on

strings. That is, the material can move freely along the lines of force, but in motion perpendicular to the lines of force the material must carry the lines of force with it or be carried along by them. The changes in the magnetic field are the same as if the electrical conductivity were infinite; they are given by the equation

$$\frac{\partial \mathbf{H}}{\partial t} = \text{curl} (\mathbf{v} \times \mathbf{H}). \quad (2.4)$$

In discussing certain surface phenomena, it is insufficient to regard the lines of force as frozen into the material; in discussing these, equation (2.4) must be modified to include the effects of electrical resistance.

The magnetic field can be regarded as a sort of "strain," possessing a potential energy  $W$  given by the volume integral

$$W = \int \frac{H^2}{8\pi} d\tau. \quad (2.5)$$

The field produces mechanical effects equivalent to the action of Maxwell's stresses, i.e., a tension  $H^2/8\pi$  per unit area along the lines of force and an equal lateral pressure.

Finally, a heat equation is needed. Let  $\epsilon$  be the rate of generation of energy per unit mass,  $\mathbf{F}$  be the heat flux per unit area, and  $Q$  be the total heat energy per unit mass. Then, if viscous and electromagnetic heating are ignored,

$$\rho \frac{dQ}{dt} = \frac{p}{\rho} \frac{d\rho}{dt} + \rho\epsilon - \text{div} \mathbf{F}. \quad (2.6)$$

If the material is regarded as a perfect gas,

$$Q = \frac{p}{(\gamma - 1)\rho}, \quad (2.7)$$

where  $\gamma$  is the ratio of specific heats, assumed constant. Thus

$$\rho^\gamma \frac{d}{dt} \left( \frac{p}{\rho^\gamma} \right) = (\gamma - 1)(\rho\epsilon - \text{div} \mathbf{F}). \quad (2.8)$$

If the effects of energy generation and heat flow are negligible, this reduces to the ordinary adiabatic equation.

### § 3. THE VIRIAL THEOREM

Chandrasekhar and Fermi (1953) have used a form of the virial theorem to fix an upper limit for the magnetic field of a star. Take the scalar product of equation (2.3) with the vector displacement  $\mathbf{r}$  from a fixed point, say the center of the star. Then, on integration throughout all space,

$$\int \rho \mathbf{r} \cdot \frac{d\mathbf{v}}{dt} d\tau = \int \mathbf{r} \cdot (\rho \mathbf{g} - \text{grad } p + \mathbf{j} \times \mathbf{H}) d\tau. \quad (3.1)$$

Since  $\mathbf{v} = d\mathbf{r}/dt$  and  $\rho d\tau$  is constant following the motion,

$$\int \rho \mathbf{r} \cdot \frac{d\mathbf{v}}{dt} d\tau = \frac{1}{2} \frac{d^2 I}{dt^2} - 2T, \quad (3.2)$$

where  $T$  is the total kinetic energy, corresponding to the velocity  $\mathbf{v}$ , and  $I$  is the "moment of inertia,"

$$I = \int \rho r^2 d\tau.$$

The terms on the right of equation (3.1) can be expressed, either by partial integration or by considering the work done in dissipating the mass to infinity, in terms of the magnetic energy,  $W$ , the total heat energy,  $\mathfrak{H}$ , and the gravitational energy,  $-\Omega$ . In fact,

$$\int \mathbf{r} \cdot (\mathbf{j} \times \mathbf{H}) d\tau = W, \quad (3.3)$$

$$\int \mathbf{r} \cdot \rho \mathbf{g} d\tau = -\Omega, \quad (3.4)$$

$$-\int \mathbf{r} \cdot \text{grad } p d\tau = 3 \int p d\tau = 3(\gamma - 1)\mathfrak{H}. \quad (3.5)$$

Substituting all these results in equation (3.1), we get

$$\frac{1}{2} \frac{d^2 I}{dt^2} = 2T + W + 3(\gamma - 1)\mathfrak{H} - \Omega, \quad (3.6)$$

which is the appropriate form of the virial theorem. In particular, for a star in equilibrium,

$$W + 3(\gamma - 1)\mathfrak{H} = \Omega. \quad (3.7)$$

This equation expresses, in integral form, the fact that the star is supported against gravity partly by the magnetic forces, partly by the pressure. Comparing equations (2.5), (3.5), and (3.7), we see that the magnetic pressure  $H^2/8\pi$  is equivalent, on an average, to a gas pressure  $p$  one-third as big. The reason for the one-third factor is roughly as follows. Take  $Oz$  parallel to the field  $H$ ,  $Ox$ , and  $Oy$  perpendicular to it; then the magnetic pressure acts only along  $Ox$  and  $Oy$  and is replaced by an equal tension along  $Oz$ . Thus the mean pressure in the three directions is one-third of  $H^2/8\pi$ .

Equation (3.7) indicates an upper limit to the magnetic field consistent with equilibrium, since it implies that

$$W < \Omega. \quad (3.8)$$

In fact, if  $W = \Omega$ , the whole of the weight is supported by the magnetic forces, no support being required from gas pressure. Actually, the upper limit on  $W$  is likely to be less than  $\Omega$ ; equation (3.7) is derived by integrating over the whole star, and, though at some points it may be possible to balance the whole of gravity by magnetic forces, it is highly unlikely that magnetic forces can support the material everywhere without assistance from the pressure (cf. Prendergast 1958).

The upper limit given by relation (3.8) is, however, unlikely even to be ap-

proached for actual stars. For a uniform star of mass  $M$  and radius  $R$ ,  $\Omega = \frac{3}{8}GM^2R^{-1}$ , where  $G$  is the gravitational constant; for a sphere with a uniform field  $H_0$  in the interior and a dipole field outside,  $W = \frac{1}{4}H_0^2R^3$ ; if these values are used, as giving the correct orders of magnitude, the condition  $W < \Omega$  gives

$$H_0 < (\frac{12}{5}G)^{1/2}MR^{-2}.$$

If one takes  $R = 2R_\odot$ ,  $M = 2.4M_\odot$ , this becomes

$$H_0 < 10^8 \text{ gauss}.$$

Comparing this with the observed surface fields of stars, a few thousand gauss in magnitude, we see that the upper limit could be approached only if the sub-surface field is inordinately greater than that observed. Indeed, even allowing for a fairly substantial increase inward, this argument suggests that magnetic fields are not likely, in general, to produce serious modifications in a star's internal structure.

### 3.1. THE VIRIAL THEOREM AND STABILITY

Chandrasekhar and Fermi used the virial equation to discuss stability of equilibrium of stars. The total energy,  $E$ , of a star in equilibrium is

$$\begin{aligned} E &= W + \mathfrak{S} - \Omega \\ &= -(3\gamma - 4)\mathfrak{S}, \end{aligned} \quad (3.9)$$

using equation (3.7). One would expect explosive instability if  $E > 0$ , since then the star would have enough energy to expand it to infinity against gravity. By equation (3.9), since  $\mathfrak{S} > 0$ , this condition is realized only if  $\gamma < \frac{4}{3}$ , which is the condition valid in the absence of a magnetic field.

An alternative form to equation (3.9) is

$$E = -\frac{(3\gamma - 4)}{3(\gamma - 1)}(\Omega - W). \quad (3.10)$$

Thus, in the stable case  $\gamma > \frac{4}{3}$ ,  $E$  increases through negative values toward zero as  $W$  increases toward its upper limit,  $\Omega$ . Hence, in a certain sense, one may say that the stability of a star decreases as its magnetic field increases. For example, if a star pulsates more or less radially, its pulsations are slower when it has a large magnetic field than when it has none. One can, in fact, get a rough approximation to the fundamental period of such oscillations by assuming that the star oscillates in such a way that at any instant the displacement  $r$  of each element of mass from the center is increased in the same ratio  $1 + x$ , where  $x$  is small. Then  $I$ ,  $W$ ,  $\mathfrak{S}$ , and  $\Omega$  increase, respectively, in the ratios  $(1 + x)^2$ ,  $(1 + x)^{-1}$ ,  $(1 + x)^{2-3\gamma}$ , and  $(1 + x)^{-1}$ , or approximately  $1 + 2x$ ,  $1 - x$ ,  $1 - 3(\gamma - 1)x$ , and  $1 - x$ . Using these results in equation (3.6) and remembering that the equilibrium values  $I_0$ ,  $W_0$ ,  $\mathfrak{S}_0$ , and  $\Omega_0$  satisfy equation (3.7), we find the period of oscillation to be  $2\pi/\sigma$ , where

$$\sigma^2 I_0 = (3\gamma - 4)(\Omega_0 - W_0). \quad (3.11)$$

This illustrates the decrease in stability in a star as its magnetic field increases (Chandrasekhar and Limber 1954).

Some authors have gone further and have suggested that a sufficiently great magnetic field might make a star explosively unstable. As equation (3.9) indicates, the virial theorem lends no support to this view. It indicates that, if  $\gamma > \frac{4}{3}$ , a star in equilibrium has insufficient energy to dissipate its mass to infinity. A magnetic field may indeed produce instability, but not such instability as blows up the whole star. The type of instability most commonly to be expected is one that simply leads to a reduction in magnetic energy through a readjustment of the lines of force, e.g., by the extrusion of arched lines of force through the surface. The virial theorem cannot readily be applied to instabilities of this type, whose consequence may be violent, but not catastrophic to the whole star.

#### § 4. SURFACE DISTORTIONS DUE TO A MAGNETIC FIELD

As noted in § 3, the aggregate effect of a magnetic field on a star is similar to that of increasing the mean material pressure  $\bar{p}$  by an amount equal to one-third the mean magnetic pressure  $\bar{p}_H$ . Thus the star is distended by the field, the effect being roughly the same as that of a decrease in molecular weight. The increase in radius is by a fraction comparable with  $\bar{p}_H/3\bar{p}$ , i.e., with the ratio  $W/\mathfrak{S}$  of the magnetic and thermal energies. This is in general small, since  $W + 3(\gamma - 1)\mathfrak{S} = \Omega$  and  $W/\Omega$  is small.

In addition to the distention, the star is, in general, distorted from a spherical form. A field in meridian planes through a diameter in general corresponds to an oblate form of the free surface; one whose lines of force are circles with a diameter as axis corresponds, in general, to a prolate form; with an appropriate combination of the two kinds of field, prolate, oblate, or spherical forms of the free surface are possible (cf. Prendergast 1956; Wentzel 1960, 1961). The ellipticity of the surface is of order  $\bar{p}_H/\bar{p}$ , i.e., of order  $W/\mathfrak{S}$  or  $W/\Omega$ .

##### 4.1. FERRARO'S EQUILIBRIUM SOLUTION

The ellipticity produced by a magnetic field may be illustrated by results for a model studied by Ferraro (1954). Suppose that the state is barotropic, so that the density  $\rho$  is a function  $f(p)$  of the pressure  $p$ . If  $\Phi$  is the gravitational potential,  $\mathbf{g}$  is  $-\text{grad } \Phi$ , and so the equilibrium form of equation (2.3) is

$$\text{grad } \Phi + [f(p)]^{-1} \text{grad } p = \frac{\mathbf{j} \times \mathbf{H}}{\rho}.$$

The left-hand side of this equation is the gradient of a scalar; hence the curl of the equation is

$$\text{curl } (\rho^{-1} \mathbf{j} \times \mathbf{H}) = 0. \quad (4.1)$$

Thus only those fields which satisfy this equation are consistent with equilibrium.

Suppose that the field is symmetric about a diameter of the star, the lines of force lying in planes through this diameter and the current  $j$  flowing in circles with the diameter as axis. Then equation (4.1) can be shown to imply that

$$(\mathbf{H} \cdot \text{grad}) \frac{j}{\rho \varpi} = 0, \quad (4.2)$$

where  $j$  is the magnitude of  $j$  and  $\varpi$  is the distance from the diameter. This indicates that  $j/\rho\varpi$  is constant along a line of force.

Ferraro considered a star of uniform density, so that the barotropic condition is automatically satisfied. He assumed  $j/\rho\varpi$  to be constant everywhere within the star and not simply along a line of force; thus

$$4\pi j = \kappa \varpi, \quad (4.3)$$

where  $\kappa$  is a constant. The actual value of  $\kappa$  was assumed to be so small that powers of  $\kappa$  higher than the second can be neglected. The form adopted by the star's surface was then found to be an oblate spheroid of eccentricity  $e$ , where

$$e^2 = \frac{\kappa^2 R^2}{16G\pi^2 \rho^2} = \frac{\kappa^2 R^8}{9GM^2}, \quad (4.4)$$

$R$  being the undistorted radius. The external magnetic field is a dipole field; its intensity at the poles of the star is

$$H_p = \frac{2}{15} \kappa R^2. \quad (4.5)$$

The field at the center of the star is  $\frac{5}{2}H_p$ .

In terms of  $H_p$ , the expression for  $e^2$  is

$$e^2 = \frac{25}{4} \frac{H_p^2 R^4}{GM^2}. \quad (4.6)$$

The magnetic energy is

$$W = \frac{5}{14} H_p^2 R^3. \quad (4.7)$$

Combining these equations with the equation  $\Omega = \frac{3}{5}GM^2R^{-1}$  valid for the undistorted gravitational energy, we find

$$e^2 = \frac{21}{2} \frac{W}{\Omega}. \quad (4.8)$$

This equation implies that the surface distortion produced by the magnetic field is small if  $W/\Omega$  is small, as would be expected from the results derived from the virial theorem. Numerically, take  $R = 2R_\odot$ ,  $M = 2.4M_\odot$ ,  $H_p = 7000$  gauss; then  $e$  is  $3 \times 10^{-4}$ , indicating a negligible distortion. However, for a giant star, taking  $M = 15M_\odot$ ,  $R = 300R_\odot$ ,  $H_p = 1000$  gauss, Ferraro found  $e = 0.15$ , indicating that the distortion is becoming appreciable.<sup>1</sup>

<sup>1</sup> Wentzel (1960) gave results for a particular type of axisymmetric field, possessing an azimuthal component as well as one in meridian planes, in a star of uniform density. With



Ferraro's solution gives an internal field that is nowhere much larger than the surface field. One might expect a larger distortion, for given  $H_p$ , if the sub-surface field were considerably greater than that at the surface. On the other hand, the internal pressure  $p$  is greater for a real star, whose mass is strongly concentrated toward the center, than for a uniform globe of the same mass and radius, and this may in part offset the increased magnetic pressure toward the center. These possibilities can be investigated by assuming a polytropic relation  $p = K\rho^{1+1/n}$ , which implies a condensation of the mass toward the center; correspondingly, Ferraro's equation (4.3) is replaced by

$$4\pi j = \kappa\rho\omega, \quad (4.9)$$

so that the field-generating currents are also concentrated toward the center.

Detailed calculations have been made (Cowling 1959) for the polytrope  $n = 3$ , assuming currents given by equation (4.9). In this case the central field is found to be about  $39 H_p$ , so that the internal field is a good deal larger than that at the surface. On the other hand, the values of  $W$  and  $\Omega$  are given by

$$W = 2.922 H_p^2 R^3, \quad \Omega = \frac{3}{2} GM^2 R^{-1}. \quad (4.10)$$

Thus the increase in  $W$  over the value given by Ferraro's solution (eq. [4.7]) is less marked than the increase in the central field and is, in part, offset by a corresponding change in  $\Omega$  above the value for a uniform mass. The eccentricity of the surface is now given by

$$e^2 = 7.914 \frac{W}{\Omega} = 15.43 \frac{H_p^2 R^4}{GM^2}, \quad (4.11)$$

a value of  $e^2$  about 2.5 times that given by Ferraro's model for the same values of  $H_p$ ,  $M$ , and  $R$ . Thus the polytropic model supplies no reason to modify the view that magnetic fields are unlikely to produce any appreciable distortion in normal stars. To give appreciable surface distortion, the internal field must be far greater, compared with the surface field, than in the polytropic model, and the increased field must not be limited simply to the central regions.

The polytrope  $n = 3$  is an unsatisfactory model for illustrating the distention of a star by a magnetic field. It is in neutral equilibrium; that is, it remains in equilibrium if it undergoes an arbitrary uniform expansion, the pressure still obeying the same polytropic law  $p = K\rho^{4/3}$ . Thus the introduction of a magnetic field does not simply alter the radius by a proportionate amount; it completely destroys the possibility of equilibrium, if the constant  $K$  in the poly-

---

this field he found for the surface eccentricity, to a first approximation,

$$e^2 = (\frac{21}{2}W_p - \frac{1}{2}W_T)/\Omega,$$

where  $W_p$  and  $W_T$  are the energies of the meridional and azimuthal parts of the field;  $W_T < \frac{1}{2}W_p$  for the field considered. The appearance of the same factor  $21/2$  as in eq. (4.8) is to be regarded as fortuitous, since Wentzel's field was very different from Ferraro's.

tropic law is left unaltered. It is found, in fact, that, with a field given by equation (4.9), equilibrium is possible, for a star of given mass, only if  $K$  is reduced in the ratio  $1-1.002W/\Omega$ . That is, the pressure which corresponds to a given density must be reduced in this ratio, because of the part of the weight supported by magnetic forces.

#### 4.2. BAROCLINE STARS

Ferraro's model and the polytropic model just considered both refer to barotropic stars. For the equilibrium of such stars, equation (4.1) must be satisfied; this imposes a severe limitation on the magnetic fields consistent with equilibrium. The reason for such a limitation is to be found in the fact that, in the absence of a magnetic field, the equilibrium of a barotropic star is neutral to all internal displacements that leave the density unaltered everywhere. Thus, when a magnetic field is actually present, internal displacements are possible in which the magnetic forces alone do work, and in equilibrium the magnetic energy  $W$  must be stationary for all small displacements of this type. This implies that the force  $\mathbf{j} \times \mathbf{H}$  of magnetic origin must satisfy an equilibrium condition on its own, completely independent of the other forces acting; this condition is embodied in equation (4.1).

However, in general, the magnetic force  $\mathbf{j} \times \mathbf{H}$  cannot be considered on its own, independent of the other forces acting. Any internal displacement possessing a vertical part must, in a stable region of the star, evoke a strong restoring force (the stability force); thus, when the force  $\mathbf{j} \times \mathbf{H}$  tries to produce an internal displacement such that equation (4.1) is satisfied, it is immediately countered by this stability force. Hence the star may never reach a barotropic equilibrium state in which equation (4.1) is satisfied; it may attain a barocline state, in which the surfaces of constant density and constant pressure are slightly tilted relative to each other.

Mestel (1956) has, in fact, shown that a whole class of magnetic fields, differing widely from those satisfying equation (4.1), are consistent with virtual equilibrium. His argument is essentially as follows. Suppose that an initial magnetic field (which can, for simplicity, be regarded as axisymmetric, in planes through a diameter) is present in a star and that the star is in the state that would give equilibrium in the absence of the field. The state is then not one of equilibrium, because of the force  $\mathbf{j} \times \mathbf{H}$ ; this force accordingly distorts the star to an equilibrium state in which stability forces comparable with  $\mathbf{j} \times \mathbf{H}$  are evoked. The force  $\mathbf{j} \times \mathbf{H}$  is, by equation (2.1), in general comparable with  $H^2/4\pi L$ , where  $L$  is a length characteristic of the dimensions of the field. The stability force is comparable with  $g\rho\xi\Delta/T$ , where  $\xi$  is the vertical displacement,  $T$  the temperature, and  $\Delta$  the difference between the actual temperature gradient and the adiabatic gradient. Thus the force  $\mathbf{j} \times \mathbf{H}$  is neutralized after producing a vertical displacement such that

$$\frac{g\rho\xi\Delta}{T} \sim \frac{H^2}{4\pi L}.$$

In this,  $\Delta/T$  can be equated to (say)  $(8L_s)^{-1}$ , where  $L_s$  is the scale height,  $p/\rho g$ . Thus we get

$$\xi = \frac{H^2}{4\pi p} \frac{8L_s^2}{L}. \quad (4.12)$$

In estimating  $\xi$  from this relation, we may note that  $H^2/8\pi$  is the magnetic pressure. This is, in general, small compared with the gas pressure  $p$ ; the ratio of the mean values of  $H^2/8\pi$  and  $p$  is, by equations (2.5), (3.5), and (3.7), equal to  $3W/(\Omega - W)$ , and this can be estimated as of order  $10^{-7}$  or less. Again, for a large-scale magnetic field,  $L$  is comparable with the stellar radius  $R$ ;  $L_s$  is somewhat smaller—near the star's surface, a good deal smaller. Hence  $\xi$  is, in general, an insignificant fraction of the scale height  $L_s$ ; that is, the magnetic force  $j \times H$  is able to produce only an insignificant distortion of the surfaces of constant density before it is neutralized by the stability forces.

However, this does not end the matter. The distortion of the surfaces of constant density leads to a state that is not one of radiative equilibrium. Radiative transfer tends to restore thermal equilibrium and so to destroy the stability forces that neutralize the magnetic force  $j \times H$ . Let  $\tau$  be the time required to restore thermal equilibrium; then, to keep the magnetic force in check, the displacement  $\xi$  must be renewed after every time  $\tau$ , i.e., there must be a vertical velocity  $\xi/\tau$ . If this velocity carries the material a distance comparable with  $L$ , the magnetic field will have succeeded in adjusting itself into the new configuration that it desires to take up, in spite of the stability forces.

The time required for this adjustment is of order  $L\tau/\xi$ , or

$$\tau \frac{4\pi p}{H^2} \frac{L^2}{8L_s^2}. \quad (4.13)$$

In the deep interior, if one is considering distortions of the temperature structure with a scale length comparable with the stellar radius,  $\tau$  is comparable with the Kelvin time scale, say  $\tau \sim 10^7$  years. If the gas pressure  $p$  is  $10^7$  times the magnetic pressure  $H^2/8\pi$  and if  $L_s$  is  $\frac{1}{4}L$ , the time given by expression (4.13) is of order  $10^7 \tau$ , or  $10^{14}$  years. This is much longer than the time required for the field to decay because of the finite conductivity of the material (a time of order  $10^{10}$  years, comparable with stellar lifetimes). Thus modifications in the field in the deep interior are more likely to be due to decay than to the efforts of the magnetic field to attain an equilibrium on its own.

Near the star's surface, on the other hand,  $p$  may be not much greater than the magnetic pressure. Also  $\tau$  is small compared with the Kelvin time scale, because of the much smaller heat content per unit volume of the material near the surface. Thus an arbitrarily assigned initial field must, in general, undergo appreciable surface modifications within a time small compared with the stellar lifetime. These make the field settle down into an equilibrium configuration consistent with thermal equilibrium, in which the force  $j \times H$  is small compared

with its starting value. Were it not for distortion of the isobaric surfaces from a spherical form due to magnetic forces nearer to the star's center,  $j \times H$  would probably have to vanish; as it is,  $j \times H$  is not rigorously zero, but it is likely to be very small.

### § 5. FORCE-FREE MAGNETIC FIELDS

The magnetic pressure  $H^2/8\pi$  due to a field of 2000 gauss is  $1.6 \times 10^5$  dynes/cm<sup>2</sup>. This is comparable with the material pressure  $p$  in a star's photosphere and much larger than  $p$  in the high-level atmosphere above the photosphere. Thus in the high-level atmosphere no force is available that is large enough to balance the magnetic stresses, and so the magnetic field must attain mechanical equilibrium by itself. That is, the body magnetic force  $j \times H$  must be far smaller than the order of magnitude  $H^2/4\pi L$  to be expected on dimensional grounds alone ( $L$  being, as before, a scale length for the variations of the field). A field such that  $j \times H = 0$  is called a "force-free field"; thus the magnetic field above a star's surface is very nearly force-free. Force-free fields have been considered by Lundquist (1950), by Lüster and Schlüter (1955), by Chandrasekhar and his co-workers (1956, 1957, 1958), and by others.

#### 5.1. GENERAL PROPERTIES OF FORCE-FREE FIELDS

Force-free fields include fields for which  $j = 0$ ; these fields are derivable from a magnetic potential. If  $j \neq 0$ , the condition  $j \times H = 0$  implies that the electric currents flow along the magnetic lines of force; thus

$$\text{curl } H \equiv 4\pi j = \alpha H, \quad (5.1)$$

where  $\alpha$  is, in general, a function of position.

If  $\alpha$  is not simply a constant, then, since  $\text{div } j = 0$  and  $\text{div } H = 0$ ,

$$0 = \text{div } (\alpha H) = H \cdot \text{grad } \alpha. \quad (5.2)$$

This shows that the lines of force (which are also the current lines) lie on the surfaces  $\alpha = \text{const.}$  These surfaces cannot be simply connected; for if they were, the lines of force would have to be closed curves on the surfaces. This would imply that an area  $S$  could be found, lying wholly on such a surface, whose bounding curve  $s$  is a line of force, and, by Stokes's theorem,

$$\oint H \cdot ds = \iint \text{curl } H \cdot dS = \iint \alpha H \cdot dS.$$

But, since the magnetic field on  $S$  is wholly tangential, the last of these integrals is zero; the first integral is not zero, since the field is everywhere directed in the same sense round  $s$ . Hence the assumption that the surfaces  $\alpha = \text{const.}$  are simply connected leads to a contradiction.

We are therefore led to picture a force-free field as a field in which the lines of force (and current lines) lie on a set of torus-like surfaces packed one inside another (see Fig. 1). The limiting curve  $AB$  in this figure, which can be re-

garded as a torus of zero cross-section, is itself a current line; because of the current flowing along  $AB$ , the lines of force on the surrounding surfaces spiral around  $AB$ . This picture is valid only if  $\alpha$  does not reduce to a constant; the assumption that  $\alpha$  is constant introduces a degeneracy into the problem, as a result of which the lines of force need not lie on closed surfaces. Nevertheless, even though in this case the picture of the lines of force as twisted on a bundle of tubular surfaces is not valid in the large, it gives a correct local picture of the field.

No isolated field, or field infinite in extent which falls off more rapidly than  $r^{-2}$ , can be force-free everywhere; for, as equation (3.3) implies, a field that is force-free everywhere has zero magnetic energy and so must vanish. One can conceive a field that is force-free within a certain region and pent in this region by a gas pressure increasing by  $\Delta p$  at its bounding surface  $S$ ;  $\Delta p$  then balances

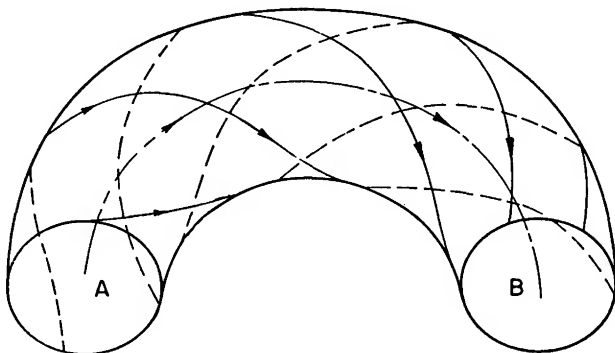


FIG. 1.—Lines of force in a force-free field

a surface force due to surface electric currents flowing in  $S$ . In this case, by a modified form of the virial theorem, the magnetic energy  $W$  is connected with  $\Delta p$  by

$$W = \int \Delta p \mathbf{r} \cdot d\mathbf{S}, \quad (5.3)$$

where  $\mathbf{r}$  is the position vector of  $d\mathbf{S}$  relative to any arbitrary origin. If  $\Delta p$  were constant, the integral on the right would be  $3\Delta p$  times the volume  $\tau$  inclosed by  $S$ ; also  $W$  is  $\tau$  times the mean value of the magnetic pressure  $H^2/8\pi$ . Hence equation (5.3) implies that an appropriate mean value of  $\Delta p$  is one-third the mean magnetic pressure. That is, by postulating a force-free field, one does not wholly get rid of forces of magnetic origin; one transfers them, without change in order of magnitude, from one point to another.

Force-free fields will not be considered in the interior of a star; as noted in § 4.1, in the interior the forces of magnetic origin are unlikely to be appreciable compared with the other forces maintaining equilibrium. Equally, in the star's atmosphere one need not consider force-free fields pent in an isolated region by

surface pressures; the magnetic pressures are too large to be balanced by gas pressure in the atmosphere. The type of field to be considered is one emanating from the deep interior of the star and force-free only above the photosphere. It may be pictured as originating when an original field above the photosphere, derivable from a magnetic potential, is twisted either as a result of subphotospheric motions or through interaction with interstellar material.

For example, lines of force of a dipole-like stellar field can be twisted by a difference in angular velocity between the two hemispheres, thus giving the field an azimuthal component. Lines of force of a sunspot field may similarly be twisted by a rotation of the central spot relative to the regions where the lines of force return to the photosphere. Fields above sunspots in fact appear to possess greater complexity than is consistent with their being derivable from a magnetic potential. Stellar fields may reasonably be expected to possess similar complexities above violently disturbed areas of the stellar surface.

## 5.2. MAGNETIC BRAKING

Lüst and Schlüter (1955) have invoked force-free fields in attempting to explain why stars of late spectral type generally rotate slowly, though they were presumably, like early-type stars, born with a rapid rotation. The basic idea, similar to one due to Alfvén, is that angular momentum can be transmitted outward along the lines of force of a force-free field and ultimately be dispersed into the surrounding interstellar material. As Lüst and Schlüter admitted, their discussion was incomplete in certain respects. A somewhat modified discussion will therefore be presented, it being indicated later how this discussion differs from that of Lüst and Schlüter.

When a star is born from the condensation of interstellar matter, it acquires a magnetic field from the lines of force imprisoned in that matter (cf. § 7.1, below). Initially, this field links up with the surrounding interstellar field; but when the condensation has proceeded so far that the field in the protostar greatly exceeds the interstellar field, a configuration in which the two fields are fully linked is no longer consistent with equilibrium. The lines of force linking the two fields begin to break, and the stellar field separates off from the interstellar. Ultimately, the two fields can be regarded as completely disconnected; a few lines of force, coming from near the star's magnetic poles, may still continue to link the two fields, but essentially the stellar field is an isolated field confined within a surface  $\Sigma$  inclosing the star.

The magnetic field within  $\Sigma$  must rotate with the angular velocity of the star, carrying with it the material in which it is imbedded. Interstellar material outside  $\Sigma$ , on the other hand, moves independently. Because matter inside  $\Sigma$  shares the star's rotation and because that just outside  $\Sigma$  is held back by the surrounding interstellar medium, turbulence can be expected to arise at the boundary of  $\Sigma$ . Matter impinging from outside may be expected to produce corrugations in  $\Sigma$ , and the resulting roughness will enable angular momentum

to be transmitted across  $\Sigma$  to the external matter. There is effectively a shearing stress across  $\Sigma$ ; the moment of this is transmitted to the star as a braking moment by the (force-free) magnetic field between the disturbed neighborhood of  $\Sigma$  and the star, the lines of force being twisted by the braking moment.

The field (which will be supposed symmetric about the star's axis of rotation) must accordingly possess an azimuthal component  $H_2$ , as well as a component  $H_1$  in meridian planes. The size of the surface  $\Sigma$  can be expected to be determined by the condition that the external matter exerts just enough material pressure  $p_m$  (gas pressure and Reynolds stresses, chiefly the latter) to balance the magnetic pressures pushing from inside. Thus

$$p_m = \frac{H_1^2 + H_2^2}{8\pi}. \quad (5.4)$$

The shearing stress transmitted along the lines of force of  $H_1$  as a consequence of the twisting of the field is  $p_s$ , where

$$p_s = \frac{H_1 H_2}{4\pi}. \quad (5.5)$$

If, as we shall assume, the shearing stress across  $\Sigma$  is less than, but comparable with, the material pressure, these equations imply that  $H_2/H_1$  is less than, but comparable with unity near  $\Sigma$ .

However, the ratio  $H_2/H_1$  is small well inside  $\Sigma$ . The azimuthal component of the force-free condition  $\mathbf{j} \times \mathbf{H} = 0$  in fact gives

$$\mathbf{H}_1 \cdot \text{grad} (\varpi H_2) = 0, \quad (5.6)$$

$\varpi$  denoting the distance from the axis of rotation. Thus  $\varpi H_2$  is constant along a line of force of  $\mathbf{H}_1$ . This shows that  $H_2$  increases more slowly with decreasing distance from the star than does  $H_1$ , which increases more like a dipole field (roughly proportional to  $1/r^3$ ). Since  $H_2/H_1$  measures the twist of the field out of meridian planes, this twist cannot be large except near  $\Sigma$ . Indeed, except near  $\Sigma$ , the star's field is unlikely to deviate greatly from one derivable from a potential.

Assume that  $\Sigma$  can be approximated adequately by a sphere of radius  $r_m$  and that  $H_1$  and  $q \equiv H_2/H_1$  can be regarded as constant on it. Then

$$p_m = \frac{H_1^2 (1 + q^2)}{8\pi}.$$

If  $H_1$  varies roughly as  $1/r^3$  and is equal to  $H_0$  at the surface  $r = R$  of the star, this gives

$$p_m r_m^6 = H_0^2 R^6 \frac{1 + q^2}{8\pi}, \quad (5.7)$$

which is an equation to determine  $r_m$ . The braking couple is comparable with that due to the shearing stress  $p_s$  over the boundary of  $\Sigma$ ; this is

$$C = 4\pi r_m^3 p_s = 4\pi r_m^3 p_m \frac{2q}{1+q^2}. \quad (5.8)$$

Lüst and Schlüter estimated  $p_m$  from a theory of turbulence, which gave the root-mean-square velocity of turbulence as  $a\omega r_m$ , where  $a$  is about  $\frac{1}{5}$ . Thus, if  $\rho$  is the density just outside  $\Sigma$ ,

$$p_m = \frac{1}{3}\rho a^2 \omega^2 r_m^2. \quad (5.9)$$

Combining this with equations (5.7) and (5.8), the radius  $r_m$  is to be estimated from

$$r_m^8 = \left(\frac{3}{8\pi}\right) H_0^2 R^6 (1+q^2) (\rho a^2 \omega^2)^{-1}, \quad (5.10)$$

and the couple  $C$  is given by

$$C = q \left[ \frac{8\pi\rho a^2 \omega^2}{3(1+q^2)} \right]^{3/8} \times (H_0 R^3)^{5/4}. \quad (5.11)$$

Lüst and Schlüter obtained rather different results, mainly because they assumed  $H_1$  to be wholly radial, so that  $H_1 \propto 1/r^2$ . This assumption may be not unreasonable for the sun because the sun's field may be extended radially by emitted streams of corpuscles. However, in this case the field is radial precisely because it is not force-free and a bounding surface  $\Sigma$  does not exist. Equations (5.10) and (5.11) will accordingly be used; they give rather smaller values of  $r_m$  and  $C$  than the formulae of Lüst and Schlüter.

For a star of the mass, radius, and angular velocity of the sun, taking  $\rho = 10^{-20.5} \text{ gm cm}^{-3}$ ,  $a = \frac{1}{5}$ ,  $q = 1$ , one obtains, from equations (5.10) and (5.11),

$$r_m = 1.5 \times 10^{12} H_0^{1/4} \text{ cm}, \quad C = 3.7 \times 10^{28} H_0^{5/4} \text{ gm cm}^2 \text{ sec}^{-2},$$

where  $H_0$  is the surface field in gauss; and the rate of braking is such as would bring the star to rest in  $10^{12} H_0^{-5/4}$  years. Thus, for a field of the order of the sun's present field ( $\sim 1$  gauss), the braking would be inappreciable; for a field of  $10^3$  gauss, on the other hand, the braking would take only a few times  $10^8$  years. The braking time is proportional to  $\omega^{1/4}$ , and so increases only slowly with increasing angular velocity. It therefore appears possible that a sufficiently strong magnetic field may be effective in braking a star. The magnetic field exerts its braking moment primarily along lines of force which meet the star near its poles; in this connection it is tempting to recall the slower rotation of the sun at its poles than near the equator.

As Lüst and Schlüter recognized, any numerical estimates are based on a number of precarious assumptions. The value assumed above for  $\rho$  just outside  $\Sigma$  was based on the density estimated to be present in the solar system near the



orbit of Mercury; since the matter present there may be due to ejection from the sun, it is not clear that this value is appropriate in the present connection. The turbulence theory used in estimating  $p_m$  (eq. [5.9]) is also not particularly firmly based. Again, the material just inside  $\Sigma$  may have so large a velocity that centrifugal force actually exceeds gravity; this may affect the pressure estimates, though the effect is not likely to be very great. Finally, certain lines of force of the star may not disconnect themselves from the interstellar field, and some braking effect may be transmitted along these. Thus the work of Lüst and Schlüter does not give a final solution to the problem of magnetic braking; but it provides a very interesting suggestion.

An alternative mechanism has been proposed by Schatzman (1959, 1962). He supposes that, as on the sun, streams of particles are continuously being ejected from a star, carrying magnetic field with them. The streams tend to conserve their angular momentum and so have a smaller angular velocity than the star. Thus the magnetic lines of force linking them to the stellar surface become twisted by differential rotation and are able to exert a braking torque on the star. Ultimately the magnetic connection with the star will be broken, by much the same mechanism as operates in solar flares (§ 5.3). But if the transfer of angular momentum from the star persists until the outward streams have gone a distance from the star equal to several stellar radii, the loss of a relatively small part of the star's mass may lead to the loss of a large part of its angular momentum.

Schatzman's proposed mechanism is attractive, since the sun is not likely to be the only star from which vigorous emission can occur. Very fast emission does not help braking, both because the magnetic connection with the star is rapidly broken and because the braking stresses are transmitted back to the star with the Alfvén velocity relative to the moving material: if the material is ejected with too great a velocity, the braking effects cannot get back to the star. The braking effect works best when the magnetic field is strong, but not so strong that it impedes emission.

### 5.3. THEORIES OF FLARES

Certain recent theories of flares are also related to force-free magnetic fields. Flares were considered in *The Sun*, chapter 8 (Cowling 1953), where it was concluded that none of the electromagnetic theories then existing was adequate. However, more recent work by Dungey (1953, 1958), Sweet (1958), Piddington (1956, 1958), and Gold and Hoyle (1960) has removed some of the theoretical inadequacies, and Severny's (1958*a, b*) recent observations have indicated cogently that solar flares result when magnetic fields are rapidly varying, and are accompanied by a considerable loss of magnetic energy. It is therefore appropriate to consider the topic afresh, the more so because flares are likely to occur on other stars as well as on the sun.

The essentially force-free property of fields in the sun's outer atmosphere is

attained because the magnetic stresses have to reach mechanical equilibrium on their own, there being no other forces present that are able to balance them. At the flare-producing level, the gas pressure is 1 or 2 dynes/cm<sup>2</sup>, whereas the magnetic pressure due to a field of 500 gauss is 10<sup>4</sup> dynes/cm<sup>2</sup>. Thus if sub-photospheric convection alters the field at the base of the sun's atmosphere, the lines of force at higher levels must be twisted and compressed until the magnetic stresses at these levels again balance out.

However, at neutral points of the field the magnetic stresses vanish. For this reason it is, in general, impossible for a field, after an arbitrary photospheric change, to adjust itself to be in equilibrium at a neutral point. To illustrate this, we consider a two-dimensional field; Dungey (1953, 1958) has shown that the argument applies with no essential change to a three-dimensional field.

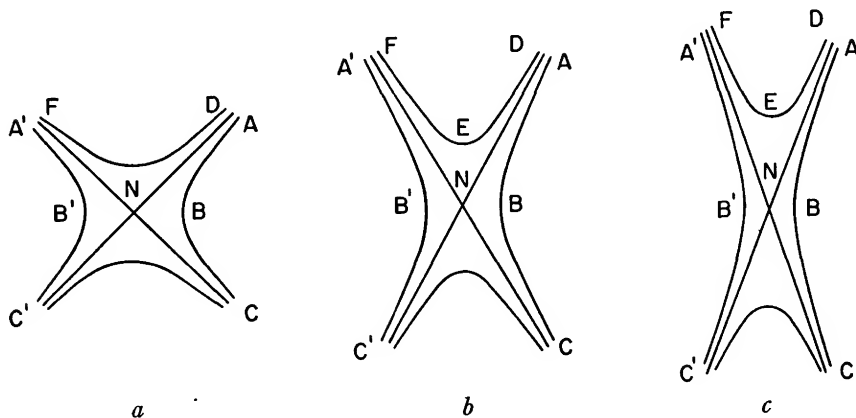


FIG. 2.—Lines of force during the development of a neutral-point flare

Consider a field initially in equilibrium, the lines of force near a neutral point  $N$  being as shown in Figure 2, *a*. As a result of some initial disturbance, let the lines of force be displaced as shown in Figure 2, *b*. In Figure 2, *a*, the force due to the magnetic tension along the curved line of force  $ABC$  just balances the gradient of magnetic pressure, pushing  $B$  toward  $N$ . In Figure 2, *b*, the curvature effect is smaller, whereas the gradient of magnetic pressure is increased by the lateral compression of the field. Hence the line of force moves still farther toward  $N$ . Similarly, the line of force  $DEF$  is subject to an increased effect of curvature and is pulled away from  $N$ . The field (the material moves with the field) is urged toward a configuration like that of Figure 2, *c*, and the squeezing process does not stop.

It follows that, so long as the assumption that the field is frozen into the material is correct, the system cannot reach any position of equilibrium whatever. We are obliged to assume that when the field has undergone sufficient lateral compression, dissipative effects arise near  $N$  which unlink the top and bottom

parts of lines of force like  $ABC$  and  $A'B'C'$  and relink them above and below  $B'B$ . The need for such a change in linking can be seen from Figure 3, due to Sweet (1958), which shows (again in a two-dimensional model) the field changes brought about by the relative displacement of two bipolar groups of spots. A two-dimensional magnetic field can be force-free only if it is derivable from a potential, and Figure 3 shows the change in the potential field when the bipolar groups approach each other. In attaining the new equilibrium field, the lines of force marked 3, which used to be internal to the two bipolar systems, have had to be broken and relinked above and below  $N$ .

The dissipative effects which may unfreeze the lines of force from the ma-

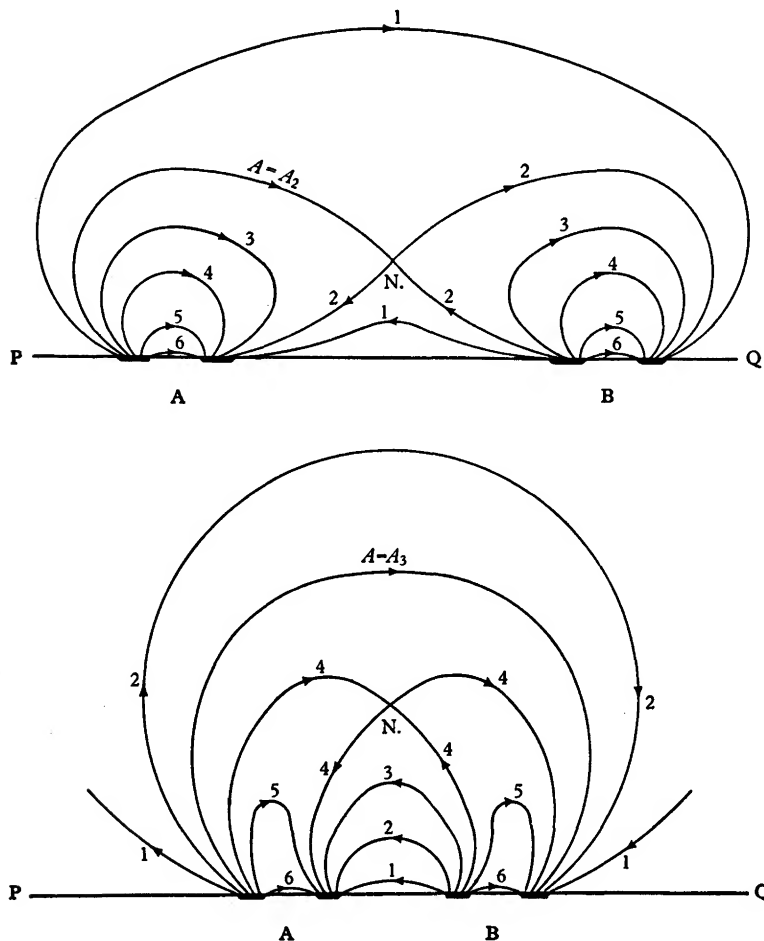


FIG. 3.—Lines of force of the potential field of two bipolar systems. *Upper figure*: undisturbed field; *lower figure*: field after a relative displacement of the bipolar systems. (After Sweet 1958, p. 124.)

terial, and so permit their breaking and relinking, are numerous. First, there is the ordinary ohmic resistance. In *The Sun*, chapter 8 (Cowling 1953), it was thought that this was too small to give appreciable effects. The work of Piddington (1956, 1958) and Cowling (1956) has shown that the resistance may be very materially enhanced by the fact that the charged particles may undergo violent collisions with any neutral atoms that may be present, since these are not, like the charged particles, dragged along by the lines of force. However, recent work by Parker (1963) has indicated that, even when this enhancement is taken into account, ohmic resistance by itself is unable to produce adequate dissipation of magnetic energy.

Next, the field adjusts itself with a velocity comparable with the velocity  $H/\sqrt{4\pi\rho}$  of Alfvén waves; taking  $\rho = 10^{-11}$  gm/cm<sup>3</sup>,  $H = 500$  gauss, one finds this velocity to be  $4.5 \times 10^7$  cm/sec. So large a velocity, and its rapid variation from place to place near a neutral point, imply that the disturbance may approach the neutral point as a shock wave. Hydromagnetic shock waves are subject to special dissipative effects, due not only to collisions between particles but also to plasma oscillations, converting energy of mass motion and magnetic energy into thermal energy. Finally, if two shock waves converge on a neutral point from opposite sides, a proportion of the particles present may be accelerated to cosmic-ray energies.

The mechanism just described goes far to meet the objections raised in *The Sun* to electromagnetic theories of flares. One objection was that, to provide the necessary heating by ohmic resistance, the electric currents would have to be generated in an impossibly narrow layer; the argument just given indicates that there may be other, and more effective, heating mechanisms, and, in any case, it shows that the layer of rapid space variation of the field, in which the strongest electric currents flow, may be very thin. A second objection was that the earlier theory ascribed flares to changes in the conductivity, which cannot appreciably affect the currents flowing in a short time; this does not apply to the present theory, which explains the flare as due to a failure in mechanical equilibrium. Finally, the new theory ascribes the energy of a flare not to some process of transport but to the actual destruction of a considerable part of the magnetic energy of an irregular field.

The new theory still needs clarification and development. In particular, it appears to overstress the role of neutral points of the magnetic field. It suggests that a minor flare should occur as soon as the field near a neutral point undergoes any disturbance whatsoever; also it indicates that a flare should be restricted to the immediate vicinity of a neutral point, whereas observed flares spread to cover a wide area. To avoid nearly continuous flares at a neutral point, one must suppose that some opposing agency (e.g., gas pressure) limits the effects of sufficiently small disturbances. To explain the spread of a flare, one must assume that the destruction of a field near a neutral point leads to instability elsewhere. Thus a flare arises when the magnetic field over an extensive region is on the

verge of instability; it is touched off by events at the neutral point but leads to destruction of magnetic energy throughout the surrounding region.

However, these limitations of the new theory should not conceal the definite advance which it represents. It emphasizes the essentially catastrophic nature of flares; the dissipative processes which it envisages are not limited to Joule heating and take place in regions where the field changes nearly discontinuously. Also it accepts as basic the concepts of hydromagnetics, whereas the standpoint of earlier theories was still not far from that of more conventional laboratory physics.

The most recent development in flare theory is in a paper by Gold and Hoyle (1960). These assumed that two arched bundles of lines of force are side by side, the fields in the two bundles being in opposite directions, and that motions in subphotospheric layers twist the bundles in opposite directions. Then the fields of the two bundles are in opposite senses in their region of contact: there is a minimum of magnetic pressure between them, which results in their being pushed together. Thus the fields along the arches begin to neutralize each other, like the fields considered by Sweet. After the fields begin to merge, lines of force which have been reconnected encircle both bundles and pull them together. The ideas of Gold and Hoyle are not fully worked out, and they may have overestimated the rate of dissipation of magnetic energy. But their theory provides an indication of one way in which magnetic instabilities can arise.

#### § 6. CONVECTION AND TURBULENCE

It has already been seen that a magnetic field is unable to distort a star appreciably unless the internal field is enormously stronger than that at the surface. It remains to consider whether the field can affect the observed properties of the star by modifying the composition or the distribution of brightness over the surface. So far as the brightness is concerned, radiative transfer cannot be affected by the field; thus we are led to consider, first, the possible effects on convection.

The work of Chandrasekhar (1952) has shown that the presence of a magnetic field has little influence on the actual condition for thermal instability. On the other hand (cf. Cowling 1953, p. 570), the magnetic field can profoundly affect motions due to thermal instability when the magnetic pressure is comparable with the material pressure. Motions tending to twist the field are strongly resisted; those which are encouraged are largely up-and-down motions, especially those along the lines of force or carrying the lines of force bodily with them. Thus the convective transfer of energy is impeded, and the degree of interference with it depends both on the field and on its inclination to the vertical. One cannot speak with too much confidence, since one is extrapolating from results at the limit of stability to results for developed convection; but it appears that a horizontal field may actually affect the convection of heat less than a vertical field. In a horizontal field a type of motion is possible, virtually

unaffected by the field, in which first one horizontal bunch of lines of force is carried to the surface, then another; if the field is vertical, it is much less easy to find motions that do not appreciably distort it.

Convection zones may be present either in the core or in the outermost layers of a star. Magnetic effects on convection in the core are not likely to be serious. If the field in the core is not enormously greater than that at the surface, the magnetic pressure in the core is very small compared with the gas pressure. It is conceivable, of course, that convection in the core may twist and stretch the lines of force, leading to a field that is irregular but greatly increased in strength. However, such an irregular field would impede convection similarly at all latitudes and would not have any latitude effect on the emergent radiation. Its sole effect would be to increase the slight excess of the temperature gradient above the adiabatic value, which is required to generate the convection.

Near the surface the magnetic pressure is certainly large enough for the magnetic field to interfere with surface convection of heat. However, a latitude effect on the emergent radiation is unlikely. Appreciable latitude differences in the efficiency of convection of heat are limited to a thin surface layer, only 10,000 or so km thick; below this layer, either the magnetic pressure is too small compared with the gas pressure to exert appreciable effects, or, if the magnetic field is enhanced by interaction with a turbulent convection, it is irregular and so exerts much the same effect on the convection at all latitudes. The thinness of the layer affected by differences of convective efficiency means that the layer hardly affects the heat actually getting through. Heat piles up behind the more "opaque" parts of the layer; the increased temperature gradient across the layer enables the heat to escape across it long before it can leak away horizontally through the much greater distance to the layer's less opaque parts.

It follows that a magnetic star should be essentially spherical both in form and in its emission. Small-scale phenomena like sunspots may, however, occur. The essential condition is the existence of a vigorous surface convection zone. If the magnetic field becomes compressed together in a given surface region, its greater strength enables it to interfere more with convection in that region. Thus heat is dammed back below the region, escaping sideways through a relatively short path or simply accumulating for a day or two. The surface layers become cooler; the reduction in their gas pressure is compensated for by the local increase in magnetic pressure. The state of affairs is similar to that in the theory of sunspots outlined in *The Sun*, chapter 8. In magnetic stars, however, no separate explanation of the origin of the "spot" field is necessary; the latter field is just the general field, strengthened by compression. Any estimate of the possible spot fields must be little more than a guess, but fields of order  $10^5$  gauss do not appear impossible.

The main difficulty of a theory of "spots" in magnetic stars is simply that a large part of the known magnetic stars are of spectral type A. Stars of this type

appear to possess no surface convection zone or, at best, only a weak one (Vitense 1951, Pecker 1953). However, the fact that many magnetic stars show irregular field variations suggests some convection in the surface layers, so that the existence of spots of some kind appears possible. The spots may differ in some respects from sunspots; e.g., they may be larger and show less contrast with their surroundings. But they may exist and, in certain cases, be accompanied by flares.

One of the most intriguing properties of magnetic A stars is the large abundance of certain elements, particularly of rare earths. Results obtained by E. M. and G. R. Burbidge (1955*a, b*) for  $\alpha_2$  Can Ven and HD 133029 show that for Eu and some other rare earths the abundance may be several hundred times as great as in normal stars, and certain commoner elements (Si, Mn, Cr) may show a tenfold increase. In magnetic variables the apparent abundances vary during the period of magnetic variation, presumably because of the separation of elements in localized areas of the stellar surface.

There is no reason to think that the anomalous abundances are more than a surface phenomenon. Though nuclear processes involving neutrons can theoretically lead to anomalous abundances throughout the whole star, such processes occur only late in a star's evolution, and all evidence strongly indicates that magnetic A stars are relatively young. The variations of abundance over the stellar surface also suggest that the anomalies are limited to surface layers and are inconsistent with any process involving mixing. This is reasonable if, as suggested by theory, the outer convection zone in A stars is relatively shallow.

Two theories of the anomalies invoke, respectively, magnetic sorting and surface nuclear reactions. In the magnetic-sorting theory, suggested by Babcock (1951), diffusive separation of different kinds of atoms is postulated, as a consequence either of differential forces or of differences in diffusive properties produced by the magnetic field. The excess of abundance over that in a normal star, in general, increases with the atomic weight; thus the general run of the anomalies can be explained by a mechanism that assists heavy elements to rise to the surface. However, no force acting selectively on the heavy elements has been suggested, and diffusion is, in any case, a very slow process. From dimensional considerations applied to the diffusion equation,

$$\frac{\partial n}{\partial t} = \text{div} (D \text{ grad } n) \quad (6.1)$$

( $D$  = diffusion coefficient), it follows that the time to produce diffusive equilibrium across a layer of thickness  $L$  is of order  $L^2/D$ . Since  $D$  is comparable with  $10 \text{ cm}^2/\text{sec}$  in the outer layers of a star, the equilibrium time is of order  $3 \times 10^9$  years for a layer only 10,000 km thick. Thus no magnetic-sorting process seems adequate to explain the anomalies.

The possible explanation in terms of surface nuclear reactions has been discussed by E. M. and G. R. Burbidge and W. A. Fowler (1955, 1958), who assume that flares can occur in magnetic stars. Nuclear synthesis of heavy elements occurs whenever neutrons are present. Now solar flares produce high-energy particles like cosmic rays; evidence also exists that they produce deuterium, which, in turn, implies that neutrons are first produced. Hence flares in magnetic stars may be able to provide the conditions for the synthesis of heavy elements.

Free neutrons can be produced by  $(p, n)$ ,  $(\alpha, n)$ , and similar reactions, involving moderately light nuclei like carbon. The threshold energies for such reactions are, say, 3–20 Mev. Thus the prerequisite for the production of the observed abundance anomalies is a copious supply of protons and  $\alpha$ -particles with energies of a few Mev. A large proportion of the available neutrons will be used in producing deuterium. Hence, to insure that the synthesis of heavy elements is not accompanied by an excessive abundance of deuterium, it is postulated that less energetic flares also occur, in which deuterons undergo fission into protons and neutrons as a result of collisions with protons with energies of order 1 Mev. The resulting neutrons are then available for further synthesis of heavy elements.

Biermann (1956) has pointed out that if proton energies exceed about 20 Mev, heavy elements will tend to be degraded into lighter ones by proton collisions, and the synthesis may be reversed. He therefore suggests that the synthesis can occur only if proton energies in the flare region lie within narrow limits. Burbidge, Burbidge, and Fowler, however, anticipate that the energy distribution of fast particles shows such a rapid decrease with increasing energy that the synthesizing processes are always dominant.

Up to the present, only the over-all problem of the general superabundance of heavy elements has been considered. The details of the superabundance ratios for different atoms and, in particular, anomalies like the underabundance of Ba have not been discussed. Equally, the causes of the zoning of distribution of certain elements, suggested by the alternate strengthening of lines of chromium and the rare earths in the spectrum of certain magnetic variables, is not discussed.

The theory stands or falls on the assumption of superflares in magnetic stars. These are supposed to generate their energy at a level where the density is  $10^{-7}$  gm/cm<sup>3</sup>, corresponding to a pressure of about  $10^5$  dynes/cm<sup>2</sup>. A deeper level is ruled out because ionization losses of energy would be too great for effective acceleration of protons and  $\alpha$ -particles; a much higher level would give too few accelerated particles—and these with excessive energies. Solar flares generate most of their energy in a region where the magnetic pressure is, say, 1000 times the gas pressure. If a similar ratio applies to flares in magnetic stars, the magnetic pressure in them is  $10^8$  dynes/cm<sup>2</sup>, corresponding to a magnetic field of  $5 \times 10^4$  gauss. This is large, but not excessively large if there are “spots”



of enhanced field. The existence of such spots is, in any case, essential to the theory; flares can occur only when differently directed fields are brought into close proximity, and this implies that the general field is locally perturbed by still stronger fields.

However, the immediate cause of a flare is the distortion of the magnetic field as a consequence of motion at a level where the gas pressure dominates the magnetic stresses. If the gas pressure at this level is taken to be ten times the magnetic pressure, it follows that strong convective motions are possible down to a depth where the pressure is  $10^9$  dynes/cm<sup>2</sup>. This will be at a depth of 10,000 km or more below the photosphere. Such a depth raises difficulties; according to Vitense (1951) and Pecker (1953), the convective layer extends only to a depth of 1000 km or so, and Burbidge, Burbidge, and Fowler based their numerical estimates of the flare activity required on the assumption that mixing cannot occur below a depth of 10,000 km.

The theory is accordingly not free of difficulties, as well as incomplete. At the same time, no alternative theory exists that does not appear to encounter even stronger objections.

One may note in passing that theories of surface nuclear reactions in flares have been proposed to explain the superabundance of Li in T Tauri stars (Bonsack and Greenstein 1960) and of He<sup>3</sup> and other elements in 3 Centauri A (Wallerstein 1962). The reactions here must be spallation reactions, in which heavier nuclei are degraded by collisions with fast protons. Direct evidence of the present existence of strong magnetic fields in these stars is lacking and, so far as 3 Centauri A is concerned, the anomalous abundances would need to have arisen in an earlier phase of the star's evolution. Difficulties of the flare hypothesis in regard to the latter star have been emphasized by Bashkin and Middlehurst (1962).

## § 7. ORIGIN OF STELLAR MAGNETIC FIELDS

Magnetic fields appear to be nearly ubiquitous in nature. No completely satisfactory theory of stellar fields has been given, but in the last few years definite progress has been made toward such a theory. Earlier ideas were reviewed in *The Sun*, chapter 8, and elsewhere. It is therefore necessary only to give an account of recent work.

Recent attempts to explain stellar magnetism in terms of a fundamental theory of magnetization by rotation have met with no success. Laboratory tests with large rotating bodies failed to show any magnetic effect (Blackett 1952), and evidence has been given that the earth, whose magnetic field should, on such a theory, be invariable in sign, has, more than once, reversed the direction of its field in the past (Nagata 1954). Equally there has been no progress with theories based on thermoelectric currents; indeed, Mestel (1956) has shown that fields due to such currents are likely to be severely limited by the mechanical effects that they produce. The only theories that have undergone recent development are those of fossil magnetism and dynamo maintenance.

## 7.1. FOSSIL MAGNETISM

The theory of fossil magnetization asserts that the magnetic field at present existing in a star is a relic of the field with which it was born. The time of free decay of a stellar magnetic field, due to the slow leak of the lines of force through the material, is comparable with  $10^{10}$  years (Cowling 1953, p. 545). Since this is far greater than the probable age of A-type stars, it follows that free decay is unlikely to reduce a star's magnetic field appreciably if it is born with such a field.

A star is, moreover, likely to be born with a substantial field, because of the field permeating interstellar material. The light from distant stars is observed to be polarized as a result of scattering by interstellar particles aligned preferentially with their long axes perpendicular to the galactic plane (Hall and Mikesell 1949; Hiltner 1949). The aligning force is normally assumed to be a magnetic field. Its direction appears to be sensibly uniform over wide ranges in the galactic plane; to produce the observed alignment, its strength must be of order  $10^{-6}$ – $10^{-5}$  gauss. A galactic magnetic field is also invoked in most theories of cosmic rays and of cosmic radio emission.

Suppose, now, that a star is formed by condensation from interstellar material in a region where the magnetic field is sensibly uniform in direction. The lines of force can be taken as frozen into the material during the contraction unless the conductivity falls to an excessively low figure. During the condensation the density increases by a factor of, say,  $10^{24}$ ; thus, assuming the same degree of contraction in all directions, the linear dimensions of the contracting mass are reduced in the ratio  $10^8$ :1. If the lines of force are frozen into the material, the total magnetic flux through the mass remains constant during the contraction; thus the magnetic field increases in the ratio  $10^{16}$ :1. Assuming an initial field of  $10^{-6}$ – $10^{-5}$  gauss, this implies a final field of  $10^{10}$ – $10^{11}$  gauss. Thus there is no difficulty in getting a large stellar field by condensation from the galactic field.

The difficulty is, indeed, that the condensation gives an excessively large field. The magnetic pressure due to a field of  $10^{10}$  gauss is  $4 \times 10^{18}$  dynes/cm<sup>2</sup>, greater than gas pressures likely to exist in a star. Thus the mechanical effects of so great a field would be strong enough to prevent gravitational forces from pulling the material together into a star. The difficulty might be partly overcome by supposing that more of the contraction takes place along the lines of force than perpendicular to them, but one cannot rely too much on such anisotropy. It appears necessary to suppose, with Mestel and Spitzer (1956), that, when the mass has condensed sufficiently far, it becomes opaque to external radiation and the number of atomic ions and electrons becomes so low that the lines of force are able to some extent to leak through the mass. The difficulty belongs to the theory of stellar origin rather than to the theory of stellar magnetic fields; in the present context it is sufficient to observe that, since stars are, in fact, able to form, the magnetic stresses can never build up

to such a strength as to prevent condensation. There is, however, no reason why stars should not be born with fields of, say,  $10^6$  gauss.

The "fossil" theory has, however, other difficulties. For example, the time of decay of stellar fields was estimated as of order  $10^{10}$  years, assuming the material to be at rest. But if large-scale motions take place in a star, in addition to field changes due to decay there are much greater changes due to convection of the field with the material. The generalization of equation (2.4) to take account of the finite conductivity  $\sigma$  of the material is

$$\frac{\partial \mathbf{H}}{\partial t} = \text{curl} \left( \mathbf{v} \times \mathbf{H} - \frac{1}{4\pi\sigma} \text{curl} \mathbf{H} \right). \quad (7.1)$$

The ratio of the decay effects, represented by the  $\sigma$ -term, to the convective effects, represented by the  $\mathbf{v} \times \mathbf{H}$  term, is comparable with  $(4\pi\sigma VL)^{-1}$ , where  $V$  and  $L$  are quantities of the order of the velocity and the length scale of variation of the field. Taking  $\sigma = 10^{-6}$  e.m.u.,  $V = 10^2$  cm/sec,  $L = 10^{10}$  cm, we find that this ratio is comparable with  $10^{-8}$ , which is very small.

Elsasser (1956) has therefore suggested that, just as molecular diffusion can in large-scale problems be supplemented by a much larger mixing effect due to turbulence, so the slow decay due to finite conductivity can be supplemented by a much larger decay due to turbulence. The effect is, roughly, that turbulent motion may split the field into much smaller elements, whose smaller size means that they can be destroyed in a much shorter time. Elsasser's argument was given added point by the recognition that (as in the theory of flares) an enhanced dissipation of magnetic energy can occur when two oppositely directed magnetic fields are pressed together.

Spitzer (1958) has examined the question in the case of axial symmetry. He concluded that, though turbulence may well lead to a reduction of the field in the interior of the turbulent region, it leads to no appreciable change in the total magnetic moment of a star. Thus turbulence in certain zones of a star should lead to the lines of force shunning the interior of those zones but being crowded together in their outer layers. Matters may be somewhat different if axial symmetry is not assumed.

In any case, however, if a large part of the body of a star is stable against convection, the time of decay of a field in that part ought to be unaffected by convection. Moreover, too great an insistence on the role of turbulent dissipation would lead to a *reductio ad absurdum*, since it would imply that virtually no agency whatsoever could maintain an observable magnetic field. None the less, convective dissipation does provide a real difficulty to the "fossil" theory, especially in view of Hayashi's (1961) suggestion that massive stars, during the course of their formation, may pass through a wholly convective phase.

A second difficulty of the "fossil" theory is that it gives a reasonably constant field, whereas the fields of most magnetic stars are decidedly variable. A considerable degree of variation can, of course, be superimposed on a relatively

constant field by assuming extensive convection currents in the outer layers. But virtually the only way of getting regular magnetic variations with a "fossil" field is on the oblique-rotator hypothesis (§ 8.1).

Finally, an explanation in terms of a general galactic field is incomplete until an explanation of the latter field has been supplied. Such an explanation is usually sought in a variant of the dynamo theory; a tiny initial "seed" field is supposed to grow steadily as turbulent motions extend the lines of force and crowd them together. This theory is defective to the extent that the main effect of turbulence may be to twist the lines of force into a steadily more confused tangle, thus increasing dissipation rather than augmenting the field. However, once again one cannot press the objection too far, since observations do appear clearly to suggest the existence of a galactic field.

To summarize, the "fossil" theory makes a number of assumptions which require further investigation. But if these assumptions are not too wide of the truth, very large stellar fields ought certainly to result from the "fossil" mechanism.

## 7.2. DYNAMO THEORIES

A dynamo theory of a magnetic field supposes that the motion of material across the lines of force of an existing field generates electric currents which maintain the field, much as the magnetism in a self-exciting dynamo is maintained by the currents which it generates.

Earlier work on this theory was subject to a number of objections. In a terrestrial dynamo the currents generated are able to flow in insulated conductors from the place where they are generated to that where they exert their magnetic field. In a body like a star, there is no similar separation between the places where the currents are generated and where they exert their magnetic field. Thus a comparison with a terrestrial dynamo is justified only if it can be shown that the changed conditions in a star do not vitiate the comparison. This, for a long time, workers were unable to show.

Much of the recent work on dynamo theories has been directed toward explaining the earth's magnetic field and so can be mentioned only cursorily here. Bullard and Gellman (1954) considered a steady pattern of convection within a conducting-fluid globe, based on motions to be expected in the earth's core—a non-uniform rotation and convective cells giving rising and falling motions near the equator. They found that, with appropriate magnitudes of the two parts of the motion, it was possible to secure maintenance of a steady magnetic field. This field, while resembling a dipole field well away from the globe, has a large toroidal component in its interior.

Bullard and Gellman employed series expansions in their work, and some doubts as to the convergence of these expansions were possible. Such doubts were fully met in work by Herzenberg (1958). The latter considered, as resembling eddies in the earth's core, a large, solid conducting sphere at rest, in which are imbedded two small conducting spheres, A and B. The small spheres are

supposed to be constrained to rotate uniformly about appropriate diameters, maintaining electrical contact with the surrounding matter all over their boundaries. Herzenberg found that, with appropriately rapid rotations of the spheres A and B, dynamo maintenance of a steady field was possible for about half the possible orientations of the two axes of rotation.

In both the work of Herzenberg and that of Bullard and Gellman, the dynamo motions were postulated; the detailed problem of their maintenance was not discussed. Bullard and Gellman went as far as to verify that the forces required to maintain them were of the order of magnitude of those likely to be met in the earth's core. A complete discussion of dynamo maintenance would have to discuss the motions as well as the field. Since the motions to be expected are not likely to be steady, the difficulties of such a complete discussion are at present altogether prohibitive. One can simply say that the work to date has shown that, in certain circumstances, magnetic fields in large fluid conductors can be maintained by dynamo interaction with convection.

One comment, however, needs to be made. The high conductivity of stellar material is not altogether an advantage to a dynamo theory of stellar fields. As Bondi and Gold (1950) have pointed out, if lines of force were exactly frozen into the material of a star, no new lines of force could emerge from the surface, and so dynamo action would be unable ever to build up an external field. In fact, the theories of Bullard and Gellman and of Herzenberg both rely explicitly on the finiteness of the conductivity, which permits the lines of force to leak through the material. Such leaking is very slow in stars, even when account is taken of the enhanced dissipation possible when two fields are pressed together (§§ 5.3 and 7.1). However, it may be supplemented near the surface by a "tearing" of the surface, in which arched lines of force are thrust above the initial surface by magnetic stresses, the material elevated with them then sliding down the lines of force to uncover new surface material.

A theory involving such "tearing," as well as leakage due to finite conductivity, was suggested by Parker (1955) to explain the solar cycle; it may be capable of extension to magnetic stars. This theory regards solar magnetic fields as maintained by dynamo interaction with non-uniform rotation and with convective upwellings in the outer convection zone. The magnetic field is assumed to be largely confined to the sun's outer layers; it includes both azimuthal and meridian components, the former being assumed to be dominant at low latitudes and the latter near the poles.

It is assumed that, initially, loops of magnetic force are present in meridian planes. The non-uniform rotation (supposed to be mainly a variation of angular velocity with depth) then pulls out the vertical parts of the loops in the azimuthal direction, thereby creating an azimuthal field. Next, convective upsurges lift the lines of force of the azimuthal field; because of Coriolis forces, the inflow at the base of an upsurge creates a whirling motion round the vertical, so that the convection twists the lines of force about the vertical, as well as lifting

them (cf. Fig. 4). Hence new loops of magnetic force are created in meridian planes, which supplement the original field in those planes.

The new field, being derived from the original vertical field, consists of loops of opposite signs on the two sides of one of the original loops. Thus it reinforces the original field on one side (which turns out to be the side nearer to the equator) and tends to reverse it on the other. Thus loops in meridian planes are moved toward the equator, as well as being reinforced by the dynamo effects. The process is supposed to generate a field effectively periodic in structure, traveling toward the equator from both sides. The azimuthal field, which gives rise to the field of sunspots, is strongest near the equator because the greater rotational velocities there lead to an enhanced azimuthal extension of the lines of force. The theory relies on the finiteness of the electrical conductivity to

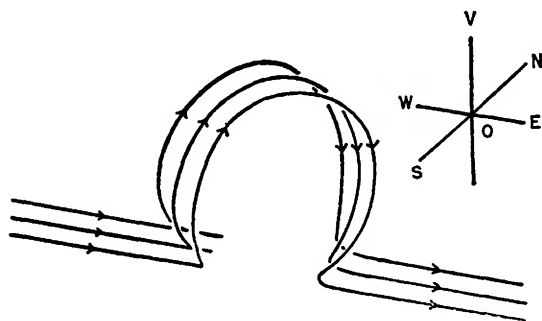


FIG. 4.—Parker's upsurges. Lines of force lifted by an upsurge in the northern hemisphere are rotated forward (to south) on the left and backward on the right. *OV*, *EW*, and *NS* indicate the vertical, east-west, and north-south directions. (Reprinted with permission from T. G. Cowling, *Magnetohydrodynamics* [New York: Interscience Publishers, 1957], p. 89, Fig. 17.)

merge loops arising from different convective cells into one regular field, and on the "tearing" of the surface as new magnetic arches are pushed through it, to explain the arrival of the field above the surface.

A theory of this kind, based on an irregular phenomenon like convection, cannot be given a complete mathematical basis, and, to this extent, Parker's theory is incomplete. The theory is also somewhat unsatisfactory in other respects. For example, the new loops of magnetic force created by upsurges are at a higher level than those from which they originate. Also downsurges may be expected to create loops in the reverse sense. Again, why should magnetic fields in the two hemispheres synchronize in a sunspot cycle if they are due to waves advancing independently from north and south? Finally, the field is supposed to be limited to layers only a few tens of thousands of kilometers thick; but even in these layers are the effects of finite conductivity strong enough to smooth out irregularities of the field in a few years? With a conductivity of  $10^{-7}$  e.m.u. and with no enhancement of dissipation by turbulence, a field in a region of size 10,000 km would take a time of order 10,000 years for smoothing.

A theory with a family resemblance to that of Parker has been proposed by Babcock (1961). Like Parker, he begins with a (dipolar) field in meridian planes, which is pulled out azimuthally and amplified by non-uniform rotation. If "ropes" of locally enhanced azimuthal field occur, the gas pressure in them is less than that elsewhere at the same level, since the sum of gas pressure and magnetic pressure is constant. Hence the density is reduced in the ropes, which accordingly acquire a sort of magnetic buoyancy. This carries the field to the surface, producing bipolar magnetic regions.

It is now assumed (consistent with the observed behavior of sunspots) that, as the bipolar regions age, their "preceding" parts drift toward the equator from both sides, to be neutralized there by merging. "Following" parts are assumed to migrate poleward, where their lines of force neutralize and finally reverse the initial dipolar field. The process then repeats itself, the field reversing itself during each 11-year solar cycle.

Babcock's theory is subject to difficulties similar to those which are met by that of Parker. It does not indicate why the parts of the bipolar region migrate in latitude, and the subphotospheric field changes which accompany field reversal must be complicated and require elucidation. Nevertheless, like Parker's theory, it provides a courageous attempt to knit together all the phenomena of solar fields and should be taken into account in considering stellar magnetic variation in general.

#### § 8. MAGNETIC VARIABLE STARS

Stellar magnetic fields are normally variable. Often their variation is irregular; sometimes, however, it has a more or less regular cycle. The more irregular variations are presumably due to some equally irregular convection. Here consideration will be limited to the regular variations; even these pose a theoretical problem of some difficulty, especially when actual reversal of the observed field occurs during a magnetic cycle. Three theories of the variations will be considered: (*a*) the oblique-rotator, (*b*) the magnetic-oscillator, and (*c*) the hydro-magnetic-cycle theories.

In the oblique-rotator theory, the star is supposed to rotate about an axis inclined at a considerable angle to the line of sight, its magnetic axis being also inclined at a large angle to its rotational axis. The rotation may bring patches of positive and negative magnetic polarity alternately into view and so lead to reversals in the observed field. In the magnetic-oscillator theory, the star is supposed to undergo a periodic oscillation, controlled by the magnetic forces and other mechanical forces; the reversals in magnetic polarity are supposed to result from the interaction of the oscillations with the magnetic field. The hydro-magnetic-cycle theory is less definitely formulated than the others. It ascribes reversals of polarity to a hydromagnetic dynamo effect, similar to that (whatever it may be) which is responsible for the solar cycle. It leads to variations in the field that are cyclic rather than actually periodic; moreover, the cycle must be overlaid by large, irregular fluctuations.

On the oblique-rotator theory a magnetic variable is like an eclipsing variable, in that the apparent variations are due to "occultation" of different patches of polarity. The other two theories make the star to be an intrinsic variable. Babcock (1958) has grouped these two theories under one heading; but the two are sufficiently different to justify their consideration separately.

### 8.1. THE OBLIQUE-ROTATOR THEORY

The most detailed study that has been made of the oblique-rotator theory is that of Deutsch (1954, 1958). Deutsch showed that, for regularly reversing magnetic variables, the period of variations is roughly inversely proportional to the spectral line width. Assuming that the line width is due mainly to the star's rotation and that the radius does not vary much among the stars in question, this is consistent with the magnetic period being equal to the period of rotation. The theory is also able to account satisfactorily for the so-called crossover effect. This effect is that, when the observed average polarity is changing from (say) positive to negative, the widths of the Zeeman components of the spectral lines are consistent with the simultaneous presence, on the visible hemisphere, of patches of positive and negative polarity, of which those of positive polarity are receding, those of negative polarity are approaching. Clearly, this effect is consistent with any theory that ascribes changes of polarity to the motion of patches of different polarity from the visible hemisphere to the invisible, and vice versa.

The theory has been strongly criticized by Babcock (1958). Deutsch's result that the magnetic period is inversely proportional to the line width suggests that it is directly proportional to the rotational period; it does not show that the two periods are actually equal. Babcock brings evidence that the rotations required to explain magnetic reversals would produce line widths perhaps twice as big as those observed. Deutsch does not regard this evidence as altogether convincing, in view of difficulties in interpreting the observations; but the onus appears to be on him rather than on Babcock to substantiate his contentions.

Babcock also points out that field reversals are observed in nearly all periodic magnetic variables and that field reversals are explicable on the oblique-rotator theory only if the star's axis of rotation is not far from perpendicular to the line of sight. However, an appreciable fraction of the existing magnetic stars should have their axes inclined at relatively small angles to the line of sight; these should, moreover, be the ones in which a magnetic field is most easily detectable, since in them the Zeeman shift would be the least obscured by rotational broadening. Again, to give field reversal, the magnetic axis must be inclined at a large angle to the axis of rotation; with a dynamo theory of the origin of the field, at any rate, one would expect the magnetic and rotational axes to tend to be coincident.

If a star's magnetic field is roughly a dipole field, on the oblique-rotator theory the apparent field should vary more or less sinusoidally. The observed field variation departs considerably from a sinusoidal form, suggesting a non-



dipole field. Deutsch has attempted to determine the true form of the field for the star HD 125248 on the oblique-rotator theory. His calculations were complicated by the fact that certain elements appear to show systematic differences in abundance from point to point of the star's surface, and the consequent fluctuations in line strength affect the apparent strength of the field. The results of the calculations are exhibited in Figures 5 and 6. They are interesting chiefly as illustrating the considerable complication that a star's magnetic field and the distribution of elements over its surface might need to possess on this theory.

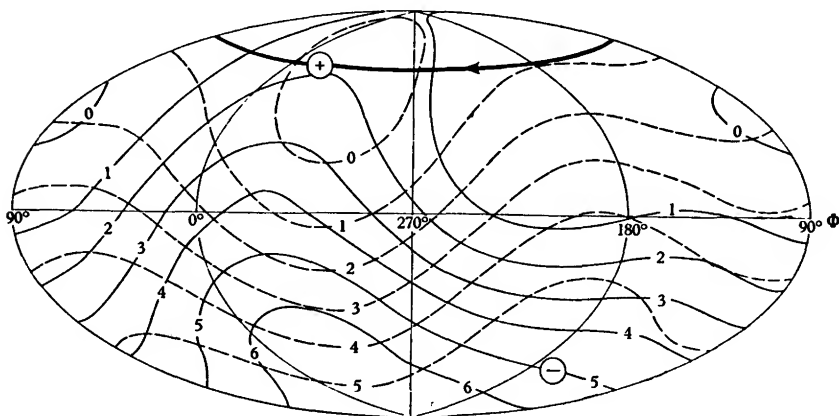


FIG. 5.—Curves of constant equivalent width for lines of the groups Eu II, Gd II, and Ce II (*full curves*) and Cr I, Cr II, and Sr II (*broken curves*). The subsolar point describes the heavy curve in the direction indicated;  $\Phi$  is the phase angle. The plus and minus signs mark the axis of the dipole part of the field. Aitoff equal-area projection. (After Deutsch 1958, p. 219.)

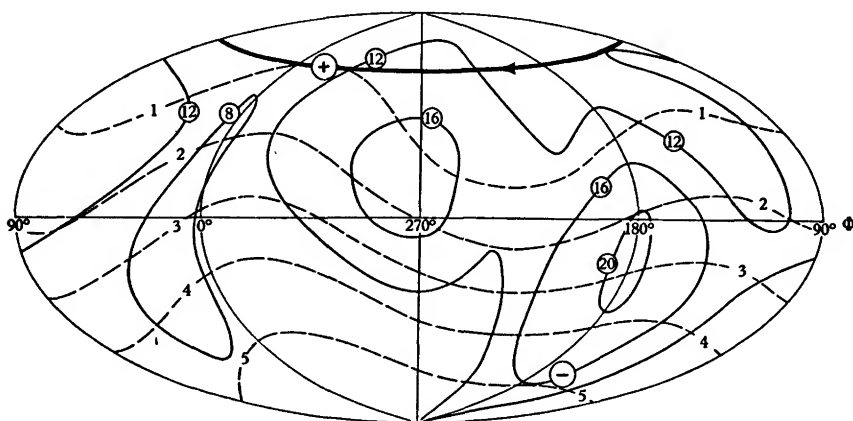


FIG. 6.—The dashed curves are curves of constant local equivalent width for lines of the group Fe I, Fe II, Ti II. The full curves are the contours of constant  $|H|$ . The heavy curve and the plus and minus signs have the same significance as in Fig. 5. (After Deutsch 1958, p. 219.)

The fact that the maximum equivalent widths for lines of each group occur in the unobserved zone of the star casts some doubt on the details of the picture.

The question of the validity of the oblique-rotator model must in large part be left to the observers to settle. From the theoretician's standpoint, the model is attractive because of its simplicity and definiteness. This definiteness is, however, in one respect a disadvantage, since it implies a lack of adjustable parameters; the complication of the field shown in Figure 6 is the obverse of the rigidity of the theory. In any case, the oblique-rotator model is inadequate as a total explanation of magnetic variations, because of the irregular changes often superposed on magnetic cycles.

## 8.2. THE MAGNETIC-OSCILLATOR THEORY

The theory that cyclic changes in stellar magnetic fields are due to mechanical oscillations was studied first in a preliminary fashion by Schwarzschild (1949). He assumed that the star was seen nearly pole-on and that it oscillated between prolate and oblate spheroidal configurations. In estimating the period of oscillation, he took into account only the forces of magnetic origin; he found that, in order to get a period comparable with the 9 days observed for HD 125248, he had to assume a field of order  $10^6$  gauss. To reconcile this with the observed surface field, he assumed the  $10^6$  gauss to refer to the central field, the field falling off to a value less than  $10^4$  gauss at the surface. However, Ferraro and Memory (1952) found that the field of order  $10^6$  gauss must not be limited to the central regions. Assuming a surface field of order 7000 gauss and a reasonably fast increase in field strength toward the center, they found a period comparable with a year, much greater than that observed.

However, they were assuming, like Schwarzschild, that the oscillations were controlled by magnetic forces only. In actual stars, gravitational forces are far more important than the magnetic forces, and, in consequence (Cowling 1952), the majority of the important free periods of a star like HD 125248 must be *smaller* than the observed—only a few hours or so. There are two types of oscillations which might give periods of the right order. One is a high-overtone oscillation, with a number of spherical nodal surfaces; motion between these surfaces is mainly horizontal, but gravitational effects due to the small parts of the motion that are vertical drive the whole motion and are correspondingly attenuated in their effect. The other is a torsional oscillation in which the motion is virtually wholly horizontal and along closed curves in any sphere concentric with the star; the controlling forces are magnetic, arising from the twisting of the lines of force.

Oscillations of the first type are unlikely to be able to explain the observed magnetic variations. A large number of oscillations of this type are likely to possess periods of the right order, and it is difficult to see why one of them should be excited and not the others. Again, the maintenance of the oscillations presents difficulties, since dissipation is likely to be rapid in a high-overtone oscillation. Finally, it is only with extreme difficulty that the oscillations can

be made to give magnetic reversal. At first, it was thought that an oscillation in a star seen pole-on might carry the lines of force to and fro, so that they bow first toward, then away from, the observer, like cornstalks in the wind. But this is not so; the field above and in surface layers is limited in its variations by the fact that, first, the same lines of force cross the surface of the star at all phases and, second, the field above the surface is force-free (in the case of a field in meridian planes, derivable from a potential) at all phases. When these facts are taken into account, it becomes virtually impossible to get reversal by the lines of force bowing to and fro (Cowling 1952; Sweet 1954).

In any case, the crossover effect strongly suggests that magnetic reversals are due to the passage of patches of polarity from the visible hemisphere to the invisible, and vice versa. Such passage is secured by oscillations of the type under consideration only with a patchy field—one oriented in a very special manner to the line of sight. However, magnetic reversals are the rule rather than the exception in actual magnetic variables.

The situation with regard to torsional oscillations is a little better, but only a little. These oscillations are, essentially, controlled by magnetic forces; thus, like the oscillations of Schwarzschild and of Ferraro and Memory, they are too slow to give the observed periods of magnetic stars unless the subsurface field is far greater than that observed at the surface. Also, in some torsional oscillations at least, it is possible for thin shells within the star to oscillate independently, each with its own period, so that no over-all oscillation with a definite period would be observable (Plumpton and Ferraro 1955). These difficulties can be overcome by assuming, as Walén did in a theory of the solar cycle (1949), that the internal field is tangled and increased in strength as a result of convection, so that both the effective stiffness is increased and the star is made to vibrate as a whole. Interaction with the star's rotation may also help to keep the star oscillating as a whole (Cowling 1955).

However, to produce magnetic reversals, the regions of opposite polarity must appear alternately on the visible hemisphere. This means that the magnetic axis must, in the mean position, be nearly perpendicular to the line of sight, and that the oscillations twist it toward and away from the observer. Since magnetic fields are most readily observed if the rotational axis points toward the observer, such a preferential orientation would imply that, contrary to most expectations, the magnetic axis tends to be perpendicular to the axis of rotation.

To summarize, torsional oscillations can be made to give magnetic reversals with the observed periods only if a rather large number of favorable assumptions are made. No other type of mechanical oscillation appears to be able to give polarity reversals.

### 8.3. THE HYDROMAGNETIC-CYCLE THEORY

This theory, which attempts to explain stellar magnetic variations by an analogy with the solar cycle, is much less definitely formulated than the others.

No generally accepted theory of the solar cycle exists. Walén (1949) has proposed a theory of it in terms of torsional oscillations; Parker (1955) and Babcock (1961), theories in terms of hydromagnetic interaction between the field, convective motions, and Coriolis forces (cf. § 7.2); and other theories can be expected. Thus a hydromagnetic-cycle theory of stellar magnetic variation may take many forms. We shall consider here the form in which actual reversal of the field occurs, as in the solar cycle.

One obvious difference between solar and stellar fields is in magnitude. The general solar field observed at high latitudes is only 1 gauss or so, and stellar fields are a thousand times as big. Thus if the two fields are extended over similar volumes, a stellar field has a million times the energy of the solar field. Its energy is very considerable. If a stellar field extends more or less uniformly through the interior, then (cf. § 4.1) its energy is comparable with  $\frac{5}{14}H_p^2R^3$ ; taking  $H_p = 2000$  gauss,  $R = 2R_\odot$ , this is  $4 \times 10^{39}$  ergs, equal to the energy radiated by the sun in about 12 days. This cannot greatly overestimate the energy, even if the field does not penetrate into the deep interior, since the external field provides a considerable fraction of the total energy; it may, however, be an underestimate (cf. eq. [4.10]).

So considerable an energy is not likely to be drawn from the heat flux of a magnetic variable in the day or two in which the field builds up to its maximum. However, it can easily be drawn from the kinetic energy of internal motions; an energy of  $4 \times 10^{39}$  ergs corresponds to giving a mass  $2.4M_\odot$  a velocity of 1300 cm/sec. Thus a magnetic cycle could be regarded as arising from the conversion of kinetic into magnetic energy to give the field maxima and the reconversion of magnetic energy into kinetic, so that kinetic energy becomes dominant again at the phases when zero average magnetic field is observed.

Even so, the actual magnitudes and periods of variation of stellar fields are hard to explain on the cycle theory. The magnitude of a field presumably depends only on the star's angular velocity and on convection near its surface (fields generated by deeper convection cannot leak through to the surface in so short a time as a few days). The surface convection zone is believed to be far weaker in A stars than in the sun; the angular velocity may be, say, 30 times as great as the sun's. Thus, to explain a field 1000 times as great as the sun's, the field produced must increase at least as fast as the square of the angular velocity. Since dynamo effects are proportional to the velocities involved, this means that the angular velocity must be effective at least twice in the field-generating process. Dynamo mechanisms depending on the angular velocity do, in fact, often involve the angular velocity at two points, but a greater dependence would appear excessive.

Assuming that a mechanism can be found to give the desired dependence, one must next explain how the field can appear at the surface. Leakage through the material because of its finite conductivity is far too slow; the field must burst its way out because of the mechanical forces that it exerts, much as the field of

a sunspot pair appears to burst out. However, the field of a sunspot, which is similar in order of magnitude to the field of a magnetic star but is local, already takes a day or two to reach the surface; a stellar field, which is not local, might be expected to take a far longer time to emerge. If, as observations indicate, the field builds up in only a day or so, it would have to burst out in a catastrophic fashion. Observational evidence of the catastrophe should be recognizable; moreover, it should be accompanied by a stirring that would rapidly end any zoning of the distribution of elements on the surface.

Another difficulty is to explain the difference in period between HD 188041 (226 days) and other fairly regular variables (5–9 days). The spectral type is not very different (A5p for HD 188041, A0p–A4p for the others); the magnetic field is also not very different in magnitude, though rather less in HD 188041 than in most of the rest. Thus the discrepancy in periods is difficult to explain if the period depends on the same physical properties as the magnitude of the field.

Little more than this can be said about the hydromagnetic-cycle theory because of its incomplete formulation. However, it clearly does not evade difficulties as great as those met by other theories; also it appears unable to explain the crossover effect. Thus a completely satisfactory theory of magnetic variation must be left for the future to provide. In the meantime, a good deal of further work, both theoretical and observational, is required.

## § 9. CONCLUSION

The reader will have noted how frequently it has been stated that the effect of a magnetic field on stellar properties is negligible, provided that the internal field is not far greater than that at the surface. A field increase in the ratio 50:1 in going from the surface to the center is regarded as quite reasonable, since a decaying field tends to be concentrated in the more highly conducting central regions. If no greater increase than this is permitted, the field is unable to distort or distend a star appreciably or to exert any decisive influence on the period of stellar oscillations. An increase in the ratio of 1000:1, on the other hand, would make the field begin to exert appreciable effects.

Though to the present author it appears more reasonable to suppose that such a large increase does not occur, the increase is not impossible. On the fossil theory of stellar magnetism, a central field of  $10^7$  gauss is perfectly possible. If this were a violently tangled field, it might not imply a large surface field. Such a tangled field would decay faster than a regular one, but a moderate increase in rates of decay is perfectly permissible. A very considerable magnetic variation would be possible if the moderately deep field reached the surface from time to time.

Prendergast (1956) and Wentzel (1961) have, in fact, found relatively simple twisted fields that are wholly internal to a star and recognizable from outside

only by the surface distortions and distentions which they produce. Fields approximating to these would be far stronger internally than would be indicated by observations of the surface field.

Such fields compose a very restricted subclass of all the possible fields, and there are difficulties in the way of believing that they are representative of the majority of actual stellar fields. There is no obvious reason why such fields should preferentially be set up in the first instance or why, once set up, they should not, through finite conductivity, leak through the outer layers to the surface. For this reason, too much weight should not be attached to the possibility of a very great internal field. Nevertheless, it would not be appropriate to close this chapter without drawing attention to it.

#### REFERENCES

- |  |       |  |
|--|-------|--|
| BABCOCK, H. W.   | 1951  | <i>Ap. J.</i> , <b>114</b> , 1.  |
|  | 1958  | <i>Ibid.</i> , <b>128</b> , 228.   |
|  | 1960  | <i>Ibid.</i> , <b>132</b> , 521.   |
|  | 1961  | <i>Ibid.</i> , <b>133</b> , 572.   |
| BASHKIN, S., and<br>MIDDLEHURST, B. M.                   | 1962  | <i>Comm. of Lunar and Planetary Laboratory</i> , Univ. of Arizona, No. 20.   |
| BIERMANN, L.   | 1956  | <i>Zs. f. Ap.</i> , <b>41</b> , 46.  |
| BLACKETT, P. M. S.                                       | 1952  | <i>Phil. Trans. R. Soc., London, ser. A</i> , <b>245</b> , 309.              |
| BONDI, H., and GOLD, T.                                  | 1950  | <i>M.N.</i> , <b>110</b> , 607.  |
| BONSACK, W. K., and<br>GREENSTEIN, J. L.                 | 1960  | <i>Ap. J.</i> , <b>131</b> , 83.   |
| BULLARD, E., and<br>GELLMAN, H.                          | 1954  | <i>Phil. Trans. R. Soc., London, ser. A</i> , <b>247</b> , 213.              |
| BURBIDGE, E. M., and<br>BURBIDGE, G. R.                  | 1955a | <i>Ap. J., Suppl.</i> , <b>1</b> , 43.                                       |
|  | 1955b | <i>Ap. J.</i> , <b>122</b> , 396.  |
| BURBIDGE, E. M.<br>BURBIDGE, G. R., and<br>FOWLER, W. A. | 1955  | <i>Ap. J., Suppl.</i> , <b>2</b> , 167.                                      |
|  | 1958  | <i>I.A.U. Symp.</i> , No. 6 (Cambridge: Cambridge University Press), p. 222. |
| CHANDRASEKHAR, S.  | 1952  | <i>Phil. Mag.</i> , <b>43</b> , 501.   |
|  | 1956  | <i>Proc. Nat. Acad. Sci.</i> , <b>42</b> , 1.                                |
| CHANDRASEKHAR, S., and<br>FERMI, E.                      | 1953  | <i>Ap. J.</i> , <b>118</b> , 116.  |
| CHANDRASEKHAR, S., and<br>KENDALL, P. C.                 | 1957  | <i>Ap. J.</i> , <b>126</b> , 457.  |
| CHANDRASEKHAR, S., and<br>LIMBER, D. N.                  | 1954  | <i>Ap. J.</i> , <b>119</b> , 10.   |
| CHANDRASEKHAR, S., and<br>WOLTJER, L.                    | 1958  | <i>Proc. Nat. Acad. Sci.</i> , <b>44</b> , 285.                              |

- COWLING, T. G. 1952 *M.N.*, **112**, 527.  
 1953 *The Sun*, ed. G. P. KUIPER (Chicago: University of Chicago Press), chap. 8.  
 1955 *Proc. R. Soc., London, ser. A*, **233**, 319.  
 1956 *M.N.*, **116**, 114.  
 1959 Unpublished result.
- DEUTSCH, A. J. 1954 *Trans. I.A.U.*, **8**, 801.  
 1958 *I.A.U. Symp.*, No. 6 (Cambridge: Cambridge University Press), p. 209.
- DUNGEY, J. W. 1953 *Phil. Mag.*, **44**, 725.  
 1958 *Cosmic Electrodynamics* (Cambridge: Cambridge University Press).
- ELSASSER, W. M. 1956 *Rev. Mod. Phys.*, **28**, 135.
- FERRARO, V. C. A. 1954 *Ap. J.*, **119**, 407.
- FERRARO, V. C. A., and  
 MEMORY, D. J. 1952 *M.N.*, **112**, 361.
- GOLD, T., and HOYLE, F. 1960 *M.N.*, **120**, 89.
- HALL, J. S., and  
 MIKESELL, A. H. 1949 *A.J.*, **54**, 187.
- HAYASHI, C. 1961 *Pub. Astr. Soc. Japan*, **13**, 450.
- HERZENBERG, A. 1958 *Phil. Trans. R. Soc., London, ser. A*, **250**, 543.
- HILTNER, W. A. 1949 *Ap. J.*, **109**, 471.
- LÜST, R., and  
 SCHLÜTER, A. 1954 *Zs. f. Ap.*, **34**, 263.  
 1955 *Ibid.*, **38**, 190.
- LUNDQUIST, S. 1950 *Ark. f. Fys.*, **2**, 361.
- MESTEL, L. 1956 *M.N.* **116**, 324.
- MESTEL, L., and  
 SPITZER, L., JR. 1956 *M.N.*, **116**, 503.
- NAGATA, T. (ed.) 1954 *J. Geomag. Geoelec., Kyoto*, Vol. **6**, No. 4.
- PARKER, E. N. 1955 *Ap. J.*, **122**, 293.  
 1963 *Ap. J., Suppl.*, **8**, 177.
- PECKER, CH. 1953 *Ann. d'ap.*, **16**, 321.
- PIDDINGTON, J. H. 1956 *M.N.*, **116**, 314.  
 1958 *I.A.U. Symp.*, No. 6 (Cambridge: Cambridge University Press), p. 141.
- PLUMPTON, C., and  
 FERRARO, V. C. A. 1955 *Ap. J.*, **121**, 168.
- PRENDERGAST, K. H. 1956 *Ap. J.*, **123**, 498.  
 1958 *Ibid.*, **128**, 361.
- SCHATZMAN, E. 1959 *I.A.U. Symp.*, No. 10 (Cambridge: Cambridge University Press), p. 129.  
 1962 *Ann. d'ap.*, **25**, 1.
- SCHWARZSCHILD, M. 1949 *Ann. d'ap.*, **12**, 148.
- SEVERNY, A. B. 1958a *Crimean Obs. Pub.*, **20**, 12.  
 1958b *A.J., U.S.S.R.*, **35**, 335.

- SPITZER, L. 1958 *I.A.U. Symp.*, No. 6 (Cambridge: Cambridge University Press), p. 169.
- SWEET, P. A. 1954 *M.N.*, 114, 549.  
1958 *I.A.U. Symp.*, No. 6 (Cambridge: Cambridge University Press), p. 123.
- VITENSE, E. 1951 *Zs. f. Ap.*, 28, 81.
- WALÉN, C. 1949 *On the Vibratory Rotation of the Sun* (Stockholm: Henrik Lindstahls Bokhandel).
- WALLERSTEIN, G. 1962 *Phys. Rev., Letters*, 9, 143.
- WENTZEL, D. G. 1960 *Ap. J., Suppl.*, 5, 187.  
1961 *Ap. J.*, 133, 170.





## CHAPTER 9

# *Meridian Circulation in Stars*

L. MESTEL

*University of Cambridge, England*

THIS chapter is concerned with large-scale laminar circulation generated by non-spherical perturbations—centrifugal and magnetic force. For radiative zones there exists a fairly well-developed theory, which may be applied with confidence to studies of stellar evolution, stellar rotation, and perhaps surface phenomena in hot stars. For convective zones there is the beginning of a phenomenological theory of laminar flow superimposed on the small-scale turbulence; this is the more promising field for future work, because of probable applications to the solar cycle.

### § 1. HYDROSTATIC EQUILIBRIUM OF GASEOUS STARS

Consider first a non-rotating, non-magnetic homogeneous star of mass  $M$ , maintained in hydrostatic equilibrium as a sphere of radius  $R$ . Its gravitational potential energy  $\mathfrak{B}$  is  $-\eta GM^2/R$ ,  $G$  being the gravitational constant and  $\eta$  a numerical factor depending on the mass distribution. By the non-relativistic virial theorem (Eddington 1926), the total random kinetic energy  $K = -\mathfrak{B}/2$ . If the star is non-degenerate, so that the pressure  $p$ , the density  $\rho$ , and the temperature  $T$  are related by the perfect gas law

$$p = \frac{\Re}{\mu} \rho T, \quad (1.1)$$

then the mean temperature through the star is  $\eta GM\mu/3\Re R$ ,  $\mu$  being the mean molecular weight. Even at a radius several powers of ten above the main-sequence value this temperature is far greater than any that could be maintained at the surface by galactic radiation. Thus hydrostatic equilibrium enforces a temperature gradient from center to surface, with a consequent energy leak through the opaque gas: if there are no active nuclear sources the star loses energy and contracts. For hydrostatic equilibrium to hold at a smaller radius the thermal energy  $K$  must increase. Provided the ratio  $\gamma$  of the two principal

specific heats exceeds  $\frac{4}{3}$  over the bulk of the star, the gravitational energy released by the contraction is able to supply the surface loss, the energy absorbed by the non-kinetic degrees of freedom of the gas, and the required increase in  $K$ . The contraction is then non-catastrophic, through a sequence of states in hydrostatic equilibrium (Kelvin-Helmholtz contraction). It is halted at a central temperature high enough for nuclear energy generation to balance the leak to the surface: the extra condition of thermal equilibrium selects a unique member from the class of models in hydrostatic equilibrium (the Vogt-Russell theorem, e.g., Chandrasekhar 1939).

The assumption of purely radiative transport of energy often yields temperature gradients which are locally superadiabatic and therefore convectively unstable. Main sequence stars more massive than the sun have convective cores, because of the extreme temperature-sensitivity of the Bethe cycle. Stars with surface temperatures below the ionization temperature of hydrogen have subphotospheric convective zones, which can extend deep into the star, yielding marked overluminosity (Osterbrock 1953; Hoyle and Schwarzschild 1955; Kippenhahn, Temesváry, and Biermann 1958). Hayashi (1961) has shown that a similar effect occurs in the earlier stages of the pre-main-sequence contraction, shortening considerably the Kelvin-Helmholtz time scale, and insuring that the bulk of the star suffers violent turbulence between formation and the achievement of thermal equilibrium.

Now let a rotation field  $\Omega$  and a magnetic field  $H$  be introduced. The steady state virial theorem becomes (Chandrasekhar and Fermi 1953)

$$2\mathfrak{T} + \mathfrak{M} + 2K + \mathfrak{B} = 0, \quad (1.2)$$

where  $\mathfrak{T}$  is the macroscopic (here rotational) kinetic energy and  $\mathfrak{M}$  the magnetic energy; surface magnetic stresses and thermal pressure are again assumed negligible. The new terms are both positive, magnetic and centrifugal force both being essentially disruptive. In fact it is possible to construct equilibrium models in which the magnetic and centrifugal forces bear the brunt of the self-gravitation, with the thermal energy just a small perturbation: for example, a flattened structure, analogous to a disk-like galaxy, in which centrifugal force balances two components of gravity, and the isothermal pressure merely keeps the disk of finite thickness; or a slightly flattened model in which a magnetic field perpendicular to the rotation axis exerts the necessary pressure in the third dimension. Study of these models and of their stability is highly relevant to the condensation problem; but since the models lack the essential property of a high internal temperature, they bear no resemblance to stars. We take as a defining property of a non-degenerate star that its thermal energy must be comparable with its gravitational energy, so that it must radiate: the magnetic and centrifugal fields are treated as perturbations on the zero-order, spherically symmetrical state.

As the thermal and dynamical properties of radiative and convective zones

differ so much, it is convenient to bifurcate the discussion here, postponing discussion of convective zones until § 8. As a further simplifying restriction, the star's magnetic field is assumed symmetric about the axis of rotation, so that in the equilibrium state  $\rho$ ,  $p$  and  $T$  are also axially symmetric. The equation of hydrostatic support is now

$$-\frac{\nabla p}{\rho} + \nabla\phi + \Omega^2\tilde{\omega} + \left[ \frac{(\nabla \times \mathbf{H}) \times \mathbf{H}}{4\pi\rho} \right]_p = 0, \quad (1.3)$$

where the suffix  $p$  selects the poloidal (i.e., meridional) component of the magnetic force, and  $\tilde{\omega}$  is the vectorial distance from the axis. The gravitational potential  $\phi$  is related to  $\rho$  by Poisson's equation

$$\nabla^2\phi = -4\pi G\rho. \quad (1.4)$$

We now note an essential difference between (a) an incompressible liquid "star" (e.g., a planetary core), or a star with a barytropic equation of state  $\rho = \rho(p)$  (such as a degenerate "black" dwarf); and (b) a star obeying the normal gas law (1.1). In case (a), the hydrostatic condition (1.3) implies that

$$\begin{aligned} \Omega^2\tilde{\omega} + \left[ \frac{(\nabla \times \mathbf{H}) \times \mathbf{H}}{4\pi\rho} \right]_p &= \nabla \left[ \int \frac{dp}{\rho} - \phi \right] \\ &= \nabla V : \end{aligned} \quad (1.5)$$

in an equilibrium state the perturbing force per unit mass must be derivable from a potential  $V$ . Equation (1.3) may then be rewritten

$$\nabla p = \rho(\nabla\phi + \nabla V) = \rho\nabla\Psi, \quad (1.6)$$

say. Thus  $p$  is a constant on a surface of constant  $\Psi$  (known as a level surface); we may write

$$p = p(\Psi); \quad \rho = \rho(\Psi) = \frac{dp}{d\Psi}. \quad (1.7)$$

The simplest case is the non-magnetic star: the constraint (1.5) implies that  $\Omega = \Omega(\tilde{\omega})$  ( $\Omega$  must be constant on cylindrical surfaces). If  $\Omega = 0$  and  $\rho$  is constant, then a magnetic field of given angular dependence, e.g., a dipole type, has its radial variation restricted to a special class of function (Ferraro 1954). In a rotating magnetic star, the  $\Omega$  and  $\mathbf{H}$  fields are jointly constrained. If  $\rho$  is constant, the constraint is linear in the perturbing forces. In a barytropic star, the density  $\rho$  will itself depend on the perturbing forces because of the change in the pressure, so that, strictly speaking, the constraint (1.5) is a complicated non-linear relation. However, if the perturbing forces are small compared with gravity, the unperturbed density  $\rho_0$  may be written for  $\rho$ , so that the constraint is approximately linear. The important point is that one cannot imagine arbi-

trary, non-spherical perturbations imposed on a liquid or barytropic star without a consequent breakdown in hydrostatic equilibrium. The resulting mass motions would distort the  $\Omega$  and  $\mathbf{H}$  fields by convecting angular momentum and magnetic flux. The system would oscillate about an equilibrium state that satisfies the relation (1.5), until dissipation of energy reduced it to rest.

By contrast, in case (b) the star has no difficulty in satisfying the hydrostatic condition (1.3), whether or not the perturbation fields satisfy the constraint (1.5). In either case the perturbing fields require a non-spherical temperature as well as a non-spherical density field to provide hydrostatic support (Sweet 1950*b*; Mestel 1956; §§ 2 and 3 below). With  $p \propto \rho T$ ,  $\rho$  is not a unique function of  $p$  and condition (1.5) is not enforced by (1.3): the star has at each point an extra degree of freedom with which to balance the non-thermal force fields. If the perturbation field happens to be conservative, then again a joint potential  $\Psi$  exists, and in equilibrium the  $\rho$  and  $p$  fields will be functions of  $\Psi$ ; but if the perturbation field is more general, so are the  $\rho$  and  $p$  fields.

This degree of freedom is relevant because of the high degree of thermal stability in a radiative zone with a strongly subadiabatic temperature gradient. In order to interchange two elements of gas, energy must be supplied of the order of the difference in gravitational potential energy of the two elements. The possibility of an interchange instability will limit the arbitrariness of the perturbing fields only if they exert forces comparable with gravity; and even then, there is no guarantee that the new perturbing forces that result will be conservative. There is thus no reason to expect that, in general, a non-conservative force field will spontaneously transform itself into a conservative field of lower energy, unless the perturbation is comparable in strength with the gravitational field.

Just as for a spherical star, hydrostatic equilibrium alone does not specify a unique model, and appeal must be made to the condition of thermal equilibrium. For both mathematical and historical reasons it is convenient to study separately the cases with conservative and non-conservative perturbing forces.

## § 2. THERMAL EQUILIBRIUM: CONSERVATIVE PERTURBING FORCES

The case studied in the greatest detail in the literature (von Zeipel 1924; Eddington 1925, 1929; Vogt 1925, 1943; Öpik 1951; Sweet 1950*b*) is the uniformly rotating, non-magnetic homogeneous star, for which there exists a centrifugal potential  $V = \Omega^2 \varpi^2/2$ . More recently, Baker and Kippenhahn (1959) have studied the general conservative rotation field  $\Omega(\varpi)$ . As a simple generalization, we suppose there exists a potential  $V$  defined by equation (1.5), so that  $\rho$ ,  $p$ , and  $T$  are functions of the joint potential  $\Psi \equiv (\phi + V)$ . In the usual notation, the radiative flux is

$$\mathbf{F} = -\frac{4}{3} \frac{a c T^3}{\kappa \rho} \nabla T = \left( -\frac{4}{3} \frac{a c T^3}{\kappa \rho} \frac{dT}{d\Psi} \right) \nabla \Psi, \quad (2.1)$$

where the opacity  $\kappa$  is also a function of  $\Psi$  by virtue of its dependence only on  $\rho$  and  $T$ . Hence

$$\nabla \cdot \mathbf{F} = \frac{d}{d\Psi} \left( -\frac{4}{3} \frac{a c T^3}{\kappa \rho} \frac{dT}{d\Psi} \right) (\nabla \Psi)^2 + \left( -\frac{4}{3} \frac{a c T^3}{\kappa \rho} \frac{dT}{d\Psi} \right) (\nabla^2 V - 4\pi G \rho), \quad (2.2)$$

where Poisson's equation (1.4) has been used.

If  $H = 0$  and  $\Omega$  is constant,  $\nabla^2 V = 2\Omega^2$ , and  $\nabla \cdot \mathbf{F}$  takes on the form originally derived by von Zeipel (1924); his celebrated paradox results when the condition of *radiative equilibrium* is imposed, so that the energy generation  $\rho\epsilon$  per unit volume is forced to balance  $\nabla \cdot \mathbf{F}$ . Since  $\nabla^2 V$  is a function of  $\Psi$  (in fact, constant over the whole star), all the terms in  $\nabla \cdot \mathbf{F}$  are constant on level surfaces except  $(\nabla \Psi)^2$ , which on the contrary must vary from pole to equator, since level surfaces are not everywhere parallel. But in a homogeneous star  $\rho\epsilon$  is also a function of  $\rho$  and  $T$ , and hence of  $\Psi$ , so that the coefficient of  $(\nabla \Psi)^2$  in  $\nabla \cdot \mathbf{F}$  must vanish separately:

$$-\frac{4}{3} \frac{a c T^3}{\kappa \rho} \frac{dT}{d\Psi} = \text{constant}, \quad (2.3)$$

or, by equation (2.1),  $\mathbf{F} \propto \nabla \Psi$ . The remaining terms, all constant on level surfaces, yield

$$\epsilon \propto \left( 1 - \frac{\nabla^2 V}{4\pi G \rho} \right) = \left( 1 - \frac{\Omega^2}{2\pi G \rho} \right) \quad (2.4)$$

in von Zeipel's case.

This result is clearly untenable—at low enough densities it demands negative energy generation. But the correct conclusion from this *reductio ad absurdum* is not that the energy equation restricts the class of allowed perturbing fields, for example forbidding uniform rotation, but rather that strict radiative equilibrium must break down. It is this assumption that has put a severe constraint on  $\nabla \cdot \mathbf{F}$ . In the limit of zero perturbing force,  $\Psi \equiv \phi$ , and there is no requirement that the first term in  $\nabla \cdot \mathbf{F}$  should vanish independently of the second. In particular, if at the radius considered there are no active nuclear sources, e.g., in the cool envelope of a Cowling-type star, then in thermal equilibrium the two terms in equation (2.2) must be equal and opposite. But according to von Zeipel's argument, an infinitesimal uniform rotation forces the first term to vanish separately, and demands that the second be balanced by a spurious energy generation. This discontinuity as  $V \rightarrow 0$  is a further indication that von Zeipel's result is just a mathematical peculiarity.

Vogt (1925) and Eddington (1925, 1929) pointed out that the breakdown in radiative equilibrium tends to set up slight variations of temperature and pressure over a level surface, which start a meridian circulation. A steady state is reached when the convection of energy, the local nuclear generation, and the divergence of the radiation flux sum to zero. In a convectively stable zone, the temperature gradient normal to a level surface is subadiabatic; hence if an element acquires an energy excess it rises, and at such a rate that the excess of

adiabatic cooling over the energy supply always keeps the rising element at the appropriate temperature and density, as fixed by the hydrostatic conditions. The argument applies whether or not  $\nabla^2 V$  is constant over a level surface, i.e., whether or not a generalized von Zeipel paradox can be deduced from the constraint of strict radiative equilibrium.

The heat equation is

$$C_v \rho \frac{dT}{dt} = \frac{p}{\rho} \frac{d\rho}{dt} + (\rho\epsilon - \nabla \cdot \mathbf{F}), \quad (2.5)$$

where  $C_v$  is the specific heat at constant volume and  $d/dt$  is the derivative following the motion. This equation balances the rate of increase of the internal energy with the rate of compressional heating, the supply from the nuclear sources and from the radiation field. Radiation pressure can be included by suitable definitions of  $C_v$  and  $p$ ; terms dropped from the right-hand side are the viscous heating and the energy exchanges between the thermal and magnetic fields (Cowling 1945; Biermann 1950). In a steady state, with  $\rho$ ,  $p$ , and  $T$  functions of  $\Psi$ , equation (2.5) becomes

$$\rho G(\Psi)(\mathbf{v} \cdot \nabla \Psi) = (\rho\epsilon - \nabla \cdot \mathbf{F}), \quad (2.6)$$

where

$$G(\Psi) = C_v \left[ \frac{dT}{d\Psi} - (\gamma - 1) \frac{T}{\rho} \frac{d\rho}{d\Psi} \right]. \quad (2.7)$$

Since the flux of matter across a level surface  $\Psi = \Psi_0$  must vanish,

$$\int_{\Psi=\Psi_0} \rho(\Psi) \left( \mathbf{v} \cdot \frac{\nabla \Psi}{|\nabla \Psi|} \right) dS = \int_{\Psi=\Psi_0} \frac{(\rho\epsilon - \nabla \cdot \mathbf{F})}{G(\Psi) |\nabla \Psi|} dS = 0. \quad (2.8)$$

If  $\tau$  is the volume between two neighboring level surfaces, condition (2.8) is equivalent to

$$\int_{\tau} (\rho\epsilon - \nabla \cdot \mathbf{F}) d\tau = 0; \quad (2.9)$$

although radiative equilibrium breaks down locally, in a steady state the average of  $(\rho\epsilon - \nabla \cdot \mathbf{F})$  over a suitable volume vanishes.

It is now convenient to write

$$\nabla \cdot \mathbf{F} = \langle \nabla \cdot \mathbf{F} \rangle + (\nabla \cdot \mathbf{F})', \quad (2.10)$$

where the broken brackets refer to the mean over the level surface through the point considered, and the prime refers to the remainder with zero mean. Thus,

$$\begin{aligned} \langle \nabla \cdot \mathbf{F} \rangle &= \frac{d}{d\Psi} \left( -\frac{4}{3} \frac{a c T^3}{\kappa \rho} \frac{dT}{d\Psi} \right) \langle (\nabla \Psi)^2 \rangle \\ &\quad + \left( -\frac{4}{3} \frac{a c T^3}{\kappa \rho} \frac{dT}{d\Psi} \right) [\langle \nabla^2 V \rangle - 4\pi G \rho], \end{aligned} \quad (2.11)$$

and

$$(\nabla \cdot \mathbf{F})' = \frac{d}{d\Psi} \left( -\frac{4}{3} \frac{a c T^3}{\kappa \rho} \frac{dT}{d\Psi} \right) [(\nabla \Psi)^2]' + \left( -\frac{4}{3} \frac{a c T^3}{\kappa \rho} \frac{dT}{d\Psi} \right) (\nabla^2 V)'. \quad (2.12)$$

If the perturbing forces are small compared with gravity, the approximation that ignores quadratic terms in primed quantities transforms (2.8) into

$$\rho\epsilon - \langle \nabla \cdot \mathbf{F} \rangle = 0. \quad (2.13)$$

The vertical component  $v_r$  of the circulation velocity is given, from (2.6) and (2.12), as

$$\begin{aligned} \rho_0 g_0 \frac{n_0 - 1/(\gamma - 1)}{n_0 + 1} v_r = & - \frac{(L_r)_0}{4\pi r^2 g_0} (\nabla^2 V)' \\ & + [(\nabla \Psi)^2]' \left[ \frac{\rho_0}{g_0^2} \left( \frac{L_r}{M_r} - \epsilon \right) \right]_0. \end{aligned} \quad (2.14)$$

Zero-order approximations have been used in the coefficients of  $v_r$ ,  $(\nabla^2 V)'$  and  $[(\nabla \Psi)^2]'$ ;  $g_0$  is the local zero-order gravitational acceleration, and  $n_0 = d(\log \rho_0)/d(\log T_0)$  is the local polytropic index;  $L_r$  and  $M_r$  refer to the radius  $r$ . The equation of continuity yields the horizontal component of velocity

$$v_\theta = - \frac{1}{\rho_0 r \sin \theta} \frac{\partial}{\partial r} \left( \rho_0 r^2 \int_0^\theta v_r \sin \theta d\theta \right). \quad (2.15)$$

The details of the circulation depend on both the perturbation and the stellar model. For example, a star with a uniform nuclear source  $\epsilon$ , such as Eddington's standard model, and in uniform rotation has a vanishing first order circulation field, since  $\epsilon = L_r/M_r$ , and also  $(\nabla^2 V)' = (2\Omega^2)' = 0$  (Schwarzschild 1942). In a more realistic model, such as the Cowling point-convective model, we have  $\epsilon = 0$  and  $L_r = L$  in the radiative envelope, so that even if  $(\nabla^2 V)' = 0$  the circulation field does not vanish. An accurate calculation of the perturbed gravitational field and hence of  $[(\nabla \Psi)^2]'$  is best done by the technique outlined in § 3. However, it is clear that under small perturbations the fractional change in  $\phi$  must be of the order of  $|\nabla V|/|\nabla \phi_0|$ , so that  $|[(\nabla \Psi)^2]'| \simeq g_0^2 |\nabla V|/g_0$ , and

$$v_r \simeq \frac{n_0 + 1}{n_0 - 1/(\gamma - 1)} \left[ \frac{L_0}{(M_r)_0} \frac{|\nabla V|}{g_0^2} - \frac{(\nabla^2 V)'}{4\pi \rho_0 r^2} \frac{L_0}{g_0^2} \right]. \quad (2.16)$$

Over the bulk of the star the two terms in the brackets are comparable, unless  $|\nabla V|$  has locally large derivatives. The order of the velocities is  $10^{-5} (\bar{L}\bar{R}^2/\bar{M}^2) \times |\nabla V|/g_0$  (barred quantities being expressed in solar units). For example, the rotationally driven currents over the bulk of the sun have a speed  $\simeq 10^{-10}$  cms/sec, assuming for  $\Omega$  its surface value  $\simeq 3 \times 10^{-6}$ . But if the theory can be applied to the low density surface regions (see § 8), then the second term in the brackets is larger than the average by the factor  $\bar{\rho}_0/\rho_0$  ( $\bar{\rho}_0$  being the mean density), except when the perturbation field satisfies the constraint  $(\nabla^2 V)' = 0$ . In the earlier discussion this condition was required in order to derive von Zeipel's paradox from the hypothesis of strict radiative equilibrium. Now it is the condition that the first-order vertical velocities be of the same order of magnitude all over the non-convective regions of the star (Baker and Kippenhahn 1959).<sup>1</sup>

<sup>1</sup> Even when  $(\nabla^2 V) = 0$ , the second-order expression for  $v_r$  contains a term in  $\bar{\rho}_0/\rho_0$  (Öpik 1951, Kippenhahn, private communication).



In a non-magnetic star, with  $\Omega$  a function of  $\varpi$  only,  $\nabla^2 V = d(\Omega^2 \varpi^2)/\varpi d\varpi$ . Since the level surfaces are not surfaces of constant  $\varpi$ , the relevant condition is the constancy of  $d(\Omega^2 \varpi^2)/d\varpi^2$  over the whole star. As  $\Omega$  must be finite on the axis, this reduces to  $\Omega$  constant over the whole star.

To sum up, if  $\lambda$  is a parameter measuring the ratio of the (conservative) perturbing force to gravity, the order of the velocities generated over the bulk of the radiative zone is (dropping the suffix zero)

$$\lambda \frac{L}{M} \frac{1}{g}. \quad (2.17)$$

Near the surface the vertical velocity is of order

$$\lambda \frac{L}{M} \left( \frac{\bar{\rho}}{\rho} \right) \frac{1}{g}, \quad (2.18)$$

except for those exceptional perturbing fields for which the factor  $\bar{\rho}/\rho$  is replaced by unity. In general, the equation of continuity (2.15) yields a horizontal component of the same order as (2.17) or (2.18), but for the exceptional cases the horizontal velocity is of order

$$\lambda \frac{L}{M} \left| \frac{r \rho'}{\rho} \right| \frac{1}{g}. \quad (2.19)$$

As  $n$  approaches the adiabatic value  $1/(\gamma - 1)$  near a convective zone, the vertical velocity becomes large like  $1/[n - (1/\gamma - 1)]$ , and the horizontal like  $1/[n - (1/\gamma - 1)]^2$ .

### § 3. THERMAL EQUILIBRIUM: GENERAL PERTURBING FORCES

We have seen that for a real star, the condition of hydrostatic support does not constrain the perturbing force density to be conservative; a more general theory is therefore required. We now describe a systematic scheme of approximation for computing the perturbed  $\rho$ ,  $\phi$ , and  $T$  fields, and the meridian circulation field, as series in the perturbing parameter, applicable whether or not a potential  $V$  exists.

Consider an arbitrary perturbing force  $\lambda f$  per unit mass, where  $\lambda$  is a suitable non-dimensional parameter (e.g., the ratio of gravity to centrifugal force at a standard point). The hydrostatic condition becomes

$$-\nabla p + \rho \nabla \phi + \rho \lambda f = 0. \quad (3.1)$$

Provided  $\lambda f/g \ll 1$ , we may expand about the zero-order, spherically symmetrical state (Sweet 1950*b*; Sweet and Roy 1953). For example,

$$\begin{aligned} \phi(r, \theta) &= \phi_0(r) + \lambda \phi_1(r, \theta) + \dots \\ &= \phi_0(r) + \lambda [\phi_{11}(r) + \phi_{12}(r, \theta)] + \dots, \end{aligned} \quad (3.2)$$

where

$$\phi_{11}(r) = \int_0^\pi \phi_1(r, \theta) \sin \theta d\theta, \quad (3.3)$$

and  $\phi_{12}(\mathbf{r}, \theta)$  is the part of  $\phi_1(\mathbf{r}, \theta)$  that vanishes on averaging over a *sphere*. There are, therefore, eight first-order quantities to determine. The  $r$ -component of (3.1) yields two conditions, the  $\theta$ -component yields one, and (1.1) and (1.4) yield two conditions each, making seven in all. If we now tried to impose strict radiative equilibrium, the eight quantities would have to satisfy nine conditions. It is the vector character of the equation of support that overdetermines the problem: under spherical symmetry each physical equation implies just one constraint. Thus radiative equilibrium implies a restriction on the perturbation field; in general, radiative equilibrium must break down, and thermal equilibrium is maintained by meridian circulation. The argument is clearly valid to all orders in  $\lambda$ ; it is logically prior to the expansion procedure.

We may regard the circulation as the relic of the flow in a contracting non-spherical star, after the central temperatures have become high enough for nuclear energy generation to balance the surface loss, and so halt the over-all contraction. In fact, the theory may be applied to a contracting or expanding star, yielding a meridian circulation superimposed on the mean radial motion.

In a steady state the energy equation (2.5) reduces to

$$C_v \rho T \mathbf{v} \cdot \nabla \left( \log \frac{T}{\rho^{\gamma-1}} \right) = (\rho \epsilon - \nabla \cdot \mathbf{F}). \quad (3.4)$$

The zero-order approximation is  $(\rho \epsilon - \nabla \cdot \mathbf{F})_0 = 0$ —radiative equilibrium in the unperturbed state. Since there is no net outflow of matter from a sphere in a steady state, we have

$$0 = \int_0^\pi \rho_0 (v_r)_1 \sin \theta d\theta \propto (\rho \epsilon - \nabla \cdot \mathbf{F})_{11}, \quad (3.5)$$

so that

$$\left( C_v \rho_0 T_0 \frac{d}{dr} \log \frac{T_0}{\rho_0^{\gamma-1}} \right) (v_r)_1 = (\rho \epsilon - \nabla \cdot \mathbf{F})_{12}. \quad (3.6)$$

Instead of being required to vanish,  $(\rho \epsilon - \nabla \cdot \mathbf{F})_{12}$  determines the radial velocity  $(v_r)_1$ . With nine quantities and nine equations the system is now determinate,  $(v_\theta)_1$  again being fixed by continuity. It should be noted that in higher approximations the average of  $(\rho \epsilon - \nabla \cdot \mathbf{F})$  over a sphere does not vanish, because, for example, convection by the *first-order* velocity field of *first-order* perturbations to the thermal field contributes *second-order* terms to the energy balance. To compute the  $n$ 'th-order contribution to the circulation one needs the  $(n-1)$ 'th-order perturbation to the mean state (Sweet and Roy 1953).

If viscosity is ignored, the pressure-density field in a steady state is, to the first order, unaltered by the circulation, since the time-independent inertial terms are quadratic in  $\mathbf{v}$ : pressure variations in excess of those satisfying equation (3.1) are required to start up the circulation, but not, in this approximation, to maintain it. The conditions for strictly steady circulation are discussed in § 4. For the moment, we note that even if the circulation distorts the perturbation field, e.g., through convection of angular momentum, the instantane-

ous *first-order* velocity field may still be calculated from the present theory, for the consequent time-derivatives of  $\rho$  and  $T$  are necessarily quadratic in the perturbation.

Only first-order theory has been treated in detail in the literature (Sweet 1950*b*). From equations (1.4) and (3.1), we have

$$\nabla^2 \left( \frac{\partial \phi_{12}}{\partial \theta} \right) - \frac{4\pi G \rho'_0}{(-\phi'_0)} \frac{\partial \phi_{12}}{\partial \theta} = \frac{4\pi G}{\phi'_0} \left[ \frac{\partial}{\partial r} (r \rho_0 f_\theta) - \rho_0 \frac{\partial f_r}{\partial \theta} \right]. \quad (3.7)$$

Provided the Reynolds stresses in turbulent zones are small compared with the centrifugal energy, this equation is valid through the whole star. At  $r = 0$  and  $r = \infty$ ,  $\phi_{12}$  vanishes. To the first order, the continuity of  $\phi_{12}$  and its normal derivative at the distorted stellar surface is equivalent to the continuity of  $\phi_{12}$  and  $d\phi_{12}/dr$  at  $r = R$ . Expansion of  $f_r$ ,  $f_\theta$ , and  $\phi_{12}$ ,

$$\begin{aligned} f_r &= \sum_{s=0}^{\infty} a_s(r) P_s(\cos \theta), & f_\theta &= - \sum_{s=1}^{\infty} b_s(r) \frac{\partial P_s}{\partial \theta}, \\ \phi_{12} &= - \sum_{s=1}^{\infty} c_s(r) \frac{\partial P_s}{\partial \theta}, \end{aligned} \quad (3.8)$$

reduces (3.7) to a set of ordinary differential equations for  $c_s$ , with boundary conditions identical with those for  $\phi_{12}$ .

From  $\phi_{12}$  we find  $\rho_{12}$ ,  $p_{12}$ , and  $T_{12}$ ; whence

$$\begin{aligned} (v_r)_1 \left( \rho_0 g_0 \frac{n_0 - 1/\gamma - 1}{n_0 + 1} \right) &= \rho_0 \epsilon_0 \left\{ T_{12} \frac{\partial}{\partial T_0} [\log(\rho_0 \epsilon_0)] \right. \\ &+ \rho_{12} \frac{\partial}{\partial \rho_0} [\log(\rho_0 \epsilon_0)] \left. \right\} - \frac{1}{r^2} \frac{\partial}{\partial r} \left\{ r^2 F_0 \left[ T_{12} \frac{\partial}{\partial T_0} \log \left( \frac{T_0^3}{\kappa_0 \rho_0} \right) \right. \right. \\ &+ \rho_{12} \frac{\partial}{\partial \rho_0} \left( \log \frac{T_0^3}{\kappa_0 \rho_0} \right) + \frac{1}{T_0'} \frac{\partial}{\partial r} T_{12} \left. \right] \left. \right\} \\ &- \frac{F_0}{r^2 T_0'} \frac{\partial}{\partial \theta} \left( \frac{1}{\sin \theta} \frac{\partial}{\partial \theta} T_{12} \sin \theta \right), \end{aligned} \quad (3.9)$$

with  $(v_\theta)_1$  given by (2.15).

The simplest problem is again the uniformly rotating star, for which

$$f_r = \frac{2}{3} \Omega^2 r [1 - P_2(\cos \theta)], \quad f_\theta = -\frac{1}{3} \Omega^2 r \frac{\partial P_2}{\partial \theta}. \quad (3.10)$$

Sweet's technique yields

$$\phi_{12} = P_2(\cos \theta) \left[ \frac{1}{3} r^2 (1 - h) \Omega^2 \right], \quad (3.11)$$

where

$$r h'' + 6 h' + \frac{4\pi G \rho'_0 r}{\phi'_0} h = 0. \quad (3.12)$$

The velocity field in the envelope of a Cowling-type star is (dropping the suffixes 0 and 1)

$$v_r = \frac{2}{3} \frac{n+1}{n-\frac{3}{2}} \frac{L}{M_r} \frac{\Omega^2 r}{g^2} \left[ h \left( 4 - \frac{4\pi G \rho r}{g} \right) + r h' \right] P_2(\cos \theta) \quad (3.13)$$

$$= \dot{p}(r) P_2(\cos \theta),$$

and

$$v_\theta = -\frac{1}{2\rho r} \frac{d}{dr}(\rho r^2 \dot{p}) \sin \theta \cos \theta. \quad (3.14)$$

Sweet's detailed calculations confirm the order of magnitude estimate (2.17) for  $v$  (thus correcting Eddington's gross overestimate [1929], which for many years misled workers in stellar evolution). The streamlines are as in Figure 1, *a*: the slow increase with  $r$  of  $r^2 \dot{p}$  is not enough to offset the drop in  $\rho$ , so that the

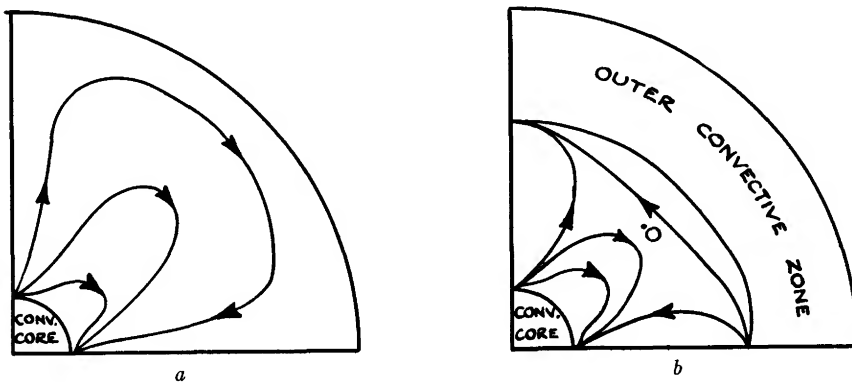


FIG. 1.—Schematic streamlines in uniformly rotating stars. When the  $\mu$ -current velocities are included (§§ 5 and 6), the streamlines do not enter the core, but are diverted horizontally in a thin boundary layer.

direction of the horizontal flow is from pole to equator through the whole envelope. However, if the star has an outer convective zone, so that after reaching a maximum, the polytropic index decreases again to the adiabatic value  $\frac{3}{2}$ , the increased suction of the vertical velocity field reverses the horizontal component. The streamlines are then as in Figure 1, *b*, with a stagnation point at 0.

As noted in the last section, uniform rotation is that special member of the class of conservative rotation fields that yields a finite first-order  $v_r$  as  $\rho \rightarrow 0$  near the surface; other conservative fields yield  $v_r$  and  $v_\theta \propto 1/\rho$ . If we now generalize the rotation law to simple non-conservative forms, such as  $\Omega(r)$ , then Sweet's technique shows that uniform rotation is again a special case: near the surface there are in general dominant terms like  $\{[r(\Omega^2)']r/g\}(L/M)(\bar{p}/\rho)$  in both horizontal and vertical components (Baker and Kippenhahn 1959). In fact, the estimated orders of the velocities due to conservative perturbations (eqs. [2.17], [2.18], and [2.19]) are applicable to the more general case.

The Eddington-Sweet theory assumes that not only the non-linear inertial force, but also the linear viscous force is negligible compared with the perturbing centrifugal or magnetic forces. This approximation is excellent as long as the velocities are of order (2.17). However, even in the simple case of a uniformly rotating star, for which  $v_r$  remains finite as  $\rho \rightarrow 0$ , the computed circulation has singular features. At the surface,  $v_\theta$  becomes large like  $r\rho'/\rho$ . As a convective zone is approached,  $v_r$ ,  $v_\theta$ , and  $v_\theta/v_r$  all diverge. Further, consider a star with its radiative zone divided in two by a discontinuity in  $\mu$ , with a compensating density jump. Such a surface cannot be distorted from its equilibrium position without bringing into play restoring gravitational forces, since temperature discontinuities are forbidden (see § 6). Therefore, meridional currents cannot cross from one zone into the other, but must be deflected horizontally by the “ $\mu$ -barrier”; each zone has its own circulation independently of the other. But at an infinitesimal distance from the barrier the breakdown in radiative equilibrium persists, driving a vertical velocity field; hence if  $v_r$  is to vanish at the barrier, continuity requires that  $v_\theta$  become infinite. The energy available to drive the circulation is not used up because of the constraining barrier. For since there is no zero-order horizontal entropy gradient, a non-viscous gas is accelerated indefinitely. And even if  $v_\theta$  were finite, the discontinuity in  $v_\theta$  at the barrier would imply an inadmissible infinite shear.

All these singularities can be removed by the introduction of the small but finite viscosity (Mestel 1953). Near a  $\mu$ -barrier at a radius  $\bar{r}$  deep in the radiative envelope of a uniformly rotating star, a velocity field that approximately satisfies both the field equations and the boundary conditions is

$$\begin{aligned} v_r &= p(\bar{r})[1 - e^{K(r-\bar{r})^3}]P_2(\cos \theta), \\ v_\theta &= \frac{3}{2}p(\bar{r})(\bar{r}K)(r - \bar{r})^2 e^{K(r-\bar{r})^3} \sin \theta \cos \theta, \\ &[K(r - \bar{r}) \leq 0], \end{aligned} \quad (3.15)$$

where  $|K|^{-1/3}$  must be much less than the scale height, and  $p(r)P_2$  is Sweet's vertical velocity in the absence of the barrier. The viscous force density on  $v_\theta$  has a dominant term  $\eta \nabla^2 v_\theta$ , where  $\eta$  is the radiative viscosity  $2aT^4/15\kappa\rho c$  (Cowling 1953). The magnitude must be adjusted so that the local change in the thermal field resulting from both centrifugal and viscous force yields  $\nabla \cdot \mathbf{F} = 0$  at the barrier. The order of  $|K|$  is found to be  $\simeq 10^{-14}$  cgs, so that the “boundary layer” (the narrow region in which the viscous force on the circulation is comparable with the centrifugal) is about a kilometer wide. At its maximum,  $v_\theta$  is about  $10^6$  times the normal Sweet value.<sup>2</sup>

A similar type of analysis yields a thin boundary layer near a convective zone: at the base of the solar Unsöld zone the vertical and horizontal compo-

<sup>2</sup> The theory of the boundary layer near a  $\mu$ -barrier given in Mestel (1953) is inaccurate, as the modulating factor assumed there, while reducing  $v_r$  to zero, still leaves a discontinuity in  $v_\theta$  at the barrier (see also § 4).

nents are respectively about  $10^{-4}$  and 3 cm/sec. It is remarkable that even in a slowly rotating star like the sun the very slight thermal disequilibrium can lead, near an unstable region, to horizontal velocities of an observable order (although in fact, because of the penetration of the turbulent convection into adjacent subadiabatic layers, a theory based on a zero-order stable stratification is unlikely to be realistic).

Strong horizontal shearing can sometimes give rise to local turbulence, the energy in the flow being available to overturn the otherwise stable density stratification. A sufficient criterion for *stability* is that the Richardson number  $J = g(-\rho'/\rho)/(dv_\theta/dr)^2$  should be greater than about  $\frac{1}{4}$  (Chandrasekhar 1961). In a boundary layer near a  $\mu$ -barrier deep in a star,  $J$  is infinite at  $\bar{r}$  (since  $dv_\theta/dr$  vanishes there); but near the edge of the layer  $J$  attains a minimum value  $\simeq 10^{-7}/p^2$ . In the sun, with  $p \simeq 10^{-10}$ , stability is assured. However, since  $p \propto \bar{L}\bar{R}^5\bar{\Omega}^2/\bar{M}^3$ ,  $J$  could approach the value  $\frac{1}{4}$  in rapidly rotating bright stars, e.g., if  $\bar{\Omega} = 10^2$ , and  $\bar{M} = 10$  (assuming  $\bar{L} \propto \bar{M}^3$  and  $\bar{R} \propto \bar{M}^{0.7}$ ). The instability would reconvert kinetic energy of the circulation into gravitational potential energy, and so assist the viscous force in keeping the flow finite.

#### § 4. CONDITIONS FOR STEADY CIRCULATION

So far, the perturbing  $\Omega$  and  $\mathbf{H}$  fields have been thought of as prescribed, and procedures have been outlined for computing the consequent meridian circulation. A great variety of streamline patterns can be generated in this way (e.g., Kippenhahn 1958). However, a circulation fast enough to be of interest tends to alter the driving perturbing fields. The circulation is “inexorable”—its speed and direction are determined by the instantaneous distortion of the thermal field. At each instance the perturbing forces are balanced by perturbations in the pressure and gravitational field: the circulation is driven by the slight *excesses* and *defects* in pressure due to the consequent breakdown in radiative equilibrium. Thus, although the energy of the circulation is normally small compared with the centrifugal and magnetic energies, amply justifying the neglect of inertia, the circulation still convects angular momentum and magnetic flux. Further, the interaction between the  $\Omega$  and  $\mathbf{H}$  fields is affected by the circulation. To follow the changing circulation pattern is a formidable task; we shall merely study possible self-consistent steady states.

Suppose again that the star is rotating, and has a large-scale magnetic field symmetric about the rotation axis, with both a poloidal component  $\mathbf{H}_p$  and a toroidal component  $\mathbf{H}_t$ . In the absence of circulation, the steady state conditions are (1)  $\Omega$  approximately constant along individual field lines (Ferraro’s law of isorotation, 1937); and (2) the poloidal currents  $j_p$  maintaining the toroidal field  $\mathbf{H}_t$  flow parallel to  $\mathbf{H}_p$ , so that the magnetic torque vanishes (viscous force and radiation braking being negligible [see below]). Both conditions are modified by the circulation (Mestel 1961). Provided the time of circulation is short compared with the ohmic decay time of the field, the magnetic Reynolds num-

ber of the circulation is high, and the poloidal component of the steady state hydromagnetic equation yields approximately

$$v_p = kH_p, \quad (4.1)$$

with  $k$  a scalar. An "inexorable" circulation in a highly conducting medium forces the poloidal field lines to follow closely the streamlines; in particular, it allows only a few field lines to leak out of the stellar surface. The theoretical and observational consequences of this result will be noted later (§ 7).

Further, the convection of angular momentum causes non-uniform rotation. This generates a further toroidal component and a magnetic torque, which in turn changes the angular momentum of the circulating elements. The convection of the toroidal field by the circulation must be included along with the twisting of the poloidal component by rotational shear. The non-steady problem would be difficult even if the circulation field could be taken as fixed. However, if we assume a steady state has been achieved, there are the following integrals:

$$\Omega - \frac{kH_t}{\varpi} = \alpha, \quad (4.2)$$

$$\rho k = \frac{\rho v_p}{H_p} = \eta, \quad (4.3)$$

$$-\frac{\varpi H_t}{4\pi} + \rho k \Omega \varpi^2 = -\frac{\beta}{4\pi}, \quad (4.4)$$

where  $\alpha$ ,  $\eta$ , and  $\beta$  are constants on the streamlines. Equation (4.2) is the toroidal component of the hydromagnetic equation: together with equation (4.1) it implies that the most general, steady, axially symmetrical flow consists of an arbitrary uniform rotation of each poloidal loop, superimposed on a velocity  $kH$  parallel to the field. Equation (4.3) expresses conservation of mass and magnetic flux. The integral (4.4) is derived from the toroidal equation of motion: it balances the convection of angular momentum by the circulation against its transport by the magnetic stresses (Lüst and Schlüter 1955).

Equations (4.2), (4.3), and (4.4) combine to give

$$\Omega = \frac{\alpha + \eta\beta/\rho\varpi^2}{1 - 4\pi\eta^2/\rho}, \quad (4.5)$$

and (writing now  $H_\phi$  instead of  $H_t$ )

$$H_\phi = \frac{\beta/\varpi + 4\pi\eta\alpha\varpi}{1 - 4\pi\eta^2/\rho}. \quad (4.6)$$

If  $\eta = 0$  (no circulation), (4.5) and (4.6) reduce as required to Ferraro's law  $\Omega = \alpha$ , and the torque-free condition  $\varpi H_\phi = \beta$  (Lüst and Schlüter 1954). With  $\eta$  finite, the non-dimensional parameter  $4\pi\eta^2/\rho$  can be written as  $(v_p/v_A)^2$ , where  $v_A$  is the local speed of Alfvén waves along the poloidal field. Non-singular

solutions without discontinuities are possible only if  $v_p/v_A$  is either less than or greater than unity all over the radiative zone—the flow must be either “sub-Alfvén” or “super-Alfvén.” The quantities  $\alpha$  and  $\beta$  are free, except for the constraint of constancy along the poloidal field-streamlines; they can easily be related to the toroidal magnetic flux between neighboring poloidal loops, and the angular momentum in the volume between the associated magnetic shells (Mestel 1961).

The self-consistency problem arises because the circulation  $v_p$  assumed in deriving the above integrals is itself a complicated functional of the  $\Omega$  and  $H$  fields. In principle, one can proceed by introducing a stream function  $S$  for the undetermined circulation; prescribing  $\alpha(S)$ ,  $\beta(S)$ , and also  $\eta(S)$  (so fixing the strength as well as the direction of  $H_p$ ); and then, using the technique given in § 3 to compute the stream function, arriving at an integro-differential equation for  $S$ . In practice, self-consistent solutions have been derived only in two extreme cases, for which the driving perturbation can be defined effectively independently of the circulation it generates (Roxburgh 1963).

In the first, and more important case, one can find conditions for the radiative zone to rotate nearly uniformly, in spite of the convection of angular momentum by Sweet’s rotationally driven circulation. By (4.5),  $\alpha$  must be constant over the whole zone; also

$$\frac{v_p^2}{v_A^2} = \frac{v_p^2}{H_p^2/4\pi\rho} = \frac{4\pi\eta^2}{\rho} \ll 1, \quad (4.7)$$

and

$$\left| \frac{\eta\beta}{\rho\omega^2} \right| \ll |\alpha|. \quad (4.8)$$

Since the currents are assumed rotationally driven, for consistency both the toroidal and poloidal magnetic energy must be less than the centrifugal:

$$H_t^2 \ll 4\pi\rho\Omega^2\varpi^2 \quad (4.9)$$

and, from (4.7),

$$4\pi\rho v_p^2 \ll H_p^2 \ll 4\pi\rho\Omega^2\varpi^2. \quad (4.10)$$

There is no difficulty in satisfying condition (4.10), for not even in the singular regions discussed earlier in § 3 does the circulation inertia become comparable with the centrifugal force. For example, even in a B-star rotating near the stability limit,  $H_p$  as weak as  $10^{-1}$  gauss satisfies the left-hand inequality. The circulation indirectly generates a toroidal field of order  $4\pi\eta a\omega$  (Mestel 1961), which certainly satisfies (4.9) and (4.8). If the star has, in addition, a stronger, torque-free toroidal field  $\beta/\omega$ , independent of the circulation, then again, provided the energy condition (4.9) is satisfied, condition (4.8) holds, and the solution is self-consistent.

An incidental consequence of this self-consistent solution is a likely modifica-



tion of the "boundary layer" theory of the preceding section (Roxburgh 1962, private communication). When  $v_\theta$  becomes large, so (by eqs. [4.1] and [4.5]) does  $H_\theta$ , and the consequent poloidal magnetic force may be locally larger than the centrifugal, thus contradicting a basic assumption, and requiring a new theory of the zone in which  $\mathbf{v}$  is diverted horizontally. One may surmise that the thickness of this zone will be fixed by the condition that the local magnetic and centrifugal force densities are, in fact, comparable.

The other simply computable self-consistent case is derived by taking as an approximation to (4.2) and (4.3)

$$H_\phi = -\frac{\alpha}{\eta} \rho \varpi = \gamma \rho \varpi, \quad (4.11)$$

where  $\gamma$  is again constant on streamlines. This field is easily seen to be a consequence of the freezing of the flux into a circulating toroidal tube, provided the twisting of the poloidal field by non-uniform rotation makes a negligible contribution to the variation in  $H_\phi$ . For consistency with the torque equation (4.4), we require

$$\left| \frac{\Omega \varpi \rho}{\eta H_\phi} \right| \frac{4\pi \eta^2}{\rho} > 1; \quad (4.12)$$

since by hypothesis  $|\Omega \varpi \rho / \eta H_\phi| \ll 1$ , we have

$$\frac{4\pi \eta^2}{\rho} \gg 1. \quad (4.13)$$

That is, the poloidal field must be weak enough for the flow to be "super-Alfvén." If in addition  $H_\phi^2/8\pi \gg \frac{1}{2}\rho\Omega^2\varpi^2$ , or

$$\frac{1}{(4\pi \eta^2/\rho)^{1/2}} \gg \left| \frac{\Omega \varpi \rho}{\eta H_\phi} \right|, \quad (4.14)$$

then the toroidal magnetic field is the dominant perturbation, and the streamlines must be computed from the distortion of the thermal field by the toroidal field (4.11). Conditions (4.12) and (4.14) together yield

$$\frac{1}{4\pi \eta^2/\rho} < \left| \frac{\Omega \varpi \rho}{\eta H_\phi} \right| \ll \frac{1}{(4\pi \eta^2/\rho)^{1/2}}. \quad (4.15)$$

If  $\eta \rightarrow \infty$  (zero-poloidal field), the left-hand inequality can be satisfied with  $\Omega = 0$ . The magnetic torque is zero, and so no Coriolis force is required to balance it.

To complete the problem one has to assume that  $\gamma$  is constant over the whole zone, so that again the properties of the circulation do not enter even implicitly into the definition of the driving parameter (Roxburgh 1963). The magnetic force per unit mass is then

$$\frac{(\nabla \times \mathbf{H}_t) \times \mathbf{H}_t}{4\pi \rho} = -\frac{\gamma^2}{4\pi} \nabla(\rho \varpi^2). \quad (4.16)$$

Thus there exists a joint potential and associated level surfaces. However,  $\nabla^2(\rho\omega^2)$  is certainly not constant over the level surfaces, so that both the vertical and horizontal components near the surface become large (cf. § 2). The circulation consists of an inner zone with currents descending at the pole and rising at the equator, and an outer zone with the signs reversed.

However, condition (4.13) is a very severe restriction on the allowed poloidal field, simply because the circulation speeds are generally so slow. Over the bulk of the star, even if  $H_\phi$  has its maximum allowed value (about  $10^8$  gauss),  $H_p$  (from eq. [4.13]) must be well below  $10^{-2}$  gauss; while with more realistic, lower values for  $H_\phi$ , the upper limit on  $H_p$  decreases like  $H_\phi^2$ . Near the surface  $H_\phi$  decreases like  $\rho$ , but  $4\pi\rho v_p^2$  stays approximately constant; the maximum allowed ratio  $H_p/H_\phi$  is now larger, but still well below unity. If the star's magnetic field is primeval, or dynamo-maintained, it is very unlikely that the ratio of poloidal- to toroidal-field strength should be less than  $10^{-10}$ . (A purely *toroidal* field will be slowly built up in an initially non-magnetic rotating star by the electron partial pressure [Biermann 1950]. However, this field's structure is quite different from [4.11]. Its energy is never greater than the centrifugal energy, and is usually less, so that the neglect of the centrifugal perturbation to the thermal field would be unjustified; and the presence of even a very weak poloidal field is sufficient to prevent Biermann's "battery" from operating [Mestel and Roxburgh 1962].) We conclude that the self-consistent solution generated by the toroidal field (4.11) is unlikely to be realized in any real star.

Other extreme cases may be easily defined, but have so far eluded computation. If the poloidal magnetic energy is much greater than either the centrifugal or the toroidal energy, then  $\Omega$  and  $H_\phi$ , whether or not satisfying the steady-state conditions (4.5) and (4.6), are irrelevant to the computation of the circulation. Again, assuming the magnetic Reynolds number much larger than unity, we have to satisfy the steady-state hydromagnetic condition (4.1). If the radial component  $H_r$  were proportional to  $P_n(\cos\theta)$ , the field would exert a force with a radial component  $(\partial P_n/\partial\theta)^2$ , which is a sum of terms in  $P_{2n}, P_{2n-2}, \dots, P_2, P_0$ , and so generates a radial velocity involving  $P_2, \dots, P_{2n}$ . Thus a strong poloidal field, generating a circulation parallel to itself, must have a very complicated structure, with only even-order Legendre functions appearing in  $H_r$ ; no model has appeared in the literature.

At the other extreme, we may imagine a rotating star with a magnetic field so weak that, not only is its effect on the thermal field negligible, but also its constraining effect on the rotation may be ignored, so that the steady-state condition (4.4) reduces to  $\Omega\omega^2$  constant on individual streamlines. From (4.2) and (4.4), a necessary condition is that  $4\pi\eta^2/\rho \gg 1$ . But again the streamlines are not known a priori, but are complicated functionals of the rotation field itself. If the streamlines are closed loops within the radiative zone, there is the possibility (Randers 1941) that the rotation field would be subject to Rayleigh instability (though the subadiabatic temperature gradient would tend to stabi-

lize). If streamlines enter and leave a uniformly rotating convective core, the circulation would need to be *upward* near the equator and *downward* near the pole: otherwise the only steady state would be with zero angular momentum in the envelope. Again, no example has been computed; still less has it been shown that a non-magnetic star with an arbitrary initial rotation field would evolve by convection of angular momentum toward a state with a self-maintained circulation. It is possible that, in the absence of a magnetic constraint, the rotation field will asymptotically approach a state which satisfies radiative equilibrium, i.e., the circulation will *choke* rather than *maintain* itself.

It remains to check that other toroidal forces are negligible in radiative zones. Molecular and radiative viscosity are far too small to affect any but the most violent  $\Omega$ -gradients within the stellar lifetime (Cowling 1953). More important is radiation braking: the effect of the convection of angular momentum by the radiation flux (Jeans 1926). This can be represented approximately as a torque-density  $(F/c^2) \cdot \nabla(\Omega \varpi^2)$ ,  $c$  being the velocity of light (Cowling 1953). The convection of angular momentum by the circulation dominates if

$$1 \ll \frac{\rho v c^2}{F} \simeq \rho \left( \frac{\Omega^2 r}{g^2} \right) \frac{L}{M} \frac{\bar{\rho}}{\rho} c^2 \left( \frac{4\pi r^2}{L} \right) \simeq 10^6 \left( \frac{\Omega^2 r}{g} \right), \quad (4.17)$$

where the Baker-Kippenhahn estimate (2.18) for  $v$  has been used, since  $\Omega$  is sure to be non-uniform. Thus, even in the sun, where the rotational currents are negligibly slow, the radiation braking is smaller than the Coriolis force by a factor of ten, and so is a fortiori negligible.

There is one remaining possibility. We have noted that in a non-magnetic star an initial circulation may tend to choke itself by building up a rotation field satisfying  $\nabla \cdot \mathbf{F} = 0$ . Subsequent radiation braking may then modify the  $\Omega$ -field so as to allow a slow circulation. The steady-state condition would then be

$$\left( \rho v + \frac{F}{c^2} \right) \cdot \nabla(\Omega \varpi^2) = 0: \quad (4.18)$$

$\Omega \varpi^2$  constant along the lines of the vector field  $[v + (F/\rho c^2)]$ , and  $v$ , the circulation driven by this  $\Omega$ -field, of order  $F/\rho c^2$ .

## § 5. MERIDIAN CIRCULATION AND STELLAR EVOLUTION

The evolution of a star of given mass and composition from its "initial main-sequence" state is by transmutation of hydrogen into helium in the hot central regions. In stars rather more massive than the sun, the dominant nuclear process is the highly temperature-sensitive Bethe cycle, so that the star has a convective core that is kept homogeneous by turbulent mixing. The evolutionary tracks are critically dependent on how much, if any, mixing of matter between core and envelope takes place. The path in the Hertzsprung-Russell diagram of a fully mixed star is up and slightly to the left of the initial main sequence. Also, since the luminosity depends strongly on  $\mu$  as well as on  $M$ , the mass-luminosity

relation for the "observational main sequence" would be markedly blurred (Fesenkov 1954). By contrast, a star in which not all, but a substantial fraction, of the mass is mixed moves to the right into the giant region as  $\mu$  increases in the inner part (Hoyle and Lyttleton 1949; Bondi and Bondi 1950, 1951); while if no mixing occurs, the star begins by burning out its core, staying close to the main sequence.

Hoyle and Schwarzschild (1955) have followed in detail the subsequent evolution of an unmixed star of mass  $\simeq 1.2 M_{\odot}$ . The star acquires a structure with a partially degenerate, nearly isothermal core, surrounded by a shell energy source in radiative equilibrium, a radiative envelope, and an outer convective zone; it evolves further by increase in the mass of the burnt-out core following exhaustion of the shell hydrogen. With certain assumptions about the efficiency of convection in the outer zone, the authors are able to obtain a Hertzsprung-Russell diagram very similar to that for the globular clusters, including the highly overluminous red giants. For the present study, it is necessary again to emphasize that if non-turbulent mixing, though by hypothesis forbidden in the main-sequence stage, were to start up at any epoch in the shell-source stage of evolution, the subsequent tracks would be radically altered, since the continual increase in the mass of the burnt-out core would cease. The evolution of more massive stars has not yet been studied in such detail, but again one can be sure that the presence or absence of mixing is crucial.

We now study in detail the conditions for our thermally-driven meridian circulation to be effective in mixing matter across radiatively stable zones. This is equivalent to asking that the perturbing centrifugal and magnetic forces play an important role in stellar evolution, so that a track in the Hertzsprung-Russell diagram depends not only on the star's mass and initial composition, but also on its angular momentum or its magnetic field. But the remarkable feature of the diagrams of both globular and galactic clusters that have been published in the last decade (e.g., Sandage 1958) is the comparative absence of smear, as compared with the classical diagrams (e.g., Eddington 1926), where the giants form a blot to the right of the main sequence. The most plausible conclusion is that stars of a cluster, which can be presumed to have a common age and the same initial composition, can be described, as a good zero-order approximation, in terms of one parameter, namely the mass. This is consistent with mixing being negligible, as indeed is assumed in current evolutionary computations. However, should the theory predict mixing to occur for a plausible parameter range, e.g., for angular velocities as observed in main sequence stars of type earlier than  $F$ , then one would have a hint that the apparent extra degrees of freedom in the evolutionary problem are, in fact, closely enough correlated with the mass, so that we can still obtain fairly precise evolutionary tracks for a cluster.

Suppose now that the theory of circulation as developed so far required no essential amendment. For definiteness, consider the radiative envelope of a

Cowling model star, kept in nearly uniform rotation by a magnetic field, so that the circulation streamlines are as in Figure 1*a*. We may define a time  $\bar{t}(r, \theta)$  for matter streaming out of the core to reach the point  $(r, \theta)$  along the relevant streamline. At time  $t > \bar{t}$ ,  $\mu(r, \theta)$  will have the value  $\mu_c$  of  $\mu$  in the core at the earlier time  $[t - \bar{t}(r, \theta)]$ ; at time  $t < \bar{t}$ ,  $\mu(r, \theta)$  will retain the initial value  $\mu_c$  (presumed uniform over the star). An analogous but more complicated statement can be made if a significant increase in  $\mu$  occurs within the radiative zone. The star stays effectively "homogeneous" if the circulation is able to keep the spatial variations in  $\mu$  below the level at which they sensibly affect the structure.

The time of travel from core to surface is (Sweet 1950*b*)

$$1.6 \times 10^8 \frac{(\bar{M}^2/\bar{L}\bar{R})}{(\Omega^2 R^3/GM)} \text{ years,} \quad (5.1)$$

where barred quantities are expressed in solar units. As the currents are slower deep in the star than near the surface, this time is essentially the time for any noticeable partial mixing to have occurred. With  $\Omega_\odot = 2.85 \times 10^{-6}$ ,  $(\Omega^2 R^3/GM)_\odot \simeq 2 \times 10^{-5}$ , yielding a travel time for the sun of  $8 \times 10^{12}$  years—much longer than the time of solar evolution, so that rotational mixing can certainly be ignored for the sun. But if  $\Omega^2 R^3/GM$  is stepped up to  $\frac{1}{10}$  (thus approaching the limit allowed by rotational instability at the surface), the travel time (5.1) becomes  $1.6 \times 10^9 (\bar{M}^2/\bar{L}\bar{R})$  years. The Bethe cycle liberates  $6 \times 10^{18}$  ergs per gram of hydrogen consumed (Schwarzschild 1958), so that during one circulation time a fraction  $[2 \times (1.6 \times 10^9)(3.2 \times 10^7) \bar{M}^2/\bar{L}\bar{R}]/6 \times 10^{18} (\bar{M}/\bar{L}) = 1.7 \times 10^{-2} \bar{M}/\bar{R}$  would be converted into helium: since  $\bar{M}/\bar{R}$  varies slowly with  $\bar{M}$  (roughly as  $\bar{M}^{0.3}$ ), the fraction converted is at most about 5 per cent. If, for example, the initial helium content of the star were 10 per cent,  $\mu_c$  would increase from 0.53 to 0.55: the consequent 2 per cent radial variation in  $\mu$  would change the model only slightly from the strictly homogeneous. Thus the present naïve application of the theory predicts near homogeneity during the evolution of a rapidly rotating O or B star, and perhaps substantial mixing in Type A.

However, these conclusions are premature; for it has been assumed in the theory of §§ 2 and 3 that the region considered is chemically homogeneous, whereas in fact the  $\mu$ -field set up by Sweet's circulation is necessarily inhomogeneous, and in particular non-spherical. Just as the non-radial perturbation  $\Omega^2 r/g$  generates " $\Omega$ -current" velocities  $v^\Omega$  of order  $(L/Mg)(\Omega^2 r/g)$ , so we may expect the temperature variations over a sphere resulting from horizontal  $\mu$ -variations  $\Delta\mu/\mu$  to generate " $\mu$ -current" velocities  $v^\mu$  of order  $(L/Mg)(\Delta\mu/\mu)$ . We have seen that Sweet's circulation acting alone would set up horizontal  $\mu$ -variations  $\Delta\mu/\mu \simeq 0.008/(\Omega^2 R^3/GM)$  deep in the star. In a Cowling-model star, the mean density decreases by a factor 30 between the core and the surface (Gardiner 1951), so that deep in the star  $(\Omega^2 r/g) \simeq (1/30)(\Omega^2 R^3/GM)$ ; hence

the  $\mu$ -current and  $\Omega$ -current velocities are roughly comparable when  $\Omega^2 R^3 / GM \simeq \frac{1}{2}$ , with the star on the verge of rotational disruption.

This rough estimate for the critical angular velocity is so high that we are forced to study the  $\mu$ -current field in detail, not only to get a better estimate for the critical parameter, but also to determine the *sign* of the  $\mu$ -currents. If Sweet's circulation tends to set up a  $\mu$ -current field that opposes the driving circulation, then our estimate suggests that the chance of mixing is much reduced: matter from the core, with a slightly higher helium content, is unable to flow into the envelope. On the other hand, if the  $\mu$ -currents enhance the  $\Omega$ -currents, then, with rotation less than the critical value, the  $\mu$ -current velocities would dominate: the asymptotic state would be a *self-maintained* circulation, almost independent of the rotational perturbation, in which nuclear synthesis in the core and the  $\mu$ -current velocity field together preserve the  $\mu$ -field required to drive the circulation. If such a parameter-independent circulation were to arise it would be of particular interest for stellar evolution, in that it would not lead to blurring of tracks in the Hertzsprung-Russell diagram.

### § 6. CONDITIONS FOR STEADY MIXING

The derivation of the  $\mu$ -current field follows closely the theory of § 3. Given a non-spherical  $\mu$ -field  $\mu(r, \theta)$ , we introduce a parameter  $\lambda(r, \theta)$  defined by

$$\frac{\mu(r, \theta) - \mu_0(r)}{\mu_0(r)} = \lambda(r, \theta). \quad (6.1)$$

Here  $\mu_0(r)$  can be the average of  $\mu(r, \theta)$  over the sphere  $r$ ; or the average over the zone considered, and so independent of  $r$ ; or the original spherical  $\mu$ -field, before the  $\Omega$ -current distortion. The only condition imposed is that  $\lambda$  be small, so that first-order perturbation theory can be applied to a spherically symmetrical zero-order state: the effects of the perturbing force and the  $\lambda$ -field may then be superposed. The perturbations  $\rho_1$ ,  $\phi_1$ , and  $p_1$  are all spherically symmetrical, while

$$T_1(r, \theta) = \lambda(r, \theta)T_0(r) + \bar{T}(r) \quad (6.2)$$

to the first order in  $\lambda$ . If

$$\int_0^\pi \lambda(r, \theta) \sin \theta d\theta = 0, \quad (6.3)$$

it is readily seen that there is no first-order change in the mean physical quantities, but otherwise  $\phi_1$ ,  $p_1$ ,  $\rho_1$ , and  $\bar{T}$  adjust themselves to yield radiative equilibrium in the mean. Again, the local breakdown in radiative equilibrium generates a circulation field.

We now assume that  $\lambda$  has equatorial symmetry, and write

$$\lambda(r, \theta) = a_0(r) + a_2(r)P_2(\cos \theta) + a_4(r)P_4(\cos \theta) + \dots \quad (6.4)$$

For convenience, we take for  $\mu_0$  the mean of  $\mu$  over the whole radiative zone; all the radial variation of the  $\theta$ -average of  $\mu(r, \theta)$  is absorbed into  $a_0(r)$ . The energy equation (3.4) then yields for the vertical component  $v_r$  of the  $\mu$ -current velocity

$$v_r^\mu = K_2(r)P_2 + K_4(r)P_4 + \dots, \quad (6.5)$$

where

$$\begin{aligned} & \rho g \left( \frac{n-3}{n+1} \right) K_{2n}(r) \left( \frac{4\pi r^2}{L} \right) = \left( -\frac{T}{T'} \right) \left( \frac{L_r}{L} \right) a_{2n}'' \\ & - \left\{ \frac{L_r}{L} \left[ 1 + T \frac{\partial}{\partial T} \log \left( \frac{T^3}{\kappa \rho} \right) + \frac{4}{5(1+X_0)\mu_0} \right] - \left( -\frac{T}{T'} \frac{L_r}{L} \right)' \right\} a_{2n}' \\ & + \left[ \left( \frac{L_r}{L} \right)' \left\{ \left( \gamma - \frac{4}{5\mu_0 X_0} \right) - \left[ 1 + T \frac{\partial}{\partial T} \log \left( \frac{T^3}{\kappa \rho} \right) \right. \right. \right. \right. \\ & \left. \left. \left. + \frac{4}{5(1+X_0)\mu_0} \right\} \right\} - \left[ -\frac{2n(2n+1)T}{r^2 T'} \right] \right] a_{2n}. \end{aligned} \quad (6.6)$$

We have assumed here a Bethe-cycle type of law:  $\epsilon = \alpha \rho T^\gamma$ , with  $\gamma$  constant, and  $\alpha$  proportional to  $X$ , the fraction by weight of hydrogen.  $\mu$  is given by  $4/(3+5X-Z)$ ,  $Z$  being the fraction of heavy elements (effectively constant). The factor  $(1+X)$  in the opacity coefficient is included. In the envelope of a Cowling-type star,  $L_r/L = 1$ ; in a shell-source model, energy generation occurs in the radiative zone, but only in a shell so narrow that within it  $\rho$ ,  $T$ , and  $r$  are nearly constant. In both cases (6.5) simplifies (Mestel 1953, 1954, 1957). The computation of the velocity field with neglect of the time derivatives, in spite of the steady changes in the star's structure through nuclear transmutations, is again fully justified in a first-order theory.

Before estimating the effect of  $\mu$ -currents on the mixing problem, we digress and see how sharp the variation in  $\lambda$  has to be before the whole basis of the theory is invalid, i.e., before the  $\mu$ -current speeds are comparable with the free-fall speed. If  $l$  is the scale of radial variation of  $\lambda$ , and  $l/r$  is so much less than unity that the  $a_{2n}''$  term in (6.5) dominates, then  $v_r^\mu \simeq (L/Mg)(r/l)^2 a_{2n}$  and  $v_\theta^\mu \simeq (L/Mg)(r/l)^3 a_{2n}$ . As an example, consider a star with two zones with their respective values of  $\mu$  differing by about unity, separated by a sharp transition layer. If the layer is distorted markedly from the spherical, so that  $a_2 \simeq 1$ , then the  $\mu$ -current speeds reach  $\simeq (L/Mg)(r/l)^3$ . For the sun this is of the order of the free-fall speed when  $l/r \simeq 2 \times 10^{-4}$ , or  $l \simeq 6 \times 10^6$ . Thus, with such sharp radial variations in  $\mu$ , one cannot discuss even moderate distortions of the spherical  $\mu$ -field in terms of hydrostatic equilibrium,  $\theta$ -variations in  $T$ , and slow  $\mu$ -currents; rather one has to think in terms of a near discontinuity in  $\mu$ , continuity in  $T$ , and dynamical oscillations about the spherically symmetrical state.

A *very slight* non-spherical distortion of a  $\mu$ -barrier can be described in terms of  $\mu$ -currents; and in fact in a rotating star, such a barrier must generate within

it just the  $\mu$ -current field that cancels out the  $\Omega$ -current field, so that the distortion is brought to a halt. Just outside the barrier region there will be no  $\mu$ -currents to interfere with the  $\Omega$ -currents, and the flow near the barrier is as described by the boundary layer theory of § 3.

We now return to the evolution of the uniformly rotating Cowling-model star. At any instant the total velocity field is  $\mathbf{v} = \mathbf{v}^a + \mathbf{v}^\mu$ ; the rate of change of  $\mu$  at a fixed point is given by

$$\frac{\partial \mu}{\partial t} + \mathbf{v} \cdot \nabla \mu = \left( \frac{d\mu}{dt} \right)_{\text{nuclear processes}}. \quad (6.7)$$

At this point the theory becomes non-linear, for the changes in  $\mu$  at a point are a result of the transport of spatial variations in  $\mu$  by velocities that depend in part on these instantaneous spatial variations. The mean of equation (6.7) over a sphere yields

$$\mu_0 \dot{a}_0 + \sum_{s=1}^{\infty} \frac{(\rho r^2 \mu_0 a_{2s} f_{2s})'}{\rho r^2 (4s+1)} = \frac{5}{4} \frac{\mu_0^2 a \rho T \gamma}{6 \times 10^{18}}, \quad (6.8)$$

where we have written

$$v_r = f_2(r)P_2 + f_4(r)P_4 + \dots, \quad (6.9)$$

and used the equation of continuity for  $v_\theta$ . The equations for the variation of  $a_2$ ,  $a_4$ , etc. are much more complicated. However, a good deal of information can be gained from equation (6.8), provided only the first term in the series is retained. This is a plausible first approximation when the driving velocity is Sweet's function  $p(r)P_2$  (cf. [3.13]). In the radiative envelope of a Cowling-type star, (6.8) reduces to

$$\dot{a}_0 + \frac{\{\rho r^2 a_2 [p(r) + K_2(r)]\}'}{5\rho r^2} = 0, \quad (6.10)$$

with

$$K_2(r) = a_2 a_2'' + \beta_2 a_2' + \gamma_2 a_2 \quad (6.11)$$

as defined in (6.6).

We now look for a "quasi-static" solution, in which  $a_0$  increases uniformly with time throughout a sphere of mass  $M'$ , so that  $\dot{a}_0 \propto L/M'$ . From (6.10) we deduce the equation of mixing

$$\rho r^2 a_2 (a_2 a_2'' + \beta_2 a_2' + \gamma_2 a_2 + p) = \frac{5}{4\pi} \dot{a}_0 [M' - M(r)]. \quad (6.12)$$

This is simply the integral of (6.7) (with zero right-hand side) over the mass  $[M' - M(r)]$ : the net transport of  $\mu$  across the sphere  $r$  is sufficient to increase the mean of  $\mu$  over the zone  $[M' - M(r)]$  at the rate  $\mu_0 \dot{a}_0$ . As boundary conditions we have that  $a_2$  must vanish at the surface of the core and at the edge of the zone; for at both radii the horizontal velocities become large compared with the vertical.

For details of the solutions of equation (6.12) for a star with Kramers opacity,



and a discussion of the correct interpretations of the results, the reader is referred to Mestel (1953). The principal conclusions are as follows:

(1) Near the core, the  $\mu$ -current velocities always oppose the driving  $\Omega$ -currents so that a self-maintained circulation, without a driving mechanical perturbation, is not possible. This disposes of the possibility of parameter-independent mixing.

(2) If the  $\Omega$ -currents are just able to overcome the  $\mu$ -current choke at the core surface  $r_c$ , the parameter  $q(r_c) = \Omega^2 r_c^3 / GM(r_c)$  must exceed the critical value  $q' \simeq 1/30$ . Since the mean density increases by a factor 30 between the surface and the core of a Cowling-model star, the centrifugal force at the surface of a *uniformly* rotating star would then cancel one component of gravity. The rough estimate of § 5 is thus confirmed.

(3) A very slight increase in  $q$  (by a factor 1.2) would enable the whole star to be mixed. Although near the core the  $\mu$ -currents oppose the  $\Omega$ -currents, over most of the envelope they actually enhance the circulation: once the choke near the core is overcome by a large enough rotation, the distribution of  $\mu$  set up by the circulation yields a positive  $v_{r,\mu}$ . This feature is partly responsible for the remarkable sensitivity of the mass of the mixing zone to slight increases in  $q$  above  $q'$ .

(4) If the parameter  $q$  is between  $q'$  and  $1.2q'$ , it is probable, though not rigorously proved, that about one quarter of the star will be continuously mixed. If the star has a fairly deep subphotospheric convection zone, the currents should be able to flow across the intervening radiative zone, even if  $q$  is a little less than  $1.2q'$ , so that again the star would be fully mixed.

It should be emphasized that with  $q$  below  $q'$ , what the theory shows is that there can be no continuous flow of matter between core and envelope: a  $\mu$ -barrier is built up at the core surface. Away from the core, however, the Eddington-Sweet circulation continues, as there are no  $\mu$ -variations to interfere.<sup>3</sup> At the core surface, the currents are again deflected horizontally in a thin boundary layer. The possible shearing instability mentioned in § 3 is unlikely to upset the sharp separation of core and envelope, for the shear is violent near the edge of the boundary layer but not at the interface, where it is in fact zero.

Similar methods have been applied (Mestel 1957) to shell-source stars. Again, it was found that the system cannot set up a self-maintained circulation, effectively independent of any centrifugal or magnetic perturbation: with  $a_2 > 0$  ( $\mu$  greater at the poles than at the equator), it is impossible to find a solution with  $v_{r,\mu}$  non-negative at all points along the polar axis, as would be required. One can again estimate the angular velocity required to maintain a finite mixing zone: it is found that, if anything, the conditions are more stringent than in a

<sup>3</sup> In a star with an appreciable initial helium content, the  $\mu$ -gradient associated with gravitational stratification of the elements could interfere with the  $\Omega$ -currents even away from the core surface. However, the time of diffusion from an initially homogeneous distribution is so much longer than the age of the star (Eddington 1926) that the effect can be ignored.

Cowling-model star. Incidentally, it is also shown that the perturbing effect of one component of a binary on the other will never be strong enough to cause mixing, except possibly in circumstances when other evolutionary processes, such as exchange of mass, are likely to swamp it.

With these results for the uniformly rotating star, we may lay down conditions for rotational mixing to be possible in a realistic model. Clearly, the star must rotate much more rapidly inside than at the surface, otherwise the ratio at the core of centrifugal to gravitational force could not exceed  $1/30$ , without implying rotational instability at the surface. Uniform rotation of the mixing zone demands a weak magnetic field to offset the convection of angular momentum by the currents; but the field must be kept well within the star, otherwise it will equalize the angular velocities of the inner and outer parts, so allowing the  $\mu$ -current choke to suppress the mixing. A circulation as in Figure 1, *a*, will inevitably drag the field through the whole star. If the angular velocity in the subphotospheric convection zone were to increase sharply with depth (cf. § 8), a low surface rotation could be consistent with a sufficiently high inner rotation, thus allowing complete mixing by the circulation of Figure 1, *b*. Also, if the star already has a  $\mu$ -barrier in its radiative zone, so that currents leaving the core are prevented from reaching the surface, and if the angular velocity within the  $\mu$ -barrier is sufficiently high, and kept uniform by a magnetic field that is confined by the circulation to lie within the  $\mu$ -barrier, then continuous mixing of the inner part of the star can take place. But it is difficult to see why such a state should be achieved: any  $\mu$ -barrier set up in the star is likely to arise at the core surface, and stop all non-turbulent mixing.

The other steady circulation field discussed in § 4 does not lead to the same sort of difficulty. With  $H_\phi = \gamma\rho\omega$ , the ratio of the magnetic to the gravitational force density decreases to zero at the surface, so that a high perturbing parameter at the core does not imply impossibly large forces at the surface. However, the conditions for this steady state to occur are so implausible that it is hardly a serious possibility.

If a non-magnetic, rapidly rotating star were to develop a non-vanishing circulation field, with  $\Omega\omega^2$  constant on streamlines that leave the core near the equator and enter it near the pole, then mixing may be possible; for there is now no magnetic constraint on the rotation field, and a low surface rotation is not inconsistent with a high interior rotation. Since the driving circulation does not have a simple  $P_2$  form, the  $\mu$ -current theory for this case is likely to be much more complicated; and there is always the strong possibility that without a constraining magnetic field, the star steadily adjusts its rotation field to approach radiative equilibrium and zero circulation.

As already noted, the evidence to date from stellar evolution is consistent with the hypothesis of zero mixing. The approximate  $\mu$ -current theory strongly supports this hypothesis, in that it shows how stringent are the conditions under which mixing can occur. Further refinements of the theory are likely to make

the conditions even more stringent: for example, in the uniform rotation case, the  $\mu$ -current terms in  $P_4$ ,  $P_6$ , etc., all tend to choke the circulation near the core. If evolutionary studies continue to be consistent with zero mixing, no further work is likely to be called for. But if the evidence should point to non-turbulent mixing at some stage, then the conditions on the  $\Omega$  and  $H$  fields found so far should be regarded as the best possible, and likely to become more stringent if a more accurate treatment is attempted.

### § 7. OTHER THEORETICAL CONSEQUENCES OF MERIDIAN CIRCULATION

With mixing of matter much less probable than was once thought, interest in meridian circulation has declined. However, there are other theoretical predictions that may be observationally relevant. We have noted that any observational evidence that during their evolution stars retain nearly uniform rotation is easily reconciled with conservation of angular momentum, simply by the introduction of a weak poloidal magnetic field throughout the bulk of the star. Equally, contrary evidence would be a powerful argument against such a field. If the star rotates slowly, so that the meridian circulation is too slow to alter the angular momentum field during the star's lifetime, then each mass shell in the radiative layers of a non-magnetic star would conserve its angular momentum as the star evolves; but in a rapidly rotating star the rotation field would be determined by the circulation as well as by radial expansion or contraction through stellar evolution.

Proto-stars forming out of magnetic gas clouds may be expected to retain at least part if not all of the primeval magnetic flux (Mestel and Spitzer 1956; Mestel 1963). However, the Hayashi phase of total convection through which stars pass en route to the main sequence (1961) introduces a further uncertainty. It is possible that the initial field may be tangled up and rapidly destroyed by ohmic dissipation (Sweet 1950*a*). Alternatively a turbulent dynamo may operate, maintaining a field with some energy in large-scale components, though with the bulk concentrated in the loops of the same size as the mean eddy size. Again, it has been argued (Spitzer 1957) that even if dynamo regeneration does not occur, the turbulence does not destroy the magnetic flux, but rather keeps it compressed near the axis and below the surface; with subsequent decay of the turbulence, the field lines would leak back fairly rapidly so as to thread the bulk of the star. With the theoretical position so uncertain, it would be useful to have from observation any hints as to whether stars do in fact have large-scale internal fields.

Abt (1957) has claimed that the surface rotations of a random sample of ten A- and F-type giants are consistent with evolution from main sequence B-stars, provided the giants do *not* rotate as rigid bodies: reasonable agreement is obtained if each shell is assumed to retain its initial angular momentum. However, Abt's conclusions are based on the Sandage-Schwarzschild evolutionary tracks

(1952), which assume radiative equilibrium in the envelope. The effect of convection on the rotation field is uncertain: it is possible that agreement with observation can be reached by accepting that the radiative zones are magnetically constrained to rotate uniformly, while the non-isotropic subphotospheric convection maintains a rotation that increases sharply inward (cf. § 8). If Abt's stars have evolved along tracks in the Hertzsprung-Russell diagram that slope more than the Sandage-Schwarzschild tracks, then the main-sequence stars from which they have evolved will be less massive and so of presumably lower rotation than the O and B stars. Again, an increase in the moment of inertia, due to a change in the model adopted, could yield the result that uniform rotation is, after all, not inconsistent with observation. However, if further research confirms that Abt's giants do rotate non-uniformly, we have two possibilities: either (1) the whole of the anomaly in the surface rotation can be explained by a reasonable postulate about the effect of the convection on the rotation field, with the rotation field of the inner, radiative regions not relevant; or (2) there is no marked non-uniformity of rotation in the convective zone, but in the radiative zone meridian circulation builds up a non-uniform rotation field, which absorbs some angular momentum from the convective zone. We have already noted (§ 4) how formidable is the problem of computing the evolving rotation field when the convection of angular momentum is by a circulation that itself depends on the rotation field; we now see that this unsolved problem may have to be faced.

Consider now the circulation in a radiative zone near the surface of an early-type star. If the angular velocity is non-uniform, the Baker-Kippenhahn formula (2.18) is applicable and can yield remarkably high speeds, up to  $10^3$  cm/sec or more. Although, through the bulk of the star, a very weak field  $H_p$  is able to offset the convection of angular momentum by the circulation, keeping the parameter (4.7) much smaller than unity, near the surface a moderate field, of order one gauss, may be unable to prevent a noticeable departure from uniform rotation (as is required for formula [2.18] to be relevant). What is remarkable is that the coupling between  $H_p$ ,  $\Omega$ , and the circulation, as summarized in (4.5) can lead to an *increase* in  $\Omega$  with distance from the axis (Mestel 1961). For example, suppose the streamlines near the surface are as in Figure 1, *a*, as is the case if the main variation of  $\Omega$  is radial rather than horizontal. Along a horizontal streamline  $\rho$  is nearly constant, so that by (4.5)  $\Omega$  varies only because of  $\varpi$ . If the flow is everywhere sub-Alfvén ( $4\pi\eta^2/\rho \ll 1$ ), but with  $H_p$  such that in the low density surface regions  $4\pi\eta^2/\rho$  is comparable with unity, then (4.5) predicts equatorial *acceleration* as long as  $\eta\beta/\alpha < 0$ . This will be the case, for example, if the toroidal field is merely a consequence of the non-uniform rotation generated by the circulation, so that the field lines are closed in space. But the same result holds for a whole class of fields.

In his model of the solar cycle, Babcock (1961) uses the energy stored in the equatorial acceleration to generate from the poloidal field a toroidal field which

subsequently annihilates and reverses the initial poloidal field. Some mechanism must be invoked to maintain the equatorial acceleration, and a picture that appeals to meridian circulation is attractive, in that the energy supply of the circulation comes from the nuclear sources, which last as long as the star lasts. However, even if the theory summarized in equations (4.1), (4.2), (4.3), and (4.4) could be generalized so as to yield both magnetic variability and constant equatorial acceleration, it could not in fact be applied unmodified to the sun. Implicit in the theory is the neglect of the toroidal viscous force, legitimate in a radiative zone, but dubious in the subphotospheric convection zone, where eddy viscosity is likely to be dominant. But the results for radiative zones do strongly encourage study of laminar circulation in convective zones.

The steady state condition (4.1) deserves some comment. If the centrifugal energy of the star is much greater than the magnetic, the circulation will be rotationally driven. A poloidal field able to maintain approximate uniformity of rotation will necessarily have more energy than the *circulation* (see eq. [4.10]) but the "inexorable" circulation will proceed notwithstanding, carrying the magnetic field with it. For example, if the magnetic field has a dipole structure, the quadrupole circulation will not satisfy equation (4.1), and the field will be progressively distorted. Provided the local magnetic force does not become comparable with the centrifugal force, so altering the circulation field, we may expect the distortion of the surface field to continue until local ohmic diffusion is able to separate the internal and external parts of the field. The external field, no longer anchored in the stellar surface, could be blown away by a stellar wind, and the star left with just an internal field satisfying (4.1). The conclusion is that the absence of an *external* field is *not* a conclusive argument for the *internal* field being negligible. Thus if the star is born with a field that it retains in spite of the Hayashi convection phase, subphotospheric circulation may prevent all but a few field lines from leaking out to the surface.

The argument applies equally to a laminar circulation superimposed on the small-scale turbulence in a surface convective zone. It is perhaps significant that the *external* general magnetic field of the sun appears confined to the polar regions, where we have no evidence for large-scale circulation, whereas in the sunspot latitudes the magnetic fields observed are local. The suggested explanation is that the large-scale poloidal field in the sunspot latitudes is kept beneath the surface by circulation. Theory must then account for the postulated circulation and its special structure: once again we are led to a study of circulation in convective zones.

## § 8. MERIDIAN CIRCULATION IN CONVECTIVE ENVELOPES

In this final section, we summarize the pioneer work in this field, due to Biermann (1951, 1958) and Kippenhahn (1959, 1960, 1963). The discussion is limited to two extreme cases: (1) zones of efficient convection, in which the convective energy transport keeps the temperature-density relation closely adia-

batic; and (2) zones of inefficient convection, in which the turbulent energy transport is negligible, so that radiative equilibrium under superadiabatic temperature gradients is the correct zero-order approximation. On the main sequence the subphotospheric convection zone goes over from case (1) to case (2) near spectral type A5.

(1) In convective regions fairly deep within the star, even the crudest estimates of the energy transport show that not more than the slightest deviation from adiabacy is allowed. In such a zone it is not possible, as in a radiative zone, to prescribe arbitrary perturbing fields to which the thermal field adjusts itself—the efficient convection deprives the star of its extra degree of freedom. Thus in hydrostatic equilibrium, with no meridian circulation, the perturbing centrifugal and magnetic fields must satisfy the constraint (1.5) (assuming that the Reynolds stresses of the turbulence are negligible). In particular, a non-magnetic star must have its rotation law of the form  $\Omega(\varpi)$ . But the actual form of the rotation field is determined by the toroidal forces acting; if  $\mathbf{H} = 0$  and if there is no meridian circulation, the only remaining force is the toroidal component of friction. The turbulent “mean free path,” the mixing length  $l$ , is usually taken of the order of the scale height, which is far greater than the mean free path of a photon or an ion. Thus, whereas in a radiative zone the viscous force is negligible except for enormous velocity gradients, in a turbulent zone the force due to eddy viscosity can quickly alter the rotation field.

If the turbulence is assumed isotropic, then the condition of zero torque implies uniform rotation over the whole zone; and this also satisfies the constraint  $\Omega = \Omega(\varpi)$ , required by the condition of poloidal equilibrium. However, Biermann (1951) has pointed out that the gravitational field which drives the convection implies a preferred direction, and so a degree of anisotropy in the turbulent field. He considers a simple model, with a monotropic velocity distribution superimposed on an isotropic distribution, with the magnitude (and indeed the sign) of the anisotropy left as a parameter, constant over the zone. Thus with  $v_t$  a typical turbulent velocity, Biermann adopts an eddy viscosity  $\rho l v_t$  in the vertical direction, and  $s \rho l v_t$  in the two horizontal directions. An initially uniform rotation field would be altered by transport of angular momentum across spherical shells, until a steady state is reached with the law

$$\Omega = \Omega_0 \left( \frac{r}{R} \right)^{-2(1-s)}. \quad (8.1)$$

Thus if  $s \neq 1$ , the radially dependent law (8.1) is inconsistent with poloidal equilibrium under the adiabatic  $p - \rho$  relation. The non-potential centrifugal field, forced on the star by the non-isotropic turbulence, sets up a large-scale circulation; in a steady state, the work done by the centrifugal field is dissipated by the turbulent viscous drag on the circulation. With  $0 < s < 1$ —greater vertical than horizontal turbulent motions—the circulation rises at the equator and sinks at the pole; with  $s > 1$ , the circulation is reversed.

Biermann (1958) and Kippenhahn (1960) show in detail that the actual slight departures from adiabacy do not alter these conclusions. It should be noted that in contrast to the von Zeipel–Eddington case, it is the necessity to conserve *momentum*, rather than energy, that drives the circulation.

For slow enough rotation, the convection of angular momentum by the circulation can be treated as a perturbation, which adds a non-spherical part to the zero-order rotation field (8.1). Kippenhahn (1963) shows that a poleward surface circulation ( $0 < s < 1$ ) yields equatorial deceleration, while the opposite circulation ( $s > 1$ ) yields equatorial acceleration. He finds that even in a slowly rotating star like the sun, the correction to the zero-order expression (8.1) is not small if  $s = 1.5$ : the turbulent viscosity is not high enough to keep small the Coriolis distortion of the  $\Omega$ -field. However, it is possible that a small anisotropy ( $|1 - s| \ll 1$ ) will be sufficient to yield circulation speeds and equatorial acceleration of the correct orders of magnitude.

The Biermann-Kippenhahn assumptions are reasonable in the limit of zero rotation, for which the back reaction of the rotation on the turbulence may be ignored. In the sun, however, the rotation is high enough to reduce the efficiency of convection with increasing latitude (Chandrasekhar 1961). Even if the consequent departures from adiabacy are still small, doubt is cast on the assumption that the dynamical properties of the turbulence are spherically symmetrical. In the same phenomenological spirit, it would be worthwhile exploring the consequences of a latitude-dependent parameter  $s$ .<sup>4</sup>

Further complications are introduced by a large-scale magnetic field. A magnetic torque generated by non-uniform rotation may assist the turbulent friction and the Coriolis force in determining the rotation field. Also, the poloidal magnetic force could be, at least locally, comparable with the centrifugal force, and so could help fix the circulation.

Some postulate must be made concerning the interaction of the turbulence and the magnetic field. If the Batchelor criterion (1950) is accepted, there should be no spontaneous build-up of even a small-scale field, and any large-scale field would be confined to the edge of the zone, and would have to be re-generated externally (e.g., Babcock 1961). A different view is urged by Malkus (1959), who admittedly bypasses the dynamo problem, but suggests that a spontaneous small-scale field does arise, and reaches the level required to maximize the efficiency of convection, by canceling out or minimizing the constraints that inhibit the convection. Among these constraints are the non-linear inertial terms in the equations of motion—just the terms which in a turbulent field are parameterized into the form of the Reynolds pressure and the eddy viscous force. Thus if Malkus' argument is correct, the basis of the Biermann-Kippenhahn theory is altered.

Clearly, we are still feeling our way in this field. The problems are challenging: to explain the solar cycle, the apparently steady equatorial acceleration,

<sup>4</sup> I owe this suggestion to Drs. E. A. Spiegel and W. V. R. Malkus.

and the laminar circulation suggested by sunspot motions (Tuominen 1954). One can conjecture that a laminar flow superimposed on the small-scale turbulence will be an essential feature of future theory. And since a deductive theory of turbulence convection is still a long way off, the Biermann-Kippenhahn phenomenological approach is inevitable.

Amid all the uncertainties and conceptual difficulties of any theory of turbulence, there is one clear advantage of principle. In studying the interaction of the circulation with the magnetic and rotation fields in a radiative zone, we were restricted to steady states mainly because of the difficulty of finding time-dependent solutions. But since the viscous and ohmic dissipation times are so long, there is no strong physical reason for expecting the system to settle down into a steady or slowly varying state: the steady solutions are best looked on as mean states about which the system actually oscillates. By contrast, in a turbulent zone the characteristic dissipation time is of the order of the eddy lifetime, which is much shorter than the period of the solar cycle, so that we may expect the system to evolve through statistically steady states.

(2) In the outer layers of B-stars and the hotter giants and supergiants, the hydrogen convection zone is very shallow and hardly affects the energy transport (Böhm-Vitense 1958). The convective velocities are of the order of 10 or 100 cm/sec, instead of the kilometer/sec estimated for the solar convection zone. As pointed out by Kippenhahn (1959), the perturbation theory as developed for radiative zones may be applied to these zones of weak convection, even though the zero-order state is not one of rest. An arbitrary centrifugal field requires a non-adiabatic temperature density field to balance it, but as the convection is so inefficient, any slight modification to the convection field will not sensibly affect the thermal field, which will, therefore, generate an Eddington-type circulation in order to conserve energy. Since the zero-order temperature-gradient is superadiabatic, the velocity field, e.g., in a uniformly rotating zone, would be down at the pole and up at the equator.

At the edge of the narrow convective zone the temperature gradient approaches the adiabatic value (cf. eq. [3.9]), yielding large circulation speeds; as discussed earlier in § 3, it is the friction acting on the circulation that keeps the velocities finite. The eddy viscosity of the weak thermal turbulence exerts some drag, but not enough to keep the circulation *dynamically* stable. Kippenhahn, therefore, pictures the circulation as generating its own "proper-turbulence," with velocities of the same order as the circulation itself, and it is the drag of this dynamically generated turbulence that keeps the circulation speed finite. With these assumptions, it is shown that the surface layers of O and B stars, of giants hotter than  $6500^\circ$ , and supergiants hotter than  $5000^\circ$ , all have a dynamical turbulence, with velocities of several km/sec, thus compensating for the weakening of the thermal turbulence. There is, therefore, every reason to expect these stars to have coronas like the sun's, heated presumably by the dissipation of shock waves generated in the turbulent layers; and it is possible that the consequent mass loss from giants may be significant for stellar evolution.



Much of the final draft of this chapter was prepared when the author was visiting lecturer at the School on Geophysical Fluid Dynamics at the Woods Hole Oceanographic Institution, during the summer of 1962. The author wishes to acknowledge stimulating discussions with Drs. M. Stern, E. A. Spiegel, W. V. R. Malkus, G. Veronis, and D. W. Moore. He is also indebted to Dr. R. Kippenhahn for sending him a paper before its publication, and to Mr. I. W. Roxburgh for helpful comments on the manuscript.

## REFERENCES

- |                                     |      |  |
|-------------------------------------|------|--|
| ABT, H. A.                          | 1957 | <i>Ap. J.</i> , <b>126</b> , 503.  |
| BABCOCK, H. W.                      | 1961 | <i>Ap. J.</i> , <b>133</b> , 572.  |
| BAKER, N., and<br>KIPPENHAHN, R.    | 1959 | <i>Zs. f. Ap.</i> , <b>48</b> , 140.   |
| BATCHELOR, G. K.                    | 1950 | <i>Proc. R. Soc. London A</i> , <b>201</b> , 405.  |
| BIERMANN, L.                        | 1950 | <i>Zs. f. Naturforsch.</i> , <b>5a</b> , 65.   |
|                                     | 1951 | <i>Zs. f. Ap.</i> , <b>28</b> , 304.   |
|                                     | 1958 | <i>Electromagnetic Phenomena in Cosmical Physics</i> ,<br>ed. B. LEHNERT (Cambridge: Cambridge Uni-<br>versity Press), p. 248. |
| BÖHM-VITENSE, E.                    | 1958 | <i>Zs. f. Ap.</i> , <b>46</b> , 108.   |
| BONDI, C. M., and<br>BONDI, H.      | 1950 | <i>M.N.</i> , <b>110</b> , 287.  |
|                                     | 1951 | <i>Ibid.</i> , <b>111</b> , 397.   |
| CHANDRASEKHAR, S.                   | 1939 | <i>An Introduction to the Study of Stellar Structure</i><br>(Chicago: University of Chicago Press).                            |
|                                     | 1961 | <i>Hydrodynamic and Hydromagnetic Stability</i> (Ox-<br>ford: Oxford University Press).  |
| CHANDRASEKHAR, S., and<br>FERMI, E. | 1953 | <i>Ap. J.</i> , <b>118</b> , 116.  |
| COWLING, T. G.                      | 1945 | <i>M.N.</i> , <b>105</b> , 166.  |
|                                     | 1953 | "Solar Electrodynamics," in <i>The Sun</i> , ed. G. P.<br>KUIPER (Chicago: University of Chicago<br>Press), chap. 8.           |
| EDDINGTON, A. S.                    | 1925 | <i>Observatory</i> , <b>48</b> , 73.   |
|                                     | 1926 | <i>The Internal Constitution of the Stars</i> (Cambridge:<br>Cambridge University Press).                                      |
|                                     | 1929 | <i>M.N.</i> , <b>90</b> , 54.  |
| FERRARO, V. C. A.                   | 1937 | <i>M.N.</i> , <b>97</b> , 458.   |
|                                     | 1954 | <i>Ap. J.</i> , <b>119</b> , 407.  |
| FESENKOV, V. G.                     | 1954 | <i>Trans. I.A.U., Rome</i> , <b>8</b> (1952), 702.   |
| GARDINER, J. G.                     | 1951 | <i>M.N.</i> , <b>111</b> , 94.   |
| HAYASHI, C.                         | 1961 | <i>Pub. Astr. Soc. Japan</i> , <b>13</b> , 450.  |
| HOYLE, F., and<br>LYTTLETON, R. A.  | 1949 | <i>M.N.</i> , <b>109</b> , 614.  |
| HOYLE, F., and<br>SCHWARZSCHILD, M. | 1955 | <i>Ap. J. Suppl.</i> No. 13.   |

- JEANS, J. H. 1926 *M.N.*, **86**, 328 and 444.
- KIPPENHAHN, R. 1958 *Zs. f. Ap.*, **46**, 26.  
 1959 *Ibid.*, **48**, 203.  
 1960 *Mém. Soc. R. Liège, Ser. 5*, **3**, 249.  
 1963 *Ap. J.*, **137**, 664.
- KIPPENHAHN, R.,  
 TEMESVÁRY, ST., and  
 BIERMANN, L. 1958 *Zs. f. Ap.*, **46**, 257.
- LÜST, R., and  
 SCHLÜTER, A. 1954 *Zs. f. Ap.*, **34**, 263.  
 1955 *Ibid.*, **38**, 190.
- MALKUS, W. V. R. 1959 *Ap. J.*, **130**, 259.
- MESTEL, L. 1953 *M.N.*, **113**, 716.  
 1954 *Ibid.*, **114**, 500 (errata).  
 1956 *Ibid.*, **116**, 324.  
 1957 *Ap. J.*, **126**, 550.  
 1961 *M.N.*, **122**, 473.  
 1964 *Ibid.*, in preparation.
- MESTEL, L., and  
 ROXBURGH, I. W. 1962 *Ap. J.*, **136**, 615.
- MESTEL, L., and  
 SPITZER, L., JR. 1956 *M.N.*, **116**, 503.
- ÖPIK, E. J. 1951 *M.N.*, **111**, 278.
- OSTERBROCK, D. 1953 *Ap. J.*, **118**, 529.
- RANDERS, G. 1941 *Ap. J.*, **94**, 109.
- ROXBURGH, I. W. 1963 *M.N.*, **126**, 67.
- SANDAGE, A. R. 1958 *Stellar Populations*, ed. D. J. K. O'CONNELL (Amsterdam: North Holland Pub. Co.), p. 41.
- SANDAGE, A. R., and  
 SCHWARZSCHILD, M. 1952 *Ap. J.*, **116**, 463.
- SCHWARZSCHILD, M. 1942 *Ap. J.*, **95**, 441.  
 1958 *Structure and Evolution of the Stars* (Princeton: Princeton University Press).
- SPITZER, L. JR. 1957 *Ap. J.*, **125**, 525.
- SWEET, P. A. 1950a *M.N.*, **110**, 69.  
 1950b *Ibid.*, p. 548.
- SWEET, P. A., and  
 ROY, A. E. 1953 *M.N.*, **113**, 701.
- TUOMINEN, J. 1954 *Mém. Soc. R. Liège, Ser. 4*, **14**, 221.
- VOGT, H. 1925 *A.N.*, **223**, 229.  
 1943 *Aufbau und Entwicklung der Sterne* (Leipzig: Akademische Verlagsgesellschaft, Beiker und Erler Kom.-Ges.).
- ZEIPEL, H. VON 1924 *Festschrift f. H. von Seeliger*, p. 144.



## CHAPTER 10

# *Stellar Stability*

P. LEDOUX

*Institut d'Astrophysique de l'Université de Liège*

### § 1. INTRODUCTION

THE aim of this chapter is to summarize the present state of our knowledge concerning the stability of a star considered as a *whole* when it has reached a state of pure hydrostatic equilibrium or is, at least, very close to it.

Incidentally, some attention will be paid to local<sup>1</sup> instabilities such as may arise from superadiabatic gradients of temperature or differential rotation because, although they do not endanger the existence of the star, they lead to readjustments of the equilibrium conditions and may present interesting interactions with instabilities of the first type.

On the other hand, questions of *gravitational instability* related to the condensation of stars from interstellar material will be omitted because, in that case, as opposed to the stability problem considered here, the properties of the general medium outside the contracting mass (which is still very far from any kind of stellar equilibrium) play a predominant role. This is true whether gravitational instability occurs simply under the mutual gravitational attraction of the particles (Jeans) or is initiated or accelerated by other factors, such as radiation pressure (Whipple, Spitzer) or the external material pressure due to turbulence or the expansion of an H II region (Ebert, Bonnor, McCrea).<sup>2</sup>

The study of stellar stability yields criteria which have to be satisfied by all stellar models and fixes the possible ranges of some of their most significant parameters, providing a welcome complement to the usual purely hydrostatic

<sup>1</sup> This term is not used here to imply that, in all cases, the corresponding criteria of stability depend only on local conditions or that they can always be derived from the consideration of a purely local perturbation as in the "parcel method," although this often provides a significant first approximation.

<sup>2</sup> Cf., for instance, the three essays by G. R. Burbidge (1960), F. D. Kahn (1960) and R. Ebert, S. v. Hoerner, and St. Temesváry (1960) in *Die Entstehung von Sternen durch Kondensation diffuser Materie*.

approach. In the long run, it should also reveal the ultimate causes of the different types of instability that give rise to many of the most interesting manifestations in the stellar world (novae and supernovae, pulsating stars, flare stars, etc.) or to some phenomena, such as a continuous loss of mass, which may play an important role in some phases of stellar evolution.

We cannot linger here on the difficult question of the best possible and most embracing definition of stability for a continuous system, but the interested reader may be referred to a previous article by the present author (Ledoux 1958) and to the introduction of the recent book by S. Chandrasekhar (1961b). Here, we shall say that a given state is stable, provided that,  $\epsilon_1$  being an arbitrary small quantity, it is always possible to define another small quantity  $\epsilon_2$  such that any initial perturbation smaller than  $\epsilon_2$  gives rise to natural motions in which all "displacements" (excluding, if necessary, non-palpable co-ordinates such as angular variables) remain smaller than  $\epsilon_1$ .

One should be aware that this definition does not exclude some types of instability (such as metastability or the kind that gives rise to hard self-excited oscillations) that manifest themselves only for finite perturbations in excess of a certain critical value and which might also be significant in the stellar case.

We shall deal here mainly with the stability of configurations in absolute equilibrium, since, for compressible masses, we know very little in any other case. The application of the definition of stability adopted above has taken two forms. In the energy method, a generalized potential (including the effects of thermodynamic or other non-mechanical factors; cf. Ledoux 1958, §§ 9 and 10) must go through an absolute minimum (i.e., minimum with respect to all independent variables) in any stable equilibrium state. In the other method, a small perturbation is applied to the equilibrium configuration, and its further behavior under the natural forces of the system is studied. It is assumed that if the perturbation is small enough, the solutions of the *linearized* equations of motion will approximate closely enough to the actual solutions of the complete non-linear problem to reveal the trend of the motion in a small region around the equilibrium state and thus will permit us to decide whether or not the general definition above is satisfied.

In the stellar case, most of the known results have been established by the small perturbation method and the attempts by L. H. Thomas (1930a) and R. C. Tolman (1939) to base the discussion on the energy method have remained isolated. Anyway, as shown in detail (Ledoux 1958, §§ 11, 12, 13) for the case of purely radial perturbations, the two methods, if worked out completely, are rigorously equivalent at least as far as dynamical stability is concerned. While the Euler equation (first-order condition), which expresses the condition that the energy be stationary, gives the ordinary hydrostatic equation, the discussion of the Jacobi equation (second-order condition), insuring that the energy is a true minimum, can be reduced to that of an eigenvalue problem,

which is exactly the same as the one arrived at by the small-perturbation method. It does not seem either that the local Weierstrass-Legendre conditions could introduce anything significantly new.

Of course, it may seem easier (and sometimes is) to prove that a given configuration is unstable by showing that there is at least one permitted type of perturbation for which the variation of the generalized potential is negative (or that the work of the fictitious external forces needed to bring about the corresponding modification is negative) than to solve completely the equations of small motion. However, the same end is achieved in the small-perturbation method by the variational interpretation of the equations. Nevertheless, in really complicated problems, the physical directness of the energy method may still prove an important advantage.

However, as the emphasis has been put on the energy method in an earlier paper (Ledoux 1958), here we shall adopt the small-perturbation method. In that case, since the equations of motion are linear, we can always represent the time dependence by a factor of the type  $e^{st}$ , where  $s$  may be complex. It is clear that if all the characteristic values  $s$  have negative real parts, the equilibrium state is certainly stable. On the other hand, if at least one of the characteristic values  $s$  has a positive real part, the configuration is certainly unstable.

As shown by Liapounoff (1907), if one or more of the real parts of the characteristic values are rigorously equal to zero, then the situation becomes more complicated, and, in general, the discussion must be pushed one step further to include at least the first non-linear terms before a decision as to the stability can be reached unless the principle of the exchange of stability is applicable.

In a star, the dissipation of energy associated with any kind of motion is very small compared with the gravitational and internal energy and, in a first approximation, we may treat the system as *conservative*. Then only  $s^2$  appears in the equations, and its values are all real. Writing  $s^2 = -\sigma^2$ , the motion will reduce to an oscillation if  $\sigma^2$  is positive (*dynamical stability*) or will give rise to an exponentially increasing displacement if  $\sigma^2$  is negative (*dynamical instability*). The time scale of these motions (period of the oscillation or time needed for an increase in the displacement by a factor  $e$ ) is fixed by the square root of the ratio of the moment of inertia to the potential energy, so that it can be characterized by a time  $\tau_0$ , defined by

$$\tau_0 \simeq \left( \frac{R^3}{GM} \right)^{1/2} = \left( \frac{3}{4\pi G \bar{\rho}} \right)^{1/2}, \quad (1.1)$$

where  $G$  is the Newtonian constant of gravitation,  $M$  the mass,  $R$  the radius, and  $\bar{\rho}$  the mean density of the star.

Let us now take into account the dissipation, in which we include all factors that may affect the entropy of a mass element, i.e., not only the effects of viscosity but also those of all heat exchanges and of heat generation by thermo-

nuclear reactions. Then  $s$  becomes complex, and, assuming dynamical stability, it can be written

$$s = i\sigma - \sigma',$$

where the generalized damping coefficient  $\sigma'$  may either be positive (*vibrational stability*) or negative (*vibrational instability* or *overstability*).

The damping time  $\tau' = 1/\sigma'$  is of the same order as the ratio of the total energy of the oscillation to the rate of dissipation. Neglecting viscosity, as is often permissible in stars, it is *proportional* to the gravitational time scale defined by

$$\tau_G \simeq \frac{GM^2}{RL}, \quad (1.2)$$

where  $L$  is the luminosity of the star.

As  $\tau_G$  is very much larger than  $\tau_0$ , this will also be true, in general, of the damping time  $\tau'$ . In case of dynamical stability, this means that the amplitude of the oscillation will slowly decrease or increase according to the sign of  $\sigma'$ , while, if dynamical instability occurs, it will be much more violent than any form of vibrational instability.

Because of its radiation into space, a star evolves continually, but, normally, its luminosity  $L$  is so small compared with the internal reserves of energy that this change is very slow and can be thought of as a succession of quasi-equilibrium states. If the energy radiated away is liberated by gravitational contraction, the time scale is fixed by equation (1.2), but if its source is a given nuclear reaction, say  $i$ , the characteristic time, which, in general, is even much larger than  $\tau_G$ , is given by

$$(\tau_N)_i = \frac{(E_N)_i}{\bar{L}_i}, \quad (1.3)$$

where  $(E_N)_i$  is the total energy capable of liberation by the considered reaction and  $\bar{L}_i$  is the average luminosity during the corresponding phase of the star's life.

We must verify whether these evolutionary changes always remain very slow. If this is the case, we say that the condition of *secular stability* is verified, while if they tend to accelerate, the star is said to be *secularly unstable*.

Secular stability is thus intimately connected with stellar evolution, and, with the present emphasis on the latter, its study, which lags well behind that of dynamical or vibrational stability, deserves to be much extended. But even in the last two cases, improvements may be necessary if we are to face successfully all the problems raised by stellar evolution. In any case, we shall certainly be led to modify somewhat the way in which we use the corresponding criteria.

Up to now, we had only to decide whether a given static, *isolated* model was stable or not. But from now on, if we discover some kind of instability in a model, we shall have to investigate at which stage in the previous evolution of the star it first appeared and, in the case of a mild instability, at which later

stage it will disappear again, as this information might be essential to assess the real significance of the instability.

More drastic changes in our approach might also be advantageous if we have at our disposal large enough electronic computers; in that respect, attempts have already been made (Cox and Brownlee 1960) to set up the time-dependent equation of stellar structure on these computers in such a way that instabilities, or at least some of them, if present, should manifest themselves automatically. However, the large differences between the time scales of the different instabilities make this a rather complex and difficult problem.

## § 2. GENERAL EQUATIONS AND LOCAL STABILITY

The small-perturbation method rests on the discussion of the linearized equations of motion obtained by taking the first variation with respect to the dependent variables of the general non-linear equations expressing the conservation of mass, momentum, and energy.

Since we have to deal with extended continuous systems, the hydrodynamic approach is convenient, and we may use either the Eulerian representation in which the spatial co-ordinates ( $r; x, y, z$ ) are independent geometrical variables, the velocity field  $v$  being defined as a function of  $r$  and  $t$ , or the Lagrangian representation in which the spatial co-ordinates ( $r; x, y, z$ ) are attached to the particles and are dependent mechanical variables, functions of  $t$  and parameters characterizing the particle considered—for instance, the initial values ( $r_0; x_0, y_0, z_0$ ) of its co-ordinates.

In the first case, the variations denoted by a *prime* are taken locally, and all spatial operators are invariant. In the second, the variations denoted by  $\delta$  are taken following the motion, and the spatial operators are not invariant. When more than one spatial co-ordinate is involved, this complicates the equations appreciably, so that, in general, we shall use Eulerian co-ordinates, although the energy equation and some of the boundary conditions, for instance, usually take a simpler form in the Lagrangian representation. Anyway, the following relations between total and local time derivatives or between Eulerian and Lagrangian variations may be useful:

$$\dot{f} = \frac{\partial f}{\partial t} + v \cdot \text{grad } f, \quad \dot{f} = \frac{\partial f}{\partial t} + (v \text{ grad})f, \quad (2.1)$$

$$\delta f = f' + \delta r \cdot \text{grad } f, \quad \delta f = f' + (\delta r \text{ grad})f. \quad (2.2)$$

Since the general equations have been established in great detail in a recent article (Ledoux and Walraven 1958), we shall be content here to summarize their most useful forms. The peculiarities of the stellar problem arise from two facts: (a) factors such as radiative stresses and energy or ionization and subatomic energy alter somewhat the usual hydrodynamic and thermodynamic equations; (b) the field of forces which usually reduces to gravity is affected by



the modifications of the system, and, in general, its resulting perturbations are not negligible, as is the case in laboratory experiments or even in the terrestrial atmosphere and oceans.

### 2.1. EFFECTS OF RADIATION

As far as the description of the radiation field in a fluid in motion and their interaction is concerned, the question has been satisfactorily cleared up by L. H. Thomas (1930*b*), and a covariant treatment has been recently published by Hazlehurst and Sargent (1959). A succinct summary up to the first-order terms in  $v/c$  may also be found in the review article by Ledoux and Walraven (1958, § 49- $\beta$ ).

Provided that the coefficients of opacity  $\kappa$  and emission  $j$ , the radiative flux  $F_R$ , and the density of radiative energy  $u_R$  are given their proper values (i.e., measured in a system moving with the matter at the point considered), the following generalizations are valid:

a) The energy density associated with the gas, for our purpose, may be written

$$u_G = \frac{3}{2} n k T + \rho I, \quad (2.3)$$

where  $n$  is the number density of particles,  $T$  the absolute temperature,  $\rho$  the material density, and  $I$  the ionization energy per unit mass. To this must be added

$$u_R = a T^4, \quad (2.4)$$

where  $a$  is the Stefan-Boltzmann constant. Thus the total internal energy per unit mass becomes

$$U = \frac{u_G + u_R}{\rho} = \frac{3}{2} \frac{\Re T}{\bar{\mu}} + \frac{a T^4}{\rho} + I, \quad (2.5)$$

where  $\Re = k/m_H$  is the gas constant and  $\bar{\mu}$  is the mean molecular weight.

b) The radiative flux must be taken into account and is defined by

$$F_R = -\frac{c}{3 \kappa \rho} \text{grad } u_R = -\frac{4a c T^3}{3 \kappa \rho} \text{grad } T, \quad (2.6)$$

corresponding to a coefficient of conduction,

$$K = \frac{4a c T^3}{3 \kappa \rho}, \quad (2.7)$$

where we shall adopt, for  $\kappa$ , a law of the general form

$$\kappa = \kappa_0 \rho^m T^{-n}. \quad (2.8)$$

c) For all time rates of variation and material velocities likely to be encountered here, the radiative stresses may be separated into an isotropic pressure,

$$p_R = \frac{1}{3} a T^4, \quad (2.9)$$

and viscous stresses exactly similar to the material ones. The ordinary coefficient of dynamic viscosity,

$$\eta_G \simeq \frac{1}{3} \rho \bar{c} \bar{l}, \quad (2.10)$$

must in this case be replaced by a coefficient of radiative viscosity,

$$\eta_R = \frac{4u_R}{15 c_{\kappa} \rho}, \quad (2.11)$$

which is of the same form as relation (2.10) with a density and a mean-free path for the radiation defined by

$$\rho_R = \frac{u_R}{c^2}, \quad \bar{l}_R = \frac{1}{\kappa \rho}. \quad (2.12)$$

Radiative and molecular viscous stresses are roughly of the same order and may often be neglected in the present context.

d) From the general definition of the entropy,

$$dS = \frac{dQ}{T} = \frac{dU}{T} - \frac{p}{T} \frac{d\rho}{\rho^2}, \quad (2.13)$$

using (2.5) (where, for the time being, we neglect the ionization energy), and, for the total pressure,

$$p = p_G + p_R = \frac{\Re \rho T}{\bar{\mu}} + \frac{1}{3} a T^4, \quad (2.14)$$

we obtain

$$S = \frac{4}{3} \frac{a T^3}{\rho} + \int \frac{c_v dT}{T} - \frac{\Re}{\bar{\mu}} \ln \rho, \quad (2.15)$$

where  $c_v$  is the specific heat of the gas at constant volume.

When this mixture is subjected to an adiabatic transformation, the relations between the variations of  $p$ ,  $T$ , and  $\rho$  may be expressed as

$$\frac{1}{p} \frac{dp}{dt} = \Gamma_1 \frac{1}{\rho} \frac{d\rho}{dt}; \quad \frac{1}{T} \frac{dT}{dt} = (\Gamma_3 - 1) \frac{1}{\rho} \frac{d\rho}{dt} = \frac{\Gamma_2 - 1}{\Gamma_2} \frac{1}{p} \frac{dp}{dt}, \quad (2.16)$$

while the variation of  $\beta = p_G/p$  is given by

$$\frac{1}{\beta} \frac{d\beta}{dt} = (\Gamma_3 - \Gamma_1) \frac{1}{\rho} \frac{d\rho}{dt},$$

where the coefficients have the following values:

$$\begin{aligned} \Gamma_1 &= \beta + \frac{(4 - 3\beta)^2(\gamma - 1)}{\beta + 12(\gamma - 1)(1 - \beta)}, \\ \Gamma_3 - 1 &= \frac{(4 - 3\beta)(\gamma - 1)}{\beta + 12(\gamma - 1)(1 - \beta)} = \frac{\Gamma_1 - \beta}{4 - 3\beta} = \Gamma_1 \frac{\Gamma_2 - 1}{\Gamma_2}. \end{aligned} \quad (2.17)$$

## 2.2. LOCAL INSTABILITY, CONVECTION, AND TURBULENCE, AND THEIR EFFECTS

2.2.1. *Local thermal instability*.—The most common form of local instability in stars is the convective instability that arises in a layer where Schwarzschild's criterion,

$$\begin{aligned} g \cdot A &= g \left( \frac{1}{\rho} \text{grad } \rho - \frac{1}{\Gamma_1 p} \text{grad } p \right) \\ &= -g \frac{4-3\beta}{\beta} \left( \frac{1}{T} \text{grad } T - \frac{\Gamma_2-1}{\Gamma_2} \frac{1}{p} \text{grad } p \right) > 0, \end{aligned} \quad (2.18)$$

is violated,  $g$  being the local gravity acceleration.

As far as the stellar interior is concerned, it is generally assumed that, when this occurs, turbulent convection sets in, mixing the relevant layer and tending to reduce the actual gradients of density and temperature to their adiabatic values.

However, rigorously speaking, there must always persist a small superadiabatic excess  $D$  sufficiently large to maintain the convective motions against the effects of viscosity and conduction and to enable convection currents to carry the required energy flux. In the case of spherical symmetry, if  $A$  denotes the radial component of  $A$  in equation (2.18),  $D$  will be defined by

$$\begin{aligned} D &= \frac{\beta}{4-3\beta} A = - \left( \frac{1}{T} \frac{dT}{dr} - \frac{\Gamma_2-1}{\Gamma_2} \frac{1}{p} \frac{dp}{dr} \right) \\ &= \frac{1}{T} \left| \frac{dT}{dr} \right| - \frac{\Gamma_2-1}{\Gamma_2} \frac{1}{p} \left| \frac{dp}{dr} \right|, \end{aligned} \quad (2.19)$$

since, in all cases of interest,  $dT/dr$  and  $dp/dr$  are simultaneously negative. The radial convective flux of energy must be of the form

$$F_t = \rho C_p T c_t l_t D, \quad (2.20)$$

where  $C_p$  is the specific heat at constant pressure and  $c_t$  and  $l_t$  characterize, respectively, the mean absolute velocity and the scale of the turbulent motions.

In a region where Schwarzschild's criterion is violated, i.e.,

$$D > 0, \quad (2.21)$$

$F_t$  is naturally positive.  $c_t$  is usually only a small fraction of the velocity

$$v = l_t \sqrt{gD} \quad (2.22)$$

communicated by the buoyancy force in a gravitational field  $g(g_r = -g, 0, 0)$  to an element of matter describing a distance  $l_t$  along the radius. But even in that case, if in equation (2.20)  $F_t$  and  $l_t$  are given typical stellar values,  $D$  turns out to be so small (of the order of  $10^{-16}$  in the interior of the sun) that, as far

as the distribution of  $\rho$  and  $T$  is concerned, one may assume (Schwarzschild 1958) that, in a convection zone,

$$\frac{1}{T} \text{grad } T = \frac{\Gamma_2 - 1}{\Gamma_2} \frac{1}{p} \text{grad } p, \quad \frac{1}{\rho} \text{grad } \rho = \frac{1}{\Gamma_1 p} \text{grad } p. \quad (2.23)$$

On the other hand,  $D$  is still much too large to allow cellular convection. Indeed, adopting Jeffreys' (1930) generalization<sup>3</sup> of Rayleigh's criterion to compressible fluids, one finds that cellular convection will be established in a plane layer of thickness  $h$  for a critical value of  $D$  of the order of

$$D_c \simeq \frac{27\pi^4 \kappa_T \eta}{4g h^4 \rho} \cdot \frac{\beta}{4 - 3\beta} \quad (2.24)$$

or, for a critical Rayleigh number,

$$\mathcal{R}_c = \frac{g D h^4 \rho}{\kappa_T \eta} \cdot \frac{4 - 3\beta}{\beta} \simeq 10^3, \quad (2.25)$$

the work of the buoyancy force being then exactly balanced by the dissipation due to viscosity and conduction (Chandrasekhar 1958, p. 103).

The numerical factors in equations (2.24) and (2.25) depend somewhat on the boundary conditions and on the geometry<sup>4</sup> if one departs from the plane case. But, on the whole, one may consider that  $\mathcal{R}_c$  is comprised between  $10^3$  and  $10^5$ . In a star, the effects of radiation should be taken into account by means of formulae (2.7) and (2.11) when evaluating the viscosity and, especially, the thermometric conductivity  $\kappa_T$ , which is related to the effective conductivity  $\kappa$  by

$$\kappa_T = \frac{\kappa}{\rho \epsilon_p}.$$

For a spherical layer of thickness  $(r_2 - r_1)$  at a distance  $r$  from the center, we get roughly

$$\mathcal{R} = \frac{4\pi G \bar{\rho}(r) \rho D}{3\kappa_T \eta} \frac{4 - 3\beta}{\beta} (r_2 - r_1)^4 r. \quad (2.26)$$

Applying this formula to a central core in the sun of radius  $r \simeq 0.1R_\odot$  and mean conditions, say  $T \simeq 10^7$ ,  $\rho \simeq 10^2$ , we find

$$\mathcal{R} \simeq 10^{37} D;$$

even for the small value of  $D$  referred to above,  $\mathcal{R}$  is still of the order of  $10^{21}$ , which is much larger than the critical value (2.25).

Laboratory experiments indicate that, in such cases, irregular turbulent motions tend to replace laminar convection. Then, with this kind of values for  $D$ ,

<sup>3</sup> See also Spiegel and Veronis (1960).

<sup>4</sup> Cf. Wasiutynski (1946), Jeffreys and Bland (1951), and Chandrasekhar (1952a, 1953), where the discussion is extended to the spherical case in view essentially of geophysical applications.

it is only for extremely small values of the core radius (or for very thin layers) of the order of  $R_c^* \simeq 3 \times 10^{-5} R_\odot \simeq 2 \times 10^6$  cm that  $\mathcal{R}$  may approach its critical value.

However, one may also be tempted to consider that, on the large scale appropriate for stars, some kind of general organized circulation may exist, even if the motions become turbulent, as seems to be the case in the earth's atmosphere. Then the coefficient of molecular and radiative viscosity in equation (2.26) should be replaced by the appropriate value for turbulent viscosity, which may be  $10^{10}$  times larger. For thick regions, this would not yet reduce  $\mathcal{R}$ , at least in the sun, to anything comparable with its critical value, but the resulting increase by a factor of the order of  $10^2$  in the critical radius  $R_c^*$  of the central core or in the critical thickness of a thin layer may be of some interest (Schwarzschild 1959).

**2.2.2. Turbulent convection.**—For large convective zones such as might be of interest here, it seems that the only picture available for convection at the present time is one of irregular quasi-isotropic turbulent motions. Unfortunately, the substantial advances (Chandrasekhar 1949, 1957; Batchelor 1953) made in the theory of homogeneous isotropic turbulence in incompressible fluids either through the statistical approach of Taylor and von Karman or through the introduction of the notion of a turbulence spectrum following Kolmogoroff, Onsager, Heisenberg, and others have been of little avail for the present problem. The main factors to incorporate in any generalization relate, on the one hand, to the buoyancy which is here the cause of the motion and should be included explicitly in the theory and, on the other hand, to the fact that the motion may extend over several scale heights, which makes it more difficult to allow properly for compressibility. The first point has been the object of some extension of both the statistical (Chandrasekhar 1952*b*) and Heisenberg's heuristic approach (cf. Ledoux, Schwarzschild, and Spiegel 1961), while the second point remains mainly unexplored.

In those circumstances, we still have to use the elementary picture in which the turbulent elements are supposed to detach themselves from a given layer with the average properties of that layer and move a certain distance (mixing length:  $l_i$ ), keeping their individuality before being reabsorbed in another layer with different average properties.

Let us resolve the velocity, at each point, into an average velocity of components  $\bar{v}^i$  defined in such a way that the usual equation of continuity remains valid for the mean motion,

$$\frac{\partial \bar{\rho}}{\partial t} + \text{div} (\bar{\rho} \bar{\mathbf{v}}) = 0, \quad (2.27)$$

and a velocity of turbulence  $V^i$ , which, on the average, does not give rise to any transfer of mass,

$$\langle \rho V_i \rangle = 0, \quad \bar{V}^i = \frac{\langle (\bar{\rho} - \rho) V^i \rangle}{\rho}.$$

Then the main dynamical effect of turbulence is to introduce, in the mean equation of motion, new stresses of the form  $\langle \rho V^i V^k \rangle$ , which, at least in a first approximation (cf. Ledoux and Walraven 1958, § 49), can be divided into an isotropic pressure of turbulence,

$$p_t = \langle \rho V^i V_i \rangle = \langle \frac{1}{3} \rho |V|^2 \rangle = \frac{1}{3} \bar{\rho} c_t^2, \quad (2.28)$$

and "viscous stresses," which, in terms of the average velocity  $\bar{v}_i$  and a coefficient of turbulent viscosity

$$\eta_t \simeq \frac{1}{3} \bar{\rho} \bar{l}_t c_t, \quad (2.29)$$

take exactly the same form as the usual gaseous stresses.

The equation governing the variation of the kinetic energy of turbulence (Cowling 1935, Wasiutynski 1946) takes the form

$$\begin{aligned} \bar{\rho} \frac{d}{dt} \left( \frac{1}{2} \frac{\langle \rho V^2 \rangle}{\bar{\rho}} \right) + p_t \operatorname{div} \bar{\mathbf{v}} &= \frac{\partial}{\partial t} \left( \frac{1}{2} \langle \rho V^2 \rangle \right) + \operatorname{div} \left( \frac{1}{2} \langle \rho V^2 \rangle \bar{\mathbf{v}} \right) \\ &+ p_t \operatorname{div} \bar{\mathbf{v}} = \rho \epsilon_4 - \rho \epsilon_2 - \operatorname{div} \bar{\mathbf{F}}_2 - \langle \mathbf{V} \cdot \operatorname{grad} p \rangle, \end{aligned} \quad (2.30)$$

where  $\epsilon_2$ , which is of the order of  $c_t^3/\bar{l}_t$ , represents the total rate of dissipation per unit mass of the kinetic energy of turbulence due to molecular and radiative viscosity;  $\epsilon_4$  represents the rate of transformation of kinetic energy of mean motion into turbulent kinetic energy due to the turbulent stresses; and

$$\bar{\mathbf{F}}_2 = \frac{1}{2} \langle \rho V^2 \mathbf{V} \rangle$$

corresponds to the convective flux of turbulent energy.

The last term in equation (2.30) represents the transformation of gravitational potential energy into kinetic energy of turbulence, and one may also introduce the rate of transformation of thermal energy into kinetic energy of turbulence,

$$\epsilon_3 = \frac{1}{\bar{\rho}} \langle p \operatorname{div} \mathbf{V} \rangle, \quad (2.31)$$

which does not appear explicitly in the form adopted for (2.30) but which is convenient to express the conservation of thermal energy. In that respect, we must also introduce the turbulent flux of thermal energy,

$$\mathbf{F}_t = \langle \rho U \mathbf{V} \rangle,$$

with  $U$  defined by equation (2.5).

As we shall mainly deal with spherical masses, in which the only non-vanishing components of  $\bar{\mathbf{V}}$  and  $\mathbf{F}_t$  are the radial ones, their explicit expressions are of special interest:

$$\bar{V}_r = l_t c_t \left( \frac{4 - 3\beta}{\beta} \right) D, \quad (2.32)$$

$$F_{t,r} = \bar{\rho} \dot{t} c_t c_v T \left\{ 1 + \frac{2(1-\beta)}{\beta} \left[ 5 + \frac{4(1-\beta)}{\beta} \right] \right\} D, \quad (2.33)$$

where  $c_v$  is the specific heat of the gas.

It is sometimes advantageous to introduce, instead of  $F_{t,r}$ , a generalized turbulent flux  $F_{t,r}^*$  which includes the rate of work by the pressure on the turbulent elements:

$$F_{t,r}^* = F_{t,r} + \bar{p} \bar{V}_r = \bar{\rho} \dot{t} c_t C_p D. \quad (2.34)$$

Here  $C_p$  is a generalized specific heat at constant pressure, given by

$$C_p = c_v \left\{ \frac{5}{3} + \frac{8(1-\beta)}{3\beta} \left[ 5 + \frac{4(1-\beta)}{\beta} \right] \right\} \quad (2.35)$$

if the gas is treated as monatomic, which is a good approximation nearly everywhere in a star. In the same conditions, one may define a generalized specific heat at constant volume,

$$C_v = c_v \left[ 1 + \frac{8(1-\beta)}{\beta} \right]. \quad (2.36)$$

In general, the net value of the right-hand member of equation (2.30) is small, and, by analogy with the equation of thermal energy, one may consider an "adiabatic" approximation in which it is supposed to vanish exactly, so that, using equations (2.27) and (2.28), it becomes

$$\frac{1}{\dot{p}_t} \frac{d\dot{p}_t}{dt} = \frac{5}{3} \frac{1}{\bar{\rho}} \frac{d\bar{\rho}}{dt}. \quad (2.37)$$

### 2.3. EFFECTS OF IONIZATION

With the very high abundances of H and He that prevail in most stars, the ionization of heavier elements has negligible effects, and, since H and He are already completely ionized at fairly low temperatures, the gas in the main interior may be treated as monatomic and  $\gamma$  put equal to  $\frac{5}{3}$ .

In the external layers, it may be necessary to take into account the effects of the ionizations of H I, He I, and He II; but, as they occur in fairly well-separated ranges of temperature, it is often sufficient to consider that only one ion at a time is in a critical stage of ionization. In that case, denoting the total numbers of electrons and ions per unit mass, respectively, by  $N_e$  and  $M$  (which is invariant) and the total number of particles  $N_e + M$  by  $N$ , we have

$$N_e = M \sum_Z X_Z (r + x_Z^{r+1}) = Mx; \quad n = \rho (N_e + M) = \rho N, \quad (2.38)$$

where, for each value of  $Z$ ,  $r$  takes one of the values  $r \leq (Z-1)$ ;  $X_Z$  is the abundance by number of the element of atomic number  $Z$ ;  $x_Z^{r+1} = M_Z^{r+1}/M_Z$  is the fraction of the atoms  $Z$  which have lost  $(r+1)$  electrons; and  $x$  is the relative abundance of electrons with respect to ions.

We must add Saha's equation,

$$\frac{x_i^{r+1}}{1 - x_i^{r+1}} = \frac{2(2\pi m_e kT)^{3/2}}{h^3 \rho M z} \frac{u_i^{r+1}}{u_i^r} e^{-\chi_i^r/kT}, \quad (2.39)$$

where the index  $i$  refers to the element in the process of getting ionized and the  $u_i^r$ 's are the partition functions and  $\chi_i^r$  is the ionization potential of the ion having lost  $r$  electrons.

Noting that, from equation (2.39) with

$$p_G = N k \rho T = M(1+x) k \rho T = \frac{\Re \rho T}{\bar{\mu}}$$

and

$$dx = X_i dx_i^{r+1}, \quad \frac{d\bar{\mu}}{\bar{\mu}} = -\frac{dN}{N} = -\frac{dx}{1+x},$$

we get

$$\frac{X_i dx_i^{r+1}}{(1+x)B} = \left(\frac{5}{2} + \frac{\chi_i^r}{kT}\right) \frac{dT}{T} - \frac{dp_G}{p_G}, \quad (2.40)$$

where

$$B = \frac{X_i x x_i^{r+1} (1 - x_i^{r+1})}{x(1+x) + X_i x_i^{r+1} (1 - x_i^{r+1})}.$$

Expressing  $dp_G/p_G$  in (2.40) successively in terms of  $dT/T$  and  $d\rho/\rho$  or  $dT/T$  and  $dp/p$ , we find

$$\begin{aligned} A_{\rho, T} &= \left(\frac{\partial \ln N}{\partial \ln \rho}\right)_T = -\frac{B}{(1+B)}, \\ A_{T, \rho} &= \left(\frac{\partial \ln N}{\partial \ln T}\right)_\rho = B \left[ \frac{5}{2} + \frac{\chi_i^r}{kT} + \frac{4(1-\beta)}{\beta} \right], \\ A_{T, \rho} &= \left(\frac{\partial \ln N}{\partial \ln T}\right)_\rho = \frac{B}{1+B} \left( \frac{3}{2} + \frac{\chi_i^r}{kT} \right). \end{aligned} \quad (2.41)$$

Equation (2.13), where  $dS$  is put equal to zero,  $dU$  is evaluated from (2.5) with

$$dI = -\chi_i^r dM_i^r = \chi_i^r dN_e = \chi_i^r dN,$$

and  $(p, \rho)$  and  $(\rho, T)$  are successively adopted as independent variables, yields for the generalized adiabatic coefficients,

$$\Gamma_1 = \frac{\{16 - 12\beta - (\frac{3}{2})\beta^2 + \beta[4 - (\frac{3}{2})\beta + \beta\chi_i^r/kT] A_{T, \rho}\} (1 + A_{\rho, T})}{12 - 10.5\beta + \beta(\frac{3}{2} + \chi_i^r/kT) A_{T, \rho}}, \quad (2.42)$$

$$\begin{aligned} \Gamma_3 - 1 &= \frac{\Gamma_2 - 1}{\Gamma_2} \Gamma_1 = \frac{4 - 3\beta + \beta A_{T, \rho}}{12 - 10.5\beta + \beta(\frac{3}{2} + \chi_i^r/kT) A_{T, \rho}} \\ &= \frac{\Gamma_1 - \beta(1 + A_{\rho, T})}{[(4 - 3\beta) + \beta A_{T, \rho}]}, \end{aligned} \quad (2.43)$$

in terms of which the adiabatic relation (2.16) is still valid.



The generalized specific heats become

$$C_p = c_v \left\{ \frac{5}{3} + \frac{8(1-\beta)}{3\beta} \left[ 5 + \frac{4(1-\beta)}{\beta} \right] + \frac{2}{3} \frac{A_{T,p}^2}{B} \right\}, \quad (2.44)$$

$$C_v = c_v \left[ 1 + \frac{8(1-\beta)}{\beta} - \frac{2}{3} \frac{A_{T,p}^2}{A_{p,T}} \right]. \quad (2.45)$$

The expression (2.34) for  $F_{t,r}^*$  remains valid with this new value of  $C_p$ , while the expression (2.32), for the mean radial velocity of turbulence, becomes

$$\bar{V}_r = \bar{l}_t c_t \left( \frac{4-3\beta}{\beta} + A_{T,p} \right) D. \quad (2.46)$$

Of course, in the absence of a critical ionization,  $B$  and all the  $A$ 's vanish, and one obtains the usual expression for a mixture of a monatomic gas and radiation.

#### 2.4. EFFECTS OF NUCLEAR PROCESSES

Up to now, annihilation or materialization processes do not play any role in stellar structure, and, in all other types of nuclear reactions, the mass loss is so small as to be negligible.

The energy liberated in all other types of nuclear reactions is very quickly transformed into ordinary thermal energy in local equilibrium except for the fraction carried away by neutrinos. Usually this is fairly small, and, since it does not interact with the stellar material in any appreciable way, we may simply drop the corresponding part from the variation of the subatomic energy per unit mass,  $E_s$ . The conservation of thermal energy may then be written

$$\frac{d(U + E_s)}{dt} - \frac{p}{\rho^2} \frac{d\rho}{dt} = -\frac{1}{\rho} \operatorname{div} F_R, \quad (2.47)$$

assuming radiative equilibrium and neglecting viscosity and conduction.

For thermonuclear reactions,  $-dE_s/dt$  is a function of  $\rho$  and  $T$  and is denoted here by  $\epsilon_1$ , which is positive in all cases of interest. In limited ranges of  $T$  and  $\rho$ , it may be represented as

$$-\frac{dE_s}{dt} = \epsilon_1 = \epsilon_0 \rho T^\nu, \quad (2.48)$$

and equation (2.47) is usually written

$$\frac{dU}{dt} - \frac{p}{\rho^2} \frac{d\rho}{dt} = \epsilon_1 - \frac{1}{\rho} \operatorname{div} F_R. \quad (2.49)$$

The two terms on the right-hand side are very small as compared with  $U$  and may be neglected for a perturbation on a short time scale (cf. [1.1]), which may thus be treated, in a first approximation, as adiabatic.

However, it has been suggested by Hoyle (1946) and it is a fundamental step in the theory of the stellar formation of the chemical elements (Burbidge,

Burbidge, Fowler, and Hoyle 1957) that, in the course of its evolution, a star may reach a state of sufficiently high temperature and density for the establishment of a true nuclear equilibrium between the different chemical elements. In that case,  $E_s$  itself must be considered as a function of  $\rho$  and  $T$ , and

$$\frac{dE_s}{dt} = \frac{\partial E_s}{\partial T} \frac{dT}{dt} + \frac{\partial E_s}{\partial \rho} \frac{d\rho}{dt} \quad (2.50)$$

will no longer be small as compared with  $dU/dt$ , so that, in this case, an adiabatic modification will be characterized by (2.47), where the second member is dropped:

$$\frac{d(U + E_s)}{dt} - \frac{p}{\rho^2} \frac{d\rho}{dt} = 0. \quad (2.51)$$

Since in the conditions considered here all the elements will be completely ionized, we may use for  $U$  its expression (2.5) with  $I \equiv 0$ . Developing equation (2.51) in terms of  $p$  and  $\rho$  or  $T$  and  $\rho$ , we may define new generalized adiabatic coefficients,

$$\Gamma_1^* = \frac{16 - 12\beta - 1.5\beta^2 + 6\beta(1-\beta)A_{\rho,p} - \beta(4-3\beta)(\rho/NkT)(\partial E_s/\partial \rho)_p}{12 - 10.5\beta - 6\beta(1-\beta)A_{p,\rho} + \beta(4-3\beta)(p/NkT)(\partial E_s/\partial p)_p} \quad (2.52)$$

and

$$(\Gamma_3^* - 1) = \frac{4 - 3\beta - 1.5\beta A_{\rho,T} - (\beta\rho/NkT)(\partial E_s/\partial \rho)_T}{12 - 10.5\beta + 1.5\beta A_{T,\rho} + (\beta T/NkT)(\partial E_s/\partial T)_\rho}, \quad (2.53)$$

where the  $A$ 's have the same general definitions as in equation (2.41) but cannot, of course, be defined in terms of  $B$  and  $\chi_i^*$ . Since the energies involved are very large, one may expect the derivatives of  $E_s$  with respect to the state variables to be large too and the effects on the  $\Gamma$ 's to be considerable.

If  $\rho$  and  $T$  are to be preferred as independent variables,  $\Gamma_1$  may also be expressed in terms of the partial derivatives with respect to them by means of the relations

$$\begin{aligned} A_{p,\rho} &= A_{T,\rho} [(4-3\beta) + \beta A_{T,\rho}]^{-1}, \\ A_{\rho,p} &= [(4-3\beta)A_{\rho,T} - \beta A_{T,\rho}] [(4-3\beta) + \beta A_{T,\rho}]^{-1}, \\ \left(\frac{\partial E_s}{\partial \rho}\right)_p &= \left(\frac{\partial E_s}{\partial \rho}\right)_T - \left(\frac{\partial E_s}{\partial T}\right)_\rho \frac{T}{\rho} \frac{\beta(1 + A_{\rho,T})}{[(4-3\beta) + \beta A_{T,\rho}]}, \\ \left(\frac{\partial E_s}{\partial p}\right)_\rho &= \left(\frac{\partial E_s}{\partial T}\right)_\rho \frac{T}{p} \frac{1}{[(4-3\beta) + \beta A_{T,\rho}]}. \end{aligned}$$

The integrability condition for the entropy also yields

$$A_{T,\rho} = -\frac{3}{2}A_{\rho,T} - \frac{\rho}{NkT} \left(\frac{\partial E_s}{\partial \rho}\right)_T.$$

In general, a relation of the form

$$dE_s = \chi dN$$

will still exist which will permit us to relate the partial derivatives of  $E_s$  and  $T$  and to simplify (2.52) and (2.53). In particular, for conditions of temperatures and density of the order of those envisaged by Hoyle (1946) (cf. BBFH 1957, § XII):  $T \simeq 3 \times 10^9$  to  $7 \times 10^9$  °K,  $\rho \simeq 10^8$  gm cm<sup>-3</sup>,  $\beta \simeq 1$ , and, if  $\chi/kT$  is greater than unity which is likely in the range considered,  $\Gamma_1$  reduces to

$$\Gamma_1^* = \frac{5(1 + A_{T,\rho}) + 2(\chi/kT) A_{T,\rho}}{3(1 + A_{T,\rho}) + 2(\chi/kT) A_{T,\rho}}.$$

In the lower range of temperatures around  $3 \times 10^9$  °K when the elements of the iron peak are being built,  $dE_s$  and  $dN$  are both negative for  $dT$  positive ( $\chi: +$ ,  $A_{T,\rho}: -$ ) and values of  $\Gamma_1$  appreciably larger than  $\frac{5}{3}$  would seem possible.

In the upper range around  $7 \times 10^9$  °K, when the iron is converted into He again with rising temperature,  $dE_s$  and  $dN$  are both positive ( $\chi: +$ ,  $A_{T,\rho}: +$ ) and  $\Gamma_1$  may certainly become much smaller than  $\frac{5}{3}$ , probably fairly close to 1.

In both cases, the cosmological consequences could be very important. In the second, which has already been discussed qualitatively by Hoyle on the basis of general physical arguments, an extremely strong dynamical instability may arise, which, after a phase of violent collapse, is supposed to lead, in the end, to the dispersal of a large fraction of the material of the star into the surrounding interstellar space. But if, in the first case, which in the course of normal evolution always precedes the second,  $\Gamma_1^*$  becomes large enough in a sufficiently large core, the resulting decrease in compressibility, if coupled with sufficiently fast rotation, may renew the interest in the possibilities of fission explored by Poincaré, Jeans, Darwin, and Cartan (cf. Lyttleton 1953; Ledoux 1958, Part A, §§ 7 and 8).

## 2.5. GENERAL EQUATIONS

Omitting the broken brackets around mean values (except when necessary to avoid misunderstanding), the general equations of motion may be written with the same notations as above:

### 2.5.1. Conservation of mass.—

$$\frac{\partial \rho}{\partial t} + \text{div}(\rho \mathbf{v}) = 0. \quad (2.54)$$

### 2.5.2. Conservation of momentum.—In the absence of turbulence, we have

$$\frac{d\mathbf{v}}{dt} = \frac{\partial \mathbf{v}}{\partial t} + (\mathbf{v} \cdot \text{grad}) \mathbf{v} = \mathbf{F} - \frac{1}{\rho} \text{grad } p + \frac{1}{\rho} \text{div } \mathfrak{G}, \quad (2.55)$$

or, more explicitly, in a general system of co-ordinates,

$$\frac{\partial v^k}{\partial t} + v^i \Delta_i v^k = F^k - \frac{1}{\rho} g^{ik} \Delta_i p + \frac{1}{\rho} \Delta_i \mathfrak{G}^{ik}, \quad (2.56)$$

where  $\mathfrak{G}$  represents the tensor of the viscous stresses due to molecular and radiative viscosity, which, to the same order of approximation as in § 2.1,  $c$ , has exactly the same form as the usual molecular tensor with a global coefficient of dynamical viscosity

$$\eta = \eta_R + \eta_G,$$

and where  $\Delta_i$  represents the usual covariant derivative, which, in Cartesian co-ordinates, reduces to  $\partial/\partial x^i$ .

In any case, those viscous terms are small, and, in the presence of turbulence, we shall neglect their effects on the mean motion, since they are very small compared with those of turbulent viscosity, but we shall retain them for the turbulent motion in which the spatial variations of the turbulent velocity  $V$  may be very large, writing

$$\frac{\partial v^k}{\partial t} + v^i \Delta_i v^k = F^k - \frac{1}{\rho} g^{ik} \Delta_i (p + p_t) + \frac{1}{\rho} \Delta_i [\mathfrak{G}_i^{ik}(v) + \mathfrak{G}^{ik}(V)], \quad (2.57)$$

where again  $\mathfrak{G}_i^{ik}$  has the same form as the molecular stresses but with the viscosity coefficient  $\eta_i$  defined by (2.29).

In our problem, the external force  $F$  reduces most often to gravitation, and we have

$$F = -\text{grad } \phi, \quad (2.58)$$

with

$$\nabla^2 \phi = 4\pi G\rho. \quad (2.59)$$

**2.5.3. Conservation of mechanical energy.**—For laminar flow, we have, per unit mass,

$$\begin{aligned} \frac{d}{dt}(\tfrac{1}{2} v^2) &= \frac{\partial}{\partial t}(\tfrac{1}{2} v^2) + (v \cdot \text{grad})(\tfrac{1}{2} v^2) \\ &= v \cdot F - \frac{v}{\rho} \cdot \text{grad } p + \frac{v}{\rho} \text{div } \mathfrak{G}(v), \end{aligned} \quad (2.60)$$

or, by unit volume,

$$\frac{\partial}{\partial t}(\tfrac{1}{2} \rho v^2) + \text{div}(\tfrac{1}{2} \rho v^2 v) = \rho F \cdot v - v \cdot \text{grad } p + v \cdot \text{div } \mathfrak{G}(v). \quad (2.61)$$

In the presence of turbulence, with the same kind of approximations as before, we get

$$\frac{\partial}{\partial t}(\tfrac{1}{2} v^2) + v^i \Delta_i (\tfrac{1}{2} v^2) = F^k v_k - \frac{v^i}{\rho} \Delta_i (p + p_t) + \frac{v_k}{\rho} \Delta_i \mathfrak{G}_i^{ik}(v). \quad (2.62)$$

The conservation of turbulent energy has already been expressed in a convenient form in equation (2.30).

**2.5.4. Conservation of thermal energy.**—For laminar flow, we have

$$\frac{dQ}{dt} = \frac{dU}{dt} + \frac{p}{\rho} \text{div } v = \epsilon_1 + \frac{1}{\rho} \Sigma \mathfrak{G}^{ik}(v) \Delta_i v_k - \frac{1}{\rho} \text{div } F_R,$$

which can also be written

$$\begin{aligned} \frac{d\mathcal{P}}{dt} - \frac{\Gamma_1 \mathcal{P}}{\rho} \frac{d\rho}{dt} &= \frac{\partial \mathcal{P}}{\partial t} + \mathbf{v} \cdot \text{grad } \mathcal{P} - \frac{\Gamma_1 \mathcal{P}}{\rho} \left( \frac{\partial \rho}{\partial t} + \mathbf{v} \cdot \text{grad } \rho \right) \\ &= (\Gamma_3 - 1) \rho \left[ \epsilon_1 + \frac{1}{\rho} \Sigma \mathfrak{G}^{ik}(\mathbf{v}) \Delta_i v_k - \frac{1}{\rho} \text{div } \mathbf{F}_R \right]. \end{aligned} \quad (2.63)$$

The second term in the brackets represents the heat liberated by ordinary viscosity in the mean motion, and, in the presence of turbulence, we shall neglect it, as compared with that liberated in the turbulent elements, writing

$$\frac{d}{dt} \left( \frac{\langle \rho U \rangle}{\bar{\rho}} \right) + \frac{\mathcal{P}}{\rho} \text{div } \mathbf{v} = \left[ \epsilon_1 + \epsilon_2 - \epsilon_3 - \frac{1}{\rho} \text{div} (\mathbf{F}_R + \mathbf{F}_t) \right],$$

or, transforming it as before,

$$\frac{d\mathcal{P}}{dt} - \frac{\Gamma_1 \mathcal{P}}{\rho} \frac{d\rho}{dt} = (\Gamma_3 - 1) \rho \left[ \epsilon_1 + \epsilon_2 - \epsilon_3 - \frac{1}{\rho} \text{div} (\mathbf{F}_R + \mathbf{F}_t) \right], \quad (2.64)$$

with the notations introduced in § 2.2.2.

In all this, we have assumed the nuclear processes to be of the thermonuclear type with a rate of energy generation given by a function  $\epsilon_1$  of  $\rho$  and  $T$ , and we have neglected, in the first member of the equation, a term

$$\frac{1}{\bar{\mu}} \frac{d\bar{\mu}}{dt} \frac{6\beta(1-\beta)\mathcal{P}}{(\frac{3}{2})\beta + 12(1-\beta)} = -\frac{1}{N} \frac{dN}{dt} \frac{6\beta(1-\beta)\mathcal{P}}{(\frac{3}{2})\beta + 12(1-\beta)}$$

corresponding to the variation of the chemical composition or the total number of particles  $N$  per unit mass. In the case of thermonuclear reactions, this is justified since

$$\frac{1}{\bar{\mu}} \frac{d\bar{\mu}}{dt} = \alpha \bar{\mu} \frac{\epsilon_1}{e_N}$$

is then very small,  $\epsilon_1$  being only a small fraction of the total energy  $e_N$  which can be released per unit mass by the relevant reaction. The proportionality factor  $\alpha$  depends on the type of reactions considered and takes the value  $\frac{5}{4}$  for the conversion of H into He and  $\frac{1}{16}$  for the conversion of He into C<sup>12</sup>. The above expression remains very small until the temperatures reach values of the order of  $10^9$  to  $10^{10}$  °K.

But, at these high temperatures, nuclear equilibrium processes will be at work, and it might be better to use directly the definitions (2.50) and (2.52–2.53), although it is possible to obtain the same final result by substituting (2.50) for  $\epsilon_1$  in (2.63) or (2.64), in the first members of which the above term is developed in terms of  $(\partial N / \partial \rho)_p$  and  $(\partial N / \partial p)_p$ . For instance, (2.64) becomes

$$\frac{d\mathcal{P}}{dt} - \frac{\Gamma_1^* \mathcal{P}}{\rho} \frac{d\rho}{dt} = (\Gamma_3^* - 1) \rho \left[ \epsilon_2 - \epsilon_3 - \frac{1}{\rho} \text{div} (\mathbf{F}_R + \mathbf{F}_t) \right]. \quad (2.65)$$

## 2.6. SMALL MOTIONS AND LINEARIZED EQUATIONS

To obtain the linearized form of any one of the above equations, one has simply to take the first variation of that equation with respect to the dependent

variables. Since, in general, we use the Eulerian representation, space co-ordinates must be treated as independent and the space operators as invariant, but one must remember that all absolute time derivatives should be expanded as in equations (2.1) before the first variation is taken.

Here we shall limit ourselves to the case where the perturbation is applied to an equilibrium state with, possibly, convection zones and characterized by

$$\begin{aligned} v &= 0, \\ \frac{1}{\rho} \operatorname{grad} (p + p_t) &= -\operatorname{grad} \phi, \\ \nabla^2 \phi &= 4\pi G \rho, \\ \epsilon_1 + \epsilon_2 - \epsilon_3 &= \frac{1}{\rho} \operatorname{div} (F_R + F_t), \end{aligned} \quad (2.66)$$

or, using definition (2.34),

$$\begin{aligned} \epsilon_1 &= \frac{1}{\rho} \operatorname{div} (F_R + F_t^* + F_2), \\ \epsilon_2 + \frac{1}{\rho} V \cdot \operatorname{grad} p &= \frac{1}{\rho} \operatorname{div} F_2. \end{aligned}$$

This is the only case which has been studied so far, and the review article by Ledoux and Walraven (1958, § 56) may be consulted for more general circumstances. Then the linearized equations become

$$\frac{\partial \rho'}{\partial t} + \operatorname{div} (\rho v') = 0, \quad (2.67)$$

$$\begin{aligned} \frac{\partial v'}{\partial t} &= -\operatorname{grad} \phi' + \frac{\rho'}{\rho^2} \operatorname{grad} (p + p_t) - \frac{1}{\rho} \operatorname{grad} (p' + p'_t), \\ &\quad - \frac{\rho'}{\rho^2} \operatorname{div} \mathfrak{G}(V) + \frac{1}{\rho} \operatorname{div} [\mathfrak{G}_t(v') + \langle \mathfrak{G}(V') \rangle], \end{aligned} \quad (2.68)$$

$$\nabla^2 \phi' = 4\pi G \rho', \quad (2.69)$$

$$\begin{aligned} \frac{\partial p'}{\partial t} + v' \cdot \operatorname{grad} p - \frac{\Gamma_1 p}{\rho} \left( \frac{\partial \rho'}{\partial t} + v' \cdot \operatorname{grad} \rho \right) \\ = (\Gamma_3 - 1) \rho \left[ \epsilon_1 + \epsilon_2 - \epsilon_3 - \frac{1}{\rho} \operatorname{div} (F_R + F_t) \right]', \end{aligned} \quad (2.70)$$

$$\begin{aligned} \frac{\partial p'_t}{\partial t} + v' \cdot \operatorname{grad} p_t - \frac{5}{3} \frac{p_t}{\rho} \left( \frac{\partial \rho'}{\partial t} + v' \cdot \operatorname{grad} \rho \right) \\ = \frac{2}{3} \rho \left( \epsilon_4 - \epsilon_2 - \frac{1}{\rho} \operatorname{div} F_2 - \frac{1}{\rho} \langle V \cdot \operatorname{grad} p \rangle \right)', \end{aligned} \quad (2.71)$$

where  $v'$  denotes the small velocity associated with the perturbation.

According to equations (2.2), we may interchange at will the Eulerian and Lagrangian perturbations  $f'$  and  $\delta f$  of any quantity  $f$  which, in the equilibrium state, is identically zero or for which  $\operatorname{grad} f = 0$ . This is the case for the second

members of (2.70) and (2.71), which then take their simplest form in Lagrangian notation,

$$\frac{d\delta p}{dt} - \frac{\Gamma_1 p}{\rho} \frac{d\delta \rho}{dt} = (\Gamma_3 - 1) \rho \delta \left[ \epsilon_1 + \epsilon_2 - \epsilon_3 - \frac{1}{\rho} \operatorname{div}(\mathbf{F}_R + \mathbf{F}_t) \right], \quad (2.72)$$

$$\frac{d\delta p}{dt} - \frac{5}{3} \frac{p_t}{\rho} \frac{d\delta \rho}{dt} = \frac{2}{3} \rho \delta \left( \epsilon_4 - \epsilon_2 - \frac{1}{\rho} \operatorname{div} \mathbf{F}_2 - \frac{1}{\rho} \langle \mathbf{V} \cdot \operatorname{grad} p \rangle \right). \quad (2.73)$$

The corresponding generalization of the second adiabatic relation (2.16) between  $\delta T$  and  $\delta \rho$  can be obtained by eliminating  $\delta p$  from (2.72) by means of the general relation

$$\frac{\delta p}{p} = (4 - 3\beta) \frac{\delta T}{T} + \beta \frac{\delta \rho}{\rho} + \beta \left( A_{\rho, T} \frac{\delta \rho}{\rho} + A_{T, \rho} \frac{\delta T}{T} \right)$$

derived from the equation of state (2.14), taking into account the possible variation of  $\bar{\mu}$ . One then finds

$$\frac{1}{T} \frac{d\delta T}{dt} = (\Gamma_3 - 1) \frac{1}{\rho} \frac{d\delta \rho}{dt} + \frac{1}{C_p T} \delta \left[ \epsilon_1 + \epsilon_2 - \epsilon_3 - \frac{1}{\rho} \operatorname{div}(\mathbf{F}_R + \mathbf{F}_t) \right], \quad (2.74)$$

using definitions (2.41), (2.43), and (2.45).

Let us note also that, in this case, the total or partial time derivatives are equivalent when applied to any first-order quantity.

## 2.7. BOUNDARY CONDITIONS

We limit ourselves to the case of *free surfaces* and surfaces of discontinuity of the type of contact surfaces, i.e., surfaces through which no mass is flowing, contrary to what happens at a shock front. Let

$$f(x, y, z, t) = 0 \quad (2.75)$$

represent such a surface and indices 1 and 2 distinguish between values taken on each side of it.

The velocities must satisfy the kinematic conditions

$$\frac{\partial f}{\partial t} + \mathbf{v}_i \cdot \operatorname{grad} f = 0, \quad i = 1, 2, \quad (2.76)$$

which express the fact that, on both sides, the normal material velocities are equal to the normal velocity of the surface. In other words, material particles belonging to either side of the surface always remain on it, and new particles cannot appear except at singularities. By subtraction, one also gets

$$(\mathbf{v}_1 - \mathbf{v}_2) \cdot \operatorname{grad} f = 0. \quad (2.77)$$

Of course, on a free surface, only one of equations (2.76) is valid.

If, as assumed above, the original state is purely static, these conditions for the perturbed motion reduce to the following:

(a) on a free surface:

$$\frac{\partial f'}{\partial t} + \mathbf{v}' \cdot \text{grad } f = 0; \quad (2.78)$$

(b) on a contact surface:

$$(\mathbf{v}'_1 - \mathbf{v}'_2) \cdot \text{grad } f = 0. \quad (2.79)$$

Furthermore, surface forces must satisfy dynamical conditions which may be written, if these forces reduce to a pure isotropic pressure field,

$$p_1(x_1, y_1, z_1, t) - p_2(x_2, y_2, z_2, t) = 0 \quad (2.80)$$

for all points  $(x_1, y_1, z_1) \equiv (x_2, y_2, z_2)$  on the surface (2.75) at any time  $t$ . Since this equality always refers to points facing each other across the surface and since material points may have different tangential motions, this condition cannot be expressed, during a perturbation, directly in terms of either the Eulerian or the Lagrangian variations, but we can write

$$\Delta p_1 = \Delta p_2$$

if  $\Delta$  corresponds to a variation following a given point of the surface during its motion. Of course, we may also follow a given material particle (say 1) on *one* side of the surface, but then, on the other side, we must evaluate the changes of pressure for the particle (2) which coincide, at each instant, with the point reached by particle (1). This can be written

$$\delta p_1 = \delta p_2 + (\delta \mathbf{r}_1 - \delta \mathbf{r}_2) \cdot (\text{grad } p)_2 \quad (2.81)$$

or

$$\delta p_2 = \delta p_1 + (\delta \mathbf{r}_2 - \delta \mathbf{r}_1) \cdot (\text{grad } p)_1.$$

If the surface  $f = 0$  coincides with an isobaric surface, then equations (2.81) reduce to

$$\delta p_1 = \delta p_2, \quad (2.82)$$

since then  $(\delta \mathbf{r}_1 - \delta \mathbf{r}_2)$ , which is always tangential to  $f = 0$ , is normal to  $\text{grad } p_1$  and  $\text{grad } p_2$ .

Using equation (2.2), the conditions (2.81) become

$$\begin{aligned} p'_1 - p'_2 + \delta \mathbf{r}_1 [(\text{grad } p)_1 - (\text{grad } p)_2] &= 0, \\ p'_1 - p'_2 + \delta \mathbf{r}_2 [(\text{grad } p)_1 - (\text{grad } p)_2] &= 0. \end{aligned} \quad (2.83)$$

Since all points  $(x_1, y_1, z_1) \equiv (x_2, y_2, z_2)$  which satisfy equation (2.80) must automatically be on the surface (2.75), one may also substitute  $(p_1 - p_2)$  for  $f$  in equation (2.76) and get the mixed conditions

$$\begin{aligned} \frac{\partial p_1}{\partial t} - \frac{\partial p_2}{\partial t} + \mathbf{v}_1 [(\text{grad } p)_1 - (\text{grad } p)_2] &= 0, \\ \frac{\partial p_1}{\partial t} - \frac{\partial p_2}{\partial t} + \mathbf{v}_2 [(\text{grad } p)_1 - (\text{grad } p)_2] &= 0. \end{aligned} \quad (2.84)$$



Applied to a perturbation of a static equilibrium state, they simply yield the time derivatives of (2.83).

On a free surface ( $p = 0$ ), condition (2.82) becomes

$$\delta p = 0 \quad \text{or} \quad p' + \delta \mathbf{r} \cdot \text{grad } p = 0. \quad (2.85)$$

If the viscous forces are taken into account, the order of the system of the differential equations of motion is raised, and the dynamical condition (2.80) must be replaced by the three conditions

$$P_1^i \equiv [-g^{ik} p(\mathbf{r}) n_k + \mathfrak{G}^{ik}(\mathbf{r}, \mathbf{v}) n_k]_1 = [-g^{ik} p(\mathbf{r}) n_k + \mathfrak{G}^{ik}(\mathbf{r}, \mathbf{v}) n_k]_2 \equiv P_2^i \quad (2.86)$$

$$i = 1, 2, 3,$$

where the  $n_k$ 's are the components of the normal to the surface (2.75). They express that the complete stress vector  $\mathbf{P}$  is the same on both sides, and, of course, on a free surface, it must vanish identically:

$$\mathbf{P} = 0. \quad (2.87)$$

Furthermore, the kinematic conditions are also modified. For a perfect fluid, according to equation (2.77), the particles on each side of (2.75) can have different tangential motions. But, in the presence of viscosity, this would result in a frictional force exerted, say by fluid (1) on fluid (2), usually taken as being proportional to the difference between the tangential velocities  $v_{t,i}$  and which must be balanced by the tangential component of the stress vector in fluid (2) (and vice versa):

$$[\mathbf{P} - (\mathbf{P} \cdot \mathbf{n})\mathbf{n}]_2 = \eta_{12}(\mathbf{v}_{t,1} - \mathbf{v}_{t,2}), \quad (2.88)$$

where  $\eta_{12}$  characterizes the mutual friction of the two fluids. Since it is usually extremely large while the first member of equation (2.88) remains finite, the latter implies

$$\mathbf{v}_{t,1} = \mathbf{v}_{t,2}. \quad (2.89)$$

Thus, in this case, material particles keep facing each other across the surface of discontinuity while it moves, and the conditions for the perturbed motion may be derived from equations (2.86) by taking directly their Lagrangian variations and noting that, if the original state is static, the correct first-order terms corresponding to the viscous tensions are obtained simply by substituting  $\mathbf{v}'$  for  $\mathbf{v}$  in them. On a free surface, of course, we should always have

$$\delta \mathbf{P} = 0. \quad (2.90)$$

In some cases, depending on the fields of force present, other boundary conditions may have to be written down explicitly. For instance, the gravitational potential  $\phi$  and its gradient should always be continuous. In the presence of an electromagnetic field, extra conditions will also appear (Simon 1959).

### § 3. THE GENERAL PROBLEM AND ITS ILLUSTRATION FOR PURELY RADIAL MOTION

The elimination of  $\rho'$  and  $p'$  by means of equations (2.67) and (2.70) from equation (2.68) requires a differentiation of the last equation with respect to time. If we introduce the displacement  $\delta r$  and note that

$$v = \frac{\partial \delta r}{\partial t},$$

this means that the problem, as already pointed out by Jeans (1928, § 108), is of the third order in  $t$ , since all other eliminations will not involve new time differentiation. We may then expect, quite generally, that our discussion should be subdivided into three parts corresponding to motions on different time scales.

To illustrate the problem, let us consider the case of purely radial motions, disregarding viscosity and turbulence for the time being. The relevant equations may then be written as follows:

$$\frac{\partial \rho'}{\partial t} + \frac{1}{r^2} \frac{\partial}{\partial r} \left( r^2 \rho \frac{\partial \delta r}{\partial t} \right) = 0 \quad \text{or} \quad \frac{\partial}{\partial t} \left( \frac{\delta \rho}{\rho} \right) = -\frac{1}{r^2} \frac{\partial}{\partial r} \left( r^2 \frac{\partial \delta r}{\partial t} \right), \quad (3.1)$$

$$\frac{\partial^2 \delta r}{\partial t^2} = -\frac{\partial \phi'}{\partial r} + \frac{\rho'}{\rho^2} \frac{\partial p}{\partial r} - \frac{1}{\rho} \frac{\partial p'}{\partial r}, \quad (3.2)$$

$$\begin{aligned} \frac{\partial p'}{\partial t} + \frac{\partial \delta r}{\partial t} \cdot \frac{\partial p}{\partial r} - \frac{\Gamma_1 p}{\rho} \left( \frac{\partial \rho'}{\partial t} + \frac{\partial \delta r}{\partial t} \frac{\partial \rho}{\partial r} \right) \\ = (\Gamma_3 - 1) \rho \left[ \delta \epsilon_1 - \frac{d \delta L(r)}{d m} \right], \end{aligned} \quad (3.3)$$

where  $L(r) = 4\pi r^2 F(r)$  is the total flux across the sphere of radius  $r$ , and  $m$  the mass contained in it;  $m$  is invariant following the motion. In this case, after a differentiation with respect to  $t$  and using equation (3.1), Poisson's equation (2.69) may be integrated once with respect to  $r$ , yielding

$$\frac{\partial}{\partial r} \left( \frac{\partial \phi'}{\partial t} \right) = -4\pi G \rho \frac{\partial \delta r}{\partial t}. \quad (3.4)$$

Taking the time derivative of (3.3) and eliminating  $(\partial \rho'/\partial t)$ ,  $(\partial p'/\partial t)$ , and  $(\partial \phi'/\partial t)$ , we obtain the following equation:

$$\begin{aligned} \frac{\partial^3 \delta r}{\partial t^3} = \frac{1}{\rho} \frac{\partial}{\partial r} \left[ \frac{\Gamma_1 p}{r^2} \frac{\partial}{\partial r} \left( r^2 \frac{\partial \delta r}{\partial t} \right) \right] - \frac{4}{\rho r} \frac{\partial p}{\partial r} \frac{\partial \delta r}{\partial t} \\ - \frac{1}{\rho} \frac{\partial}{\partial r} \left[ (\Gamma_3 - 1) \rho \left( \delta \epsilon - \frac{d \delta L}{d m} \right) \right]. \end{aligned} \quad (3.5)$$

Let us separate  $t$  and  $r$ , writing, for the relative displacement,

$$\frac{\delta r}{r} = \xi(r) e^{st}. \quad (3.6)$$

In all generality,  $\xi$  as well as  $s$  may be complex; however, the imaginary part of  $\xi$  is always very small, except, in some cases, in the very external layers. Here, for the sake of simplicity, we shall treat  $\xi$  as real throughout the star, but it is easy to generalize the discussion for complex  $\xi$ , the main effect being that any solution which, in the present approximation, corresponds to a purely standing oscillation would then acquire a slight progressive component. As far as the aperiodic solutions are concerned, some for which  $s^3$  is negligible would remain unaltered because  $\xi$  is actually real, while, for the others, the periodic modulation of extremely long period which might result has no physical significance, the increase in amplitude during a quarter of this period being so large as to take us out of the range of the linear approximation.

Using the relation (3.6), equation (3.5) becomes

$$s^3 r \xi = \frac{s}{\rho} \frac{1}{r^3} \left\{ \frac{d}{dr} \left( \Gamma_1 p r^4 \frac{d\xi}{dr} \right) + r^3 \xi \frac{d}{dr} [ (3\Gamma_1 - 4) p ] \right\} - \frac{1}{\rho} \frac{d}{dr} \left[ (\Gamma_3 - 1) \rho \left( \delta\epsilon - \frac{d\delta L}{dm} \right) \right]. \quad (3.7)$$

According to the boundary conditions,

$$\begin{aligned} \delta r &= 0, \quad \text{at} \quad r = 0, \\ \delta p &= -\Gamma_1 p \left( 3\xi + r \frac{d\xi}{dr} \right) + \frac{(\Gamma_3 - 1)}{s} \rho \left( \delta\epsilon - \frac{d\delta L}{dm} \right) = 0 \\ &\text{at } r = R, \quad \text{where} \quad p = 0, \end{aligned} \quad (3.8)$$

the quantity  $\xi$  remains finite everywhere. If we integrate equation (3.7) multiplied by  $4\pi\rho r^3 \xi dr$  over the whole star, we obtain an average equation for  $s$  which can be written

$$s^3 + s(A - B) + C = 0. \quad (3.9)$$

If  $J$  is defined by

$$J = \int_0^M \xi^2 r^2 dm, \quad (3.10)$$

the different constants in equation (3.9) take the values

$$\begin{aligned} A &= (J)^{-1} \int_0^R 4\pi \Gamma_1 p r^4 \left( \frac{d\xi}{dr} \right)^2 dr, \\ B &= (J)^{-1} \int_0^R \xi^2 \frac{d}{dr} [ (3\Gamma_1 - 4) p ] 4\pi r^3 dr, \\ C &= (J)^{-1} \int_0^R 4\pi \xi r^3 \frac{d}{dr} \left[ (\Gamma_3 - 1) \rho \left( \delta\epsilon - \frac{d\delta L}{dm} \right) \right] dr \\ &= (J)^{-1} \int_0^M \left( \frac{\delta T}{T} \right)_a \left( \delta\epsilon - \frac{d\delta L}{dm} \right) dm. \end{aligned}$$

Here  $C$  has been transformed by using an integration by parts, the boundary conditions (3.8), and the second relation (2.16) (or [2.74] with the second member neglected), which relates the adiabatic variations of  $T$  (denoted here by an index  $a$ ) to those of  $\rho$  given by equation (3.1).

Equation (3.9) admits a real root of opposite sign to  $C$  which we shall represent by  $s_1$ , so that the equation may be written

$$(s^2 + 2Ps + Q)(s - s_1) = 0,$$

with

$$s_1 = \frac{C}{Q}, \quad Q = (A - B) + s_1^2, \quad P = \frac{s_1}{2} = -\frac{C}{2Q}.$$

The two other roots are given by

$$s = -P \pm \sqrt{(P^2 - Q)}. \quad (3.11)$$

Generally  $C$ , which corresponds to the "dissipation" in the system, is much smaller than  $A$  or  $B$ , and  $P$  is much smaller than  $Q$ , so that, neglecting the dissipation (adiabatic approximation), the roots (3.11) become

$$s_a = \pm i \sqrt{Q_a}$$

or

$$s_a^2 = -\sigma^2 = -Q_a = -\frac{1}{J_a} \left\{ \int_0^R 4\pi \Gamma_1 p r^4 \left( \frac{d\xi_a}{dr} \right)^2 dr - \int_0^R \xi_a^2 \frac{d}{dr} [(3\Gamma_1 - 4)p] 4\pi r^3 dr \right\}, \quad (3.12)$$

where, of course,  $\xi_a$  should be the appropriate adiabatic solution.

If we treat  $\xi_a$  as a constant, which is not too bad an approximation for the fundamental mode (Ledoux and Pekeris 1941), we get

$$\sigma^2 = \langle (3\Gamma_1 - 4) \rangle \frac{\int_0^M \frac{Gm(r) dm(r)}{r}}{\int_0^M r^2 dm} = -\langle (3\Gamma_1 - 4) \rangle \frac{V}{I}, \quad (3.13)$$

with the usual definitions of the gravitational potential energy  $V$  and the moment of inertia  $I$  with respect to the center.

This defines a time scale of the same order as (1.1), and the corresponding motion will be either an oscillation or an exponentially increasing motion, according to whether  $\sigma^2$  is positive or negative. We have thus isolated the solution of (3.5), which is significant for the *dynamical stability* of the star, and, in this respect, the main result is already apparent, namely, that the star can be dynamically unstable only if the mean value of  $\Gamma_1$  taken with respect to the pressure over the whole star is smaller than  $\frac{4}{3}$ .

In the usual case of well-marked dynamical stability, the roots (3.11) may be written

$$s = \pm i\sigma_a - \sigma' = \pm i\sqrt{(Q_a) - P},$$

with

$$\sigma' = P = -\frac{1}{2\sigma_a^2 J_a} \int_0^M \left(\frac{\delta T}{T}\right)_a \left(d\epsilon_1 - \frac{d\delta L}{dm}\right)_a dm, \quad (3.14)$$

where, since  $P$  is very small compared with  $Q$ , we have introduced, as a first approximation for  $\xi$ ,  $\delta\rho/\rho$ ,  $\delta T/T$ , etc., the same adiabatic solution as used in equation (3.12). The amplitude of the adiabatic oscillation will decrease or increase, depending on whether the damping coefficient is positive or negative, and, correspondingly, the star will be said to be *vibrationally stable* or *unstable*.

The last root,  $s_1$ , is also given by the evaluation of the small dissipation term  $C$ , but this time using a solution  $\xi$  of the general equation (3.7), which can no longer be approximated by the solution of the *adiabatic* equation, since the time scale here is very long ( $s_1$ , very small) and the deviations from adiabacy very large. In fact, the appropriate solution must be found from equation (3.7), where the left-hand member may be neglected but where the last term on the right must be expressed explicitly in terms of  $\xi$  and its derivatives. This is the problem of *secular stability*.

Let us note that if we had separated the time by means of equation (3.6) directly in equations (3.1)–(3.4), the elimination could have been carried out directly, yielding, instead of equation (3.7), an equation of the second degree in  $s$  in which the third root,  $s_1$ , would not appear and the corresponding motion would escape notice.

Having thus recognized the reasons why our study is naturally subdivided into three parts and having already isolated their main characteristics, we shall now turn to a somewhat more detailed account of each. One should however note that, in this approach, the last term in the right-hand member of (3.5) has not been developed explicitly in terms of  $\delta r$ . Carrying this out will in general raise the order of the equation in time. This is especially true if the variations of the abundances of the different elements entering the thermonuclear reactions (cf. § 5.13, eqs. [5.12]) are taken explicitly into account. This means that, apart from the three main cases discussed here, there might still be other characteristic time scales associated with other modes of instability which have been little studied until now.

#### § 4. DYNAMICAL STABILITY

From § 3, we already know that, as far as dynamical stability is concerned, we may limit the discussion to the adiabatic approximation, i.e., neglect the right-hand members in equations (2.72), (2.73), and (2.74) and separate the time directly in equations (2.67)–(2.74) by writing, for the perturbation of any quantity  $a$ ,

$$a'(x^i, t) = a_0(x^i) e^{i\sigma t}, \quad (4.1)$$

with

$$v' = \frac{\partial \delta r}{\partial t} = i\sigma \eta(x^i) e^{i\sigma t}.$$

As to the space co-ordinates  $x^i$ , as long as we have to deal with spherical stars in absolute equilibrium, polar co-ordinates  $(r, \theta, \varphi)$  are indicated, and they are always separable in terms of spherical harmonics. Writing, for the amplitude,

$$a_0(r, \theta, \varphi) = a(r)y_l^m(\theta, \varphi) = a(r)P_l^m(\cos \theta)e^{im\varphi}, \quad -l \leq m \leq l, \quad (4.2)$$

we are left, after elimination of all but one of the dependent variables, with an ordinary differential equation for  $a(r)$  depending on  $l$  and  $m$  and containing the undetermined parameter  $\lambda = \sigma^2$ .

Taking the boundary conditions into account, this equation usually admits solutions only for an infinite discrete set of eigenvalues  $\lambda_1, \lambda_2, \lambda_3, \dots$ , to each of which corresponds one (more than one in case of degeneracy) eigenfunction  $a_i(r)$ . The problem being hermitian, all the  $\lambda_j = (\sigma_j)^2$ 's are real, and, if all are positive, the star is said to be dynamically stable.

However, strictly speaking, this conclusion is warranted only if the system of eigenfunctions (4.2) is complete, since, otherwise, perturbations may exist which could not be represented by a series development in terms of the eigen-solutions and would thus escape our analysis. This is a rather delicate problem which has not been solved in all cases so that, sometimes, our discussion will only yield *necessary* conditions of stability (all  $\lambda_i$ 's positive) and *sufficient* conditions of instability (one  $\lambda_i$ , at least, negative).

#### 4.1. RADIAL PERTURBATIONS

This is by far the simplest case where  $l = m = 0$ , and all perturbations are, from the start, pure functions of  $r$ . We have already outlined the eliminations leading to equation (3.7) in which the last term on the right may now be neglected. Dividing then by  $s = i\sigma$ , we are led to the eigenvalue problem

$$\frac{d}{dr} \left( r^4 \Gamma_1 p \frac{d\xi}{dr} \right) + \xi \left\{ \sigma^2 \rho r^4 + r^3 \frac{d}{dr} [ (3\Gamma_1 - 4) p ] \right\} = 0,$$

$$\delta r = 0, \quad \text{at} \quad r = 0, \quad (4.3)$$

$$\delta p = p' + \delta r \frac{\partial p}{\partial r} = p' = -\Gamma_1 p \left( 3\xi + r \frac{d\xi}{dr} \right) = 0, \quad \text{at} \quad r = R,$$

since the non-adiabatic part in the secondary boundary condition (3.8) may also be neglected and since  $\partial p / \partial r = -(Gm/r^2)\rho$  vanishes at the surface.

Rigorously speaking, in any convection zone,  $p$  should be replaced by  $(p + p_1)$  (cf. § 2.2.2), but the turbulent pressure  $p_1$  could become an appreciable fraction of  $p$  only in a very external layer whose mass anyway is too small to affect  $\sigma^2$ , so that  $p_1$  may be neglected everywhere. Except for the terms in  $d\Gamma_1/dr$ , this problem is identical with the one set up by Eddington (1919) in his first papers on the subject.

Despite the singularities at  $r = 0$  and  $r = R$ , where  $\Gamma_1 p r^4$  vanishes, the general properties of the classical Sturm-Liouville problem subsist for all physi-

cal models. The eigen-solutions  $\xi_i$  corresponding to the infinite discrete set of eigenvalues  $\sigma_i^2$ , supposed ordered by increasing values, form a complete orthogonal set of functions, which may be used to represent the most general radial perturbation. Thus, in this case, the necessary and sufficient condition of dynamical stability is that all the  $\sigma_i^2$ 's be positive.

Physically, these eigenfunctions correspond to the different modes of radial oscillations, the fundamental mode  $\xi_0$  having no nodes in  $0 \leq r \leq R$ , while the first mode  $\xi_1$  has one node, etc.

Since  $\sigma_0^2$  is the smallest eigenvalue, it is through the fundamental mode that dynamical instability ( $\sigma^2 < 0$ ) will first arise, and consequently, as far as we are concerned here, it is the most interesting one. The variational method (cf. Ledoux and Pekeris 1941; Ledoux and Walraven 1957, § 58) shows that it is given by the minimum of the right-hand member of equation (3.12) when  $\xi(r)$  is varied among the set of regular functions in  $0 \leq r \leq R$ , the minimum occurring for the actual eigen-solution  $\xi_0$ .

If  $\Gamma_1$  is constant and since  $d\rho/dr$  is always negative, the right-hand side of (3.12) is definitely positive, provided that  $\Gamma_1 > \frac{4}{3}$ , and  $\sigma_0^2$  is then always positive, and the star is stable. This can also be seen, if one remembers that  $\xi_0$  keeps the same sign over the whole interval  $0 \leq r \leq R$ , from the value of  $\sigma^2$  derived from the virial theorem (Ledoux 1945, 1949),

$$\sigma_0^2 = - \frac{\int_0^R 4\pi r^2 \xi_0 \frac{d}{dr} [(3\Gamma_1 - 4)\rho] dr}{\int_0^R 4\pi r^4 \xi_0 dr}, \quad (4.4)$$

which, for  $\Gamma_1$  equal to a constant, becomes

$$\sigma_0^2 = - \frac{(3\Gamma_1 - 4) \int_0^V \xi_0 dV}{\int_0^I \xi_0 dI}, \quad (4.5)$$

with the same definitions of  $V$  and  $I$  as in (3.13).

Thus, in this case, the stability decreases with  $\Gamma_1$ , and it vanishes for  $\Gamma_1 = \frac{4}{3}$ . Consequently, radiation which reduces  $\Gamma_1$  (cf. eq. [2.17]) decreases the dynamical stability of a star; however, instability cannot arise on this account alone, since the critical value  $\Gamma_1 = \frac{4}{3}$  is reached only for an infinite value of  $p_R/p_G$ , and this occurs only in stars of infinite mass.

Actually,  $\Gamma_1$  is never a constant, as the ionization of an electronic shell of an abundant element can lower its value appreciably and even render it smaller than  $\frac{4}{3}$  in the region where it takes place. From equation (3.12) or (4.4), it is apparent that a sufficient condition for stability is that  $(3\Gamma_1 - 4)\rho$  decrease everywhere as  $r$  increases. In other words, regions where  $\Gamma_1$  is greater than  $\frac{4}{3}$  and increases with  $r$  have a destabilizing influence, and regions where  $\Gamma_1$  is greater than  $\frac{4}{3}$  and decreases with increasing  $r$  have a stabilizing influence.

If  $\Gamma_1$  is smaller than  $\frac{4}{3}$ , the effects of its variations are reversed. Tolman (1939) and Ledoux (1949) have shown that, in general, the variations of  $\Gamma_1$  occurring somewhere around the middle of the star's radius have the strongest influence and that, all conditions in this region being equal, the most favorable case for instability occurs when  $(3\Gamma_1 - 4)$  has the deepest possible minimum both at the center and close to the surface. However, with the large abundances of H and He now favored, only the last minimum is possible, and  $\Gamma_1$  remains sufficiently well above  $\frac{4}{3}$  everywhere else, even in the most massive stars known, to preclude dynamical instability.

If we do not limit ourselves to actual stars, the extension of this discussion to the early stages of gravitational contraction may be worthwhile. Biermann and Cowling (1939) have shown that, for masses of the order of  $1-10 M_\odot$ , there are phases corresponding to values of the radius between  $30$  and  $100 R_\odot$ , where, because of the ionization of the heavy elements, dynamical stability requires the presence of a fairly high hydrogen content. But, in the presence of a large abundance of hydrogen, dynamical instability would probably be encountered at an earlier stage ( $R \simeq 100-1000 R_\odot$ ) unless the contracting hydrogen had previously been ionized by the ultraviolet radiation of pre-existing stars or by collisional ionization (Hoyle 1953) and is maintained in that stage all through the subsequent evolution.

Of course, dynamical instability in these early phases of star formation would probably mean simply a rapid collapse, with the ionization spreading rapidly through the whole mass, although a careful study of the resulting motions may reveal unexpected effects.<sup>5</sup>

On the other hand, at the opposite extreme of stellar evolution when very high densities and temperatures may bring about a state of nuclear statistical equilibrium,  $\Gamma_1^*$ , as already noted at the end of § 2.4, could become much smaller than  $\frac{4}{3}$  through a fairly extensive region producing a violent dynamical instability characterized, at those high densities, by a very short time scale and providing the necessary mechanism for redistributing the newly formed elements in interstellar space, perhaps in a supernova explosion (Hoyle 1946; Burbidge *et al.* 1956, 1957). However, up to now, the discussion of this case has remained purely qualitative, and a new approach through the proper evaluation of the  $\Gamma^*$ 's might prove fruitful.<sup>6</sup>

Another similar case concerns the equilibrium between electron captures and  $\beta$ -radioactivity, which may become established at the very high densities encountered in white dwarfs and perhaps, in somewhat different circumstances, the equilibrium between  $e^+$ ,  $e^-$ , and radiation may also play a role (Souffrin 1960).

<sup>5</sup> Cameron (1962) has recently emphasized the importance of these early phases of dynamical instability.

<sup>6</sup> Compare, however, the papers by Colgate *et al.* (1960, 1962) and by Ono and Sakashita (1961) in which a direct attack on the complete non-linear problem is attempted.



In white dwarfs, assuming complete degeneracy, the adiabatic coefficient relating  $\delta p$  and  $\delta \rho$  is given (Sauvenier-Goffin 1950*a*, *b*) by

$$\Gamma_1' = \frac{8x^5}{3(x^2 + 1)^{1/2}f(x)}, \quad (4.6)$$

where  $x = p_0/m_e c$ ,  $p_0$  being the maximum value of the electron momentum under the conditions considered, and  $f(x)$  is the usual function appearing in the expression for the electron pressure (Chandrasekhar 1939, chaps. 10 and 11).

As  $x$  tends toward  $\infty$  (extreme relativistic degeneracy),  $\Gamma_1'$  tends toward  $\frac{4}{3}$ , and, at the same time, the radius of the configuration tends toward zero, defining Chandrasekhar's critical mass  $M_e$  above which degeneracy of the electron gas is impossible. One might have thought that these two circumstances were related and that the existence of the critical mass  $M_e$  was bound in some way to the limit of dynamical stability. However, as shown by Sauvenier-Goffin (1950*a*), this is not the case because, at the same time as  $(3\Gamma_1' - 4)$  tends toward zero, the factor which multiplies this quantity in the expression (4.4) for  $\sigma^2$  tends toward  $\infty$ ,  $\sigma^2$  remaining finite.

On the other hand, taking into account the nuclear equilibrium mentioned above, Schatzman (1958) has shown that  $\Gamma_1'$  is decreased appreciably below its value (4.6) for sufficiently high  $x$  and densities, and this leads to dynamical instability for a critical radius of the order of  $2.7 \times 10^{-3} R_\odot$ .

#### 4.2. NON-RADIAL PERTURBATIONS

In this case, the displacement  $\delta \mathbf{r}$  has three distinct components— $\delta r$ ,  $r\delta\theta$ ,  $r \sin \theta \delta\varphi$ —of which  $\delta r$ , like all other perturbations  $\rho'$ ,  $p'$ ,  $\phi'$ , must be represented by an expression of the general form (4.1) and (4.2), while  $r\delta\theta$  and  $r \sin \theta \delta\varphi$  will be proportional to  $\partial Y_l^m / \partial \theta$  and  $\partial Y_l^m / \partial \varphi$ , respectively. In this case, the elimination of all but one of the dependent variables will, in general, lead to a fourth-order differential equation whose unwieldy coefficients depend in a complicated fashion on  $\sigma^2$  (Ledoux and Walraven 1958, § 75).

Here the boundary conditions for the perturbation  $\phi'$ ,

$$\phi'_{i,R} = \phi'_{e,R} = \frac{C}{R^{l+1}}, \quad (4.7)$$

$$\left( \frac{\partial \phi'_i}{\partial r} \right)_R + \frac{l+1}{R} \phi'_{i,R} = - (4\pi G \rho \delta r)_R,$$

where the indices  $i$  and  $e$  refer, respectively, to the internal and external side of the surface, must be taken explicitly into account. Up to now, the complete general problem has not been solved.

In a few special instances, either  $\phi'$  may be estimated directly, or its elimination may be carried out without the repeated use of Laplace's equation (2.69), which, in the general case, is the operation responsible for the raising of the order of the equation.

The simplest example of the first type is provided by the homogeneous incompressible sphere (Thomson 1863) which is capable of non-radial oscillations only and for which  $\phi'$  is determined entirely by the radial displacement of the surface. Despite the fact that this model is very far from an actual star, it is interesting for two reasons. First, its frequencies are known explicitly, and their expressions,

$$\sigma_l^2 = \frac{4\pi G \rho}{3} l \frac{2l-2}{2l+1}, \quad l \geq 2, \quad (4.8)$$

show that they are independent of  $m$ , and this degeneracy ( $2l+1$  eigenfunctions associated with each  $\sigma_l$ ) will be encountered in all models as long as perturbing factors such as rotation, magnetic field, or tides are absent.

On the other hand, if one neglects  $\phi'$  in the problem, the last factor in equation (4.8) is replaced by 1, but since, in any case, it tends rapidly toward unity with increasing  $l$ , this suggests that, in more complicated cases, a reasonable approximation for  $\sigma_l$  might be obtained by simply dropping the term in  $\phi'$  in the equation of motion.

This is confirmed by the discussion (Sauvenier-Goffin 1951) of the non-radial perturbations of the homogeneous compressible model, which, as shown by Pekeris (1938; cf. also Ledoux and Walraven 1958, § 75), are also governed by a second-order differential equation which may be written

$$(1-x^2) \frac{d^2 a}{dx^2} + \frac{da}{dx} \cdot \frac{2-6x^2}{x} + a \left[ \frac{2\omega^2}{\Gamma_1} + \frac{8}{\Gamma_1} - 6 - \frac{2l(l+1)}{\Gamma_1 \omega^2} - l(l+1) \frac{1-x^2}{x^2} \right] = 0, \quad (4.9)$$

$$x = \frac{r}{R}, \quad a = \frac{\rho'}{\rho}, \quad \omega^2 = \frac{3\sigma^2}{4\pi G \rho}. \quad (4.10)$$

Although still far from a significant stellar model, this case illustrates another important aspect of the problem. Using an argument introduced by Cowling (1941), we see that, if  $\omega^2$  is very large ( $1/\omega^2$  negligible), the problem reduces essentially to a Sturm-Liouville problem admitting a discrete spectrum of positive eigenvalues  $\omega^2$  increasing indefinitely. On the other hand, if  $\omega^2$  is sufficiently small (term in  $\omega^2$  negligible), we get an infinite positive discrete spectrum for  $(-1/\omega^2)$ . Reverting to the complete problem, we may expect two distinct discrete spectra for  $\omega^2$ , one starting at a minimum positive value and tending to  $+\infty$  (stable modes) and another one starting at a minimum negative value and converging toward zero.

This is confirmed by the exact polynomial solutions

$$a_{l,k} = x^l \sum_{j=0}^k C_{2j} x^{2j}, \quad k = 0, 1, 2, \dots; \quad l = 2, 3, 4, \dots, \quad (4.11)$$

corresponding to the exact eigenvalues,

$$\omega_{l,k}^2 = D_k \pm [D_k^2 + l(l+1)]^{1/2}, \quad (4.12)$$

where

$$D_k = -4 + \Gamma_1[k(2k+2l+5) + 3 + 2l].$$

Each pair of eigenvalues (4.12) always contains a positive and a negative one except if  $l = 0$ , when one of the spectra vanishes and the other reduces to that for purely radial oscillations, with the usual instability entering through the fundamental mode ( $k = 0$ ) for  $\Gamma_1 < \frac{4}{3}$ .

Although, as far as  $a = \rho'/\rho$  is concerned, there corresponds only one solution to each pair of eigenvalues (4.12), the corresponding displacements are different, the stable mode having always one more node ( $\delta r = 0$ ) than the unstable one.

Contrary to the case of radial oscillations, the amplitudes of  $\rho' = a\rho$  and  $p'$  vanish at the center. This is a general property of the non-radial oscillations which always have a loop as well as a node at the center. For a given  $k$ ,  $|\omega^2|$  increases with  $l$ , so that, in particular, the strength of the dynamical instability increases when the horizontal dimensions of the perturbation decrease. On the other hand, for a given  $l$ , the two sets of  $\omega^2$  increase algebraically with  $k$ , so that, in particular, the instability decreases with the vertical wave length.

The origin of the instability here can be traced back to the fact that, for this model, the radial component  $A$  of  $\mathbf{A}$  (cf. [2.18] and [2.19]) reduces to  $-(1/\Gamma_1 p)dp/dr$ , which is everywhere positive and thus violates Schwarzschild's criterion at every point in the star. When this happens, dynamical instability always occurs for some type of non-radial perturbation, while the stability toward purely radial displacement is not at all affected by the value of  $A$ .

Another interesting example is also provided by Roche's model, in which an envelope with a density distribution  $\rho = a/r^2$  surrounds a point mass  $M(1 - 3a/R^2\bar{\rho})$  at the center. This model has the interesting property that, while for  $\Gamma_1 < \frac{3}{2}$  it is everywhere convectively unstable, for  $\Gamma_1 > \frac{3}{2}$  the convective instability extends only over the region

$$\frac{r}{R} > \left(1 - \frac{3}{2\Gamma_1}\right)^{1/3}.$$

Furthermore, for  $a \rightarrow 0$ , the differential equation is of the second order again. Unfortunately, in general, it possesses an irregular singularity at the center which, up to now, has prevented a general discussion.

However, for  $\Gamma_1 = \frac{3}{2}$ ,  $A = 0$  at  $r = 0$ ,  $A > 0$  everywhere else, this difficulty disappears, and Ottelet (1960) has shown that, in this case, the eigen-solutions are polynomials in  $r$  and that the spectrum still falls into two parts but that, if  $N$  is the degree of the polynomials and  $l$  that of the spherical harmonics, negative eigenvalues (unstable modes) occur only when

$$l \geq 3N + 3.$$

This means that instability will occur only if the horizontal wavelength ( $\propto 1/l$ ) is small enough compared with the vertical wavelength ( $\propto 1/N$ ), a result already hinted at in the case of the homogeneous compressible model and which was emphasized in the general case by Ledoux (1949, chap. iii).

Applying Cowling's reasoning when  $\Gamma_1 \neq \frac{3}{2}$ , the equation reduces for large  $\omega^2$  ( $\omega^2 \gg l^2$ ) to

$$\frac{d^2\xi}{dx^2} + \frac{d\xi}{dx} \left[ \frac{1-4x^3}{x(1-x^3)} \right] + \xi \left[ \frac{3\omega^2 x}{\Gamma_1(1-x^3)} - \frac{l(l+1)}{x^2} - \frac{3(3\Gamma_1-4)}{\Gamma_1 x^2(1-x^2)} \right] = 0,$$

which is again of the Sturm-Liouville type and admits an infinite discrete spectrum of positive  $\omega^2$ . On the other hand, for  $\omega^2$  very small (in particular  $\omega^2 \ll l^2$ ), the equation becomes

$$\frac{d^2\xi}{dx^2} + \frac{d\xi}{dx} \frac{4}{x} + \xi \left\{ -\frac{2}{\omega^2} \frac{l(l+1)}{x^5} \left[ \frac{3}{2\Gamma_1(1-x^3)} - 1 \right] - \frac{l(l+1)}{x^2} - \frac{3}{\Gamma_1} \frac{1+4x^3}{x^2(1-x^3)^2} \right\} = 0,$$

where  $(-1/\omega^2)$  plays the role of the parameter. For  $\Gamma_1 < \frac{3}{2}$ , the coefficient of  $(-1/\omega^2)$  is positive everywhere, and, although the problem is no longer strictly of the Sturm-Liouville type, one may still expect for  $\omega^2$  an infinite discrete spectrum of negative eigenvalues converging toward zero, in agreement with the superadiabatic gradient prevailing in the whole star. But if  $\Gamma_1 > \frac{3}{2}$ , the coefficient of  $(-1/\omega^2)$  changes sign in the interval  $0 \leq x \leq 1$  and now a part of the spectrum for  $(-1/\omega^2)$  should be negative (Ince 1944), corresponding to eigen-solutions having small amplitudes in the superadiabatic part of the star. Thus, as the convectively unstable region shrinks, the more restricted do the unstable modes become.

In the case of the polytropes, neglecting the perturbation  $\phi'$  of the gravitational field, Cowling (1941) found that the spectrum for  $\sigma^2$  falls into two parts also, one tending toward  $+\infty$  and the other to zero, and he denoted the corresponding modes, respectively, as  $p$  and  $g$  modes. He also showed that if  $n$  is the polytropic index and if  $\Gamma_1$  is a constant, the eigenvalues  $\sigma_o^2$  all become negative if

$$\frac{n}{n+1} < \frac{1}{\Gamma_1},$$

which is also the condition for the gradient to be superadiabatic throughout ( $A > 0$ ). On the other hand, in the case of a subadiabatic gradient [ $A < 0$ ,  $n/(n+1) > 1/\Gamma_1$ ], the  $\sigma_o^2$ 's, as well as the  $\sigma_p^2$ 's, are all positive.

If we now come to the general physical case (cf. Ledoux and Walraven 1958, §§ 74, 75, and 79) and again neglect  $\phi'$ , as well as the turbulent and non-

adiabatic terms, the second-order differential equation for the radial displacement  $\delta r$  may be written

$$\frac{d}{dr} \left\{ \frac{\rho}{p^{2/\Gamma_1} \{ [\bar{l}(l+1)/\sigma^2] - (\rho r^2/\Gamma_1 p) \}} \frac{dv}{dr} \right\} = \frac{1}{r^2} (\sigma^2 + A g) \frac{\rho}{p^{2/\Gamma_1}} v, \quad (4.13)$$

where  $g$  is the absolute value of the gravity at  $r$  and

$$v = r^2 p^{1/\Gamma_1} \delta r$$

must satisfy the boundary conditions

$$v = 0 \quad \text{at} \quad r = 0 \quad \text{and} \quad r = R.$$

Equation (4.13) multiplied by  $v$  and integrated from 0 to  $R$ , taking the above conditions into account, yields

$$\begin{aligned} \sigma^2 \int_0^R \frac{\rho v^2}{r^2 p^{2/\Gamma_1}} dr + \int_0^R \frac{A g \rho}{r^2 p^{2/\Gamma_1}} v^2 dr \\ + \int_0^R \frac{\rho (dv/dr)^2 dr}{\{ [\bar{l}(l+1)/\sigma^2] - (\rho r^2/\Gamma_1 p) \} p^{2/\Gamma_1}} = 0. \end{aligned} \quad (4.14)$$

If  $\sigma^2$  is large ( $p$ -modes of high orders), this reduces to

$$\sigma_p^2 = \frac{\int_0^R \frac{\Gamma_1}{r^2 p^{2/\Gamma_1-1}} \left( \frac{dv}{dr} \right)^2 dr - \int_0^R \frac{A g \rho}{r^2 p^{2/\Gamma_1}} v^2 dr}{\int_0^R \frac{\rho v^2}{r^2 p^{2/\Gamma_1}} dr}, \quad (4.15)$$

which shows that if  $A$  is everywhere negative (subadiabatic gradient),  $\sigma_p^2$  is always positive. If the gradient is superadiabatic in some part of the star ( $A > 0$ ), we see that, at least for high enough modes ( $dv/dr$  large),  $\sigma_p^2$  is still positive and increases indefinitely with the order of the mode.

On the other hand, if  $\sigma^2$  is small ( $g$ -modes), equation (4.14), where  $\rho r^2/\Gamma_1 p$  is neglected as compared with  $(1/\sigma^2)$  in the last integral, leads to

$$\sigma_g^2 = - \frac{l(l+1) \int_0^R \frac{A g \rho v^2}{r^2 p^{2/\Gamma_1}} dr}{l(l+1) \int_0^R \frac{\rho v^2}{r^2 p^{2/\Gamma_1}} dr + \int_0^R \frac{\rho}{p^{2/\Gamma_1}} \left( \frac{dv}{dr} \right)^2 dr}, \quad (4.16)$$

which shows that the  $\sigma_g^2$ 's are always positive if  $A$  is everywhere negative (subadiabatic gradient). If  $A$  is positive everywhere (superadiabatic gradient throughout), the  $\sigma_g^2$ 's all become negative, leading to dynamical instability. If  $A$  is positive in some part of the star only, the occurrence of negative  $\sigma_g^2$ 's depends on the relative extent of these superadiabatic regions.

In all cases, the absolute value of  $\sigma_g^2$  decreases when the order of the mode increases ( $dv/dr$  increases). Also, for a mode of a given order,  $|\sigma_g^2|$  increases

with  $l$ . Thus, as long as the dissipative effects of viscosity and conduction are neglected, the instability, if present, will be the stronger, the smaller the horizontal wavelength and the longer the vertical wavelength, a result already referred to above and which has also been confirmed by Skumanich (1955) for a polytropic atmosphere.

Let us note also that the integral in the numerator of equation (4.16) is simply the total work of the buoyancy force counted positively in a superadiabatic region. In fact, in the case of small horizontal and large vertical wavelengths, formula (4.16) may be written

$$\sigma_g^2 = - \frac{\int_0^M A g (\delta r)^2 dm}{\int_0^M (\delta r)^2 dm} = \frac{\int_0^V (A r) \xi^2 dV}{\int_0^I \xi^2 dI}, \quad (4.17)$$

with  $\xi = \delta r/r$  and the same notation as in equation (3.13). Thus essentially, this type of instability will occur when the gravitational potential energy available for release in the superadiabatic regions is larger than the necessary work against gravitation in the stable ones.

The fact that this type of instability, just like ordinary convection, finds its origin in the existence of superadiabatic gradients renders the appraisal of its physical significance rather delicate. If, by somewhat artificial boundary conditions at the top and the bottom of a superadiabatic region, all motions could be made to vanish outside, formula (4.16) or (4.17) would then always yield negative values for the  $\sigma_g^2$ 's. Thus, whatever the extent of a superadiabatic region, if motions are limited to it, which is essentially the point of view adopted in the treatment of convection, some instability will always manifest itself *locally*, leading to a mixing of this zone and lowering the gradient close to its adiabatic value.

Since, in the course of stellar evolution, superadiabatic gradients are likely to develop very gradually, starting first in thin zones and growing in extent very slowly, it seems reasonable to expect that convection would always follow very closely, preventing the occurrence of extensive regions with appreciable superadiabatic gradients such as those once advocated by Unsöld (1930) and Biermann (1939) to explain ordinary novae.

Of course, convection does not reduce the gradients exactly to their adiabatic values but, as recalled previously (cf. § 2.2.1), the subsisting superadiabacy is extremely small in most of the star. Nevertheless, in the case of a star with a large convection zone involving most of its mass, it might be interesting to assess the existence and the type of non-radial modes of motion leading to the kind of dynamical instability discussed here. But, even if this is realized, it does not mean that the star would actually be shattered into pieces, but, occasionally, the fortuitous building-up of a suitable perturbation might lead to the ejection

of matter in the form of local jets. More important probably, it might result in a general remixing of the star, involving the stable as well as the unstable regions, the star settling down afterward in a state of lower total potential energy.

In the very external layers, fairly large superadiabatic gradients may persist because of the inefficiency of the convective energy transport there. But, in this case, the mass involved and the gravitational potential energy available are usually very small, and no large-scale consequences can be expected, although privileged displacements giving rise to local ejections or surges might still exist.

### § 5. VIBRATIONAL STABILITY

We have already seen in § 3, at least for radial motions, that if we assume dynamical stability, the effect of the non-adiabatic terms on the corresponding short time-scale oscillations of frequencies  $\sigma$  is to introduce a "damping term,"  $\exp(-\sigma' t)$ , which will lead to an increase or a decrease of the amplitude in time, depending on whether  $\sigma'$  as given by equation (3.14) is negative (vibrational instability) or positive (vibrational stability). The same will, of course, remain true for more general motions such as the non-radial oscillations considered in § 4, but for the sake of simplicity we shall again divide the discussion into two parts.

#### 5.1. RADIAL PERTURBATIONS

If viscous forces and the possible existence of convection zones are taken into account, expression (3.14) of  $\sigma'$  must be generalized, and the perturbation method (Rosseland 1931, 1932) yields, for each mode  $k$  of radial oscillation, a "damping constant,"

$$\sigma'_k = \frac{2}{3J_{k,a}} \int_0^M \frac{\eta r^2}{\rho} \left( \frac{d\xi_k}{dr} \right)_a^2 dm - \frac{1}{2\sigma_{k,a}^2 J_{k,a}} \int_0^M \left[ \frac{\delta T}{T} \delta(\dots) + \frac{2}{3} \frac{\delta \rho}{\rho} \delta(\dots) \right]_{a,k} dm, \quad (5.1)$$

with the same definition of  $J$  as in (3.10) and where the brackets represent the corresponding expressions in (2.72) and (2.73) or (5.2) below. The indices  $k$  and  $a$  recall that the evaluation of the second member should be carried out, using the solution corresponding to the  $k$ -mode of adiabatic pulsation.

The dissipation by viscous forces takes a particularly simple form for radial motions and is represented by the first term on the right of equation (5.1). In radiative regions, assuming that purely radial motions do not create turbulence,  $\eta$  is the sum of the radiative and molecular coefficients of viscosity, while, in a convective zone, at least if the period of oscillation is larger than the mean lifetime of a turbulent element, it should be identified with  $\eta_t$ , the coefficient of turbulent viscosity, which is much larger than the first two.

The form (5.1) of  $\sigma'$  is obtained only after an integration by parts, using the complete boundary condition at  $r = R$ , generalizing equation (3.8), namely,

$$\begin{aligned}
\delta(p + p_t) = & -(\Gamma_1 p + \frac{5}{3} p_t) \left( 3\xi + r \frac{d\xi}{dr} \right) \\
& + \frac{\Gamma_3 - 1}{i\sigma} \rho \delta \left\{ \epsilon_1 + \epsilon_2 - \epsilon_3 - \frac{d[4\pi r^2(F_R + F_t)]}{dm} \right\} \\
& + \frac{2}{3} \frac{\rho}{i\sigma} \delta \left[ \epsilon_4 - \epsilon_2 - \frac{d(4\pi r^2 F_2)}{dm} - \frac{1}{\rho} \langle V \text{grad } p \rangle \right] = 0,
\end{aligned} \quad (5.2)$$

and noting that the dynamical coefficient of viscosity  $\eta$  decreases to zero with  $\rho$  at the surface. In practice, since the turbulent terms, as well as the energy generation, vanish before reaching the surface, condition (5.2) reduces to

$$\delta p = -\Gamma_1 p \left( 3\xi + r \frac{d\xi}{dr} \right) - \frac{\Gamma_3 - 1}{i\sigma} \frac{d\delta L_R(r)}{4\pi r^2 dr} = 0 \quad \text{at } r = R, \quad (5.3)$$

where

$$L_R(r) = 4\pi r^2 F_R(r).$$

With  $p$  vanishing at  $r = R$ , this implies that, close enough to the surface,  $\delta L_R(r)$  ceases to vary appreciably with  $r$ , i.e.,

$$\left( \frac{d\delta L_R(r)}{dr} \right)_{r \rightarrow R} \rightarrow 0. \quad (5.4)$$

We shall see later that this makes it necessary to exercise some care in the evaluation of the integrand in equation (5.1) close to the surface, but we shall first discuss the influence of the different terms in the main interior.

**5.1.1. The main stellar interior.**—From now on, except when specifically mentioned, we shall be concerned with the fundamental mode, and we shall omit the  $k$ -indices.

In a radiative region, the effects of viscosity will be small, and equation (5.1) reduces to equation (3.14). The term corresponding to the energy generation (cf. eq. [2.48]),

$$\delta\epsilon_1 = \epsilon_1 \left( \frac{\delta\rho}{\rho} + \nu \frac{\delta T}{T} \right)_a = \epsilon_1 \left( \frac{1}{\Gamma_3 - 1} + \nu \right) \left( \frac{\delta T}{T} \right)_a, \quad (5.5)$$

is always of the same sign as  $(\delta T/T)_a$  and always tends to render  $\sigma'$  negative and thus contributes to the instability. On the other hand, the second term, in which the variation of the total radiative flux  $L_R$  is given, for the opacity law (2.8), by

$$\delta L_R(r) = L_R(r) \left[ 4\xi + (4+n) \frac{\delta T}{T} - m \frac{\delta\rho}{\rho} + \frac{(d/dr)(\delta T/T)}{(1/T)(dT/dr)} \right]_a, \quad (5.6)$$

usually contributes a positive part to  $\sigma'$  and thus favors stability.

In all stellar models for ordinary masses and comprising an important radiative zone, all the amplitudes  $\xi_a$ ,  $(\delta\rho/\rho)_a$ , and  $(\delta T/T)_a$  increase fairly rapidly from the center to the surface. Since for any of the known thermonuclear reac-



tions,  $\epsilon_1$  is appreciable only close to the center, the corresponding destabilizing term in (5.1) or (3.14), as pointed out by Cowling (1935), is weighted by a small factor as compared with the conduction term in  $\delta L_R$ , which can be large in the external layers.

In those conditions, one should expect ordinary stars to be very stable, and, indeed, one finds (Cowling 1935, Ledoux 1941) that the critical value of  $\nu$ , say  $\nu_c$ , bringing about vibrational instability is much larger, say of the order of  $10^3$ – $10^4$ , than the actual values of  $\nu$ .

However, for larger and larger masses,  $(1 - \beta) = p_R/p$  increases and  $\Gamma_1$ ,  $\Gamma_2$ , and  $\Gamma_3$  decrease and tend toward  $\frac{4}{3}$ , a limiting case ( $M \rightarrow \infty$ ) for which  $\xi_a$ ,  $(\delta p/p)_a$  and  $(\delta T/T)_a$  would all become constant throughout the star and  $\nu_c$  would become of the order of 1.5–0.5, depending on whether the opacity is mainly due to photoionization and free-free transitions or to electron scattering. These critical values of  $\nu_c$  are now so small that, for any law of energy generation of the type (2.48), one should expect that there is a finite critical mass, say  $M_c$ , for which  $\nu_c$  will be reduced to a value of the order of the actual  $\nu$  and which will be on the verge of vibrational instability.

Using the standard model and Kramers' law of opacity ( $m = 1$ ,  $n = 3.5$ ), Ledoux (1941) found that, for the carbon cycle, the critical mass was approximately  $M_c \simeq 100 M_\odot \bar{\mu}^{-2}$ . Recently, Schwarzschild and Härm (1959), using refined models for massive stars and noting that, with the large predominance of H and He admitted now, electron scattering ( $m = 0$ ,  $n = 0$ ) is the main source of opacity, have reduced the limit of stable masses to  $M_c \simeq 60 M_\odot$ . The reduction is mainly due to the different opacity laws used and, to a smaller extent, to the fact that the actual models possess a large convective core, which makes the rate of increase of  $\xi_a$  through the star somewhat smaller than in the standard model.

For stars formed initially from pure hydrogen, as may have been the case for primeval stars, the critical mass  $M_c$  is likely to be much larger. Ledoux and Boury (1960), taking only the proton-proton chain into account, found  $M_c \simeq 1200 M_\odot$ .

However, as pointed out by other authors (Levéé and Hilton 1960, Ezer 1961), enough carbon may already have been built in the central region (an abundance of the order of  $10^{-12}$  is sufficient) by the end of the gravitational contraction to make the carbon cycle more efficient than the  $p$ - $p$  chain. In the relevant range of physical conditions, the temperature and density sensitivity of the carbon cycle itself is very small, but nevertheless its influence reduces  $M_c$  to a value of the order of  $300 M_\odot$  (Boury 1963). On the other hand, the continued production of carbon raises new problems, but, although it makes for a rather rapid evolution, it seems that when all factors are properly taken into account, the latter could still be represented by a series of quasi-static models. Although highly speculative this study should be continued to clear up the starting point of element synthesis in stars and to follow the history of such

large masses even if the discussion of their stability becomes entangled with that of difficult phases of stellar evolution.

Anyway, even for smaller masses, it is only in the light of stellar evolution that the real significance of the criterion of vibrational instability can be ascertained. Up to now, the critical masses given above refer to stellar models having just reached a state in which the luminosity is exactly balanced by the energy generated in the interior by thermonuclear reactions (cf. eq. [2.66]). Schwarzschild and Härm (1959) have already pointed out that, as evolution proceeds, the changes brought about in the stellar model by the conversion of hydrogen into helium will restore the pulsational stability of masses slightly larger than  $M_e$  so soon that hardly any serious consequences can follow. Using the condition that, to be of consequence, the instability should persist long enough for the velocity amplitude to reach the escape velocity at the surface, they could raise the effective limit of possible masses to  $M'_e \simeq 65 M_\odot$ .

However, the evolution previous to reaching the main sequence is also of interest. For  $M > M_e$ , vibrational instability should occur some distance above the main sequence, where a part of the radiated energy is already generated by thermonuclear reactions and a part is still due to gravitational contraction, which, however, will not affect the instability directly, as it is proportional to the time rate of the variation of  $T$ . This distance above the main sequence will depend on  $(M - M_e)$ , but it will probably never be very large, as  $\epsilon_1$  depends on a high power of  $T$  and decreases very rapidly with this distance. Anyway, this means that vibrational instability will always begin by being very mild ( $\sigma' \simeq 0$ ), but, as the contraction proceeds, it will strengthen, and a study of its interaction with the general contraction, including possibly some of the second-order terms, would be very welcome.

Moving the generation of energy from the center toward the exterior favors instability. However, to get an appreciable effect, one has to push the energy-producing shell much farther out than permitted by the Chandrasekhar-Schönberg limit (Chandrasekhar and Schönberg 1942) for the isothermal core (cf. Ledoux 1941).

Of course, in special cases, nuclear reactions may take place in the external regions, but the energy liberated is only a very small fraction of the luminosity, and, in the presence of different types of nuclear reactions, only those contributing appreciably to the total flux influence its vibrational stability.

The influence of the model itself on vibrational stability can best be discussed in terms of its central condensation  $\rho_c/\bar{\rho}$ . As this ratio increases,  $\xi_a$  increases more and more rapidly from the center to the surface (cf. Ledoux and Walraven 1958, Table 12), and, as we have seen, this reinforces the vibrational stability of the model (cf., for instance, J. P. Cox 1955). Conversely, the smaller the central condensation, the easier it is to bring about vibrational instability.

The white dwarfs provide an example (Ledoux and Sauvenier-Goffin 1950) in which the combination of this factor with low values of the  $\Gamma$ 's in the interior

reduces the variation of  $\xi$ , so much that practically any type of nuclear reactions would render the star vibrationally unstable.

The white dwarf stage is also incompatible with nuclear reactions in the degenerate interior from the point of view of secular stability (Mestel 1952), but, in the discussion of the approach to this stage, the consideration of vibrational instability may be important. In those phases of the star's life, most of the hydrogen in the interior must already have been burned, and, according to Schatzman (1945), the rest will diffuse rapidly into the external layers where the temperature may become high enough for nuclear reactions to proceed while the interior becomes at least partially degenerate. This state is not so different from some of the models discussed by Ledoux and Sauvenier-Goffin (1950), and vibrational instability would again be rather likely to lead to oscillations of increasing amplitude until, at expansion phases, the velocity in the external layers reaches the velocity of escape, allowing the star to rid itself of its last hydrogen and to settle definitely in the white dwarf stage. Chapter 5 (§ 2.3) of the present volume, by L. Mestel, provides a more detailed and up to date summary of the present situation as far as the applications of these stability considerations to white dwarfs are concerned.

For normal stars, the physical model with the smallest mass concentration ( $\rho_c/\bar{\rho} \simeq 6$ ) is the polytrope  $n = \frac{3}{2}$ , which can be used to represent a star of fairly small mass ( $\beta \rightarrow 1$ ,  $\Gamma_1 \rightarrow \gamma = \frac{5}{3}$ ) in convective equilibrium throughout. In fact, it was once suggested by Biermann (1935) that such stars should be vibrationally unstable. However, Cowling (1938) pointed out that a fairly small external zone in which radiative transfer prevails and in which the variation of the total flux is again given by equation (5.6) would restore an appreciable stability to the star. In this case, a rough estimate yields for  $\nu_c$  a value of the order of 9. As this is smaller than the actual  $\nu$  for the carbon cycle, the latter would render such stars unstable. However, at present, the available evidence (Limber 1958) suggests that such models are significant only for small, cool stars in which the energy generation is due to the  $p$ - $p$  chain with a  $\nu$  of the order of 4 or 5, i.e., smaller than  $\nu_c$ .

Nevertheless, the margin of stability is relatively small, and it may be worthwhile to rediscuss the problem carefully, trying to evaluate as well as one can the effects of convection. This encounters two types of difficulty. The most fundamental one relates to the question of knowing whether or not the convection adjusts itself to the oscillation. It has been suggested (cf., for instance, Schwarzschild and Härm 1959) that if the mean lifetime of a turbulent element is large compared with the pulsation period, this adjustment would be slight and with more or less random phase lags, so that all the variations of the convective terms and especially  $\delta L_i$  may as well be neglected. However, it might be more reasonable to consider that this applies only to  $\bar{l}_i$  and  $\bar{e}_i$  while the other factors in the expressions of  $L_i$  and  $\epsilon_2$  will vary in phase with the pulsation, and the corresponding values of  $\delta L_i$  and  $\delta \epsilon_2$  are not at all negligible.

If, on the contrary, one treats the adjustment as instantaneous, which is reasonable only if the relaxation time of convection is short compared with the period, one has to use the general expression of  $\sigma'$ , which after elimination of  $\delta\epsilon_3$ , using its definition (2.31), may be written

$$\begin{aligned}
 2\sigma_a^2\sigma'J_a = & \frac{4\sigma_a^2}{3} \int_{M_i} \frac{\eta_i r^2}{\rho} \left( \frac{d\xi}{dr} \right)_a^2 dm - \int_0^M \left( \frac{\delta T}{T} \right)_a \left( \delta\epsilon_1 - \frac{d\delta L_R}{dm} \right)_a dm \\
 & + \int_{M_i} \left( \frac{\delta T}{T} \frac{d\delta L_i^*}{dm} + \frac{2}{3} \frac{\delta\rho}{\rho} \frac{d\delta L_2}{dm} \right)_a dm \\
 & - \int_{M_i} \left( \Gamma_3 - \frac{5}{3} \right) \left( \frac{\delta\rho}{\rho} \right)_a \left[ \delta\epsilon_2 + \delta \left( 4\pi r^2 \bar{V}_r \frac{d\rho}{dm} \right) \right]_a dm,
 \end{aligned} \tag{5.7}$$

where the index  $M_i$  to some of the integrals indicates that they bear only on the regions in convective equilibrium and where  $L_i^*$  and  $L_2$  correspond to  $F_i^*$  and  $F_2$  as defined in § 2.2.2.

At this stage, one encounters the second difficulty that arises in the evaluation of the variations of the different convective terms due to the lack of an adequate theory of stellar convection. It is generally assumed that  $F_2$  and  $L_2$  and their variations are negligible, as well as the effects of  $\epsilon_4$ , which gives rise to a third-order term, and that

$$\frac{\delta \bar{l}_i}{\bar{l}_i} \simeq \frac{\delta r}{r} = \xi.$$

The variations of all the other relevant quantities  $\bar{c}_i$ ,  $D$ ,  $\bar{V}_r$ ,  $\epsilon_2$ , and  $L_i^*$  may then be computed from their definitions (cf. Ledoux and Walraven 1958, §§ 65 and 67) and, in particular if  $\Gamma_1$ ,  $\Gamma_2$ , and  $\Gamma_3$  reduce to a constant  $\gamma$ , we get the simple expression

$$\frac{\delta L_i^*}{L_i^*} = \xi \left( 1 - 3\gamma \right) - \left( \gamma + \frac{4}{3} \right) r \frac{d\xi}{dr}.$$

Taking all this into account, the third integral in (5.7) reduces after an integration by parts to

$$- \int_{M_i} \delta L_i^* d/dm \left( \delta T/T \right)_a dm,$$

since  $\delta L_i^*$  as well as  $L_i^*$  should vanish at the boundaries of a convective region. According to its expression above,  $\delta L_i^*$  is positive at compression while, at the same phase,  $(\delta T/T)$  increases with  $m$  so that this integral contributes always negatively to  $\sigma'$  and thus exerts a destabilizing influence. If, furthermore, as in the small, cool stars referred to above,  $\gamma = \frac{5}{3}$ , the last term in (5.7) vanishes altogether, and the amount of numerical work involved in taking the effects of convection into account is reduced to a minimum.

In the external layers, where convection is usually due to the ionization of H and He, the problem becomes much more complex, as we must study the dis-

placement of the ionization equilibrium in the course of the pulsation to evaluate  $\delta[(\Gamma_2 - 1)/\Gamma_2]$ ,  $\delta A_{T,p}$ , and  $\delta C_p$  as given by (2.41), (2.43), and (2.44). However, according to our previous remark that, at any place, only one type of ion (say  $i$ ) is in a critical stage of ionization, equation (2.40) and the definitions above it, where the Lagrangian variation  $\delta$  may be substituted for  $d$ , will enable us to carry out all necessary computations.

**5.1.2. Influence of the external layers.**—However, in these external layers, we encounter another type of difficulty. Expression (5.1) for  $\sigma'$  implies that the non-adiabatic terms are small everywhere, but this ceases to be the case very close to the surface. Indeed, the rate of non-adiabatic heating as seen from the second term on the right of equation (2.74) is simply equal to the ratio of the energy accumulated per unit mass and unit time to the heat content of the material. This ratio is extremely small in the interior but increases rapidly close to the surface, and we may take, as an upper limit to the adiabatic region, the layer where the two terms on the right of equation (2.74) become of the same order of magnitude. The corresponding critical radius  $R_a$  or critical mass  $M_a$  are best determined numerically in each case, and they correspond usually to temperatures of the order of a few  $10^4$  degrees (cf. Ledoux and Walraven 1958, § 67).

As we go higher up and approach or enter the atmosphere proper, the heat capacity finally becomes very small, and the relaxation time of radiative equilibrium becomes very short (Whitney 1955), or, in other words, the diffusion speed of a photon there becomes large compared with the velocity of sound, so that, past a certain level (say  $R^*$  or  $M^*$ ), the spatial variations of  $\delta L_R$  must become very small and the layers above  $R^*$  have a negligible influence on vibrational stability. In fact, there is a real danger in using the adiabatic solution to compute  $d\delta L/dr$  in this region because this would yield values which, instead of vanishing at  $r = R$  in agreement with equation (5.4), would tend to a finite limit, the non-adiabatic part of  $\delta T$  tending toward infinity. This is, of course, due to the fact that the adiabatic solution satisfies only the adiabatic boundary condition (3.8) and not the complete condition (5.2) or (5.3).

As a consequence, the integrals in the previous expressions for  $\sigma'$  should actually be limited to  $M_a$ , and, to the value thus obtained, say  $\sigma'_a$ , should be added the generalized contribution of the region  $M_a$  to  $M^*$ , so that  $\sigma'$  becomes (Ledoux and Walraven 1958, §§ 63 and 70)

$$\sigma' = \sigma'_a + \frac{1}{2\pi J_a \sigma_a} \int_{M_a}^{M^*} \int_0^{2\pi/\sigma_a} \left[ \left( \frac{\delta T}{T} \right)_a + \left( \frac{\delta T}{T} \right)_{n.a.} \right] \frac{d\delta L}{dm} dm dt, \quad (5.8)$$

noting that  $\epsilon_1$  vanishes there and assuming that the effects of convection are negligible.

It can be argued (Eddington 1941, 1942) that, between  $M_a$  and  $M^*$ , the non-

adiabatic part of the pressure perturbation  $(\delta p/p)_{n.a.}$  always remains very small, and then equations (2.72) and (2.74) give the relation

$$\frac{d}{dt} \left( \frac{\delta T}{T} \right)_{n.a.} = \left[ \frac{3\beta(\Gamma_3 - 1)^2 C_v}{2 c_v} - \Gamma_1 \right] \frac{1}{\Gamma_1 C_v T} \frac{d\delta L}{dm} \simeq - \frac{1}{\Gamma_1 C_v T} \frac{d\delta L}{dm}.$$

This shows that the term in  $(\delta T/T)_{n.a.}$  in equation (5.8) integrated over a period vanishes, so that the last term reduces to

$$\frac{1}{2\pi\sigma_a J_a} \int_{M_a}^{M^*} dm \int_0^{2\pi/\sigma_a} \left( \frac{\delta T}{T} \right)_a \frac{d\delta L}{dm} dt.$$

Its value depends both on the phase shift  $\varphi$  which arises between  $\delta L$  and  $(\delta T)_a$  across the layer  $(M_a - M^*)$  and on their variations in absolute value, especially in the case of  $\delta L$ .

A pure phase shift  $\varphi$  would always favor instability, and the effect would be maximum for  $\varphi = 180^\circ$ . However, such values can be reached only if the heat capacity of the layer  $(M^* - M_a)$  is large, as may be the case when this region comprises the ionization zone of H and (or) part at least of those of He. Let us note, however, that in extremely massive stars along the main sequence, where these ionizations occur practically in the atmosphere around or above  $M^*$ , their effects will be negligible, and our previous conclusion on the limiting mass of stable stars remains unaffected. In ordinary main-sequence stars, on the other hand, the two levels  $M_a$  and  $M^*$  tend to become very close, and layers above  $M_a$  may probably be safely neglected.

In cool supergiants, the situation is more favorable, and a large phase lag of the order of  $90^\circ$  attributed to the ionization of H was first advocated by Eddington (1941, 1942) as the source of instability causing the pulsation of the cepheids. Physically, it means that heat is accumulated in the critical region  $(M^* - M_a)$  in the form of ionization energy at the expense of the flux during the contraction and liberated at expansion.

It is now doubtful whether the ionization of H alone could actually lead to instability (cf. Ledoux and Walraven 1958, §§ 69 and 70), but Jevakhin (1959*a*, *b*, *c*) in a series of papers has come to the conclusion that the second ionization of He could be more efficient. However, as it occurs deeper in the star, the departure from adiabacy may not yet be very large there, and the destabilizing influence may be due more to the lowering of the generalized  $\Gamma$ 's and the corresponding reductions in the amplitude of  $(\delta T)_a$  and  $(\delta \kappa)_a$  than to pure non-adiabatic effects such as a phase lag in  $\delta L$ . In that case, it would be worthwhile to take this effect into account in all stars except the most massive ones.

Actually, the question of separating the adiabatic and non-adiabatic effects and their proper evaluation is a rather complex problem which has recently been tackled by Cox (1960), using an elaborate numerical method, and its first results, to a certain extent, support Jevakhin's conclusions.

Although this question is a very important one for the theory of variable stars, we shall not linger on it here (cf. Ledoux and Whitney 1961) because obviously this "valve mechanism," as it was called by Eddington, cannot endanger the existence of the star, since, even in the absence of any extra damping terms, the limited heat capacity of the ionization zones would always limit the amplitude of an increasing oscillation to some fairly small finite value.

5.1.3. *Phase delays in energy generation.*—As already pointed out by Eddington (cf. Rosseland 1949), the abundances of the different nuclei entering the thermonuclear reactions may vary with the pulsation, and the effective exponent  $\nu_e$  of  $T$  to be used in the expression (5.5) for  $\delta\epsilon$  may be appreciably different from the equilibrium value  $\nu$  which we have used up to now.

Let us consider a chain of nuclear reactions involving a certain number of reactions between pairs of elements  $i$  and  $j$  liberating the energies  $Q_{ij}$  in Mev and a certain number of disintegrations of elements  $k$  of mean life  $\bar{\tau}_k$  and constant  $\lambda_k = 1/\bar{\tau}_k$  liberating the energies  $Q_k$ . The rate of energy production may be written

$$\epsilon = 6.05 \times 10^{23} \sum_{i,j} Q_{ij} K_{ij} \rho \frac{X_i X_j}{A_i A_j} + \sum_k Q_k \lambda_k \frac{X_k}{A_k}, \quad (5.9)$$

where the  $X$ 's represent the abundances by mass. The  $K_{ij}$ 's are defined by

$$K_{ij} = 4.38 \times 10^6 a_{ij} S_{ij} (A_{ij} Z_i Z_j)^{-1} \tau_{ij}^2 e^{-\tau_{ij}},$$

where  $a_{ij} = 1$  or  $\frac{1}{2}$ , depending on whether  $j$  is different from, or equal to,  $i$ ;  $S_{ij}$  is the nearly constant factor in the cross-section of the reaction expressed in kev-barns;  $A_{ij}$  is the reduced mass in atomic units of the two nuclei and  $Z_i$  and  $Z_j$ , their charges. With

$$\tau_{ij} = 42.483 \left( \frac{Z_i^2 Z_j^2 A_{ij}}{T_6} \right)^{1/3},$$

where  $T_6$  is the temperature expressed in millions of degrees,  $K_{ij}$  may be approximated in a given range of temperature by

$$K_{ij} = CT^{\nu_{ij}}, \quad \nu_{ij} = \frac{1}{3}(\tau_{ij} - 2). \quad (5.10)$$

Neglecting the gradients of chemical composition, which are usually very small, the variation in time of the abundance of element  $l$  is given by

$$\begin{aligned} \frac{\partial X_l}{\partial t} = & \sum_{i,j} n_{ij}^l K_{ij}^l \rho \frac{A_l}{A_i A_j} X_i X_j - \sum_i n_{li} K_{li} \frac{\rho}{A_j} X_l X_j \\ & + \sum_k n_k^l \lambda_k \frac{A_l}{A_k} X_k - \lambda_l X_l; \quad l = 1, 2, \dots, \end{aligned} \quad (5.11)$$

where  $n_{ij}^l$  and  $n_k^l$  are, respectively, the numbers of nuclei  $l$  produced in the reaction  $(i, j)$  and the disintegration  $k$ , and  $n_{li}$ , the number of nuclei  $l$  destroyed

in the reaction  $(l, j)$ . In the course of an infinitesimal oscillation of frequency  $\sigma$ , the linearization of (5.11) yields

$$\begin{aligned} \frac{\partial \delta X_l}{\partial t} = & \sum_{ij} n_{ij}^l K_{ij}^l \rho \frac{A_l X_i X_j}{A_i A_j} \left( \frac{\delta X_i}{X_i} + \frac{\delta X_j}{X_j} + \frac{\delta \rho}{\rho} + \frac{\delta K_{ij}^l}{K_{ij}^l} \right) \\ & - \sum_j n_{lj} K_{lj} \frac{\rho}{A_j} X_l X_j \left( \frac{\delta X_l}{X_l} + \frac{\delta X_j}{X_j} + \frac{\delta \rho}{\rho} + \frac{\delta K_{lj}}{K_{lj}} \right) \\ & + \sum_k n_k^l \lambda_k^l \frac{A_l}{A_k} X_k \left( \frac{\delta X_k}{X_k} \right) - \lambda_l X_l \frac{\delta X_l}{X_l}; \quad l = 1, 2, \dots, \end{aligned} \quad (5.12)$$

where

$$\frac{\delta \rho}{\rho} \propto e^{i\sigma t}, \quad \frac{\delta K_{ij}^l}{K_{ij}^l} = \nu_{ij}^l \frac{\delta T}{T} \propto \nu_{ij}^l e^{i\sigma t}, \quad \frac{\delta K_{lj}}{K_{lj}} \propto \nu_{lj} e^{i\sigma t}.$$

After substitution of the solutions of these equations in the linearized form of equation (5.9), we obtain

$$\delta \epsilon = \epsilon \left( \alpha \frac{\delta \rho}{\rho} + \beta \frac{\delta T}{T} \right).$$

However only the real part of  $\delta \epsilon$  will affect the stability, while the imaginary part will modify very slightly the frequency, and, as far as we are concerned here, we may define the effective exponents characterizing the sensitivity of the reactions to  $\rho$  and  $T$  by

$$\mu_e = \Re \alpha, \quad \nu_e = \Re \beta.$$

The solution of the system (5.12) may be greatly simplified by using the equilibrium abundances, which are inversely proportional to the mean lifetimes of the different elements and noting that steps in the chain which liberate little energy may be neglected.

The abundances of the elements with mean lifetimes short compared with the period of oscillation will vary in phase with the pulsation, nuclear equilibrium values being reached at each instant. If this is the case for all elements entering the reactions,  $\mu_e$  and  $\nu_e$  will be identical with their values in the static model.

On the other hand, the variations of the abundances of elements with mean lives long compared with the period of oscillation will exhibit phase shifts of the order of  $\pm \pi/2$  and will contribute only imaginary parts to  $\alpha$  and  $\beta$ , so that we may treat the corresponding abundances as constant and equal to those in the static model. If this is true of all the elements entering the considered chain of reactions,  $\mu_e = \mu$ , and  $\nu_e$  is a mean value of the different  $\nu_{ij}$ 's weighted with respect to the energy:  $\nu_e = (\sum Q_{ij} \nu_{ij}) / (\sum Q_{ij})$ . This is the case, for instance, for all collision processes in the carbon cycle in ordinary stars. Since the two disintegrations liberate a relatively small fraction of the total energy and since the  $\nu_{ij}$ 's corresponding to the collision processes are not very different from each



other,  $\nu_e$  will remain close to its equilibrium value. It is only at very high temperatures that a detailed discussion may prove necessary.

On the other hand, in the case of the  $p$ - $p$  chain,  $(\nu_e - \nu)$  may become rather important under various circumstances (Ledoux and Sauvenier-Goffin 1950; Schatzman 1951).

Very generally, the  $K_{ij}$ 's depend only on  $T$ , and  $\mu_e$  is equal to 1, but in special cases (as for the reactions of some nuclei with electrons in white dwarfs) the sensitivity to the density may become considerable (Schatzman 1954) and  $\mu_e$  much larger than 1. This, of course, would favor the onset of vibrational instability.

5.1.4. *Effects of friction and progressive waves.*—The effect of the dissipation by viscosity is represented by the first term in expressions (5.1) and (5.7) for  $\sigma'$ . For ordinary molecular or radiative viscosity this is very small, at least for the first few modes (Counson, Ledoux, and Simon 1956).

As the coefficient of turbulent viscosity  $\eta_t$  is much larger than  $\eta_G$  or  $\eta_R$ , its influence could be considerable even on the fundamental mode of radial pulsation, provided that this notion itself be applicable, which again probably requires that the mean lifetime of a turbulent element be short compared with the period of oscillation. However, in the presence of a spectrum of turbulence, one may expect this condition to be satisfied, at least for a part of the spectrum. Even if this means a considerable reduction of  $\eta_t$  as compared with its value computed on the simple picture of one global mean mixing-length and mean turbulent velocity, the effect could still remain important in a star with an extensive convection zone. Apart from the general energy dissipation, the associated transfer of momentum may have to be taken explicitly into account in the equation of motion, as it might reduce considerably the increase of  $\xi$  from the center to the surface and thus again enhance the role of the nuclear reactions in the central core (Longe 1956).

If the exact structure of the outermost layers of the star does not insure the perfect reflection that is implied by our previous boundary conditions, the oscillation there will take on a more or less marked progressive character, and the wave energy escaping or destroyed in the surrounding medium will contribute to the damping of the pulsation.

The author does not know of any realistic discussion of this problem and the usual *linearized* treatment of infinite idealized atmospheres<sup>7</sup> is not very satisfactory. Perhaps Schatzman's model (1956) comprising a finite isothermal layer at temperature  $T$  supporting an infinite atmosphere at temperature  $T'$  ( $T' \gg T$ ) is one of the most interesting. The result which may be derived from it (cf. Ledoux and Walraven 1958, § 68,  $\beta$ ), that the damping due to the outgoing wave in the upper layer can be appreciable, even if the progressive character of the oscillation in the lower layer remains very slight, may be of general significance.

<sup>7</sup> Cf. Rosseland (1949, § 6.4), Simon (1957a), Ledoux and Walraven (1958, § 68,  $\beta$ ).

At least, this is true of stars which, like the sun, may possess a chromosphere and an extensive corona in which even waves of very large wavelength ( $\lambda \simeq R$ ) may develop fairly sharp fronts and dissipate their kinetic energy of motion into heat at great heights. If we schematize the region of large density gradient in the chromosphere by a discontinuity and denote by  $\rho^*$  the density on the outside of it, the contribution to  $\sigma'$  due to the outgoing wave may be written

$$\sigma_{\text{prog}} = -\frac{1}{2} \frac{\Delta K}{K_M}, \quad (5.13)$$

where

$$\Delta K = -2rR^2c[\tfrac{1}{2}\rho^*\sigma^2(\delta r)_R^2]$$

represents the average loss of energy per second and  $K_M$  the maximum kinetic energy of pulsation,

$$K_M = \frac{\sigma^2}{2} \int_0^M (\delta r)^2 dm.$$

In these expressions  $\delta r$  represents the amplitude and  $c$  is the velocity of sound, which, in these very external layers, may be taken as close to the Newtonian velocity.

A rather large upper limit to the value of equation (5.13) may be obtained by replacing  $\rho^*$  by the photospheric density, as was done, for instance, by Schwarzschild and Härm (1959), who found an appreciable contribution to the general damping.

Apart from this effect, the progressive character of the wave under the photosphere, which, on the basis of Schatzman's model, may be expected to be rather weak, does not as such appreciably affect  $\sigma'$ .

5.1.5. *Vibrational stability toward the higher modes of pulsation.*—For the first few modes, the situation remains very much the same as for the fundamental one, except that, at the surface, the amplitudes reach even higher values compared with those at the center. Thus, in the evaluation of  $\sigma'_k$ , the external layers are even more heavily weighted than for the fundamental mode.

If, as is usually the case, the variations of the flux in these layers favor stability, the star will then be much more stable with respect to these higher modes. But if destabilizing factors are at work in these layers (such as the variations of the ionization of H and He, as recalled above), they may also be more efficient for these first few higher modes, which should then be amplified, as well as the fundamental one.

As we go to higher and higher modes, the amplitude  $\xi$  starts by decreasing appreciably on leaving the center and rises again to very large values only very close to the surface.<sup>8</sup> At the same time, the most external mode approaches the surface more and more closely, and finally it should reach the critical level  $(R^*, M^*)$ , where, as we have seen, the integrals in  $\sigma'$  should be terminated. But

<sup>8</sup> See A. Boursy and Mme Hustin-Breton (1961) and Ledoux (1962).

in this case, interior to  $R^*$ , the relative amplitude  $(\xi/\xi_c)$  will remain fairly small. Of course,  $\delta\rho/\rho = -(3\xi + r d\xi/dr)$  will increase more rapidly toward the surface, but again, for high enough modes, it seems that it could be made relatively small everywhere in the region contributing to  $\sigma'$ .

This means that, for high enough modes, the stabilizing effect of heat conduction in the external layers could be reduced very much. On the other hand, two other sources of dissipation will increase rapidly and might very well more than compensate for this tendency. First, the effects of viscosity as compared with those of heat conduction (cf. eq. [5.1]) will increase at least as  $\sigma_k^2$ . Furthermore, the higher the frequency, the larger the fraction of the wave energy escaping across any density discontinuity which may occur at the stellar surface, and, as we have seen in the preceding section, this could lead to a large dissipation.

As a corollary, the last factor implies that, as we go to higher and higher modes, the wave would take on a stronger and stronger progressive character, and, for high enough values of  $\sigma_k$ , the discussion might be more significant if applied to a purely progressive wave than to a purely standing oscillation. Relatively little work has been done on this subject and mainly for purely adiabatic waves (cf. Ledoux and Walraven 1958, Part VI). A discussion of the influence of the non-adiabatic terms on the propagation of waves in stars would be very welcome. It is very likely that, on this account, the amplitude will first increase because of the nuclear reactions as the wave progresses from the center outward (cf. Rosseland 1931, § 3) and will then tend to get damped out by viscosity and heat conduction as it moves outside the energy-producing region, causing a net transfer of heat from the central part to the outside. Assuming that, in the energy-generation zone, there are always small irregularities capable of exciting this type of waves, could this mechanism play a role in the general heat transfer inside the star, remembering that, in the stellar interior, the velocity of sound is much larger than the speed of diffusion of the photons?

## 5.2. NON-RADIAL OSCILLATIONS

In this case, as we have seen in § 4.2, the perturbations of  $\rho$  and  $T$  vanish at the center, so that the variation of  $\epsilon$  and the destabilizing influence of the energy generation are smaller than for radial pulsations.

To the same order of approximation as the one adopted in § 4.2, where we have neglected the perturbation of the gravitational potential, it is easy to verify that the eigen-solutions  $\delta\mathbf{r}$  of the adiabatic problem are orthogonal with respect to the mass, and, as before, the perturbation method may be used to derive the coefficient of vibrational stability  $(\sigma'_k)_l^m$  toward the  $k$ -mode of the pulsation represented by the spherical harmonic of degree  $l$  and order  $m$ . As shown by Simon (1957b), it is actually independent of  $m$  and can be written, neglecting viscosity and convection,

$$\sigma'_{k,l} = - \frac{1}{2(\sigma_{k,l})^2} \frac{\iint \left( \frac{\delta T}{T} \right)_{l,k} \left( \epsilon - \frac{1}{\rho} \operatorname{div} \mathbf{FR} \right)'_{k,l} \rho r^2 \sin \theta dr d\theta d\varphi}{\iiint (\delta \mathbf{r})_{l,k} \cdot (\delta \mathbf{r})_{l,k} \rho r^2 \sin \theta dr d\theta d\varphi}, \quad (5.14)$$

where all the terms in the second member are to be evaluated by means of the corresponding adiabatic solution.

We have kept here explicitly the Eulerian variation (denoted by a prime) for the bracket because, for non-radial oscillations, the solution will be commonly expressed in terms of these variations and, furthermore, the evaluation of the Eulerian variation of  $\operatorname{div} \mathbf{FR}$  is somewhat easier because the operator is then invariant.

The explicit expression of (5.14) has been worked out by Simon and applied to one of the modes ( $l = 2$ ) of the standard model. Simon's results not only confirm the general expectation that the influence of the energy generation is smaller here but also show that, in contrast to the case of radial oscillations, the vibrational stability toward non-radial oscillations is reinforced when the exponent  $\nu$  of  $T$  in  $\epsilon$  increases. This is due to the fact that, at the same time, the energy-producing core shrinks so that the average values of  $T'$  and  $\rho'$  across it decrease. Although, on this basis, one may expect that, in general, vibrational instability will appear first for purely radial perturbations, detailed applications of equation (5.14) to a few other cases would be very welcome.

Of course, one could also expect that viscous dissipation would be somewhat larger in this case, the viscous damping time decreasing with the degree  $l$  of the spherical harmonics somewhat as  $l^2$ . But, since we are mainly interested in relatively small values of  $l$ , this means that the damping times (Counson, Ledoux, and Simon 1956) for gaseous or radiative viscosity remain very large ( $10^{11}$ – $10^{12}$  years). However, these non-radial oscillations might easily become turbulent, and turbulent friction could reduce these damping times by a very large factor.

## § 6. SECULAR STABILITY

### 6.1. GENERAL CONSIDERATIONS

While the problems of dynamical and vibrational stability have been the object of extensive studies that led to precise criteria, secular stability has been rather neglected up to now. Its discussion seems to stem from a remark by H. N. Russell a long time ago, when very little was known of nuclear reactions in stellar interiors except that they should provide a much longer lifetime for ordinary stars than that allowed by the Helmholtz-Kelvin contraction hypothesis (cf. eq. [1.2]). In this connection, Russell pointed out that these reactions should depend on  $\rho$  and  $T$  in such a way that the star behaves as a self-controlled system in which any excess (defect) of the luminosity with respect to the energy generated can be compensated for by a small contraction (expansion) and the simultaneous increase (decrease) in  $\rho$  and  $T$ . If this condition is not satisfied, then, although an exact fortuitous balance between energy generation and

luminosity may still be reached instantaneously, any small departure from it will start a gaseous star contracting or expanding at a rate characterized again by a time scale proportional to equation (1.2).

This may perhaps be illustrated most simply by means of the virial theorem, which for a spherical star in the absence of rotation, magnetic fields, or tidal effects, becomes

$$\frac{1}{2} \frac{d^2 I}{dt^2} = 2K + V + 3 \int_0^M \frac{p}{\rho} dm, \quad (6.1)$$

where  $I$  and  $V$  have the same meanings as in equation (3.13) and  $K$  is the kinetic energy of mass motion.

Since we expect the motion to be very slow, we may neglect the acceleration term on the left of equation (6.1) as well as  $K$ , and we are left with the ordinary expression of the virial theorem as applied to a series of quasi-equilibrium states:

$$\Delta V + 3 \int_0^M \Delta \left( \frac{p}{\rho} \right) dm = 0, \quad (6.2)$$

where  $\Delta$  denotes the variation from one configuration to the next.

With the same hypothesis, the conservation of total energy yields for a star in which  $\beta = p_R/p_G$  is a constant (generalized expressions can easily be derived by introducing appropriate averages of  $\beta$ ,  $\Gamma_1$ , and  $\Gamma_3$ ):

$$\begin{aligned} -L\Delta t &= \int_0^M \Delta \left( \frac{3}{2} \frac{p_G}{\rho} \right) dm + \int_0^M \Delta \left( \frac{3p_R}{\rho} \right) dm + \Delta V + \Delta E \\ &= - \int_0^M \Delta \left( \frac{3}{2} \frac{p_G}{\rho} \right) dm + \Delta E, \end{aligned}$$

where  $E$  denotes the subatomic energy and

$$\Delta E = -\Delta t \int_0^M \epsilon_1 dm.$$

If we expand the integrand, taking into account the variations of the mean molecular weight  $\bar{\mu}$  due to the thermonuclear reactions, we get

$$-L\Delta t = \frac{1}{2} \left( \frac{\beta}{4-3\beta} \right) \Delta V - \frac{3\beta(1-\beta)}{2(4-3\beta)} \int_0^M \frac{p}{\rho} \left( \frac{\Delta \rho}{\rho} - 4 \frac{\Delta \bar{\mu}}{\bar{\mu}} \right) dm + \Delta E. \quad (6.3)$$

Proceeding in the same way with the integral in equation (6.2), eliminating  $\Delta p/p$  by means of equation (2.64), including the extra term proportional to  $(\Delta \bar{\mu}/\bar{\mu})$  discussed there with  $\alpha = \frac{5}{4}$  ( $H \rightarrow He$ ), and solving for  $\Delta \rho/\rho$ , which we introduce in equation (6.3), we obtain

$$-L\Delta t = \frac{\beta}{2} \Delta V - \Delta t \int_0^M \epsilon_1 dm + \frac{6\beta(1-\beta)}{(4-3\beta)} \frac{\Delta t}{e_N} \frac{5}{4} \int_0^M \bar{\mu} \frac{p}{\rho} \epsilon_1 dm, \quad (6.4)$$

with the same notations as in the remark under equation (2.64). One also finds for the variation of the internal thermal energy,  $U$ ,

$$\Delta U = -\Delta V \left( 1 - \frac{\beta}{2} \right) - \frac{6\beta(1-\beta)}{(4-3\beta)} \frac{\Delta t}{e_N} \frac{5}{4} \int_0^M \bar{\mu} \frac{p}{\rho} \epsilon_1 dm.$$

The terms due to variation in chemical composition are normally very small and quite negligible in many respects. However, before dropping them, let us note that equation (6.4) may be written in the limit

$$\frac{dV}{dt} = \frac{2}{\beta} \left( \int_0^M \epsilon_1 dm - L \right) + \frac{4(1-\beta)}{(4-3\beta)} \frac{5}{4e_N} (\langle \epsilon_1 \bar{\mu} \rangle) V, \quad (6.5)$$

where  $\langle \epsilon_1 \bar{\mu} \rangle$  is an average fairly close to the value at the center of the star.

During the evolutionary phase controlled by nuclear energy generation and if Russell's condition is satisfied, we may admit that, at each instant,

$$L = \int_0^M \epsilon_1 dm.$$

In a star in radiative equilibrium (or at least possessing an external zone in radiative equilibrium),  $(1-\beta)$  is related to the luminosity and the mass by a relation of the type (cf. Chandrasekhar 1939, chap. vi)

$$(1-\beta) \simeq \frac{\langle \kappa \eta \rangle}{4\pi cG} \cdot \frac{L}{M},$$

where  $\langle \kappa \eta \rangle$  is an appropriate average of the opacity times the mean rate of energy generation normalized to unity at the surface. Using this relation in equation (6.5), we get

$$\frac{1}{V} \frac{dV}{dt} = \frac{5\langle \kappa \eta \rangle \cdot \langle \epsilon_1 \bar{\mu} \rangle}{(4-3\beta) 4\pi cG E_N} \frac{L}{E_N},$$

where  $E_N = Me_N$ . Thus the time scale of the evolution due to the burning-up of nuclear fuel is given by

$$\tau_N = \frac{(4-3\beta) 4\pi cG E_N}{5\langle \kappa \eta \rangle \langle \epsilon_1 \bar{\mu} \rangle} \frac{1}{L}, \quad (6.6)$$

which is of the same order as that defined by equation (1.3).

This will remain true as long as any perturbation of the equilibrium state decays at a rate characterized by equation (1.2), the star then resuming its slow evolution at the rate defined by equation (6.6). The corresponding condition of secular stability may be derived by perturbing equation (6.5), where all terms due to changes in chemical composition can now be neglected. This leads to

$$\frac{\beta}{2} \frac{d\delta V}{dt} = \int_0^M \delta \epsilon_1 dm - \delta L,$$

which can be transformed, using expressions (5.5) and (5.6), into

$$\begin{aligned} \frac{\beta}{2} \int_0^M \frac{Gm}{r} \frac{d}{dt} \left( \frac{\delta r}{r} \right) dm &= \int_0^M \left( \mu \frac{\delta \rho}{\rho} + \nu \frac{\delta T}{T} \right) \epsilon_1 dm \\ &- L \left[ 4 \frac{\delta r}{r} + (n+4) \frac{\delta T}{T} - m \frac{\delta \rho}{\rho} + \frac{d}{dm} \left( \frac{\delta T}{T} \right) / \frac{1}{T} \frac{dT}{dm} \right]_{\text{Ex}}. \end{aligned} \quad (6.7)$$

Although, in all this,  $L$  and  $\delta L$  refer to the total luminosity or its total variation as observed at the surface of the star, it is obvious that in the present connection there is no need to use a refined theory of the atmospheric layers, since in fact the latter will adapt themselves to the flux coming from the interior. On the other hand, it would seem that the details of the energy transport in the deep interior are also of little consequence, and that, as indicated, the last bracket in equation (6.7) should be evaluated for the mean conditions prevailing toward the exterior but nevertheless deep enough for the usual "interior" approximations to hold.

The general form (6.7) is of little use as long as  $\delta T/T$  and  $\delta \rho/\rho$  are not eliminated. Rigorously, this is rather difficult, and we shall return to it later. However, even during the perturbation, we may consider that the hydrostatic equation is satisfied at each step, and it has been known since Lane and Kelvin that, together with the equation expressing the conservation of mass, they admit of a homology transformation,

$$r' = tr, \quad \rho' = t^{-3}\rho, \quad p' = t^{-4}p.$$

For a gas, the equation of state also implies  $T' = t^{-1}T$ , and this remains true for a mixture of gas and radiation when  $\beta$  is a constant.

It has usually been considered that, these equations being dominant in the problem, there is at least one possible type of motion that does not deviate very much from this homology transformation, so that we may introduce in equation (6.7)

$$\frac{\delta \rho}{\rho} = -3\xi, \quad \frac{\delta T}{T} = -\xi, \quad \frac{\delta p}{p} = -4\xi,$$

with  $\xi = \delta r/r$  constant throughout the star. This immediately yields

$$\frac{1}{\xi} \frac{d\xi}{dt} = \frac{2}{\beta} [n - 3m]_{\text{Ex}} - (3\mu + \nu) - \frac{L}{V}, \quad (6.8)$$

which shows that any such perturbation will decay or grow at a rate characterized by the gravitational time scale (1.2), depending on whether the bracket is negative or positive. The condition

$$n - 3m < 3\mu + \nu \quad (6.9)$$

is usually referred to as the condition of secular stability, and it was first obtained by Jeans (1928, § 108). It is difficult to judge how much the result is affected by the homology solution adopted, but one may note that, in the critical case  $n - 3m = 3\mu + \nu$ , it satisfies the complete system of equations. Anyway, this condition is amply satisfied in any gaseous star living on thermonuclear reactions, since the first member of relation (6.9) is very small (0, for electron scattering, 0.5 for Kramers' opacity law), while in the second member  $\mu$  is at least 1 and  $\nu$  is always larger than 4.

## 6.2. THE DETAILED PROBLEM

The only other original investigation of the problem is due to L. H. Thomas (1930*a*), who started from the energy principle, using the entropy as the dependent variable. This approach might seem particularly appropriate because the secular motions that we consider here are essentially due to the changes in entropy and Thomas' method, which leads to a rather complex integrodifferential problem, was reviewed in detail by the author (Ledoux 1958). Some suggestions were also made there concerning a possible attack on this problem by means of series development in terms of the eigen-modes of adiabatic radial oscillations. Further attempts in that direction, however, have proved rather disappointing, as the amount of numerical work becomes rapidly prohibitive.

In fact, it seems that the direct method of Jeans, which need not be limited to the case of a homology transformation, may prove more fruitful. As we pointed out toward the end of § 3, the problem is actually governed by equation (3.7), in which we neglect the first member but where the last term on the right must be expressed explicitly in terms of  $\xi$  and its derivatives.

Integrating, first, this equation from any level  $r$  to the surface and taking the boundary condition (3.8) into account, it becomes

$$s_1 \left[ \frac{\Gamma_1 p}{r^2} \frac{d}{dr} \left( \frac{r^3}{p'} \frac{da}{dr} \right) - 4a \right] = (\Gamma_3 - 1) \rho \left( \delta \epsilon_1 - \frac{d\delta L}{dm} \right), \quad (6.10)$$

where

$$a = - \int_r^R \xi \frac{dp}{dr} dr = \int_0^R \xi \frac{Gm(r)}{r^2} \rho dr,$$

and  $p'$  denotes  $dp/dr$ .

Note that equation (3.2), where, in this case, the left-hand member can be neglected, shows that  $4a = -\delta p$ , so that

$$\frac{\delta T}{T} = - \frac{\beta}{4-3\beta} \frac{\delta \rho}{\rho} - \frac{4a}{(4-3\beta)p}. \quad (6.11)$$

Eliminating  $\delta \rho/\rho$  and  $\delta T/T$  by means of equations (3.1) and (6.11) from the usual expressions (5.5) and (5.6) of  $\delta \epsilon_1$  and  $\delta L$  in equation (6.10), yields the fourth-order equation (Ledoux 1960)

$$\begin{aligned} s_1 p \left[ \frac{\Gamma_1}{r^2} \frac{d}{dr} \left( \frac{r^3}{p'} \frac{da}{dr} \right) - \frac{4a}{p} \right] &= (\Gamma_3 - 1) \rho \epsilon \left[ \left( \frac{\beta \nu}{4-3\beta} - \mu \right) \frac{1}{r^2} \right. \\ &\times \frac{d}{dr} \left( \frac{r^3}{p'} \frac{da}{dr} \right) - \frac{4\nu a}{(4-3\beta)p} \left. \right] - \frac{\Gamma_3 - 1}{4\pi r^2} \frac{d}{dr} \left[ \frac{4L(r)}{p'} \frac{da}{dr} \right. \\ &+ L(r) \left\{ \left[ \frac{(4+n)\beta}{4-3\beta} + m \right] \frac{1}{r^2} \frac{d}{dr} \left( \frac{r^3}{p'} \frac{da}{dr} \right) - \frac{4(4+n)a}{(4-3\beta)p} \right\} \\ &\left. + \frac{L(r)T}{(dT/dr)} \frac{d}{dr} \left[ \frac{\beta}{4-3\beta} \frac{1}{r^2} \frac{d}{dr} \left( \frac{r^3}{p'} \frac{da}{dr} \right) - \frac{4a}{(4-3\beta)p} \right] \right], \end{aligned} \quad (6.12)$$



which should be solved subject to the boundary conditions

$$\begin{aligned} \frac{da}{dr} &= 0 & \text{at } r &= 0, \\ a &= 0, \quad \frac{da}{dr} = 0, \quad \text{and} \quad \frac{d\delta L}{dr} = 0 & \text{at } r &= R. \end{aligned} \quad (6.13)$$

The general properties of this boundary-value problem have not been discussed, and it is possible that really useful results could be obtained only by numerical integrations in particular cases. One could, of course, define a mean value of  $s_1$  by integrating equation (6.12) multiplied by  $4\pi r^2 a dr$  over the whole star, but, in the general case, the derived expressions are too cumbersome and yield little information. However, if we set  $\xi$  equal to a constant, which again restricts the solutions to those corresponding to purely homologous motions, the expression for  $s_1$  immediately reduces to

$$s_1 = \frac{[(n-3m)_{\text{Ex}} - (3\mu + \nu)]L}{\langle [(\Gamma_1 - 4)/3(\Gamma_3 - 1)] \rangle (-V)},$$

which defines the same time scale as equation (6.8) and leads to the same condition of secular stability (6.9).

However, the limited significance of this condition is immediately apparent here, since the differential equation reduces, for  $\xi = c'$ , to

$$s_1(3\Gamma_1 - 4)p = (\Gamma_3 - 1)\rho\epsilon[(n-3m) - (3\mu + \nu)], \quad (6.14)$$

which, apart from the critical case:  $s_1 = 0$ ,  $(n-3m) = (3\mu + \nu)$  at each point, cannot be satisfied.

In particular, it does not yield any information as to the possibility of secular motions in which a part of the star is contracting and the rest expanding. According to Sandage and Schwarzschild (1952), such a phase is encountered, for instance, in the evolution of a star when a growing isothermal core resulting from the exhaustion of nuclear fuel reaches the Schönberg-Chandrasekhar limit. But one should note that, apart from a reasonable mathematical treatment of the equations, such a case would also require a more general approach, as the changes in chemical composition due to nuclear reactions should be taken explicitly into account here, at least as far as they are at the origin of the increase in mass of the isothermal core.

In other cases, the unstable character of the situation might not manifest itself immediately in the form of motions. For instance, as was pointed out by Mestel (1952; see also chap. 5, § 2.3, of this volume), the pressure in a white dwarf, being essentially determined by the degenerate electron gas, depends very little on the temperature, and the regulating mechanism discussed above, which tends to maintain the balance between nuclear energy generation and radiation, is lacking. In this case, if at any time the energy generation exceeds the luminosity, heat accumulates in the star, raising the temperature, which, in

its turn, increases the energy generation so that after a while a very fast rate of change of the temperature may be reached (Härm and Schwarzschild 1961) unless some new process of energy transfer comes into play. Although, for a while, this increasing temperature will not imply any dynamical consequences, as the pressure remains largely independent of  $T$ , it is obvious that the situation is potentially "explosive," since, sooner or later,  $T$  will become large enough to lift the degeneracy of the electron gas.

With the increasing importance of evolutionary considerations, the need for an adequate solution to the general problem of secular stability will probably be felt more urgently. In fact, it is on this basis that the method of treating stellar evolution (series of equilibrium or quasi-equilibrium configurations), the type of time derivatives to be kept, the time step to be adopted, should be justified. It may also throw new light on particularly complex phases of stellar evolution when the non-linear character of the general problem and error feedback in the time derivatives makes it difficult (Hoyle 1960), starting from a given quasi-equilibrium solution, to determine the one immediately following after a finite time step. Furthermore, there is always a possibility that, in continuing a series of models by finite steps, one might overpass the critical point where stability is lost without noticing it, at least for some time.

In all these respects, a comparison with the classical problem of the evolution of a mechanical system depending on a slowly varying parameter might be of interest. In that case the theory of linear series of equilibrium configurations and of the exchange or loss of stability at their bifurcation, turning, or terminating points as developed by Poincaré (for a short summary cf. Ledoux 1958, §§ 3-7) yields a global view of the stability problem which, for instance, has proved very useful in the discussion of the evolution of an incompressible mass in solid rotation with a slowly increasing angular velocity.

Geometrically, our problem is simpler, since, as far as we are concerned here (absence of rotation, magnetic field, or tidal effects), the star may be considered as spherical at all times. On the other hand, in this case the slowly variable parameter is the chemical composition, which we may characterize by the distribution of the mean molecular weight  $\bar{\mu}$ , and it is of a much more complex analytical nature because its instantaneous values and their variations depend on the position in the star.

It would seem that the direct extrapolation of Poincaré's method would consist in linearizing the equation of stellar structure for the general Lagrangian perturbation associated with the variation of the chemical composition resulting from the distribution of the nuclear energy sources at the time considered. To reinforce the analogy with a mechanical system having a finite number of degrees of freedom, let us treat the star as formed of a series of  $n$  concentric shells and substitute for the derivatives their expressions in terms of the finite differences between the perturbations in consecutive shells. Taking the boundary conditions into account, this will lead, in general, to an algebraic system

of  $(4n + 4)$  non-homogeneous linear equations in  $(4n + 4)$  unknowns, the second members of which are expressed in terms of the imposed variation in chemical composition.

Obviously, the necessary and sufficient condition for this system to admit a solution is that the determinant of rank  $(4n + 4)$  formed with the coefficients of the unknowns in the left-hand members of the equations be different from zero, and, in that case, we can be sure that there exists an infinitely close neighboring equilibrium configuration. On the other hand, any point where the determinant vanishes marks a break in the linear series, which must be associated with some kind of instability. For instance, it is relatively easy to verify that, in agreement with our discussion of equation (6.14), this happens if  $(n - 3m) = (3\mu + \nu)$  at each point in the star.

This approach also has the advantage that it could easily be incorporated in some of the practical methods (Henyey *et al.* 1959, Huang 1960) of computing evolutionary sequences. Any change of sign of the determinant computed at each step would automatically call attention to the existence of a critical point in the sequence.

However, in a purely mechanical system, which is free or in which the constraints are independent of the parameter, the connection with the potential energy is straightforward and enables us to show immediately that the non-vanishing of the determinant implies that the potential remains a minimum for each of the successive configurations in the evolutionary sequence that thus satisfy the stability criteria. But here the situation is appreciably more complex. First, the effective potential energy comprises a thermodynamical part, so that the variation of the gravitational potential energy is not converted entirely into kinetic energy of mass motion but, in part, into thermal energy. This implies changes in the state variables  $p$  and  $T$ , which, in general, are not negligible even for slow motions, as is the case for the kinetic energy. Thus, in general, we cannot, as above, limit our discussion to the perturbation of the equilibrium equations but must add, at least in the energy budget, terms depending explicitly on time derivatives. The fact that these extra terms will in their turn affect the rate of change of the parameter  $\mu$  complicates the problem further.

Thus, although the fairly simple procedure outlined above may be sufficient in the slowest phases of stellar evolution, it would have to be generalized considerably before it could be applied in the general case.

## § 7. SOME COMMENTS ON THE EFFECTS OF ROTATION, MAGNETIC FIELDS, OR EXTERNAL GRAVITATIONAL FIELDS

In the preceding sections the discussion has been limited to the case of spherical configurations in absolute equilibrium under the effect of their own gravity. The presence of rotation, magnetic fields, or external gravitational fields, which is a fairly common occurrence in stars, introduces new fields of forces and actuates new degrees of freedom that complicate the problem to such

an extent that progress in the detailed discussion of their effects is extremely slow. Most often, all that we can do, at the present time, is to try to foresee, by rough arguments, the main consequences of these factors.

### 7.1. DYNAMICAL AND SECULAR STABILITY

At the present stage, it is not always so easy to distinguish between dynamical and secular instabilities caused by one of these factors.

7.1.1. *Effects of a rotation.*—The effects of a rotation are probably those that have been most studied but mainly for ideal configurations composed either of a homogeneous incompressible fluid or of a central particle comprising practically all the mass and surrounded by a tenuous envelope (Roche's model) or a combination of the two formed of a central incompressible core surrounded by a Roche's envelope (cf. Jeans 1919; Lyttleton 1953; Ledoux 1958, §§ 3–8).

Physically, we are looking either for upper limits to the value of the angular momentum  $\mathfrak{S}$  or the angular velocity  $\Omega$  past which hydrostatic equilibrium is impossible or for critical values of  $\Omega$  or  $\mathfrak{S}$  at which instabilities arise in the course of the evolution of a mass endowed originally with a given angular momentum.

For an incompressible fluid of density  $\rho$ , it is well known that there are no equilibrium configurations for

$$\frac{\Omega^2}{2\pi G\rho} > 0.2247. \quad (7.1)$$

In this case the evolution of a given mass  $M$  with a given value of  $\mathfrak{S}$  through a series of equilibrium states of increasing density is usually described in terms of configurations of increasing  $\mathfrak{S}$  at constant  $\rho$ , since the two problems are mathematically equivalent. It is then found that, as  $\mathfrak{S}$  increases from zero, the equilibrium configuration passes through a series of flatter and flatter Maclaurin spheroids ( $a = b > c$ ) until, for an eccentricity  $e = 0.8127$  corresponding to

$$\frac{\Omega^2}{2\pi G\rho} = 0.1868 \quad \text{or} \quad \frac{\mathfrak{S}}{(GM^3R)^{1/2}} = 0.3035, \quad R = (abc)^{1/3}, \quad (7.2)$$

they become secularly unstable and are replaced by a series of Jacobi ellipsoids ( $a > b > c$ ), which, in their turn, become unstable for

$$\frac{b}{a} = 0.4322, \quad \frac{c}{a} = 0.3451, \quad \frac{\Omega^2}{2\pi G\rho} = 0.1420, \quad \frac{\mathfrak{S}}{(GM^3R)^{1/2}} = 0.3896, \quad (7.3)$$

giving place to pear-shaped configurations. But while the Maclaurin spheroids remain dynamically stable past the critical point (7.2), up to

$$e = 0.9529, \quad \frac{\Omega^2}{2\pi G\rho} = 0.2201, \quad \frac{\mathfrak{S}}{(GM^3R)^{1/2}} = 0.5092,$$

the Jacobi ellipsoids, following E. Cartan, lose both their secular and their dynamical stability at the point defined by (7.3), so that slow evolution is im-

possible past this point and a detailed discussion of the dynamics of the motions which set in becomes very difficult.

As far as Roche's model is concerned, if it does not represent a compressible mass, it gives at least some idea of one of the effects of compressibility, namely, the heterogeneity which results from it, with the density increasing toward the center.

In this case, neglecting the mass of the tenuous envelope, the expression of the total potential, including that of the centrifugal force, is very simple. For given  $M$  and  $\Omega$ , there is always a critical equipotential surface with a sharp edge in the equatorial plane at a distance  $(R_E)_c$  from the center, defined by

$$\Omega^2 (R_E)_c = \frac{GM}{(R_E)_c^2}, \quad (7.4)$$

along which the centrifugal force balances exactly the gravitational attraction. If  $(R_P)_c$  is the corresponding polar radius,

$$\left(\frac{R_E}{R_P}\right)_c = \frac{3}{2},$$

and the volume inclosed is

$$\mathfrak{V}_c = 4\pi(R_E)_c^3 \times 0.1804. \quad (7.5)$$

For a given mass  $M$ ,  $(R_E)_c$ ,  $(R_P)_c$ , and  $\mathfrak{V}_c$  decrease as  $\Omega$  increases.

Let us now endow this very idealistic model with finite physical dimensions by imposing the volume  $\mathfrak{V}$  occupied by the envelope or the mean density

$$\bar{\rho} = \frac{M}{\mathfrak{V}}$$

of the configuration. If  $\mathfrak{V}$  is smaller than  $\mathfrak{V}_c$ , then all the particles composing  $M$  are on smooth equipotential surfaces and submitted to a net attraction toward the interior which can be balanced by a pressure gradient, so that an equilibrium configuration is possible. But if  $\mathfrak{V} = \mathfrak{V}_c$  or if, according to equations (7.4) and (7.5),  $\bar{\rho}$  is such that

$$\frac{\Omega^2}{2\pi G\bar{\rho}} = 0.3607, \quad (7.6)$$

the particles on the sharp edge will just be revolving on circular orbits and can no longer be considered as belonging properly to the configuration. As soon as  $\mathfrak{V}$  becomes larger than  $\mathfrak{V}_c$ , some of the particles in the equator or close to it will fall on equipotential surfaces corresponding to repulsive forces, and, in the absence of imposed external constraints, no equilibrium configurations are possible.

Physically, these results are often applied to the evolution by contraction of a highly centrally condensed configuration of mass  $M$  and volume  $\mathfrak{V}$  supposed

to possess a small but finite angular momentum  $\mathfrak{S}$  such that, initially, the condition

$$\frac{\Omega^2}{2\pi G \bar{\rho}} < 0.3607$$

is satisfied. As the configuration shrinks,  $\bar{\rho}$  varies as  $\mathfrak{B}^{-1}$ , while, because of the conservation of angular momentum,  $\Omega$  varies as  $\mathfrak{B}^{-2/3}$ , so that  $\Omega^2/2\pi G \bar{\rho}$  increases as  $\mathfrak{B}^{-1/3}$ . As soon as it overshoots the critical value (7.6), matter will start leaving the main mass through the sharp edge in the equatorial plane.

It is generally concluded, on this basis, that a rotating compressible mass evolves very differently from an incompressible one, all the allowed configurations keeping the symmetry of revolution and the unique type of instability arising at the critical point defined by equation (7.6) leading to the shedding of material mainly in the equatorial plane.

More elaborate versions of this model have also been studied, in which the central mass, instead of reducing to a point, forms a homogeneous incompressible core, which, if we again neglect the gravitational potential of the envelope, will take the different possible forms discussed above. Adding to the corresponding external gravitational potential that of the centrifugal force, the critical equipotential surface in the envelope and its volume  $\mathfrak{B}_e$  can be discussed as before. As long as the core remains spheroidal, this surface still has a sharp edge in the equatorial plane, while, if the core becomes a Jacobi ellipsoid, the critical surface takes the form of a pseudo-ellipsoid with pointed ends at the extremities of the long axis. In terms of evolution, this means that if the critical volume  $\mathfrak{B}_e$  is reached while the core is still spheroidal, loss of mass will occur as before all along the equatorial sharp edge, but, if this is delayed until the core has become truly ellipsoidal, the instability of the envelope will lead to the shedding of streams of material through the pointed ends of the critical surface.

The study of a somewhat more realistic model, in which the pressure and the density obey a polytropic relation

$$p = \kappa \rho^\gamma - p_0,$$

was tackled by Jeans and led him to the conclusion that, at least up to the order of the approximation used, this compressible mass could follow two distinct patterns of evolution, modeled, respectively, on the behavior of an incompressible mass or on that of Roche's model, depending on whether  $\gamma$  is greater or smaller than a critical value of the order of 2.2.

Excepting, perhaps, very special phases of the nuclear evolution of stellar material,  $\gamma$  is at most equal to  $\frac{5}{3}$ , and thus it would seem that the rotational instability of physical interest is essentially exhibited by Roche's model.

However, many idealizations and approximations remain at the basis of this discussion, and essential effects of compressibility, such as differential rotation and meridional currents, have been entirely neglected. On the other hand, one

should be aware of the fact that the formal difficulties that beset the general problem are not trivial. For instance, in the case of an incompressible but non-homogeneous fluid in solid-body rotation, an exact treatment becomes mathematically difficult because, as shown by the classical work of Hamy and Volterra and the more recent discussions of Dive and Wavre (1932), the level surfaces in that case are no longer ellipsoids, nor can they be general homothetic surfaces.

Nevertheless, as far as the existence of an upper limit to the ratio of the rotational energy to the gravitational potential energy is concerned, the critical values (7.1) and (7.6) give significant orders of magnitude which can be checked immediately. For instance, applying the virial theorem (6.1) to a quasi-static configuration in which, for simplicity, we shall treat the pressure of radiation as negligible, we have

$$2K + V + 3(\gamma - 1)U = 0, \quad (7.7)$$

where  $K$  is now the kinetic energy of the stationary mass motions associated with the rotation. Since the internal energy  $U$  must be positive, this implies that no equilibrium configuration is possible unless

$$2K < -V. \quad (7.8)$$

For a uniformly rotating body, this reduces, in a first approximation, to

$$\frac{\Omega^2}{2\pi G\rho} < 0.5,$$

which is of the same order as the critical values found above.

Furthermore, as long as the main kinetic energy of mass motion remains associated with the rotation corresponding to the angular momentum, the constancy of the latter implies that  $K$  varies about as  $\mathfrak{B}^{-2/3}$ , while the gravitational potential energy  $V$  varies as  $\mathfrak{B}^{-1/3}$ . Thus we have approximately

$$K = K_0 \left( \frac{V}{V_0} \right)^2. \quad (7.9)$$

This shows that, starting from a configuration  $(K_0, V_0)$  which satisfies condition (7.8)—say,  $2K_0 = -\alpha V_0$  ( $\alpha < 1$ )—a continuous shrinking of the volume  $\mathfrak{B}$  will always lead to a state in which relation (7.8) is just violated ( $\mathfrak{B} \simeq \alpha^3 \mathfrak{B}_0$ ) and some kind of rotational instability sets in that prevents any further contraction or leads to a shedding of stellar material.

On the other hand, the virial theorem applied to two neighboring configurations yields

$$3(\gamma - 1)\Delta U + 2\Delta K + \Delta V = 0,$$

while, according to equation (7.9), one has

$$\Delta K = 2 \frac{K}{V} \Delta V,$$

so that

$$\Delta U = -\frac{\Delta V [4(K/V) + 1]}{3(\gamma - 1)}.$$

We see that, in this case, the fraction of the liberated potential energy which is transformed into internal energy depends on the ratio  $K/V$ . In particular, if  $K = -V/4$ ,  $\Delta U$  vanishes, and it becomes negative for higher values of  $K$ .

In the same way, using the equation of conservation of the total energy  $J$ , we get

$$\begin{aligned}\Delta J &= -L\Delta t = \Delta K + \Delta U + \Delta V + \Delta E \\ &= \frac{\Delta V}{3(\gamma - 1)} \left[ \frac{2K}{V} (3\gamma - 5) + (3\gamma - 4) \right] + \Delta E.\end{aligned}$$

In particular, in phases when the liberation of subatomic energy  $\Delta E$  is negligible, we have

$$\Delta J = -L\Delta t = \frac{\Delta V}{3(\gamma - 1)} \left[ \frac{2K}{V} (3\gamma - 5) + (3\gamma - 4) \right]. \quad (7.10)$$

Again, the fraction of the liberated gravitational energy that is radiated away during a contraction depends on the ratio  $K/V$ . However, as long as  $\gamma$  is in the usual physical range  $\frac{4}{3} \leq \gamma \leq \frac{5}{3}$ ,  $\Delta J$  remains negative. Even the value  $\gamma = \frac{4}{3}$  ceases to be critical and is replaced by

$$\gamma_c = \frac{(10/3)(K/V) + 4/3}{2K/V + 1},$$

which decreases from  $\frac{4}{3}$  to 0 as  $K/V$  varies from 0 to  $-0.4$ , which anyway is already very close to the limit defined by relation (7.8). In principle,  $\gamma_c$  may also be greater than  $\frac{5}{3}$ , but this occurs only for  $K > -V/2$ , i.e., for values which violate the condition (7.8).

**7.1.2. Effects of a magnetic field.**—The general effects of a magnetic field may also be estimated in the same way (Chandrasekhar and Fermi 1953, Cowling 1960). Neglecting the magnetic energy outside the star and assuming static equilibrium, the virial theorem yields

$$\mathfrak{M} + V + 3(\gamma - 1)U = 0, \quad (7.11)$$

where the total magnetic energy  $\mathfrak{M}$  is given by

$$\mathfrak{M} = \int_{\mathfrak{V}} \frac{H^2}{8\pi} d\mathfrak{V}$$

if  $\mathfrak{V}$  is the total volume of the star. Since in any equilibrium configuration  $U$  must be positive, we must have

$$\mathfrak{M} < -V, \quad (7.12)$$

or, in order of magnitude,

$$\bar{H}^2 < 4 \times 10^{16} \frac{M^2}{R^4}, \quad (7.13)$$



where the average field  $\bar{H}$  is expressed in gauss and  $M$  and  $R$  in units of the solar mass and radius.

If the magnetic flux is assumed constant as it should be if the conductivity is high enough, we have, approximately, when the volume varies,

$$H \propto \mathfrak{B}^{-2/3}, \quad \mathfrak{M} \propto \mathfrak{B}^{-1/3}, \quad V \propto \mathfrak{B}^{-1/3}, \quad (7.14)$$

and we see that the ratio  $\mathfrak{M}/V$  remains constant. Thus, contrary to what happens in the case of rotation, if condition (7.12) is satisfied in the original configuration, it will remain satisfied forever after, so that the magnetic field will not prevent further contraction.

Let us note, however, that, as far as the formation of stars from interstellar matter pervaded by a magnetic field is concerned, this does not solve the problem because, for reasonable initial values  $H \simeq 10^{-6}$ ,  $\rho \simeq 10^{-23}$ , the smallest mass that can start contracting according to (7.13) is of the order of a few thousand times the solar mass. To get down to ordinary stellar masses, it is absolutely necessary that lines of force could straighten out of the contracting mass, decreasing the magnetic flux through the material (Mestel and Spitzer 1956, Spitzer 1958).

On the other hand, combining equation (7.11) with the conservation of the total energy,

$$J = U + V + \mathfrak{M}, \quad (7.15)$$

where we have neglected the subatomic energy  $E$ , we find

$$J = (3\gamma - 4)(V + \mathfrak{M}),$$

which, for  $\gamma > \frac{4}{3}$ , leads to the same condition (7.12) for the existence of an equilibrium configuration.

The application of these relations to the variations between two neighboring quasi-static configurations yields, with the help of (7.14),

$$\Delta U = -\frac{\Delta V}{3(\gamma - 1)} \left( 1 + \frac{\mathfrak{M}}{V} \right)$$

and

$$\Delta J = \frac{\Delta V}{3(\gamma - 1)} \left( 1 + \frac{\mathfrak{M}}{V} \right) (3\gamma - 4). \quad (7.16)$$

Here again the fractions of the liberated gravitational energy that are transformed into internal energy or radiated away depend on the ratio  $(\mathfrak{M}/V)$ , which, however, in our approximation, keeps a constant value depending on the initial conditions. In this case, the value  $\gamma = \frac{4}{3}$  remains critical.

If rotation and magnetic field are simultaneously present, the virial theorem yields, for stationary configurations,

$$2K + V + 3(\gamma - 1)U + \mathfrak{M} = 0,$$

and the total energy  $J$  takes the form

$$J = K + V + U + \mathfrak{M},$$

whence we get

$$U = -\frac{2K + V + \mathfrak{M}}{3(\gamma - 1)}$$

and

$$J = \frac{K(3\gamma - 5) + (V + \mathfrak{M})(3\gamma - 4)}{3(\gamma - 1)} = -K - (3\gamma - 1)U.$$

For  $U$  to be positive, we must have

$$2K + \mathfrak{M} < -V, \quad (7.17)$$

which automatically renders  $J$  negative for all physically possible values of  $\gamma$ .

Since, in the magnetohydrodynamic approximation considered here, the constancy of the total angular momentum is still satisfied (Chandrasekhar 1960), we can still use equations (7.9) and (7.14) to relate the variations of  $K$  and  $\mathfrak{M}$  to those of  $V$  in going from one quasi-static configuration to the next and write

$$\Delta U = -\frac{\Delta V}{3(\gamma - 1)} \left( 4\frac{K}{V} + \frac{\mathfrak{M}}{V} + 1 \right)$$

and

$$\Delta J = \frac{\Delta V}{3(\gamma - 1)} \left[ (3\gamma - 5)\frac{2K}{V} + (3\gamma - 4)\left(\frac{\mathfrak{M}}{V} + 1\right) \right]. \quad (7.18)$$

One verifies readily that, starting from an equilibrium configuration in which (7.17) is satisfied, there are no critical values of  $\gamma$  in the physical range  $\frac{4}{3} \leq \gamma \leq \frac{5}{3}$  capable of making the right-hand member of (7.18) vanish.

The above treatment of the magnetic field calls for some general remarks. From our definition,  $\mathfrak{M}$  is the magnetic energy inside the star. Rigorously speaking, this implies that the magnetic field  $\mathbf{H}$  vanishes at the same time as the pressure  $p$  on the surface of the star. Actually, we know that  $\mathbf{H}$  may extend to very large distances outside the material body, and the corresponding magnetic energy, say  $\mathfrak{M}_e$ , should really be added to  $\mathfrak{M}$  in all the above expressions (Piddington 1957). However, as the external field of an isolated object decreases at least as rapidly as that of a dipole, the corresponding correction does not affect the order of magnitude of the previous results.

The situation is more complicated if the magnetic field originating in the star interacts with matter outside it, and, in this case, some care is required (Piddington 1957) in the application of the general theorems considered above. However, although this kind of situation may be very important for the detailed study of the evolution of the star, especially as far as its rotation is concerned, it is unlikely to lead by itself to new types of instability (Lüst and Schlüter 1955; Mestel 1959; Schatzman 1959, 1960).

7.1.3. *Effects of an external gravitational field.*—In the same way, the virial theorem yields easily useful qualitative information on the effects of an external gravitational field. Let us consider two masses  $M_1$  and  $M_2$  whose centers of gravity, a distance  $d$  apart, revolve on circular orbits around the center of gravity of the system with an angular velocity

$$\Omega^2 = \frac{G(M_1 + M_2)}{d^3}, \quad (7.19)$$

each mass turning on itself at the same rate.

Adopting Cartesian axes  $(O, x, y, z)$  with  $O$  at the center of  $M_1$ , and  $x$  and  $z$  in the orbital plane, so that  $z$  is directed from  $M_1$  to  $M_2$ , the potential of the force exerted by  $M_2$  on a point of  $M_1$ , provided that  $M_2$  may be considered as collected at its center, is given, in a first approximation, by

$$\phi_{21} = -\frac{GM_2}{d} \left( 1 + \frac{z}{d} - \frac{x^2 + y^2 - 2z^2}{2d^2} \right).$$

We may neglect the first term, since it is a constant in our co-ordinates, the corresponding force being balanced by the centrifugal force associated with the revolution of the center of  $M_1$  defined by equation (7.19), and consider only the tidal potential,

$$\phi'_{21} = -\frac{GM_2}{d} \left( \frac{z}{d} - \frac{x^2 + y^2 - 2z^2}{2d^2} \right). \quad (7.20)$$

If  $\phi_1$  is the gravitational potential exerted by  $M_1$  on one of its internal points and  $I_1$  is the moment of inertia of  $M_1$  with respect to its center, the usual procedure yields the following expression for the virial theorem applied to  $M_1$ :

$$\begin{aligned} \frac{1}{2} \frac{d^2 I_1}{dt^2} = & V_1 - 2V'_{21} - 3(\gamma - 1)U_1 + \int_{M_1} (\dot{x}^2 + \dot{y}^2 + \dot{z}^2) dm \\ & + \Omega^2 \int_{M_1} (x^2 + y^2) dm - \frac{2\Omega^2 M_2 d}{(M_1 + M_2)} \int_{M_1} z dm - 2\Omega \int_{M_1} (x\dot{z} - \dot{x}z) dm, \end{aligned} \quad (7.21)$$

where the potential energy of  $M_1$  in the tidal field of  $M_2$  is given by

$$V'_{21} = \int_M \phi'_{21} dm.$$

In the stationary case ( $\dot{x} = \dot{y} = \dot{z} = 0$ ), equation (7.21) becomes

$$V_1 - 2V''_{21} + 3(\gamma - 1)U = 0, \quad (7.22)$$

where  $V''_{21}$  corresponds to the generalized potential  $\phi''_{21}$  of the tidal forces plus the centrifugal forces due, respectively, to the revolution of the origin and the rotation of the axes:

$$\phi''_{21} = \phi'_{21} + \frac{\Omega^2 M_2 d}{(M_1 + M_2)} z - \frac{\Omega^2}{2} (x^2 + y^2).$$

With the help of equations (7.19) and (7.20), this may be transformed into

$$\phi_{21}'' = \frac{GM_2}{2d^3}(x^2 + y^2 - 2z^2) - \frac{G(M_1 + M_2)}{2d^3}(x^2 + z^2)$$

or, in polar co-ordinates  $(r, \theta, \varphi)$ ,  $\theta$  being measured from the  $z$ -axis and  $\varphi$  from the  $x$ -axis in the  $(x, y)$  plane,

$$\begin{aligned} \phi_{21}'' = & -\frac{GM_2}{d^3} r^2 \left( 1 + \frac{M_1 + M_2}{2M_2} \right) \\ & + \frac{3}{2} \frac{GM_2}{d^3} r^2 \sin^2 \theta \left( 1 + \frac{1}{3} \frac{M_1 + M_2}{M_2} \sin^2 \varphi \right). \end{aligned} \quad (7.23)$$

Since  $U$  must always be positive, we deduce from (7.22) that, in a stationary configuration, we necessarily have

$$2V_{21}'' = 2 \int_M \phi_{21}'' dm > V_1.$$

More explicitly, using equation (7.23) to compute  $V_{21}''$ , we obtain

$$2 \frac{GM_2}{d^3} \left[ - \left( 1 + \frac{M_1 + M_2}{2M_2} \right) I_1 + \frac{3}{2} \left( 1 + \frac{M_1 + M_2}{6M_2} \right) I_{1,z} \right] > V_1, \quad (7.24)$$

where we have assumed that  $M_1$  has symmetry of revolution around the  $z$ -axis, so that  $\sin^2 \varphi$  may be replaced by its average value  $\frac{1}{2}$  and  $I_{1,z}$  denotes the moment of inertia about the  $z$ -axis.

Let us apply relation (7.24) to a homogeneous incompressible mass  $M_1$ , which, in these circumstances, takes the shape of a prolate spheroid along the  $z$ -axis. Assuming that  $M_1$  is small compared with  $M_2$  and that  $c/a \simeq 2$ , we find, for the necessary condition of stability of  $M_1$  in the field of  $M_2$ ,

$$\frac{M_1}{R_1^3} > 4.5 \frac{M_2}{d^3},$$

where  $R_1 = (a^2 c)^{1/3}$ . The corresponding equality may be taken as defining a critical distance  $d_c$  such that, for any  $d < d_c$ ,  $M_1$  is pulled apart by the tidal effect of  $M_2$ . Denoting by  $\rho_2$  the actual density of  $M_2$  and by  $\rho_2'$  the fictitious density of  $M_2$  supposed spread over the sphere of radius  $d$ , the condition may be written

$$\rho_1 > 4.5 \rho_2 \left( \frac{R_2}{d} \right)^3 \quad \text{or} \quad \rho_1 > 4.5 \rho_2', \quad (7.25)$$

which is analogous to the well-known Roche limit, although the exact discussion leads to a value of the constant about three times larger. This shows that, in some cases, the virial theorem may yield a necessary condition that is, however, quite far from being sufficient.

The case of two incompressible fluid masses both of finite volume so that each

is subject to distortion in the gravitational field of the other is appreciably more difficult. The numerical work of Darwin (1906) for two masses of the *same density* indicates that, ignoring the instability of the orbits due to tidal friction, which is of no interest to us here, the critical distance  $d'_c$  for which the configuration becomes unstable is fairly insensitive to the ratio  $M_1/M_2$  and remains always of the order of 2.5 times the radius of the combined mass assumed spherical.

As far as the effects of compressibility are concerned, very little is actually known. Equation (7.24) shows that, as compared with an incompressible mass, a compressible one of the same mean density will be more stable, since  $I_1$  and  $I_{1,z}$  decrease and  $V_1$  increases in absolute value as the central condensation (say  $\rho_c/\bar{\rho}$ ) increases.

Going to the extreme limit of Roche's model, in which practically all the mass is concentrated in a central point surrounded by a tenuous envelope of vanishing density, the instability, by breaking up as discussed above, disappears altogether. However, the total potential field of two masses built according to this model and revolving around their common center of gravity on circular orbits presents singularities at five Lagrangian points, three of which are on the line joining the two masses—one, say  $L_1$ , between them and two, say  $L_2$  and  $L_3$ , on both sides of the masses. The two other Lagrangian points, say  $L_4$  and  $L_5$ , are at the summits of the equilateral triangles built, in the plane of the orbit, on the segment joining the two masses. These points correspond to well-known particular solutions of the three-body problem in which a particle brought to any of these points with zero velocity remains indefinitely at rest in these positions with respect to axes centered at the center of gravity and rotating with the system. However, the straight-line solutions  $L_1$ ,  $L_2$ , and  $L_3$  are unstable, while  $L_4$  and  $L_5$  may be stable or unstable depending on the ratio of the masses. In particular,  $L_1$  is at the junction of the two lobes of a dumbbell-like equipotential surface surrounding the two masses.

If we assume that all this remains true for highly centrally condensed stars, they will both be stable as long as their volumes are smaller than that of the lobes inclosing them. But if, in the course of evolution, one of them expands, instability will set in as soon as its surface touches the first critical equipotential surface, and matter will be lost to the second star through  $L_1$ . Eventually, of course, the system as a whole can also lose mass through the external points  $L_2$  and  $L_3$ .

It is generally believed that these instabilities play an important role in the evolution of close binary stars whose observations, indeed, often reveal material streams circulating around and between the components or drifting away from them. This has given rise in recent years to many interesting papers by Struve, Kuiper, Kopal, Crawford, Huang, Sahade, Morton, and others.<sup>9</sup>

<sup>9</sup> For general accounts see Struve and Huang (1957), Sahade (1960), Morton (1960).

7.1.4. *Effects on the small perturbations of an equilibrium state.*—One may also attempt to use the complete form of the virial theorem (cf. eq. [6.1] or [7.21]), with the appropriate terms due to the above factors added, to improve somewhat the previous conclusions or complete them. In particular, if it is applied to a small perturbation of an equilibrium state depending on the time by a factor  $e^{i\sigma t}$ , it yields an expression for  $\sigma$  that, with the help of some reasonable assumption for the displacement, gives some quantitative indications on the effects of these factors.

For instance, for pseudo-radial pulsations of a rotating star, Ledoux (1945) obtained

$$\sigma^2 = - (3\gamma - 4) \frac{V}{I} + (5 - 3\gamma) \frac{2K}{I},$$

which gives the appropriate correction to the expression (3.13) valid in the absence of rotation. This formula shows that, if equilibrium is at all possible (grad  $p$  inward everywhere), no dynamical instability could arise from the rotation for the kind of displacement adopted. However, one should be aware that the latter is justified only for fairly slow angular velocities.

In the same way, in the presence of a magnetic field vanishing at the surface of the star or decreasing sufficiently rapidly outside it, Chandrasekhar and Limber (1954) get

$$\sigma^2 = - (3\gamma - 4) \frac{V + \mathfrak{M}}{I},$$

which confirms the previous conclusion (cf. eq. [7.12]). However, here also the result is valid only for pseudo-radial displacements. But a large magnetic field (Wentzel 1960) will distort the star considerably from the spherical shape, just as will a fast rotation, and Chandrasekhar's (1960) general tensorial formulation of the virial theorem may provide a more appropriate approach in these cases, although the choice of the displacement will remain critical.<sup>10</sup>

The origin of these difficulties is really our lack of adequate equilibrium models for stars in the presence of a fast rotation, a strong magnetic field, or a large external gravitational field. The problem is difficult enough for incompressible fluids without thermal properties. The heterogeneity introduced by compressibility already considerably increases the difficulty of building hydrostatic models. Furthermore, according to von Zeipel's theorem, in a rotating star the generation of energy and the heat transfer are incompatible with a solid-body rotation and cause meridional circulations. Because of the conservation of angular momentum, these acquire zonal components, which leads to differential rotation.

If the rotation is so slow that condition (7.8) is amply satisfied, approximate discussions are still possible<sup>11</sup> and yield the order of magnitude of the speed

<sup>10</sup> Since this was written, a long series of papers by Chandrasekhar and Lebovitz have appeared in the *Astrophysical Journal*, in which the power of this method has been demonstrated.

<sup>11</sup> See Sweet (1950), Öpik (1951), Mestel (1960).

of the meridional currents, which turns out to be very small. But, in the case of fast rotation, which is more interesting from the stability point of view, practically nothing is known of the possible stationary configurations. The same may be said in the case of a large external gravitational field whose effects are formally very similar to those of a fast "imaginary" rotation.

The situation is perhaps even more hopeless in the presence of a large magnetic field, despite some recent progress by Woltjer (1959) and Wentzel (1960) in the approach to the problem. But we are still very far from being able to take properly into account factors such as compressibility, energy generation, and heat transfer (Mestel 1956).

In these conditions it is understandable that the only cases where a detailed discussion of the effects of these various factors on the eigenvalues of the stability problem has been possible reduce to those where these factors can be treated as small perturbations (Cowling and Newing 1949, Ledoux and Simon 1957). Although this yields information on the perturbed frequencies of stable oscillations that may be useful, for instance, in the theory of intrinsic variable stars, it cannot lead to significant results concerning the instabilities capable of arising for large values of these factors.

## 7.2. LOCAL STABILITY

We have already seen that solid-body rotation is incompatible with energy generation and that the resulting steady state is characterized by a system of meridional and zonal circulations. For slow over-all rotation, the speed of these currents, however, is so small that they can hardly affect the structure of the star and that the resulting mixing between layers at different depths can be neglected (Sweet 1950, Öpik 1951, Mestel 1960). The situation must be very similar as far as the effects of a fairly weak external gravitational field are concerned. We know very little of what happens in the presence of a magnetic field and energy generation, although, far from the critical cases discussed in the preceding section, it is rather unlikely that fast motions and appreciable mixing could arise on this basis.

However, these various factors have other effects on local stability, which, as far as rotation and magnetic field are concerned, are discussed very completely at least for plane layers of idealized fluid in Chandrasekhar's (1961) book on hydrodynamical stability. Here we recall only the most significant features for stellar structure. A somewhat more detailed summary has also been presented elsewhere (Ledoux 1958, § 17).

**7.2.1. *Effects of a rotation.***—Differential rotation by itself can create a local type of instability similar in many respects to thermal convective instability. Let us consider, for instance, an incompressible fluid rotating with an angular velocity  $\Omega(R)$  depending only on the distance  $R$  to the axis. Because of the conservation of angular momentum, an element of matter displaced outward arrives in its new surroundings with an angular velocity larger than the local one if, in the unperturbed state,  $\Omega R^2$  decreases when  $R$  increases. Hence it is subject

to a stronger centrifugal force than its neighbors, and its outward motion is accelerated. This instability tends to result in meridional convective motions, which can be fairly fast and could provide an efficient means of mixing. On the other hand, if Rayleigh's criterion,

$$\frac{d[\Omega(R)R^2]}{aR} > 0, \quad (7.26)$$

is satisfied, the resulting field of centrifugal force stabilizes the medium at least against displacement normal to the axis of rotation.

In a compressible medium, the buoyancy of the displaced element must be composed with the excess or defect of centrifugal force to obtain the net force acting upon it, and one may expect that the global condition for stability will involve a combination of the terms on the left of (2.18) and (7.26).

In particular, we see from equation (7.26) that a solid-body rotation ( $\Omega = \text{const.}$ ) should have a stabilizing influence at least in some directions. In the stellar case, this has been discussed, first, by Randers (1942) and more completely by Cowling (1945, 1951), who found that, in the presence of a super-adiabatic gradient ( $D$  or  $A > 0$ ; cf. eq. [2.21]), instability would persist for a displacement characterized by wave numbers  $l_R, l_z, l_\varphi$ , provided that

$$g \cdot A[l_\varphi^2 + (l_R \cos \alpha - l_z \sin \alpha)^2] < -4\Omega^2 l_z^2, \quad (7.27)$$

where  $\alpha$  is the angle between  $-g$  and the  $z$ -axis oriented along  $\Omega$ . For the slow rotations considered here,  $\alpha$  is always very close to the co-latitude  $\theta$ , and one easily verifies that, for radial displacements, this condition reduces to

$$gA > 4\Omega^2 \sin^2 \theta,$$

which shows that convection parallel to the equatorial plane is always hindered by a solid-body rotation, while the ordinary Schwarzschild criterion of stability applies to motions parallel to the axis of rotation. However, the general condition (7.27) also shows that there are always displacements with non-vanishing components along  $R$  and  $\varphi$  which lead to instability for arbitrary small positive values of  $A$ , provided that the wave number  $l_z$  tends toward zero. But the corresponding motions are rather special and may be unimportant as far as the transfer of heat is concerned.

The case of a non-uniform rotation has been tackled by Solberg and Høiland (1939, 1941), who endeavored to interpret the problem in terms of the circulation theorems of Bjerknes applied to closed-stream tubes implying axial symmetry in the displacement. This method leads to a very general criterion which can be reduced to the following necessary and sufficient conditions of stability:

$$\frac{2\Omega}{R} \frac{\partial(\Omega R^2)}{\partial R} + g \cdot A > 0, \quad g_z A_z > 0, \quad (7.28)$$

$$g_z \left[ \frac{\partial(\Omega R^2)}{\partial R} A_z - \frac{\partial(\Omega R^2)}{\partial z} A_R \right] > 0. \quad (7.29)$$



If rotation is absent, one recovers Schwarzschild's criterion, while if the fluid is in adiabatic equilibrium ( $A_R = 0$ ,  $A_z = 0$ ), condition (7.28) reduces to Rayleigh's criterion (7.26).

Wasiutynski (1946, §§ 6.2, 6.3, and 26.1) considers that some of the possibilities of instability implied by relations (7.28) and (7.29) would disappear if the discussion was limited to displacements along the stream tubes of steady motions, which are actually possible when dissipation by conduction and viscosity is taken into account, as was done, for instance, in establishing Rayleigh's criterion (2.24) for thermal instability toward cellular convection. In the general stellar case of a compressible fluid with pseudo-spherical symmetry, this is a highly complex problem that has not been tackled.

On the other hand, the influence of a solid-body rotation on the Rayleigh-Jeffreys problem (convection in a horizontal layer of fluid treated as incompressible except for the variations of the weight  $g\rho$  due to the varying temperature) has been extensively studied by Chandrasekhar, and a full account of the results and complete references will be found in his book (Chandrasekhar 1961).

If the axis of rotation is vertical, one finds that the Coriolis force inhibits the onset of cellular convection, the critical Rayleigh number (cf. eq. [2.25]) being larger than the value (2.25) by an amount that increases with the Taylor number

$$\mathfrak{T} = \frac{4h^4\Omega^2}{\nu^2}, \quad (7.30)$$

the cells getting more and more elongated along the vertical at the same time.

Chandrasekhar also found that, in presence of sufficiently strong Coriolis forces,  $\mathfrak{T}$  greater than a critical  $\mathfrak{T}^*$ , and if the ratio  $\kappa/\nu$  of the conductivity to the kinematic viscosity is larger than another critical value depending somewhat on the boundary condition (1.478 in case of two "free" surfaces), instability arises as oscillations of increasing amplitude (overstability or vibrational instability) before convection can start. Considering the assumptions on which it rests, this theory can probably be applied safely only to fairly thin external layers in a star. But, in that case, if the only form of viscosity is of molecular or radiative origin,  $\kappa/\nu$  becomes so large that, according to Chandrasekhar, we should expect local instability due to superadiabatic gradients to manifest itself much more frequently as oscillations of increasing amplitude than as cellular convection. However, turbulent friction, if present, could very well reverse this conclusion.

When the axis of rotation is inclined to the vertical by an angle  $\theta$ , the previous conclusions remain valid for convective instability starting as elongated rolls parallel to the plane ( $\Omega$ ,  $g$ ), provided that  $\Omega$  be replaced by  $\Omega \cos \theta$  in equation (7.30). For other types of displacements, however, the situation is more difficult and has not been cleared up completely.

Finally, the most interesting case, in some respects—namely, that of non-uniform rotation—has hardly been considered.

7.2.2. *Effects of an external gravitational field.*—To the best of my knowledge, no discussion of this case exists in the literature, and it does not seem that an external field will have much direct influence on the onset of local convection. But in a superadiabatic region ( $A > 0$ ) the motions at right angles to the direction of the external field will be enhanced, a slow meridional circulation then probably being necessary to compensate for this.

7.2.3. *Effects of a magnetic field.*—In many respects, the effects of a magnetic field on local stability are similar to those of a rotation. As was suggested by Biermann (1941), if convection results in motions characterized by closed stream lines, it must be hindered by the presence of a general uniform magnetic field, since a highly conducting fluid tends to stick to the magnetic lines of force. An interesting qualitative account of the main features of this situation may be found in Cowling's (1957) book.

To illustrate the stabilizing influence of the magnetic field, let us consider a horizontal layer with a vertical superadiabatic gradient ( $A > 0$ ) and subjected to a horizontal magnetic field  $H$ , neglecting viscosity and conduction. In the absence of  $H$ , the layer would be convectively unstable, but, in the presence of the field, a simple argument (Walen 1949) shows that instability arises only if

$$A > \frac{\pi H^2}{\lambda^2 g \rho},$$

the instability being the greater, for a given  $A$ , the larger the wavelength  $\lambda$  along the magnetic field (Kruskal and Schwarzschild 1954).

The corresponding extension of the Rayleigh-Jeffreys problem has been discussed quantitatively by Thomson (1951) and more extensively by Chandrasekhar (1961) especially for the case where  $H$  and  $g$  are parallel. As in the case of rotation, one finds that the critical Rayleigh number above which convection sets in is larger than in the case without a magnetic field by an amount that increases with the Hartmann number,

$$\mathcal{M} = \frac{H^2 h^2 \sigma}{\rho \nu}, \quad (7.31)$$

where  $\sigma$  is the electrical conductivity.

Overstability may also occur here before convection, provided that  $\mathcal{M}$  is large enough and the thermal conductivity  $\kappa$  appreciably greater than the electrical resistance  $(4\pi\sigma)^{-1}$ . As, in a stellar atmosphere,  $\kappa \gg (4\pi\sigma)^{-1}$ , one should expect that, in presence of a magnetic field, overstability would be fairly frequent. However, it is likely that, for many types of displacements, the damping due to second-order terms could limit the amplitudes to relatively small values. Furthermore, as pointed out by Cowling, a stellar layer has no fixed boundaries, as in the theoretical case, and the resulting effect is more likely to be a limited increase in the amplitude of progressive waves traveling through the unstable region than the building-up of large standing oscillations.

Chandrasekhar has shown that the previous results remain valid, if  $H$  makes

an angle  $\theta$  with  $\mathbf{g}$ , for convection starting in elongated rolls parallel to the plane  $(\mathbf{H}, \mathbf{g})$ , provided that  $H$  be replaced by  $H \cos \theta$  in equation (7.31). On the contrary, convection in transverse rolls is much more difficult to excite. Chandrasekhar has also studied the combined effect of a rotation and a magnetic field and discussed the way in which the shape of the most favored cells varies with  $\mathfrak{T}$  and  $\mathfrak{M}$ .

As far as non-uniform magnetic fields are concerned, even less is known, at least in the stellar context, than in the case of non-uniform rotation, although, in some problems, perturbation of wavelengths comparable to the scale of variation of the field may be the more interesting.

Finally, the general interaction between rotation and magnetic field would certainly deserve a better treatment than the rough arguments based on the "frozen-in field" picture commonly used when this problem arises, namely, in the discussion of stellar evolution. For instance, is it not possible that the often invoked braking action on rotation of a stellar magnetic field interacting with interstellar or expelled stellar material would result in a gradient of  $(\Omega R^2)$  inside the star violating Rayleigh's condition (7.26) and leading to a fairly active convective instability which could have important consequences for the further evolution of the star? In the same way, is it true, as assumed by Hoyle and others, that if a rotating star possesses a magnetic field, its angular velocity remains uniform throughout when it evolves by contraction of a dense central core and expansion of the surrounding envelope? In the absence of a magnetic field, this type of evolution would most probably, as mentioned once by Schlüter, lead to intense differential rotation, violating equation (7.26), and remixing of the interior, with no doubt very important consequences for the evolution. One would expect that, at least for a weak enough magnetic field, these conclusions would remain valid, but they are so different from the surface rotational instability to which the first assumption leads that, certainly, a careful discussion of the whole problem would be justified.

#### REFERENCES

- |   |      |  |
|---|------|--|
| BATCHELOR, G. K.  | 1953 | <i>The Theory of Homogeneous Turbulence</i> (Cambridge: Cambridge University Press). |
| BIERMANN, L.  | 1935 | <i>A.N.</i> , <b>257</b> , 269.  |
|   | 1939 | <i>Zs. f. Ap.</i> , <b>18</b> , 344.   |
|   | 1941 | <i>Vjschr. Astr. Gesellsch.</i> , <b>76</b> , 194.                                   |
| BIERMANN, L., and<br>COWLING, T. G.                                     | 1939 | <i>Zs. f. Ap.</i> , <b>19</b> , 1.   |
| BOURY, A.   | 1963 | <i>Ann d'ap.</i> , <b>26</b> , 354.  |
| BOURY, A., and<br>MME HUSTIN-BRETON                                     | 1961 | <i>Bull. Acad. R. Belg., Cl. Sci.</i> , 5th ser., <b>47</b> , 543.                   |
| BURBIDGE, E. M.,<br>BURBIDGE, G. R.,<br>FOWLER, W. A., and<br>HOYLE, F. | 1957 | <i>Rev. Mod. Phys.</i> , <b>29</b> , 547.  |

- BURBIDGE, G. R. 1960 *Die Entstehung von Sternen durch Kondensation diffuser Materie* (Berlin: Springer-Verlag), p. 1.
- BURBIDGE, G. R., HOYLE, F., BURBIDGE, E. M., CHRISTY, R. F., and FOWLER, W. A. 1956 *Phys. Rev.*, **103**, 1145.
- CAMERON, A. G. W. 1962 *Icarus*, **1**, 13.
- CHANDRASEKHAR, S. 1939 *An Introduction to the Study of Stellar Structure* (Chicago: University of Chicago Press), chaps. 10 and 11.
- 1949 *Ap. J.*, **110**, 329.
- 1952a *Phil. Mag.*, ser. 7, **43**, 1317.
- 1952b *Phil. Trans. R. Soc. London*, ser. A, **244**, 357.
- 1953 *Phil. Mag.*, ser. 7, **44**, 233.
- 1957 *J. U. Madras, B*, **27**, 251.
- 1958 *Max Planck Festschrift*, p. 103.
- 1960 *J. Math. Anal. and Appl.*, **1**, 240.
- 1961 *Hydrodynamic and Hydromagnetic Stability* (Oxford: Clarendon Press).
- CHANDRASEKHAR, S., and FERMI, E. 1953 *Ap. J.*, **118**, 116.
- CHANDRASEKHAR, S., and LIMBER, D. N. 1954 *Ap. J.*, **119**, 10.
- CHANDRASEKHAR, S., and SCHÖNBERG, M. 1942 *Ap. J.*, **96**, 161.
- COLGATE, S. A., GRASBERGER, W. H., and WHITE, R. A. 1962 *J. Phys. Soc., Japan, suppl. A*, Vol. 3.
- COLGATE, S. A., and JOHNSON, M. H. 1960 *Phys. Rev., Letters*, **5**, 235.
- COUNSON, J., LEDOUX, P., and SIMON, R. 1956 *Bull. Soc. R. Sci. Liège*, **25**, 144.
- COWLING, T. G. 1935 *M.N.*, **96**, 42.
- 1938 *Ibid.*, **98**, 528.
- 1941 *Ibid.*, **101**, 367.
- 1945 *Ibid.*, **105**, 166.
- 1951 *Ap. J.*, **114**, 272.
- 1957 *Magnetohydrodynamics* (New York and London: Interscience Publishers), chap. 4.
- 1960 *M.N.* **121**, 393.
- COWLING, T. G., and NEWING, R. A. 1949 *Ap. J.*, **109**, 149.
- COX, A. N., and BROWNEE, R. R. 1960 *Mém. Soc. R. Sci. Liège*, 5th ser., **3**, 469.
- COX, J. P. 1955 *Ap. J.*, **122**, 286.
- 1960 *Ibid.*, **132**, 594.
- DARWIN, G. H. 1906 *Phil. Trans. R. Soc. London*, ser. A, **206**, 161.

- EBERT, R., HOERNER,  
S. VON, and  
TEMESVÁRY, ST. 1960 *Die Entstehung von Sternen durch Kondensation  
diffuser Materie* (Berlin: Springer-Verlag), p. 184.
- EDDINGTON, A. S. 1919 *M.N.*, **79**, 2 and 177.  
1941 *Ibid.*, **101**, 182.  
1942 *Ibid.*, **102**, 154.
- EZER, D. 1961 *Ap. J.*, **133**, 159.
- HÄRM, R., and  
SCHWARZSCHILD, M. 1961 *A.J.*, **66**, 45.
- HAZLEHURST, J., and  
SARGENT, W. L. 1959 *Ap. J.*, **130**, 276.
- HENYEY, L. G., WILETS,  
L., BÖHM, K. H.,  
LELEVIER, R., and  
LEVÉE, R. D. 1959 *Ap. J.*, **129**, 628.
- HØILAND, E. 1939 *Arch. Mat. Naturvidensk.* (Oslo), Vol. **42**, No. 5.  
1941 *Avhandl. Norsk. Vidensk. Akad., Mat.-Naturv. Kl.*  
(Oslo), No. 11.
- HOYLE, F. 1946 *M.N.*, **106**, 343.  
1953 *Ap. J.*, **118**, 513.  
1960 *Mém. Soc. R. Sci. Liège*, 5th ser., **3**, 445.
- HUANG, SU-SHU 1960 *Ap. J.*, **131**, 452.
- INCE, E. L. 1944 *Ordinary Differential Equations* (New York:  
Dover Publications).
- JEANS, J. H. 1919 *Problems of Cosmogony and Stellar Dynamics*  
(Cambridge: Cambridge University Press).  
1928 *Astronomy and Cosmogony* (Cambridge: Cam-  
bridge University Press), § 108.  
1930 *Proc. Cambridge Phil. Soc.*, **26**, 170.
- JEFFREYS, H.  
JEFFREYS, H., and  
BLAND, M. E. M. 1951 *M.N., Geophys. Suppl.*, **6**, 148.
- JEVAKHIN, S. A. 1959a *A.J. (U.S.S.R.)*, **36**, 269.  
1959b *Ibid.*, p. 394.  
1959c *Ibid.*, p. 996.
- KAHN, F. D. 1960 *Die Entstehung von Sternen durch Kondensation  
diffuser Materie* (Berlin: Springer-Verlag), p. 104.
- KRUSKAL, M., and  
SCHWARZSCHILD, M.  
LEDoux, P. 1954 *Proc. R. Soc. London, A*, **223**, 348.  
1941 *Ap. J.*, **94**, 537.  
1945 *Ibid.*, **102**, 143.  
1949 *Mém. Soc. R. Sci. Liège*, 4th ser., Vol. **9**, chaps. 4  
and 5.  
1958 *Hdb. d. Phys.*, ed. S. FLÜGGE (Berlin: Springer-  
Verlag), **51**, 605.  
1960 *Bull. Acad. R. Belg., Cl. Sci.*, 5th ser., **46**, 429.  
1962 *Ibid.*, **48**, 240.

- LEDOUX, P., and  
BOURY, A. 1960 *Mém. Soc. R. Sci. Liège*, 5th ser., **3**, 298.
- LEDOUX, P., and  
PEKERIS, C. L. 1941 *Ap. J.*, **94**, 124.
- LEDOUX, P., and  
SAUVENIER-GOFFIN, E. 1950 *Ap. J.*, **111**, 611.
- LEDOUX, P.,  
SCHWARZSCHILD, M.,  
and SPIEGEL, E. 1961 *Ap. J.*, **133**, 184.
- LEDOUX, P., and  
SIMON, R. 1957 *Ann. d'ap.*, **20**, 185.
- LEDOUX, P., and  
WALRAVEN, TH. 1958 *Hdb. d. Phys.*, ed. S. FLÜGGE (Berlin: Springer-Verlag), **51**, 353.
- LEDOUX, P., and  
WHITNEY, C. A. 1961 *I.A.U. Symp. No. 12 (Nuovo Cimento*, ser. 10, **22**, Suppl. No. 1), p. 131.
- LEVÉE, R. D., and  
HILTON, P. L. 1960 *Mém. Soc. R. Sci. Liège*, 5th ser., **3**, 514.
- LIPOUNOFF, M. A. 1907 *Ann. Toulouse*, ser. 2, Vol. **9**.
- LIMBER, D. N. 1958 *Ap. J.*, **127**, 363 and 387.
- LONGE, P. 1956 *Bull. Soc. R. Sci. Liège*, **25**, 541.
- LÜST, R., and  
SCHLÜTER, A. 1955 *Zs. f. Ap.*, **38**, 190.
- LYTTLETON, R. A. 1953 *The Stability of Rotating Liquid Masses* (Cambridge: Cambridge University Press).
- MESTEL, L. 1952 *M.N.* **112**, 583.  
1956 *Ibid.*, **116**, 324.  
1959 *Ibid.*, **119**, 223 and 249.  
1960 *Mém. Soc. R. Sci. Liège*, 5th ser., **3**, 235.
- MESTEL, L., and  
SPITZER, L., JR. 1956 *M.N.*, **116**, 503.
- MORTON, D. C. 1960 *Ap. J.*, **132**, 146.
- ÖPIK, E. 1951 *M.N.*, **111**, 94.
- ONO, Y., and  
SAKASHITA, S. 1961 *Pub. Astr. Soc. Japan*, **13**, 146, and *Progress of Theoret. Phys.*, Suppl. No. 20, p. 85.
- OTTELET, I. 1960 *Ann. d'ap.*, **23**, 218.
- PEKERIS, C. L. 1938 *Ap. J.*, **88**, 189.
- PIDDINGTON, J. H. 1957 *Australian J. Phys.*, **10**, 530.
- RANDERS, G. 1942 *Ap. J.*, **95**, 454.
- ROSSELAND, S. 1931 *Pub. Obs. U. Oslo*, No. 1.  
1932 *Ibid.*, No. 2.  
1949 *The Pulsation Theory of Variable Stars* (Oxford: Clarendon Press), §§ 5.3–5.5.
- SAHADE, J. 1960 *Mém. Soc. R. Sci. Liège*, 5th ser., **3**, 76.

- SANDAGE, A. R., and  
SCHWARZSCHILD, M. 1952 *Ap. J.*, **116**, 463.
- SAUVENIER-GOFFIN, E. 1950a *Mém. Soc. R. Sci. Liège*, 4th ser., **10**, 1.  
1950b *Bull. Soc. R. Sci. Liège*, **19**, 47.  
1951 *Ibid.*, **20**, 20.
- SCHATZMAN, E. 1945 *Ann. d'ap.*, **8**, 143.  
1951 *Ibid.*, **14**, 305.  
1954 *Mém. Soc. R. Sci. Liège*, 4th ser., **14**, 163.  
1956 *Ann. d'ap.*, **19**, 45.  
1958 *White Dwarfs* (Amsterdam: North Holland Publishing Co.).  
1959 *I.A.U. Symp. No. 10*, p. 129.  
1960 *Mt. Wilson and Palomar Obs., Tech. Rept., No. 3*.
- SCHWARZSCHILD, M. 1958 *Structure and Evolution of the Stars* (Princeton: Princeton University Press), § 7.  
1959 *Ap. J.*, **130**, 355.
- SCHWARZSCHILD, N., and  
HÄRM, R. 1959 *Ap. J.*, **129**, 637.
- SIMON, R. 1957a *Bull. Acad. R. Belg., Cl. Sci.*, 5th ser., **43**, 471.  
1957b *Ibid.*, **43**, 610.  
1959 *Ann. d'ap.*, **22**, 712.
- SKUMANICH, A. 1955 *Ap. J.*, **121**, 408.
- SOUFFRIN, P. 1960 *Mém. Soc. R. Sci. Liège*, 5th ser., **3**, 245.
- SPIEGEL, E. A., and  
VERONIS, G. 1960 *Ap. J.*, **131**, 442.
- SPITZER, L., JR. 1958 *I.A.U. Symp.*, **6**, 169.
- STRUVE, O., and  
HUANG, SU-SHU 1957 *Occ. Notes R.A.S.*, **3**, 161.
- SWEET, P. A. 1950 *M.N.*, **110**, 548.
- THOMAS, L. H. 1930a *M.N.*, **91**, 122 and 619.  
1930b *Quart. J. Math.*, **1**, 239.
- THOMSON, W. 1863 *Phil. Trans. R. Soc.*, **153**, 612.
- THOMSON, W. B. 1951 *Phil. Mag.*, **42**, 1417.
- TOLMAN, R. C. 1939 *Ap. J.*, **90**, 541.
- UNSÖLD, A. 1930 *Zs. f. Ap.*, **1**, 138.
- WALEN, C. 1949 *On the Vibratory Rotation of the Sun* (Stockholm: Lindstahl's Bokhandel).
- WASIUTYNSKI, J. 1946 *Ap. Norveg.*, Vol. **4**, Sec. 22.2.
- WAVRE, R. 1932 *Figures planétaires et géodésie* (Paris: Gauthier-Villars).
- WENTZEL, D. G. 1960 *Ap. J., Suppl.*, **5**, 187.
- WHITNEY, C. 1955 "Stellar Pulsation," Thesis, Harvard University, unpublished.
- WOLTJER, L. 1959 *Ap. J.*, **130**, 400 and 405.

## CHAPTER 11

# *Stellar Evolution and Age Determinations*

R. L. SEARS\*

*Kellogg Radiation Laboratory, California Institute of Technology*

AND

ROBERT R. BROWNLEE†

*Astronomy Department, University of California at Los Angeles*

### § 1. INTRODUCTION

AT THE conclusion of his *Internal Constitution of the Stars*, Sir Arthur Eddington (1926) stated: “. . . it is reasonable to hope that in a not too distant future we shall be competent to understand so simple a thing as a star.”

Great progress has been made since that time in the study of stellar structure, but the limitations of our knowledge were well stated in the remark addressed to a distinguished member of his audience by Martin Schwarzschild at the conclusion of the second Invited Discourse at the Eleventh General Assembly of the International Astronomical Union, at Berkeley, California, in 1961:

Indeed, I would think that it must be to you, Professor Hertzprung, cause of appreciable puzzlement to have watched throughout your life a stream of eager theoreticians working hard on these problems and even now being able to understand only the most obvious feature in the diagram which you plotted for the first time more than 50 years ago.

Up to about 1950 studies of stellar interiors were concerned primarily with the structure of equilibrium models. Although some early efforts were made to

\* Work supported by the National Aeronautics and Space Administration and the Office of Naval Research.

† On Professional Research and Teaching leave from Los Alamos Scientific Laboratory, University of California, Los Alamos, New Mexico; the author was partially sponsored by the AEC when this contribution was first written. Revisions and typing done at Los Alamos under the sponsorship of the AEC.



investigate the evolution of main-sequence stars (e.g., Schönberg and Chandrasekhar 1942), the principal approaches to explaining the positions of various kinds of stars in the Hertzsprung-Russell diagram lay in deriving individual, isolated models. A review by Strömgren (1952) summarizes the state of affairs at the close of this earlier era.

In the past decade, attention has turned to the construction of evolutionary sequences of stellar models, following upon the classical paper of Sandage and Schwarzschild (1952) which showed how red giant stars would occur as the inevitable consequence of natural evolutionary processes. This paper was by no means the first to suggest possible models for red giants (e.g., Öpik 1938; see Oke and Schwarzschild 1952, and references given there), but it came just after the first Hertzsprung-Russell diagrams (color-magnitude arrays) for globular clusters had been achieved down to the main sequence (Arp, Baum, and Sandage 1952), and presented such a strikingly natural explanation of the observations as to mark a breakthrough into new fields of research in stellar interiors.

Developments in the past decade have been described in Schwarzschild's (1958) book, *Structure and Evolution of the Stars* (hereafter referred to as SES); in a general article by the Burbidges (1958) which reviews much of the history of the subject, the observational basis for stellar evolution, and the first developments of modern notions of nucleosynthesis; and in an extensive review by Hayashi, Hoshi, and Sugimoto (1962) which gives many details of stellar models in all evolutionary phases. The present chapter, although we hope self-contained, to some extent complements these recent reviews. Thus, in § 2, we summarize current descriptions of the physics of stellar evolution with particular attention to recent work. In § 3, we take up details of construction of evolutionary sequences by methods, not covered explicitly in Schwarzschild's book, which have particular advantages for automatic, high-speed computers. In § 4, we review the application of the theory of stellar evolution to age determinations of stars, with attention to some of the major uncertainties which beset this application at the present time.

## § 2. PHYSICAL DESCRIPTION OF STELLAR EVOLUTION

The simplest observational fact about stars is that they shine; and an immediate conclusion from this observation is that they must evolve. The sun radiates energy at the rate of  $3.90 \times 10^{33}$  erg/sec (Allen 1963) at the present time; what are the sources of this energy, and how will the structure of the star change as these sources are drained in the march of cosmic time? The answer to the first question can be illustrated by reference to the sun, for which the available gravitational potential energy between the present state and a white dwarf state (Savardoff 1963) is  $+7 \times 10^{50}$  ergs, the thermal energy (including ionization, kinetic, and radiant energies) is  $3 \times 10^{48}$  ergs, and the nuclear energy (from conversion of hydrogen to iron) is  $9 \times 10^{51}$  ergs. There are no other known sources of energy in comparable amounts if we exclude the total

rest-mass energy,  $1.8 \times 10^{54}$  ergs, which is not considered to be available except for the  $\frac{1}{2}$  per cent released through nuclear reactions. Thus, for the sun, and by extension for other stars, only three main energy sources are important in evolution: gravitational, thermal, and nuclear.

The life of a star may be viewed as a continuous struggle to maintain equilibrium against the forces of gravity, nourished only by the steadily draining energy sources. In terms of such a picture the answer to our second question above involves following this struggle in minute detail, step by step in time. That this is possible, at least in part at the present time, is due to the mathematical completeness of a realistic theory of stellar structure, the last essential part of which was fitted into the puzzle by Bethe (1939) and others with their descriptions of the details of thermonuclear energy generation. In this section we shall review the subsequent developments in the theory of structural evolution, concentrating upon developments in recent years and stressing some of the large gaps that remain. In § 3 we shall take up details of computing the struggle.

### 2.1. PRE-MAIN-SEQUENCE STAGES

The very earliest stage in the evolution of a star has not been satisfactorily explained, though a growing number of attempts to delimit the problem have been made in recent years (see, e.g., Burbidge, Kahn, Ebert, von Hoerner, and Temesváry 1960). There is today little doubt that stars are formed from the interstellar medium (see Vol. 7 of this series); a great variety of observations support this view. As Baade (1944) emphasized in his classical paper on stellar populations, O and B stars, whose great luminosities preclude existence as such for more than a few millions of years, are invariably to be found in intimate association with extensive clouds of gas and dust, in our own and other galaxies. Their space motions are too small, relative to the gas clouds, for them to be simply transient passers-by. Moreover, these motions can in a few cases be measured with sufficient accuracy to show that groups of these stars are undergoing kinematic, if not dynamic, expansions from common origins (Blaauw 1952, 1961) that have been going on for only about  $10^7$  years. In addition to OB stars, T Tauri stars, whose light variability and characteristic emission-line spectrum indicate that they are similarly passing through a short stage of stellar evolution (Herbig 1962*a*), are also found embedded in interstellar gas and dust clouds (Joy 1945). Occasionally we see projected on the bright backgrounds of emission nebulae small dark spheroidal globules (Bok and Reilly 1947), which hint at the existence of protostars in a preluminous state. There has even been an observation by Herbig (1957; cf. Haro and Minkowski 1960) of the possible birth of a star.

Despite the wealth of qualitative observations, however, theoreticians have encountered frustrating barriers in attempting to provide a quantitative explanation. It has been remarked by Burbidge (1960) that, "If stars did not exist, it would be easy to prove that this is what we expect." Analyses of the

interstellar medium, as reviewed, e.g., by Spitzer (1966), have shown that there are turbulent motions within it, and we are probably quite safe in believing that the material for the initial stellar state is thoroughly mixed. However, the amount of angular momentum possessed by a cloud as gravitational contraction begins may be determined in a random manner. Since the star's history during the contraction phase may be strongly dependent on the angular momentum present, the usual assumption of non-rotation made in the calculation of models may be largely unrealistic.

There are additional problems, as yet unsolved, associated with the determination of the structure and energy of a contracting cloud. Of fundamental importance is the precise role played by the galactic magnetic field and the ensuing field of the cloud (Burbidge and Burbidge 1958, p. 154; Mestel 1962). Eventually, gravitational contraction will force a compression of the magnetic field and a simultaneous increase in the rotational kinetic energy due to the conservation of angular momentum. The existing magnetic fields can thus become distorted and, in a partially ionized plasma, high potentials may be produced (Greenstein 1961). These high potentials can be responsible for the acceleration of charged particles, which in turn can produce further ionization and effect changes in the magnetic field. Detailed calculations on the appropriate time scale of such complex events and their ultimate effects upon the cloud are, of course, desirable but not yet practicable.

For the present we will ignore the effects of the rotation and magnetic fields and describe current ideas of a star's evolutionary history as though the star is well behaved, condensing from a homogeneous cloud of material whose internal motions are such that the net angular momentum is zero.

More than a century ago H. von Helmholtz (1854) proposed that the source of energy for the sun and other stars was the gravitational energy released by the star as it contracted. Since the work done on a shell of material of radius  $r$ , thickness  $dr$ , and mass  $dM(r)$  in bringing it from infinity to  $r$  is

$$d\Omega = -GM(r) dM(r) \int_r^\infty \frac{dr'}{r'^2} = \frac{-GM(r) dM(r)}{r},$$

the total potential energy (negative) of a stellar mass of radius  $R$  is

$$\Omega = \int_0^R d\Omega = -G \int_0^R \frac{M(r) dM(r)}{r}.$$

The distribution of mass within the sun is still imperfectly known. However, the uncertainty is not so large as to preclude a good value for the total potential energy, about  $-6 \times 10^{48}$  ergs. Roughly, this amounts to about  $3 \times 10^{15}$  erg/gm. Since the energy output of the sun corresponds to approximately  $2 \text{ erg gm}^{-1} \text{ sec}^{-1}$ , the total time the present solar luminosity could have been maintained from gravitational potential energy alone is  $1.5 \times 10^{15}$  seconds, or about  $5 \times 10^7$  years. Considering our knowledge of the age of the solar system,

clearly this interval of time is very short, and gravitational energy cannot be the sole source of supply for the sun. Nevertheless, we shall see that it is the gravitational contraction which enables the sun—and any star—to proceed from one evolutionary stage to another in a smooth and orderly manner.

Initially then, as the interstellar cloud becomes sufficiently dense, contraction begins. In general, about one half of the gravitational potential energy is converted into internal energy and hence goes to heat the stellar material. The remaining energy is radiated away and the cloud becomes slightly luminous. Were the ratio,  $\gamma$ , of the specific heats of the stellar material precisely  $C_p/C_v = \frac{5}{3}$ , where  $C_p$  and  $C_v$  are the specific heat per mole at constant pressure and at constant volume, respectively, then exactly one-half the gravitational potential energy would be radiated away. Generally, however,  $\gamma$  will be slightly less than  $\frac{5}{3}$ , and the internal energy will benefit as slightly more than one half of the gravitational potential energy goes to heat the star. Thus, as the contraction proceeds, the radius decreases steadily and the temperature and luminosity rise.

But what of the energy that is being radiated away? The mode of energy transport which prevails at this early time is crucial in fixing the time scale and the variation of luminosity in the contracting stellar mass. Our present knowledge of these physical conditions is weak. The basic difficulty is lack of detailed information about the behavior of matter under the extreme conditions which evidently prevail in the primordial cloud. In particular, much of the mass of the cloud is so rarefied and the temperature is so low that we can do little more than guess at or make crude approximations for the equation of state and the opacity of the material. The presence of water vapor and various other molecules would seriously impede the flow of radiation, yet few (see Gaustad 1963) calculations of opacity arising from these sources have been made to the present. Because the opacity of the material ultimately determines the rate at which gravitational energy is released and, therefore, the rate of contraction, this lack of knowledge may be very serious. Further, the boundary conditions for our models, which are critically important to the question of convective transport, are sufficiently complex that no entirely satisfactory method has yet been devised for their determination. Suffice it to say that recent work on contracting models differs, in the main, dramatically from earlier work due to the use of improved boundary conditions (see below; see also Upton 1966).

Recent work has indicated that within our initial assumptions, i.e., that there is no stellar rotation or magnetic field, the opacity of material of a reasonable composition is sufficiently high that the radiative gradient exceeds the adiabatic gradient, and therefore the energy will be transported by convection (Hayashi 1961). Convective transport is in general so much more efficient than radiation transport that there is a dramatic and rapid collapse of the mass (Ezer and Cameron 1962). As a consequence, the gravitational energy is given up very quickly in, say, five million years or so, and the protostar is quite luminous and the effective temperature may be nearly that of the primordial main sequence

for much of that time (cf. Hayashi 1961; Cameron 1962*a, b*; Weymann and Moore 1962).

It should be noted that convection could be inhibited by hydromagnetic forces and that Coriolis force is a stabilizing influence. Until these effects are considered carefully, no definitive decision between a convective and a radiative model can be made (Alfvén, private communication).

If it should happen that convection is inhibited sufficiently to be relatively unimportant as the protostar collapses (see Faulkner, Griffiths, and Hoyle 1963), then the sequence of events might be more nearly like that originally calculated by Brownlee and Cox (1961). They found, for example, that when the central temperature of one solar mass has reached  $5 \times 10^5$  ° K and the central density about 0.02 gm/cm<sup>3</sup>, the radius of the model was only about 25 to 30 times the present solar radius. Further, the effective temperature was only about 450° K. Now, these central material conditions are just beginning to be sufficient to support the first of the nuclear reactions, namely, the burning of deuterium if any should be present. Evidently no nuclear transformations have occurred prior to this time unless they have occurred in the presence of magnetic fields or other sources of energy.

For stars of greater mass, the radii will of course be appreciably larger when the central temperature is  $5 \times 10^5$  ° K. Homology transformations indicate that a star of 10 solar masses would have such a central temperature when the stellar radius was about 30 per cent greater than that of the earth's orbit. Clearly at earlier contractive stages the temperature throughout the entire star is very low and all difficulties mentioned above pertain.

Because the radius of the star is certain to be even smaller for the same central temperature when convection plays a dominant role, apparently the central temperatures and densities of stars cannot sustain nuclear reactions until the protostar has collapsed to at least a size which is only an order of magnitude larger than when it reaches the main sequence.

Of the various nuclei which might conceivably be present in the primordial cloud, the deuteron would probably be the first to participate significantly in nuclear reactions. It now seems unlikely that deuterium is present in the interstellar medium from which stars are formed (Bashkin and Peaslee 1961; Fowler, Greenstein, and Hoyle 1962). However, if deuterium were present in the same abundance as found on earth and in meteorites, the amount is sufficient to cause a considerable pause in the contraction (Salpeter 1954). Calculations for a solar mass have shown that the contraction could be delayed by about 100 million years for a "radiative" model (Brownlee and Cox 1961), or by about 500 thousand years for the convective model (Ezer and Cameron 1963).

The calculated behavior of the "radiative" model of one solar mass in the  $M_{\text{bol}}$ , log  $T_e$  diagram at the onset of deuterium burning is very similar to that of a model approaching the main sequence, i.e., the luminosity decreases simultaneously with a very slight decrease in the effective temperature. This char-

acteristic “hook” suggests that it is probably fair to describe this region of the  $M_{\text{bol}}$ ,  $\log T_e$  diagram as the deuterium-burning main sequence in the same way that the zero-age main sequence can be described as the hydrogen-burning main sequence. Protostars of different masses would exhibit similar pauses. Those with masses less than the sun’s mass would pause for an appreciable time relative to the total contraction time, while the contractions for stars of greater mass would be delayed for shorter intervals.

A subtle but interesting effect of the aforementioned reaction is an altered stellar abundance before the hydrogen-burning main sequence is reached. The deuterium is converted to  $\text{He}^3$  and, together with any initial abundance of  $\text{He}^3$ , becomes a new source of energy just as the protostar approaches the main sequence. The behavior is altered slightly in that the contraction is stopped while the protostar’s radius is somewhat larger than its “final” value. If  $\text{He}^3$  is sufficiently abundant, a convective core may be present until it is depleted.

If other nuclei were sufficiently abundant, e.g.,  $\text{Li}^6$ ,  $\text{Li}^7$ ,  $\text{Be}^9$ ,  $\text{B}^{10}$ ,  $\text{B}^{11}$ , these too could be responsible for supplying energy to the protostar and could, thereby, delay the contraction. However, in spite of the fact that all of the above have large nuclear transmutation probabilities for relatively low temperatures and densities, they do not occur with sufficient frequency to merit more than a cursory consideration.

## 2.2. MAIN-SEQUENCE STAGES

The beginning of the main-sequence stage in the evolution of a star is defined as occurring when the nuclear energy-production rate has risen to achieve exact balance with the luminosity. The end of this stage can be precisely specified for those more massive stars in which a convective core of homogeneous composition exists: the end comes when hydrogen is completely exhausted in the core. Theory (SES, § 29) indicates that evolution proceeds rapidly subsequent to the end of the main-sequence stage for stars more massive than about  $1.5 M_{\odot}$ ; and observation (Sandage 1957*a*) indicates the same, in terms of the “main-sequence turnoff points” for galactic clusters and the Hertzsprung gap in the HR diagram. For stars less massive than about  $1.5 M_{\odot}$ , in which the hydrogen is depleted non-uniformly, no precise end to the main-sequence stage can be distinguished. Both theory (Hoyle 1959) and observation (color-magnitude diagrams of old galactic and globular clusters; see Sandage 1962) show that a smooth transition takes place toward the giant stages.

The evolution of main-sequence stellar models (see chap. 4 of this volume) has been extensively studied. We omit here considerations of mixing throughout a star (see SES, § 21) and of mass loss (see Burbidge and Burbidge 1958, § 24), and shall confine our physical description to qualitative features with emphasis on the implications for evolutionary tracks in the HR diagram. Specifically, we wish to characterize the evolutionary changes of luminosity and radius for a star of given initial mass and homogeneous composition. Studies of this problem in recent years have generally begun with an initial model in

equilibrium and have then proceeded through a discrete sequence of “quasi-equilibrium” models whose chemical composition changes progressively with time (see § 3 below on techniques of model construction). For a qualitative description it is necessary to understand first the structure of the equilibrium stellar model.

In an illuminating passage in his book (SES, pp. 43–44), Schwarzschild points out that “the luminosity of a star is not determined by the rate of energy generation by nuclear processes.” As emphasized long ago by Eddington, for a star *in equilibrium* “the cause of the flow [or radiation] within the star must be a gradually increasing temperature from the surface to the centre” (Eddington 1926, pp. 3–4; see, further, Hoyle and Lyttleton 1948, pp. 98–100). This temperature gradient owes its existence to the pressure gradient in the stellar gas. The pressure gradient is determined by the requirement of hydrostatic equilibrium: at each point in the star the gravitational force of the interior mass is assumed to be balanced by a pressure gradient at that point. (The dramatic consequences of failure to adhere to this assumption have been noted by Schwarzschild [SES, pp. 32–33] and by Hoyle [1955, pp. 127–29].) In an over-all sense it is clear that, the larger the mass, the larger will be the average pressure gradient, and hence the temperature gradient, and hence the luminosity. The luminosity of a star in equilibrium, and of given chemical composition, is thus determined basically by its mass.

The rate of energy generation comes in only when we introduce a second requirement, conservation of energy. It is assumed that the luminosity is balanced by the rate of energy generation over the whole star, viz., that

$$L = \int_0^M \epsilon dM_r = \int_0^M \epsilon_0 f(X) \rho T^\nu dM_r, \quad (2.1)$$

where  $L$  is the luminosity,  $M$  is the total mass,  $M_r$  is the mass interior to distance  $r$  from the center,  $\epsilon$  is the local rate of energy generation per unit mass. The right-hand side contains an approximation formula for  $\epsilon$  due to nuclear energy generation:  $\epsilon_0$  is a reaction cross-section constant,  $f(X)$  involves the local hydrogen concentration by mass,  $\rho$  is the gas density,  $T$  is the temperature, and  $\nu$  is  $\approx 4$  for the proton-proton chain and  $\approx 16$  to 20 for the CNO cycle. Now since  $L$  is determined, *not* by (2.1), but basically by the mass of the star, any change in one of the factors on the right-hand side of (2.1) must be accompanied by compensating changes in another factor there, if we require conservation of energy. As an example, computations by Morton (1959) for a model of  $10 M_\odot$  show that for a *reduction* of  $\epsilon_0$  in the CNO cycle by a factor of 100, the central density and temperature, and therefore the pressure and temperature gradients, increase to such an extent that the luminosity is *increased* by 13 per cent. Note that the luminosity is not completely insensitive to the energy-generation rate. Our point of view is that the latter affects the equilibrium structure of a star, and thus the luminosity—but very weakly, and in a direction quite the opposite of what might

naïvely be expected. A more relevant illustration for present purposes is the reduction in  $f(X)$ , which is  $X$  for the CNO cycle and  $X^2$  for the  $p$ - $p$  chain, as time proceeds, with a consequent increase in the temperature gradient, from equation (2.1). Thus, the evolutionary depletion of hydrogen leads to an increase with time of the luminosity of a main-sequence star, owing to the requirement of conservation of energy. It should be noted that the evolutionary change in chemical composition, from hydrogen to helium, also increases the luminosity in two other ways, even more important than the above: through a reduction in the radiative opacity and through an increase in the mean molecular weight per free particle, which in an ideal gas implies a greater temperature (hence temperature gradient, from center to surface) to maintain hydrostatic equilibrium.

The evolutionary change in radius of a main-sequence star is more subtle, owing to the non-linearity of the differential equations, and can best be understood by referring to detailed computations. These show (see, e.g., Henyey, LeLevier, and LeVée [hereafter referred to as HLL] 1959, Fig. 1) that the inner mass of a main-sequence star contracts during evolution and the outer mass expands, with a net increase in radius. The inner contraction provides the increase in temperature and density needed to satisfy the energy conservation in equation (2.1). The resulting rearrangement of the density distribution produces the expansion (see Hayashi, Hoshi, and Sugimoto 1962, eq. [6A.1]). These effects could hardly be predicted a priori; the subtle rearrangement of the stellar structure could only become evident after the carrying out of computations. It is interesting that only one paper to date has taken into account the actual conversion of radiant flux in the outer parts of the star into potential energy (HLL 1959, Fig. 3); though this is a very small effect in main-sequence stars it becomes more important in red giants, as noted by Sandage and Schwarzschild (1952, p. 471).

The evolutionary tracks of main-sequence stars in the HR diagram are thus characterized by increasing luminosity and radius. There is, in particular, a striking and important difference between stars which satisfy (2.1) through the CNO cycle and those which do so through the  $p$ - $p$  chain. In the former case, owing to the high temperature sensitivity of the energy-production rate, only a small rise in central temperature and thus a small contraction of the inner mass are necessary to maintain conservation of energy. At  $10 M_{\odot}$ , for example, according to Kushwaha's (1957) models as given in Tables 28.1 and 28.5 in SES, the contracting inner mass is only about 15 per cent of the total mass. The result is a considerable increase in radius for a given increase in luminosity; in consequence, the evolutionary track in the HR diagram is directed sharply away from the initial main-sequence locus toward the red giant region. Tracks for various masses are shown, e.g., in Figure 13 of HLL (1959); noteworthy in that illustration is the decreasing track slope with decreasing mass, which follows from the above argument because the temperature sensitivity of the CNO cycle increases with decreasing temperature (SES, Table 10.1 and Fig. 10.1). Below about 1.5



$M_{\odot}$ , however, where the  $p$ - $p$  chain is more important than the CNO cycle, a sudden change in track slope occurs.

Owing to the relatively low temperature sensitivity of the  $p$ - $p$  chain (and also to the dependence on the square of the hydrogen concentration), compared to the CNO cycle, in the lower mass stars a large rise in central temperature, and thus a large contraction of the inner mass, is necessary to maintain conservation of energy as the hydrogen is depleted with time. At  $1 M_{\odot}$ , for example, according to independent model sequences by each of the writers (unpublished), the contracting inner mass is about 85 per cent of the total mass. The result is a rather small increase in radius for a given increase in luminosity, such that the evolutionary track in the HR diagram is directed nearly *along* the initial main-sequence locus (Haselgrove and Hoyle 1956*b*, Sears 1959, Hoyle 1959). Realization of this characteristic track for the less massive stars has had important consequences in the recent dramatic increases in the computed ages of old galactic and globular clusters (Sandage 1962; § 4 below), as was pointed out by Hoyle (1958, p. 226; 1959).

The most extensive recent calculations of evolution for a range of masses in the main-sequence stages have been carried out by HLL (1959), Hoyle (1960), and Schwarzschild and Härm (1958). The last of these showed that the mass of the convective core increases with time in very massive stars, contrary to the decrease found in less massive stars by Kushwaha (1957; cf. Savedoff and van Dyck 1960). The reason is that the adiabatic temperature gradient is reduced relative to the pressure gradient when radiation pressure is important (see, e.g., Chandrasekhar 1951, eq. [54]), and since this is the case in very massive stars the condition for stability against convection,  $|dT|_{\text{rad}} < |dT|_{\text{ad}}$ , is weakened, relative to less massive stars where radiation pressure is negligible. Schwarzschild and Härm (1958, pp. 353–54) found that the transition point occurs at about  $10 M_{\odot}$ , for an initial composition of  $X = 0.75$ ,  $Y = 0.22$ ,  $Z = 0.03$ ; in stars more massive than  $10 M_{\odot}$  the convective core grows in mass. They also found that a discontinuity in composition at a convective-radiative interface implies convective instability on the radiative side when electron scattering is the dominant opacity source. To avoid this physical inconsistency they introduce a “semiconvective” zone (cf. Ledoux 1947) outside the convective core, which maintained convective neutrality by modifying the chemical composition continuously, but which did not contribute to the energy transport. In the evolutionary sequences of very massive stars the consequent growth of the convective core permits a much larger fraction of the mass of the star to be involved in hydrogen burning than would be expected from the Schönberg-Chandrasekhar limit (Sandage 1957*a*), and the lifetime in the main-sequence stage is correspondingly longer; this effect has been noted in the very young galactic cluster NGC 6611 by Walker (1961*a*). Another peculiarity of the evolutionary tracks of the very massive stars is that the increased radiation pressure allows a considerable evolutionary increase in radius for a small increase in luminosity;

thus, the tracks are flatter in the HR diagram than those for less massive stars. However, when the hydrogen is exhausted in the central convective core, the subsequent contraction of the entire star produces a leftward motion toward higher effective temperature, as found by HLL (1955*b*) for  $2.3 M_{\odot}$ . The lower limit to the effective temperature in the main-sequence stage for stars of  $28 M_{\odot}$  and higher (corresponding to  $M_{\text{bol}} < -5$ ) is about  $30000^{\circ}\text{K}$ , according to the computations of Schwarzschild and Härm. They did not compare their tracks with observations, asserting with good reason that the relation between effective temperature and spectral type for very hot stars was too uncertain. It is interesting that there exist several B- and A-type supergiants of high luminosity in the double cluster  $\eta$  and  $\chi$  Persei (Johnson and Morgan 1955) which, using the temperature scale of Keenan and Morgan (1951) or Aller (1963), would have temperatures below  $30000^{\circ}\text{K}$ ; according to an interpretation of these stars as belonging to main-sequence stages (Johnson and Hiltner 1956; Burbidge and Burbidge 1958, Table 4 and § 44*a*) they would be inconsistent with the results of Schwarzschild and Härm. Recent work by Hayashi and Cameron (1962; see § 2.3 below) indicates, however, that these stars may belong to a much more advanced evolutionary stage (see also Masevitch 1957).

### 2.3. POST-MAIN-SEQUENCE STAGES

The present state of our knowledge of the internal structure of stars after they leave the main sequence is pointedly summed up in Schwarzschild's remark quoted at the beginning of the chapter. The post-main-sequence stages remain the frontier of the theory of stellar evolution today, some twenty years after Schönberg and Chandrasekhar (1942) showed that, for an evolutionary sequence of idealized models consisting of a hydrogen-rich exterior and a hydrogen-burning shell atop a growing, hydrogen-exhausted isothermal core, there is an upper limit to the mass of the core (cf. Chandrasekhar 1951; SES, § 24), corresponding to the end of the main-sequence stage. The impasse was broken, a decade later, by Sandage and Schwarzschild (1952; SES, § 25), who showed that an evolutionary sequence subsequent to the Schönberg-Chandrasekhar limit could be constructed by taking into account gravitational contraction of the isothermal core. This work produced red giant models which, instead of being isolated models constructed to fit a characteristic luminosity and radius for red giants, were natural steps in an evolutionary sequence starting from the initial, chemically homogeneous main-sequence state.

In the past decade, despite the interest aroused by the Sandage-Schwarzschild paper, the accumulation of HR diagrams showing the relation of red giants to main-sequence stars in various stellar populations (galactic clusters of a range of ages, globular clusters, the Magellanic clouds), the increasing availability of powerful automatic computers, and the vigorous insouciance of the nucleosynthesists—in spite of all these stimulating factors, construction of post-main-sequence evolutionary sequences has proceeded at a slow pace. Here

we can only summarize the evolutionary changes in structure as far as they have been studied at present. It is convenient to distinguish two areas of activity in terms of stellar mass: the evolution of stars of around one solar mass, owing to their relevance to the HR diagrams of globular clusters, has been more thoroughly investigated than that of more massive stars. We discuss the less massive stars first.

After the work of Sandage and Schwarzschild (1952; see also Sandage 1954), it was realized by Hoyle and Schwarzschild (1955) that two essential features needed to be included in the solar-mass models for application to globular-cluster stars: degeneracy (cf. Gamow and Keller 1945) and convective envelopes. The central density of evolving stars of solar mass reaches sufficiently high values that, although the ions continue to fulfil the ideal gas law, the electrons begin to be affected by the exclusion principle in phase space (see, e.g., SES, § 8; Chandrasekhar 1939, chap. 10). Hence, partial-degeneracy pressure of the electrons must be included in addition to the ideal-gas pressure. A consequence of this is that the Schönberg-Chandrasekhar limit to the mass of an (ideal-gas) isothermal core can be exceeded, since the additional pressure is sufficient to support the outer layers. In other words, it is possible to construct a sequence of equilibrium models with an isothermal core surrounded by a hydrogen-burning shell source growing to contain a large portion of the mass of the star, without gravitational contraction of the core taking place. Taking the partial degeneracy into account, Hoyle and Schwarzschild found that the evolutionary sequence fitted the lower part of the subgiant region of the globular cluster color-magnitude diagram, as did Sandage and Schwarzschild; but where the earlier work contained contracting cores with a temperature gradient and a central temperature that rose in time to almost the value at which helium burning would set in, the later work contained isothermal cores at lower temperatures.

The other essential feature of the Hoyle-Schwarzschild work was the recognition that convective envelopes play an important, even dominant, role in the structure of red giants. Models computed with "zero boundary conditions,"  $P=T=0$  (see SES, § 11), and with radiative envelopes gave too large radii and too low surface temperatures to fit the cluster HR diagrams. In examining the models in detail, Hoyle and Schwarzschild noticed that the density just below the surface was extremely low. From the standpoint of the theory of stellar atmospheres the radiative-envelope models were not self-consistent, since optical depth unity (defining the photosphere, from which the radiation escapes into space) occurred deep down at higher temperatures than the effective temperature at the surface. Adopting the physical boundary conditions that the temperature must tend to the effective temperature at the surface and the density must tend to a photospheric value at the surface (cf. SES, § 11), Hoyle and Schwarzschild found that convective-envelope models would satisfy these conditions, since (going outward in the star) the decline of density with tem-

perature in an adiabatic convective region,  $\rho \sim T^{1.5}$ , is less steep than that in a radiative region,  $\rho \sim T^{3.25}$  for a Kramers opacity law. As the authors put it, "the star can indeed find a solution to its problem." With their treatment of the convective envelope (cf. those by Kippenhahn, Temesváry, and Biermann 1958; Hayashi and Hoshi 1961; Demarque and Geisler 1963), strict adherence to the boundary conditions in a given model demanded a particular convective-envelope extent, characterized by the parameter  $K$  in the adiabatic relation  $P = KT^{2.5}$ . With a remarkable combination of ingenuity and insight, Hoyle and Schwarzschild were able to construct a sequence of models which satisfied the boundary conditions and progressively increased in luminosity as the mass of the isothermal core grew by addition of hydrogen-exhausted layers. At a certain point the core extended to regions of such low density that the temperature had to rise to maintain the conservation-of-energy condition (eq. [2.1]). Although this could apparently be achieved with an isothermal core increasing its temperature as a whole over a short interval, eventually the luminosity became so high that the rate of release of gravitational contraction energy from addition of mass to the core required taking this contraction into account. Despite the degeneracy and consequent low opacity, the contraction was sufficiently rapid to set up a radiative temperature gradient in the core. The central temperature increased until a value of  $1.2 \times 10^8$  °K was reached; at the density of the order of  $10^5$  gm/cm<sup>3</sup>, this condition was sufficient to initiate helium burning and end the evolutionary increase of luminosity. In perhaps the most remarkable triumph of their paper, Hoyle and Schwarzschild found that the helium burning set in when the sequence was nearly at the tip of the red giant branch in the globular-cluster HR diagram.

The commencement of an exothermic nuclear reaction in a partially degenerate region of a star creates an unstable situation (Mestel 1952). In an ideal gas, the rise in temperature is accompanied by a rise in pressure. The situation can be followed with a sequence of equilibrium models and, as has been found in the case of contracting stars just reaching the main sequence (§ 2.1 above; HLL 1955a; Brownlee and Cox 1961; SES, § 19), the changes in structure are minor. But in a gas in which the electrons follow a degenerate gas law (with the pressure-density relation affected little or not at all by the temperature), the heating from the nuclear energy serves mainly to increase the energy of the ion gas (helium nuclei in the red giants), and thus to accelerate the nuclear reactions, without a cooling, stabilizing expansion. This unstable stage can end only when the helium is exhausted or when the temperature has risen sufficiently high to remove the degeneracy and permit a pressure increase, expansion, and cooling.

This stage, called the "helium flash" by Härm and Schwarzschild (1961; Schwarzschild and Härm 1962), has been followed by them with extremely short time steps (as low as two seconds!) between successive models. They find, in a red giant of  $1.3 M_{\odot}$ , that the temperature rises to  $3.5 \times 10^8$  °K before the

degeneracy is removed; there remains sufficient helium to continue the burning in the ideal gas. A question of crucial importance for the evolutionary path in the HR diagram is whether the temperature gradient will be so steep that the convective core extends out to the deep convective envelope. Should this happen, the entire star may become mixed and chemically homogeneous: the point in the HR diagram corresponding to a stable model having a higher helium content than initially might fall near the *left* end of the horizontal branch of the globular-cluster color-magnitude array, in the conventional plot (cf. Oke 1961, Cox and Giuli 1961, Cox and Salpeter 1961). Such a possibility was mentioned by Schwarzschild (SES, p. 228; Schwarzschild and Härm 1962).

An alternate possibility is that, after the helium flash has removed the degeneracy, the stellar model retains an inhomogeneous structure consisting of a helium-burning core, a hydrogen-burning shell, and a hydrogen-rich envelope. Such a double energy-source model was first investigated by Hoyle and Schwarzschild (1955), who found that a model of  $1.2 M_{\odot}$  with  $q_1 = 0.60$  (a helium core comprising 60 per cent of the stellar mass) lay near the right end of the horizontal branch (cf. Haselgrove and Hoyle 1958). However, it was pointed out by Nishida (1960) that the radius of a double energy-source model is extremely sensitive to the ratio of the burning rates of the two energy sources, and that since the rate of the CN cycle had been revised downward by a factor of 100 since the work of Hoyle and Schwarzschild their model stood in need of revision. Nishida found that a model of  $1.2 M_{\odot}$  with  $q_1 = 0.60$  lay near the *left* end of the horizontal branch; the reduced rate of the shell source led to a reduction by a factor of 4 in the radius. Recently Nishida and Sugimoto (1962) have considered the evolution of a  $1.2 M_{\odot}$  double energy-source model with  $q_1 = 0.45$  as helium is burned into carbon and oxygen via  $3 \text{ He}^4 \rightarrow \text{C}^{12} (\alpha, \gamma) \text{O}^{16}$  in a convective core containing 14 per cent of the mass; they find that the luminosity remains nearly constant while the radius first decreases and then increases. The excursion in the HR diagram during exhaustion of the helium in the convective core is surprisingly small, being confined very nearly to the RR Lyrae gap. Nishida and Sugimoto note that a change of an order of magnitude either way in the CN-cycle rate (or, equivalently, in their assumed  $\text{N}^{14}$  abundance) could displace the sequence to either end of the horizontal branch.

The calculations of evolutionary sequences for low-mass models have been stimulated primarily by the globular-cluster color-magnitude diagrams, though as yet we do not have a complete understanding of the horizontal branch or of the apparently inevitable descent to the white dwarf stage (see, e.g., SES, chap. 8). A second stimulus for work on low-mass models has been the development of the theory of nucleosynthesis in stars (Burbidge, Burbidge, Fowler, and Hoyle 1957; see also Bashkin's chapter in this volume), following the indication by Hoyle and Schwarzschild (1955) that the crucial process  $3 \text{ He}^4 \rightarrow \text{C}^{12}$  can take place in the evolution of a low-mass star. Perhaps it can be shown that nuclear species up to the iron abundance peak are produced in an evolutionary

scheme that involves exhaustion of a particular nuclear fuel in the stellar core, followed by contraction and a rise of the central temperature to a value sufficient for the next nuclear energy source to help maintain the conservation of energy. However, to explain the heavy-element abundances observed in the solar system and in the Galaxy, it would seem more pertinent to consider models for stars more massive than the sun, since the bulk of nucleosynthesis has taken place in the distant past, perhaps even in the very early stages of galactic evolution. For the post-main-sequence stages of massive stars progress has come only very recently, principally from the work of Hayashi and his colleagues at Kyoto (Hayashi, Hoshi, and Sugimoto 1962).

The evolutionary sequences of models subsequent to the Schönberg-Chandrasekhar limit constructed by Sandage and Schwarzschild (1952) were applied by them to the globular-cluster stars. But as was shown by Hoyle and Schwarzschild degeneracy and convective envelopes needed to be taken into account. These corrections are not so important for more massive stars, since the central densities are lower and the zero boundary conditions suffice for them. Hence the Sandage-Schwarzschild models remain of interest for the more massive stars, and their evolutionary tracks have been utilized, for example, in discussions of the properties of Cepheid variables (Sandage 1958*a*, eq. [5]; Kraft 1961, § 4). It has only been recently that more detailed evolutionary sequences than those by Sandage and Schwarzschild have been constructed.

The essential difficulty has been the handling of the partial differential equation for energy conservation including gravitational contraction and expansion (eq. [3.19] below); this is required subsequently to the Schönberg-Chandrasekhar limit for stars where partial degeneracy pressure is not sufficient to support the stellar envelope. Sandage and Schwarzschild (1952; see also SES, § 25) computed the *total* gravitational energy release per unit time from contraction of an isothermal core, without considering in detail the distribution of the energy production through the core. To do the latter evidently requires a high-speed computer; such work has been reported by Hoyle (1960) for  $3.89 M_{\odot}$  and by Polak (1962) for  $5 M_{\odot}$ . They find in particular that the core contraction is so rapid as to raise the temperature and density to values sufficient for helium burning at an even earlier stage than was the case in the Sandage-Schwarzschild work, in fact on the left-hand side of the Hertzsprung gap.

However, Hayashi, Hoshi, and Sugimoto (1962) find for  $4 M_{\odot}$  and  $15.6 M_{\odot}$  that helium burning begins on the right side of the Hertzsprung gap but that the stars move quickly to higher surface temperature and spend much of their helium-burning lives in the gap. Figure 7-1 of Hayashi *et al.* (1962) illustrates regions of helium burning in the HR diagram. These regions may be compared with the observed region of Cepheid instability (Sandage 1958*a*; Kraft 1963, Fig. 9); the agreement is suggestive but not striking. It will be necessary to attach calculations of pulsating stellar envelopes (e.g., Christy 1964) to models such as those by Hayashi *et al.* before an appropriate comparison of theory and

observation can be made. Recent work in this direction, for  $7 M_{\odot}$ , has been reported in a series of papers by Hoffmeister, Kippenhahn, and Weigert (1964).

Evolution of more massive stars ( $15.6 M_{\odot}$ ) has been studied in a series of papers by Hayashi and his collaborators (Sakashita, Ono, and Hayashi 1959; Hayashi, Jugaku, and Nishida 1959, 1960; Hayashi and Cameron 1962). The last of these follows the evolution from the initial main-sequence state through hydrogen exhaustion and helium exhaustion in the core, to the onset of carbon burning. Although the work contains a number of approximations along the

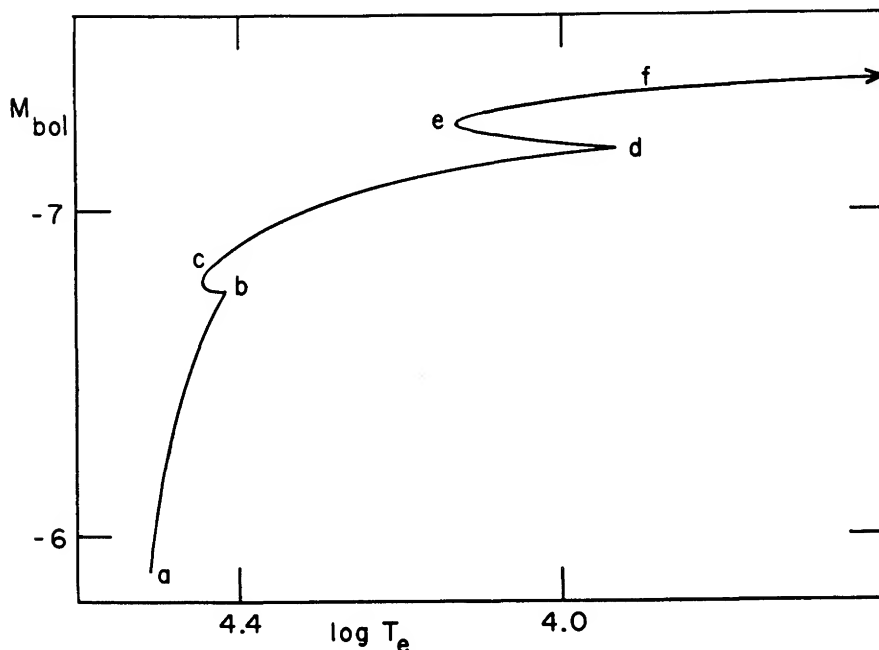


FIG. 1.—Evolutionary track of a star of  $15.6 M_{\odot}$  in the  $M_{\text{bol}}, \log T_e$  diagram, from Hayashi and Cameron (1962). Letters indicating various stages of evolution are explained in text.

way, it represents the farthest advance yet made in the evolution of massive stars. Figures 1 and 2 show the evolutionary track obtained by Hayashi and Cameron (1962), in the  $M_{\text{bol}}, \log T_e$  diagram (Fig. 1) and in a color-magnitude diagram (Fig. 2) containing observations of the galactic double cluster  $\eta$  and  $\chi$  Persei. The rather large differences between the shapes of the track in the figures are due to the bolometric corrections and effective temperature-versus- $B-V$  scale used in Figure 2, from Arp (1958).

Point  $a$  in Figure 1 is the initial position for a star of mass  $15.6 M_{\odot}$  and composition  $X = 0.90$ ,  $Y = 0.08$ ,  $Z = 0.02$ , with  $X_{\text{CNO}} = \frac{1}{3} Z$ . The evolutionary track from  $a$  to  $b$  was taken from the earlier work by Sakashita, Ono, and Hayashi (1959) and represents depletion of hydrogen in the convective core

down to  $X = 0.02$  at  $b$ . The short segment from  $b$  to  $c$  is the hydrogen-exhaustion phase, during which the whole star contracts to keep its energy production up with its luminosity. The corresponding turn of the track toward higher effective temperature (bluer  $B - V$ ) was also found in a similar phase by HLL (1955*b*) at  $2.3 M_{\odot}$  and by Kushwaha (1957) at  $10 M_{\odot}$ . Hayashi and Cameron took into account the detailed distribution of gravitational energy release in this phase, though using an interpolation formula in place of equation (3.19) (below). They give the time from  $a$  to  $b$  as  $156 \times 10^5$  years, and from  $b$  to  $c$  as  $1.4 \times 10^5$  years. They note that when the central hydrogen content has fallen as low as  $X = 10^{-4}$ ,

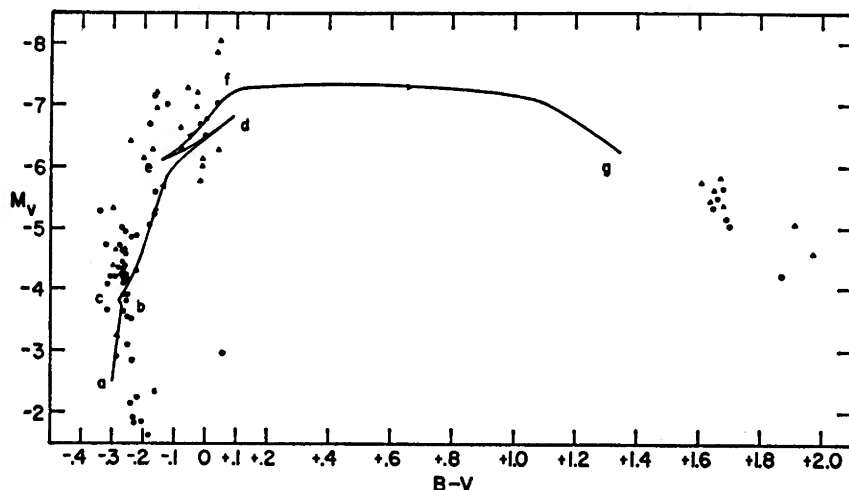


FIG. 2.—Evolutionary track of a star of  $15.6 M_{\odot}$  in the color-magnitude diagram, from Hayashi and Cameron (1962). Letters indicating various stages of evolution are the same as in Figure 1, except that  $g$  represents the last stage of central helium burning. The filled circles represent observed stars within  $23'$  of the nucleus of either  $h$  or  $\chi$  Persei; filled triangles represent stars out to  $4^{\circ}$  from the clusters' center.

the temperature at the interface between convective core and hydrogen-rich radiative envelope has become large enough for hydrogen burning to arise there and create a shell source, leading to an expansion of the envelope and a turn to the right after  $c$ .

The evolution from  $c$  to  $d$  represents the gravitational contraction of a helium core, surrounded by the hydrogen-burning shell source; at point  $d$  the central temperature becomes sufficiently high for helium burning to commence and halt the contraction. Having noted that the gravitational energy release in the core was quite uniform in the preceding phase, Hayashi and Cameron assume that the Sandage-Schwarzschild (1952) approximation is sufficient for the gravitational-contraction phase from  $c$  to  $d$ . They find that the star spends a remarkably short time,  $0.7 \times 10^5$  years, in this phase and they note a correspondingly



sparse region in the observed color-magnitude diagrams of  $\eta$  and  $\chi$  Persei (Fig. 2) and of Arp's (1959*a, b*) blue clusters in the Small Magellanic cloud.

At point *d* the energy generation due to helium burning rises to surpass that due to gravitational contraction, and the latter ceases. The center of the star is non-degenerate, and so the "helium flash" at the corresponding point in less massive stars (Schwarzschild and Härm 1962) does not occur here. In the early stages of the helium burning the helium core expands and the star contracts as a whole, according to Hayashi and Cameron, producing the leftward movement in the HR diagram. At point *e* the central helium content has fallen to  $Y = 0.35$  and the central temperature begins a rapid rise to maintain conservation of energy (the energy-generation rate being proportional to  $Y^3$ ); this gives rise to contraction of the core and expansion of the envelope, producing a rightward movement in the HR diagram (cf. the similar antics at  $4 M_{\odot}$ , described in § 4 of the paper by Hayashi, Nishida, and Sugimoto 1961). At point *f* the central helium content is down to  $Y = 0.04$ ; the evolution time from *d* to *f* is  $11.3 \times 10^5$  years, and Hayashi and Cameron show that the ratio of this time to that spent in the hydrogen-burning phase (from *a* to *b*) is comparable to the ratio of the numbers of stars in the corresponding regions in the diagram of  $\eta$  and  $\chi$  Persei. Subsequent to point *f* a very brief gravitational contraction raises the central temperature to a value appropriate for carbon burning ( $C^{12} + C^{12}$ ), at about  $8 \times 10^8$  ° K. (The possibility that  $C^{12}(\alpha, \gamma)O^{16}(\alpha, \gamma)Ne^{20}$  might deplete the carbon would lead to neon burning, but the low cross-section for  $O^{16}(\alpha, \gamma)Ne^{20}$  [Gove, Litherland, and Clark 1961; Litherland, Kuehner, Gove, Clark, and Almqvist 1961] reduces this possibility.) A recent discussion of carbon, oxygen, and neon reaction rates has been given by Reeves (1962); see also his chapter in this volume. Hayashi and Cameron constructed a carbon-burning model, but the radius was so enormous that they noted that a convective envelope should be taken into account (cf. Hoyle and Schwarzschild 1955). The position of the carbon-burning model is not indicated in Figures 1 and 2, but they conjectured that it would fall in the red giant region when the convective envelope is included. They estimated the remaining lifetime from carbon burning to formation of iron to be approximately the same as the helium-burning lifetime, which is consistent with the observations as given in Figure 2. Also, they pointed out that neutrino energy losses might be important in the carbon-burning stage.

The work by Hayashi and Cameron represents the furthest development of post-main-sequence-stages for massive stars yet carried out. Although a number of approximations were made, the qualitative agreement with observation in the case of  $\eta$  and  $\chi$  Persei (cf. the previous subsection; also, Masevitch 1957) is sufficiently good to warrant further work along the lines indicated by Hayashi and Cameron. Perhaps the most intriguing conclusion of their paper is that, while the low-mass red giants in globular clusters and the oldest galactic clusters, thanks to the inhibition of core contraction by electron degeneracy, are in

a hydrogen-burning shell phase (prior to the helium flash), the massive red supergiants in luminous galactic clusters (and in the Magellanic clouds) may be in evolutionary phases more advanced than helium burning.

### § 3. CONSTRUCTION OF EVOLUTIONARY SEQUENCES

#### 3.1. INTRODUCTION

In this section we shall review the techniques of construction of evolutionary sequences of stellar models. These techniques are essentially computational: the problem is the mathematical one of finding a solution to a set of partial differential equations, with time and one or more space variables as independent variables, and since the equations do not in general have closed analytic solutions we have to deal with numerical integration techniques.

The mathematical problem has not been stated with broad generality, since the state of the art now and for some time to come will involve mathematical descriptions of new physical situations as they arise in the course of following the evolution of a stellar model. Thus, for example, the occurrence of the helium flash in low-mass red giant models, first treated by Härm and Schwarzschild (1961), forced these workers to modify considerably their computational scheme which had sufficed for earlier stages (Schwarzschild and Harm 1962, Schwarzschild and Selberg 1962). It is evident that, when such physical phenomena as fast rotation, violent mass ejection, magnetic fields, and endothermic nuclear reactions come up in the course of evolution, allowance for these must be made in the mathematical description of the problem. Proposals have indeed been made to write a general computer program which will follow a star from the primordial gas-cloud state to the final white dwarf state (Haselgrove and Hoyle 1956*a*), but presently available techniques are quite surely inadequate to deal with all the phenomena displayed to us by observations. Consequently, the techniques to be described here cannot be represented as definitive; we confine ourselves to procedures that are being followed in current efforts.

The physical approach can be stated in general: to construct an initial model representing a star and to compute its changes in structure with time as a function of some evolutionary variable, e.g., the chemical composition. Note the implied separation of the physical problem into a "space part" and a "time part": to deal with the full mathematical problem mentioned in the first paragraph above would require solving the general partial differential equations of hydrodynamics. There have been three specific computational approaches to the solution of the physical problem in recent years. The first, which has led to the furthest developments so far in the theory of stellar evolution, has been to solve the differential equations partly by numerical integrations on a desk computer and partly by analysis of the march of characteristic differential invariants on simple graph paper. This procedure, which was foreshadowed in the extensive analysis of the mathematical character of the equations of stellar structure by Chandrasekhar (1939) in his treatise, *An Introduction to the Study*

of *Stellar Structure*, has been elegantly refined and extensively applied by Schwarzschild and Härm and their collaborators at Princeton (see also Bondi and Bondi 1949), and has recently been vigorously pursued for advanced phases of stellar evolution by Hayashi and his colleagues at Kyoto (Hayashi, Hoshi, and Sugimoto 1962). Happily, for our purposes here, as well as for all workers in the field, these techniques have been fully described in Schwarzschild's (1958) lucid monograph, *Structure and Evolution of the Stars*.

The other two approaches have basically consisted of retaining the full constitutive relations in the problem and solving the equations in physical variables on electronic computers. The principal workers, in terms of these two approaches, have been Hoyle (Haselgrove and Hoyle 1956a), who has dealt with the differential equations directly and written programs to integrate them by classical techniques such as the Runge-Kutta method, and Henyey (HLL 1955a; Henyey, Wilets, Böhm, LeLevier, and Levée [hereafter referred to as HWBLL] 1959; Henyey, Forbes, and Gould [hereafter referred to as HFG] 1964), who has transformed the differential equations explicitly to difference equations and solved them by modern techniques such as relaxation procedures. Since the present writers have some experience with these respective approaches we shall describe them in the next two subsections. Not the least of our motivations has been the feeling that, with fast electronic computers becoming more and more widely available, these potentially powerful tools of astrophysical research (see Wrubel 1960) should be utilized much more extensively than they have been in the past.

### 3.2. FITTING METHOD

The construction of evolutionary sequences of stellar models by the method of the present subsection involves separating the problem into a "space part" and a "time part." The first of these is the construction of a single stellar model, that is, the derivation of the march of physical variables between center and surface. The second part is the calculation of the evolutionary time change of some basic characteristics of this model, for example, the change of chemical composition at each point, the work done by gravitational contraction, or the amount of total mass loss. The second part provides the input data for calculating a new model; and the procedure is thence repeated indefinitely to build up an evolutionary sequence of models. We note that it is not at all necessary to choose time as the evolutionary parameter. In certain cases, other variables may be more convenient, such as Schwarzschild's eigenvalue  $C$  for radiative envelopes (SES, § 20) or the mass fraction of a growing hydrogen-exhausted core (Hoyle and Schwarzschild 1955). In the techniques described here, however, we shall implicitly restrict the discussion to time  $t$  as the evolutionary independent variable, in keeping with a direct physical approach.

In the method of this subsection, the bulk of the work in constructing an evolutionary sequence is in obtaining the space part of the solution, since this

requires solving a non-linear fourth-order boundary-value problem. Linear equations suffice for the time part if we ask only for the time changes in chemical composition at each point in a model, though in cases of fast thermal and dynamical evolution just now coming under attack, the time part will soon become more complex (cf. Hoyle 1959; SES, eq. [12.10]; Sobolev 1960; Sampson 1961; and the following subsection). We shall therefore discuss the space part separately first.

This involves four first-order differential equations of equilibrium, in four dependent variables and one independent variable. It will suffice at the outset to consider any added variables as functions only of the dependent variables and of the chemical composition. The equations for a spherical stellar model have been derived in several expositions (e.g., Wrubel 1958, Schwarzschild 1958, Aller 1954, Chandrasekhar 1951); in conventional notation they are as follows:

$$\frac{dP}{dM_r} = -\frac{G}{4\pi} \frac{M_r}{r^4}, \quad (3.1)$$

$$\frac{dr}{dM_r} = \frac{1}{4\pi} \cdot \frac{1}{r^2 \rho}, \quad (3.2)$$

$$\frac{dT}{dM_r} = -\frac{3}{64\pi^2 a c} \frac{L_r \kappa}{T^3 r^4} \quad (\text{radiative transfer}), \quad (3.3a)$$

$$\frac{dT}{dM_r} = \frac{\Gamma - 1}{\Gamma} \frac{T}{P} \frac{dP}{dM_r} \quad (\text{convective transport}), \quad (3.3b)$$

$$\frac{dL_r}{dM_r} = \epsilon. \quad (3.4)$$

These represent, respectively, at each point in a star, hydrostatic equilibrium, conservation of mass, space rate of energy transfer, and conservation of energy. The dependent variables are  $P$ , total pressure;  $r$ , distance from center;  $T$ , temperature; and  $L_r$ , energy per unit time emerging from the sphere of radius  $r$ .  $M_r$ , the mass interior to  $r$ , is here taken as the independent variable rather than  $r$ , since the dependence of chemical composition on  $M_r$  with time is unaltered by expansion or contraction (Haselgrove and Hoyle 1956*a*), both of which occur in virtually all stars during evolution. The constitutive variables, which as noted depend here only on the dependent variables and the chemical composition, are  $\rho$ , gas density in mass per unit volume;  $\kappa$ , opacity to radiation in area per unit mass;  $\Gamma$ , adiabatic exponent (Chandrasekhar 1939, pp. 55–59); and  $\epsilon$ , energy released per unit mass and per unit time.  $G$  is the gravitation constant,  $a$  is the radiation density constant, and  $c$  is the velocity of light (Allen 1963).

Thus, we have four equations in four unknowns, plus the chemical composition. We need four initial conditions or boundary conditions on the dependent variables. For the present discussion of the mathematical structure of the problem it will suffice to use the simplest boundary conditions. These conditions are

not sufficient for models of the sun and cooler stars; reference may be made to SES, § 11, for a more detailed discussion. At the surface, there are natural boundary conditions on pressure and temperature which are generally sufficient for stars hotter than the sun; we have

$$P = 0, \quad T = 0, \quad \text{at } M_r = M, \quad (3.5)$$

where  $M$  is the total mass of the star. At the center there are natural boundary conditions on the other two variables:

$$r = 0, \quad L_r = 0, \quad \text{at } M_r = 0. \quad (3.6)$$

With these boundary conditions, and *given* a specified mass,  $M$ , and (distribution of) composition, we have sufficient provisions to obtain a solution. The Vogt-Russell theorem (Vogt 1926; Russell, Dugan, and Stewart 1927) asserts further that the solution is unique; however, there is some question whether this has ever been rigorously proven, as pointed out by Odgers (1957). We shall accept Schwarzschild's conclusion of uniqueness, with his caveat with regard to mathematical degeneracy (SES, p. 97), since physically reasonable multiple solutions have not been encountered. (Haselgrove and Hoyle [1956a, p. 523] have reported instances of multiple solutions, but with a more general energy-generation expression than  $\epsilon = f[\rho, T, \text{composition}]$ , which is, of course, basic to the theorem [Chandrasekhar 1939, p. 253].)

To solve the boundary-value problem as stated above, we resort to numerical integration of the differential equations, in the technique of this subsection. Since equations (3.1), (3.2), and (3.3) have singularities at the center, and (3.2) and (3.3) at the surface, it is not possible to proceed all the way from one boundary to the other. (In several cases of interest, however, it is not necessary to do so; see, e.g., Gardiner 1951, Ib  n and Ehrman 1962.) In general, a "fitting" procedure is required: a pair of trial integrations, one starting from the center and one from the surface, is carried forward until they meet at a common value of the independent variable, the fitting point. If the four dependent variables, respectively from the outward and inward integrations, are continuous across the fitting point, then the boundary-value problem is solved and the model completed. If the dependent variables do not match at the fitting point, as is quite generally the case with the first trial pair, then subsequent trial integrations are necessary. With the boundary conditions as stated, and a given mass and (distribution of) composition, two parameters characterize each integration:  $P_c$  and  $T_c$ , the central pressure and temperature, characterize the outward trial; and  $R$  and  $L$ , the radius and luminosity, characterize the inward trial. The procedure may be visualized as a search in a four-dimensional space for a point, with coordinates  $P_c$ ,  $T_c$ ,  $R$ , and  $L$ , which will characterize a pair of integrations having continuity in the dependent variables at the fitting point.

It will be apparent that, in general, the search for a solution will require a large number of trial integrations. The recent successes in the theory of stellar

evolution are due, in large part, to recognition of special circumstances where the number of trial integrations can be ingeniously reduced, as in the classical Cowling (1935; see Schwarzschild 1946; Wrubel 1958, § 40) model, and as illustrated throughout SES. However, we are interested here in a general procedure which will ideally be appropriate for any reasonable stellar model, and which will, moreover, be suitable for automatic computers.

A first attempt at such a procedure has been introduced by Haselgrove and Hoyle (1956a). It depends essentially on the fact that there are four dependent variables to be made continuous at the fitting point, and four parameters for each pair of trial integrations. If the rates of change of the dependent variables at the fitting point with respect to each of the four boundary parameters can be found, then in principle it is possible to find a set of boundary parameters which will give continuous dependent variables across the fitting point, as will now be illustrated.

Denote the four dependent variables by  $Y_j (j = 1, \dots, 4)$ . Let the values of these at the fitting point,  $M_{r,f}$ , from the *outward* trial integration from the center be indicated with superscript  $o$ . Let the values at the fitting point from the *inward* trial integration from the surface be indicated with superscript  $i$ . For a particular pair of trial integrations, the dependent variables will not be continuous at the fitting point, i.e.,

$$\Delta Y_j = Y_j^i - Y_j^o \neq 0 \quad (j = 1, \dots, 4).$$

Denote the four trial parameters at the boundaries by  $E_k (k = 1, \dots, 4)$ .  $E_1 = P_c$  and  $E_3 = T_c$  pertain to the outward trial integration;  $E_2 = R$  and  $E_4 = L$ , to the inward trial integration. Small changes,  $\delta E_k$ , in each one of these will, after a trial integration, produce variations,  $\delta Y_j$ , in the dependent variables at the fitting point. Comparison of, say, two trial outward integrations, one with  $E_1, E_3$ , and the other with  $E_1, E_3 + \delta E_3$ , will give the rates of change of the  $Y_j^o$  with respect to  $E_3$ . A total of six integrations to the fitting point, three outward and three inward, suffices to give the rates of change of the  $Y_j$  with respect to the  $E_k$ :

$$\frac{\delta Y_j^o}{\delta E_1}, \frac{\delta Y_j^i}{\delta E_2}, \frac{\delta Y_j^o}{\delta E_3}, \frac{\delta Y_j^i}{\delta E_4} \quad (j = 1, \dots, 4). \quad (3.7)$$

Figure 3 shows schematically the marches of a particular dependent variable,  $Y_j$ , in an outward trial integration, characterized by  $P_c, T_c$ , and in an inward trial integration, characterized by  $R, L$ . The discrepancy at the fitting point  $M_{r,f}$  is indicated by  $\Delta Y_j$ , where  $\Delta Y_j > 0$  in the figure. The partial discrepancy in  $Y_j$  between the value given by the inward trial and that of the (unknown) solution may be written as  $-\Delta^i Y_j^i$ ; and similarly for the outward trial we have  $+\Delta^o Y_j^o$  (the minus sign is appropriate to the case illustrated in Fig. 3). The sum of these is the total discrepancy:

$$\Delta Y_j = -\Delta^i Y_j^i + \Delta^o Y_j^o. \quad (3.8)$$

Since the inward trial depends on  $E_2$  and  $E_4$ , then  $Y_j^i = Y_j^i(E_2, E_4)$ ; and a small change in  $Y_j^i$  is related to small changes in  $E_2$  and  $E_4$  by (to first order)

$$\Delta Y_j^i = \frac{\partial Y_j^i}{\partial E_2} \Delta E_2 + \frac{\partial Y_j^i}{\partial E_4} \Delta E_4. \quad (3.9)$$

If we identify the left-hand side with the partial discrepancy  $\Delta^i Y_j^i$ , the quantities  $\Delta E_2$  and  $\Delta E_4$  are then the changes to be made in the original trial values  $E_2$

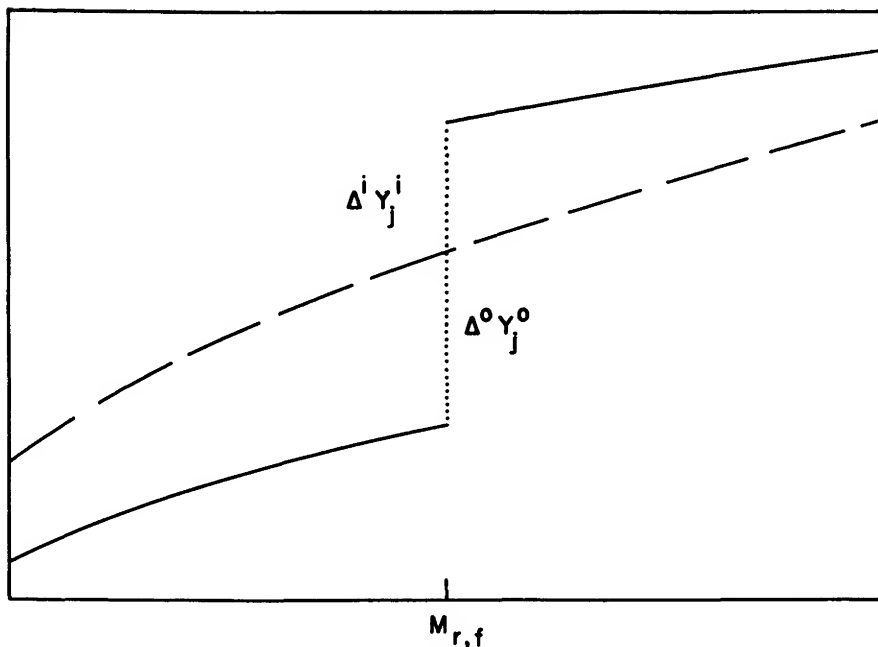


FIG. 3.—Schematic march of  $Y_j$  near the fitting point,  $M_{r,f}$ . Top curve: on an inward trial integration from the surface. Bottom curve: on an outward trial integration from the center. Dashed curve: desirable continuous march of  $Y_j$ . Dotted line: total fitting discrepancy,  $\Delta Y_j = \Delta^o Y_j^o - \Delta^i Y_j^i$ .

and  $E_4$  to produce an inward solution integration, i.e., for  $Y_j$  a march along the dashed curve in Figure 3—if the first-order representation of equation (3.9) is sufficient. The partial derivatives are obtained from the appropriate quantities in equation (3.7) above. Thus, equation (3.9) becomes

$$\Delta^i Y_j^i = \frac{\partial Y_j^i}{\partial E_2} \Delta E_2 + \frac{\partial Y_j^i}{\partial E_4} \Delta E_4. \quad (3.10)$$

Similarly for the outward integration, we have

$$\Delta^o Y_j^o = \frac{\partial Y_j^o}{\partial E_1} \Delta E_1 + \frac{\partial Y_j^o}{\partial E_3} \Delta E_3. \quad (3.11)$$

Hence, from equation (3.8), the discrepancies at the fitting point in each of the dependent variables are given by

$$\Delta Y_j = \frac{\delta Y_j^o}{\delta E_1} \Delta E_1 - \frac{\delta Y_j^i}{\delta E_2} \Delta E_2 + \frac{\delta Y_j^o}{\delta E_3} \Delta E_3 - \frac{\delta Y_j^i}{\delta E_4} \Delta E_4 \quad (j = 1, \dots, 4), \quad (3.12)$$

$$\Delta Y_j = \sum_{k=1}^4 (-1)^{k+1} \frac{\delta Y_j^o}{\delta E_k} \Delta E_k \quad (j = 1, \dots, 4). \quad (3.13)$$

In these four equations the four  $\Delta Y_j$ 's are the discrepancies at the fitting point between an original pair of trial integrations. The sixteen derivatives  $\delta Y_j^o, \delta Y_j^i / \delta E_k$  may be calculated by varying each of the original trial values by  $\delta E_k$  and, after performing the respective integrations, obtaining the variations  $\delta Y_j^o$  or  $\delta Y_j^i$  with respect to the values from the original pair. The four equations may then be solved simultaneously for the unknowns,  $\Delta E_1, \dots, \Delta E_4$ . Adding these to the original trial values  $E_k$  gives new values,  $E'_k$ , which can be used for a presumably improved pair of integrations.

This method of solving the space part of our over-all problem clearly can be programmed for an automatic computer; an illustrative flow diagram is shown in Figure 4. It will be evident, however, that because of the non-linear character of the differential equations, the convergence implied by the linear approximation of equation (3.9) may even not exist if the first trial pair is very far off in the values of  $E_k (k = 1, \dots, 4)$ . Although the procedure has been used successfully in a few cases (Haselgrove and Hoyle 1956*b*, 1958, 1959; Blackler 1958; Hoyle 1959, 1960; Sears 1959, 1960; cf. Schwarzschild and Selberg 1962), no proper analysis of its range of effectiveness has been undertaken. It would be desirable, for example, to investigate various values of the fitting point to see if some one value were peculiarly appropriate for convergence. Such analyses would of necessity require extensive numerical integrations. Experience indicates that computers with add times of the order of a millisecond require from half an hour to an hour for a single pair of integrations; this would probably be too long for an adequate analysis, and a computer with a ten-microsecond add time would be more suitable.

The remaining part of the over-all problem is the time part. Having constructed a single model for a given epoch, we wish to determine the change in the stellar structure over a time interval  $\Delta t$ . The simplest approach, which has proved generally useful in the stages of stellar evolution investigated in recent years, is suggested by the Vogt-Russell theorem: given the mass and the distribution of composition, it is possible to construct a stellar model. Accordingly, if we assume the mass to be constant over the time interval  $\Delta t$ , we can obtain the new distribution of composition at the end of this time from the burning rate  $\epsilon$  in the previous model. In linear approximation, the new mass fraction of hydrogen at the point  $M_r$  in a hydrogen-burning star is given by

$$X_2(M_r) = X_1(M_r) - \left( \frac{\epsilon_1 M_r}{E} \right) \Delta t, \quad (3.14)$$



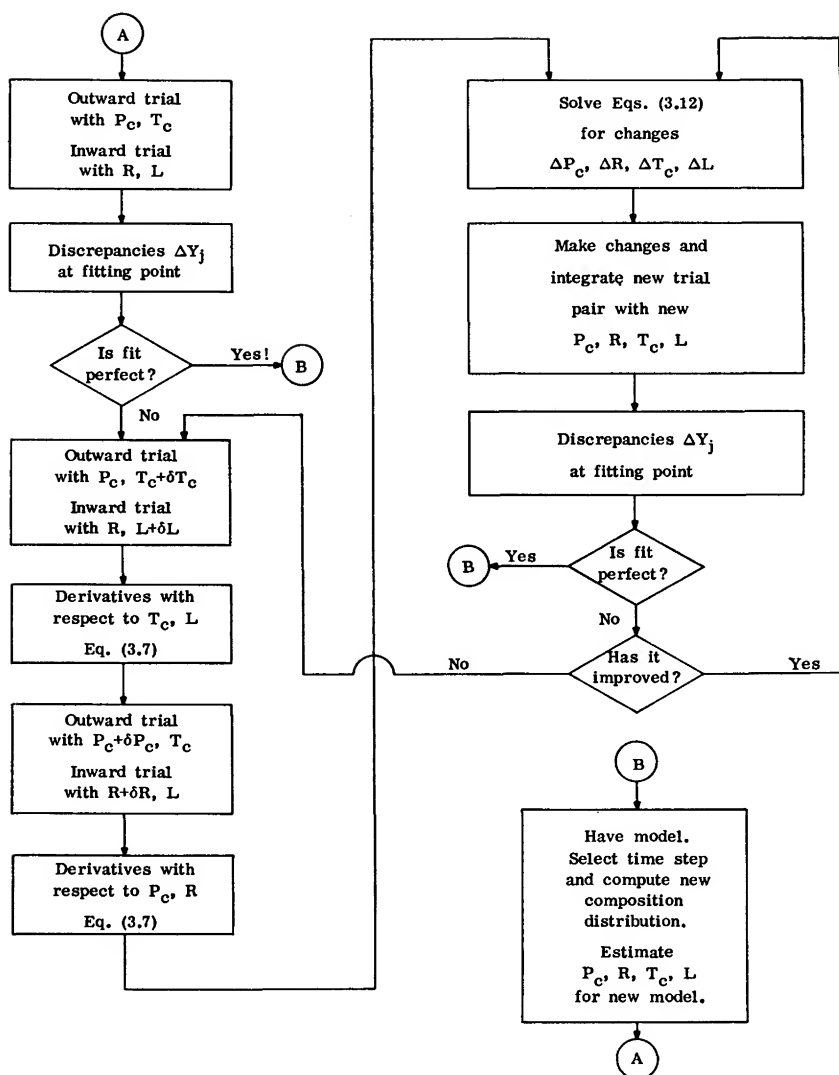


FIG. 4.—Flow diagram for construction of evolutionary sequence of stellar models by fitting trial integrations. Path leading from (A) traces construction of single model. Path leading from (B) indicates how time step is taken between models in an evolutionary sequence.

where subscripts 1 and 2 refer respectively to the previous model (known) and the new model.  $E$  is the energy released per unit mass of hydrogen consumed, which is about  $6 \times 10^{18}$  ergs per gram. Equation (3.14), evaluated at each point in model 1, thus gives the new composition at each point in model 2; and one can now return to the space part of the problem and construct model 2 (see Fig. 4). The procedure is repeated indefinitely to build up an evolutionary sequence of stellar models. Equation (3.14) is of course to be supplemented by analogous equations when other nuclear processes than hydrogen-burning have effects on the composition. It may be noted that mixing in a convective region may effectively change the composition homogeneously over a region, in which case an average of equation (3.14) is to be taken over the region (see, e.g., SES, p. 100).

The degree of accuracy of the linear approximation of equation (3.14) depends on the size of the time interval  $\Delta t$ ; for too large a value, the implicit assumption of constant burning rate  $\epsilon(M_r)$  over  $\Delta t$  will not be satisfactory. In the case of the sun, for example, three steps of  $\Delta t = 1.5 \times 10^9$  years, starting from the initial main-sequence state, give hardly different results from a single step of  $\Delta t = 4.5 \times 10^9$  years (Sears 1959); but for later stages of evolution it may be expected that the structure will change more rapidly, as witness the step of  $\Delta t = 1.6$  *seconds* needed between two of the models undergoing the helium flash, computed by Schwarzschild and Härm (1962). In general, it may be said that a little experience with the method of this subsection in a particular case soon reveals a practical upper limit to the time step, since, for the space part, rather accurate values of the  $E_k$ 's are needed for the first trials—an automatic computer will eventually “lose” the evolutionary sequence if it is permitted to take too big jumps between models.

As noted in the previous section, it has been realized since the work of Sandage and Schwarzschild (1952) and of HLL (1955*a*) that energy release via gravitational contraction plays a vital role in certain stages of stellar evolution. To see how this is taken into account in the time part of the problem we must generalize the conservation-of-energy equation (3.4) above to include other than nuclear energy production. We start from the first law of thermodynamics:

$$dU = dQ - PdV, \quad (3.15)$$

where  $U$  = internal energy,  $Q$  = heat energy, and  $PdV$  = mechanical energy (compression), with  $P$  = total pressure and  $dV$  = volume change. Let us now specify these quantities per gram. The internal energy of an ideal gas (see, e.g., Limber 1958 for a degenerate gas) is, including radiation energy density,

$$U = \frac{3}{2} \frac{k}{\mu H} T + \frac{aT^4}{\rho} = \frac{3}{2} \frac{P'}{\rho} + \frac{aT^4}{\rho}, \quad (3.16)$$

where  $k$  = Boltzmann's constant,  $H$  = mass of unit molecular weight ( $\mu$ ),  $a$  = radiation density constant, and  $P'$  = gas pressure. The time rate of change

of heat energy at the point  $M_r$  is the energy produced minus the flux out, i.e.,

$$\frac{\partial Q}{\partial t} = +\epsilon - \frac{dL_r}{dM_r}. \quad (3.17)$$

And the work done is

$$-PdV = -Pd\left(\frac{1}{\rho}\right). \quad (3.18)$$

Hence the time rate of change of the internal energy is, upon differentiation of (3.15) and substitution of (3.16)–(3.18),

$$\frac{3}{2} \frac{\partial}{\partial t} \left( \frac{P'}{\rho} \right) + a \frac{\partial}{\partial t} \left( \frac{T^4}{\rho} \right) = \epsilon - \frac{dL_r}{dM_r} - P \frac{\partial}{\partial t} \left( \frac{1}{\rho} \right).$$

Rearranging terms, we have the desired generalization of equation (3.4) (cf. SES, eq. [5.10]):

$$\frac{dL_r}{dM_r} = \epsilon - P \frac{\partial}{\partial t} \left( \frac{1}{\rho} \right) - \frac{3}{2} \frac{\partial}{\partial t} \left( \frac{P'}{\rho} \right) - a \frac{\partial}{\partial t} \left( \frac{T^4}{\rho} \right). \quad (3.19)$$

The first term on the right-hand side is the nuclear energy-production rate; the second, the mechanical compression rate; the third, the rate of change of internal particle kinetic energy (we neglect ionization, etc., energy changes); the fourth, the rate of change of internal radiant energy. The last term is usually small: it is neglected in SES, equation (5.10), but not by Hayashi and Cameron (1962, eqs. [12] and [13]) for their work on massive stars.

In constructing an initial model, we have to set to zero the time-derivative terms in (3.19) since we have no knowledge of the previous state. For the time part of the problem, between models 1 and 2, we may write (3.19) in differential approximation, following SES, pp. 100–101:

$$\begin{aligned} \frac{dL_r}{dM_r} = \epsilon - \frac{P}{\Delta t} \left[ \left( \frac{1}{\rho} \right)_2 - \left( \frac{1}{\rho} \right)_1 \right] - \frac{3}{2} \cdot \frac{1}{\Delta t} \left[ \left( \frac{P'}{\rho} \right)_2 - \left( \frac{P'}{\rho} \right)_1 \right] \\ - \frac{a}{\Delta t} \left[ \left( \frac{T^4}{\rho} \right)_2 - \left( \frac{T^4}{\rho} \right)_1 \right]. \end{aligned} \quad (3.20)$$

Having obtained model 1, we can store the quantities with subscript 1 as functions of  $M_r$ . Then, for each trial integration for model 2, we can evaluate at each point the quantities in square brackets and hence (3.20), which replaces (3.4) as the basic differential equation for conservation of energy. This procedure is quite beyond the resources of hand computation; we have referred in § 2.3 above to approximations that have been made in the past to reduce the complications. Presently available electronic computers, however, are fully capable of dealing with equation (3.20) as it stands; see, e.g., Haselgrove and Hoyle (1956a). Nevertheless, we see that the space part and the time part of the problem have become linked; and the experiences of various workers have indicated that the approach of this subsection may reach a point of rapidly diminishing returns

in the intriguing advanced phases of stellar evolution (Schwarzschild and Härm 1962). It seems appropriate to consider a more modern approach, to which we now turn.

### 3.3. DIFFERENCE METHODS

A more modern approach to the computation of stellar evolution than that described in the previous subsection is to regard the problem essentially as a hydrodynamic one, in which time and a space coordinate are given equal weight as independent variables, and to solve the problem by machine-oriented finite-difference techniques for dealing with partial differential equations, as described by, e.g., Richtmyer (1957). Such an approach to the construction of evolutionary sequences of stellar models was first applied by Henyey and his colleagues at the University of California at Berkeley (HLL 1955*a, b*, 1959; Henyey 1956; HWBLL 1959; HFG 1964), with notable success not only in establishing the general utility of their method but also in demonstrating the automatic nature of the computation. A similar approach has been developed and applied by Cox and Brownlee (1960; Brownlee and Cox 1960, 1961) at the Los Alamos Scientific Laboratory. We shall describe outlines of these workers' methods in this subsection.

In these methods the independent variables are defined only at a finite number of discrete points. One considers a two-dimensional grid or mesh of points, in which one axis represents a space variable and the other represents a time variable. Corresponding to the differential equations of the previous subsection, finite-difference equations may be written for the dependent variables at each point in the grid. To obtain the values of the dependent variables over the range of the space variable at one value of the time variable (i.e., to obtain a stellar model at a particular time), one may start with an approximate solution and improve it with the difference equations, hopefully in a stable and convergent manner. The procedure invoked has been called "relaxation," with reference to boundary-value problems such as the two-dimensional Laplace equation; here we are concerned with an initial-value problem and it will suffice to call the procedure for solution "iteration." The procedures used by the two active groups mentioned above are quite different. The Berkeley workers use what might be called a mathematical iteration: they expand the difference equations to first order in a Taylor series to obtain variational equations, and then improve the approximate trial solution by solving the variational equations for corrections in the dependent variables; this is in essence a Newton-Raphson iteration procedure (see, e.g., Wrubel 1963). The Los Alamos workers use what might be called a physical iteration: they consider the approximate trial solution to be in effect in neither hydrostatic nor thermal equilibrium, and they use Newton's second law of motion and the first law of thermodynamics as equations of condition to obtain an equilibrium solution. The time variable is used differently in the two procedures: in the former, time derivatives are used implicitly (Richtmyer 1957, pp. 16–17) to iterate for a solution at a given epoch; in the latter,

each successive iteration is made at successive epochs (which may be separated by very short time intervals) to achieve equilibrium solutions. It will be apparent that in both procedures the great speed of an electronic computer is necessary to perform the iterations. From these sketchy characterizations of these two procedures we now turn to details.

The Los Alamos workers begin with an arbitrary starting configuration at a time  $t^n$  ( $n$  is an index). This configuration can be obtained, for example, by a crude homology transformation from a known model; it need not be in hydrostatic or thermal equilibrium. The given data of the configuration are the mass distribution, the temperature distribution, and the chemical-composition distribution. These are specified as discrete functions in terms of the following notation. Consider the configuration to consist of  $J$  spherical shells, or zones, and let the interfaces between successive zones be labeled by  $x_0, x_1, \dots, x_i, x_{i+1}, \dots, x_J$ . The variable  $x_i$  represents the (inner) distance of the  $i$ th zone from the center of the configuration; note that  $x_0 = 0$  in the first zone. The distributions mentioned above are specified for each zone as follows: for the  $i$ th zone lying between  $x_i$  and  $x_{i+1}$  the mass of the zone is denoted by  $M_{i+(1/2)}$ ; and the chemical composition (for simplicity, only the hydrogen content is referred to) by  $X_{i+(1/2)}$ . These numbers are taken to represent the entire  $i$ th zone.

With these data at the start, several physical quantities can be computed for each zone as shown in Figure 5, the basic flow diagram for this method. The specific volume (reciprocal of the gas density) can be calculated from the equation of conservation of mass:

$$V_{i+(1/2)} = \frac{1}{\rho_{i+(1/2)}} = \frac{4}{3} \frac{\pi}{M_{i+(1/2)}} (x_{i+1}^3 - x_i^3). \quad (3.21)$$

The acceleration of gravity at each interface is given by

$$g_i = \frac{GM(x_i)}{x_i^2}, \quad (3.22)$$

where  $M(x_i)$  is the mass interior to  $x_i$ . The total pressure  $P_{i+(1/2)}$  in each zone can be calculated from an equation of state involving the temperature, density, and composition. Also, partial derivatives of the pressure with respect to temperature and specific volume can be obtained for each zone, and the pressure differential,  $\Delta P_i = P_{i-(1/2)} - P_{i+(1/2)}$ , across each interface.

The internal energy of a zone is given by

$$U_{i+(1/2)} = \frac{3}{2} P'_{i+(1/2)} V_{i+(1/2)} + a T_{i+(1/2)}^4 V_{i+(1/2)} + U_{\text{ion}} + U_{\text{excit}}, \quad (3.23)$$

where  $P'_{i+(1/2)}$  is the gas pressure and  $a$  is Stefan's radiation constant. The partial derivatives of  $U_{i+(1/2)}$  with respect to temperature and specific volume are also obtained for each zone.

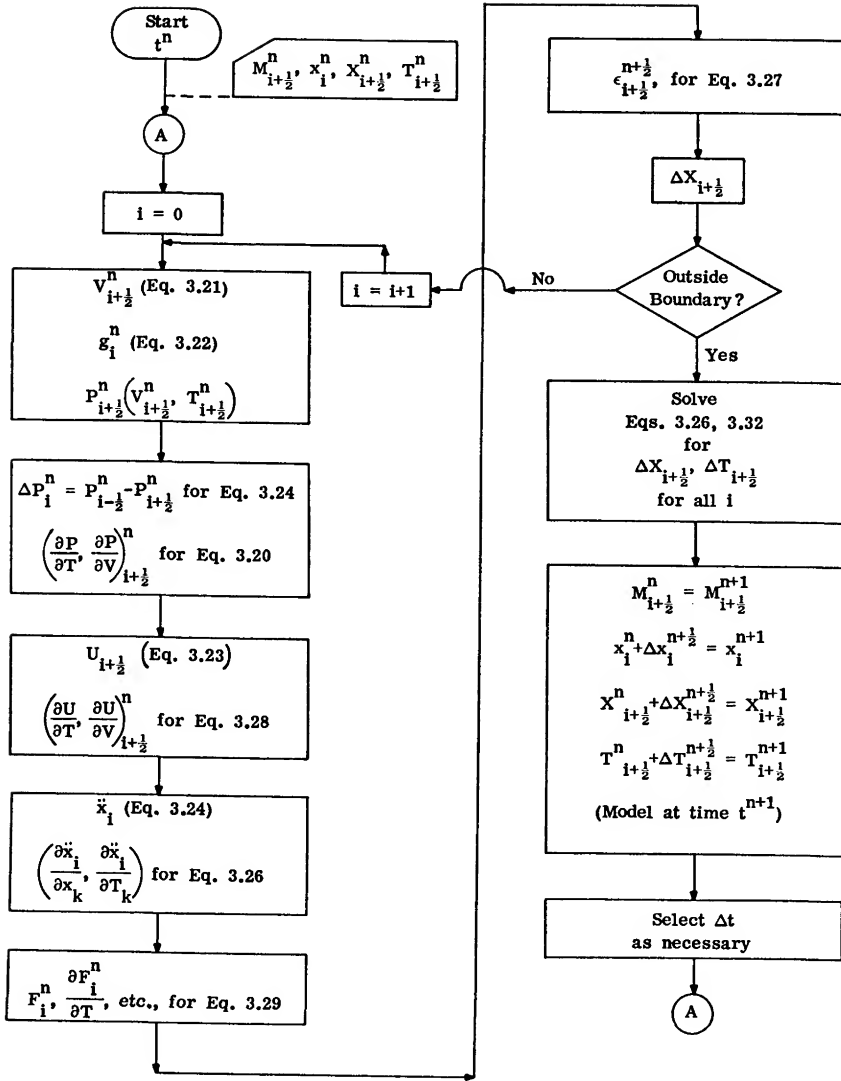


FIG. 5.—Flow diagram for construction of evolutionary sequence of stellar models by Los Alamos method. Left-hand path refers to calculations for each zone. Lower right-hand path refers to calculations in making time step.

The acceleration  $\ddot{x}_i$  of each interface is determined by the momentum conservation equation (Newton's second law),

$$\ddot{x}_i = -g_i - V_i \left( \frac{\Delta P}{\Delta x} \right)_i. \quad (3.24)$$

This quantity will generally be extremely small, except in such cases as pulsating stars (Cox and Olsen 1963; Cox, Cox, and Olsen 1963; Christy 1964); but its partial derivatives with respect to temperature and position are needed here (in eq. [3.28]). As may be imagined, the expressions for these derivatives are quite complex.

The next quantity to be calculated in this portion of the flow diagram (Fig. 5) is the flux across each interface and its partial derivatives with respect to temperature and specific volume. The total flux is the sum of the radiative, convective, and conduction fluxes. The final quantities to be calculated concern the energy-generation rate,  $\epsilon_{i+(1/2)}$ , which is discussed below. All the preceding quantities have been evaluated for all zones and interfaces at time  $t^n$  (the superscript  $n$  has been omitted for simplicity) and  $X_{i+(1/2)}$ .

Since the goal is to obtain the quantities needed for times  $t^{n+1}$ , viz.,  $x_i^{n+1}$ ,  $M_{i+(1/2)}^{n+1}$  ( $= M_{i+(1/2)}^n$ ),  $T_{i+(1/2)}^{n+1}$ , and  $X_{i+(1/2)}^{n+1}$ , the procedure is to form a set of implicit difference equations by evaluating all quantities at an intermediate time, which here is chosen to be at  $t^{n+(1/2)}$ . In order to insure stability, such centering of the equations is necessary (see Richtmyer 1957, pp. 16, 201). Many quantities will be dependent upon the magnitude of the time interval,  $\Delta t$ , and, indeed, the time dependence of all quantities must be carefully determined.

One of the two equations of condition used in this method arises from the requirement that at the end of the time step, the model should be in hydrostatic equilibrium. In general, the model will also be in thermal equilibrium but a succession of near-equilibrium states is possible. The requirement takes the form

$$\ddot{x}_i^{n+1} = 0, \quad (3.25)$$

i.e., at the end of the time step,  $\Delta t$ , the model will be in balance. To accomplish this a Taylor expansion containing the partial derivatives of (3.24) is made:

$$\ddot{x}_i^{n+1} = \ddot{x}_i^n + \sum_{k=i-1}^{i+1} \left( \frac{\partial \ddot{x}_i}{\partial x_k} \right)_T \Delta x_k^{n+(1/2)} + \sum_{k=i-(1/2)}^{i+(1/2)} \left( \frac{\partial \ddot{x}_i}{\partial T_k} \right)_V \Delta T_k^{n+(1/2)} = 0. \quad (3.26)$$

The terms of higher order are assumed to be negligible. The partial derivatives of the accelerations at time  $t^n$  are thus the known coefficients of the two variables,  $\Delta x_i^{n+(1/2)}$  and  $\Delta T_{i+(1/2)}^{n+(1/2)}$ , which are treated as unknowns.

The second equation of condition is determined from the following considerations. Within a time step,  $\Delta t$ , the total change of heat energy,  $\Delta \mathcal{E}$ , within a zone is

$$\Delta \mathcal{E}_{i+(1/2)}^{n+(1/2)} = M_{i+(1/2)} \left( \frac{\partial Q}{\partial t} \right)_{i+(1/2)}^{n+(1/2)} \Delta t = M_{i+(1/2)} \epsilon_{i+(1/2)}^{n+(1/2)} \Delta t + 4\pi (x_i^2 F_i^{n+(1/2)} - x_{i+1}^2 F_{i+1}^{n+(1/2)}) \Delta t, \quad (3.27)$$

the units being ergs. Another expression for the change in heat energy follows directly from the first law of thermodynamics:

$$\Delta \mathfrak{E}_{i+(1/2)}^{n+(1/2)} = \left( \frac{\partial U}{\partial T} \Big|_V \right)_{i+(1/2)}^n \Delta T_{i+(1/2)}^{n+(1/2)} + \left[ \left( \frac{\partial U}{\partial V} \Big|_T \right)_{i+(1/2)}^n + P_{i+(1/2)}^{n+(1/2)} \right] \Delta V_{i+(1/2)}^{n+(1/2)}. \quad (3.28)$$

Equations (3.27) and (3.28) are equated and all terms except  $\Delta T_{i+(1/2)}^{n+(1/2)}$  and  $\Delta V_{i+(1/2)}^{n+(1/2)}$  are evaluated. In equation (3.27), only  $F_i^n$ , the flux for time  $t^n$  across each interface  $i$ , is known. The flux for time  $t^{n+(1/2)}$  may be found, for example, by using a Taylor expansion:

$$F_i^{n+(1/2)} = F_i^n + \sum_{k=i-(1/2)}^{i+(1/2)} \left( \frac{\partial F_k}{\partial T_k} \right)^n \frac{\Delta T_k^{n+(1/2)}}{2}. \quad (3.29)$$

Other expansions are of course possible and indeed, the convective flux  $F_{c_i}^{n+(1/2)}$  generally needs to be obtained by an iterative process. Nevertheless, the above equation serves to illustrate the procedure.

The evaluation of  $\epsilon_{i+(1/2)}^{n+(1/2)}$ , also needed for (3.27), is somewhat difficult in that the rate of change of the chemical composition,  $\Delta x_{i+(1/2)}^{n+(1/2)}$ , must be determined at the time  $t^{n+(1/2)}$ , i.e., equilibrium abundances must be found for the middle of the time step. In addition, care must be taken to see that the time interval is not too long at a moment when any particular abundance is changing rapidly, for in that event an accurate evaluation of  $\epsilon_{i+(1/2)}^{n+(1/2)}$  is difficult.

For equation (3.28), while the partial derivatives of the internal energies with respect to  $V$  and  $T$  are in hand, an evaluation must be made for  $P_{i+(1/2)}^{n+(1/2)}$ . This is accomplished through the use of the following Taylor expansion:

$$P_{i+(1/2)}^{n+(1/2)} = P_{i+(1/2)}^n + \left( \frac{\partial P}{\partial V} \Big|_T \right)_{i+(1/2)}^n \Delta V_{i+(1/2)}^{n+(1/2)} + \left( \frac{\partial P}{\partial T} \Big|_V \right)_{i+(1/2)}^n \Delta T_{i+(1/2)}^{n+(1/2)}. \quad (3.30)$$

Thus the combination of (3.27) and (3.28) results in an expression  $\Psi$ , where

$$\Psi = \Psi(\Delta V_{i+(1/2)}^{n+(1/2)}, \Delta T_{i+(1/2)}^{n+(1/2)}) = 0. \quad (3.31)$$

With the use of a boundary condition at the center, this equation can become

$$\Psi = \Psi(\Delta x_i^{n+(1/2)}, \Delta T_{i+(1/2)}^{n+(1/2)}) = 0. \quad (3.32)$$

The two systems of condition, (3.26) and (3.32), containing the two unknowns for each zone, are now solved simultaneously by Gaussian elimination, and the corrections to the interface positions and the zone temperatures are applied.

We now have, at time  $t^{n+1}$ , all the data that were available for the starting configuration at time  $t^n$ ; we have completed one cycle. To follow the evolution,



then, the procedure is repeated for successive cycles, as in the flow diagram given in Figure 5.

The basic procedure has been described only schematically. Many technical problems arise in the course of a practical calculation; and deeper questions of stability, convergence, and accuracy arise in constructing a computer program and in evaluating the results. It is inappropriate to consider these details here since a sufficiently broad analysis to cover all types of stellar models of interest has not yet been developed. However, a few remarks based on past experience may be made in order to amplify the above outline.

One of the first problems to consider is the selection of values of the independent variables,  $x$  and  $t$ . For the former the equivalent problem is one of selecting the mass distribution in the space zones, i.e., how many zones should there be, and how should the mass be distributed among the zones? As to the number of zones, there are conflicting desires for accuracy and for minimum calculation time. In the case of configurations representing the contracting, pre-main-sequence sun, Brownlee and Cox (1961) have found that 30 zones are minimally adequate. The same number serves well enough for the main-sequence stage; but for later evolution toward the red giant stage, where pressure and density gradients may become exceedingly large, the number of zones required for particular regions may need to be substantially increased. Hence, an automatic method of subdividing (or combining) zones during the course of the calculation becomes necessary.

As to the relative masses to be contained in the various zones, the obvious necessity of having well-defined central temperatures and densities dictates that the central zone should have a very small mass fraction, of the order of  $10^{-4}$  of the total. Also, because of the steep density gradient toward the surface, the outer zones should have small mass fractions, the outermost zone containing less than  $10^{-4}$  of the total mass. This restriction creates an interesting problem in the type of calculation described here in that the heat content of the outer zones may be considerably less than the total energy flowing through them in a particular time interval which may be chosen appropriate to the evolutionary changes in the center of the configuration. Hence, in certain situations the choice of outer-zone masses may affect the choice of time intervals, and it may even be necessary to follow the evolution of the inner and outer portions on different time scales.

For the selection of a time scale in general, one possible choice is a time interval such that sound waves could be followed. But obviously this requires cycles with time intervals of the order of minutes or hours: even with the fastest available machines, a star would actually age faster than its evolution could be computed! There are situations, such as the helium flash in the partially degenerate cores of red giants, or Cepheid pulsation, where very short time intervals may well be necessary, but for many problems longer intervals will provide sufficient information. In the contracting sun (Brownlee and Cox 1961), time

intervals averaging  $2 \times 10^5$  years were used; and typical accelerations of the zone interfaces were usually no more than  $10^{-16}$  times the local gravitational accelerations. In general, it may be said that time intervals should be chosen such that the results are reasonable. Analogously with the choice of space zones described above, an automatic choice of time intervals during the course of the calculation may be programmed so that the intervals are decreased if various time derivatives become large, or increased, for the sake of economy, if feasible.

We turn now to a description of the basic procedure used by the Berkeley workers to obtain evolutionary sequences of stellar models. The details of this procedure have been described by HFG (1964), and so only a brief outline of the essence of the method is necessary here.

Let the two independent variables be denoted by  $\xi_j$  and  $t^n$ , representing respectively discrete space and time variables. The variable  $\xi_j$  does not necessarily have physical dimensions: it is defined by a functional relationship to the mass distribution, and that relationship is chosen such that  $\xi_j$  varies reasonably gently toward the center and the surface of the stellar model (an illustration is given in Fig. 1 of HLL 1959). We shall omit discussion of this and other details in order to concentrate on the essentials of the method.

It will be helpful first to summarize the steps in the method. As in the Los Alamos method just described the two independent variables do not enter entirely symmetrically: in essence, the equations are solved over the range of  $\xi_j$  for a fixed  $t^n$ . However, time derivatives are implicitly involved, as will be seen. The basic steps are as follows.

(1) Write the algebraic *difference* equations analogous to the differential equations of stellar structure. The number of difference equations will, at least in principle, equal the number of unknowns (dependent variables).

(2) Solve the difference equations for the unknowns. Since the equations are non-linear, more than a simple matrix inversion is needed. Schematically, a procedure for solution, analogous to the classical Newton-Raphson iteration procedure for solving non-linear equations, is as follows: (a) Expand the difference equations at each point to first order in a Taylor series in the dependent variables; i.e., obtain a set of first-order linear variational equations. The unknowns in this set are the *variations* in the dependent variables. (b) Compute the values of the coefficients in the variational equations from the dependent variables in a *trial model*. (c) Solve the linear variational equations for the variations in the dependent variables. These now represent corrections to be added to the previous trial values of the dependent variables, giving new trial values. (d) Iterate the procedure, from step (b), until the corrections become satisfactorily small. The dependent variables then represent the solution, i.e., the model, at the time  $t^n$ .

(3) To proceed along an evolutionary sequence, select a time  $t^{n+1}$ , obtain a first trial model by extrapolation from the dependent variables at time  $t^n$  and at  $t^{n-1}$ , and repeat the preceding steps.

To be more explicit, we display the difference equations. Consider the hydrostatic equation (3.1):

$$\frac{dP}{dM_r} = -\frac{G}{4\pi} \frac{M_r}{r^4}.$$

Transforming to a new independent variable,  $\xi$ , a pre-chosen function of  $M_r$ , we have

$$\frac{\partial P}{\partial \xi} = -\frac{G}{4\pi} \frac{M_r(\xi)}{r^4} \frac{dM_r}{d\xi}. \quad (3.33)$$

The derivative on the left-hand side is written as partial to emphasize its time dependence, in contrast to  $dM_r/d\xi$ . The corresponding difference equation is

$$\frac{P_{j+1}^n - P_j^n}{\xi_{j+1} - \xi_j} = -\frac{G}{4\pi} M'_{j+(1/2)} M_{j+(1/2)} \left( \frac{2}{r_{j+1}^n - r_j^n} \right)^4. \quad (3.34)$$

Here, the difference quotient on the left-hand side, giving the rate of change of pressure between adjacent points  $\xi_j$  and  $\xi_{j+1}$ , is an approximation to the derivative giving the rate of change at a single point. The variable  $r^4$  has been replaced by the simple average shown; it must be emphasized that this is not the only way of making a discretization representation (see HFG [1964] for a discussion of this point, including the technique of replacing some of the dependent variables by non-linear functions of them more suitable for differencing).  $M_{j+(1/2)}$  is the arithmetic mean of the mass interior to  $\xi_j$  and the mass interior to  $\xi_{j+1}$ ;  $M'_{j+(1/2)}$  is a similar mean of the derivatives  $(dM/d\xi)_j$  and  $(dM/d\xi)_{j+1}$ . The superscript  $n$  indicates the time dependence; the variables so labeled are understood to refer to the time  $t^n$ .

The difference equations analogous to the three remaining differential equations, (3.2), (3.3a), and (3.4), follow in a similar way:

$$\frac{r_{j+1}^n - r_j^n}{\xi_{j+1} - \xi_j} = \frac{M'_{j+(1/2)}}{4\pi} \left( \frac{2}{r_{j+1}^n + r_j^n} \right)^2 \frac{1}{\rho_{j+(1/2)}^n}, \quad (3.35a)$$

$$\frac{T_{j+1}^n - T_j^n}{\xi_{j+1} - \xi_j} = -\frac{3M'_{j+(1/2)}}{64\pi^2 a c} \kappa_{j+(1/2)}^n \frac{(L_{j+1}^n + L_j^n) \cdot 2^7}{(T_{j+1}^n + T_j^n)^3 (r_{j+1}^n + r_j^n)^4 \cdot 2}, \quad (3.35b)$$

$$\begin{aligned} \frac{L_{j+1}^n - L_j^n}{\xi_{j+1} - \xi_j} = & M'_{j+(1/2)} \left( \epsilon_{j+(1/2)}^n - \frac{U_{j+(1/2)}^{n-1}}{t^n - t^{n-1}} \right. \\ & \left. - P_{j+(1/2)}^n \frac{V_{j+(1/2)}^n - V_{j+(1/2)}^{n-1}}{t^n - t^{n-1}} \right). \end{aligned} \quad (3.35c)$$

In these equations the subscript  $j + \frac{1}{2}$  refers to an arithmetic mean between values at  $\xi_j$  and  $\xi_{j+1}$ —except for the nuclear energy-generation rate  $\epsilon_{j+(1/2)}^n$  which, because of its rapid variation, Henyey *et al.* find to be more satisfactorily repre-

sented by a geometric mean. In equation (3.35c) we have included the generalization given in equation (3.19);  $U$  is the internal energy and  $V$  is the specific volume. The time  $t^{n-1}$  is referred to in the last equation: a solution for that time must be available, or at least the needed quantities must be guessed.

If we consider the variable  $\xi_j$  to be specified for  $j = 0, 1, 2, \dots, J$ , then there are  $4J$  difference equations to be solved and  $4J + 4$  unknowns ( $P_j^n, r_j^n, T_j^n, L_j^n, j = 0, 1, 2, \dots, J$ ). Four of the unknowns can be obtained from the boundary conditions, e.g., at  $\xi_0$ , the center,  $r_0^n = 0$  and  $L_0^n = 0$ , and at  $\xi_J$ , the surface,  $P_J^n = 0$  and  $T_J^n = 0$ . The last two relations are the simple "classical" boundary conditions which we adopt for the present purpose; more realistic surface boundary conditions of course are necessary for the sun and cooler stars, and the incorporation of these into the method is discussed by HFG (1964). Thus we have  $4J$  equations in  $4J$  unknowns, and the next step is to solve them by the variational procedure as mentioned.

Let us write the difference equations symbolically in functional form (dropping the time superscript):

$$F^i(P_j, r_j, T_j, L_j, P_{j+1}, r_{j+1}, T_{j+1}, L_{j+1}) = 0 \quad (i = 1, \dots, 4).$$

$F^1, F^2, F^3$ , and  $F^4$  represent the four equations; for example, the hydrostatic equation is

$$F^1 = (P_{j+1} - P_j)(r_{j+1} + r_j)^4 + \frac{G}{4\pi} (M_{j+1} - M_j)M_{j+(1/2)} \cdot 2^4 = 0. \quad (3.36)$$

The Taylor expansions to first order may be written as

$$\begin{aligned} F^i + \frac{\partial F^i}{\partial P_j} \delta P_j + \frac{\partial F^i}{\partial r_j} \delta r_j + \frac{\partial F^i}{\partial T_j} \delta T_j + \frac{\partial F^i}{\partial L_j} \delta L_j + \frac{\partial F^i}{\partial P_{j+1}} \delta P_{j+1} \\ + \frac{\partial F^i}{\partial r_{j+1}} \delta r_{j+1} + \frac{\partial F^i}{\partial T_{j+1}} \delta T_{j+1} + \frac{\partial F^i}{\partial L_{j+1}} \delta L_{j+1} \quad (i = 1, \dots, 4). \end{aligned} \quad (3.37)$$

These are to be regarded as variational equations with the variations,  $\delta P_j, \delta r_j, \dots$ , as unknowns and with the partial derivatives as coefficients. For the hydrostatic equation, for example, the coefficients are

$$\begin{aligned} \frac{\partial F^1}{\partial P_j} &= - (r_{j+1} + r_j)^4 = - \frac{\partial F^1}{\partial P_{j+1}}, \\ \frac{\partial F^1}{\partial r_j} &= 4 (r_{j+1} + r_j)^3 (P_{j+1} - P_j) = \frac{\partial F^1}{\partial r_{j+1}}, \\ \frac{\partial F^1}{\partial T_j} &= 0 = \frac{\partial F^1}{\partial T_{j+1}}, \\ \frac{\partial F^1}{\partial L_j} &= 0 = \frac{\partial F^1}{\partial L_{j+1}}. \end{aligned} \quad (3.38)$$

These coefficients and the quantities  $F^i$  in the variational equations are to be explicitly evaluated from a trial model, as previously noted. Then the  $4J$  linear variational equations are to be solved for the  $4J$  unknowns, comprising  $\delta P_j$ ,  $\delta r_j$ ,  $\delta T_j$ , and  $\delta L_j$  (for  $j = 0, 1, 2, \dots, J$ ) minus  $\delta P_J = \delta r_0 = \delta T_J = \delta L_0 = 0$ . The solution of the variational equations is easy in principle, but if  $J = 50$ , say, the solution of two hundred simultaneous equations is a rather lengthy chore even for a fast computer. However, the structure of the equations, which contain only eight unknowns each and which are suggestively linked for successive values of  $j$ , practically demands a reduction procedure. Such procedures have been well developed for systems of the present type, since they occur in treating the classical partial differential equations of mathematical physics by difference methods. It would take us too far afield to write out the details of such procedures here. We refer to Richtmyer (1957, p. 103) and to Wrubel (1963) for simple illustrations of the reduction procedure and solution of the equations, and to HFG (1964) for a compact and complete description of the procedure appropriate to the present system.

Once the variational equations have been solved and the variations found, these latter are examined to see if they are all sufficiently small according to a reasonable criterion. If not, the variations are regarded as corrections to be made to the trial values of the dependent variables, new trial values are derived, the coefficients and constant terms in the variational equations are re-evaluated, and the equations solved anew. Eventually, the corrections may be expected to become small and a model is obtained. Then, to obtain the next model in an evolutionary sequence, extrapolation to the next time is made to provide a trial model for that time (the extrapolation of course includes a calculation of the expected chemical composition distribution at the new time). With a trial model for the new time, the procedure just described is repeated. A flow diagram for the whole process has been given by HFG (1964, Fig. 2).

The preceding discussion is only a crude outline of the techniques developed at Berkeley and we have omitted many important details, such as boundary conditions, specification of the function  $\xi_j$ , treatment of convective-radiative interfaces, stability and convergence rate of the iterations, etc., which arise in a practical calculation. The papers by Henyey and his colleagues already cited discuss some of these details, and no doubt new problems which we cannot point out here will come up as the techniques are extended to study various stages of stellar evolution. We wish to emphasize that the work on the evolution stages already studied by the Berkeley workers, namely the gravitational-contraction and main-sequence stages, has amply demonstrated the feasibility and power of these techniques. They are currently being applied by several groups, and it may be expected that such machine-oriented methods as those described in this subsection will carry the theory of stellar evolution as far forward again in this decade as the desk-computer methods applied at Princeton and elsewhere did in the previous decade.

## § 4. AGE DETERMINATIONS

## 4.1. INTRODUCTION

One of the most exciting developments in modern astronomy has been the contribution of the theory of stellar structure to the determination of ages of the stars. Indeed, this development has so strongly influenced the imaginations of astronomers that attempts to answer the fundamental questions of cosmogony and cosmology take age determinations from the theory of stellar evolution as primary data (see Sandage 1961*a*, *b*). The situation has changed radically since a few years ago, when Bok (1946), in a general survey of astronomical dating methods, considered that arguments from stellar and galactic dynamics gave much more definite evidence of a time scale for the universe than the then current ideas of stellar evolution.

The subsequent developments of the theory have gained widespread acceptance, in view of several points of contact with observations; and a variety of investigations, in such problems as nucleosynthesis, cluster dynamics, structure of galaxies, evolution of binary stars, etc., have been carried out with ideas of a time scale in mind. It seems, therefore, appropriate to review here methods of age determination from the theory of stellar evolution. It should not be forgotten, however, that there are various uncertainties and even inconsistencies in the applications of the theory at the present time. That the "contraction ages" of very young star clusters differ from "nuclear ages" (Sandage 1958*c*; Pesch 1961; cf. Walker 1961*a*; Hayashi 1961; Herbig 1962*a*, *b*), or that the latter may differ from "expansion ages" of stellar associations, may only be apparent irritations caused by limitations of observational data—or they may be subtle warning signs that theory and assumptions need closer examination, not to say revision. As for uncertainties, one need only note that the computed ages of the globular clusters have increased by an order of magnitude in the past decade (Sandage and Schwarzschild 1952, Sandage 1962). This particular change has been due to revision and extension of both observations and theory. It is out of place to consider here the effect of observations on age determinations; reference may be made to Sandage's chapter in Volume 4 of this series (see also Arp 1962*b*). Of present interest is the effect on age determinations of uncertainties in such "input data" of the theory as nuclear cross-sections, radiative opacities, and assumed initial chemical composition. Discussions of these, even for equilibrium models, have been carried out by few workers in recent years (e.g., Morton 1959; Demarque 1960, 1961). We shall, therefore, examine the effects of some of these uncertainties.

We cannot, however, assess here the possible effects on age determinations of such extensions to the theory as magnetic fields in stars, stellar rotation, stellar stability, mass loss (see Deutsch 1960), or occurrence of exotic nuclear reactions at critical evolution phases. These topics have only begun to be explored for static stellar models, as indicated elsewhere in this volume, and their relevance

to age determinations is not yet clear. Before invoking speculations to explain inconsistencies and gloss over imprecise knowledge we need to know the limitations of the theory as it has been applied. The next two subsections consist of a description of the method of age determination and a discussion of effects of inaccuracies in the input data in the present theory.

#### 4.2. METHOD OF AGE DETERMINATION

The recent applications of the theory of stellar evolution to the determination of stellar ages have utilized the Hertzsprung-Russell diagram as the area of contact between theory and observation. The basis for the applications is the Vogt-Russell theorem (§ 3.2), according to which a star of specified mass, initial chemical composition, and age will occupy a unique location in the diagram. (Note that the possibility is not excluded that a star of another mass, initial composition, or age may occupy the same location.) In general, therefore, the method is to reproduce the coordinates of a point, or a locus of points, with a theoretical configuration of a calculated age. This procedure is not without ambiguities, as hinted above and as will be illustrated below; some further hypotheses and arguments are usually needed. But the principle of the method is clearly defined; Strömgren (1958), in his Halley lecture, has described an observational procedure for directly determining the locations in the HR diagram of individual stars, and hence their ages (see also Crawford 1958; Bappu, Chandra, Sanwal, and Sinval 1962; Strömgren 1963).

The coordinates in the HR diagram are measures of luminosity (ordinate) and surface temperature (abscissa); it is pertinent to recall the definitions of these because the relations between the "theoretical" and "observational" HR diagrams have caused some confusion in the past and are likely to continue to do so, since these relations are in a state of flux at present. The "theoretical" HR diagram has coordinates  $M_{\text{bol}}$  (or  $\log L/L_{\odot}$ ) and  $\log T_e$ . A computed stellar model has values of luminosity  $L$  and radius  $R$  in cgs. units; the former is transformed to bolometric magnitude by the definition of the stellar magnitude scale:

$$M_{\text{bol}} = M_{\text{bol}}(\odot) - 2.5 \log \frac{L}{L_{\odot}}.$$

The luminosity of the sun is  $L_{\odot} = 3.90 \times 10^{33}$  erg sec<sup>-1</sup> (Allen 1963). The bolometric magnitude of the sun is  $M_{\text{bol}}(\odot) = +4.77$ , from the absolute visual magnitude of the sun,  $M_V(\odot) = 4.84$  (Stebbins and Kron 1957), and the bolometric correction,  $B.C.(\odot) = -0.07$  (Popper 1959, Fig. 2). These numbers are, of course, subject to change; we do not discuss them here, except to note that the  $M_{\text{bol}}(\odot)$  given above is 0.14 mag. fainter than that given in SES, p. 8 (cf. Harris 1961, 1963; Sandage 1962). The radius of a stellar model is related to the effective temperature by the definition of the latter, from the Stefan black-body radiation law:

$$\log T_e \equiv 0.25 (\log L - 2 \log R - \log 4\pi\sigma).$$

The Stefan-Boltzmann constant is  $\sigma = 5.6692 \times 10^{-5} \text{ erg cm}^{-2} \text{ deg}^{-4} \text{ sec}^{-1}$  (Allen 1963, p. 16). Using the two relations above, the computer of stellar models can directly describe his results in terms of an HR diagram, either with  $M_{\text{bol}}$ ,  $\log T_e$ , or with  $\log L/L_\odot$ ,  $\log T_e$  as coordinates.

The coordinates of the original HR diagram, constructed by Russell in 1913 (Russell 1918), were absolute visual magnitude and spectral type. Nowadays, observed HR diagrams are most frequently presented in terms of  $M_V$  and  $B - V$ , the absolute visual magnitude and blue - visual color index of the  $UBV$  system (Johnson and Morgan 1953, Johnson and Harris 1954, Johnson 1955, 1963). The relation between  $M_V$  and bolometric magnitude is

$$M_{\text{bol}} = M_V + \text{B.C.} \quad (\text{B.C.} \leq 0),$$

where the bolometric correction as a function of color index  $B - V$  has been recently discussed by Popper (1959), by Harris (1963), and by Aller (1963). The usual procedure for transforming color index to  $\log T_e$  is given schematically by

$$B - V \rightarrow \text{spectral type} \rightarrow T_e,$$

where the first of these relations is given by Johnson and Morgan (1953, Table 14), and the second by Keenan and Morgan (1951, Table 1.3). More recent discussions and tables have been given by Arp (1958), Popper (1959), Sandage (1962, Appendix A), Aller (1963), Harris (1963), and Keenan (1960, 1963). A table relating  $B - V$  to  $\log T_e$  is given in SES (Table 1.1); it should be noted that the  $T_e$ 's given there for  $B - V \geq +0.9$  are appropriate to luminosity class III.

Transformations between computed and observed quantities in the HR diagram are thus available, but not necessarily as accurate as might be desired. Estimates of statistical uncertainty are probably of little meaning since the transformations are doubtless subject to appreciable systematic errors, particularly in the high and low temperature ranges of the HR diagram. More serious is the recent demonstration that the relation between color index and effective temperature is dependent on chemical composition, in the sense that dwarfs of abnormally low heavy-element abundance have bluer  $B - V$  color indices than do normal dwarfs of the same effective temperature. This subject is under active investigation (Sandage and Eggen 1959; Melbourne 1960; Burbidge, Burbidge, Sandage, and Wildey 1960; Wildey, Burbidge, Sandage, and Burbidge 1962; Wallerstein 1962; Eggen and Sandage 1962; Sandage and Smith 1963). It should be emphasized that the relations described above can be said to hold only for normal stars; for such stars as subdwarfs, metal-weak giants, and globular cluster stars, similar relations simply do not exist at the present time.

Having seen the relation between observed and "theoretical" coordinates in the HR diagram, we turn to the problem of age determination. The "age" of a star is generally defined as the time interval between the present state and the



beginning of the main-sequence stage (§ 2.2 above). This definition has the advantage that "zero age" is well defined both from the standpoint of computation, where it represents a natural starting point for an evolutionary sequence, and from that of observation, since the majority of stars in a sample volume of space (for the solar neighborhood, see, e.g., Sandage 1958*d*) are on the main sequence and thus at or near zero age. The definition above does not include pre-main-sequence contraction times; ages in this stage are usually time intervals between some arbitrary initial configuration and the age-zero main-sequence state (cf. HLL 1955*a*, Brownlee and Cox 1961). Since so little is known about the details of star formation from interstellar material (cf. § 2.1) the initial epoch of the contraction stage is poorly defined; in general, however, the lifetime of a star in the contraction stage is less than one per cent of the main-sequence-stage lifetime (Herbig 1958; Struve 1960, 1962), and the former may be neglected in comparison with the latter.

For a specific example of age determination we consider a classical subgiant star,  $\zeta$  Her A: this is an MK standard for spectral type G0 IV (Johnson and Morgan 1953, Table 2), with a well-determined parallax of 0".104 (Wyller 1955). The absolute visual magnitude is  $M_V = +2.98$ , from the apparent magnitude (Johnson and Morgan 1953), corrected for the light of the secondary (van den Bos 1959) and the parallax. The  $B - V$  color index is +0.64 (Johnson and Morgan 1953), for which  $T_e = 5730^\circ \text{K}$  (Arp 1958); for the spectral type,  $T_e = 5750^\circ \text{K}$  (Keenan and Morgan 1951). We adopt  $\log T_e = 3.760$ ; and B.C. is  $-0.09$  (Popper 1959, Table 2), and hence  $M_{\text{bol}} = +2.89$ . These coordinates are plotted in the "theoretical" HR diagram of Figure 6, which also contains an evolutionary sequence computed by Hoyle (1959): it will be seen that  $\zeta$  Her A falls nearly on Hoyle's track,<sup>1</sup> at a point where the time since departure from the main sequence is  $9.1 \times 10^9$  years. This is the age of the star. We do not discuss the many uncertainties in the result, which is presented only as an illustration of the method. However, to complete the illustration with reference to the ambiguity mentioned in the first paragraph above, we note that a gravitationally contracting track could, in principle, be passed through the same point, giving a much younger age; but the spectrum of  $\zeta$  Her A, an MK standard, is not known to be characteristic of contracting stars (cf. Herbig 1962*a*). Also, the spectrum and mass of the companion (van de Kamp 1954) place it on the main

<sup>1</sup> Figure 6 contains Hoyle's (1959, Table 2) evolutionary track, with  $M_{\text{bol}}$  as defined above, and shifted in  $\log T_e$  so that the initial model falls on the observed age-zero main sequence, following Sandage (1962, p. 351). Sandage (1962, p. 350, footnote) notes erroneously an error in Hoyle's Table 2; one of us has recomputed Hoyle's initial model and finds  $L_{\text{bol}} = 4.12 \times 10^{33}$  ergs sec<sup>-1</sup>. With Hoyle's radius,  $R_S = 0.62352 \times 10^{11}$  cm, the surface temperature becomes  $T_S = 6210^\circ \text{K}$ . These three data fit smoothly in the Type I main sequence of Haselgrove and Hoyle (1959, Table 1). Coincidentally, the shift in  $\log T_e$  to fit the initial model to Sandage's (1962, Table 3) age-zero main sequence is identical to his value, viz.,  $\Delta \log T_e = -0.021$ ; hence Sandage's results (specifically, the first and second columns of his Table 4, except for the first items in each) are not affected.

sequence. Finally, we must note that an excellent value of the mass of  $\zeta$  Her A is available (observed masses are not essential to age determinations in the HR diagram); according to Wyller (1955; van de Kamp 1958) it is  $1.07 M_{\odot}$ , which is in striking agreement with the mass used in Hoyle's (1959) computation,  $1.09 M_{\odot}$ , and provides a most valuable check (though not a complete one!)<sup>2</sup> of the theory (see Sandage 1954).

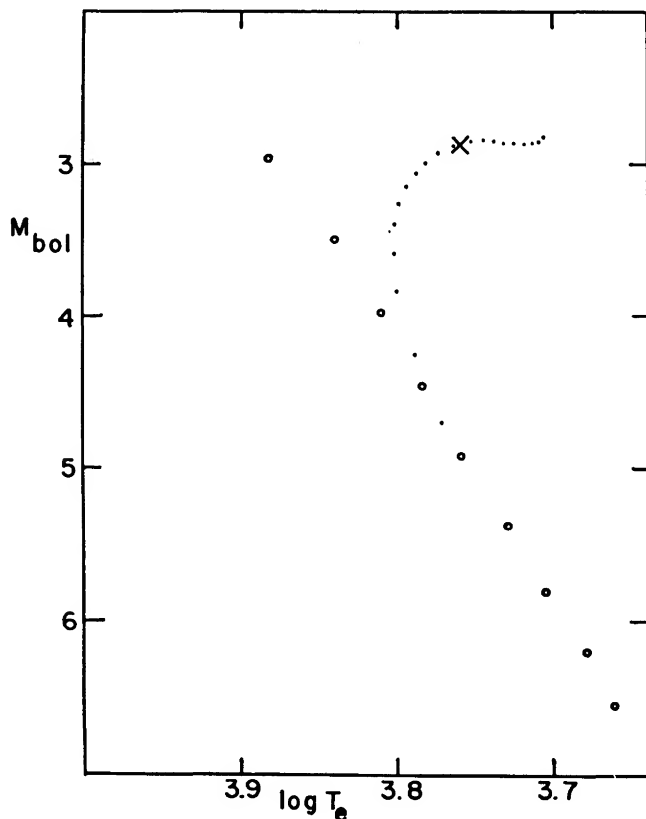


FIG. 6.—Age determination of a single star in the HR diagram. Circles: Sandage's (1962) initial main sequence. Dots: Hoyle's (1959) evolutionary track for a Type I star of  $1.09 M_{\odot}$ , with  $X = 0.75$ ,  $Y = 0.24$ ,  $Z = 0.01$ . Cross: position of  $\zeta$  Her A.

Age determinations of individual stars require of course accurate determinations of luminosities. It is only in recent years that these have become possible on a large scale, through the techniques of spectrophotometric absolute-magnitude measurement developed by Strömgren, Chalonge, Crawford, Wilson and

<sup>2</sup> It should perhaps be noted that the above illustration of age determination may be only schematic, in the light of Underhill's (1963) recent observations of radial-velocity variations in  $\zeta$  Her A.

Bappu, Oke, and others. It seems likely that age determinations of individual stars will add a valuable new dimension in studies of stellar kinematics and galactic structure and evolution (Strömberg 1958, 1963). Extensive computations of evolutionary tracks will be needed to achieve this promise.

Most of the applications of the theory of stellar evolution in the past decade have been to the determination of ages of star *clusters*. This was stimulated by the characteristic HR diagrams of globular clusters (Arp, Baum, and Sandage 1952) and of galactic clusters (Johnson 1954; cf. Trumpler 1925), in which the brighter stars deviate from the main sequence while the fainter stars are still on it. The former observation is interpreted as direct evidence for stellar evolution; the latter leads to photometric distance moduli of clusters (Johnson 1957*a*; Sandage, Vol. 4 of this series), and thus to the determination of luminosities of the cluster members. Hence, the observations give a locus of points in the HR diagram; to determine an age, the computer's task is to reproduce this locus. Since it represents a "snapshot" of the cluster's state in the HR diagram at a particular time, two steps are, in principle, necessary: (1) compute evolutionary tracks for models of a range of masses (loci of constant mass); and (2) draw lines in the HR diagram, connecting points of equal age on these tracks, to obtain loci of constant time. Comparison of these latter loci with that of the cluster then yields the cluster age. This procedure has been carried through explicitly by only a few workers (Mitchell and Johnson 1957, HLL 1959, Sandage 1962), primarily because extensive series of evolutionary tracks have not been available.

Of the various hypotheses underlying this method of age determination, the most fundamental one is that the cluster under investigation consists of stars of the same age. Here we must adapt our definition of age (given above for a single star as the time since it first reached the initial main-sequence state) to the cluster problem, since Walker (1956 *et seq.*) has found clusters with some stars in the contracting stage and others in the main-sequence stage. The hypothesis is that all stars of various masses in the cluster were formed at the same time from the interstellar material. The time interval from that epoch to the present is the cluster age, during which the more massive stars have passed through perhaps several stages owing to their higher luminosities, while the less massive (and less luminous) stars may still be in the contracting stage. Recently, suggestions have been made that in some instances the basic hypothesis may not be true: Blaauw (1958) has reported different HR diagrams in inner and outer parts of some O-associations; Roberts (1960) has noted the possibility of dust clouds and young stars in the globular cluster M3; Pesch (1961) and Herbig (1962*b*) find in the Pleiades, disagreement between ages obtained for the contracting stars and those for the brightest, H-burning stars. It appears that the best procedure at the present time is to assume initially the basic hypothesis, and then to scrutinize individual cases for disagreement. In this regard, an early tendency of observers to assign cluster membership on the basis of a

star's position in an HR diagram is to be considered with caution; in the case of the Hyades it has been shown by Johnson, Mitchell, and Iriarte (1962) that a careful discussion is necessary.

Before illustrating the procedure of cluster age determination described above we refer to an earlier and simpler method used particularly by Sandage (1957*a*). The "turnoff point" (the brightest  $M_V$  and corresponding  $B - V$ ) on the observed main sequence of a cluster is identified with the state of the model at the Schönberg-Chandrasekhar (1942) limit, at which point hydrogen has been exhausted in 12 per cent of its mass (Sandage 1957*b*, Appendix). Since the mass fraction of hydrogen burnt is proportional to the age and the (average) luminosity, Sandage (1957*a*, eq. [1]; 1958*b*) obtains

$$\text{Ages-c} = 1.1 \times 10^{10} \frac{M}{L_T} \text{ years}, \quad (4.1)$$

where  $M$  and  $L_T$  are the total mass and the "turnoff" luminosity in solar units. In recent years it has been found that the fraction of hydrogen burnt before the model leaves the main-sequence band (Hoyle 1960) varies up to half of the total mass for very massive stars (Schwarzschild and Härm 1958); but Sandage's relation is still useful for order-of-magnitude age estimates (possibly not, however, for such luminous clusters as  $\eta$  and  $\chi$  Persei, according to the work of Hayashi and Cameron 1962). A review of this and similar approaches has been given by the Burbidges (1958, pp. 202-3; see also Limber 1960).

As an illustration of the detailed procedure of cluster age determination, we show in Figure 7 an HR diagram constructed by Sandage (1962) for the galactic clusters M67 and NGC 188. The heavy lines represent the observed loci for the two clusters, in terms of the coordinates  $M_{\text{bol}}$  and  $\log T_e$ . The thin lines are the theoretical loci of constant time, obtained from Hoyle's (1959) single evolutionary track for  $1.09 M_\odot$  (shown in Fig. 6). Sandage (1962) extrapolated this track to somewhat lower masses and connected points of equal age from track to track to give the loci of constant time. Comparison of these and the observed loci gives formal ages of  $9-10 \times 10^9$  years for M67 and  $14-16 \times 10^9$  years for NGC 188, according to Sandage. He notes that the imperfect fit of observed and theoretical loci is due to details in the theoretical surface boundary conditions, specifically, the uncertainty in convective transport theory; this affects the model radii (which are larger than would be derived from the observational data in Fig. 7) but not the luminosities, and hence a fair comparison of loci is possible along the horizontal portions. (The situation for the *globular* clusters is much less satisfactory, according to Sandage's Fig. 2.) It will be clear that the derived ages depend upon, among other things, (1) the validity of the extrapolation of Hoyle's single evolutionary track, and (2) the relation of Hoyle's choice of initial chemical composition, given in the upper right corner of Figure 7, to that in the two clusters. These points have been noted by Sandage.

We wish to emphasize that proper applications of the method of age determi-

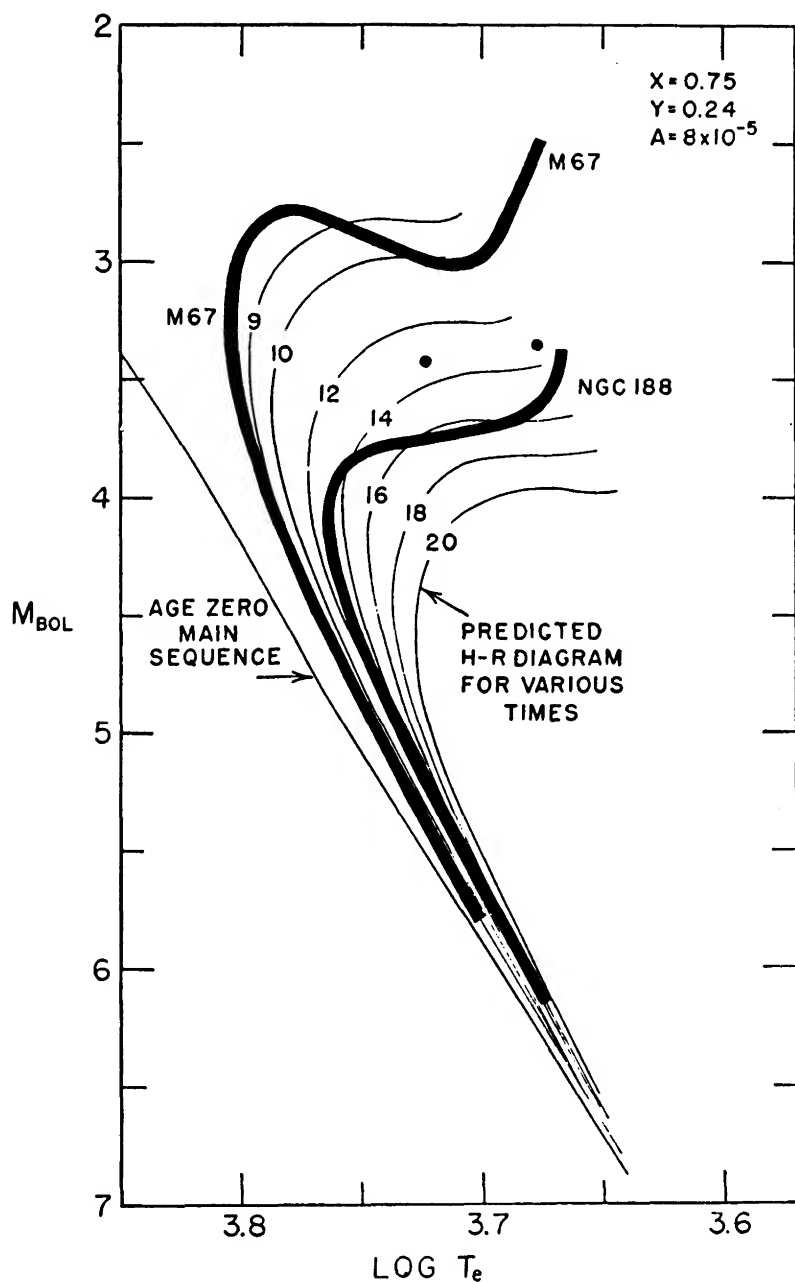


FIG. 7.—Age determination of star clusters in the HR diagram, following Sandage (1962). Heavy lines: observed loci of M67 and NGC 188. Thin lines: computed loci of constant time (attached numbers are ages in billions of years). Dots (left to right):  $\mu$  Her A and  $\delta$  Eri.

nation in the HR diagram require extensive computations of evolutionary tracks for a range of masses and a wide variety of initial chemical compositions. The theoretical foundations have been laid, and such computations as those by HLL (1959) show that the work is well within the capabilities of existing automatic computers. At the present time the observers are well ahead of the theoreticians in these problems.

#### 4.3. ACCURACY OF AGE DETERMINATIONS

Assuming that the theory of stellar evolution developed in the past generation is at least a valid and useful working hypothesis, what degree of accuracy can we ascribe to the ages determined by applications of the theory? It will be evident to the reader that this question is not to be answered in a statistical sense: one could, in principle, go to a computing machine and calculate several sets of evolutionary tracks, each time changing a punched card or two to find the effects of probable errors in the input data; and hence one could obtain a formal statistical error, " $\pm$  (some number)," to attach to derived ages. But this would be a purely academic exercise. Recent history, in particular that of the ages of globular clusters (which we shall review below), shows that quite drastic revisions of input data occur over the years with a frequency that some find amusing and others find annoying. Hence, our purpose in this subsection is simply to point out some of the factors to which age determinations are sensitive, and some to which they are not, in order to indicate where more active attention may be needed. Also relevant is a discussion of external checks and comparisons with ages otherwise determined.

It is instructive, if not indeed sobering, to examine the inflation in globular cluster ages that has taken place in the past decade. As recently as 1958 it was authoritatively stated (SES, p. 271), not without considerable reserve, that the then-available age determination for globular clusters,  $6 \times 10^9$  years, "may well be wrong by 30 per cent." At the present time we have to deal with ages several times greater than that value! What has been going on? As will shortly be apparent, there have been major advances in both observation and theory—in the latter, not the theory itself but rather in the data used for the computations. It should perhaps be emphasized that the chronological review below is not meant as a criticism of individual papers: the purpose is to illustrate how the accuracy of age determinations is affected by scientific progress.

In the classical paper by Sandage and Schwarzschild (1952), the observed "turnoff point" on the main sequence of the globular clusters M3 and M92 (Arp, Baum, and Sandage 1952) was identified with the Schönberg-Chandrasekhar limit. Using the relation (4.1) and a standard mass-luminosity relation, they estimated an approximate age of  $3 \times 10^9$  years. Shortly afterward, Sandage (1953, 1954) took into account the details of the Schönberg-Chandrasekhar evolutionary tracks and constructed a locus of constant time at  $5.1 \times 10^9$  years, which fitted the observations. Sandage did not make explicit use of a mass-

luminosity relation in the age determination, though he did use an "original" main sequence constructed from nearby stars by Johnson and Morgan (1953, Fig. 5). In 1955, Hoyle and Schwarzschild (1955) followed essentially the procedure of Sandage and Schwarzschild (1952), except that they integrated over the change in luminosity from the initial model to an advanced model (beyond which, they noted, the evolution was sufficiently rapid to be negligible). Using a main-sequence mass-luminosity relation to get the luminosity of the initial model, for which they used a mass of  $1.1 M_{\odot}$ , Hoyle and Schwarzschild obtained an age of  $6 \times 10^9$  years.

In 1956, Johnson and Sandage (1956) carried out UBV photometry of M3 which indicated that the apparent magnitude at the turnoff point in the cluster diagram was 0.2 mag. brighter than that obtained in the early work by Sandage (1953). (See also Eggen and Sandage 1959, § 4.) Since the evolution time from an initial state to any later state, such as the turnoff point, is approximately inversely proportional to the luminosity, Johnson and Sandage noted that a reduction in the age by approximately 20 per cent would follow. At the same time, however, Haselgrove and Hoyle (1956*b*) computed for the first time an evolutionary sequence of models of  $1.26 M_{\odot}$ , starting from the initial main sequence and involving the proton-proton chain, which meant that the hydrogen was burnt out non-uniformly over a large mass fraction before the central temperature rose sufficiently to initiate the CN cycle in a small, homogeneous convective core and produce the turn off the main sequence toward the red giant region (see § 2.2). These effects, and the increase in the age that would follow, were noted by Hoyle (1958, p. 226; 1959); and he further noted in the latter reference that the age was sensitive to the point of transition from the  $p$ - $p$  chain to the CN cycle. In 1956, the comparison of the Johnson-Sandage M3 photometry and the Haselgrove-Hoyle evolutionary track resulted in an age of  $6 \times 10^9$  years for M3, in essential agreement, however coincidental, with the earlier work.

The computations by Haselgrove and Hoyle (1956*b*) and also those by Hoyle and Schwarzschild (1955), used a nuclear energy-generation rate for the CN cycle based on the assumption that  $C^{12}(p, \gamma)N^{13}$  was the slowest reaction. In 1957, however, Burbidge, Burbidge, Fowler, and Hoyle (1957, pp. 571-72) expressed the conviction that  $N^{14}(p, \gamma)O^{15}$  is non-resonant at stellar energies and is the slowest and rate-governing reaction in the CN cycle (see, e.g., Honsaker 1960; Caughlan and Fowler 1962). Using new measurements on the  $N^{14}(p, \gamma)O^{15}$  cross-section, Burbidge *et al.* (1957) derived an energy-generation rate for the CN cycle some 100 times less than that used by Haselgrove and Hoyle (1956*b*), and consequently the point of transition from the  $p$ - $p$  chain to the CN cycle occurs at a later stage tending to increase the derived age. Hoyle (1959) computed an evolutionary sequence with the new rate and found an age for M3, using the same observational data as did Haselgrove and Hoyle (1956*b*), of  $8.7 \times 10^9$  years. Those data, however, were based on a mean absolute visual magnitude  $\bar{M}_V = 0.00$  for the RR Lyrae gap in M3 (Johnson and Sandage

1956), and Hoyle noted that revisions toward fainter values had been suggested and were in progress. He therefore abandoned a direct fit to the globular cluster HR diagram and derived an age for two stars of large parallax ( $\delta$  Eri and  $\mu$  Her A) of  $1.2 \times 10^{10}$  years (cf. the discussion of  $\zeta$  Her A in § 4.2). On the reasonable assumption that M3 must be at least as old as these Type I stars, he found a corresponding bright limit to the magnitudes of the RR Lyrae stars,  $\bar{M}_V \geq +0.6$ , which was in agreement with the available data. Hoyle's principal conclusion was that the age of the Galaxy was in excess of  $10^{10}$  years. It may be noted that he did not take into account all the complications in the proton-proton chain discussed by Fowler (1958, 1960).

A major advance in the observations was made by Baum, Hiltner, Johnson, and Sandage (1959), who carried out extensive faint photometry in M13 (extending work by Arp and Johnson 1955). They obtained the distance modulus by fitting the observed main sequence of M13 to a standard age-zero main sequence, after correcting the former for the effect of the differences in chemical composition upon the colors. The absolute magnitude of the turnoff point was 0.8 mag. fainter in M13 than the value Johnson and Sandage (1956, p. 382) found in M3, and consequently a considerably greater age was to be expected for M13. Baum *et al.* gave an estimate of  $10^{10}$  years from a preliminary comparison with the Hoyle (1959) Type II evolutionary sequence; but from a detailed comparison, Arp (1959c) and, independently, one of us (unpublished) found  $20 \times 10^9$  years. It is to be noted that this very considerable increase over all previous estimates was due to the observational work of Baum, Hiltner, Johnson, and Sandage (1959), in particular to their revision of the method of obtaining cluster distances and consequent lowering of the luminosities of the cluster stars. They discuss the observational errors in some detail; the uncertainty in age due to their quoted uncertainty in distance modulus *alone* is about 30 per cent.

The most recent episode in this story is the work by Sandage (1962), who has extrapolated Hoyle's (1959) Type II track to construct loci of constant time (cf. Fig. 7 above, containing Sandage's loci for Type I). Comparing these with the observational data on M13 (Baum *et al.* 1959), M5 (Arp 1962a), and M3 (Sandage 1962, Table 6), he finds formal ages ranging from  $22 \times 10^9$  to  $26 \times 10^9$  years for these clusters. "But, obviously," he writes, "little weight can be attached to these numbers." Aside from the several uncertainties, he notes in particular (1) the very poor match between the observed and computed loci in the HR diagram, and (2) Woolf's (1962a, b) penetrating observation that, over such a long time scale, stars now at the end of the horizontal branch in these clusters would have consumed more than their available energy store! Elsewhere, Sandage (1961a, b) has commented on the inconsistency of the globular-cluster time scale with cosmological data in terms of *any* extant cosmological theory. Despite Sandage's (1962) clearly stated reserve about the cluster ages, they have been given some weight: e.g., Dicke (1962) has considered their general implications for cosmology from the standpoints of a variety of theories.



It is apparent that the age determinations for globular clusters are far from being definitive at the present time. The many revisions in both observation and theory in the past decade indicate that further progress may be expected in the near future. On the observational side, for example, we may hope for an answer to the question raised by Arp (1962*b*) as to the interstellar reddening hitherto assumed (*viz.*, none) for the clusters. On the theoretical side we may hope for further computations of evolutionary tracks, to examine the validity of Sandage's (1962) extrapolation of Hoyle's (1959) single sequence.

Since age determinations are evidently sensitive to many factors, it is of interest to investigate the effects of uncertainties in these factors. How are age determinations affected by uncertainties in such input data as opacity, initial chemical composition, stellar mass, energy-generation rates, etc.? As pointed out previously a thorough investigation of these matters would be a sterile academic exercise; but an approximate analysis reveals that some factors are more important than others.

We first examine the effects on a single stellar model, specifically its radius and luminosity, which are relevant to the coordinates in the HR diagram. It will suffice to use homologous transformations strictly true only for models in radiative equilibrium, of homogeneous chemical composition, and following the ideal gas law; the degree of approximation to actual stars will be sufficient to illustrate the major effects. For an opacity law of the form  $\kappa = \kappa_0 \rho^{1-\alpha} T^{-3-S}$  and an energy-generation law of the form  $\epsilon = \epsilon_0 \rho T^\nu$ , where  $\kappa_0$ ,  $\epsilon_0$ ,  $\alpha$ ,  $S$ , and  $\nu$  are constants (the first two containing the chemical composition), we have

$$R \propto \left( \frac{\kappa_0 \epsilon_0 M^{\nu-3-\alpha-S}}{\mu^{7-\nu+S}} \right)^{1/(3+\nu-3\alpha-S)}, \quad (4.2)$$

$$L \propto \left( \frac{\mu^{21+7\nu-3\nu\alpha+3S} M^{15+5\nu-2\nu\alpha-3\alpha+S}}{\kappa_0^3 + \nu \epsilon_0^3 \alpha + S} \right)^{1/(3+\nu-3\alpha-S)} \quad (4.3)$$

The derivations of these may be obtained following procedures described by Chandrasekhar (1939, pp. 233 ff.) or Wrubel (1958, pp. 45 ff.) (cf. SES, eqs. [13.9] and [13.10]). Note that equation (4.3) is the explicit form of the theoretical mass-luminosity relation, not involving the radius. These forms have been given elsewhere, e.g., by Massevitch (1954, eqs. [7] and [8]) and by Hayashi, Hoshi, and Sugimoto (1962, eqs. [5B.4] and [5B.5]).

Equations (4.2) and (4.3) exhibit the dependences of radius and luminosity on mass, chemical composition (through  $\mu$ ,  $\kappa_0$ , and  $\epsilon_0$ ), opacity, and energy generation. The constants of proportionality can be determined by integrating the differential equations of equilibrium between specified boundary conditions: i.e., the constants are characteristic values of a model. For the present purposes, however, these are not needed.

For a Kramers opacity law (SES, § 9), with bound-free and free-free atomic transitions, the density and temperature exponents are represented with  $\alpha = 0$

and  $S = +0.5$ . For  $p$ - $p$  chain energy generation the temperature exponent is approximately  $\nu = 4$ ; equations (4.2) and (4.3) become

$$R \propto (\kappa_0 \epsilon_0)^{0.15} \mu^{-0.54} M^{0.08}, \quad (4.4)$$

$$L \propto \kappa_0^{-1.08} \epsilon_0^{-0.08} \mu^{7.8} M^{5.5}, \quad (4.5)$$

and, with  $L \propto R^2 T_e^4$ , the effective temperature is given by

$$T_e \propto \kappa_0^{-0.35} \epsilon_0^{-0.10} \mu^{2.2} M^{1.33}. \quad (4.6)$$

For the CN cycle, we choose  $\nu = 17$  and obtain

$$R \propto (\kappa_0 \epsilon_0)^{0.051} \mu^{0.49} M^{0.69}, \quad (4.7)$$

$$L \propto \kappa_0^{-1.02} \epsilon_0^{-0.02} \mu^{7.3} M^{5.2}, \quad (4.8)$$

$$T_e \propto \kappa_0^{-0.28} \epsilon_0^{-0.03} \mu^{1.6} M^{0.94}. \quad (4.9)$$

These relations may be compared with those given by, e.g., Strömgren (1952, eqs. [7] and [8]) for the Kramers law and  $\nu = 20$ ; Mashevitch (1954, eqs. [9] and [10]) for a modified Kramers law and  $\nu = 17$  and for electron scattering ( $\alpha = 1$ ,  $S = -3$ ) and  $\nu = 17$ . See also Huang (1962) for a detailed investigation at  $10 M_\odot$  involving radiation pressure and a mixed opacity law.

Equations (4.5) and (4.8) show that the luminosity is nearly inversely proportional to the opacity coefficient. If calculated values of opacity are systematically too high or too low, by 50 per cent, say (cf. Keller and Meyerott 1955; Cox, this volume), then the luminosity of a model of given mass and composition will be correspondingly low or high. However, if the luminosity is given instead, and the mass or composition is uncertain, then it is evident from equations (4.5) and (4.8) that an error in the opacity can be compensated for by very small changes in mass or composition, because of the high sensitivity of the luminosity to each of these. We shall see below that, as a consequence of this, age determinations are little affected by opacity errors. It may be noted that the effects of line opacities (Cox, this volume) viz., bound-bound transitions between atomic states, are not expected to be serious with regard to the luminosity: line opacities are important at temperatures mainly below  $5 \times 10^6$  °K, while the luminosity is established mainly by temperature gradients over hotter regions. But a detailed investigation of models with line opacities has not yet been carried out. A preliminary investigation by Iben (1962) suggests that line opacities do affect quite strongly the radius and effective temperature of a model.

Equations (4.5) and (4.8) show that the luminosity is very insensitive to the energy-generation coefficient, as expected on physical grounds from our discussion in § 2.2 above. The radius and effective temperature, however, according to equations (4.4), (4.6), (4.7), and (4.9) are more sensitive to  $\epsilon_0$  than is the luminosity, in terms of the relative accuracy with which these coordinates are

known in the HR diagram. Haselgrove and Hoyle (1959) have noted an application of this result to the sun, where the accurately observed radius offers a fairly strong condition on  $\epsilon_0$  for the  $p$ - $p$  chain; but the uncertain structure of the convective envelope renders this application impotent at present.

Equations (4.4)–(4.9) show that the chemical composition strongly affects both model coordinates in the HR diagram. The hydrogen content,  $X$ , and the helium content,  $Y$ , affect  $L$  and  $T_e$  principally via  $\mu$ , the mean molecular weight: e.g., increasing  $Y$  leads to increases in both  $L$  and  $T_e$ . The heavy-element content,  $Z = 1 - X - Y$ , enters mainly through  $\kappa_0$ , which is essentially proportional to  $Z$  in stars where bound-free absorption is important. In stars of very low  $Z$ , however, such as those in some globular clusters, free-free absorption by hydrogen and helium is paramount;  $Z$  then is important via  $\epsilon_0$  for the CN cycle, and it is only recently that the uncertainty in the absolute abundances of carbon and nitrogen has been reduced to perhaps less than a factor of 10 (Baschek 1959, Aller and Greenstein 1960, Wallerstein 1962). For detailed results of the effects of chemical composition on stellar interiors we refer to work by Strömberg (1952), Blackler (1958), Haselgrove and Hoyle (1959), Morton (1959), Demarque (1960, 1961), and Huang (1962).

The preceding discussion holds strictly only for homologous stellar models, i.e., those which differ from each other by scale factors in one or more of their physical variables (Chandrasekhar 1939, p. 235, eq. [91]), and, further, models of a restricted type. (See Hayashi, Nishida, and Sugimoto 1961 and Hayashi, Hoshi, and Sugimoto 1962 for illustrations of the curious properties of double energy-source models.) In order to examine the effects on age determinations of uncertainties in  $\kappa_0$ ,  $\epsilon_0$ , etc., we shall next consider homologous evolutionary tracks in the HR diagram, following Hoyle (1959) and Sandage (1962). The applicability of this notion to nature may be considered to be only approximate, but it should suffice for indicating gross effects. Let us consider the energy released by a star in a time interval,  $\Delta t$ , per unit mass of stellar material: this is  $(L/M)\Delta t$ . Let the mass fraction of hydrogen exhausted in time  $\Delta t$  be  $X_0\Delta q$ , where  $X_0$  is the initial mass of hydrogen per unit mass of stellar material and  $q$  is  $M_r/M$ . The terminology is that of Sandage (1958*b*, p. 45); cf. SES, p. 196. Then the energy release in the hydrogen burning is  $EX_0\Delta q$ , where  $E$  is the energy released per unit mass of hydrogen burned ( $6 \times 10^{18}$  erg/gm), and so

$$(L/M)\Delta t = EX_0\Delta q. \quad (4.10)$$

Integrating from the time when hydrogen burning begins ( $t = 0$ ) to the time subsequent to which the evolution is rapid (e.g., the subgiant turn-up point of Hoyle's (1959, Fig. 1) Type I evolutionary track; or the Schönberg-Chandrasekhar limit), we have, for the age,

$$t = \int_0^{q'} \frac{M}{L} EX_0 dq = \frac{EMX_0}{L_0} \int_0^{q'} \frac{L_0}{L} dq, \quad (4.11)$$

where  $q'$  is the mass fraction in which hydrogen has been exhausted, in time  $t$ , and  $L_0$  is the initial luminosity. Now the notion of homologous evolutionary tracks involves the assumption that the integral on the right-hand side of equation (4.11) is constant for small changes of the starting point on the main sequence. With this assumption we have (cf. eq. [4.1])

$$t \propto \frac{MX_0}{L_0}. \quad (4.12)$$

Specifically, the notion of homologous evolutionary tracks in the HR diagram as used by Hoyle (1959) and Sandage (1962) requires the assumption that  $L'/L_0 = \text{const.}$ , where  $L'$  is the luminosity at  $q'$ . Hence

$$t \propto \frac{MX_0}{L'}. \quad (4.13)$$

Let us illustrate the meaning of this equation by considering its application to  $\zeta$  Her A for which an age was derived in § 4.2. The values of  $M$  and  $L'$  are obtained from observation, and, therefore, from equation (4.13), the age is linearly proportional to the initial hydrogen content. This result, however, needs some qualification. If  $X_0$  were changed from the value used previously, 0.75, and the initial helium content changed correspondingly, the evolutionary track for the same mass  $M$  would not necessarily pass through the observed point (see Fig. 6). However, another degree of freedom is available in the heavy-element content,  $Z$ , small changes in which affect the initial luminosity strongly through the opacity. Hence, in principle at least, a change in  $X_0$  would be accompanied by a small change in  $Z$  to fit the observations. With this procedure in mind the result from equation (4.13) may be understood. It should be noted that, although the present discussion is by no means new, specific computations to check its range of validity have not been carried out.

The application of (4.13) to the ages of clusters is different from the application to a star of known mass because the masses of stars in clusters are not known, except for a few cases in the nearest ones. We may, however, invoke a mass-luminosity relation to replace  $M$  in (4.13) by a function of luminosity—specifically, by the function of  $L$ ,  $\kappa_0$ ,  $\epsilon_0$ , and chemical composition given in equation (4.3). Then we can examine the uncertainty in ages due to uncertainties in, respectively, the opacity coefficient, the energy-generation rate coefficient, and the initial chemical composition, all for a fixed  $L'$  given by observation. Implicit in such an analysis is an extension of the qualification procedure in the preceding paragraph; sets of evolutionary tracks to fit a given cluster diagram are needed. We remark that the extensive computations required would serve to give the masses of the cluster stars, if all the other input data were taken as valid (only the *slope* of the mass-luminosity relation [Haselgrove and Hoyle 1959] is used).

We consider first the effect of systematic opacity errors on age determina-

tions. The two typical mass-luminosity relations, equations (4.5) and (4.8), show that, for a fixed luminosity,  $\kappa_0$  varies approximately as the fifth power of  $M$ . Hence, equation (4.13) becomes

$$t \propto \frac{\kappa_0^{1/5} X_0}{L'};$$

i.e., quite large errors in the opacity will not affect an age determination appreciably because small changes in the stellar mass, well within any observational uncertainties, can compensate for the opacity errors. This conclusion was first noted by Hoyle (1959, p. 131).

As for the energy-generation rate, (4.5) and (4.8) show that  $\epsilon_0$  varies with an enormous power of  $M$ , and, hence, uncertainties in the cross-section for a particular process have no effect on ages—as long as a single process holds throughout the time considered. This is not the case in the mass range relevant to globular clusters, as noted above, since there is a transition from the  $p$ - $p$  chain to the CN cycle during the evolution of stars involved in age determination. Hoyle (1959) has shown that a reduction of  $\epsilon_0$  for the CN cycle by a factor of 100 leads to an increase of 50 per cent in the age. Although future changes of this size in either the CN cycle or  $p$ - $p$  chain are not expected (see Fowler 1960), recent history suggests that a certain reserve be maintained in this regard. Also, of course,  $\epsilon_0$  is directly proportional to the absolute abundance of the reacting nuclei; the ratio of  $N^{14}$  to H is, therefore, important in the CN cycle. It may be noted that Sandage's homologous extrapolation of Hoyle's evolutionary track does not allow for the transitions between various branchings of the  $p$ - $p$  chain; the resulting uncertainty may be minor, but it needs to be studied with detailed computations.

Finally we consider the effect of chemical composition on ages, particularly the initial hydrogen content of globular cluster stars,  $X_0$ . Here, equation (4.5) is appropriate: the composition factors are, for  $\kappa_0$ ,  $(X + Y)(1 + X)$ , from SES, equation (9.18), for free-free transitions; for  $\epsilon_0$ ,  $X^2$ , from the  $p$ - $p$  chain; and for  $\mu$ ,  $(5X + 3)^{-1}$ , where  $Z$  is negligible. The whole composition factor in equation (4.5) is thus

$$(1 + X)^{-1.08} X^{-0.16} (5X + 3)^{-7.8},$$

and a brief tabulation shows that, for  $X$  ranging from 1.0 to 0.5, this factor varies very nearly as  $X^{-5}$  (cf. Strömberg 1952). Hence, in equation (4.5), for a given luminosity,  $X$  varies nearly linearly with  $M$ ; equation (4.13) becomes

$$t \propto \frac{X_0^2}{L'}, \quad (4.14)$$

i.e., the age depends on approximately the square of the initial hydrogen content. In the case of the globular clusters, Sandage's (1962) age determination was based on Hoyle's (1959) Type II evolutionary sequence with  $X_0 = 0.99$ ;

if  $X_0$  were the same as a currently popular value for the sun, 0.72 (Gaustad 1964), the ages would be about 50 per cent of Sandage's values, according to the above relation. Sandage (1962) compared a second Type II sequence, with  $X_0 = 0.75$  (Hoyle 1959), with the observations and deduced a reduction factor of 60 per cent, which is about the same as obtained from the above relation. Evidently an observational measure of  $X_0$ , or of the helium-hydrogen ratio, for the globular clusters is of crucial importance in determining their ages. One star in M13 has recently been analyzed by Traving (1962), with the result that the helium-hydrogen ratio corresponds to  $X = 0.8$ ; but it is not certain that this represents the original hydrogen content,  $X_0$ , since the star is in an advanced evolutionary state lying above the blue end of the horizontal branch of M13. Nature, perversely, does not excite strong helium lines in the cooler stars in earlier evolutionary states; apparently recourse must be had to indirect methods (see SES, p. 145). It would appear that, assuming Hoyle's models and Sandage's extrapolation of them are correct, the principal uncertainties in the existing age determinations for globular clusters are (1) the assumed initial hydrogen content,  $X_0 = 0.99$ , according to which the current ages are upper limits, and (2) the distance moduli derived from observation, which, as noted earlier, are uncertain by  $\pm 0.3$  mag, leading to an uncertainty of approximately 30 per cent in the ages. We have also noted earlier Arp's (1962*b*) suggestion of interstellar reddening for globular clusters, with respect to which current ages are upper limits.

The effect of chemical composition on ages for old galactic clusters, such as M67 and NGC 188, has been recently discussed by Schmidt-Kaler (1961), who uses homology considerations and finds a composition factor varying as  $Z^{-0.3}X^{-5.0}$  for an equation corresponding to (4.8) above. The age is thus again proportional to  $X_0^2$ , and Schmidt-Kaler finds, after adopting  $X_0 = 0.62$  from the sun and other objects, a corresponding reduction of 70 per cent in the ages of M67 and NGC 188 as obtained by Sandage (1962) on the basis of Hoyle's (1959) Type I sequence with  $X_0 = 0.75$ . If we assume that the proportionality of age to  $X_0^2$  holds quite generally, at least in rough approximation, we may also comprehend a discrepancy between the age of the Pleiades as derived by Mitchell and Johnson (1957), on the basis of Tayler's (1954, 1956) models with  $X_0 = 1.00$ , and the age derived by HLL (1959) with  $X_0 = 0.68$ . These ages were, respectively,  $1.5 \times 10^8$  years and  $6 \times 10^7$  years; the ratio of these nearly equals the ratio of the  $X_0^2$  values. We conclude that computations of evolutionary sequences with a variety of initial chemical compositions are needed before age determinations in terms of the HR diagram can be placed on a firm footing.

It is appropriate to turn to consideration of possible external checks on age determinations derived from the theory of stellar evolution. The current time scale of the globular clusters is so long that it has prompted comparisons with time scales obtained from cosmology (Sandage 1961*a*, 1962; Dicke 1962; Sérsic 1962) and from nucleosynthesis (Fowler and Hoyle 1960, Fowler 1962); but

such comparisons are not direct checks, even though dissatisfactions with stellar-evolution theory may be expressed. More relevant are specific checks with items derived as directly as possible from observation.

One such item is the rate and total amount of hydrogen burning in globular clusters, as derived from semi-empirical evolutionary tracks (Sandage 1957*b*). Woolf (1962*a*) describes the method briefly. The observed number density of stars in various parts of a cluster's HR diagram equals the relative rates of evolution through these parts. The times can be computed as fractions of the cluster age, and hence, using the luminosities, the total amount of energy released over an assumed cluster age can be found. Woolf (1962*a*) found that the most advanced stars on the horizontal branch in M3 would have used up their fuel supply in approximately 50 per cent of the time indicated by Sandage's (1962) age of M3. A later note (Woolf 1962*b*) utilized Hoyle's (1959) evolutionary track to recover the initial luminosity function and changed the factor from 50 per cent to 80 per cent; Woolf noted that this was still serious. It would seem that this sort of check on ages, which is simple in principle, would be of considerable value in sufficiently well-populated clusters. In practice, an extensive observational effort is necessary to obtain accurate faint luminosity functions in clusters.

An intriguing check on age determinations would seem to be possible in expanding stellar associations, predicted by Ambarzumian (1949) and observed by Blaauw (1952). For the II Persei ( $\zeta$  Persei) association, Delhaye and Blaauw (1953) find a kinematical expansion age of  $1.5 \times 10^6$  years. From the HR diagram of the brighter stars, as obtained by Seyfert, Hardie, and Grenchik (1960) and interpreted on the basis of the Hoyle (1960; cf. Hayashi and Cameron 1962) evolutionary tracks, the age is approximately  $6 \times 10^6$  years. From the HR diagram for somewhat fainter stars, from B5 to F2 (Seyfert *et al.* 1960; Harris, Morgan, and Roman 1954), it appears that stars later than about type A0 have not yet reached the main sequence, which on the computations of HLL (1955*a*) would lead to an age of approximately  $3 \times 10^6$  years (cf. Walker 1956). The differences among these various ages are not significantly larger than the errors involved; we would rather conclude that they show essential agreement. (Compare Herbig [1962*a*, *b*].)

The existence of pre-main-sequence stars in young galactic clusters, as observed by Walker (1956, 1957, 1959, 1961*a*) and Johnson (1957*b*), suggests a comparison of H-burning ages obtained for the brighter stars and of gravitational-contraction ages obtained for the fainter stars by noting at which point the brightest of these latter reached the age-zero main sequence and comparing with the calculations of pre-main-sequence tracks by HLL (1955*a*). This was first done by Walker (1956) for NGC 2264, and he found essential agreement between the two ages. However, NGC 6611 (Walker 1961*a*) provides a fuller sample of bright early-type stars, and for it Walker finds a contraction age of  $1.8 \times 10^6$  years (using equation [7] from Sandage 1958*c*) and an H-burning

age of  $1-2 \times 10^6$  years, using the Schwarzschild-Härm (1958) evolutionary tracks. The agreement is satisfactory, in view of the uncertainty of the bolometric corrections and  $\log T_e$  scale needed for the H-burning O stars, as noted by Walker and by Schwarzschild and Härm. Insofar as the two ages represent determinations from different states of stellar structure, the agreement represents a useful check on the theory.

The general application of this check, however, appears to be beset with difficulties at the present time. The arrays of contracting stars in the color-magnitude diagrams by Walker and Johnson show considerable scatter and do not diverge from the main sequence going to fainter magnitudes, as the theory would suggest (HLL 1955*a*). These difficulties have been discussed by Sandage (1958*c*); suggestions as to the scatter have been made by Varsavsky (1960), and as to the theory, by Hayashi (1961). Another problem is the existence of yellow giants in some of these clusters (the question of membership is discussed by Walker [1961*a*, p. 451, and 1961*b*]) at an absolute magnitude which is difficult to explain in terms of post-main-sequence stages (at constant mass); Walker suggests that they may be contracting laggards, *younger* than the bulk of the observed stars. A general spread in ages in any one cluster would dissolve any check, and indeed any application, of the theory of age determinations in the cluster; for those so far observed by Walker and by Johnson (*op. cit.*) the spread does not seem to be general.

A more serious difficulty in the comparison of H-burning age against contraction age has recently arisen in the case of the Pleiades: Pesch (1961) and Herbig (1962*a, b*) have pointed out that stars exist *on* the age-zero main sequence to considerably fainter magnitudes than would be expected from the H-burning age of  $6 \times 10^7$  years estimated by HLL (1959) and the contraction tracks obtained by HLL (1955*a*). The latter, according to Herbig (1962*a*), who does not find pre-main-sequence stars down to  $M_V = +10$ , would indicate an age in excess of  $2 \times 10^8$  years. Unfortunately, each of these disparate ages for this cluster is open to question at present. The calculations by HLL (1955*a*) did not include convective envelopes: these are unnecessary for the early-type stars involved in the contraction-age determinations by Walker, described above, but for late-type stars they play a vital role in stellar structure (SES, § 11), and very possibly in the rate of stellar evolution. Hayashi (1961) has recently investigated the latter question and finds, in a preliminary computation, that deep convective envelopes transfer the energy so efficiently that the contraction ages for late-type stars are reduced to half or less of the ages from the radiative models. At present, work on Hayashi's suggestion is under way in various quarters (e.g., Faulkner, Griffiths, and Hoyle 1963); qualitatively, at least, it seems unassailable. It tends to reduce the divergence of late-type stars from the main sequence: this is predicted by the radiative models, but not observed (Walker 1957). As for the H-burning age as derived from the bright stars, we have previously noted the dependence of this age on approxi-



mately the square of the assumed initial hydrogen content. Further, the comparison of the Pleiades color-magnitude diagram with the theoretical loci of constant time is not completely satisfactory because the brightest stars fall outside the main-sequence band, as noted by Hoyle (1960) (see also Crampin and Hoyle 1960, Struve and Wade 1960, Crampin 1961) and as is also evident in comparing the observations by Johnson and Mitchell (1958) with the calculations by HLL (1959), using the transformations by Arp (1958). Hoyle (1960) suggested an aspect effect on the relation between  $B - V$  and  $\log T_e$ , owing to the rapid rotation of the pertinent stars; Crampin (1961) found that these stars fell in the main-sequence band if an empirical, rather than a computed, age-zero main sequence was used. In either case the theory is incomplete; and it is not possible at present to make a clear-cut comparison between contraction ages and H-burning ages in this important cluster, and in older ones. It may be mentioned that Herbig's (1962*a, b*) suggestion that stars of a cluster may be formed over a long period of time does not depend solely on the Pleiades difficulty; his papers contain an intriguing hypothesis of star formation in large dark clouds that seems more attractive than the simple assumption that stars of all masses are created simultaneously in a cloud.

A basic check on age determinations would seem to be available in the sun, since the age of the earth is well determined (Fowler 1962) by lead isotope measurements in the earth's crust and meteorites at  $4.55 \times 10^9$  years (Patterson 1956). A test of the theory of stellar evolution is to fit the present luminosity and radius of the sun with an evolutionary sequence of models with solar mass, at an age equal to the number above. Unfortunately, the observed solar radius is a useless condition in this test, since a calculated radius depends on the theory of convection for the envelope and present theories involve a free parameter which can be adjusted to give a radius fit without affecting the rest of the model (Schwarzschild, Howard, and Härm 1957; Sears 1959, 1960). This leaves only the present luminosity to be fitted; and we have two parameters of the original chemical composition available as input data for the computation, e.g.,  $Z/X$  and  $Y$ . Adopting a value of 0.028 for  $Z/X$  from a recent discussion by Gaustad (1964) of spectroscopic and rocket data, Sears (1964) finds that the present solar luminosity can be reached by an evolutionary sequence over  $4.5 \times 10^9$  years with an initial helium content of  $Y = 0.27$  (with  $X = 0.71$  and  $Z = 0.02$ ). This helium content is quite consistent with currently fashionable values for old Population I material (see the discussion by Schmidt-Kaler 1961); but we do not obtain a precise check of the "observed" solar age, since the calculated age depends severely on the composition. In other words, at present it is not possible to compute the age of the sun from the theory of stellar evolution; an explicit theory of convective transport is a prerequisite (cf. SES, § 7).

All these checks on age determinations could be made more useful by more extensive computations of evolutionary sequences of stellar models. The theory

of stellar evolution as it stands has hardly been fully exploited: more computations will help, not only in making detailed applications of the theory, but in revealing the inconsistencies and disagreements that point the way toward new advances.

## REFERENCES

- ALLEN, C. W. 1963 *Astrophysical Quantities* (2d ed.; London: Athlone Press).
- 1954 *Nuclear Transformations, Stellar Interiors, and Nebulae* (New York: Ronald Press), chap. 2.
- ALLER, L. H. 1963 *The Atmospheres of the Sun and Stars* (2d ed.; New York: Ronald Press), chap. 6.
- ALLER, L. H., and GREENSTEIN, J. L. 1960 *Ap. J. Suppl.*, **5**, 139.
- AMBARZUMIAN, V. A. 1949 *A.J., U.S.S.R.*, **26**, 3 [translation in *Source Book in Astronomy 1900-1950*, ed. H. SHAPLEY (Cambridge: Harvard University Press, 1960), p. 130].
- ARP, H. C. 1958 *Hdb. d. Phys.*, ed. S. FLÜGGE (Berlin: Springer-Verlag), **51**, 75.
- 1959a *A.J.*, **64**, 175.
- 1959b *Ibid.*, 254.
- 1959c *Ibid.*, 441.
- 1962a *Ap. J.*, **135**, 311.
- 1962b *Ibid.*, 971.
- ARP, H. C., BAUM, W. A., and SANDAGE, A. R. 1952 *A.J.*, **57**, 4.
- ARP, H. C., and JOHNSON, H. L. 1955 *Ap. J.*, **122**, 171.
- BAADE, W. 1944 *Ap. J.*, **100**, 137.
- BAPPU, M. K. V., CHANDRA, S., SANWAL, N. B., and SINVHAL, S. D. 1962 *M.N.*, **123**, 521.
- BASCHEK, B. 1959 *Zs. f. Ap.*, **48**, 95.
- BASHKIN, S., and PEASLEE, D. C. 1961 *Ap. J.*, **134**, 981.
- BAUM, W. A., HILTNER, W. A., JOHNSON, H. L., and SANDAGE, A. R. 1959 *Ap. J.*, **130**, 749.
- BETHE, H. 1939 *Phys. Rev.*, **55**, 434.
- BLAAUW, A. 1952 *B.A.N.*, **11**, No. 433, 405.
- 1958 *A.J.*, **63**, 186.
- 1961 *B.A.N.*, **15**, No. 505, 265.
- BLACKLER, J. M. 1958 *M.N.*, **118**, 37.
- BOK, B. J. 1946 *M.N.*, **106**, 61.

- BOK, B. J., and  
REILLY, E. 1947 *Ap. J.*, **105**, 255.
- BONDI, C. M., and  
BONDI, H. 1949 *M.N.*, **109**, 62.
- BOS, W. H., VAN DEN  
BROWNLEE, R. R., and  
COX, A. N. 1959 *Ap. J. Suppl.*, **4**, 45.
- BURBIDGE, E. M.,  
BURBIDGE, G. R.,  
FOWLER, W. A., and  
HOYLE, F. 1957 *Rev. Mod. Phys.*, **29**, 547.
- BURBIDGE, E. M.,  
BURBIDGE, G. R.,  
SANDAGE, A. R., and  
WILDEY, R. 1960 "Modèles d'étoiles et évolution stellaire," *Mém. Soc. Roy. Sci. Liège*, Ser. 5, **3**, 427.
- BURBIDGE, G. R. 1960 Lecture on star formation, NUFFIC International Summer Course in Science.
- BURBIDGE, G. R., and  
BURBIDGE, E. M. 1958 *Hdb. d. Phys.*, ed. S. FLÜGGE (Berlin: Springer-Verlag), **51**, 134.
- BURBIDGE, G. R.,  
KAHN, F. D., EBERT, R.,  
VON HOERNER, S., and  
TEMESVÁRY, S. 1960 *Die Entstehung von Sternen* (Berlin: Springer-Verlag).
- CAMERON, A. G. W. 1962a *Sky and Telescope*, **23**, 244 and 325.  
1962b *Icarus*, **1**, 13.
- CAUGHLAN, G. R., and  
FOWLER, W. A. 1962 *Ap. J.*, **136**, 453.
- CHANDRASEKHAR, S. 1939 *An Introduction to the Study of Stellar Structure* (Chicago: University of Chicago Press; reprinted by Dover Publications, New York, 1957).  
1951 *Astrophysics*, ed. J. A. HYNEK (New York: McGraw-Hill Book Co.), chap. 14.
- CHRISTY, R. F. 1964 *Rev. Mod. Phys.*, **36**, 555.
- COWLING, T. G. 1935 *M.N.*, **96**, 42.
- COX, A. N., and  
BROWNLEE, R. R. 1960 "Modèles d'étoiles et évolution stellaire," *Mém. Soc. Roy. Sci. Liège*, Ser. 5, **3**, 469.
- COX, A. N., and  
OLSEN, K. H. 1963 *A.J.*, **68**, 276.
- COX, J. P., COX, A. N.,  
and OLSEN, K. H. 1963 *A.J.*, **68**, 276.
- COX, J. P., and  
GIULI, R. T. 1961 *Ap. J.*, **133**, 755.

- COX, J. P., and  
SALPETER, E. E. 1961 *Ap. J.*, **133**, 764.
- CRAMPIN, J. 1961 *Observatory*, **81**, 150.
- CRAMPIN, J., and  
HOYLE, F. 1960 *M.N.*, **120**, 33.
- CRAWFORD, D. 1958 *Ap. J.*, **128**, 185.
- DELHAYE, J., and  
BLAAUW, A. 1953 *B.A.N.*, **12**, No. 448, 72.
- DEMARQUE, P. 1960 *Ap. J.*, **132**, 366.  
1961 *Ibid.*, **134**, 9.
- DEMARQUE, P., and  
GEISLER, J. E. 1963 *Ap. J.*, **137**, 1102.
- DEUTSCH, A. J. 1961 *Stellar Atmospheres*, ed. J. L. GREENSTEIN (Chicago: University of Chicago Press), chap. 15.
- DICKE, R. H. 1962 *Rev. Mod. Phys.*, **34**, 110.
- EDDINGTON, A. S. 1926 *The Internal Constitution of the Stars* (Cambridge: Cambridge University Press; reprinted by Dover Publications, New York, 1959).
- EGGEN, O. J., and  
SANDAGE, A. R. 1959 *M.N.*, **119**, 255.  
1962 *Ap. J.*, **136**, 735.
- EZER, D., and  
CAMERON, A. G. W. 1962 *Sky and Telescope*, **24**, 328.  
1963 "The Early Evolution of the Sun," unpublished report, Goddard Institute for Space Studies, New York.
- FAULKNER, J.,  
GRIFFITHS, K., and  
HOYLE, F. 1963 *M.N.*, **126**, 1.
- FOWLER, W. A. 1958 *Ap. J.*, **127**, 551.  
1960 "Modèles d'étoiles et évolution stellaire," *Mém. Soc. Roy. Sci. Liège*, Ser. 5, **3**, 207.  
1962 *Proceedings of the Rutherford Jubilee International Conference*, ed. J. B. BIRKS (London: Heywood and Co., Ltd.), p. 640.
- FOWLER, W. A.,  
GREENSTEIN, J. L., and  
HOYLE, F. 1962 *Geophys. J. of the R.A.S.*, **6**, 148.
- FOWLER, W. A., and  
HOYLE, F. 1960 *Ann. of Phys.*, **10**, 280.
- GAMOW, G., and  
KELLER, G. 1945 *Rev. Mod. Phys.*, **17**, 125.
- GARDINER, J. 1951 *M.N.*, **111**, 94.
- GAUSTAD, J. E. 1963 *Ap. J.*, **138**, 1050.  
1964 *Ap. J.*, **139**, 406.
- GOVE, H. E.,  
LITHERLAND, A. E., and  
CLARK, M. A. 1961 *Nature*, **191**, 1381.

- GREENSTEIN, J. L. 1961 *Amer. Scientist*, **49**, 471.
- HÄRM, R., and  
SCHWARZSCHILD, M. 1961 *A.J.*, **66**, 45.
- HARO, G., and  
MINKOWSKI, R. 1961 *A.J.*, **65**, 490.
- HARRIS, D. L., III 1961 *Planets and Satellites*, ed. G. P. KUIPER and B. M. MIDDLEHURST (Chicago: University of Chicago Press), chap. 8.
- 1963 *Basic Astronomical Data*, ed. K. AA. STRAND (Chicago: University of Chicago Press), chap. 14.
- HARRIS, D. L.,  
MORGAN, W. W., and  
ROMAN, N. G. 1954 *Ap. J.*, **119**, 622.
- HASELGROVE, C. B., and  
HOYLE, F. 1956a *M.N.*, **116**, 515.
- 1956b *Ibid.*, p. 527.
- 1958 *Ibid.*, **118**, 519.
- 1959 *Ibid.*, **119**, 112.
- HAYASHI, C. 1961 *Pub. Astr. Soc. Japan*, **13**, 450.
- HAYASHI, C., and  
CAMERON, R. C. 1962 *Ap. J.*, **136**, 166.
- HAYASHI, C., and  
HOSHI, R. 1961 *Pub. Astr. Soc. Japan*, **13**, 442.
- HAYASHI, C., HOSHI, R.,  
and SUGIMOTO, D. 1962 *Progress of Theoret. Phys., Suppl.* (Kyoto), No. 22.
- HAYASHI, C., JUGAKU, J.,  
and NISHIDA, M. 1959 *Progress of Theoret. Phys.*, **22**, 531.
- 1960 *Ap. J.*, **131**, 241.
- HAYASHI, C., NISHIDA, M.,  
and SUGIMOTO, D. 1961 *Progress of Theoret. Phys.*, **25**, 1053.
- HELMHOLTZ, H. VON 1854 Lecture, Königsberg.
- HENYEY, L. G. 1956 *Pub. A.S.P.*, **68**, 503.
- HENYEY, L. G.,  
FORBES, J. E., and  
GOULD, N. 1964 *Ap. J.*, **139**, 306.
- HENYEY, L. G.,  
LELEVIER, R., and  
LEVÉE, R. D. 1955a *Pub. A.S.P.*, **67**, 154.
- 1955b *Ibid.*, p. 341.
- 1959 *Ap. J.*, **129**, 2.
- HENYEY, L. G.,  
WILETS, L., BÖHM,  
K.-H., LELEVIER, R.,  
and LEVÉE, R. D. 1959 *Ap. J.*, **129**, 628.
- HERBIG, G. H. 1957 *Non-stable Stars*, ed. G. H. HERBIG (Cambridge: Cambridge University Press), p. 3.

- 1958 *Stellar Populations*, ed. D. J. O'CONNELL (Amsterdam: North Holland Publishing Co.), p. 127.
- 1962a *Advances in Astronomy and Astrophysics* (New York: Academic Press), **1**, 47.
- 1962b *Ap. J.*, **135**, 736.
- HOFMEISTER, E., KIPPENHAHN, R., and WEIGERT, A. 1964 *Zs. f. Ap.*, **59**, 215, 242.
- HONSAKER, J. L. 1960 *Ap. J.*, **132**, 516.
- HOYLE, F. 1955 *Frontiers of Astronomy* (New York: Harper).
- 1958 *Stellar Populations*, ed. D. J. O'CONNELL (Amsterdam: North Holland Publishing Co.).
- 1959 *M.N.*, **119**, 124.
- 1960 *Ibid.*, **120**, 22.
- HOYLE, F., and  
LYTTLETON, R. A. 1948 *Occasional Notes, R.A.S.*, **2**, No. 12.
- HOYLE, F., and  
SCHWARZSCHILD, M. 1955 *Ap. J. Suppl.*, **2**, 1.
- HUANG, S.-S. 1962 *Ap. J.*, **136**, 193.
- IBEN, I. 1962 *A.J.* **67**, 274.
- IBEN, I., and  
EHRMAN, J. R. 1962 *Ap. J.*, **135**, 770.
- JOHNSON, H. L. 1954 *Ap. J.*, **120**, 325.
- 1955 *Ann. d'ap.*, **18**, 292.
- 1957a *Ap. J.*, **126**, 121.
- 1957b *Ibid.*, p. 134.
- 1963 *Basic Astronomical Data*, ed. K. AA. STRAND (Chicago: University of Chicago Press), chap. 11.
- JOHNSON, H. L., and  
HARRIS, D. L., III 1954 *Ap. J.*, **120**, 196.
- JOHNSON, H. L., and  
HILTNER, W. A. 1956 *Ap. J.*, **123**, 267.
- JOHNSON, H. L., and  
MITCHELL, R. I. 1958 *Ap. J.*, **128**, 31.
- JOHNSON, H. L.,  
MITCHELL, R. I., and  
IRIARTE, B. 1962 *Ap. J.*, **136**, 75.
- JOHNSON, H. L., and  
MORGAN, W. W. 1953 *Ap. J.*, **117**, 313.
- 1955 *Ibid.*, **122**, 429.
- JOHNSON, H. L., and  
SANDAGE, A. R. 1956 *Ap. J.*, **124**, 379.
- JOY, A. H. 1945 *Ap. J.*, **102**, 168.
- KAMP, P. VAN DE 1954 *A.J.*, **59**, 447.
- 1958 *Hdb. d. Phys.*, ed. S. FLÜGGE (Berlin: Springer-Verlag), **50**, 187.

- KEENAN, P. C. 1962 *Stellar Atmospheres*, ed. J. L. GREENSTEIN (Chicago: University of Chicago Press), chap. 14.  
 1963 *Basic Astronomical Data*, ed. K. AA. STRAND (Chicago: University of Chicago Press), chap. 8.
- KEENAN, P. C., and MORGAN, W. W. 1951 *Astrophysics*, ed. J. A. HYNEK (New York: McGraw-Hill Book Co.), chap. 1.
- KELLER, G., and MEYEROTT, R. E. 1955 *Ap. J.*, **122**, 32.
- KIPPENHAHN, R., TEMESVÁRY, S., and BIERMANN, L. 1958 *Zs. f. Ap.*, **46**, 257.
- KRAFT, R. P. 1961 *Ap. J.*, **134**, 616.  
 1963 *Basic Astronomical Data*, ed. K. AA. STRAND (Chicago: University of Chicago Press), chap. 21.
- KUSHWAHA, R. S. 1957 *Ap. J.*, **125**, 242.
- LEDoux, P. 1947 *Ap. J.*, **105**, 305.
- LIMBER, D. N. 1958 *Ap. J.*, **127**, 387.  
 1960 *Ibid.*, **131**, 168.
- LITHERLAND, A. E., KUEHNER, J. A., GOVE, H. E., CLARK, M. A., and ALMQVIST, E. 1961 *Phys. Rev., Letters*, **7**, 98.
- MASSEVITCH, A. G. 1954 "Les processus nucléaires dans les astres," *Mém. Soc. Roy. Sci. Liège*, Ser. 4, **14**, 170.  
 1957 *Astr. Zh.*, **34**, 176 (= *Soviet Astr., A.J., U.S.S.R.*, **1**, 177).
- MELBOURNE, W. 1960 *Ap. J.*, **132**, 101.
- MESTEL, L. 1952 *M.N.*, **112**, 583.  
 1962 *Simposia sobre Evolución Estelar*, ed. J. SAHADE (La Plata: Observatorio Astronómico), p. 77.
- MITCHELL, R. I., and JOHNSON, H. L. 1957 *Ap. J.*, **125**, 414.
- MORTON, D. C. 1959 *Ap. J.*, **129**, 20.
- NISHIDA, M. 1960 *Progress of Theoret. Phys.*, **23**, 896.
- NISHIDA, M., and SUGIMOTO, D. 1962 *Progress of Theoret. Phys.*, **27**, 145.
- ODGERS, G. J. 1957 *Pub. Dom. Ap. Obs. Victoria*, **10**, 393.
- ÖPIK, E. 1938 *Pub. Obs. Tartu*, **30**, Nos. 3 and 4.
- OKE, J. B. 1961 *Ap. J.*, **133**, 166.
- OKE, J. B., and SCHWARZSCHILD, M. 1952 *Ap. J.*, **116**, 317.
- OSTERBROCK, D. E., and ROGERSON, J. B. 1961 *Pub. A.S.P.*, **73**, 129.
- PATTERSON, C. 1956 *Geochim. et Cosmochim. Acta*, **10**, 230.
- PESCH, P. 1961 *Ap. J.*, **133**, 1085.
- POLAK, E. 1962 *Ap. J.*, **136**, 465.

- POPPER, D. M. 1959 *Ap. J.*, **129**, 647.
- REEVES, H. 1962 *Ap. J.*, **135**, 779.
- RICHTMYER, R. D. 1957 *Difference Methods for Initial-Value Problems* (New York: Interscience Publishers, Inc.)
- ROBERTS, M. S. 1960 *A.J.*, **65**, 457.
- RUSSELL, H. N. 1918 *Pub. A.A.S.*, **3**, 22.
- RUSSELL, H. N.,  
DUGAN, R. S., and  
STEWART, J. Q. 1927 *Astronomy* (Boston: Ginn and Co.), **2**, 910.
- SAKASHITA, S.,  
ONO, Y., and  
HAYASHI, C. 1959 *Progress of Theoret. Phys.*, **21**, 315.
- SALPETER, E. E. 1954 "Les processus nucléaires dans les astres," *Mém. Soc. Roy. Sci. Liège*, Ser. 4, **14**, 116.
- SAMPSON, D. H. 1961 *Ap. J.*, **134**, 482.
- SANDAGE, A. R. 1953 *A.J.*, **58**, 61.
- 1954 "Les processus nucléaires dans les astres," *Mém. Soc. Roy. Sci. Liège*, Ser. 4, **14**, 254.
- 1957a *Ap. J.*, **125**, 435.
- 1957b *Ibid.*, **126**, 326.
- 1958a *Ibid.*, **127**, 513.
- 1958b *Stellar Populations*, ed. D. J. O'CONNELL (Amsterdam: North Holland Publishing Co.), p. 41.
- 1958c *Ibid.*, p. 149.
- 1958d *Ibid.*, p. 287.
- 1961a *Ap. J.*, **133**, 355.
- 1961b *A.J.*, **66**, 53.
- 1962 *Ap. J.*, **135**, 349. [See also: *Symposia sobre Evolución Estelar*, ed. J. SAHADE (La Plata: Observatorio Astronómico, 1962).]
- SANDAGE, A. R., and  
EGGEN, O. J. 1959 *M.N.*, **119**, 278.
- SANDAGE, A. R., and  
SCHWARZSCHILD, M. 1952 *Ap. J.*, **116**, 463.
- SANDAGE, A. R., and  
SMITH, L. L. 1963 *Ap. J.*, **137**, 1057.
- SAVEDOFF, M. P. 1963 *Ap. J.*, **138**, 291.
- SAVEDOFF, M. P., and  
VAN DYCK, S. R. 1960 "Modèles d'étoiles et évolution stellaire," *Mém. Soc. Roy. Sci. Liège*, Ser. 5, **3**, 523.
- SCHMIDT-KALER, T. 1961 *Observatory*, **81**, 226.
- SCHÖNBERG, M., and  
CHANDRASEKHAR, S. 1942 *Ap. J.*, **96**, 161.
- SCHWARZSCHILD, M. 1946 *Ap. J.*, **104**, 203.
- 1958 *Structure and Evolution of the Stars* (Princeton, N.J.: Princeton University Press).



- SCHWARZSCHILD, M., and  
HÄRM, R. 1958 *Ap. J.*, **128**, 348.  
1962 *Ibid.*, **136**, 158.
- SCHWARZSCHILD, M.,  
HOWARD, R. F., and  
HÄRM, R. 1957 *Ap. J.*, **125**, 233.
- SCHWARZSCHILD, M., and  
SELBERG, H. 1962 *Ap. J.*, **136**, 150.
- SEARS, R. L. 1959 *Ap. J.*, **129**, 489.  
1960 "Modèles d'étoiles et évolution stellaire," *Mém. Soc. Roy. Sci. Liège*, Ser. 5, **3**, 479.  
1964 *Ap. J.*, **140**, 477.  
1962 *Ann. d'ap.*, **25**, 206.
- SÉRSIC, J. 1962 *Ann. d'ap.*, **25**, 206.
- SEYFERT, C. K.,  
HARDIE, R., and  
GRECHIK, R. T. 1960 *Ap. J.*, **132**, 58.
- SOBOLEV, V. 1960 *Astr. Zh.*, **37**, 387 (= *Soviet Astr.*, *A.J.*, *U.S.S.R.*, **4**, 372).
- SPITZER, JR., L. 1966 Vol. 7, this series.
- STEBBINS, J., and  
KRON, G. E. 1957 *Ap. J.*, **126**, 266.
- STRÖMGREN, B. 1952 *A.J.*, **57**, 65.  
1958 *Observatory*, **78**, 137.  
1963 *Basic Astronomical Data*, ed. K. AA. STRAND (Chicago: University of Chicago Press), chap. 9.
- STRUVE, O. 1960 "Modèles d'étoiles et évolution stellaire," *Mém. Soc. Roy. Sci. Liège*, Ser. 5, **3**, 17.  
1962 *The Universe* (Cambridge: Massachusetts Institute of Technology Press).
- STRUVE, O., and  
WADE, M. S. 1960 *Observatory*, **80**, 229.
- TAYLER, R. 1954 *Ap. J.*, **120**, 332.  
1956 *M.N.*, **116**, 25.
- TRAVING, G. 1962 *Ap. J.*, **135**, 439.
- TRUMPLER, R. J. 1925 *Pub. A.S.P.*, **37**, 307.
- UNDERHILL, A. B. 1963 *Pub. Dom. Ap. Obs. Victoria*, **12**, No. 6.
- UPTON, E. K. L. 1966 Vol. 7, this series.
- VARSAVSKY, C. M. 1960 *Ap. J.*, **132**, 354.
- VOGT, H. 1926 *A.N.*, **226**, 301.
- WALKER, M. F. 1956 *Ap. J. Suppl.*, **2**, 365.  
1957 *Ap. J.*, **125**, 636.  
1959 *Ibid.*, **130**, 57.  
1961a *Ibid.*, **133**, 438.  
1961b *Ibid.*, **133**, 1081.
- WALLERSTEIN, G. 1962 *Ap. J. Suppl.*, **6**, 407.
- WEYMANN, R., and  
MOORE, E. 1962 *Ap. J.*, **137**, 552.

- WILDEY, R. L.,  
BURBIDGE, E. M.,  
SANDAGE, A. R., and  
BURBIDGE, G. R.      1962    *Ap. J.*, **135**, 94.  
WOOLF, N. J.      1962a   *Ap. J.*, **135**, 644.  
                     1962b   *A.J.*, **67**, 286.  
WRUBEL, M. H.    1958    *Hdb. d. Phys.*, ed. S. FLÜGGE (Berlin: Springer-Verlag), **51**, 1.  
                     1960    *Vistas in Astronomy*, ed. A. BEER (London: Pergamon Press), **3**, 107.  
                     1963    *Proceedings of the International School of Physics "Enrico Fermi," Course XXVIII: Star Evolution*, ed. L. GRATTON (New York and London: Academic Press), p. 50.  
WYLLER, A. A.    1955    *A.J.*, **60**, 39.



# Index

[Page numbers for sections are in *italics*]

- A pec stars; *see* Magnetic stars
- Absolute magnitudes; *see* Luminosities
- Absorption coefficients; *see* Opacity sources
- Abundances of nuclear species; *see* Elements, abundances
- Accretion of matter, 65
- Adiabatic coefficients, 505, 511, 513, 528
- Adiabatic temperature gradient, 492, 493, 495, 506
- Adiabatic transformations, 505
- Age of astronomical objects, 87–98, 613–33
  - accuracy of determinations, 620–33
  - checks on, 629–33
  - of clusters, 618–24
  - of earth; *see* Earth, age
  - of Galaxy, 98, 622
  - of meteorites, 84–90
  - of solar system; *see* Sun and solar system, age
  - of star, 93–98, 314, 615, 616
- Alpha particles, 73, 197
- Alpha process, 3, 4, 23, 24–25, 44, 45, 56, 57, 176, 354
- Anomalous elemental abundances; *see* Elements, abundances, anomalous
- Anomalous stars, 55–60
- Atmospheres; *see* Stellar atmospheres
  
- Beryllium, 60 ff., 70, 132
- Beta decay, 3, 23, 29, 31, 32–35, 43, 44, 47, 130, 133, 145, 146, 176, 177, 178, 303, 357
- Binary stars, 305, 331, 343
  - evolution, 322, 564
- Blackbody energy distribution; *see* Planck's law
- Black dwarfs, 297, 312, 314
- Bolometric magnitude, 615
- Boltzmann equation, 208, 237
- Boron, 60 ff., 70, 71, 79
- Bose-Einstein particles, 301
- Bound-free absorption; *see* Opacity, sources of
- Boundary conditions
  - for differential equations method, 596 ff.
  - for hydrodynamic equations, 518–20, 525, 528, 534, 535, 552, 568
- Bremsstrahlung, 358, 359
  
- Carbon, energy-level diagrams, 46, 160
- Carbon burning, 29, 30, 31, 33, 46, 170, 175, 176, 184
- Carbon-nitrogen cycle, 2, 3, 5, 22, 126, 127, 130, 135–47, 155, 157, 203, 271, 536, 543, 583
- Carbon stars, 50, 55, 67
- Central condensation in stars, 537
- Cepheid variables, 52, 330
- Charged-particle reactions, 3
- Chemical composition of stars, 1–98, 197, 203, 210, 256, 446–48, 549, 553, 626, 628, 629
- Chondrites; *see* Meteorites
- Circulation
  - in convective envelopes, 492–95
  - and evolution, 482–85
  - meridional in rotating stars, 465–96, 565, 566–68
  - steady, conditions for, 272, 477–82, 485–90
  - and stellar evolution, 482–85
- Clusters; *see* Star clusters
- Coherent scattering; *see* Opacity, sources of
- Collisional broadening, 217
- Color index, 615
- Composition; *see* Chemical composition
- Conduction of energy; *see* Energy transport
- Contracting core, 184, 204
- Contraction, gravitational; *see* Gravitational contraction
- Convective core; *see* Stellar cores
- Convective energy transport; *see* Energy transport
- Convective envelopes; *see* Stellar envelopes
- Convective equilibrium, 204, 328, 450, 469, 517, 530, 531, 533, 538, 539, 568
  - cellular convection, 507
  - in magnetic stars, 444–48
- Convective zones; *see* Stellar envelopes, convective
- Cores of stars; *see* Stellar cores
- Coriolis forces, 452, 482, 494, 568
- Cosmic rays, 66, 72, 74, 401, 418, 420
- Cowling model; *see* Point-source model
- Crab Nebula, 368, 395, 396, 400, 416
  
- Degeneracy, electron gas, 125, 148, 180, 181, 183, 196, 209, 210, 213–15, 221, 222, 226, 228, 231, 239, 247, 257, 297, 298, 300, 309, 310, 319, 332, 336, 352, 361, 362, 418, 483, 528, 586
  - rigid-lattice model, 301, 302, 311
- Deuterium, 29, 60–66, 580, 581
- Distortion, in rotating stars; *see* Perturbations, radial
- Distortion, tidal, 562
- Doppler broadening, 217
- Dwarf novae; *see* Novae, dwarf

- Earth  
 and abundances in crust, 4, 5, 22, 23, 25,  
 60, 66, 70, 72, 76  
 age, 87–90, 98, 202  
 atmosphere, 220  
 magnetic field, 451
- Eddington approximation for stellar interiors,  
 205
- Einstein shift, 305, 306, 307, 308, 319
- Electron gas, 125, 133, 181, 196, 297, 298,  
 300, 528, 552
- Electron pressure, 208, 225, 226, 239, 258,  
 260, 298, 302, 481, 528
- Electron scattering; *see* Opacity, sources of
- Electron screening, 124, 125, 127, 134, 158,  
 159, 171, 174, 175, 341
- Elements  
 abundances, anomalous, 50–60, 426, 446–  
 48  
 abundances, initial conditions, 31, 272  
 abundances, isotopic ratios, *1 ff.*, 4, 5, 22,  
 23, 25, 28, 37, 56, 67, 79, 80, 146, 147,  
 167  
 abundances of chemical, *1 ff.*, 4, 5, 6–21,  
 23, 25, 27, 153, 204, 272, 355, 418, 543,  
 581  
 abundances of nuclei, 4, 5, 23, 60–87, (D)  
 66, 71–73, (Li) 66–70, (Be) 70, (B) 70,  
 86, 303  
 masses of stable, 44, 118  
 metals in galactic plane, 54, 55  
 metals in protostars, 581  
 nuclear species, relative abundance, 4, 5,  
 22 *ff.*  
 origin of, 1–98, 512, 513  
 in solar system, 90–92  
 temperature dependence, tables, 61, 63
- Emden function, 298
- Emission  
 free-bound; *see* Opacity, sources of  
 free-free; *see* Opacity, sources of  
 induced, 199, 225, 246
- Energy, conservation of mechanical, 515
- Energy generation in stars, *1 ff.*, 113–89, 197,  
 273, 535  
 rates of, 114, 115, 116, 120, 126, 153, 175,  
 332–34, 341, 542, 628  
 from H-burning stage, 152–56  
 from He-burning, 164, 169, 170
- Energy sources  
 of stars, 113–89, 199, 577  
 of sun, 577, 578
- Energy transport, in stars, 195, 196  
 conduction, 196, 221–24, 228, 247, 252, 253,  
 259, 260, 311, 337  
 convection, 444, 506, 533, 534  
 radiation, 197, 198, 199, 202, 205, 219, 221,  
 223, 228, 239, 247, 252, 253, 466, 535
- Entropy, 501, 505, 513, 546, 551
- Envelopes of stars; *see* Stellar envelopes
- Equation of state, 208, 209, 230, 231, 239–45,  
 243, 263, 297, 298, 302, 310, 336, 579  
 barytropic, 467–68  
 ideal gas, 465
- Equilibrium conditions; *see* Convective; Hy-  
 drostatic; Radiative; Thermal equilib-  
 rium; etc.
- Equilibrium (*e-*) process, 3, 4, 23, 25–27, 37,  
 45, 49, 52, 71, 86
- Eta Carinae, 368, 410, 411
- Evolution of Galaxy, 53, 54
- Evolution of stars, 2, 3, 31, 33, 37, 52, 53, 55,  
 57, 59, 64, 65, 94, 113, 114, 202–4, 262,  
 319–22, 328, 330, 332, 342, 489, 490,  
 502, 513, 527, 533, 536, 537, 549, 552,  
 553, 554, 557, 564, 570, 575–633  
 and age determinations, 575–633  
 main-sequence stages, 482, 581–85  
 and meridian circulation, 482–85  
 and neutrinos, 183–85  
 post-main-sequence stages, 585–93  
 pre-main-sequence stages, 272, 537, 577–81  
 zero-age stars, 272, 274, 275, 286  
*see also* Stellar models
- Evolutionary tracks in HR diagram, 275,  
 320, 482, 483, 490, 491
- Exclusion energy, 313, 314, 315
- External gravitational fields, effects on stars,  
 554, 555, 561–64, 569
- Fermi-Dirac statistics, 209, 214, 215, 222,  
 226, 227, 231, 246, 297, 301
- Fermi-Thomas atomic model, 300, 301, 302
- 53 Tauri, anomalous abundances, 58
- Fission processes, 3, 44
- Flares, 74, 75, 77, 82, 441, 447, 448  
 theories of, 440–44
- Fluorine, energy-level diagrams, 141, 142
- Formation of stars; *see* Star formation
- Free-bound emission; *see* Opacity, sources of
- Free-free absorption; *see* Opacity, sources of
- Galaxies  
 age of, 98, 622  
 classified; *see* Luminosities, of galaxies  
 model, 96
- Gaunt factor, 207, 208, 209, 210, 211, 212,  
 213, 214, 215, 227, 228, 238, 245, 246, 249
- Giants; *see* Red giants; Supergiants; etc.
- Gravitational contraction, 78, 79, 113, 184,  
 202, 320, 327, 328, 329, 330, 332, 342,  
 352, 353, 354, 355, 360, 419, 466, 473,  
 502, 527, 536, 537, 589, 601  
 of Galaxy, 54
- Gravitational energy, 65, 113, 313, 328, 332,  
 337, 352, 355, 428, 431, 465, 466, 467,  
 468, 509, 515, 554, 559, 578, 589
- Guillotine factor, 205, 207, 212, 228, 311
- Helium  
 abundance, 22, 23, 53, 55, 126  
 -burning, 3, 25, 46, 49, 113, 114, 156–70,  
 184, 197, 203, 589  
 stars, 23, 50  
*see also* Triple-alpha process
- Helium core, 30, 113, 167, 332
- Helium flash, 159, 587
- Helmholtz contraction; *see* Gravitational con-  
 traction

- Hertzsprung-Russell diagram, 52, 93, 113, 202, 275, 277, 286, 288, 314, 315, 320, 342, 482, 483, 485, 615, 618, 619  
 turn-off point, 619, 620, 621, 622  
 homologous evolutionary tracks, 626 *ff.*  
 High-velocity stars, 51, 52, 54  
 Homology transformations, 343, 550  
 Hubble age of Galaxy, 98  
 Hydrogen burning, 30, 52, 113, 126–56, 197, 271, 282  
 Hydrogen-exhaustion phase, 279  
 Hydrostatic equilibrium, 198, 297, 299, 313, 465–68, 472, 499  
 Hyperon stars, 419  
 Induced emission of photons, 199, 225, 246  
 Inhomogeneous composition, 203  
 Instabilities in stars, 114, 315, 328, 339–41  
   convective, 272, 506, 530, 531  
   differential rotation, 566–68  
   dynamical, 329, 330, 495, 501, 502, 514, 524–34, 555–66  
   general problem and radial motion, 521–24  
   gravitational, 499  
   local, 503–20, 566–70  
     magnetic, 569, 570  
     rotational, 566–68  
     thermal, 506–8  
   and magnetic fields, 429, 430, 443, 444, 559–61  
   and rotation, 328, 329, 477, 484, 485, 555–59  
   secular, 316, 330, 336, 337, 502, 524, 547–66  
   superadiabatic temperature gradients, 506, 531, 532, 533, 534, 568, 569  
   thermal, 444  
   turbulent convection, 506, 508–10, 515, 516  
   vibrational, 318, 330, 331, 337, 338, 342, 348, 502, 524, 534–47  
 Interstellar absorption, 579  
 Ionization zones, 510–12, 541, 542  
 Iron group of elements, 26, 27, 35–37, 49, 114, 303, 354, 360, 514  
 Iron-poor stars, 56  
 Isobars and nuclear decay, 3, 44, 75, 81, 82, 83, 95  
 Isothermal core; *see* Stellar cores  
 Isothermal gas sphere, 382  
 Lead, abundance and ages of astronomical objects, 88–90  
 Lithium, 60 *ff.*, 66–70  
 Local thermodynamic equilibrium, 67, 195, 197  
 Luminosities  
   of galaxies, 371, 384, 385  
   of novae and supernovae, 339, 341, 384, 385, 389, 401, 416, 420  
   of stars, 117, 297, 307, 309, 312, 313, 367, 582, 624, 625  
   *see also* Mass-luminosity relation  
 Magnesium, energy-level diagram, 172  
 Magnesium stars, 304  
 Magnetic braking, 437–40  
 Magnetic fields in stars, 48, 54, 55, 57, 58, 65, 70, 73, 74, 76, 78, 79, 425–61, 466, 467, 477–82, 489, 490, 492, 494, 559–61, 565–66  
   force-free, 435–44  
   force-free and flares, 440–44  
   origin, 448–54  
     fossil magnetism, 449–51, 490  
     dynamo theories, 451–54, 490  
   and rotating stars, 465 *ff.*  
   and surface distortions, 430–35  
   and virial theorem, 427–30  
 Magnetic-oscillator theory, 454, 457–58  
 Magnetic stars, 50, 54, 55, 308, 309, 425–61  
   anomalous abundances, 57, 58, 425  
   basic equations, 426, 427  
   convection and turbulence, 444–48  
   hydromagnetic-cycle theory, 454, 458–60  
   oblique-rotator theory, 454, 455–57  
   surface distortion, 307, 308, 309, 430–35  
     barocline stars, 433–35  
     Ferraro's solution, 430–33  
   variables, 447, 454–60  
 Magnitude-redshift relation for galaxies, 391–412  
 Main sequence, 2, 82, 113, 130, 202, 269–92, 308, 482, 483, 541  
 Manganese stars, anomalous abundances in, 58  
 Mass ejection, 1, 2, 37, 329, 330, 337, 338, 342, 347, 351, 360, 420, 440  
 Mass-luminosity relation, 205, 272, 273, 482, 483, 549, 627  
 Mass-radius relation for white dwarfs; *see* White dwarfs  
 Maxwell-Boltzmann distribution, 54, 119, 209, 213  
 Mechanical energy conservation theorem, 515  
 Metal-hydrogen ratio, 2, 50, 52, 54  
 Metals  
   in galactic plane, 54, 55  
   in protostars, 581  
 Meteorites, 4, 5, 23, 60, 66, 70, 82, 87–90, 92, 98  
   carbonaceous chondrites, 89  
   chondrites, 4, 5, 22, 70, 89  
 Mira, 322  
 Mixing, 4, 29, 59, 485–90, 533, 534; *see also* Circulation; Convective equilibrium  
 Mixing length, 493, 508  
 Molecular weight, 205, 476, 482–90, 553  
 Molecules and opacity, 196, 208, 220, 221, 240, 245  
 Monochromatic radiative flux, definition, 200; *see also* Opacity, calculations; Stellar atmospheres  
 Morse opacities; *see* Opacity, calculations  
 Natural broadening, 216  
 Neon burning, 175  
   energy-level diagram, 165

- Neutrino reactions, 29, 30, 35, 46, 113, 114,  
117, 145–52, 176–85  
and collapse, 29, 30, 352  
from H-burning stage, 113, 145–52  
and late stages of stellar evolution, 183–85,  
356–60  
spectrum, 148, 149
- Neutron  
capture, 3, 23, 30, 33, 35, 38, 43, 44, 46, 80  
capture cross-sections, 38, 39–43  
production, 28–31, 38, 78, 80  
sources, 28–31
- Neutron stars, 305, 352, 419  
mass-radius relation, 353
- Nitrogen, energy-level diagrams, 136, 137
- Novae, 183, 327–50, 368, 369, 370  
dwarf, 329, 338, 348, 349, 370  
slow, 329  
theory, 331–50
- Nuclear abundances; *see* Elements, abundances, isotopic ratios
- Nuclear equilibrium, 513, 516, 527, 528
- Nuclear reactions in stars, 23, 24–49, 27, 35,  
73, 113, 114, 151, 186–89, 195, 197, 317,  
447, 512, 542, 544  
and age determinations, 621  
*e*-process; *see e*-process  
endothermic, 30, 355  
exothermic, 31  
and novae, 332, 333, 339  
*p*-process; *see p*-process  
production of light nuclei, 75, 76  
pynonuclear reactions, 304, 317, 318  
*r*-process; *see r*-process  
rates, 3, 116, 119–24, 127, 130–45, 166,  
185–89, 340  
*s*-process; *see s*-process
- Nuclear resonances, 120, 121, 124, 136, 138,  
139, 156, 159, 161, 165
- Occupation numbers for atomic states, 212,  
231–34, 236–38, 242, 243, 249, 258
- Opacity, calculations, 195 *ff.*, 224 *ff.*  
Eddington, 201–2, 225, 303, 319, 471, 474,  
476  
Heney, 262  
Hoyle-Hazelgrove, 262  
ionic method, 239–45  
Keller and Meyerott, 207, 209–10, 217,  
232, 254, 255, 262  
Kramers', 202, 206, 208, 211, 212, 225, 228,  
234, 238, 309, 311, 624  
Los Alamos, 239  
Lyast, 255, 256  
Mayer, 228–37, 245  
monochromatic absorption, 206–8, 237–39,  
255, 260  
Morse, 207, 217, 227, 228, 231, 232  
Moszkowski and Meyerott, 210, 218  
Strömgren, 203, 206, 207, 217, 245, 224–27,  
231, 232, 256  
Vitense, 208, 237–39, 255  
Zirin, 253, 254
- Opacity, coefficient, 260, 625  
effect of errors in, 627  
Rosseland mean, 201, 202, 205, 219, 224
- Opacity, sources of, 195 *ff.*  
absorption and scattering processes, 211 *ff.*  
bound-bound absorption, 217, 218, 228,  
233, 234, 235, 237, 245, 246, 257, 262  
bound-free, 206, 208, 211–12, 219, 225, 227,  
228, 233, 234, 235, 236, 237, 238, 245,  
247, 249, 254  
coherent scattering, 219, 220, 245, 246,  
262  
collisional broadening, 217  
Compton effect, 199, 207, 215–17, 219, 221,  
229, 236, 245, 251, 262  
electron scattering, 209, 215, 217, 227, 229,  
230, 236, 246  
free-bound emission, 211  
free-free emission, 206–8, 209, 211, 213–15,  
219, 220, 225, 226–28, 230, 236, 238,  
239, 245–47, 249, 251  
 $H^-$ , 204, 206, 208, 219, 220, 239, 245  
line absorption, 218, 228, 247, 252, 257,  
262  
molecular absorption, 220, 221, 245, 247  
natural broadening, 216  
nuclear absorption, 221  
pair production, 216, 221, 250  
photo-electric absorption, 311  
photon-photon scattering, 221  
radiation damping, 215, 216  
Raman scattering, 219  
Rayleigh scattering, 60, 200, 208, 219, 220,  
229, 239  
Thomson scattering, 198, 200, 207, 208,  
216, 217, 219, 220, 229, 239, 246
- Opacity  
graphs, 251–54, 256–61  
in stellar interiors, 202–4, 262, 263, 287,  
311, 536, 579  
tables, 236, 248, 249, 250
- Oxygen burning, 173, 175, 176  
energy-level diagrams, 138, 140
- p*-process, 3, 45, 49, 54  
Pair annihilation neutrino process, 181–83  
Pauli exclusion principle, 35, 196, 297  
Perturbations, non-radial, 528–34, 546, 547  
Perturbations, radial, 525–28, 534–46  
Phosphorus star, 58, 66  
Photo-beta process, 31, 32, 33, 34, 177  
Photo disintegration of nuclei, 3, 23, 29, 71,  
73, 114, 133, 170, 175, 221  
Photo processes, 3, 26, 27, 31, 32, 43, 216,  
219, 229  
Photon absorption; *see* Opacity  
Photon scattering; *see* Opacity, sources of  
Photoneutrino, 181, 183  
Planck's law, 189, 199  
Planetary nebulae, 4, 24, 25, 53, 321  
Point-source model, 471, 475, 484, 486–88,  
538, 597  
Polytrope models, 300, 327, 432, 531, 533  
Polytropic index, 471, 475, 531, 557

- Potential energy, gravitational; *see* Gravitational energy
- Pre-main-sequence contraction; *see* Gravitational contraction
- Pressure ionization, 298, 300, 301, 310
- Proton capture, 3, 49, 137, 138, 139
- Proton-proton cycle, 2, 51, 53, 59, 60, 61, 126–34, 203, 283, 319, 544, 583
- Protons, 73, 186–89
- Protostars, 319, 577
- Quantum statistics; *see* Fermi-Dirac statistics
- R Coronae Borealis, 56
- r*-process, 3, 4, 23, 27, 37, 38, 43–49, 50, 52, 55, 59, 86, 90, 91, 95, 96
- Radiation-braking, 482
- Radiation pressure, 65, 196, 201, 205
- Radiation temperature, 199
- Radiative cores; *see* Stellar cores
- Radiative envelopes; *see* Stellar envelopes
- Radiative equilibrium, 328, 469, 470, 473, 476, 482, 483, 485, 489, 491, 504–5, 512, 535, 540
- Radiative transfer, equation of, 198, 199, 200, 216, 468, 504; *see also* Energy transport
- Radiative processes, 3, 27, 30, 46, 161
- Radiative stresses, 504
- Radius of stars, evolutionary changes in, 583, 584, 624
- Raman scattering; *see* Opacity, sources of
- Rayleigh scattering; *see* Opacity, sources of
- Red dwarfs, 64, 204
- Red giant branch of HR diagram, 113, 114
- Red giants, 2, 3, 22, 28, 29, 30, 33, 64, 65, 483
- Relativistic degeneracy; *see* Degeneracy
- Roche's model, 530, 556, 564
- Rotation of stars, 307, 308, 320, 437, 465 *ff.* differential, 478
- Rotational distortion; *see* Instabilities
- Rotational mixing; *see* Circulation
- RR Lyrae stars, 50, 331, 425
- RT Serpentis; *see* Novae, slow
- Russell mixture, 205, 206, 207, 225, 227, 228, 310, 311
- s*-process, 3, 4, 23, 28–38, 45, 50, 54, 86, 90
- Saha equation, 208, 239, 310, 511
- Schuster-Schwarzschild atmosphere model; *see* Stellar atmospheres
- Secular instability; *see* Instabilities
- Shell source, 332, 338, 339, 483, 486, 488
- Spallation
  - cosmic-ray induced, 66–87
  - cross-sections, 77, 81–85
  - reactions, source of light nuclei, 77–87
- Specific heats, 505, 510, 512
- Spectral energy distribution, 198
- Spontaneous emission of photons, 199
- SS Cygni, 329, 338, 348, 349, 370
- Standard model, 471, 536
- Star clusters, 65, 483
  - and abundances of chemical elements in, 51–55
  - ages of, 618–24
  - galactic, 53, 93
  - globular, 52, 53, 93
  - HR diagrams, 618–20
- Star formation, 49, 54, 60, 62, 94, 95, 577–81
- Stark effect, 66, 217, 218, 246, 258
- Stellar absorption coefficient; *see* Opacity
- Stellar atmospheres, 23, 49, 50, 61, 65, 73, 79, 82, 198, 200, 202, 204, 206, 208, 217, 218, 220, 237, 239, 247, 260, 435, 436, 544
  - Schuster-Schwarzschild, 204
- Stellar cores, 29, 114, 197, 287, 304, 305, 311, 312, 314, 331, 332, 336, 337, 354, 535–40, 583, 584
  - convective, 203, 204, 209, 271, 445, 466, 482, 507, 508, 535 *ff.*, 581, 584
  - degenerate, 311, 312, 316, 320, 332–36, 536
  - and energy generation, 2, 4, 50, 60, 61, 62, 65, 156, 170, 184, 316, 547
  - helium, 30, 113, 167, 332
  - isothermal, 316, 332, 338, 339, 483, 552, 586, 587
  - radiative, 535
  - Schönberg-Chandrasekhar limit, 552
- Stellar diameters; *see* Radius of stars
- Stellar energy sources; *see* Energy sources, of stars
- Stellar envelopes, 200, 316, 320
  - convective, 64, 66, 67, 205, 262, 270, 271, 286, 441, 445, 459, 466, 475, 476, 483, 488, 489, 491, 492–95, 540–42, 586
  - radiative, 476, 483, 487, 491, 586
- Stellar evolution; *see* Evolution of stars
- Stellar models, 33, 78, 93, 202, 203, 207, 210, 262, 300, 303, 304, 312, 313, 317, 318, 338, 535, 536, 537, 538, 575, 576, 580, 588
  - boundary-value problem, 595, 596
  - construction of evolutionary sequence, 269–92, 318, 576 *ff.*, 593–612
  - difference methods, 603–14
  - differential equations method, 594–603
  - iteration, 603
  - pure hydrogen-helium stars, 289, 290
  - pure hydrogen stars, 289
  - pure hydrogen white dwarfs, 304, 319
  - relaxation method, 603
  - zero-age line, 289, 290
- Stellar populations, 2, 31, 50, 52, 55
  - population I, 2, 272, 273, 289, 290, 314
  - population II, 31, 288, 289–91
- Stellar radii; *see* Radius of stars
- Stellar stability, 499–560
  - defined, 500
- Subdwarfs, 288–91
  - A-type, 288
  - F-type, 288
  - G-type, 56
  - UBV photometry of, 288
- Sulphur, energy-level diagram, 174



- Sun and solar system, 4, 5, 72, 73, 74, 75, 76,  
77, 81, 82, 85, 94, 96, 149, 203, 284, 285,  
286, 576  
age, 44, 90-92, 202  
chemical abundances and composition, 2,  
3, 4, 5, 23, 26, 31, 35-38, 47, 49, 50,  
58, 70, 74, 283, 589  
energy, 576  
neutrinos, 149-51  
Superadiabatic temperature gradient, 466,  
493, 495  
Supergiants, 22, 54, 56, 184, 541  
Supernovae, 2, 3, 23, 25-27, 31, 38, 45, 47-49,  
55, 71, 72, 92, 114, 183, 185, 350-63  
and chain reactions, 362, 363  
classification, 392-412  
type I, 26, 47, 48, 351, 361, 372, 373,  
380, 381, 391, 392, 393-401, 414, 416,  
417, 418  
type II, 26, 351, 360, 372, 373, 380, 401,  
402, 414, 418  
type III, 402-7  
type IV, 407-10  
type V, 367, 373, 410-12  
distribution, 379-83, 385-91  
frequency, 372, 378-84  
light-curves, 47, 389, 393-95, 403, 404,  
407, 410  
list of Known, 375, 376  
magnitude-redshift relation, 391, 392  
origin of solar system, 90, 91  
and radio galaxies, 363, 416  
remnants, 415, 416  
spectra, 373, 374, 395-401, 402, 405, 406,  
408, 409, 411, 412-15  
theories, 26, 27, 367 *ff.*, 417-20  
Surface nuclear reactions, 4, 50, 57, 59, 447  
Synchrotron radiation, 48
- Technetium, 2, 28, 33  
Temperature, effective, 313, 615  
initial conditions, 31  
Thermal energy, 48, 184, 355, 466, 509, 510,  
512, 515, 548, 554  
Thermal equilibrium, 49, 317, 466, 468-77  
Thermal instability; *see* Instabilities, thermal  
Thermodynamic equilibrium, 49, 73, 198, 434  
Thermonuclear reactions, 1 *ff.*, 119 *ff.*, 122  
(Table), 130-45, 159-65, 185-89, 342,  
501, 512, 516, 537; *see also* Nuclear reac-  
tions in stars  
Thomson scattering; *see* Opacity  
Three-alpha process; *see* Triple-alpha process  
Tidal distortion, 562  
Tidal potential, 562  
Trans-bismuth elements, 3, 44, 49  
Transmutation of elements, 1 *ff.*  
from H, 142-52  
from He, 166-69, 185  
Triple-alpha process, 2, 27, 28, 29, 56, 354  
Turbulent convection, 506, 508-10; *see also*  
Instabilities
- U Geminorum stars, 322, 336, 346, 348-50  
URCA process, 176-78, 356, 359
- Virial theorem, 184, 427-30, 465, 466, 526,  
548, 558, 559, 560, 561, 562, 565  
and stability, 429, 430  
Viscosity, 328, 476, 477, 493, 507, 515, 516,  
520, 534, 544, 546, 547  
dynamical, 505, 515  
kinematic, 328  
molecular, 509  
radiative, 505, 509  
turbulent, 508, 509, 515, 534, 544  
Vogt-Russell theorem, 466, 596, 614
- Weak interaction process and neutrino pro-  
duction, 178-83
- White dwarfs, 196, 204, 297-323, 327, 336,  
337, 361, 363, 527, 528, 537, 538, 553  
AC 70°8247, 306  
Chandrasekhar limiting mass, 300, 308  
defined, 297  
40 Eridani B, 305, 306, 314  
mass-radius relation, 303, 305, 352, 353,  
362  
origin and evolution, 319-22  
Procyon B, 305, 307  
Ross 627, 307  
Wolf 219, 307  
*see also* Degeneracy
- Zero-age stars; *see* Evolution of stars, zero-  
age stars; Stellar models, zero-age line  
Zero-temperature stars, 297-309

## **STARS AND STELLAR SYSTEMS**

### ***Compendium of Astronomy and Astrophysics***

This series, comprising nine volumes is intended to present the basic empirical information in each area of astrophysics and stellar astronomy with an appropriate background of theory, relevant to the current status and development of the science. Extreme specialization has been avoided in order to make the chapters suitable to graduate students and also to the increasing number of scientists in other fields requiring astronomical information.

Separate editors have been appointed for each volume. The volume editors together with the general editors form the editorial board which is responsible for the over-all planning of the series.

#### ***General Editor . . .***

GERARD P. KUIPER, head of the Lunar and Planetary Laboratory, University of Arizona, was formerly director of Yerkes Observatory, University of Chicago.

#### ***Associate General Editor . . .***

BARBARA M. MIDDLEHURST, Research Associate at the Steward Observatory of the University of Arizona, was formerly lecturer in astronomy, St. Andrews University, Scotland.

# STARS AND STELLAR SYSTEMS

## VOLUME TITLES:

I

TELESCOPES

II

ASTRONOMICAL TECHNIQUES

III

BASIC ASTRONOMICAL DATA

IV

CLUSTERS AND BINARIES

V

GALACTIC STRUCTURE

VI

STELLAR ATMOSPHERES

VII

NEBULAE AND INTERSTELLAR MATTER

VIII

STELLAR STRUCTURE

IX

GALAXIES AND THE UNIVERSE

STELLAR  
STRUCTURE

ALLER and  
McLAUGHLIN

STARS  
AND  
STELLAR  
SYSTEMS  
VOLUME  
VIII



CHICAGO